On Spin Locks in AUTOSAR: Blocking Analysis of FIFO, Unordered, and Priority-Ordered Spin Locks

Alexander Wieder Björn B. Brandenburg
Max Planck Institute for Software Systems (MPI-SWS)

***Abstract*—Motivated by the widespread use of spin locks in embedded multiprocessor real-time systems, the worst-case blocking in spin locks is analyzed using mixed-integer linear programming. Four queue orders and two preemption models are studied: (i) FIFO-ordered spin locks, (ii) unordered spin locks, (iii) priority-ordered spin locks with unordered tie-breaking, and (iv) priority-ordered spin locks with FIFO-ordered tie-breaking, each analyzed assuming both preemptable and non-preemptable spinning. Of the eight lock types, seven have not been analyzed in prior work. Concerning the sole exception (non-preemptable FIFO spin locks), the new analysis is asymptotically less pessimistic and typically much more accurate since no critical section is accounted for more than once. The eight lock types are empirically compared in schedulability experiments. While the presented analysis is generic in nature and applicable to real-time systems in general, it is specifically motivated by the recent inclusion of spin locks into the AUTOSAR standard, and four concrete suggestions for an improved AUTOSAR spin lock API are derived from the results.**

I. INTRODUCTION

Spin locks are widely used in (embedded) multiprocessor real-time systems to coordinate mutually exclusive access to shared resources. For instance, the use of spin locks is mandated by the AUTOSAR real-time operating system (RTOS) standard [1] for inter-core synchronization. Unfortunately, although many different types of spin locks are used in practice, worst-case blocking analysis is available only for a single spin lock type, namely FIFO-ordered spin locks [7, 8, 13, 16]. In this work, we fill this gap by developing a novel worst-case blocking analysis approach suitable for analyzing a wide range of different spin lock types. Notably, this analysis approach can be applied even if the type of spin lock is unknown. While our analysis is generic in nature and applicable to real-time systems in general, it is motivated specifically by the recent inclusion of spin locks into the AUTOSAR standard, which we consider in this paper as a representative case study indicative of current industrial practice.

A. Motivation: Spin Locks in Theory and Practice

From an implementation point of view, spin locks are highly attractive in embedded systems because they require little OS support and typically cause very low runtime overheads. However, in hard real-time embedded systems (such as many of the automotive systems targeted by AUTOSAR), low runtime overheads by themselves are insufficient. Rather, it is equally important for an RTOS to guarantee *predictable* blocking times. That is, it must be possible to derive *a priori* bounds on each task's *worst-case response time*, which in turn requires bounding the maximum delays due to lock contention. To this end, formal *blocking analysis* of the employed locking primitives is required.

Unfortunately, such analysis is not yet available for all relevant lock types. Prior analysis of spin locks in real-time systems (reviewed in Sec. I-C) has focused on *non-preemptable FIFO spin locks*, where jobs busy-wait non-preemptably in FIFO order in case of contention. Such locks are easy to analyze, and appropriate bounds on worst-case blocking have been derived [7, 8, 13, 16]. However, while non-preemptable FIFO spin locks are analytically most convenient, other sometimes incompletely specified spin lock types are also used in practice.

For instance, AUTOSAR mandates the availability of spin locks, but does not specify any particular type. Hence, instead of FIFO-ordered locks, AUTOSAR-compliant RTOSs may in fact offer *priority-ordered* spin locks, or even *unordered* spin locks without any progress guarantees. In particular, unordered spin locks are likely used frequently in practice due to their simple implementation and minimal space requirements, as we review in Sec. II. To the best of our knowledge, no suitable worst-case analysis for unordered and priority-ordered non-preemptable spin locks has been proposed to date. Thus, while desirable from an implementation point of view, these spin lock types currently cannot be employed in predictable hard real-time systems.

Another limitation in existing analysis is the reliance on non-preemptable spinning, which can be unacceptable in the presence of latency-sensitive tasks (*i.e.*, tasks that must be scheduled immediately when activated) as such spinning can cause scheduling latencies linear in the number of processors. To avoid long non-preemptable sections, prior work has explored the design and implementation of *preemptable spin locks* [3, 12, 19], where busy-waiting jobs can be preempted at any time and only the actual critical sections are executed non-preemptably. The primary benefit of preemptable spinning is that the maximum non-preemptable section length is independent of the number of processors (which, given rising core counts, is highly desirable), albeit at the cost of increased worst-case blocking, which arises because preempted jobs must "reissue" their lock requests after a preemption (*e.g.*, in FIFO-ordered spin locks, preempted jobs must re-queue again at the end of the queue [3, 12]). While preemptable spinning may be unavoidable in demanding latency-sensitive applications, no analysis of the associated increase in blocking has been proposed to date, which renders such locks unsafe in the context of predictable hard real-time systems.

B. Contributions

In this paper, we address the lack of blocking analysis for common spin lock types with a comprehensive framework for the formal analysis of spin delays under *partitioned fixed-priority* (P-FP) scheduling,[1] a scheduling approach widely

[1] Under *partitioned* scheduling, each task is statically allocated to a processor and each processor is scheduled using a uniprocessor policy. In contrast, under *global* scheduling, all processors serve a single ready queue and tasks migrate.

The conference version of this extended tech report appears in the *Proceedings of the 34th IEEE Real-Time Systems Symposium (RTSS 2013)*, December 2013, IEEE.

employed in practice (*e.g.*, in AUTOSAR [1]). In particular, we provide new blocking analysis for eight types of spin locks: **(i)** FIFO-ordered spin locks, **(ii)** unordered spin locks, **(iii)** priority-ordered spin locks with unordered tie-breaking, and **(iv)** priority-ordered spin locks with FIFO-ordered tie-breaking, each analyzed assuming both preemptable and non-preemptable spinning. Of the eight considered spin lock types, seven have not been formally analyzed in prior work.

The second major contribution of this paper pertains to *how* delays due to spin locks are analyzed. A key problem with spin locks is that they give rise to *transitive blocking*—when a high-priority job busy-waits due to a spin lock, it occupies a processor and prevents lower-priority jobs from executing, which are thus transitively delayed by lock contention encountered by the higher-priority job. To obtain sound bounds on worst-case blocking, such transitive delays must be fully accounted for. Prior analysis [7, 8, 13, 16] has dealt with this issue by inflating job execution costs. That is, prior to computing response-time bounds, each task's worst-case execution time is inflated to reflect the maximum time spent busy-waiting. This is safe, but, as we show in Sec. III, also pessimistic as it can cause the impact of individual critical sections to be overestimated by a factor of $\Omega(n \cdot \phi)$, where n is the number of tasks and ϕ is the ratio of the longest and the shortest period. In this paper, we propose a new, asymptotically less pessimistic analysis approach that ensures that no critical section is accounted for more than once. Our approach extends a recently proposed analysis technique for semaphore protocols [9] based on *linear programming*, and is shown to yield often much improved blocking bounds (Sec. V).

Finally, we provide guidelines—backed by empirical evidence based on the new analysis—as to when each of the eight considered lock types is most appropriate (Secs. IV and V), and conclude with suggestions for possible future improvements of AUTOSAR's spin lock API (Sec. VI).

C. Related Work

Spin lock algorithms have long been studied in the literature on general-purpose multiprocessing; comprehensive overviews of classic solutions to the shared-memory mutual exclusion problem are provided by Raynal [24] and Anderson *et al.* [4]. The seminal work on efficient, list-based spin locks with FIFO semantics is due to Mellor-Crummey and Scott [22]. Based on their technique, priority-ordered variants for use in real-time systems were later developed [12, 18, 21], as were extensions that allow spinning jobs to be preempted [3, 12, 19]. Most preemptable spin locks, and especially list-based spin locks, require OS support to reliably detect preempted jobs [19]. If preempted, spinning jobs are automatically dequeued in such locks, thus forcing them to requeue after the preemption, which may occur repeatedly during a single lock acquisition attempt.

Takada and Sakamura [27] proposed a preemptable FIFO spin lock in which preempted tasks are not dequeued, but merely skipped (*i.e.*, preempted jobs do not requeue at the end of the FIFO queue after a preemption), which lessens the delay incurred by the preempted job. However, skipping also leads to worse blocking bounds for tasks that are *not* preempted since, in the worst case, up to $n - 1$ other tasks may already be queued and become eligible in time to block later-queued tasks. Due to this inherent pessimism, we do not consider skipping-based preemptable spin locks any further. We also do not consider "spin-lock-like" synchronization mechanisms based on *restartable critical sections* [17] or *helping* techniques [28], because such mechanisms are less general than ordinary spin locks (*e.g.*, neither approach can deal gracefully with side effects in critical sections such as writes to shared I/O ports) and thus are ill-suited for use as a generic, RTOS-provided locking primitive.

Gai *et al.* [16] were the first to formally analyze blocking due to spin locks in partitioned multiprocessor real-time systems. They proposed the *Multiprocessor Stack Resource Policy* (MSRP), which combines Baker's classic uniprocessor *Stack Resource Policy* [6] for processor-local synchronization with non-preemptable FIFO spin locks for inter-processor synchronization, and derived corresponding bounds on worst-case blocking. Notably, if a task contains more than one critical section, Gai *et al.*'s analysis considers each critical section individually. We review the MSRP in Sec. II.

Devi *et al.* [13] presented an analysis of non-preemptable FIFO spin locks analogous to Gai *et al.*'s analysis [16] assuming global instead of partitioned scheduling. Non-preemptable FIFO spin locks were also integrated into Block *et al.*'s *Flexible Multiprocessor Locking Protocol* (FMLP) [7], which supports both global and partitioned scheduling. Motivated by the FMLP and subsequently developed protocols, *holistic blocking analysis* was developed [8, Ch. 5], which improves upon Gai *et al.*'s and Devi *et al.*'s approach [13, 16] by considering all of a task's critical sections together to reduce pessimism in the presence of infrequent long critical sections. Nonetheless, holistic analysis of spin locks [8] is still subject to considerable pessimism because it requires inflating each task's execution cost (see Sec. II). The new analysis in Sec. III overcomes this limitation.

A well-studied alternative to spin locks are *semaphore protocols*, wherein blocked tasks yield the processor to lower-priority tasks by suspending instead of busy-waiting until the lock becomes available. While busy-waiting conceptually wastes processor cycles, it has the dual advantage of maintaining cache affinity (cache contents are likely perturbed when tasks suspend) and of avoiding scheduler invocations and context switches (which can be costly compared to typical spin lock overheads). *Provided that critical sections are suitably short*, spin locks are often more efficient in practice [8]. For inherently long critical sections, semaphore protocols are more appropriate. (See *e.g.* [8] for a recent survey of such protocols.)

Two notable hybrid approaches exist. Lakshmanan *et al.* [20] proposed the *Multiprocessor Priority Ceiling Protocol with Virtual Spinning*, a semaphore protocol that emulates busy-waiting by letting suspended tasks "virtually spin" to prevent other tasks from acquiring locks. Their analysis still assumes that tasks suspend and is thus not directly applicable to actual spin locks. And finally, Faggioli *et al.* [15] proposed a locking protocol for reservation-based schedulers that includes preemptable spinning. Their protocol differs from the preemptable spin locks considered herein in that even lock holders remain preemptable, which in turn requires considerable scheduling machinery to ensure resource-holder progress. In contrast, we focus on true lightweight spin locks that do not require scheduler invocations.

D. System Model and Notation

We consider a real-time workload consisting of n sporadic tasks $\tau = \{T_1, \ldots, T_n\}$ scheduled on m identical processors $P_1, \ldots, P_m$. We denote a task T_i's *worst-case execution time* (WCET) as e_i and its *period* as p_i, and let J_i denote a job of T_i. A task's *utilization* is defined as $u_i = e_i/p_i$. A job J_i is *pending* from its release until it completes. T_i's *worst-case response time* r_i denotes the maximum duration that any J_i remains pending. For simplicity, we assume implicit deadlines and that tasks do not self-suspend (*i.e.*, pending jobs are always ready). We define ϕ to be the ratio of the maximum and the minimum period; formally $\phi = \max_i\{p_i\}/\min_i\{p_i\}$.

We assume P-FP scheduling. Each task is statically assigned to a processor, and each processor schedules pending jobs preemptably in order of decreasing task priority (unless preemptions are temporarily restricted, see Sec. II). We let $P(T_i)$ denote the processor to which T_i has been assigned, and let π_i denote the scheduling priority of T_i, where $\pi_i < \pi_x$ implies that T_i has higher priority than T_x.

Besides the m processors, the tasks share a set Q of n_r serially-reusable resources $Q = \{\ell_1, \ldots, \ell_{n_r}\}$ (*e.g.*, I/O ports, data structures, *etc.*). We let $N_{i,q}$ denote the maximum number of times that any J_i accesses ℓ_q, and let $L_{i,q}$ denote T_i's *maximum critical section length*, that is, the maximum time that any J_i uses ℓ_q as part of a single access ($L_{i,q} = 0$ if $N_{i,q,} = 0$). We assume that jobs must be scheduled in order to use shared resources, and that jobs release all shared resources prior to completion.

Finally, we make the simplifying assumption that jobs request and hold at most one resource at a time. That is, we do not consider *nested* critical sections in this paper. Nested critical sections are certainly relevant in practice, but cause severe analytical challenges even when considering only "nesting-friendly" spin lock types. Given that our focus is a comprehensive exploration of *all* major spin lock types, we postpone a discussion of nesting support, which we are actively investigating, to future work. None of the prior detailed analyses of spin locks [7, 8, 13, 16, 29] supports *fine-grained* nested critical sections.[2]

II. Spin Locks in Practice

Although the blocking analysis presented in this work is of general relevance, we focus in the following on AUTOSAR as a representative example of spin lock support in practice.

In partitioned multiprocessor systems, there are two types of shared resources: *local resources* and *global resources*, with the distinction that global resources are used on multiple processors, whereas local resources are shared only among tasks on a single processor. Local resources are simpler to deal with since they require only uniprocessor synchronization, for which optimal locking protocols such as the *Priority Ceiling Protocol* (PCP) [26] and the *Stack Resource Policy* (SRP) [6] have long been known. In AUTOSAR, local resources are managed with the PCP via the `GetResource()` and `ReleaseResource()` APIs.

[2]Nesting can be trivially supported under any locking protocol with *group locks* [7, 8], which reduce fine-grained resource nesting to coarse-grained, unnested (group) locking, albeit with a loss of parallelism and analysis accuracy. Ward and Anderson [29] recently showed how to support nested critical sections without loss of asymptotic optimality under a variety of locking protocols, including non-preemptable FIFO spin locks. Their technique, however, requires additional runtime support (a partial order of all resources that may be nested is required to defer certain requests), which puts it beyond the realm of AUTOSAR for now. Further, [29] does not include fine-grained analysis (the focus of [29] is asymptotic optimality), which puts it outside the scope of this paper.

Algorithm 1 Non-preemptable spin lock in AUTOSAR.

```
1: SuspendAllInterrupts()
2: GetSpinLock(lock)
3: // critical section
4: ReleaseSpinLock(lock)
5: ResumeAllInterrupts()
```

Global resources are more challenging to support as they require inter-core synchronization. As discussed in Sec. I, the AUTOSAR standard mandates spin locks for this purpose. In particular, the AUTOSAR API [1, p.110] includes the functions `GetSpinLock()` and `ReleaseSpinLock()` to acquire and release a spin lock. When a task T_x holds the lock for a global resource ℓ_q and a second task T_i tries to acquire the lock for ℓ_q with `GetSpinLock()`, T_i busy-waits (*i.e.*, spins) until it successfully acquires the lock. After obtaining the associated lock for a resource, a critical section can safely be executed without interference from other tasks.

To ensure a timely completion of critical sections, preemptions due to higher-priority tasks during the execution of a critical section must be avoided. To this end, AUTOSAR provides the `SuspendAllInterrupts()` API to temporarily disable interrupts [1, p.46]. After the critical section, interrupts must be re-enabled with the `ResumeAllInterrupts()` call. With this API, non-preemptable spin locks can be trivially implemented in AUTOSAR by disabling all interrupts prior to calling `GetSpinLock()`, as illustrated in Algorithm 1.

Notably, AUTOSAR mandates the availability of spin locks, but does not specify a concrete algorithm or specific spin lock semantics (beyond the assurance of mutual exclusion). That is, spin locks in AUTOSAR are not required to satisfy lock requests in any specific order. This leaves considerable leeway to OS implementors, who can choose whichever algorithm and semantics are easiest to support on their target platforms, but is problematic from the point of view of worst-case analysis.

However, if `GetSpinLock()` ensures that conflicting critical sections are executed in FIFO order, then Gai *et al*.'s analysis of spin locks [16] is applicable to AUTOSAR, as we review next.

A. The Multiprocessor Stack Resource Policy

Gai *et al*. introduced the *Multiprocessor Stack Resource Policy* (MSRP) [16], a multiprocessor extension of the classic SRP [6]. Under the MSRP, non-preemptable FIFO-ordered spin locks are used to coordinate access to global resources, and the SRP is used for local resources. While AUTOSAR mandates the PCP (and not the SRP), the two protocols are in fact quite similar and result in equivalent worst-case blocking. Thus, assuming spin locks are employed as illustrated in Algorithm 1, and assuming that `GetSpinLock()` implements spin locks with FIFO semantics (*e.g.*, ticket or queue locks [22]), Gai *et al*.'s analysis of the MSRP [16] directly applies to AUTOSAR as well.

Under the MSRP, jobs are subject to three types of blocking: *local blocking* due to the SRP, and *non-preemptive blocking* and *remote blocking* due to spin locks. The former two types both cause *priority inversions* [10, 26], whereas the latter results in spinning. We briefly review the analysis of each blocking type.

a) Local Blocking: The SRP (and the PCP) are based on *resource ceilings*. The resource ceiling $\Pi(\ell_q)$ of a local resource ℓ_q is the highest priority among all tasks accessing ℓ_q: $\Pi(\ell_q) = \min_{T_i}\{\pi_i | N_{i,q} > 0\}$. Further, a dynamic *system ceiling* $\hat{\Pi}(t)$ is defined to be the highest resource ceiling of any resource in use at time t: $\hat{\Pi}(t) = \min_{\ell_q}\big\{\{\Pi(\ell_q) |\, \ell_q \text{ is locked at time } t\} \cup \{n+1\}\big\}$, where $\hat{\Pi}(t) = n+1$ indicates that no resource is locked. The key scheduling rule of the SRP is that a newly released job J_i may only start executing at time t if $\pi_i < \hat{\Pi}(t)$, which ensures the availability of all local resources that J_i might access.

A job J_i incurs local blocking if, at the time of J_i's release, a job of a local lower-priority task T_l executes a request for a local resource ℓ_q with $\Pi(\ell_q) \leq \pi_i$. Under the SRP, T_l's request for ℓ_q causes the system ceiling $\hat{\Pi}(t)$ to be set to *at least* $\Pi(\ell_q)$. If T_i releases a job while T_l is holding ℓ_q, J_i is delayed since $\hat{\Pi}(t) \leq \pi_i$, and hence J_i is blocked by T_l's job.

Each job of T_i can be locally blocked at most once (upon release) for a duration of at most β_i^{loc} time units, where

$$\beta_i^{loc} = \max_{T_l,q}\{L_{l,q} | N_{l,q} > 0 \wedge \Pi(\ell_q) \leq \pi_i < \pi_l \wedge \ell_q \text{ is local}\}.$$

For brevity of notation, we define $\max(\emptyset) \triangleq 0$ in this paper.

b) Remote Blocking: When using non-preemptable spin locks, a job J_i that requested a global resource ℓ_q spins non-preemptably until gaining access. Due to the strong progress guarantee of FIFO spin locks, the maximum spin time per request, denoted as $S_{i,q}$, is bounded by the sum of the maximum critical section lengths on each other processor (w.r.t. ℓ_q):

$$S_{i,q} = \begin{cases} \sum\limits_{P_k \neq P(T_i)} \max\{L_{x,q} | P(T_x) = P_k\} & \text{if } N_{i,q} > 0, \\ 0 & \text{if } N_{i,q} = 0. \end{cases}$$

This implies an upper bound β_i^{rem} on the maximal total remote blocking incurred by any J_i, where $\beta_i^{rem} = \sum_{\ell_q} N_{i,q} \cdot S_{i,q}$.

c) Non-Preemptive Blocking: A lower-priority job J_l spinning or executing non-preemptably can cause a job of T_i to incur a priority inversion upon release. The maximum duration β_i^{NP} of such blocking is bounded by T_l's worst-case spin time and critical length for a single request:

$$\beta_i^{NP} = \max\big\{S_{l,q} + L_{l,q} \mid P(T_i) = P(T_l) \wedge \pi_i < \pi_l \wedge \ell_q \text{ is global}\big\}.$$

d) Schedulability Analysis: Finally, response-time analysis [5] is used to check if T_i is schedulable. Under the MSRP, a safe bound on T_i's maximum response time r_i is given by a solution to the following recurrence [16]:

$$r_i = e_i + \beta_i^{rem} + \max\big\{\beta_i^{NP}, \beta_i^{loc}\big\} + \sum_{\substack{\pi_h < \pi_i \\ P(T_i) = P(T_h)}} \left\lceil \frac{r_i}{p_h} \right\rceil \cdot e'_h,$$

where $e'_h = e_h + \beta_h^{rem}$ denotes T_h's *inflated* execution cost. Given the response-time bound r_i, T_i is schedulable if $r_i \leq p_i$. Thus, schedulability under AUTOSAR can be verified *a priori*, provided that `GetSpinLock()` implements FIFO semantics.

However, as noted in Sec. I, non-preemptable FIFO spin locks can have a detrimental effect on worst-case scheduling latencies. This is apparent in the above analysis: the worst-case non-preemptive blocking β_i^{NP} depends on the remote blocking $S_{l,q}$ of any lower-priority tasks T_l, and $S_{l,q}$ in turn depends on the sum of the maximum critical section length *on each processor*. The worst-case scheduling latency (*i.e.*, $\max(\beta_i^{NP}, \beta_i^{LOC})$) can thus increase linearly with m.

Given the trend towards rising core counts, non-preemptable spinning is thus unlikely to be the appropriate choice in all cases. To avoid tying β_i^{NP} to the number of processors, the preemption of spinning jobs must be permitted. While not explicitly supported, this can be readily realized with the current AUTOSAR specification, as described next.

Algorithm 2 Preemptable unordered spin lock in AUTOSAR.

```
1: SuspendAllInterrupts()
2: if TryToGetSpinLock(lock) ≠ TRYTOGETSPINLOCK_SUCCESS then
3:     ResumeAllInterrupts()
4:     go to 1
5: // critical section
6: ReleaseSpinLock(lock)
7: ResumeAllInterrupts()
```

B. Unordered Preemptable Spin Locks

First of all, it is worth emphasizing that even in the case of preemptable spinning, the actual critical section must still be executed non-preemptably (*e.g.*, see [3, 12, 27]). This is required to avoid the preemption of a lock-holding job, which could result in excessive delays (*i.e.*, if lock holders could be preempted, bounds on worst-case blocking would have to reflect entire job execution costs, which is undesirable since job execution costs are typically much larger than critical sections). Therefore, it is *not* sufficient to simply exchange lines 1 and 2 in Algorithm 1, because then a task that successfully acquired a spin lock could still be preempted just before calling `SuspendAllInterrupts()`, thereby allowing the lock-holder preemption problem to occur. That is, simply calling `GetSpinLock()` with interrupts enabled—although permitted by AUTOSAR—does not yield a proper *predictable* spin lock.

However, it is possible to implement preemptable spin locks within the scope of AUTOSAR using the `TryToGetSpinLock()` API [1, p.105], which acquires the requested lock if it is available, and otherwise fails immediately without spinning. As illustrated in Algorithm 2, the `TryToGetSpinLock()` procedure can be used to realize proper preemptable spin locks.

The presented approach allows for preemptions during spinning (lines 3 and 4), yet still ensures that lock holders are not preempted. Unfortunately, this is only possible at the expense of all ordering guarantees (if any): even if the underlying spin lock implementation serves requests in a specific order (*e.g.*, in FIFO order as considered in Sec. II-A), the construction shown in Algorithm 2 does not preserve this ordering, nor does it guarantee any particular order. The resulting lack of any ordering guarantees makes it challenging to derive non-trivial bounds on worst-case blocking, and to the best of our knowledge, no analysis of such *unordered* spin locks has been proposed to date.

C. A Hypothetical API For Preemptable Spin Locks

Of course, preemptable spinning does not inherently imply a lack of ordering guarantees [3, 12, 27]. However, the current

Algorithm 3 Proposed API for preemptable spin locks.

```
1: GetPreemptableSpinLock(lock)
   // atomically disables interrupts on lock acquisition
2: // critical section
3: ReleaseSpinLock(lock)
4: ResumeAllInterrupts()
```

AUTOSAR specification [1] does not provide a high-level API suitable for accommodating spin locks that both are preemptable and ensure a specific order, which would be much more analysis-friendly. To address this shortcoming, we assume the availability of a hypothetical API for spin locks with preemptable spinning: `GetPreemptableSpinLock()`.

To facilitate analysis, `GetPreemptableSpinLock()` is defined to have the following semantics. In the presence of contention, `GetPreemptableSpinLock()` ensures that the task remains fully preemptable, as is the case in Algorithm 2. However, there are important differences. First, unlike `GetSpinLock()`, the envisioned `GetPreemptableSpinLock()` API *atomically* disables interrupts as part of acquiring the lock (which may require OS support [3, 12, 27]). Second, unlike Algorithm 2, we assume that `GetPreemptableSpinLock()` enforces a specified order among conflicting critical sections. Algorithm 3 shows how the envisioned API could be used to combine preemptable spinning with arbitrary order guarantees.

D. Considered Spin Lock Types

A primary motivation driving this work is that AUTOSAR does not specify any particular ordering for `GetSpinLock()`; a compliant RTOS can thus implement any order. Similarly, the envisioned API for preemptable spin locks, `GetPreemptableSpinLock()`, *can* be combined with any order. This poses the question: when implementing an AUTOSAR-compliant OS, which order *should* be chosen (from a real-time point of view)? Further, should the AUTOSAR specification itself perhaps mandate a specific order?

We have identified four orderings that warrant closer study for reasons of either practical relevance or analytical suitability: unordered, FIFO-ordered, and two variants of priority-ordered spin locks (explained below). Each of these four orderings can be combined with either non-preemptable spinning (Algorithm 1) or preemptable spinning (Algorithm 3), for a total of eight considered lock types, as summarized in Table I.

The inclusion of *FIFO-ordered* spin locks is obvious given that they offer the strongest progress guarantee—starvation freedom—and given that applicable analysis already exists [16].

Unordered spin locks (*i.e.*, spin locks that do not guarantee any particular order) are decidedly unattractive from an analytical point of view, but have practical relevance nonetheless. First, since AUTOSAR does not specify any particular ordering for `GetSpinLock()`, unordered spin locks must be assumed when analyzing current systems. (Assuming unordered spin locks is a safe assumption, as any analysis of unordered spin locks is necessarily also correct for any specific order.) Second, basic *test-and-set* (TAS) locks, which are "the simplest mutual exclusion lock[s] found in all operating system textbooks and widely used in practice" [22], are inherently unordered. TAS locks are further attractive because they can be realized with minimal memory, namely only a single bit, which makes them suitable for even the most memory-constrained environments (*e.g.*, TAS locks can be embedded into other data structures). And finally, Algorithm 2 yields unordered preemptable spin locks, regardless of the underlying spin lock implementation.

TABLE I
OVERVIEW OF SPIN LOCK TYPES CONSIDERED IN THIS PAPER

short name	guaranteed order of requests	preemptable spinning	representative implementation(s)
U|N	unordered	no	test-and-set
U|P	unordered	yes	Algorithm 2
F|N	FIFO	no	[22]
F|P	FIFO	yes	[12, 19, 27]
P|N	priority/unordered	no	[23]
P|P	priority/unordered	yes	[23]
PF|N	priority/FIFO	no	[12, 18, 21]
PF|P	priority/FIFO	yes	[12, 18, 21]

Finally, in a real-time system, it is natural to consider *priority-ordered* spin locks, based on the intuition that urgent tasks with higher scheduling priorities should also receive preferential treatment when contending for resources other than processor time [12, 18, 21]. However, a task's scheduling priority and the locking priority considered for request ordering do not necessarily have to coincide. For one, depending on the employed implementation, the number of available distinct locking priorities may be limited, and further, as we show in Sec. V, it can be beneficial to apply locking priorities only selectively. It is thus necessary to specify how to break ties in locking priority, that is, how to order conflicting critical sections of equal priority. In list-based priority-ordered spin locks [12, 18, 21], *FIFO-ordered tie-breaking* is natural. However, it is also possible to construct priority-ordered spin locks using other techniques [23] (or simply from TAS locks), in which case *unordered tie-breaking* must be assumed (*i.e.*, critical sections of equal priority are executed in arbitrary order). We consider both tie-breaking variants in this paper.

For brevity, we refer to each of the eight lock types using a short name as listed in Table I. To the best of our knowledge, only F|N locks (*i.e.*, **F**IFO locks with **n**on-preemptable spinning) have been considered in the context of worst-case blocking analysis before. As part of this work, we derived new blocking analysis for all of the eight spin lock types listed in Table I.

III. AN IMPROVED ANALYSIS OF SPIN LOCKS

All prior analyses of spin locks [7, 8, 13, 16] rely on inflating job execution costs to (indirectly) account for transitive blocking effects (*e.g.*, the delay that a job incurs when a higher-priority spinning job occupies the processor). While this approach is attractively simple, we chose to follow a different, more explicit approach [9] in our analysis instead.

The fundamental weakness in inflating job execution costs is that an individual critical section may be accounted for multiple times. In particular, in the analysis of a job J_i that is repeatedly preempted by jobs of a higher-priority task T_h, any inflation of the execution cost of T_h will be reflected $\lceil r_i/p_h \rceil$ times due to the mechanics of response-time analysis. With $\Omega(n)$ higher-priority tasks and $\lceil r_i/p_h \rceil \approx \phi$, considerable pessimism accumulates. We summarize this observation as follows (a formal proof is given in Appendix A).

Theorem 1. *Any blocking analysis relying on the inflation of job execution costs can be pessimistic by a factor of* $\Omega(\phi \cdot n)$.

To avoid such inherent pessimism altogether, we instead extend a recent analysis framework for semaphores [9].

A. A Mixed-Integer Linear Program to Bound Blocking

In a nutshell, our blocking analysis works by constructing a *mixed-integer linear program* (ILP) to bound the maximum cumulative blocking that any job of a task T_i can incur.

We distinguish between two blocking types: *spin delay* and *arrival blocking*. A request for resource ℓ_q can cause a job J_i to incur spin delay in two cases: **(S1)** J_i requests ℓ_q and busy-waits until it gains access to ℓ_q; or **(S2)** a local higher-priority job requests ℓ_q, busy-waits until it gains access, and by this transitively delays J_i's job. Requests from local lower-priority jobs may cause J_i to incur arrival blocking if at the time that J_i is released **(A1)** a local lower-priority job is non-preemptably busy-waiting or executes a critical section pertaining to a global resource, or **(A2)** a local lower-priority job is accessing a local resource with a priority ceiling higher or equal to T_i's priority.

To analyze the worst-case blocking incurred by an arbitrary job J_i of T_i, we enumerate all requests of other tasks that could overlap with the interval during which J_i is pending, and we define two *blocking variables* [9] for each such request. Let $R_{x,q,v}$ denote the v^{th} request of task T_x for resource ℓ_q while J_i is pending. For each request $R_{x,q,v}$, we define two blocking variables $X^S_{x,q,v}$ and $X^A_{x,q,v}$ that give $R_{x,q,v}$'s contribution to T_i's spin delay and arrival blocking, resp.

These blocking variables have the following interpretation: with respect to an arbitrary, but fixed schedule, $R_{x,q,v}$ contributes to J_i's arrival blocking (resp., spin delay) with exactly $X^A_{x,q,v} \cdot L_{x,q}$ (resp., $X^S_{x,q,v} \cdot L_{x,q}$) time units. Thus, if $X^A_{x,q,v} = 0$, then $R_{x,q,v}$ does not cause any arrival blocking (in the fixed schedule). Similarly, if $X^S_{x,q,v} = 0.5$, then $R_{x,q,v}$ contributes $L_{x,q}/2$ time units to J_i's spin delay (again, in the fixed schedule). Given a *concrete schedule* (*i.e.*, a trace of the task set), it is trivial to determine the values of each critical section's blocking variables.

The blocking analysis approach that we adopt [9] uses blocking variables to express constraints on the set of *all possible* schedules. In particular, each blocking variable is used as a variable in a linear program that, when maximized, yields a safe upper bound on the worst-case blocking incurred by any J_i.

More specifically, our goal is to compute for each task T_i a blocking bound $b_i(r_1, \ldots, r_n)$ such that the recurrence

$$r_i = e_i + b_i(r_1, \ldots, r_n) + I_i(r_i)$$

yields a safe upper bound on T_i's maximum response time r_i, where $I_i(r_i)$ denotes the worst-case interference due to preemptions by local higher-priority jobs, *excluding* any blocking these jobs may incur, and where $b_i(r_1, \ldots, r_n)$ denotes a bound on *all* blocking that affects T_i (either directly or transitively).

With P-FP scheduling, the worst-case interference $I_i(r_i)$ is simply $I_i(r_i) = \sum_{T_h \in \tau^{lh}} \left\lceil \frac{r_i}{p_h} \right\rceil \cdot e_h$ [5], where $\tau^{lh} \triangleq \{T_h \mid P(T_h) = P(T_i) \wedge \pi_h < \pi_i\}$ denotes the set of local higher-priority tasks. Finding $b_i(r_1, \ldots, r_n)$ is the purpose of the analysis presented in the following. It should be noted that, in contrast to Gai *et al.*'s MSRP analysis [16] and similar to Brandenburg's holistic analysis [8], the blocking term $b_i(r_1, \ldots, r_n)$ depends on the response times of *all* tasks, which implies that blocking bounds and response-time bounds must be determined iteratively in alternating fashion until a fixpoint is reached [8, 9]. Nonetheless, for brevity, we denote the blocking term simply as b_i in the following. The response time r_i is then given by

$$r_i = e_i + b_i + \sum_{T_h \in \tau^{lh}} \left\lceil \frac{r_i}{p_h} \right\rceil \cdot e_h.$$

Note that this recurrence does *not* rely on inflated execution costs; b_i must thus reflect all possible transitive delays.

TABLE II
SUMMARY OF NOTATION

b_i	total blocking contributing to T_i's response time
P_k	kth processor in the system with $1 \leq k \leq m$
$P(T_x)$	processor that task T_x is assigned to
τ^i	set of all tasks except T_i
$\tau(P_k)$	set of all tasks assigned to processor P_k
τ^R	set of all remote tasks
τ^{ll} / τ^{lh}	set of lower-priority / higher-priority tasks on $P(T_i)$
Q / Q^g / Q^l	set of all / global / local resources
$pc(T_i)$	set of resources with priority ceiling at least π_i
$N^i_{T_x,q}$	number of requests by T_x for ℓ_q while J_i is pending
$ncs(T_i, q)$	maximum number of requests for ℓ_q issued by any jobs of tasks in $\tau^{lh} \cup \{T_i\}$ while J_i is pending
$R_{x,q,v}$	vth request issued by jobs of T_x while J_i is pending
$X^S_{x,q,v}$	contribution of $R_{x,q,v}$ to T_i's spin delay
$X^A_{x,q,v}$	contribution of $R_{x,q,v}$ to T_i's arrival blocking
$njobs(T_x, t)$	maximum number of jobs of T_x pending in any interval of length t

For brevity, let $\tau^i \triangleq \tau \setminus \{T_i\}$ (see Table II for a summary of notation). Further, let $N^i_{x,q}$ denote an upper bound on the number of requests for ℓ_q issued by jobs of task T_x while a job of T_i is pending, and let $njobs(T_x, t)$ denote an upper bound on the number of jobs of T_x that can be pending in any interval of length t. Then $N^i_{x,q} = njobs(T_x, r_i) \cdot N_{x,q}$. For a sporadic task T_x, $njobs(T_x, t)$ is given by $njobs(T_x, t) \triangleq \left\lceil \frac{t + r_x}{p_x} \right\rceil$ [8].

The **optimization objective** is then to maximize

$$b_i \triangleq \sum_{T_x \in \tau^i} \sum_{\ell_q \in Q} \sum_{v=1}^{N^i_{x,q}} \left(X^S_{x,q,v} + X^A_{x,q,v} \right) \cdot L_{x,q}, \qquad (1)$$

where $X^A_{x,q,v} \in [0, 1]$ and $X^S_{x,q,v} \in [0, 1]$ for each $R_{x,q,v}$. Note that only $njobs(T_x, t)$ ties b_i to the sporadic task model. By substituting a proper definition of $njobs(T_x, t)$, our analysis can be applied to more expressive task models as well (*e.g.*, [25]).

When maximized, Eq. (1) yields the maximum blocking possible across the set of all schedules not shown to be impossible. In the following, we impose constraints on the blocking variables that b_i depends on to rule out scenarios that we prove to be impossible. Note that this approach substantially differs from approaches that directly compute an upper bound on worst-case blocking by enumerating critical sections that *can* block (*e.g.*, [8, 16])—in our analysis, all critical sections are presumed to be blocking unless shown otherwise, which is more robust [9].

B. Generic Constraints Applicable to All Spin Lock Types

With the objective function in place, we next specify constraints to eliminate impossible scenarios. We begin by observing that direct spin delay and (indirect) arrival blocking are mutually exclusive. To ensure that each request $R_{x,q,v}$ is counted at most once in b_i, we establish the following constraint.

Constraint 1. *In any schedule of τ:*

$$\forall T_x \in \tau^i : \ \forall \ell_q \in Q : \ \forall v : \ X^A_{x,q,v} + X^S_{x,q,v} \leq 1.$$

Proof: Suppose not. Then there exists a schedule such that a single request $R_{x,q,v}$ causes T_i to incur both spin delay and arrival blocking simultaneously at some point in time t. Both arrival blocking conditions A1 and A2 require a lower-priority job to be scheduled on processor $P(T_i)$ at time t, whereas spin delay condition S1 (resp., S2) requires J_i (resp., a higher-priority job) to be scheduled on $P(T_i)$ at time t. However, at any point in time, at most one job can be scheduled on T_i's processor. ■

We consider arrival blocking next. Since a job is released only once (and since we assume that jobs do not self-suspend), each job can incur arrival blocking only once (upon release). To express this, we require an *indicator variable* A_q, with the following interpretation: given a fixed, concrete schedule, $A_q = 1$ if and only if J_i incurred arrival blocking due to a critical section accessing ℓ_q, and $A_q = 0$ otherwise. In an ILP interpretation, each A_q is a binary decision variable. This allows us to formalize that at most one resource causes arrival blocking.

Constraint 2. *In any schedule of τ:* $\sum_{\ell_q \in Q} A_q \leq 1$.

Proof: Suppose not. Then there exists a schedule in which requests for two different resources ℓ_1 and ℓ_2 both contribute to T_i's arrival blocking. Arrival blocking conditions A1 and A2 require a lower-priority job J_l to be scheduled on processor $P(T_i)$. Since we assume that J_i does not self-suspend, this is only possible if J_l was already scheduled at the time of J_i's release. Clearly, only one such J_l exists. Since jobs become preemptable at the end of a critical section, J_l would have to be accessing ℓ_1 and ℓ_2 simultaneously. Since we assume that jobs hold at most one resource at a time, this is impossible. ■

Of course, in order for a resource ℓ_q to cause arrival blocking, it must actually be accessed by local lower-priority tasks. Let $\tau^{ll} \triangleq \{T_l \mid P(T_l) = P(T_i) \wedge \pi_l > \pi_i\}$ denote such tasks.

Constraint 3. *In any schedule of τ:*

$$\forall \ell_q \in Q : \ A_q \leq \sum_{T_x \in \tau^{ll}} N_{x,q}$$

Proof: Suppose not. Then, since A_q is binary, $1 = A_q > \sum_{T_x \in \tau^{ll}} N_{x,q} = 0$ for some resource ℓ_q. By the definition of A_q, this implies that T_i incurs arrival blocking due to requests for ℓ_q by local lower-priority jobs although ℓ_q is not accessed by any local lower-priority tasks, which is clearly impossible. ■

In a similar vein, we can rule out arrival blocking due to local resources with priority ceilings lower than π_i (condition A2). To this end, we define the *conflict set* $pc(T_i)$ of T_i to be the set of local resources with a priority ceiling of at least T_i's priority. Let Q^l denote the set of local resources on processor $P(T_i)$. Then $pc(T_i) \triangleq \left\{\ell_q \;\middle|\; \ell_q \in Q^l \wedge \Pi(\ell_q) \leq \pi_i\right\}$.

Constraint 4. *In any schedule of τ:*

$$\forall \ell_q \in Q^l \setminus pc(T_i) : \ A_q \leq 0$$

Proof: Follows from the definitions of the conflict set $pc(T_i)$ and each A_q, as $A_q = 1$ only if J_i is arrival-blocked due to a request for ℓ_q, which is possible only if $\ell_q \in pc(T_i)$. ■

Another straightforward constraint on arrival blocking is that requests from local higher-priority tasks cannot arrival-block T_i.

Constraint 5. *In any schedule of τ:* $\sum_{T_x \in \tau^{lh}} \sum_{\ell_q} \sum_{v=1}^{N^i_{x,q}} X^A_{x,q,v} \leq 0.$

Proof: Follows immediately from conditions A1 and A2, which require a lower-priority job to be scheduled on $P(T_i)$, whereas any job of tasks in τ^{lh} has higher priority than J_i. ■

As a final generic constraint pertaining to arrival blocking, we link the indicator variable A_q with the blocking variables for ℓ_q.

Constraint 6. *In any schedule of τ:*

$$\forall \ell_q \in Q : \ \sum_{T_x \in \tau^{ll}} \sum_{v=1}^{N^i_{x,q}} X^A_{x,q,v} \leq A_q.$$

Proof: Suppose not. If $A_q = 0$, this would imply, by definition of $X^A_{x,q,v}$, that in some schedule $R_{x,q,v}$ arrival-blocked J_i, even though by definition of A_q no request for ℓ_q arrival-blocked J_i, which is clearly impossible. If $A_q = 1$, at least two requests by local lower-priority tasks caused arrival blocking. Analogously to Constraint 2, this is impossible because at most one request can be in progress on $P(T_i)$ when J_i is released. ■

Finally, we observe that spin delay is necessarily due to remote tasks, since it is impossible to spin while waiting for local tasks.

Constraint 7. *In any schedule of τ:* $\sum_{T_x \in \tau^{ll} \cup \tau^{lh}} \sum_{\ell_q} \sum_{v=1}^{N^i_{x,q}} X^S_{x,q,v} \leq 0.$

Proof: Suppose not. Then there exists a schedule in which at some point in time t the execution of a request $R_{x,q,v}$ issued by a local task T_x causes J_i to incur spin delay. By conditions S1 and S2, a job on processor $P(T_i)$ is also spinning at time t. However, the job scheduled on $P(T_i)$ at time t cannot both be spinning and executing $R_{x,q,v}$ at the same time. ■

This concludes our discussion of generic constraints. The above constraints are generic in that they apply to all considered spin lock types. Next, we derive constraints specific to individual spin lock types. We focus on three lock types herein: F|N locks, F|P locks, and P|N locks, which together illustrate the main analysis techniques employed in this work. Due to space constraints, analyses of the other lock types, which are analyzed using simple combinations of the techniques developed for F|N, F|P, and P|N locks, can be found in Appendix C.

We begin with F|N locks, because they are the easiest to analyze, and because baseline analysis exists in the form of Gai *et al.*'s classic MSRP analysis (recall Sec. II-A).

C. Constraints for FIFO-ordered Non-Preemptable Spin Locks

As discussed in Sec. III-A, our analysis must explicitly account for transitive delays to avoid the pessimism inherent in inflating job execution costs (Theorem 1). In particular, the final blocking bound b_i must represent all delays that J_i may

"accumulate" when higher-priority jobs that preempted J_i spin. Thus, not only do we need to consider J_i's requests for global resources, but also any requests issued by higher-priority tasks. To this end, we let $ncs(T_i, q)$ denote an upper bound on the number of requests (or *number of critical sections*) for ℓ_q issued by either by J_i itself or by preempting higher-priority jobs (while J_i is pending): $ncs(T_i, q) \triangleq N_{i,q} + \sum_{T_h \in \tau^{lh}} N^i_{h,q}$.

In conjunction with the strong progress guarantee in F|N locks, $ncs(T_i, q)$ implies an immediate upper bound on the number of requests for ℓ_q that cause J_i to incur spin delay. Let $\tau(P_k) \triangleq \{T_x \mid P(T_x) = P_k\}$ be the set of tasks assigned to P_k.

Constraint 8. *In any schedule of τ with F|N locks:*

$$\forall \ell_q \in Q : \forall P_k, P_k \neq P(T_i) : \sum_{T_x \in \tau(P_k)} \sum_{v=1}^{N^i_{x,q}} X^S_{x,q,v} \leq ncs(T_i, q).$$

Proof: Suppose not. Then there exists a schedule in which more than $ncs(T_i, q)$ requests for some ℓ_q of tasks on processor P_k cause J_i to incur spin delay. Then, by the pigeon-hole principle, at least one request for ℓ_q issued by T_i or a local higher-priority task is delayed by more than one request for ℓ_q from processor P_k. However, since jobs spin non-preemptably, and since F|N locks serve requests in FIFO order, each request for ℓ_q can be preceded by at most one request for ℓ_q from each other processor. Contradiction. ■

The above constraint, even though it may appear to be quite simple, is considerably more effective at limiting blocking than prior analyses, as will become evident in Sec. V. Next, we apply the reasoning underlying Constraint 8 to arrival blocking.

A remote job J_r can contribute to J_i's arrival blocking if a local lower-priority job J_l spins non-preemptably while waiting for J_r to release a lock. However, at most one request from each processor can contribute to J_i's arrival blocking in this way.

Constraint 9. *In any schedule of τ with F|N locks:*

$$\forall P_k, P_k \neq P(T_i) : \ \forall \ell_q \in Q : \sum_{T_x \in \tau(P_k)} \sum_{v=1}^{N^i_{x,q}} X^A_{x,q,v} \leq A_q.$$

Proof: Suppose not. If $A_q = 0$, then some request from a remote processor P_k for resource ℓ_q causes J_i to incur arrival blocking. However, by the definition of A_q, no requests for ℓ_q causes J_i to incur arrival blocking if $A_q = 0$. If $A_q = 1$, then at least two requests for ℓ_q issued from processor P_k contribute to T_i's arrival blocking. Analogously to Constraint 2, at most one request of a local lower-priority job J_l causes J_i to incur arrival blocking. Hence, at least two requests from P_k must delay J_l. Analogously to Constraint 8, this is impossible in F|N locks. ■

This concludes our analysis of F|N locks. As is apparent in Constraints 8 and 9, FIFO-ordering is a strong property, as is non-preemptable spinning. We relax the latter aspect next.

D. Constraints for FIFO-ordered Preemptable Spin Locks

In contrast to non-preemptable spin locks analyzed so far, preemptable spin locks allow jobs to be preempted while busy-waiting for global resources. Hence, while busy-waiting, jobs are subject to normal fixed-priority scheduling; spinning thus never causes a priority inversion. Requests from remote tasks thus cannot cause (transitive) arrival blocking.

Constraint 10. *In any schedule of τ with preemptable spin locks:* $\sum_{T_x \in \tau^R} \sum_{\ell_q \in Q} \sum_{v=1}^{N^i_{x,q}} X^A_{x,q,v} \leq 0$.

Proof: Follows from the preceding discussion. ■

Preemptable spinning solves the transitive arrival blocking problem, but it does so at the expense of increasing spin delays. To accurately account for "retries" due to preemptions, we introduce a new indicator variable: for each resource ℓ_q, with respect to an arbitrary, but fixed schedule, let C_q denote the number of times that a request for resource ℓ_q by J_i or a job of a task in τ^{lh} is *cancelled* due to a preemption. From an ILP point of view, each C_q is an integer variable. A trivial bound on the sum of all C_q is given by the number of higher-priority job releases that can possibly occur while J_i is pending.

Constraint 11. *In any schedule of τ with preemptable spin locks:* $\sum_{\ell_q} C_q \leq \sum_{T_h \in \tau^{lh}} \left\lceil \frac{r_i}{p_h} \right\rceil$.

Another trivial observation is that $C_q = 0$ if neither J_i nor any higher-priority jobs access ℓ_q.

Constraint 12. *In any schedule of τ with preemptable spin locks:* $\forall \ell_q$ *if* $ncs(T_i, q) = 0$ *then* $C_q = 0$.

As C_q bounds the number of times that a particular resource is re-requested, we can almost directly apply the argument of Constraint 8; the only change is that each time that ℓ_q is re-requested, other processors may "skip ahead" once.

Constraint 13. *In any schedule of τ with F|P locks:* $\forall \ell_q \in Q$:

$$\forall P_k, P_k \neq P(T_i) : \sum_{T_x \in \tau(P_k)} \sum_{v=1}^{N^i_{x,q}} X^S_{x,q,v} \leq ncs(T_i, q) + C_q.$$

Proof: Suppose not. Then more than $ncs(T_i, q) + C_q$ requests by tasks on a remote processor P_k for a resource ℓ_q contribute to T_i's spin delay. As requests are issued sequentially and served in FIFO order, T_i and local higher-priority jobs issue at most $ncs(T_i, q) + C_q$ requests for ℓ_q (counting requests re-issued after a preemption as individual requests). By the pigeon-hole principle, this implies that one *uninterrupted* request for ℓ_q was blocked by more than one request issued by jobs on P_k. With FIFO-ordered spin locks, this is impossible. ■

This concludes our analysis of F|P locks. Preemptable spinning increases the analysis complexity (additional integer variables are required) and increases spin delays (Constraint 13 permits more blocking than Constraint 8), but with our ILP-based analysis approach, both aspects can be easily integrated. To the best of our knowledge, this is the first analysis of preemptable spin locks from a worst-case blocking point of view. Next, we shift the focus away from FIFO-ordered spin locks and present our analysis of priority-ordered spin locks.

E. Priority-ordered Non-Preemptable Spin Locks

P|N locks ensure that a request is blocked at most once by another request with lower priority at the expense that there is no immediate bound on the number of blocking higher-priority requests. In the following, we denote the locking priority of requests for resource ℓ_q issued by jobs of a task T_x as $\pi_{x,q}$.

We apply response-time analysis [5] on a per-request basis to obtain an upper bound on per-request delay. For a resource ℓ_q and task T_i, let $W_q^{\mathrm{P|N}}(T_i, \pi)$ denote the smallest positive value (if any) that satisfies the following recurrence:

$$W_q^{\mathrm{P|N}}(T_i, \pi) = S(\ell_q, \pi) + LP(\ell_q, \pi) + 1 \quad \text{where} \tag{2}$$
$$S(\ell_q, \pi) = \sum_{T_x \in \tau^R \wedge \pi_{x,q} \leq \pi} njobs(T_x, W_q^{\mathrm{P|N}}(T_i, \pi)) \cdot N_{x,q} \cdot L_{x,q},$$
$$LP(\ell_q, \pi) = \max_{T_x \in \tau^R} \{L_{x,q} | \pi_{x,q} > \pi\}.$$

Lemma 1. *Let t_0 be the time a job J_i of task T_i attempts to lock resource ℓ_q with locking priority π, and let t_1 be the time that J_i subsequently acquires ℓ_q. With P\|N locks, $t_1 - t_0 \leq W_q^{\mathrm{P|N}}(T_i, \pi)$.*

Proof: Analogous to the response-time analysis of non-preemptive fixed-priority scheduling. The response-time of J_i's request—that is, the maximum wait time $W_q^{\mathrm{P|N}}(T_i, \pi)$—depends on the maximum length of one lower-priority request $LP(\ell_q, \pi)$ and all higher-priority requests of all remote tasks issued during an interval of length $W_q^{\mathrm{P|N}}(T_i, \pi)$, that is, $S(\ell_q, \pi)$. Thus after at most $W_q^{\mathrm{P|N}}(T_i, \pi)$ time units ℓ_q is available. ■

To simplify the notation of the following constraints, we define $\pi_q^{minLP} \triangleq \max_{T_x \in \tau^{ll}} \{\pi_{x,q} | N_{x,q} > 0\}$ and $\pi_q^{minHP} \triangleq \max_{T_x \in (\tau^{lh} \cup \{T_i\})} \{\pi_{x,q} | N_{x,q} > 0\}$ to be the minimum locking priority of any lower-priority and higher-priority task, resp., on T_i's processor that accesses the global resource ℓ_q.

Given $W_q^{\mathrm{P|N}}(T_i, \pi)$ (*i.e.*, if it exists), we can constrain the the number of requests for ℓ_q that can contribute to T_i's spin delay. First, we consider requests issued with higher or equal priority.

Constraint 14. *In any schedule of τ with P\|N locks:*

$$\forall P_k, P_k \neq P(T_i) \colon \forall \ell_q \in Q^g \colon \forall T_x \in \tau(P_k), \pi_{x,q} \leq \pi_q^{minHP} \colon$$
$$\sum_{v=1}^{N_{x,q}^i} X_{x,q,v}^S \leq njobs(T_x, W_q^{\mathrm{P|N}}(T_i, \pi_q^{minHP})) \cdot N_{x,q} \cdot ncs(T_i, q).$$

Proof: Let R denote a request for a resource ℓ_q by T_i or a local higher-priority task. By the definition of π_q^{minHP}, R has at least the locking priority π_q^{minHP} and, by Lem. 1, is hence delayed by at most $W_q^{\mathrm{P|N}}(T_i, \pi_q^{minHP})$ time units (note that $W_q^{\mathrm{P|N}}(T_i, \pi_q^{minHP}) \geq W_q^{\mathrm{P|N}}(T_h, \pi_{h,q})$ if $T_h \in \tau^{lh}$ and $\pi_q^{minHP} \geq \pi_{h,q}$). During an interval of length $W_q^{\mathrm{P|N}}(T_i, \pi_q^{minHP})$, jobs of a remote task T_x issue at most $njobs(T_x, W_q^{\mathrm{P|N}}(T_i, \pi_q^{minHP})) \cdot N_{x,q}$ requests for ℓ_q. The stated bound follows as at most $ncs(T_i, q)$ such requests R for ℓ_q are issued by T_i or local higher-priority tasks. ■

Requests with lower priority cause J_i to incur (transitive) spin delay at most once for each request by T_i or a task in τ^{lh}.

Constraint 15. *In any schedule of τ with P\|N locks:*

$$\forall \ell_q \in Q^g : \sum_{\substack{T_x \in \tau^R \\ \pi_{x,q} > \pi_q^{minHP}}} \sum_{v=1}^{N_{x,q}^i} X_{x,q,v}^S \leq ncs(T_i, q).$$

Proof: Suppose not. Then at least one request for global resource ℓ_q issued by T_i or a local higher-priority task is delayed more than once by a request for ℓ_q from a different processor issued with a lower priority. However, by definition P\|N locks ensure that each request is blocked at most once by a lower-priority request for the same resource. Contradiction. ■

Next, we consider arrival blocking. The number of lower-priority requests that cause arrival blocking is bounded by A_q.

Constraint 16. *In any schedule of τ with P\|N locks:*

$$\forall \ell_q \in Q^g : \sum_{\substack{T_x \in \tau^R \\ \pi_{x,q} > \pi_q^{minLP}}} \sum_{v=1}^{N_{x,q}^i} X_{x,q,v}^A \leq A_q.$$

Proof: Suppose not. In case $A_q = 0$, by definition of A_q, T_i incurs transitive arrival blocking due to a request for ℓ_q, although no access for ℓ_q from a local lower-priority task causes T_i to incur arrival blocking, which is impossible. In case $A_q = 1$, a request for ℓ_q with priority at least π_q^{minLP} is delayed more than once by requests for ℓ_q issued on other processors with a locking priority of less than π_q^{minLP}. However, with P\|N locks, a request for a resource ℓ_q cannot be delayed by more than one lower-priority request for ℓ_q. Contradiction. ■

Next, we constrain the arrival blocking due to requests with higher priority issued on other processors.

Constraint 17. *In any schedule of τ with P\|N locks:*

$$\forall \ell_q \in Q^g : \forall T_x \in \tau^R, \pi_{x,q} \leq \pi_q^{minLP} :$$
$$\sum_{v=1}^{N_{x,q}^i} X_{x,q,v}^A \leq njobs(T_x, W_q^{\mathrm{P|N}}(T_i, \pi_q^{minLP})) \cdot N_{x,q} \cdot A_q$$

Proof: Let R denote the request by a local lower-priority job that causes T_i to incur arrival blocking. By definition of π_q^{minLP}, R has a priority of at least π_q^{minLP}, and, by Lem. 1, is hence delayed by at most $W_q^{\mathrm{P|N}}(T_i, \pi_q^{minLP})$ time units (note that $W_q^{\mathrm{P|N}}(T_i, \pi_q^{minLP}) \geq W_q^{\mathrm{P|N}}(T_l, \pi_{l,q})$ if $T_l \in \tau^{ll}$ and $\pi_q^{minLP} \geq \pi_{l,q}$). During an interval of length $W_q^{\mathrm{P|N}}(T_i, \pi_q^{minLP})$, jobs of a remote task T_x issue at most $njobs(T_x, W_q^{\mathrm{P|N}}(T_i, \pi_q^{minLP})) \cdot N_{x,q}$ requests for ℓ_q. The bound follows as T_i is arrival-blocked via ℓ_q only if $A_q = 1$. ■

Note that the preceding analysis does not assume any particular ordering among requests issued with the same locking priority. This fact can be leveraged to analyze unordered spin locks: if all tasks have the same locking priority (for all resources), no particular ordering among requests can be assumed, just as with unordered spin locks. Therefore, we do not explicitly present constraints for unordered spin locks and instead treat the unordered spin lock types (*i.e.*, U\|N and U\|P locks) as special cases of the corresponding priority-ordered spin locks with unordered tie-breaking (*i.e.*, P\|N and P\|P locks) in which all tasks have the lowest-possible locking priority. Due to space constraints, we provide the analysis of the remaining spin lock types (*i.e.*, P\|P, PF\|N, and PF\|P locks) in Appendix C.

IV. Qualitative Comparison of Spin Lock Types

With analysis available for eight different lock types, it may be challenging to select an appropriate lock for a given application.

The choice of spin lock algorithm depends on many factors in practice, among them hardware-dependent considerations such as memory availability and support for atomic operations. Besides such engineering concerns, there are also analytical concerns that may force the use of a specific lock type.

Clearly, there are no analytical reasons to *choose* unordered spin locks, but our ILP-based analysis makes it possible to *tolerate* locks with such weak guarantees. In contrast, FIFO-ordered spin locks offer strong progress guarantees, which not only allow for an effective analysis, but also completely rule out starvation effects without a need to assign locking priorities or other parameters—FIFO-ordered locks are a simple, appealing solution, and particularly so with non-preemptable spinning.

However, despite their many benefits, FIFO-ordered locks are fundamentally unsuitable for some workloads. For instance, suppose an engine control unit is being realized on a (future) 16-core platform, and a high-frequency, hard real-time control task with a period of $250\mu s$ and a worst-case execution cost of at least $110\mu s$ shares a data structure (*e.g.*, a message box) with tasks on every other core. Even with a short maximum critical section length of only $10\mu s$, the system is inherently infeasible when using FIFO-ordered locks. In general, if some tasks have less than $(m-1) \cdot L^{max}$ slack, where L^{max} denotes the maximum (task-independent) critical section length, then FIFO-ordered locks are inappropriate and locking priorities are fundamentally required.

Similarly, there exist (practical) workloads in which preemptable spinning is unavoidable. For example, suppose the above $250\mu s$-task must be co-hosted with a $1000ms$ maintenance task that accesses a shared resource with a maximum critical section length of $100\mu s$. Regardless of which lock order is employed, the (lower-priority) maintenance task must not spin without allowing preemptions, for otherwise the maximum arrival blocking of the control task would be *at least* $200\mu s$, rendering it unschedulable. Preemptable spinning is fundamentally required in the presence of latency-sensitive tasks.

However, for workloads in which none of the lock types can be ruled out based on qualitative considerations, the choice is considerably more difficult. To provide guidance in such scenarios, we present an empirical comparison.

V. Empirical Comparison of Spin Lock Types

We implemented the proposed ILP-based analysis using the GNU Linear Programming Kit and conducted a large-scale schedulability study to **(i)** determine whether the proposed analysis improves upon prior approaches, and **(ii)** to empirically compare the eight considered spin lock types in a variety of different scenarios in which each choice was potentially viable. Our implementation is freely available as part of the SchedCAT open source project [2].

a) Setup: We considered platforms with $m \in \{4, 8, 16\}$ processors; quad-core embedded processors are readily available today, whereas 8-core and 16-core platforms are slightly more forward-looking scenarios. Task sets with up to 10 tasks per processor (*i.e.*, $n \in \{m, 2m, \ldots, 10m\}$) were generated using Emberson *et al.*'s task set generator [14]. Periods were randomly chosen from a log-uniform distribution over the interval $[1ms, 1000ms]$, which covers a wide range of periods commonly encountered in automotive applications [11]. We assigned rate-monotonic scheduling priorities.

Each task set shared either $m/2$, m, or $2m$ resources. For each resource ℓ_q, we randomly determined $rsf \cdot n$ tasks to access ℓ_q, where the *resource sharing factor* rsf was varied across $rsf \in \{0.1, 0.25, 0.4, 0.75\}$. The accessing tasks were chosen independently for each resource. If a task T_i was determined to access a resource ℓ_q, the number of requests per job $N_{i,q}$ was chosen uniformly at random from the range $[1, \ldots, N^{max}]$, where N^{max} was varied across $N^{max} \in \{1, 2, 5, 10, 15\}$, unless specified otherwise. The critical section length $L_{i,q}$ was chosen randomly from either $[1\mu s, 15\mu s]$ (*short*) or $[1\mu s, 100\mu s]$ (*medium*). To ensure plausibility, we enforced that $e_i \geq \sum_{\ell_q} N_{i,q} \cdot L_{i,q}$.

Locking priorities were assigned by first assigning all tasks the same priority and by then iteratively raising priorities to benefit unschedulable tasks as described in Appendix B.

We conducted two sets of experiments. First, to study the impact of increasing load, we evaluated schedulability as a function of n with a task-set-size-dependent total utilization of $U \in \{0.1n, 0.2n, 0.3n\}$. In the second set of experiments, to study the impact of increasing contention, we fixed the total utilization at $U = 0.5m$, set the number of tasks to $n \in \{U/0.1, U/0.2, U/0.3\}$ (rounding up if necessary), and then varied N^{max} across $[1, 40]$.

In total, we evaluated 1296 different parameter configurations, and generated and tested at least 1000 task sets for each choice of n (resp., N^{max}) in the first (resp., second) set of experiments. For each configuration and each n (resp., N^{max}), we applied eleven blocking analyses: the eight ILP-based analyses from Sec. III (labeled as listed in Table I), Gai *et al.*'s classic [16] and Brandenburg's holistic [8] analysis of F|N locks (labeled "MSRP-classic" and "MSRP-holistic," resp.), and a configuration labeled "no blocking," which reflects best-case schedulability assuming all resources are private (*i.e.*, the schedulability of independent tasks). In the case of F|N and PF|N locks, we first applied the computationally cheap holistic analysis of F|N locks [8], and applied our ILP-based analysis of F|N and PF|N locks only if the holistic analysis resulted in an unschedulable task set. This approach is possible for PF|N locks as task sets schedulable with F|N locks are schedulable with PF|N locks as well.[3] All results are available online (see Appendix H); due to the large volume of results, we focus herein on major trends and discuss selected graphs that exhibit the discussed effects. We start with the impact of increasing load.

b) Varying n: First of all, we note that if blocking is not a "bottleneck" for timeliness—for instance, in case of low resource contention—then the choice of spin lock type is of course irrelevant. However, even with moderate contention, significant differences become apparent with increasing system load.

Fig. 1 depicts such a case, which is representative for a wide range of the evaluated configurations. Here, the holistic analysis of F|N locks leads to somewhat higher schedulability than Gai *et al.*'s MSRP analysis [16], due to a modest decrease in pessimism. In contrast, with our new ILP-based analysis of the same lock type, a much larger number of tasks can be supported—in the scenario depicted in Fig. 1, more than ten additional tasks

[3] F|N can be considered as a special case of PF|N locks in which all requests are issued with the same locking priority.

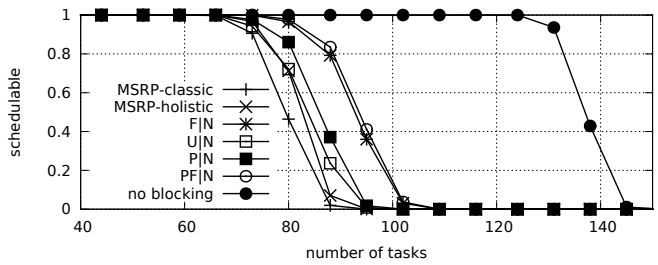

Fig. 1. Schedulability under non-preemptable spin locks for $m = 16$, $U = 0.1n$, 16 shared resources, $rsf = 0.4$, $N^{max} = 2$, and short critical sections.

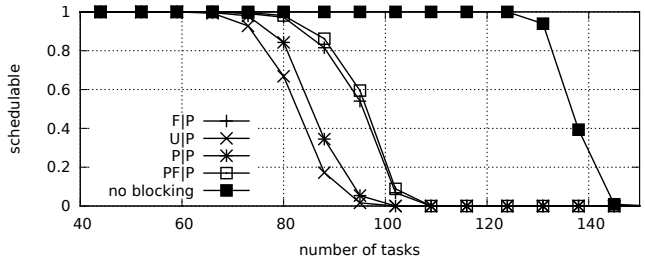

Fig. 2. Schedulability under preemptable spin locks for $m = 16$, $U = 0.1n$, 8 shared resources, $rsf = 0.25$, $N^{max} = 10$, and short critical sections.

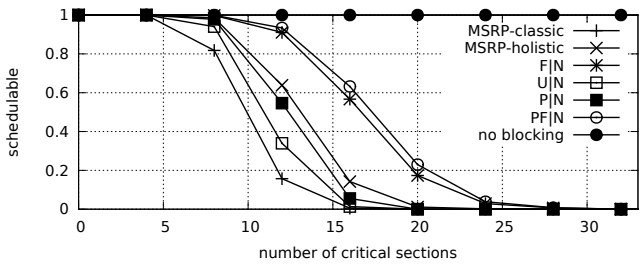

Fig. 3. Schedulability under non-preemptable spin locks for $m = 16$, $U = 0.1n$, 8 shared resources, $rsf = 0.25$, and short critical sections.

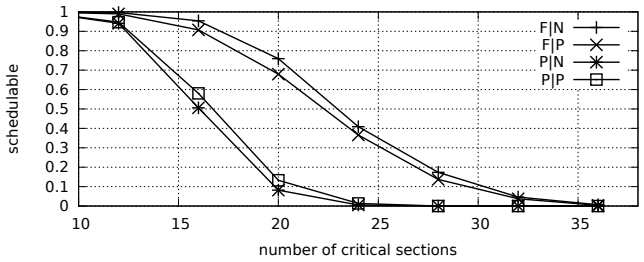

Fig. 4. Schedulability under preemptable spin locks for $m = 16$, $U = 0.1n$, 32 shared resources, $rsf = 0.10$, and short critical sections.

can be supported on the same platform—which highlights the typically much less pessimistic nature of our ILP-based analysis.

Interestingly, the ILP-based analysis of unordered spin locks (*i.e.*, U|N locks) also yields equal or even slightly higher schedulability than both prior MSRP analysese in this configuration. This is particularly remarkable since the ILP-based analysis of U|N locks cannot make any assumptions about the ordering of requests for global resources, while the analysis of the MSRP can exploit the guaranteed FIFO ordering. Of course, U|N locks are not *always* preferable to the classic MSRP analysis, but the fact that they are sometimes preferable at all shows that the ILP approach is typically much more accurate.

Adding locking priorities (*i.e.*, comparing U|N to P|N locks and F|N to PF|N locks) leads to slight improvements. In this configuration, as in many others, PF|N locks yield the highest schedulability. The schedulability results for preemptable spin locks, shown in Fig. 2, exhibit in large parts the same trends as their non-preemptable counterparts (Fig. 1). This shows that, *for the considered parameter ranges*, arrival blocking is rarely the deciding factor. Nonetheless, we note that preemptable spinning can have a significant impact in the presence of latency-sensitive tasks (*i.e.*, if some tasks simply cannot tolerate scheduling delays due to non-preemptable spinning).

A general trend observed in a wide range of different configurations is that FIFO-ordered spin locks (*i.e.*, F|N, PF|N, F|P, and PF|P locks) generally achieve significantly higher schedulability than the other lock types, which highlights the analytical benefits of strong progress guarantees. Also, as might be expected, the use of unordered spin locks generally results in equal or lower schedulability than priority-ordered spin locks.

c) Varying N^{max}: In our second set of experiments, we studied the impact of increasing contention for a given number of tasks. The results for one representative configuration are shown in Fig. 3. In general, the trends mostly follow the patterns already observed in the first set of experiments. In Fig. 3, PF|N locks again perform slightly better than F|N locks, and both FIFO-ordered choices perform much better than either U|N or P|N locks (and also better than F|N locks under prior analysis).

Interestingly, the effect of enabling preemptions during spinning is highly dependent on the configuration and the type of spin lock. For instance, Fig. 4 depicts a case wherein, in the same configuration, preemptable spinning *improves* schedulability for prioritized spin locks (with unordered tie-breaking), while it *decreases* the schedulability of FIFO-ordered spin locks. We conclude from such effects that preemptable spinning, while helpful or even essential for *some* workloads, it is not a magic bullet that is universally applicable to *all* real-time workloads.

VI. Conclusion and Recommendations

Motivated by the widespread use of spin locks for synchronization in embedded multiprocessor systems, we studied eight types of spin locks from a blocking analysis point of view, seven of which had not been previously considered in this context. Notably, we derived a novel analysis method that is asymptotically less pessimistic than prior analyses since it never accounts for any critical section more than once.

Based on qualitative and quantitative considerations, we explored the suitability of the various lock types in the context of AUTOSAR, which we selected as a representative case study. In short, the status quo is highly undesirable from a real-time perspective, as unordered spin locks—the only safe assumption if no order is specified, and which could not be efficiently analyzed prior to our ILP-based analysis—yield generally the lowest schedulability of all spin lock types.

On the basis of our results, we arrive at the following recommendations for improved spin lock support in AUTOSAR.

(1) AUTOSAR should fully specify the semantics of the spin locks provided, to enable an efficient worst-case analysis such as the one that we have presented in Sec. III.

(2) AUTOSAR should mandate the availability of FIFO-ordered spin locks since they achieve the highest schedulability in a wide range of scenarios (Sec. V). Nevertheless,

(3) AUTOSAR should also provide flexible priority-ordered spin locks, as there exist workloads that inherently require such locks (Sec. IV). Importantly, locking priorities should not depend on scheduling priorities (see Appendix B). And, finally,

(4) the AUTOSAR API should be extended to allow preemptable spinning without sacrificing request ordering guarantees. Preemptable spinning is unavoidable for some latency-sensitive workloads (Sec. IV), but from an analysis perspective, the benefits of preemptable spinning can be completely voided by the loss of ordering guarantees. Hence, the API should allow explicit control over preemptability without affecting the request ordering, as proposed in Sec. II-C and Algorithm 3.

In future work, we will extend our analysis to support nested locking, and plan to apply our approach to reader-writer locks.

REFERENCES

[1] "AUTOSAR Release 4.1, Specification of Operating System," http://www.autosar.org, 2013.

[2] "SchedCAT: Schedulability test collection and toolkit," web site, http://www.mpi-sws.org/~bbb/projects/schedcat.

[3] J. Anderson, R. Jain, and K. Jeffay, "Efficient object sharing in quantum-based real-time systems," in *RTSS'98*, 1998, pp. 346–355.

[4] J. H. Anderson, Y.-J. Kim, and T. Herman, "Shared-memory mutual exclusion: major research trends since 1986," *Distributed Computing*, vol. 16, no. 2-3, pp. 75–110, 2003.

[5] N. Audsley, A. Burns, M. Richardson, K. Tindell, and A. Wellings, "Applying new scheduling theory to static priority pre-emptive scheduling," *Software Eng. J.*, vol. 8, no. 5, pp. 284–292, 1993.

[6] T. Baker, "Stack-based scheduling for realtime processes," *Real-Time Systems*, vol. 3, no. 1, pp. 67–99, 1991.

[7] A. Block, H. Leontyev, B. Brandenburg, and J. Anderson, "A flexible real-time locking protocol for multiprocessors," in *RTCSA'07*, 2007.

[8] B. Brandenburg, "Scheduling and locking in multiprocessor real-time operating systems," Ph.D. dissertation, The University of North Carolina at Chapel Hill, 2011.

[9] ——, "Improved analysis and evaluation of real-time semaphore protocols for P-FP scheduling," in *RTAS'13*, 2013.

[10] B. Brandenburg and J. Anderson, "Optimality results for multiprocessor real-time locking," in *RTSS'10*, 2010, pp. 49–60.

[11] D. Buttle, "Real-time in the prime-time," Keynote at ECRTS'12.

[12] T. Craig, "Queuing spin lock algorithms to support timing predictability," in *RTSS'93*, 1993, pp. 148–157.

[13] U. Devi, H. Leontyev, and J. Anderson, "Efficient synchronization under global EDF scheduling on multiprocessors," in *ECRTS'06*, 2006, pp. 75–84.

[14] P. Emberson, R. Stafford, and R. Davis, "Techniques for the synthesis of multiprocessor tasksets," in *WATERS'10*, 2010.

[15] D. Faggioli, G. Lipari, and T. Cucinotta, "The multiprocessor bandwidth inheritance protocol," in *ECRTS'10*, 2010, pp. 90–99.

[16] P. Gai, G. Lipari, and M. Di Natale, "Minimizing memory utilization of real-time task sets in single and multi-processor systems-on-a-chip," in *RTSS'01*. IEEE, 2001, pp. 73–83.

[17] T. Johnson and K. Harathi, "Interruptible critical sections," Dept. of Computer Science, University of Florida, Tech. Rep., 1994.

[18] ——, "A prioritized multiprocessor spin lock," *IEEE Transactions on Parallel and Distributed Systems*, vol. 8, no. 9, pp. 926–933, 1997.

[19] L. I. Kontothanassis, R. W. Wisniewski, and M. L. Scott, "Scheduler-conscious synchronization," *ACM Transactions on Computer Systems*, vol. 15, no. 1, pp. 3–40, 1997.

[20] K. Lakshmanan, D. Niz, and R. Rajkumar, "Coordinated task scheduling, allocation and synchronization on multiprocessors," in *RTSS'09*, 2009, pp. 469–478.

[21] E. P. Markatos and T. J. LeBlanc, "Multiprocessor synchronization primitives with priorities," in *Eighth IEEE Workshop on Real-Time Operating Systems and Software*, 1991, pp. 1–7.

[22] J. Mellor-Crummey and M. Scott, "Algorithms for scalable synchronization on shared-memory multiprocessors," *ACM Transactions on Computer Systems*, vol. 9, no. 1, pp. 21–65, 1991.

[23] L. D. Molesky, C. Shen, and G. Zlokapa, "Predictable synchronization mechanisms for multiprocessor real-time systems," *Real-Time Systems*, vol. 2, no. 3, pp. 163–180, 1990.

[24] M. Raynal, *Algorithms for mutual exclusion*. MIT Press, 1986.

[25] S. Schliecker, M. Negrean, and R. Ernst, "Response Time Analysis on Multicore ECUs With Shared Resources," *IEEE Trans. Ind. Informat.*, vol. 5, no. 4, pp. 402–413, 2009.

[26] L. Sha, R. Rajkumar, and J. Lehoczky, "Priority inheritance protocols: an approach to real-time synchronization," *IEEE Trans. Comput.*, vol. 39, no. 9, pp. 1175–1185, 1990.

[27] H. Takada and K. Sakamura, "Predictable spin lock algorithms with preemption," in *RTOSS '94*, 1994, pp. 2–6.

[28] ——, "A novel approach to multiprogrammed multiprocessor synchronization for real-time kernels," in *RTSS'97*, 1997, pp. 134–143.

[29] B. Ward and J. Anderson, "Supporting nested locking in multiprocessor real-time systems," in *ECRTS'12*, 2012, pp. 223–232.

APPENDIX

A. Proof of Theorem 1

Let α denote a given, arbitrary non-negative integer parameter. We construct a scenario in which $\Omega(n \cdot \alpha)$ delay is accounted for, actual blocking is $O(1)$, and where $\phi = \alpha$.

Consider a system consisting of two processors, P_1 and P_2, a single shared resource ℓ_1, and a task set consisting of $n \geq 3$ tasks. The tasks $T_1, \ldots, T_{n-2}$ are assigned to P_1 and have parameters $p_i = 2n - 3$ and $e_i = 1$, and and access ℓ_1 once per job with a negligible critical section length of $L_{i,1} = \epsilon > 0$. Task T_{n-1} is assigned to P_2 and has parameters $p_{n-1} = \alpha \cdot (2n - 3)$ and $e_{n-1} = 1$, and requests ℓ_1 once per job with $L_{n-1,1} = 1$. Finally, the lowest-priority task T_n with $p_n = \alpha \cdot (2n - 3)$ and $e_n = \alpha$ is assigned to P_1 and does not access ℓ_1.

Let r_n^{inf} denote T_n's response-time bound obtained by inflating execution costs. We have $r_n^{inf} = e_n + \sum_{h=1}^{n-2} \left\lceil \frac{r_n^{inf}}{p_h} \right\rceil e'_h$, where e'_h denotes the inflated execution time of T_h. Since each $T_h \in \{T_1, \ldots, T_{n_2}\}$ directly conflicts with T_{n-1} via ℓ_1, we have $e'_h \geq e_h + L_{n-1,1} = e_h + 1$ under any (mutual exclusion) locking protocol. Suppose $e'_h = e_h + 1 = 2$. Then $r_n^{inf} = \alpha + \sum_{h=1}^{n-2} \left\lceil \frac{r_n^{inf}}{2n-3} \right\rceil 2 = \alpha \cdot (2n - 3)$.

Observe that T_{n-1} issues only a single request for ℓ_1, and hence $T_1, \ldots, T_{n-2}$ are blocked by at most one request in total while a job J_n is pending. The *actual* remote blocking that contributes to T_n's response time (*i.e.*, the time that any job on processor P_1 spins while J_n is pending) is hence limited to $L_{n-1,1} = 1$. Hence we have $r_n^{real} = e_n + L_{n-1,1} + \sum_{h=1}^{n-2} \left\lceil \frac{r_n^{real}}{p_h} \right\rceil \cdot e_h$, and, since $r_n^{real} \leq r_n^{inf}$, also $r_n^{real} \leq e_n + L_{n-1,1} + \sum_{h=1}^{n-2} \left\lceil \frac{r_n^{inf}}{p_h} \right\rceil \cdot e_h$.

The pessimism due to execution cost inflation is given by the difference of r_n^{real} and r_n^{inf}, where $r_n^{inf} - r_n^{real} \geq e_n + \sum_{h=1}^{n-2} \left\lceil \frac{r_n^{inf}}{p_h} \right\rceil (e_h + 1) - \left(e_n + L_{n-1,1} + \sum_{h=1}^{n-2} \left\lceil \frac{r_n^{inf}}{p_h} \right\rceil \cdot e_h \right) = \sum_{h=1}^{n-2} \left\lceil \frac{r_n^{inf}}{p_h} \right\rceil - L_{n-1,1} = \sum_{h=1}^{n-2} \left\lceil \frac{\alpha \cdot (2n-3)}{(2n-3)} \right\rceil - 1 = (n-2) \cdot \alpha - 1 = \Omega(n \cdot \alpha)$. Since $\phi = \alpha$ and because actual blocking is limited to $L_{n-1,1} = O(1)$, this establishes that r_n^{inf} overestimates the impact of blocking by a factor of $\Omega(\phi \cdot n)$. ■

B. Assigning Locking Priorities

Priority-ordered spin locks pose the problem of assigning locking priorities in addition to scheduling priorities. In our experiments, each task had a single locking priority (*i.e.*, $\pi_{i,q} = \pi_{i,r}$ for all ℓ_q, ℓ_r). We used a simple iterative scheme that aims to improve schedulability with the selective use of priorities.

Given a task set, we started by assigning the lowest-possible locking priority to all tasks and computed response-time bounds. If some task T_i was deemed unschedulable, we elevated the locking priority of the failing task and, in the case of non-preemptable spin locks, all other local lower-priority tasks (to lessen the non-preemptive blocking incurred by T_i).

We iteratively bounded response times and raised locking priorities until either the task set was deemed schedulable or a simple heuristic (based on the number of prior priority increases) established that further priority increases were unlikely to help. More sophisticated priority assignment heuristics are an interesting future subject, but are beyond the scope of this paper.

In the remainder of the appendix, we provide analyses of PF|N locks, P|P locks, and PF|P locks that were omitted from the conference version due to space constraints. We start with PF|N locks.

C. Constraints for Priority-Ordered Non-Preemptable Spin Locks with FIFO-Ordered Tie-Breaking

PF|N locks are a hybrid of the P|N locks and F|N locks considered previously: they ensure that within each priority level requests are satisfied in FIFO order, and each request can be delayed at most once by a lower-priority request.

To begin with, we establish a wait-time bound that provides a bound on the maximum delay encountered as part of single request for a resource ℓ_q issued with priority π. This wait-time bound is then used in turn to bound the maximum interference due to higher-priority requests. To this end, for a global resource ℓ_q, a task T_i, and a priority π, let $W_q^{\mathrm{PF|N}}(T_i, \pi)$ denote the smallest positive value that satisfies the following recurrence:

$$W_q^{\mathrm{PF|N}}(T_i, \pi) \triangleq HP(\ell_q, \pi) + SP(\ell_q, \pi) + LP(\ell_q, \pi) + 1. \tag{3}$$

Here, $HP(\ell_q, \pi)$ denotes the maximum delay remote requests with a priority higher than π can contribute to the wait time of J_i's request, which can be bounded based on the maximum number of jobs that exist during any interval of length $W_q^{\mathrm{PF|N}}(T_i, \pi)$:

$$HP(\ell_q, \pi) = \sum_{\substack{T_x \in \tau^R \\ \pi > \pi_{x,q}}} \Big(njobs\big(T_x,\, W_q^{\mathrm{PF|N}}(T_i, \pi)\big) \cdot N_{x,q} \cdot L_{x,q} \Big).$$

$SP(\ell_q, \pi)$ accounts for the delay J_i's request can incur due to remote requests with priority π, which are served in FIFO order:

$$SP(\ell_q, \pi) = \sum_{P_k, P_k \neq P(T_i)}^{m} \max_{T_x \in \tau(P_k)} \{L_{x,q} | \pi_{x,q} = \pi\}.$$

Finally, $LP(\ell_q, \pi)$ accounts for the delay J_i's request can incur due to remote lower-priority requests, which in a PF|N lock is limited to at most one critical section:

$$LP(\ell_q, \pi) = \max_{T_x \in \tau^R} \{L_{x,q} | \pi_{x,q} > \pi\}.$$

Lemma 2. *Let t_0 denote the time a job J_i of task T_i attempts to lock a resource ℓ_q with locking priority π, and let t_1 denote the time that J_i subsequently acquires the lock for ℓ_q. With PF|N locks, $t_1 - t_0 \leq W_q^{\mathrm{PF|N}}(T_i, \pi)$.*

Proof: Let R denote J_i's request for ℓ_q. In a PF|N lock, at any point in time $t \in [t_0, t_1)$, J_i is spinning non-preemptably because either **(i)** ℓ_q is being used by a job with locking priority (w.r.t. ℓ_q) lower than π, **(ii)** ℓ_q is being used by a job with locking priority equal to π, or **(iii)** ℓ_q is being used by a job with a locking priority greater than π. We bound the maximum duration for which each of these conditions can hold during an interval of length $W_q^{\mathrm{PF|N}}(T_i, \pi)$.

Case (i): Since requests are satisfied in priority order when using PF|N locks, R can be delayed by at most one lower-priority request for ℓ_q, which is accounted for by $LP(\ell_q, \pi)$.

Case (ii): Since requests of equal priority are satisfied in FIFO order when using PF|N locks, w.r.t. each other processor, R can be delayed by at most one remote request for ℓ_q with priority π, for a total of at most $SP(\ell_q, \pi)$ time units.

Case (iii): When using PF|N locks, any number of higher-priority requests can delay R. However, analogous to the response-time analysis of non-preemptive fixed-priority scheduling, the maximum number of higher-priority requests for ℓ_q that exist during $[t_0, t_1)$ bounds the length of the interval since J_i ceases spinning and acquires ℓ_q as soon as ℓ_q is no longer contended. In any interval of length $W_q^{\mathrm{PF|N}}(T_i, \pi)$, at most $njobs\big(T_x, W_q^{\mathrm{PF|N}}(T_i, \pi)\big)$ jobs of each remote task T_x with a locking priority $\pi_{x,q}$ higher than π exist. Each such job issues at most $N_{x,q}$ requests for ℓ_q, and holds ℓ_q for at most $L_{x,q}$ time units as part of each request. Each remote task T_x with a higher locking priority (w.r.t. ℓ_q) hence holds ℓ_q for at most $njobs\big(T_x, W_q^{\mathrm{PF|N}}(T_i, \pi)\big) \cdot N_{x,q} \cdot L_{x,q}$ during any interval of length $W_q^{\mathrm{PF|N}}(T_i, \pi)$. The term $HP(\ell_q, \pi)$ thus bounds the cumulative length that J_i is spinning while a job with a higher locking priority uses ℓ_q during any interval of length $W_q^{\mathrm{PF|N}}(T_i, \pi)$.

Since $W_q^{\mathrm{PF|N}}(T_i, \pi)$ is by definition the smallest value that satisfies Eq. (3) (if one exists), after at most $W_q^{\mathrm{PF|N}}(T_i, \pi)$ time units after J_i started spinning, ℓ_q is no longer unavailable due to a lower-priority (w.r.t. ℓ_q) request (case (i)), ℓ_q is no longer unavailable due to earlier-issued equal-priority requests (case (ii)), and ℓ_q is no longer contended by jobs of tasks with higher locking priority (case (iii)). J_i hence acquires ℓ_q at time t_1 no more than $W_q^{\mathrm{PF|N}}(T_i, \pi)$ time units after it started spinning at time t_0. ∎

If $W_q^{\mathrm{PF|N}}(T_i, \pi)$ does not exist, that is, if the recurrence Eq. (3) does not converge, then starvation cannot be ruled out and Constraints 18 and 19 do not apply.

In the following constraints, we exploit two simple monotonicity properties of $W_q^{\mathrm{PF|N}}(T_i, \pi)$, which we next state explicitly for the sake of clarity. First, $W_q^{\mathrm{PF|N}}(T_i, \pi)$ is monotonic with respect to scheduling priority. That is, the wait time of a request for ℓ_q issued by a local higher-priority task T_h with the same

locking priority π is no longer than the wait time of T_i's request. (In fact, the per-request wait-time bound for PF|N locks is independent of scheduling priority since jobs spin non-preemptably.) Formally,

$$\forall T_h \in \tau^{lh} : \; W_q^{\mathrm{PF|N}}(T_i, \pi) \geq W_q^{\mathrm{PF|N}}(T_h, \pi). \tag{4}$$

The second monotonicity property that we exploit pertains to the locking priority π: in a PF|N lock, requests issued with higher locking priority naturally do not incur more spin delay than requests issued with lower locking priority:

$$\pi' < \pi \rightarrow W_q^{\mathrm{PF|N}}(T_i, \pi) \geq W_q^{\mathrm{PF|N}}(T_i, \pi'). \tag{5}$$

Based on the wait-time bound $W_q^{\mathrm{PF|N}}(T_i, \pi)$, we next present constraints on the maximum spin delay incurred by any J_i when using PF|N locks. Recall from Sec. III-E that π_q^{minLP} and π_q^{minHP} denote the minimum locking priority of any lower-priority and higher-priority task, resp., on T_i's processor that accesses the global resource ℓ_q. For convenience, we repeat the definitions here:

$$\pi_q^{minLP} \triangleq \max_{T_x \in \tau^{ll}} \{\pi_{x,q} | \ell_q \in Q \wedge N_{x,q} > 0\},$$
$$\pi_q^{minHP} \triangleq \max_{T_x \in (\tau^{lh} \cup \{T_i\})} \{\pi_{x,q} | \ell_q \in Q \wedge N_{x,q} > 0\}.$$

These two definitions are needed because J_i might be delayed transitively due to requests of local tasks with locking priorities lower than T_i's own locking priority. To obtain valid (and simple) constraints, we make the following two simplifications: first, for a given resource ℓ_q, we assume that J_i and all higher-priority jobs that preempt J_i issue requests with locking priority π_q^{minHP} (the lowest locking priority that any such job uses), and second, we assume that all local lower-priority jobs request ℓ_q with locking priority π_q^{minLP} (again, the lowest locking priority used by any local, lower-priority job). Both of these are safe assumption due to the monotonicity property stated in Eq. (5). However, we note that these simplifications are a potential source of pessimism that could be avoided with a significantly more complicated analysis setup, which we leave to future work.

With these assumptions in place, we obtain a simple constraint on the maximum spin delay due to higher-priority requests.

Constraint 18. *In any schedule of τ with PF|N locks:*

$$\forall P_k, P_k \neq P(T_i) : \; \forall \ell_q \in Q^g :$$
$$\forall T_x \in \tau(P_k), \pi_{x,q} < \pi_q^{minHP} :$$
$$\sum_{v=1}^{N_{x,q}^i} X_{x,q,v}^S \leq njobs\big(T_x, W_q^{\mathrm{PF|N}}(T_i, \pi_q^{minHP})\big) \cdot N_{x,q} \cdot ncs(T_i, q).$$

Proof: Analogous to Constraint 14. Each request R for ℓ_q issued by J_i remains incomplete for at most $W_q^{\mathrm{PF|N}}(T_i, \pi)$ time units. Due to the monotonicity property stated in Eq. (4), this also holds true for any request issued for ℓ_q by a job of a higher-priority task that preempted J_i. At most $ncs(T_i, q)$ requests are issued for ℓ_q by T_i and local higher-priority tasks while J_i is pending. Hence at most $ncs(T_i, q) \cdot njobs\big(T_x, W_q^{\mathrm{PF|N}}(T_i, \pi)\big) \cdot N_{x,q}$ requests of each remote task T_x with higher locking priority delay J_i. ■

Next, we establish a constraint on arrival blocking due to the non-preemptable spinning of lower-priority jobs that are delayed by remote requests with higher locking priority.

Constraint 19. *In any schedule of τ with PF|N locks:*

$$\forall \ell_q \in Q^g : \forall T_x \in \tau^R, \pi_{x,q} < \pi_q^{minLP} :$$
$$\sum_{v=1}^{N_{x,q}^i} X_{x,q,v}^A \leq njobs\big(T_x, W_q^{\mathrm{PF|N}}(T_i, \pi_q^{minLP})\big) \cdot N_{x,q} \cdot A_q.$$

Proof: Analogous to Constraint 17. A request R issued by a local lower-priority task (with priority at least π_q^{minLP}) can be delayed by all remote requests for ℓ_q with higher locking priorities. Exploiting Eqs. (4) and (5), R remains incomplete for at most $W_q^{\mathrm{PF|N}}(T_i, \pi_q^{minLP})$ time units, which limits the maximum number of jobs of each remote task T_x with a (potentially) higher locking priority to $njobs\big(T_x, W_q^{\mathrm{PF|N}}(T_i, \pi_q^{minLP})\big)$. The stated bound on the maximum number of transitively blocking remote requests with higher locking priorities follows. ■

Requests issued with the same locking priority are satisfied in FIFO order. Hence, the spin delay due to remote equal-priority requests can be constrained similarly to how it is constrained in the analysis of F|N locks.

Constraint 20. *In any schedule of τ with PF|N locks:*

$$\forall P_k, P_k \neq P(T_i) : \; \forall \ell_q \in Q^g :$$
$$\sum_{\substack{T_x \in \tau(P_k) \\ \pi_{x,q} = \pi_q^{minHP}}} \sum_{v=1}^{N_{x,q}^i} X_{x,q,v}^S \leq ncs(T_i, q).$$

Proof: Analogous to Constraint 8. Due to the FIFO-ordering of equal-priority requests, it follows that, w.r.t. each remote processor, at most one earlier-issued, equal-priority request can delay each of the $ncs(T_i, q)$ requests for ℓ_q issued by J_i and local higher-priority jobs. ■

As mentioned before, assuming that all requests for ℓ_q issued by J_i and local higher-priority jobs are issued with locking priority π_q^{minHP} is safe due to the monotonicity property stated in Eq. (5); the blocking incurred by any J_i does not exceed the bound implied by Constraint 20 if in the actual schedule some requests of J_i or local higher-priority jobs are issued with a locking priority higher than π_q^{minHP} .

Next, we constrain the maximum transitive delay due to the non-preemptable spinning of lower-priority jobs that are delayed by earlier-issued remote requests with equal locking priority.

Constraint 21. *In any schedule of τ when using PF|N locks:*

$$\forall \ell_q \in Q^g : \; \forall P_k, P_k \neq P(T_i) :$$
$$\sum_{\substack{T_x \in \tau(P_k) \\ \pi_{x,q} = \pi_q^{minLP}}} \sum_{v=1}^{N_{x,q}^i} X_{x,q,v}^A \leq A_q.$$

Proof: Analogous to Constraint 9. Since requests with the same priority are served in FIFO-order, at most one request per processor for a resource ℓ_q issued with the same locking priority

can contribute to T_i's arrival blocking. ∎

Finally, we constrain the maximum spin delay due to remote requests with lower locking priority.

Constraint 22. *In any schedule of τ with PF|N locks:*

$$\forall \ell_q \in Q^g : \sum_{\substack{T_x \in \tau^R \\ \pi_{x,q} > \pi_q^{minHP}}} \sum_{v=1}^{N_{x,q}^i} X_{x,q,v}^S \leq ncs(T_i, q).$$

Proof: Analogous to Constraint 15. Each request for ℓ_q issued by T_i or a local higher-priority job can be delayed at most once by a remote request for ℓ_q issued with a lower priority. ∎

Similar reasoning applies to the maximum transitive delay due to the non-preemptable spinning of a lower-priority job that is delayed by a remote request with a lower locking priority.

Constraint 23. *In any schedule of τ with PF|N locks:*

$$\forall \ell_q \in Q^g : \sum_{\substack{T_x \in \tau^R \\ \pi_{x,q} > \pi_q^{minLP}}} \sum_{v=1}^{N_{x,q}^i} X_{x,q,v}^A \leq A_q.$$

Proof: Analogous to Constraint 16. If J_i is transitively blocked due to a request for ℓ_q (*i.e.*, if $A_q = 1$), then at most one remote request for ℓ_q issued with a priority less than π_q^{minLP} can contribute to T_i's arrival blocking. ∎

This concludes our analysis of PF|N locks. Together with the generic Constraints 1–7, the PF|N-specific Constraints 18–23 define an ILP that bounds the maximum blocking incurred by any J_i. In the unlikely case that the recurrence given in Eq. (3) does not converge for some ℓ_q, the constraints on blocking due to ℓ_q that depend on the wait-time bound $W_q^{\mathrm{PF|N}}(T_i, \pi)$, namely Constraints 18 and 19, must be omitted from the ILP.

Next, we consider the remaining preemptable spin lock types, namely P|P and PF|P locks. We start by briefly revisiting the generic constraints for preemptable spin locks already introduced in Sec. III-D.

D. Generic Constraints for Preemptable Spin Locks

Recall that preemptable spin locks allow busy-waiting jobs to be preempted. This has the advantage that critical sections executed on remote processors do not cause (transitive) arrival blocking, which, however, comes at the cost that the length of the interval during which an individual request is susceptible to contention is increased (due to preemptions by higher-priority jobs). To integrate these aspects into our analysis, we introduced in Sec. III-D three constraints in the analysis of F|P locks that in fact apply to all preemptable spin lock types: Constraints 10–12 are generic constraints applicable to all preemptable spin locks, including the P|P and PF|P locks considered in the following.

To simplify the notation of the constraints for P|P and PF|P locks, we denote the set of resources accessed by higher-priority tasks, which is frequently referenced in the analysis of preemptable spin locks, as Q^{lh}. Formally,

$$Q^{lh} \triangleq \left\{ \ell_q \;\middle|\; T_h \in \tau^{lh} \wedge N_{h,q} > 0 \right\}.$$

With the generic definitions in place, we next present an analysis of P|P locks.

E. Constraints for Priority-Ordered Preemptable Spin Locks with Unordered Tie-Breaking

Priority-ordered preemptable spin locks ensure that each request is delayed at most once by a different request with a lower priority. For requests with the same priority no particular ordering is specified.

To analyze P|P locks, we first establish a wait-time bound to bound the worst-case delay that a job of T_i can incur after issuing a request for a resource ℓ_q (with priority $\pi_{i,q}$) until the request is satisfied. This bound is later used to constrain the number of requests that can contribute to T_i's overall blocking.

For a global resource ℓ_q and a task T_i, let $W_q^{\mathrm{P|P}}(T_i)$ denote the smallest positive value that satisfies the following recurrence:

$$\begin{aligned} W_q^{\mathrm{P|P}}(T_i) = {} & S(T_i, \ell_q) + LP^i(T_i, \ell_q) + LP^{lh}(T_i, \ell_q) \\ & + I(T_i, \ell_q) + LP^P(T_i, \ell_q) + 1. \end{aligned} \tag{6}$$

The individual components of $W_q^{\mathrm{P|P}}(T_i)$ are defined as follows and justified in the proof of Lem. 3 below.

$S(T_i, \ell_q)$ bounds the maximum delay remote requests of equal or higher priority can contribute to the wait time of T_i's request. However, since J_i can be preempted while spinning, "equal or higher priority" has to be interpreted with respect to the lowest locking priority used by either T_i (when accessing ℓ_q) or a local higher-priority job (when accessing any resource). $S(T_i, \ell_q)$ thus accounts for all delays due to both T_i's request and requests of local higher-priority tasks being blocked by remote requests of higher or equal priority:

$$S(T_i, \ell_q) = \sum_{\ell_r \in Q^{lh} \cup \{\ell_q\}} \sum_{\substack{T_x \in \tau^R \\ \pi_{x,r} \leq \pi'_r}} \Bigg(njobs\big(T_x, W_q^{\mathrm{P|P}}(T_i)\big) \cdot N_{x,r} \cdot L_{x,r} \Bigg),$$

where $\pi'_r = \max\{\pi_{h,r} \mid T_h \in \tau^{lh} \wedge N_{h,r} > 0\}$ if $\ell_r \neq \ell_q$ and $\pi'_r = \max\{\pi_{h,r} \mid T_h \in \tau^{lh} \cup \{T_i\} \wedge N_{h,r} > 0\}$ if $\ell_r = \ell_q$.

$LP^i(T_i, \ell_q)$ accounts for the time J_i's request can be delayed by a remote lower-priority request that already held ℓ_q when J_i issued its request:

$$LP^i(T_i, \ell_q) = \max_{T_x \in \tau^R} \{L_{x,q} | \pi_{x,q} > \pi_{i,q}\}.$$

$LP^{lh}(T_i, \ell_q)$ accounts for requests from local higher-priority jobs that are delayed by remote lower-priority requests:

$$LP^{lh}(T_i, \ell_q) = \sum_{\ell_r \in Q^{lh}} \sum_{T_h \in \tau^{lh}} \left\lceil \frac{W_q^{\mathrm{P|P}}(T_i)}{p_h} \right\rceil \cdot N_{h,r} \cdot \max_{T_x \in \tau^R} \{L_{x,q} | \pi_{x,r} > \pi_{h,r}\}.$$

In a P|P lock, J_i can be preempted while busy-waiting, and hence interference due to the execution of local higher-priority jobs needs to be accounted for with $I(T_i, \ell_q)$:

$$I(T_i, \ell_q) = \sum_{T_h \in \tau^{lh}} \left\lceil \frac{W_q^{\mathrm{P|P}}(T_i)}{p_h} \right\rceil \cdot e_h.$$

Finally, $LP^P(T_i, \ell_q)$ accounts for the (possibly transitive) delay that results from J_i or a higher-priority job being preempted while spinning:

$$LP^P(T_i, \ell_q) = prts\big(T_i,\, W_q^{\mathrm{P|P}}(T_i)\big) \cdot cpp(T_i, \ell_q).$$

Here, $prts(T_i, t)$ denotes the maximum number of preemptions that occur on T_i's processor throughout any interval of length t while a job of T_i is pending:

$$prts(T_i, t) \triangleq \sum_{T_h \in \tau^{lh}} \left\lceil \frac{t}{p_h} \right\rceil.$$

And $cpp(T_i, \ell_q)$ denotes the worst-case cost per preemption (of either J_i or a local higher-priority job) with respect to the increase in J_i's waiting time due to a remote lower-priority request acquiring a contested resource:

$$cpp(T_i, \ell_q) = \max\{cpp^{lh}(T_i),\ \ cpp^{i}(T_i, \ell_q)\},$$

where $cpp^{lh}(T_i)$ denotes the worst-case cost per preemption of a higher-priority job, formally,

$$\begin{aligned} cpp^{lh}(T_i) = \max\{L_{x,r} \mid\ & T_x \in \tau^R \ \wedge\ \ell_r \in Q^{lh} \ \wedge \\ & T_h \in \tau^{lh} \ \wedge\ N_{h,r} > 0 \ \wedge \\ & \pi_{h,r} < \pi_{x,r}\}, \end{aligned}$$

and where $cpp^{i}(T_i, \ell_q)$ denotes the worst-case cost per preemption of J_i, formally,

$$cpp^{i}(T_i, \ell_q) = \max\{L_{x,q} \mid T_x \in \tau^R \ \wedge \pi_{i,q} < \pi_{x,q}\}.$$

Lemma 3. *Let t_0 denote the time a job J_i of task T_i attempts to lock a resource ℓ_q (with its assigned locking priority $\pi_{i,q}$), and let t_1 denote the time that J_i subsequently acquires the lock for ℓ_q. With P\|P locks, $t_1 - t_0 \leq W_q^{\mathrm{P|P}}(T_i)$.*

Proof: Analogous to Lem. 2. Let R denote J_i's request for ℓ_q. In any point in time $t \in [t_0, t_1)$, J_i is either spinning or has been preempted by a local higher-priority job. We distinguish among seven different cases, depending on whether J_i is scheduled or preempted, whether a spinning job was already preempted, and whether a lower- or higher-priority request causes blocking at time t.

If J_i is spinning at time t, then R is blocked because ℓ_q is being used by a remote job J_x at time t. We consider three distinct cases: **(i)** J_x has a locking priority (w.r.t. ℓ_q) of at least $\pi_{i,q}$, **(ii)** J_x has a locking priority (w.r.t. ℓ_q) lower than $\pi_{i,q}$ and J_i has *not* been preempted during $[t_0, t]$, or **(iii)** J_x has a locking priority (w.r.t. ℓ_q) lower than $\pi_{i,q}$ and J_i *has* previously been preempted during $[t_0, t)$.

Otherwise, if J_i has been preempted and a local higher-priority job J_h is scheduled at time t, then J_h is either **(iv)** executing normally, or it is spinning (which transitively delays J_i). If J_h is spinning, it requested some resource ℓ_r (not necessarily ℓ_q) that is currently in use by a remote job J_x. We again distinguish among three cases: **(v)** J_x's locking priority is at least as high as J_h's locking priority (both w.r.t. ℓ_r), **(vi)** J_x's locking priority is lower than J_h's locking priority (both w.r.t. ℓ_r) and J_h has *not* been preempted while busy-waiting for ℓ_r, and **(vii)** J_x's locking priority is lower than J_h's locking priority (both w.r.t. ℓ_r) and J_h *has* been preempted while busy-waiting for ℓ_r.

We bound the maximum duration for which each of these conditions can hold during an interval of length $W_q^{\mathrm{P|P}}(T_i)$. We begin with requests of equal or higher priority delaying either J_i or a local higher-priority job.

Cases (i) and (v): In cases (i) and (v), in order for a remote task T_x to (transitively) delay J_i, it must either be using ℓ_q and have a locking priority $\pi_{x,q} \leq \pi_{i,q}$, or it must be using some $\ell_r \in Q^{lh}$ (where possibly $\ell_q = \ell_r$) and have a locking priority higher than or equal to the locking priority of some task $T_h \in \tau^{lh}$ that accesses ℓ_r (*i.e.*, $N_{h,r} > 0$ and $\pi_{x,q} \leq \pi_{h,r}$). The cumulative length of all critical sections of all remote tasks satisfying either condition, which is given by $S(T_i, \ell_q)$, thus bounds the total duration during which either case (i) or case (v) occurs during an interval of length $W_q^{\mathrm{P|P}}(T_i)$.

Case (ii): If J_i is delayed by a job J_x using ℓ_q, and J_x has a lower locking priority than J_i and J_i has not been preempted during $[t_0, t]$, then J_x must have continuously used ℓ_q during $[t_0, t]$ since P\|P locks ensure that jobs with lower locking priority cannot acquire ℓ_q while J_i is spinning. The maximum critical section length of any remote task T_x with $\pi_{x,q} > \pi_{i,q}$, as given by $LP^i(T_i, \ell_q)$, thus bounds the maximum duration during which case (ii) occurs.

Cases (iii) and (vii): In P\|P locks, if J_i is preempted while busy-waiting, then remote jobs with a locking priority lower than $\pi_{i,q}$ may acquire ℓ_q while J_i is preempted, which may lead to case (iii). Similarly, if a local higher-priority job J_h is preempted while busy-waiting for a resource $\ell_r \in Q^{lh}$, remote jobs with a locking priority lower than $\pi_{h,r}$ may acquire ℓ_r while J_h is preempted, which may lead to case (vii). In both cases, additional (transitive) delay is caused by the preemption as J_i's wait time is increased by the length of one lower-priority critical section. That is, each time that J_i is preempted, J_i may spin for up to an additional $cpp^i(T_i, \ell_q)$ time units when resuming execution, and each time that a local higher-priority job J_h is preempted while spinning, J_i may be transitively delayed for up to an additional $cpp^{lh}(T_i)$ time units when J_h resumes execution, for a worst-case cost per preemption of $cpp(T_i, \ell_q)$. During an interval of length $W_q^{\mathrm{P|P}}(T_i)$, at most $prts\big(T_i,\, W_q^{\mathrm{P|P}}(T_i)\big)$ higher-priority jobs are released on J_i's processor, which bounds the total number of preemptions. Hence the total cumulative duration during which either case (iii) or case (vii) occurs over the course of an interval of length $W_q^{\mathrm{P|P}}(T_i)$ is bounded by $LP^P(T_i, \ell_q)$.

Case (iv): Analogously to the regular response-time analysis of (preemptive) fixed-priority scheduling [5], during an interval of length $W_q^{\mathrm{P|P}}(T_i)$ starting at time t_0 (at which no higher-priority jobs can be pending because J_i is scheduled and tasks are assumed to not self-suspend), each local higher-priority task $T_h \in \tau^{lh}$ releases at most $\left\lceil \frac{W_q^{\mathrm{P|P}}(T_i)}{p_h} \right\rceil$ jobs, each of which executes for at most e_h time units (not counting any spinning). The total delay due to the regular execution of higher-priority jobs during an interval of length $W_q^{\mathrm{P|P}}(T_i)$ starting at time t_0 is hence bounded by $I(T_i, \ell_q)$.

Case (vi): Analogously to case (ii), if a higher-priority job J_h trying to lock a resource $\ell_r \in Q^{lh}$ is not preempted, it spins waiting for a task $T_x \in \tau^R$ with $\pi_{x,r} > \pi_{h,r}$ to release ℓ_r for at most the duration of one critical section. During an interval of

length $W_q^{\mathrm{P|P}}(T_i)$, each higher-priority task T_h releases at most $\left\lceil \frac{W_q^{\mathrm{P|P}}(T_i)}{p_h} \right\rceil$ jobs, each of which accesses each $\ell_r \in Q^{lh}$ at most $N_{h,r}$ times. As part of each such access, case (vi) occurs for the duration of at most one critical section. The total duration of case (vi) occurring during an interval of length $W_q^{\mathrm{P|P}}(T_i)$ is hence bounded by $LP^{lh}(T_i, \ell_q)$.

This covers all possible ways in which J_i may be (transitively) delayed when trying to lock a resource ℓ_q. Therefore, during an interval of length $W_q^{\mathrm{P|P}}(T_i)$, the total delay incurred by J_i—that is, the total duration during which one of the seven analyzed cases occurs—is limited to $S(T_i, \ell_q) + LP^{i}(T_i, \ell_q) + LP^{P}(T_i, \ell_q) + I(T_i, \ell_q) + LP^{lh}(T_i, \ell_q) = W_q^{\mathrm{P|P}}(T_i) - 1$. In other words, during an interval of length $W_q^{\mathrm{P|P}}(T_i)$ starting at time t_0, J_i is unable to lock ℓ_q for at most $W_q^{\mathrm{P|P}}(T_i) - 1$ time units. J_i thus ceases to spin and acquires ℓ_q at time t_1 at most $W_q^{\mathrm{P|P}}(T_i)$ time units after initially trying to lock ℓ_q. ∎

In the following, we assume that the wait-time bound $W_q^{\mathrm{P|P}}(T_i)$, *i.e.*, the smallest integer to satisfy Eq. (6), can be computed via fixed-point iteration. If, however, the fixed-point iteration does not converge, then the per-request maximum wait time of J_i (w.r.t. ℓ_q) cannot be bounded with the presented approach and Constraint 24 below cannot be applied. (Constraint 25 remains valid in either case.)

As before in the analysis of PF|N locks, we exploit that $W_q^{\mathrm{P|P}}(T_i)$ is monotonic with respect to scheduling priority. That is, the wait-time bound for a local higher-priority task T_h is no longer than the wait-time bound for T_i. Formally,

$$\forall T_h \in \tau^{lh} : \; W_q^{\mathrm{P|P}}(T_i, \pi) \geq W_q^{\mathrm{P|P}}(T_h, \pi). \tag{7}$$

Note that Eq. (7) depends specifically on the definitions of $S(T_i, \ell_q)$, since $S(T_i, \ell_q)$ is defined in terms of the minimum locking priority of T_i and all local higher-priority tasks, which ensures the required monotonicity.

Given the wait-time bound $W_q^{\mathrm{P|P}}(T_i)$, we can constrain the the number of requests for ℓ_q that can contribute to T_i's spin delay, similar to Constraint 14. First, we consider requests issued with higher or equal priority. As in the analysis of PF|N locks, we make the simplifying assumption that all higher-priority jobs issue requests for each ℓ_q with locking priority π_q^{minHP}.

Constraint 24. *In any schedule of τ when using P|P locks:*

$$\begin{aligned}
&\forall P_k, P_k \neq P(T_i) : \forall \ell_q \in Q^g : \\
&\quad \forall T_x \in \tau(P_k), \pi_{x,q} \leq \pi_q^{minHP} : \\
&\qquad \sum_{v=1}^{N_{x,q}^i} X_{x,q,v}^S \leq njobs\big(T_x,\, W_q^{\mathrm{P|P}}(T_i)\big) \\
&\qquad\qquad \cdot N_{x,q} \cdot ncs(T_i, q).
\end{aligned}$$

Proof: Analogous to Constraint 14. Due to the monotonicity property stated in Eq. (7), it is safe to use $W_q^{\mathrm{P|P}}(T_i)$ to bound the maximum duration of any request issued by J_i or any local higher-priority tasks. Each request R for ℓ_q issued by T_i or a local higher-priority task has a locking priority of at least π_q^{minHP}. During any interval of length $W_q^{\mathrm{P|P}}(T_i)$, jobs of a remote task T_x with locking priority at least π_q^{minHP} (w.r.t. ℓ_q) issue at most $njobs\big(T_x,\, W_q^{\mathrm{P|P}}(T_i)\big) \cdot N_{x,q}$ requests for ℓ_q. The stated bound follows since J_i and higher-priority jobs issue at most $ncs(T_i, q)$ requests for ℓ_q. ∎

Next, we consider blocking requests of lower locking priority. Requests with lower locking priority can (possibly transitively) cause T_i to incur spin delay at most once for each request issued by T_i or a local higher-priority task. Further, J_i can be (possibly transitively) blocked by a remote lower-priority request each time J_i or a local higher-priority job is preempted. (Recall that J_i and local higher-priority jobs are preempted at most C_q times in total while busy-waiting for ℓ_q, which is enforced with Constraints 11 and 12.)

Constraint 25. *In any schedule of τ when using P|P locks:*

$$\forall \ell_q \in Q^g : \sum_{\substack{T_x \in \tau^R \\ \pi_{x,q} > \pi_q^{minHP}}} \sum_{v=1}^{N_{x,q}^i} X_{x,q,v}^S \leq ncs(T_i, q) + C_q.$$

Proof: Analogous to Constraints 13 and 15. Each request R for ℓ_q issued by T_i or a local higher-priority task has a locking priority of at least π_q^{minHP}. J_i can be directly or transitively delayed be remote lower-priority requests for a resource ℓ_q each time J_i or a local higher-priority task is preempted or issues a request for ℓ_q. Hence the total number of times that J_i or local higher-priority jobs busy-wait for ℓ_q, in addition to the number of times that J_i or local higher-priority jobs need to restart busy-waiting after being preempted, limits the number of requests issued with locking priority lower than π_q^{minHP} that (transitively) delay J_i. ∎

This concludes our analysis of P|P locks. Together with the generic Constraints 1–7 (for any lock type), and the generic Constraints 10–12 (for preemptable spin locks), the P|P-specific Constraints 24 and 25 define an ILP that bounds the maximum blocking incurred by any J_i. If the recurrence given in Eq. (6) does not converge for some ℓ_q, Constraint 24 must be omitted from the ILP.

Next, we present our analysis of PF|P locks.

F. Constraints for Priority-Ordered Preemptable Spin Locks with FIFO-Ordered Tie-Breaking

Like their non-preemptable counterpart PF|N locks, PF|P locks are a hybrid of FIFO-ordered and priority-ordered spin locks. For requests with different priorities, PF|P locks behave similar to P|P locks: a request can be blocked by at most once one other request for the same resource issued with lower locking priority, while a request can be blocked by all concurrent higher-priority requests for the same resource. Requests with the same locking priority, however, are served in FIFO-order. This similarity of PF|P locks to P|P locks is also reflected in the approach that we employ to analyze PF|P locks: similar to P|P locks, we first establish a wait-time bound on the worst-case delay that a job of T_i can incur when attempting to lock a resource ℓ_q. This bound is later used in Constraint 26 to limit the number of requests that can contribute to T_i's overall blocking.

For a global resource ℓ_q and a task T_i, let $W_q^{\mathrm{PF|P}}(T_i)$ denote the smallest positive value that satisfies the following recurrence:

$$W_q^{\mathrm{PF|P}}(T_i) = HP(T_i, \ell_q) + LSP^{i}(T_i, \ell_q) + LSP^{lh}(T_i, \ell_q)$$

$$+ LSP^P(T_i, \ell_q) + I(T_i, \ell_q) + 1. \quad (8)$$

The individual components of $W_q^{\mathrm{PF|P}}(T_i)$ are defined as follows and justified in the proof of Lem. 4.

$HP(T_i, \ell_q)$ denotes the maximum delay that remote higher-priority requests for ℓ_q or any other resources requested by local higher-priority tasks can contribute to the wait time of T_i's request:

$$HP(T_i, \ell_q) = \sum_{\ell_r \in Q^{lh} \cup \{\ell_q\}} \sum_{\substack{T_x \in \tau^R \\ \pi_{x,r} < \pi'_r}} \Big(njobs\big(T_x,\, W_q^{\mathrm{PF|P}}(T_i)\big) \cdot N_{x,r} \cdot L_{x,r} \Big).$$

where $\pi'_r = \max\{\pi_{h,r} \mid T_h \in \tau^{lh} \wedge N_{h,r} > 0\}$ if $\ell_r \neq \ell_q$ and $\pi'_r = \max\{\pi_{h,r} \mid T_h \in \tau^{lh} \cup \{T_i\} \wedge N_{h,r} > 0\}$ if $\ell_r = \ell_q$.

To define the remaining terms, we first define a generic helper bound $spin^{LS}(P_a, \ell_r, \pi)$ that bounds the maximum delay *due to requests of equal and lower priority only* that any job J_a that starts (or restarts) busy-waiting on a processor P_a for a resource ℓ_r with locking priority π incurs before either acquiring ℓ_r or being preempted (and thus being forced to restart busy-waiting). There are two cases that must be considered: J_a could be delayed by up to $m-1$ requests issued by remote jobs with equal locking priority, or by one request issued by a remote job with lower locking priority and up to $m-2$ requests issued by remote jobs with equal locking priority. We therefore define $spin^{LS}(P_a, \ell_r, \pi)$ as:

$$spin^{LS}(P_a, \ell_r, \pi) = \max\big\{ spin^{S}(P_a, \ell_r, \pi),\, spin^{L}(P_a, \ell_r, \pi) \big\},$$

where $spin^S(P_a, \ell_r, \pi)$ bounds the maximum delay when (up to) $m-1$ jobs with equal locking priority precede J_a in the queue for ℓ_r, and where $spin^L(P_a, \ell_r, \pi)$ bounds the case of J_a being preceded by one lower-priority and up to $m-2$ equal-priority requests.

A safe bound on $spin^S(P_a, \ell_r, \pi)$ is given by the sum of the maximum critical lengths on each remote processor:

$$spin^{S}(P_a, \ell_r, \pi) = \sum_{P_k \neq P_a} \max\{L_{x,r} \mid T_x \in \tau(P_k) \wedge \pi_{x,r} = \pi\}.$$

If a job with a lower locking priority holds ℓ_r when J_a starts busy-waiting, only (up to) $m-2$ jobs with equal locking priority precede J_a in the queue for ℓ_r (recall that jobs are removed from the queue when they are preempted, and that only one job per processor is spinning at any time). Suppose that the job with lower locking priority executes on processor P_l. Then a safe bound is given by:

$$spin^{L'}(P_a, \ell_r, \pi, P_l) = \max\{L_{x,q} | T_x \in \tau(P_l) \wedge \pi_{x,q} > \pi\} + \sum_{\substack{P_k \neq P(T_i) \\ P_k \neq P_l}} \max\{L_{x,q} | T_x \in \tau(P_k) \wedge \pi_{x,q} = \pi\}.$$

Since the job with lower locking priority could potentially reside on any processor (other than P_a), $spin^L(P_a, \ell_r, \pi)$ is defined as follows:

$$spin^{L}(P_a, \ell_r, \pi) = \max_{P_l \neq P_a} \Big\{ spin^{L'}(P_a, \ell_r, \pi, P_l) \Big\}.$$

With the definition of $spin^{LS}(P_a, \ell_r, \pi)$ in place, it is easy to express the remaining terms.

$LSP^i(T_i, \ell_q)$ accounts for the time J_i's request can be delayed by remote requests with a lower or equal locking priority (before J_i is preempted, if at all):

$$LSP^i(T_i, \ell_q) = spin^{LS}(P(T_i), \ell_q, \pi_{i,q}).$$

$LSP^{lh}(T_i, \ell_q)$ accounts for spinning local higher-priority jobs that are delayed by remote requests issued with the same or lower locking priority:

$$LSP^{lh}(T_i, \ell_q) = \sum_{l_r \in Q^{lh}} \sum_{T_h \in \tau^{lh}} \left\lceil \frac{W_q^{\mathrm{PF|P}}(T_i)}{p_h} \right\rceil \cdot N_{h,r} \cdot spin^{LS}(P(T_i), \ell_r, \pi_{h,r}).$$

Since busy-waiting jobs can be preempted in PF|P locks, $I(T_i, \ell_q)$ accounts for the interference that J_i can incur due to the execution of local higher-priority jobs:

$$I(T_i, \ell_q) = \sum_{T_h \in \tau^{lh}} \left\lceil \frac{W_q^{\mathrm{PF|P}}(T_i)}{p_h} \right\rceil \cdot e_h.$$

Preemptions can also cause additional spinning because other jobs may "skip ahead" in the wait queue when a busy-waiting job is preempted. To account for this, $LSP^P(T_i, \ell_q)$ bounds the additional delay J_i can incur (possibly transitively) due to the preemption of J_i and local higher-priority jobs:

$$LSP^P(T_i, \ell_q) = cpp(T_i, \ell_q) \cdot prts\big(T_i,\, W_q^{\mathrm{PF|P}}(T_i)\big),$$

where $prts(T_i, t)$ is defined as before in the analysis of P|P locks. The definition of $cpp(T_i, \ell_q)$, which denotes the worst-case cost per preemption (of either J_i or a local higher-priority job) with respect to the increase in J_i's wait time due to a remote request acquiring a contested resource, is also defined as in the analysis of P|P locks:

$$cpp(T_i, \ell_q) = \max\big\{ cpp^{lh}(T_i), cpp^{i}(T_i, \ell_q) \big\}.$$

The definitions of $cpp^{lh}(T_i)$ and $cpp^i(T_i)$, however, must be adjusted to reflect the FIFO-ordering of equal-priority requests in PF|P locks. $cpp^i(T_i, \ell_q)$ bounds the maximum additional delay incurred by J_i when it is forced to restart its request for ℓ_q after being preempted, where

$$cpp^{i}(T_i, \ell_q) = spin^{LS}(P(T_i), \ell_q, \pi_{i,q}).$$

Analogously, $cpp^{lh}(T_i)$ bounds the maximum additional delay transitively incurred by J_i after a preemption of a higher-priority job J_h that is busy-waiting for a resource $\ell_r \in Q^{lh}$. Since a higher-priority job might be waiting for any resource in Q^{lh} when it is preempted, and since the identity of J_h is not known *a priori*, a safe bound is given by:

$$cpp^{lh}(T_i) = \max\big\{ spin^{LS}(P(T_i), \ell_r, \pi_{h,r}) \mid T_h \in \tau^{lh} \wedge N_{h,r} > 0 \big\}.$$

Lemma 4. *Let t_0 denote the time a job J_i of task T_i attempts to lock a resource ℓ_q (with its assigned locking priority $\pi_{i,q}$), and let t_1 denote the time that J_i subsequently acquires the lock for ℓ_q. With PF\|P locks, $t_1 - t_0 \leq W_q^{\mathrm{PF|P}}(T_i)$.*

Proof: Analogous to the proof of Lem. 3. Let R denote J_i's request for ℓ_q. In any point in time $t \in [t_0, t_1)$, J_1 is spinning or preempted by a local higher-priority job. We distinguish among eleven different scenarios, which together cover all possible ways in which J_i can be prevented from acquiring ℓ_q at time t.

If J_i is spinning at time t, then R is blocked because ℓ_q is being used by a remote job J_x at time t. We consider five distinct cases: **(i)** J_x has a locking priority (w.r.t. ℓ_q) exceeding $\pi_{i,q}$, **(ii)** J_x has a locking priority (w.r.t. ℓ_q) equal to $\pi_{i,q}$ and J_i has *not* been preempted during $[t_0, t]$, **(iii)** J_x has a locking priority (w.r.t. ℓ_q) equal to $\pi_{i,q}$ and J_i *has* previously been preempted during $[t_0, t]$, **(iv)** J_x has a locking priority (w.r.t. ℓ_q) lower than $\pi_{i,q}$ and J_i has *not* been preempted during $[t_0, t)$, or **(v)** J_x has a locking priority (w.r.t. ℓ_q) lower than $\pi_{i,q}$ and J_i *has* previously been preempted during $[t_0, t)$.

Otherwise, if J_i has been preempted and a local higher-priority job J_h is scheduled at time t, then J_h is either **(vi)** executing normally, or it is spinning. If J_h is spinning, it requested some resource $\ell_r \in Q^{lh}$ that is currently in use by a remote job J_x. We again distinguish among five cases: **(vii)** J_x's locking priority is higher than J_h's locking priority (both w.r.t. ℓ_r), **(viii)** J_x's locking priority is equal to J_h's locking priority (both w.r.t. ℓ_r) and J_h has *not* been preempted while busy-waiting for ℓ_r, **(ix)** J_x's locking priority is equal to J_h's locking priority (both w.r.t. ℓ_r) and J_h *has* been preempted while busy-waiting for ℓ_r, **(x)** J_x's locking priority is lower than J_h's locking priority (both w.r.t. ℓ_r) and J_h has *not* been preempted while busy-waiting for ℓ_r, and **(xi)** J_x's locking priority is lower than J_h's locking priority (both w.r.t. ℓ_r) and J_h *has* been preempted while busy-waiting for ℓ_r.

We bound the maximum duration for which each of these conditions can hold during an interval of length $W_q^{\mathrm{PF|P}}(T_i)$.

Cases (i) and (vii): In order for a remote job J_x to (transitively) delay J_i with a higher-priority request, it must either be using ℓ_q and have a locking priority $\pi_{x,q} < \pi_{i,q}$, or it must be using some $\ell_r \in Q^{lh}$ and have a locking priority higher than the locking priority of some task $T_h \in \tau^{lh}$ that accesses ℓ_r (*i.e.*, $N_{h,r} > 0$ and $\pi_{x,q} < \pi_{h,r}$). The cumulative length of all critical sections of all remote tasks satisfying either condition, which is given by $HP(T_i, \ell_q)$, thus bounds the total duration during which either case (i) or case (vii) occurs during an interval of length $W_q^{\mathrm{FP|P}}(T_i)$.

Cases (ii) and (iv): If J_i has not been preempted during $[t_0, t]$, then, due to the FIFO ordering of equal-priority requests in PF|P locks, any equal-priority request blocking J_i must have been already issued at time t_0. Further, if J_i is blocked by a request with issued by a job J_l with a lower locking priority at time t, then J_l must have already held ℓ_q at time t_0 because jobs with lower locking priority cannot acquire a PF|P lock while jobs with higher locking priority are busy-waiting.

Consider the priority of the job that holds ℓ_q when J_i starts busy-waiting. If ℓ_q is held by a job with equal locking priority when J_i starts busy-waiting, then up to $m-1$ additional requests of jobs with equal locking priority that were issued at or before time t_0 may precede J_i in the queue for ℓ_q as there is only one spinning job per processor at any time, and since the requests of preempted jobs are cancelled (and thus cannot delay J_i). The sum of the longest critical section (w.r.t. ℓ_q) on each remote processor, as given by $spin^S(P(T_i), \ell_q, \pi_{i,q})$, thus bounds the total duration for which case (ii) can occur.

If ℓ_q is held by a job with lower locking priority when J_i starts busy-waiting, then case (iv) can occur for at most the duration of one critical section executed by a task with lower locking priority (on any one processor), and case (ii) can occur for the sum of durations of the longest critical section executed by a job with equal locking priority on each of the $m-2$ other processors. $spin^L(P(T_i), \ell_q, \pi_{i,q})$ thus bounds the cumulative duration during which cases (ii) and (iv) occur, assuming case (iv) occurs at all.

Combining the two cases, the maximum total duration that J_i is unable to lock ℓ_q due to cases (ii) and (iv) is hence limited to $LSP^i(T_i, \ell_q) = spin^{LS}(P(T_i), \ell_q, \pi_{i,q})$ time units.

(Note that any delay due to requests of higher locking priority fall under case (i); if ℓ_q is held by a job with higher locking priority when J_i starts busy-waiting, then case (ii) persists for the duration of at most $m-2$ equal-priority requests, which is a non-worst-case scenario with less total blocking that is subsumed by the preceding analysis).

Cases (iii), (v), (ix), and (xi): With PF|P locks, if a spinning job is preempted, its lock request is cancelled and must be reissued after resuming execution. This gives jobs on other cores with a lower or equal locking priority a chance to "skip ahead," which causes J_i to incur additional delay. Due to the FIFO ordering of equal-priority requests, and because the requests of preempted jobs are cancelled, at most $m-1$ requests of equal or lower priority can "skip ahead" each time that J_i or a local higher-priority job is preempted. Further, of the additional $m-1$ requests causing delays, at most one request is of lower locking priority. When J_i restarts its request for ℓ_q after being preempted, it hence faces a worst-case situation (w.r.t. to lower- and equal-priority requests) that is equivalent to the scenarios discussed in cases (ii) and (iv) above. Analogously, the worst-case cost per preemption in terms of the additional spin delay incurred by J_i when resuming execution is hence bounded by $cpp^i(T_i, \ell_q) = spin^{LS}(P(T_i), \ell_q, \pi_{i,q})$.

If a local higher-priority job J_h is preempted while busy-waiting (instead of J_i), it similarly can be faced with renewed contention from lower- and equal-priority requests just like when J_h initially issued its request. However, in this case, the locking priority of the preempting job J_h is relevant (and not the locking priority of J_i), and J_h could be busy-waiting for any resource in Q^{lh} (and not just ℓ_q). Therefore, when a local higher-priority, busy-waiting job is preempted, J_i is subject to transitive delays due to either up to $m-1$ equal-priority requests, or due to up $m-2$ equal-priority requests and one lower-priority request for potentially any resource in Q^{lh}. Applying the same reasoning as in cases (ii) and (iv) above to each potentially preempted task and each accessed resource leads to the bound $cpp^{lh}(T_i)$.

The maximum additional delay due to additional spinning of J_i or a local higher-priority job after one preemption is limited to the maximum of $cpp^i(T_i, \ell_q)$ and $cpp^{lh}(T_i)$, as given by $cpp(T_i, \ell_q)$. As there are at most $prts\big(T_i, W_q^{\mathrm{PF|P}}(T_i)\big)$ preemp-

tions during an interval of length $W_q^{\mathrm{PF|P}}(T_i)$, the maximum cumulative duration during which cases (iii), (v), (ix), and (xi) occur is hence limited to $LSP^P(T_i, \ell_q)$.

Case (vi): Analogously to regular response-time analysis of (preemptive) fixed-priority scheduling, during an interval of length $W_q^{\mathrm{PF|P}}(T_i)$ starting at time t_0 (at which no higher-priority jobs can be pending because J_i is scheduled and tasks are assumed to not self-suspend), each local higher-priority task $T_h \in \tau^{lh}$ releases at most $\left\lceil \frac{W_q^{\mathrm{PF|P}}(T_i)}{p_h} \right\rceil$ jobs, each of which executes for at most e_h time units (not counting any spinning). The total delay due to the regular execution of higher-priority jobs during an interval of length $W_q^{\mathrm{PF|P}}(T_i)$ starting at time t_0 is hence bounded by $I(T_i, \ell_q)$.

Cases (viii) and (x): When a local higher-priority job J_h issues a request for a resource $\ell_r \in Q^{hl}$, reasoning similar to cases (ii) and (iv) applies. Hence each time that any job J_h requests a resource ℓ_r, the transitive delay incurred by J_i until J_h is either preempted or acquires ℓ_r is limited to $spin^{LS}(P(T_i), \ell_r, \pi_{h,r})$. During an interval of length $W_q^{\mathrm{PF|P}}(T_i)$, each higher-priority task $T_h \in \tau^{lh}$ releases at most $\left\lceil \frac{W_q^{\mathrm{PF|P}}(T_i)}{p_h} \right\rceil$ jobs, each of which requests each resource $\ell_r \in Q^{lh}$ at most $N_{h,r}$ times. The total duration during which J_i is transitively delayed due to cases (viii) and (x) during an interval of length $W_q^{\mathrm{PF|P}}(T_i)$ hence does not exceed $LSP^{lh}(T_i, \ell_q)$.

This covers all possible ways in which J_i may be (transitively) delayed when trying to lock a resource ℓ_q. Therefore, during an interval of length $W_q^{\mathrm{PF|P}}(T_i)$, the total delay incurred by J_i—the total duration during which one of the eleven analyzed cases occurs—is limited to $HP(T_i, \ell_q) + LSP^i(T_i, \ell_q) + LSP^P(T_i, \ell_q) + I(T_i, \ell_q) + LSP^{lh}(T_i, \ell_q) = W_q^{\mathrm{PF|P}}(T_i) - 1$. In other words, during an interval of length $W_q^{\mathrm{PF|P}}(T_i)$ starting at time t_0, J_i is unable to lock ℓ_q for at most $W_q^{\mathrm{PF|P}}(T_i) - 1$ time units. J_i thus ceases to spin and acquires ℓ_q at time t_1 at most $W_q^{\mathrm{PF|P}}(T_i)$ time units after initially trying to lock ℓ_q. ■

Similar to PF|N locks and P|P locks, we exploit that $W_q^{\mathrm{PF|P}}(T_i)$ is monotonic with respect to scheduling priority. The wait time of a request for ℓ_q issued by a local higher-priority task T_h is no longer than the wait time of T_i's request. Formally,

$$\forall T_h \in \tau^{lh} : \; W_q^{\mathrm{PF|P}}(T_i) \geq W_q^{\mathrm{PF|P}}(T_h). \tag{9}$$

Again, as is the case with $W_q^{\mathrm{P|P}}(T_i)$, this monotonicity property stems from a suitably monotonic bound on the delays due to requests issued with "higher" locking priority, *i.e.*, $HP(T_i, \ell_q)$, in the definition $W_q^{\mathrm{PF|P}}(T_i)$.

Next, based on the wait-time bound $W_q^{\mathrm{PF|P}}(T_i)$, we present constraints on spin delay due to higher-priority requests. As in the preceding analyses, we assume that $W_q^{\mathrm{PF|P}}(T_i)$ has been determined using fixed-point iteration; in cases where this is not possible, the following constraint cannot be applied. Further, as in the analyses of PF|N and P|P locks, we make the simplifying assumption that all higher-priority jobs issue requests for each ℓ_q with locking priority π_q^{minHP}.

Constraint 26. *In any schedule of τ with PF|P locks:*

$$\forall P_k, P_k \neq P(T_i) : \; \forall \ell_q \in Q^g : \\ \forall T_x \in \tau(P_k), \pi_{x,q} < \pi_q^{minHP} : \\ \sum_{v=1}^{N_{x,q}^i} X_{x,q,v}^S \leq njobs\big(T_x, W_q^{\mathrm{PF|P}}(T_i)\big) \cdot N_{x,q} \cdot ncs(T_i, q).$$

Proof: Analogous to Constraint 24. Due to the monotonicity property stated in Eq. (9), it is safe to use $W_q^{\mathrm{PF|P}}(T_i)$ to bound the maximum duration of any request issued by J_i or any local higher-priority tasks. Each request R for ℓ_q issued by T_i or a local higher-priority task has a locking priority of at least π_q^{minHP}. During any interval of length $W_q^{\mathrm{PF|P}}(T_i)$, jobs of a remote task T_x with locking priority higher than π_q^{minHP} (w.r.t. ℓ_q) issue at most $njobs\big(T_x, W_q^{\mathrm{PF|P}}(T_i)\big) \cdot N_{x,q}$ requests for ℓ_q. The stated bound follows since J_i and higher-priority jobs issue at most $ncs(T_i, q)$ requests for ℓ_q. ■

Requests issued with the same locking priority are satisfied in FIFO order. Hence, in this case, the constraints on spin delay are similar to those for F|P locks. We constrain the number of requests issued with equal locking priority that can contribute to T_i's spin delay with the next constraint.

Constraint 27. *In any schedule of τ with PF|P locks:*

$$\forall P_k, P_k \neq P(T_i) : \; \forall \ell_q \in Q^g : \\ \sum_{\substack{T_x \in \tau(P_k) \\ \pi_{x,q} = \pi_q^{minHP}}} \sum_{v=1}^{N_{x,q}^i} X_{x,q,v}^S \leq ncs(T_i, q) + C_q.$$

Proof: Analogous to Constraints 13 and 25. Each request R for ℓ_q issued by T_i or a local higher-priority task has a locking priority of at least π_q^{minHP}. J_i can be directly or transitively delayed by remote equal-priority requests for a resource ℓ_q each time J_i or a local higher-priority task is preempted or issues a request for ℓ_q. Hence the total number of times that J_i or local higher-priority jobs busy-wait for ℓ_q, in addition to the number of times that J_i or local higher-priority jobs need to restart busy-waiting after being preempted, limits the number of requests issued with locking priority equal to π_q^{minHP} that delay J_i. ■

Requests with lower priority can (possibly transitively) cause T_i to incur spin delay at most once per request issued by T_i or a local higher-priority job.

Constraint 28. *In any schedule of τ with PF|P locks:*

$$\forall \ell_q \in Q^g : \sum_{\substack{T_x \in \tau^R \\ \pi_{x,q} > \pi_q^{minHP}}} \sum_{v=1}^{N_{x,q}^i} X_{x,q,v}^S \leq ncs(T_i, q) + C_q.$$

Proof: Analogous to Constraints 15 and 26. J_i can be directly or transitively delayed by remote lower-priority requests for a resource ℓ_q each time J_i or a local higher-priority task is preempted or issues a request for ℓ_q. ■

This concludes our analysis of PF|P locks. Together with the generic Constraints 1–7 (for any lock type), the generic Constraints 10–12 (for preemptable spin locks), and the PF|P-

specific Constraints 26–28 define an ILP that bounds the maximum blocking incurred by any J_i. If the recurrence given in Eq. (8) does not converge for some ℓ_q, Constraint 26 must be omitted from the ILP.

Next, we discuss some opportunities for future improvements.

G. Analysis Refinements

The analyses of several spin lock types presented in this work demonstrate how integer linear programming can be leveraged to find fine-grained worst-case blocking bounds. For most of the lock types, the presented ILP-based analysis is the first worst-case blocking analysis proposed to date, which we attribute in part to the difficulty of expressing reasonably accurate bounds using prior analysis approaches. Case in point, the wait-time bounds established in Lemmas 1–4, which resemble the per-request analysis approach used in the classic MSRP analysis [16], are both much more complicated to reason about than each ILP constraint (which can be reasoned about in isolation), and are also *much* more pessimistic than the bounds obtained with the ILP-based analysis (*e.g.*, just avoiding to account for any request more than once already makes a big difference).

From theoretical point of view, we have shown that the presented analysis approach can be asymptotically less pessimistic than any approach that relies on the inflation of per-job execution costs (Theorem 1). This result, however, should not be mistaken to mean that the proposed ILP-based analysis is *always* superior. For one, we make no claim of optimality with regard to the set of proposed constraints—with additional knowledge of each task's synchronization behavior, and also simply with more involved analysis, it is possible to derive tighter constraints for many of the considered lock types.

Further, in the specific case of F|N locks, our ILP-based analysis yields slightly higher bounds than holistic analysis [8] in (somewhat rare) corner cases due to constant factors. This effect, however, does not lessen the usability of our approach in practice since it can be used together with prior analysis techniques, just as we did in our experiments described in Sec. V.

Nonetheless, our approach could be further improved in various ways to yield more accurate blocking bounds, as we show with three examples next.

1) Reduced pessimism in transitive blocking bounds: Recall that one form of transitive blocking is caused when local higher-priority jobs incur direct blocking when accessing global resources, which then transitively delays pending lower-priority jobs. In the aforementioned corner cases in which our ILP-based analysis of F|N locks is less accurate than the prior holistic analysis, we identified pessimism in the analysis of transitive blocking as the primary cause.

To account for transitive blocking, we use the function $ncs(T_i, q)$ to determine the number of requests issued by T_i or local higher-priority jobs for a resource ℓ_q while T_i's job is pending. As defined in Sec. III, $ncs(T_i, q)$ can in some cases overestimate the number of critical sections that may cause T_i to incur transitive blocking since it is defined in terms of $N^i_{h,q}$ for each local higher-priority task T_h, which in term depends on the term $njobs(T_h, r_i)$.

The bound $njobs(T_h, r_i)$, however, can be pessimistic for local higher-priority jobs because it does not consider the fact that the local processor does not idle while J_i is pending (*i.e.*, the bound does not reflect proper response-time analysis). Thus there exist certain corner cases wherein $njobs(T_h, r_i) = 2$ when in fact only a single job of a given T_h could preempt any J_i, which leads to pessimistic bounds on worst-case transitive blocking.

This could be easily avoided by integrating more accurate estimates of the number of preempting higher-priority jobs into the definition of $N^i_{h,q}$. For example, a more accurate bound on the number of preempting jobs could be extracted from response-time analysis based on holistic blocking analysis.

2) Additional constraints: The pessimism in transitive blocking can be further reduced with additional constraints that we present next. In case a job of T_i incurs transitive blocking due to requests for a remote resource ℓ_q that T_i does not access, the number of blocking requests can be constrained by considering the maximum number of remote requests that a local higher-priority task is *exposed* to while T_i's job is pending. In particular, let $E(T_h, T_x, \ell_q, t)$ denote the *exposure*, that is, the number of requests for ℓ_q issued by jobs of a remote task T_x that can be pending while jobs of T_h are pending throughout any interval of length t:

$$E(T_h, T_x, \ell_q, t) = njobs(T_h, t) \cdot N^h_{x,q}.$$

By considering an interval of length r_i, $E(T_h, T_x, \ell_q, r_i)$ bounds the number of requests for ℓ_q issued by jobs of T_x that can block jobs of T_h while T_i's job is pending, and hence, bounds the number of requests that can transitively block T_i's job (via T_h). For each global resource ℓ_q not accessed by T_i, the following generic constraint exploits this observation to impose a constraint on the total transitive blocking due to requests of local higher-priority requests for ℓ_q.

Constraint 29. *In any schedule of τ:*

$$\forall \ell_q \in Q^g, N_{i,q} = 0 : \forall T_x \in \tau^r : \sum_{v=1}^{N^i_{x,q}} X^S_{x,q,v} \leq \sum_{\substack{T_h \in \tau^{lh} \\ N_{h,q} > 0}} E(T_h, T_x, \ell_q, r_i)$$

Proof: Suppose not. Then, for some resource ℓ_q not accessed by T_i, a job of T_i is transitively blocked by more than

$$\sum_{T_h \in \tau^{lh} \wedge N_{h,q} > 0} E(T_h, T_x, \ell_q, r_i)$$

requests from a remote task T_x. Then, by the pigeon-hole principle, a local higher-priority task $T_h \in \tau^{lh}$ with $N_{h,q} > 0$ is directly blocked by more than $E(T_h, T_x, \ell_q, r_i)$ requests for ℓ_q issued by T_x while T_i's job is pending. Then, by the definition of $E(T_h, T_x, \ell_q, t)$ and the pigeon-hole principle, one of T_h's jobs is blocked by more than $N^h_{x,q}$ requests for ℓ_q issued by T_x. However, $N^h_{x,q}$ bounds the number of requests for ℓ_q issued by jobs of T_x that can be pending while a job of T_h is pending. Contradiction. ■

The previous constraint is generic in the sense that it applies to all types of spin locks. Tighter constraints building on the same idea can be derived by exploiting properties of specific spin lock types. In the case of F|N locks, we can derive a tighter constraint that also exploits the fact that each request of either

T_i or a local higher-priority tasks can be delayed by at most one request from each other processor.

Constraint 30. *In any schedule of τ when using F\|N locks:*

$$\forall \ell_q : \forall P_k \neq P(T_i) : \forall T_x \in \tau(P_k) : \sum_{v=1}^{N^i_{x,q}} X^S_{x,q,v} \leq N_{i,q} + \sum_{\substack{T_h \in \tau^{lh} \\ N_{h,q}>0}} E(T_h, T_x, \ell_q, r_i)$$

The proof follows the same pattern as the proof of Constraint 29. The same approach can be adopted in the analysis of F|P locks, P|P locks and PF|P locks, which we leave to future work. We note that the experiments reported on in this paper did not employ Constraints 29 and 30.

3) Reduced pessimism in wait-time bounds: The wait-time bounds established in Lemmas 1–4 are used to bound the "lifetime" of a single request for a given resource, which is in turn used to bound the maximum number of requests that can precede J_i's request repeatedly. The accuracy of the wait-time bounds thus is not directly reflected in the final results, but any pessimism in the wait-time bounds does potentially have an indirect impact because a pessimistic per-request wait-time bound increases the analyzed "lifetime" of a request and hence also its "window of exposure" with respect to contention.

Improved wait-time bounds could thus lead to (somewhat) improved blocking bounds for unordered and priority-ordered spin locks. One way in which the existing wait-time bounds could be improved would be to apply holistic analysis [8] instead of the per-request analysis employed herein. One could further even imagine a "bootstrapping" approach, wherein the presented ILP-based analysis is employed to derive much more accurate wait-time bounds, which are then fed into a second round of ILP-based analysis.

To summarize, our ILP-based analysis is asymptotically less pessimistic than prior approaches, but could still be improved by reducing the impact of certain constant factors. As our focus is to demonstrate the principles behind ILP-based analysis, we leave these and other possible detail improvements to future work.

H. Full Results

For the sake of transparency and completeness, the entire set of results is made available in the following. The graphs are organized as follows.

Figs. 5–2164 show results depending on task set size n

- Figs. 5–724 show results for 4 processors.
  - Figs. 5–244 show results for 2 resources.
    - Figs. 5–64 show results for $rsf = 0.1$.
      - Figs. 5–24 show results for $U = 0.1n$.
      - Figs. 25–44 show results for $U = 0.2n$.
      - Figs. 45–64 show results for $U = 0.3n$.
    - Figs. 65–124 show results for $rsf = 0.25$.
      - Figs. 65–84 show results for $U = 0.1n$.
      - Figs. 85–104 show results for $U = 0.2n$.
      - Figs. 105–124 show results for $U = 0.3n$.
    - Figs. 125–184 show results for $rsf = 0.4$.
      - Figs. 125–144 show results for $U = 0.1n$.
      - Figs. 145–164 show results for $U = 0.2n$.
      - Figs. 165–184 show results for $U = 0.3n$.
    - Figs. 185–244 show results for $rsf = 0.75$.
      - Figs. 185–204 show results for $U = 0.1n$.
      - Figs. 205–224 show results for $U = 0.2n$.
      - Figs. 225–244 show results for $U = 0.3n$.
  - Figs. 245–484 show results for 4 resources.
    - Figs. 245–304 show results for $rsf = 0.1$.
      - Figs. 245–264 show results for $U = 0.1n$.
      - Figs. 265–284 show results for $U = 0.2n$.
      - Figs. 285–304 show results for $U = 0.3n$.
    - Figs. 305–364 show results for $rsf = 0.25$.
      - Figs. 305–324 show results for $U = 0.1n$.
      - Figs. 325–344 show results for $U = 0.2n$.
      - Figs. 345–364 show results for $U = 0.3n$.
    - Figs. 365–424 show results for $rsf = 0.4$.
      - Figs. 365–384 show results for $U = 0.1n$.
      - Figs. 385–404 show results for $U = 0.2n$.
      - Figs. 405–424 show results for $U = 0.3n$.
    - Figs. 425–484 show results for $rsf = 0.75$.
      - Figs. 425–444 show results for $U = 0.1n$.
      - Figs. 445–464 show results for $U = 0.2n$.
      - Figs. 465–484 show results for $U = 0.3n$.
  - Figs. 485–724 show results for 8 resources.
    - Figs. 485–544 show results for $rsf = 0.1$.
      - Figs. 485–504 show results for $U = 0.1n$.
      - Figs. 505–524 show results for $U = 0.2n$.
      - Figs. 525–544 show results for $U = 0.3n$.
    - Figs. 545–604 show results for $rsf = 0.25$.
      - Figs. 545–564 show results for $U = 0.1n$.
      - Figs. 565–584 show results for $U = 0.2n$.
      - Figs. 585–604 show results for $U = 0.3n$.
    - Figs. 605–664 show results for $rsf = 0.4$.
      - Figs. 605–624 show results for $U = 0.1n$.
      - Figs. 625–644 show results for $U = 0.2n$.
      - Figs. 645–664 show results for $U = 0.3n$.
    - Figs. 665–724 show results for $rsf = 0.75$.
      - Figs. 665–684 show results for $U = 0.1n$.
      - Figs. 685–704 show results for $U = 0.2n$.
      - Figs. 705–724 show results for $U = 0.3n$.
- Figs. 725–1444 show results for 8 processors.
  - Figs. 725–964 show results for 4 resources.
    - Figs. 725–784 show results for $rsf = 0.1$.
      - Figs. 725–744 show results for $U = 0.1n$.
      - Figs. 745–764 show results for $U = 0.2n$.
      - Figs. 765–784 show results for $U = 0.3n$.
    - Figs. 785–844 show results for $rsf = 0.25$.
      - Figs. 785–804 show results for $U = 0.1n$.
      - Figs. 805–824 show results for $U = 0.2n$.
      - Figs. 825–844 show results for $U = 0.3n$.
    - Figs. 845–904 show results for $rsf = 0.4$.
      - Figs. 845–864 show results for $U = 0.1n$.
      - Figs. 865–884 show results for $U = 0.2n$.
      - Figs. 885–904 show results for $U = 0.3n$.

    - Figs. 905–964 show results for $rsf = 0.75$.
      - Figs. 905–924 show results for $U = 0.1n$.
      - Figs. 925–944 show results for $U = 0.2n$.
      - Figs. 945–964 show results for $U = 0.3n$.
  - Figs. 965–1204 show results for 8 resources.
    - Figs. 965–1024 show results for $rsf = 0.1$.
      - Figs. 965–984 show results for $U = 0.1n$.
      - Figs. 985–1004 show results for $U = 0.2n$.
      - Figs. 1005–1024 show results for $U = 0.3n$.
    - Figs. 1025–1084 show results for $rsf = 0.25$.
      - Figs. 1025–1044 show results for $U = 0.1n$.
      - Figs. 1045–1064 show results for $U = 0.2n$.
      - Figs. 1065–1084 show results for $U = 0.3n$.
    - Figs. 1085–1144 show results for $rsf = 0.4$.
      - Figs. 1085–1104 show results for $U = 0.1n$.
      - Figs. 1105–1124 show results for $U = 0.2n$.
      - Figs. 1125–1144 show results for $U = 0.3n$.
    - Figs. 1145–1204 show results for $rsf = 0.75$.
      - Figs. 1145–1164 show results for $U = 0.1n$.
      - Figs. 1165–1184 show results for $U = 0.2n$.
      - Figs. 1185–1204 show results for $U = 0.3n$.
  - Figs. 1205–1444 show results for 16 resources.
    - Figs. 1205–1264 show results for $rsf = 0.1$.
      - Figs. 1205–1224 show results for $U = 0.1n$.
      - Figs. 1225–1244 show results for $U = 0.2n$.
      - Figs. 1245–1264 show results for $U = 0.3n$.
    - Figs. 1265–1324 show results for $rsf = 0.25$.
      - Figs. 1265–1284 show results for $U = 0.1n$.
      - Figs. 1285–1304 show results for $U = 0.2n$.
      - Figs. 1305–1324 show results for $U = 0.3n$.
    - Figs. 1325–1384 show results for $rsf = 0.4$.
      - Figs. 1325–1344 show results for $U = 0.1n$.
      - Figs. 1345–1364 show results for $U = 0.2n$.
      - Figs. 1365–1384 show results for $U = 0.3n$.
    - Figs. 1385–1444 show results for $rsf = 0.75$.
      - Figs. 1385–1404 show results for $U = 0.1n$.
      - Figs. 1405–1424 show results for $U = 0.2n$.
      - Figs. 1425–1444 show results for $U = 0.3n$.
- Figs. 1445–2164 show results for 16 processors.
  - Figs. 1445–1684 show results for 8 resources.
    - Figs. 1445–1504 show results for $rsf = 0.1$.
      - Figs. 1445–1464 show results for $U = 0.1n$.
      - Figs. 1465–1484 show results for $U = 0.2n$.
      - Figs. 1485–1504 show results for $U = 0.3n$.
    - Figs. 1505–1564 show results for $rsf = 0.25$.
      - Figs. 1505–1524 show results for $U = 0.1n$.
      - Figs. 1525–1544 show results for $U = 0.2n$.
      - Figs. 1545–1564 show results for $U = 0.3n$.
    - Figs. 1565–1624 show results for $rsf = 0.4$.
      - Figs. 1565–1584 show results for $U = 0.1n$.
      - Figs. 1585–1604 show results for $U = 0.2n$.
      - Figs. 1605–1624 show results for $U = 0.3n$.
    - Figs. 1625–1684 show results for $rsf = 0.75$.
      - Figs. 1625–1644 show results for $U = 0.1n$.
      - Figs. 1645–1664 show results for $U = 0.2n$.
      - Figs. 1665–1684 show results for $U = 0.3n$.
  - Figs. 1685–1924 show results for 16 resources.
    - Figs. 1685–1744 show results for $rsf = 0.1$.
      - Figs. 1685–1704 show results for $U = 0.1n$.
      - Figs. 1705–1724 show results for $U = 0.2n$.
      - Figs. 1725–1744 show results for $U = 0.3n$.
    - Figs. 1745–1804 show results for $rsf = 0.25$.
      - Figs. 1745–1764 show results for $U = 0.1n$.
      - Figs. 1765–1784 show results for $U = 0.2n$.
      - Figs. 1785–1804 show results for $U = 0.3n$.
    - Figs. 1805–1864 show results for $rsf = 0.4$.
      - Figs. 1805–1824 show results for $U = 0.1n$.
      - Figs. 1825–1844 show results for $U = 0.2n$.
      - Figs. 1845–1864 show results for $U = 0.3n$.
    - Figs. 1865–1924 show results for $rsf = 0.75$.
      - Figs. 1865–1884 show results for $U = 0.1n$.
      - Figs. 1885–1904 show results for $U = 0.2n$.
      - Figs. 1905–1924 show results for $U = 0.3n$.
  - Figs. 1925–2164 show results for 32 resources.
    - Figs. 1925–1984 show results for $rsf = 0.1$.
      - Figs. 1925–1944 show results for $U = 0.1n$.
      - Figs. 1945–1964 show results for $U = 0.2n$.
      - Figs. 1965–1984 show results for $U = 0.3n$.
    - Figs. 1985–2044 show results for $rsf = 0.25$.
      - Figs. 1985–2004 show results for $U = 0.1n$.
      - Figs. 2005–2024 show results for $U = 0.2n$.
      - Figs. 2025–2044 show results for $U = 0.3n$.
    - Figs. 2045–2104 show results for $rsf = 0.4$.
      - Figs. 2045–2064 show results for $U = 0.1n$.
      - Figs. 2065–2084 show results for $U = 0.2n$.
      - Figs. 2085–2104 show results for $U = 0.3n$.
    - Figs. 2105–2164 show results for $rsf = 0.75$.
      - Figs. 2105–2124 show results for $U = 0.1n$.
      - Figs. 2125–2144 show results for $U = 0.2n$.
      - Figs. 2145–2164 show results for $U = 0.3n$.

Figs. 2165–2596 show results depending on the number of critical sections

- Figs. 2165–2308 show results for 4 processors.
  - Figs. 2165–2212 show results for 2 resources.
    - Figs. 2165–2176 show results for $rsf = 0.1$.
      - Figs. 2165–2168 show results for $U = 0.1n$.
      - Figs. 2169–2172 show results for $U = 0.2n$.
      - Figs. 2173–2176 show results for $U = 0.3n$.
    - Figs. 2177–2188 show results for $rsf = 0.25$.
      - Figs. 2177–2180 show results for $U = 0.1n$.
      - Figs. 2181–2184 show results for $U = 0.2n$.
      - Figs. 2185–2188 show results for $U = 0.3n$.
    - Figs. 2189–2200 show results for $rsf = 0.4$.
      - Figs. 2189–2192 show results for $U = 0.1n$.
      - Figs. 2193–2196 show results for $U = 0.2n$.
      - Figs. 2197–2200 show results for $U = 0.3n$.
    - Figs. 2201–2212 show results for $rsf = 0.75$.

· Figs. 2201–2204 show results for $U = 0.1n$.
· Figs. 2205–2208 show results for $U = 0.2n$.
· Figs. 2209–2212 show results for $U = 0.3n$.

– Figs. 2213–2260 show results for 4 resources.
∗ Figs. 2213–2224 show results for $rsf = 0.1$.
· Figs. 2213–2216 show results for $U = 0.1n$.
· Figs. 2217–2220 show results for $U = 0.2n$.
· Figs. 2221–2224 show results for $U = 0.3n$.
∗ Figs. 2225–2236 show results for $rsf = 0.25$.
· Figs. 2225–2228 show results for $U = 0.1n$.
· Figs. 2229–2232 show results for $U = 0.2n$.
· Figs. 2233–2236 show results for $U = 0.3n$.
∗ Figs. 2237–2248 show results for $rsf = 0.4$.
· Figs. 2237–2240 show results for $U = 0.1n$.
· Figs. 2241–2244 show results for $U = 0.2n$.
· Figs. 2245–2248 show results for $U = 0.3n$.
∗ Figs. 2249–2260 show results for $rsf = 0.75$.
· Figs. 2249–2252 show results for $U = 0.1n$.
· Figs. 2253–2256 show results for $U = 0.2n$.
· Figs. 2257–2260 show results for $U = 0.3n$.

– Figs. 2261–2308 show results for 8 resources.
∗ Figs. 2261–2272 show results for $rsf = 0.1$.
· Figs. 2261–2264 show results for $U = 0.1n$.
· Figs. 2265–2268 show results for $U = 0.2n$.
· Figs. 2269–2272 show results for $U = 0.3n$.
∗ Figs. 2273–2284 show results for $rsf = 0.25$.
· Figs. 2273–2276 show results for $U = 0.1n$.
· Figs. 2277–2280 show results for $U = 0.2n$.
· Figs. 2281–2284 show results for $U = 0.3n$.
∗ Figs. 2285–2296 show results for $rsf = 0.4$.
· Figs. 2285–2288 show results for $U = 0.1n$.
· Figs. 2289–2292 show results for $U = 0.2n$.
· Figs. 2293–2296 show results for $U = 0.3n$.
∗ Figs. 2297–2308 show results for $rsf = 0.75$.
· Figs. 2297–2300 show results for $U = 0.1n$.
· Figs. 2301–2304 show results for $U = 0.2n$.
· Figs. 2305–2308 show results for $U = 0.3n$.

• Figs. 2309–2452 show results for 8 processors.
– Figs. 2309–2356 show results for 4 resources.
∗ Figs. 2309–2320 show results for $rsf = 0.1$.
· Figs. 2309–2312 show results for $U = 0.1n$.
· Figs. 2313–2316 show results for $U = 0.2n$.
· Figs. 2317–2320 show results for $U = 0.3n$.
∗ Figs. 2321–2332 show results for $rsf = 0.25$.
· Figs. 2321–2324 show results for $U = 0.1n$.
· Figs. 2325–2328 show results for $U = 0.2n$.
· Figs. 2329–2332 show results for $U = 0.3n$.
∗ Figs. 2333–2344 show results for $rsf = 0.4$.
· Figs. 2333–2336 show results for $U = 0.1n$.
· Figs. 2337–2340 show results for $U = 0.2n$.
· Figs. 2341–2344 show results for $U = 0.3n$.
∗ Figs. 2345–2356 show results for $rsf = 0.75$.
· Figs. 2345–2348 show results for $U = 0.1n$.
· Figs. 2349–2352 show results for $U = 0.2n$.
· Figs. 2353–2356 show results for $U = 0.3n$.

– Figs. 2357–2404 show results for 8 resources.
∗ Figs. 2357–2368 show results for $rsf = 0.1$.
· Figs. 2357–2360 show results for $U = 0.1n$.
· Figs. 2361–2364 show results for $U = 0.2n$.
· Figs. 2365–2368 show results for $U = 0.3n$.
∗ Figs. 2369–2380 show results for $rsf = 0.25$.
· Figs. 2369–2372 show results for $U = 0.1n$.
· Figs. 2373–2376 show results for $U = 0.2n$.
· Figs. 2377–2380 show results for $U = 0.3n$.
∗ Figs. 2381–2392 show results for $rsf = 0.4$.
· Figs. 2381–2384 show results for $U = 0.1n$.
· Figs. 2385–2388 show results for $U = 0.2n$.
· Figs. 2389–2392 show results for $U = 0.3n$.
∗ Figs. 2393–2404 show results for $rsf = 0.75$.
· Figs. 2393–2396 show results for $U = 0.1n$.
· Figs. 2397–2400 show results for $U = 0.2n$.
· Figs. 2401–2404 show results for $U = 0.3n$.

– Figs. 2405–2452 show results for 16 resources.
∗ Figs. 2405–2416 show results for $rsf = 0.1$.
· Figs. 2405–2408 show results for $U = 0.1n$.
· Figs. 2409–2412 show results for $U = 0.2n$.
· Figs. 2413–2416 show results for $U = 0.3n$.
∗ Figs. 2417–2428 show results for $rsf = 0.25$.
· Figs. 2417–2420 show results for $U = 0.1n$.
· Figs. 2421–2424 show results for $U = 0.2n$.
· Figs. 2425–2428 show results for $U = 0.3n$.
∗ Figs. 2429–2440 show results for $rsf = 0.4$.
· Figs. 2429–2432 show results for $U = 0.1n$.
· Figs. 2433–2436 show results for $U = 0.2n$.
· Figs. 2437–2440 show results for $U = 0.3n$.
∗ Figs. 2441–2452 show results for $rsf = 0.75$.
· Figs. 2441–2444 show results for $U = 0.1n$.
· Figs. 2445–2448 show results for $U = 0.2n$.
· Figs. 2449–2452 show results for $U = 0.3n$.

• Figs. 2453–2596 show results for 16 processors.
– Figs. 2453–2500 show results for 8 resources.
∗ Figs. 2453–2464 show results for $rsf = 0.1$.
· Figs. 2453–2456 show results for $U = 0.1n$.
· Figs. 2457–2460 show results for $U = 0.2n$.
· Figs. 2461–2464 show results for $U = 0.3n$.
∗ Figs. 2465–2476 show results for $rsf = 0.25$.
· Figs. 2465–2468 show results for $U = 0.1n$.
· Figs. 2469–2472 show results for $U = 0.2n$.
· Figs. 2473–2476 show results for $U = 0.3n$.
∗ Figs. 2477–2488 show results for $rsf = 0.4$.
· Figs. 2477–2480 show results for $U = 0.1n$.
· Figs. 2481–2484 show results for $U = 0.2n$.
· Figs. 2485–2488 show results for $U = 0.3n$.
∗ Figs. 2489–2500 show results for $rsf = 0.75$.
· Figs. 2489–2492 show results for $U = 0.1n$.
· Figs. 2493–2496 show results for $U = 0.2n$.
· Figs. 2497–2500 show results for $U = 0.3n$.

- Figs. 2501–2548 show results for 16 resources.
  - Figs. 2501–2512 show results for $rsf = 0.1$.
    - Figs. 2501–2504 show results for $U = 0.1n$.
    - Figs. 2505–2508 show results for $U = 0.2n$.
    - Figs. 2509–2512 show results for $U = 0.3n$.
  - Figs. 2513–2524 show results for $rsf = 0.25$.
    - Figs. 2513–2516 show results for $U = 0.1n$.
    - Figs. 2517–2520 show results for $U = 0.2n$.
    - Figs. 2521–2524 show results for $U = 0.3n$.
  - Figs. 2525–2536 show results for $rsf = 0.4$.
    - Figs. 2525–2528 show results for $U = 0.1n$.
    - Figs. 2529–2532 show results for $U = 0.2n$.
    - Figs. 2533–2536 show results for $U = 0.3n$.
  - Figs. 2537–2548 show results for $rsf = 0.75$.
    - Figs. 2537–2540 show results for $U = 0.1n$.
    - Figs. 2541–2544 show results for $U = 0.2n$.
    - Figs. 2545–2548 show results for $U = 0.3n$.
- Figs. 2549–2596 show results for 32 resources.
  - Figs. 2549–2560 show results for $rsf = 0.1$.
    - Figs. 2549–2552 show results for $U = 0.1n$.
    - Figs. 2553–2556 show results for $U = 0.2n$.
    - Figs. 2557–2560 show results for $U = 0.3n$.
  - Figs. 2561–2572 show results for $rsf = 0.25$.
    - Figs. 2561–2564 show results for $U = 0.1n$.
    - Figs. 2565–2568 show results for $U = 0.2n$.
    - Figs. 2569–2572 show results for $U = 0.3n$.
  - Figs. 2573–2584 show results for $rsf = 0.4$.
    - Figs. 2573–2576 show results for $U = 0.1n$.
    - Figs. 2577–2580 show results for $U = 0.2n$.
    - Figs. 2581–2584 show results for $U = 0.3n$.
  - Figs. 2585–2596 show results for $rsf = 0.75$.
    - Figs. 2585–2588 show results for $U = 0.1n$.
    - Figs. 2589–2592 show results for $U = 0.2n$.
    - Figs. 2593–2596 show results for $U = 0.3n$.

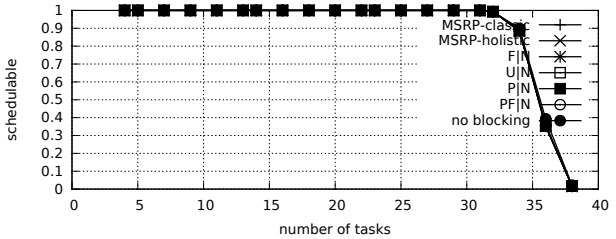

Fig. 5. Schedulability under non-preemptable spin locks for $m = 4$, $U = 0.1n$, 2 resources, $rsf = 0.1$, $N^{max} = 1$, and medium critical sections. The schedulability of the considered preemptable lock types in this configuration is shown in Fig. 15.

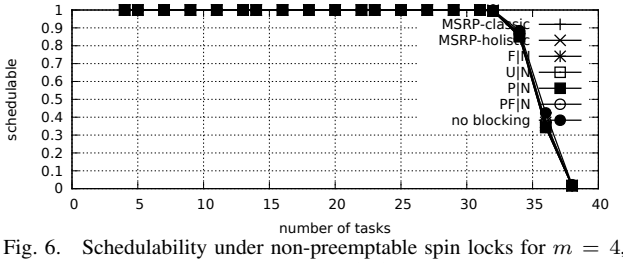

Fig. 6. Schedulability under non-preemptable spin locks for $m = 4$, $U = 0.1n$, 2 resources, $rsf = 0.1$, $N^{max} = 2$, and medium critical sections. The schedulability of the considered preemptable lock types in this configuration is shown in Fig. 16.

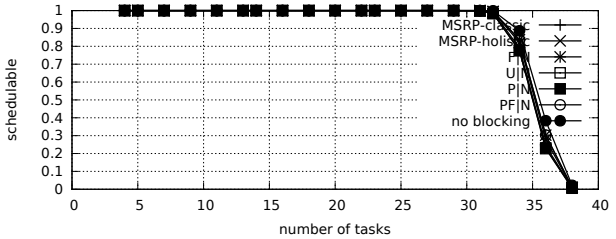

Fig. 7. Schedulability under non-preemptable spin locks for $m = 4$, $U = 0.1n$, 2 resources, $rsf = 0.1$, $N^{max} = 5$, and medium critical sections. The schedulability of the considered preemptable lock types in this configuration is shown in Fig. 17.

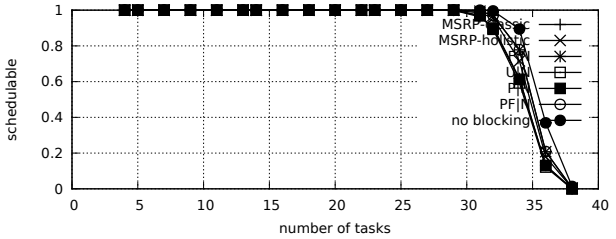

Fig. 8. Schedulability under non-preemptable spin locks for $m = 4$, $U = 0.1n$, 2 resources, $rsf = 0.1$, $N^{max} = 10$, and medium critical sections. The schedulability of the considered preemptable lock types in this configuration is shown in Fig. 18.

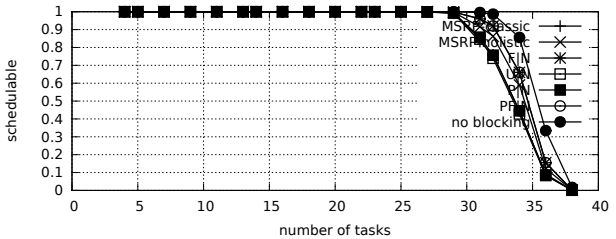

Fig. 9. Schedulability under non-preemptable spin locks for $m = 4$, $U = 0.1n$, 2 resources, $rsf = 0.1$, $N^{max} = 15$, and medium critical sections. The schedulability of the considered preemptable lock types in this configuration is shown in Fig. 19.

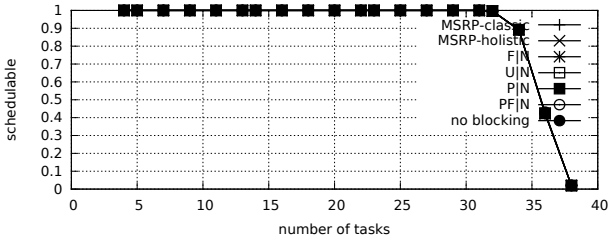

Fig. 10. Schedulability under non-preemptable spin locks for $m = 4$, $U = 0.1n$, 2 resources, $rsf = 0.1$, $N^{max} = 1$, and short critical sections. The schedulability of the considered preemptable lock types in this configuration is shown in Fig. 20.

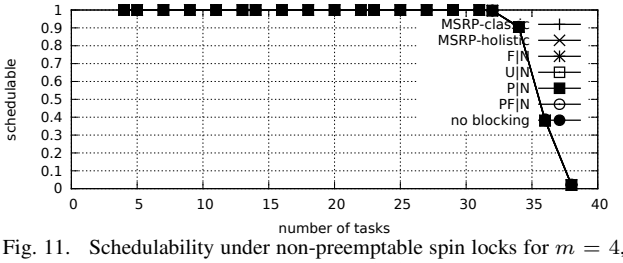

Fig. 11. Schedulability under non-preemptable spin locks for $m = 4$, $U = 0.1n$, 2 resources, $rsf = 0.1$, $N^{max} = 2$, and short critical sections. The schedulability of the considered preemptable lock types in this configuration is shown in Fig. 21.

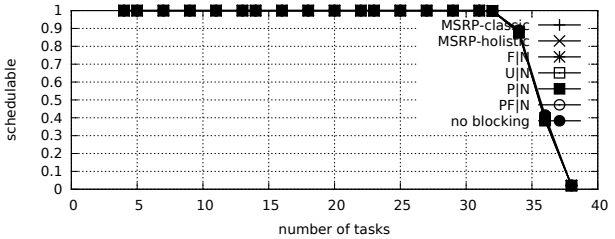

Fig. 12. Schedulability under non-preemptable spin locks for $m = 4$, $U = 0.1n$, 2 resources, $rsf = 0.1$, $N^{max} = 5$, and short critical sections. The schedulability of the considered preemptable lock types in this configuration is shown in Fig. 22.

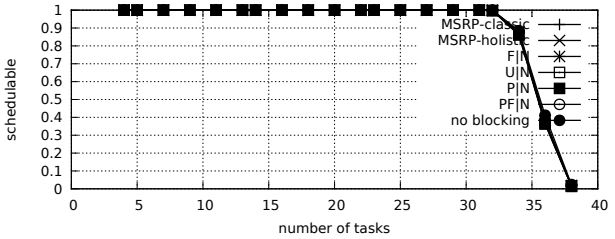

Fig. 13. Schedulability under non-preemptable spin locks for $m = 4$, $U = 0.1n$, 2 resources, $rsf = 0.1$, $N^{max} = 10$, and short critical sections. The schedulability of the considered preemptable lock types in this configuration is shown in Fig. 23.

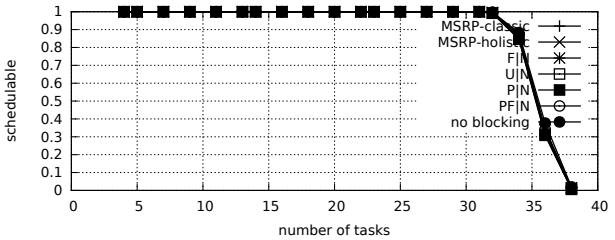

Fig. 14. Schedulability under non-preemptable spin locks for $m = 4$, $U = 0.1n$, 2 resources, $rsf = 0.1$, $N^{max} = 15$, and short critical sections. The schedulability of the considered preemptable lock types in this configuration is shown in Fig. 24.

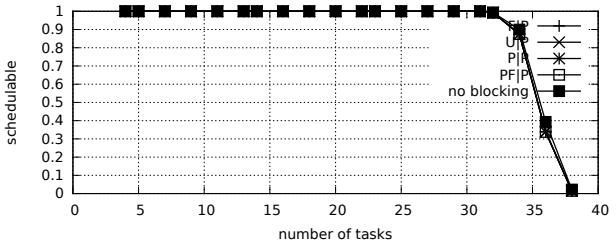

Fig. 15. Schedulability under preemptable spin locks for $m = 4$, $U = 0.1n$, 2 resources, $rsf = 0.1$, $N^{max} = 1$, and medium critical sections. The schedulability of the considered non-preemptable lock types in this configuration is shown in Fig. 5.

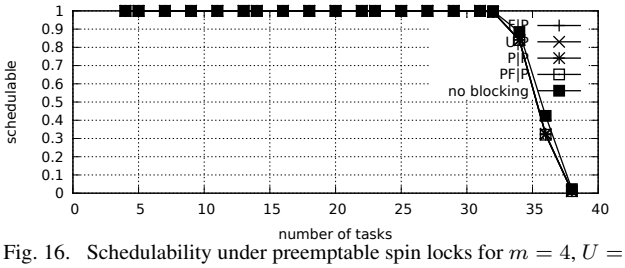

Fig. 16. Schedulability under preemptable spin locks for $m = 4$, $U = 0.1n$, 2 resources, $rsf = 0.1$, $N^{max} = 2$, and medium critical sections. The schedulability of the considered non-preemptable lock types in this configuration is shown in Fig. 6.

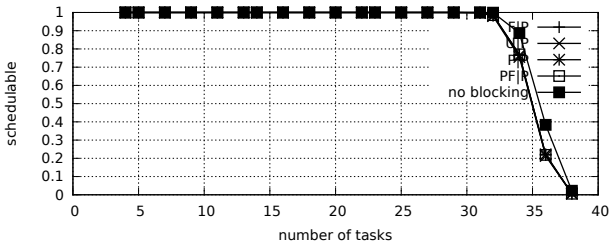

Fig. 17. Schedulability under preemptable spin locks for $m = 4$, $U = 0.1n$, 2 resources, $rsf = 0.1$, $N^{max} = 5$, and medium critical sections. The schedulability of the considered non-preemptable lock types in this configuration is shown in Fig. 7.

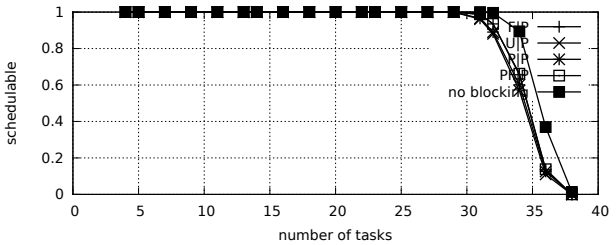

Fig. 18. Schedulability under preemptable spin locks for $m = 4$, $U = 0.1n$, 2 resources, $rsf = 0.1$, $N^{max} = 10$, and medium critical sections. The schedulability of the considered non-preemptable lock types in this configuration is shown in Fig. 8.

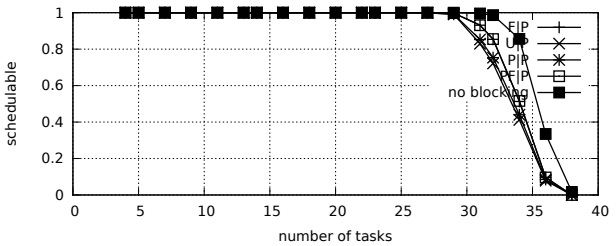

Fig. 19. Schedulability under preemptable spin locks for $m = 4$, $U = 0.1n$, 2 resources, $rsf = 0.1$, $N^{max} = 15$, and medium critical sections. The schedulability of the considered non-preemptable lock types in this configuration is shown in Fig. 9.

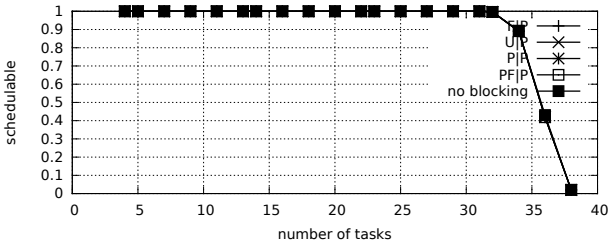

Fig. 20. Schedulability under preemptable spin locks for $m = 4$, $U = 0.1n$, 2 resources, $rsf = 0.1$, $N^{max} = 1$, and short critical sections. The schedulability of the considered non-preemptable lock types in this configuration is shown in Fig. 10.

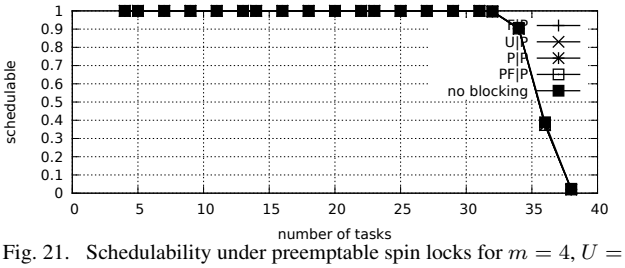

Fig. 21. Schedulability under preemptable spin locks for $m = 4$, $U = 0.1n$, 2 resources, $rsf = 0.1$, $N^{max} = 2$, and short critical sections. The schedulability of the considered non-preemptable lock types in this configuration is shown in Fig. 11.

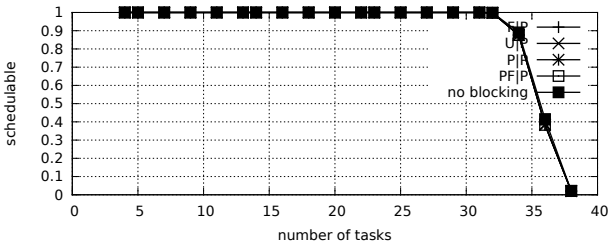

Fig. 22. Schedulability under preemptable spin locks for $m = 4$, $U = 0.1n$, 2 resources, $rsf = 0.1$, $N^{max} = 5$, and short critical sections. The schedulability of the considered non-preemptable lock types in this configuration is shown in Fig. 12.

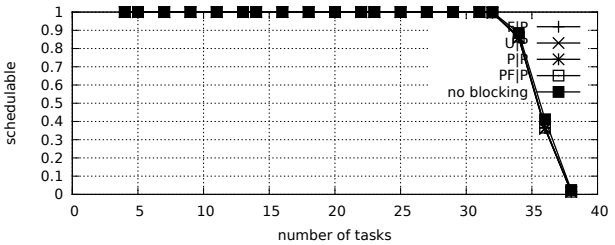

Fig. 23. Schedulability under preemptable spin locks for $m = 4$, $U = 0.1n$, 2 resources, $rsf = 0.1$, $N^{max} = 10$, and short critical sections. The schedulability of the considered non-preemptable lock types in this configuration is shown in Fig. 13.

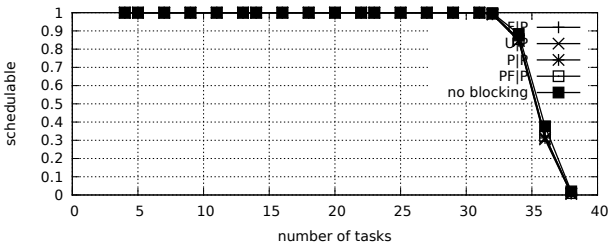

Fig. 24. Schedulability under preemptable spin locks for $m = 4$, $U = 0.1n$, 2 resources, $rsf = 0.1$, $N^{max} = 15$, and short critical sections. The schedulability of the considered non-preemptable lock types in this configuration is shown in Fig. 14.

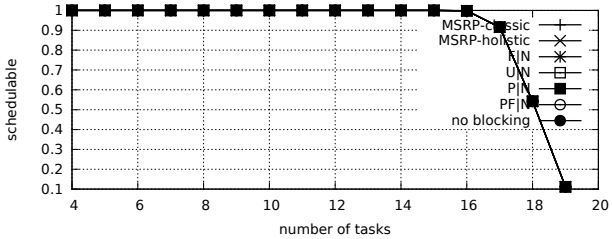

Fig. 25. Schedulability under non-preemptable spin locks for $m = 4$, $U = 0.2n$, 2 resources, $rsf = 0.1$, $N^{max} = 1$, and medium critical sections. The schedulability of the considered preemptable lock types in this configuration is shown in Fig. 35.

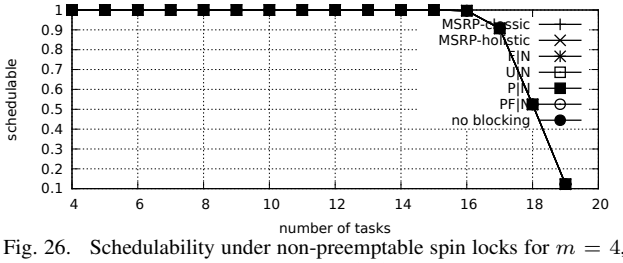

Fig. 26. Schedulability under non-preemptable spin locks for $m = 4$, $U = 0.2n$, 2 resources, $rsf = 0.1$, $N^{max} = 2$, and medium critical sections. The schedulability of the considered preemptable lock types in this configuration is shown in Fig. 36.

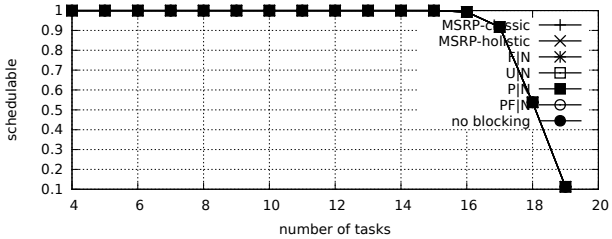

Fig. 27. Schedulability under non-preemptable spin locks for $m = 4$, $U = 0.2n$, 2 resources, $rsf = 0.1$, $N^{max} = 5$, and medium critical sections. The schedulability of the considered preemptable lock types in this configuration is shown in Fig. 37.

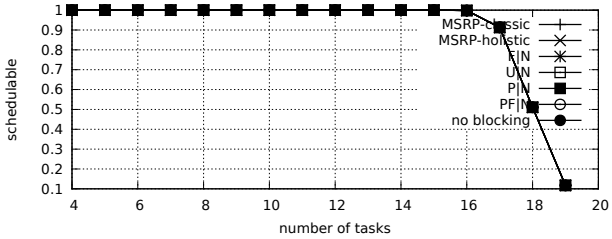

Fig. 28. Schedulability under non-preemptable spin locks for $m = 4$, $U = 0.2n$, 2 resources, $rsf = 0.1$, $N^{max} = 10$, and medium critical sections. The schedulability of the considered preemptable lock types in this configuration is shown in Fig. 38.

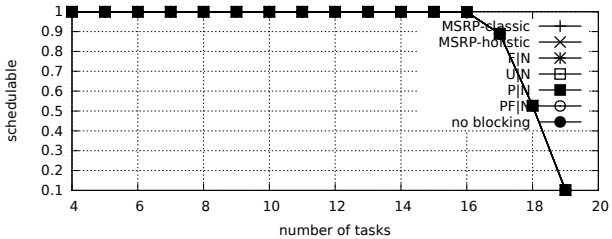

Fig. 29. Schedulability under non-preemptable spin locks for $m = 4$, $U = 0.2n$, 2 resources, $rsf = 0.1$, $N^{max} = 15$, and medium critical sections. The schedulability of the considered preemptable lock types in this configuration is shown in Fig. 39.

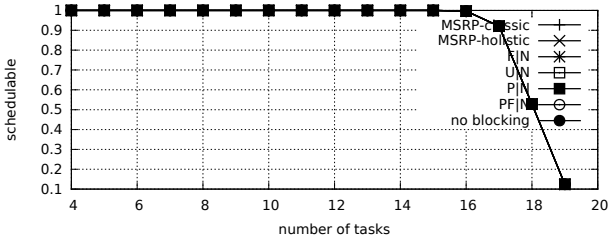

Fig. 30. Schedulability under non-preemptable spin locks for $m = 4$, $U = 0.2n$, 2 resources, $rsf = 0.1$, $N^{max} = 1$, and short critical sections. The schedulability of the considered preemptable lock types in this configuration is shown in Fig. 40.

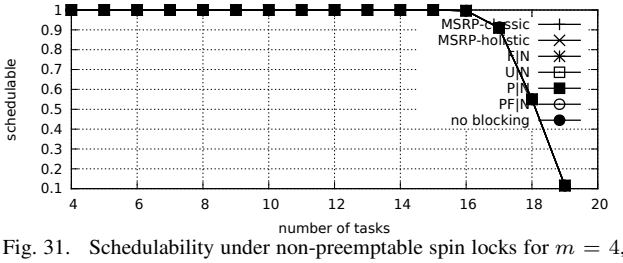

Fig. 31. Schedulability under non-preemptable spin locks for $m = 4$, $U = 0.2n$, 2 resources, $rsf = 0.1$, $N^{max} = 2$, and short critical sections. The schedulability of the considered preemptable lock types in this configuration is shown in Fig. 41.

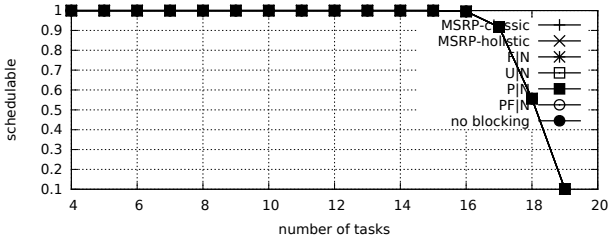

Fig. 32. Schedulability under non-preemptable spin locks for $m = 4$, $U = 0.2n$, 2 resources, $rsf = 0.1$, $N^{max} = 5$, and short critical sections. The schedulability of the considered preemptable lock types in this configuration is shown in Fig. 42.

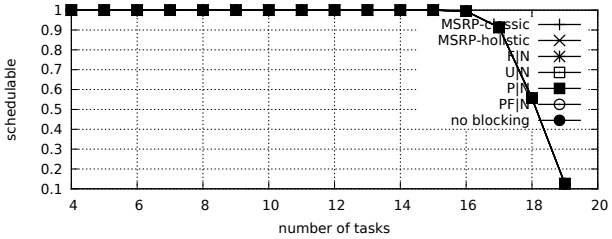

Fig. 33. Schedulability under non-preemptable spin locks for $m = 4$, $U = 0.2n$, 2 resources, $rsf = 0.1$, $N^{max} = 10$, and short critical sections. The schedulability of the considered preemptable lock types in this configuration is shown in Fig. 43.

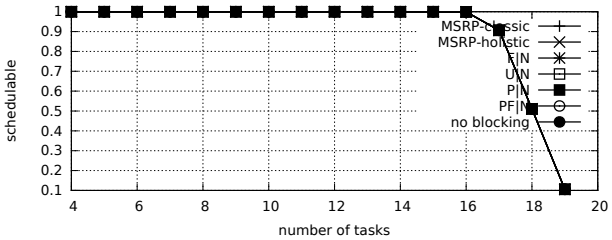

Fig. 34. Schedulability under non-preemptable spin locks for $m = 4$, $U = 0.2n$, 2 resources, $rsf = 0.1$, $N^{max} = 15$, and short critical sections. The schedulability of the considered preemptable lock types in this configuration is shown in Fig. 44.

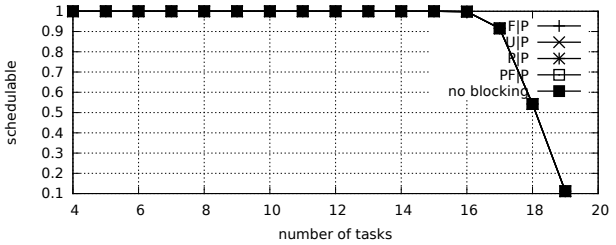

Fig. 35. Schedulability under preemptable spin locks for $m = 4$, $U = 0.2n$, 2 resources, $rsf = 0.1$, $N^{max} = 1$, and medium critical sections. The schedulability of the considered non-preemptable lock types in this configuration is shown in Fig. 25.

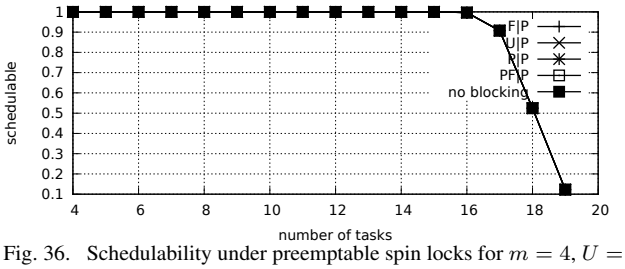

Fig. 36. Schedulability under preemptable spin locks for $m = 4$, $U = 0.2n$, 2 resources, $rsf = 0.1$, $N^{max} = 2$, and medium critical sections. The schedulability of the considered non-preemptable lock types in this configuration is shown in Fig. 26.

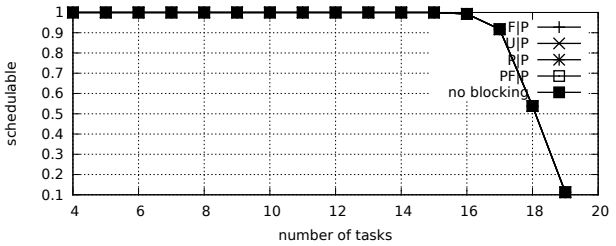

Fig. 37. Schedulability under preemptable spin locks for $m = 4$, $U = 0.2n$, 2 resources, $rsf = 0.1$, $N^{max} = 5$, and medium critical sections. The schedulability of the considered non-preemptable lock types in this configuration is shown in Fig. 27.

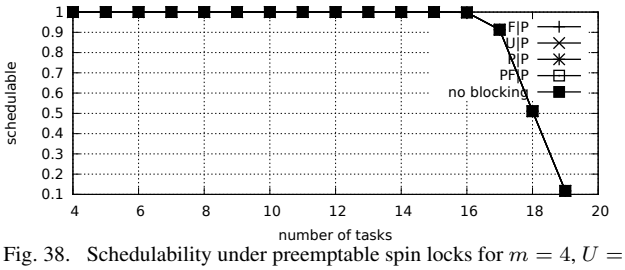

Fig. 38. Schedulability under preemptable spin locks for $m = 4$, $U = 0.2n$, 2 resources, $rsf = 0.1$, $N^{max} = 10$, and medium critical sections. The schedulability of the considered non-preemptable lock types in this configuration is shown in Fig. 28.

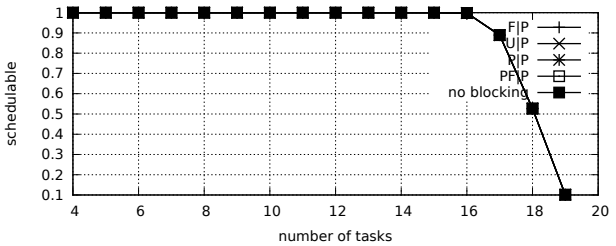

Fig. 39. Schedulability under preemptable spin locks for $m = 4$, $U = 0.2n$, 2 resources, $rsf = 0.1$, $N^{max} = 15$, and medium critical sections. The schedulability of the considered non-preemptable lock types in this configuration is shown in Fig. 29.

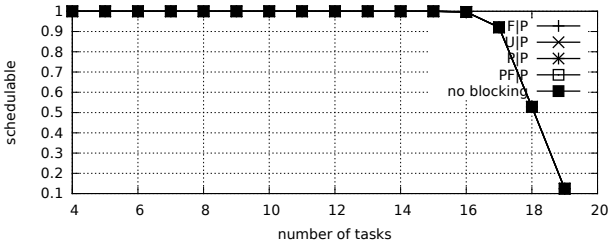

Fig. 40. Schedulability under preemptable spin locks for $m = 4$, $U = 0.2n$, 2 resources, $rsf = 0.1$, $N^{max} = 1$, and short critical sections. The schedulability of the considered non-preemptable lock types in this configuration is shown in Fig. 30.

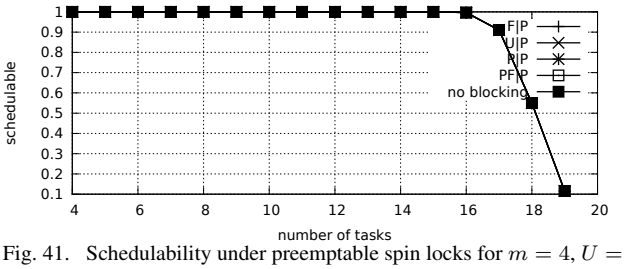

Fig. 41. Schedulability under preemptable spin locks for $m = 4$, $U = 0.2n$, 2 resources, $rsf = 0.1$, $N^{max} = 2$, and short critical sections. The schedulability of the considered non-preemptable lock types in this configuration is shown in Fig. 31.

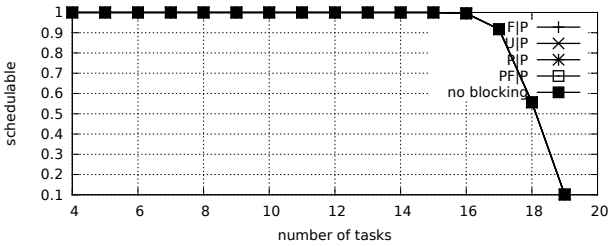

Fig. 42. Schedulability under preemptable spin locks for $m = 4$, $U = 0.2n$, 2 resources, $rsf = 0.1$, $N^{max} = 5$, and short critical sections. The schedulability of the considered non-preemptable lock types in this configuration is shown in Fig. 32.

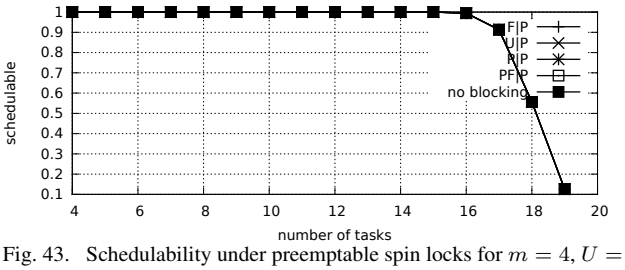

Fig. 43. Schedulability under preemptable spin locks for $m = 4$, $U = 0.2n$, 2 resources, $rsf = 0.1$, $N^{max} = 10$, and short critical sections. The schedulability of the considered non-preemptable lock types in this configuration is shown in Fig. 33.

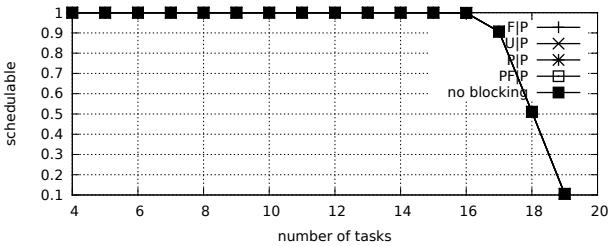

Fig. 44. Schedulability under preemptable spin locks for $m = 4$, $U = 0.2n$, 2 resources, $rsf = 0.1$, $N^{max} = 15$, and short critical sections. The schedulability of the considered non-preemptable lock types in this configuration is shown in Fig. 34.

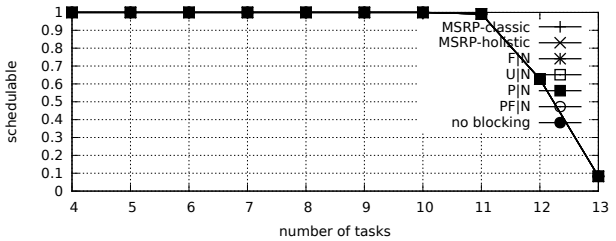

Fig. 45. Schedulability under non-preemptable spin locks for $m = 4$, $U = 0.3n$, 2 resources, $rsf = 0.1$, $N^{max} = 1$, and medium critical sections. The schedulability of the considered preemptable lock types in this configuration is shown in Fig. 55.

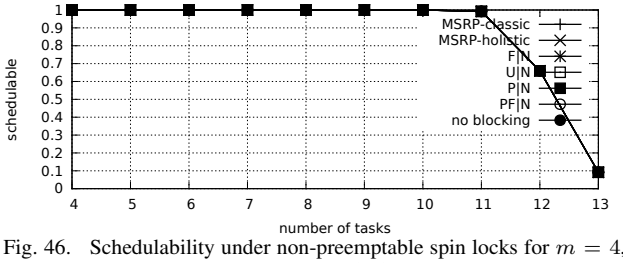

Fig. 46. Schedulability under non-preemptable spin locks for $m = 4$, $U = 0.3n$, 2 resources, $rsf = 0.1$, $N^{max} = 2$, and medium critical sections. The schedulability of the considered preemptable lock types in this configuration is shown in Fig. 56.

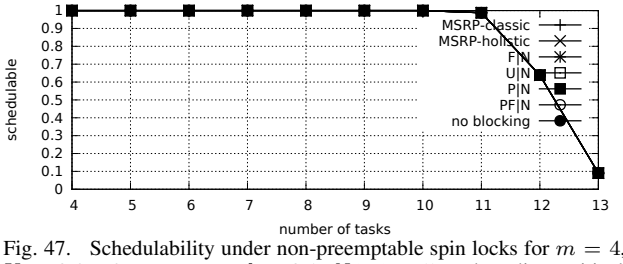

Fig. 47. Schedulability under non-preemptable spin locks for $m = 4$, $U = 0.3n$, 2 resources, $rsf = 0.1$, $N^{max} = 5$, and medium critical sections. The schedulability of the considered preemptable lock types in this configuration is shown in Fig. 57.

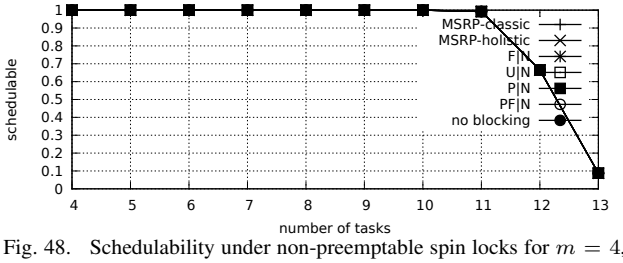

Fig. 48. Schedulability under non-preemptable spin locks for $m = 4$, $U = 0.3n$, 2 resources, $rsf = 0.1$, $N^{max} = 10$, and medium critical sections. The schedulability of the considered preemptable lock types in this configuration is shown in Fig. 58.

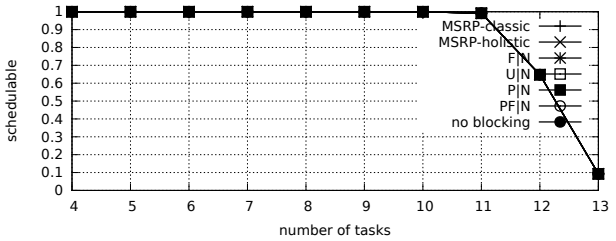

Fig. 49. Schedulability under non-preemptable spin locks for $m = 4$, $U = 0.3n$, 2 resources, $rsf = 0.1$, $N^{max} = 15$, and medium critical sections. The schedulability of the considered preemptable lock types in this configuration is shown in Fig. 59.

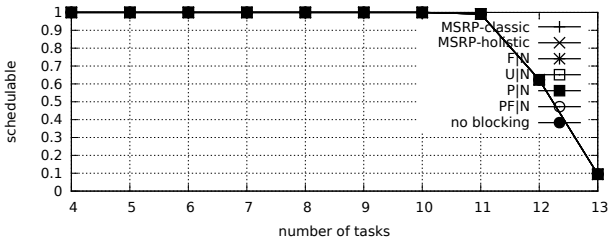

Fig. 50. Schedulability under non-preemptable spin locks for $m = 4$, $U = 0.3n$, 2 resources, $rsf = 0.1$, $N^{max} = 1$, and short critical sections. The schedulability of the considered preemptable lock types in this configuration is shown in Fig. 60.

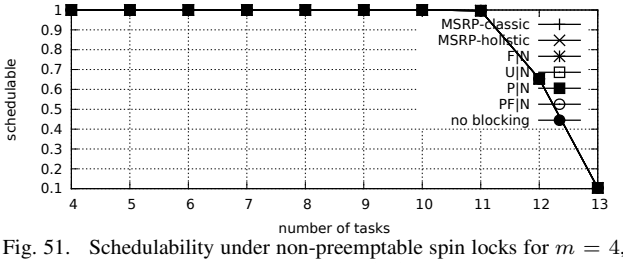

Fig. 51. Schedulability under non-preemptable spin locks for $m = 4$, $U = 0.3n$, 2 resources, $rsf = 0.1$, $N^{max} = 2$, and short critical sections. The schedulability of the considered preemptable lock types in this configuration is shown in Fig. 61.

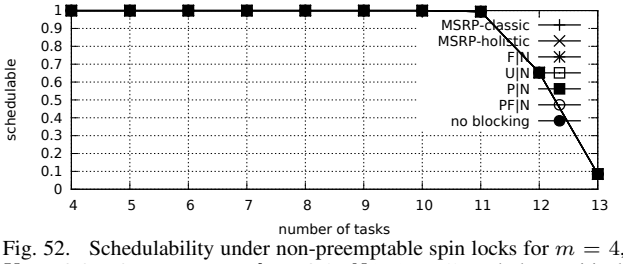

Fig. 52. Schedulability under non-preemptable spin locks for $m = 4$, $U = 0.3n$, 2 resources, $rsf = 0.1$, $N^{max} = 5$, and short critical sections. The schedulability of the considered preemptable lock types in this configuration is shown in Fig. 62.

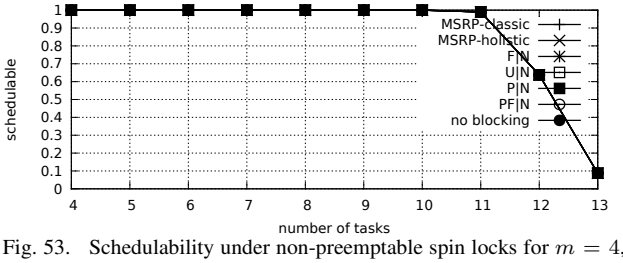

Fig. 53. Schedulability under non-preemptable spin locks for $m = 4$, $U = 0.3n$, 2 resources, $rsf = 0.1$, $N^{max} = 10$, and short critical sections. The schedulability of the considered preemptable lock types in this configuration is shown in Fig. 63.

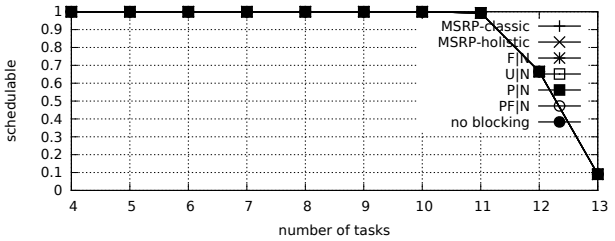

Fig. 54. Schedulability under non-preemptable spin locks for $m = 4$, $U = 0.3n$, 2 resources, $rsf = 0.1$, $N^{max} = 15$, and short critical sections. The schedulability of the considered preemptable lock types in this configuration is shown in Fig. 64.

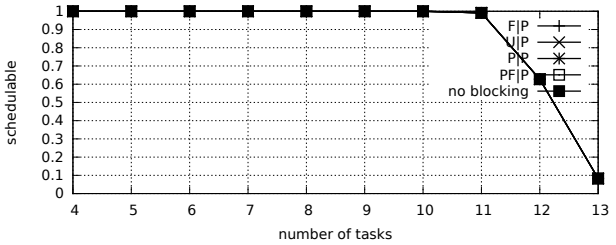

Fig. 55. Schedulability under preemptable spin locks for $m = 4$, $U = 0.3n$, 2 resources, $rsf = 0.1$, $N^{max} = 1$, and medium critical sections. The schedulability of the considered non-preemptable lock types in this configuration is shown in Fig. 45.

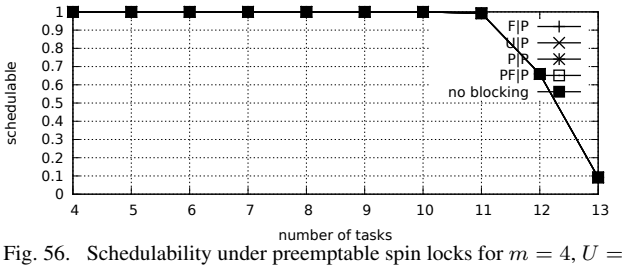

Fig. 56. Schedulability under preemptable spin locks for $m = 4$, $U = 0.3n$, 2 resources, $rsf = 0.1$, $N^{max} = 2$, and medium critical sections. The schedulability of the considered non-preemptable lock types in this configuration is shown in Fig. 46.

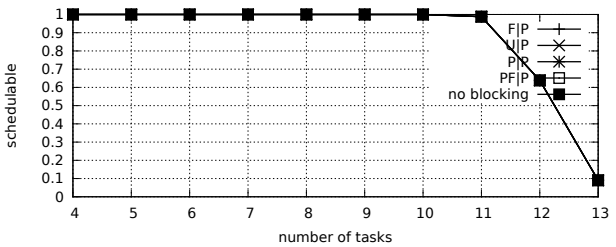

Fig. 57. Schedulability under preemptable spin locks for $m = 4$, $U = 0.3n$, 2 resources, $rsf = 0.1$, $N^{max} = 5$, and medium critical sections. The schedulability of the considered non-preemptable lock types in this configuration is shown in Fig. 47.

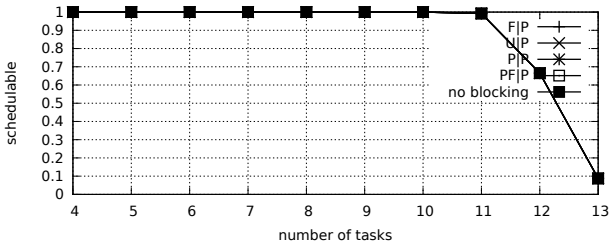

Fig. 58. Schedulability under preemptable spin locks for $m = 4$, $U = 0.3n$, 2 resources, $rsf = 0.1$, $N^{max} = 10$, and medium critical sections. The schedulability of the considered non-preemptable lock types in this configuration is shown in Fig. 48.

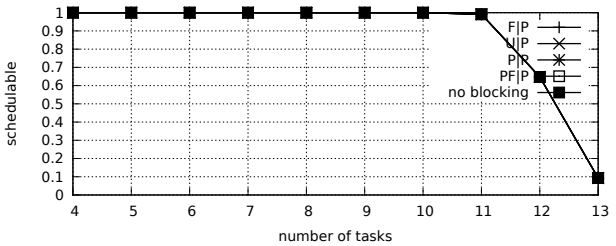

Fig. 59. Schedulability under preemptable spin locks for $m = 4$, $U = 0.3n$, 2 resources, $rsf = 0.1$, $N^{max} = 15$, and medium critical sections. The schedulability of the considered non-preemptable lock types in this configuration is shown in Fig. 49.

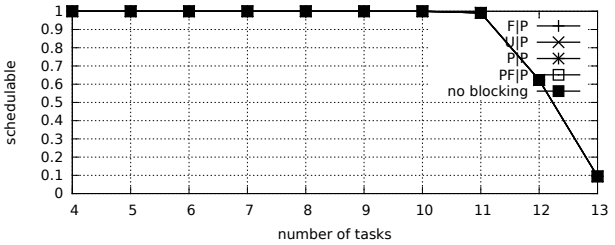

Fig. 60. Schedulability under preemptable spin locks for $m = 4$, $U = 0.3n$, 2 resources, $rsf = 0.1$, $N^{max} = 1$, and short critical sections. The schedulability of the considered non-preemptable lock types in this configuration is shown in Fig. 50.

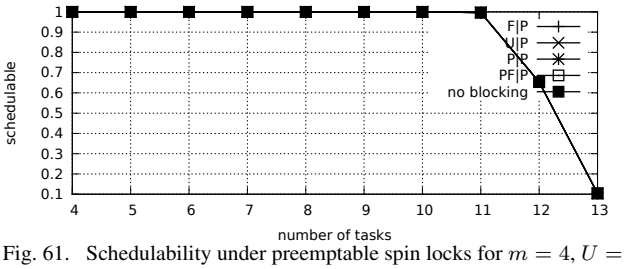

Fig. 61. Schedulability under preemptable spin locks for $m = 4$, $U = 0.3n$, 2 resources, $rsf = 0.1$, $N^{max} = 2$, and short critical sections. The schedulability of the considered non-preemptable lock types in this configuration is shown in Fig. 51.

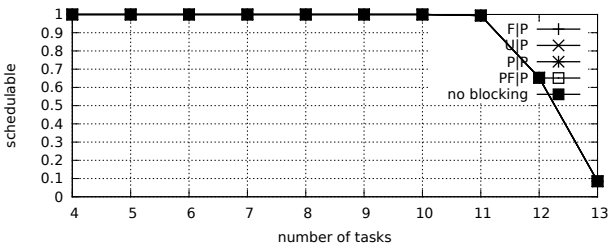

Fig. 62. Schedulability under preemptable spin locks for $m = 4$, $U = 0.3n$, 2 resources, $rsf = 0.1$, $N^{max} = 5$, and short critical sections. The schedulability of the considered non-preemptable lock types in this configuration is shown in Fig. 52.

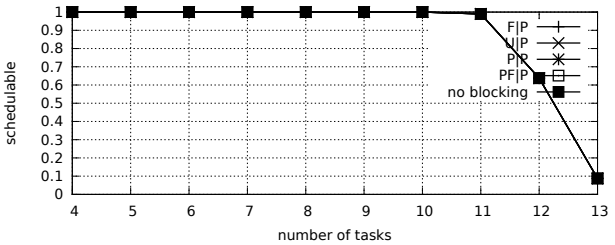

Fig. 63. Schedulability under preemptable spin locks for $m = 4$, $U = 0.3n$, 2 resources, $rsf = 0.1$, $N^{max} = 10$, and short critical sections. The schedulability of the considered non-preemptable lock types in this configuration is shown in Fig. 53.

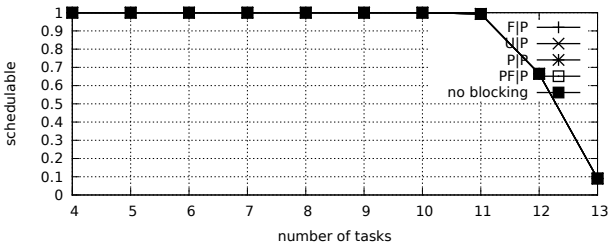

Fig. 64. Schedulability under preemptable spin locks for $m = 4$, $U = 0.3n$, 2 resources, $rsf = 0.1$, $N^{max} = 15$, and short critical sections. The schedulability of the considered non-preemptable lock types in this configuration is shown in Fig. 54.

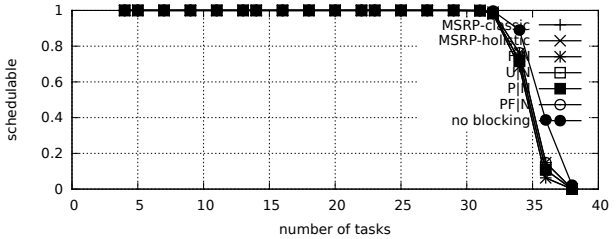

Fig. 65. Schedulability under non-preemptable spin locks for $m = 4$, $U = 0.1n$, 2 resources, $rsf = 0.25$, $N^{max} = 1$, and medium critical sections. The schedulability of the considered preemptable lock types in this configuration is shown in Fig. 75.

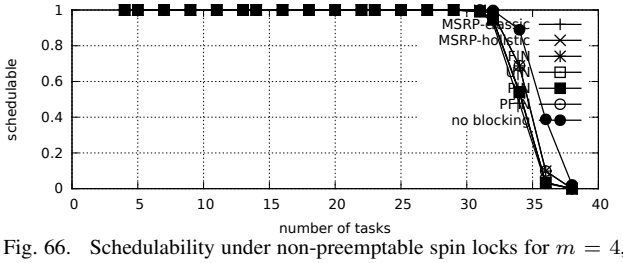

Fig. 66. Schedulability under non-preemptable spin locks for $m = 4$, $U = 0.1n$, 2 resources, $rsf = 0.25$, $N^{max} = 2$, and medium critical sections. The schedulability of the considered preemptable lock types in this configuration is shown in Fig. 76.

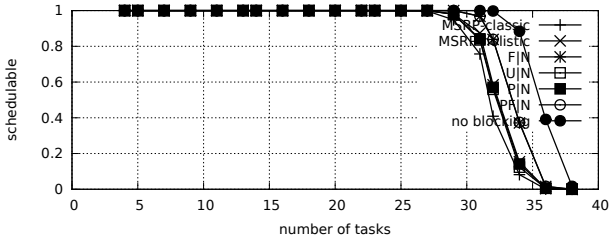

Fig. 67. Schedulability under non-preemptable spin locks for $m = 4$, $U = 0.1n$, 2 resources, $rsf = 0.25$, $N^{max} = 5$, and medium critical sections. The schedulability of the considered preemptable lock types in this configuration is shown in Fig. 77.

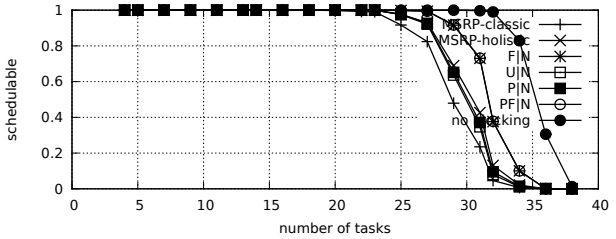

Fig. 68. Schedulability under non-preemptable spin locks for $m = 4$, $U = 0.1n$, 2 resources, $rsf = 0.25$, $N^{max} = 10$, and medium critical sections. The schedulability of the considered preemptable lock types in this configuration is shown in Fig. 78.

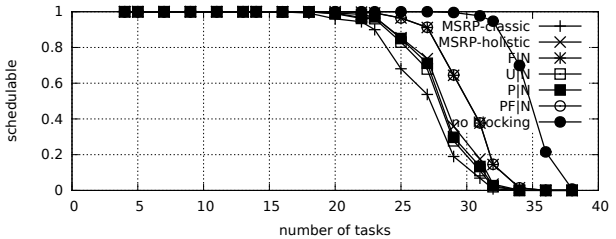

Fig. 69. Schedulability under non-preemptable spin locks for $m = 4$, $U = 0.1n$, 2 resources, $rsf = 0.25$, $N^{max} = 15$, and medium critical sections. The schedulability of the considered preemptable lock types in this configuration is shown in Fig. 79.

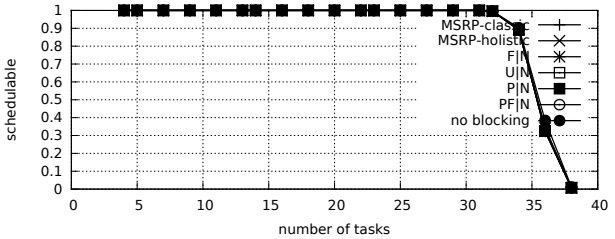

Fig. 70. Schedulability under non-preemptable spin locks for $m = 4$, $U = 0.1n$, 2 resources, $rsf = 0.25$, $N^{max} = 1$, and short critical sections. The schedulability of the considered preemptable lock types in this configuration is shown in Fig. 80.

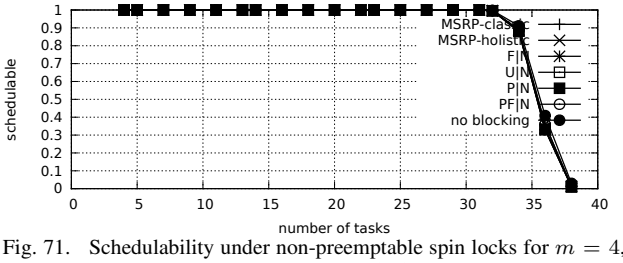

Fig. 71. Schedulability under non-preemptable spin locks for $m = 4$, $U = 0.1n$, 2 resources, $rsf = 0.25$, $N^{max} = 2$, and short critical sections. The schedulability of the considered preemptable lock types in this configuration is shown in Fig. 81.

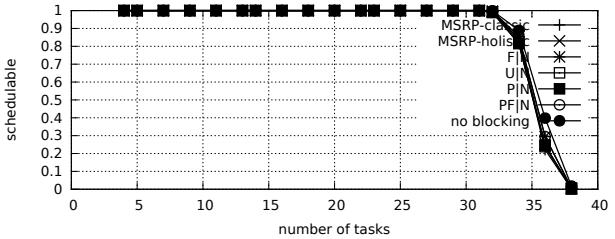

Fig. 72. Schedulability under non-preemptable spin locks for $m = 4$, $U = 0.1n$, 2 resources, $rsf = 0.25$, $N^{max} = 5$, and short critical sections. The schedulability of the considered preemptable lock types in this configuration is shown in Fig. 82.

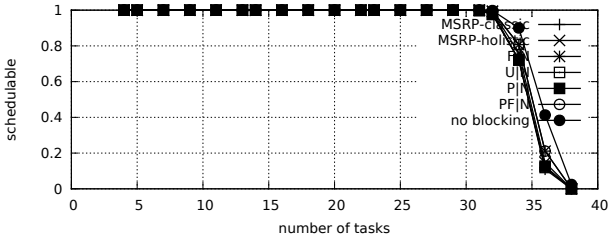

Fig. 73. Schedulability under non-preemptable spin locks for $m = 4$, $U = 0.1n$, 2 resources, $rsf = 0.25$, $N^{max} = 10$, and short critical sections. The schedulability of the considered preemptable lock types in this configuration is shown in Fig. 83.

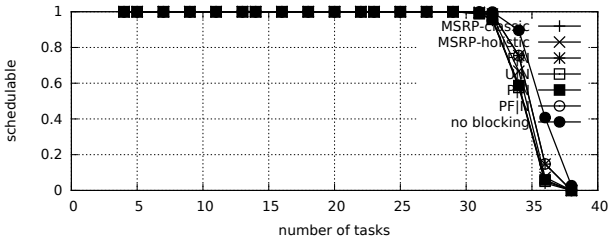

Fig. 74. Schedulability under non-preemptable spin locks for $m = 4$, $U = 0.1n$, 2 resources, $rsf = 0.25$, $N^{max} = 15$, and short critical sections. The schedulability of the considered preemptable lock types in this configuration is shown in Fig. 84.

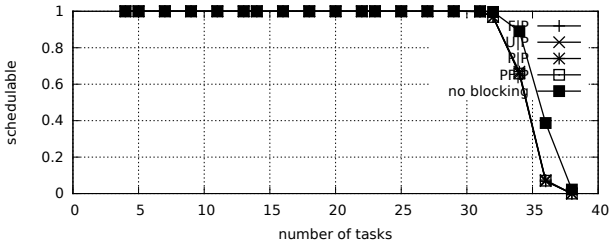

Fig. 75. Schedulability under preemptable spin locks for $m = 4$, $U = 0.1n$, 2 resources, $rsf = 0.25$, $N^{max} = 1$, and medium critical sections. The schedulability of the considered non-preemptable lock types in this configuration is shown in Fig. 65.

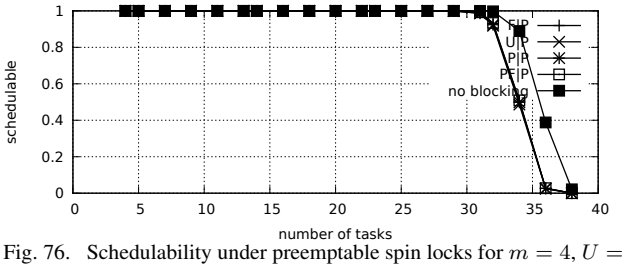

Fig. 76. Schedulability under preemptable spin locks for $m = 4$, $U = 0.1n$, 2 resources, $rsf = 0.25$, $N^{max} = 2$, and medium critical sections. The schedulability of the considered non-preemptable lock types in this configuration is shown in Fig. 66.

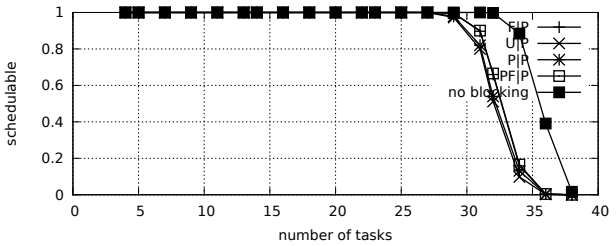

Fig. 77. Schedulability under preemptable spin locks for $m = 4$, $U = 0.1n$, 2 resources, $rsf = 0.25$, $N^{max} = 5$, and medium critical sections. The schedulability of the considered non-preemptable lock types in this configuration is shown in Fig. 67.

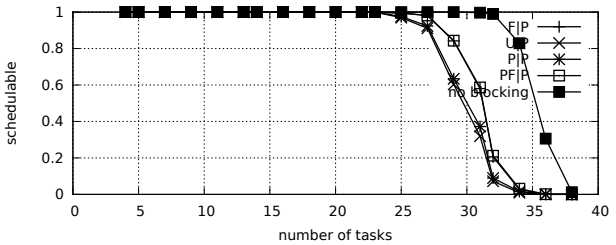

Fig. 78. Schedulability under preemptable spin locks for $m = 4$, $U = 0.1n$, 2 resources, $rsf = 0.25$, $N^{max} = 10$, and medium critical sections. The schedulability of the considered non-preemptable lock types in this configuration is shown in Fig. 68.

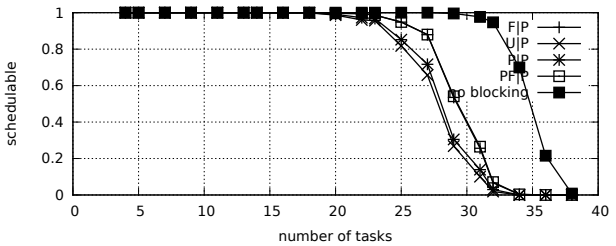

Fig. 79. Schedulability under preemptable spin locks for $m = 4$, $U = 0.1n$, 2 resources, $rsf = 0.25$, $N^{max} = 15$, and medium critical sections. The schedulability of the considered non-preemptable lock types in this configuration is shown in Fig. 69.

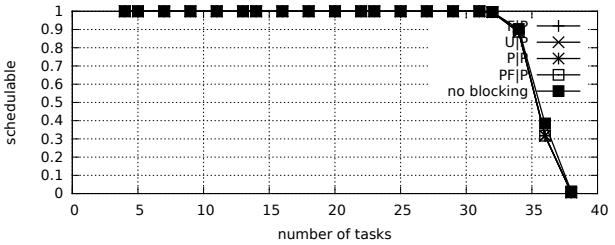

Fig. 80. Schedulability under preemptable spin locks for $m = 4$, $U = 0.1n$, 2 resources, $rsf = 0.25$, $N^{max} = 1$, and short critical sections. The schedulability of the considered non-preemptable lock types in this configuration is shown in Fig. 70.

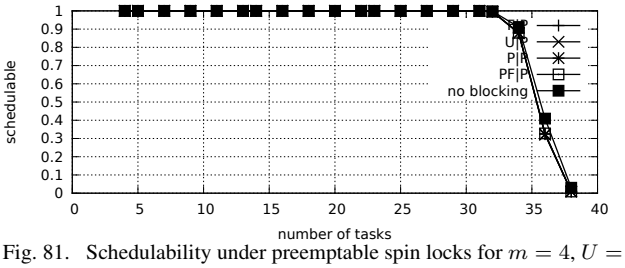

Fig. 81. Schedulability under preemptable spin locks for $m = 4$, $U = 0.1n$, 2 resources, $rsf = 0.25$, $N^{max} = 2$, and short critical sections. The schedulability of the considered non-preemptable lock types in this configuration is shown in Fig. 71.

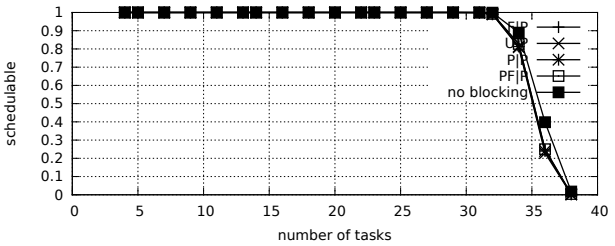

Fig. 82. Schedulability under preemptable spin locks for $m = 4$, $U = 0.1n$, 2 resources, $rsf = 0.25$, $N^{max} = 5$, and short critical sections. The schedulability of the considered non-preemptable lock types in this configuration is shown in Fig. 72.

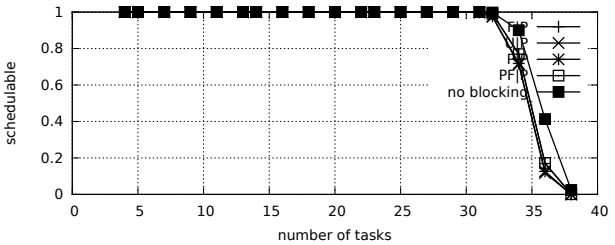

Fig. 83. Schedulability under preemptable spin locks for $m = 4$, $U = 0.1n$, 2 resources, $rsf = 0.25$, $N^{max} = 10$, and short critical sections. The schedulability of the considered non-preemptable lock types in this configuration is shown in Fig. 73.

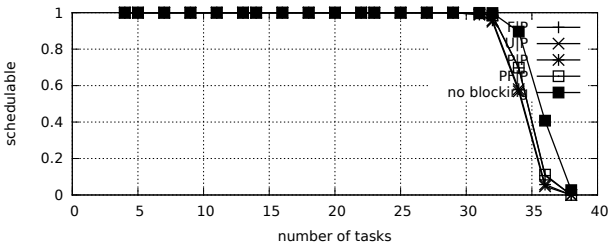

Fig. 84. Schedulability under preemptable spin locks for $m = 4$, $U = 0.1n$, 2 resources, $rsf = 0.25$, $N^{max} = 15$, and short critical sections. The schedulability of the considered non-preemptable lock types in this configuration is shown in Fig. 74.

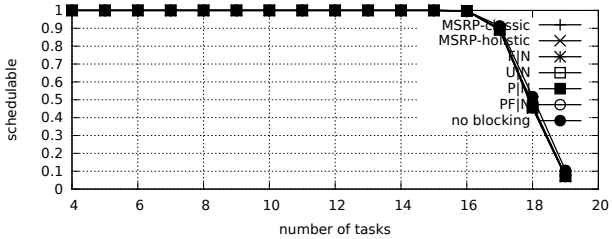

Fig. 85. Schedulability under non-preemptable spin locks for $m = 4$, $U = 0.2n$, 2 resources, $rsf = 0.25$, $N^{max} = 1$, and medium critical sections. The schedulability of the considered preemptable lock types in this configuration is shown in Fig. 95.

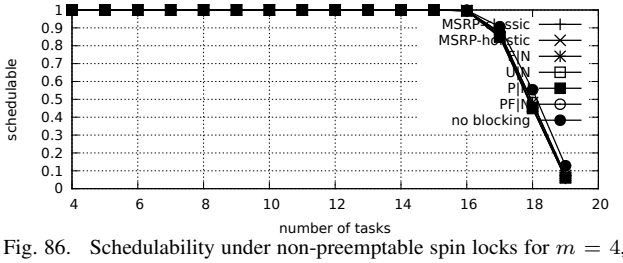

Fig. 86. Schedulability under non-preemptable spin locks for $m = 4$, $U = 0.2n$, 2 resources, $rsf = 0.25$, $N^{max} = 2$, and medium critical sections. The schedulability of the considered preemptable lock types in this configuration is shown in Fig. 96.

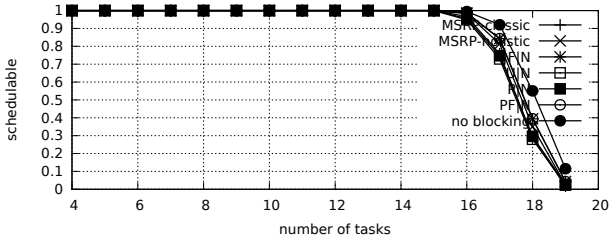

Fig. 87. Schedulability under non-preemptable spin locks for $m = 4$, $U = 0.2n$, 2 resources, $rsf = 0.25$, $N^{max} = 5$, and medium critical sections. The schedulability of the considered preemptable lock types in this configuration is shown in Fig. 97.

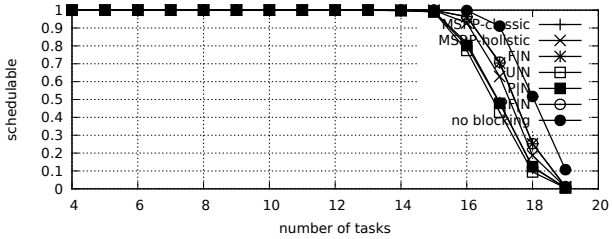

Fig. 88. Schedulability under non-preemptable spin locks for $m = 4$, $U = 0.2n$, 2 resources, $rsf = 0.25$, $N^{max} = 10$, and medium critical sections. The schedulability of the considered preemptable lock types in this configuration is shown in Fig. 98.

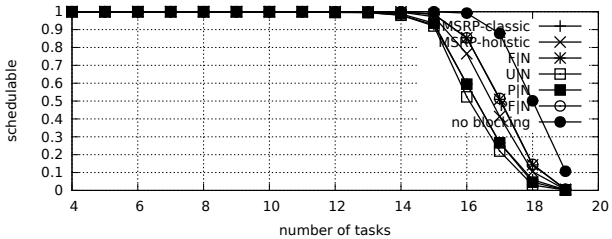

Fig. 89. Schedulability under non-preemptable spin locks for $m = 4$, $U = 0.2n$, 2 resources, $rsf = 0.25$, $N^{max} = 15$, and medium critical sections. The schedulability of the considered preemptable lock types in this configuration is shown in Fig. 99.

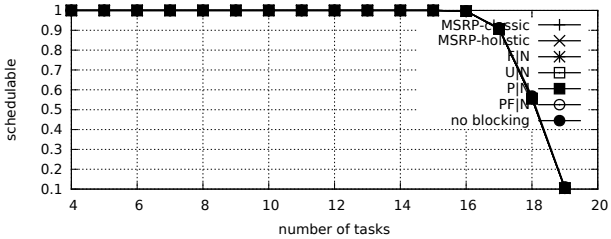

Fig. 90. Schedulability under non-preemptable spin locks for $m = 4$, $U = 0.2n$, 2 resources, $rsf = 0.25$, $N^{max} = 1$, and short critical sections. The schedulability of the considered preemptable lock types in this configuration is shown in Fig. 100.

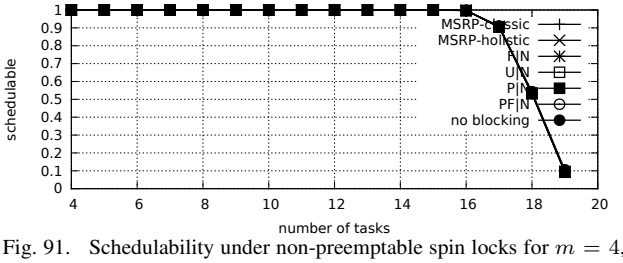

Fig. 91. Schedulability under non-preemptable spin locks for $m = 4$, $U = 0.2n$, 2 resources, $rsf = 0.25$, $N^{max} = 2$, and short critical sections. The schedulability of the considered preemptable lock types in this configuration is shown in Fig. 101.

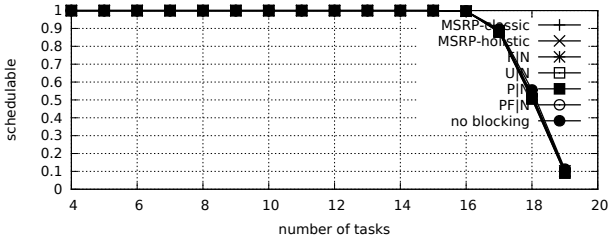

Fig. 92. Schedulability under non-preemptable spin locks for $m = 4$, $U = 0.2n$, 2 resources, $rsf = 0.25$, $N^{max} = 5$, and short critical sections. The schedulability of the considered preemptable lock types in this configuration is shown in Fig. 102.

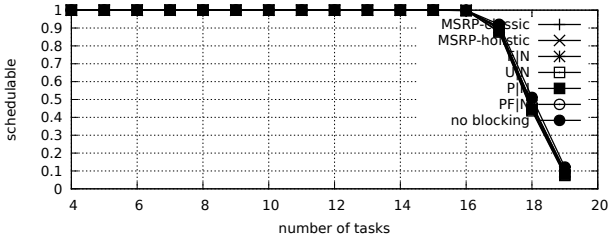

Fig. 93. Schedulability under non-preemptable spin locks for $m = 4$, $U = 0.2n$, 2 resources, $rsf = 0.25$, $N^{max} = 10$, and short critical sections. The schedulability of the considered preemptable lock types in this configuration is shown in Fig. 103.

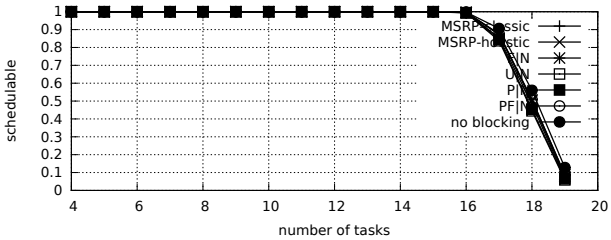

Fig. 94. Schedulability under non-preemptable spin locks for $m = 4$, $U = 0.2n$, 2 resources, $rsf = 0.25$, $N^{max} = 15$, and short critical sections. The schedulability of the considered preemptable lock types in this configuration is shown in Fig. 104.

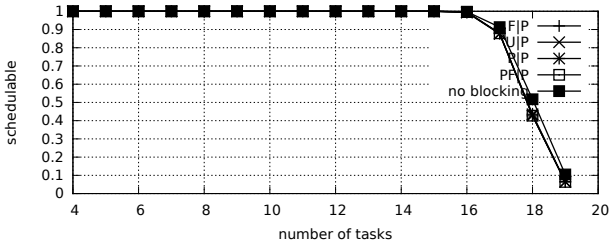

Fig. 95. Schedulability under preemptable spin locks for $m = 4$, $U = 0.2n$, 2 resources, $rsf = 0.25$, $N^{max} = 1$, and medium critical sections. The schedulability of the considered non-preemptable lock types in this configuration is shown in Fig. 85.

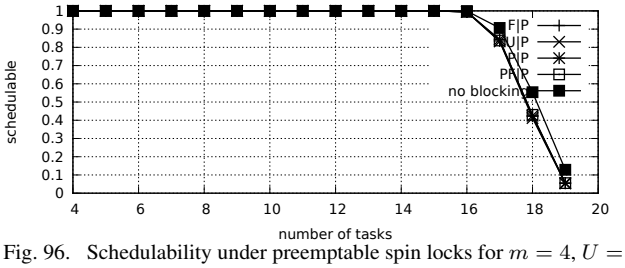

Fig. 96. Schedulability under preemptable spin locks for $m = 4$, $U = 0.2n$, 2 resources, $rsf = 0.25$, $N^{max} = 2$, and medium critical sections. The schedulability of the considered non-preemptable lock types in this configuration is shown in Fig. 86.

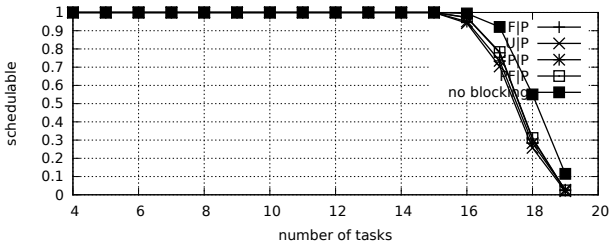

Fig. 97. Schedulability under preemptable spin locks for $m = 4$, $U = 0.2n$, 2 resources, $rsf = 0.25$, $N^{max} = 5$, and medium critical sections. The schedulability of the considered non-preemptable lock types in this configuration is shown in Fig. 87.

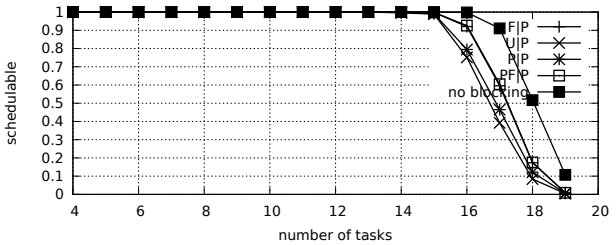

Fig. 98. Schedulability under preemptable spin locks for $m = 4$, $U = 0.2n$, 2 resources, $rsf = 0.25$, $N^{max} = 10$, and medium critical sections. The schedulability of the considered non-preemptable lock types in this configuration is shown in Fig. 88.

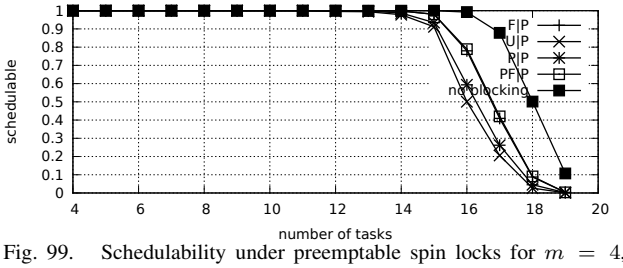

Fig. 99. Schedulability under preemptable spin locks for $m = 4$, $U = 0.2n$, 2 resources, $rsf = 0.25$, $N^{max} = 15$, and medium critical sections. The schedulability of the considered non-preemptable lock types in this configuration is shown in Fig. 89.

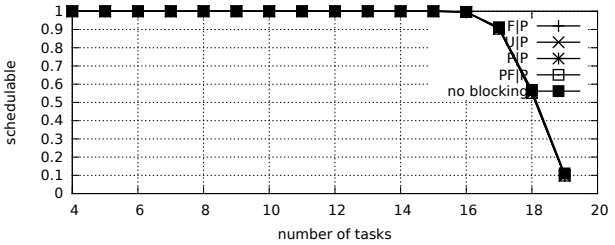

Fig. 100. Schedulability under preemptable spin locks for $m = 4$, $U = 0.2n$, 2 resources, $rsf = 0.25$, $N^{max} = 1$, and short critical sections. The schedulability of the considered non-preemptable lock types in this configuration is shown in Fig. 90.

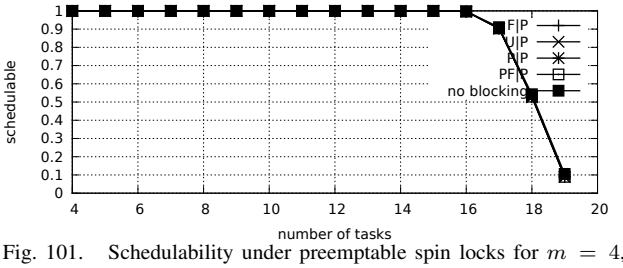

Fig. 101. Schedulability under preemptable spin locks for $m = 4$, $U = 0.2n$, 2 resources, $rsf = 0.25$, $N^{max} = 2$, and short critical sections. The schedulability of the considered non-preemptable lock types in this configuration is shown in Fig. 91.

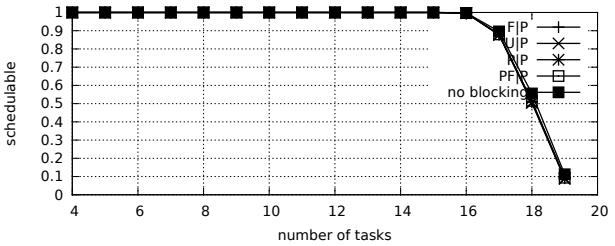

Fig. 102. Schedulability under preemptable spin locks for $m = 4$, $U = 0.2n$, 2 resources, $rsf = 0.25$, $N^{max} = 5$, and short critical sections. The schedulability of the considered non-preemptable lock types in this configuration is shown in Fig. 92.

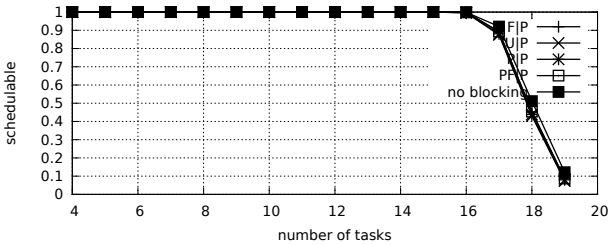

Fig. 103. Schedulability under preemptable spin locks for $m = 4$, $U = 0.2n$, 2 resources, $rsf = 0.25$, $N^{max} = 10$, and short critical sections. The schedulability of the considered non-preemptable lock types in this configuration is shown in Fig. 93.

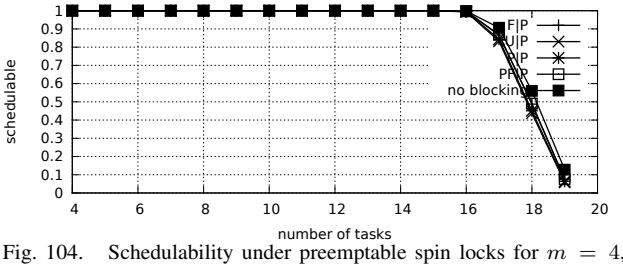

Fig. 104. Schedulability under preemptable spin locks for $m = 4$, $U = 0.2n$, 2 resources, $rsf = 0.25$, $N^{max} = 15$, and short critical sections. The schedulability of the considered non-preemptable lock types in this configuration is shown in Fig. 94.

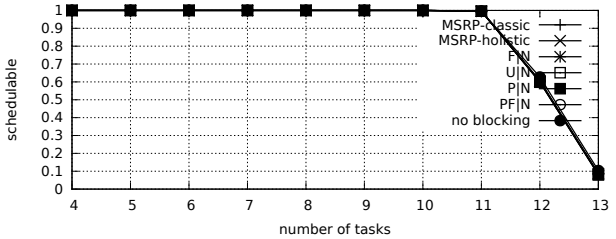

Fig. 105. Schedulability under non-preemptable spin locks for $m = 4$, $U = 0.3n$, 2 resources, $rsf = 0.25$, $N^{max} = 1$, and medium critical sections. The schedulability of the considered preemptable lock types in this configuration is shown in Fig. 115.

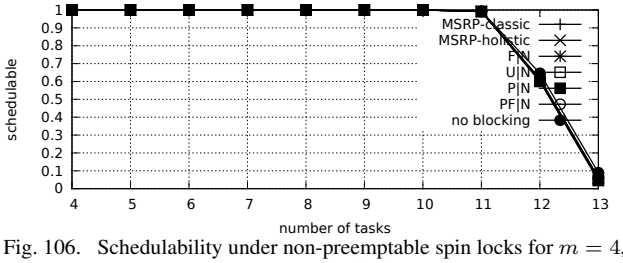

Fig. 106. Schedulability under non-preemptable spin locks for $m = 4$, $U = 0.3n$, 2 resources, $rsf = 0.25$, $N^{max} = 2$, and medium critical sections. The schedulability of the considered preemptable lock types in this configuration is shown in Fig. 116.

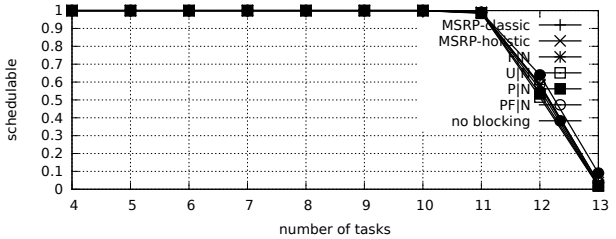

Fig. 107. Schedulability under non-preemptable spin locks for $m = 4$, $U = 0.3n$, 2 resources, $rsf = 0.25$, $N^{max} = 5$, and medium critical sections. The schedulability of the considered preemptable lock types in this configuration is shown in Fig. 117.

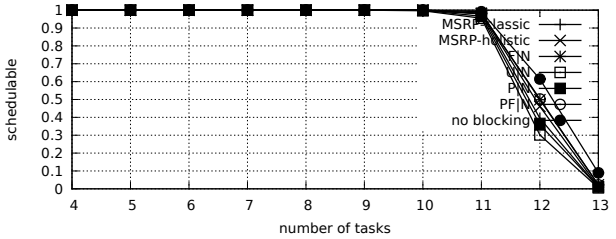

Fig. 108. Schedulability under non-preemptable spin locks for $m = 4$, $U = 0.3n$, 2 resources, $rsf = 0.25$, $N^{max} = 10$, and medium critical sections. The schedulability of the considered preemptable lock types in this configuration is shown in Fig. 118.

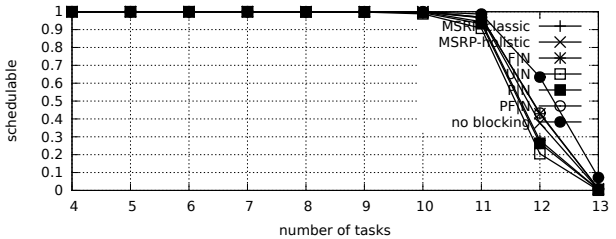

Fig. 109. Schedulability under non-preemptable spin locks for $m = 4$, $U = 0.3n$, 2 resources, $rsf = 0.25$, $N^{max} = 15$, and medium critical sections. The schedulability of the considered preemptable lock types in this configuration is shown in Fig. 119.

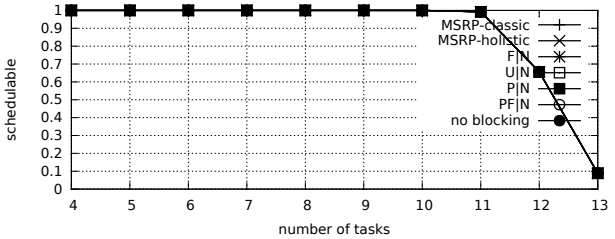

Fig. 110. Schedulability under non-preemptable spin locks for $m = 4$, $U = 0.3n$, 2 resources, $rsf = 0.25$, $N^{max} = 1$, and short critical sections. The schedulability of the considered preemptable lock types in this configuration is shown in Fig. 120.

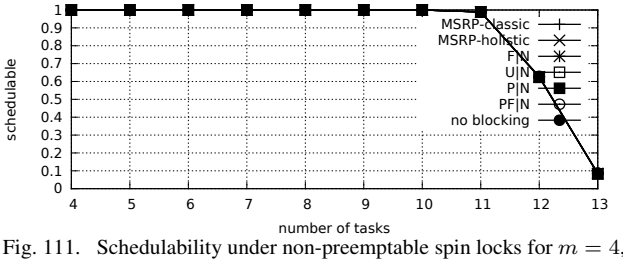

Fig. 111. Schedulability under non-preemptable spin locks for $m = 4$, $U = 0.3n$, 2 resources, $rsf = 0.25$, $N^{max} = 2$, and short critical sections. The schedulability of the considered preemptable lock types in this configuration is shown in Fig. 121.

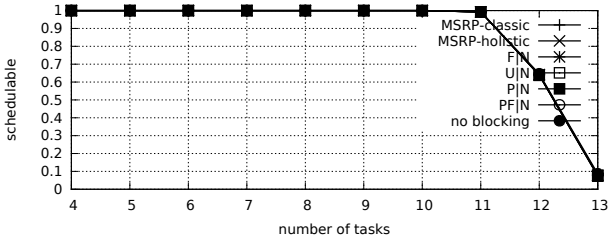

Fig. 112. Schedulability under non-preemptable spin locks for $m = 4$, $U = 0.3n$, 2 resources, $rsf = 0.25$, $N^{max} = 5$, and short critical sections. The schedulability of the considered preemptable lock types in this configuration is shown in Fig. 122.

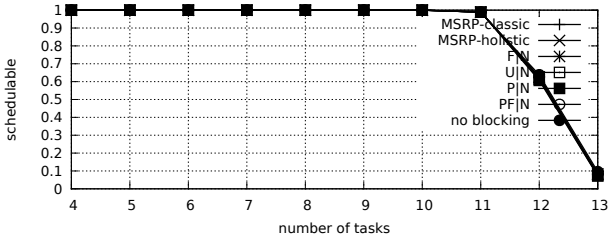

Fig. 113. Schedulability under non-preemptable spin locks for $m = 4$, $U = 0.3n$, 2 resources, $rsf = 0.25$, $N^{max} = 10$, and short critical sections. The schedulability of the considered preemptable lock types in this configuration is shown in Fig. 123.

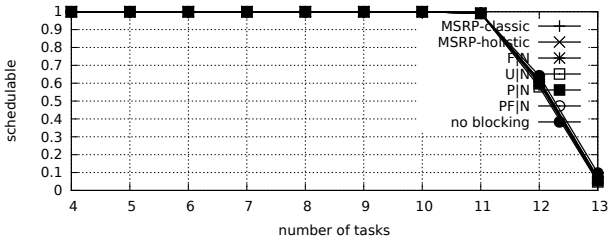

Fig. 114. Schedulability under non-preemptable spin locks for $m = 4$, $U = 0.3n$, 2 resources, $rsf = 0.25$, $N^{max} = 15$, and short critical sections. The schedulability of the considered preemptable lock types in this configuration is shown in Fig. 124.

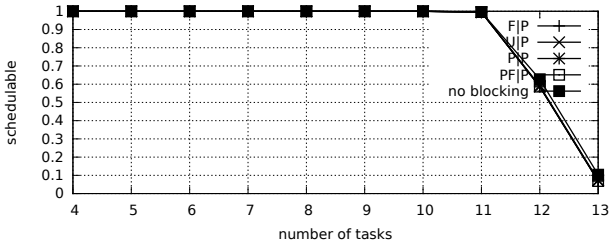

Fig. 115. Schedulability under preemptable spin locks for $m = 4$, $U = 0.3n$, 2 resources, $rsf = 0.25$, $N^{max} = 1$, and medium critical sections. The schedulability of the considered non-preemptable lock types in this configuration is shown in Fig. 105.

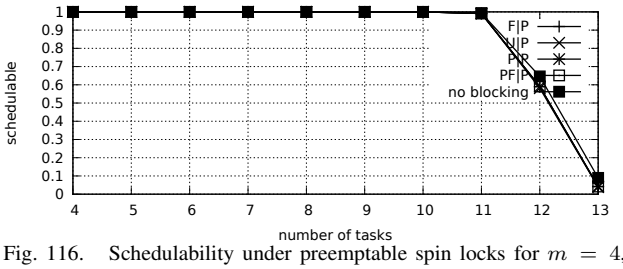

Fig. 116. Schedulability under preemptable spin locks for $m = 4$, $U = 0.3n$, 2 resources, $rsf = 0.25$, $N^{max} = 2$, and medium critical sections. The schedulability of the considered non-preemptable lock types in this configuration is shown in Fig. 106.

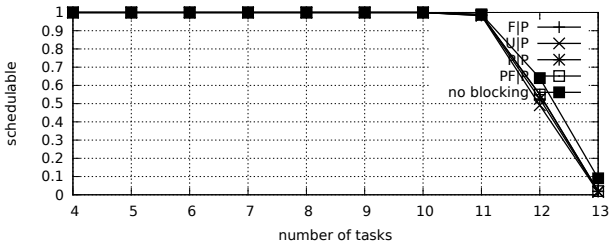

Fig. 117. Schedulability under preemptable spin locks for $m = 4$, $U = 0.3n$, 2 resources, $rsf = 0.25$, $N^{max} = 5$, and medium critical sections. The schedulability of the considered non-preemptable lock types in this configuration is shown in Fig. 107.

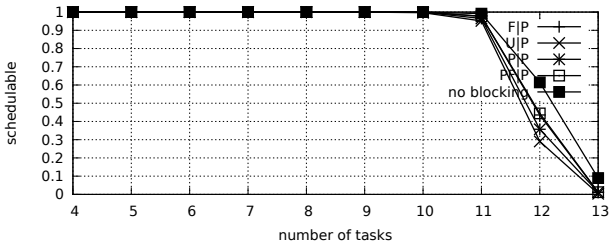

Fig. 118. Schedulability under preemptable spin locks for $m = 4$, $U = 0.3n$, 2 resources, $rsf = 0.25$, $N^{max} = 10$, and medium critical sections. The schedulability of the considered non-preemptable lock types in this configuration is shown in Fig. 108.

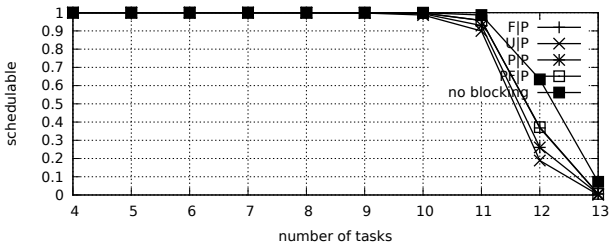

Fig. 119. Schedulability under preemptable spin locks for $m = 4$, $U = 0.3n$, 2 resources, $rsf = 0.25$, $N^{max} = 15$, and medium critical sections. The schedulability of the considered non-preemptable lock types in this configuration is shown in Fig. 109.

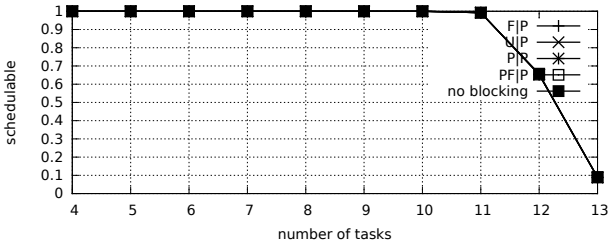

Fig. 120. Schedulability under preemptable spin locks for $m = 4$, $U = 0.3n$, 2 resources, $rsf = 0.25$, $N^{max} = 1$, and short critical sections. The schedulability of the considered non-preemptable lock types in this configuration is shown in Fig. 110.

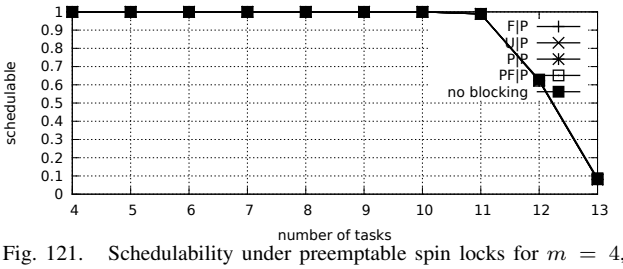

Fig. 121. Schedulability under preemptable spin locks for $m = 4$, $U = 0.3n$, 2 resources, $rsf = 0.25$, $N^{max} = 2$, and short critical sections. The schedulability of the considered non-preemptable lock types in this configuration is shown in Fig. 111.

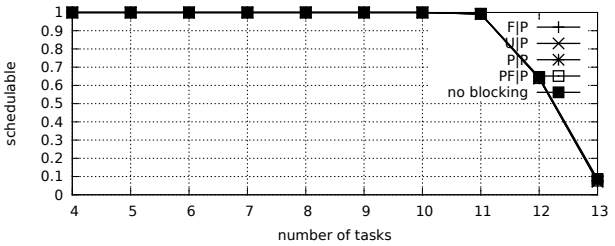

Fig. 122. Schedulability under preemptable spin locks for $m = 4$, $U = 0.3n$, 2 resources, $rsf = 0.25$, $N^{max} = 5$, and short critical sections. The schedulability of the considered non-preemptable lock types in this configuration is shown in Fig. 112.

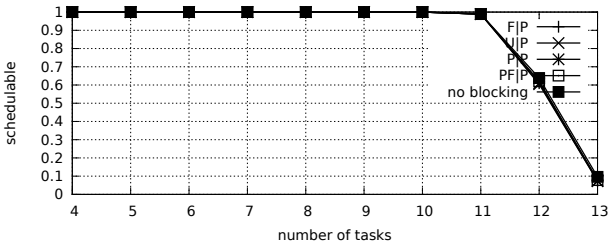

Fig. 123. Schedulability under preemptable spin locks for $m = 4$, $U = 0.3n$, 2 resources, $rsf = 0.25$, $N^{max} = 10$, and short critical sections. The schedulability of the considered non-preemptable lock types in this configuration is shown in Fig. 113.

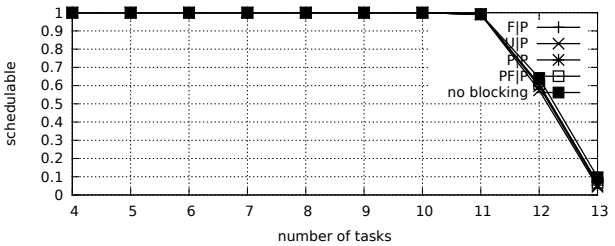

Fig. 124. Schedulability under preemptable spin locks for $m = 4$, $U = 0.3n$, 2 resources, $rsf = 0.25$, $N^{max} = 15$, and short critical sections. The schedulability of the considered non-preemptable lock types in this configuration is shown in Fig. 114.

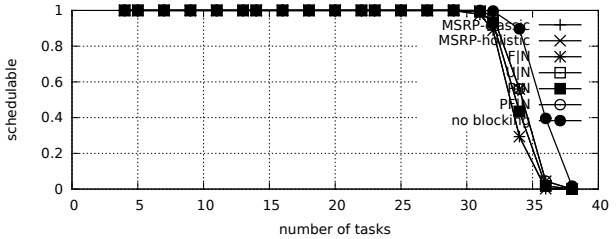

Fig. 125. Schedulability under non-preemptable spin locks for $m = 4$, $U = 0.1n$, 2 resources, $rsf = 0.4$, $N^{max} = 1$, and medium critical sections. The schedulability of the considered preemptable lock types in this configuration is shown in Fig. 135.

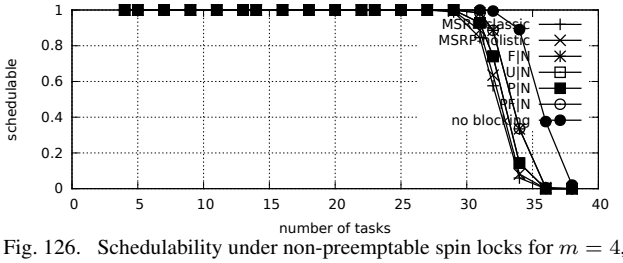

Fig. 126. Schedulability under non-preemptable spin locks for $m = 4$, $U = 0.1n$, 2 resources, $rsf = 0.4$, $N^{max} = 2$, and medium critical sections. The schedulability of the considered preemptable lock types in this configuration is shown in Fig. 136.

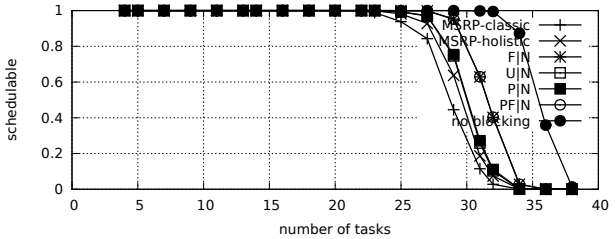

Fig. 127. Schedulability under non-preemptable spin locks for $m = 4$, $U = 0.1n$, 2 resources, $rsf = 0.4$, $N^{max} = 5$, and medium critical sections. The schedulability of the considered preemptable lock types in this configuration is shown in Fig. 137.

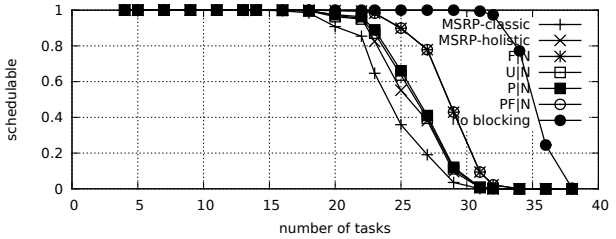

Fig. 128. Schedulability under non-preemptable spin locks for $m = 4$, $U = 0.1n$, 2 resources, $rsf = 0.4$, $N^{max} = 10$, and medium critical sections. The schedulability of the considered preemptable lock types in this configuration is shown in Fig. 138.

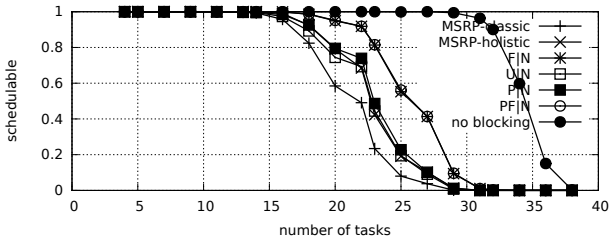

Fig. 129. Schedulability under non-preemptable spin locks for $m = 4$, $U = 0.1n$, 2 resources, $rsf = 0.4$, $N^{max} = 15$, and medium critical sections. The schedulability of the considered preemptable lock types in this configuration is shown in Fig. 139.

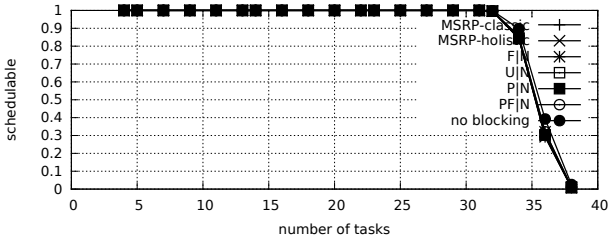

Fig. 130. Schedulability under non-preemptable spin locks for $m = 4$, $U = 0.1n$, 2 resources, $rsf = 0.4$, $N^{max} = 1$, and short critical sections. The schedulability of the considered preemptable lock types in this configuration is shown in Fig. 140.

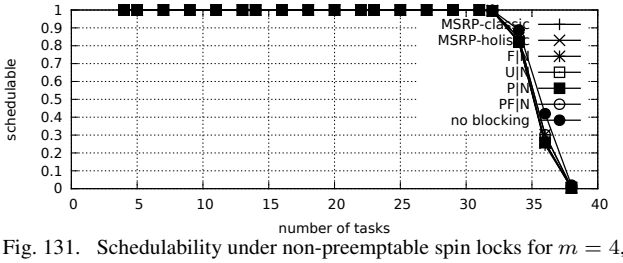

Fig. 131. Schedulability under non-preemptable spin locks for $m = 4$, $U = 0.1n$, 2 resources, $rsf = 0.4$, $N^{max} = 2$, and short critical sections. The schedulability of the considered preemptable lock types in this configuration is shown in Fig. 141.

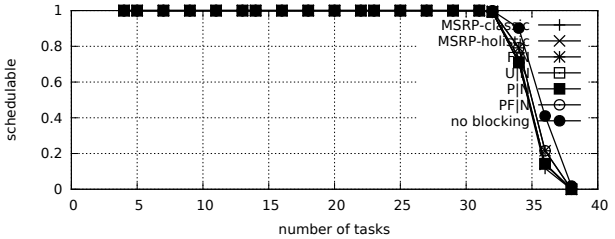

Fig. 132. Schedulability under non-preemptable spin locks for $m = 4$, $U = 0.1n$, 2 resources, $rsf = 0.4$, $N^{max} = 5$, and short critical sections. The schedulability of the considered preemptable lock types in this configuration is shown in Fig. 142.

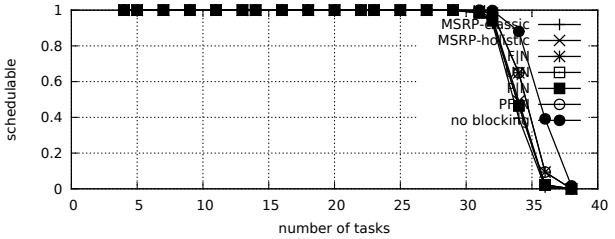

Fig. 133. Schedulability under non-preemptable spin locks for $m = 4$, $U = 0.1n$, 2 resources, $rsf = 0.4$, $N^{max} = 10$, and short critical sections. The schedulability of the considered preemptable lock types in this configuration is shown in Fig. 143.

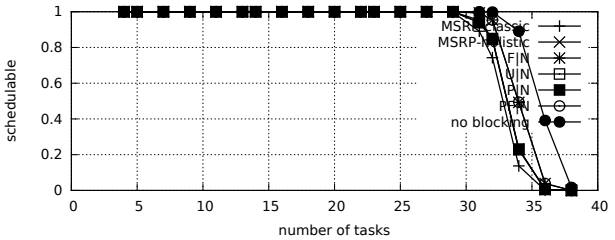

Fig. 134. Schedulability under non-preemptable spin locks for $m = 4$, $U = 0.1n$, 2 resources, $rsf = 0.4$, $N^{max} = 15$, and short critical sections. The schedulability of the considered preemptable lock types in this configuration is shown in Fig. 144.

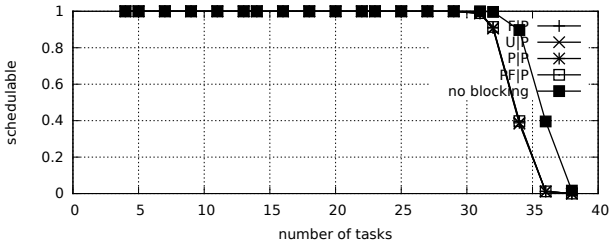

Fig. 135. Schedulability under preemptable spin locks for $m = 4$, $U = 0.1n$, 2 resources, $rsf = 0.4$, $N^{max} = 1$, and medium critical sections. The schedulability of the considered non-preemptable lock types in this configuration is shown in Fig. 125.

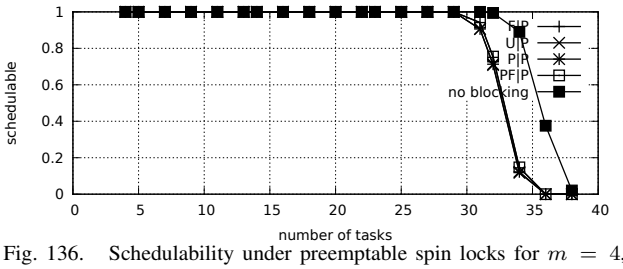

Fig. 136. Schedulability under preemptable spin locks for $m = 4$, $U = 0.1n$, 2 resources, $rsf = 0.4$, $N^{max} = 2$, and medium critical sections. The schedulability of the considered non-preemptable lock types in this configuration is shown in Fig. 126.

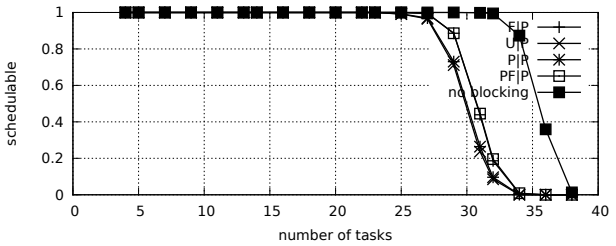

Fig. 137. Schedulability under preemptable spin locks for $m = 4$, $U = 0.1n$, 2 resources, $rsf = 0.4$, $N^{max} = 5$, and medium critical sections. The schedulability of the considered non-preemptable lock types in this configuration is shown in Fig. 127.

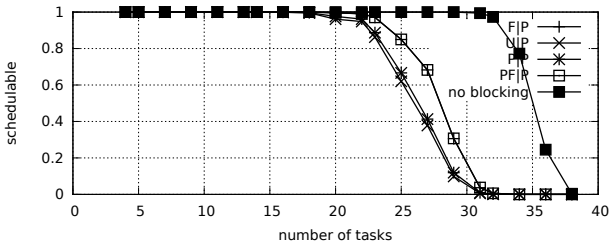

Fig. 138. Schedulability under preemptable spin locks for $m = 4$, $U = 0.1n$, 2 resources, $rsf = 0.4$, $N^{max} = 10$, and medium critical sections. The schedulability of the considered non-preemptable lock types in this configuration is shown in Fig. 128.

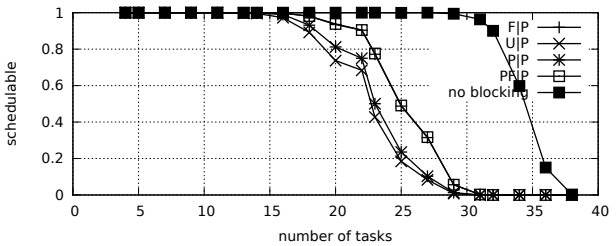

Fig. 139. Schedulability under preemptable spin locks for $m = 4$, $U = 0.1n$, 2 resources, $rsf = 0.4$, $N^{max} = 15$, and medium critical sections. The schedulability of the considered non-preemptable lock types in this configuration is shown in Fig. 129.

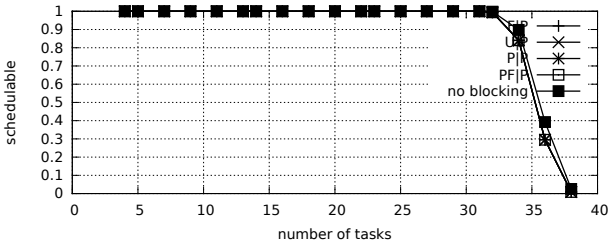

Fig. 140. Schedulability under preemptable spin locks for $m = 4$, $U = 0.1n$, 2 resources, $rsf = 0.4$, $N^{max} = 1$, and short critical sections. The schedulability of the considered non-preemptable lock types in this configuration is shown in Fig. 130.

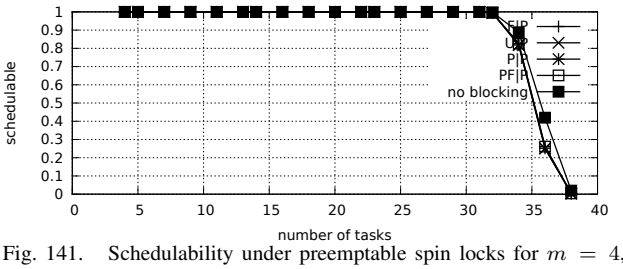

Fig. 141. Schedulability under preemptable spin locks for $m = 4$, $U = 0.1n$, 2 resources, $rsf = 0.4$, $N^{max} = 2$, and short critical sections. The schedulability of the considered non-preemptable lock types in this configuration is shown in Fig. 131.

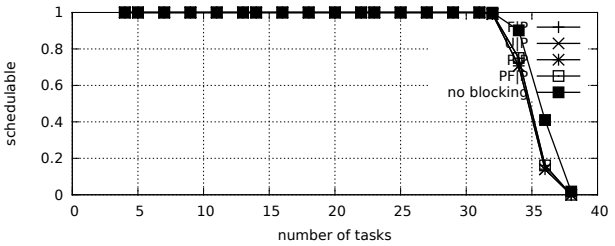

Fig. 142. Schedulability under preemptable spin locks for $m = 4$, $U = 0.1n$, 2 resources, $rsf = 0.4$, $N^{max} = 5$, and short critical sections. The schedulability of the considered non-preemptable lock types in this configuration is shown in Fig. 132.

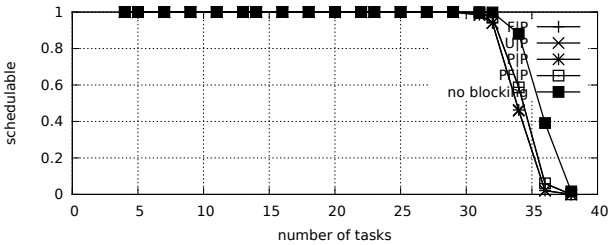

Fig. 143. Schedulability under preemptable spin locks for $m = 4$, $U = 0.1n$, 2 resources, $rsf = 0.4$, $N^{max} = 10$, and short critical sections. The schedulability of the considered non-preemptable lock types in this configuration is shown in Fig. 133.

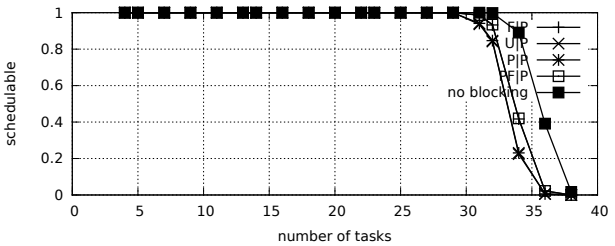

Fig. 144. Schedulability under preemptable spin locks for $m = 4$, $U = 0.1n$, 2 resources, $rsf = 0.4$, $N^{max} = 15$, and short critical sections. The schedulability of the considered non-preemptable lock types in this configuration is shown in Fig. 134.

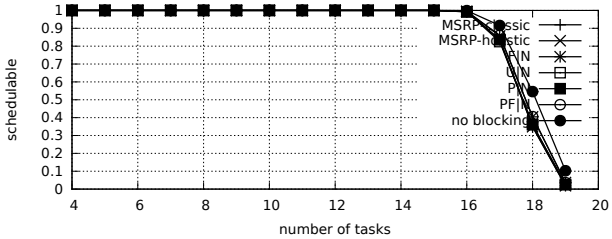

Fig. 145. Schedulability under non-preemptable spin locks for $m = 4$, $U = 0.2n$, 2 resources, $rsf = 0.4$, $N^{max} = 1$, and medium critical sections. The schedulability of the considered preemptable lock types in this configuration is shown in Fig. 155.

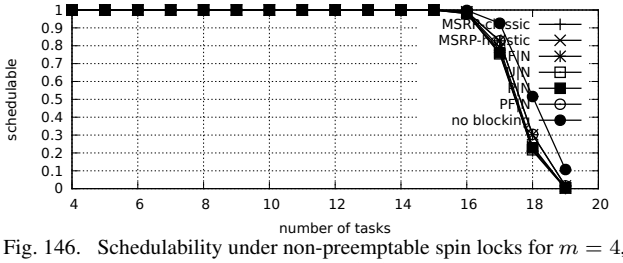

Fig. 146. Schedulability under non-preemptable spin locks for $m = 4$, $U = 0.2n$, 2 resources, $rsf = 0.4$, $N^{max} = 2$, and medium critical sections. The schedulability of the considered preemptable lock types in this configuration is shown in Fig. 156.

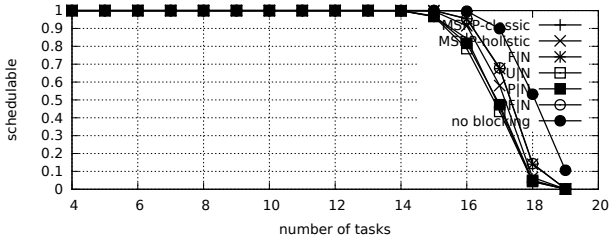

Fig. 147. Schedulability under non-preemptable spin locks for $m = 4$, $U = 0.2n$, 2 resources, $rsf = 0.4$, $N^{max} = 5$, and medium critical sections. The schedulability of the considered preemptable lock types in this configuration is shown in Fig. 157.

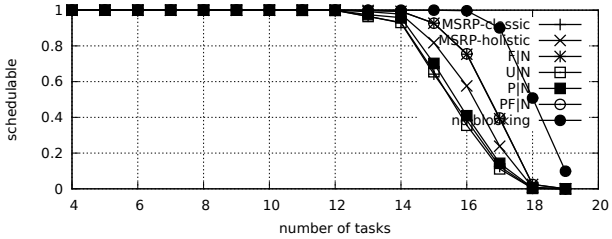

Fig. 148. Schedulability under non-preemptable spin locks for $m = 4$, $U = 0.2n$, 2 resources, $rsf = 0.4$, $N^{max} = 10$, and medium critical sections. The schedulability of the considered preemptable lock types in this configuration is shown in Fig. 158.

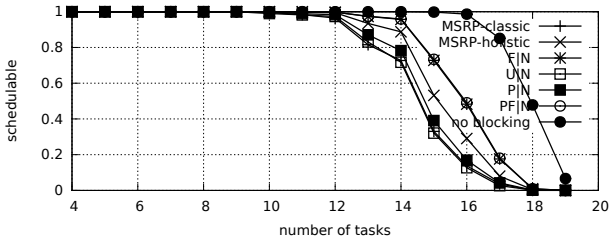

Fig. 149. Schedulability under non-preemptable spin locks for $m = 4$, $U = 0.2n$, 2 resources, $rsf = 0.4$, $N^{max} = 15$, and medium critical sections. The schedulability of the considered preemptable lock types in this configuration is shown in Fig. 159.

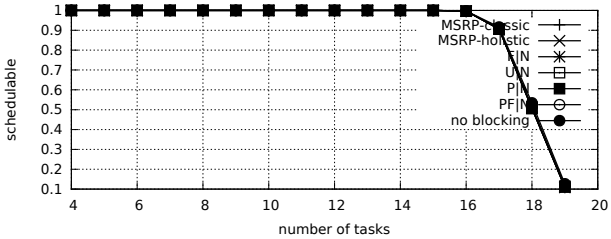

Fig. 150. Schedulability under non-preemptable spin locks for $m = 4$, $U = 0.2n$, 2 resources, $rsf = 0.4$, $N^{max} = 1$, and short critical sections. The schedulability of the considered preemptable lock types in this configuration is shown in Fig. 160.

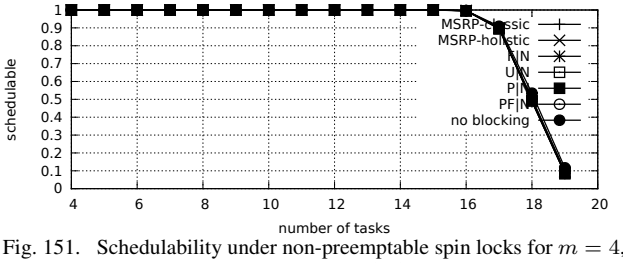

Fig. 151. Schedulability under non-preemptable spin locks for $m = 4$, $U = 0.2n$, 2 resources, $rsf = 0.4$, $N^{max} = 2$, and short critical sections. The schedulability of the considered preemptable lock types in this configuration is shown in Fig. 161.

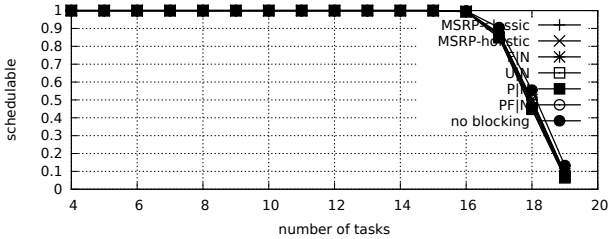

Fig. 152. Schedulability under non-preemptable spin locks for $m = 4$, $U = 0.2n$, 2 resources, $rsf = 0.4$, $N^{max} = 5$, and short critical sections. The schedulability of the considered preemptable lock types in this configuration is shown in Fig. 162.

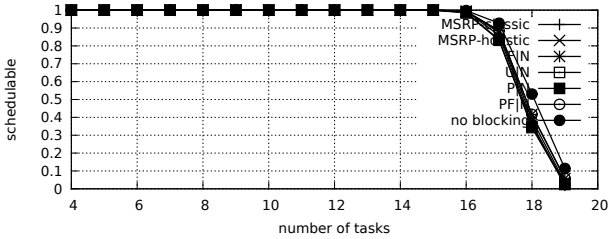

Fig. 153. Schedulability under non-preemptable spin locks for $m = 4$, $U = 0.2n$, 2 resources, $rsf = 0.4$, $N^{max} = 10$, and short critical sections. The schedulability of the considered preemptable lock types in this configuration is shown in Fig. 163.

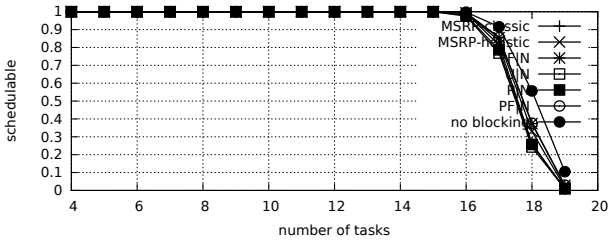

Fig. 154. Schedulability under non-preemptable spin locks for $m = 4$, $U = 0.2n$, 2 resources, $rsf = 0.4$, $N^{max} = 15$, and short critical sections. The schedulability of the considered preemptable lock types in this configuration is shown in Fig. 164.

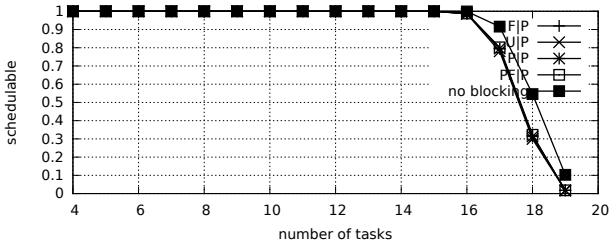

Fig. 155. Schedulability under preemptable spin locks for $m = 4$, $U = 0.2n$, 2 resources, $rsf = 0.4$, $N^{max} = 1$, and medium critical sections. The schedulability of the considered non-preemptable lock types in this configuration is shown in Fig. 145.

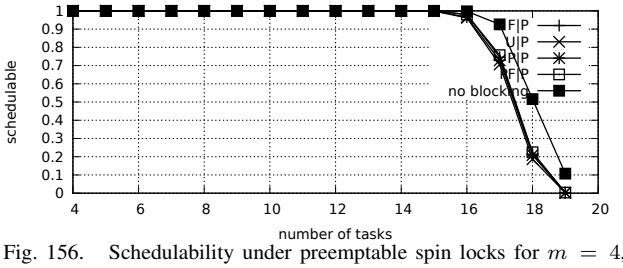

Fig. 156. Schedulability under preemptable spin locks for $m = 4$, $U = 0.2n$, 2 resources, $rsf = 0.4$, $N^{max} = 2$, and medium critical sections. The schedulability of the considered non-preemptable lock types in this configuration is shown in Fig. 146.

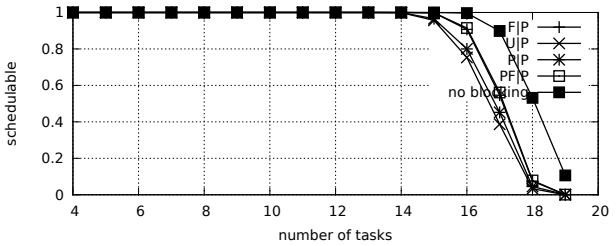

Fig. 157. Schedulability under preemptable spin locks for $m = 4$, $U = 0.2n$, 2 resources, $rsf = 0.4$, $N^{max} = 5$, and medium critical sections. The schedulability of the considered non-preemptable lock types in this configuration is shown in Fig. 147.

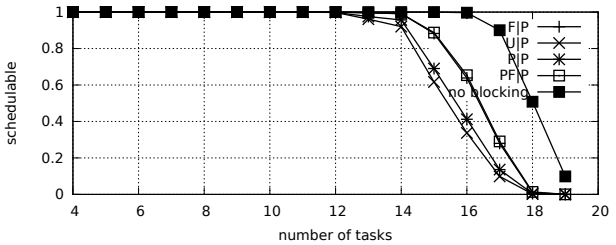

Fig. 158. Schedulability under preemptable spin locks for $m = 4$, $U = 0.2n$, 2 resources, $rsf = 0.4$, $N^{max} = 10$, and medium critical sections. The schedulability of the considered non-preemptable lock types in this configuration is shown in Fig. 148.

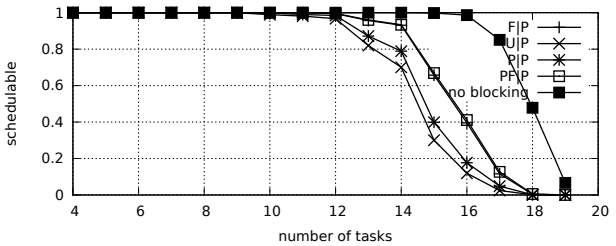

Fig. 159. Schedulability under preemptable spin locks for $m = 4$, $U = 0.2n$, 2 resources, $rsf = 0.4$, $N^{max} = 15$, and medium critical sections. The schedulability of the considered non-preemptable lock types in this configuration is shown in Fig. 149.

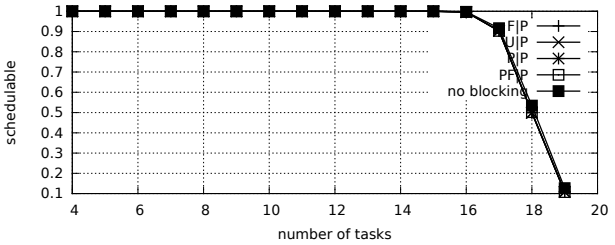

Fig. 160. Schedulability under preemptable spin locks for $m = 4$, $U = 0.2n$, 2 resources, $rsf = 0.4$, $N^{max} = 1$, and short critical sections. The schedulability of the considered non-preemptable lock types in this configuration is shown in Fig. 150.

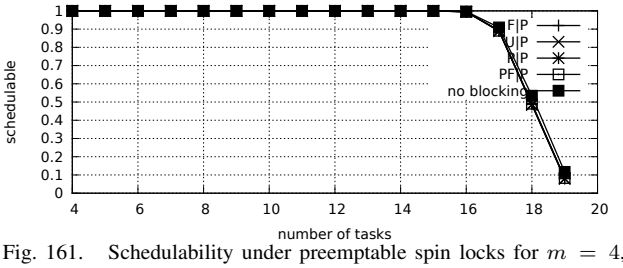

Fig. 161. Schedulability under preemptable spin locks for $m = 4$, $U = 0.2n$, 2 resources, $rsf = 0.4$, $N^{max} = 2$, and short critical sections. The schedulability of the considered non-preemptable lock types in this configuration is shown in Fig. 151.

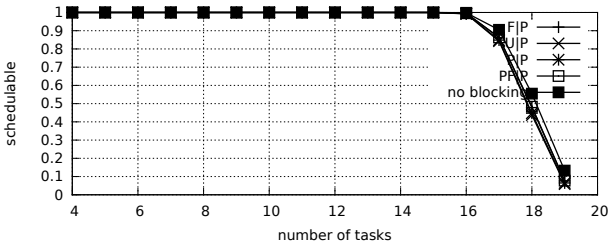

Fig. 162. Schedulability under preemptable spin locks for $m = 4$, $U = 0.2n$, 2 resources, $rsf = 0.4$, $N^{max} = 5$, and short critical sections. The schedulability of the considered non-preemptable lock types in this configuration is shown in Fig. 152.

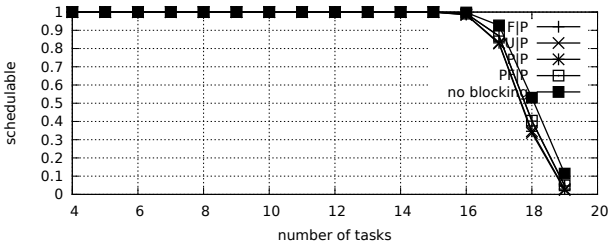

Fig. 163. Schedulability under preemptable spin locks for $m = 4$, $U = 0.2n$, 2 resources, $rsf = 0.4$, $N^{max} = 10$, and short critical sections. The schedulability of the considered non-preemptable lock types in this configuration is shown in Fig. 153.

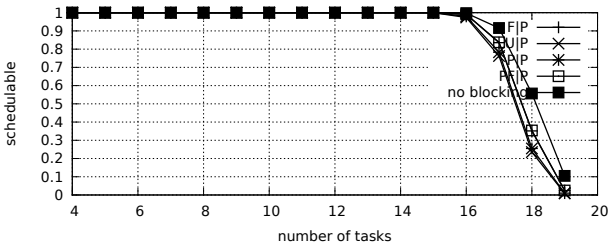

Fig. 164. Schedulability under preemptable spin locks for $m = 4$, $U = 0.2n$, 2 resources, $rsf = 0.4$, $N^{max} = 15$, and short critical sections. The schedulability of the considered non-preemptable lock types in this configuration is shown in Fig. 154.

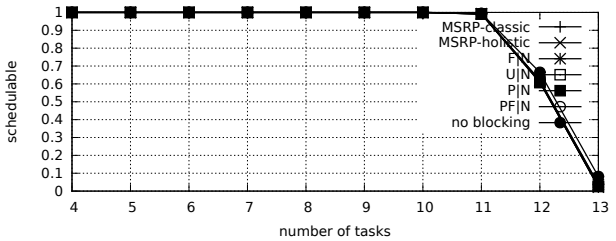

Fig. 165. Schedulability under non-preemptable spin locks for $m = 4$, $U = 0.3n$, 2 resources, $rsf = 0.4$, $N^{max} = 1$, and medium critical sections. The schedulability of the considered preemptable lock types in this configuration is shown in Fig. 175.

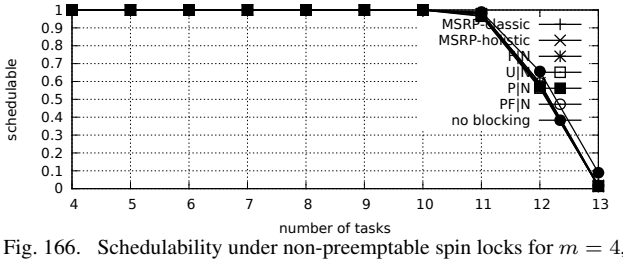

Fig. 166. Schedulability under non-preemptable spin locks for $m = 4$, $U = 0.3n$, 2 resources, $rsf = 0.4$, $N^{max} = 2$, and medium critical sections. The schedulability of the considered preemptable lock types in this configuration is shown in Fig. 176.

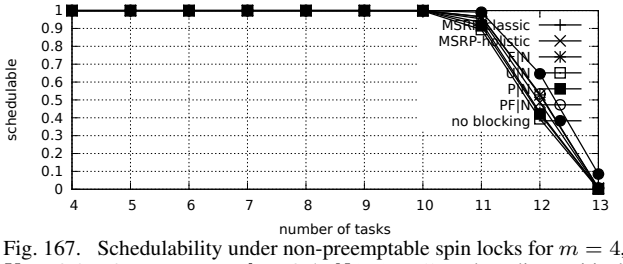

Fig. 167. Schedulability under non-preemptable spin locks for $m = 4$, $U = 0.3n$, 2 resources, $rsf = 0.4$, $N^{max} = 5$, and medium critical sections. The schedulability of the considered preemptable lock types in this configuration is shown in Fig. 177.

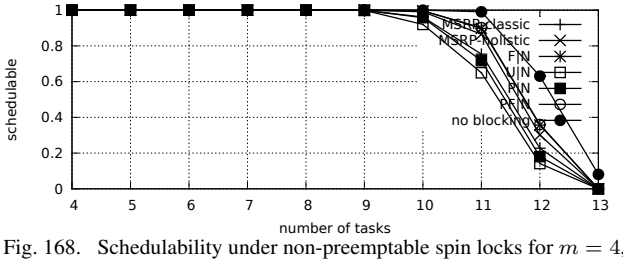

Fig. 168. Schedulability under non-preemptable spin locks for $m = 4$, $U = 0.3n$, 2 resources, $rsf = 0.4$, $N^{max} = 10$, and medium critical sections. The schedulability of the considered preemptable lock types in this configuration is shown in Fig. 178.

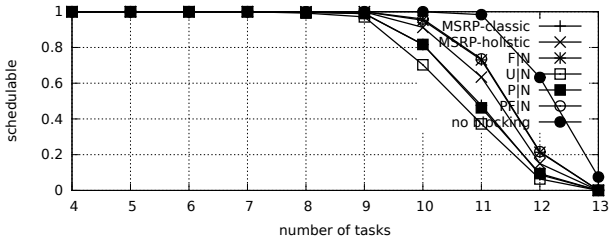

Fig. 169. Schedulability under non-preemptable spin locks for $m = 4$, $U = 0.3n$, 2 resources, $rsf = 0.4$, $N^{max} = 15$, and medium critical sections. The schedulability of the considered preemptable lock types in this configuration is shown in Fig. 179.

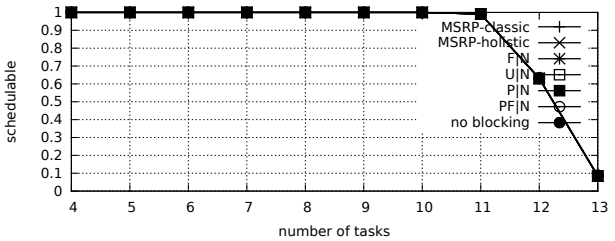

Fig. 170. Schedulability under non-preemptable spin locks for $m = 4$, $U = 0.3n$, 2 resources, $rsf = 0.4$, $N^{max} = 1$, and short critical sections. The schedulability of the considered preemptable lock types in this configuration is shown in Fig. 180.

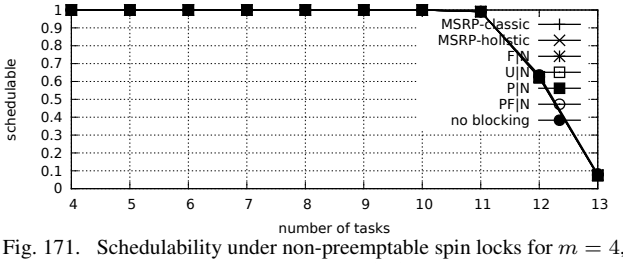

Fig. 171. Schedulability under non-preemptable spin locks for $m = 4$, $U = 0.3n$, 2 resources, $rsf = 0.4$, $N^{max} = 2$, and short critical sections. The schedulability of the considered preemptable lock types in this configuration is shown in Fig. 181.

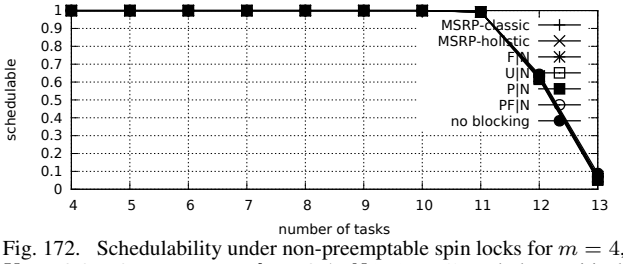

Fig. 172. Schedulability under non-preemptable spin locks for $m = 4$, $U = 0.3n$, 2 resources, $rsf = 0.4$, $N^{max} = 5$, and short critical sections. The schedulability of the considered preemptable lock types in this configuration is shown in Fig. 182.

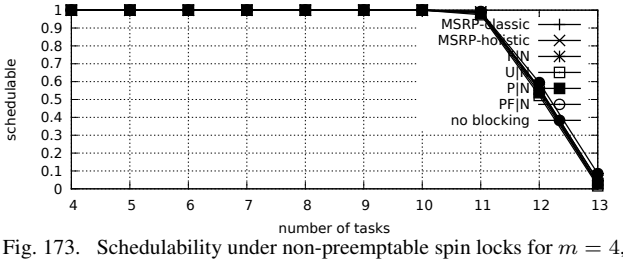

Fig. 173. Schedulability under non-preemptable spin locks for $m = 4$, $U = 0.3n$, 2 resources, $rsf = 0.4$, $N^{max} = 10$, and short critical sections. The schedulability of the considered preemptable lock types in this configuration is shown in Fig. 183.

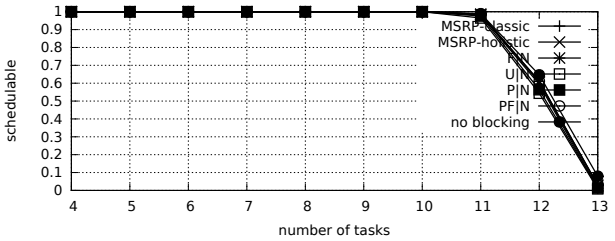

Fig. 174. Schedulability under non-preemptable spin locks for $m = 4$, $U = 0.3n$, 2 resources, $rsf = 0.4$, $N^{max} = 15$, and short critical sections. The schedulability of the considered preemptable lock types in this configuration is shown in Fig. 184.

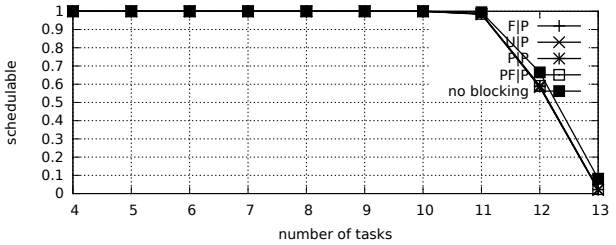

Fig. 175. Schedulability under preemptable spin locks for $m = 4$, $U = 0.3n$, 2 resources, $rsf = 0.4$, $N^{max} = 1$, and medium critical sections. The schedulability of the considered non-preemptable lock types in this configuration is shown in Fig. 165.

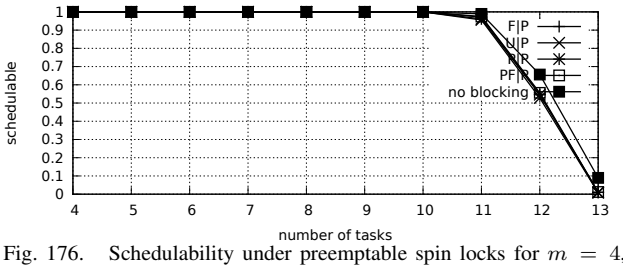

Fig. 176. Schedulability under preemptable spin locks for $m = 4$, $U = 0.3n$, 2 resources, $rsf = 0.4$, $N^{max} = 2$, and medium critical sections. The schedulability of the considered non-preemptable lock types in this configuration is shown in Fig. 166.

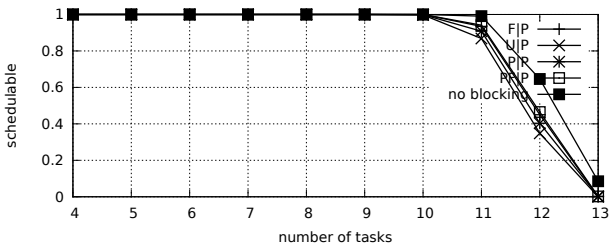

Fig. 177. Schedulability under preemptable spin locks for $m = 4$, $U = 0.3n$, 2 resources, $rsf = 0.4$, $N^{max} = 5$, and medium critical sections. The schedulability of the considered non-preemptable lock types in this configuration is shown in Fig. 167.

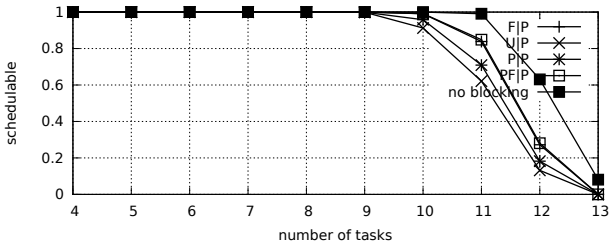

Fig. 178. Schedulability under preemptable spin locks for $m = 4$, $U = 0.3n$, 2 resources, $rsf = 0.4$, $N^{max} = 10$, and medium critical sections. The schedulability of the considered non-preemptable lock types in this configuration is shown in Fig. 168.

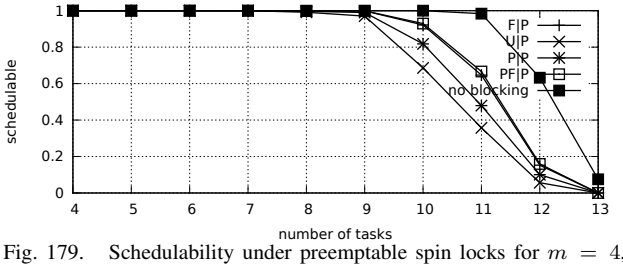

Fig. 179. Schedulability under preemptable spin locks for $m = 4$, $U = 0.3n$, 2 resources, $rsf = 0.4$, $N^{max} = 15$, and medium critical sections. The schedulability of the considered non-preemptable lock types in this configuration is shown in Fig. 169.

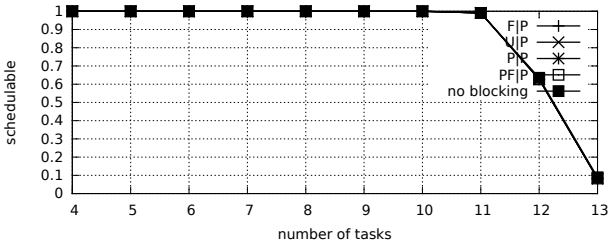

Fig. 180. Schedulability under preemptable spin locks for $m = 4$, $U = 0.3n$, 2 resources, $rsf = 0.4$, $N^{max} = 1$, and short critical sections. The schedulability of the considered non-preemptable lock types in this configuration is shown in Fig. 170.

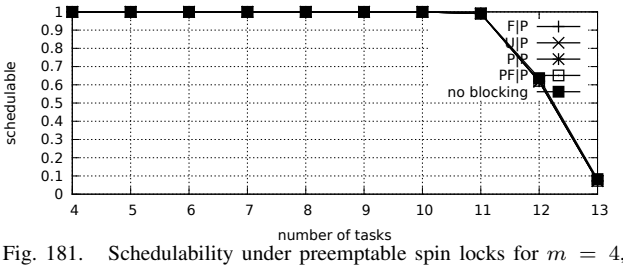

Fig. 181. Schedulability under preemptable spin locks for $m = 4$, $U = 0.3n$, 2 resources, $rsf = 0.4$, $N^{max} = 2$, and short critical sections. The schedulability of the considered non-preemptable lock types in this configuration is shown in Fig. 171.

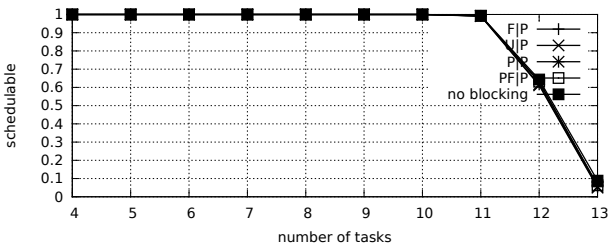

Fig. 182. Schedulability under preemptable spin locks for $m = 4$, $U = 0.3n$, 2 resources, $rsf = 0.4$, $N^{max} = 5$, and short critical sections. The schedulability of the considered non-preemptable lock types in this configuration is shown in Fig. 172.

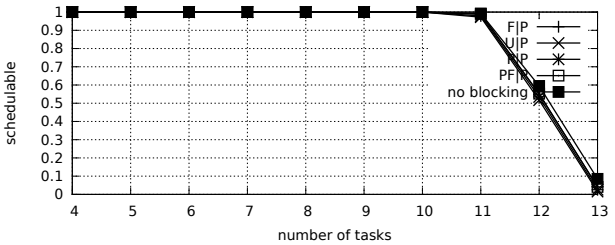

Fig. 183. Schedulability under preemptable spin locks for $m = 4$, $U = 0.3n$, 2 resources, $rsf = 0.4$, $N^{max} = 10$, and short critical sections. The schedulability of the considered non-preemptable lock types in this configuration is shown in Fig. 173.

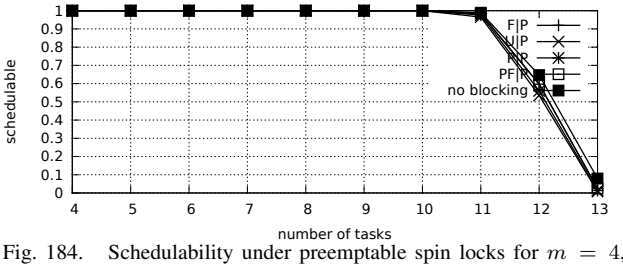

Fig. 184. Schedulability under preemptable spin locks for $m = 4$, $U = 0.3n$, 2 resources, $rsf = 0.4$, $N^{max} = 15$, and short critical sections. The schedulability of the considered non-preemptable lock types in this configuration is shown in Fig. 174.

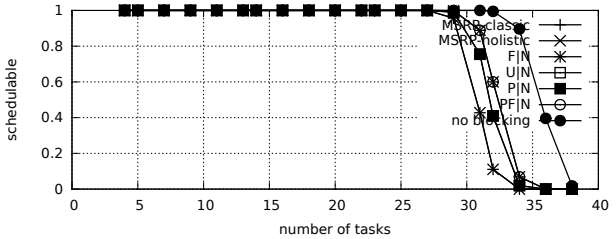

Fig. 185. Schedulability under non-preemptable spin locks for $m = 4$, $U = 0.1n$, 2 resources, $rsf = 0.75$, $N^{max} = 1$, and medium critical sections. The schedulability of the considered preemptable lock types in this configuration is shown in Fig. 195.

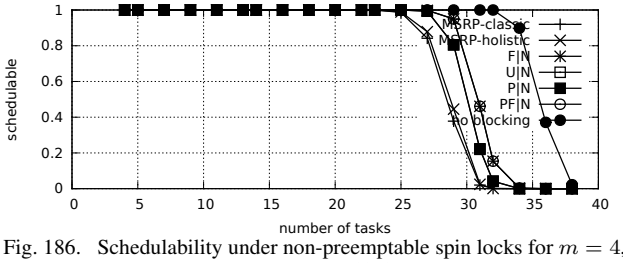

Fig. 186. Schedulability under non-preemptable spin locks for $m = 4$, $U = 0.1n$, 2 resources, $rsf = 0.75$, $N^{max} = 2$, and medium critical sections. The schedulability of the considered preemptable lock types in this configuration is shown in Fig. 196.

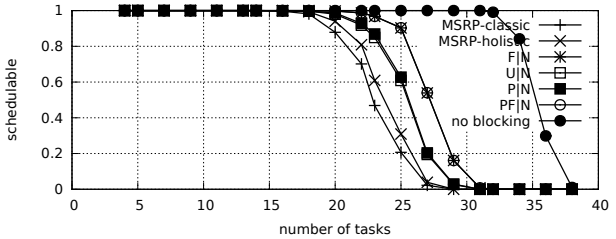

Fig. 187. Schedulability under non-preemptable spin locks for $m = 4$, $U = 0.1n$, 2 resources, $rsf = 0.75$, $N^{max} = 5$, and medium critical sections. The schedulability of the considered preemptable lock types in this configuration is shown in Fig. 197.

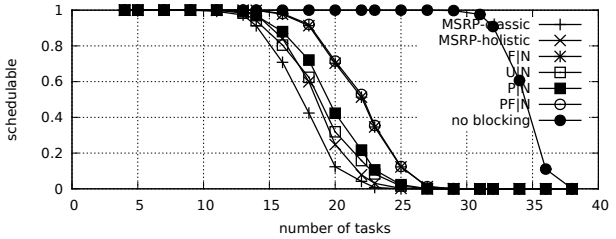

Fig. 188. Schedulability under non-preemptable spin locks for $m = 4$, $U = 0.1n$, 2 resources, $rsf = 0.75$, $N^{max} = 10$, and medium critical sections. The schedulability of the considered preemptable lock types in this configuration is shown in Fig. 198.

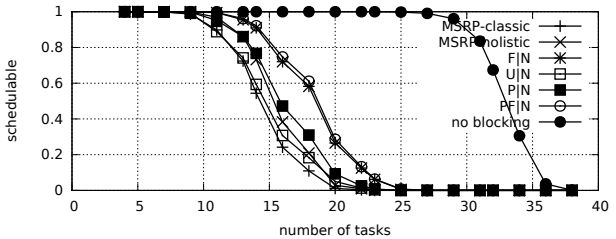

Fig. 189. Schedulability under non-preemptable spin locks for $m = 4$, $U = 0.1n$, 2 resources, $rsf = 0.75$, $N^{max} = 15$, and medium critical sections. The schedulability of the considered preemptable lock types in this configuration is shown in Fig. 199.

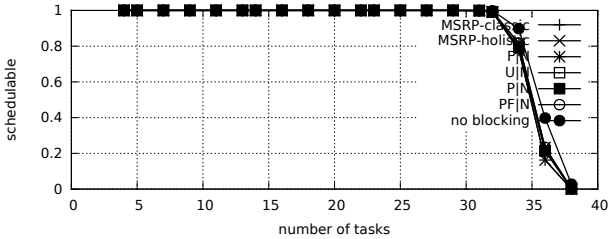

Fig. 190. Schedulability under non-preemptable spin locks for $m = 4$, $U = 0.1n$, 2 resources, $rsf = 0.75$, $N^{max} = 1$, and short critical sections. The schedulability of the considered preemptable lock types in this configuration is shown in Fig. 200.

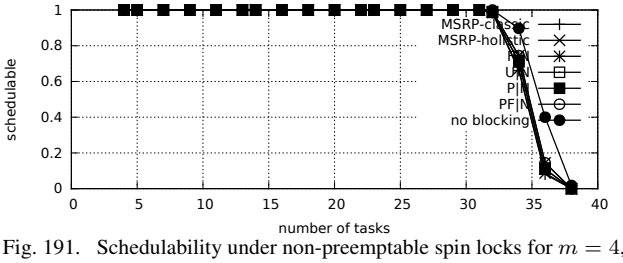

Fig. 191. Schedulability under non-preemptable spin locks for $m = 4$, $U = 0.1n$, 2 resources, $rsf = 0.75$, $N^{max} = 2$, and short critical sections. The schedulability of the considered preemptable lock types in this configuration is shown in Fig. 201.

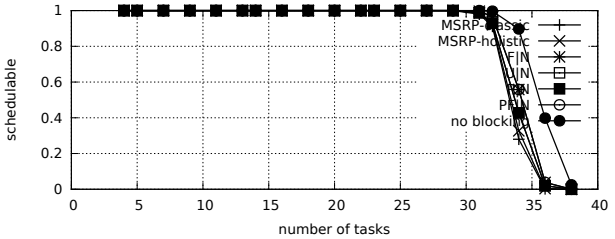

Fig. 192. Schedulability under non-preemptable spin locks for $m = 4$, $U = 0.1n$, 2 resources, $rsf = 0.75$, $N^{max} = 5$, and short critical sections. The schedulability of the considered preemptable lock types in this configuration is shown in Fig. 202.

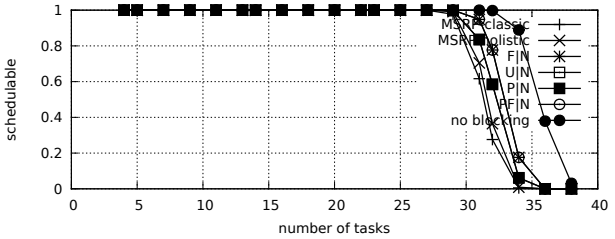

Fig. 193. Schedulability under non-preemptable spin locks for $m = 4$, $U = 0.1n$, 2 resources, $rsf = 0.75$, $N^{max} = 10$, and short critical sections. The schedulability of the considered preemptable lock types in this configuration is shown in Fig. 203.

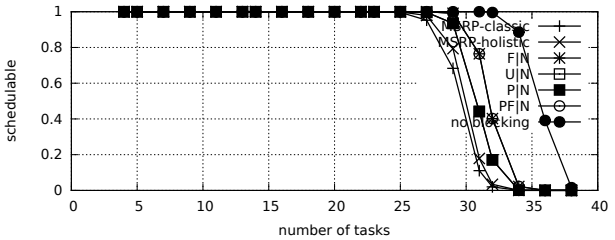

Fig. 194. Schedulability under non-preemptable spin locks for $m = 4$, $U = 0.1n$, 2 resources, $rsf = 0.75$, $N^{max} = 15$, and short critical sections. The schedulability of the considered preemptable lock types in this configuration is shown in Fig. 204.

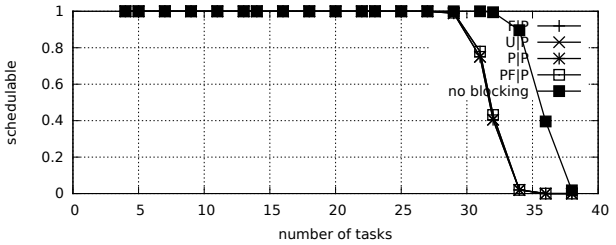

Fig. 195. Schedulability under preemptable spin locks for $m = 4$, $U = 0.1n$, 2 resources, $rsf = 0.75$, $N^{max} = 1$, and medium critical sections. The schedulability of the considered non-preemptable lock types in this configuration is shown in Fig. 185.

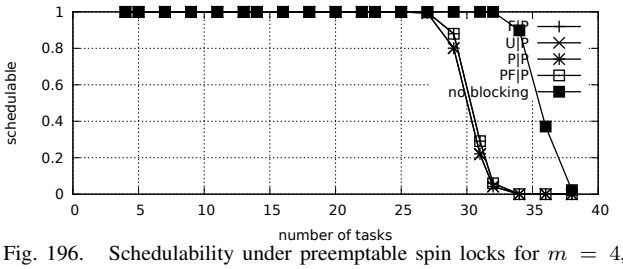

Fig. 196. Schedulability under preemptable spin locks for $m = 4$, $U = 0.1n$, 2 resources, $rsf = 0.75$, $N^{max} = 2$, and medium critical sections. The schedulability of the considered non-preemptable lock types in this configuration is shown in Fig. 186.

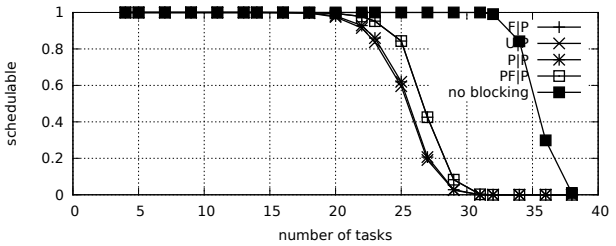

Fig. 197. Schedulability under preemptable spin locks for $m = 4$, $U = 0.1n$, 2 resources, $rsf = 0.75$, $N^{max} = 5$, and medium critical sections. The schedulability of the considered non-preemptable lock types in this configuration is shown in Fig. 187.

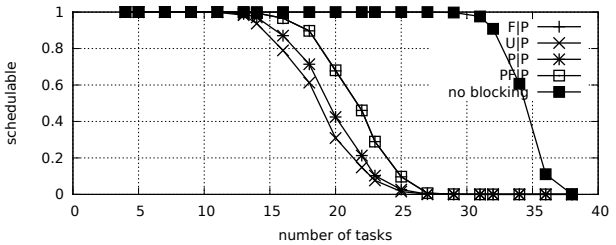

Fig. 198. Schedulability under preemptable spin locks for $m = 4$, $U = 0.1n$, 2 resources, $rsf = 0.75$, $N^{max} = 10$, and medium critical sections. The schedulability of the considered non-preemptable lock types in this configuration is shown in Fig. 188.

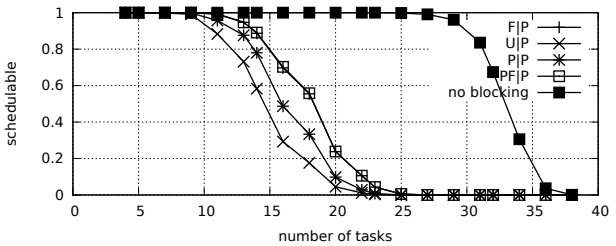

Fig. 199. Schedulability under preemptable spin locks for $m = 4$, $U = 0.1n$, 2 resources, $rsf = 0.75$, $N^{max} = 15$, and medium critical sections. The schedulability of the considered non-preemptable lock types in this configuration is shown in Fig. 189.

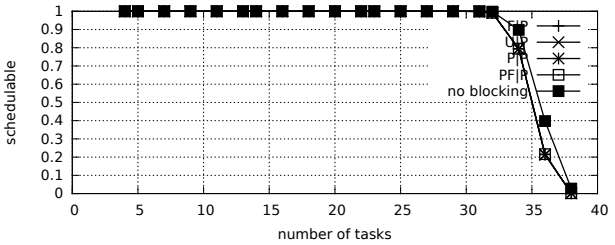

Fig. 200. Schedulability under preemptable spin locks for $m = 4$, $U = 0.1n$, 2 resources, $rsf = 0.75$, $N^{max} = 1$, and short critical sections. The schedulability of the considered non-preemptable lock types in this configuration is shown in Fig. 190.

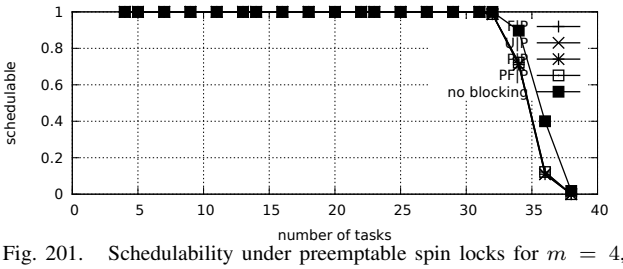

Fig. 201. Schedulability under preemptable spin locks for $m = 4$, $U = 0.1n$, 2 resources, $rsf = 0.75$, $N^{max} = 2$, and short critical sections. The schedulability of the considered non-preemptable lock types in this configuration is shown in Fig. 191.

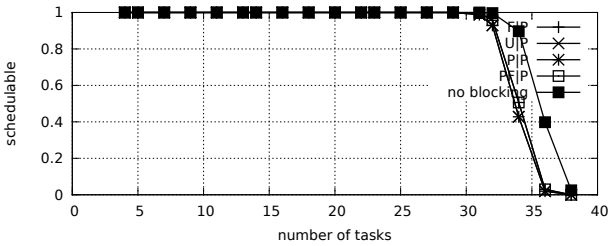

Fig. 202. Schedulability under preemptable spin locks for $m = 4$, $U = 0.1n$, 2 resources, $rsf = 0.75$, $N^{max} = 5$, and short critical sections. The schedulability of the considered non-preemptable lock types in this configuration is shown in Fig. 192.

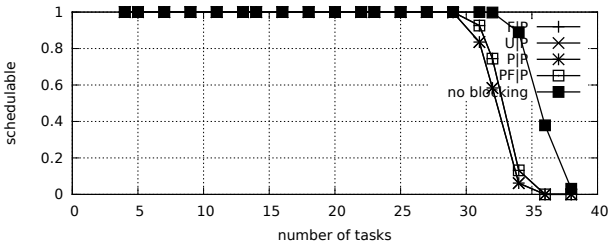

Fig. 203. Schedulability under preemptable spin locks for $m = 4$, $U = 0.1n$, 2 resources, $rsf = 0.75$, $N^{max} = 10$, and short critical sections. The schedulability of the considered non-preemptable lock types in this configuration is shown in Fig. 193.

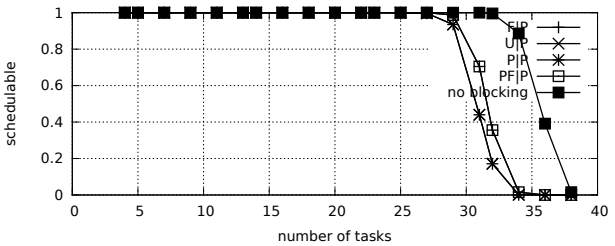

Fig. 204. Schedulability under preemptable spin locks for $m = 4$, $U = 0.1n$, 2 resources, $rsf = 0.75$, $N^{max} = 15$, and short critical sections. The schedulability of the considered non-preemptable lock types in this configuration is shown in Fig. 194.

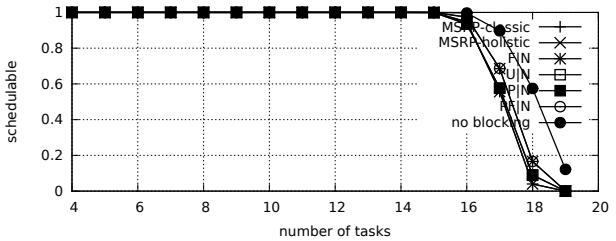

Fig. 205. Schedulability under non-preemptable spin locks for $m = 4$, $U = 0.2n$, 2 resources, $rsf = 0.75$, $N^{max} = 1$, and medium critical sections. The schedulability of the considered preemptable lock types in this configuration is shown in Fig. 215.

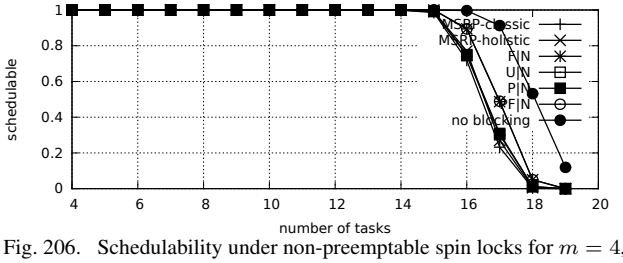

Fig. 206. Schedulability under non-preemptable spin locks for $m = 4$, $U = 0.2n$, 2 resources, $rsf = 0.75$, $N^{max} = 2$, and medium critical sections. The schedulability of the considered preemptable lock types in this configuration is shown in Fig. 216.

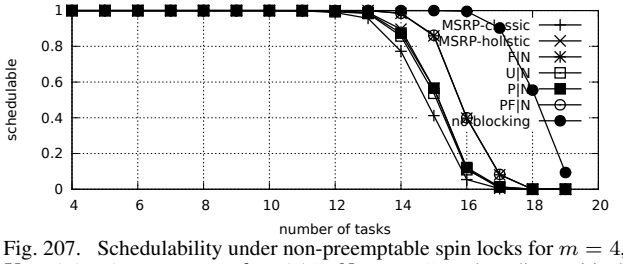

Fig. 207. Schedulability under non-preemptable spin locks for $m = 4$, $U = 0.2n$, 2 resources, $rsf = 0.75$, $N^{max} = 5$, and medium critical sections. The schedulability of the considered preemptable lock types in this configuration is shown in Fig. 217.

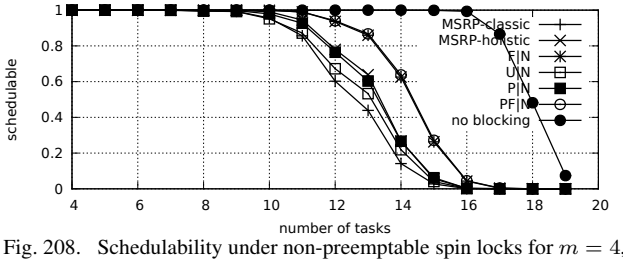

Fig. 208. Schedulability under non-preemptable spin locks for $m = 4$, $U = 0.2n$, 2 resources, $rsf = 0.75$, $N^{max} = 10$, and medium critical sections. The schedulability of the considered preemptable lock types in this configuration is shown in Fig. 218.

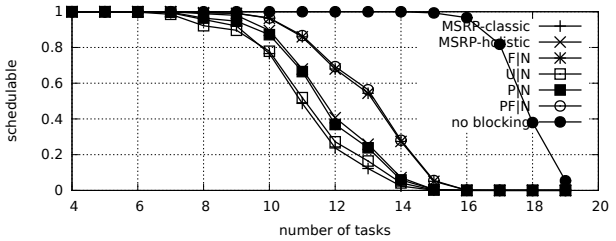

Fig. 209. Schedulability under non-preemptable spin locks for $m = 4$, $U = 0.2n$, 2 resources, $rsf = 0.75$, $N^{max} = 15$, and medium critical sections. The schedulability of the considered preemptable lock types in this configuration is shown in Fig. 219.

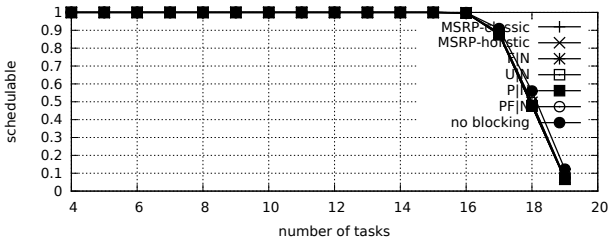

Fig. 210. Schedulability under non-preemptable spin locks for $m = 4$, $U = 0.2n$, 2 resources, $rsf = 0.75$, $N^{max} = 1$, and short critical sections. The schedulability of the considered preemptable lock types in this configuration is shown in Fig. 220.

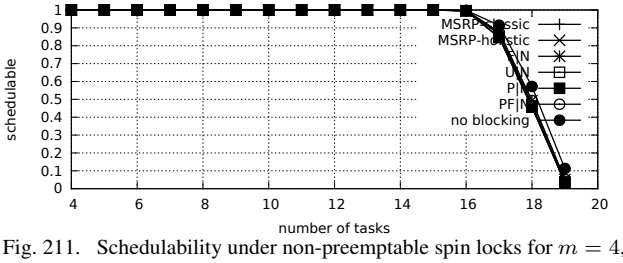

Fig. 211. Schedulability under non-preemptable spin locks for $m = 4$, $U = 0.2n$, 2 resources, $rsf = 0.75$, $N^{max} = 2$, and short critical sections. The schedulability of the considered preemptable lock types in this configuration is shown in Fig. 221.

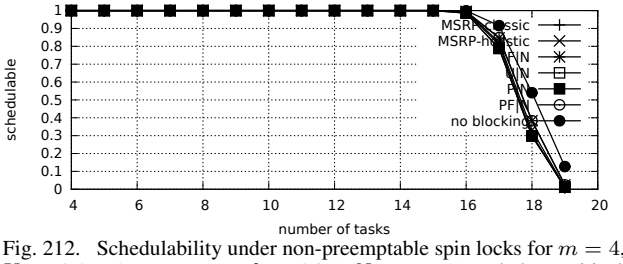

Fig. 212. Schedulability under non-preemptable spin locks for $m = 4$, $U = 0.2n$, 2 resources, $rsf = 0.75$, $N^{max} = 5$, and short critical sections. The schedulability of the considered preemptable lock types in this configuration is shown in Fig. 222.

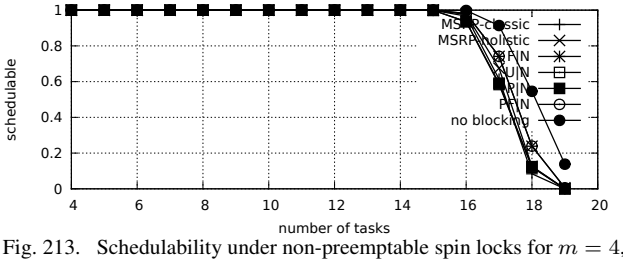

Fig. 213. Schedulability under non-preemptable spin locks for $m = 4$, $U = 0.2n$, 2 resources, $rsf = 0.75$, $N^{max} = 10$, and short critical sections. The schedulability of the considered preemptable lock types in this configuration is shown in Fig. 223.

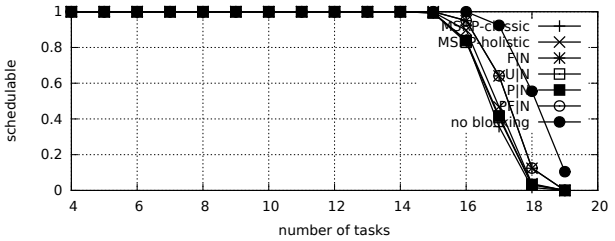

Fig. 214. Schedulability under non-preemptable spin locks for $m = 4$, $U = 0.2n$, 2 resources, $rsf = 0.75$, $N^{max} = 15$, and short critical sections. The schedulability of the considered preemptable lock types in this configuration is shown in Fig. 224.

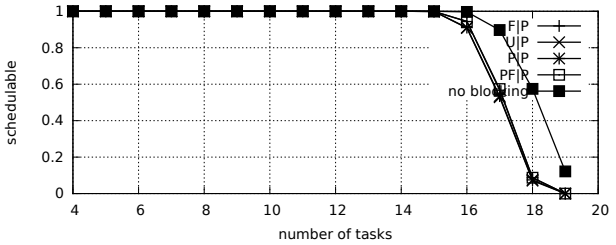

Fig. 215. Schedulability under preemptable spin locks for $m = 4$, $U = 0.2n$, 2 resources, $rsf = 0.75$, $N^{max} = 1$, and medium critical sections. The schedulability of the considered non-preemptable lock types in this configuration is shown in Fig. 205.

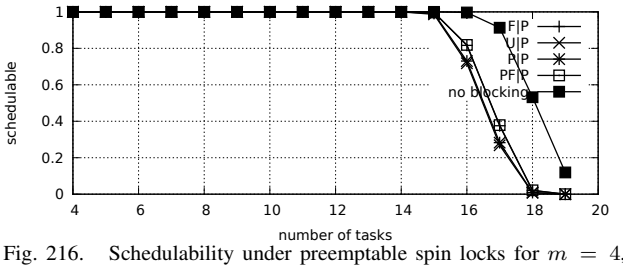

Fig. 216. Schedulability under preemptable spin locks for $m = 4$, $U = 0.2n$, 2 resources, $rsf = 0.75$, $N^{max} = 2$, and medium critical sections. The schedulability of the considered non-preemptable lock types in this configuration is shown in Fig. 206.

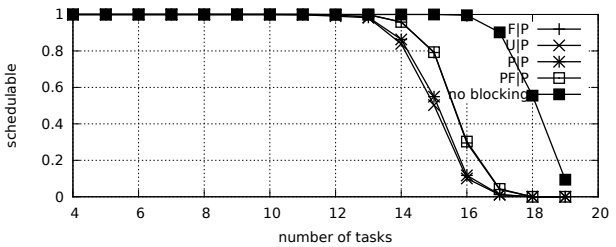

Fig. 217. Schedulability under preemptable spin locks for $m = 4$, $U = 0.2n$, 2 resources, $rsf = 0.75$, $N^{max} = 5$, and medium critical sections. The schedulability of the considered non-preemptable lock types in this configuration is shown in Fig. 207.

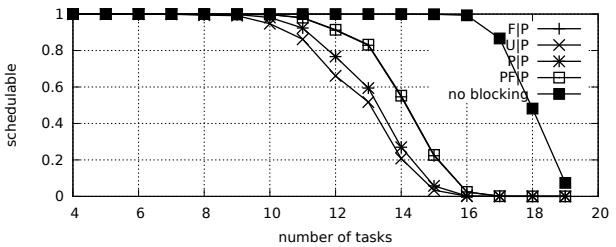

Fig. 218. Schedulability under preemptable spin locks for $m = 4$, $U = 0.2n$, 2 resources, $rsf = 0.75$, $N^{max} = 10$, and medium critical sections. The schedulability of the considered non-preemptable lock types in this configuration is shown in Fig. 208.

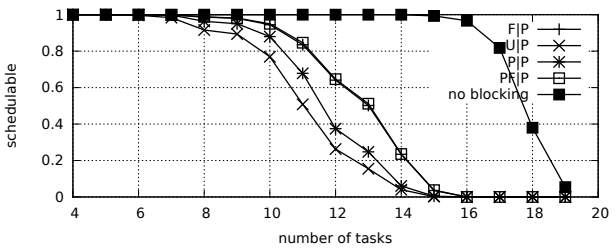

Fig. 219. Schedulability under preemptable spin locks for $m = 4$, $U = 0.2n$, 2 resources, $rsf = 0.75$, $N^{max} = 15$, and medium critical sections. The schedulability of the considered non-preemptable lock types in this configuration is shown in Fig. 209.

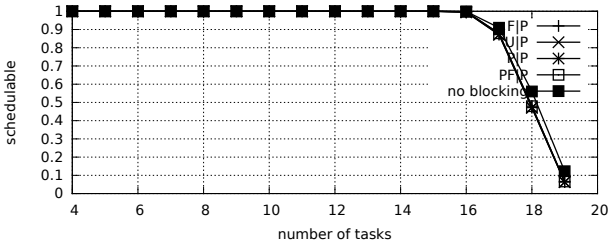

Fig. 220. Schedulability under preemptable spin locks for $m = 4$, $U = 0.2n$, 2 resources, $rsf = 0.75$, $N^{max} = 1$, and short critical sections. The schedulability of the considered non-preemptable lock types in this configuration is shown in Fig. 210.

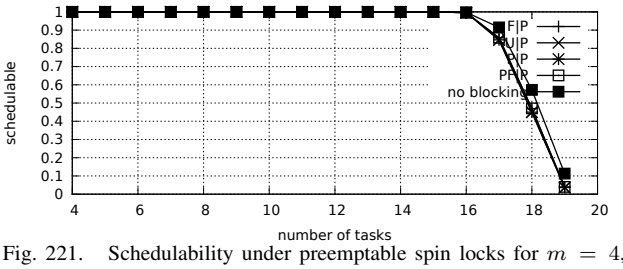

Fig. 221. Schedulability under preemptable spin locks for $m = 4$, $U = 0.2n$, 2 resources, $rsf = 0.75$, $N^{max} = 2$, and short critical sections. The schedulability of the considered non-preemptable lock types in this configuration is shown in Fig. 211.

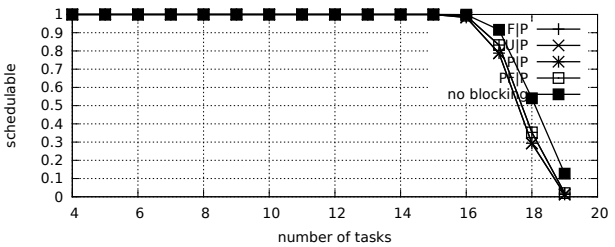

Fig. 222. Schedulability under preemptable spin locks for $m = 4$, $U = 0.2n$, 2 resources, $rsf = 0.75$, $N^{max} = 5$, and short critical sections. The schedulability of the considered non-preemptable lock types in this configuration is shown in Fig. 212.

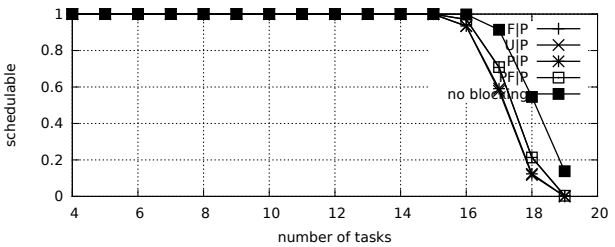

Fig. 223. Schedulability under preemptable spin locks for $m = 4$, $U = 0.2n$, 2 resources, $rsf = 0.75$, $N^{max} = 10$, and short critical sections. The schedulability of the considered non-preemptable lock types in this configuration is shown in Fig. 213.

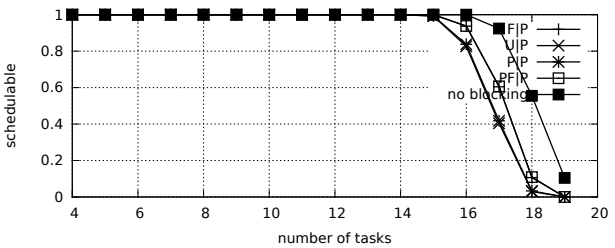

Fig. 224. Schedulability under preemptable spin locks for $m = 4$, $U = 0.2n$, 2 resources, $rsf = 0.75$, $N^{max} = 15$, and short critical sections. The schedulability of the considered non-preemptable lock types in this configuration is shown in Fig. 214.

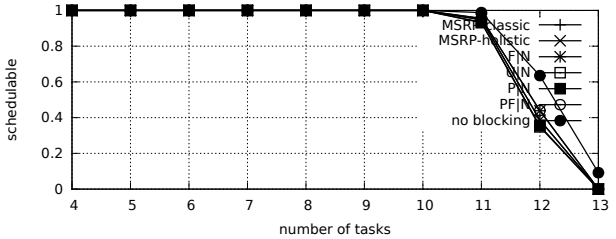

Fig. 225. Schedulability under non-preemptable spin locks for $m = 4$, $U = 0.3n$, 2 resources, $rsf = 0.75$, $N^{max} = 1$, and medium critical sections. The schedulability of the considered preemptable lock types in this configuration is shown in Fig. 235.

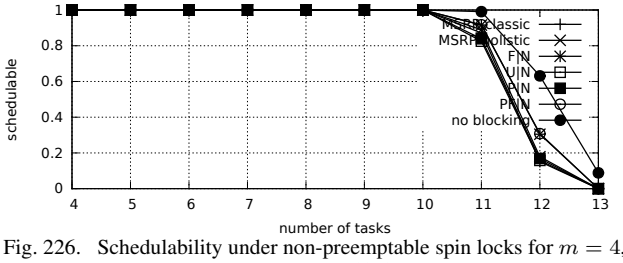

Fig. 226. Schedulability under non-preemptable spin locks for $m = 4$, $U = 0.3n$, 2 resources, $rsf = 0.75$, $N^{max} = 2$, and medium critical sections. The schedulability of the considered preemptable lock types in this configuration is shown in Fig. 236.

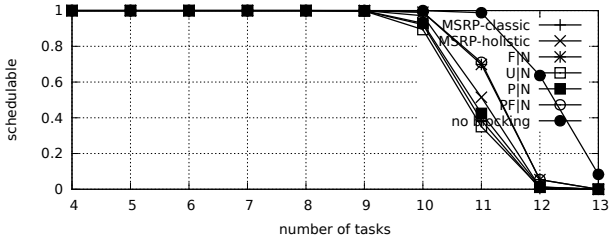

Fig. 227. Schedulability under non-preemptable spin locks for $m = 4$, $U = 0.3n$, 2 resources, $rsf = 0.75$, $N^{max} = 5$, and medium critical sections. The schedulability of the considered preemptable lock types in this configuration is shown in Fig. 237.

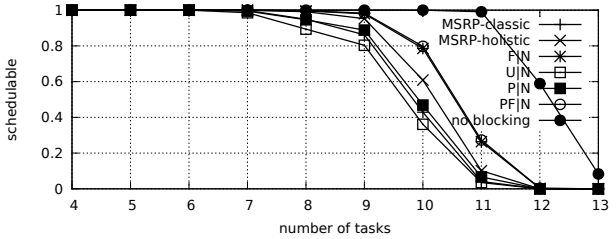

Fig. 228. Schedulability under non-preemptable spin locks for $m = 4$, $U = 0.3n$, 2 resources, $rsf = 0.75$, $N^{max} = 10$, and medium critical sections. The schedulability of the considered preemptable lock types in this configuration is shown in Fig. 238.

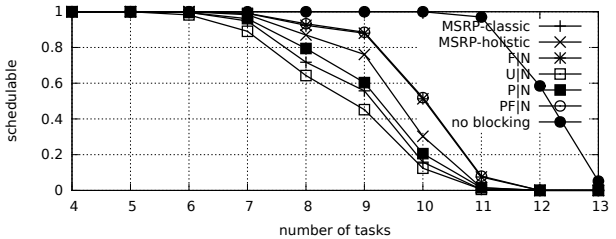

Fig. 229. Schedulability under non-preemptable spin locks for $m = 4$, $U = 0.3n$, 2 resources, $rsf = 0.75$, $N^{max} = 15$, and medium critical sections. The schedulability of the considered preemptable lock types in this configuration is shown in Fig. 239.

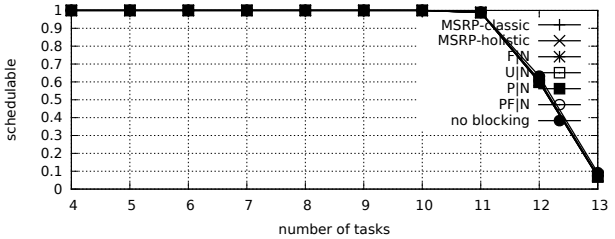

Fig. 230. Schedulability under non-preemptable spin locks for $m = 4$, $U = 0.3n$, 2 resources, $rsf = 0.75$, $N^{max} = 1$, and short critical sections. The schedulability of the considered preemptable lock types in this configuration is shown in Fig. 240.

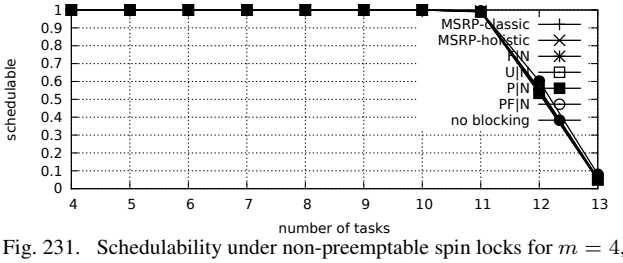

Fig. 231. Schedulability under non-preemptable spin locks for $m = 4$, $U = 0.3n$, 2 resources, $rsf = 0.75$, $N^{max} = 2$, and short critical sections. The schedulability of the considered preemptable lock types in this configuration is shown in Fig. 241.

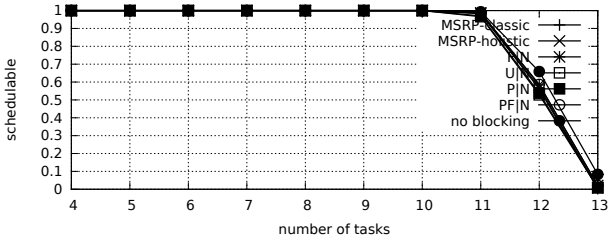

Fig. 232. Schedulability under non-preemptable spin locks for $m = 4$, $U = 0.3n$, 2 resources, $rsf = 0.75$, $N^{max} = 5$, and short critical sections. The schedulability of the considered preemptable lock types in this configuration is shown in Fig. 242.

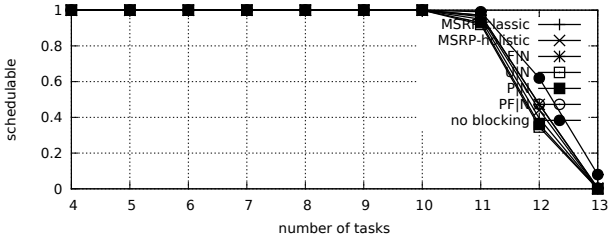

Fig. 233. Schedulability under non-preemptable spin locks for $m = 4$, $U = 0.3n$, 2 resources, $rsf = 0.75$, $N^{max} = 10$, and short critical sections. The schedulability of the considered preemptable lock types in this configuration is shown in Fig. 243.

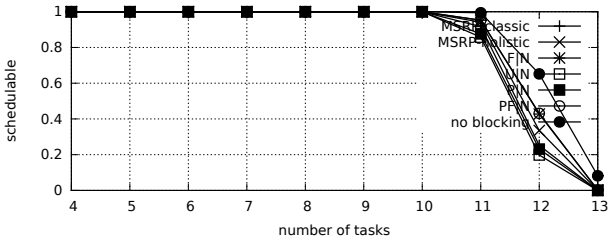

Fig. 234. Schedulability under non-preemptable spin locks for $m = 4$, $U = 0.3n$, 2 resources, $rsf = 0.75$, $N^{max} = 15$, and short critical sections. The schedulability of the considered preemptable lock types in this configuration is shown in Fig. 244.

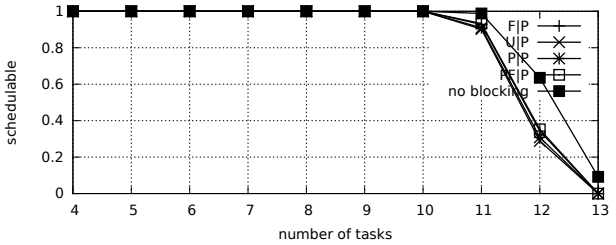

Fig. 235. Schedulability under preemptable spin locks for $m = 4$, $U = 0.3n$, 2 resources, $rsf = 0.75$, $N^{max} = 1$, and medium critical sections. The schedulability of the considered non-preemptable lock types in this configuration is shown in Fig. 225.

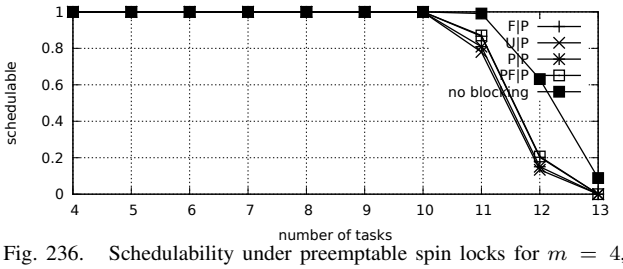

Fig. 236. Schedulability under preemptable spin locks for $m = 4$, $U = 0.3n$, 2 resources, $rsf = 0.75$, $N^{max} = 2$, and medium critical sections. The schedulability of the considered non-preemptable lock types in this configuration is shown in Fig. 226.

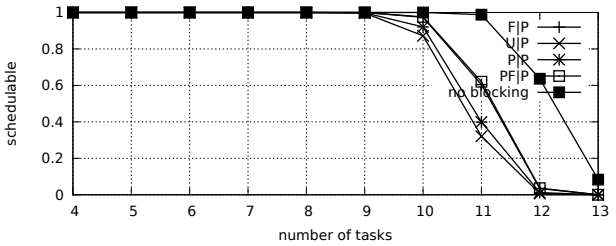

Fig. 237. Schedulability under preemptable spin locks for $m = 4$, $U = 0.3n$, 2 resources, $rsf = 0.75$, $N^{max} = 5$, and medium critical sections. The schedulability of the considered non-preemptable lock types in this configuration is shown in Fig. 227.

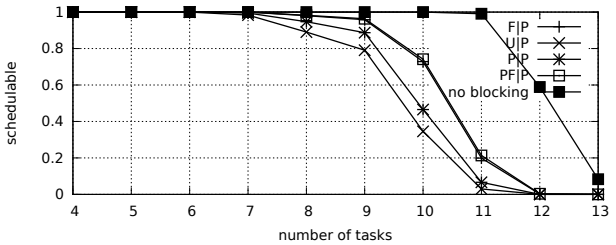

Fig. 238. Schedulability under preemptable spin locks for $m = 4$, $U = 0.3n$, 2 resources, $rsf = 0.75$, $N^{max} = 10$, and medium critical sections. The schedulability of the considered non-preemptable lock types in this configuration is shown in Fig. 228.

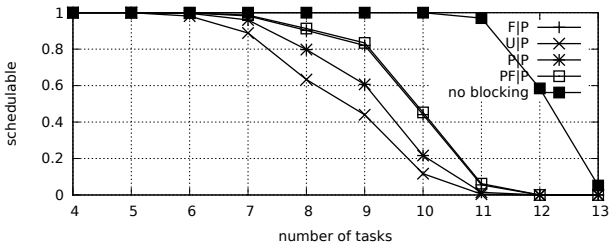

Fig. 239. Schedulability under preemptable spin locks for $m = 4$, $U = 0.3n$, 2 resources, $rsf = 0.75$, $N^{max} = 15$, and medium critical sections. The schedulability of the considered non-preemptable lock types in this configuration is shown in Fig. 229.

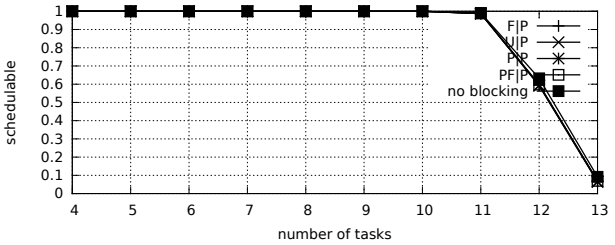

Fig. 240. Schedulability under preemptable spin locks for $m = 4$, $U = 0.3n$, 2 resources, $rsf = 0.75$, $N^{max} = 1$, and short critical sections. The schedulability of the considered non-preemptable lock types in this configuration is shown in Fig. 230.

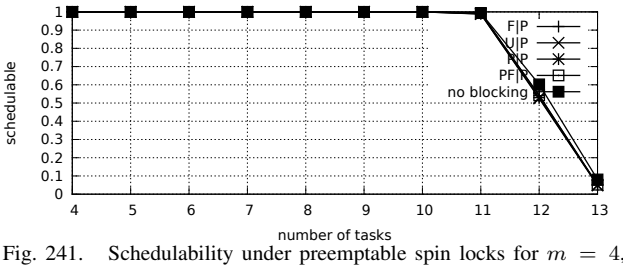

Fig. 241. Schedulability under preemptable spin locks for $m = 4$, $U = 0.3n$, 2 resources, $rsf = 0.75$, $N^{max} = 2$, and short critical sections. The schedulability of the considered non-preemptable lock types in this configuration is shown in Fig. 231.

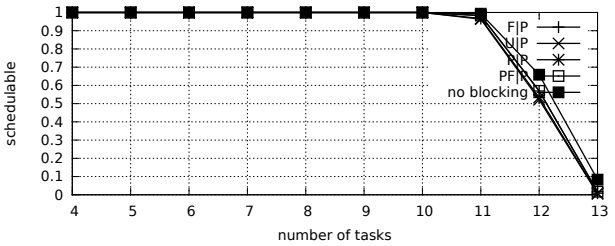

Fig. 242. Schedulability under preemptable spin locks for $m = 4$, $U = 0.3n$, 2 resources, $rsf = 0.75$, $N^{max} = 5$, and short critical sections. The schedulability of the considered non-preemptable lock types in this configuration is shown in Fig. 232.

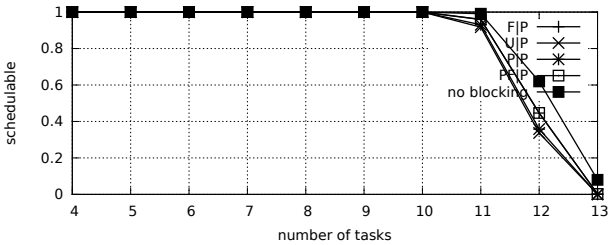

Fig. 243. Schedulability under preemptable spin locks for $m = 4$, $U = 0.3n$, 2 resources, $rsf = 0.75$, $N^{max} = 10$, and short critical sections. The schedulability of the considered non-preemptable lock types in this configuration is shown in Fig. 233.

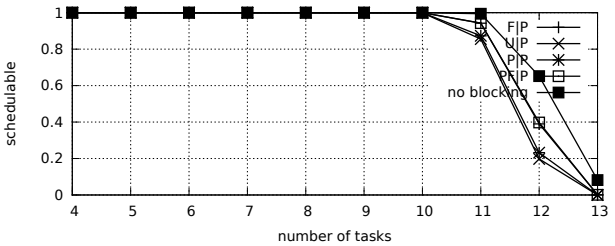

Fig. 244. Schedulability under preemptable spin locks for $m = 4$, $U = 0.3n$, 2 resources, $rsf = 0.75$, $N^{max} = 15$, and short critical sections. The schedulability of the considered non-preemptable lock types in this configuration is shown in Fig. 234.

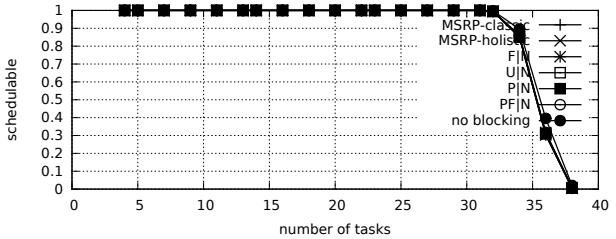

Fig. 245. Schedulability under non-preemptable spin locks for $m = 4$, $U = 0.1n$, 4 resources, $rsf = 0.1$, $N^{max} = 1$, and medium critical sections. The schedulability of the considered preemptable lock types in this configuration is shown in Fig. 255.

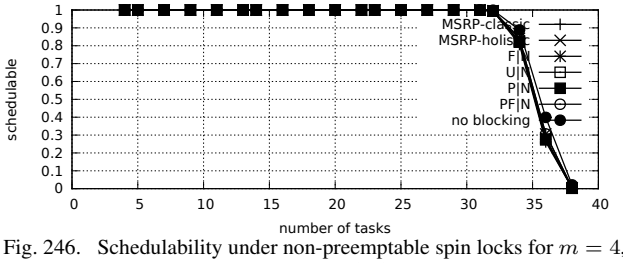

Fig. 246. Schedulability under non-preemptable spin locks for $m = 4$, $U = 0.1n$, 4 resources, $rsf = 0.1$, $N^{max} = 2$, and medium critical sections. The schedulability of the considered preemptable lock types in this configuration is shown in Fig. 256.

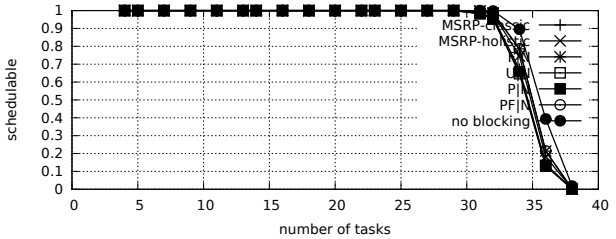

Fig. 247. Schedulability under non-preemptable spin locks for $m = 4$, $U = 0.1n$, 4 resources, $rsf = 0.1$, $N^{max} = 5$, and medium critical sections. The schedulability of the considered preemptable lock types in this configuration is shown in Fig. 257.

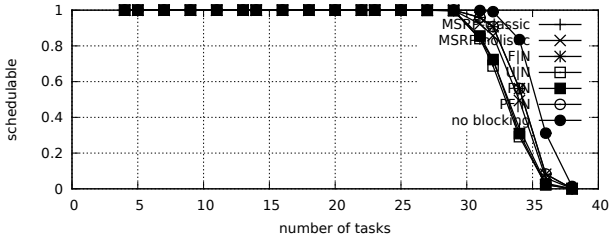

Fig. 248. Schedulability under non-preemptable spin locks for $m = 4$, $U = 0.1n$, 4 resources, $rsf = 0.1$, $N^{max} = 10$, and medium critical sections. The schedulability of the considered preemptable lock types in this configuration is shown in Fig. 258.

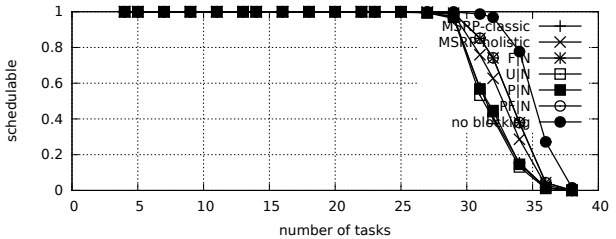

Fig. 249. Schedulability under non-preemptable spin locks for $m = 4$, $U = 0.1n$, 4 resources, $rsf = 0.1$, $N^{max} = 15$, and medium critical sections. The schedulability of the considered preemptable lock types in this configuration is shown in Fig. 259.

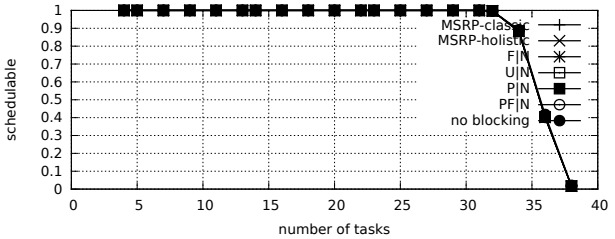

Fig. 250. Schedulability under non-preemptable spin locks for $m = 4$, $U = 0.1n$, 4 resources, $rsf = 0.1$, $N^{max} = 1$, and short critical sections. The schedulability of the considered preemptable lock types in this configuration is shown in Fig. 260.

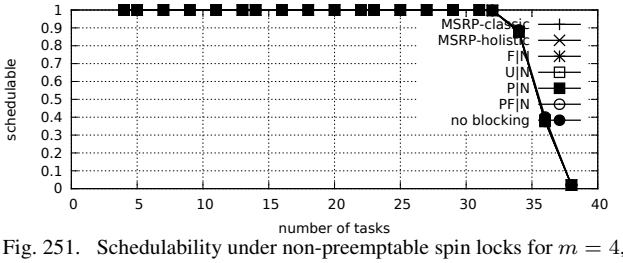

Fig. 251. Schedulability under non-preemptable spin locks for $m = 4$, $U = 0.1n$, 4 resources, $rsf = 0.1$, $N^{max} = 2$, and short critical sections. The schedulability of the considered preemptable lock types in this configuration is shown in Fig. 261.

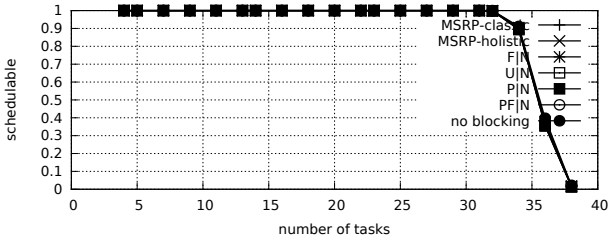

Fig. 252. Schedulability under non-preemptable spin locks for $m = 4$, $U = 0.1n$, 4 resources, $rsf = 0.1$, $N^{max} = 5$, and short critical sections. The schedulability of the considered preemptable lock types in this configuration is shown in Fig. 262.

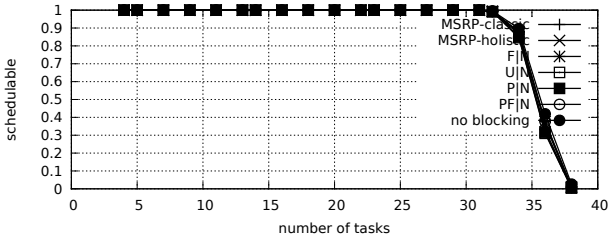

Fig. 253. Schedulability under non-preemptable spin locks for $m = 4$, $U = 0.1n$, 4 resources, $rsf = 0.1$, $N^{max} = 10$, and short critical sections. The schedulability of the considered preemptable lock types in this configuration is shown in Fig. 263.

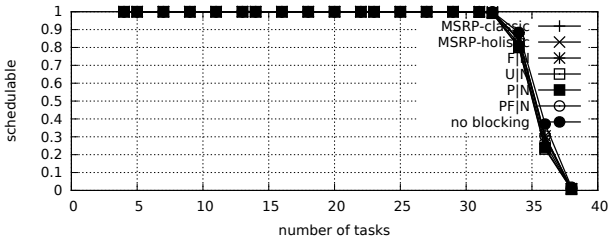

Fig. 254. Schedulability under non-preemptable spin locks for $m = 4$, $U = 0.1n$, 4 resources, $rsf = 0.1$, $N^{max} = 15$, and short critical sections. The schedulability of the considered preemptable lock types in this configuration is shown in Fig. 264.

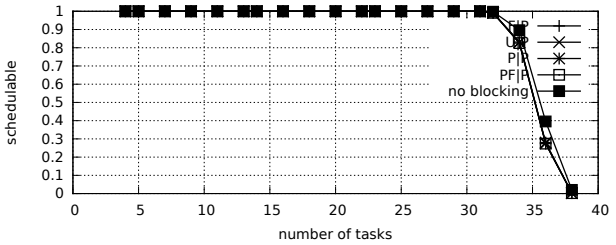

Fig. 255. Schedulability under preemptable spin locks for $m = 4$, $U = 0.1n$, 4 resources, $rsf = 0.1$, $N^{max} = 1$, and medium critical sections. The schedulability of the considered non-preemptable lock types in this configuration is shown in Fig. 245.

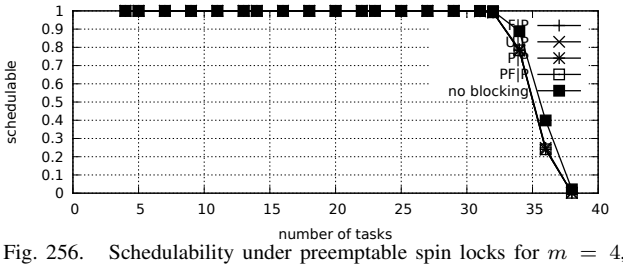

Fig. 256. Schedulability under preemptable spin locks for $m = 4$, $U = 0.1n$, 4 resources, $rsf = 0.1$, $N^{max} = 2$, and medium critical sections. The schedulability of the considered non-preemptable lock types in this configuration is shown in Fig. 246.

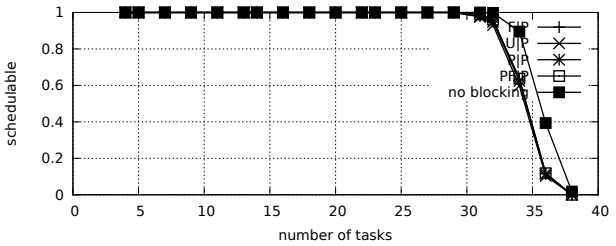

Fig. 257. Schedulability under preemptable spin locks for $m = 4$, $U = 0.1n$, 4 resources, $rsf = 0.1$, $N^{max} = 5$, and medium critical sections. The schedulability of the considered non-preemptable lock types in this configuration is shown in Fig. 247.

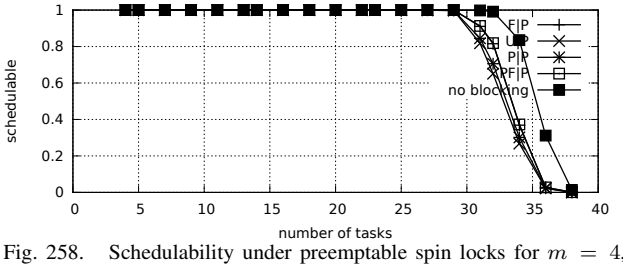

Fig. 258. Schedulability under preemptable spin locks for $m = 4$, $U = 0.1n$, 4 resources, $rsf = 0.1$, $N^{max} = 10$, and medium critical sections. The schedulability of the considered non-preemptable lock types in this configuration is shown in Fig. 248.

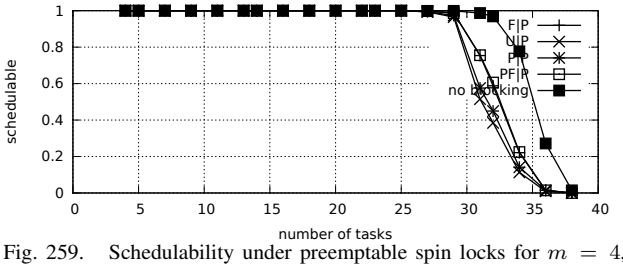

Fig. 259. Schedulability under preemptable spin locks for $m = 4$, $U = 0.1n$, 4 resources, $rsf = 0.1$, $N^{max} = 15$, and medium critical sections. The schedulability of the considered non-preemptable lock types in this configuration is shown in Fig. 249.

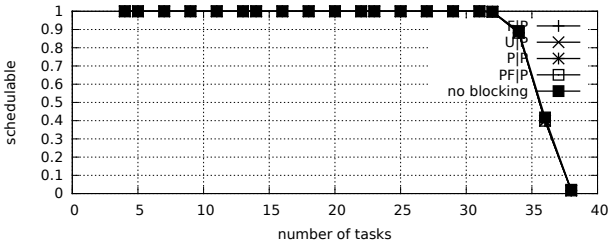

Fig. 260. Schedulability under preemptable spin locks for $m = 4$, $U = 0.1n$, 4 resources, $rsf = 0.1$, $N^{max} = 1$, and short critical sections. The schedulability of the considered non-preemptable lock types in this configuration is shown in Fig. 250.

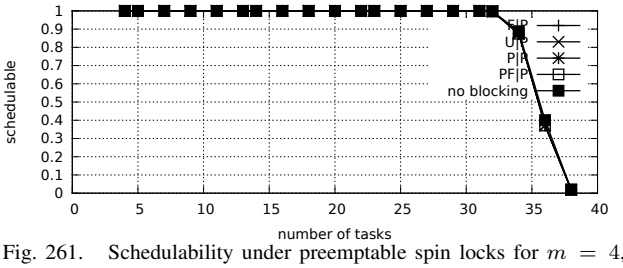

Fig. 261. Schedulability under preemptable spin locks for $m = 4$, $U = 0.1n$, 4 resources, $rsf = 0.1$, $N^{max} = 2$, and short critical sections. The schedulability of the considered non-preemptable lock types in this configuration is shown in Fig. 251.

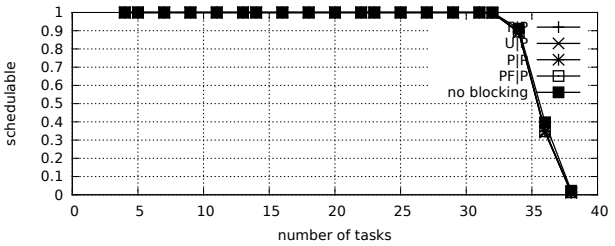

Fig. 262. Schedulability under preemptable spin locks for $m = 4$, $U = 0.1n$, 4 resources, $rsf = 0.1$, $N^{max} = 5$, and short critical sections. The schedulability of the considered non-preemptable lock types in this configuration is shown in Fig. 252.

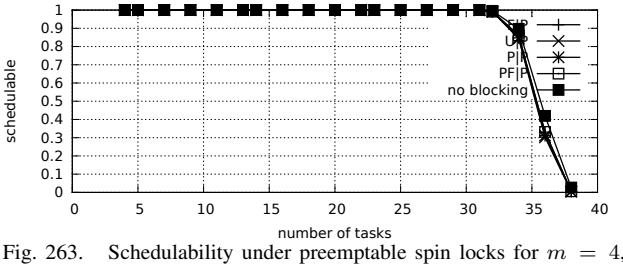

Fig. 263. Schedulability under preemptable spin locks for $m = 4$, $U = 0.1n$, 4 resources, $rsf = 0.1$, $N^{max} = 10$, and short critical sections. The schedulability of the considered non-preemptable lock types in this configuration is shown in Fig. 253.

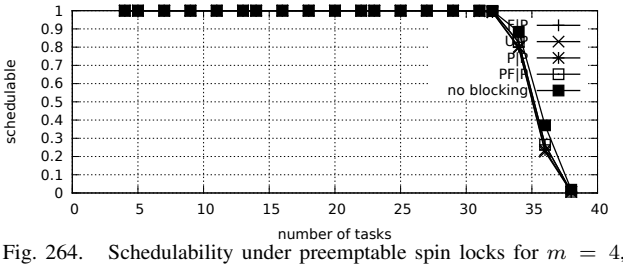

Fig. 264. Schedulability under preemptable spin locks for $m = 4$, $U = 0.1n$, 4 resources, $rsf = 0.1$, $N^{max} = 15$, and short critical sections. The schedulability of the considered non-preemptable lock types in this configuration is shown in Fig. 254.

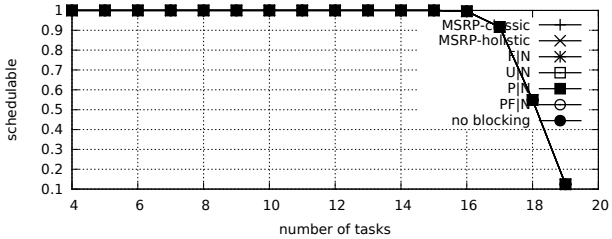

Fig. 265. Schedulability under non-preemptable spin locks for $m = 4$, $U = 0.2n$, 4 resources, $rsf = 0.1$, $N^{max} = 1$, and medium critical sections. The schedulability of the considered preemptable lock types in this configuration is shown in Fig. 275.

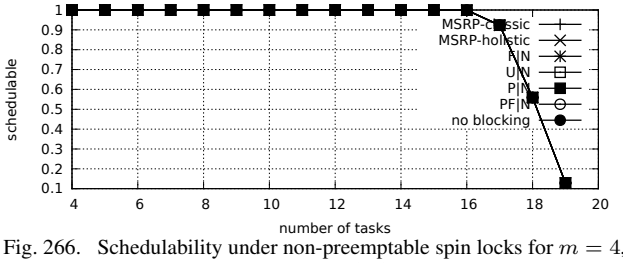

Fig. 266. Schedulability under non-preemptable spin locks for $m = 4$, $U = 0.2n$, 4 resources, $rsf = 0.1$, $N^{max} = 2$, and medium critical sections. The schedulability of the considered preemptable lock types in this configuration is shown in Fig. 276.

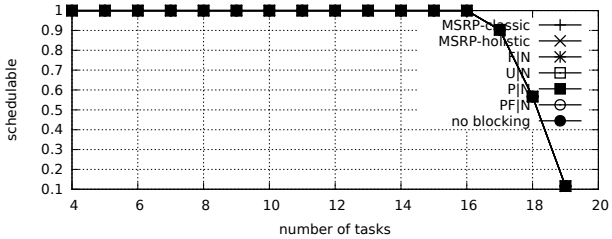

Fig. 267. Schedulability under non-preemptable spin locks for $m = 4$, $U = 0.2n$, 4 resources, $rsf = 0.1$, $N^{max} = 5$, and medium critical sections. The schedulability of the considered preemptable lock types in this configuration is shown in Fig. 277.

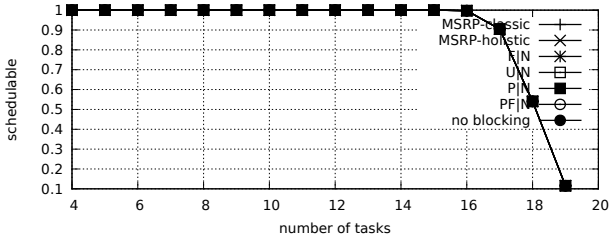

Fig. 268. Schedulability under non-preemptable spin locks for $m = 4$, $U = 0.2n$, 4 resources, $rsf = 0.1$, $N^{max} = 10$, and medium critical sections. The schedulability of the considered preemptable lock types in this configuration is shown in Fig. 278.

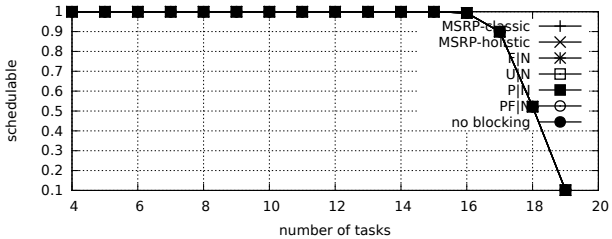

Fig. 269. Schedulability under non-preemptable spin locks for $m = 4$, $U = 0.2n$, 4 resources, $rsf = 0.1$, $N^{max} = 15$, and medium critical sections. The schedulability of the considered preemptable lock types in this configuration is shown in Fig. 279.

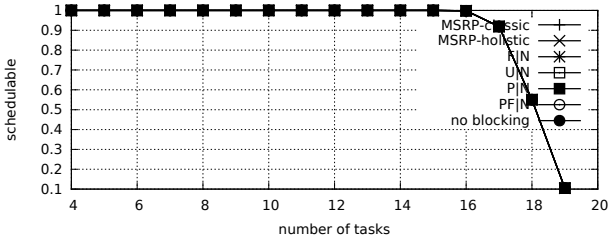

Fig. 270. Schedulability under non-preemptable spin locks for $m = 4$, $U = 0.2n$, 4 resources, $rsf = 0.1$, $N^{max} = 1$, and short critical sections. The schedulability of the considered preemptable lock types in this configuration is shown in Fig. 280.

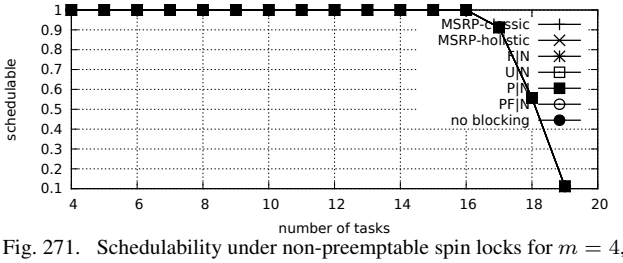

Fig. 271. Schedulability under non-preemptable spin locks for $m = 4$, $U = 0.2n$, 4 resources, $rsf = 0.1$, $N^{max} = 2$, and short critical sections. The schedulability of the considered preemptable lock types in this configuration is shown in Fig. 281.

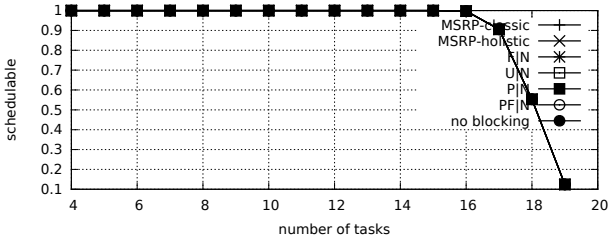

Fig. 272. Schedulability under non-preemptable spin locks for $m = 4$, $U = 0.2n$, 4 resources, $rsf = 0.1$, $N^{max} = 5$, and short critical sections. The schedulability of the considered preemptable lock types in this configuration is shown in Fig. 282.

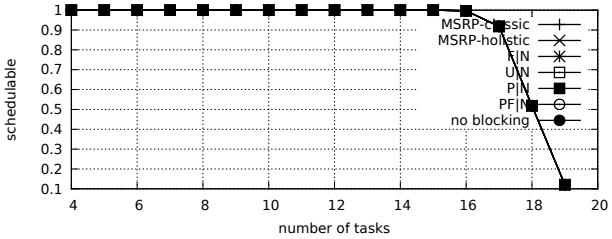

Fig. 273. Schedulability under non-preemptable spin locks for $m = 4$, $U = 0.2n$, 4 resources, $rsf = 0.1$, $N^{max} = 10$, and short critical sections. The schedulability of the considered preemptable lock types in this configuration is shown in Fig. 283.

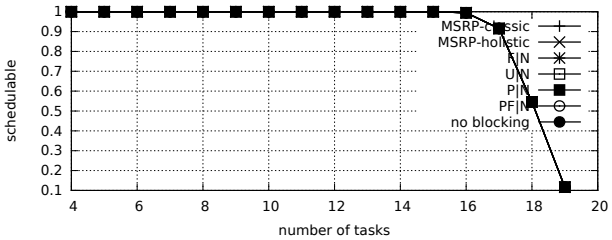

Fig. 274. Schedulability under non-preemptable spin locks for $m = 4$, $U = 0.2n$, 4 resources, $rsf = 0.1$, $N^{max} = 15$, and short critical sections. The schedulability of the considered preemptable lock types in this configuration is shown in Fig. 284.

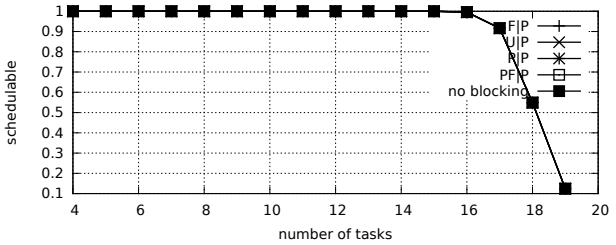

Fig. 275. Schedulability under preemptable spin locks for $m = 4$, $U = 0.2n$, 4 resources, $rsf = 0.1$, $N^{max} = 1$, and medium critical sections. The schedulability of the considered non-preemptable lock types in this configuration is shown in Fig. 265.

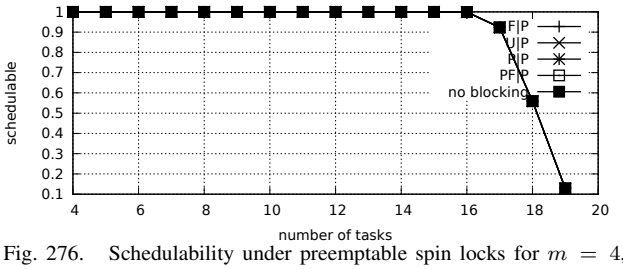

Fig. 276. Schedulability under preemptable spin locks for $m = 4$, $U = 0.2n$, 4 resources, $rsf = 0.1$, $N^{max} = 2$, and medium critical sections. The schedulability of the considered non-preemptable lock types in this configuration is shown in Fig. 266.

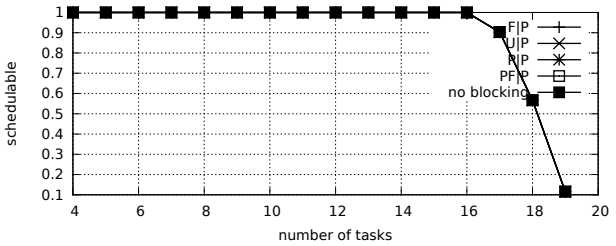

Fig. 277. Schedulability under preemptable spin locks for $m = 4$, $U = 0.2n$, 4 resources, $rsf = 0.1$, $N^{max} = 5$, and medium critical sections. The schedulability of the considered non-preemptable lock types in this configuration is shown in Fig. 267.

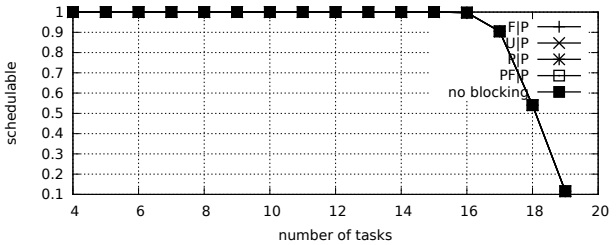

Fig. 278. Schedulability under preemptable spin locks for $m = 4$, $U = 0.2n$, 4 resources, $rsf = 0.1$, $N^{max} = 10$, and medium critical sections. The schedulability of the considered non-preemptable lock types in this configuration is shown in Fig. 268.

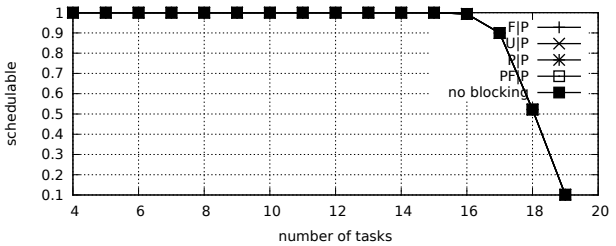

Fig. 279. Schedulability under preemptable spin locks for $m = 4$, $U = 0.2n$, 4 resources, $rsf = 0.1$, $N^{max} = 15$, and medium critical sections. The schedulability of the considered non-preemptable lock types in this configuration is shown in Fig. 269.

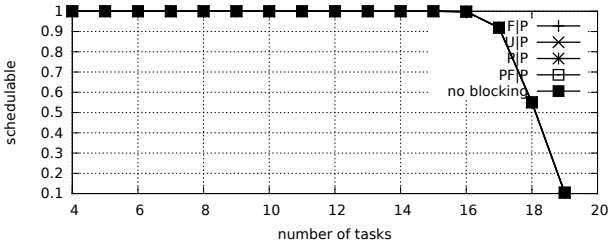

Fig. 280. Schedulability under preemptable spin locks for $m = 4$, $U = 0.2n$, 4 resources, $rsf = 0.1$, $N^{max} = 1$, and short critical sections. The schedulability of the considered non-preemptable lock types in this configuration is shown in Fig. 270.

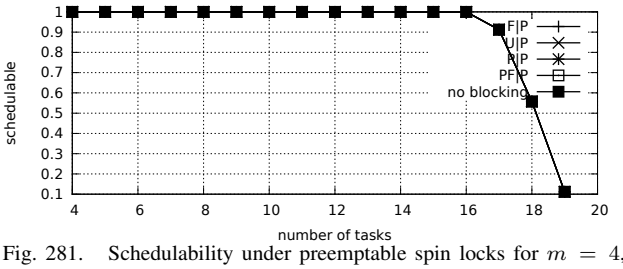

Fig. 281. Schedulability under preemptable spin locks for $m = 4$, $U = 0.2n$, 4 resources, $rsf = 0.1$, $N^{max} = 2$, and short critical sections. The schedulability of the considered non-preemptable lock types in this configuration is shown in Fig. 271.

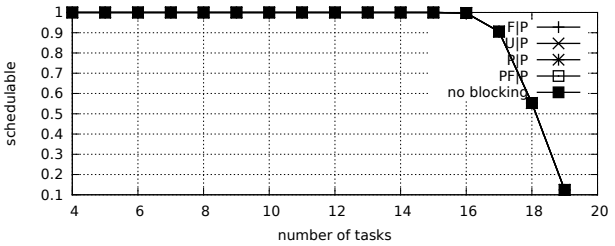

Fig. 282. Schedulability under preemptable spin locks for $m = 4$, $U = 0.2n$, 4 resources, $rsf = 0.1$, $N^{max} = 5$, and short critical sections. The schedulability of the considered non-preemptable lock types in this configuration is shown in Fig. 272.

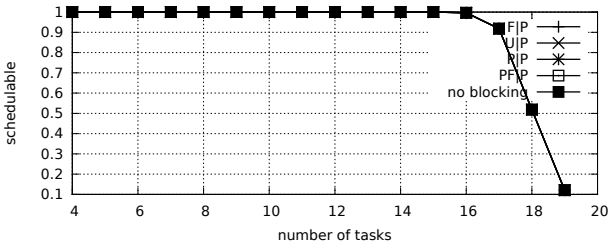

Fig. 283. Schedulability under preemptable spin locks for $m = 4$, $U = 0.2n$, 4 resources, $rsf = 0.1$, $N^{max} = 10$, and short critical sections. The schedulability of the considered non-preemptable lock types in this configuration is shown in Fig. 273.

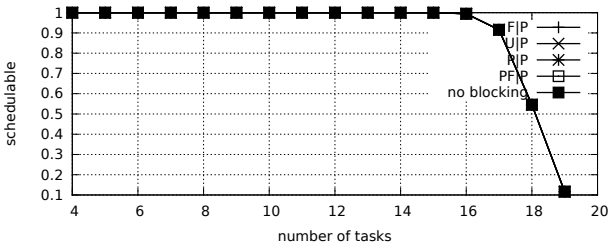

Fig. 284. Schedulability under preemptable spin locks for $m = 4$, $U = 0.2n$, 4 resources, $rsf = 0.1$, $N^{max} = 15$, and short critical sections. The schedulability of the considered non-preemptable lock types in this configuration is shown in Fig. 274.

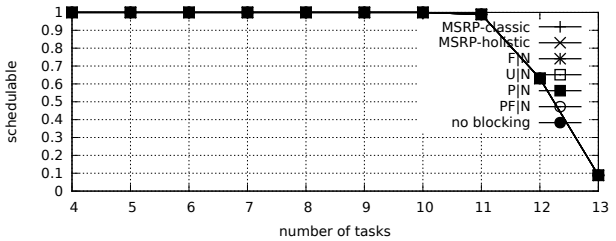

Fig. 285. Schedulability under non-preemptable spin locks for $m = 4$, $U = 0.3n$, 4 resources, $rsf = 0.1$, $N^{max} = 1$, and medium critical sections. The schedulability of the considered preemptable lock types in this configuration is shown in Fig. 295.

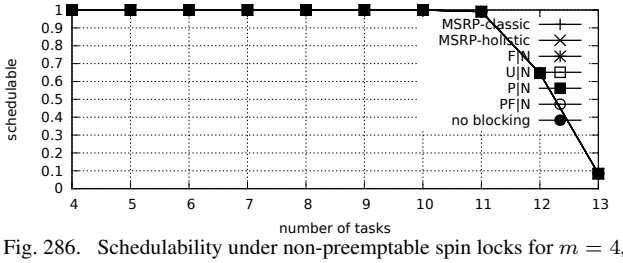

Fig. 286. Schedulability under non-preemptable spin locks for $m = 4$, $U = 0.3n$, 4 resources, $rsf = 0.1$, $N^{max} = 2$, and medium critical sections. The schedulability of the considered preemptable lock types in this configuration is shown in Fig. 296.

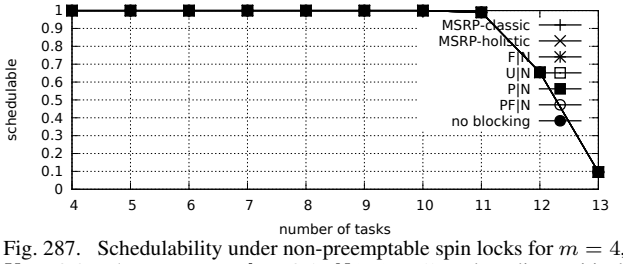

Fig. 287. Schedulability under non-preemptable spin locks for $m = 4$, $U = 0.3n$, 4 resources, $rsf = 0.1$, $N^{max} = 5$, and medium critical sections. The schedulability of the considered preemptable lock types in this configuration is shown in Fig. 297.

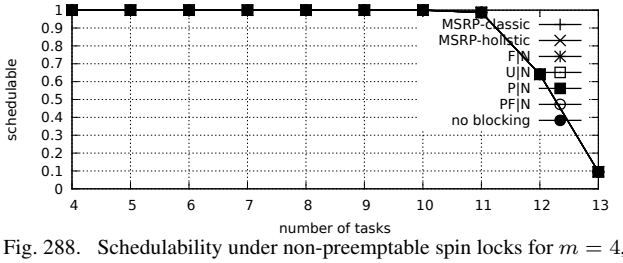

Fig. 288. Schedulability under non-preemptable spin locks for $m = 4$, $U = 0.3n$, 4 resources, $rsf = 0.1$, $N^{max} = 10$, and medium critical sections. The schedulability of the considered preemptable lock types in this configuration is shown in Fig. 298.

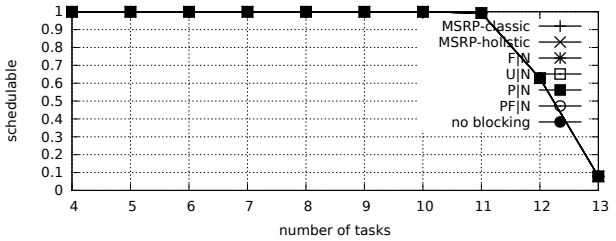

Fig. 289. Schedulability under non-preemptable spin locks for $m = 4$, $U = 0.3n$, 4 resources, $rsf = 0.1$, $N^{max} = 15$, and medium critical sections. The schedulability of the considered preemptable lock types in this configuration is shown in Fig. 299.

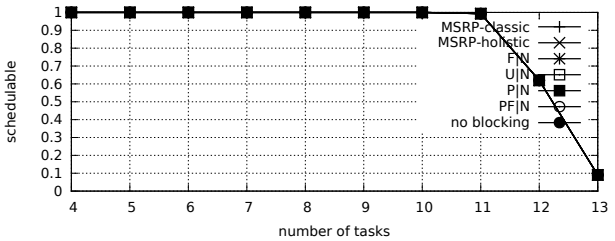

Fig. 290. Schedulability under non-preemptable spin locks for $m = 4$, $U = 0.3n$, 4 resources, $rsf = 0.1$, $N^{max} = 1$, and short critical sections. The schedulability of the considered preemptable lock types in this configuration is shown in Fig. 300.

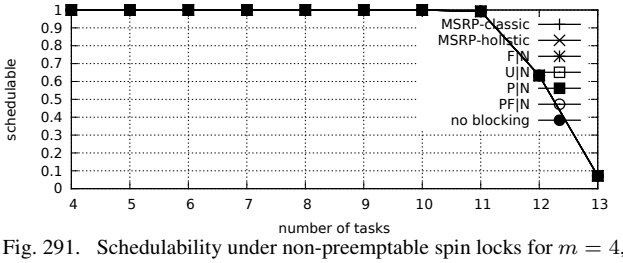

Fig. 291. Schedulability under non-preemptable spin locks for $m = 4$, $U = 0.3n$, 4 resources, $rsf = 0.1$, $N^{max} = 2$, and short critical sections. The schedulability of the considered preemptable lock types in this configuration is shown in Fig. 301.

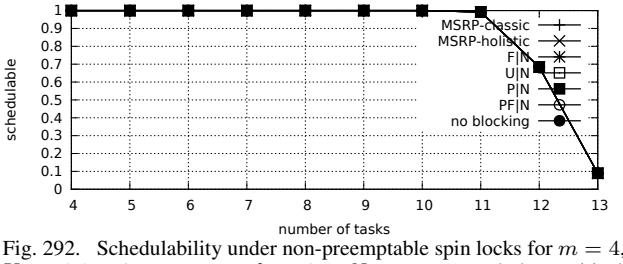

Fig. 292. Schedulability under non-preemptable spin locks for $m = 4$, $U = 0.3n$, 4 resources, $rsf = 0.1$, $N^{max} = 5$, and short critical sections. The schedulability of the considered preemptable lock types in this configuration is shown in Fig. 302.

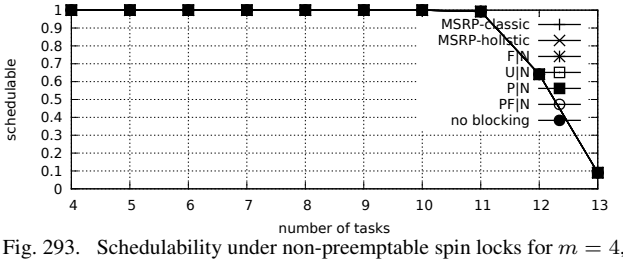

Fig. 293. Schedulability under non-preemptable spin locks for $m = 4$, $U = 0.3n$, 4 resources, $rsf = 0.1$, $N^{max} = 10$, and short critical sections. The schedulability of the considered preemptable lock types in this configuration is shown in Fig. 303.

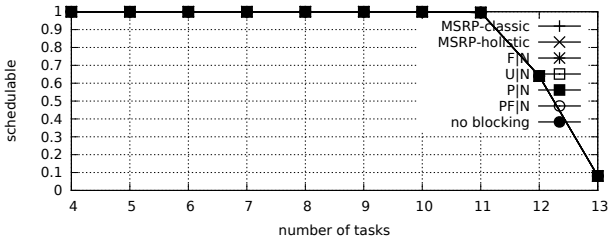

Fig. 294. Schedulability under non-preemptable spin locks for $m = 4$, $U = 0.3n$, 4 resources, $rsf = 0.1$, $N^{max} = 15$, and short critical sections. The schedulability of the considered preemptable lock types in this configuration is shown in Fig. 304.

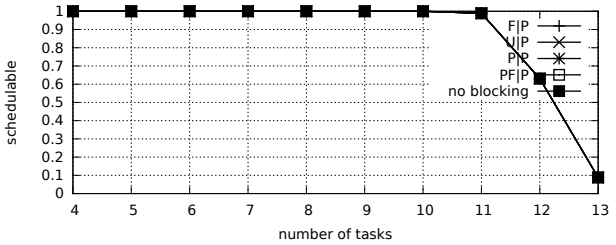

Fig. 295. Schedulability under preemptable spin locks for $m = 4$, $U = 0.3n$, 4 resources, $rsf = 0.1$, $N^{max} = 1$, and medium critical sections. The schedulability of the considered non-preemptable lock types in this configuration is shown in Fig. 285.

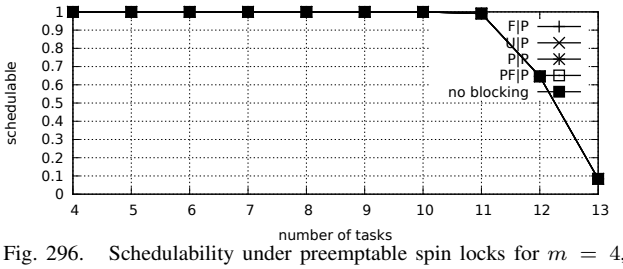

Fig. 296. Schedulability under preemptable spin locks for $m = 4$, $U = 0.3n$, 4 resources, $rsf = 0.1$, $N^{max} = 2$, and medium critical sections. The schedulability of the considered non-preemptable lock types in this configuration is shown in Fig. 286.

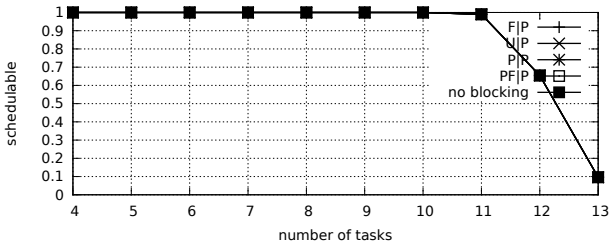

Fig. 297. Schedulability under preemptable spin locks for $m = 4$, $U = 0.3n$, 4 resources, $rsf = 0.1$, $N^{max} = 5$, and medium critical sections. The schedulability of the considered non-preemptable lock types in this configuration is shown in Fig. 287.

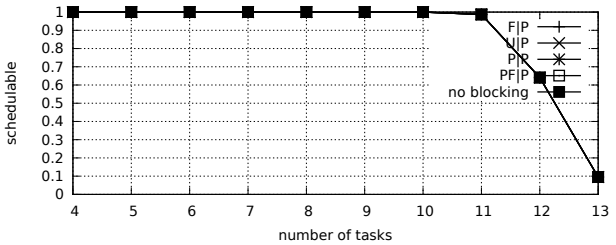

Fig. 298. Schedulability under preemptable spin locks for $m = 4$, $U = 0.3n$, 4 resources, $rsf = 0.1$, $N^{max} = 10$, and medium critical sections. The schedulability of the considered non-preemptable lock types in this configuration is shown in Fig. 288.

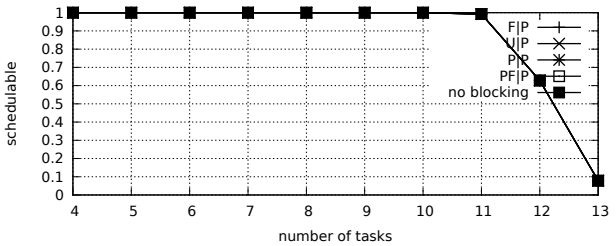

Fig. 299. Schedulability under preemptable spin locks for $m = 4$, $U = 0.3n$, 4 resources, $rsf = 0.1$, $N^{max} = 15$, and medium critical sections. The schedulability of the considered non-preemptable lock types in this configuration is shown in Fig. 289.

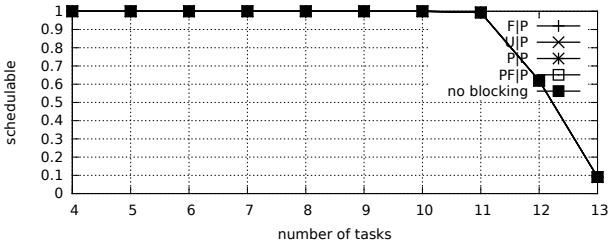

Fig. 300. Schedulability under preemptable spin locks for $m = 4$, $U = 0.3n$, 4 resources, $rsf = 0.1$, $N^{max} = 1$, and short critical sections. The schedulability of the considered non-preemptable lock types in this configuration is shown in Fig. 290.

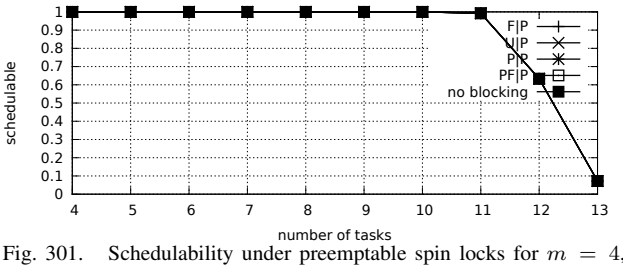

Fig. 301. Schedulability under preemptable spin locks for $m = 4$, $U = 0.3n$, 4 resources, $rsf = 0.1$, $N^{max} = 2$, and short critical sections. The schedulability of the considered non-preemptable lock types in this configuration is shown in Fig. 291.

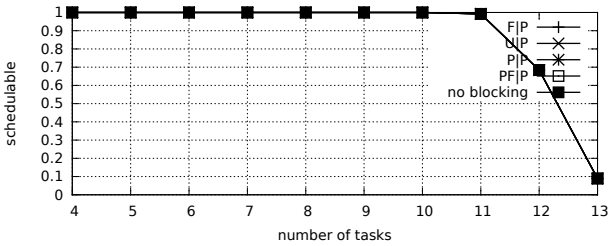

Fig. 302. Schedulability under preemptable spin locks for $m = 4$, $U = 0.3n$, 4 resources, $rsf = 0.1$, $N^{max} = 5$, and short critical sections. The schedulability of the considered non-preemptable lock types in this configuration is shown in Fig. 292.

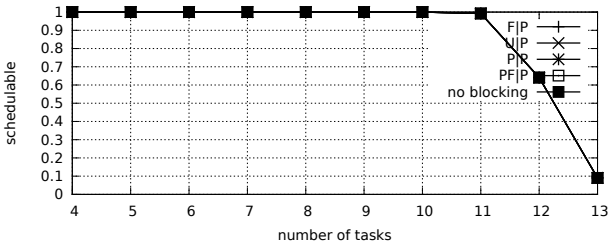

Fig. 303. Schedulability under preemptable spin locks for $m = 4$, $U = 0.3n$, 4 resources, $rsf = 0.1$, $N^{max} = 10$, and short critical sections. The schedulability of the considered non-preemptable lock types in this configuration is shown in Fig. 293.

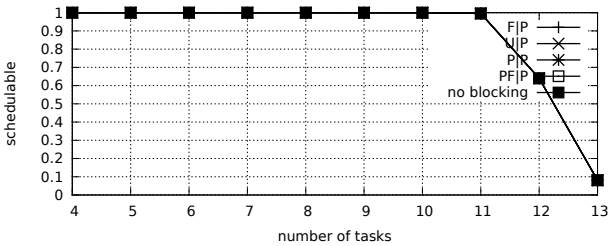

Fig. 304. Schedulability under preemptable spin locks for $m = 4$, $U = 0.3n$, 4 resources, $rsf = 0.1$, $N^{max} = 15$, and short critical sections. The schedulability of the considered non-preemptable lock types in this configuration is shown in Fig. 294.

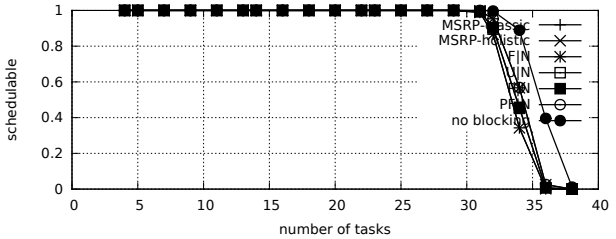

Fig. 305. Schedulability under non-preemptable spin locks for $m = 4$, $U = 0.1n$, 4 resources, $rsf = 0.25$, $N^{max} = 1$, and medium critical sections. The schedulability of the considered preemptable lock types in this configuration is shown in Fig. 315.

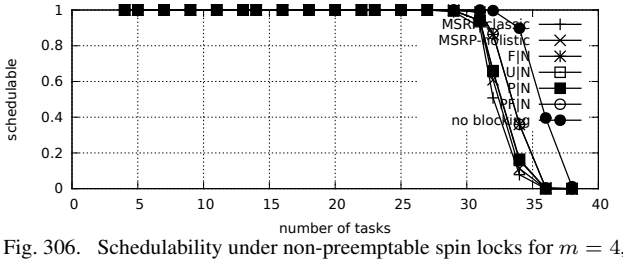

Fig. 306. Schedulability under non-preemptable spin locks for $m = 4$, $U = 0.1n$, 4 resources, $rsf = 0.25$, $N^{max} = 2$, and medium critical sections. The schedulability of the considered preemptable lock types in this configuration is shown in Fig. 316.

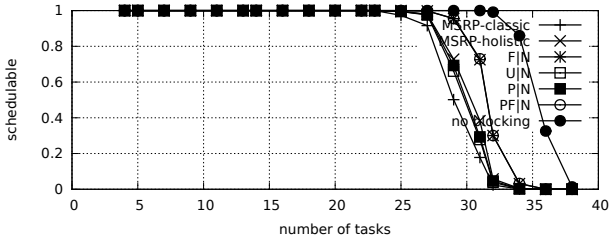

Fig. 307. Schedulability under non-preemptable spin locks for $m = 4$, $U = 0.1n$, 4 resources, $rsf = 0.25$, $N^{max} = 5$, and medium critical sections. The schedulability of the considered preemptable lock types in this configuration is shown in Fig. 317.

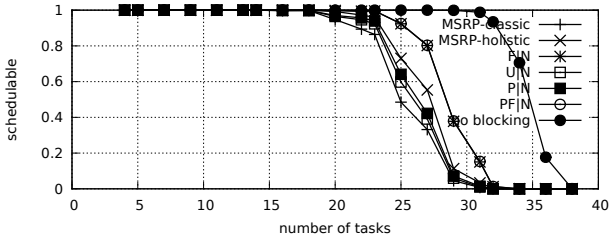

Fig. 308. Schedulability under non-preemptable spin locks for $m = 4$, $U = 0.1n$, 4 resources, $rsf = 0.25$, $N^{max} = 10$, and medium critical sections. The schedulability of the considered preemptable lock types in this configuration is shown in Fig. 318.

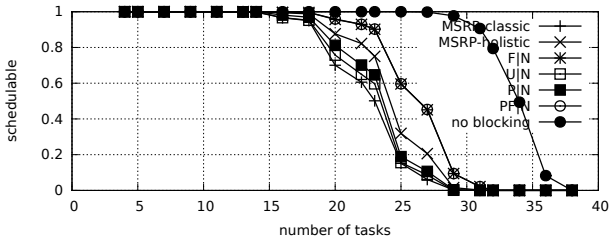

Fig. 309. Schedulability under non-preemptable spin locks for $m = 4$, $U = 0.1n$, 4 resources, $rsf = 0.25$, $N^{max} = 15$, and medium critical sections. The schedulability of the considered preemptable lock types in this configuration is shown in Fig. 319.

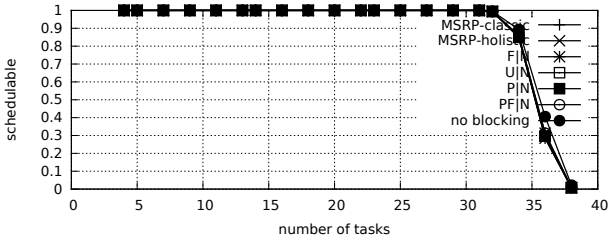

Fig. 310. Schedulability under non-preemptable spin locks for $m = 4$, $U = 0.1n$, 4 resources, $rsf = 0.25$, $N^{max} = 1$, and short critical sections. The schedulability of the considered preemptable lock types in this configuration is shown in Fig. 320.

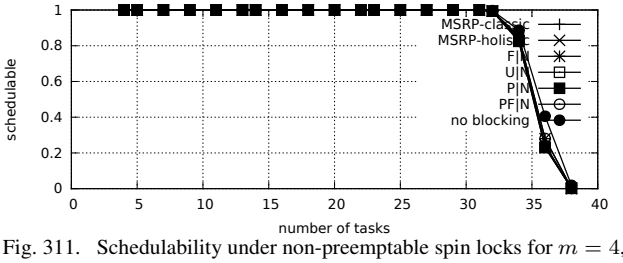

Fig. 311. Schedulability under non-preemptable spin locks for $m = 4$, $U = 0.1n$, 4 resources, $rsf = 0.25$, $N^{max} = 2$, and short critical sections. The schedulability of the considered preemptable lock types in this configuration is shown in Fig. 321.

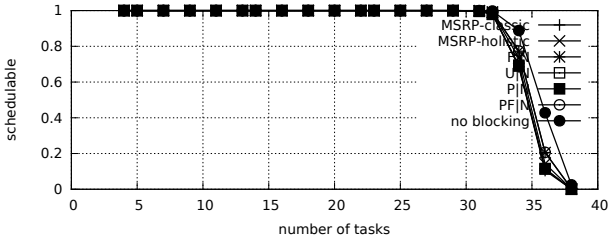

Fig. 312. Schedulability under non-preemptable spin locks for $m = 4$, $U = 0.1n$, 4 resources, $rsf = 0.25$, $N^{max} = 5$, and short critical sections. The schedulability of the considered preemptable lock types in this configuration is shown in Fig. 322.

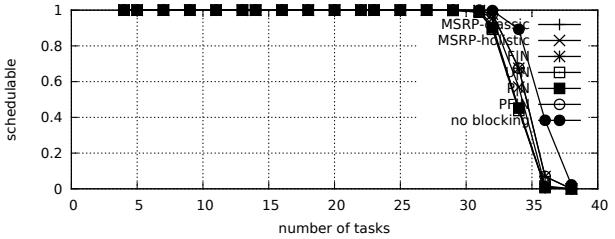

Fig. 313. Schedulability under non-preemptable spin locks for $m = 4$, $U = 0.1n$, 4 resources, $rsf = 0.25$, $N^{max} = 10$, and short critical sections. The schedulability of the considered preemptable lock types in this configuration is shown in Fig. 323.

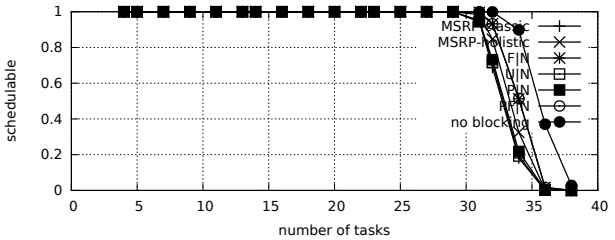

Fig. 314. Schedulability under non-preemptable spin locks for $m = 4$, $U = 0.1n$, 4 resources, $rsf = 0.25$, $N^{max} = 15$, and short critical sections. The schedulability of the considered preemptable lock types in this configuration is shown in Fig. 324.

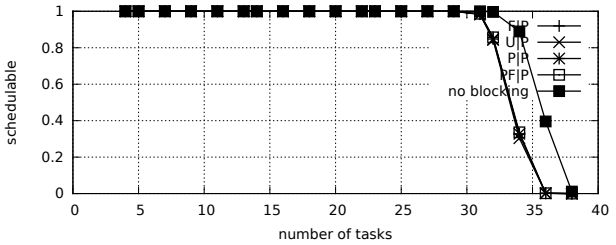

Fig. 315. Schedulability under preemptable spin locks for $m = 4$, $U = 0.1n$, 4 resources, $rsf = 0.25$, $N^{max} = 1$, and medium critical sections. The schedulability of the considered non-preemptable lock types in this configuration is shown in Fig. 305.

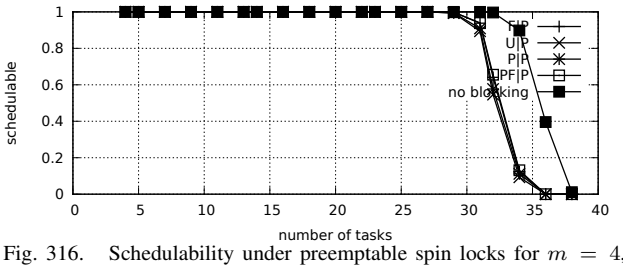

Fig. 316. Schedulability under preemptable spin locks for $m = 4$, $U = 0.1n$, 4 resources, $rsf = 0.25$, $N^{max} = 2$, and medium critical sections. The schedulability of the considered non-preemptable lock types in this configuration is shown in Fig. 306.

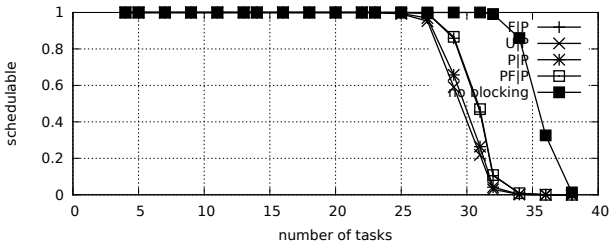

Fig. 317. Schedulability under preemptable spin locks for $m = 4$, $U = 0.1n$, 4 resources, $rsf = 0.25$, $N^{max} = 5$, and medium critical sections. The schedulability of the considered non-preemptable lock types in this configuration is shown in Fig. 307.

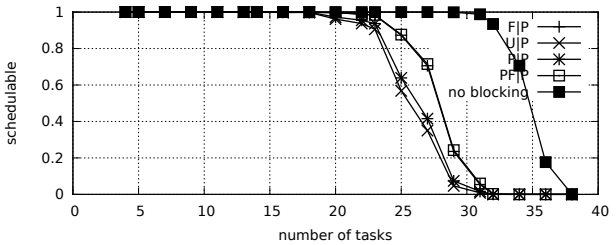

Fig. 318. Schedulability under preemptable spin locks for $m = 4$, $U = 0.1n$, 4 resources, $rsf = 0.25$, $N^{max} = 10$, and medium critical sections. The schedulability of the considered non-preemptable lock types in this configuration is shown in Fig. 308.

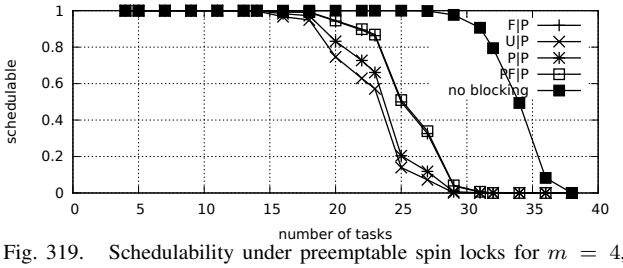

Fig. 319. Schedulability under preemptable spin locks for $m = 4$, $U = 0.1n$, 4 resources, $rsf = 0.25$, $N^{max} = 15$, and medium critical sections. The schedulability of the considered non-preemptable lock types in this configuration is shown in Fig. 309.

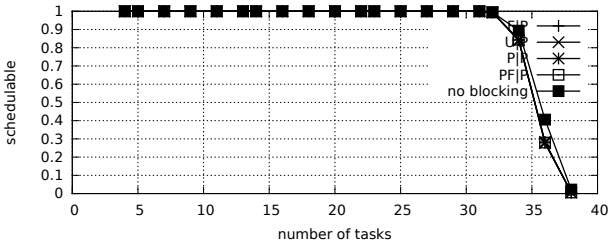

Fig. 320. Schedulability under preemptable spin locks for $m = 4$, $U = 0.1n$, 4 resources, $rsf = 0.25$, $N^{max} = 1$, and short critical sections. The schedulability of the considered non-preemptable lock types in this configuration is shown in Fig. 310.

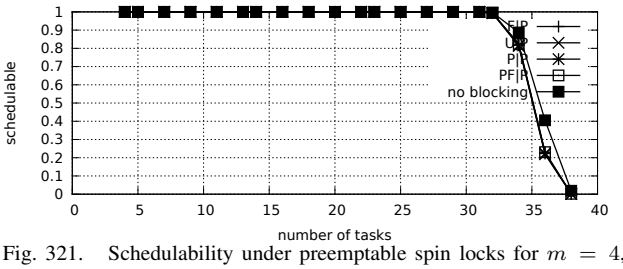

Fig. 321. Schedulability under preemptable spin locks for $m = 4$, $U = 0.1n$, 4 resources, $rsf = 0.25$, $N^{max} = 2$, and short critical sections. The schedulability of the considered non-preemptable lock types in this configuration is shown in Fig. 311.

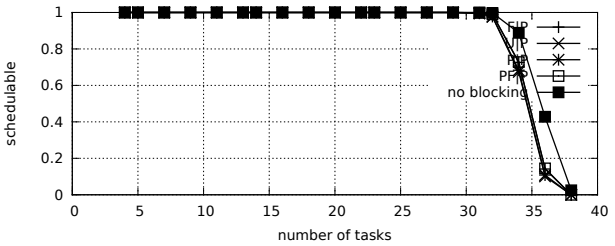

Fig. 322. Schedulability under preemptable spin locks for $m = 4$, $U = 0.1n$, 4 resources, $rsf = 0.25$, $N^{max} = 5$, and short critical sections. The schedulability of the considered non-preemptable lock types in this configuration is shown in Fig. 312.

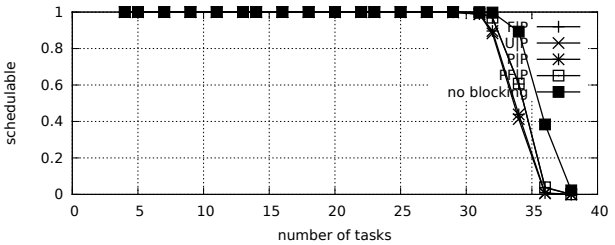

Fig. 323. Schedulability under preemptable spin locks for $m = 4$, $U = 0.1n$, 4 resources, $rsf = 0.25$, $N^{max} = 10$, and short critical sections. The schedulability of the considered non-preemptable lock types in this configuration is shown in Fig. 313.

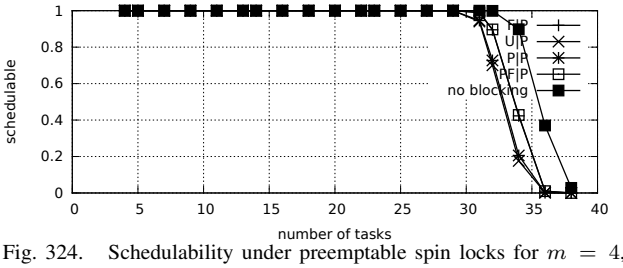

Fig. 324. Schedulability under preemptable spin locks for $m = 4$, $U = 0.1n$, 4 resources, $rsf = 0.25$, $N^{max} = 15$, and short critical sections. The schedulability of the considered non-preemptable lock types in this configuration is shown in Fig. 314.

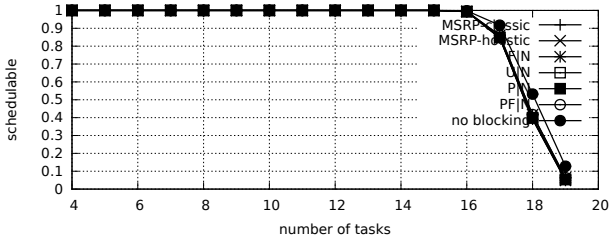

Fig. 325. Schedulability under non-preemptable spin locks for $m = 4$, $U = 0.2n$, 4 resources, $rsf = 0.25$, $N^{max} = 1$, and medium critical sections. The schedulability of the considered preemptable lock types in this configuration is shown in Fig. 335.

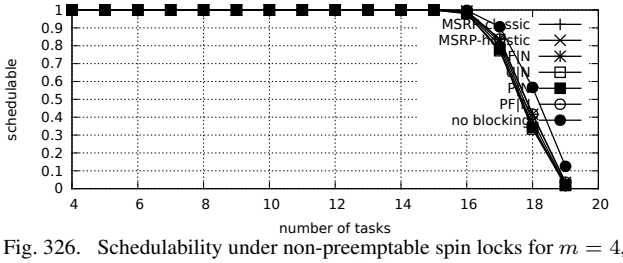

Fig. 326. Schedulability under non-preemptable spin locks for $m = 4$, $U = 0.2n$, 4 resources, $rsf = 0.25$, $N^{max} = 2$, and medium critical sections. The schedulability of the considered preemptable lock types in this configuration is shown in Fig. 336.

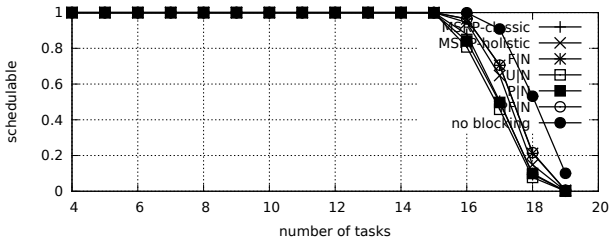

Fig. 327. Schedulability under non-preemptable spin locks for $m = 4$, $U = 0.2n$, 4 resources, $rsf = 0.25$, $N^{max} = 5$, and medium critical sections. The schedulability of the considered preemptable lock types in this configuration is shown in Fig. 337.

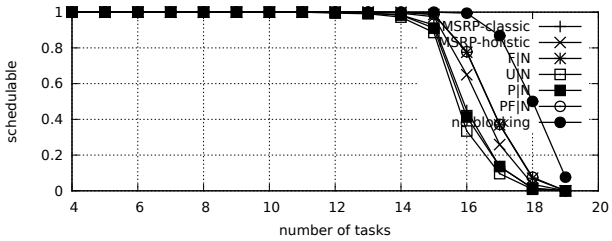

Fig. 328. Schedulability under non-preemptable spin locks for $m = 4$, $U = 0.2n$, 4 resources, $rsf = 0.25$, $N^{max} = 10$, and medium critical sections. The schedulability of the considered preemptable lock types in this configuration is shown in Fig. 338.

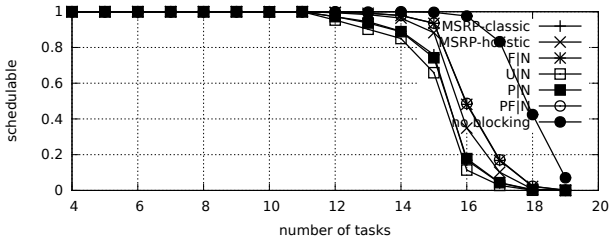

Fig. 329. Schedulability under non-preemptable spin locks for $m = 4$, $U = 0.2n$, 4 resources, $rsf = 0.25$, $N^{max} = 15$, and medium critical sections. The schedulability of the considered preemptable lock types in this configuration is shown in Fig. 339.

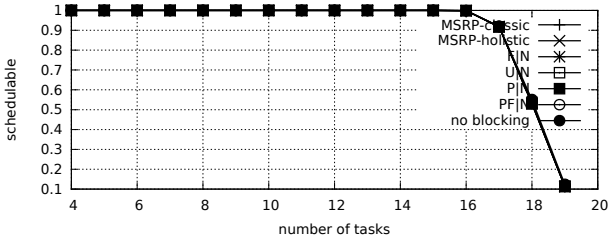

Fig. 330. Schedulability under non-preemptable spin locks for $m = 4$, $U = 0.2n$, 4 resources, $rsf = 0.25$, $N^{max} = 1$, and short critical sections. The schedulability of the considered preemptable lock types in this configuration is shown in Fig. 340.

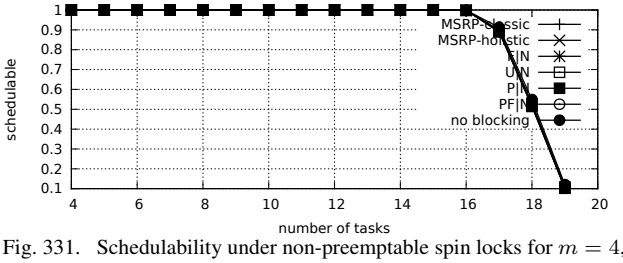

Fig. 331. Schedulability under non-preemptable spin locks for $m = 4$, $U = 0.2n$, 4 resources, $rsf = 0.25$, $N^{max} = 2$, and short critical sections. The schedulability of the considered preemptable lock types in this configuration is shown in Fig. 341.

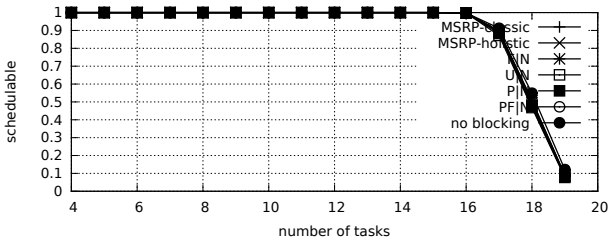

Fig. 332. Schedulability under non-preemptable spin locks for $m = 4$, $U = 0.2n$, 4 resources, $rsf = 0.25$, $N^{max} = 5$, and short critical sections. The schedulability of the considered preemptable lock types in this configuration is shown in Fig. 342.

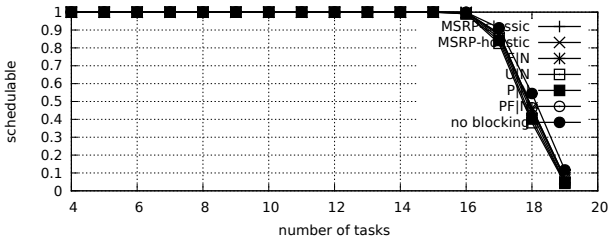

Fig. 333. Schedulability under non-preemptable spin locks for $m = 4$, $U = 0.2n$, 4 resources, $rsf = 0.25$, $N^{max} = 10$, and short critical sections. The schedulability of the considered preemptable lock types in this configuration is shown in Fig. 343.

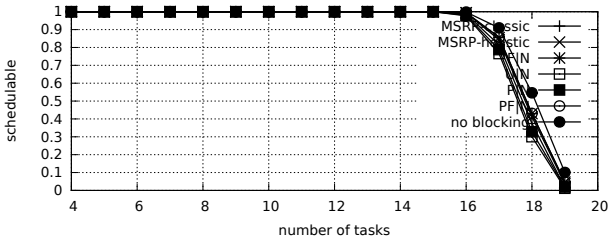

Fig. 334. Schedulability under non-preemptable spin locks for $m = 4$, $U = 0.2n$, 4 resources, $rsf = 0.25$, $N^{max} = 15$, and short critical sections. The schedulability of the considered preemptable lock types in this configuration is shown in Fig. 344.

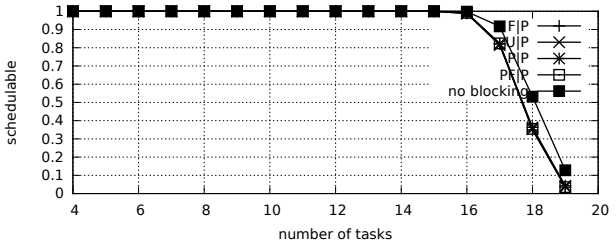

Fig. 335. Schedulability under preemptable spin locks for $m = 4$, $U = 0.2n$, 4 resources, $rsf = 0.25$, $N^{max} = 1$, and medium critical sections. The schedulability of the considered non-preemptable lock types in this configuration is shown in Fig. 325.

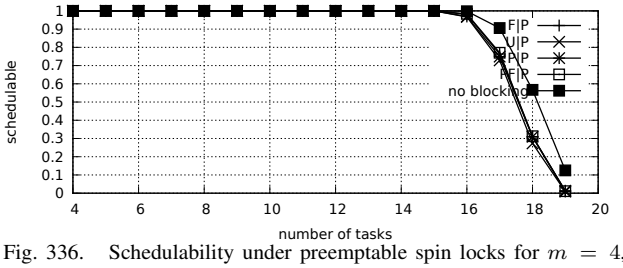

Fig. 336. Schedulability under preemptable spin locks for $m = 4$, $U = 0.2n$, 4 resources, $rsf = 0.25$, $N^{max} = 2$, and medium critical sections. The schedulability of the considered non-preemptable lock types in this configuration is shown in Fig. 326.

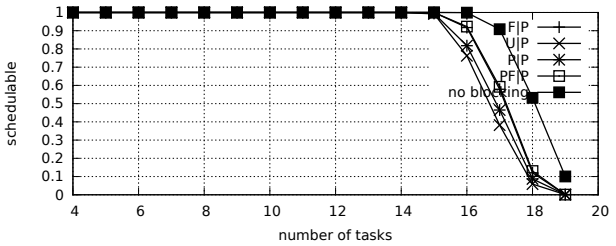

Fig. 337. Schedulability under preemptable spin locks for $m = 4$, $U = 0.2n$, 4 resources, $rsf = 0.25$, $N^{max} = 5$, and medium critical sections. The schedulability of the considered non-preemptable lock types in this configuration is shown in Fig. 327.

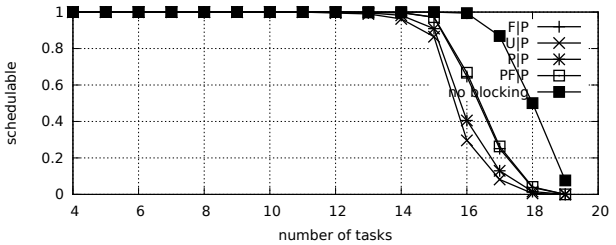

Fig. 338. Schedulability under preemptable spin locks for $m = 4$, $U = 0.2n$, 4 resources, $rsf = 0.25$, $N^{max} = 10$, and medium critical sections. The schedulability of the considered non-preemptable lock types in this configuration is shown in Fig. 328.

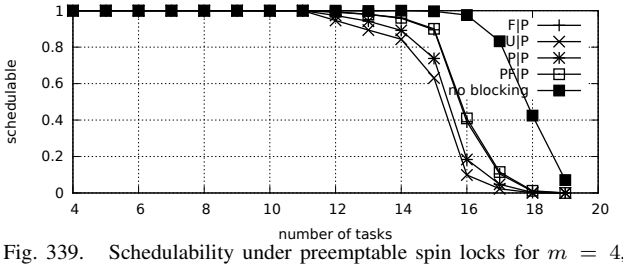

Fig. 339. Schedulability under preemptable spin locks for $m = 4$, $U = 0.2n$, 4 resources, $rsf = 0.25$, $N^{max} = 15$, and medium critical sections. The schedulability of the considered non-preemptable lock types in this configuration is shown in Fig. 329.

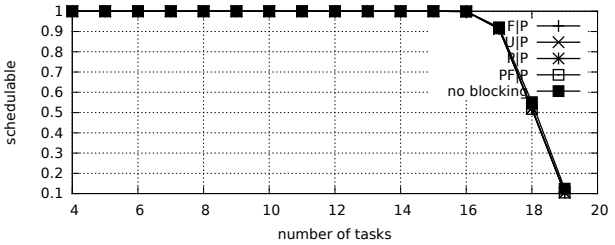

Fig. 340. Schedulability under preemptable spin locks for $m = 4$, $U = 0.2n$, 4 resources, $rsf = 0.25$, $N^{max} = 1$, and short critical sections. The schedulability of the considered non-preemptable lock types in this configuration is shown in Fig. 330.

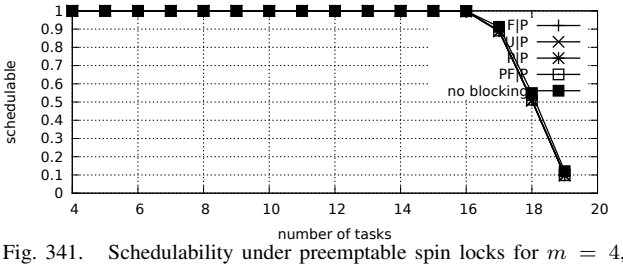

Fig. 341. Schedulability under preemptable spin locks for $m = 4$, $U = 0.2n$, 4 resources, $rsf = 0.25$, $N^{max} = 2$, and short critical sections. The schedulability of the considered non-preemptable lock types in this configuration is shown in Fig. 331.

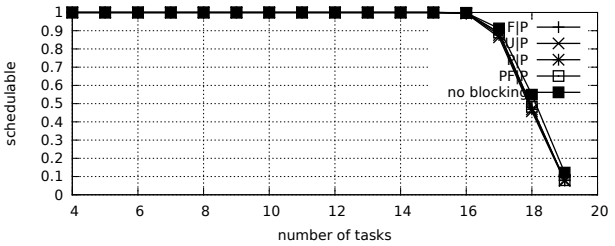

Fig. 342. Schedulability under preemptable spin locks for $m = 4$, $U = 0.2n$, 4 resources, $rsf = 0.25$, $N^{max} = 5$, and short critical sections. The schedulability of the considered non-preemptable lock types in this configuration is shown in Fig. 332.

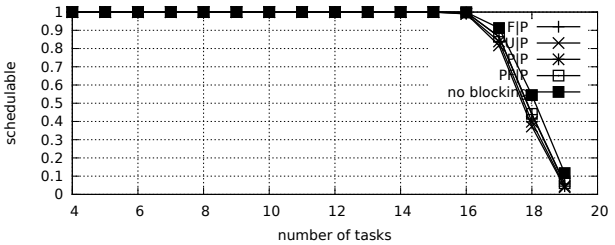

Fig. 343. Schedulability under preemptable spin locks for $m = 4$, $U = 0.2n$, 4 resources, $rsf = 0.25$, $N^{max} = 10$, and short critical sections. The schedulability of the considered non-preemptable lock types in this configuration is shown in Fig. 333.

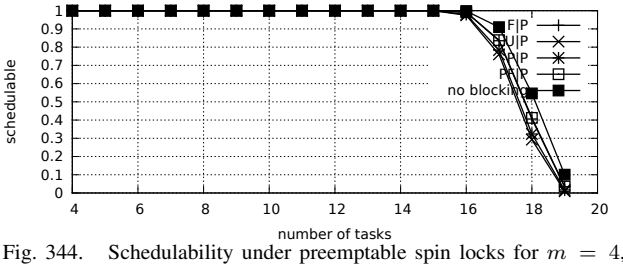

Fig. 344. Schedulability under preemptable spin locks for $m = 4$, $U = 0.2n$, 4 resources, $rsf = 0.25$, $N^{max} = 15$, and short critical sections. The schedulability of the considered non-preemptable lock types in this configuration is shown in Fig. 334.

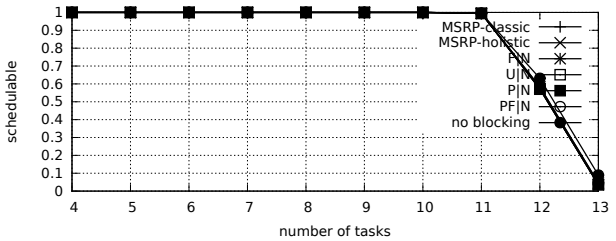

Fig. 345. Schedulability under non-preemptable spin locks for $m = 4$, $U = 0.3n$, 4 resources, $rsf = 0.25$, $N^{max} = 1$, and medium critical sections. The schedulability of the considered preemptable lock types in this configuration is shown in Fig. 355.

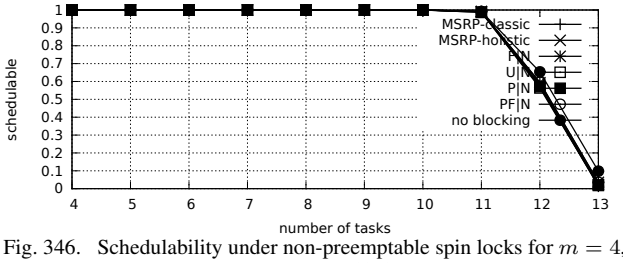

Fig. 346. Schedulability under non-preemptable spin locks for $m = 4$, $U = 0.3n$, 4 resources, $rsf = 0.25$, $N^{max} = 2$, and medium critical sections. The schedulability of the considered preemptable lock types in this configuration is shown in Fig. 356.

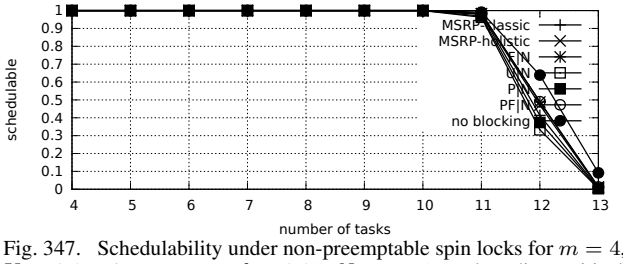

Fig. 347. Schedulability under non-preemptable spin locks for $m = 4$, $U = 0.3n$, 4 resources, $rsf = 0.25$, $N^{max} = 5$, and medium critical sections. The schedulability of the considered preemptable lock types in this configuration is shown in Fig. 357.

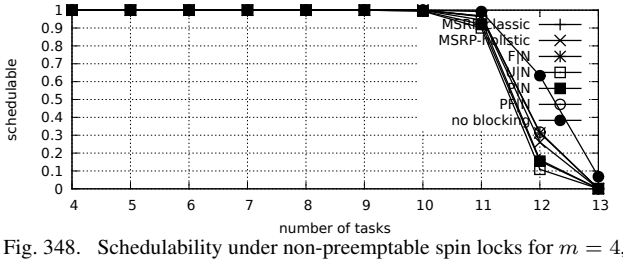

Fig. 348. Schedulability under non-preemptable spin locks for $m = 4$, $U = 0.3n$, 4 resources, $rsf = 0.25$, $N^{max} = 10$, and medium critical sections. The schedulability of the considered preemptable lock types in this configuration is shown in Fig. 358.

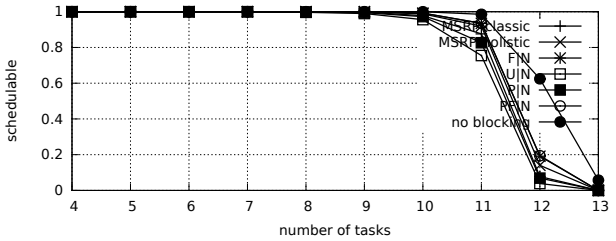

Fig. 349. Schedulability under non-preemptable spin locks for $m = 4$, $U = 0.3n$, 4 resources, $rsf = 0.25$, $N^{max} = 15$, and medium critical sections. The schedulability of the considered preemptable lock types in this configuration is shown in Fig. 359.

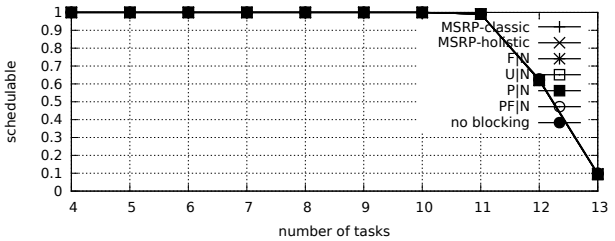

Fig. 350. Schedulability under non-preemptable spin locks for $m = 4$, $U = 0.3n$, 4 resources, $rsf = 0.25$, $N^{max} = 1$, and short critical sections. The schedulability of the considered preemptable lock types in this configuration is shown in Fig. 360.

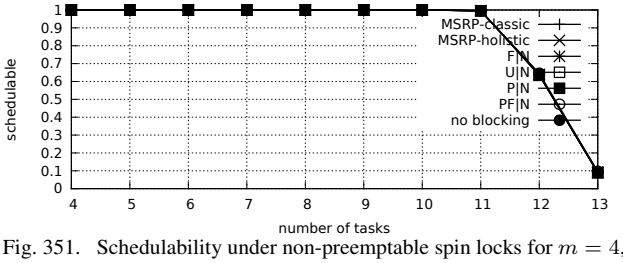

Fig. 351. Schedulability under non-preemptable spin locks for $m = 4$, $U = 0.3n$, 4 resources, $rsf = 0.25$, $N^{max} = 2$, and short critical sections. The schedulability of the considered preemptable lock types in this configuration is shown in Fig. 361.

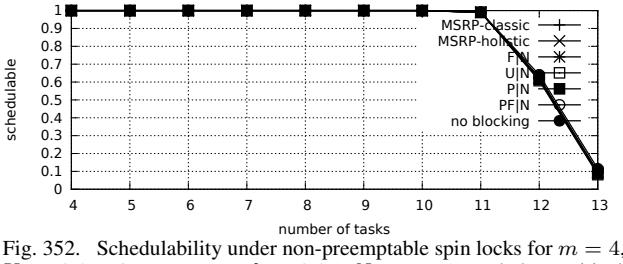

Fig. 352. Schedulability under non-preemptable spin locks for $m = 4$, $U = 0.3n$, 4 resources, $rsf = 0.25$, $N^{max} = 5$, and short critical sections. The schedulability of the considered preemptable lock types in this configuration is shown in Fig. 362.

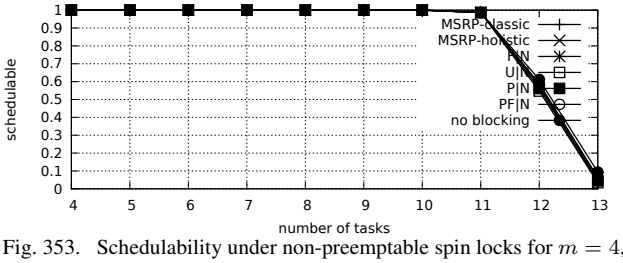

Fig. 353. Schedulability under non-preemptable spin locks for $m = 4$, $U = 0.3n$, 4 resources, $rsf = 0.25$, $N^{max} = 10$, and short critical sections. The schedulability of the considered preemptable lock types in this configuration is shown in Fig. 363.

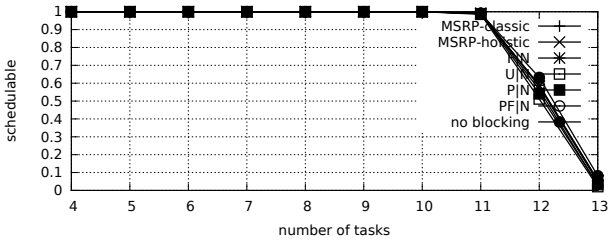

Fig. 354. Schedulability under non-preemptable spin locks for $m = 4$, $U = 0.3n$, 4 resources, $rsf = 0.25$, $N^{max} = 15$, and short critical sections. The schedulability of the considered preemptable lock types in this configuration is shown in Fig. 364.

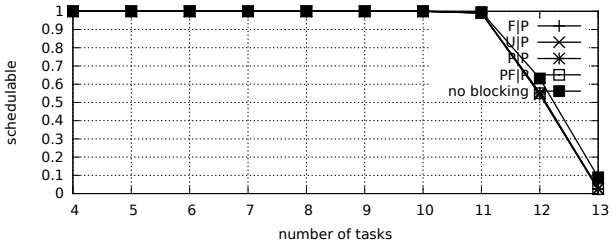

Fig. 355. Schedulability under preemptable spin locks for $m = 4$, $U = 0.3n$, 4 resources, $rsf = 0.25$, $N^{max} = 1$, and medium critical sections. The schedulability of the considered non-preemptable lock types in this configuration is shown in Fig. 345.

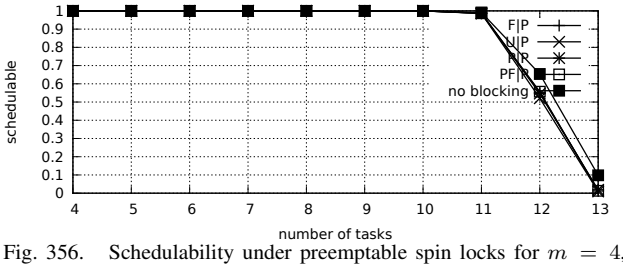

Fig. 356. Schedulability under preemptable spin locks for $m = 4$, $U = 0.3n$, 4 resources, $rsf = 0.25$, $N^{max} = 2$, and medium critical sections. The schedulability of the considered non-preemptable lock types in this configuration is shown in Fig. 346.

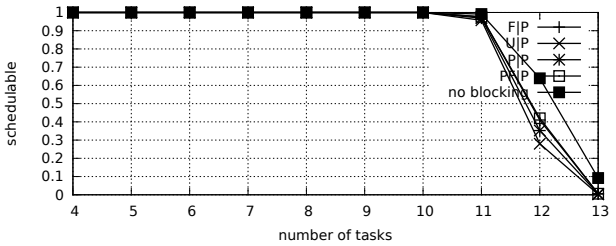

Fig. 357. Schedulability under preemptable spin locks for $m = 4$, $U = 0.3n$, 4 resources, $rsf = 0.25$, $N^{max} = 5$, and medium critical sections. The schedulability of the considered non-preemptable lock types in this configuration is shown in Fig. 347.

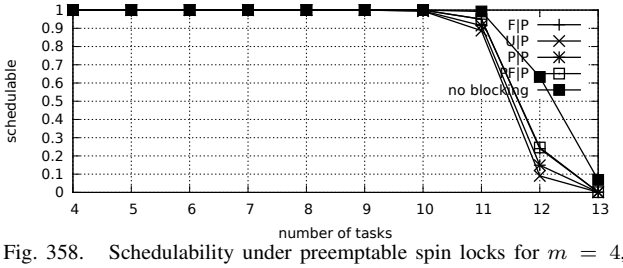

Fig. 358. Schedulability under preemptable spin locks for $m = 4$, $U = 0.3n$, 4 resources, $rsf = 0.25$, $N^{max} = 10$, and medium critical sections. The schedulability of the considered non-preemptable lock types in this configuration is shown in Fig. 348.

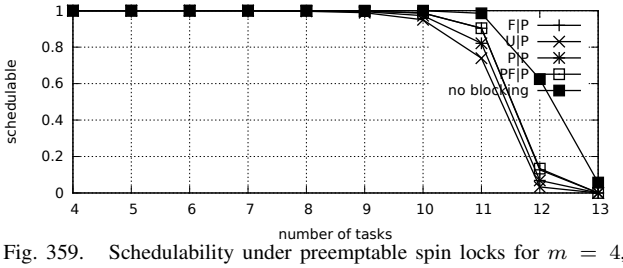

Fig. 359. Schedulability under preemptable spin locks for $m = 4$, $U = 0.3n$, 4 resources, $rsf = 0.25$, $N^{max} = 15$, and medium critical sections. The schedulability of the considered non-preemptable lock types in this configuration is shown in Fig. 349.

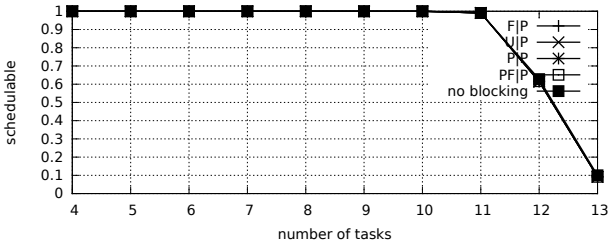

Fig. 360. Schedulability under preemptable spin locks for $m = 4$, $U = 0.3n$, 4 resources, $rsf = 0.25$, $N^{max} = 1$, and short critical sections. The schedulability of the considered non-preemptable lock types in this configuration is shown in Fig. 350.

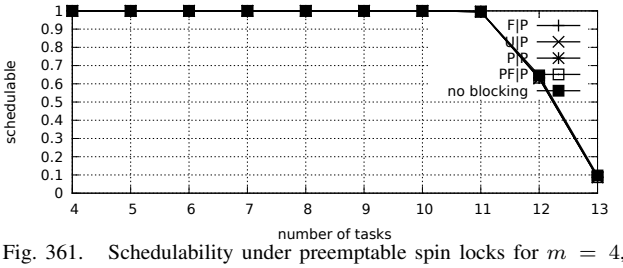

Fig. 361. Schedulability under preemptable spin locks for $m = 4$, $U = 0.3n$, 4 resources, $rsf = 0.25$, $N^{max} = 2$, and short critical sections. The schedulability of the considered non-preemptable lock types in this configuration is shown in Fig. 351.

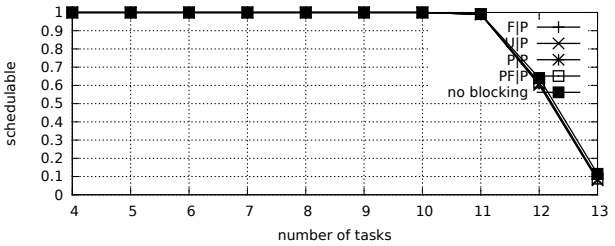

Fig. 362. Schedulability under preemptable spin locks for $m = 4$, $U = 0.3n$, 4 resources, $rsf = 0.25$, $N^{max} = 5$, and short critical sections. The schedulability of the considered non-preemptable lock types in this configuration is shown in Fig. 352.

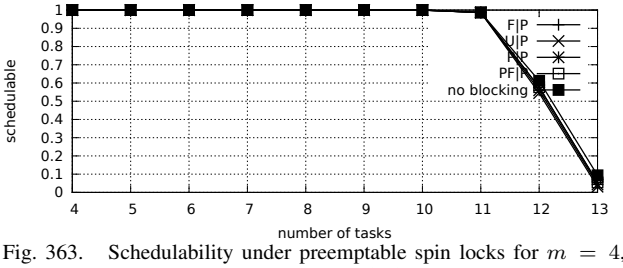

Fig. 363. Schedulability under preemptable spin locks for $m = 4$, $U = 0.3n$, 4 resources, $rsf = 0.25$, $N^{max} = 10$, and short critical sections. The schedulability of the considered non-preemptable lock types in this configuration is shown in Fig. 353.

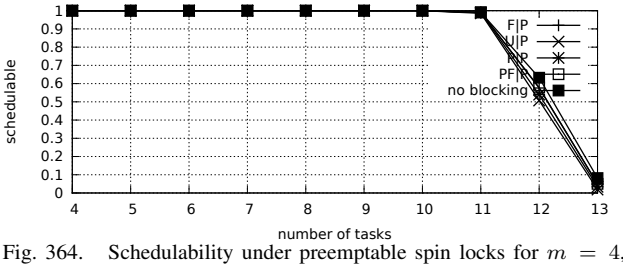

Fig. 364. Schedulability under preemptable spin locks for $m = 4$, $U = 0.3n$, 4 resources, $rsf = 0.25$, $N^{max} = 15$, and short critical sections. The schedulability of the considered non-preemptable lock types in this configuration is shown in Fig. 354.

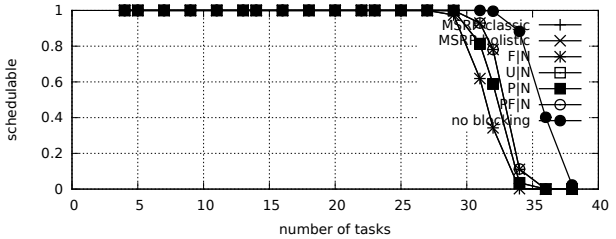

Fig. 365. Schedulability under non-preemptable spin locks for $m = 4$, $U = 0.1n$, 4 resources, $rsf = 0.4$, $N^{max} = 1$, and medium critical sections. The schedulability of the considered preemptable lock types in this configuration is shown in Fig. 375.

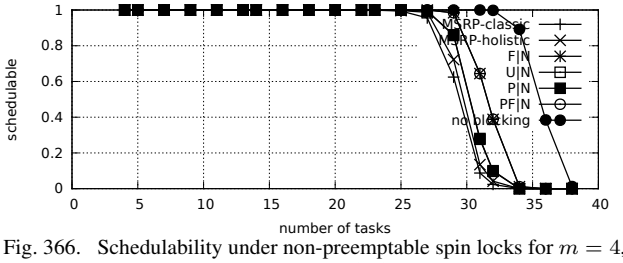

Fig. 366. Schedulability under non-preemptable spin locks for $m = 4$, $U = 0.1n$, 4 resources, $rsf = 0.4$, $N^{max} = 2$, and medium critical sections. The schedulability of the considered preemptable lock types in this configuration is shown in Fig. 376.

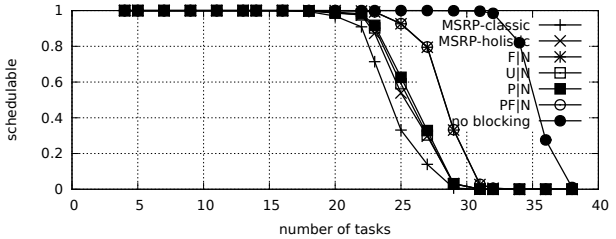

Fig. 367. Schedulability under non-preemptable spin locks for $m = 4$, $U = 0.1n$, 4 resources, $rsf = 0.4$, $N^{max} = 5$, and medium critical sections. The schedulability of the considered preemptable lock types in this configuration is shown in Fig. 377.

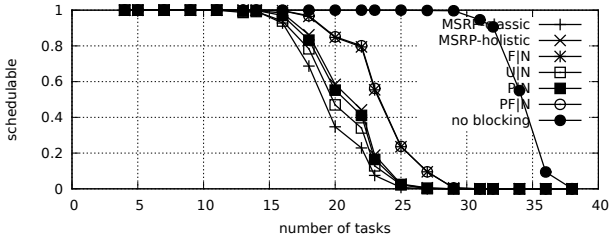

Fig. 368. Schedulability under non-preemptable spin locks for $m = 4$, $U = 0.1n$, 4 resources, $rsf = 0.4$, $N^{max} = 10$, and medium critical sections. The schedulability of the considered preemptable lock types in this configuration is shown in Fig. 378.

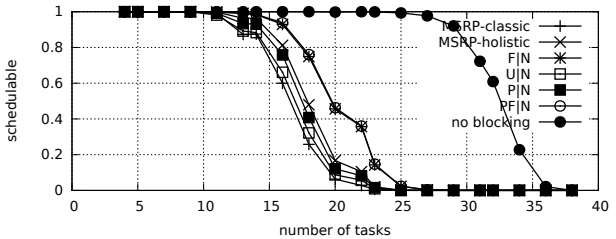

Fig. 369. Schedulability under non-preemptable spin locks for $m = 4$, $U = 0.1n$, 4 resources, $rsf = 0.4$, $N^{max} = 15$, and medium critical sections. The schedulability of the considered preemptable lock types in this configuration is shown in Fig. 379.

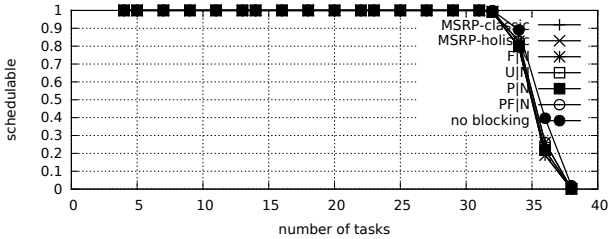

Fig. 370. Schedulability under non-preemptable spin locks for $m = 4$, $U = 0.1n$, 4 resources, $rsf = 0.4$, $N^{max} = 1$, and short critical sections. The schedulability of the considered preemptable lock types in this configuration is shown in Fig. 380.

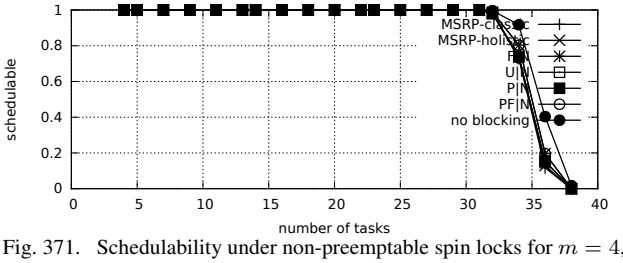

Fig. 371. Schedulability under non-preemptable spin locks for $m = 4$, $U = 0.1n$, 4 resources, $rsf = 0.4$, $N^{max} = 2$, and short critical sections. The schedulability of the considered preemptable lock types in this configuration is shown in Fig. 381.

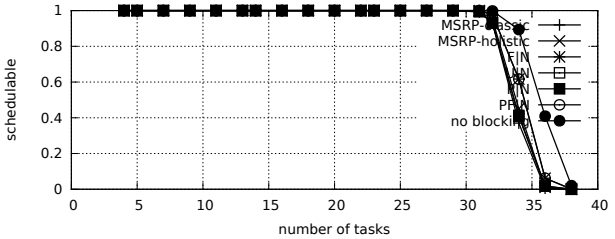

Fig. 372. Schedulability under non-preemptable spin locks for $m = 4$, $U = 0.1n$, 4 resources, $rsf = 0.4$, $N^{max} = 5$, and short critical sections. The schedulability of the considered preemptable lock types in this configuration is shown in Fig. 382.

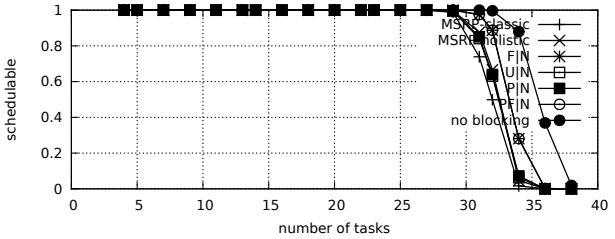

Fig. 373. Schedulability under non-preemptable spin locks for $m = 4$, $U = 0.1n$, 4 resources, $rsf = 0.4$, $N^{max} = 10$, and short critical sections. The schedulability of the considered preemptable lock types in this configuration is shown in Fig. 383.

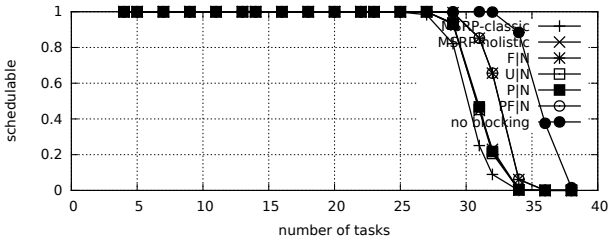

Fig. 374. Schedulability under non-preemptable spin locks for $m = 4$, $U = 0.1n$, 4 resources, $rsf = 0.4$, $N^{max} = 15$, and short critical sections. The schedulability of the considered preemptable lock types in this configuration is shown in Fig. 384.

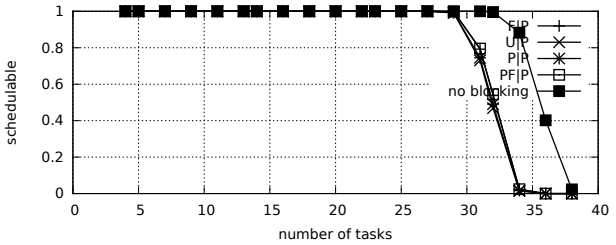

Fig. 375. Schedulability under preemptable spin locks for $m = 4$, $U = 0.1n$, 4 resources, $rsf = 0.4$, $N^{max} = 1$, and medium critical sections. The schedulability of the considered non-preemptable lock types in this configuration is shown in Fig. 365.

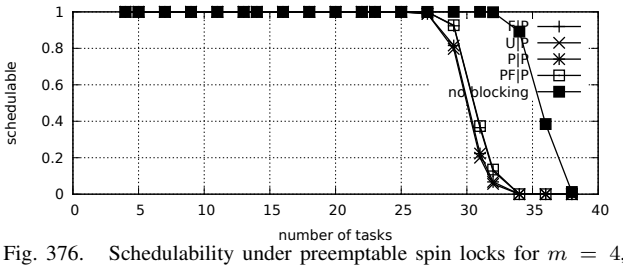

Fig. 376. Schedulability under preemptable spin locks for $m = 4$, $U = 0.1n$, 4 resources, $rsf = 0.4$, $N^{max} = 2$, and medium critical sections. The schedulability of the considered non-preemptable lock types in this configuration is shown in Fig. 366.

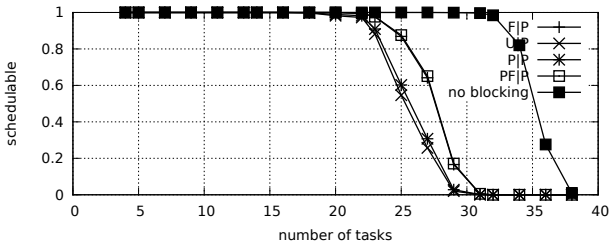

Fig. 377. Schedulability under preemptable spin locks for $m = 4$, $U = 0.1n$, 4 resources, $rsf = 0.4$, $N^{max} = 5$, and medium critical sections. The schedulability of the considered non-preemptable lock types in this configuration is shown in Fig. 367.

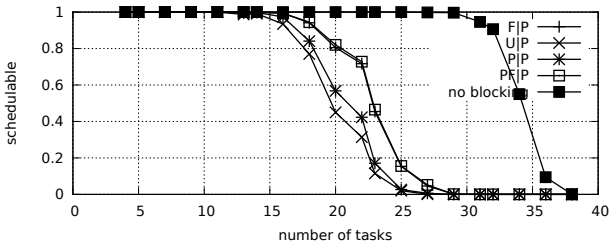

Fig. 378. Schedulability under preemptable spin locks for $m = 4$, $U = 0.1n$, 4 resources, $rsf = 0.4$, $N^{max} = 10$, and medium critical sections. The schedulability of the considered non-preemptable lock types in this configuration is shown in Fig. 368.

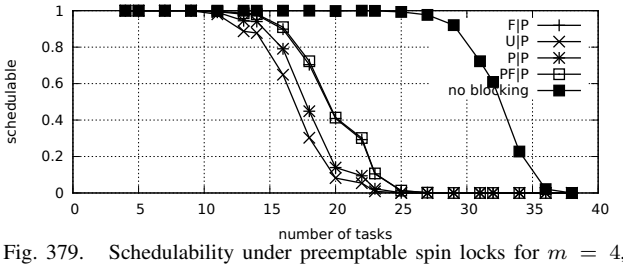

Fig. 379. Schedulability under preemptable spin locks for $m = 4$, $U = 0.1n$, 4 resources, $rsf = 0.4$, $N^{max} = 15$, and medium critical sections. The schedulability of the considered non-preemptable lock types in this configuration is shown in Fig. 369.

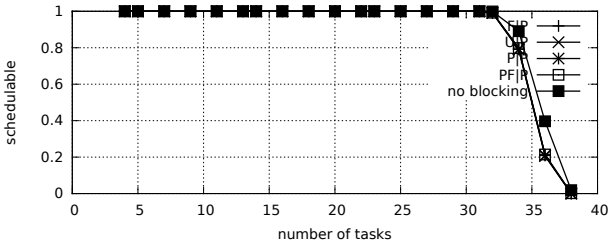

Fig. 380. Schedulability under preemptable spin locks for $m = 4$, $U = 0.1n$, 4 resources, $rsf = 0.4$, $N^{max} = 1$, and short critical sections. The schedulability of the considered non-preemptable lock types in this configuration is shown in Fig. 370.

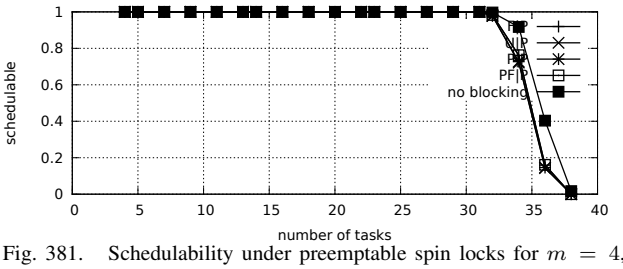

Fig. 381. Schedulability under preemptable spin locks for $m = 4$, $U = 0.1n$, 4 resources, $rsf = 0.4$, $N^{max} = 2$, and short critical sections. The schedulability of the considered non-preemptable lock types in this configuration is shown in Fig. 371.

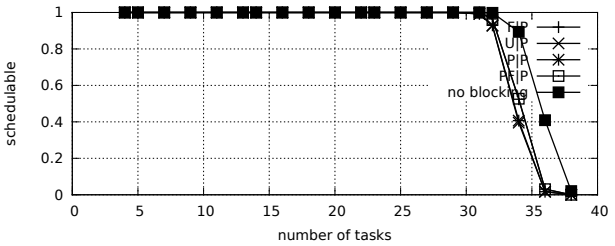

Fig. 382. Schedulability under preemptable spin locks for $m = 4$, $U = 0.1n$, 4 resources, $rsf = 0.4$, $N^{max} = 5$, and short critical sections. The schedulability of the considered non-preemptable lock types in this configuration is shown in Fig. 372.

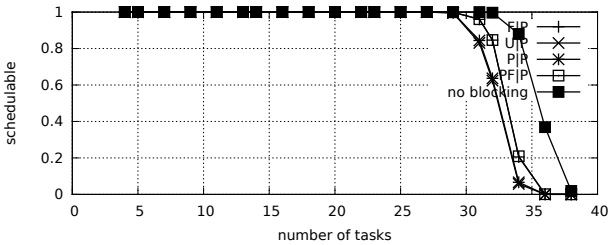

Fig. 383. Schedulability under preemptable spin locks for $m = 4$, $U = 0.1n$, 4 resources, $rsf = 0.4$, $N^{max} = 10$, and short critical sections. The schedulability of the considered non-preemptable lock types in this configuration is shown in Fig. 373.

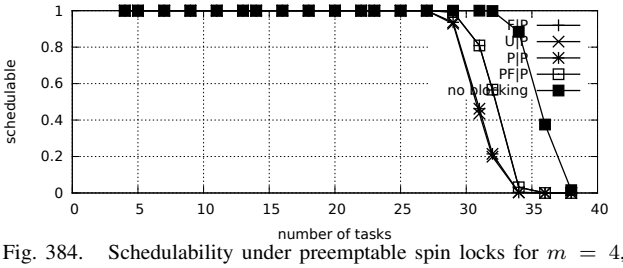

Fig. 384. Schedulability under preemptable spin locks for $m = 4$, $U = 0.1n$, 4 resources, $rsf = 0.4$, $N^{max} = 15$, and short critical sections. The schedulability of the considered non-preemptable lock types in this configuration is shown in Fig. 374.

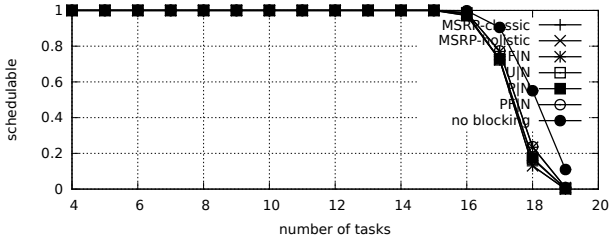

Fig. 385. Schedulability under non-preemptable spin locks for $m = 4$, $U = 0.2n$, 4 resources, $rsf = 0.4$, $N^{max} = 1$, and medium critical sections. The schedulability of the considered preemptable lock types in this configuration is shown in Fig. 395.

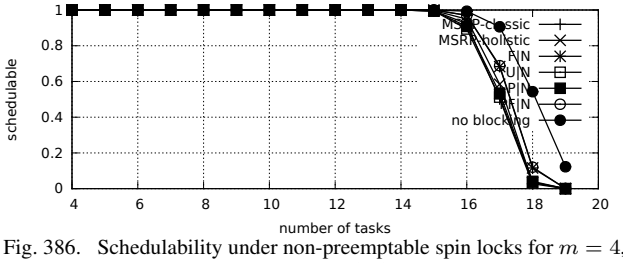

Fig. 386. Schedulability under non-preemptable spin locks for $m = 4$, $U = 0.2n$, 4 resources, $rsf = 0.4$, $N^{max} = 2$, and medium critical sections. The schedulability of the considered preemptable lock types in this configuration is shown in Fig. 396.

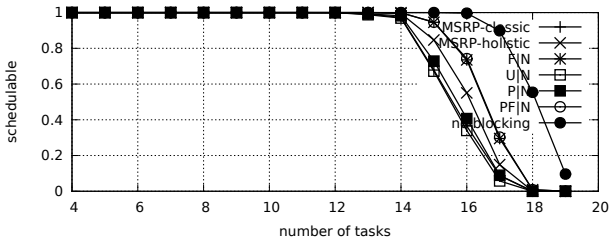

Fig. 387. Schedulability under non-preemptable spin locks for $m = 4$, $U = 0.2n$, 4 resources, $rsf = 0.4$, $N^{max} = 5$, and medium critical sections. The schedulability of the considered preemptable lock types in this configuration is shown in Fig. 397.

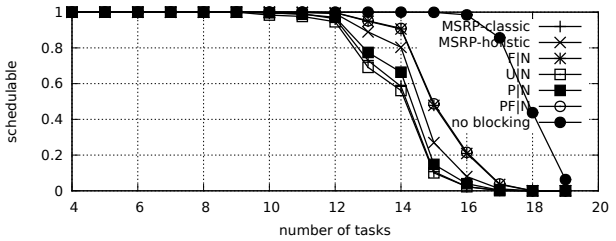

Fig. 388. Schedulability under non-preemptable spin locks for $m = 4$, $U = 0.2n$, 4 resources, $rsf = 0.4$, $N^{max} = 10$, and medium critical sections. The schedulability of the considered preemptable lock types in this configuration is shown in Fig. 398.

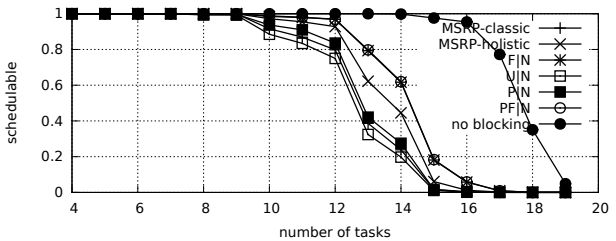

Fig. 389. Schedulability under non-preemptable spin locks for $m = 4$, $U = 0.2n$, 4 resources, $rsf = 0.4$, $N^{max} = 15$, and medium critical sections. The schedulability of the considered preemptable lock types in this configuration is shown in Fig. 399.

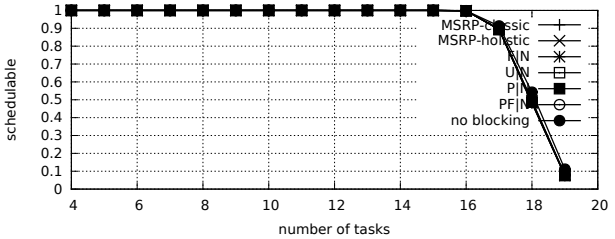

Fig. 390. Schedulability under non-preemptable spin locks for $m = 4$, $U = 0.2n$, 4 resources, $rsf = 0.4$, $N^{max} = 1$, and short critical sections. The schedulability of the considered preemptable lock types in this configuration is shown in Fig. 400.

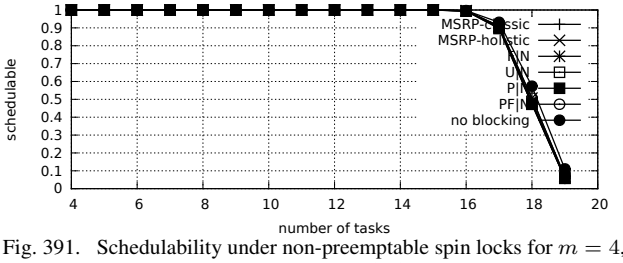

Fig. 391. Schedulability under non-preemptable spin locks for $m = 4$, $U = 0.2n$, 4 resources, $rsf = 0.4$, $N^{max} = 2$, and short critical sections. The schedulability of the considered preemptable lock types in this configuration is shown in Fig. 401.

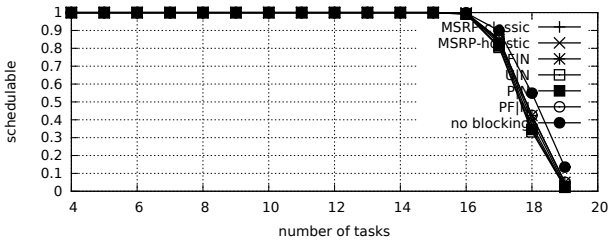

Fig. 392. Schedulability under non-preemptable spin locks for $m = 4$, $U = 0.2n$, 4 resources, $rsf = 0.4$, $N^{max} = 5$, and short critical sections. The schedulability of the considered preemptable lock types in this configuration is shown in Fig. 402.

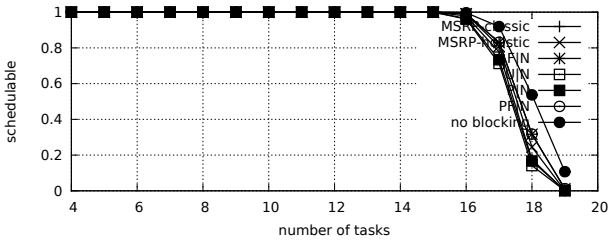

Fig. 393. Schedulability under non-preemptable spin locks for $m = 4$, $U = 0.2n$, 4 resources, $rsf = 0.4$, $N^{max} = 10$, and short critical sections. The schedulability of the considered preemptable lock types in this configuration is shown in Fig. 403.

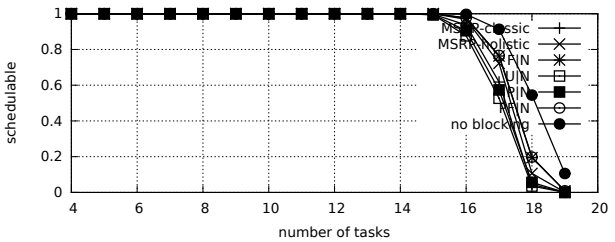

Fig. 394. Schedulability under non-preemptable spin locks for $m = 4$, $U = 0.2n$, 4 resources, $rsf = 0.4$, $N^{max} = 15$, and short critical sections. The schedulability of the considered preemptable lock types in this configuration is shown in Fig. 404.

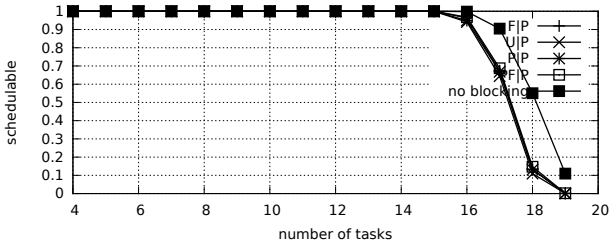

Fig. 395. Schedulability under preemptable spin locks for $m = 4$, $U = 0.2n$, 4 resources, $rsf = 0.4$, $N^{max} = 1$, and medium critical sections. The schedulability of the considered non-preemptable lock types in this configuration is shown in Fig. 385.

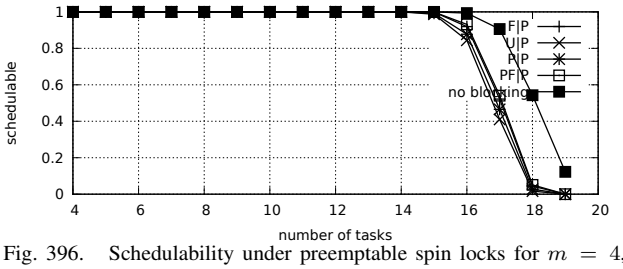

Fig. 396. Schedulability under preemptable spin locks for $m = 4$, $U = 0.2n$, 4 resources, $rsf = 0.4$, $N^{max} = 2$, and medium critical sections. The schedulability of the considered non-preemptable lock types in this configuration is shown in Fig. 386.

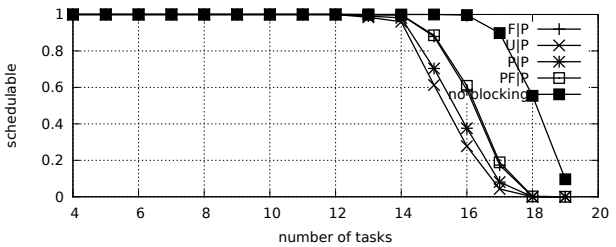

Fig. 397. Schedulability under preemptable spin locks for $m = 4$, $U = 0.2n$, 4 resources, $rsf = 0.4$, $N^{max} = 5$, and medium critical sections. The schedulability of the considered non-preemptable lock types in this configuration is shown in Fig. 387.

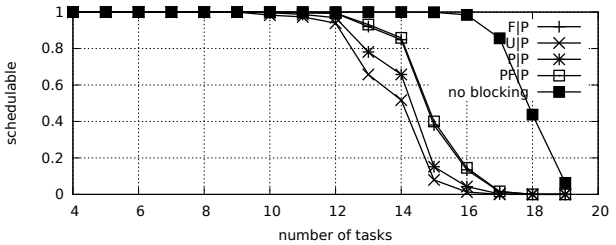

Fig. 398. Schedulability under preemptable spin locks for $m = 4$, $U = 0.2n$, 4 resources, $rsf = 0.4$, $N^{max} = 10$, and medium critical sections. The schedulability of the considered non-preemptable lock types in this configuration is shown in Fig. 388.

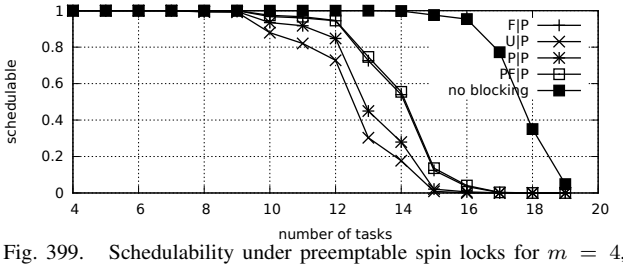

Fig. 399. Schedulability under preemptable spin locks for $m = 4$, $U = 0.2n$, 4 resources, $rsf = 0.4$, $N^{max} = 15$, and medium critical sections. The schedulability of the considered non-preemptable lock types in this configuration is shown in Fig. 389.

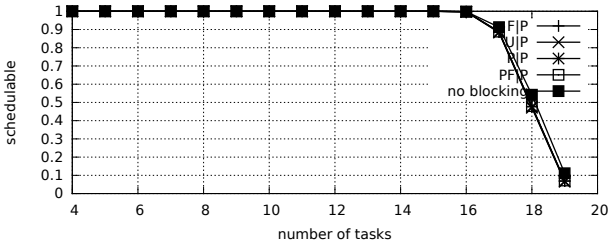

Fig. 400. Schedulability under preemptable spin locks for $m = 4$, $U = 0.2n$, 4 resources, $rsf = 0.4$, $N^{max} = 1$, and short critical sections. The schedulability of the considered non-preemptable lock types in this configuration is shown in Fig. 390.

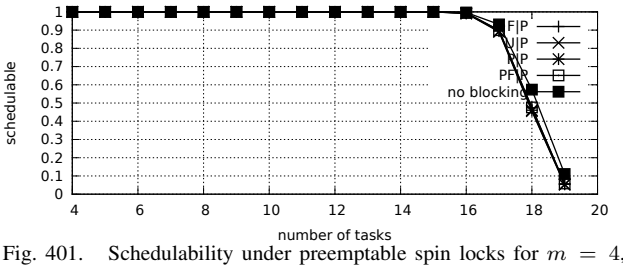

Fig. 401. Schedulability under preemptable spin locks for $m = 4$, $U = 0.2n$, 4 resources, $rsf = 0.4$, $N^{max} = 2$, and short critical sections. The schedulability of the considered non-preemptable lock types in this configuration is shown in Fig. 391.

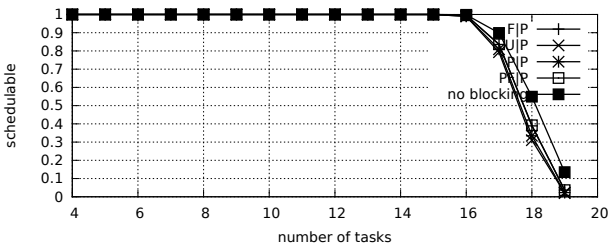

Fig. 402. Schedulability under preemptable spin locks for $m = 4$, $U = 0.2n$, 4 resources, $rsf = 0.4$, $N^{max} = 5$, and short critical sections. The schedulability of the considered non-preemptable lock types in this configuration is shown in Fig. 392.

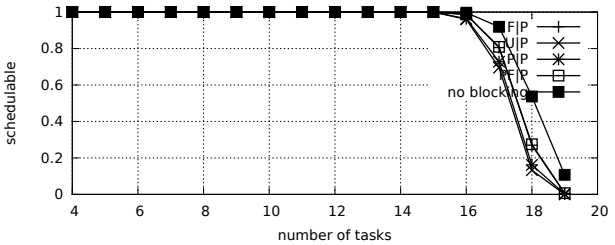

Fig. 403. Schedulability under preemptable spin locks for $m = 4$, $U = 0.2n$, 4 resources, $rsf = 0.4$, $N^{max} = 10$, and short critical sections. The schedulability of the considered non-preemptable lock types in this configuration is shown in Fig. 393.

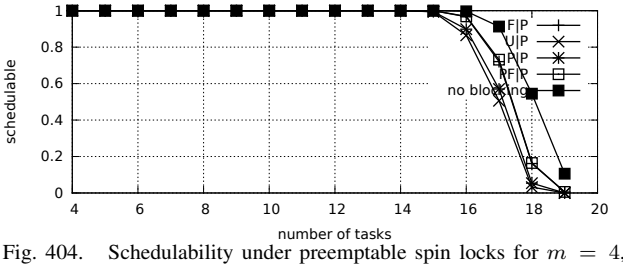

Fig. 404. Schedulability under preemptable spin locks for $m = 4$, $U = 0.2n$, 4 resources, $rsf = 0.4$, $N^{max} = 15$, and short critical sections. The schedulability of the considered non-preemptable lock types in this configuration is shown in Fig. 394.

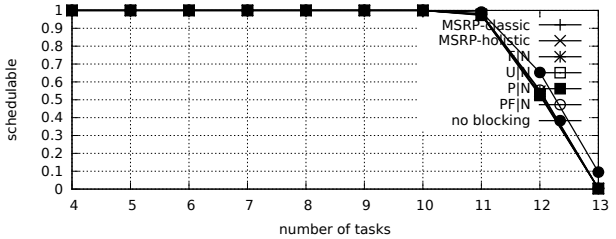

Fig. 405. Schedulability under non-preemptable spin locks for $m = 4$, $U = 0.3n$, 4 resources, $rsf = 0.4$, $N^{max} = 1$, and medium critical sections. The schedulability of the considered preemptable lock types in this configuration is shown in Fig. 415.

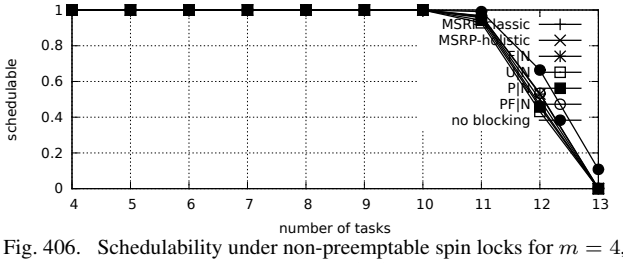

Fig. 406. Schedulability under non-preemptable spin locks for $m = 4$, $U = 0.3n$, 4 resources, $rsf = 0.4$, $N^{max} = 2$, and medium critical sections. The schedulability of the considered preemptable lock types in this configuration is shown in Fig. 416.

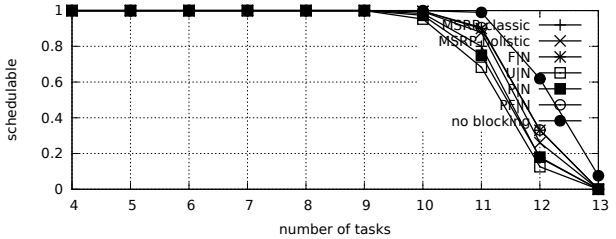

Fig. 407. Schedulability under non-preemptable spin locks for $m = 4$, $U = 0.3n$, 4 resources, $rsf = 0.4$, $N^{max} = 5$, and medium critical sections. The schedulability of the considered preemptable lock types in this configuration is shown in Fig. 417.

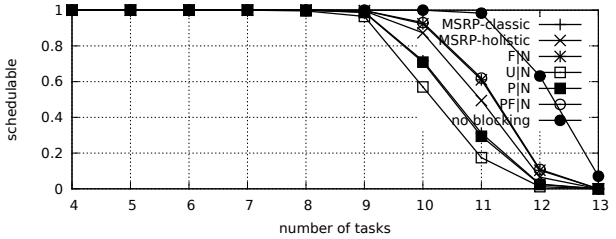

Fig. 408. Schedulability under non-preemptable spin locks for $m = 4$, $U = 0.3n$, 4 resources, $rsf = 0.4$, $N^{max} = 10$, and medium critical sections. The schedulability of the considered preemptable lock types in this configuration is shown in Fig. 418.

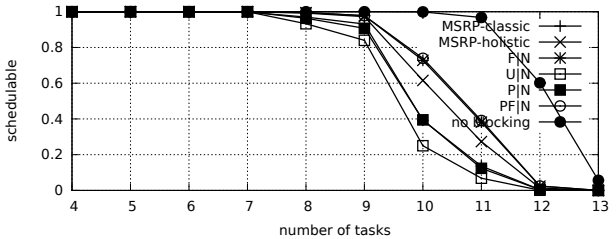

Fig. 409. Schedulability under non-preemptable spin locks for $m = 4$, $U = 0.3n$, 4 resources, $rsf = 0.4$, $N^{max} = 15$, and medium critical sections. The schedulability of the considered preemptable lock types in this configuration is shown in Fig. 419.

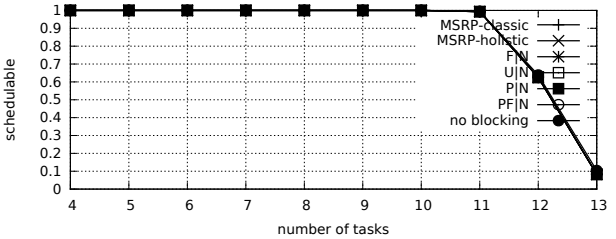

Fig. 410. Schedulability under non-preemptable spin locks for $m = 4$, $U = 0.3n$, 4 resources, $rsf = 0.4$, $N^{max} = 1$, and short critical sections. The schedulability of the considered preemptable lock types in this configuration is shown in Fig. 420.

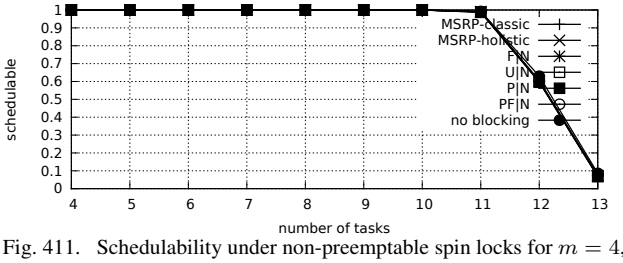

Fig. 411. Schedulability under non-preemptable spin locks for $m = 4$, $U = 0.3n$, 4 resources, $rsf = 0.4$, $N^{max} = 2$, and short critical sections. The schedulability of the considered preemptable lock types in this configuration is shown in Fig. 421.

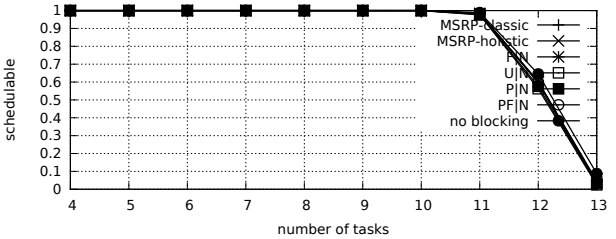

Fig. 412. Schedulability under non-preemptable spin locks for $m = 4$, $U = 0.3n$, 4 resources, $rsf = 0.4$, $N^{max} = 5$, and short critical sections. The schedulability of the considered preemptable lock types in this configuration is shown in Fig. 422.

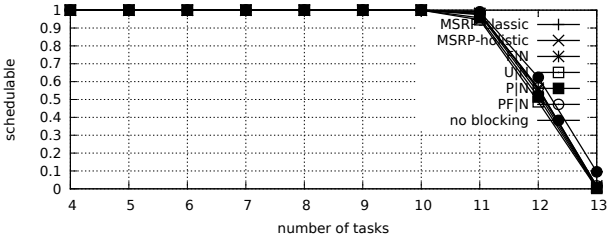

Fig. 413. Schedulability under non-preemptable spin locks for $m = 4$, $U = 0.3n$, 4 resources, $rsf = 0.4$, $N^{max} = 10$, and short critical sections. The schedulability of the considered preemptable lock types in this configuration is shown in Fig. 423.

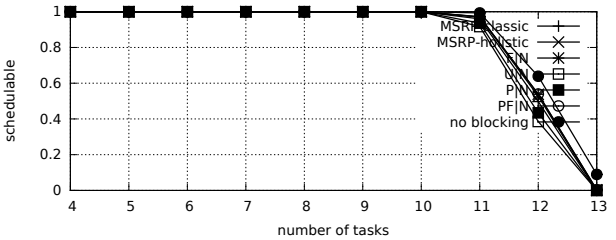

Fig. 414. Schedulability under non-preemptable spin locks for $m = 4$, $U = 0.3n$, 4 resources, $rsf = 0.4$, $N^{max} = 15$, and short critical sections. The schedulability of the considered preemptable lock types in this configuration is shown in Fig. 424.

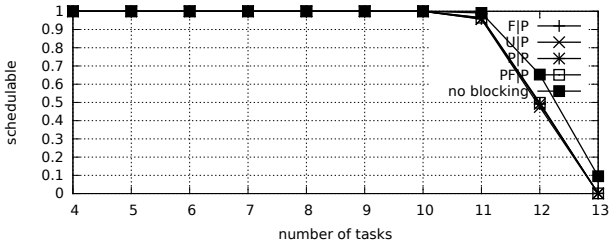

Fig. 415. Schedulability under preemptable spin locks for $m = 4$, $U = 0.3n$, 4 resources, $rsf = 0.4$, $N^{max} = 1$, and medium critical sections. The schedulability of the considered non-preemptable lock types in this configuration is shown in Fig. 405.

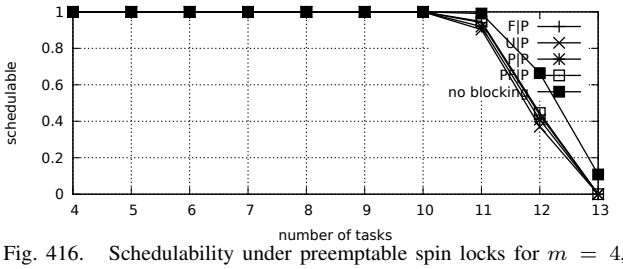

Fig. 416. Schedulability under preemptable spin locks for $m = 4$, $U = 0.3n$, 4 resources, $rsf = 0.4$, $N^{max} = 2$, and medium critical sections. The schedulability of the considered non-preemptable lock types in this configuration is shown in Fig. 406.

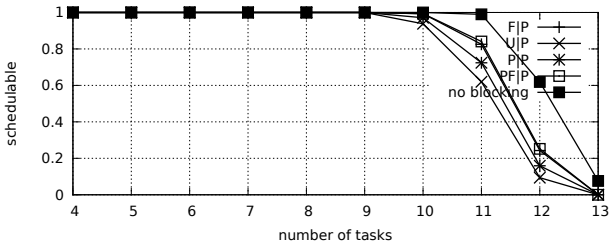

Fig. 417. Schedulability under preemptable spin locks for $m = 4$, $U = 0.3n$, 4 resources, $rsf = 0.4$, $N^{max} = 5$, and medium critical sections. The schedulability of the considered non-preemptable lock types in this configuration is shown in Fig. 407.

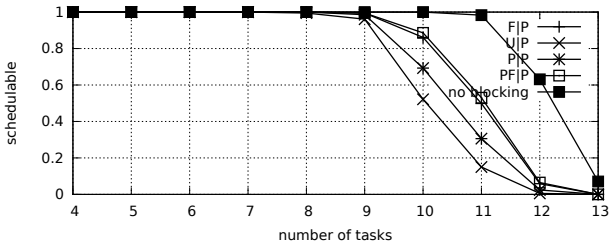

Fig. 418. Schedulability under preemptable spin locks for $m = 4$, $U = 0.3n$, 4 resources, $rsf = 0.4$, $N^{max} = 10$, and medium critical sections. The schedulability of the considered non-preemptable lock types in this configuration is shown in Fig. 408.

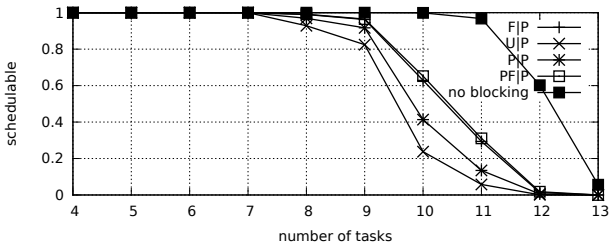

Fig. 419. Schedulability under preemptable spin locks for $m = 4$, $U = 0.3n$, 4 resources, $rsf = 0.4$, $N^{max} = 15$, and medium critical sections. The schedulability of the considered non-preemptable lock types in this configuration is shown in Fig. 409.

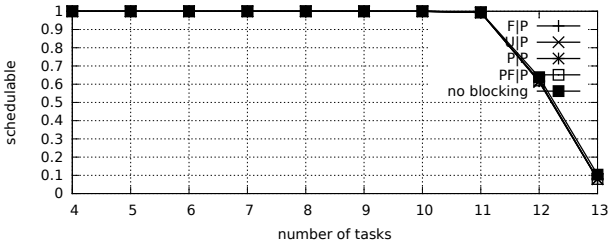

Fig. 420. Schedulability under preemptable spin locks for $m = 4$, $U = 0.3n$, 4 resources, $rsf = 0.4$, $N^{max} = 1$, and short critical sections. The schedulability of the considered non-preemptable lock types in this configuration is shown in Fig. 410.

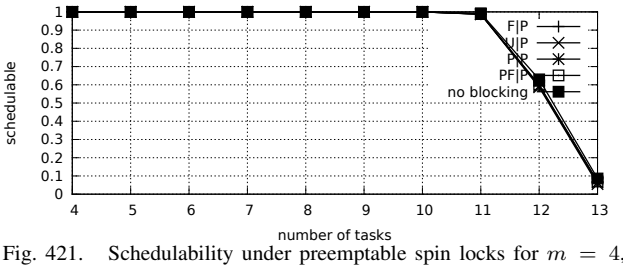

Fig. 421. Schedulability under preemptable spin locks for $m = 4$, $U = 0.3n$, 4 resources, $rsf = 0.4$, $N^{max} = 2$, and short critical sections. The schedulability of the considered non-preemptable lock types in this configuration is shown in Fig. 411.

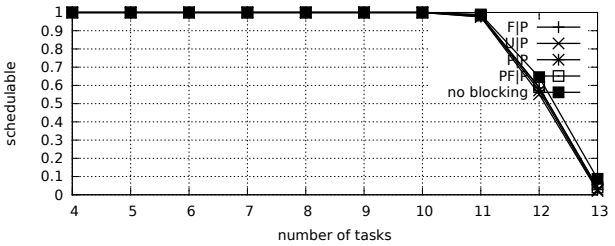

Fig. 422. Schedulability under preemptable spin locks for $m = 4$, $U = 0.3n$, 4 resources, $rsf = 0.4$, $N^{max} = 5$, and short critical sections. The schedulability of the considered non-preemptable lock types in this configuration is shown in Fig. 412.

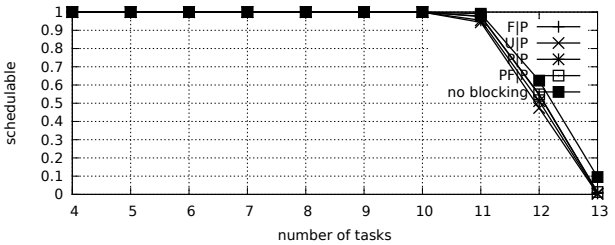

Fig. 423. Schedulability under preemptable spin locks for $m = 4$, $U = 0.3n$, 4 resources, $rsf = 0.4$, $N^{max} = 10$, and short critical sections. The schedulability of the considered non-preemptable lock types in this configuration is shown in Fig. 413.

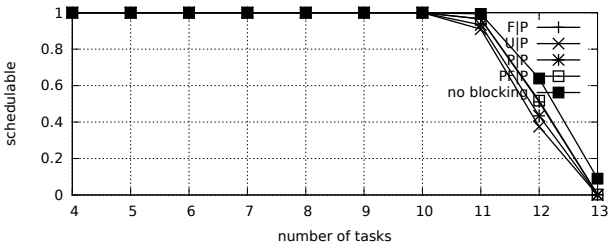

Fig. 424. Schedulability under preemptable spin locks for $m = 4$, $U = 0.3n$, 4 resources, $rsf = 0.4$, $N^{max} = 15$, and short critical sections. The schedulability of the considered non-preemptable lock types in this configuration is shown in Fig. 414.

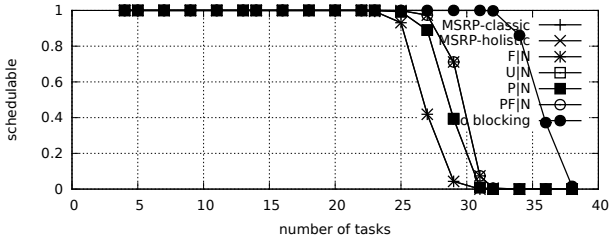

Fig. 425. Schedulability under non-preemptable spin locks for $m = 4$, $U = 0.1n$, 4 resources, $rsf = 0.75$, $N^{max} = 1$, and medium critical sections. The schedulability of the considered preemptable lock types in this configuration is shown in Fig. 435.

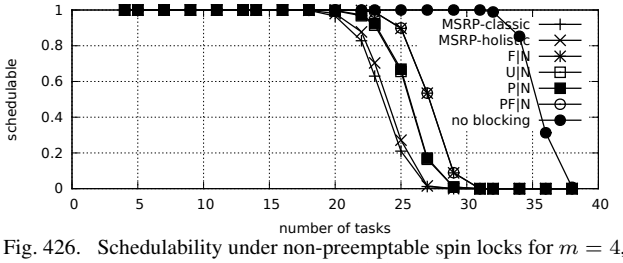

Fig. 426. Schedulability under non-preemptable spin locks for $m = 4$, $U = 0.1n$, 4 resources, $rsf = 0.75$, $N^{max} = 2$, and medium critical sections. The schedulability of the considered preemptable lock types in this configuration is shown in Fig. 436.

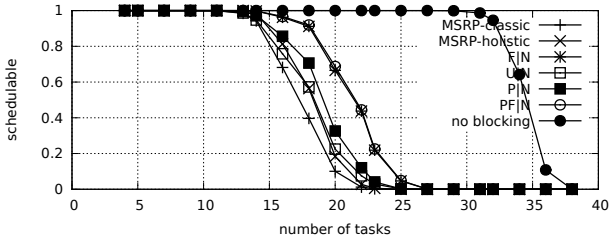

Fig. 427. Schedulability under non-preemptable spin locks for $m = 4$, $U = 0.1n$, 4 resources, $rsf = 0.75$, $N^{max} = 5$, and medium critical sections. The schedulability of the considered preemptable lock types in this configuration is shown in Fig. 437.

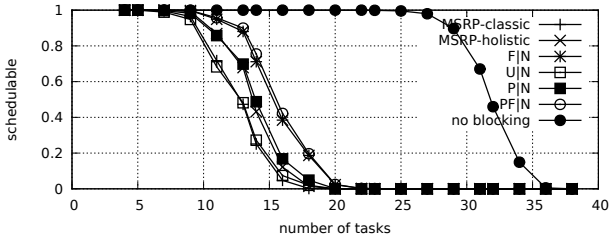

Fig. 428. Schedulability under non-preemptable spin locks for $m = 4$, $U = 0.1n$, 4 resources, $rsf = 0.75$, $N^{max} = 10$, and medium critical sections. The schedulability of the considered preemptable lock types in this configuration is shown in Fig. 438.

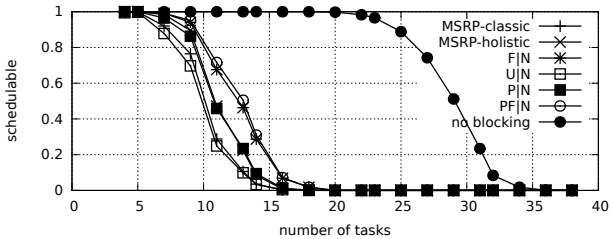

Fig. 429. Schedulability under non-preemptable spin locks for $m = 4$, $U = 0.1n$, 4 resources, $rsf = 0.75$, $N^{max} = 15$, and medium critical sections. The schedulability of the considered preemptable lock types in this configuration is shown in Fig. 439.

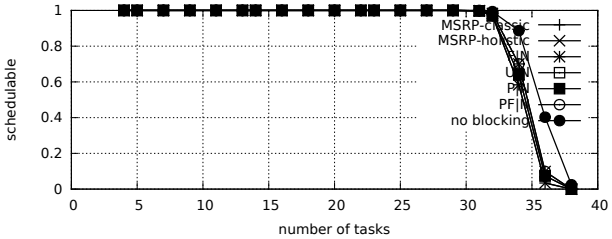

Fig. 430. Schedulability under non-preemptable spin locks for $m = 4$, $U = 0.1n$, 4 resources, $rsf = 0.75$, $N^{max} = 1$, and short critical sections. The schedulability of the considered preemptable lock types in this configuration is shown in Fig. 440.

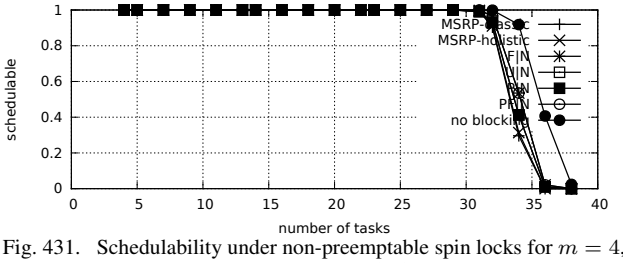

Fig. 431. Schedulability under non-preemptable spin locks for $m = 4$, $U = 0.1n$, 4 resources, $rsf = 0.75$, $N^{max} = 2$, and short critical sections. The schedulability of the considered preemptable lock types in this configuration is shown in Fig. 441.

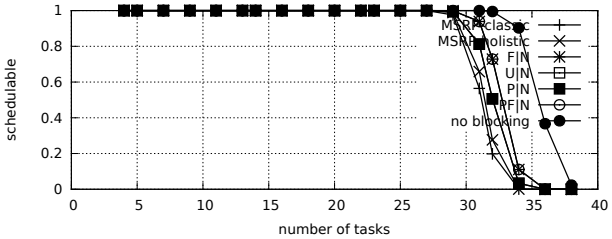

Fig. 432. Schedulability under non-preemptable spin locks for $m = 4$, $U = 0.1n$, 4 resources, $rsf = 0.75$, $N^{max} = 5$, and short critical sections. The schedulability of the considered preemptable lock types in this configuration is shown in Fig. 442.

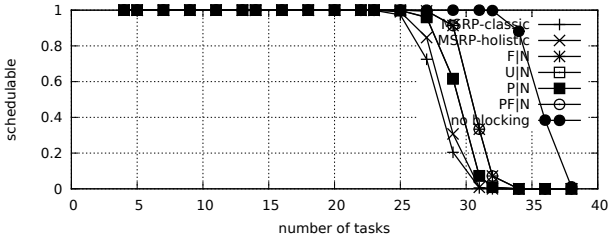

Fig. 433. Schedulability under non-preemptable spin locks for $m = 4$, $U = 0.1n$, 4 resources, $rsf = 0.75$, $N^{max} = 10$, and short critical sections. The schedulability of the considered preemptable lock types in this configuration is shown in Fig. 443.

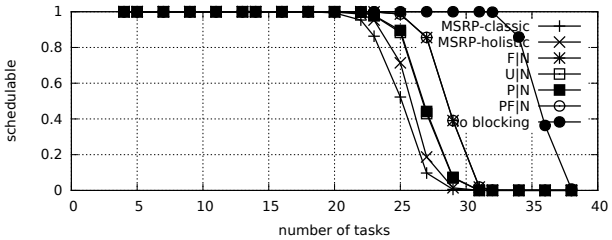

Fig. 434. Schedulability under non-preemptable spin locks for $m = 4$, $U = 0.1n$, 4 resources, $rsf = 0.75$, $N^{max} = 15$, and short critical sections. The schedulability of the considered preemptable lock types in this configuration is shown in Fig. 444.

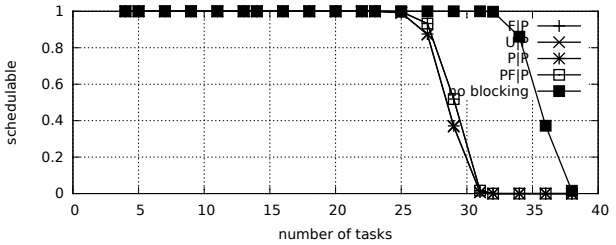

Fig. 435. Schedulability under preemptable spin locks for $m = 4$, $U = 0.1n$, 4 resources, $rsf = 0.75$, $N^{max} = 1$, and medium critical sections. The schedulability of the considered non-preemptable lock types in this configuration is shown in Fig. 425.

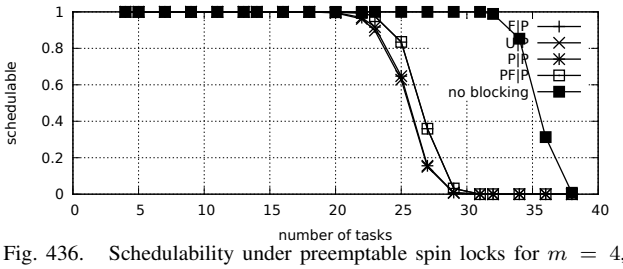

Fig. 436. Schedulability under preemptable spin locks for $m = 4$, $U = 0.1n$, 4 resources, $rsf = 0.75$, $N^{max} = 2$, and medium critical sections. The schedulability of the considered non-preemptable lock types in this configuration is shown in Fig. 426.

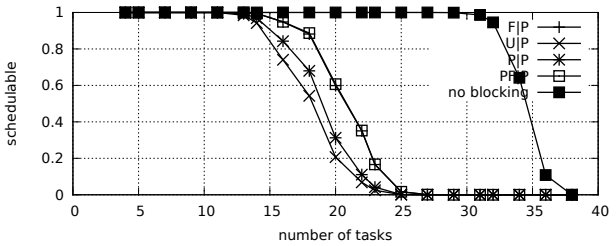

Fig. 437. Schedulability under preemptable spin locks for $m = 4$, $U = 0.1n$, 4 resources, $rsf = 0.75$, $N^{max} = 5$, and medium critical sections. The schedulability of the considered non-preemptable lock types in this configuration is shown in Fig. 427.

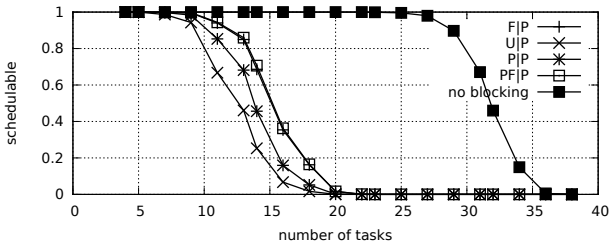

Fig. 438. Schedulability under preemptable spin locks for $m = 4$, $U = 0.1n$, 4 resources, $rsf = 0.75$, $N^{max} = 10$, and medium critical sections. The schedulability of the considered non-preemptable lock types in this configuration is shown in Fig. 428.

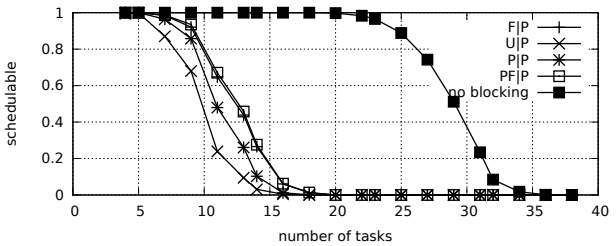

Fig. 439. Schedulability under preemptable spin locks for $m = 4$, $U = 0.1n$, 4 resources, $rsf = 0.75$, $N^{max} = 15$, and medium critical sections. The schedulability of the considered non-preemptable lock types in this configuration is shown in Fig. 429.

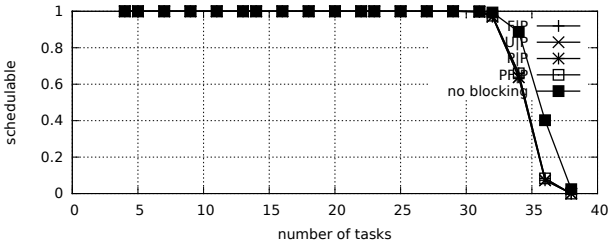

Fig. 440. Schedulability under preemptable spin locks for $m = 4$, $U = 0.1n$, 4 resources, $rsf = 0.75$, $N^{max} = 1$, and short critical sections. The schedulability of the considered non-preemptable lock types in this configuration is shown in Fig. 430.

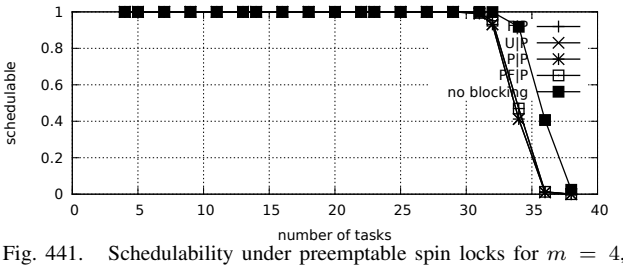

Fig. 441. Schedulability under preemptable spin locks for $m = 4$, $U = 0.1n$, 4 resources, $rsf = 0.75$, $N^{max} = 2$, and short critical sections. The schedulability of the considered non-preemptable lock types in this configuration is shown in Fig. 431.

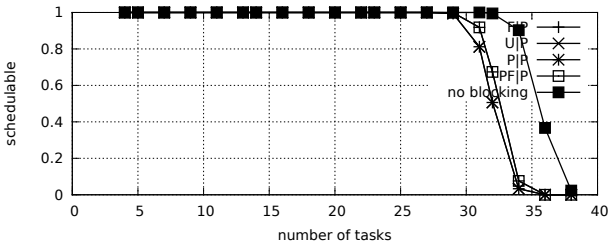

Fig. 442. Schedulability under preemptable spin locks for $m = 4$, $U = 0.1n$, 4 resources, $rsf = 0.75$, $N^{max} = 5$, and short critical sections. The schedulability of the considered non-preemptable lock types in this configuration is shown in Fig. 432.

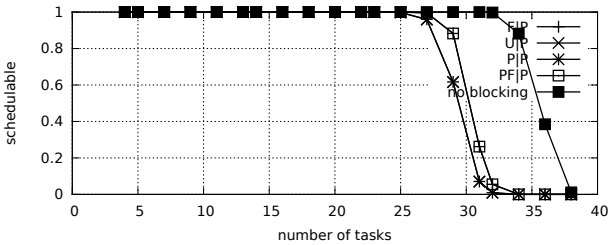

Fig. 443. Schedulability under preemptable spin locks for $m = 4$, $U = 0.1n$, 4 resources, $rsf = 0.75$, $N^{max} = 10$, and short critical sections. The schedulability of the considered non-preemptable lock types in this configuration is shown in Fig. 433.

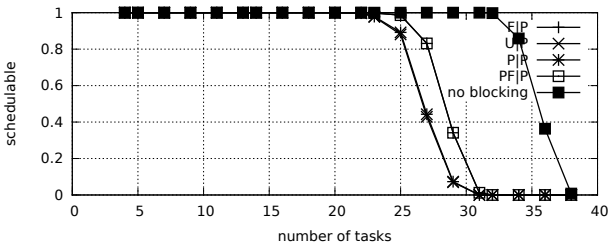

Fig. 444. Schedulability under preemptable spin locks for $m = 4$, $U = 0.1n$, 4 resources, $rsf = 0.75$, $N^{max} = 15$, and short critical sections. The schedulability of the considered non-preemptable lock types in this configuration is shown in Fig. 434.

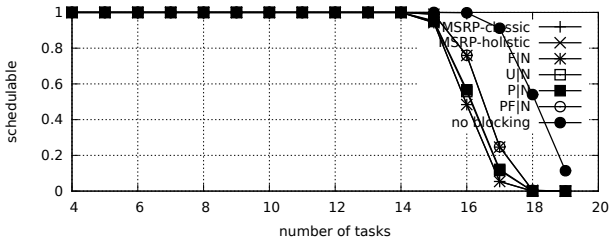

Fig. 445. Schedulability under non-preemptable spin locks for $m = 4$, $U = 0.2n$, 4 resources, $rsf = 0.75$, $N^{max} = 1$, and medium critical sections. The schedulability of the considered preemptable lock types in this configuration is shown in Fig. 455.

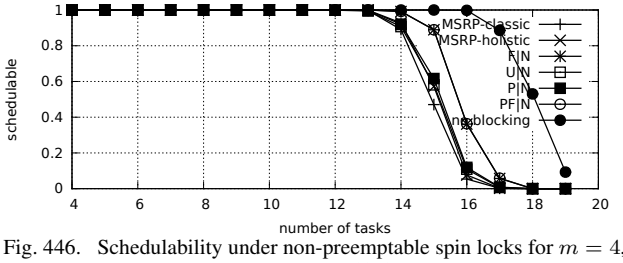

Fig. 446. Schedulability under non-preemptable spin locks for $m = 4$, $U = 0.2n$, 4 resources, $rsf = 0.75$, $N^{max} = 2$, and medium critical sections. The schedulability of the considered preemptable lock types in this configuration is shown in Fig. 456.

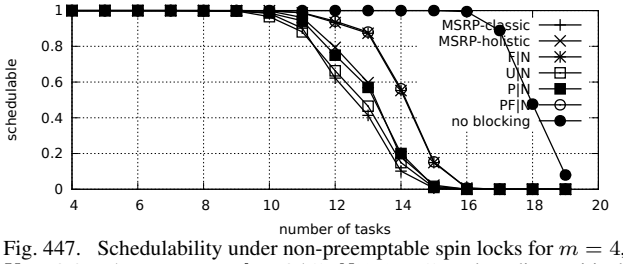

Fig. 447. Schedulability under non-preemptable spin locks for $m = 4$, $U = 0.2n$, 4 resources, $rsf = 0.75$, $N^{max} = 5$, and medium critical sections. The schedulability of the considered preemptable lock types in this configuration is shown in Fig. 457.

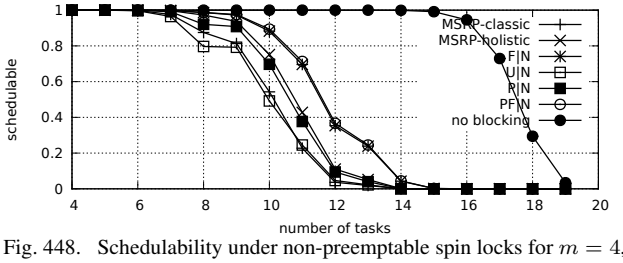

Fig. 448. Schedulability under non-preemptable spin locks for $m = 4$, $U = 0.2n$, 4 resources, $rsf = 0.75$, $N^{max} = 10$, and medium critical sections. The schedulability of the considered preemptable lock types in this configuration is shown in Fig. 458.

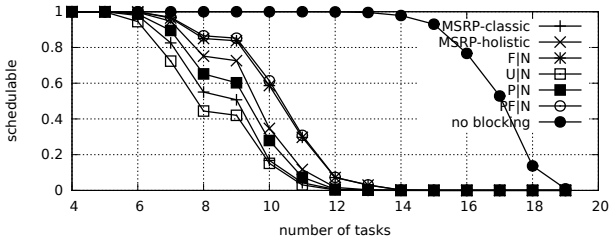

Fig. 449. Schedulability under non-preemptable spin locks for $m = 4$, $U = 0.2n$, 4 resources, $rsf = 0.75$, $N^{max} = 15$, and medium critical sections. The schedulability of the considered preemptable lock types in this configuration is shown in Fig. 459.

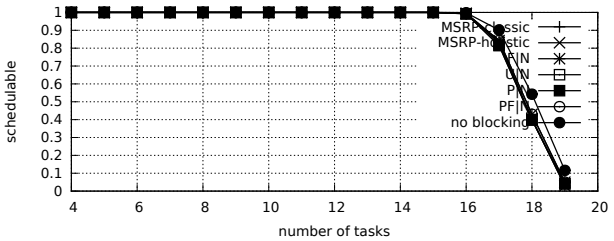

Fig. 450. Schedulability under non-preemptable spin locks for $m = 4$, $U = 0.2n$, 4 resources, $rsf = 0.75$, $N^{max} = 1$, and short critical sections. The schedulability of the considered preemptable lock types in this configuration is shown in Fig. 460.

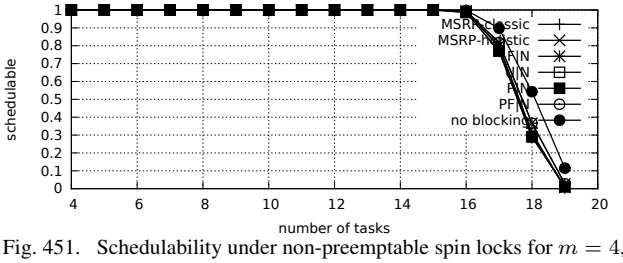

Fig. 451. Schedulability under non-preemptable spin locks for $m = 4$, $U = 0.2n$, 4 resources, $rsf = 0.75$, $N^{max} = 2$, and short critical sections. The schedulability of the considered preemptable lock types in this configuration is shown in Fig. 461.

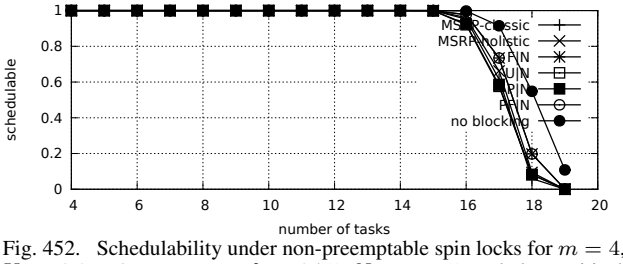

Fig. 452. Schedulability under non-preemptable spin locks for $m = 4$, $U = 0.2n$, 4 resources, $rsf = 0.75$, $N^{max} = 5$, and short critical sections. The schedulability of the considered preemptable lock types in this configuration is shown in Fig. 462.

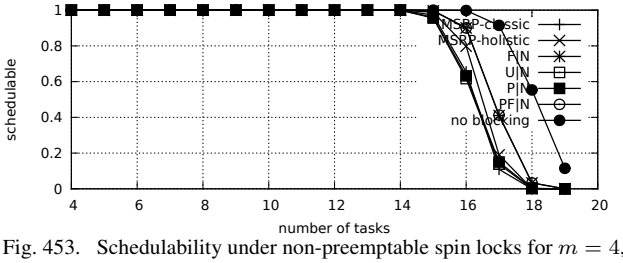

Fig. 453. Schedulability under non-preemptable spin locks for $m = 4$, $U = 0.2n$, 4 resources, $rsf = 0.75$, $N^{max} = 10$, and short critical sections. The schedulability of the considered preemptable lock types in this configuration is shown in Fig. 463.

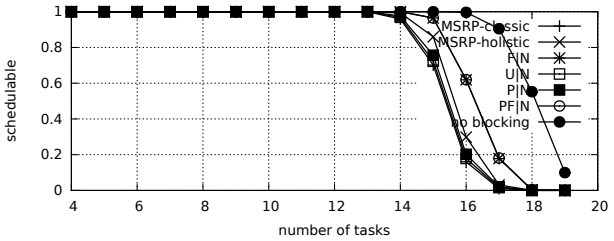

Fig. 454. Schedulability under non-preemptable spin locks for $m = 4$, $U = 0.2n$, 4 resources, $rsf = 0.75$, $N^{max} = 15$, and short critical sections. The schedulability of the considered preemptable lock types in this configuration is shown in Fig. 464.

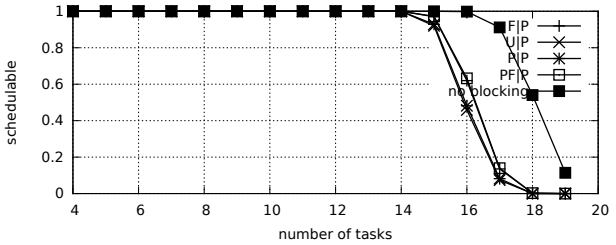

Fig. 455. Schedulability under preemptable spin locks for $m = 4$, $U = 0.2n$, 4 resources, $rsf = 0.75$, $N^{max} = 1$, and medium critical sections. The schedulability of the considered non-preemptable lock types in this configuration is shown in Fig. 445.

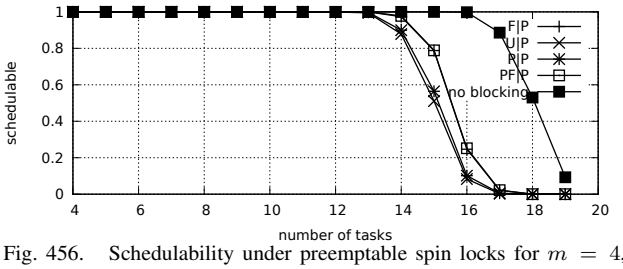

Fig. 456. Schedulability under preemptable spin locks for $m = 4$, $U = 0.2n$, 4 resources, $rsf = 0.75$, $N^{max} = 2$, and medium critical sections. The schedulability of the considered non-preemptable lock types in this configuration is shown in Fig. 446.

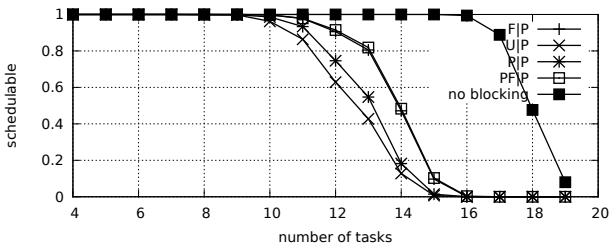

Fig. 457. Schedulability under preemptable spin locks for $m = 4$, $U = 0.2n$, 4 resources, $rsf = 0.75$, $N^{max} = 5$, and medium critical sections. The schedulability of the considered non-preemptable lock types in this configuration is shown in Fig. 447.

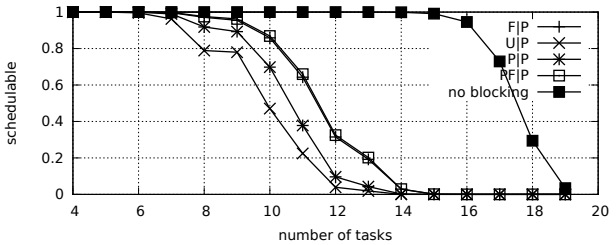

Fig. 458. Schedulability under preemptable spin locks for $m = 4$, $U = 0.2n$, 4 resources, $rsf = 0.75$, $N^{max} = 10$, and medium critical sections. The schedulability of the considered non-preemptable lock types in this configuration is shown in Fig. 448.

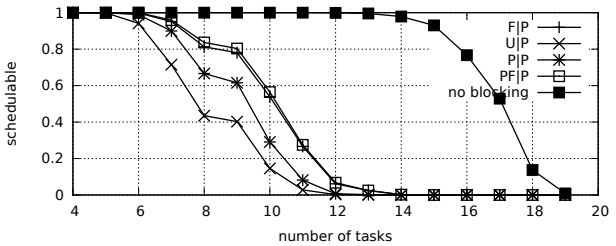

Fig. 459. Schedulability under preemptable spin locks for $m = 4$, $U = 0.2n$, 4 resources, $rsf = 0.75$, $N^{max} = 15$, and medium critical sections. The schedulability of the considered non-preemptable lock types in this configuration is shown in Fig. 449.

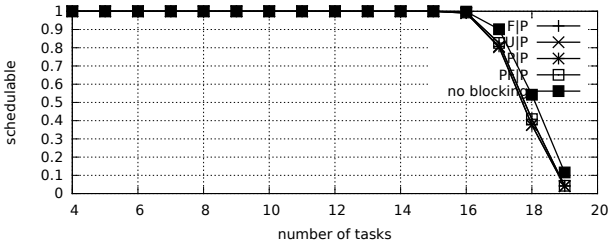

Fig. 460. Schedulability under preemptable spin locks for $m = 4$, $U = 0.2n$, 4 resources, $rsf = 0.75$, $N^{max} = 1$, and short critical sections. The schedulability of the considered non-preemptable lock types in this configuration is shown in Fig. 450.

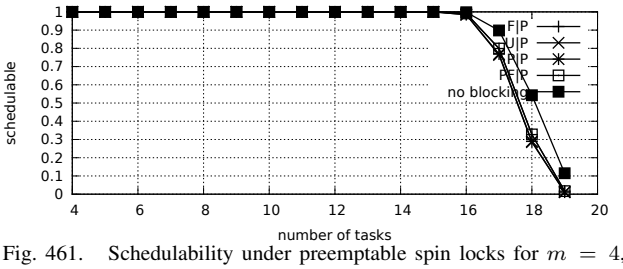

Fig. 461. Schedulability under preemptable spin locks for $m = 4$, $U = 0.2n$, 4 resources, $rsf = 0.75$, $N^{max} = 2$, and short critical sections. The schedulability of the considered non-preemptable lock types in this configuration is shown in Fig. 451.

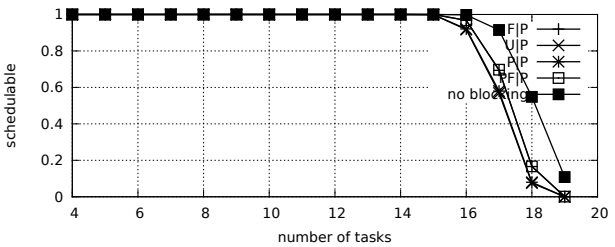

Fig. 462. Schedulability under preemptable spin locks for $m = 4$, $U = 0.2n$, 4 resources, $rsf = 0.75$, $N^{max} = 5$, and short critical sections. The schedulability of the considered non-preemptable lock types in this configuration is shown in Fig. 452.

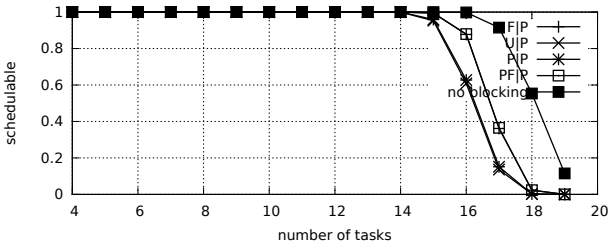

Fig. 463. Schedulability under preemptable spin locks for $m = 4$, $U = 0.2n$, 4 resources, $rsf = 0.75$, $N^{max} = 10$, and short critical sections. The schedulability of the considered non-preemptable lock types in this configuration is shown in Fig. 453.

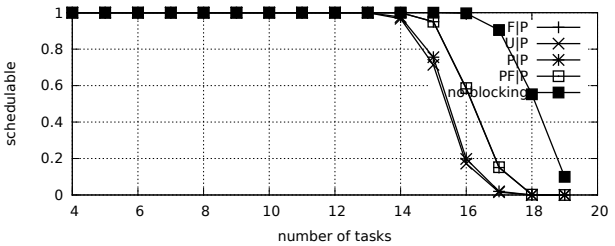

Fig. 464. Schedulability under preemptable spin locks for $m = 4$, $U = 0.2n$, 4 resources, $rsf = 0.75$, $N^{max} = 15$, and short critical sections. The schedulability of the considered non-preemptable lock types in this configuration is shown in Fig. 454.

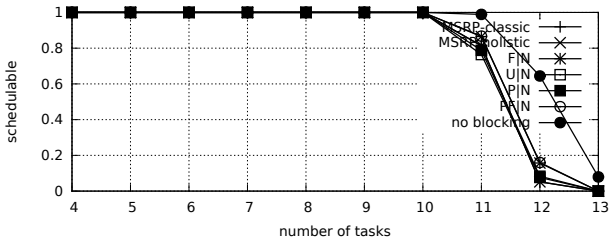

Fig. 465. Schedulability under non-preemptable spin locks for $m = 4$, $U = 0.3n$, 4 resources, $rsf = 0.75$, $N^{max} = 1$, and medium critical sections. The schedulability of the considered preemptable lock types in this configuration is shown in Fig. 475.

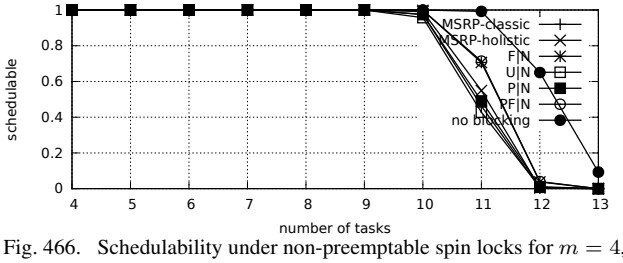

Fig. 466. Schedulability under non-preemptable spin locks for $m = 4$, $U = 0.3n$, 4 resources, $rsf = 0.75$, $N^{max} = 2$, and medium critical sections. The schedulability of the considered preemptable lock types in this configuration is shown in Fig. 476.

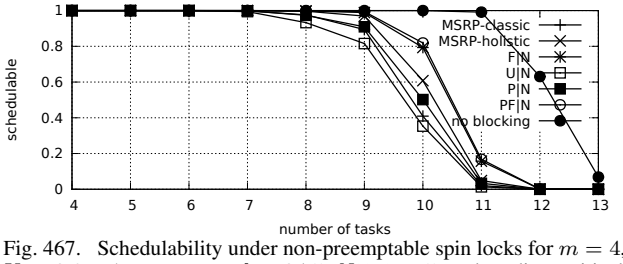

Fig. 467. Schedulability under non-preemptable spin locks for $m = 4$, $U = 0.3n$, 4 resources, $rsf = 0.75$, $N^{max} = 5$, and medium critical sections. The schedulability of the considered preemptable lock types in this configuration is shown in Fig. 477.

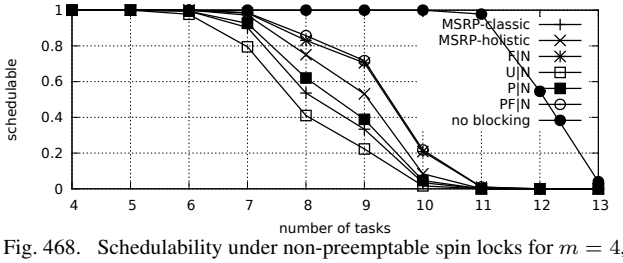

Fig. 468. Schedulability under non-preemptable spin locks for $m = 4$, $U = 0.3n$, 4 resources, $rsf = 0.75$, $N^{max} = 10$, and medium critical sections. The schedulability of the considered preemptable lock types in this configuration is shown in Fig. 478.

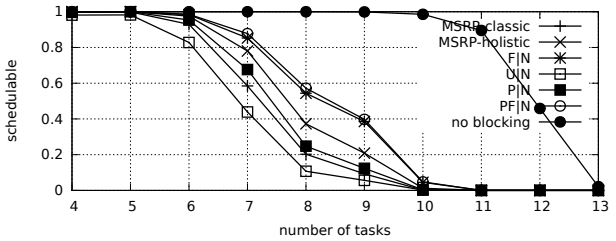

Fig. 469. Schedulability under non-preemptable spin locks for $m = 4$, $U = 0.3n$, 4 resources, $rsf = 0.75$, $N^{max} = 15$, and medium critical sections. The schedulability of the considered preemptable lock types in this configuration is shown in Fig. 479.

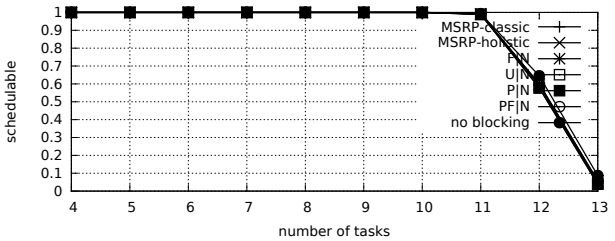

Fig. 470. Schedulability under non-preemptable spin locks for $m = 4$, $U = 0.3n$, 4 resources, $rsf = 0.75$, $N^{max} = 1$, and short critical sections. The schedulability of the considered preemptable lock types in this configuration is shown in Fig. 480.

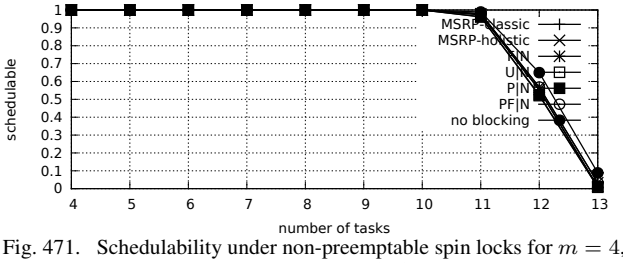

Fig. 471. Schedulability under non-preemptable spin locks for $m = 4$, $U = 0.3n$, 4 resources, $rsf = 0.75$, $N^{max} = 2$, and short critical sections. The schedulability of the considered preemptable lock types in this configuration is shown in Fig. 481.

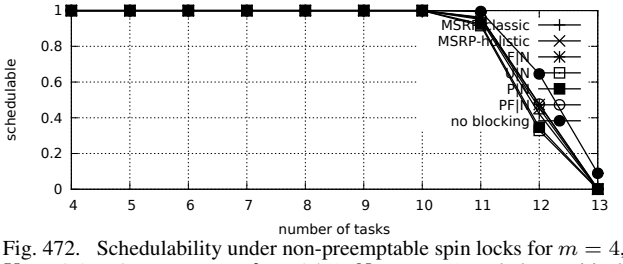

Fig. 472. Schedulability under non-preemptable spin locks for $m = 4$, $U = 0.3n$, 4 resources, $rsf = 0.75$, $N^{max} = 5$, and short critical sections. The schedulability of the considered preemptable lock types in this configuration is shown in Fig. 482.

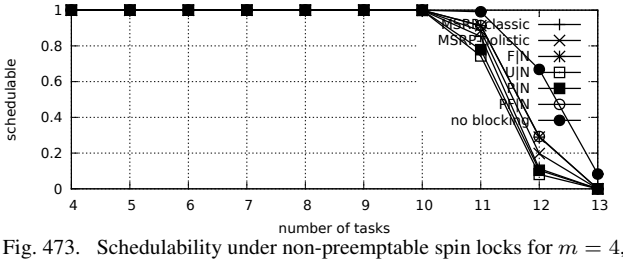

Fig. 473. Schedulability under non-preemptable spin locks for $m = 4$, $U = 0.3n$, 4 resources, $rsf = 0.75$, $N^{max} = 10$, and short critical sections. The schedulability of the considered preemptable lock types in this configuration is shown in Fig. 483.

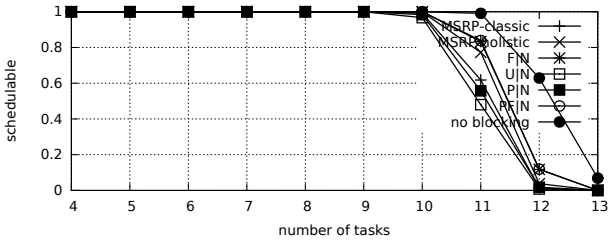

Fig. 474. Schedulability under non-preemptable spin locks for $m = 4$, $U = 0.3n$, 4 resources, $rsf = 0.75$, $N^{max} = 15$, and short critical sections. The schedulability of the considered preemptable lock types in this configuration is shown in Fig. 484.

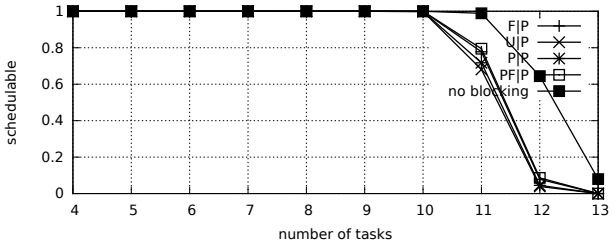

Fig. 475. Schedulability under preemptable spin locks for $m = 4$, $U = 0.3n$, 4 resources, $rsf = 0.75$, $N^{max} = 1$, and medium critical sections. The schedulability of the considered non-preemptable lock types in this configuration is shown in Fig. 465.

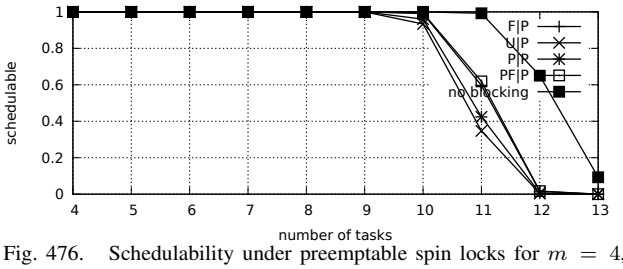

Fig. 476. Schedulability under preemptable spin locks for $m = 4$, $U = 0.3n$, 4 resources, $rsf = 0.75$, $N^{max} = 2$, and medium critical sections. The schedulability of the considered non-preemptable lock types in this configuration is shown in Fig. 466.

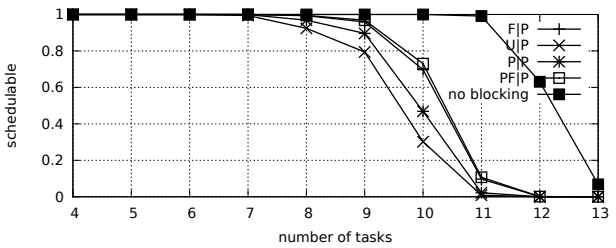

Fig. 477. Schedulability under preemptable spin locks for $m = 4$, $U = 0.3n$, 4 resources, $rsf = 0.75$, $N^{max} = 5$, and medium critical sections. The schedulability of the considered non-preemptable lock types in this configuration is shown in Fig. 467.

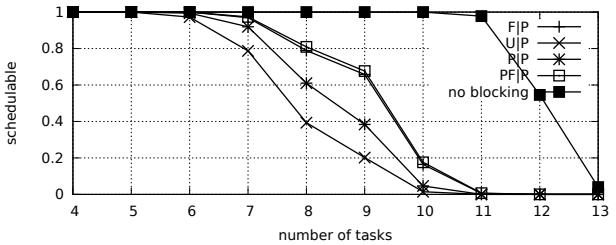

Fig. 478. Schedulability under preemptable spin locks for $m = 4$, $U = 0.3n$, 4 resources, $rsf = 0.75$, $N^{max} = 10$, and medium critical sections. The schedulability of the considered non-preemptable lock types in this configuration is shown in Fig. 468.

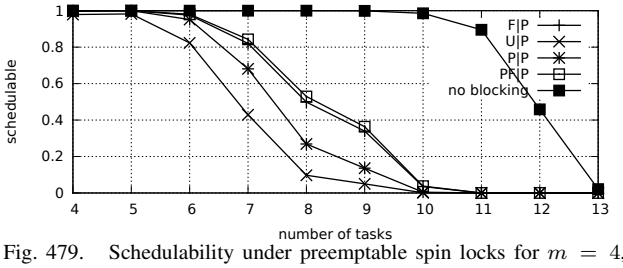

Fig. 479. Schedulability under preemptable spin locks for $m = 4$, $U = 0.3n$, 4 resources, $rsf = 0.75$, $N^{max} = 15$, and medium critical sections. The schedulability of the considered non-preemptable lock types in this configuration is shown in Fig. 469.

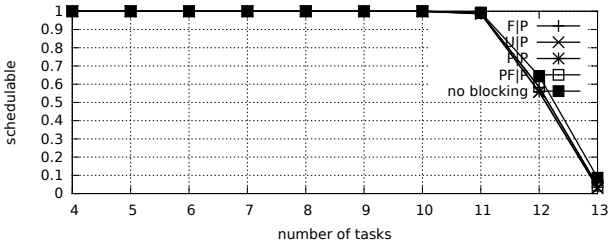

Fig. 480. Schedulability under preemptable spin locks for $m = 4$, $U = 0.3n$, 4 resources, $rsf = 0.75$, $N^{max} = 1$, and short critical sections. The schedulability of the considered non-preemptable lock types in this configuration is shown in Fig. 470.

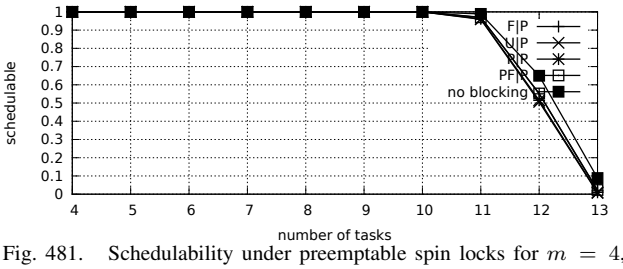

Fig. 481. Schedulability under preemptable spin locks for $m = 4$, $U = 0.3n$, 4 resources, $rsf = 0.75$, $N^{max} = 2$, and short critical sections. The schedulability of the considered non-preemptable lock types in this configuration is shown in Fig. 471.

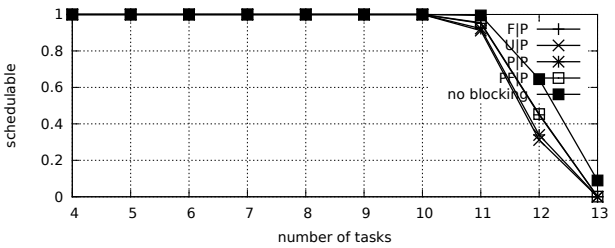

Fig. 482. Schedulability under preemptable spin locks for $m = 4$, $U = 0.3n$, 4 resources, $rsf = 0.75$, $N^{max} = 5$, and short critical sections. The schedulability of the considered non-preemptable lock types in this configuration is shown in Fig. 472.

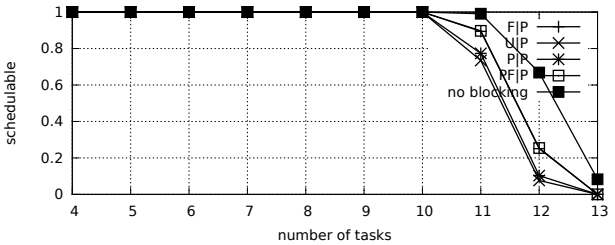

Fig. 483. Schedulability under preemptable spin locks for $m = 4$, $U = 0.3n$, 4 resources, $rsf = 0.75$, $N^{max} = 10$, and short critical sections. The schedulability of the considered non-preemptable lock types in this configuration is shown in Fig. 473.

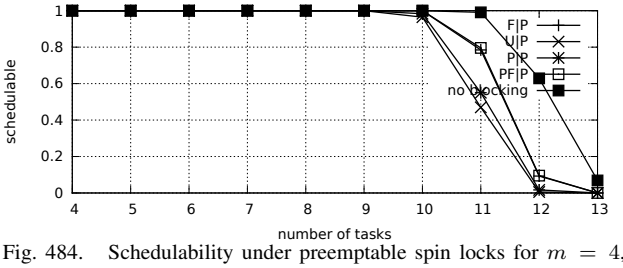

Fig. 484. Schedulability under preemptable spin locks for $m = 4$, $U = 0.3n$, 4 resources, $rsf = 0.75$, $N^{max} = 15$, and short critical sections. The schedulability of the considered non-preemptable lock types in this configuration is shown in Fig. 474.

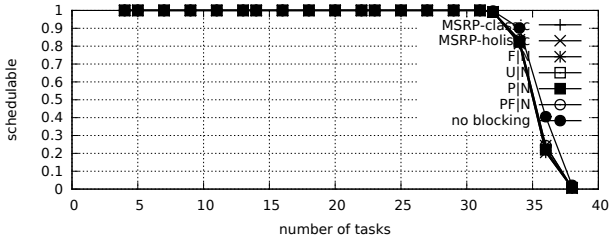

Fig. 485. Schedulability under non-preemptable spin locks for $m = 4$, $U = 0.1n$, 8 resources, $rsf = 0.1$, $N^{max} = 1$, and medium critical sections. The schedulability of the considered preemptable lock types in this configuration is shown in Fig. 495.

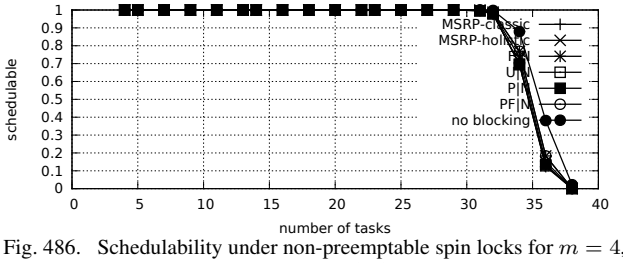

Fig. 486. Schedulability under non-preemptable spin locks for $m = 4$, $U = 0.1n$, 8 resources, $rsf = 0.1$, $N^{max} = 2$, and medium critical sections. The schedulability of the considered preemptable lock types in this configuration is shown in Fig. 496.

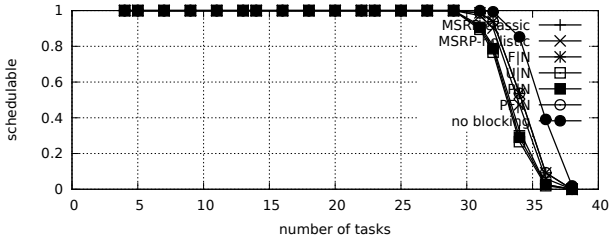

Fig. 487. Schedulability under non-preemptable spin locks for $m = 4$, $U = 0.1n$, 8 resources, $rsf = 0.1$, $N^{max} = 5$, and medium critical sections. The schedulability of the considered preemptable lock types in this configuration is shown in Fig. 497.

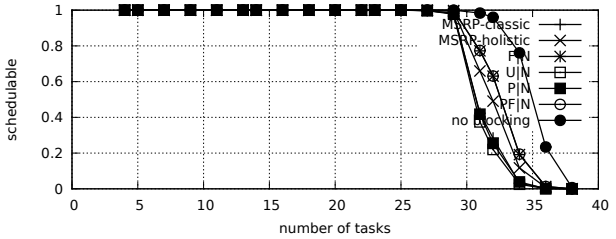

Fig. 488. Schedulability under non-preemptable spin locks for $m = 4$, $U = 0.1n$, 8 resources, $rsf = 0.1$, $N^{max} = 10$, and medium critical sections. The schedulability of the considered preemptable lock types in this configuration is shown in Fig. 498.

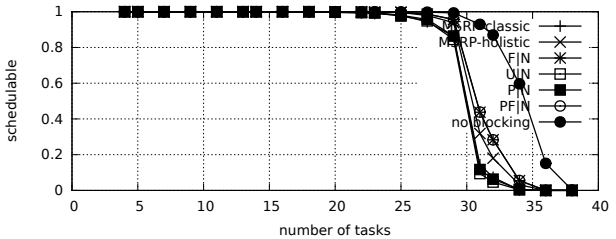

Fig. 489. Schedulability under non-preemptable spin locks for $m = 4$, $U = 0.1n$, 8 resources, $rsf = 0.1$, $N^{max} = 15$, and medium critical sections. The schedulability of the considered preemptable lock types in this configuration is shown in Fig. 499.

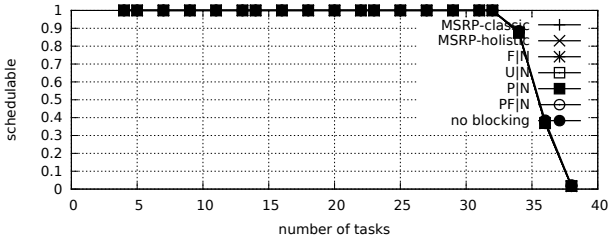

Fig. 490. Schedulability under non-preemptable spin locks for $m = 4$, $U = 0.1n$, 8 resources, $rsf = 0.1$, $N^{max} = 1$, and short critical sections. The schedulability of the considered preemptable lock types in this configuration is shown in Fig. 500.

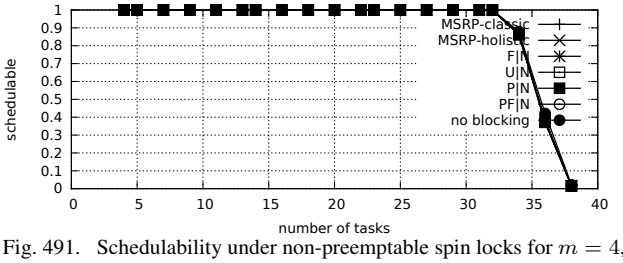

Fig. 491. Schedulability under non-preemptable spin locks for $m = 4$, $U = 0.1n$, 8 resources, $rsf = 0.1$, $N^{max} = 2$, and short critical sections. The schedulability of the considered preemptable lock types in this configuration is shown in Fig. 501.

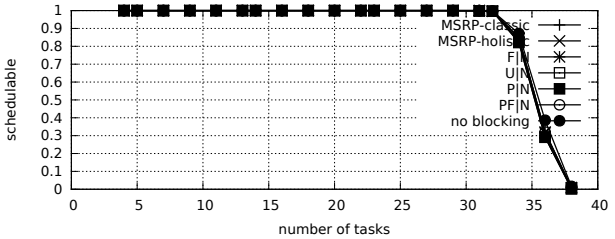

Fig. 492. Schedulability under non-preemptable spin locks for $m = 4$, $U = 0.1n$, 8 resources, $rsf = 0.1$, $N^{max} = 5$, and short critical sections. The schedulability of the considered preemptable lock types in this configuration is shown in Fig. 502.

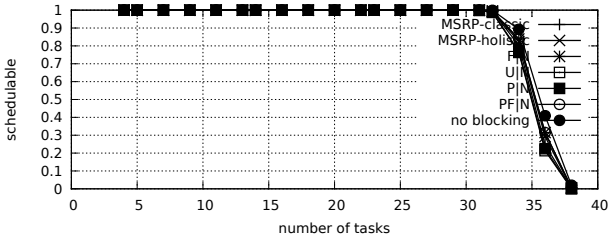

Fig. 493. Schedulability under non-preemptable spin locks for $m = 4$, $U = 0.1n$, 8 resources, $rsf = 0.1$, $N^{max} = 10$, and short critical sections. The schedulability of the considered preemptable lock types in this configuration is shown in Fig. 503.

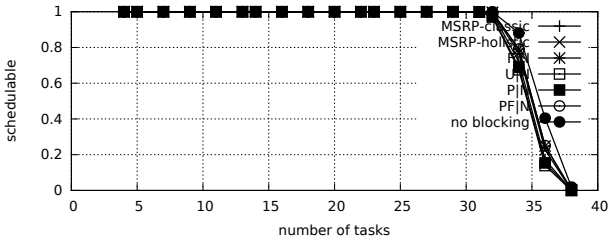

Fig. 494. Schedulability under non-preemptable spin locks for $m = 4$, $U = 0.1n$, 8 resources, $rsf = 0.1$, $N^{max} = 15$, and short critical sections. The schedulability of the considered preemptable lock types in this configuration is shown in Fig. 504.

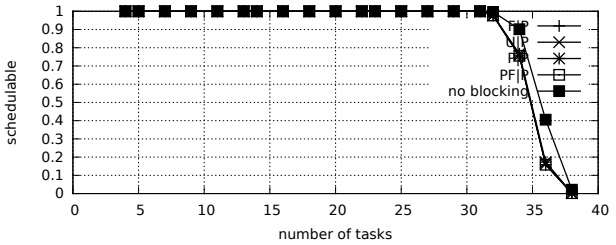

Fig. 495. Schedulability under preemptable spin locks for $m = 4$, $U = 0.1n$, 8 resources, $rsf = 0.1$, $N^{max} = 1$, and medium critical sections. The schedulability of the considered non-preemptable lock types in this configuration is shown in Fig. 485.

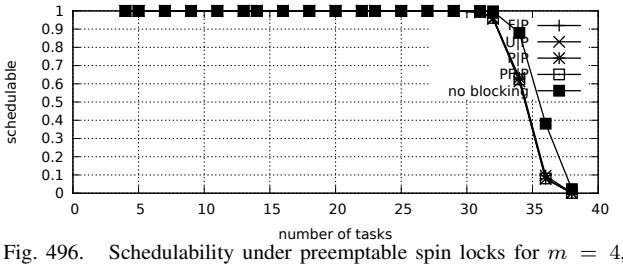

Fig. 496. Schedulability under preemptable spin locks for $m = 4$, $U = 0.1n$, 8 resources, $rsf = 0.1$, $N^{max} = 2$, and medium critical sections. The schedulability of the considered non-preemptable lock types in this configuration is shown in Fig. 486.

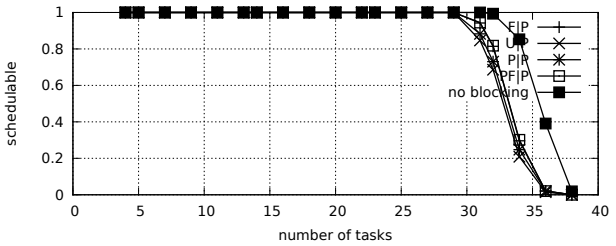

Fig. 497. Schedulability under preemptable spin locks for $m = 4$, $U = 0.1n$, 8 resources, $rsf = 0.1$, $N^{max} = 5$, and medium critical sections. The schedulability of the considered non-preemptable lock types in this configuration is shown in Fig. 487.

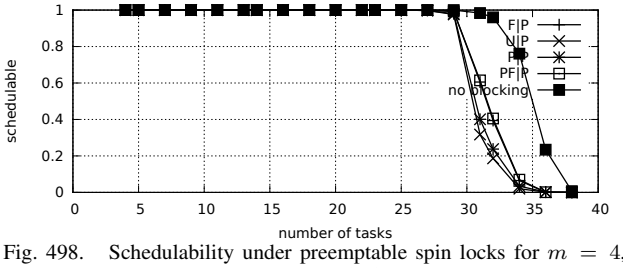

Fig. 498. Schedulability under preemptable spin locks for $m = 4$, $U = 0.1n$, 8 resources, $rsf = 0.1$, $N^{max} = 10$, and medium critical sections. The schedulability of the considered non-preemptable lock types in this configuration is shown in Fig. 488.

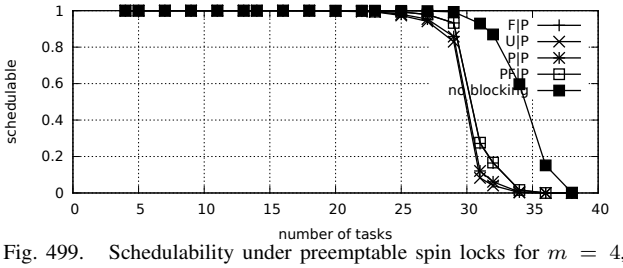

Fig. 499. Schedulability under preemptable spin locks for $m = 4$, $U = 0.1n$, 8 resources, $rsf = 0.1$, $N^{max} = 15$, and medium critical sections. The schedulability of the considered non-preemptable lock types in this configuration is shown in Fig. 489.

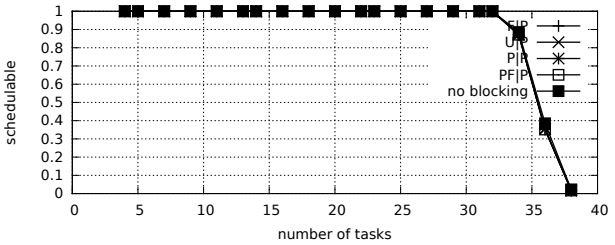

Fig. 500. Schedulability under preemptable spin locks for $m = 4$, $U = 0.1n$, 8 resources, $rsf = 0.1$, $N^{max} = 1$, and short critical sections. The schedulability of the considered non-preemptable lock types in this configuration is shown in Fig. 490.

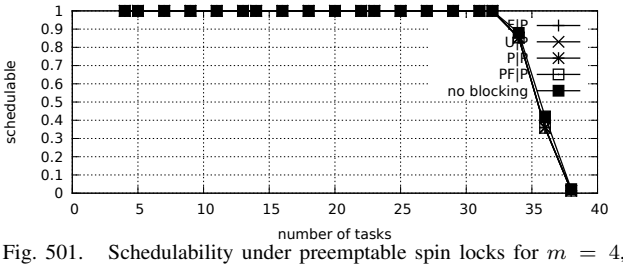

Fig. 501. Schedulability under preemptable spin locks for $m = 4$, $U = 0.1n$, 8 resources, $rsf = 0.1$, $N^{max} = 2$, and short critical sections. The schedulability of the considered non-preemptable lock types in this configuration is shown in Fig. 491.

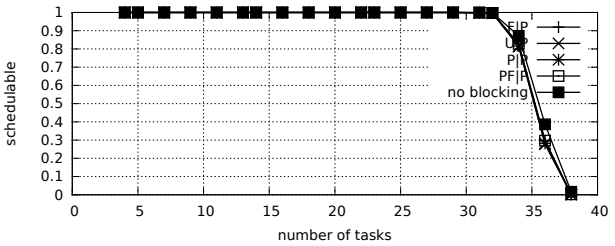

Fig. 502. Schedulability under preemptable spin locks for $m = 4$, $U = 0.1n$, 8 resources, $rsf = 0.1$, $N^{max} = 5$, and short critical sections. The schedulability of the considered non-preemptable lock types in this configuration is shown in Fig. 492.

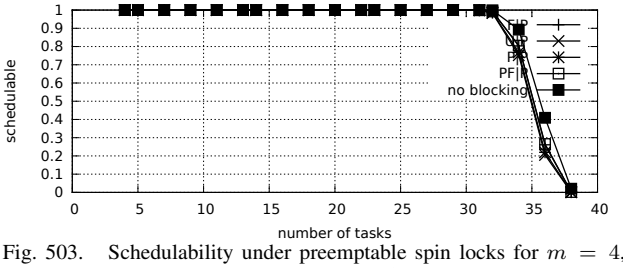

Fig. 503. Schedulability under preemptable spin locks for $m = 4$, $U = 0.1n$, 8 resources, $rsf = 0.1$, $N^{max} = 10$, and short critical sections. The schedulability of the considered non-preemptable lock types in this configuration is shown in Fig. 493.

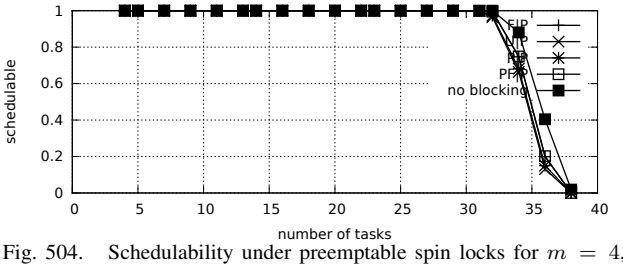

Fig. 504. Schedulability under preemptable spin locks for $m = 4$, $U = 0.1n$, 8 resources, $rsf = 0.1$, $N^{max} = 15$, and short critical sections. The schedulability of the considered non-preemptable lock types in this configuration is shown in Fig. 494.

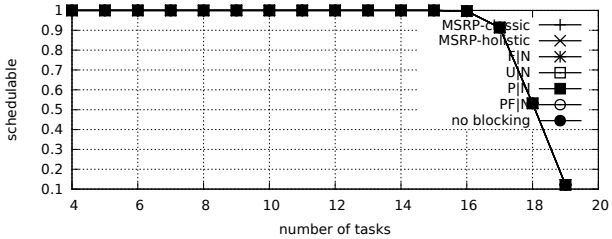

Fig. 505. Schedulability under non-preemptable spin locks for $m = 4$, $U = 0.2n$, 8 resources, $rsf = 0.1$, $N^{max} = 1$, and medium critical sections. The schedulability of the considered preemptable lock types in this configuration is shown in Fig. 515.

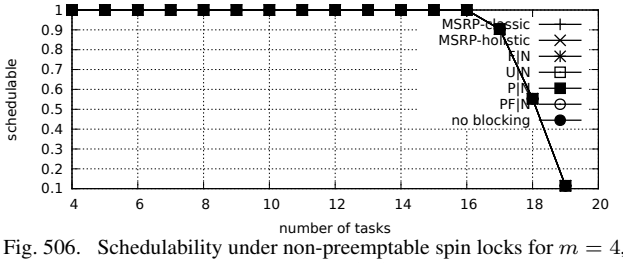

Fig. 506. Schedulability under non-preemptable spin locks for $m = 4$, $U = 0.2n$, 8 resources, $rsf = 0.1$, $N^{max} = 2$, and medium critical sections. The schedulability of the considered preemptable lock types in this configuration is shown in Fig. 516.

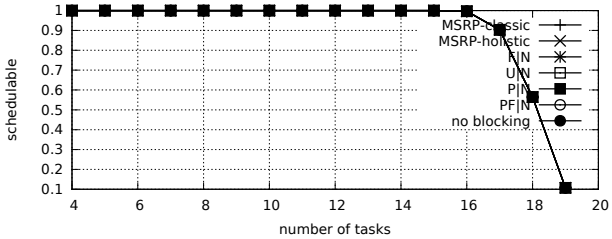

Fig. 507. Schedulability under non-preemptable spin locks for $m = 4$, $U = 0.2n$, 8 resources, $rsf = 0.1$, $N^{max} = 5$, and medium critical sections. The schedulability of the considered preemptable lock types in this configuration is shown in Fig. 517.

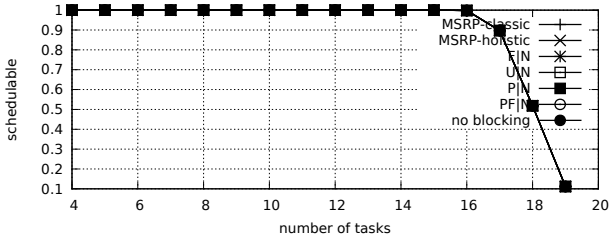

Fig. 508. Schedulability under non-preemptable spin locks for $m = 4$, $U = 0.2n$, 8 resources, $rsf = 0.1$, $N^{max} = 10$, and medium critical sections. The schedulability of the considered preemptable lock types in this configuration is shown in Fig. 518.

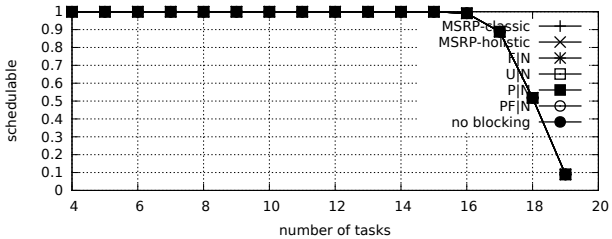

Fig. 509. Schedulability under non-preemptable spin locks for $m = 4$, $U = 0.2n$, 8 resources, $rsf = 0.1$, $N^{max} = 15$, and medium critical sections. The schedulability of the considered preemptable lock types in this configuration is shown in Fig. 519.

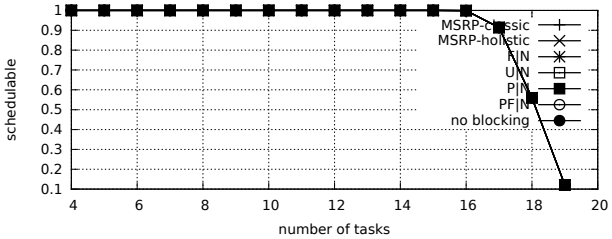

Fig. 510. Schedulability under non-preemptable spin locks for $m = 4$, $U = 0.2n$, 8 resources, $rsf = 0.1$, $N^{max} = 1$, and short critical sections. The schedulability of the considered preemptable lock types in this configuration is shown in Fig. 520.

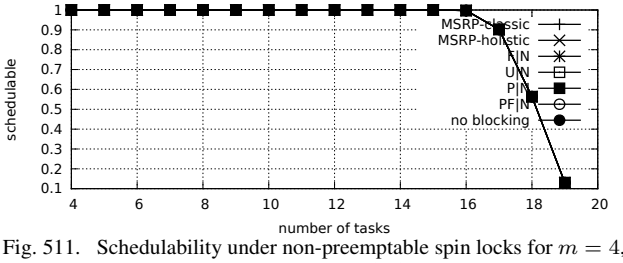

Fig. 511. Schedulability under non-preemptable spin locks for $m = 4$, $U = 0.2n$, 8 resources, $rsf = 0.1$, $N^{max} = 2$, and short critical sections. The schedulability of the considered preemptable lock types in this configuration is shown in Fig. 521.

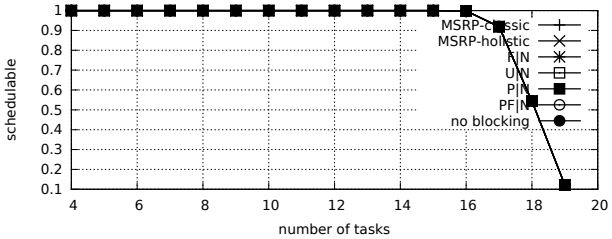

Fig. 512. Schedulability under non-preemptable spin locks for $m = 4$, $U = 0.2n$, 8 resources, $rsf = 0.1$, $N^{max} = 5$, and short critical sections. The schedulability of the considered preemptable lock types in this configuration is shown in Fig. 522.

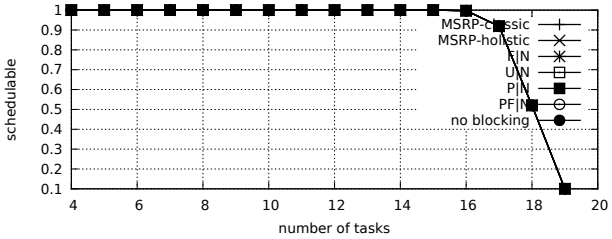

Fig. 513. Schedulability under non-preemptable spin locks for $m = 4$, $U = 0.2n$, 8 resources, $rsf = 0.1$, $N^{max} = 10$, and short critical sections. The schedulability of the considered preemptable lock types in this configuration is shown in Fig. 523.

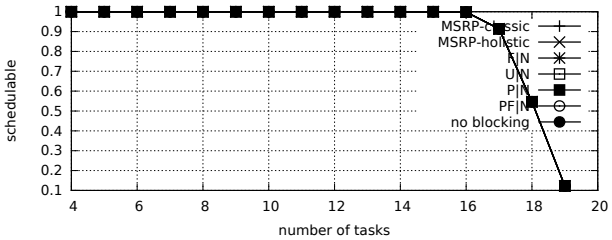

Fig. 514. Schedulability under non-preemptable spin locks for $m = 4$, $U = 0.2n$, 8 resources, $rsf = 0.1$, $N^{max} = 15$, and short critical sections. The schedulability of the considered preemptable lock types in this configuration is shown in Fig. 524.

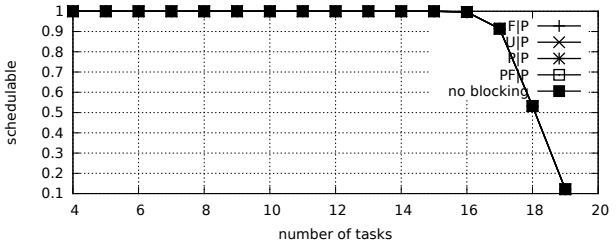

Fig. 515. Schedulability under preemptable spin locks for $m = 4$, $U = 0.2n$, 8 resources, $rsf = 0.1$, $N^{max} = 1$, and medium critical sections. The schedulability of the considered non-preemptable lock types in this configuration is shown in Fig. 505.

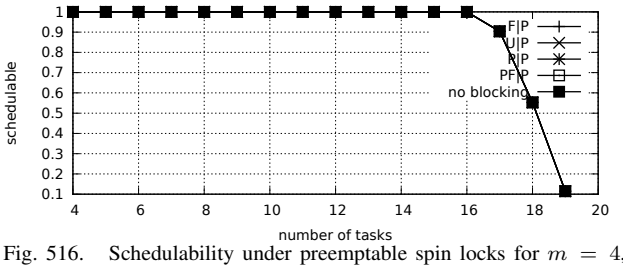

Fig. 516. Schedulability under preemptable spin locks for $m = 4$, $U = 0.2n$, 8 resources, $rsf = 0.1$, $N^{max} = 2$, and medium critical sections. The schedulability of the considered non-preemptable lock types in this configuration is shown in Fig. 506.

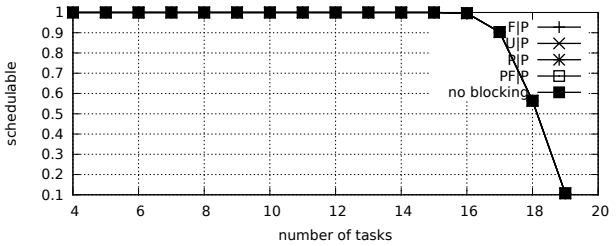

Fig. 517. Schedulability under preemptable spin locks for $m = 4$, $U = 0.2n$, 8 resources, $rsf = 0.1$, $N^{max} = 5$, and medium critical sections. The schedulability of the considered non-preemptable lock types in this configuration is shown in Fig. 507.

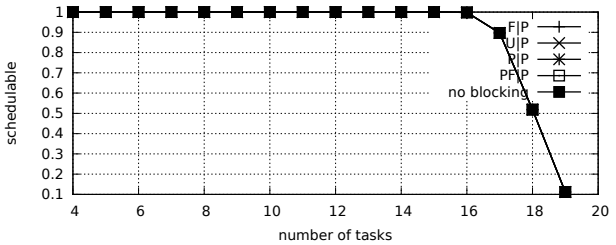

Fig. 518. Schedulability under preemptable spin locks for $m = 4$, $U = 0.2n$, 8 resources, $rsf = 0.1$, $N^{max} = 10$, and medium critical sections. The schedulability of the considered non-preemptable lock types in this configuration is shown in Fig. 508.

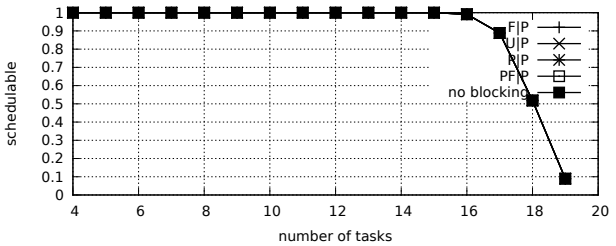

Fig. 519. Schedulability under preemptable spin locks for $m = 4$, $U = 0.2n$, 8 resources, $rsf = 0.1$, $N^{max} = 15$, and medium critical sections. The schedulability of the considered non-preemptable lock types in this configuration is shown in Fig. 509.

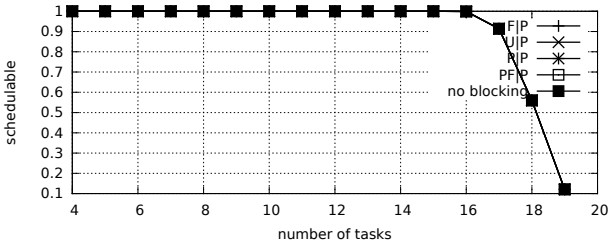

Fig. 520. Schedulability under preemptable spin locks for $m = 4$, $U = 0.2n$, 8 resources, $rsf = 0.1$, $N^{max} = 1$, and short critical sections. The schedulability of the considered non-preemptable lock types in this configuration is shown in Fig. 510.

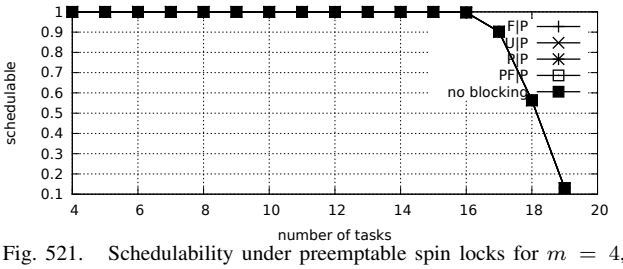

Fig. 521. Schedulability under preemptable spin locks for $m = 4$, $U = 0.2n$, 8 resources, $rsf = 0.1$, $N^{max} = 2$, and short critical sections. The schedulability of the considered non-preemptable lock types in this configuration is shown in Fig. 511.

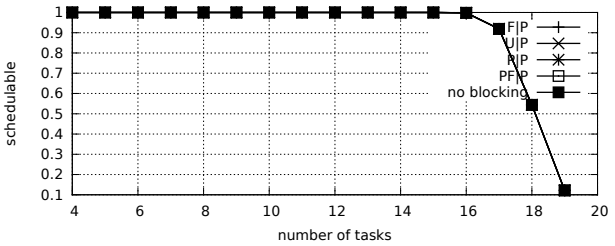

Fig. 522. Schedulability under preemptable spin locks for $m = 4$, $U = 0.2n$, 8 resources, $rsf = 0.1$, $N^{max} = 5$, and short critical sections. The schedulability of the considered non-preemptable lock types in this configuration is shown in Fig. 512.

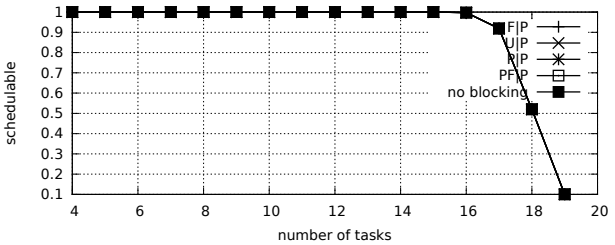

Fig. 523. Schedulability under preemptable spin locks for $m = 4$, $U = 0.2n$, 8 resources, $rsf = 0.1$, $N^{max} = 10$, and short critical sections. The schedulability of the considered non-preemptable lock types in this configuration is shown in Fig. 513.

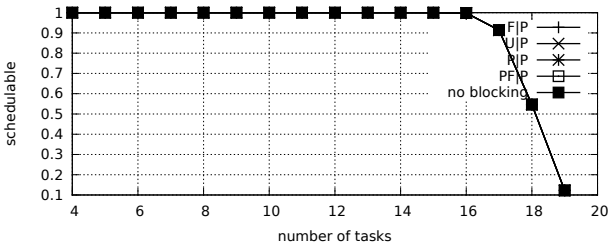

Fig. 524. Schedulability under preemptable spin locks for $m = 4$, $U = 0.2n$, 8 resources, $rsf = 0.1$, $N^{max} = 15$, and short critical sections. The schedulability of the considered non-preemptable lock types in this configuration is shown in Fig. 514.

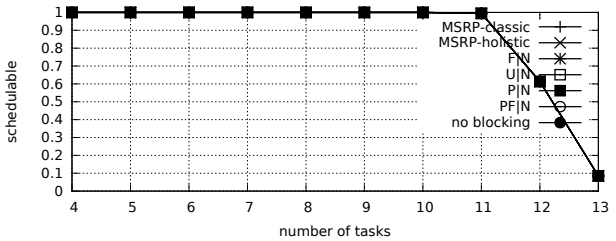

Fig. 525. Schedulability under non-preemptable spin locks for $m = 4$, $U = 0.3n$, 8 resources, $rsf = 0.1$, $N^{max} = 1$, and medium critical sections. The schedulability of the considered preemptable lock types in this configuration is shown in Fig. 535.

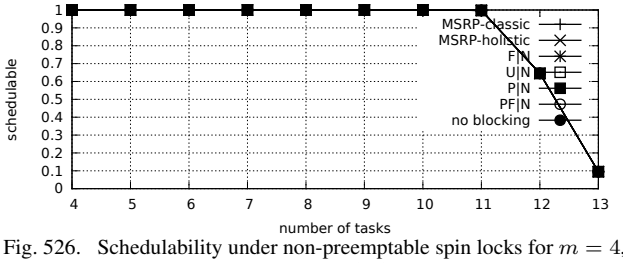

Fig. 526. Schedulability under non-preemptable spin locks for $m = 4$, $U = 0.3n$, 8 resources, $rsf = 0.1$, $N^{max} = 2$, and medium critical sections. The schedulability of the considered preemptable lock types in this configuration is shown in Fig. 536.

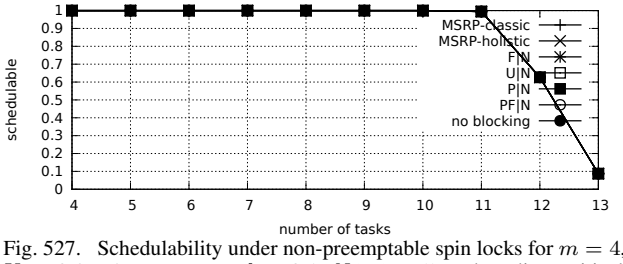

Fig. 527. Schedulability under non-preemptable spin locks for $m = 4$, $U = 0.3n$, 8 resources, $rsf = 0.1$, $N^{max} = 5$, and medium critical sections. The schedulability of the considered preemptable lock types in this configuration is shown in Fig. 537.

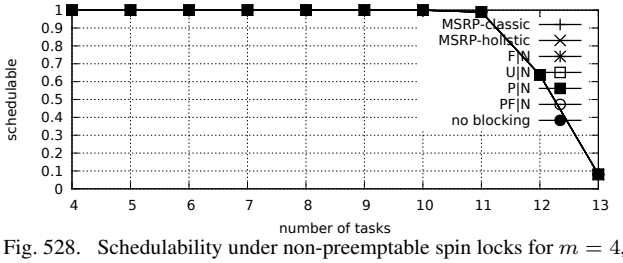

Fig. 528. Schedulability under non-preemptable spin locks for $m = 4$, $U = 0.3n$, 8 resources, $rsf = 0.1$, $N^{max} = 10$, and medium critical sections. The schedulability of the considered preemptable lock types in this configuration is shown in Fig. 538.

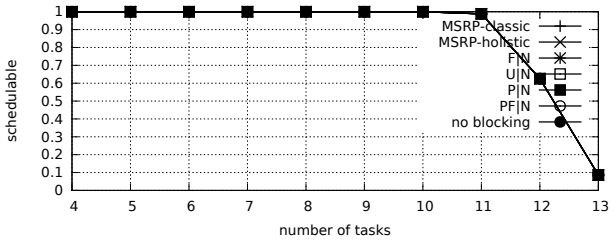

Fig. 529. Schedulability under non-preemptable spin locks for $m = 4$, $U = 0.3n$, 8 resources, $rsf = 0.1$, $N^{max} = 15$, and medium critical sections. The schedulability of the considered preemptable lock types in this configuration is shown in Fig. 539.

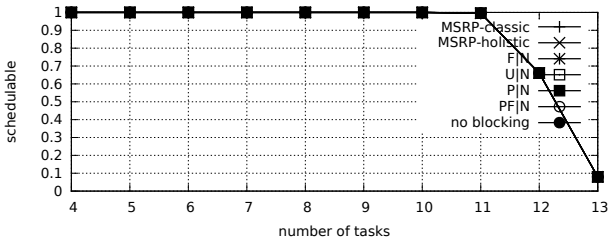

Fig. 530. Schedulability under non-preemptable spin locks for $m = 4$, $U = 0.3n$, 8 resources, $rsf = 0.1$, $N^{max} = 1$, and short critical sections. The schedulability of the considered preemptable lock types in this configuration is shown in Fig. 540.

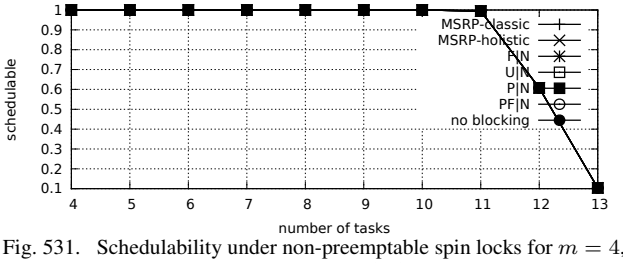

Fig. 531. Schedulability under non-preemptable spin locks for $m = 4$, $U = 0.3n$, 8 resources, $rsf = 0.1$, $N^{max} = 2$, and short critical sections. The schedulability of the considered preemptable lock types in this configuration is shown in Fig. 541.

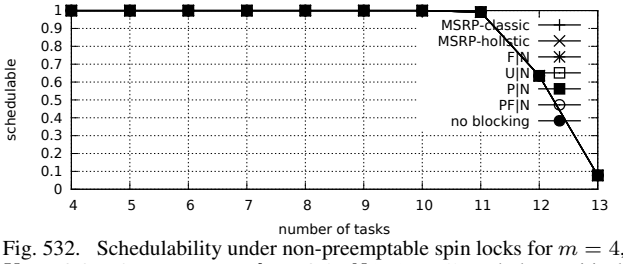

Fig. 532. Schedulability under non-preemptable spin locks for $m = 4$, $U = 0.3n$, 8 resources, $rsf = 0.1$, $N^{max} = 5$, and short critical sections. The schedulability of the considered preemptable lock types in this configuration is shown in Fig. 542.

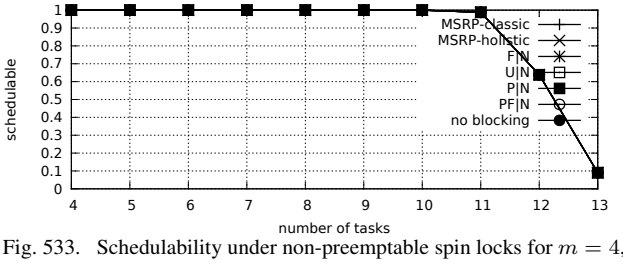

Fig. 533. Schedulability under non-preemptable spin locks for $m = 4$, $U = 0.3n$, 8 resources, $rsf = 0.1$, $N^{max} = 10$, and short critical sections. The schedulability of the considered preemptable lock types in this configuration is shown in Fig. 543.

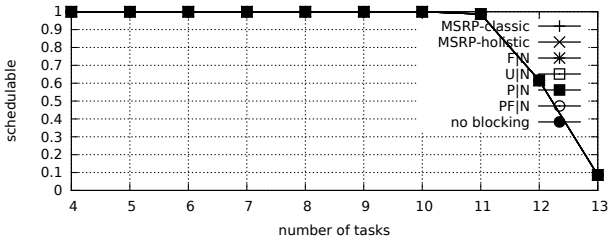

Fig. 534. Schedulability under non-preemptable spin locks for $m = 4$, $U = 0.3n$, 8 resources, $rsf = 0.1$, $N^{max} = 15$, and short critical sections. The schedulability of the considered preemptable lock types in this configuration is shown in Fig. 544.

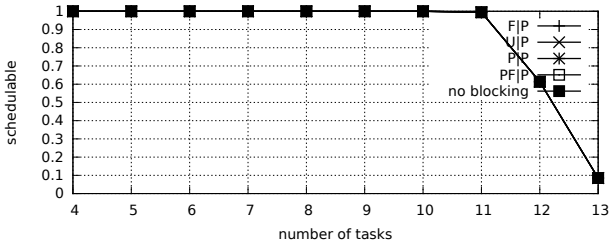

Fig. 535. Schedulability under preemptable spin locks for $m = 4$, $U = 0.3n$, 8 resources, $rsf = 0.1$, $N^{max} = 1$, and medium critical sections. The schedulability of the considered non-preemptable lock types in this configuration is shown in Fig. 525.

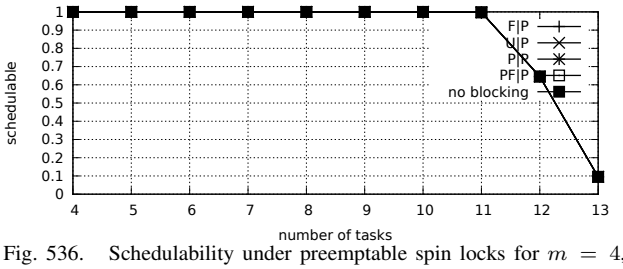

Fig. 536. Schedulability under preemptable spin locks for $m = 4$, $U = 0.3n$, 8 resources, $rsf = 0.1$, $N^{max} = 2$, and medium critical sections. The schedulability of the considered non-preemptable lock types in this configuration is shown in Fig. 526.

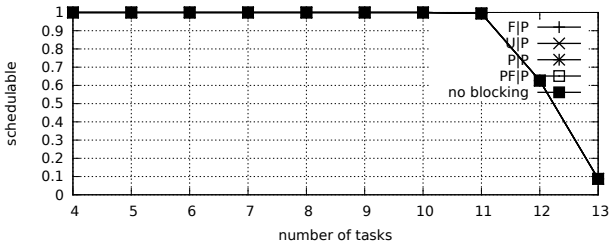

Fig. 537. Schedulability under preemptable spin locks for $m = 4$, $U = 0.3n$, 8 resources, $rsf = 0.1$, $N^{max} = 5$, and medium critical sections. The schedulability of the considered non-preemptable lock types in this configuration is shown in Fig. 527.

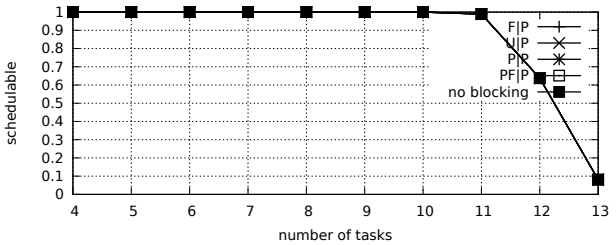

Fig. 538. Schedulability under preemptable spin locks for $m = 4$, $U = 0.3n$, 8 resources, $rsf = 0.1$, $N^{max} = 10$, and medium critical sections. The schedulability of the considered non-preemptable lock types in this configuration is shown in Fig. 528.

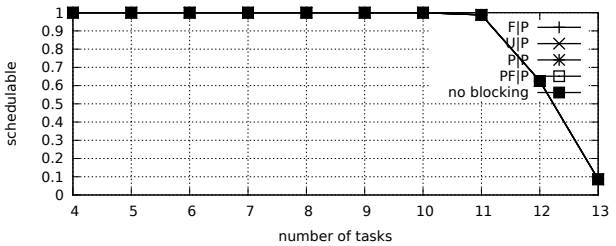

Fig. 539. Schedulability under preemptable spin locks for $m = 4$, $U = 0.3n$, 8 resources, $rsf = 0.1$, $N^{max} = 15$, and medium critical sections. The schedulability of the considered non-preemptable lock types in this configuration is shown in Fig. 529.

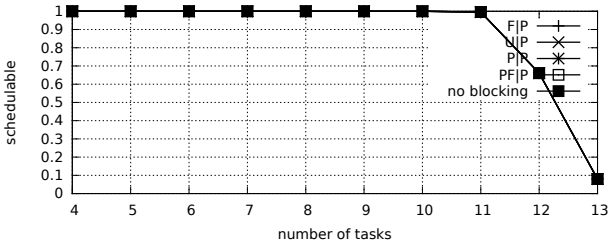

Fig. 540. Schedulability under preemptable spin locks for $m = 4$, $U = 0.3n$, 8 resources, $rsf = 0.1$, $N^{max} = 1$, and short critical sections. The schedulability of the considered non-preemptable lock types in this configuration is shown in Fig. 530.

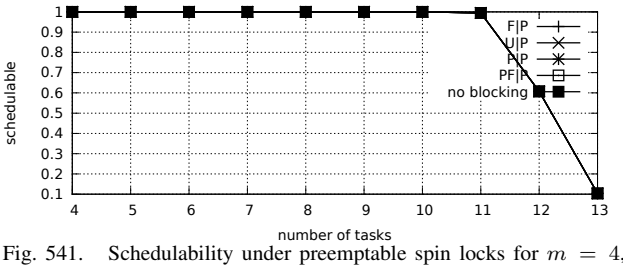

Fig. 541. Schedulability under preemptable spin locks for $m = 4$, $U = 0.3n$, 8 resources, $rsf = 0.1$, $N^{max} = 2$, and short critical sections. The schedulability of the considered non-preemptable lock types in this configuration is shown in Fig. 531.

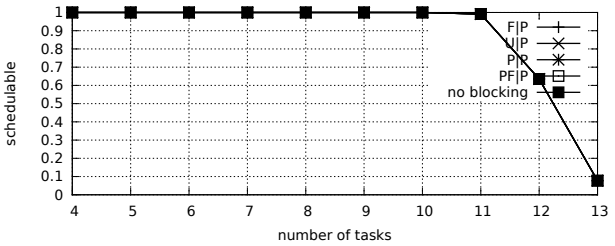

Fig. 542. Schedulability under preemptable spin locks for $m = 4$, $U = 0.3n$, 8 resources, $rsf = 0.1$, $N^{max} = 5$, and short critical sections. The schedulability of the considered non-preemptable lock types in this configuration is shown in Fig. 532.

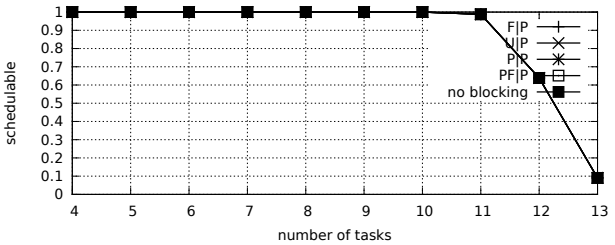

Fig. 543. Schedulability under preemptable spin locks for $m = 4$, $U = 0.3n$, 8 resources, $rsf = 0.1$, $N^{max} = 10$, and short critical sections. The schedulability of the considered non-preemptable lock types in this configuration is shown in Fig. 533.

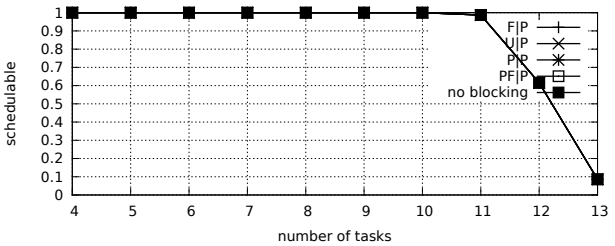

Fig. 544. Schedulability under preemptable spin locks for $m = 4$, $U = 0.3n$, 8 resources, $rsf = 0.1$, $N^{max} = 15$, and short critical sections. The schedulability of the considered non-preemptable lock types in this configuration is shown in Fig. 534.

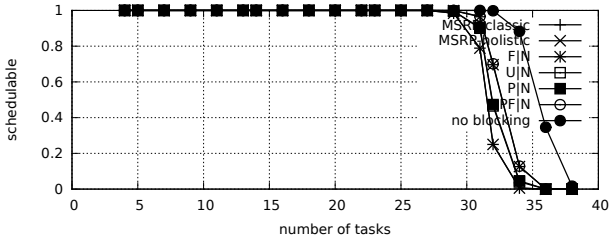

Fig. 545. Schedulability under non-preemptable spin locks for $m = 4$, $U = 0.1n$, 8 resources, $rsf = 0.25$, $N^{max} = 1$, and medium critical sections. The schedulability of the considered preemptable lock types in this configuration is shown in Fig. 555.

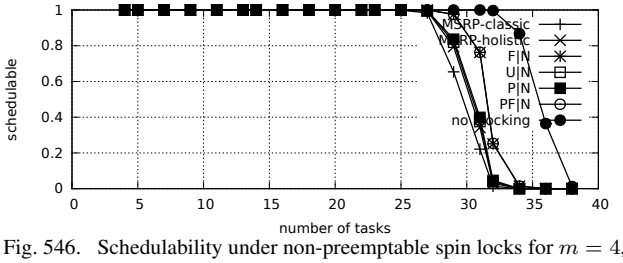

Fig. 546. Schedulability under non-preemptable spin locks for $m = 4$, $U = 0.1n$, 8 resources, $rsf = 0.25$, $N^{max} = 2$, and medium critical sections. The schedulability of the considered preemptable lock types in this configuration is shown in Fig. 556.

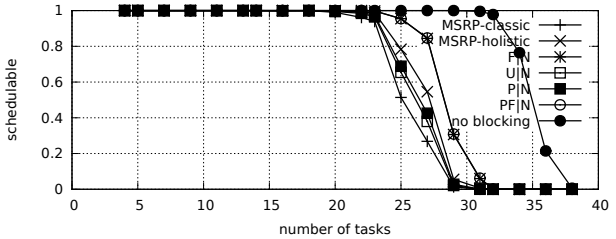

Fig. 547. Schedulability under non-preemptable spin locks for $m = 4$, $U = 0.1n$, 8 resources, $rsf = 0.25$, $N^{max} = 5$, and medium critical sections. The schedulability of the considered preemptable lock types in this configuration is shown in Fig. 557.

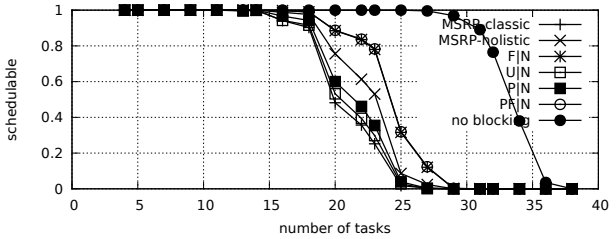

Fig. 548. Schedulability under non-preemptable spin locks for $m = 4$, $U = 0.1n$, 8 resources, $rsf = 0.25$, $N^{max} = 10$, and medium critical sections. The schedulability of the considered preemptable lock types in this configuration is shown in Fig. 558.

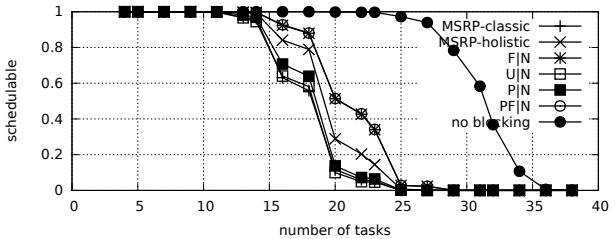

Fig. 549. Schedulability under non-preemptable spin locks for $m = 4$, $U = 0.1n$, 8 resources, $rsf = 0.25$, $N^{max} = 15$, and medium critical sections. The schedulability of the considered preemptable lock types in this configuration is shown in Fig. 559.

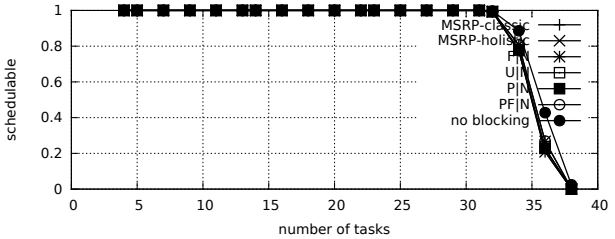

Fig. 550. Schedulability under non-preemptable spin locks for $m = 4$, $U = 0.1n$, 8 resources, $rsf = 0.25$, $N^{max} = 1$, and short critical sections. The schedulability of the considered preemptable lock types in this configuration is shown in Fig. 560.

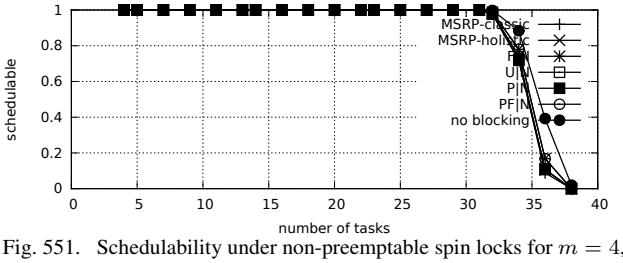

Fig. 551. Schedulability under non-preemptable spin locks for $m = 4$, $U = 0.1n$, 8 resources, $rsf = 0.25$, $N^{max} = 2$, and short critical sections. The schedulability of the considered preemptable lock types in this configuration is shown in Fig. 561.

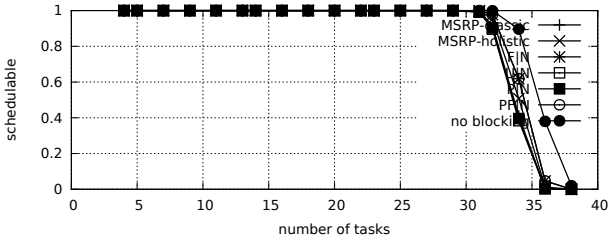

Fig. 552. Schedulability under non-preemptable spin locks for $m = 4$, $U = 0.1n$, 8 resources, $rsf = 0.25$, $N^{max} = 5$, and short critical sections. The schedulability of the considered preemptable lock types in this configuration is shown in Fig. 562.

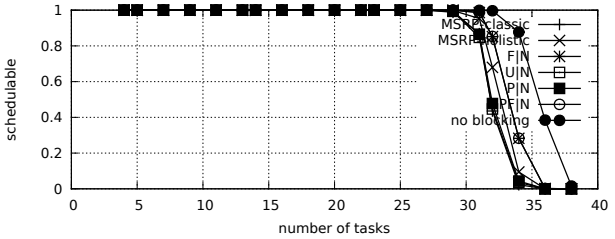

Fig. 553. Schedulability under non-preemptable spin locks for $m = 4$, $U = 0.1n$, 8 resources, $rsf = 0.25$, $N^{max} = 10$, and short critical sections. The schedulability of the considered preemptable lock types in this configuration is shown in Fig. 563.

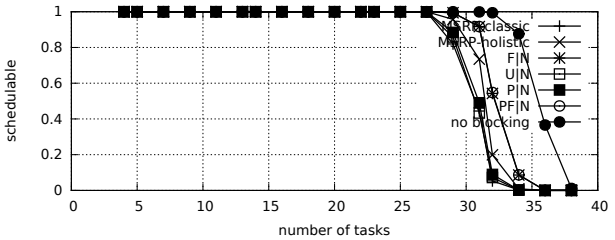

Fig. 554. Schedulability under non-preemptable spin locks for $m = 4$, $U = 0.1n$, 8 resources, $rsf = 0.25$, $N^{max} = 15$, and short critical sections. The schedulability of the considered preemptable lock types in this configuration is shown in Fig. 564.

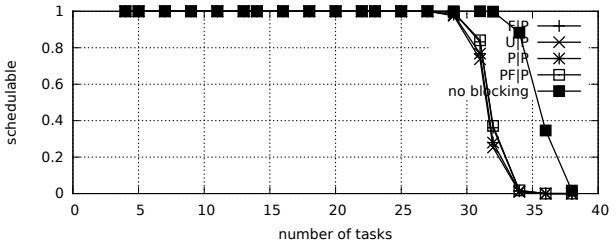

Fig. 555. Schedulability under preemptable spin locks for $m = 4$, $U = 0.1n$, 8 resources, $rsf = 0.25$, $N^{max} = 1$, and medium critical sections. The schedulability of the considered non-preemptable lock types in this configuration is shown in Fig. 545.

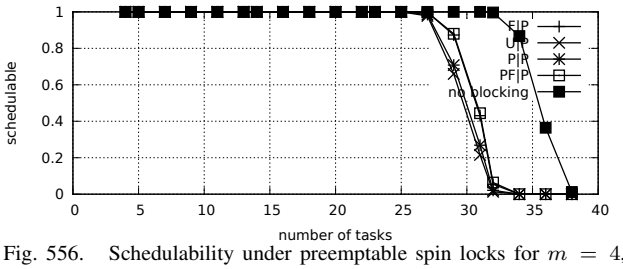

Fig. 556. Schedulability under preemptable spin locks for $m = 4$, $U = 0.1n$, 8 resources, $rsf = 0.25$, $N^{max} = 2$, and medium critical sections. The schedulability of the considered non-preemptable lock types in this configuration is shown in Fig. 546.

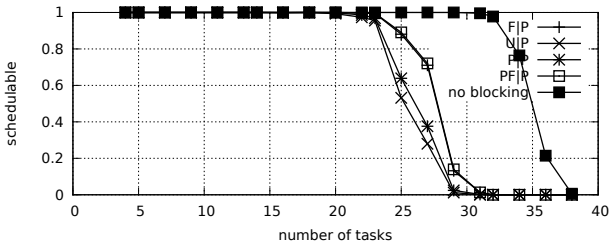

Fig. 557. Schedulability under preemptable spin locks for $m = 4$, $U = 0.1n$, 8 resources, $rsf = 0.25$, $N^{max} = 5$, and medium critical sections. The schedulability of the considered non-preemptable lock types in this configuration is shown in Fig. 547.

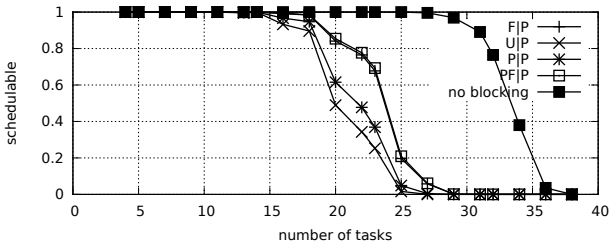

Fig. 558. Schedulability under preemptable spin locks for $m = 4$, $U = 0.1n$, 8 resources, $rsf = 0.25$, $N^{max} = 10$, and medium critical sections. The schedulability of the considered non-preemptable lock types in this configuration is shown in Fig. 548.

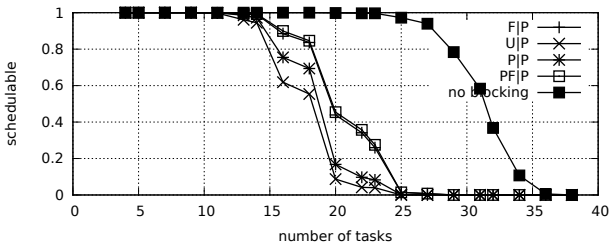

Fig. 559. Schedulability under preemptable spin locks for $m = 4$, $U = 0.1n$, 8 resources, $rsf = 0.25$, $N^{max} = 15$, and medium critical sections. The schedulability of the considered non-preemptable lock types in this configuration is shown in Fig. 549.

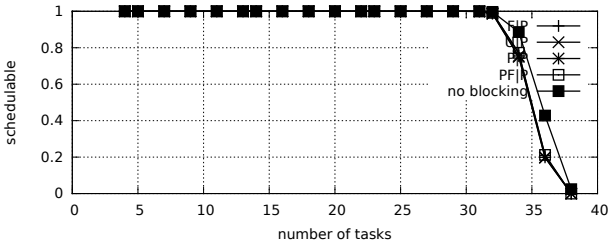

Fig. 560. Schedulability under preemptable spin locks for $m = 4$, $U = 0.1n$, 8 resources, $rsf = 0.25$, $N^{max} = 1$, and short critical sections. The schedulability of the considered non-preemptable lock types in this configuration is shown in Fig. 550.

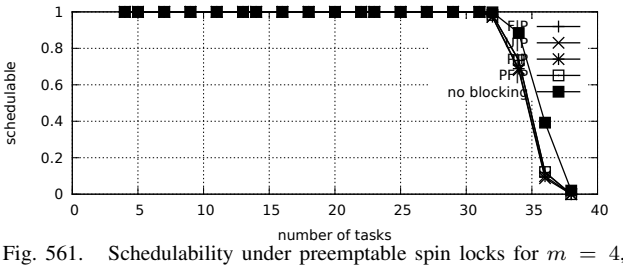

Fig. 561. Schedulability under preemptable spin locks for $m = 4$, $U = 0.1n$, 8 resources, $rsf = 0.25$, $N^{max} = 2$, and short critical sections. The schedulability of the considered non-preemptable lock types in this configuration is shown in Fig. 551.

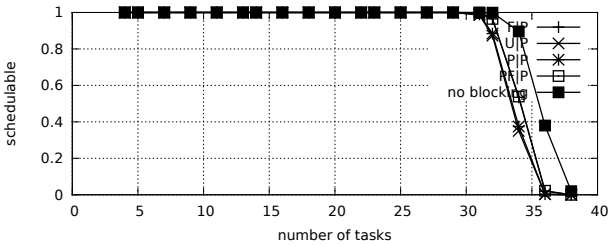

Fig. 562. Schedulability under preemptable spin locks for $m = 4$, $U = 0.1n$, 8 resources, $rsf = 0.25$, $N^{max} = 5$, and short critical sections. The schedulability of the considered non-preemptable lock types in this configuration is shown in Fig. 552.

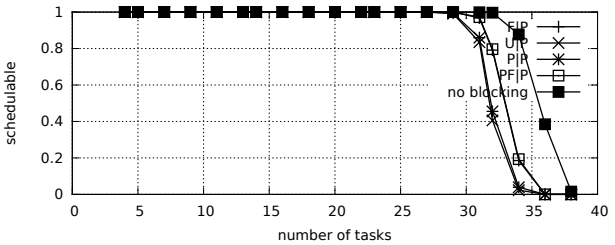

Fig. 563. Schedulability under preemptable spin locks for $m = 4$, $U = 0.1n$, 8 resources, $rsf = 0.25$, $N^{max} = 10$, and short critical sections. The schedulability of the considered non-preemptable lock types in this configuration is shown in Fig. 553.

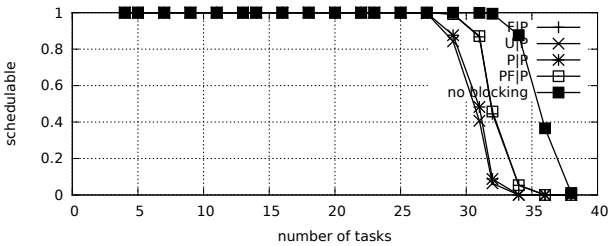

Fig. 564. Schedulability under preemptable spin locks for $m = 4$, $U = 0.1n$, 8 resources, $rsf = 0.25$, $N^{max} = 15$, and short critical sections. The schedulability of the considered non-preemptable lock types in this configuration is shown in Fig. 554.

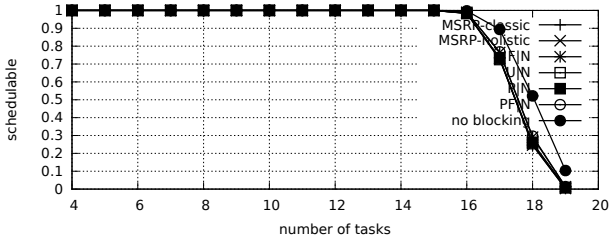

Fig. 565. Schedulability under non-preemptable spin locks for $m = 4$, $U = 0.2n$, 8 resources, $rsf = 0.25$, $N^{max} = 1$, and medium critical sections. The schedulability of the considered preemptable lock types in this configuration is shown in Fig. 575.

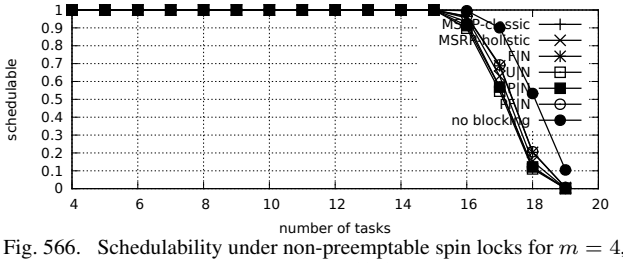

Fig. 566. Schedulability under non-preemptable spin locks for $m = 4$, $U = 0.2n$, 8 resources, $rsf = 0.25$, $N^{max} = 2$, and medium critical sections. The schedulability of the considered preemptable lock types in this configuration is shown in Fig. 576.

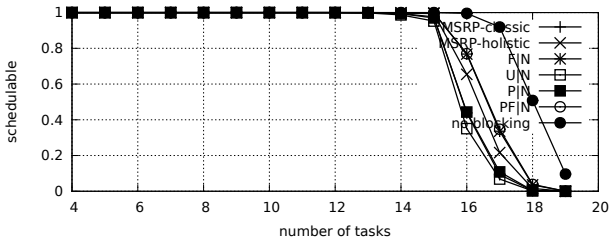

Fig. 567. Schedulability under non-preemptable spin locks for $m = 4$, $U = 0.2n$, 8 resources, $rsf = 0.25$, $N^{max} = 5$, and medium critical sections. The schedulability of the considered preemptable lock types in this configuration is shown in Fig. 577.

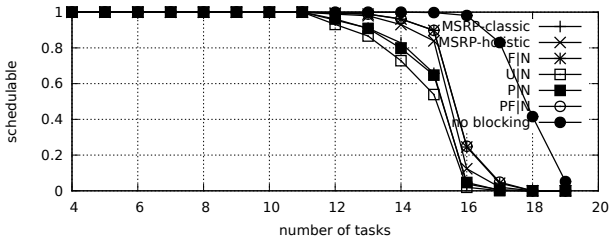

Fig. 568. Schedulability under non-preemptable spin locks for $m = 4$, $U = 0.2n$, 8 resources, $rsf = 0.25$, $N^{max} = 10$, and medium critical sections. The schedulability of the considered preemptable lock types in this configuration is shown in Fig. 578.

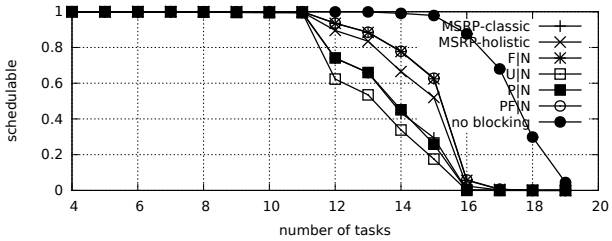

Fig. 569. Schedulability under non-preemptable spin locks for $m = 4$, $U = 0.2n$, 8 resources, $rsf = 0.25$, $N^{max} = 15$, and medium critical sections. The schedulability of the considered preemptable lock types in this configuration is shown in Fig. 579.

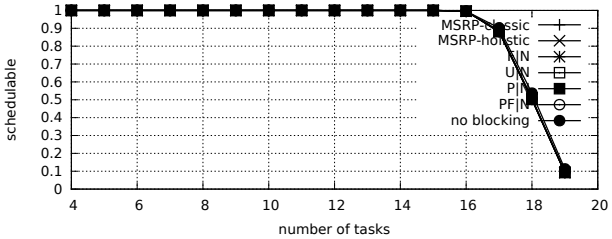

Fig. 570. Schedulability under non-preemptable spin locks for $m = 4$, $U = 0.2n$, 8 resources, $rsf = 0.25$, $N^{max} = 1$, and short critical sections. The schedulability of the considered preemptable lock types in this configuration is shown in Fig. 580.

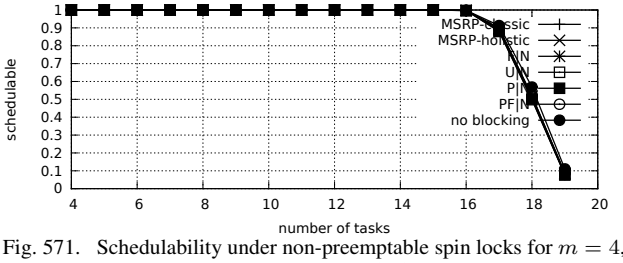

Fig. 571. Schedulability under non-preemptable spin locks for $m = 4$, $U = 0.2n$, 8 resources, $rsf = 0.25$, $N^{max} = 2$, and short critical sections. The schedulability of the considered preemptable lock types in this configuration is shown in Fig. 581.

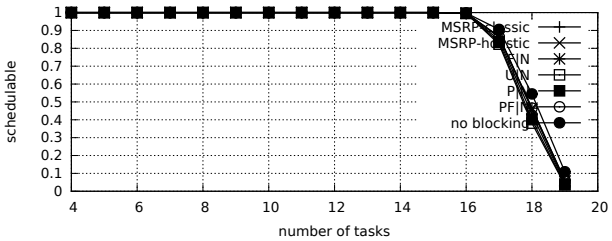

Fig. 572. Schedulability under non-preemptable spin locks for $m = 4$, $U = 0.2n$, 8 resources, $rsf = 0.25$, $N^{max} = 5$, and short critical sections. The schedulability of the considered preemptable lock types in this configuration is shown in Fig. 582.

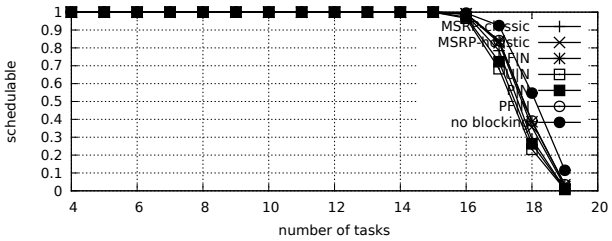

Fig. 573. Schedulability under non-preemptable spin locks for $m = 4$, $U = 0.2n$, 8 resources, $rsf = 0.25$, $N^{max} = 10$, and short critical sections. The schedulability of the considered preemptable lock types in this configuration is shown in Fig. 583.

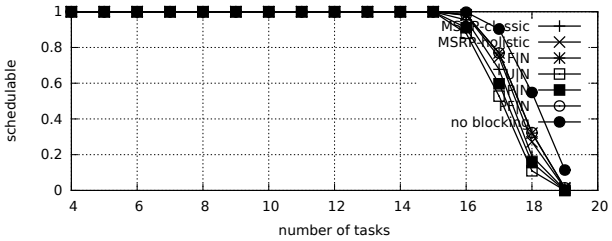

Fig. 574. Schedulability under non-preemptable spin locks for $m = 4$, $U = 0.2n$, 8 resources, $rsf = 0.25$, $N^{max} = 15$, and short critical sections. The schedulability of the considered preemptable lock types in this configuration is shown in Fig. 584.

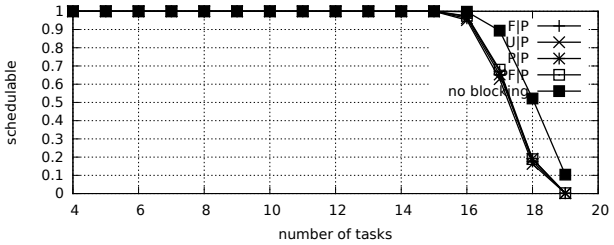

Fig. 575. Schedulability under preemptable spin locks for $m = 4$, $U = 0.2n$, 8 resources, $rsf = 0.25$, $N^{max} = 1$, and medium critical sections. The schedulability of the considered non-preemptable lock types in this configuration is shown in Fig. 565.

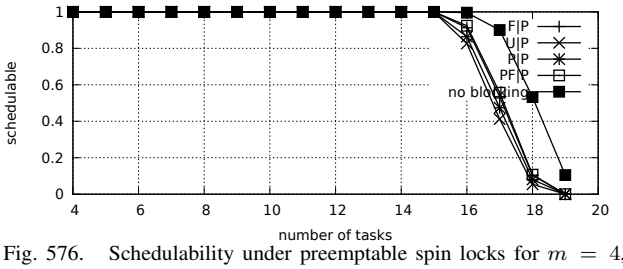

Fig. 576. Schedulability under preemptable spin locks for $m = 4$, $U = 0.2n$, 8 resources, $rsf = 0.25$, $N^{max} = 2$, and medium critical sections. The schedulability of the considered non-preemptable lock types in this configuration is shown in Fig. 566.

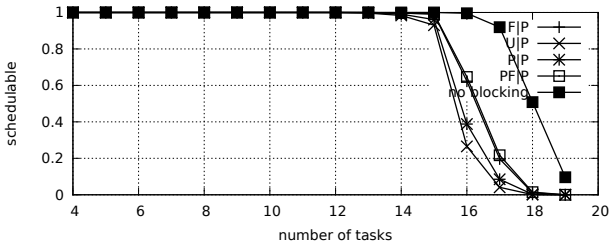

Fig. 577. Schedulability under preemptable spin locks for $m = 4$, $U = 0.2n$, 8 resources, $rsf = 0.25$, $N^{max} = 5$, and medium critical sections. The schedulability of the considered non-preemptable lock types in this configuration is shown in Fig. 567.

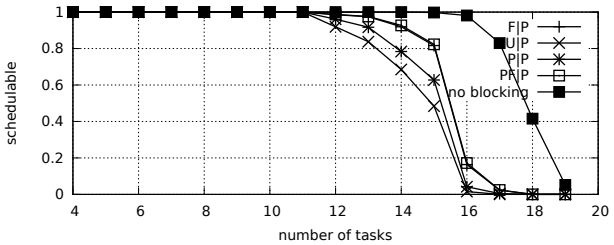

Fig. 578. Schedulability under preemptable spin locks for $m = 4$, $U = 0.2n$, 8 resources, $rsf = 0.25$, $N^{max} = 10$, and medium critical sections. The schedulability of the considered non-preemptable lock types in this configuration is shown in Fig. 568.

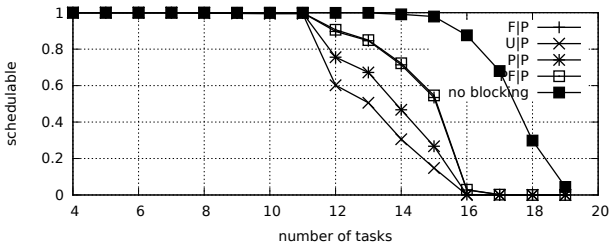

Fig. 579. Schedulability under preemptable spin locks for $m = 4$, $U = 0.2n$, 8 resources, $rsf = 0.25$, $N^{max} = 15$, and medium critical sections. The schedulability of the considered non-preemptable lock types in this configuration is shown in Fig. 569.

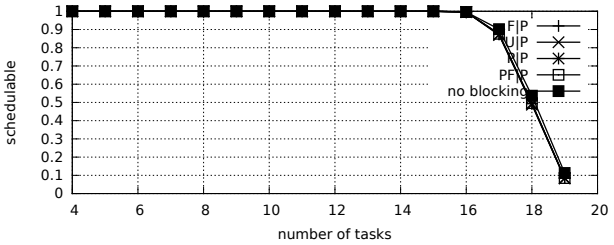

Fig. 580. Schedulability under preemptable spin locks for $m = 4$, $U = 0.2n$, 8 resources, $rsf = 0.25$, $N^{max} = 1$, and short critical sections. The schedulability of the considered non-preemptable lock types in this configuration is shown in Fig. 570.

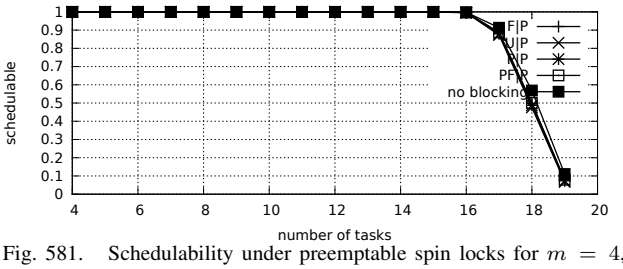

Fig. 581. Schedulability under preemptable spin locks for $m = 4$, $U = 0.2n$, 8 resources, $rsf = 0.25$, $N^{max} = 2$, and short critical sections. The schedulability of the considered non-preemptable lock types in this configuration is shown in Fig. 571.

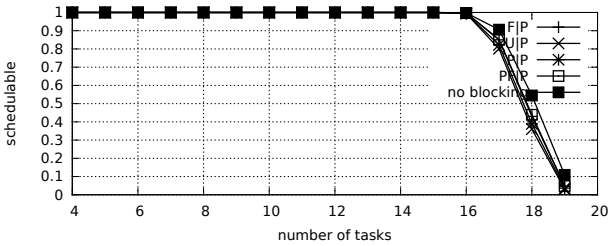

Fig. 582. Schedulability under preemptable spin locks for $m = 4$, $U = 0.2n$, 8 resources, $rsf = 0.25$, $N^{max} = 5$, and short critical sections. The schedulability of the considered non-preemptable lock types in this configuration is shown in Fig. 572.

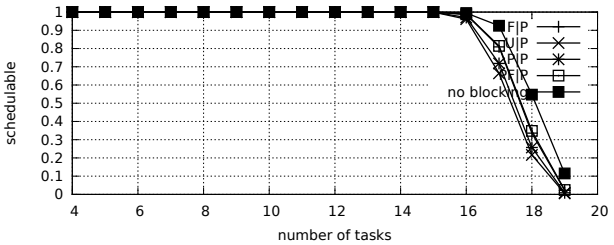

Fig. 583. Schedulability under preemptable spin locks for $m = 4$, $U = 0.2n$, 8 resources, $rsf = 0.25$, $N^{max} = 10$, and short critical sections. The schedulability of the considered non-preemptable lock types in this configuration is shown in Fig. 573.

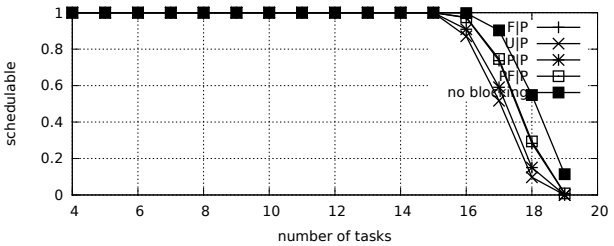

Fig. 584. Schedulability under preemptable spin locks for $m = 4$, $U = 0.2n$, 8 resources, $rsf = 0.25$, $N^{max} = 15$, and short critical sections. The schedulability of the considered non-preemptable lock types in this configuration is shown in Fig. 574.

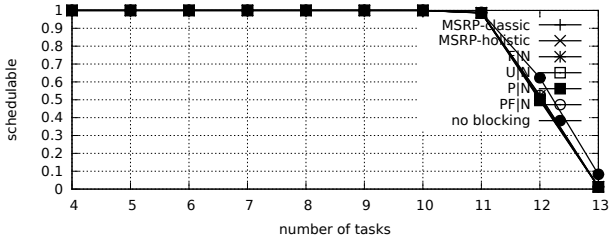

Fig. 585. Schedulability under non-preemptable spin locks for $m = 4$, $U = 0.3n$, 8 resources, $rsf = 0.25$, $N^{max} = 1$, and medium critical sections. The schedulability of the considered preemptable lock types in this configuration is shown in Fig. 595.

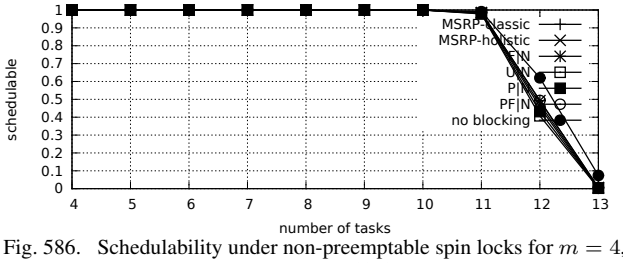

Fig. 586. Schedulability under non-preemptable spin locks for $m = 4$, $U = 0.3n$, 8 resources, $rsf = 0.25$, $N^{max} = 2$, and medium critical sections. The schedulability of the considered preemptable lock types in this configuration is shown in Fig. 596.

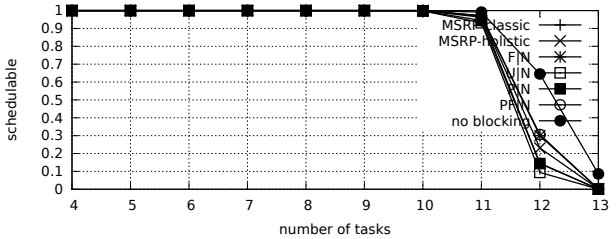

Fig. 587. Schedulability under non-preemptable spin locks for $m = 4$, $U = 0.3n$, 8 resources, $rsf = 0.25$, $N^{max} = 5$, and medium critical sections. The schedulability of the considered preemptable lock types in this configuration is shown in Fig. 597.

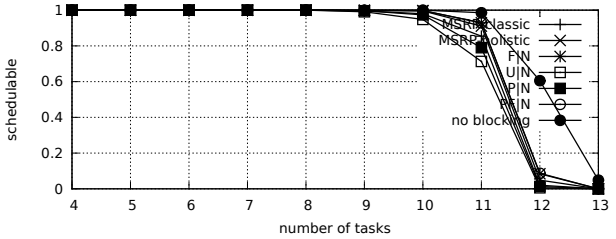

Fig. 588. Schedulability under non-preemptable spin locks for $m = 4$, $U = 0.3n$, 8 resources, $rsf = 0.25$, $N^{max} = 10$, and medium critical sections. The schedulability of the considered preemptable lock types in this configuration is shown in Fig. 598.

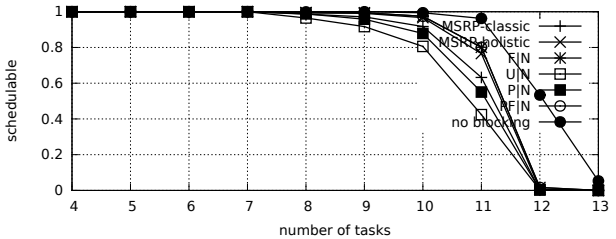

Fig. 589. Schedulability under non-preemptable spin locks for $m = 4$, $U = 0.3n$, 8 resources, $rsf = 0.25$, $N^{max} = 15$, and medium critical sections. The schedulability of the considered preemptable lock types in this configuration is shown in Fig. 599.

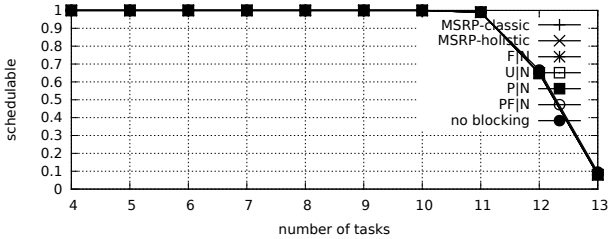

Fig. 590. Schedulability under non-preemptable spin locks for $m = 4$, $U = 0.3n$, 8 resources, $rsf = 0.25$, $N^{max} = 1$, and short critical sections. The schedulability of the considered preemptable lock types in this configuration is shown in Fig. 600.

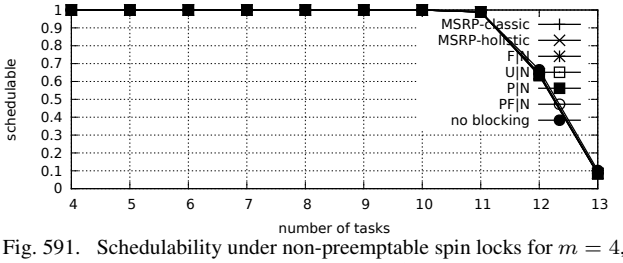

Fig. 591. Schedulability under non-preemptable spin locks for $m = 4$, $U = 0.3n$, 8 resources, $rsf = 0.25$, $N^{max} = 2$, and short critical sections. The schedulability of the considered preemptable lock types in this configuration is shown in Fig. 601.

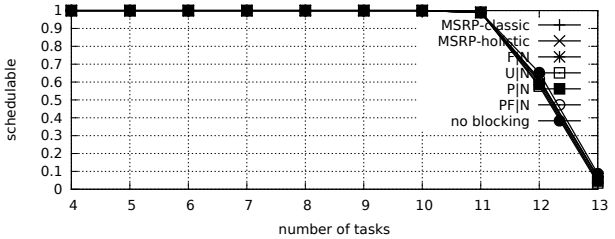

Fig. 592. Schedulability under non-preemptable spin locks for $m = 4$, $U = 0.3n$, 8 resources, $rsf = 0.25$, $N^{max} = 5$, and short critical sections. The schedulability of the considered preemptable lock types in this configuration is shown in Fig. 602.

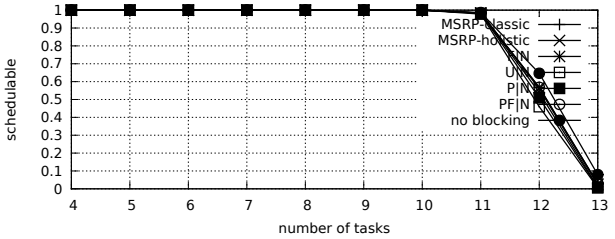

Fig. 593. Schedulability under non-preemptable spin locks for $m = 4$, $U = 0.3n$, 8 resources, $rsf = 0.25$, $N^{max} = 10$, and short critical sections. The schedulability of the considered preemptable lock types in this configuration is shown in Fig. 603.

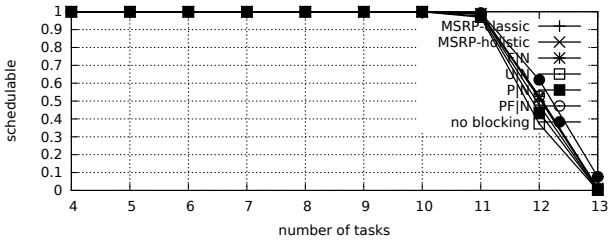

Fig. 594. Schedulability under non-preemptable spin locks for $m = 4$, $U = 0.3n$, 8 resources, $rsf = 0.25$, $N^{max} = 15$, and short critical sections. The schedulability of the considered preemptable lock types in this configuration is shown in Fig. 604.

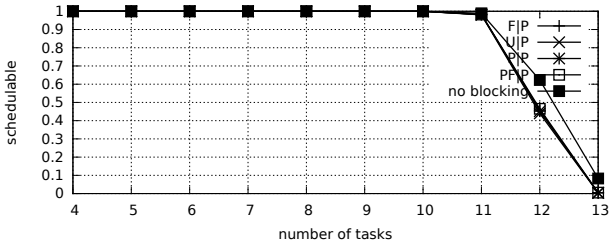

Fig. 595. Schedulability under preemptable spin locks for $m = 4$, $U = 0.3n$, 8 resources, $rsf = 0.25$, $N^{max} = 1$, and medium critical sections. The schedulability of the considered non-preemptable lock types in this configuration is shown in Fig. 585.

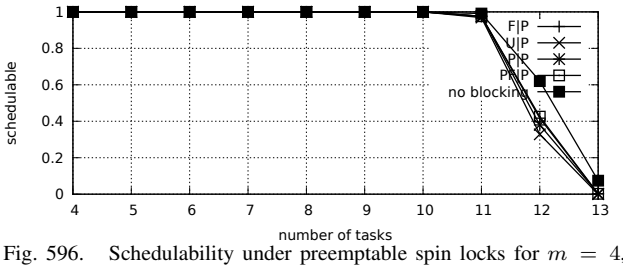

Fig. 596. Schedulability under preemptable spin locks for $m = 4$, $U = 0.3n$, 8 resources, $rsf = 0.25$, $N^{max} = 2$, and medium critical sections. The schedulability of the considered non-preemptable lock types in this configuration is shown in Fig. 586.

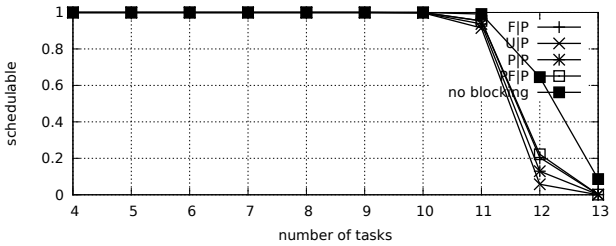

Fig. 597. Schedulability under preemptable spin locks for $m = 4$, $U = 0.3n$, 8 resources, $rsf = 0.25$, $N^{max} = 5$, and medium critical sections. The schedulability of the considered non-preemptable lock types in this configuration is shown in Fig. 587.

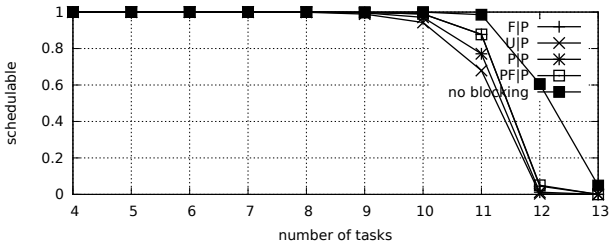

Fig. 598. Schedulability under preemptable spin locks for $m = 4$, $U = 0.3n$, 8 resources, $rsf = 0.25$, $N^{max} = 10$, and medium critical sections. The schedulability of the considered non-preemptable lock types in this configuration is shown in Fig. 588.

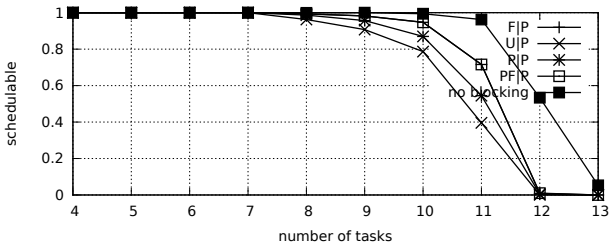

Fig. 599. Schedulability under preemptable spin locks for $m = 4$, $U = 0.3n$, 8 resources, $rsf = 0.25$, $N^{max} = 15$, and medium critical sections. The schedulability of the considered non-preemptable lock types in this configuration is shown in Fig. 589.

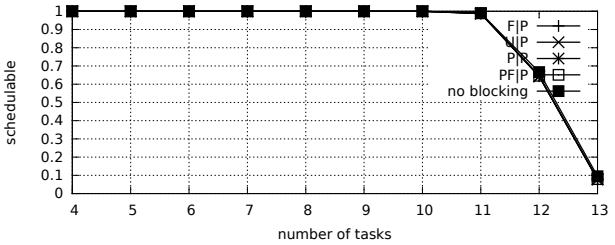

Fig. 600. Schedulability under preemptable spin locks for $m = 4$, $U = 0.3n$, 8 resources, $rsf = 0.25$, $N^{max} = 1$, and short critical sections. The schedulability of the considered non-preemptable lock types in this configuration is shown in Fig. 590.

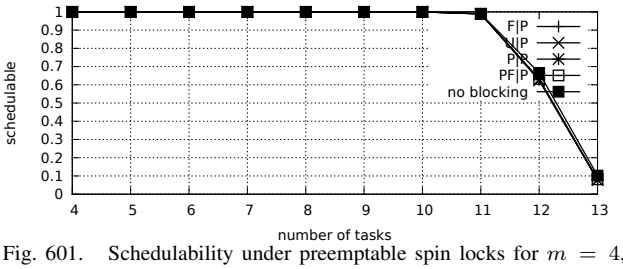

Fig. 601. Schedulability under preemptable spin locks for $m = 4$, $U = 0.3n$, 8 resources, $rsf = 0.25$, $N^{max} = 2$, and short critical sections. The schedulability of the considered non-preemptable lock types in this configuration is shown in Fig. 591.

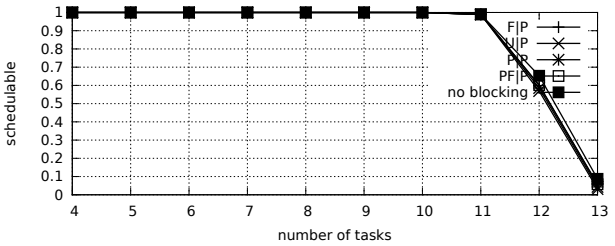

Fig. 602. Schedulability under preemptable spin locks for $m = 4$, $U = 0.3n$, 8 resources, $rsf = 0.25$, $N^{max} = 5$, and short critical sections. The schedulability of the considered non-preemptable lock types in this configuration is shown in Fig. 592.

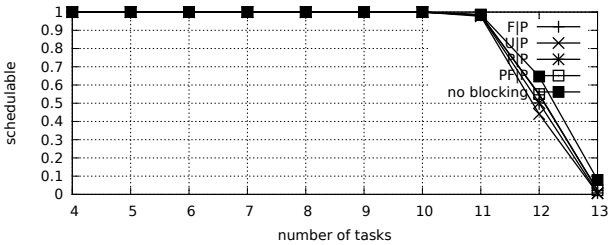

Fig. 603. Schedulability under preemptable spin locks for $m = 4$, $U = 0.3n$, 8 resources, $rsf = 0.25$, $N^{max} = 10$, and short critical sections. The schedulability of the considered non-preemptable lock types in this configuration is shown in Fig. 593.

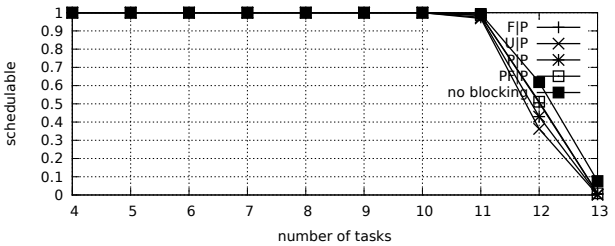

Fig. 604. Schedulability under preemptable spin locks for $m = 4$, $U = 0.3n$, 8 resources, $rsf = 0.25$, $N^{max} = 15$, and short critical sections. The schedulability of the considered non-preemptable lock types in this configuration is shown in Fig. 594.

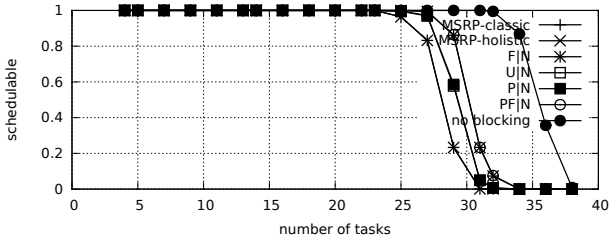

Fig. 605. Schedulability under non-preemptable spin locks for $m = 4$, $U = 0.1n$, 8 resources, $rsf = 0.4$, $N^{max} = 1$, and medium critical sections. The schedulability of the considered preemptable lock types in this configuration is shown in Fig. 615.

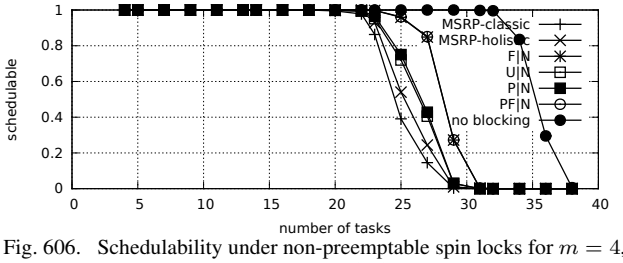

Fig. 606. Schedulability under non-preemptable spin locks for $m = 4$, $U = 0.1n$, 8 resources, $rsf = 0.4$, $N^{max} = 2$, and medium critical sections. The schedulability of the considered preemptable lock types in this configuration is shown in Fig. 616.

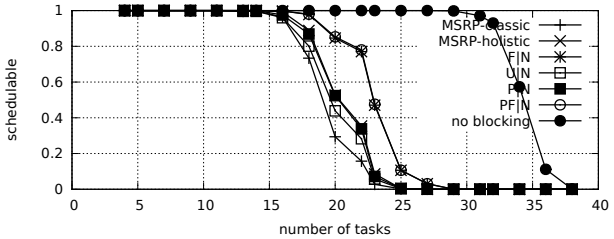

Fig. 607. Schedulability under non-preemptable spin locks for $m = 4$, $U = 0.1n$, 8 resources, $rsf = 0.4$, $N^{max} = 5$, and medium critical sections. The schedulability of the considered preemptable lock types in this configuration is shown in Fig. 617.

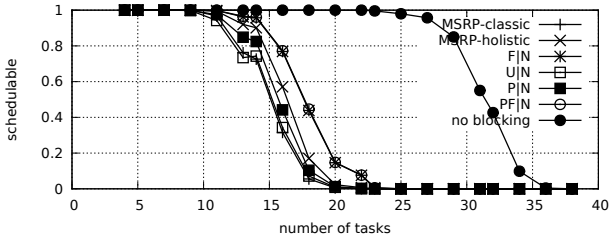

Fig. 608. Schedulability under non-preemptable spin locks for $m = 4$, $U = 0.1n$, 8 resources, $rsf = 0.4$, $N^{max} = 10$, and medium critical sections. The schedulability of the considered preemptable lock types in this configuration is shown in Fig. 618.

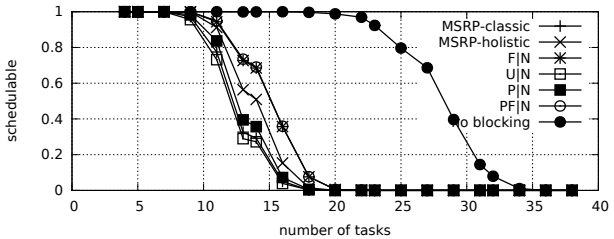

Fig. 609. Schedulability under non-preemptable spin locks for $m = 4$, $U = 0.1n$, 8 resources, $rsf = 0.4$, $N^{max} = 15$, and medium critical sections. The schedulability of the considered preemptable lock types in this configuration is shown in Fig. 619.

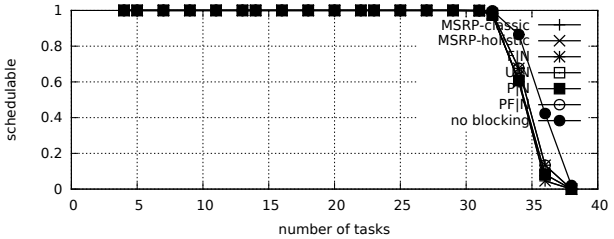

Fig. 610. Schedulability under non-preemptable spin locks for $m = 4$, $U = 0.1n$, 8 resources, $rsf = 0.4$, $N^{max} = 1$, and short critical sections. The schedulability of the considered preemptable lock types in this configuration is shown in Fig. 620.

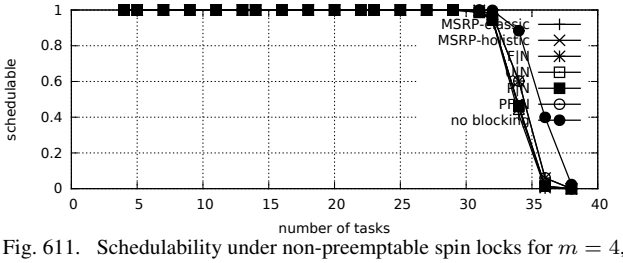

Fig. 611. Schedulability under non-preemptable spin locks for $m = 4$, $U = 0.1n$, 8 resources, $rsf = 0.4$, $N^{max} = 2$, and short critical sections. The schedulability of the considered preemptable lock types in this configuration is shown in Fig. 621.

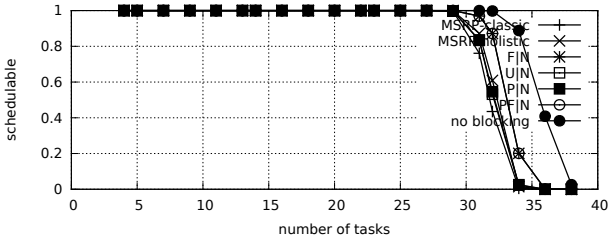

Fig. 612. Schedulability under non-preemptable spin locks for $m = 4$, $U = 0.1n$, 8 resources, $rsf = 0.4$, $N^{max} = 5$, and short critical sections. The schedulability of the considered preemptable lock types in this configuration is shown in Fig. 622.

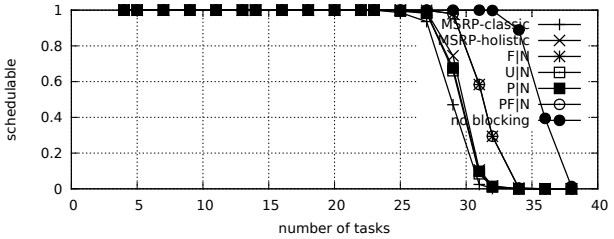

Fig. 613. Schedulability under non-preemptable spin locks for $m = 4$, $U = 0.1n$, 8 resources, $rsf = 0.4$, $N^{max} = 10$, and short critical sections. The schedulability of the considered preemptable lock types in this configuration is shown in Fig. 623.

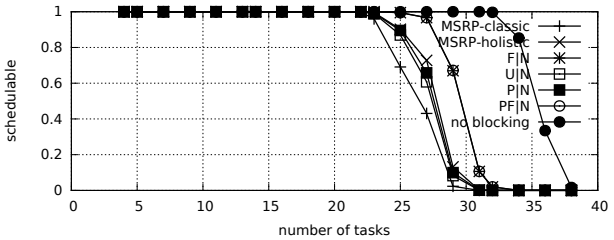

Fig. 614. Schedulability under non-preemptable spin locks for $m = 4$, $U = 0.1n$, 8 resources, $rsf = 0.4$, $N^{max} = 15$, and short critical sections. The schedulability of the considered preemptable lock types in this configuration is shown in Fig. 624.

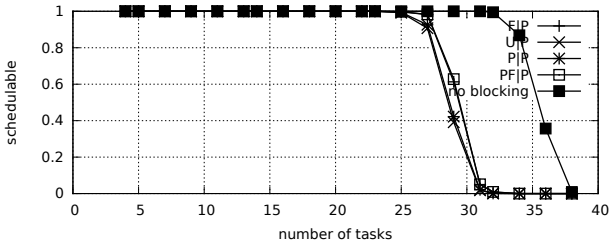

Fig. 615. Schedulability under preemptable spin locks for $m = 4$, $U = 0.1n$, 8 resources, $rsf = 0.4$, $N^{max} = 1$, and medium critical sections. The schedulability of the considered non-preemptable lock types in this configuration is shown in Fig. 605.

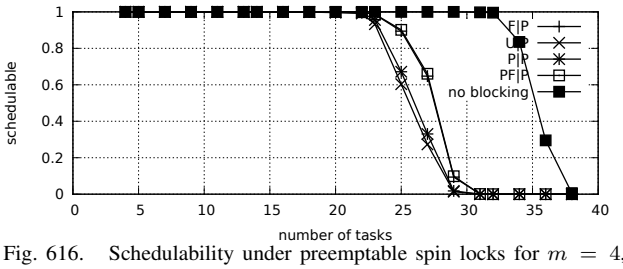

Fig. 616. Schedulability under preemptable spin locks for $m = 4$, $U = 0.1n$, 8 resources, $rsf = 0.4$, $N^{max} = 2$, and medium critical sections. The schedulability of the considered non-preemptable lock types in this configuration is shown in Fig. 606.

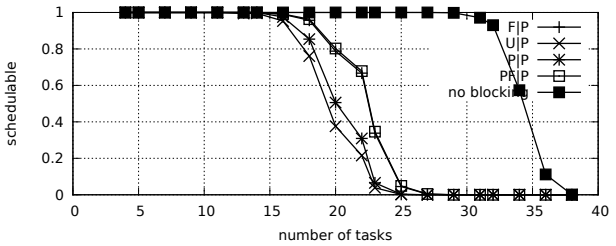

Fig. 617. Schedulability under preemptable spin locks for $m = 4$, $U = 0.1n$, 8 resources, $rsf = 0.4$, $N^{max} = 5$, and medium critical sections. The schedulability of the considered non-preemptable lock types in this configuration is shown in Fig. 607.

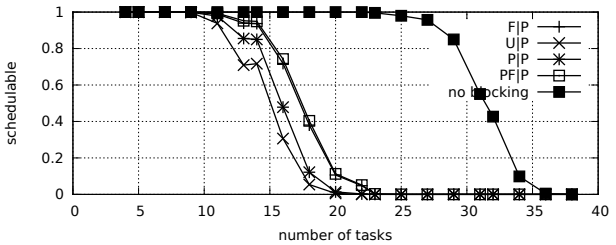

Fig. 618. Schedulability under preemptable spin locks for $m = 4$, $U = 0.1n$, 8 resources, $rsf = 0.4$, $N^{max} = 10$, and medium critical sections. The schedulability of the considered non-preemptable lock types in this configuration is shown in Fig. 608.

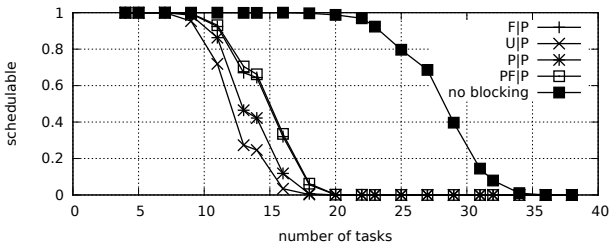

Fig. 619. Schedulability under preemptable spin locks for $m = 4$, $U = 0.1n$, 8 resources, $rsf = 0.4$, $N^{max} = 15$, and medium critical sections. The schedulability of the considered non-preemptable lock types in this configuration is shown in Fig. 609.

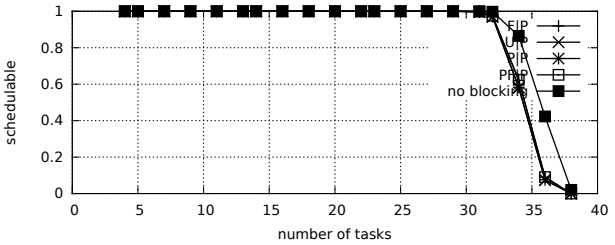

Fig. 620. Schedulability under preemptable spin locks for $m = 4$, $U = 0.1n$, 8 resources, $rsf = 0.4$, $N^{max} = 1$, and short critical sections. The schedulability of the considered non-preemptable lock types in this configuration is shown in Fig. 610.

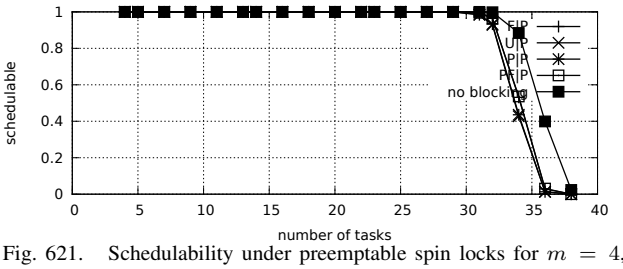

Fig. 621. Schedulability under preemptable spin locks for $m = 4$, $U = 0.1n$, 8 resources, $rsf = 0.4$, $N^{max} = 2$, and short critical sections. The schedulability of the considered non-preemptable lock types in this configuration is shown in Fig. 611.

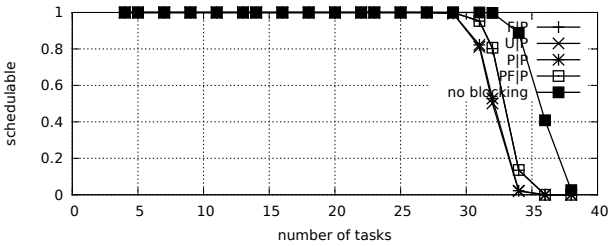

Fig. 622. Schedulability under preemptable spin locks for $m = 4$, $U = 0.1n$, 8 resources, $rsf = 0.4$, $N^{max} = 5$, and short critical sections. The schedulability of the considered non-preemptable lock types in this configuration is shown in Fig. 612.

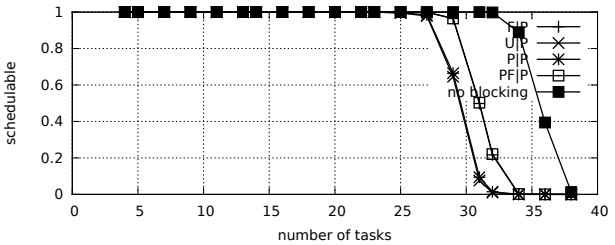

Fig. 623. Schedulability under preemptable spin locks for $m = 4$, $U = 0.1n$, 8 resources, $rsf = 0.4$, $N^{max} = 10$, and short critical sections. The schedulability of the considered non-preemptable lock types in this configuration is shown in Fig. 613.

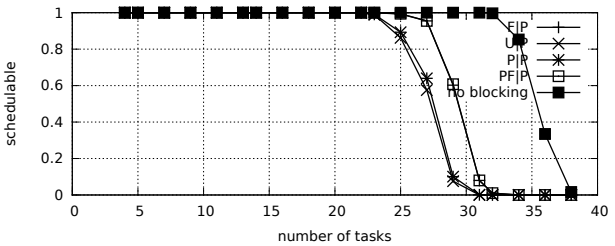

Fig. 624. Schedulability under preemptable spin locks for $m = 4$, $U = 0.1n$, 8 resources, $rsf = 0.4$, $N^{max} = 15$, and short critical sections. The schedulability of the considered non-preemptable lock types in this configuration is shown in Fig. 614.

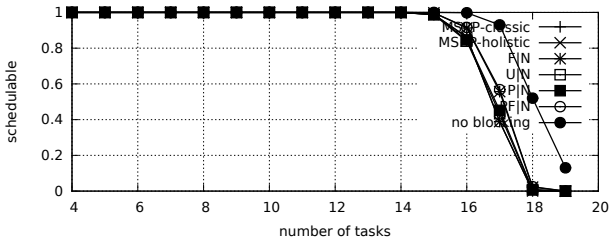

Fig. 625. Schedulability under non-preemptable spin locks for $m = 4$, $U = 0.2n$, 8 resources, $rsf = 0.4$, $N^{max} = 1$, and medium critical sections. The schedulability of the considered preemptable lock types in this configuration is shown in Fig. 635.

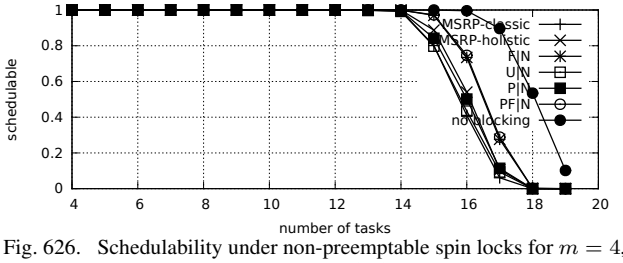

Fig. 626. Schedulability under non-preemptable spin locks for $m = 4$, $U = 0.2n$, 8 resources, $rsf = 0.4$, $N^{max} = 2$, and medium critical sections. The schedulability of the considered preemptable lock types in this configuration is shown in Fig. 636.

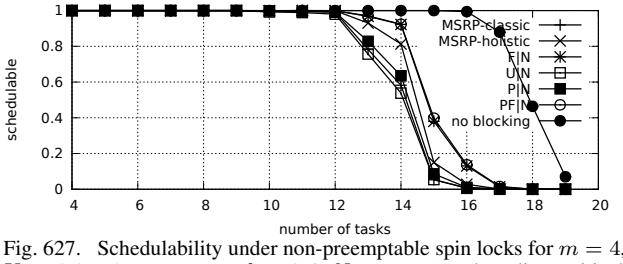

Fig. 627. Schedulability under non-preemptable spin locks for $m = 4$, $U = 0.2n$, 8 resources, $rsf = 0.4$, $N^{max} = 5$, and medium critical sections. The schedulability of the considered preemptable lock types in this configuration is shown in Fig. 637.

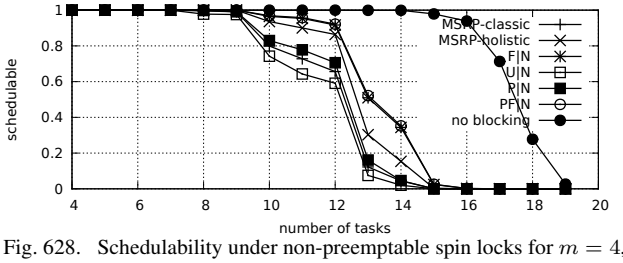

Fig. 628. Schedulability under non-preemptable spin locks for $m = 4$, $U = 0.2n$, 8 resources, $rsf = 0.4$, $N^{max} = 10$, and medium critical sections. The schedulability of the considered preemptable lock types in this configuration is shown in Fig. 638.

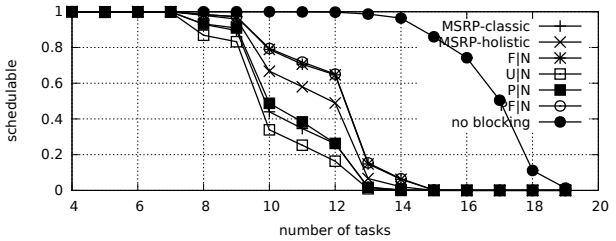

Fig. 629. Schedulability under non-preemptable spin locks for $m = 4$, $U = 0.2n$, 8 resources, $rsf = 0.4$, $N^{max} = 15$, and medium critical sections. The schedulability of the considered preemptable lock types in this configuration is shown in Fig. 639.

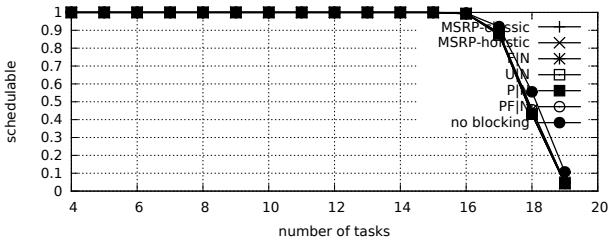

Fig. 630. Schedulability under non-preemptable spin locks for $m = 4$, $U = 0.2n$, 8 resources, $rsf = 0.4$, $N^{max} = 1$, and short critical sections. The schedulability of the considered preemptable lock types in this configuration is shown in Fig. 640.

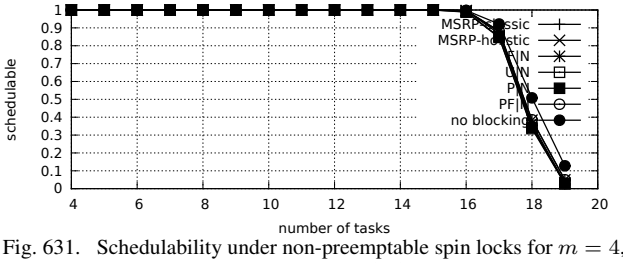

Fig. 631. Schedulability under non-preemptable spin locks for $m = 4$, $U = 0.2n$, 8 resources, $rsf = 0.4$, $N^{max} = 2$, and short critical sections. The schedulability of the considered preemptable lock types in this configuration is shown in Fig. 641.

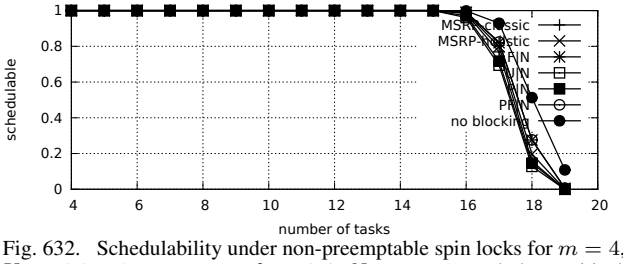

Fig. 632. Schedulability under non-preemptable spin locks for $m = 4$, $U = 0.2n$, 8 resources, $rsf = 0.4$, $N^{max} = 5$, and short critical sections. The schedulability of the considered preemptable lock types in this configuration is shown in Fig. 642.

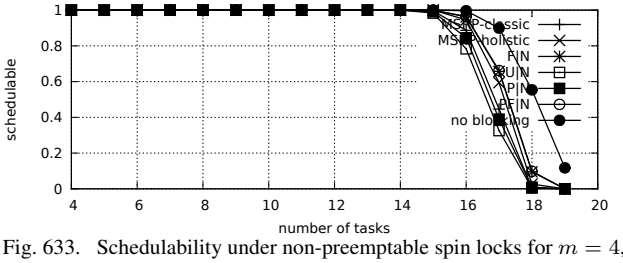

Fig. 633. Schedulability under non-preemptable spin locks for $m = 4$, $U = 0.2n$, 8 resources, $rsf = 0.4$, $N^{max} = 10$, and short critical sections. The schedulability of the considered preemptable lock types in this configuration is shown in Fig. 643.

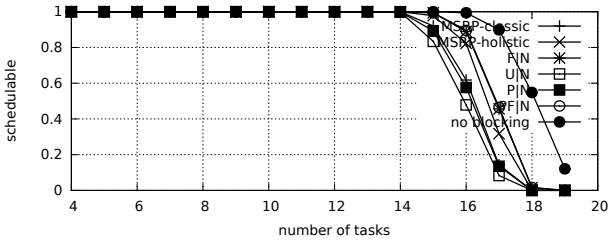

Fig. 634. Schedulability under non-preemptable spin locks for $m = 4$, $U = 0.2n$, 8 resources, $rsf = 0.4$, $N^{max} = 15$, and short critical sections. The schedulability of the considered preemptable lock types in this configuration is shown in Fig. 644.

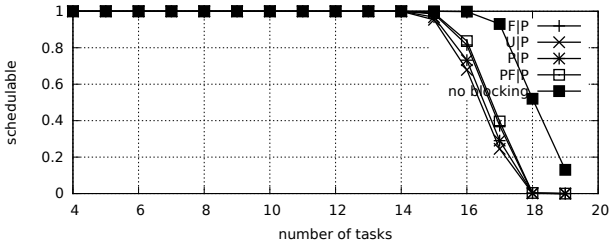

Fig. 635. Schedulability under preemptable spin locks for $m = 4$, $U = 0.2n$, 8 resources, $rsf = 0.4$, $N^{max} = 1$, and medium critical sections. The schedulability of the considered non-preemptable lock types in this configuration is shown in Fig. 625.

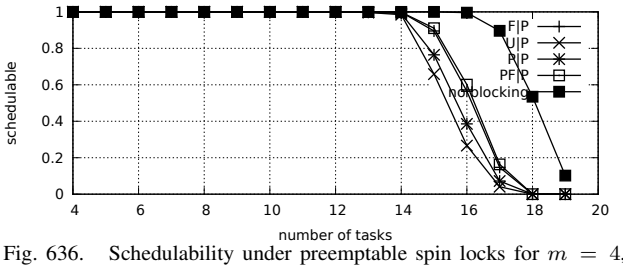

Fig. 636. Schedulability under preemptable spin locks for $m = 4$, $U = 0.2n$, 8 resources, $rsf = 0.4$, $N^{max} = 2$, and medium critical sections. The schedulability of the considered non-preemptable lock types in this configuration is shown in Fig. 626.

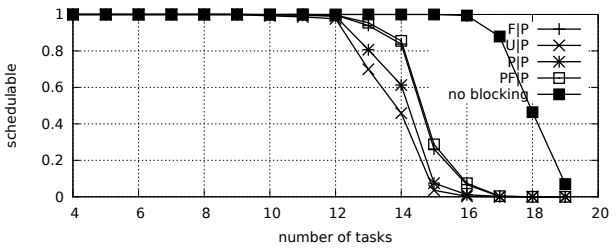

Fig. 637. Schedulability under preemptable spin locks for $m = 4$, $U = 0.2n$, 8 resources, $rsf = 0.4$, $N^{max} = 5$, and medium critical sections. The schedulability of the considered non-preemptable lock types in this configuration is shown in Fig. 627.

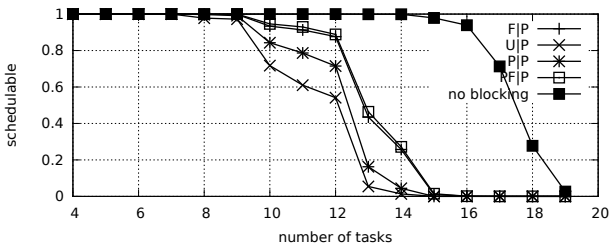

Fig. 638. Schedulability under preemptable spin locks for $m = 4$, $U = 0.2n$, 8 resources, $rsf = 0.4$, $N^{max} = 10$, and medium critical sections. The schedulability of the considered non-preemptable lock types in this configuration is shown in Fig. 628.

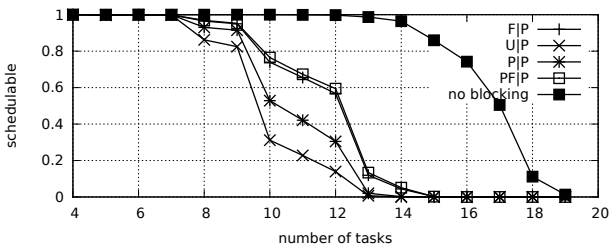

Fig. 639. Schedulability under preemptable spin locks for $m = 4$, $U = 0.2n$, 8 resources, $rsf = 0.4$, $N^{max} = 15$, and medium critical sections. The schedulability of the considered non-preemptable lock types in this configuration is shown in Fig. 629.

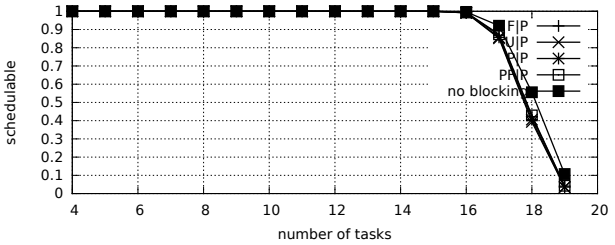

Fig. 640. Schedulability under preemptable spin locks for $m = 4$, $U = 0.2n$, 8 resources, $rsf = 0.4$, $N^{max} = 1$, and short critical sections. The schedulability of the considered non-preemptable lock types in this configuration is shown in Fig. 630.

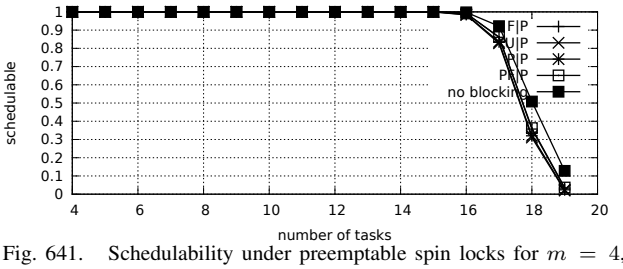

Fig. 641. Schedulability under preemptable spin locks for $m = 4$, $U = 0.2n$, 8 resources, $rsf = 0.4$, $N^{max} = 2$, and short critical sections. The schedulability of the considered non-preemptable lock types in this configuration is shown in Fig. 631.

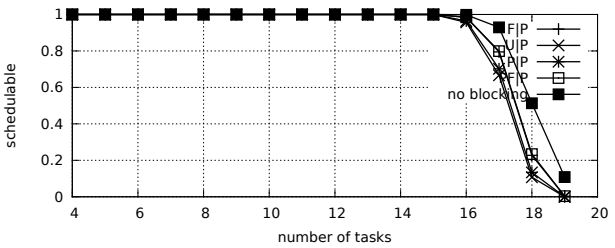

Fig. 642. Schedulability under preemptable spin locks for $m = 4$, $U = 0.2n$, 8 resources, $rsf = 0.4$, $N^{max} = 5$, and short critical sections. The schedulability of the considered non-preemptable lock types in this configuration is shown in Fig. 632.

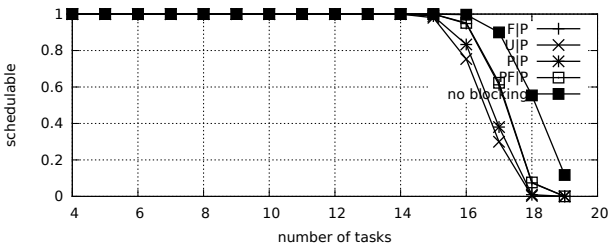

Fig. 643. Schedulability under preemptable spin locks for $m = 4$, $U = 0.2n$, 8 resources, $rsf = 0.4$, $N^{max} = 10$, and short critical sections. The schedulability of the considered non-preemptable lock types in this configuration is shown in Fig. 633.

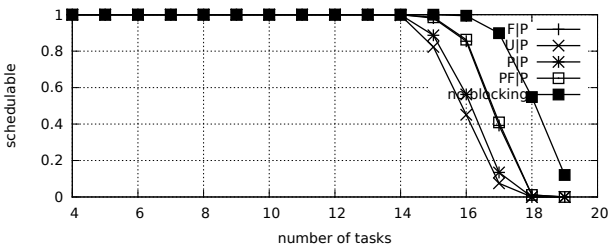

Fig. 644. Schedulability under preemptable spin locks for $m = 4$, $U = 0.2n$, 8 resources, $rsf = 0.4$, $N^{max} = 15$, and short critical sections. The schedulability of the considered non-preemptable lock types in this configuration is shown in Fig. 634.

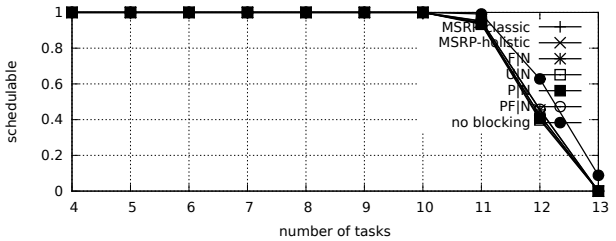

Fig. 645. Schedulability under non-preemptable spin locks for $m = 4$, $U = 0.3n$, 8 resources, $rsf = 0.4$, $N^{max} = 1$, and medium critical sections. The schedulability of the considered preemptable lock types in this configuration is shown in Fig. 655.

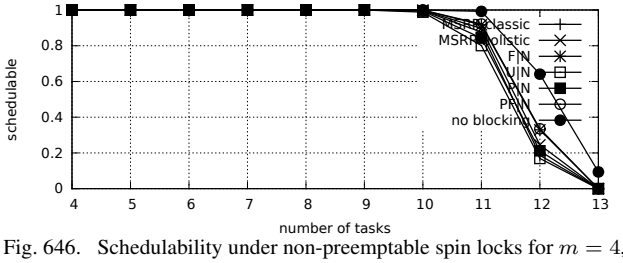

Fig. 646. Schedulability under non-preemptable spin locks for $m = 4$, $U = 0.3n$, 8 resources, $rsf = 0.4$, $N^{max} = 2$, and medium critical sections. The schedulability of the considered preemptable lock types in this configuration is shown in Fig. 656.

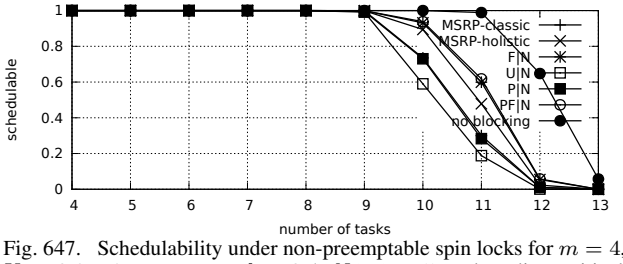

Fig. 647. Schedulability under non-preemptable spin locks for $m = 4$, $U = 0.3n$, 8 resources, $rsf = 0.4$, $N^{max} = 5$, and medium critical sections. The schedulability of the considered preemptable lock types in this configuration is shown in Fig. 657.

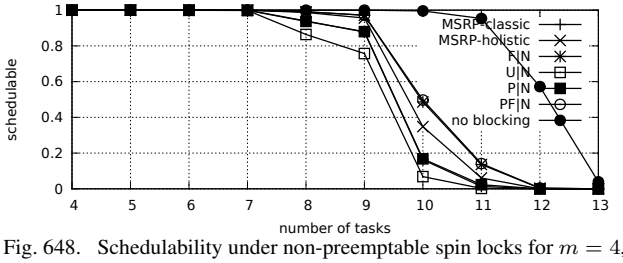

Fig. 648. Schedulability under non-preemptable spin locks for $m = 4$, $U = 0.3n$, 8 resources, $rsf = 0.4$, $N^{max} = 10$, and medium critical sections. The schedulability of the considered preemptable lock types in this configuration is shown in Fig. 658.

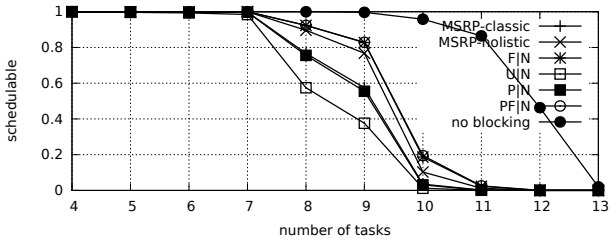

Fig. 649. Schedulability under non-preemptable spin locks for $m = 4$, $U = 0.3n$, 8 resources, $rsf = 0.4$, $N^{max} = 15$, and medium critical sections. The schedulability of the considered preemptable lock types in this configuration is shown in Fig. 659.

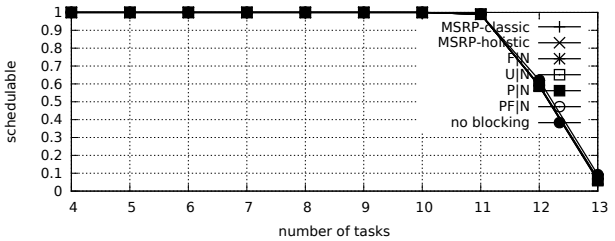

Fig. 650. Schedulability under non-preemptable spin locks for $m = 4$, $U = 0.3n$, 8 resources, $rsf = 0.4$, $N^{max} = 1$, and short critical sections. The schedulability of the considered preemptable lock types in this configuration is shown in Fig. 660.

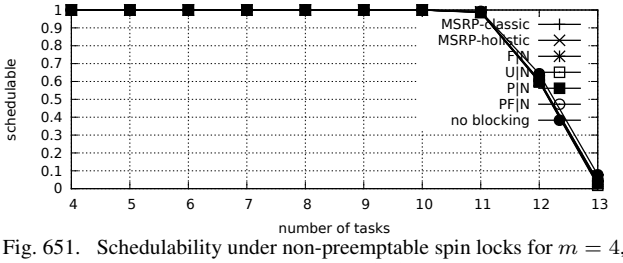

Fig. 651. Schedulability under non-preemptable spin locks for $m = 4$, $U = 0.3n$, 8 resources, $rsf = 0.4$, $N^{max} = 2$, and short critical sections. The schedulability of the considered preemptable lock types in this configuration is shown in Fig. 661.

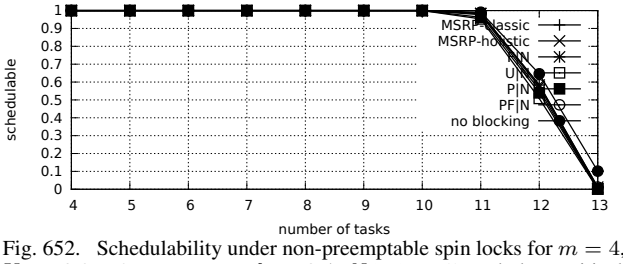

Fig. 652. Schedulability under non-preemptable spin locks for $m = 4$, $U = 0.3n$, 8 resources, $rsf = 0.4$, $N^{max} = 5$, and short critical sections. The schedulability of the considered preemptable lock types in this configuration is shown in Fig. 662.

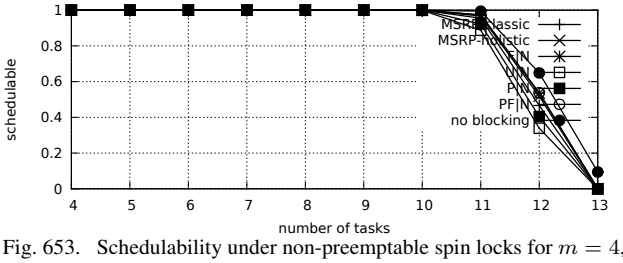

Fig. 653. Schedulability under non-preemptable spin locks for $m = 4$, $U = 0.3n$, 8 resources, $rsf = 0.4$, $N^{max} = 10$, and short critical sections. The schedulability of the considered preemptable lock types in this configuration is shown in Fig. 663.

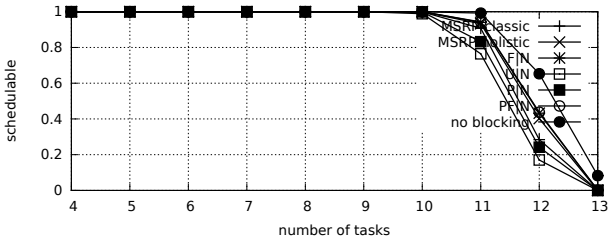

Fig. 654. Schedulability under non-preemptable spin locks for $m = 4$, $U = 0.3n$, 8 resources, $rsf = 0.4$, $N^{max} = 15$, and short critical sections. The schedulability of the considered preemptable lock types in this configuration is shown in Fig. 664.

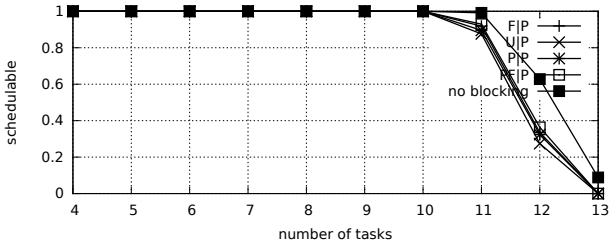

Fig. 655. Schedulability under preemptable spin locks for $m = 4$, $U = 0.3n$, 8 resources, $rsf = 0.4$, $N^{max} = 1$, and medium critical sections. The schedulability of the considered non-preemptable lock types in this configuration is shown in Fig. 645.

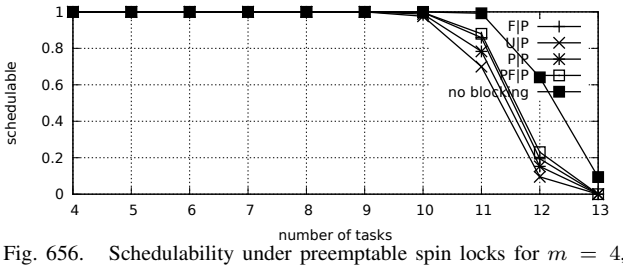

Fig. 656. Schedulability under preemptable spin locks for $m = 4$, $U = 0.3n$, 8 resources, $rsf = 0.4$, $N^{max} = 2$, and medium critical sections. The schedulability of the considered non-preemptable lock types in this configuration is shown in Fig. 646.

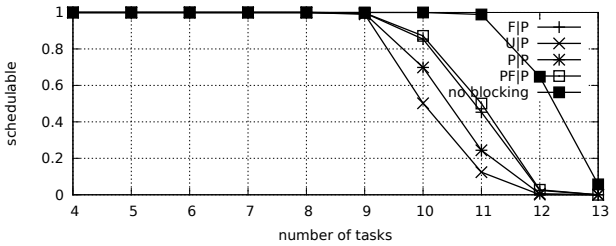

Fig. 657. Schedulability under preemptable spin locks for $m = 4$, $U = 0.3n$, 8 resources, $rsf = 0.4$, $N^{max} = 5$, and medium critical sections. The schedulability of the considered non-preemptable lock types in this configuration is shown in Fig. 647.

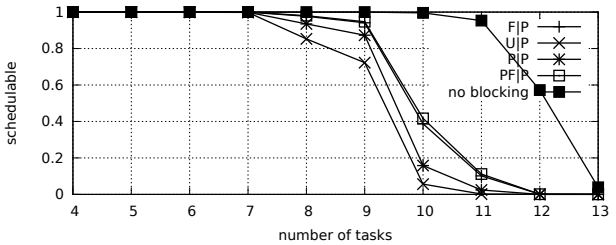

Fig. 658. Schedulability under preemptable spin locks for $m = 4$, $U = 0.3n$, 8 resources, $rsf = 0.4$, $N^{max} = 10$, and medium critical sections. The schedulability of the considered non-preemptable lock types in this configuration is shown in Fig. 648.

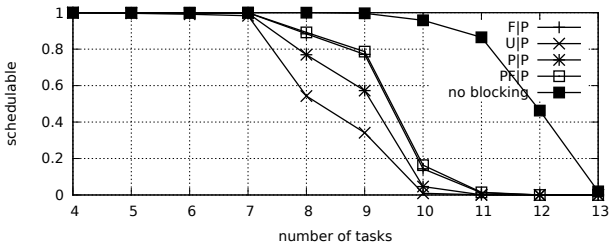

Fig. 659. Schedulability under preemptable spin locks for $m = 4$, $U = 0.3n$, 8 resources, $rsf = 0.4$, $N^{max} = 15$, and medium critical sections. The schedulability of the considered non-preemptable lock types in this configuration is shown in Fig. 649.

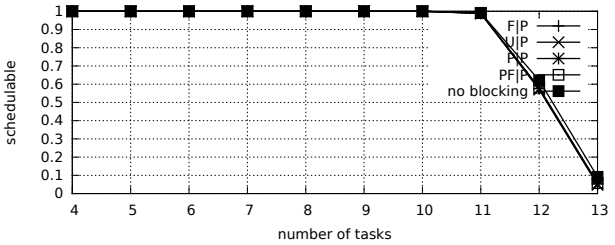

Fig. 660. Schedulability under preemptable spin locks for $m = 4$, $U = 0.3n$, 8 resources, $rsf = 0.4$, $N^{max} = 1$, and short critical sections. The schedulability of the considered non-preemptable lock types in this configuration is shown in Fig. 650.

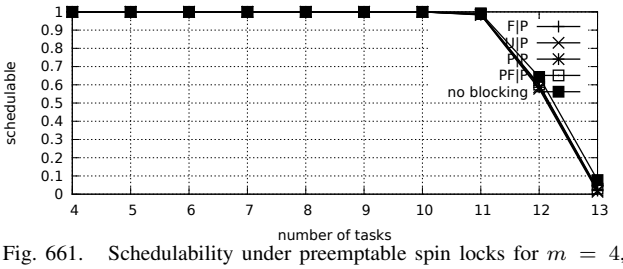

Fig. 661. Schedulability under preemptable spin locks for $m = 4$, $U = 0.3n$, 8 resources, $rsf = 0.4$, $N^{max} = 2$, and short critical sections. The schedulability of the considered non-preemptable lock types in this configuration is shown in Fig. 651.

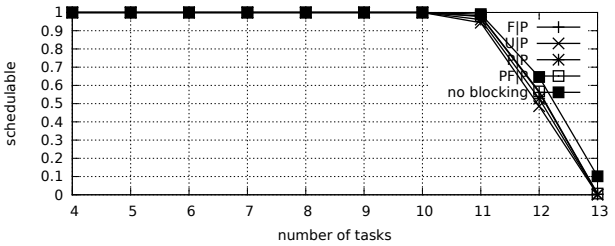

Fig. 662. Schedulability under preemptable spin locks for $m = 4$, $U = 0.3n$, 8 resources, $rsf = 0.4$, $N^{max} = 5$, and short critical sections. The schedulability of the considered non-preemptable lock types in this configuration is shown in Fig. 652.

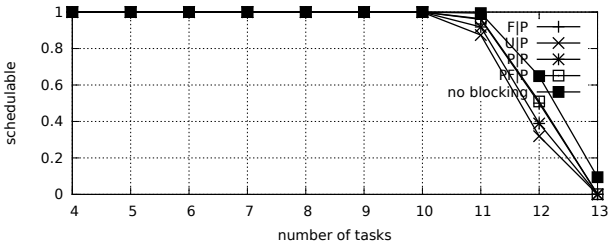

Fig. 663. Schedulability under preemptable spin locks for $m = 4$, $U = 0.3n$, 8 resources, $rsf = 0.4$, $N^{max} = 10$, and short critical sections. The schedulability of the considered non-preemptable lock types in this configuration is shown in Fig. 653.

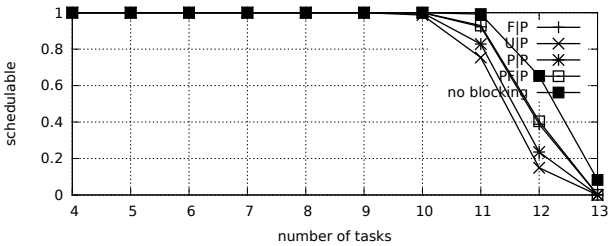

Fig. 664. Schedulability under preemptable spin locks for $m = 4$, $U = 0.3n$, 8 resources, $rsf = 0.4$, $N^{max} = 15$, and short critical sections. The schedulability of the considered non-preemptable lock types in this configuration is shown in Fig. 654.

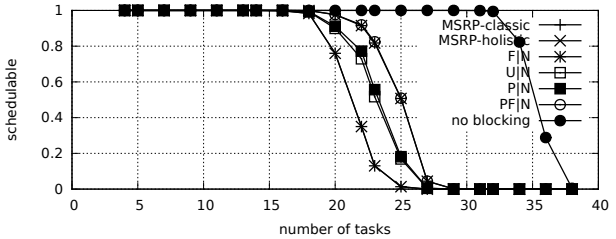

Fig. 665. Schedulability under non-preemptable spin locks for $m = 4$, $U = 0.1n$, 8 resources, $rsf = 0.75$, $N^{max} = 1$, and medium critical sections. The schedulability of the considered preemptable lock types in this configuration is shown in Fig. 675.

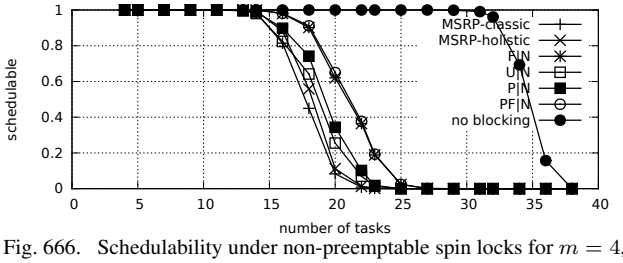

Fig. 666. Schedulability under non-preemptable spin locks for $m = 4$, $U = 0.1n$, 8 resources, $rsf = 0.75$, $N^{max} = 2$, and medium critical sections. The schedulability of the considered preemptable lock types in this configuration is shown in Fig. 676.

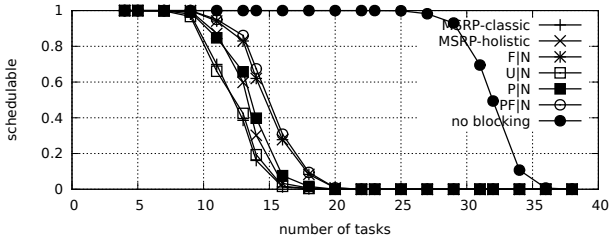

Fig. 667. Schedulability under non-preemptable spin locks for $m = 4$, $U = 0.1n$, 8 resources, $rsf = 0.75$, $N^{max} = 5$, and medium critical sections. The schedulability of the considered preemptable lock types in this configuration is shown in Fig. 677.

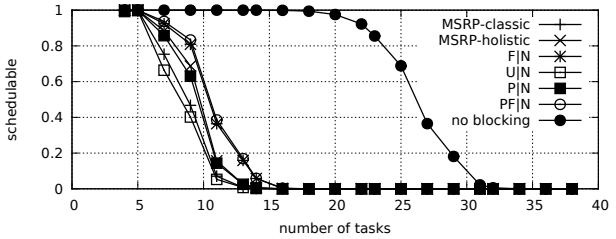

Fig. 668. Schedulability under non-preemptable spin locks for $m = 4$, $U = 0.1n$, 8 resources, $rsf = 0.75$, $N^{max} = 10$, and medium critical sections. The schedulability of the considered preemptable lock types in this configuration is shown in Fig. 678.

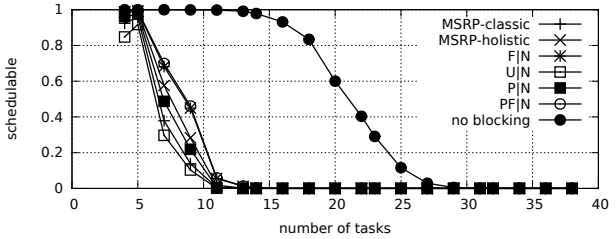

Fig. 669. Schedulability under non-preemptable spin locks for $m = 4$, $U = 0.1n$, 8 resources, $rsf = 0.75$, $N^{max} = 15$, and medium critical sections. The schedulability of the considered preemptable lock types in this configuration is shown in Fig. 679.

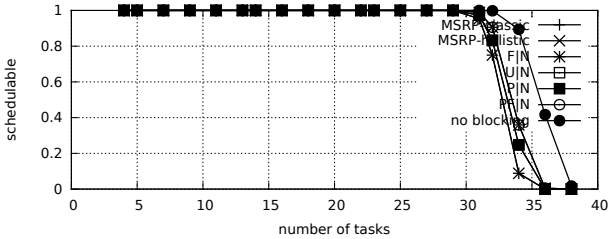

Fig. 670. Schedulability under non-preemptable spin locks for $m = 4$, $U = 0.1n$, 8 resources, $rsf = 0.75$, $N^{max} = 1$, and short critical sections. The schedulability of the considered preemptable lock types in this configuration is shown in Fig. 680.

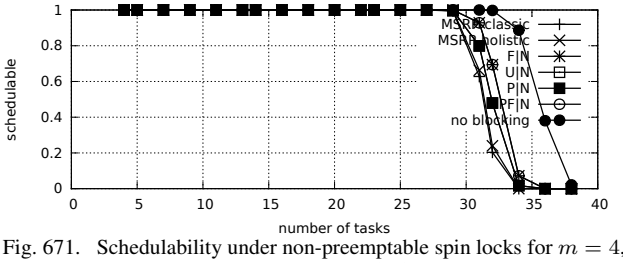

Fig. 671. Schedulability under non-preemptable spin locks for $m = 4$, $U = 0.1n$, 8 resources, $rsf = 0.75$, $N^{max} = 2$, and short critical sections. The schedulability of the considered preemptable lock types in this configuration is shown in Fig. 681.

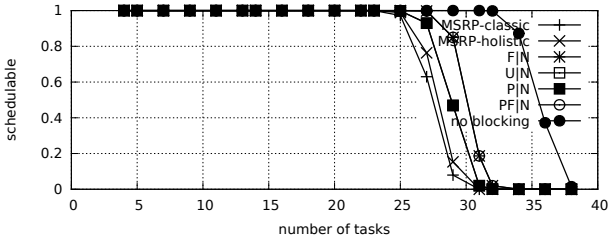

Fig. 672. Schedulability under non-preemptable spin locks for $m = 4$, $U = 0.1n$, 8 resources, $rsf = 0.75$, $N^{max} = 5$, and short critical sections. The schedulability of the considered preemptable lock types in this configuration is shown in Fig. 682.

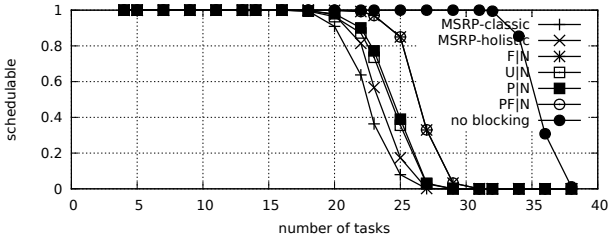

Fig. 673. Schedulability under non-preemptable spin locks for $m = 4$, $U = 0.1n$, 8 resources, $rsf = 0.75$, $N^{max} = 10$, and short critical sections. The schedulability of the considered preemptable lock types in this configuration is shown in Fig. 683.

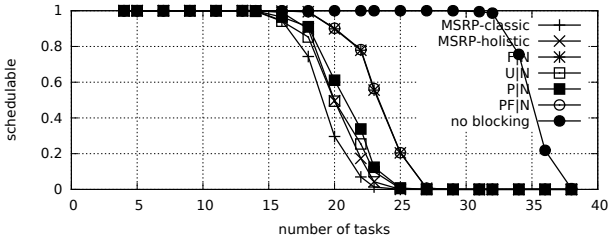

Fig. 674. Schedulability under non-preemptable spin locks for $m = 4$, $U = 0.1n$, 8 resources, $rsf = 0.75$, $N^{max} = 15$, and short critical sections. The schedulability of the considered preemptable lock types in this configuration is shown in Fig. 684.

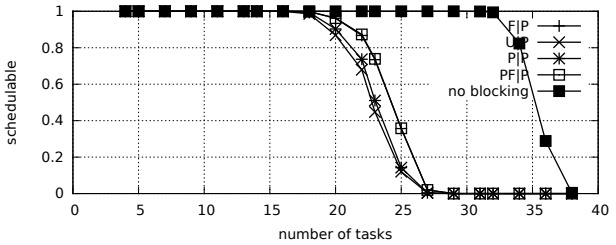

Fig. 675. Schedulability under preemptable spin locks for $m = 4$, $U = 0.1n$, 8 resources, $rsf = 0.75$, $N^{max} = 1$, and medium critical sections. The schedulability of the considered non-preemptable lock types in this configuration is shown in Fig. 665.

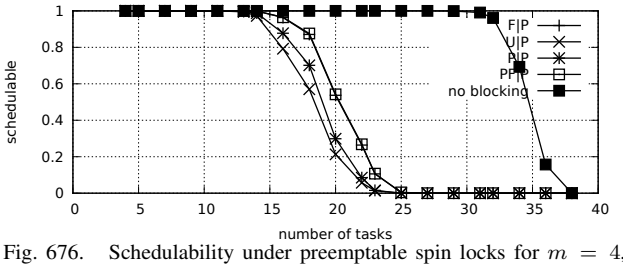

Fig. 676. Schedulability under preemptable spin locks for $m = 4$, $U = 0.1n$, 8 resources, $rsf = 0.75$, $N^{max} = 2$, and medium critical sections. The schedulability of the considered non-preemptable lock types in this configuration is shown in Fig. 666.

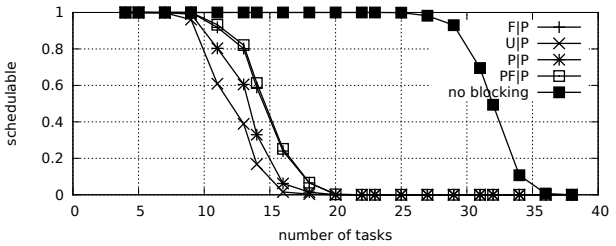

Fig. 677. Schedulability under preemptable spin locks for $m = 4$, $U = 0.1n$, 8 resources, $rsf = 0.75$, $N^{max} = 5$, and medium critical sections. The schedulability of the considered non-preemptable lock types in this configuration is shown in Fig. 667.

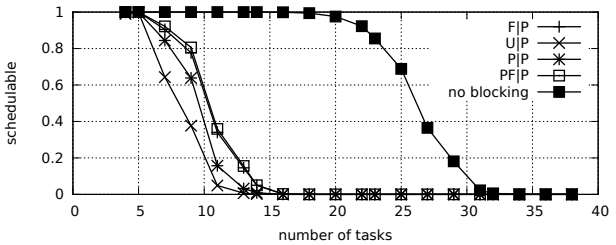

Fig. 678. Schedulability under preemptable spin locks for $m = 4$, $U = 0.1n$, 8 resources, $rsf = 0.75$, $N^{max} = 10$, and medium critical sections. The schedulability of the considered non-preemptable lock types in this configuration is shown in Fig. 668.

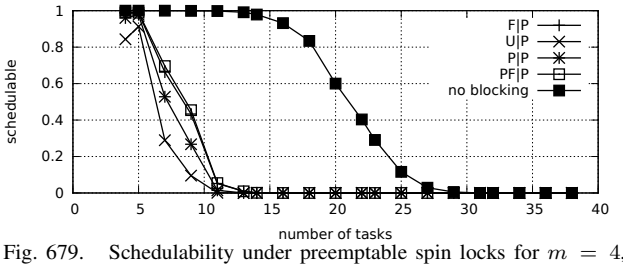

Fig. 679. Schedulability under preemptable spin locks for $m = 4$, $U = 0.1n$, 8 resources, $rsf = 0.75$, $N^{max} = 15$, and medium critical sections. The schedulability of the considered non-preemptable lock types in this configuration is shown in Fig. 669.

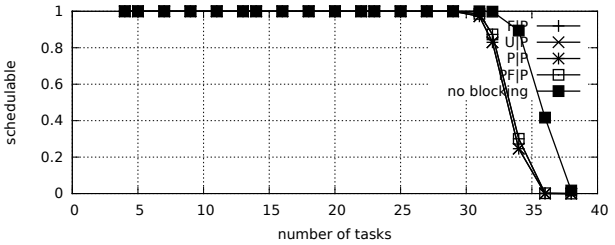

Fig. 680. Schedulability under preemptable spin locks for $m = 4$, $U = 0.1n$, 8 resources, $rsf = 0.75$, $N^{max} = 1$, and short critical sections. The schedulability of the considered non-preemptable lock types in this configuration is shown in Fig. 670.

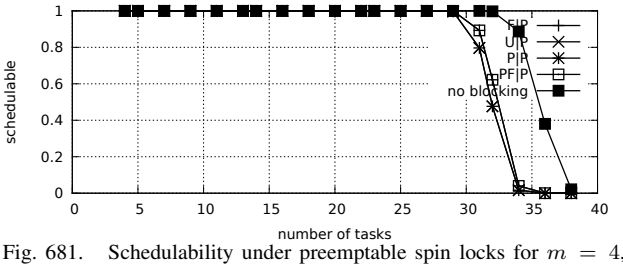

Fig. 681. Schedulability under preemptable spin locks for $m = 4$, $U = 0.1n$, 8 resources, $rsf = 0.75$, $N^{max} = 2$, and short critical sections. The schedulability of the considered non-preemptable lock types in this configuration is shown in Fig. 671.

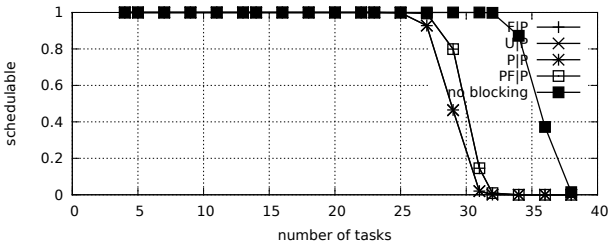

Fig. 682. Schedulability under preemptable spin locks for $m = 4$, $U = 0.1n$, 8 resources, $rsf = 0.75$, $N^{max} = 5$, and short critical sections. The schedulability of the considered non-preemptable lock types in this configuration is shown in Fig. 672.

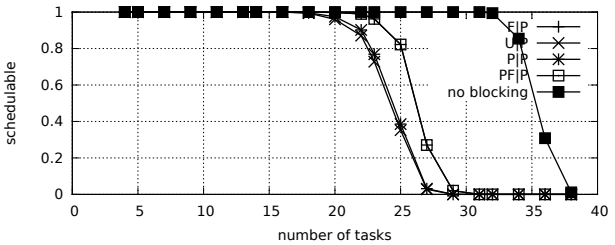

Fig. 683. Schedulability under preemptable spin locks for $m = 4$, $U = 0.1n$, 8 resources, $rsf = 0.75$, $N^{max} = 10$, and short critical sections. The schedulability of the considered non-preemptable lock types in this configuration is shown in Fig. 673.

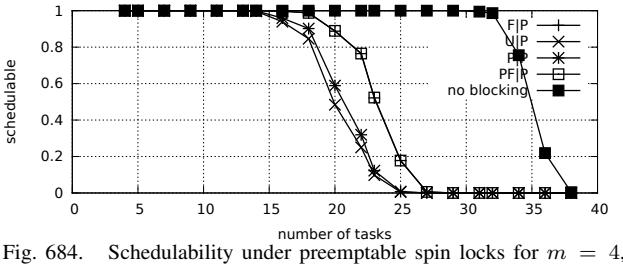

Fig. 684. Schedulability under preemptable spin locks for $m = 4$, $U = 0.1n$, 8 resources, $rsf = 0.75$, $N^{max} = 15$, and short critical sections. The schedulability of the considered non-preemptable lock types in this configuration is shown in Fig. 674.

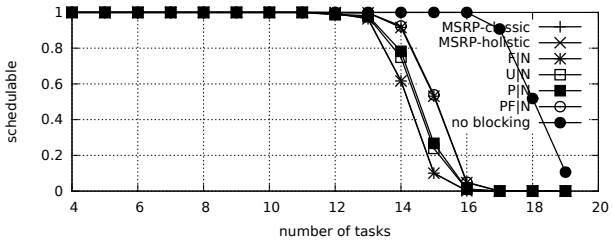

Fig. 685. Schedulability under non-preemptable spin locks for $m = 4$, $U = 0.2n$, 8 resources, $rsf = 0.75$, $N^{max} = 1$, and medium critical sections. The schedulability of the considered preemptable lock types in this configuration is shown in Fig. 695.

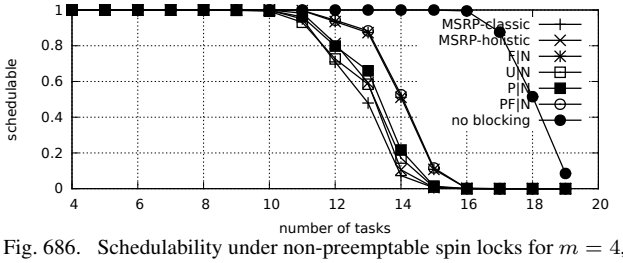

Fig. 686. Schedulability under non-preemptable spin locks for $m = 4$, $U = 0.2n$, 8 resources, $rsf = 0.75$, $N^{max} = 2$, and medium critical sections. The schedulability of the considered preemptable lock types in this configuration is shown in Fig. 696.

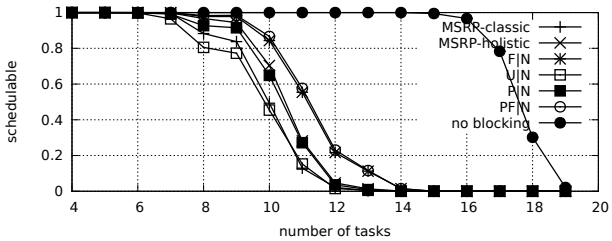

Fig. 687. Schedulability under non-preemptable spin locks for $m = 4$, $U = 0.2n$, 8 resources, $rsf = 0.75$, $N^{max} = 5$, and medium critical sections. The schedulability of the considered preemptable lock types in this configuration is shown in Fig. 697.

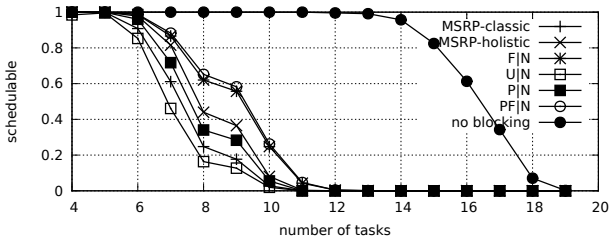

Fig. 688. Schedulability under non-preemptable spin locks for $m = 4$, $U = 0.2n$, 8 resources, $rsf = 0.75$, $N^{max} = 10$, and medium critical sections. The schedulability of the considered preemptable lock types in this configuration is shown in Fig. 698.

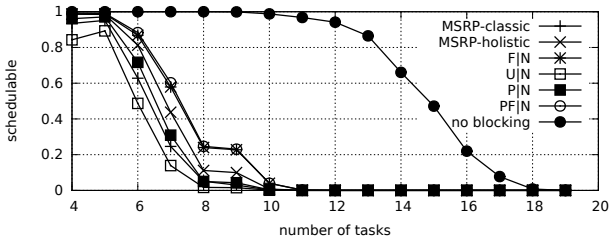

Fig. 689. Schedulability under non-preemptable spin locks for $m = 4$, $U = 0.2n$, 8 resources, $rsf = 0.75$, $N^{max} = 15$, and medium critical sections. The schedulability of the considered preemptable lock types in this configuration is shown in Fig. 699.

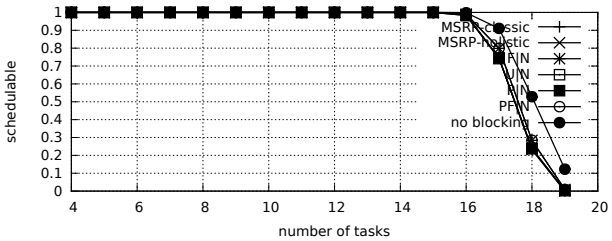

Fig. 690. Schedulability under non-preemptable spin locks for $m = 4$, $U = 0.2n$, 8 resources, $rsf = 0.75$, $N^{max} = 1$, and short critical sections. The schedulability of the considered preemptable lock types in this configuration is shown in Fig. 700.

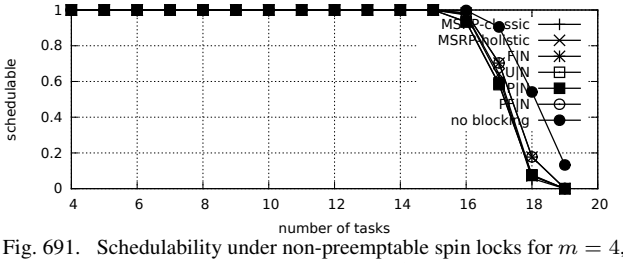

Fig. 691. Schedulability under non-preemptable spin locks for $m = 4$, $U = 0.2n$, 8 resources, $rsf = 0.75$, $N^{max} = 2$, and short critical sections. The schedulability of the considered preemptable lock types in this configuration is shown in Fig. 701.

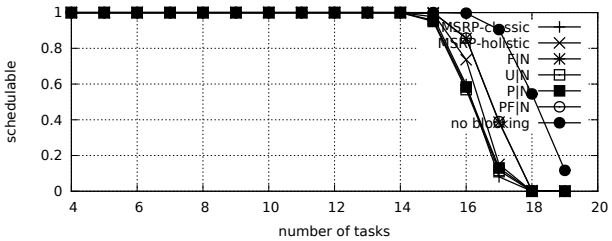

Fig. 692. Schedulability under non-preemptable spin locks for $m = 4$, $U = 0.2n$, 8 resources, $rsf = 0.75$, $N^{max} = 5$, and short critical sections. The schedulability of the considered preemptable lock types in this configuration is shown in Fig. 702.

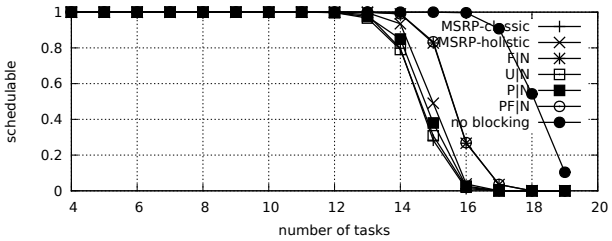

Fig. 693. Schedulability under non-preemptable spin locks for $m = 4$, $U = 0.2n$, 8 resources, $rsf = 0.75$, $N^{max} = 10$, and short critical sections. The schedulability of the considered preemptable lock types in this configuration is shown in Fig. 703.

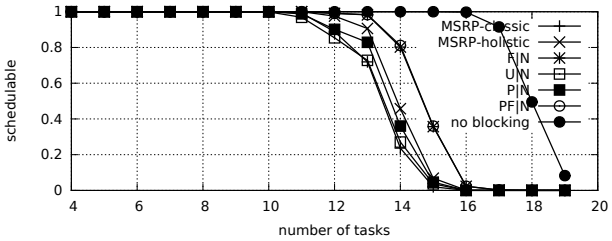

Fig. 694. Schedulability under non-preemptable spin locks for $m = 4$, $U = 0.2n$, 8 resources, $rsf = 0.75$, $N^{max} = 15$, and short critical sections. The schedulability of the considered preemptable lock types in this configuration is shown in Fig. 704.

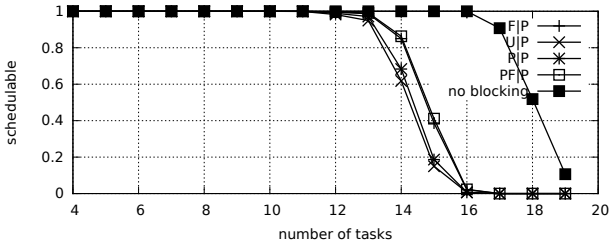

Fig. 695. Schedulability under preemptable spin locks for $m = 4$, $U = 0.2n$, 8 resources, $rsf = 0.75$, $N^{max} = 1$, and medium critical sections. The schedulability of the considered non-preemptable lock types in this configuration is shown in Fig. 685.

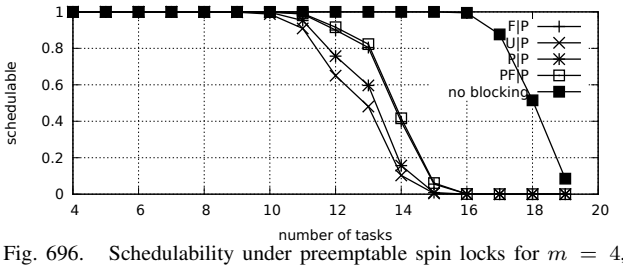

Fig. 696. Schedulability under preemptable spin locks for $m = 4$, $U = 0.2n$, 8 resources, $rsf = 0.75$, $N^{max} = 2$, and medium critical sections. The schedulability of the considered non-preemptable lock types in this configuration is shown in Fig. 686.

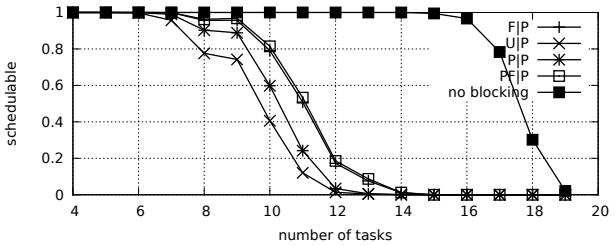

Fig. 697. Schedulability under preemptable spin locks for $m = 4$, $U = 0.2n$, 8 resources, $rsf = 0.75$, $N^{max} = 5$, and medium critical sections. The schedulability of the considered non-preemptable lock types in this configuration is shown in Fig. 687.

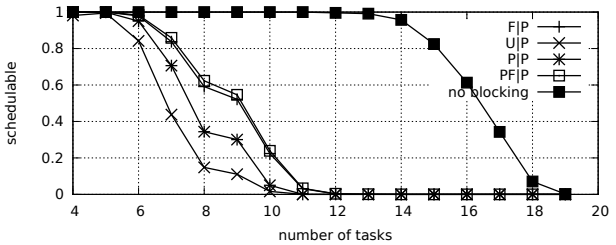

Fig. 698. Schedulability under preemptable spin locks for $m = 4$, $U = 0.2n$, 8 resources, $rsf = 0.75$, $N^{max} = 10$, and medium critical sections. The schedulability of the considered non-preemptable lock types in this configuration is shown in Fig. 688.

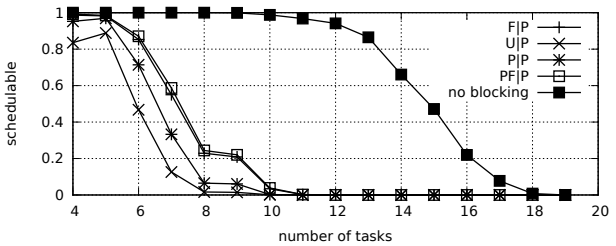

Fig. 699. Schedulability under preemptable spin locks for $m = 4$, $U = 0.2n$, 8 resources, $rsf = 0.75$, $N^{max} = 15$, and medium critical sections. The schedulability of the considered non-preemptable lock types in this configuration is shown in Fig. 689.

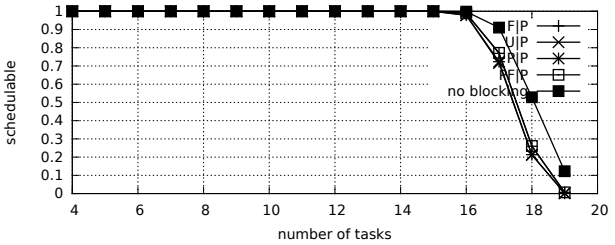

Fig. 700. Schedulability under preemptable spin locks for $m = 4$, $U = 0.2n$, 8 resources, $rsf = 0.75$, $N^{max} = 1$, and short critical sections. The schedulability of the considered non-preemptable lock types in this configuration is shown in Fig. 690.

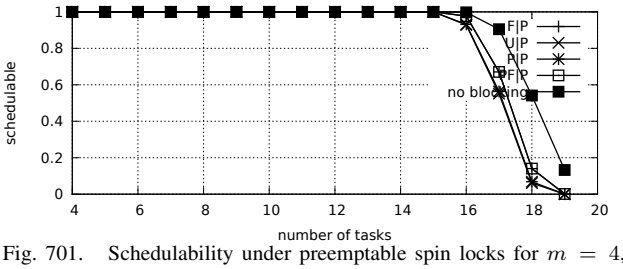

Fig. 701. Schedulability under preemptable spin locks for $m = 4$, $U = 0.2n$, 8 resources, $rsf = 0.75$, $N^{max} = 2$, and short critical sections. The schedulability of the considered non-preemptable lock types in this configuration is shown in Fig. 691.

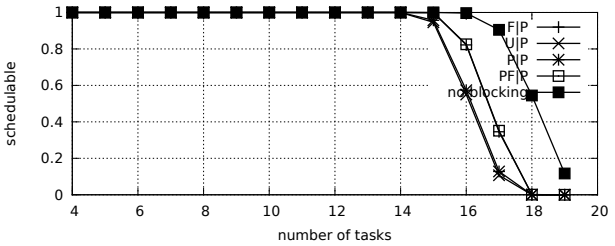

Fig. 702. Schedulability under preemptable spin locks for $m = 4$, $U = 0.2n$, 8 resources, $rsf = 0.75$, $N^{max} = 5$, and short critical sections. The schedulability of the considered non-preemptable lock types in this configuration is shown in Fig. 692.

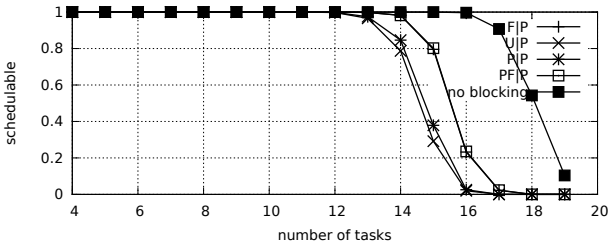

Fig. 703. Schedulability under preemptable spin locks for $m = 4$, $U = 0.2n$, 8 resources, $rsf = 0.75$, $N^{max} = 10$, and short critical sections. The schedulability of the considered non-preemptable lock types in this configuration is shown in Fig. 693.

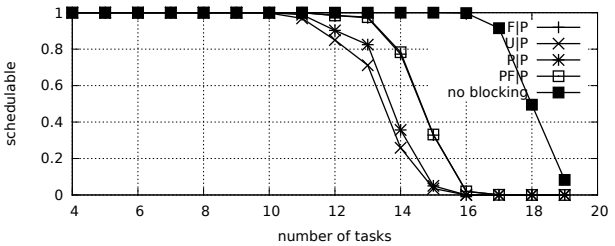

Fig. 704. Schedulability under preemptable spin locks for $m = 4$, $U = 0.2n$, 8 resources, $rsf = 0.75$, $N^{max} = 15$, and short critical sections. The schedulability of the considered non-preemptable lock types in this configuration is shown in Fig. 694.

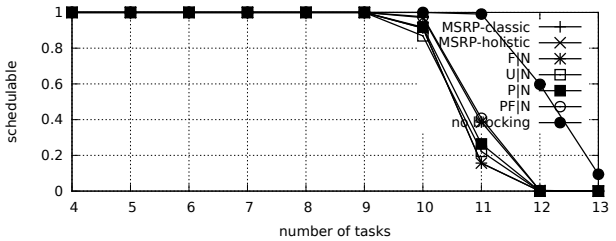

Fig. 705. Schedulability under non-preemptable spin locks for $m = 4$, $U = 0.3n$, 8 resources, $rsf = 0.75$, $N^{max} = 1$, and medium critical sections. The schedulability of the considered preemptable lock types in this configuration is shown in Fig. 715.

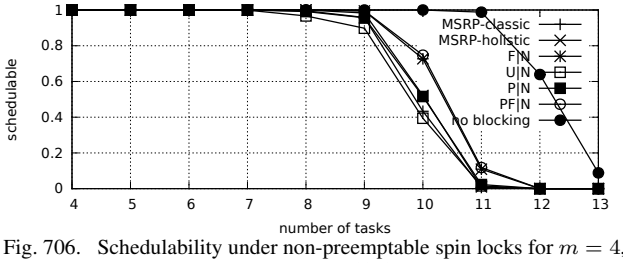

Fig. 706. Schedulability under non-preemptable spin locks for $m = 4$, $U = 0.3n$, 8 resources, $rsf = 0.75$, $N^{max} = 2$, and medium critical sections. The schedulability of the considered preemptable lock types in this configuration is shown in Fig. 716.

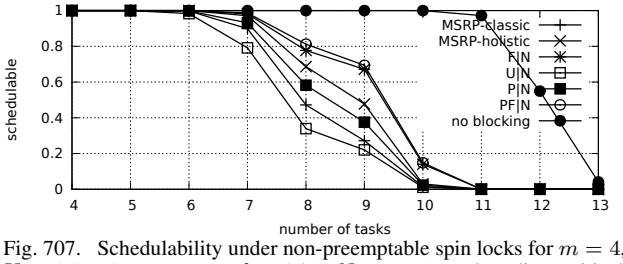

Fig. 707. Schedulability under non-preemptable spin locks for $m = 4$, $U = 0.3n$, 8 resources, $rsf = 0.75$, $N^{max} = 5$, and medium critical sections. The schedulability of the considered preemptable lock types in this configuration is shown in Fig. 717.

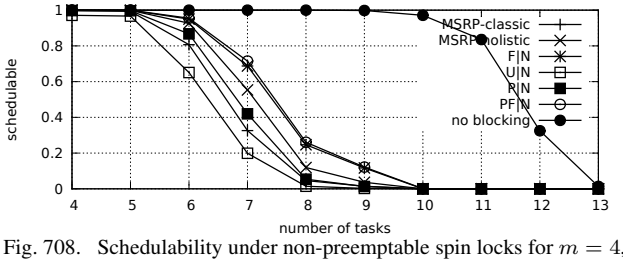

Fig. 708. Schedulability under non-preemptable spin locks for $m = 4$, $U = 0.3n$, 8 resources, $rsf = 0.75$, $N^{max} = 10$, and medium critical sections. The schedulability of the considered preemptable lock types in this configuration is shown in Fig. 718.

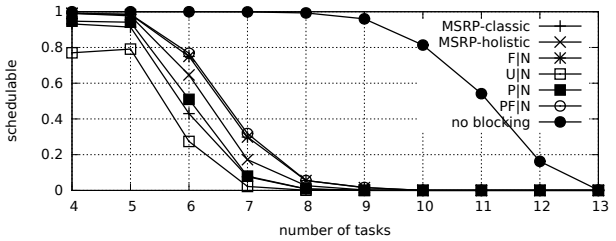

Fig. 709. Schedulability under non-preemptable spin locks for $m = 4$, $U = 0.3n$, 8 resources, $rsf = 0.75$, $N^{max} = 15$, and medium critical sections. The schedulability of the considered preemptable lock types in this configuration is shown in Fig. 719.

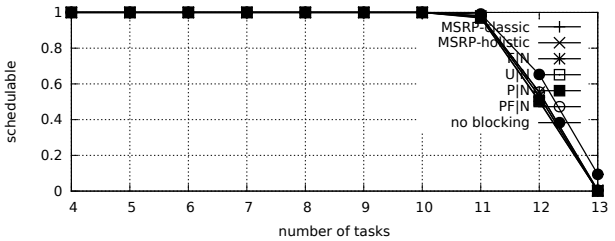

Fig. 710. Schedulability under non-preemptable spin locks for $m = 4$, $U = 0.3n$, 8 resources, $rsf = 0.75$, $N^{max} = 1$, and short critical sections. The schedulability of the considered preemptable lock types in this configuration is shown in Fig. 720.

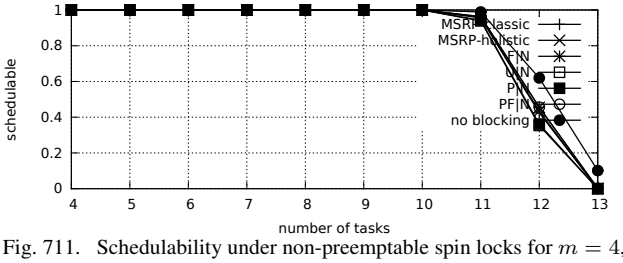

Fig. 711. Schedulability under non-preemptable spin locks for $m = 4$, $U = 0.3n$, 8 resources, $rsf = 0.75$, $N^{max} = 2$, and short critical sections. The schedulability of the considered preemptable lock types in this configuration is shown in Fig. 721.

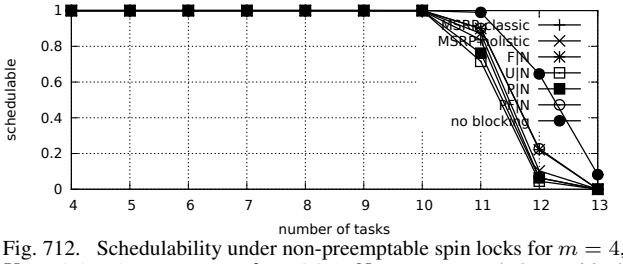

Fig. 712. Schedulability under non-preemptable spin locks for $m = 4$, $U = 0.3n$, 8 resources, $rsf = 0.75$, $N^{max} = 5$, and short critical sections. The schedulability of the considered preemptable lock types in this configuration is shown in Fig. 722.

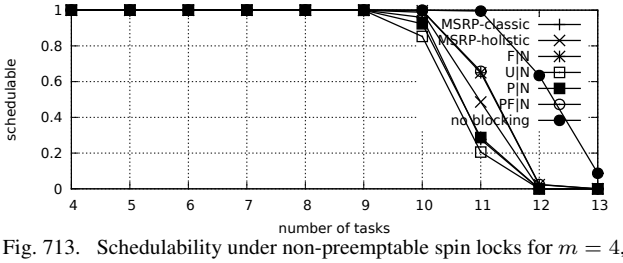

Fig. 713. Schedulability under non-preemptable spin locks for $m = 4$, $U = 0.3n$, 8 resources, $rsf = 0.75$, $N^{max} = 10$, and short critical sections. The schedulability of the considered preemptable lock types in this configuration is shown in Fig. 723.

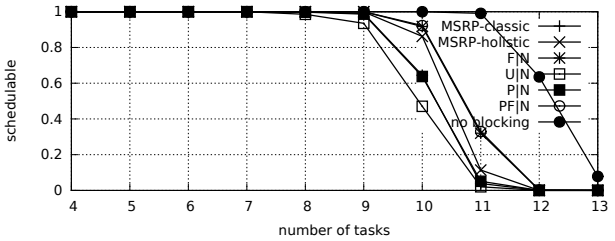

Fig. 714. Schedulability under non-preemptable spin locks for $m = 4$, $U = 0.3n$, 8 resources, $rsf = 0.75$, $N^{max} = 15$, and short critical sections. The schedulability of the considered preemptable lock types in this configuration is shown in Fig. 724.

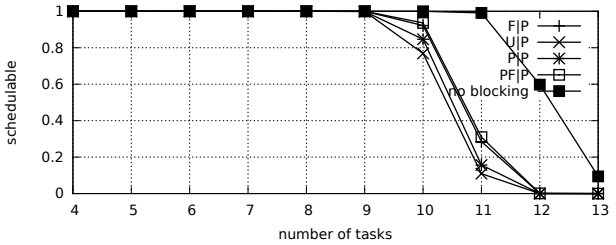

Fig. 715. Schedulability under preemptable spin locks for $m = 4$, $U = 0.3n$, 8 resources, $rsf = 0.75$, $N^{max} = 1$, and medium critical sections. The schedulability of the considered non-preemptable lock types in this configuration is shown in Fig. 705.

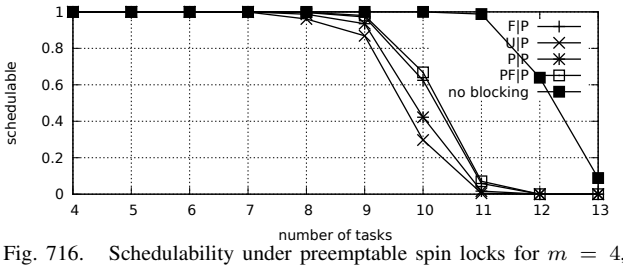

Fig. 716. Schedulability under preemptable spin locks for $m = 4$, $U = 0.3n$, 8 resources, $rsf = 0.75$, $N^{max} = 2$, and medium critical sections. The schedulability of the considered non-preemptable lock types in this configuration is shown in Fig. 706.

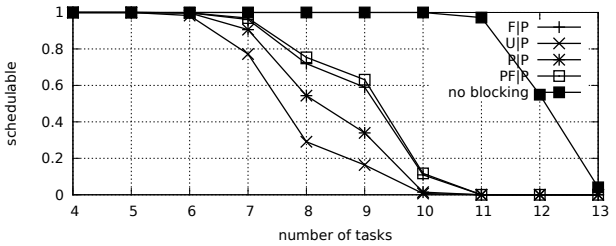

Fig. 717. Schedulability under preemptable spin locks for $m = 4$, $U = 0.3n$, 8 resources, $rsf = 0.75$, $N^{max} = 5$, and medium critical sections. The schedulability of the considered non-preemptable lock types in this configuration is shown in Fig. 707.

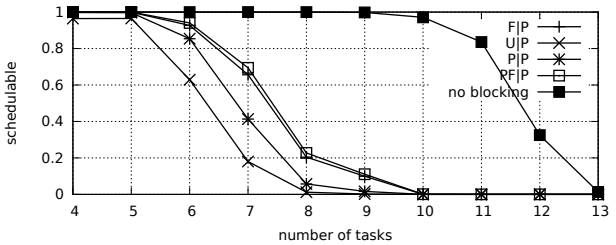

Fig. 718. Schedulability under preemptable spin locks for $m = 4$, $U = 0.3n$, 8 resources, $rsf = 0.75$, $N^{max} = 10$, and medium critical sections. The schedulability of the considered non-preemptable lock types in this configuration is shown in Fig. 708.

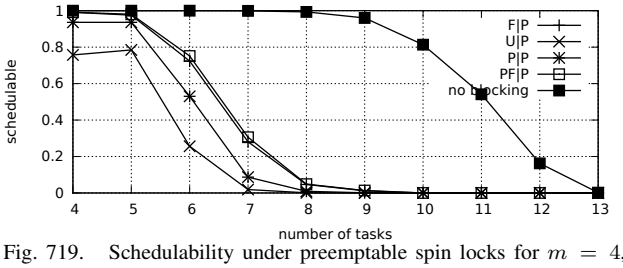

Fig. 719. Schedulability under preemptable spin locks for $m = 4$, $U = 0.3n$, 8 resources, $rsf = 0.75$, $N^{max} = 15$, and medium critical sections. The schedulability of the considered non-preemptable lock types in this configuration is shown in Fig. 709.

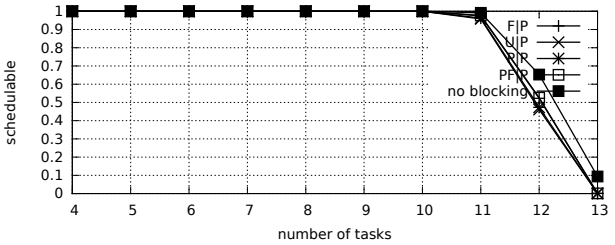

Fig. 720. Schedulability under preemptable spin locks for $m = 4$, $U = 0.3n$, 8 resources, $rsf = 0.75$, $N^{max} = 1$, and short critical sections. The schedulability of the considered non-preemptable lock types in this configuration is shown in Fig. 710.

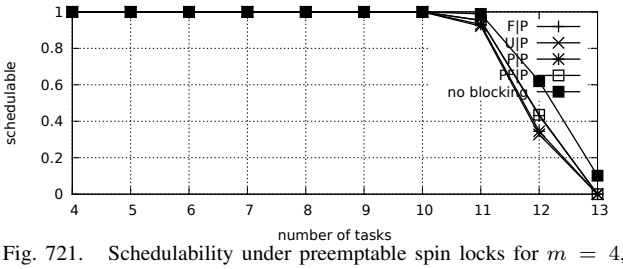

Fig. 721. Schedulability under preemptable spin locks for $m = 4$, $U = 0.3n$, 8 resources, $rsf = 0.75$, $N^{max} = 2$, and short critical sections. The schedulability of the considered non-preemptable lock types in this configuration is shown in Fig. 711.

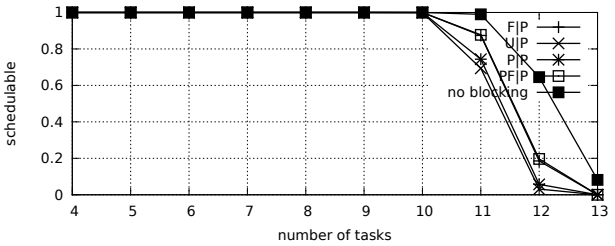

Fig. 722. Schedulability under preemptable spin locks for $m = 4$, $U = 0.3n$, 8 resources, $rsf = 0.75$, $N^{max} = 5$, and short critical sections. The schedulability of the considered non-preemptable lock types in this configuration is shown in Fig. 712.

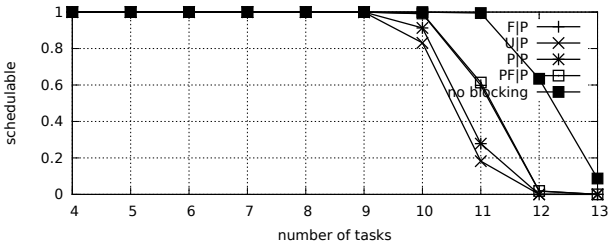

Fig. 723. Schedulability under preemptable spin locks for $m = 4$, $U = 0.3n$, 8 resources, $rsf = 0.75$, $N^{max} = 10$, and short critical sections. The schedulability of the considered non-preemptable lock types in this configuration is shown in Fig. 713.

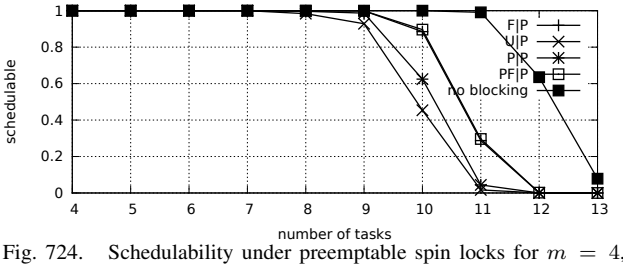

Fig. 724. Schedulability under preemptable spin locks for $m = 4$, $U = 0.3n$, 8 resources, $rsf = 0.75$, $N^{max} = 15$, and short critical sections. The schedulability of the considered non-preemptable lock types in this configuration is shown in Fig. 714.

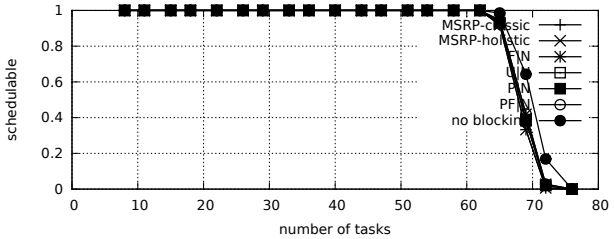

Fig. 725. Schedulability under non-preemptable spin locks for $m = 8$, $U = 0.1n$, 4 resources, $rsf = 0.1$, $N^{max} = 1$, and medium critical sections. The schedulability of the considered preemptable lock types in this configuration is shown in Fig. 735.

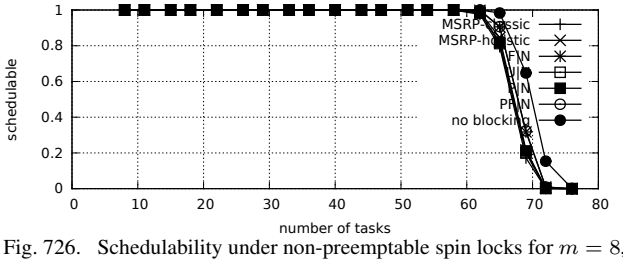

Fig. 726. Schedulability under non-preemptable spin locks for $m = 8$, $U = 0.1n$, 4 resources, $rsf = 0.1$, $N^{max} = 2$, and medium critical sections. The schedulability of the considered preemptable lock types in this configuration is shown in Fig. 736.

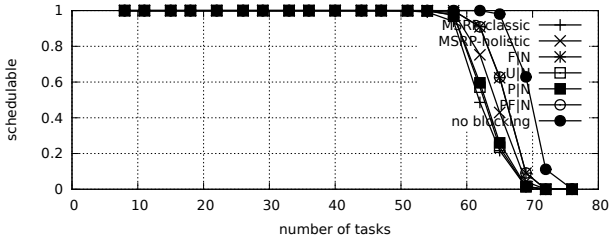

Fig. 727. Schedulability under non-preemptable spin locks for $m = 8$, $U = 0.1n$, 4 resources, $rsf = 0.1$, $N^{max} = 5$, and medium critical sections. The schedulability of the considered preemptable lock types in this configuration is shown in Fig. 737.

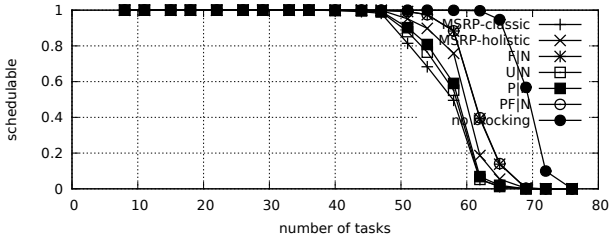

Fig. 728. Schedulability under non-preemptable spin locks for $m = 8$, $U = 0.1n$, 4 resources, $rsf = 0.1$, $N^{max} = 10$, and medium critical sections. The schedulability of the considered preemptable lock types in this configuration is shown in Fig. 738.

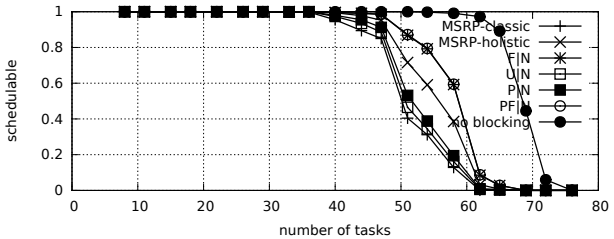

Fig. 729. Schedulability under non-preemptable spin locks for $m = 8$, $U = 0.1n$, 4 resources, $rsf = 0.1$, $N^{max} = 15$, and medium critical sections. The schedulability of the considered preemptable lock types in this configuration is shown in Fig. 739.

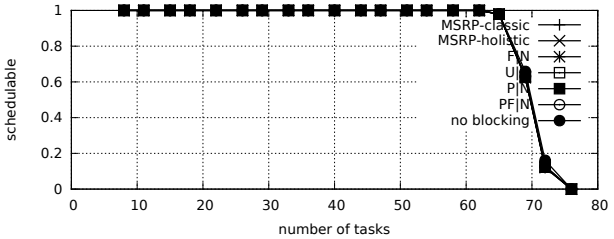

Fig. 730. Schedulability under non-preemptable spin locks for $m = 8$, $U = 0.1n$, 4 resources, $rsf = 0.1$, $N^{max} = 1$, and short critical sections. The schedulability of the considered preemptable lock types in this configuration is shown in Fig. 740.

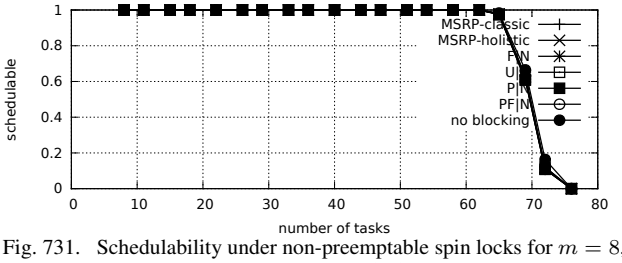

Fig. 731. Schedulability under non-preemptable spin locks for $m = 8$, $U = 0.1n$, 4 resources, $rsf = 0.1$, $N^{max} = 2$, and short critical sections. The schedulability of the considered preemptable lock types in this configuration is shown in Fig. 741.

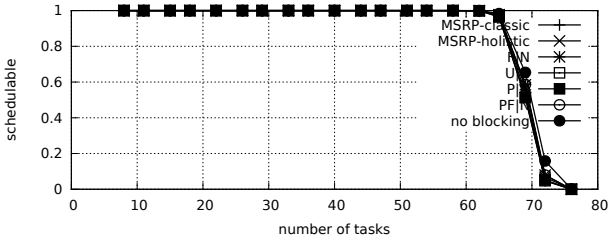

Fig. 732. Schedulability under non-preemptable spin locks for $m = 8$, $U = 0.1n$, 4 resources, $rsf = 0.1$, $N^{max} = 5$, and short critical sections. The schedulability of the considered preemptable lock types in this configuration is shown in Fig. 742.

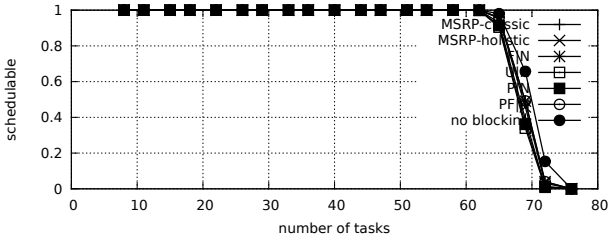

Fig. 733. Schedulability under non-preemptable spin locks for $m = 8$, $U = 0.1n$, 4 resources, $rsf = 0.1$, $N^{max} = 10$, and short critical sections. The schedulability of the considered preemptable lock types in this configuration is shown in Fig. 743.

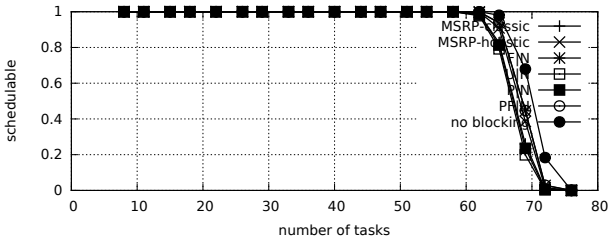

Fig. 734. Schedulability under non-preemptable spin locks for $m = 8$, $U = 0.1n$, 4 resources, $rsf = 0.1$, $N^{max} = 15$, and short critical sections. The schedulability of the considered preemptable lock types in this configuration is shown in Fig. 744.

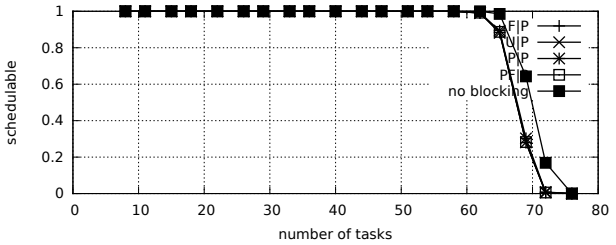

Fig. 735. Schedulability under preemptable spin locks for $m = 8$, $U = 0.1n$, 4 resources, $rsf = 0.1$, $N^{max} = 1$, and medium critical sections. The schedulability of the considered non-preemptable lock types in this configuration is shown in Fig. 725.

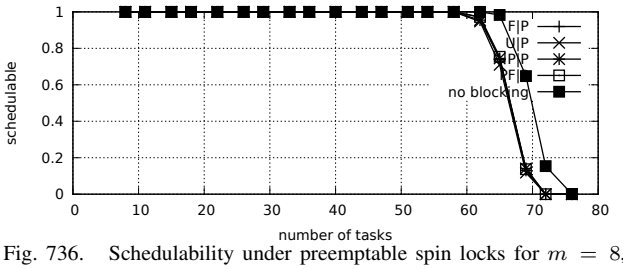

Fig. 736. Schedulability under preemptable spin locks for $m = 8$, $U = 0.1n$, 4 resources, $rsf = 0.1$, $N^{max} = 2$, and medium critical sections. The schedulability of the considered non-preemptable lock types in this configuration is shown in Fig. 726.

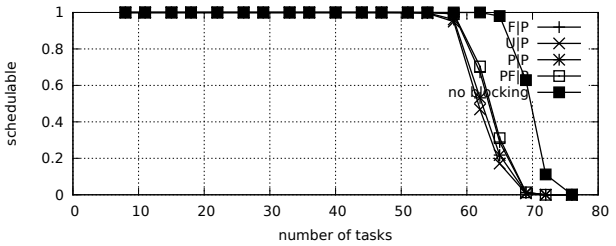

Fig. 737. Schedulability under preemptable spin locks for $m = 8$, $U = 0.1n$, 4 resources, $rsf = 0.1$, $N^{max} = 5$, and medium critical sections. The schedulability of the considered non-preemptable lock types in this configuration is shown in Fig. 727.

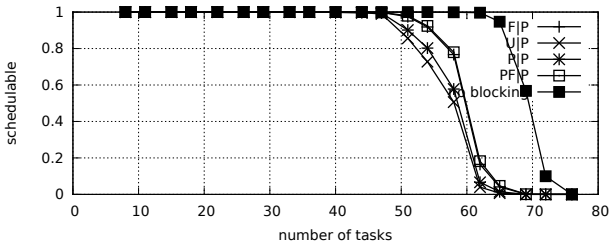

Fig. 738. Schedulability under preemptable spin locks for $m = 8$, $U = 0.1n$, 4 resources, $rsf = 0.1$, $N^{max} = 10$, and medium critical sections. The schedulability of the considered non-preemptable lock types in this configuration is shown in Fig. 728.

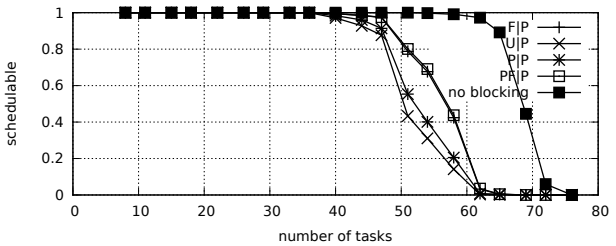

Fig. 739. Schedulability under preemptable spin locks for $m = 8$, $U = 0.1n$, 4 resources, $rsf = 0.1$, $N^{max} = 15$, and medium critical sections. The schedulability of the considered non-preemptable lock types in this configuration is shown in Fig. 729.

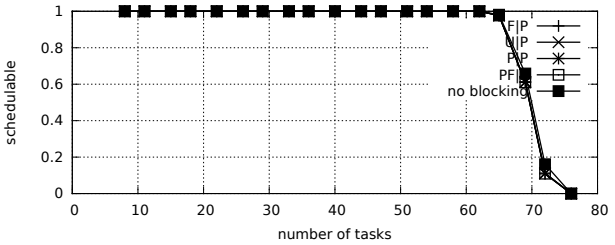

Fig. 740. Schedulability under preemptable spin locks for $m = 8$, $U = 0.1n$, 4 resources, $rsf = 0.1$, $N^{max} = 1$, and short critical sections. The schedulability of the considered non-preemptable lock types in this configuration is shown in Fig. 730.

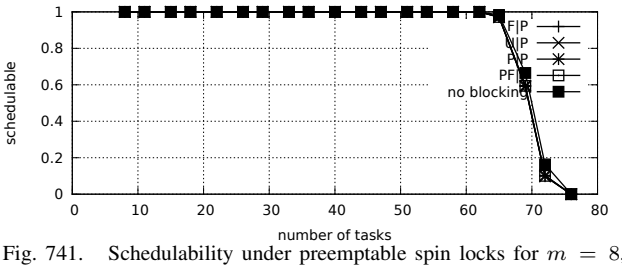

Fig. 741. Schedulability under preemptable spin locks for $m = 8$, $U = 0.1n$, 4 resources, $rsf = 0.1$, $N^{max} = 2$, and short critical sections. The schedulability of the considered non-preemptable lock types in this configuration is shown in Fig. 731.

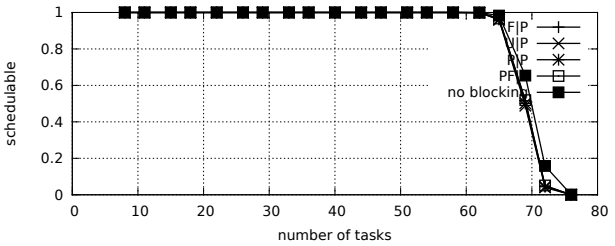

Fig. 742. Schedulability under preemptable spin locks for $m = 8$, $U = 0.1n$, 4 resources, $rsf = 0.1$, $N^{max} = 5$, and short critical sections. The schedulability of the considered non-preemptable lock types in this configuration is shown in Fig. 732.

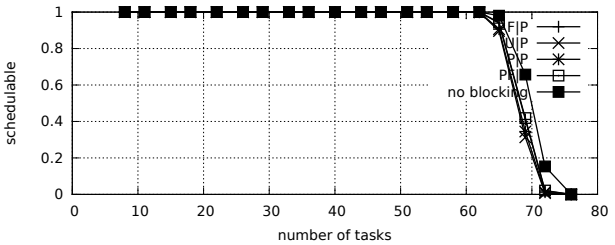

Fig. 743. Schedulability under preemptable spin locks for $m = 8$, $U = 0.1n$, 4 resources, $rsf = 0.1$, $N^{max} = 10$, and short critical sections. The schedulability of the considered non-preemptable lock types in this configuration is shown in Fig. 733.

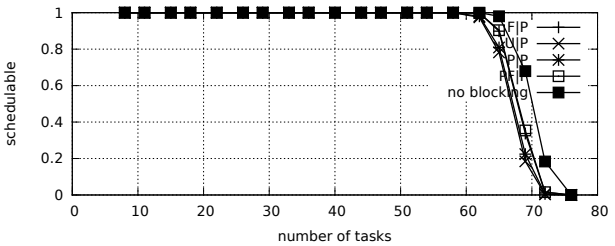

Fig. 744. Schedulability under preemptable spin locks for $m = 8$, $U = 0.1n$, 4 resources, $rsf = 0.1$, $N^{max} = 15$, and short critical sections. The schedulability of the considered non-preemptable lock types in this configuration is shown in Fig. 734.

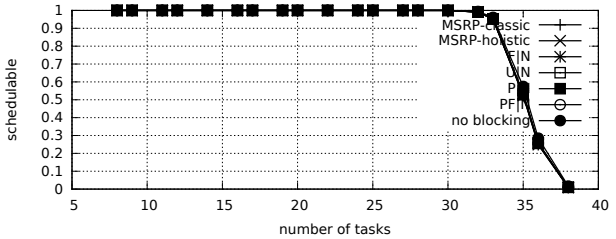

Fig. 745. Schedulability under non-preemptable spin locks for $m = 8$, $U = 0.2n$, 4 resources, $rsf = 0.1$, $N^{max} = 1$, and medium critical sections. The schedulability of the considered preemptable lock types in this configuration is shown in Fig. 755.

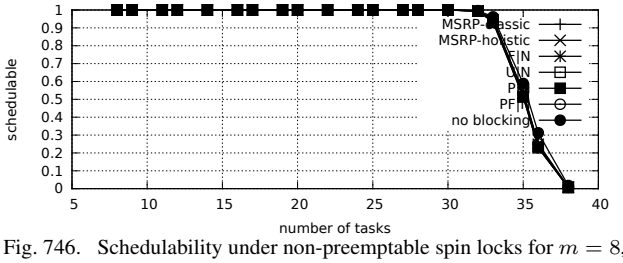

Fig. 746. Schedulability under non-preemptable spin locks for $m = 8$, $U = 0.2n$, 4 resources, $rsf = 0.1$, $N^{max} = 2$, and medium critical sections. The schedulability of the considered preemptable lock types in this configuration is shown in Fig. 756.

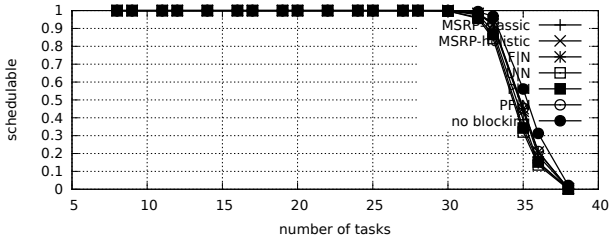

Fig. 747. Schedulability under non-preemptable spin locks for $m = 8$, $U = 0.2n$, 4 resources, $rsf = 0.1$, $N^{max} = 5$, and medium critical sections. The schedulability of the considered preemptable lock types in this configuration is shown in Fig. 757.

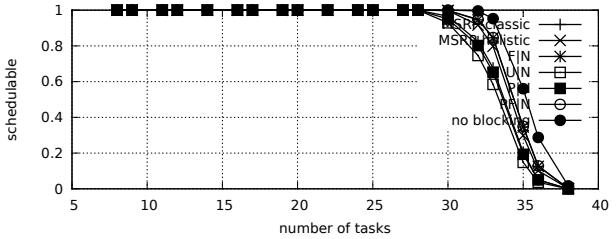

Fig. 748. Schedulability under non-preemptable spin locks for $m = 8$, $U = 0.2n$, 4 resources, $rsf = 0.1$, $N^{max} = 10$, and medium critical sections. The schedulability of the considered preemptable lock types in this configuration is shown in Fig. 758.

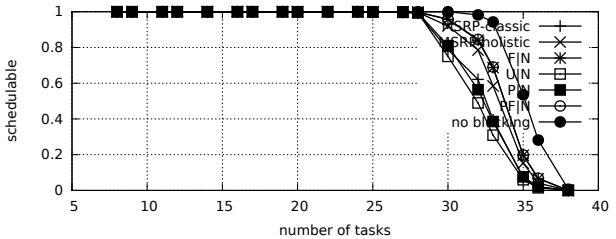

Fig. 749. Schedulability under non-preemptable spin locks for $m = 8$, $U = 0.2n$, 4 resources, $rsf = 0.1$, $N^{max} = 15$, and medium critical sections. The schedulability of the considered preemptable lock types in this configuration is shown in Fig. 759.

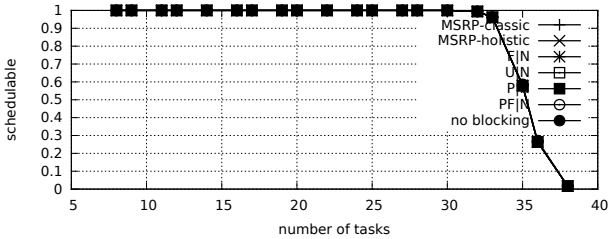

Fig. 750. Schedulability under non-preemptable spin locks for $m = 8$, $U = 0.2n$, 4 resources, $rsf = 0.1$, $N^{max} = 1$, and short critical sections. The schedulability of the considered preemptable lock types in this configuration is shown in Fig. 760.

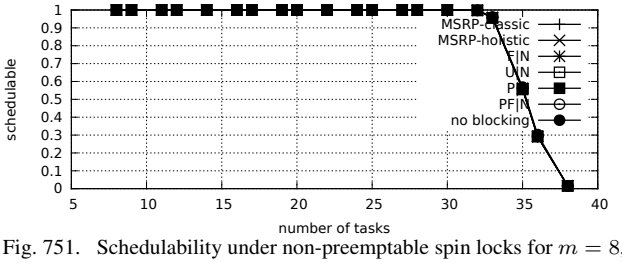

Fig. 751. Schedulability under non-preemptable spin locks for $m = 8$, $U = 0.2n$, 4 resources, $rsf = 0.1$, $N^{max} = 2$, and short critical sections. The schedulability of the considered preemptable lock types in this configuration is shown in Fig. 761.

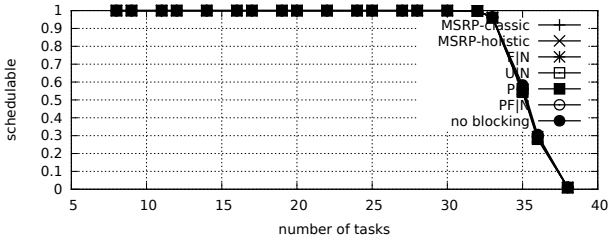

Fig. 752. Schedulability under non-preemptable spin locks for $m = 8$, $U = 0.2n$, 4 resources, $rsf = 0.1$, $N^{max} = 5$, and short critical sections. The schedulability of the considered preemptable lock types in this configuration is shown in Fig. 762.

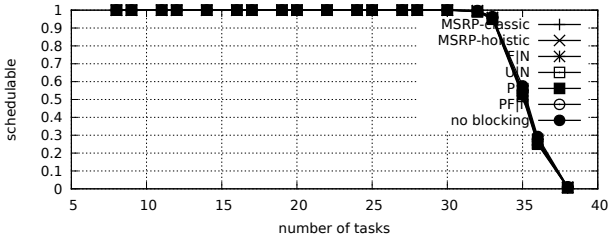

Fig. 753. Schedulability under non-preemptable spin locks for $m = 8$, $U = 0.2n$, 4 resources, $rsf = 0.1$, $N^{max} = 10$, and short critical sections. The schedulability of the considered preemptable lock types in this configuration is shown in Fig. 763.

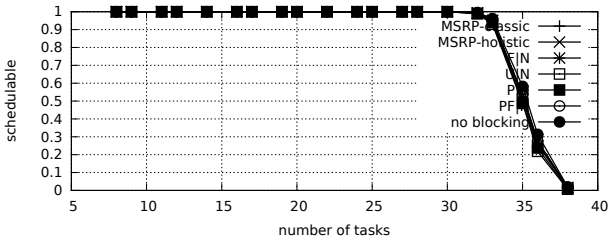

Fig. 754. Schedulability under non-preemptable spin locks for $m = 8$, $U = 0.2n$, 4 resources, $rsf = 0.1$, $N^{max} = 15$, and short critical sections. The schedulability of the considered preemptable lock types in this configuration is shown in Fig. 764.

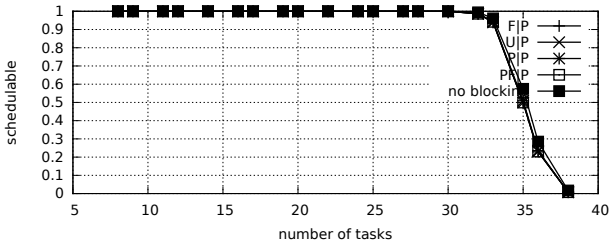

Fig. 755. Schedulability under preemptable spin locks for $m = 8$, $U = 0.2n$, 4 resources, $rsf = 0.1$, $N^{max} = 1$, and medium critical sections. The schedulability of the considered non-preemptable lock types in this configuration is shown in Fig. 745.

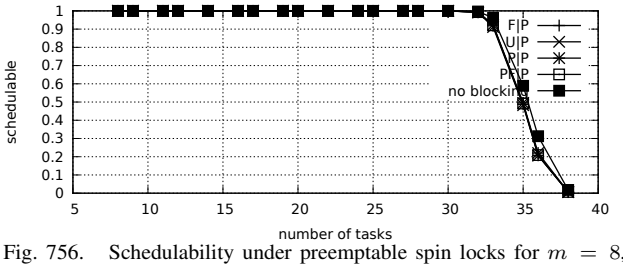

Fig. 756. Schedulability under preemptable spin locks for $m = 8$, $U = 0.2n$, 4 resources, $rsf = 0.1$, $N^{max} = 2$, and medium critical sections. The schedulability of the considered non-preemptable lock types in this configuration is shown in Fig. 746.

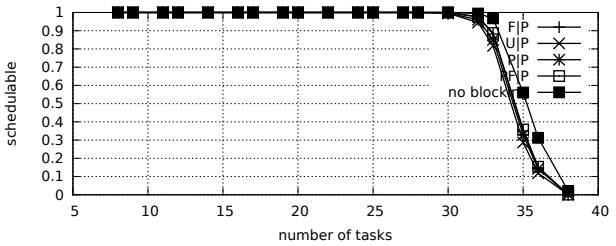

Fig. 757. Schedulability under preemptable spin locks for $m = 8$, $U = 0.2n$, 4 resources, $rsf = 0.1$, $N^{max} = 5$, and medium critical sections. The schedulability of the considered non-preemptable lock types in this configuration is shown in Fig. 747.

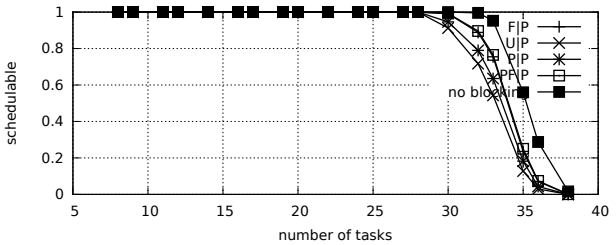

Fig. 758. Schedulability under preemptable spin locks for $m = 8$, $U = 0.2n$, 4 resources, $rsf = 0.1$, $N^{max} = 10$, and medium critical sections. The schedulability of the considered non-preemptable lock types in this configuration is shown in Fig. 748.

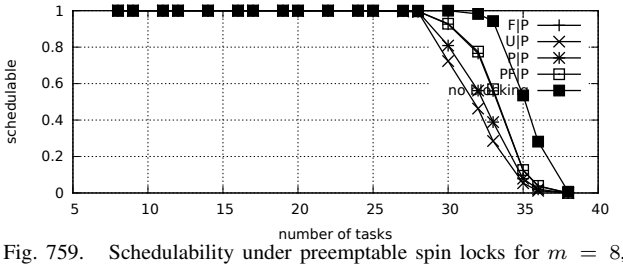

Fig. 759. Schedulability under preemptable spin locks for $m = 8$, $U = 0.2n$, 4 resources, $rsf = 0.1$, $N^{max} = 15$, and medium critical sections. The schedulability of the considered non-preemptable lock types in this configuration is shown in Fig. 749.

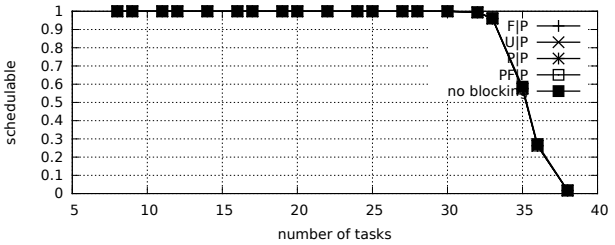

Fig. 760. Schedulability under preemptable spin locks for $m = 8$, $U = 0.2n$, 4 resources, $rsf = 0.1$, $N^{max} = 1$, and short critical sections. The schedulability of the considered non-preemptable lock types in this configuration is shown in Fig. 750.

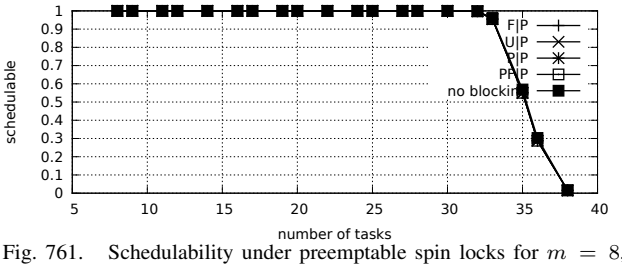

Fig. 761. Schedulability under preemptable spin locks for $m = 8$, $U = 0.2n$, 4 resources, $rsf = 0.1$, $N^{max} = 2$, and short critical sections. The schedulability of the considered non-preemptable lock types in this configuration is shown in Fig. 751.

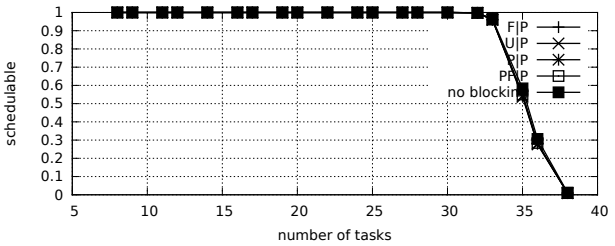

Fig. 762. Schedulability under preemptable spin locks for $m = 8$, $U = 0.2n$, 4 resources, $rsf = 0.1$, $N^{max} = 5$, and short critical sections. The schedulability of the considered non-preemptable lock types in this configuration is shown in Fig. 752.

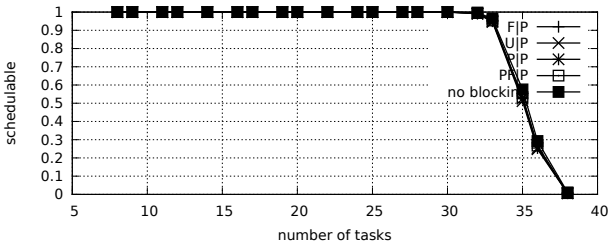

Fig. 763. Schedulability under preemptable spin locks for $m = 8$, $U = 0.2n$, 4 resources, $rsf = 0.1$, $N^{max} = 10$, and short critical sections. The schedulability of the considered non-preemptable lock types in this configuration is shown in Fig. 753.

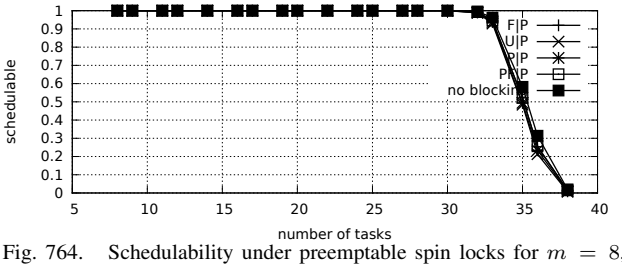

Fig. 764. Schedulability under preemptable spin locks for $m = 8$, $U = 0.2n$, 4 resources, $rsf = 0.1$, $N^{max} = 15$, and short critical sections. The schedulability of the considered non-preemptable lock types in this configuration is shown in Fig. 754.

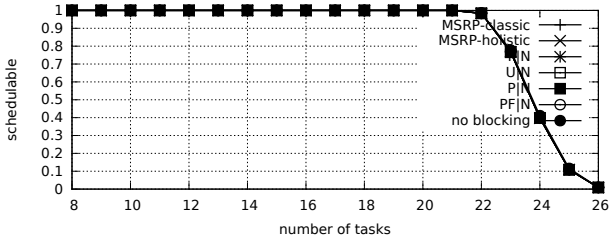

Fig. 765. Schedulability under non-preemptable spin locks for $m = 8$, $U = 0.3n$, 4 resources, $rsf = 0.1$, $N^{max} = 1$, and medium critical sections. The schedulability of the considered preemptable lock types in this configuration is shown in Fig. 775.

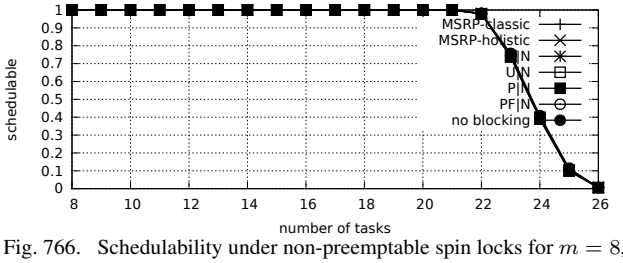

Fig. 766. Schedulability under non-preemptable spin locks for $m = 8$, $U = 0.3n$, 4 resources, $rsf = 0.1$, $N^{max} = 2$, and medium critical sections. The schedulability of the considered preemptable lock types in this configuration is shown in Fig. 776.

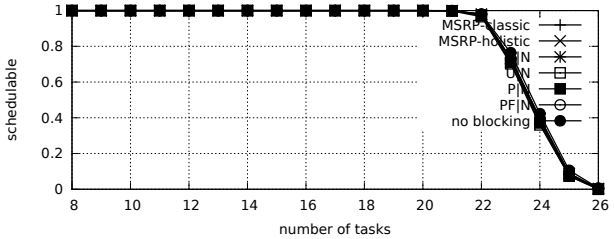

Fig. 767. Schedulability under non-preemptable spin locks for $m = 8$, $U = 0.3n$, 4 resources, $rsf = 0.1$, $N^{max} = 5$, and medium critical sections. The schedulability of the considered preemptable lock types in this configuration is shown in Fig. 777.

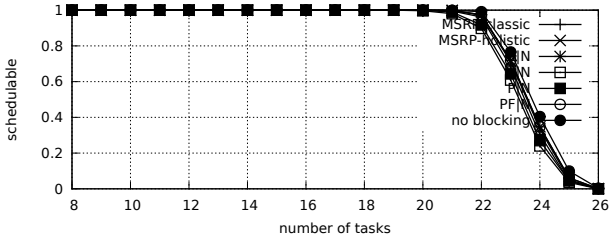

Fig. 768. Schedulability under non-preemptable spin locks for $m = 8$, $U = 0.3n$, 4 resources, $rsf = 0.1$, $N^{max} = 10$, and medium critical sections. The schedulability of the considered preemptable lock types in this configuration is shown in Fig. 778.

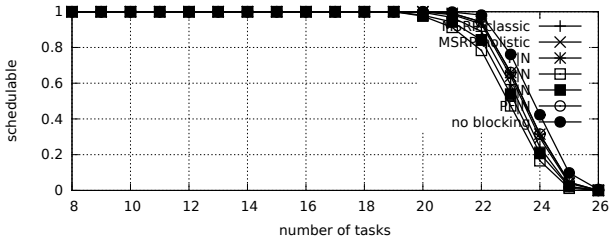

Fig. 769. Schedulability under non-preemptable spin locks for $m = 8$, $U = 0.3n$, 4 resources, $rsf = 0.1$, $N^{max} = 15$, and medium critical sections. The schedulability of the considered preemptable lock types in this configuration is shown in Fig. 779.

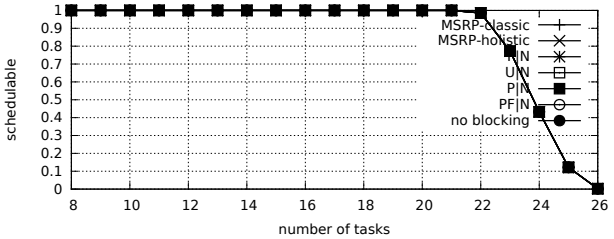

Fig. 770. Schedulability under non-preemptable spin locks for $m = 8$, $U = 0.3n$, 4 resources, $rsf = 0.1$, $N^{max} = 1$, and short critical sections. The schedulability of the considered preemptable lock types in this configuration is shown in Fig. 780.

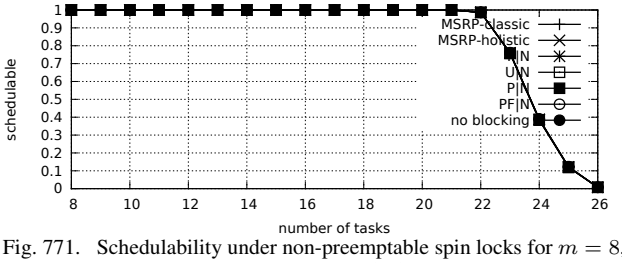

Fig. 771. Schedulability under non-preemptable spin locks for $m = 8$, $U = 0.3n$, 4 resources, $rsf = 0.1$, $N^{max} = 2$, and short critical sections. The schedulability of the considered preemptable lock types in this configuration is shown in Fig. 781.

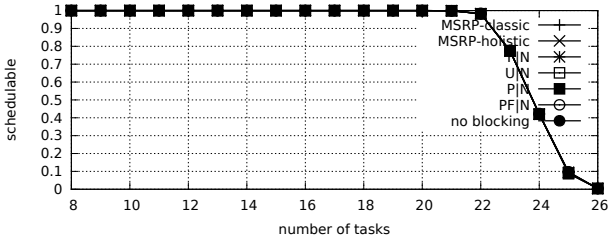

Fig. 772. Schedulability under non-preemptable spin locks for $m = 8$, $U = 0.3n$, 4 resources, $rsf = 0.1$, $N^{max} = 5$, and short critical sections. The schedulability of the considered preemptable lock types in this configuration is shown in Fig. 782.

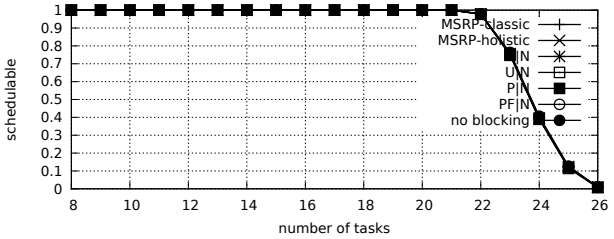

Fig. 773. Schedulability under non-preemptable spin locks for $m = 8$, $U = 0.3n$, 4 resources, $rsf = 0.1$, $N^{max} = 10$, and short critical sections. The schedulability of the considered preemptable lock types in this configuration is shown in Fig. 783.

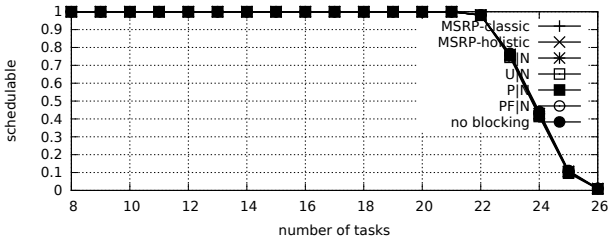

Fig. 774. Schedulability under non-preemptable spin locks for $m = 8$, $U = 0.3n$, 4 resources, $rsf = 0.1$, $N^{max} = 15$, and short critical sections. The schedulability of the considered preemptable lock types in this configuration is shown in Fig. 784.

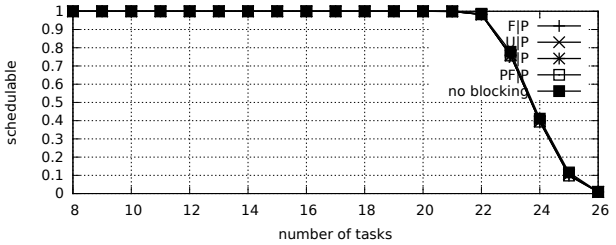

Fig. 775. Schedulability under preemptable spin locks for $m = 8$, $U = 0.3n$, 4 resources, $rsf = 0.1$, $N^{max} = 1$, and medium critical sections. The schedulability of the considered non-preemptable lock types in this configuration is shown in Fig. 765.

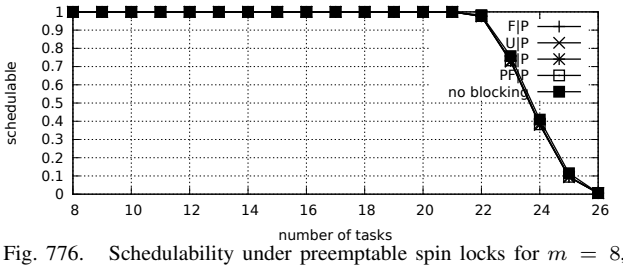

Fig. 776. Schedulability under preemptable spin locks for $m = 8$, $U = 0.3n$, 4 resources, $rsf = 0.1$, $N^{max} = 2$, and medium critical sections. The schedulability of the considered non-preemptable lock types in this configuration is shown in Fig. 766.

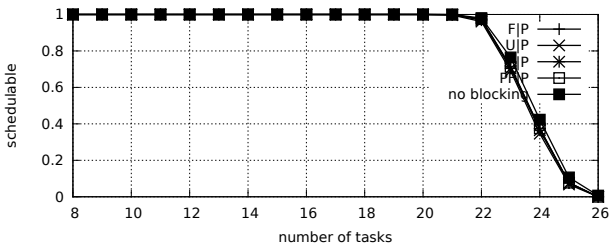

Fig. 777. Schedulability under preemptable spin locks for $m = 8$, $U = 0.3n$, 4 resources, $rsf = 0.1$, $N^{max} = 5$, and medium critical sections. The schedulability of the considered non-preemptable lock types in this configuration is shown in Fig. 767.

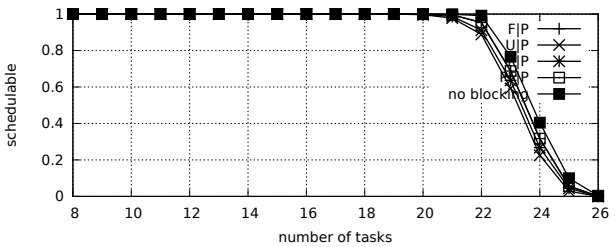

Fig. 778. Schedulability under preemptable spin locks for $m = 8$, $U = 0.3n$, 4 resources, $rsf = 0.1$, $N^{max} = 10$, and medium critical sections. The schedulability of the considered non-preemptable lock types in this configuration is shown in Fig. 768.

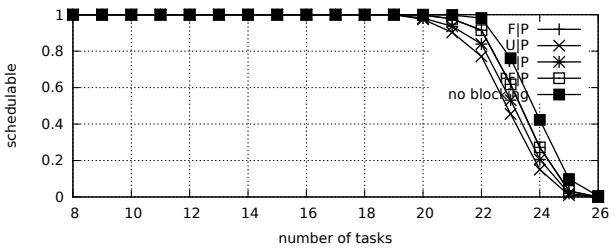

Fig. 779. Schedulability under preemptable spin locks for $m = 8$, $U = 0.3n$, 4 resources, $rsf = 0.1$, $N^{max} = 15$, and medium critical sections. The schedulability of the considered non-preemptable lock types in this configuration is shown in Fig. 769.

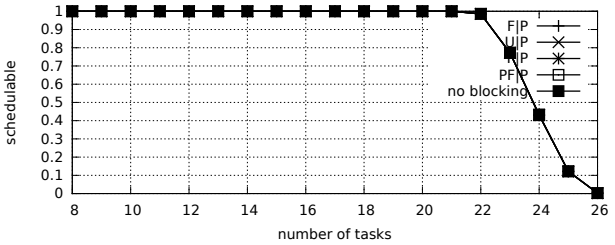

Fig. 780. Schedulability under preemptable spin locks for $m = 8$, $U = 0.3n$, 4 resources, $rsf = 0.1$, $N^{max} = 1$, and short critical sections. The schedulability of the considered non-preemptable lock types in this configuration is shown in Fig. 770.

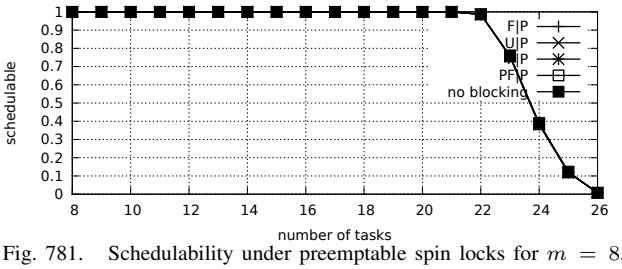

Fig. 781. Schedulability under preemptable spin locks for $m = 8$, $U = 0.3n$, 4 resources, $rsf = 0.1$, $N^{max} = 2$, and short critical sections. The schedulability of the considered non-preemptable lock types in this configuration is shown in Fig. 771.

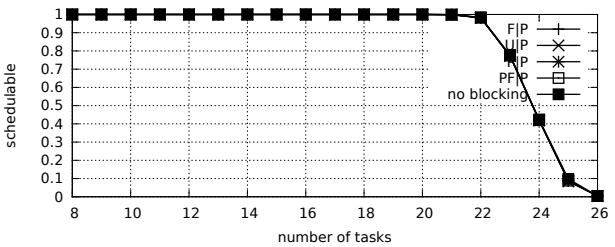

Fig. 782. Schedulability under preemptable spin locks for $m = 8$, $U = 0.3n$, 4 resources, $rsf = 0.1$, $N^{max} = 5$, and short critical sections. The schedulability of the considered non-preemptable lock types in this configuration is shown in Fig. 772.

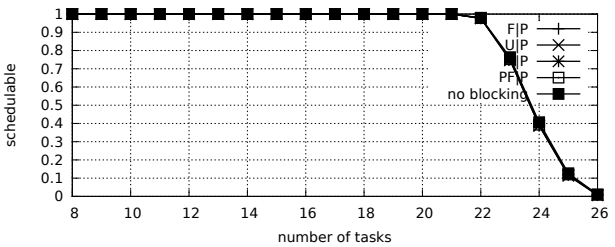

Fig. 783. Schedulability under preemptable spin locks for $m = 8$, $U = 0.3n$, 4 resources, $rsf = 0.1$, $N^{max} = 10$, and short critical sections. The schedulability of the considered non-preemptable lock types in this configuration is shown in Fig. 773.

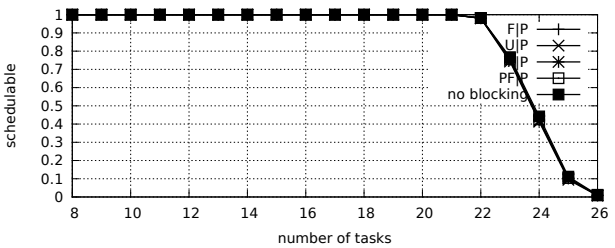

Fig. 784. Schedulability under preemptable spin locks for $m = 8$, $U = 0.3n$, 4 resources, $rsf = 0.1$, $N^{max} = 15$, and short critical sections. The schedulability of the considered non-preemptable lock types in this configuration is shown in Fig. 774.

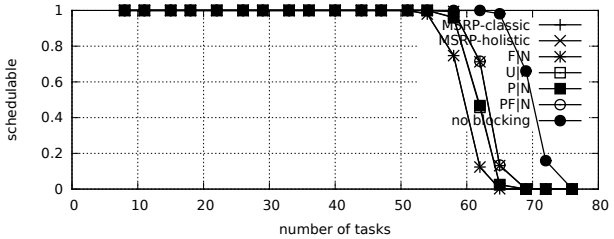

Fig. 785. Schedulability under non-preemptable spin locks for $m = 8$, $U = 0.1n$, 4 resources, $rsf = 0.25$, $N^{max} = 1$, and medium critical sections. The schedulability of the considered preemptable lock types in this configuration is shown in Fig. 795.

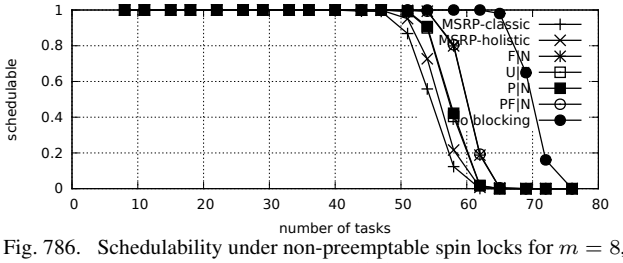

Fig. 786. Schedulability under non-preemptable spin locks for $m = 8$, $U = 0.1n$, 4 resources, $rsf = 0.25$, $N^{max} = 2$, and medium critical sections. The schedulability of the considered preemptable lock types in this configuration is shown in Fig. 796.

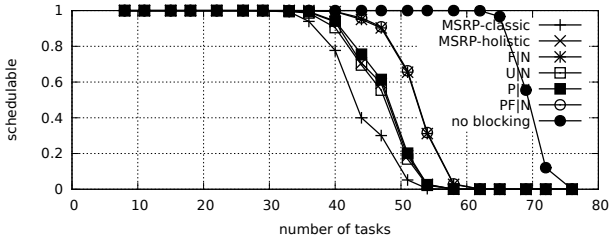

Fig. 787. Schedulability under non-preemptable spin locks for $m = 8$, $U = 0.1n$, 4 resources, $rsf = 0.25$, $N^{max} = 5$, and medium critical sections. The schedulability of the considered preemptable lock types in this configuration is shown in Fig. 797.

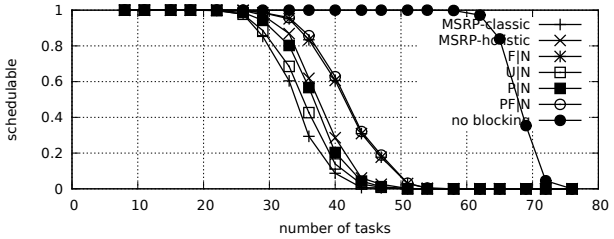

Fig. 788. Schedulability under non-preemptable spin locks for $m = 8$, $U = 0.1n$, 4 resources, $rsf = 0.25$, $N^{max} = 10$, and medium critical sections. The schedulability of the considered preemptable lock types in this configuration is shown in Fig. 798.

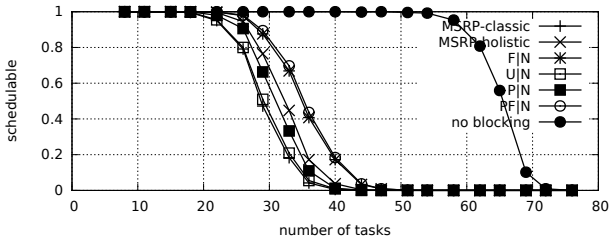

Fig. 789. Schedulability under non-preemptable spin locks for $m = 8$, $U = 0.1n$, 4 resources, $rsf = 0.25$, $N^{max} = 15$, and medium critical sections. The schedulability of the considered preemptable lock types in this configuration is shown in Fig. 799.

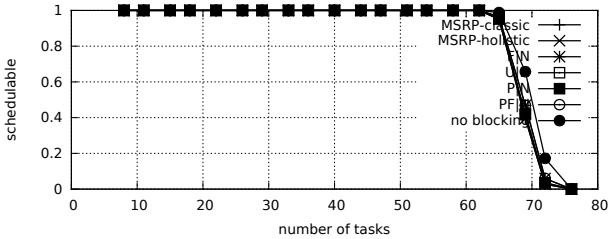

Fig. 790. Schedulability under non-preemptable spin locks for $m = 8$, $U = 0.1n$, 4 resources, $rsf = 0.25$, $N^{max} = 1$, and short critical sections. The schedulability of the considered preemptable lock types in this configuration is shown in Fig. 800.

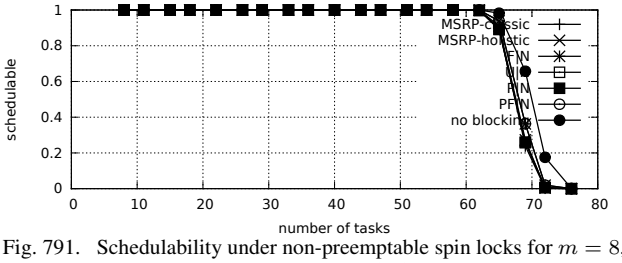

Fig. 791. Schedulability under non-preemptable spin locks for $m = 8$, $U = 0.1n$, 4 resources, $rsf = 0.25$, $N^{max} = 2$, and short critical sections. The schedulability of the considered preemptable lock types in this configuration is shown in Fig. 801.

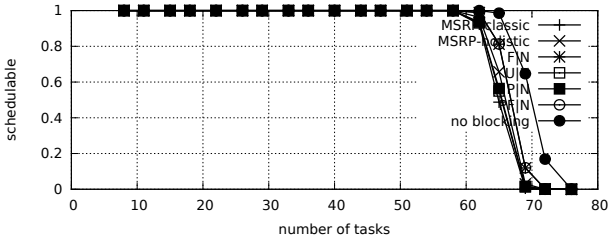

Fig. 792. Schedulability under non-preemptable spin locks for $m = 8$, $U = 0.1n$, 4 resources, $rsf = 0.25$, $N^{max} = 5$, and short critical sections. The schedulability of the considered preemptable lock types in this configuration is shown in Fig. 802.

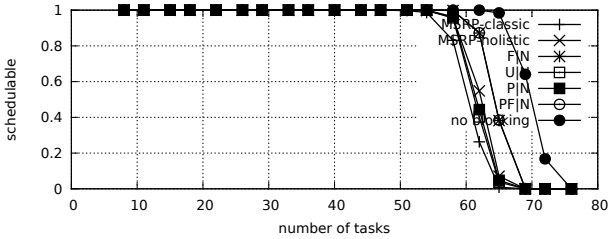

Fig. 793. Schedulability under non-preemptable spin locks for $m = 8$, $U = 0.1n$, 4 resources, $rsf = 0.25$, $N^{max} = 10$, and short critical sections. The schedulability of the considered preemptable lock types in this configuration is shown in Fig. 803.

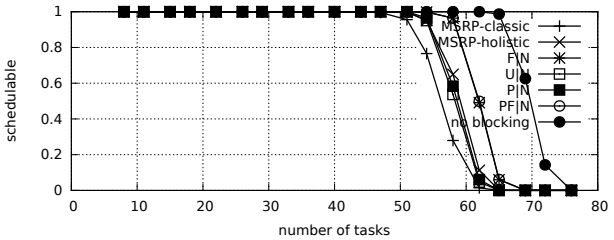

Fig. 794. Schedulability under non-preemptable spin locks for $m = 8$, $U = 0.1n$, 4 resources, $rsf = 0.25$, $N^{max} = 15$, and short critical sections. The schedulability of the considered preemptable lock types in this configuration is shown in Fig. 804.

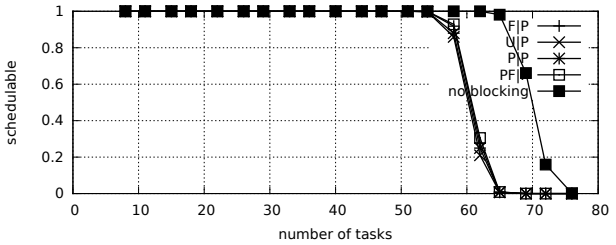

Fig. 795. Schedulability under preemptable spin locks for $m = 8$, $U = 0.1n$, 4 resources, $rsf = 0.25$, $N^{max} = 1$, and medium critical sections. The schedulability of the considered non-preemptable lock types in this configuration is shown in Fig. 785.

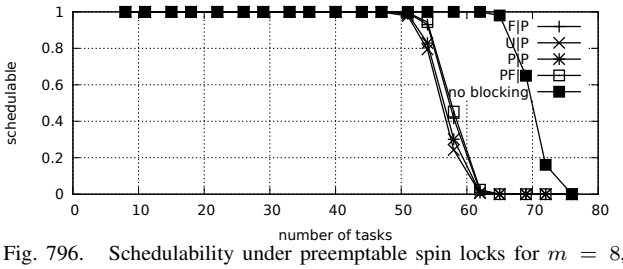

Fig. 796. Schedulability under preemptable spin locks for $m = 8$, $U = 0.1n$, 4 resources, $rsf = 0.25$, $N^{max} = 2$, and medium critical sections. The schedulability of the considered non-preemptable lock types in this configuration is shown in Fig. 786.

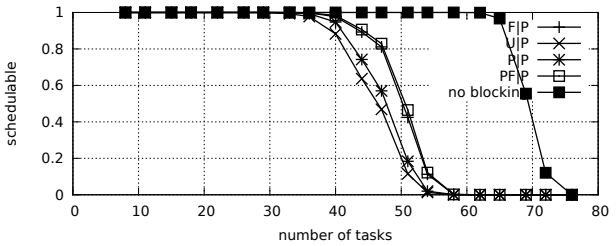

Fig. 797. Schedulability under preemptable spin locks for $m = 8$, $U = 0.1n$, 4 resources, $rsf = 0.25$, $N^{max} = 5$, and medium critical sections. The schedulability of the considered non-preemptable lock types in this configuration is shown in Fig. 787.

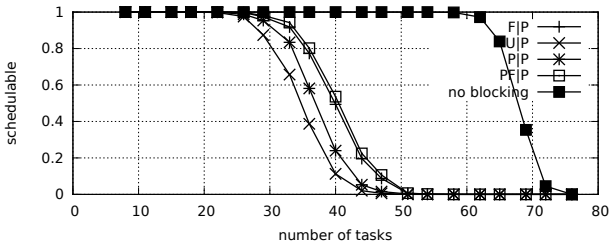

Fig. 798. Schedulability under preemptable spin locks for $m = 8$, $U = 0.1n$, 4 resources, $rsf = 0.25$, $N^{max} = 10$, and medium critical sections. The schedulability of the considered non-preemptable lock types in this configuration is shown in Fig. 788.

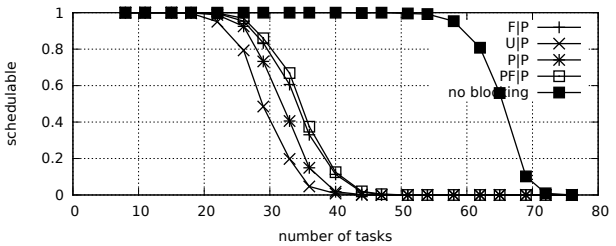

Fig. 799. Schedulability under preemptable spin locks for $m = 8$, $U = 0.1n$, 4 resources, $rsf = 0.25$, $N^{max} = 15$, and medium critical sections. The schedulability of the considered non-preemptable lock types in this configuration is shown in Fig. 789.

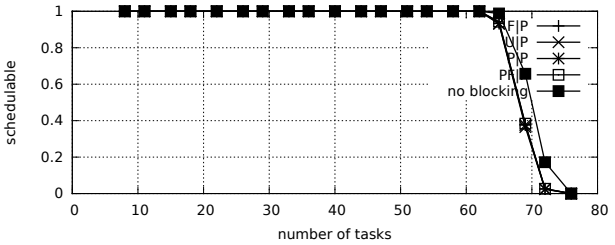

Fig. 800. Schedulability under preemptable spin locks for $m = 8$, $U = 0.1n$, 4 resources, $rsf = 0.25$, $N^{max} = 1$, and short critical sections. The schedulability of the considered non-preemptable lock types in this configuration is shown in Fig. 790.

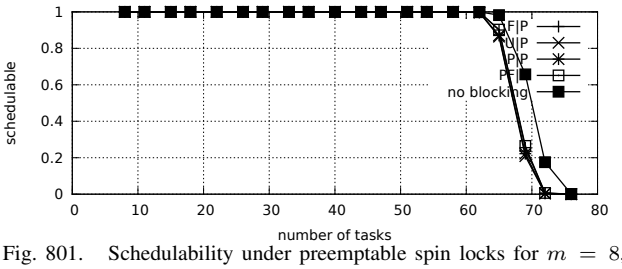

Fig. 801. Schedulability under preemptable spin locks for $m = 8$, $U = 0.1n$, 4 resources, $rsf = 0.25$, $N^{max} = 2$, and short critical sections. The schedulability of the considered non-preemptable lock types in this configuration is shown in Fig. 791.

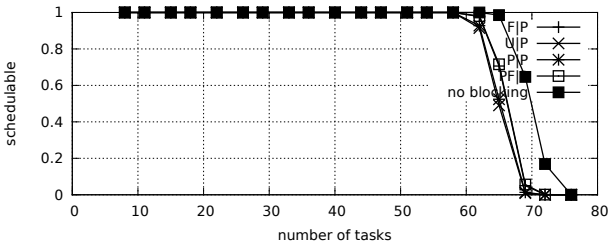

Fig. 802. Schedulability under preemptable spin locks for $m = 8$, $U = 0.1n$, 4 resources, $rsf = 0.25$, $N^{max} = 5$, and short critical sections. The schedulability of the considered non-preemptable lock types in this configuration is shown in Fig. 792.

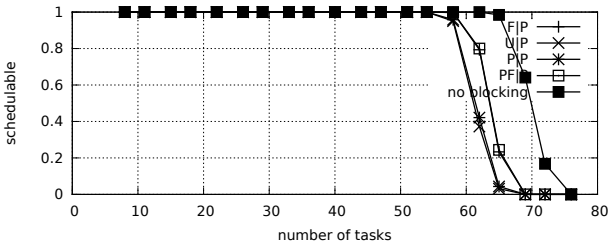

Fig. 803. Schedulability under preemptable spin locks for $m = 8$, $U = 0.1n$, 4 resources, $rsf = 0.25$, $N^{max} = 10$, and short critical sections. The schedulability of the considered non-preemptable lock types in this configuration is shown in Fig. 793.

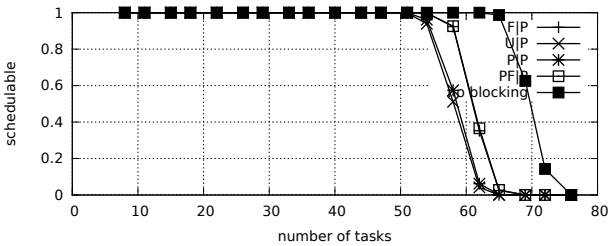

Fig. 804. Schedulability under preemptable spin locks for $m = 8$, $U = 0.1n$, 4 resources, $rsf = 0.25$, $N^{max} = 15$, and short critical sections. The schedulability of the considered non-preemptable lock types in this configuration is shown in Fig. 794.

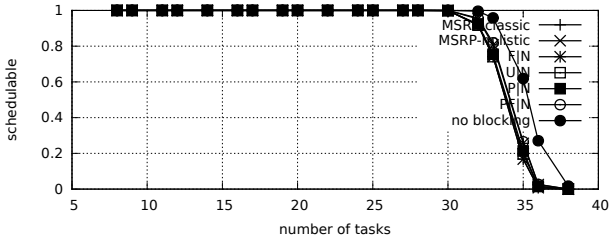

Fig. 805. Schedulability under non-preemptable spin locks for $m = 8$, $U = 0.2n$, 4 resources, $rsf = 0.25$, $N^{max} = 1$, and medium critical sections. The schedulability of the considered preemptable lock types in this configuration is shown in Fig. 815.

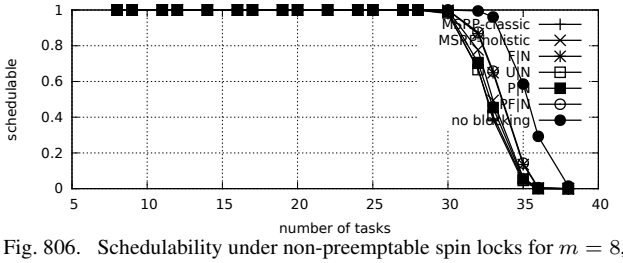

Fig. 806. Schedulability under non-preemptable spin locks for $m = 8$, $U = 0.2n$, 4 resources, $rsf = 0.25$, $N^{max} = 2$, and medium critical sections. The schedulability of the considered preemptable lock types in this configuration is shown in Fig. 816.

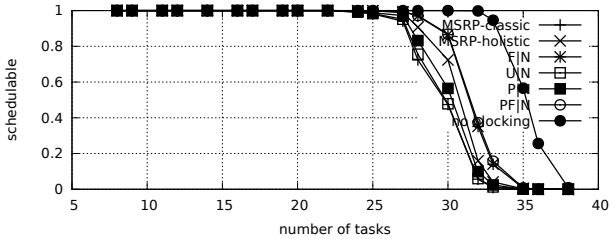

Fig. 807. Schedulability under non-preemptable spin locks for $m = 8$, $U = 0.2n$, 4 resources, $rsf = 0.25$, $N^{max} = 5$, and medium critical sections. The schedulability of the considered preemptable lock types in this configuration is shown in Fig. 817.

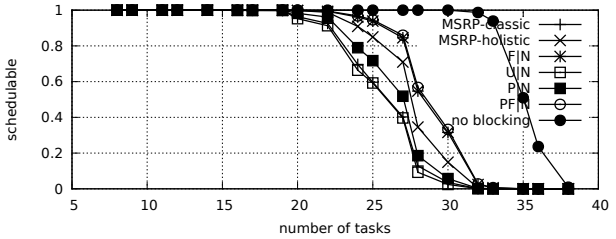

Fig. 808. Schedulability under non-preemptable spin locks for $m = 8$, $U = 0.2n$, 4 resources, $rsf = 0.25$, $N^{max} = 10$, and medium critical sections. The schedulability of the considered preemptable lock types in this configuration is shown in Fig. 818.

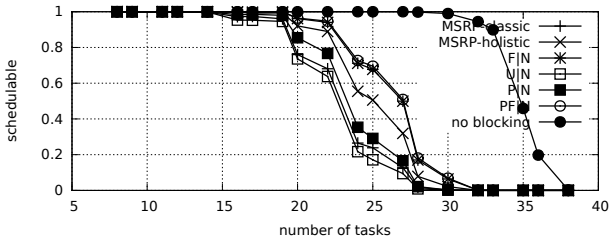

Fig. 809. Schedulability under non-preemptable spin locks for $m = 8$, $U = 0.2n$, 4 resources, $rsf = 0.25$, $N^{max} = 15$, and medium critical sections. The schedulability of the considered preemptable lock types in this configuration is shown in Fig. 819.

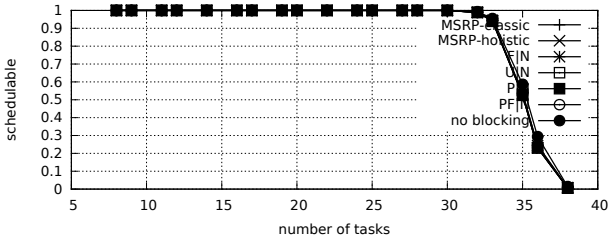

Fig. 810. Schedulability under non-preemptable spin locks for $m = 8$, $U = 0.2n$, 4 resources, $rsf = 0.25$, $N^{max} = 1$, and short critical sections. The schedulability of the considered preemptable lock types in this configuration is shown in Fig. 820.

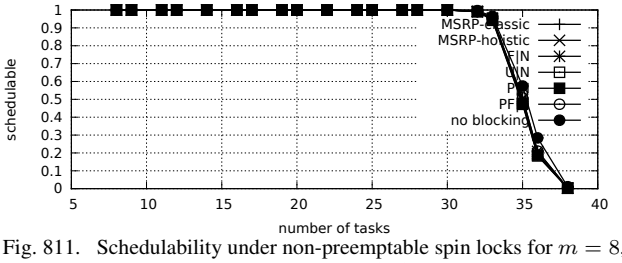

Fig. 811. Schedulability under non-preemptable spin locks for $m = 8$, $U = 0.2n$, 4 resources, $rsf = 0.25$, $N^{max} = 2$, and short critical sections. The schedulability of the considered preemptable lock types in this configuration is shown in Fig. 821.

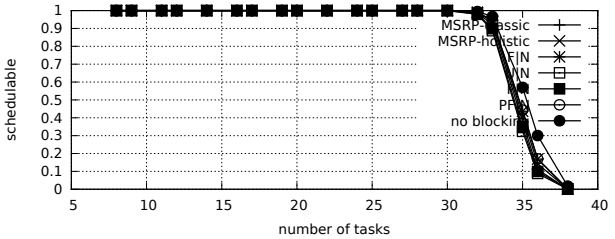

Fig. 812. Schedulability under non-preemptable spin locks for $m = 8$, $U = 0.2n$, 4 resources, $rsf = 0.25$, $N^{max} = 5$, and short critical sections. The schedulability of the considered preemptable lock types in this configuration is shown in Fig. 822.

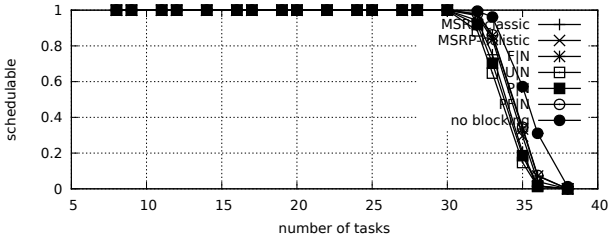

Fig. 813. Schedulability under non-preemptable spin locks for $m = 8$, $U = 0.2n$, 4 resources, $rsf = 0.25$, $N^{max} = 10$, and short critical sections. The schedulability of the considered preemptable lock types in this configuration is shown in Fig. 823.

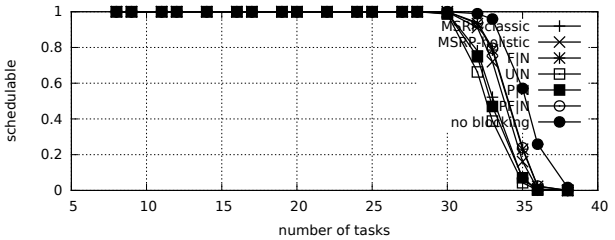

Fig. 814. Schedulability under non-preemptable spin locks for $m = 8$, $U = 0.2n$, 4 resources, $rsf = 0.25$, $N^{max} = 15$, and short critical sections. The schedulability of the considered preemptable lock types in this configuration is shown in Fig. 824.

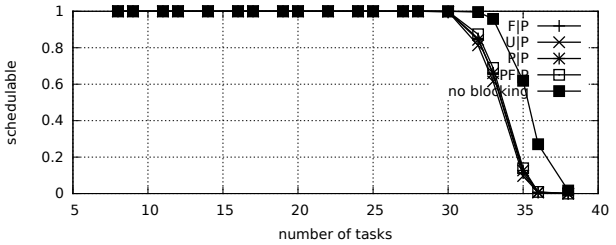

Fig. 815. Schedulability under preemptable spin locks for $m = 8$, $U = 0.2n$, 4 resources, $rsf = 0.25$, $N^{max} = 1$, and medium critical sections. The schedulability of the considered non-preemptable lock types in this configuration is shown in Fig. 805.

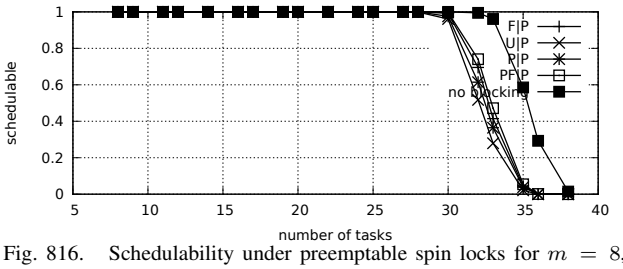

Fig. 816. Schedulability under preemptable spin locks for $m = 8$, $U = 0.2n$, 4 resources, $rsf = 0.25$, $N^{max} = 2$, and medium critical sections. The schedulability of the considered non-preemptable lock types in this configuration is shown in Fig. 806.

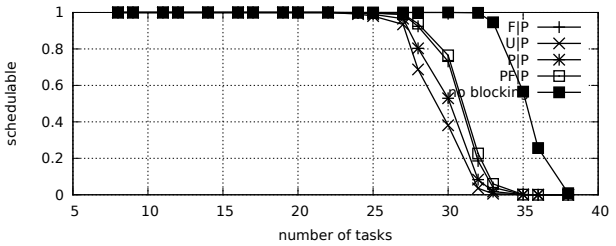

Fig. 817. Schedulability under preemptable spin locks for $m = 8$, $U = 0.2n$, 4 resources, $rsf = 0.25$, $N^{max} = 5$, and medium critical sections. The schedulability of the considered non-preemptable lock types in this configuration is shown in Fig. 807.

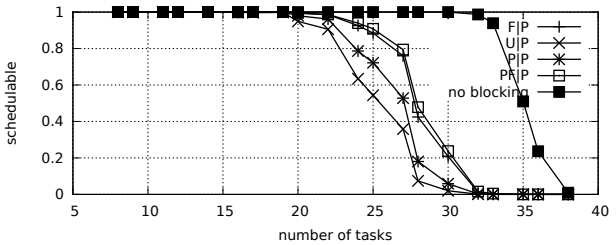

Fig. 818. Schedulability under preemptable spin locks for $m = 8$, $U = 0.2n$, 4 resources, $rsf = 0.25$, $N^{max} = 10$, and medium critical sections. The schedulability of the considered non-preemptable lock types in this configuration is shown in Fig. 808.

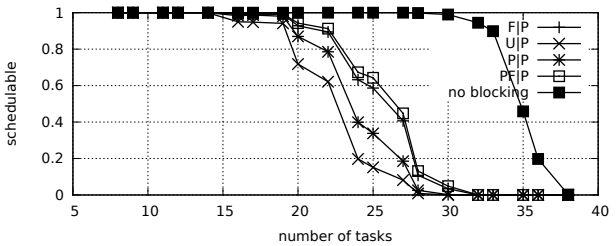

Fig. 819. Schedulability under preemptable spin locks for $m = 8$, $U = 0.2n$, 4 resources, $rsf = 0.25$, $N^{max} = 15$, and medium critical sections. The schedulability of the considered non-preemptable lock types in this configuration is shown in Fig. 809.

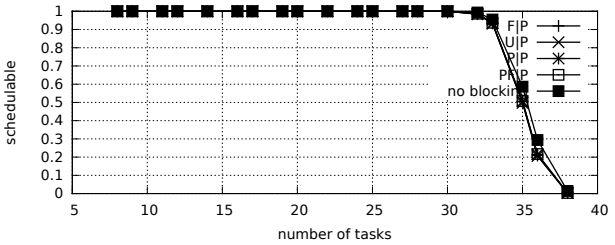

Fig. 820. Schedulability under preemptable spin locks for $m = 8$, $U = 0.2n$, 4 resources, $rsf = 0.25$, $N^{max} = 1$, and short critical sections. The schedulability of the considered non-preemptable lock types in this configuration is shown in Fig. 810.

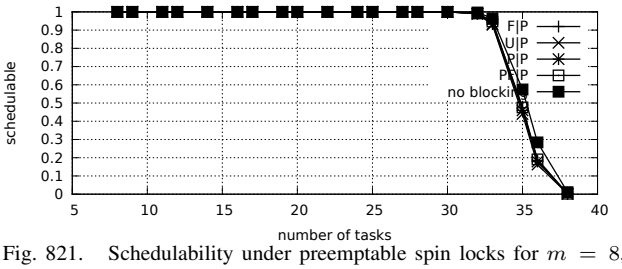

Fig. 821. Schedulability under preemptable spin locks for $m = 8$, $U = 0.2n$, 4 resources, $rsf = 0.25$, $N^{max} = 2$, and short critical sections. The schedulability of the considered non-preemptable lock types in this configuration is shown in Fig. 811.

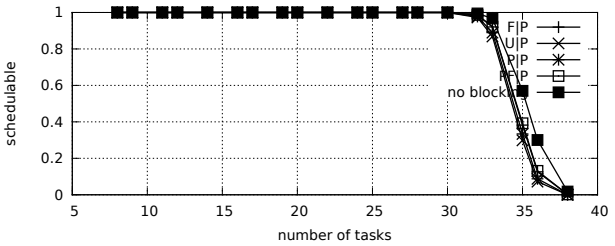

Fig. 822. Schedulability under preemptable spin locks for $m = 8$, $U = 0.2n$, 4 resources, $rsf = 0.25$, $N^{max} = 5$, and short critical sections. The schedulability of the considered non-preemptable lock types in this configuration is shown in Fig. 812.

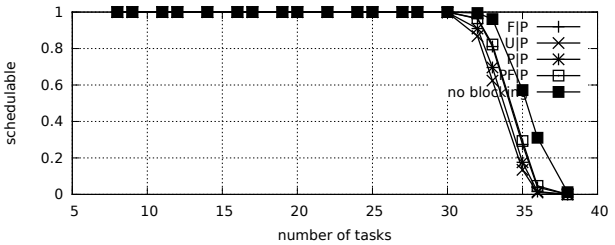

Fig. 823. Schedulability under preemptable spin locks for $m = 8$, $U = 0.2n$, 4 resources, $rsf = 0.25$, $N^{max} = 10$, and short critical sections. The schedulability of the considered non-preemptable lock types in this configuration is shown in Fig. 813.

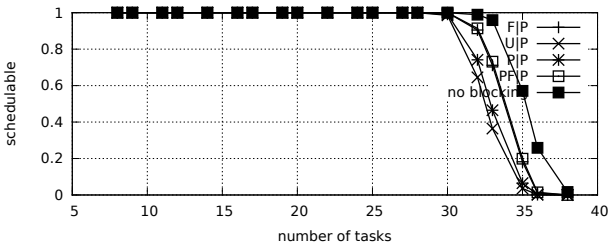

Fig. 824. Schedulability under preemptable spin locks for $m = 8$, $U = 0.2n$, 4 resources, $rsf = 0.25$, $N^{max} = 15$, and short critical sections. The schedulability of the considered non-preemptable lock types in this configuration is shown in Fig. 814.

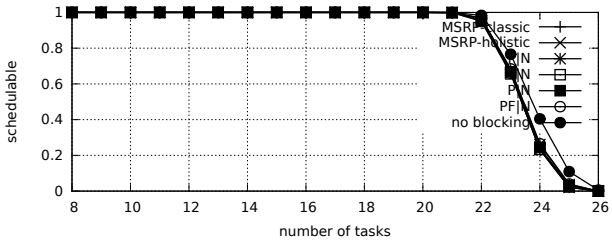

Fig. 825. Schedulability under non-preemptable spin locks for $m = 8$, $U = 0.3n$, 4 resources, $rsf = 0.25$, $N^{max} = 1$, and medium critical sections. The schedulability of the considered preemptable lock types in this configuration is shown in Fig. 835.

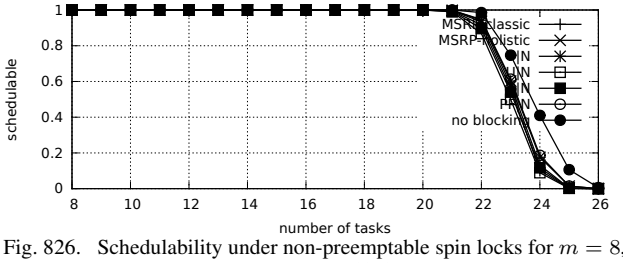

Fig. 826. Schedulability under non-preemptable spin locks for $m = 8$, $U = 0.3n$, 4 resources, $rsf = 0.25$, $N^{max} = 2$, and medium critical sections. The schedulability of the considered preemptable lock types in this configuration is shown in Fig. 836.

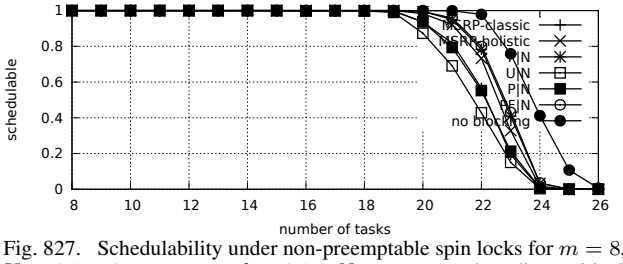

Fig. 827. Schedulability under non-preemptable spin locks for $m = 8$, $U = 0.3n$, 4 resources, $rsf = 0.25$, $N^{max} = 5$, and medium critical sections. The schedulability of the considered preemptable lock types in this configuration is shown in Fig. 837.

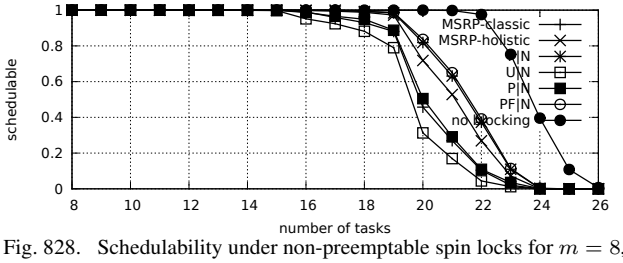

Fig. 828. Schedulability under non-preemptable spin locks for $m = 8$, $U = 0.3n$, 4 resources, $rsf = 0.25$, $N^{max} = 10$, and medium critical sections. The schedulability of the considered preemptable lock types in this configuration is shown in Fig. 838.

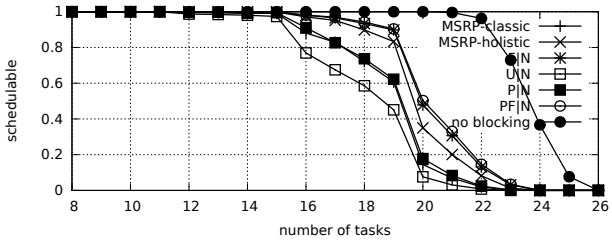

Fig. 829. Schedulability under non-preemptable spin locks for $m = 8$, $U = 0.3n$, 4 resources, $rsf = 0.25$, $N^{max} = 15$, and medium critical sections. The schedulability of the considered preemptable lock types in this configuration is shown in Fig. 839.

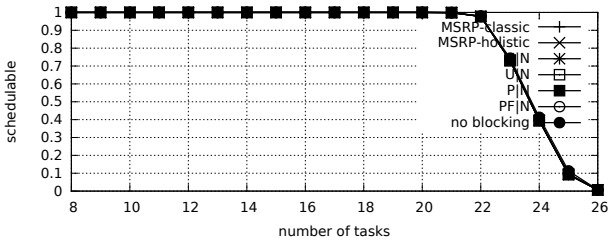

Fig. 830. Schedulability under non-preemptable spin locks for $m = 8$, $U = 0.3n$, 4 resources, $rsf = 0.25$, $N^{max} = 1$, and short critical sections. The schedulability of the considered preemptable lock types in this configuration is shown in Fig. 840.

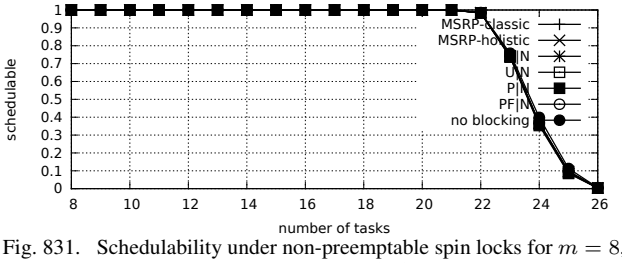

Fig. 831. Schedulability under non-preemptable spin locks for $m = 8$, $U = 0.3n$, 4 resources, $rsf = 0.25$, $N^{max} = 2$, and short critical sections. The schedulability of the considered preemptable lock types in this configuration is shown in Fig. 841.

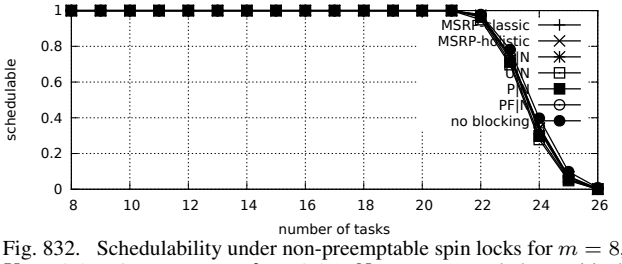

Fig. 832. Schedulability under non-preemptable spin locks for $m = 8$, $U = 0.3n$, 4 resources, $rsf = 0.25$, $N^{max} = 5$, and short critical sections. The schedulability of the considered preemptable lock types in this configuration is shown in Fig. 842.

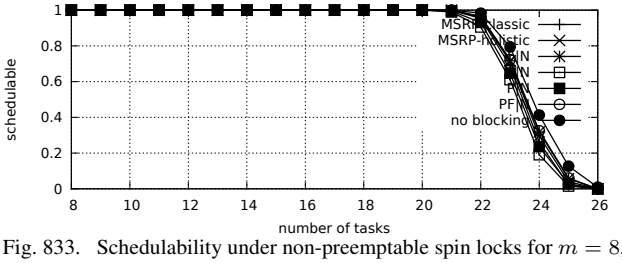

Fig. 833. Schedulability under non-preemptable spin locks for $m = 8$, $U = 0.3n$, 4 resources, $rsf = 0.25$, $N^{max} = 10$, and short critical sections. The schedulability of the considered preemptable lock types in this configuration is shown in Fig. 843.

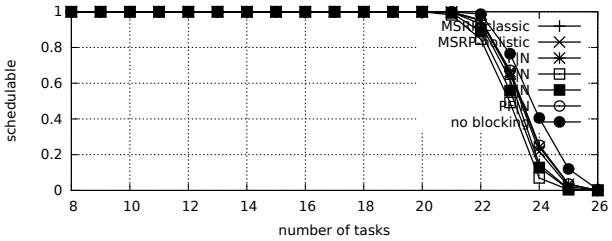

Fig. 834. Schedulability under non-preemptable spin locks for $m = 8$, $U = 0.3n$, 4 resources, $rsf = 0.25$, $N^{max} = 15$, and short critical sections. The schedulability of the considered preemptable lock types in this configuration is shown in Fig. 844.

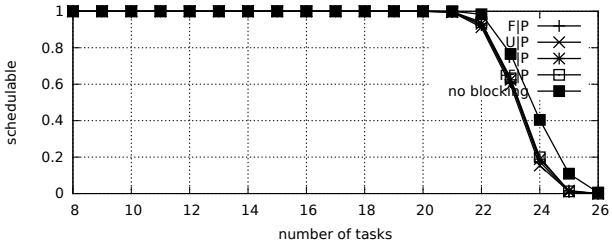

Fig. 835. Schedulability under preemptable spin locks for $m = 8$, $U = 0.3n$, 4 resources, $rsf = 0.25$, $N^{max} = 1$, and medium critical sections. The schedulability of the considered non-preemptable lock types in this configuration is shown in Fig. 825.

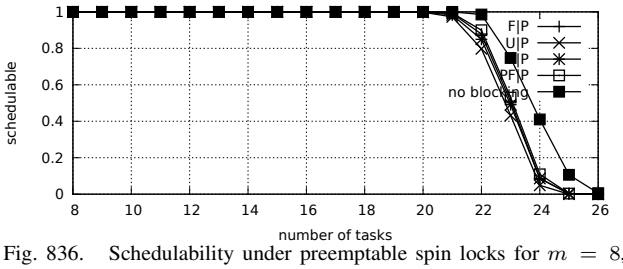

Fig. 836. Schedulability under preemptable spin locks for $m = 8$, $U = 0.3n$, 4 resources, $rsf = 0.25$, $N^{max} = 2$, and medium critical sections. The schedulability of the considered non-preemptable lock types in this configuration is shown in Fig. 826.

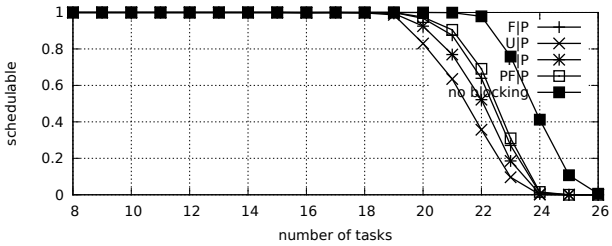

Fig. 837. Schedulability under preemptable spin locks for $m = 8$, $U = 0.3n$, 4 resources, $rsf = 0.25$, $N^{max} = 5$, and medium critical sections. The schedulability of the considered non-preemptable lock types in this configuration is shown in Fig. 827.

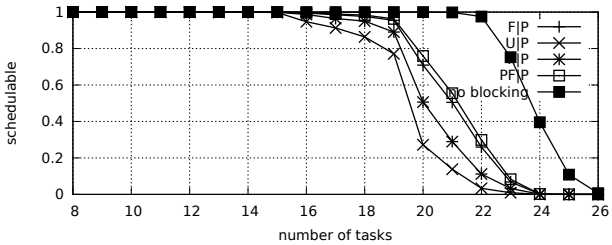

Fig. 838. Schedulability under preemptable spin locks for $m = 8$, $U = 0.3n$, 4 resources, $rsf = 0.25$, $N^{max} = 10$, and medium critical sections. The schedulability of the considered non-preemptable lock types in this configuration is shown in Fig. 828.

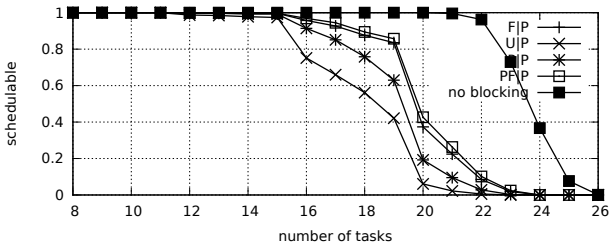

Fig. 839. Schedulability under preemptable spin locks for $m = 8$, $U = 0.3n$, 4 resources, $rsf = 0.25$, $N^{max} = 15$, and medium critical sections. The schedulability of the considered non-preemptable lock types in this configuration is shown in Fig. 829.

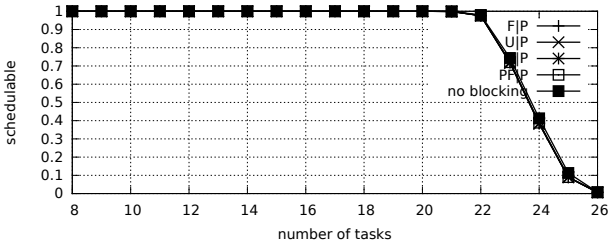

Fig. 840. Schedulability under preemptable spin locks for $m = 8$, $U = 0.3n$, 4 resources, $rsf = 0.25$, $N^{max} = 1$, and short critical sections. The schedulability of the considered non-preemptable lock types in this configuration is shown in Fig. 830.

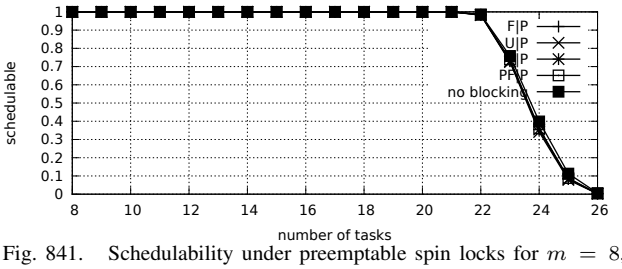

Fig. 841. Schedulability under preemptable spin locks for $m = 8$, $U = 0.3n$, 4 resources, $rsf = 0.25$, $N^{max} = 2$, and short critical sections. The schedulability of the considered non-preemptable lock types in this configuration is shown in Fig. 831.

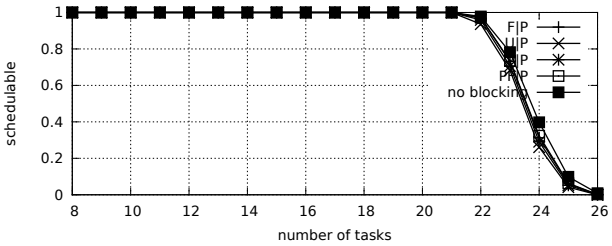

Fig. 842. Schedulability under preemptable spin locks for $m = 8$, $U = 0.3n$, 4 resources, $rsf = 0.25$, $N^{max} = 5$, and short critical sections. The schedulability of the considered non-preemptable lock types in this configuration is shown in Fig. 832.

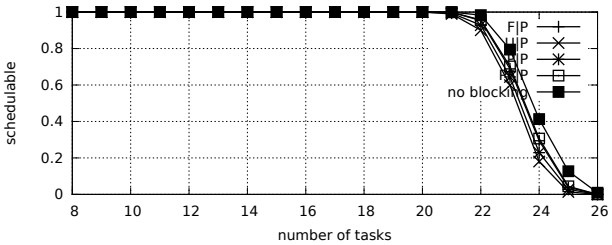

Fig. 843. Schedulability under preemptable spin locks for $m = 8$, $U = 0.3n$, 4 resources, $rsf = 0.25$, $N^{max} = 10$, and short critical sections. The schedulability of the considered non-preemptable lock types in this configuration is shown in Fig. 833.

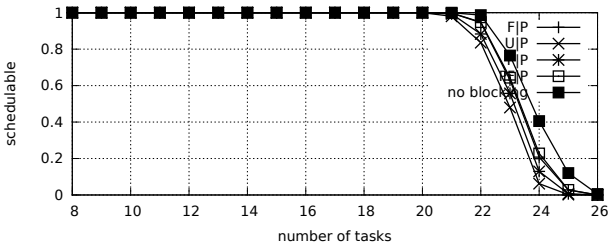

Fig. 844. Schedulability under preemptable spin locks for $m = 8$, $U = 0.3n$, 4 resources, $rsf = 0.25$, $N^{max} = 15$, and short critical sections. The schedulability of the considered non-preemptable lock types in this configuration is shown in Fig. 834.

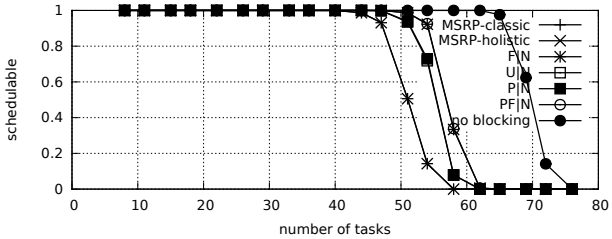

Fig. 845. Schedulability under non-preemptable spin locks for $m = 8$, $U = 0.1n$, 4 resources, $rsf = 0.4$, $N^{max} = 1$, and medium critical sections. The schedulability of the considered preemptable lock types in this configuration is shown in Fig. 855.

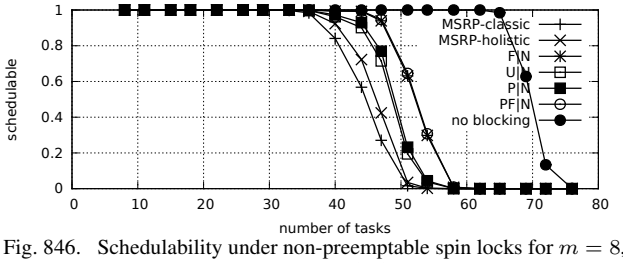

Fig. 846. Schedulability under non-preemptable spin locks for $m = 8$, $U = 0.1n$, 4 resources, $rsf = 0.4$, $N^{max} = 2$, and medium critical sections. The schedulability of the considered preemptable lock types in this configuration is shown in Fig. 856.

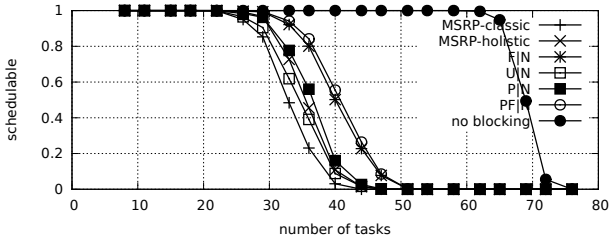

Fig. 847. Schedulability under non-preemptable spin locks for $m = 8$, $U = 0.1n$, 4 resources, $rsf = 0.4$, $N^{max} = 5$, and medium critical sections. The schedulability of the considered preemptable lock types in this configuration is shown in Fig. 857.

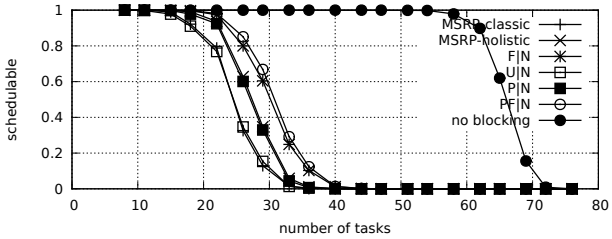

Fig. 848. Schedulability under non-preemptable spin locks for $m = 8$, $U = 0.1n$, 4 resources, $rsf = 0.4$, $N^{max} = 10$, and medium critical sections. The schedulability of the considered preemptable lock types in this configuration is shown in Fig. 858.

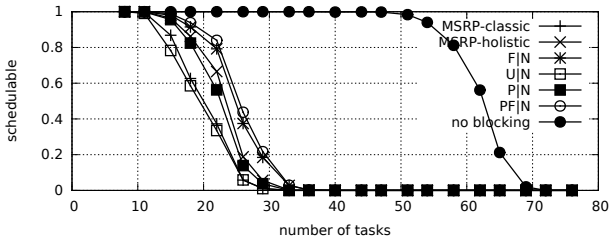

Fig. 849. Schedulability under non-preemptable spin locks for $m = 8$, $U = 0.1n$, 4 resources, $rsf = 0.4$, $N^{max} = 15$, and medium critical sections. The schedulability of the considered preemptable lock types in this configuration is shown in Fig. 859.

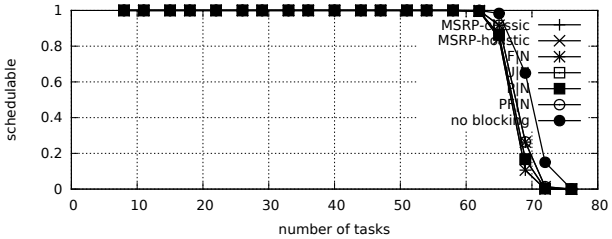

Fig. 850. Schedulability under non-preemptable spin locks for $m = 8$, $U = 0.1n$, 4 resources, $rsf = 0.4$, $N^{max} = 1$, and short critical sections. The schedulability of the considered preemptable lock types in this configuration is shown in Fig. 860.

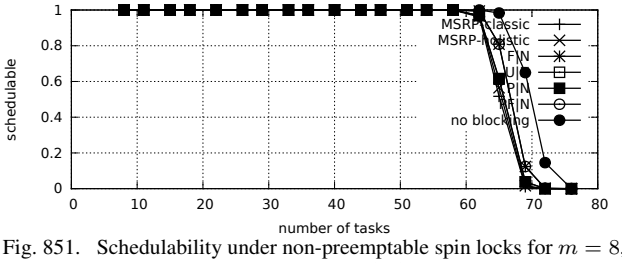

Fig. 851. Schedulability under non-preemptable spin locks for $m = 8$, $U = 0.1n$, 4 resources, $rsf = 0.4$, $N^{max} = 2$, and short critical sections. The schedulability of the considered preemptable lock types in this configuration is shown in Fig. 861.

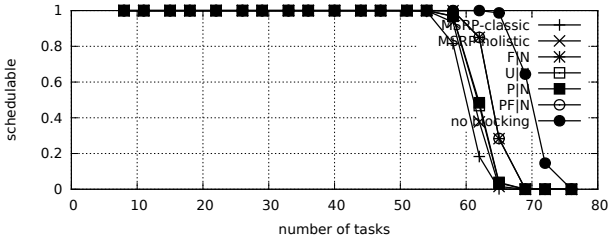

Fig. 852. Schedulability under non-preemptable spin locks for $m = 8$, $U = 0.1n$, 4 resources, $rsf = 0.4$, $N^{max} = 5$, and short critical sections. The schedulability of the considered preemptable lock types in this configuration is shown in Fig. 862.

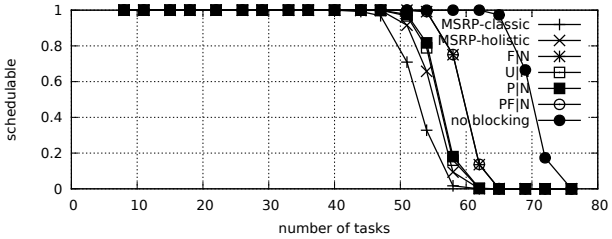

Fig. 853. Schedulability under non-preemptable spin locks for $m = 8$, $U = 0.1n$, 4 resources, $rsf = 0.4$, $N^{max} = 10$, and short critical sections. The schedulability of the considered preemptable lock types in this configuration is shown in Fig. 863.

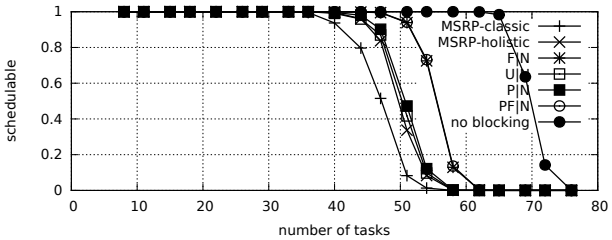

Fig. 854. Schedulability under non-preemptable spin locks for $m = 8$, $U = 0.1n$, 4 resources, $rsf = 0.4$, $N^{max} = 15$, and short critical sections. The schedulability of the considered preemptable lock types in this configuration is shown in Fig. 864.

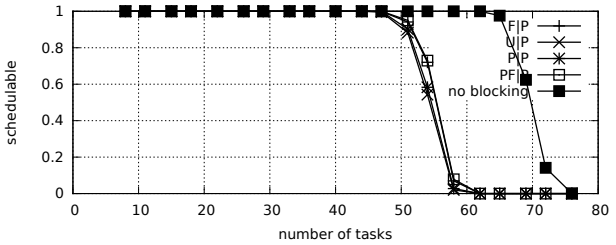

Fig. 855. Schedulability under preemptable spin locks for $m = 8$, $U = 0.1n$, 4 resources, $rsf = 0.4$, $N^{max} = 1$, and medium critical sections. The schedulability of the considered non-preemptable lock types in this configuration is shown in Fig. 845.

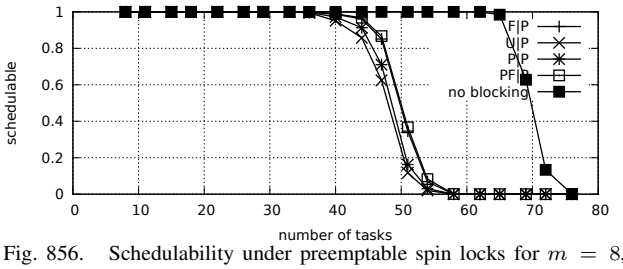

Fig. 856. Schedulability under preemptable spin locks for $m = 8$, $U = 0.1n$, 4 resources, $rsf = 0.4$, $N^{max} = 2$, and medium critical sections. The schedulability of the considered non-preemptable lock types in this configuration is shown in Fig. 846.

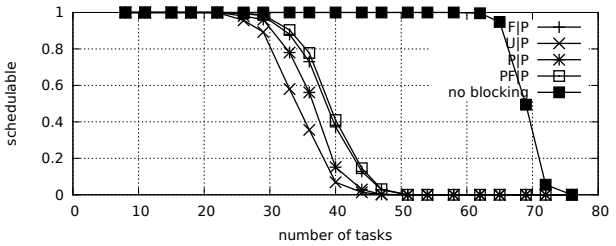

Fig. 857. Schedulability under preemptable spin locks for $m = 8$, $U = 0.1n$, 4 resources, $rsf = 0.4$, $N^{max} = 5$, and medium critical sections. The schedulability of the considered non-preemptable lock types in this configuration is shown in Fig. 847.

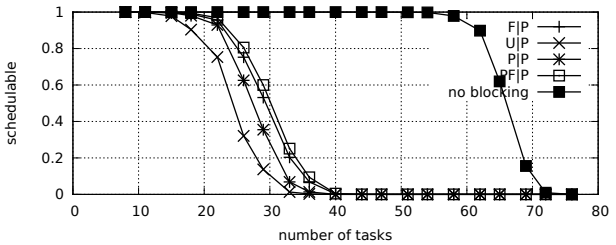

Fig. 858. Schedulability under preemptable spin locks for $m = 8$, $U = 0.1n$, 4 resources, $rsf = 0.4$, $N^{max} = 10$, and medium critical sections. The schedulability of the considered non-preemptable lock types in this configuration is shown in Fig. 848.

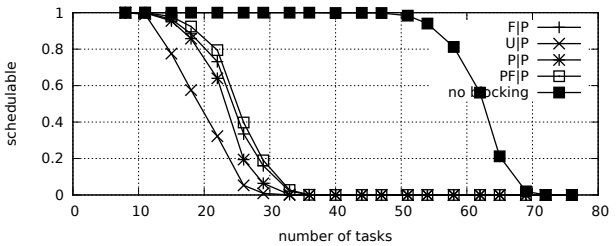

Fig. 859. Schedulability under preemptable spin locks for $m = 8$, $U = 0.1n$, 4 resources, $rsf = 0.4$, $N^{max} = 15$, and medium critical sections. The schedulability of the considered non-preemptable lock types in this configuration is shown in Fig. 849.

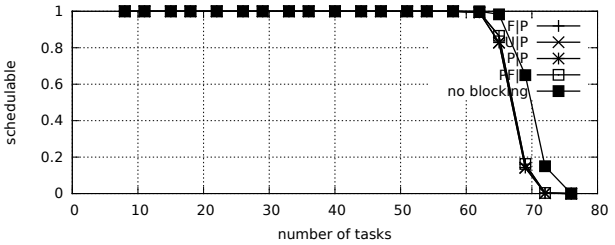

Fig. 860. Schedulability under preemptable spin locks for $m = 8$, $U = 0.1n$, 4 resources, $rsf = 0.4$, $N^{max} = 1$, and short critical sections. The schedulability of the considered non-preemptable lock types in this configuration is shown in Fig. 850.

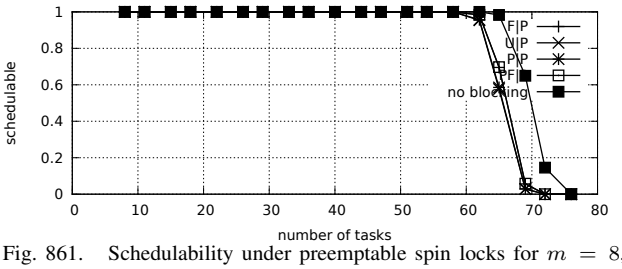

Fig. 861. Schedulability under preemptable spin locks for $m = 8$, $U = 0.1n$, 4 resources, $rsf = 0.4$, $N^{max} = 2$, and short critical sections. The schedulability of the considered non-preemptable lock types in this configuration is shown in Fig. 851.

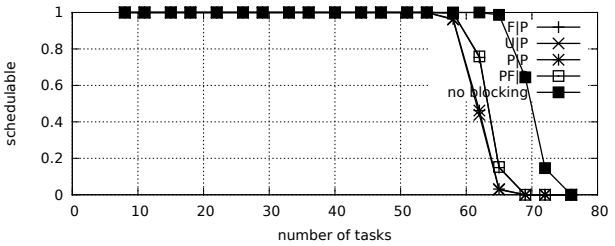

Fig. 862. Schedulability under preemptable spin locks for $m = 8$, $U = 0.1n$, 4 resources, $rsf = 0.4$, $N^{max} = 5$, and short critical sections. The schedulability of the considered non-preemptable lock types in this configuration is shown in Fig. 852.

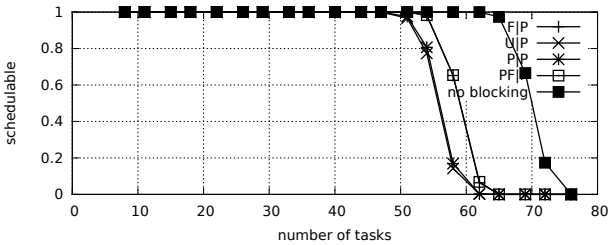

Fig. 863. Schedulability under preemptable spin locks for $m = 8$, $U = 0.1n$, 4 resources, $rsf = 0.4$, $N^{max} = 10$, and short critical sections. The schedulability of the considered non-preemptable lock types in this configuration is shown in Fig. 853.

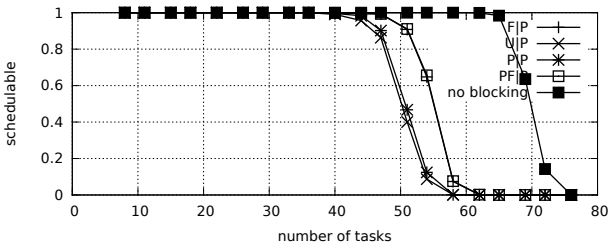

Fig. 864. Schedulability under preemptable spin locks for $m = 8$, $U = 0.1n$, 4 resources, $rsf = 0.4$, $N^{max} = 15$, and short critical sections. The schedulability of the considered non-preemptable lock types in this configuration is shown in Fig. 854.

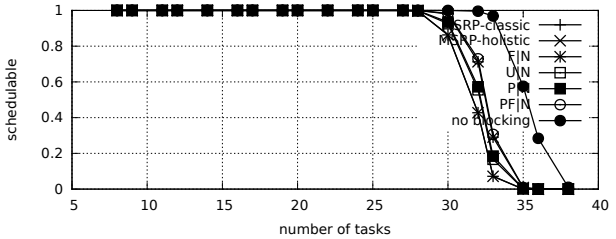

Fig. 865. Schedulability under non-preemptable spin locks for $m = 8$, $U = 0.2n$, 4 resources, $rsf = 0.4$, $N^{max} = 1$, and medium critical sections. The schedulability of the considered preemptable lock types in this configuration is shown in Fig. 875.

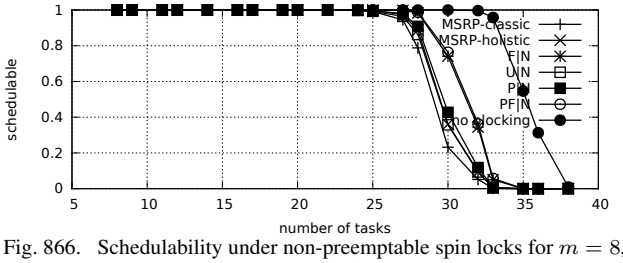

Fig. 866. Schedulability under non-preemptable spin locks for $m = 8$, $U = 0.2n$, 4 resources, $rsf = 0.4$, $N^{max} = 2$, and medium critical sections. The schedulability of the considered preemptable lock types in this configuration is shown in Fig. 876.

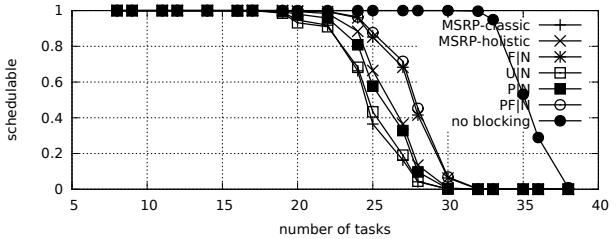

Fig. 867. Schedulability under non-preemptable spin locks for $m = 8$, $U = 0.2n$, 4 resources, $rsf = 0.4$, $N^{max} = 5$, and medium critical sections. The schedulability of the considered preemptable lock types in this configuration is shown in Fig. 877.

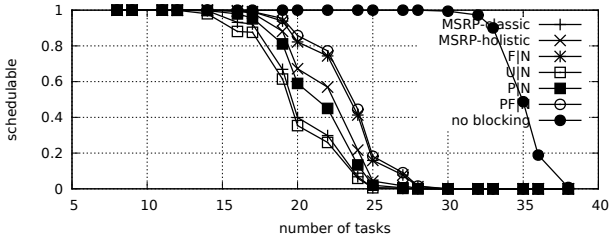

Fig. 868. Schedulability under non-preemptable spin locks for $m = 8$, $U = 0.2n$, 4 resources, $rsf = 0.4$, $N^{max} = 10$, and medium critical sections. The schedulability of the considered preemptable lock types in this configuration is shown in Fig. 878.

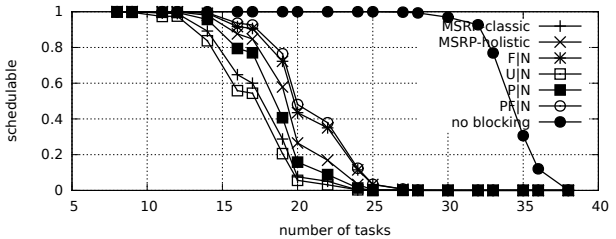

Fig. 869. Schedulability under non-preemptable spin locks for $m = 8$, $U = 0.2n$, 4 resources, $rsf = 0.4$, $N^{max} = 15$, and medium critical sections. The schedulability of the considered preemptable lock types in this configuration is shown in Fig. 879.

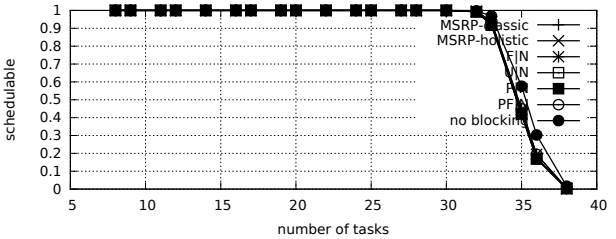

Fig. 870. Schedulability under non-preemptable spin locks for $m = 8$, $U = 0.2n$, 4 resources, $rsf = 0.4$, $N^{max} = 1$, and short critical sections. The schedulability of the considered preemptable lock types in this configuration is shown in Fig. 880.

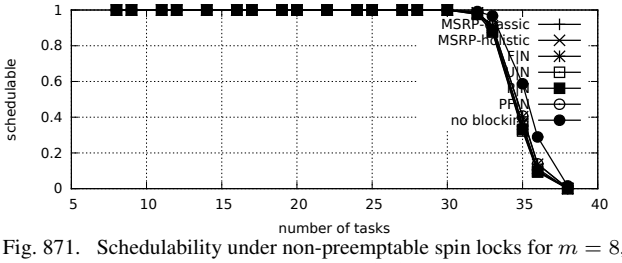

Fig. 871. Schedulability under non-preemptable spin locks for $m = 8$, $U = 0.2n$, 4 resources, $rsf = 0.4$, $N^{max} = 2$, and short critical sections. The schedulability of the considered preemptable lock types in this configuration is shown in Fig. 881.

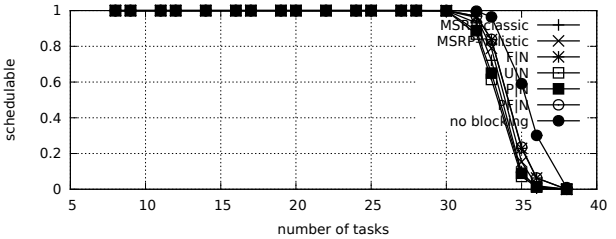

Fig. 872. Schedulability under non-preemptable spin locks for $m = 8$, $U = 0.2n$, 4 resources, $rsf = 0.4$, $N^{max} = 5$, and short critical sections. The schedulability of the considered preemptable lock types in this configuration is shown in Fig. 882.

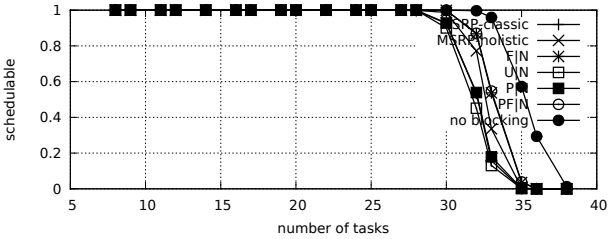

Fig. 873. Schedulability under non-preemptable spin locks for $m = 8$, $U = 0.2n$, 4 resources, $rsf = 0.4$, $N^{max} = 10$, and short critical sections. The schedulability of the considered preemptable lock types in this configuration is shown in Fig. 883.

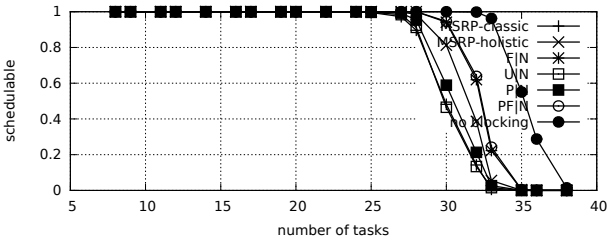

Fig. 874. Schedulability under non-preemptable spin locks for $m = 8$, $U = 0.2n$, 4 resources, $rsf = 0.4$, $N^{max} = 15$, and short critical sections. The schedulability of the considered preemptable lock types in this configuration is shown in Fig. 884.

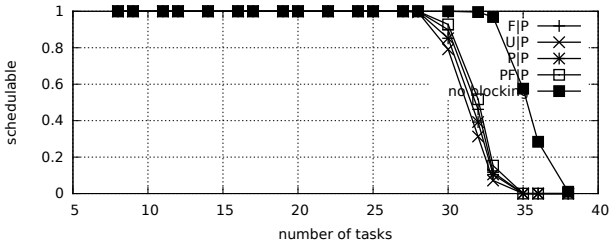

Fig. 875. Schedulability under preemptable spin locks for $m = 8$, $U = 0.2n$, 4 resources, $rsf = 0.4$, $N^{max} = 1$, and medium critical sections. The schedulability of the considered non-preemptable lock types in this configuration is shown in Fig. 865.

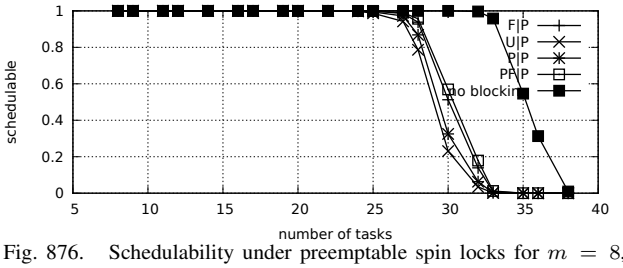

Fig. 876. Schedulability under preemptable spin locks for $m = 8$, $U = 0.2n$, 4 resources, $rsf = 0.4$, $N^{max} = 2$, and medium critical sections. The schedulability of the considered non-preemptable lock types in this configuration is shown in Fig. 866.

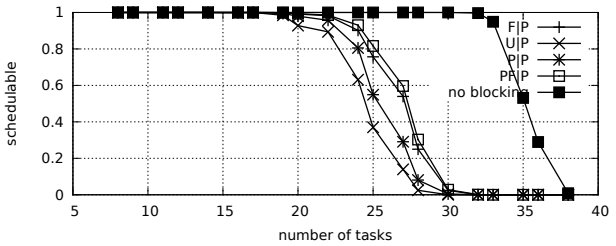

Fig. 877. Schedulability under preemptable spin locks for $m = 8$, $U = 0.2n$, 4 resources, $rsf = 0.4$, $N^{max} = 5$, and medium critical sections. The schedulability of the considered non-preemptable lock types in this configuration is shown in Fig. 867.

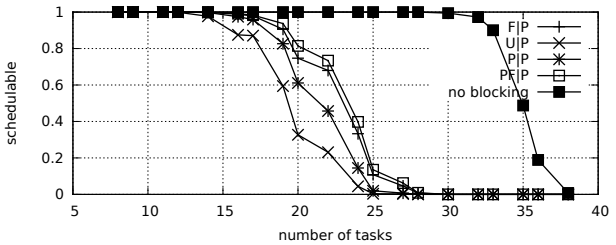

Fig. 878. Schedulability under preemptable spin locks for $m = 8$, $U = 0.2n$, 4 resources, $rsf = 0.4$, $N^{max} = 10$, and medium critical sections. The schedulability of the considered non-preemptable lock types in this configuration is shown in Fig. 868.

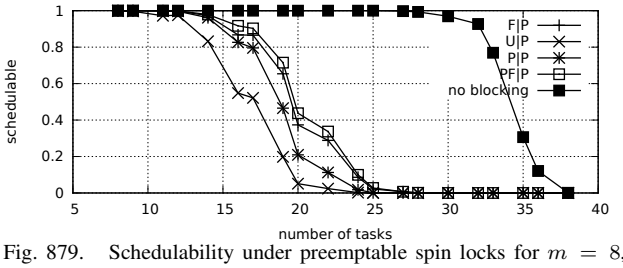

Fig. 879. Schedulability under preemptable spin locks for $m = 8$, $U = 0.2n$, 4 resources, $rsf = 0.4$, $N^{max} = 15$, and medium critical sections. The schedulability of the considered non-preemptable lock types in this configuration is shown in Fig. 869.

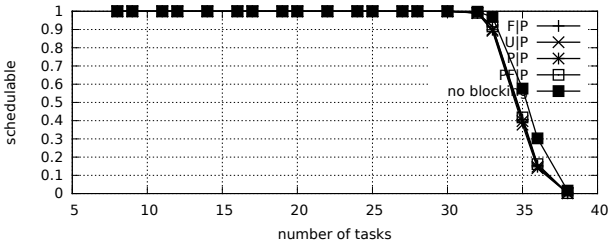

Fig. 880. Schedulability under preemptable spin locks for $m = 8$, $U = 0.2n$, 4 resources, $rsf = 0.4$, $N^{max} = 1$, and short critical sections. The schedulability of the considered non-preemptable lock types in this configuration is shown in Fig. 870.

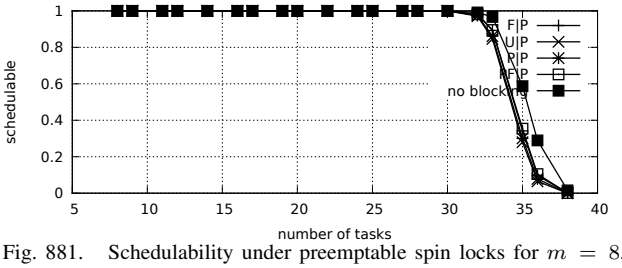

Fig. 881. Schedulability under preemptable spin locks for $m = 8$, $U = 0.2n$, 4 resources, $rsf = 0.4$, $N^{max} = 2$, and short critical sections. The schedulability of the considered non-preemptable lock types in this configuration is shown in Fig. 871.

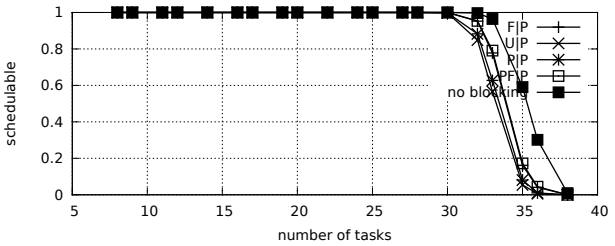

Fig. 882. Schedulability under preemptable spin locks for $m = 8$, $U = 0.2n$, 4 resources, $rsf = 0.4$, $N^{max} = 5$, and short critical sections. The schedulability of the considered non-preemptable lock types in this configuration is shown in Fig. 872.

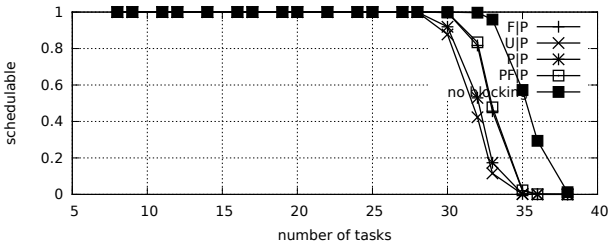

Fig. 883. Schedulability under preemptable spin locks for $m = 8$, $U = 0.2n$, 4 resources, $rsf = 0.4$, $N^{max} = 10$, and short critical sections. The schedulability of the considered non-preemptable lock types in this configuration is shown in Fig. 873.

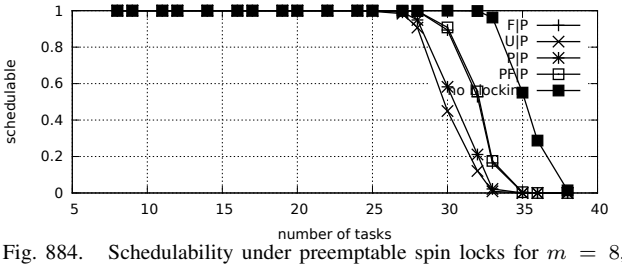

Fig. 884. Schedulability under preemptable spin locks for $m = 8$, $U = 0.2n$, 4 resources, $rsf = 0.4$, $N^{max} = 15$, and short critical sections. The schedulability of the considered non-preemptable lock types in this configuration is shown in Fig. 874.

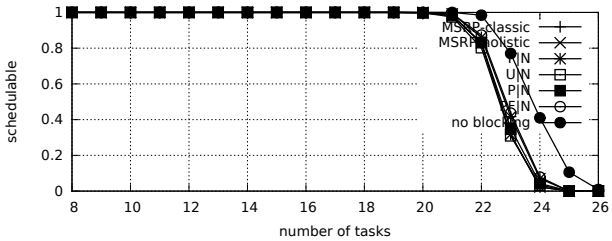

Fig. 885. Schedulability under non-preemptable spin locks for $m = 8$, $U = 0.3n$, 4 resources, $rsf = 0.4$, $N^{max} = 1$, and medium critical sections. The schedulability of the considered preemptable lock types in this configuration is shown in Fig. 895.

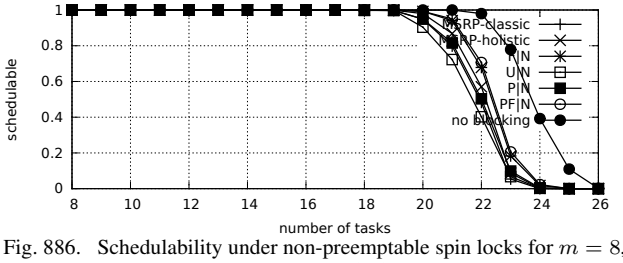

Fig. 886. Schedulability under non-preemptable spin locks for $m = 8$, $U = 0.3n$, 4 resources, $rsf = 0.4$, $N^{max} = 2$, and medium critical sections. The schedulability of the considered preemptable lock types in this configuration is shown in Fig. 896.

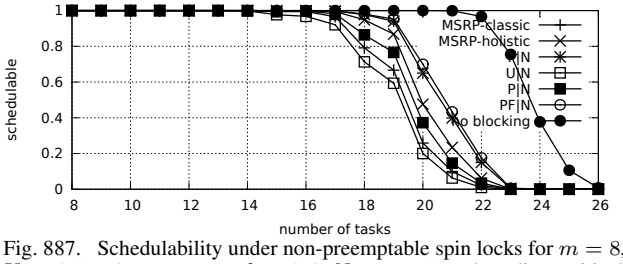

Fig. 887. Schedulability under non-preemptable spin locks for $m = 8$, $U = 0.3n$, 4 resources, $rsf = 0.4$, $N^{max} = 5$, and medium critical sections. The schedulability of the considered preemptable lock types in this configuration is shown in Fig. 897.

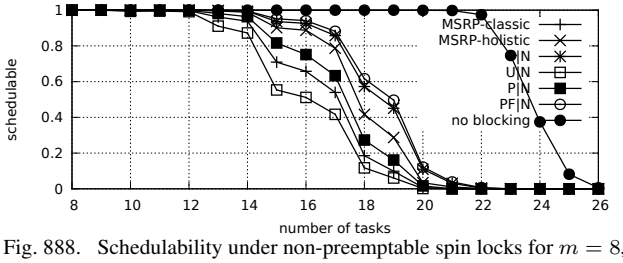

Fig. 888. Schedulability under non-preemptable spin locks for $m = 8$, $U = 0.3n$, 4 resources, $rsf = 0.4$, $N^{max} = 10$, and medium critical sections. The schedulability of the considered preemptable lock types in this configuration is shown in Fig. 898.

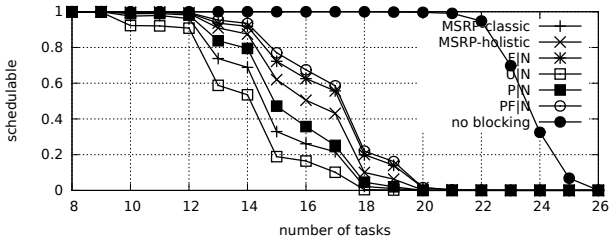

Fig. 889. Schedulability under non-preemptable spin locks for $m = 8$, $U = 0.3n$, 4 resources, $rsf = 0.4$, $N^{max} = 15$, and medium critical sections. The schedulability of the considered preemptable lock types in this configuration is shown in Fig. 899.

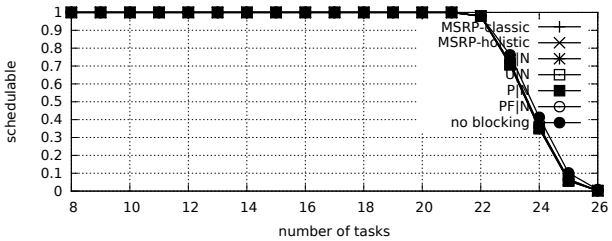

Fig. 890. Schedulability under non-preemptable spin locks for $m = 8$, $U = 0.3n$, 4 resources, $rsf = 0.4$, $N^{max} = 1$, and short critical sections. The schedulability of the considered preemptable lock types in this configuration is shown in Fig. 900.

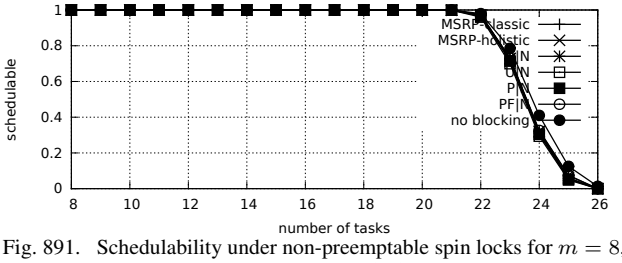

Fig. 891. Schedulability under non-preemptable spin locks for $m = 8$, $U = 0.3n$, 4 resources, $rsf = 0.4$, $N^{max} = 2$, and short critical sections. The schedulability of the considered preemptable lock types in this configuration is shown in Fig. 901.

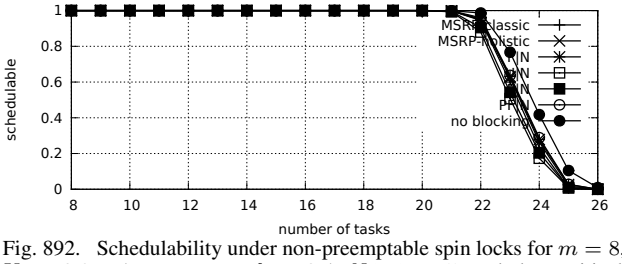

Fig. 892. Schedulability under non-preemptable spin locks for $m = 8$, $U = 0.3n$, 4 resources, $rsf = 0.4$, $N^{max} = 5$, and short critical sections. The schedulability of the considered preemptable lock types in this configuration is shown in Fig. 902.

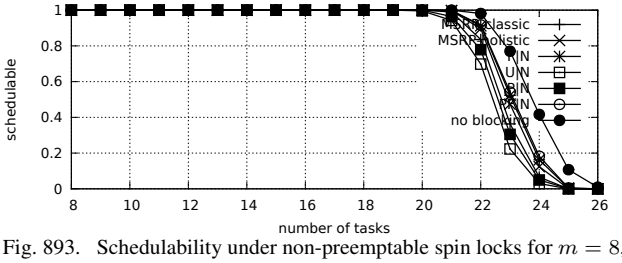

Fig. 893. Schedulability under non-preemptable spin locks for $m = 8$, $U = 0.3n$, 4 resources, $rsf = 0.4$, $N^{max} = 10$, and short critical sections. The schedulability of the considered preemptable lock types in this configuration is shown in Fig. 903.

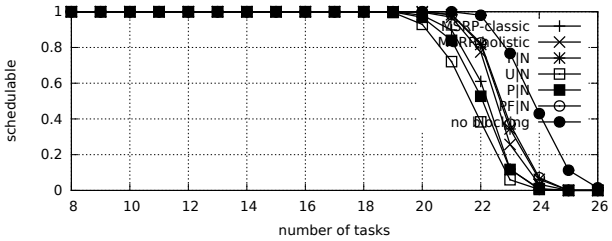

Fig. 894. Schedulability under non-preemptable spin locks for $m = 8$, $U = 0.3n$, 4 resources, $rsf = 0.4$, $N^{max} = 15$, and short critical sections. The schedulability of the considered preemptable lock types in this configuration is shown in Fig. 904.

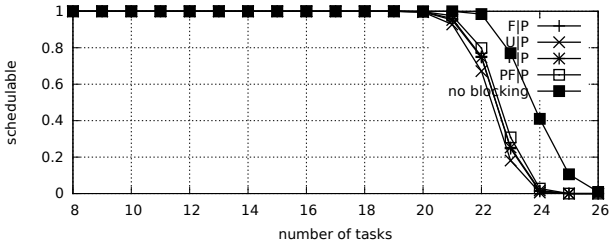

Fig. 895. Schedulability under preemptable spin locks for $m = 8$, $U = 0.3n$, 4 resources, $rsf = 0.4$, $N^{max} = 1$, and medium critical sections. The schedulability of the considered non-preemptable lock types in this configuration is shown in Fig. 885.

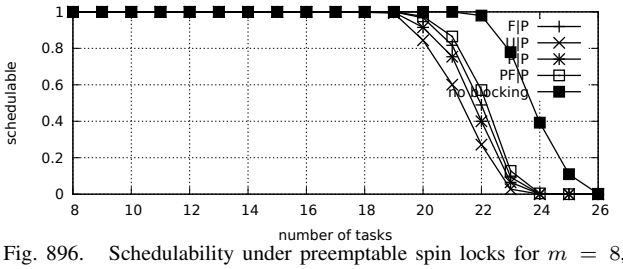

Fig. 896. Schedulability under preemptable spin locks for $m = 8$, $U = 0.3n$, 4 resources, $rsf = 0.4$, $N^{max} = 2$, and medium critical sections. The schedulability of the considered non-preemptable lock types in this configuration is shown in Fig. 886.

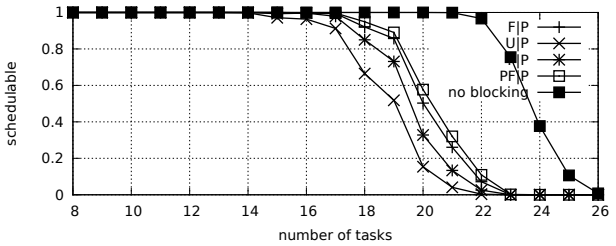

Fig. 897. Schedulability under preemptable spin locks for $m = 8$, $U = 0.3n$, 4 resources, $rsf = 0.4$, $N^{max} = 5$, and medium critical sections. The schedulability of the considered non-preemptable lock types in this configuration is shown in Fig. 887.

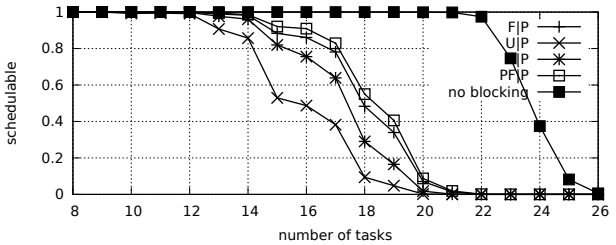

Fig. 898. Schedulability under preemptable spin locks for $m = 8$, $U = 0.3n$, 4 resources, $rsf = 0.4$, $N^{max} = 10$, and medium critical sections. The schedulability of the considered non-preemptable lock types in this configuration is shown in Fig. 888.

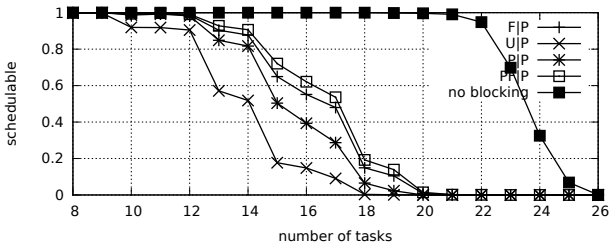

Fig. 899. Schedulability under preemptable spin locks for $m = 8$, $U = 0.3n$, 4 resources, $rsf = 0.4$, $N^{max} = 15$, and medium critical sections. The schedulability of the considered non-preemptable lock types in this configuration is shown in Fig. 889.

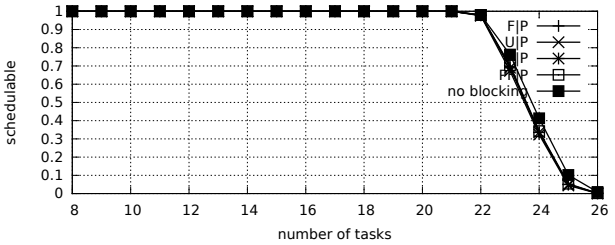

Fig. 900. Schedulability under preemptable spin locks for $m = 8$, $U = 0.3n$, 4 resources, $rsf = 0.4$, $N^{max} = 1$, and short critical sections. The schedulability of the considered non-preemptable lock types in this configuration is shown in Fig. 890.

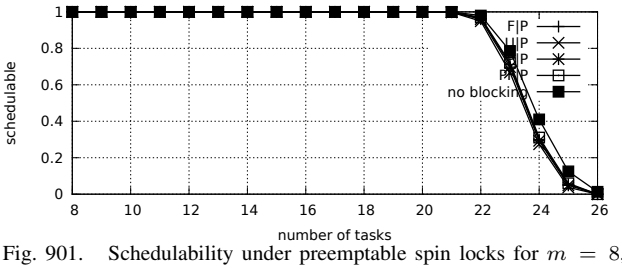

Fig. 901. Schedulability under preemptable spin locks for $m = 8$, $U = 0.3n$, 4 resources, $rsf = 0.4$, $N^{max} = 2$, and short critical sections. The schedulability of the considered non-preemptable lock types in this configuration is shown in Fig. 891.

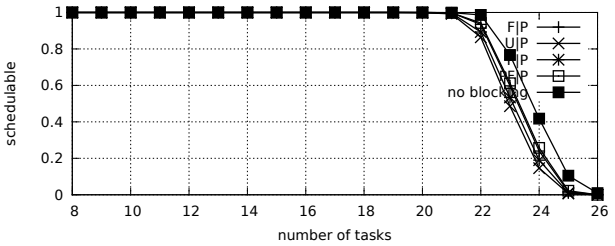

Fig. 902. Schedulability under preemptable spin locks for $m = 8$, $U = 0.3n$, 4 resources, $rsf = 0.4$, $N^{max} = 5$, and short critical sections. The schedulability of the considered non-preemptable lock types in this configuration is shown in Fig. 892.

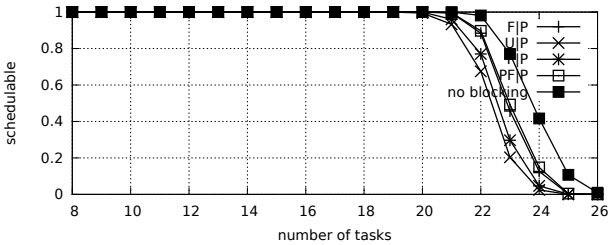

Fig. 903. Schedulability under preemptable spin locks for $m = 8$, $U = 0.3n$, 4 resources, $rsf = 0.4$, $N^{max} = 10$, and short critical sections. The schedulability of the considered non-preemptable lock types in this configuration is shown in Fig. 893.

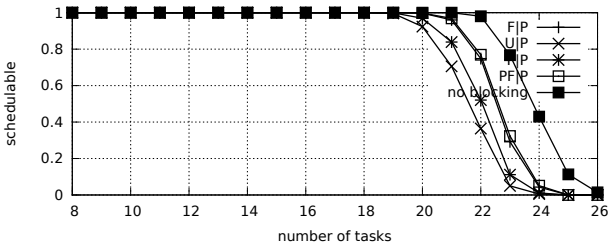

Fig. 904. Schedulability under preemptable spin locks for $m = 8$, $U = 0.3n$, 4 resources, $rsf = 0.4$, $N^{max} = 15$, and short critical sections. The schedulability of the considered non-preemptable lock types in this configuration is shown in Fig. 894.

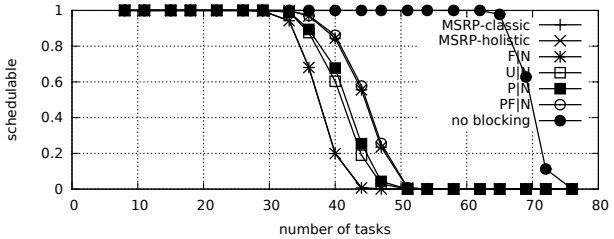

Fig. 905. Schedulability under non-preemptable spin locks for $m = 8$, $U = 0.1n$, 4 resources, $rsf = 0.75$, $N^{max} = 1$, and medium critical sections. The schedulability of the considered preemptable lock types in this configuration is shown in Fig. 915.

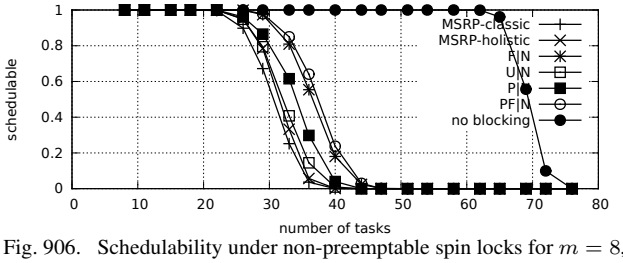

Fig. 906. Schedulability under non-preemptable spin locks for $m = 8$, $U = 0.1n$, 4 resources, $rsf = 0.75$, $N^{max} = 2$, and medium critical sections. The schedulability of the considered preemptable lock types in this configuration is shown in Fig. 916.

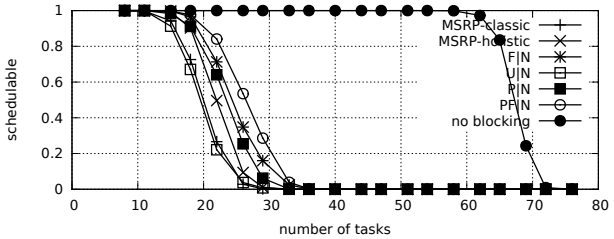

Fig. 907. Schedulability under non-preemptable spin locks for $m = 8$, $U = 0.1n$, 4 resources, $rsf = 0.75$, $N^{max} = 5$, and medium critical sections. The schedulability of the considered preemptable lock types in this configuration is shown in Fig. 917.

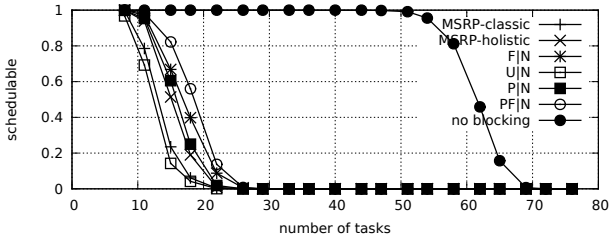

Fig. 908. Schedulability under non-preemptable spin locks for $m = 8$, $U = 0.1n$, 4 resources, $rsf = 0.75$, $N^{max} = 10$, and medium critical sections. The schedulability of the considered preemptable lock types in this configuration is shown in Fig. 918.

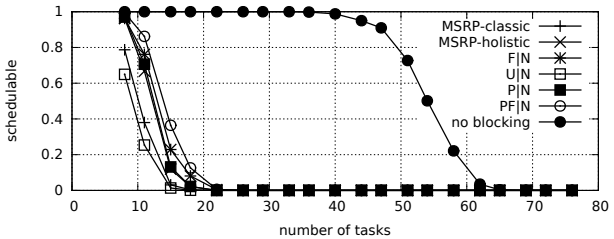

Fig. 909. Schedulability under non-preemptable spin locks for $m = 8$, $U = 0.1n$, 4 resources, $rsf = 0.75$, $N^{max} = 15$, and medium critical sections. The schedulability of the considered preemptable lock types in this configuration is shown in Fig. 919.

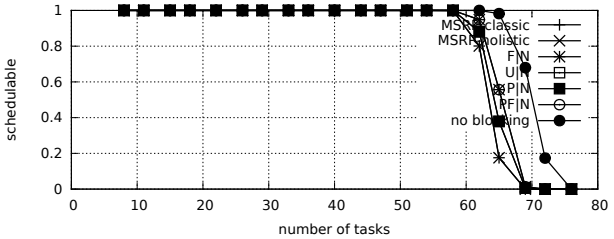

Fig. 910. Schedulability under non-preemptable spin locks for $m = 8$, $U = 0.1n$, 4 resources, $rsf = 0.75$, $N^{max} = 1$, and short critical sections. The schedulability of the considered preemptable lock types in this configuration is shown in Fig. 920.

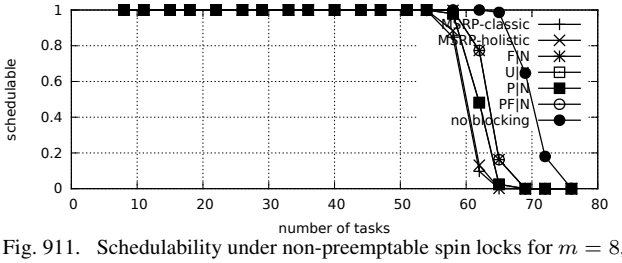

Fig. 911. Schedulability under non-preemptable spin locks for $m = 8$, $U = 0.1n$, 4 resources, $rsf = 0.75$, $N^{max} = 2$, and short critical sections. The schedulability of the considered preemptable lock types in this configuration is shown in Fig. 921.

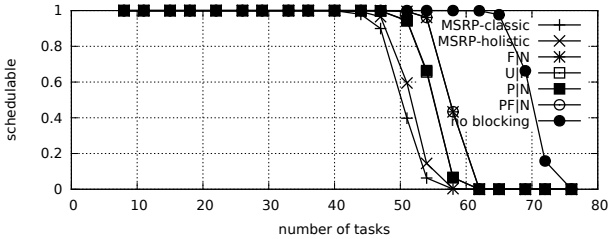

Fig. 912. Schedulability under non-preemptable spin locks for $m = 8$, $U = 0.1n$, 4 resources, $rsf = 0.75$, $N^{max} = 5$, and short critical sections. The schedulability of the considered preemptable lock types in this configuration is shown in Fig. 922.

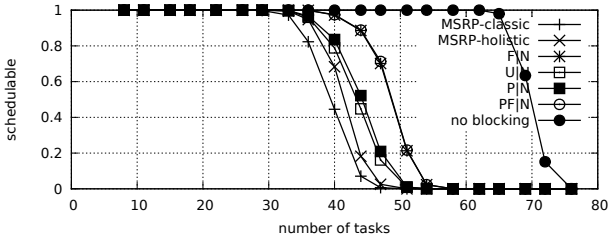

Fig. 913. Schedulability under non-preemptable spin locks for $m = 8$, $U = 0.1n$, 4 resources, $rsf = 0.75$, $N^{max} = 10$, and short critical sections. The schedulability of the considered preemptable lock types in this configuration is shown in Fig. 923.

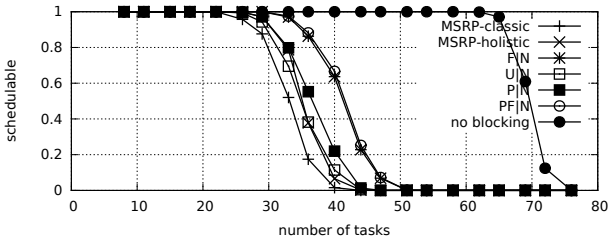

Fig. 914. Schedulability under non-preemptable spin locks for $m = 8$, $U = 0.1n$, 4 resources, $rsf = 0.75$, $N^{max} = 15$, and short critical sections. The schedulability of the considered preemptable lock types in this configuration is shown in Fig. 924.

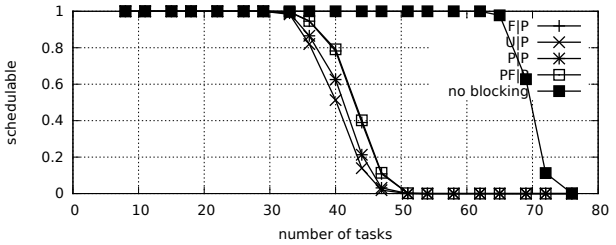

Fig. 915. Schedulability under preemptable spin locks for $m = 8$, $U = 0.1n$, 4 resources, $rsf = 0.75$, $N^{max} = 1$, and medium critical sections. The schedulability of the considered non-preemptable lock types in this configuration is shown in Fig. 905.

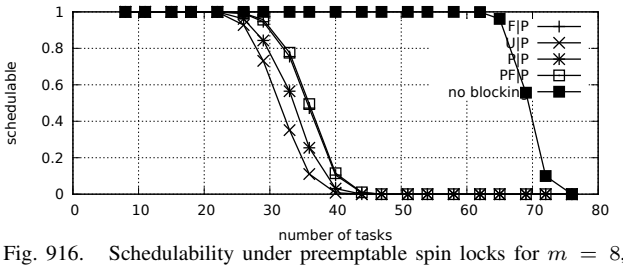

Fig. 916. Schedulability under preemptable spin locks for $m = 8$, $U = 0.1n$, 4 resources, $rsf = 0.75$, $N^{max} = 2$, and medium critical sections. The schedulability of the considered non-preemptable lock types in this configuration is shown in Fig. 906.

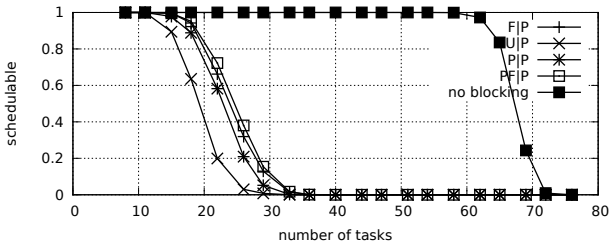

Fig. 917. Schedulability under preemptable spin locks for $m = 8$, $U = 0.1n$, 4 resources, $rsf = 0.75$, $N^{max} = 5$, and medium critical sections. The schedulability of the considered non-preemptable lock types in this configuration is shown in Fig. 907.

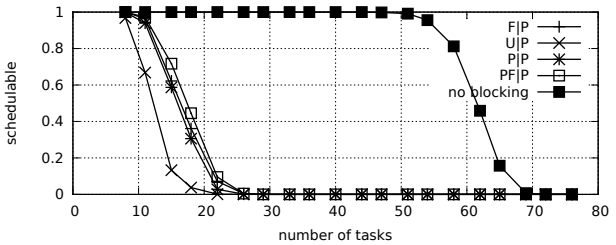

Fig. 918. Schedulability under preemptable spin locks for $m = 8$, $U = 0.1n$, 4 resources, $rsf = 0.75$, $N^{max} = 10$, and medium critical sections. The schedulability of the considered non-preemptable lock types in this configuration is shown in Fig. 908.

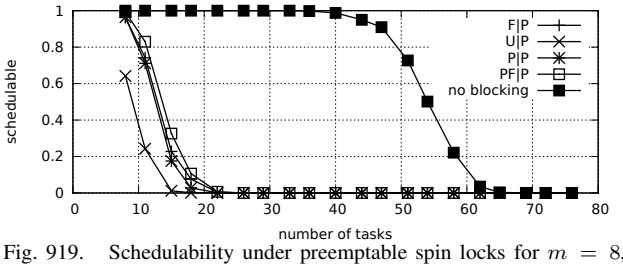

Fig. 919. Schedulability under preemptable spin locks for $m = 8$, $U = 0.1n$, 4 resources, $rsf = 0.75$, $N^{max} = 15$, and medium critical sections. The schedulability of the considered non-preemptable lock types in this configuration is shown in Fig. 909.

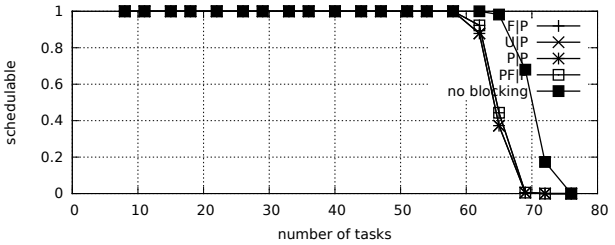

Fig. 920. Schedulability under preemptable spin locks for $m = 8$, $U = 0.1n$, 4 resources, $rsf = 0.75$, $N^{max} = 1$, and short critical sections. The schedulability of the considered non-preemptable lock types in this configuration is shown in Fig. 910.

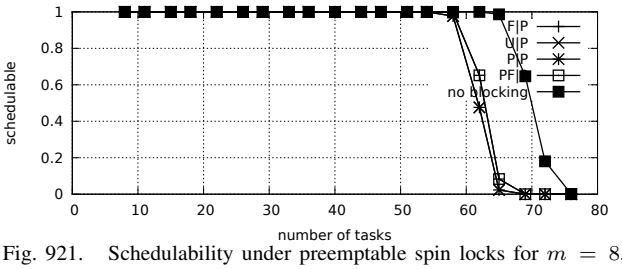

Fig. 921. Schedulability under preemptable spin locks for $m = 8$, $U = 0.1n$, 4 resources, $rsf = 0.75$, $N^{max} = 2$, and short critical sections. The schedulability of the considered non-preemptable lock types in this configuration is shown in Fig. 911.

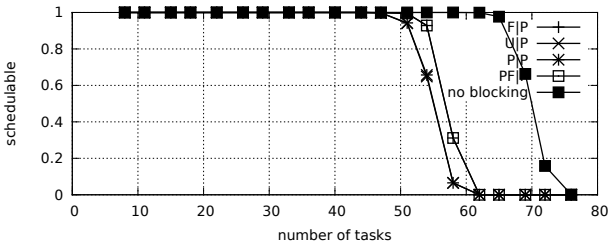

Fig. 922. Schedulability under preemptable spin locks for $m = 8$, $U = 0.1n$, 4 resources, $rsf = 0.75$, $N^{max} = 5$, and short critical sections. The schedulability of the considered non-preemptable lock types in this configuration is shown in Fig. 912.

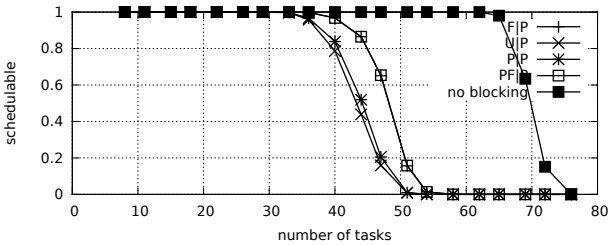

Fig. 923. Schedulability under preemptable spin locks for $m = 8$, $U = 0.1n$, 4 resources, $rsf = 0.75$, $N^{max} = 10$, and short critical sections. The schedulability of the considered non-preemptable lock types in this configuration is shown in Fig. 913.

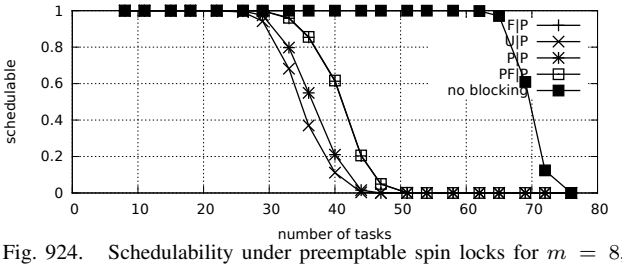

Fig. 924. Schedulability under preemptable spin locks for $m = 8$, $U = 0.1n$, 4 resources, $rsf = 0.75$, $N^{max} = 15$, and short critical sections. The schedulability of the considered non-preemptable lock types in this configuration is shown in Fig. 914.

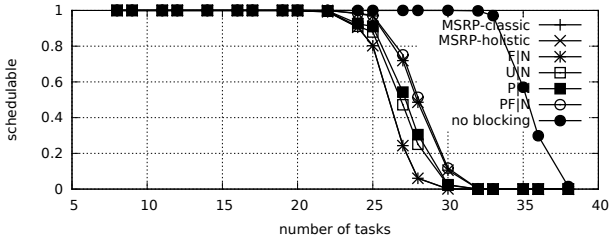

Fig. 925. Schedulability under non-preemptable spin locks for $m = 8$, $U = 0.2n$, 4 resources, $rsf = 0.75$, $N^{max} = 1$, and medium critical sections. The schedulability of the considered preemptable lock types in this configuration is shown in Fig. 935.

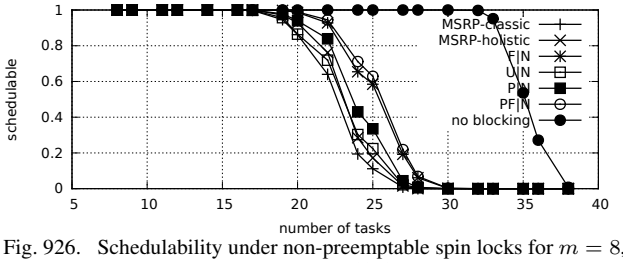

Fig. 926. Schedulability under non-preemptable spin locks for $m = 8$, $U = 0.2n$, 4 resources, $rsf = 0.75$, $N^{max} = 2$, and medium critical sections. The schedulability of the considered preemptable lock types in this configuration is shown in Fig. 936.

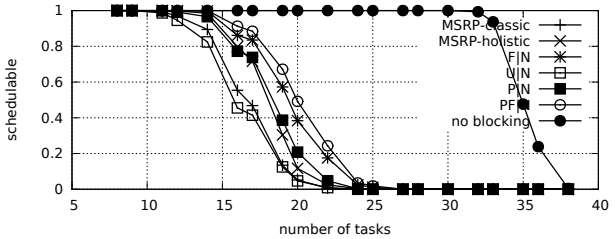

Fig. 927. Schedulability under non-preemptable spin locks for $m = 8$, $U = 0.2n$, 4 resources, $rsf = 0.75$, $N^{max} = 5$, and medium critical sections. The schedulability of the considered preemptable lock types in this configuration is shown in Fig. 937.

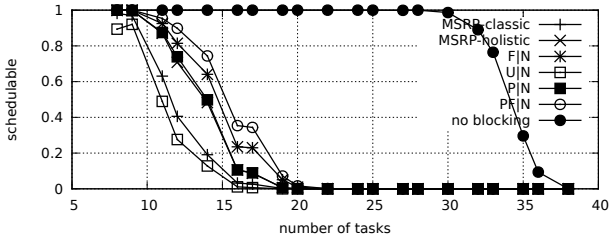

Fig. 928. Schedulability under non-preemptable spin locks for $m = 8$, $U = 0.2n$, 4 resources, $rsf = 0.75$, $N^{max} = 10$, and medium critical sections. The schedulability of the considered preemptable lock types in this configuration is shown in Fig. 938.

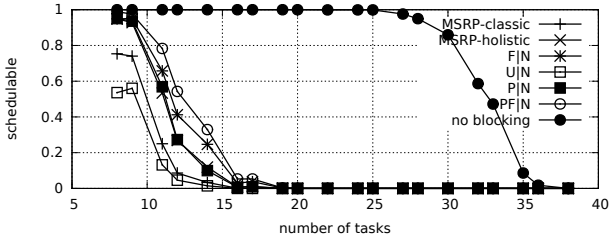

Fig. 929. Schedulability under non-preemptable spin locks for $m = 8$, $U = 0.2n$, 4 resources, $rsf = 0.75$, $N^{max} = 15$, and medium critical sections. The schedulability of the considered preemptable lock types in this configuration is shown in Fig. 939.

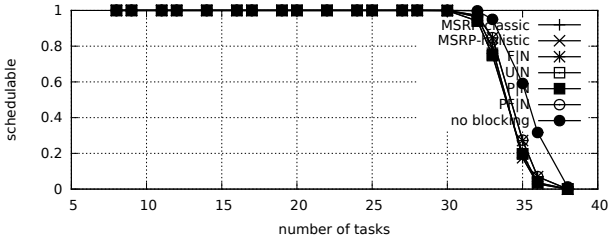

Fig. 930. Schedulability under non-preemptable spin locks for $m = 8$, $U = 0.2n$, 4 resources, $rsf = 0.75$, $N^{max} = 1$, and short critical sections. The schedulability of the considered preemptable lock types in this configuration is shown in Fig. 940.

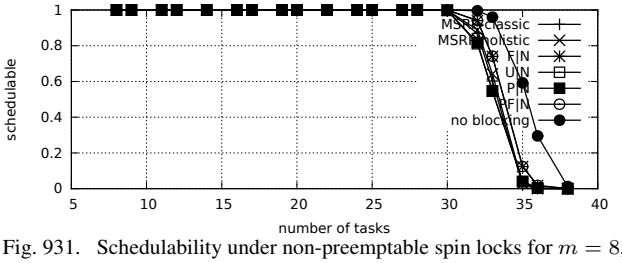

Fig. 931. Schedulability under non-preemptable spin locks for $m = 8$, $U = 0.2n$, 4 resources, $rsf = 0.75$, $N^{max} = 2$, and short critical sections. The schedulability of the considered preemptable lock types in this configuration is shown in Fig. 941.

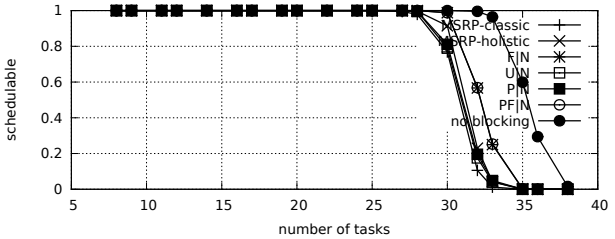

Fig. 932. Schedulability under non-preemptable spin locks for $m = 8$, $U = 0.2n$, 4 resources, $rsf = 0.75$, $N^{max} = 5$, and short critical sections. The schedulability of the considered preemptable lock types in this configuration is shown in Fig. 942.

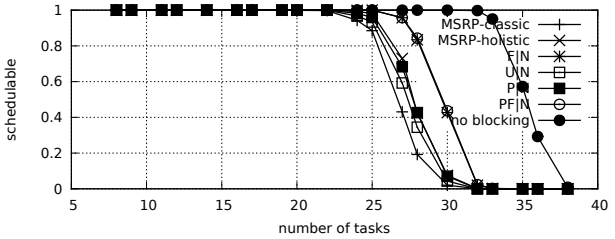

Fig. 933. Schedulability under non-preemptable spin locks for $m = 8$, $U = 0.2n$, 4 resources, $rsf = 0.75$, $N^{max} = 10$, and short critical sections. The schedulability of the considered preemptable lock types in this configuration is shown in Fig. 943.

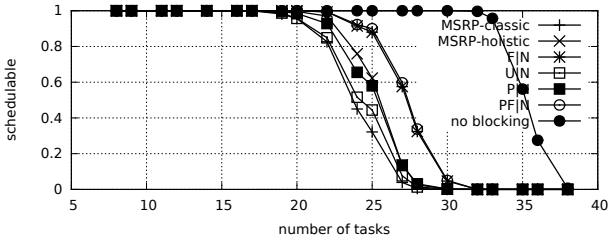

Fig. 934. Schedulability under non-preemptable spin locks for $m = 8$, $U = 0.2n$, 4 resources, $rsf = 0.75$, $N^{max} = 15$, and short critical sections. The schedulability of the considered preemptable lock types in this configuration is shown in Fig. 944.

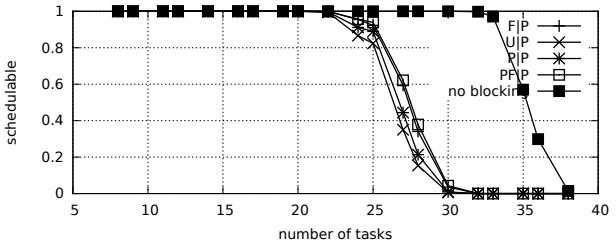

Fig. 935. Schedulability under preemptable spin locks for $m = 8$, $U = 0.2n$, 4 resources, $rsf = 0.75$, $N^{max} = 1$, and medium critical sections. The schedulability of the considered non-preemptable lock types in this configuration is shown in Fig. 925.

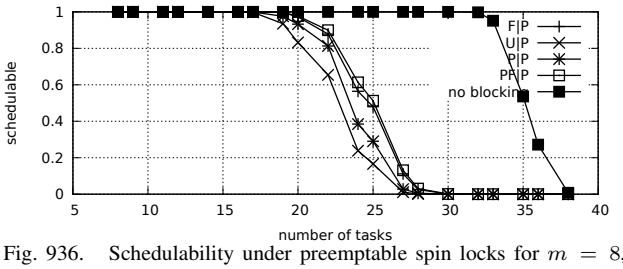

Fig. 936. Schedulability under preemptable spin locks for $m = 8$, $U = 0.2n$, 4 resources, $rsf = 0.75$, $N^{max} = 2$, and medium critical sections. The schedulability of the considered non-preemptable lock types in this configuration is shown in Fig. 926.

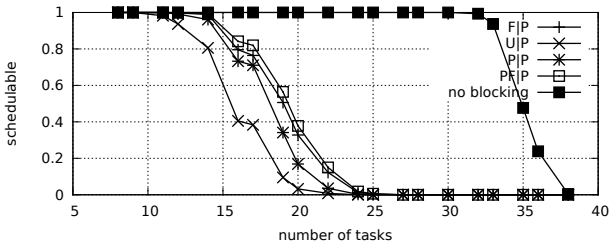

Fig. 937. Schedulability under preemptable spin locks for $m = 8$, $U = 0.2n$, 4 resources, $rsf = 0.75$, $N^{max} = 5$, and medium critical sections. The schedulability of the considered non-preemptable lock types in this configuration is shown in Fig. 927.

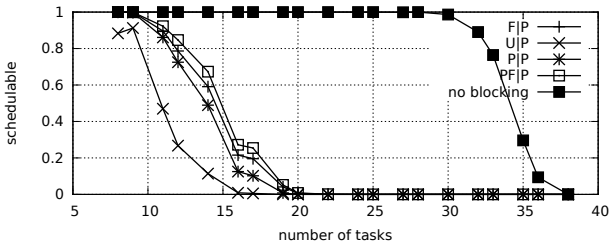

Fig. 938. Schedulability under preemptable spin locks for $m = 8$, $U = 0.2n$, 4 resources, $rsf = 0.75$, $N^{max} = 10$, and medium critical sections. The schedulability of the considered non-preemptable lock types in this configuration is shown in Fig. 928.

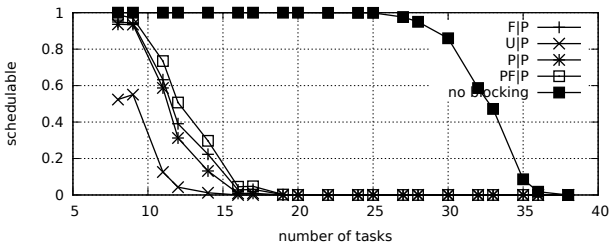

Fig. 939. Schedulability under preemptable spin locks for $m = 8$, $U = 0.2n$, 4 resources, $rsf = 0.75$, $N^{max} = 15$, and medium critical sections. The schedulability of the considered non-preemptable lock types in this configuration is shown in Fig. 929.

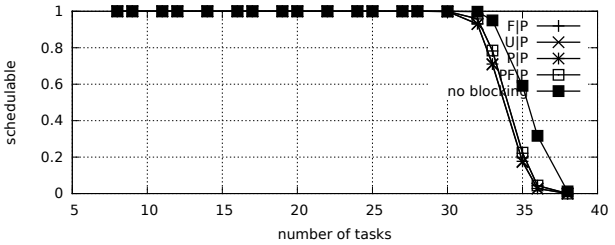

Fig. 940. Schedulability under preemptable spin locks for $m = 8$, $U = 0.2n$, 4 resources, $rsf = 0.75$, $N^{max} = 1$, and short critical sections. The schedulability of the considered non-preemptable lock types in this configuration is shown in Fig. 930.

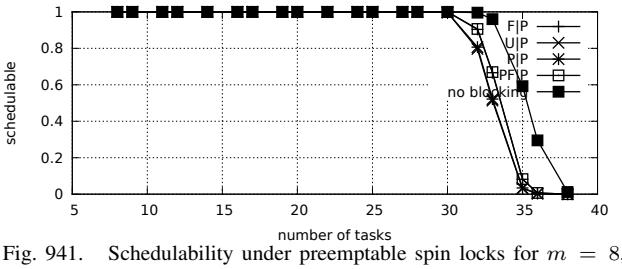

Fig. 941. Schedulability under preemptable spin locks for $m = 8$, $U = 0.2n$, 4 resources, $rsf = 0.75$, $N^{max} = 2$, and short critical sections. The schedulability of the considered non-preemptable lock types in this configuration is shown in Fig. 931.

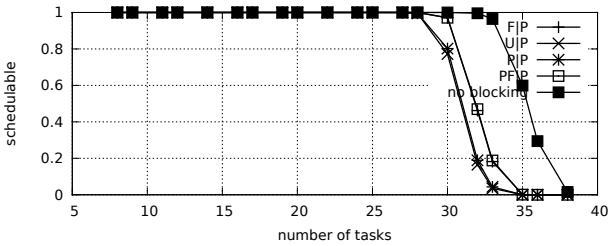

Fig. 942. Schedulability under preemptable spin locks for $m = 8$, $U = 0.2n$, 4 resources, $rsf = 0.75$, $N^{max} = 5$, and short critical sections. The schedulability of the considered non-preemptable lock types in this configuration is shown in Fig. 932.

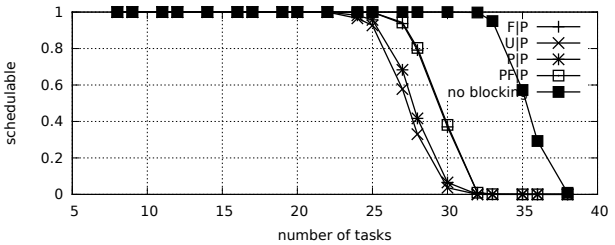

Fig. 943. Schedulability under preemptable spin locks for $m = 8$, $U = 0.2n$, 4 resources, $rsf = 0.75$, $N^{max} = 10$, and short critical sections. The schedulability of the considered non-preemptable lock types in this configuration is shown in Fig. 933.

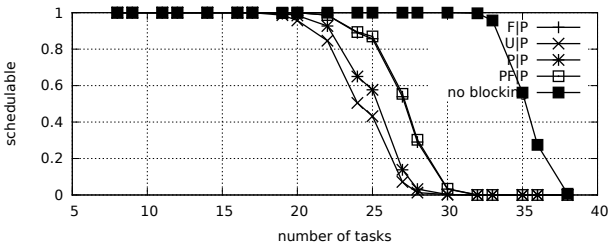

Fig. 944. Schedulability under preemptable spin locks for $m = 8$, $U = 0.2n$, 4 resources, $rsf = 0.75$, $N^{max} = 15$, and short critical sections. The schedulability of the considered non-preemptable lock types in this configuration is shown in Fig. 934.

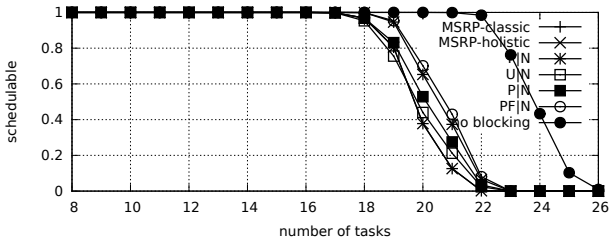

Fig. 945. Schedulability under non-preemptable spin locks for $m = 8$, $U = 0.3n$, 4 resources, $rsf = 0.75$, $N^{max} = 1$, and medium critical sections. The schedulability of the considered preemptable lock types in this configuration is shown in Fig. 955.

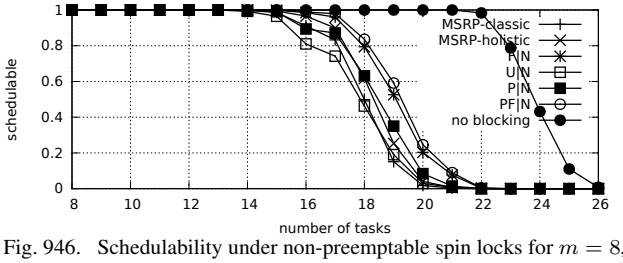

Fig. 946. Schedulability under non-preemptable spin locks for $m = 8$, $U = 0.3n$, 4 resources, $rsf = 0.75$, $N^{max} = 2$, and medium critical sections. The schedulability of the considered preemptable lock types in this configuration is shown in Fig. 956.

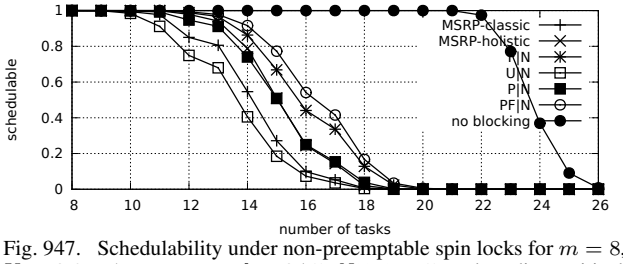

Fig. 947. Schedulability under non-preemptable spin locks for $m = 8$, $U = 0.3n$, 4 resources, $rsf = 0.75$, $N^{max} = 5$, and medium critical sections. The schedulability of the considered preemptable lock types in this configuration is shown in Fig. 957.

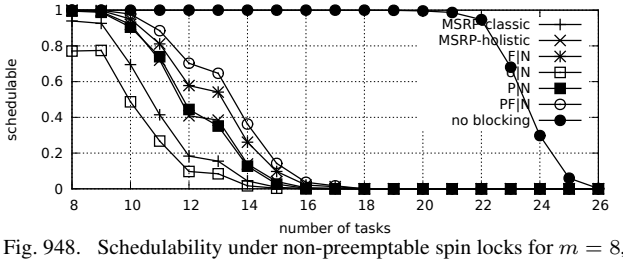

Fig. 948. Schedulability under non-preemptable spin locks for $m = 8$, $U = 0.3n$, 4 resources, $rsf = 0.75$, $N^{max} = 10$, and medium critical sections. The schedulability of the considered preemptable lock types in this configuration is shown in Fig. 958.

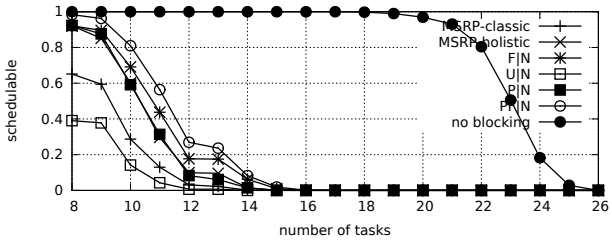

Fig. 949. Schedulability under non-preemptable spin locks for $m = 8$, $U = 0.3n$, 4 resources, $rsf = 0.75$, $N^{max} = 15$, and medium critical sections. The schedulability of the considered preemptable lock types in this configuration is shown in Fig. 959.

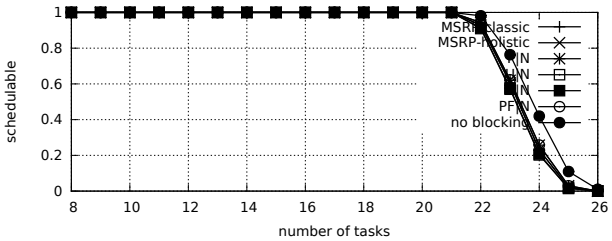

Fig. 950. Schedulability under non-preemptable spin locks for $m = 8$, $U = 0.3n$, 4 resources, $rsf = 0.75$, $N^{max} = 1$, and short critical sections. The schedulability of the considered preemptable lock types in this configuration is shown in Fig. 960.

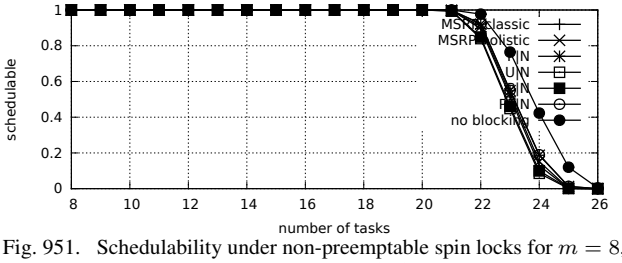

Fig. 951. Schedulability under non-preemptable spin locks for $m = 8$, $U = 0.3n$, 4 resources, $rsf = 0.75$, $N^{max} = 2$, and short critical sections. The schedulability of the considered preemptable lock types in this configuration is shown in Fig. 961.

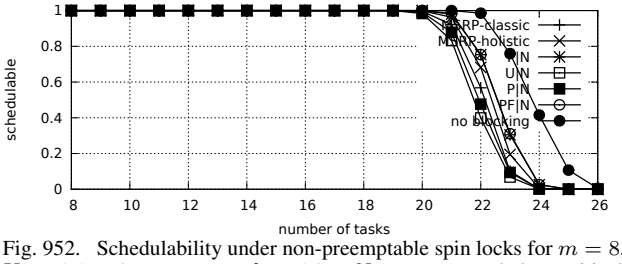

Fig. 952. Schedulability under non-preemptable spin locks for $m = 8$, $U = 0.3n$, 4 resources, $rsf = 0.75$, $N^{max} = 5$, and short critical sections. The schedulability of the considered preemptable lock types in this configuration is shown in Fig. 962.

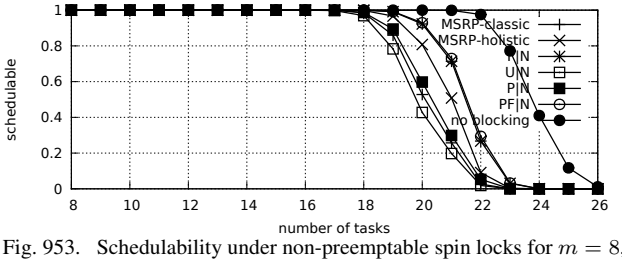

Fig. 953. Schedulability under non-preemptable spin locks for $m = 8$, $U = 0.3n$, 4 resources, $rsf = 0.75$, $N^{max} = 10$, and short critical sections. The schedulability of the considered preemptable lock types in this configuration is shown in Fig. 963.

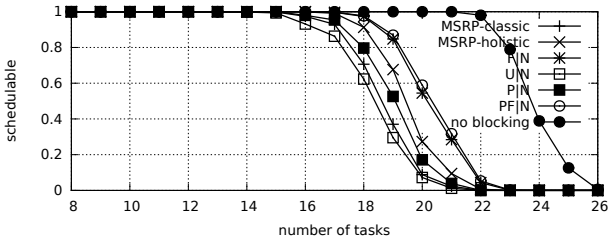

Fig. 954. Schedulability under non-preemptable spin locks for $m = 8$, $U = 0.3n$, 4 resources, $rsf = 0.75$, $N^{max} = 15$, and short critical sections. The schedulability of the considered preemptable lock types in this configuration is shown in Fig. 964.

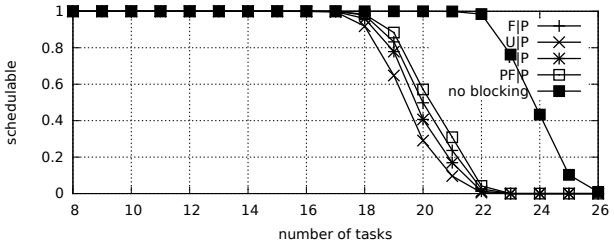

Fig. 955. Schedulability under preemptable spin locks for $m = 8$, $U = 0.3n$, 4 resources, $rsf = 0.75$, $N^{max} = 1$, and medium critical sections. The schedulability of the considered non-preemptable lock types in this configuration is shown in Fig. 945.

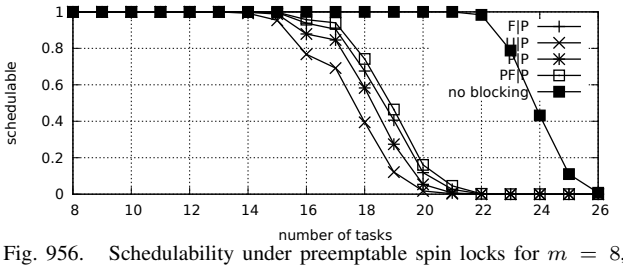

Fig. 956. Schedulability under preemptable spin locks for $m = 8$, $U = 0.3n$, 4 resources, $rsf = 0.75$, $N^{max} = 2$, and medium critical sections. The schedulability of the considered non-preemptable lock types in this configuration is shown in Fig. 946.

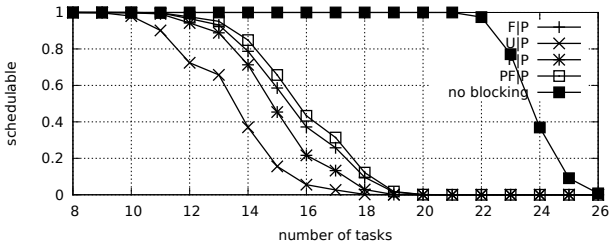

Fig. 957. Schedulability under preemptable spin locks for $m = 8$, $U = 0.3n$, 4 resources, $rsf = 0.75$, $N^{max} = 5$, and medium critical sections. The schedulability of the considered non-preemptable lock types in this configuration is shown in Fig. 947.

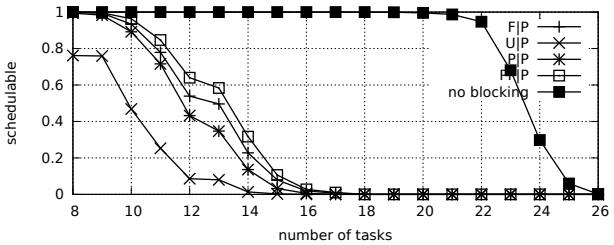

Fig. 958. Schedulability under preemptable spin locks for $m = 8$, $U = 0.3n$, 4 resources, $rsf = 0.75$, $N^{max} = 10$, and medium critical sections. The schedulability of the considered non-preemptable lock types in this configuration is shown in Fig. 948.

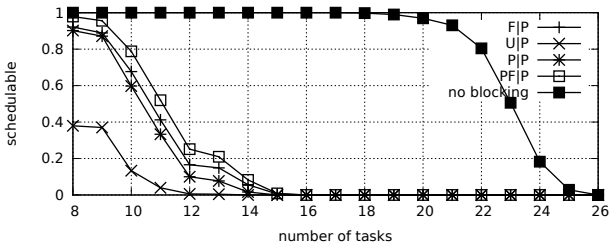

Fig. 959. Schedulability under preemptable spin locks for $m = 8$, $U = 0.3n$, 4 resources, $rsf = 0.75$, $N^{max} = 15$, and medium critical sections. The schedulability of the considered non-preemptable lock types in this configuration is shown in Fig. 949.

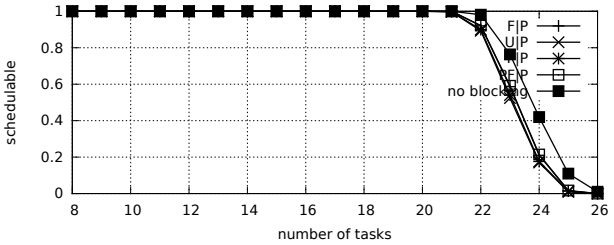

Fig. 960. Schedulability under preemptable spin locks for $m = 8$, $U = 0.3n$, 4 resources, $rsf = 0.75$, $N^{max} = 1$, and short critical sections. The schedulability of the considered non-preemptable lock types in this configuration is shown in Fig. 950.

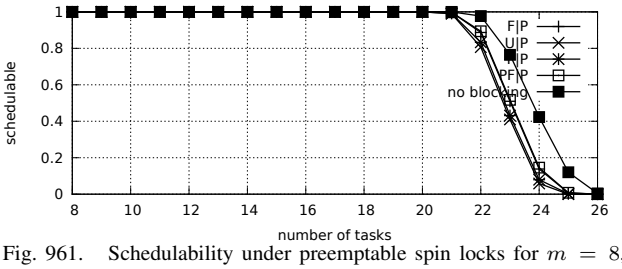

Fig. 961. Schedulability under preemptable spin locks for $m = 8$, $U = 0.3n$, 4 resources, $rsf = 0.75$, $N^{max} = 2$, and short critical sections. The schedulability of the considered non-preemptable lock types in this configuration is shown in Fig. 951.

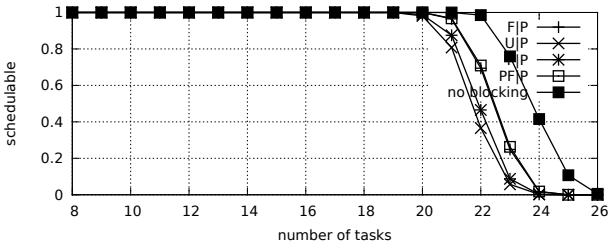

Fig. 962. Schedulability under preemptable spin locks for $m = 8$, $U = 0.3n$, 4 resources, $rsf = 0.75$, $N^{max} = 5$, and short critical sections. The schedulability of the considered non-preemptable lock types in this configuration is shown in Fig. 952.

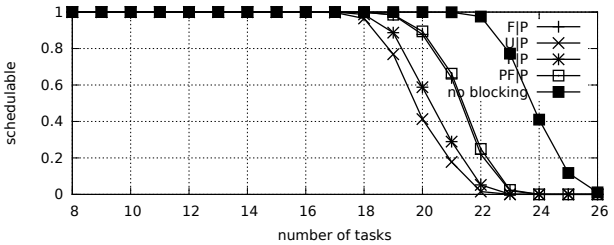

Fig. 963. Schedulability under preemptable spin locks for $m = 8$, $U = 0.3n$, 4 resources, $rsf = 0.75$, $N^{max} = 10$, and short critical sections. The schedulability of the considered non-preemptable lock types in this configuration is shown in Fig. 953.

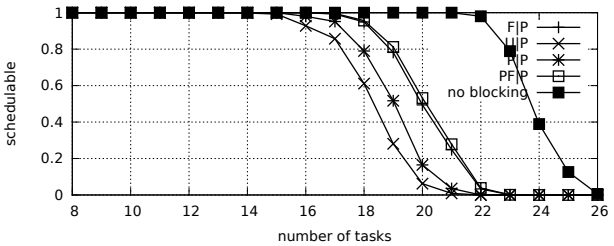

Fig. 964. Schedulability under preemptable spin locks for $m = 8$, $U = 0.3n$, 4 resources, $rsf = 0.75$, $N^{max} = 15$, and short critical sections. The schedulability of the considered non-preemptable lock types in this configuration is shown in Fig. 954.

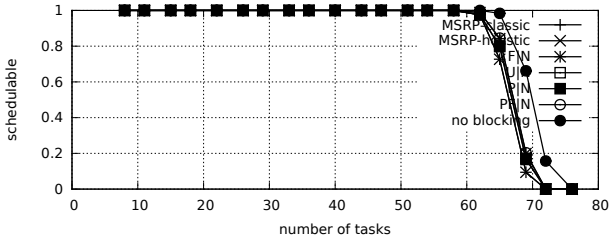

Fig. 965. Schedulability under non-preemptable spin locks for $m = 8$, $U = 0.1n$, 8 resources, $rsf = 0.1$, $N^{max} = 1$, and medium critical sections. The schedulability of the considered preemptable lock types in this configuration is shown in Fig. 975.

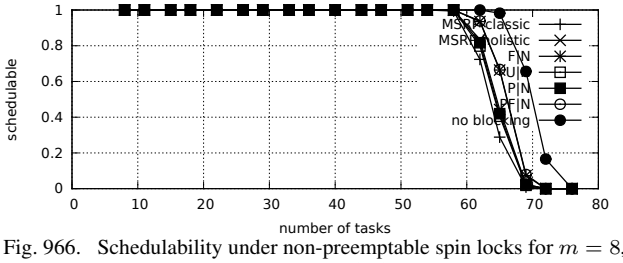

Fig. 966. Schedulability under non-preemptable spin locks for $m = 8$, $U = 0.1n$, 8 resources, $rsf = 0.1$, $N^{max} = 2$, and medium critical sections. The schedulability of the considered preemptable lock types in this configuration is shown in Fig. 976.

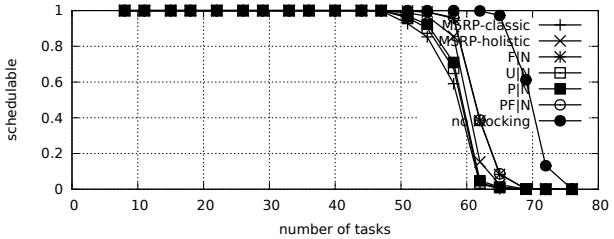

Fig. 967. Schedulability under non-preemptable spin locks for $m = 8$, $U = 0.1n$, 8 resources, $rsf = 0.1$, $N^{max} = 5$, and medium critical sections. The schedulability of the considered preemptable lock types in this configuration is shown in Fig. 977.

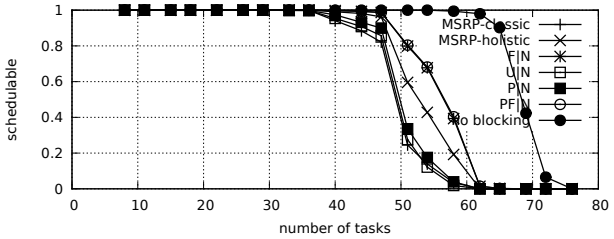

Fig. 968. Schedulability under non-preemptable spin locks for $m = 8$, $U = 0.1n$, 8 resources, $rsf = 0.1$, $N^{max} = 10$, and medium critical sections. The schedulability of the considered preemptable lock types in this configuration is shown in Fig. 978.

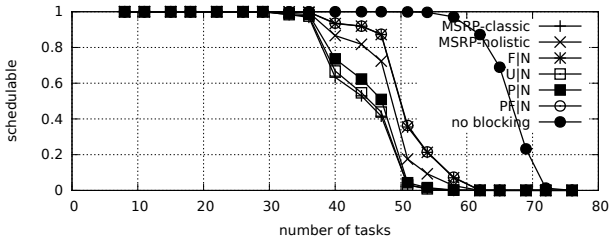

Fig. 969. Schedulability under non-preemptable spin locks for $m = 8$, $U = 0.1n$, 8 resources, $rsf = 0.1$, $N^{max} = 15$, and medium critical sections. The schedulability of the considered preemptable lock types in this configuration is shown in Fig. 979.

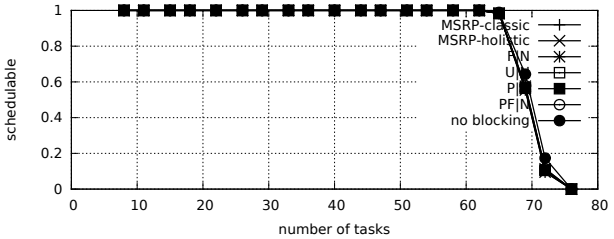

Fig. 970. Schedulability under non-preemptable spin locks for $m = 8$, $U = 0.1n$, 8 resources, $rsf = 0.1$, $N^{max} = 1$, and short critical sections. The schedulability of the considered preemptable lock types in this configuration is shown in Fig. 980.

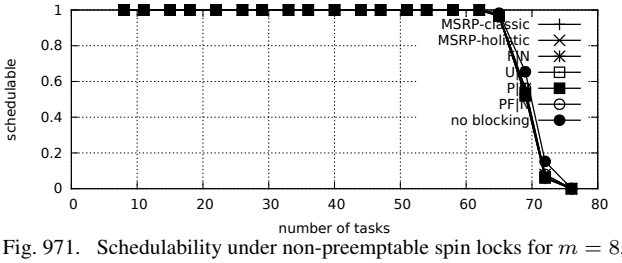

Fig. 971. Schedulability under non-preemptable spin locks for $m = 8$, $U = 0.1n$, 8 resources, $rsf = 0.1$, $N^{max} = 2$, and short critical sections. The schedulability of the considered preemptable lock types in this configuration is shown in Fig. 981.

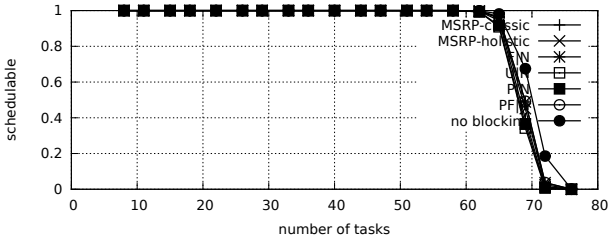

Fig. 972. Schedulability under non-preemptable spin locks for $m = 8$, $U = 0.1n$, 8 resources, $rsf = 0.1$, $N^{max} = 5$, and short critical sections. The schedulability of the considered preemptable lock types in this configuration is shown in Fig. 982.

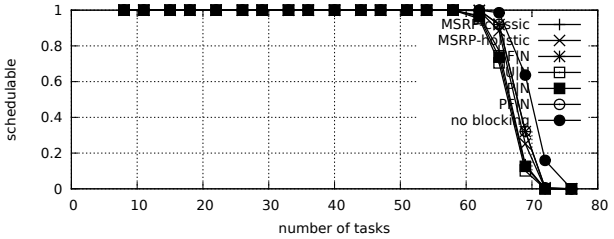

Fig. 973. Schedulability under non-preemptable spin locks for $m = 8$, $U = 0.1n$, 8 resources, $rsf = 0.1$, $N^{max} = 10$, and short critical sections. The schedulability of the considered preemptable lock types in this configuration is shown in Fig. 983.

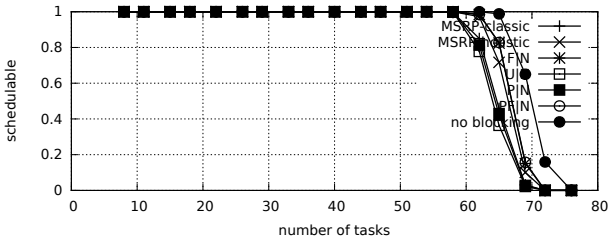

Fig. 974. Schedulability under non-preemptable spin locks for $m = 8$, $U = 0.1n$, 8 resources, $rsf = 0.1$, $N^{max} = 15$, and short critical sections. The schedulability of the considered preemptable lock types in this configuration is shown in Fig. 984.

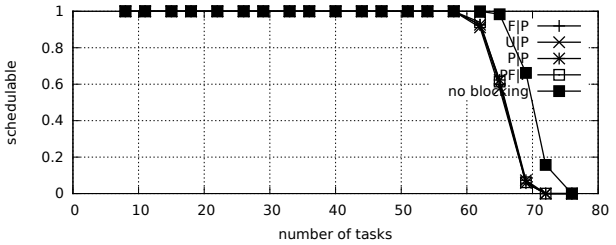

Fig. 975. Schedulability under preemptable spin locks for $m = 8$, $U = 0.1n$, 8 resources, $rsf = 0.1$, $N^{max} = 1$, and medium critical sections. The schedulability of the considered non-preemptable lock types in this configuration is shown in Fig. 965.

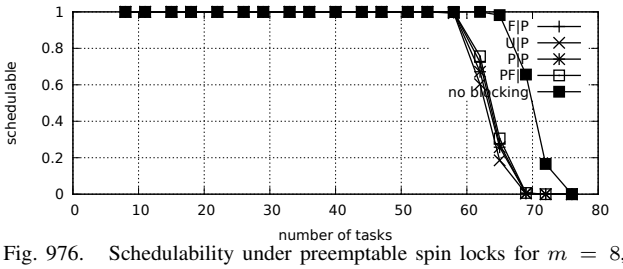

Fig. 976. Schedulability under preemptable spin locks for $m = 8$, $U = 0.1n$, 8 resources, $rsf = 0.1$, $N^{max} = 2$, and medium critical sections. The schedulability of the considered non-preemptable lock types in this configuration is shown in Fig. 966.

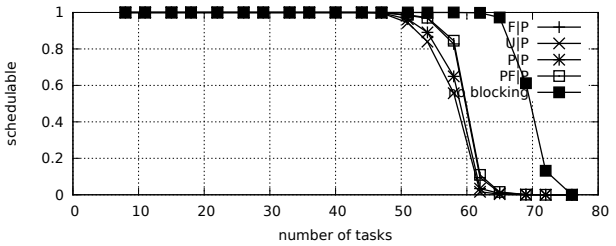

Fig. 977. Schedulability under preemptable spin locks for $m = 8$, $U = 0.1n$, 8 resources, $rsf = 0.1$, $N^{max} = 5$, and medium critical sections. The schedulability of the considered non-preemptable lock types in this configuration is shown in Fig. 967.

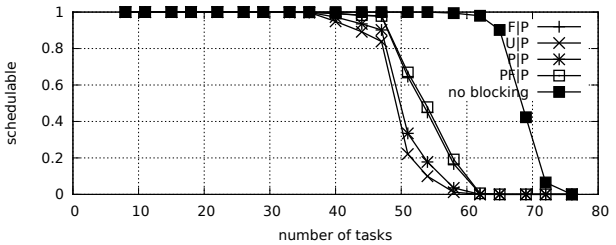

Fig. 978. Schedulability under preemptable spin locks for $m = 8$, $U = 0.1n$, 8 resources, $rsf = 0.1$, $N^{max} = 10$, and medium critical sections. The schedulability of the considered non-preemptable lock types in this configuration is shown in Fig. 968.

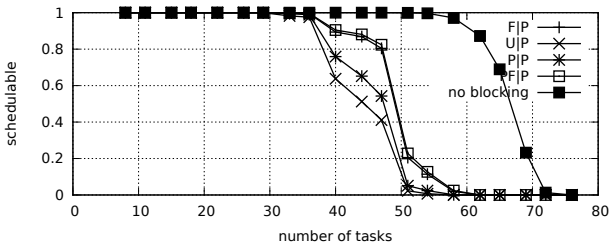

Fig. 979. Schedulability under preemptable spin locks for $m = 8$, $U = 0.1n$, 8 resources, $rsf = 0.1$, $N^{max} = 15$, and medium critical sections. The schedulability of the considered non-preemptable lock types in this configuration is shown in Fig. 969.

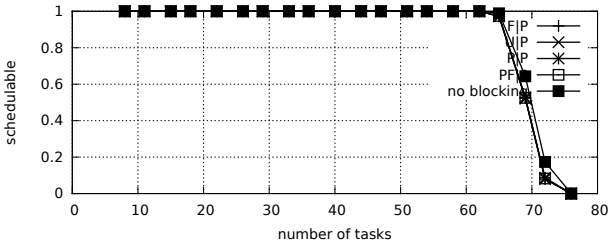

Fig. 980. Schedulability under preemptable spin locks for $m = 8$, $U = 0.1n$, 8 resources, $rsf = 0.1$, $N^{max} = 1$, and short critical sections. The schedulability of the considered non-preemptable lock types in this configuration is shown in Fig. 970.

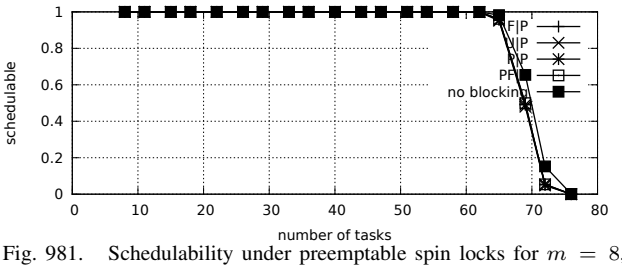

Fig. 981. Schedulability under preemptable spin locks for $m = 8$, $U = 0.1n$, 8 resources, $rsf = 0.1$, $N^{max} = 2$, and short critical sections. The schedulability of the considered non-preemptable lock types in this configuration is shown in Fig. 971.

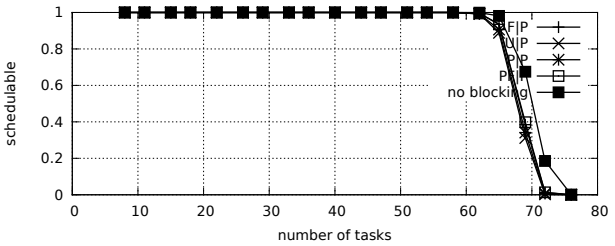

Fig. 982. Schedulability under preemptable spin locks for $m = 8$, $U = 0.1n$, 8 resources, $rsf = 0.1$, $N^{max} = 5$, and short critical sections. The schedulability of the considered non-preemptable lock types in this configuration is shown in Fig. 972.

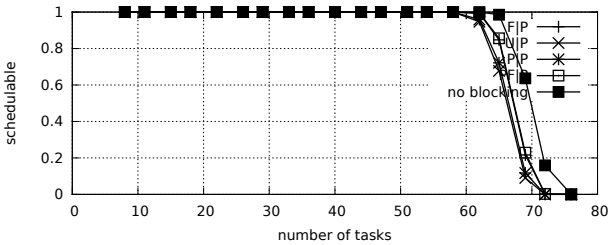

Fig. 983. Schedulability under preemptable spin locks for $m = 8$, $U = 0.1n$, 8 resources, $rsf = 0.1$, $N^{max} = 10$, and short critical sections. The schedulability of the considered non-preemptable lock types in this configuration is shown in Fig. 973.

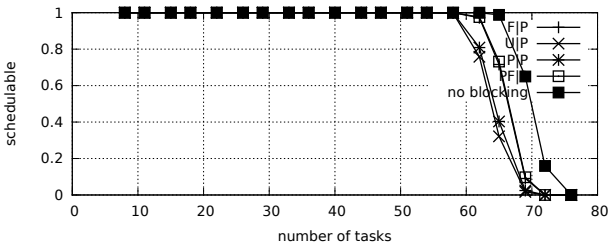

Fig. 984. Schedulability under preemptable spin locks for $m = 8$, $U = 0.1n$, 8 resources, $rsf = 0.1$, $N^{max} = 15$, and short critical sections. The schedulability of the considered non-preemptable lock types in this configuration is shown in Fig. 974.

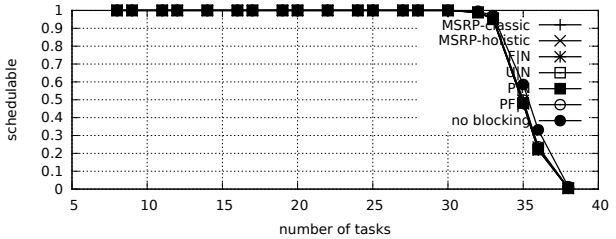

Fig. 985. Schedulability under non-preemptable spin locks for $m = 8$, $U = 0.2n$, 8 resources, $rsf = 0.1$, $N^{max} = 1$, and medium critical sections. The schedulability of the considered preemptable lock types in this configuration is shown in Fig. 995.

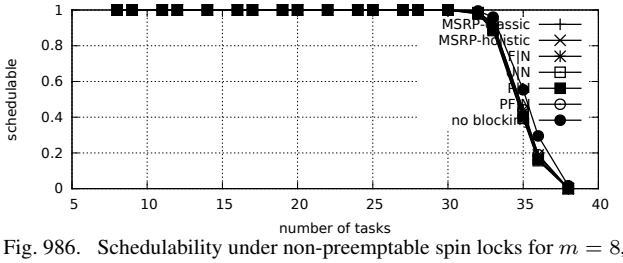

Fig. 986. Schedulability under non-preemptable spin locks for $m = 8$, $U = 0.2n$, 8 resources, $rsf = 0.1$, $N^{max} = 2$, and medium critical sections. The schedulability of the considered preemptable lock types in this configuration is shown in Fig. 996.

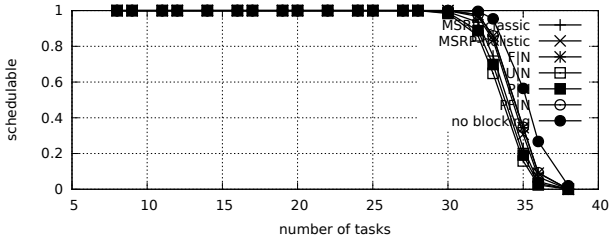

Fig. 987. Schedulability under non-preemptable spin locks for $m = 8$, $U = 0.2n$, 8 resources, $rsf = 0.1$, $N^{max} = 5$, and medium critical sections. The schedulability of the considered preemptable lock types in this configuration is shown in Fig. 997.

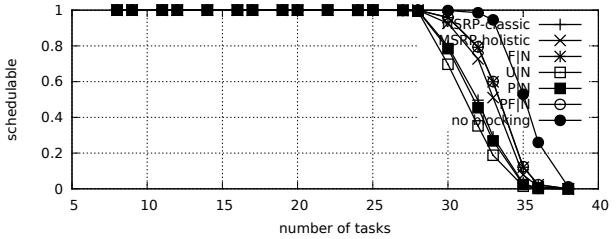

Fig. 988. Schedulability under non-preemptable spin locks for $m = 8$, $U = 0.2n$, 8 resources, $rsf = 0.1$, $N^{max} = 10$, and medium critical sections. The schedulability of the considered preemptable lock types in this configuration is shown in Fig. 998.

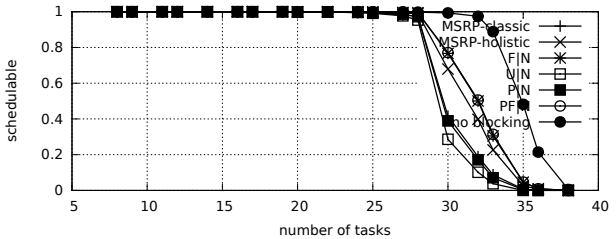

Fig. 989. Schedulability under non-preemptable spin locks for $m = 8$, $U = 0.2n$, 8 resources, $rsf = 0.1$, $N^{max} = 15$, and medium critical sections. The schedulability of the considered preemptable lock types in this configuration is shown in Fig. 999.

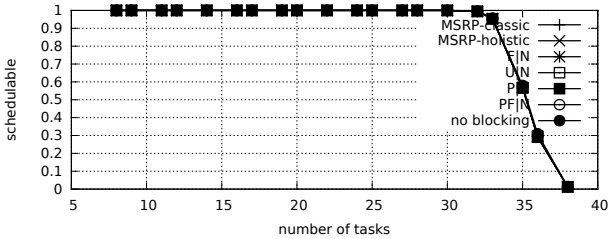

Fig. 990. Schedulability under non-preemptable spin locks for $m = 8$, $U = 0.2n$, 8 resources, $rsf = 0.1$, $N^{max} = 1$, and short critical sections. The schedulability of the considered preemptable lock types in this configuration is shown in Fig. 1000.

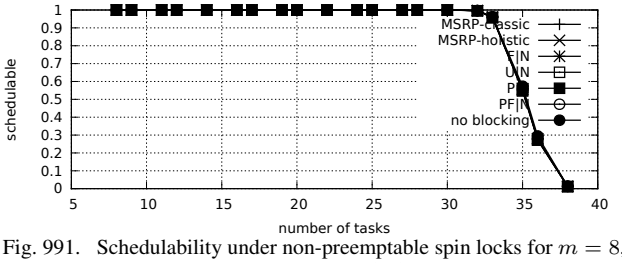

Fig. 991. Schedulability under non-preemptable spin locks for $m = 8$, $U = 0.2n$, 8 resources, $rsf = 0.1$, $N^{max} = 2$, and short critical sections. The schedulability of the considered preemptable lock types in this configuration is shown in Fig. 1001.

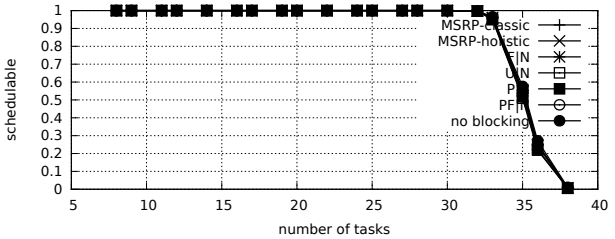

Fig. 992. Schedulability under non-preemptable spin locks for $m = 8$, $U = 0.2n$, 8 resources, $rsf = 0.1$, $N^{max} = 5$, and short critical sections. The schedulability of the considered preemptable lock types in this configuration is shown in Fig. 1002.

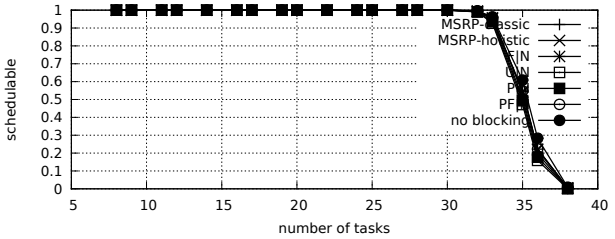

Fig. 993. Schedulability under non-preemptable spin locks for $m = 8$, $U = 0.2n$, 8 resources, $rsf = 0.1$, $N^{max} = 10$, and short critical sections. The schedulability of the considered preemptable lock types in this configuration is shown in Fig. 1003.

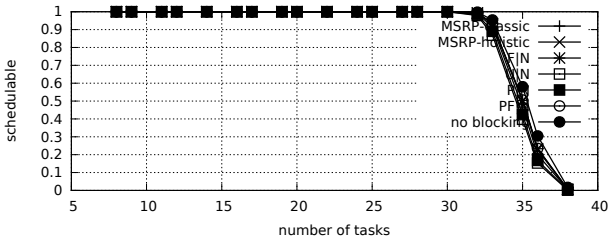

Fig. 994. Schedulability under non-preemptable spin locks for $m = 8$, $U = 0.2n$, 8 resources, $rsf = 0.1$, $N^{max} = 15$, and short critical sections. The schedulability of the considered preemptable lock types in this configuration is shown in Fig. 1004.

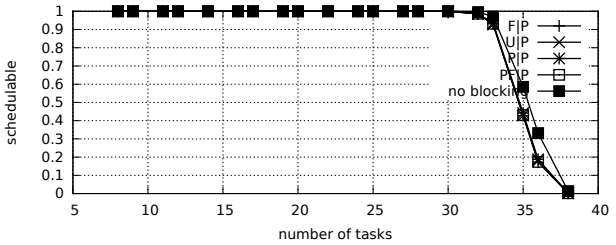

Fig. 995. Schedulability under preemptable spin locks for $m = 8$, $U = 0.2n$, 8 resources, $rsf = 0.1$, $N^{max} = 1$, and medium critical sections. The schedulability of the considered non-preemptable lock types in this configuration is shown in Fig. 985.

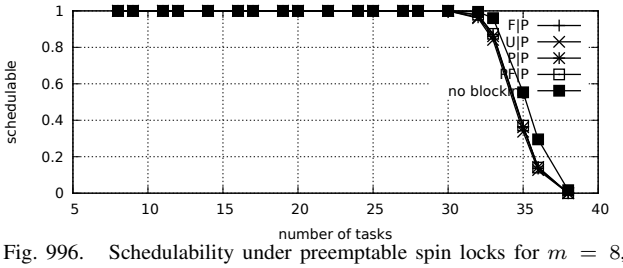

Fig. 996. Schedulability under preemptable spin locks for $m = 8$, $U = 0.2n$, 8 resources, $rsf = 0.1$, $N^{max} = 2$, and medium critical sections. The schedulability of the considered non-preemptable lock types in this configuration is shown in Fig. 986.

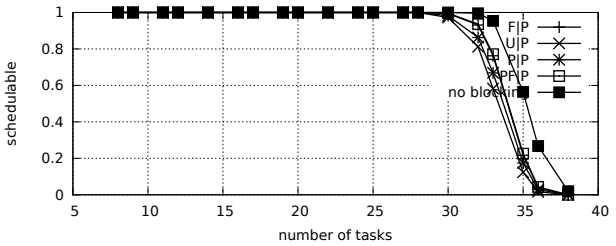

Fig. 997. Schedulability under preemptable spin locks for $m = 8$, $U = 0.2n$, 8 resources, $rsf = 0.1$, $N^{max} = 5$, and medium critical sections. The schedulability of the considered non-preemptable lock types in this configuration is shown in Fig. 987.

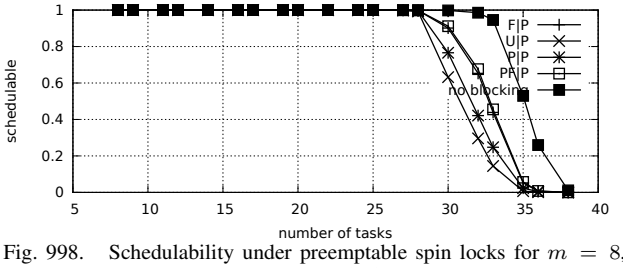

Fig. 998. Schedulability under preemptable spin locks for $m = 8$, $U = 0.2n$, 8 resources, $rsf = 0.1$, $N^{max} = 10$, and medium critical sections. The schedulability of the considered non-preemptable lock types in this configuration is shown in Fig. 988.

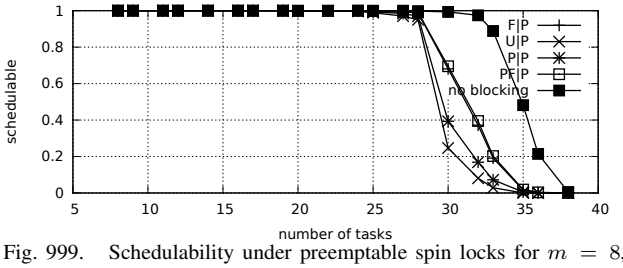

Fig. 999. Schedulability under preemptable spin locks for $m = 8$, $U = 0.2n$, 8 resources, $rsf = 0.1$, $N^{max} = 15$, and medium critical sections. The schedulability of the considered non-preemptable lock types in this configuration is shown in Fig. 989.

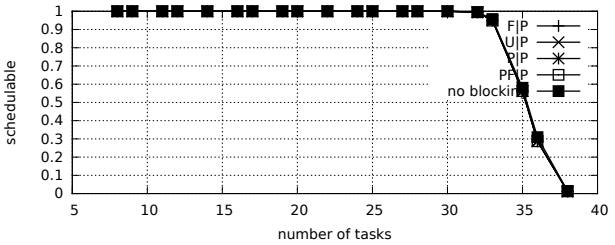

Fig. 1000. Schedulability under preemptable spin locks for $m = 8$, $U = 0.2n$, 8 resources, $rsf = 0.1$, $N^{max} = 1$, and short critical sections. The schedulability of the considered non-preemptable lock types in this configuration is shown in Fig. 990.

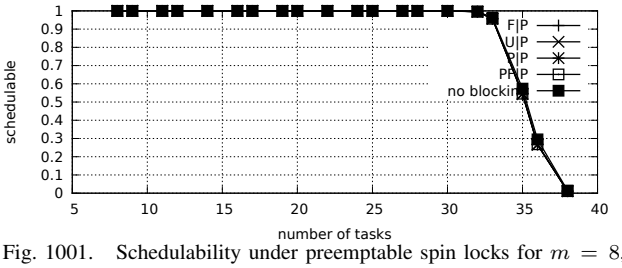

Fig. 1001. Schedulability under preemptable spin locks for $m = 8$, $U = 0.2n$, 8 resources, $rsf = 0.1$, $N^{max} = 2$, and short critical sections. The schedulability of the considered non-preemptable lock types in this configuration is shown in Fig. 991.

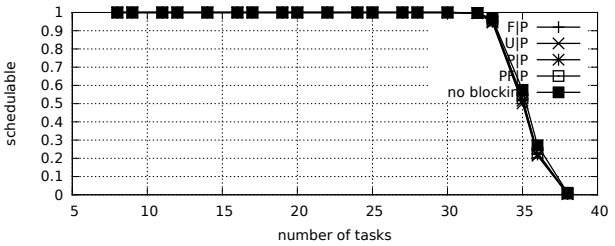

Fig. 1002. Schedulability under preemptable spin locks for $m = 8$, $U = 0.2n$, 8 resources, $rsf = 0.1$, $N^{max} = 5$, and short critical sections. The schedulability of the considered non-preemptable lock types in this configuration is shown in Fig. 992.

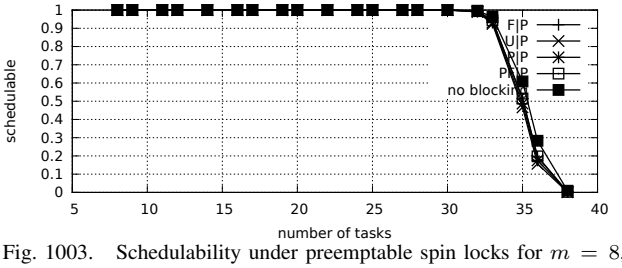

Fig. 1003. Schedulability under preemptable spin locks for $m = 8$, $U = 0.2n$, 8 resources, $rsf = 0.1$, $N^{max} = 10$, and short critical sections. The schedulability of the considered non-preemptable lock types in this configuration is shown in Fig. 993.

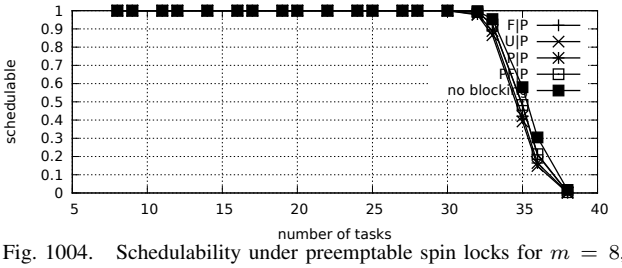

Fig. 1004. Schedulability under preemptable spin locks for $m = 8$, $U = 0.2n$, 8 resources, $rsf = 0.1$, $N^{max} = 15$, and short critical sections. The schedulability of the considered non-preemptable lock types in this configuration is shown in Fig. 994.

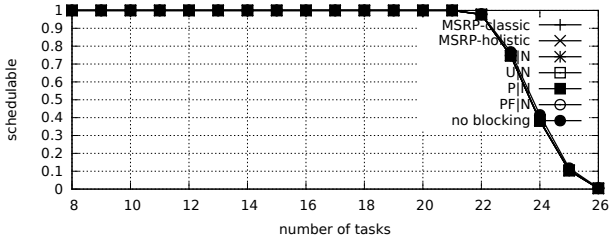

Fig. 1005. Schedulability under non-preemptable spin locks for $m = 8$, $U = 0.3n$, 8 resources, $rsf = 0.1$, $N^{max} = 1$, and medium critical sections. The schedulability of the considered preemptable lock types in this configuration is shown in Fig. 1015.

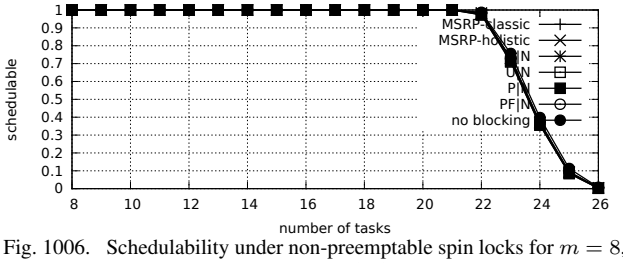

Fig. 1006. Schedulability under non-preemptable spin locks for $m = 8$, $U = 0.3n$, 8 resources, $rsf = 0.1$, $N^{max} = 2$, and medium critical sections. The schedulability of the considered preemptable lock types in this configuration is shown in Fig. 1016.

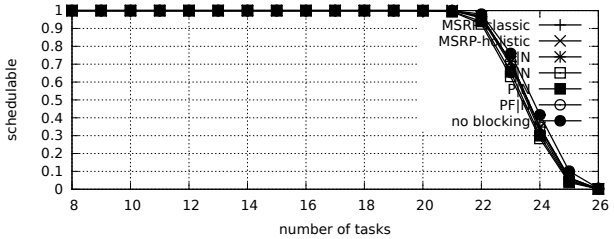

Fig. 1007. Schedulability under non-preemptable spin locks for $m = 8$, $U = 0.3n$, 8 resources, $rsf = 0.1$, $N^{max} = 5$, and medium critical sections. The schedulability of the considered preemptable lock types in this configuration is shown in Fig. 1017.

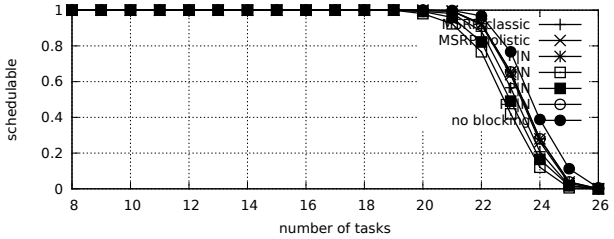

Fig. 1008. Schedulability under non-preemptable spin locks for $m = 8$, $U = 0.3n$, 8 resources, $rsf = 0.1$, $N^{max} = 10$, and medium critical sections. The schedulability of the considered preemptable lock types in this configuration is shown in Fig. 1018.

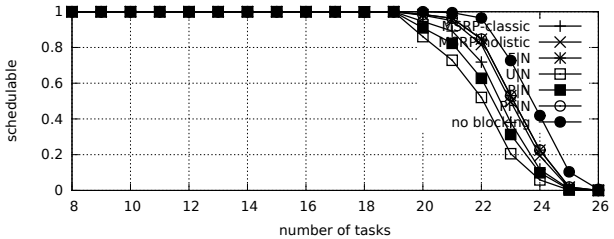

Fig. 1009. Schedulability under non-preemptable spin locks for $m = 8$, $U = 0.3n$, 8 resources, $rsf = 0.1$, $N^{max} = 15$, and medium critical sections. The schedulability of the considered preemptable lock types in this configuration is shown in Fig. 1019.

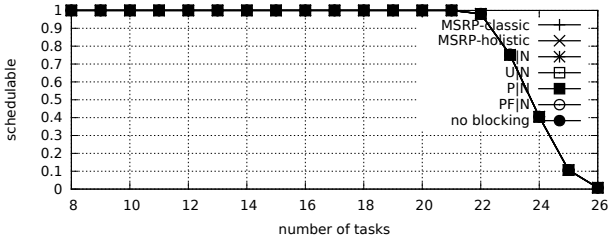

Fig. 1010. Schedulability under non-preemptable spin locks for $m = 8$, $U = 0.3n$, 8 resources, $rsf = 0.1$, $N^{max} = 1$, and short critical sections. The schedulability of the considered preemptable lock types in this configuration is shown in Fig. 1020.

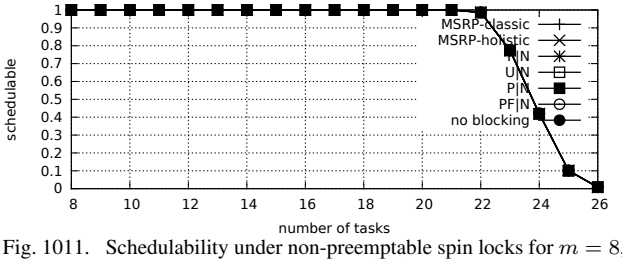

Fig. 1011. Schedulability under non-preemptable spin locks for $m = 8$, $U = 0.3n$, 8 resources, $rsf = 0.1$, $N^{max} = 2$, and short critical sections. The schedulability of the considered preemptable lock types in this configuration is shown in Fig. 1021.

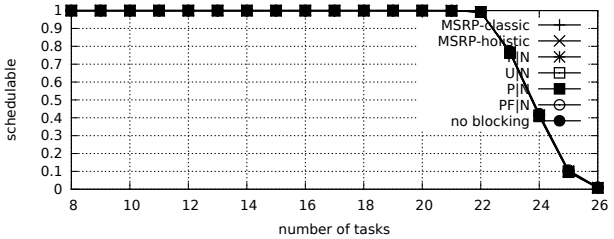

Fig. 1012. Schedulability under non-preemptable spin locks for $m = 8$, $U = 0.3n$, 8 resources, $rsf = 0.1$, $N^{max} = 5$, and short critical sections. The schedulability of the considered preemptable lock types in this configuration is shown in Fig. 1022.

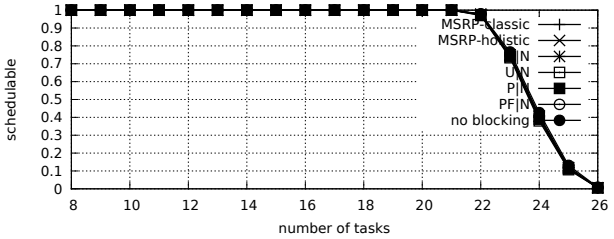

Fig. 1013. Schedulability under non-preemptable spin locks for $m = 8$, $U = 0.3n$, 8 resources, $rsf = 0.1$, $N^{max} = 10$, and short critical sections. The schedulability of the considered preemptable lock types in this configuration is shown in Fig. 1023.

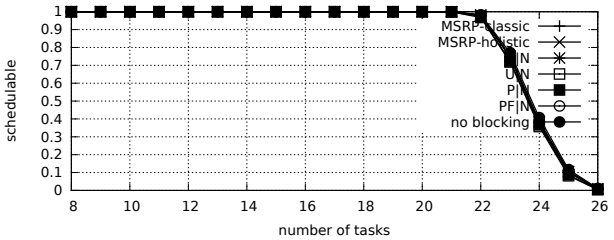

Fig. 1014. Schedulability under non-preemptable spin locks for $m = 8$, $U = 0.3n$, 8 resources, $rsf = 0.1$, $N^{max} = 15$, and short critical sections. The schedulability of the considered preemptable lock types in this configuration is shown in Fig. 1024.

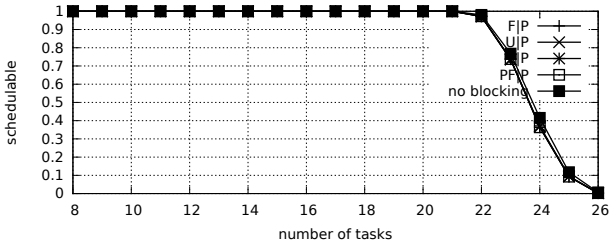

Fig. 1015. Schedulability under preemptable spin locks for $m = 8$, $U = 0.3n$, 8 resources, $rsf = 0.1$, $N^{max} = 1$, and medium critical sections. The schedulability of the considered non-preemptable lock types in this configuration is shown in Fig. 1005.

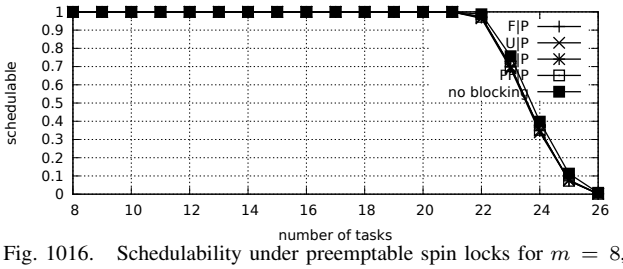

Fig. 1016. Schedulability under preemptable spin locks for $m = 8$, $U = 0.3n$, 8 resources, $rsf = 0.1$, $N^{max} = 2$, and medium critical sections. The schedulability of the considered non-preemptable lock types in this configuration is shown in Fig. 1006.

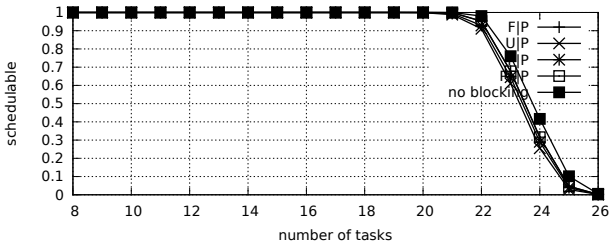

Fig. 1017. Schedulability under preemptable spin locks for $m = 8$, $U = 0.3n$, 8 resources, $rsf = 0.1$, $N^{max} = 5$, and medium critical sections. The schedulability of the considered non-preemptable lock types in this configuration is shown in Fig. 1007.

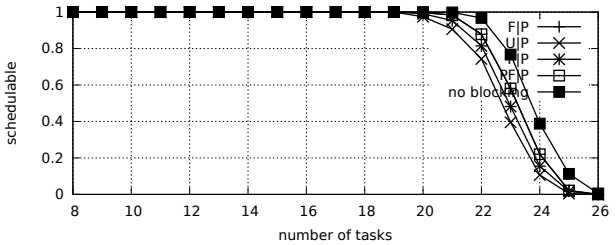

Fig. 1018. Schedulability under preemptable spin locks for $m = 8$, $U = 0.3n$, 8 resources, $rsf = 0.1$, $N^{max} = 10$, and medium critical sections. The schedulability of the considered non-preemptable lock types in this configuration is shown in Fig. 1008.

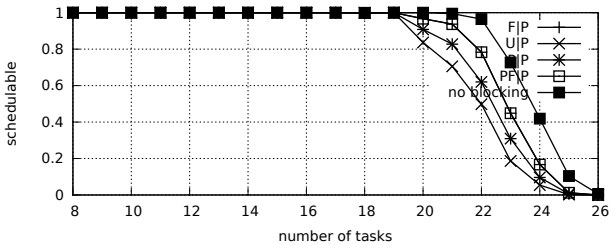

Fig. 1019. Schedulability under preemptable spin locks for $m = 8$, $U = 0.3n$, 8 resources, $rsf = 0.1$, $N^{max} = 15$, and medium critical sections. The schedulability of the considered non-preemptable lock types in this configuration is shown in Fig. 1009.

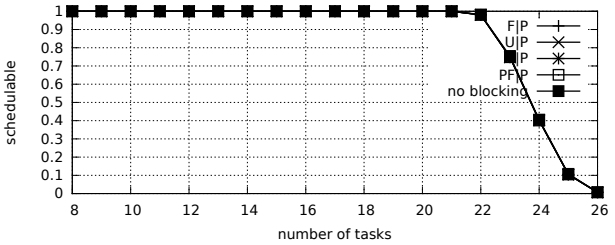

Fig. 1020. Schedulability under preemptable spin locks for $m = 8$, $U = 0.3n$, 8 resources, $rsf = 0.1$, $N^{max} = 1$, and short critical sections. The schedulability of the considered non-preemptable lock types in this configuration is shown in Fig. 1010.

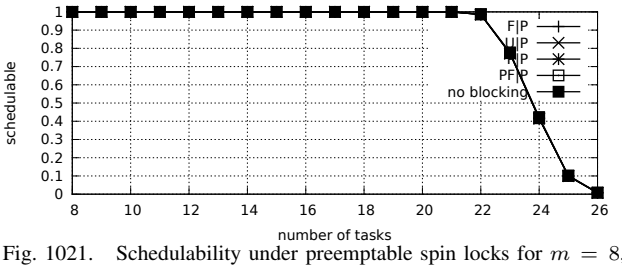

Fig. 1021. Schedulability under preemptable spin locks for $m = 8$, $U = 0.3n$, 8 resources, $rsf = 0.1$, $N^{max} = 2$, and short critical sections. The schedulability of the considered non-preemptable lock types in this configuration is shown in Fig. 1011.

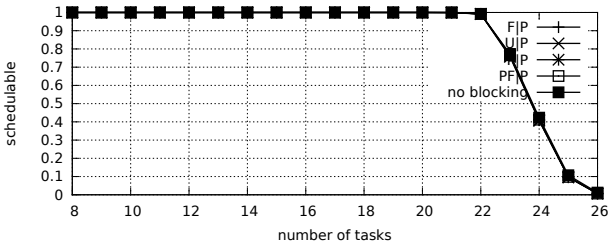

Fig. 1022. Schedulability under preemptable spin locks for $m = 8$, $U = 0.3n$, 8 resources, $rsf = 0.1$, $N^{max} = 5$, and short critical sections. The schedulability of the considered non-preemptable lock types in this configuration is shown in Fig. 1012.

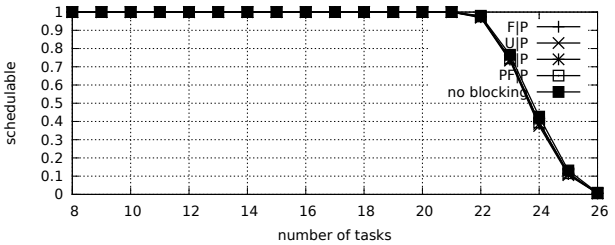

Fig. 1023. Schedulability under preemptable spin locks for $m = 8$, $U = 0.3n$, 8 resources, $rsf = 0.1$, $N^{max} = 10$, and short critical sections. The schedulability of the considered non-preemptable lock types in this configuration is shown in Fig. 1013.

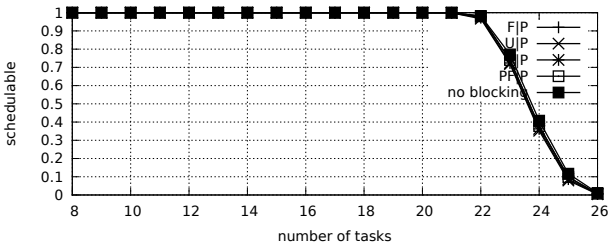

Fig. 1024. Schedulability under preemptable spin locks for $m = 8$, $U = 0.3n$, 8 resources, $rsf = 0.1$, $N^{max} = 15$, and short critical sections. The schedulability of the considered non-preemptable lock types in this configuration is shown in Fig. 1014.

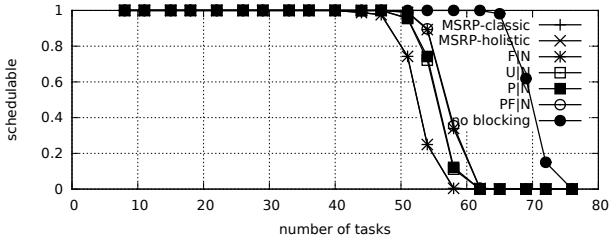

Fig. 1025. Schedulability under non-preemptable spin locks for $m = 8$, $U = 0.1n$, 8 resources, $rsf = 0.25$, $N^{max} = 1$, and medium critical sections. The schedulability of the considered preemptable lock types in this configuration is shown in Fig. 1035.

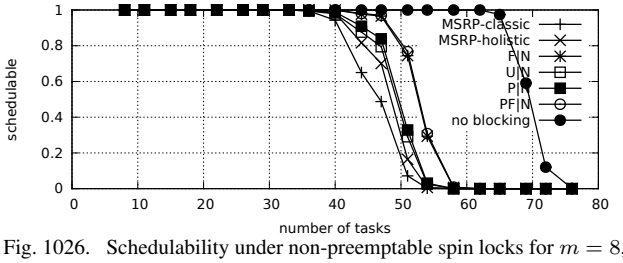

Fig. 1026. Schedulability under non-preemptable spin locks for $m = 8$, $U = 0.1n$, 8 resources, $rsf = 0.25$, $N^{max} = 2$, and medium critical sections. The schedulability of the considered preemptable lock types in this configuration is shown in Fig. 1036.

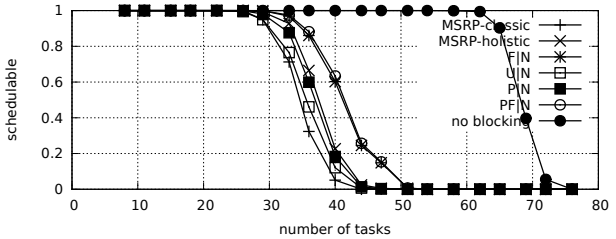

Fig. 1027. Schedulability under non-preemptable spin locks for $m = 8$, $U = 0.1n$, 8 resources, $rsf = 0.25$, $N^{max} = 5$, and medium critical sections. The schedulability of the considered preemptable lock types in this configuration is shown in Fig. 1037.

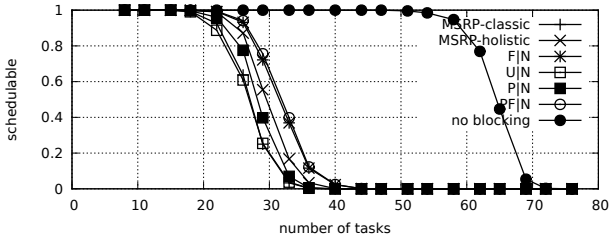

Fig. 1028. Schedulability under non-preemptable spin locks for $m = 8$, $U = 0.1n$, 8 resources, $rsf = 0.25$, $N^{max} = 10$, and medium critical sections. The schedulability of the considered preemptable lock types in this configuration is shown in Fig. 1038.

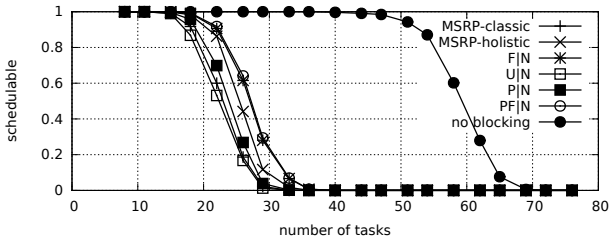

Fig. 1029. Schedulability under non-preemptable spin locks for $m = 8$, $U = 0.1n$, 8 resources, $rsf = 0.25$, $N^{max} = 15$, and medium critical sections. The schedulability of the considered preemptable lock types in this configuration is shown in Fig. 1039.

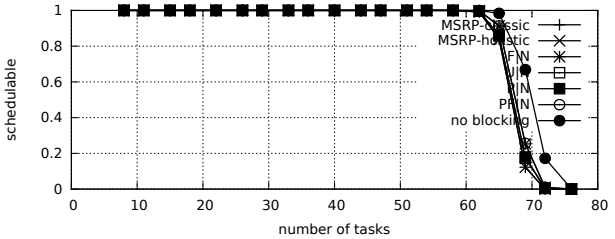

Fig. 1030. Schedulability under non-preemptable spin locks for $m = 8$, $U = 0.1n$, 8 resources, $rsf = 0.25$, $N^{max} = 1$, and short critical sections. The schedulability of the considered preemptable lock types in this configuration is shown in Fig. 1040.

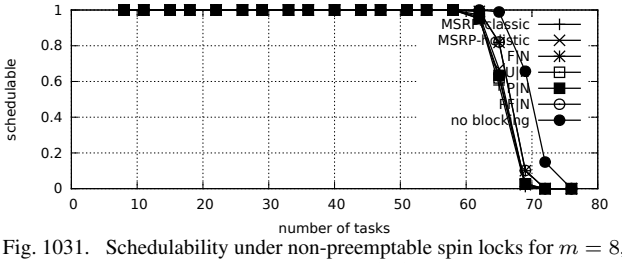

Fig. 1031. Schedulability under non-preemptable spin locks for $m = 8$, $U = 0.1n$, 8 resources, $rsf = 0.25$, $N^{max} = 2$, and short critical sections. The schedulability of the considered preemptable lock types in this configuration is shown in Fig. 1041.

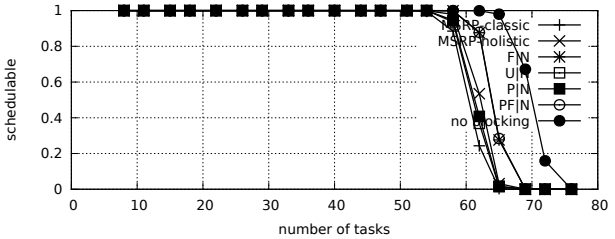

Fig. 1032. Schedulability under non-preemptable spin locks for $m = 8$, $U = 0.1n$, 8 resources, $rsf = 0.25$, $N^{max} = 5$, and short critical sections. The schedulability of the considered preemptable lock types in this configuration is shown in Fig. 1042.

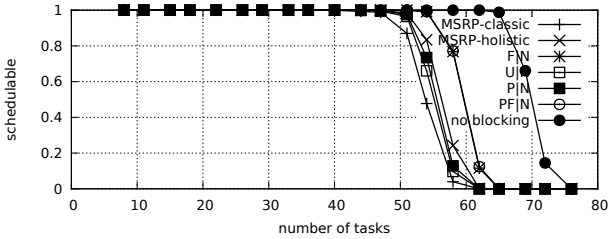

Fig. 1033. Schedulability under non-preemptable spin locks for $m = 8$, $U = 0.1n$, 8 resources, $rsf = 0.25$, $N^{max} = 10$, and short critical sections. The schedulability of the considered preemptable lock types in this configuration is shown in Fig. 1043.

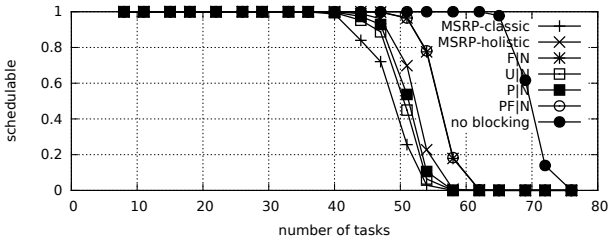

Fig. 1034. Schedulability under non-preemptable spin locks for $m = 8$, $U = 0.1n$, 8 resources, $rsf = 0.25$, $N^{max} = 15$, and short critical sections. The schedulability of the considered preemptable lock types in this configuration is shown in Fig. 1044.

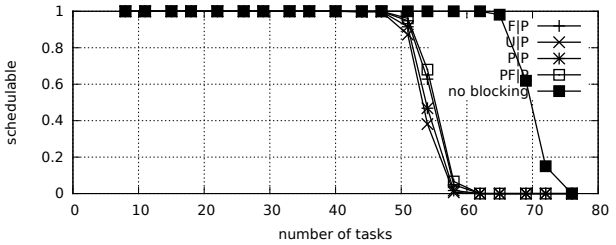

Fig. 1035. Schedulability under preemptable spin locks for $m = 8$, $U = 0.1n$, 8 resources, $rsf = 0.25$, $N^{max} = 1$, and medium critical sections. The schedulability of the considered non-preemptable lock types in this configuration is shown in Fig. 1025.

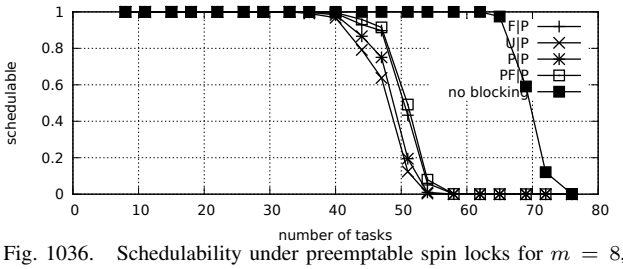

Fig. 1036. Schedulability under preemptable spin locks for $m = 8$, $U = 0.1n$, 8 resources, $rsf = 0.25$, $N^{max} = 2$, and medium critical sections. The schedulability of the considered non-preemptable lock types in this configuration is shown in Fig. 1026.

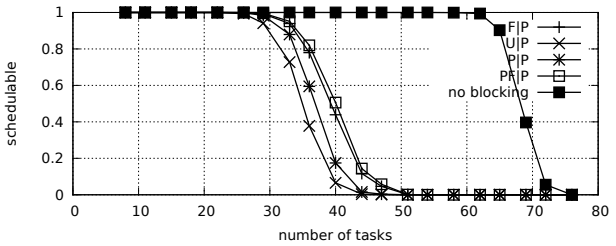

Fig. 1037. Schedulability under preemptable spin locks for $m = 8$, $U = 0.1n$, 8 resources, $rsf = 0.25$, $N^{max} = 5$, and medium critical sections. The schedulability of the considered non-preemptable lock types in this configuration is shown in Fig. 1027.

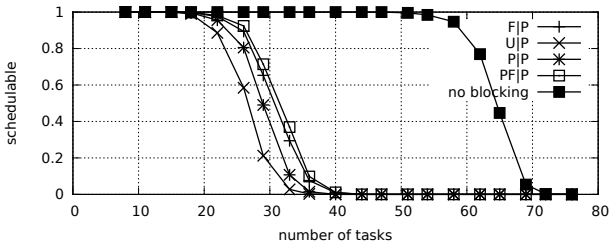

Fig. 1038. Schedulability under preemptable spin locks for $m = 8$, $U = 0.1n$, 8 resources, $rsf = 0.25$, $N^{max} = 10$, and medium critical sections. The schedulability of the considered non-preemptable lock types in this configuration is shown in Fig. 1028.

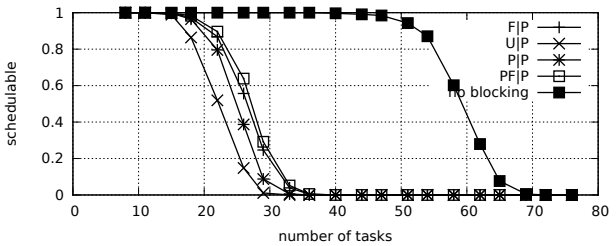

Fig. 1039. Schedulability under preemptable spin locks for $m = 8$, $U = 0.1n$, 8 resources, $rsf = 0.25$, $N^{max} = 15$, and medium critical sections. The schedulability of the considered non-preemptable lock types in this configuration is shown in Fig. 1029.

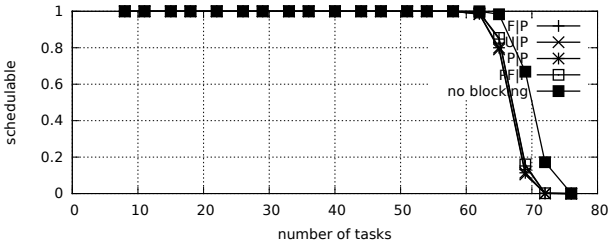

Fig. 1040. Schedulability under preemptable spin locks for $m = 8$, $U = 0.1n$, 8 resources, $rsf = 0.25$, $N^{max} = 1$, and short critical sections. The schedulability of the considered non-preemptable lock types in this configuration is shown in Fig. 1030.

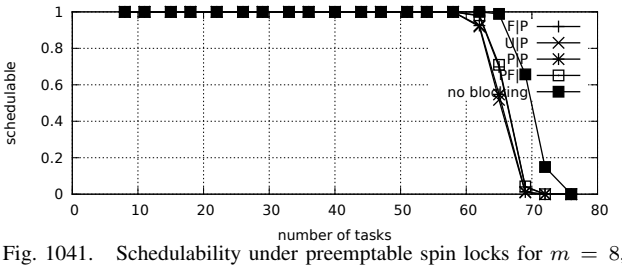

Fig. 1041. Schedulability under preemptable spin locks for $m = 8$, $U = 0.1n$, 8 resources, $rsf = 0.25$, $N^{max} = 2$, and short critical sections. The schedulability of the considered non-preemptable lock types in this configuration is shown in Fig. 1031.

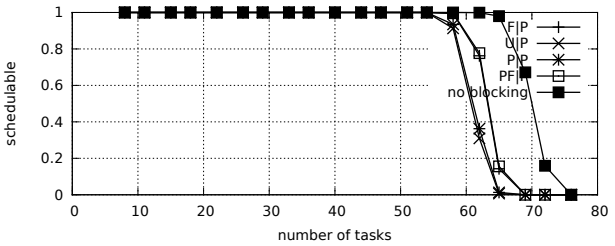

Fig. 1042. Schedulability under preemptable spin locks for $m = 8$, $U = 0.1n$, 8 resources, $rsf = 0.25$, $N^{max} = 5$, and short critical sections. The schedulability of the considered non-preemptable lock types in this configuration is shown in Fig. 1032.

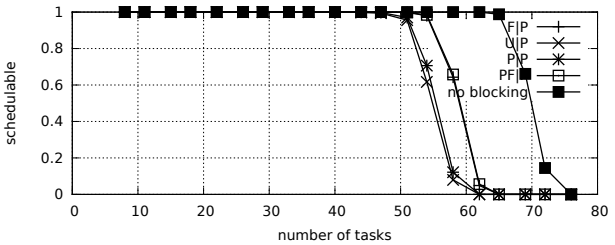

Fig. 1043. Schedulability under preemptable spin locks for $m = 8$, $U = 0.1n$, 8 resources, $rsf = 0.25$, $N^{max} = 10$, and short critical sections. The schedulability of the considered non-preemptable lock types in this configuration is shown in Fig. 1033.

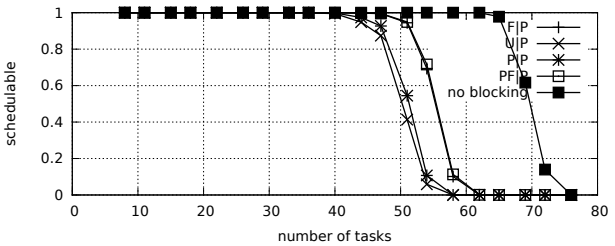

Fig. 1044. Schedulability under preemptable spin locks for $m = 8$, $U = 0.1n$, 8 resources, $rsf = 0.25$, $N^{max} = 15$, and short critical sections. The schedulability of the considered non-preemptable lock types in this configuration is shown in Fig. 1034.

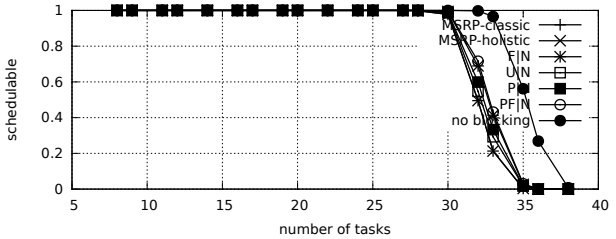

Fig. 1045. Schedulability under non-preemptable spin locks for $m = 8$, $U = 0.2n$, 8 resources, $rsf = 0.25$, $N^{max} = 1$, and medium critical sections. The schedulability of the considered preemptable lock types in this configuration is shown in Fig. 1055.

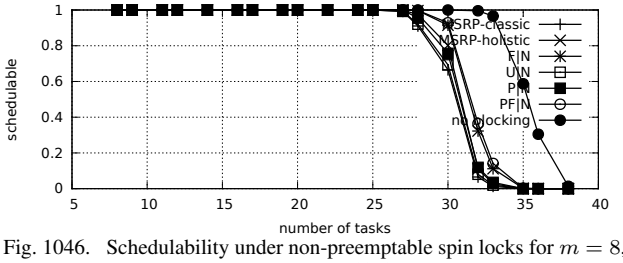

Fig. 1046. Schedulability under non-preemptable spin locks for $m = 8$, $U = 0.2n$, 8 resources, $rsf = 0.25$, $N^{max} = 2$, and medium critical sections. The schedulability of the considered preemptable lock types in this configuration is shown in Fig. 1056.

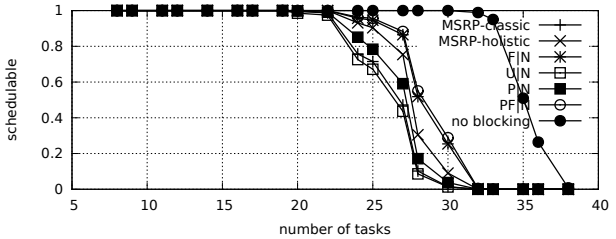

Fig. 1047. Schedulability under non-preemptable spin locks for $m = 8$, $U = 0.2n$, 8 resources, $rsf = 0.25$, $N^{max} = 5$, and medium critical sections. The schedulability of the considered preemptable lock types in this configuration is shown in Fig. 1057.

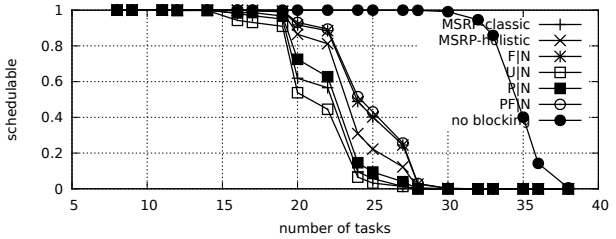

Fig. 1048. Schedulability under non-preemptable spin locks for $m = 8$, $U = 0.2n$, 8 resources, $rsf = 0.25$, $N^{max} = 10$, and medium critical sections. The schedulability of the considered preemptable lock types in this configuration is shown in Fig. 1058.

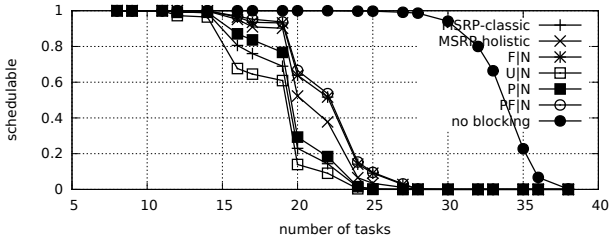

Fig. 1049. Schedulability under non-preemptable spin locks for $m = 8$, $U = 0.2n$, 8 resources, $rsf = 0.25$, $N^{max} = 15$, and medium critical sections. The schedulability of the considered preemptable lock types in this configuration is shown in Fig. 1059.

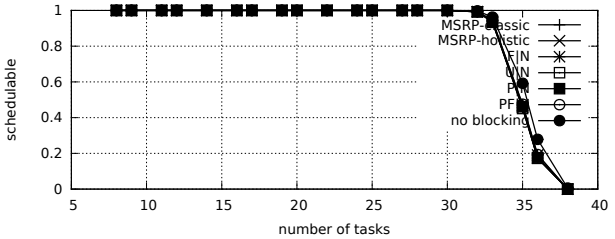

Fig. 1050. Schedulability under non-preemptable spin locks for $m = 8$, $U = 0.2n$, 8 resources, $rsf = 0.25$, $N^{max} = 1$, and short critical sections. The schedulability of the considered preemptable lock types in this configuration is shown in Fig. 1060.

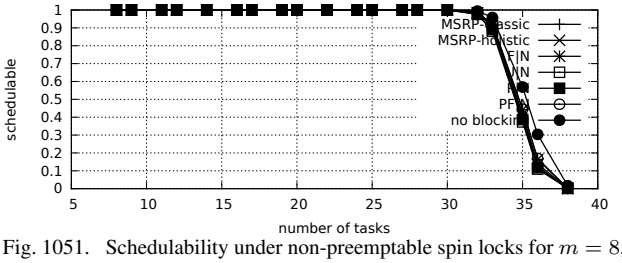

Fig. 1051. Schedulability under non-preemptable spin locks for $m = 8$, $U = 0.2n$, 8 resources, $rsf = 0.25$, $N^{max} = 2$, and short critical sections. The schedulability of the considered preemptable lock types in this configuration is shown in Fig. 1061.

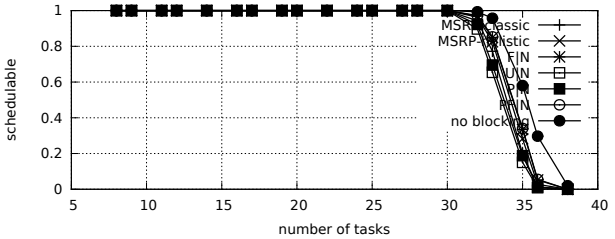

Fig. 1052. Schedulability under non-preemptable spin locks for $m = 8$, $U = 0.2n$, 8 resources, $rsf = 0.25$, $N^{max} = 5$, and short critical sections. The schedulability of the considered preemptable lock types in this configuration is shown in Fig. 1062.

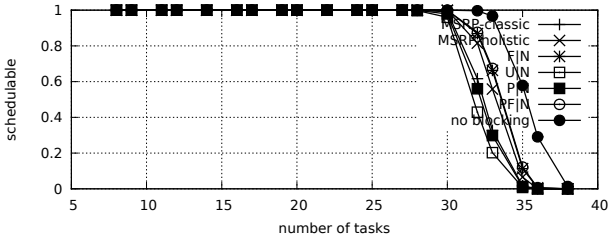

Fig. 1053. Schedulability under non-preemptable spin locks for $m = 8$, $U = 0.2n$, 8 resources, $rsf = 0.25$, $N^{max} = 10$, and short critical sections. The schedulability of the considered preemptable lock types in this configuration is shown in Fig. 1063.

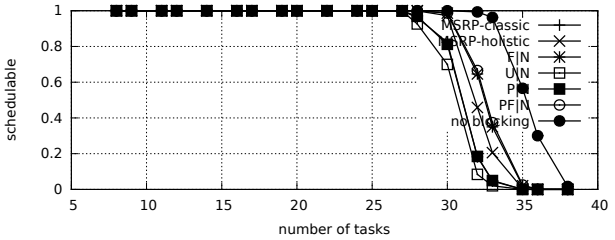

Fig. 1054. Schedulability under non-preemptable spin locks for $m = 8$, $U = 0.2n$, 8 resources, $rsf = 0.25$, $N^{max} = 15$, and short critical sections. The schedulability of the considered preemptable lock types in this configuration is shown in Fig. 1064.

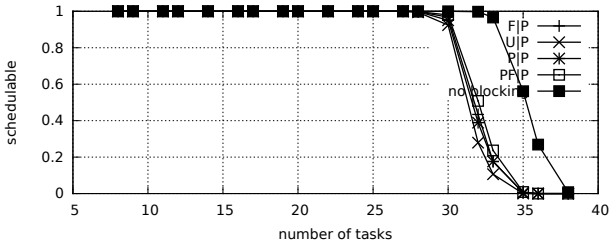

Fig. 1055. Schedulability under preemptable spin locks for $m = 8$, $U = 0.2n$, 8 resources, $rsf = 0.25$, $N^{max} = 1$, and medium critical sections. The schedulability of the considered non-preemptable lock types in this configuration is shown in Fig. 1045.

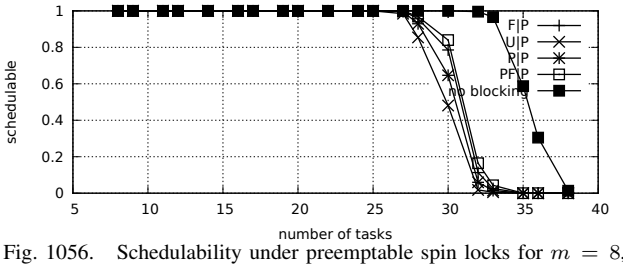

Fig. 1056. Schedulability under preemptable spin locks for $m = 8$, $U = 0.2n$, 8 resources, $rsf = 0.25$, $N^{max} = 2$, and medium critical sections. The schedulability of the considered non-preemptable lock types in this configuration is shown in Fig. 1046.

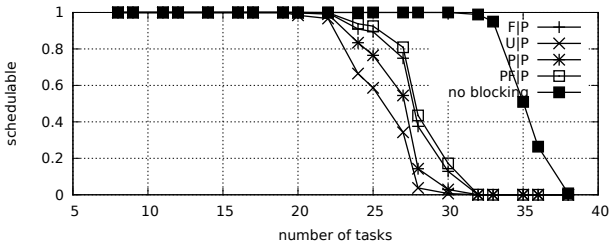

Fig. 1057. Schedulability under preemptable spin locks for $m = 8$, $U = 0.2n$, 8 resources, $rsf = 0.25$, $N^{max} = 5$, and medium critical sections. The schedulability of the considered non-preemptable lock types in this configuration is shown in Fig. 1047.

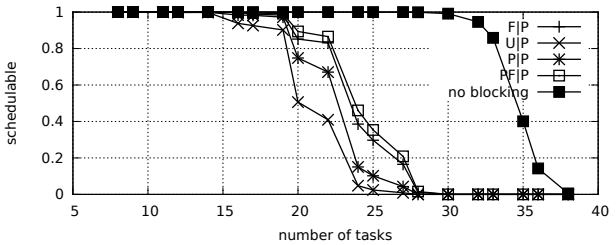

Fig. 1058. Schedulability under preemptable spin locks for $m = 8$, $U = 0.2n$, 8 resources, $rsf = 0.25$, $N^{max} = 10$, and medium critical sections. The schedulability of the considered non-preemptable lock types in this configuration is shown in Fig. 1048.

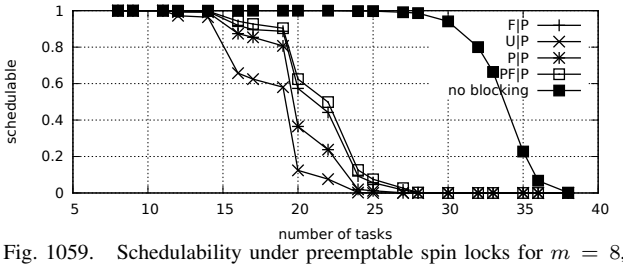

Fig. 1059. Schedulability under preemptable spin locks for $m = 8$, $U = 0.2n$, 8 resources, $rsf = 0.25$, $N^{max} = 15$, and medium critical sections. The schedulability of the considered non-preemptable lock types in this configuration is shown in Fig. 1049.

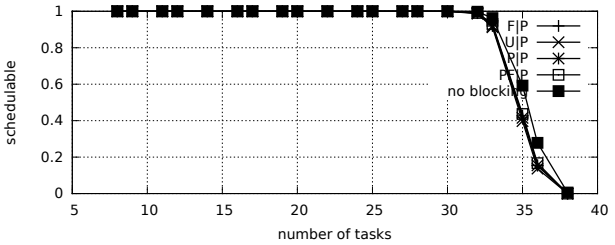

Fig. 1060. Schedulability under preemptable spin locks for $m = 8$, $U = 0.2n$, 8 resources, $rsf = 0.25$, $N^{max} = 1$, and short critical sections. The schedulability of the considered non-preemptable lock types in this configuration is shown in Fig. 1050.

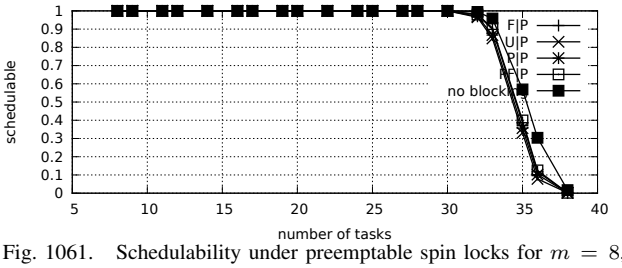

Fig. 1061. Schedulability under preemptable spin locks for $m = 8$, $U = 0.2n$, 8 resources, $rsf = 0.25$, $N^{max} = 2$, and short critical sections. The schedulability of the considered non-preemptable lock types in this configuration is shown in Fig. 1051.

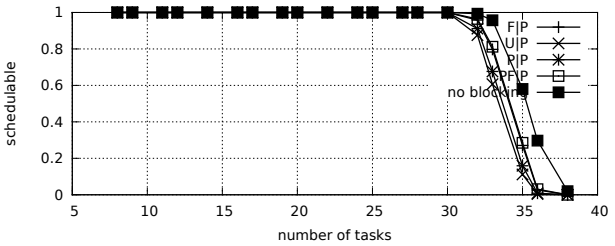

Fig. 1062. Schedulability under preemptable spin locks for $m = 8$, $U = 0.2n$, 8 resources, $rsf = 0.25$, $N^{max} = 5$, and short critical sections. The schedulability of the considered non-preemptable lock types in this configuration is shown in Fig. 1052.

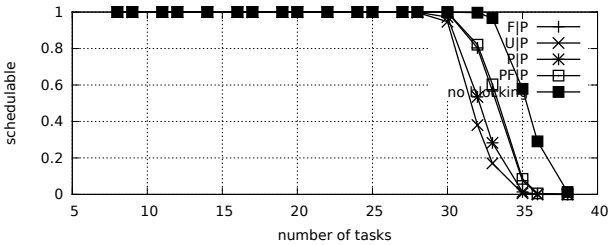

Fig. 1063. Schedulability under preemptable spin locks for $m = 8$, $U = 0.2n$, 8 resources, $rsf = 0.25$, $N^{max} = 10$, and short critical sections. The schedulability of the considered non-preemptable lock types in this configuration is shown in Fig. 1053.

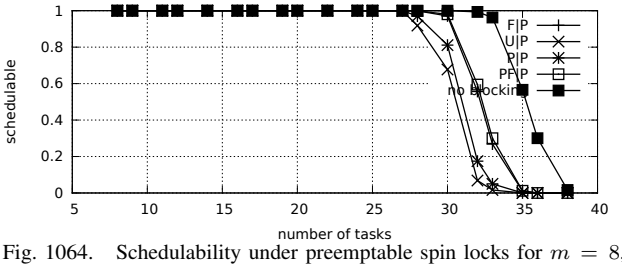

Fig. 1064. Schedulability under preemptable spin locks for $m = 8$, $U = 0.2n$, 8 resources, $rsf = 0.25$, $N^{max} = 15$, and short critical sections. The schedulability of the considered non-preemptable lock types in this configuration is shown in Fig. 1054.

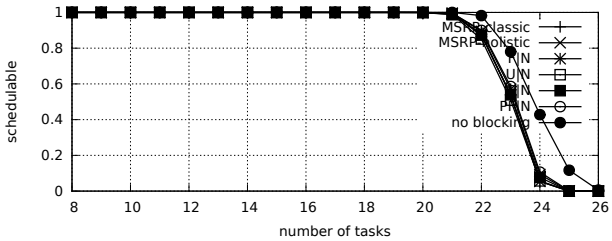

Fig. 1065. Schedulability under non-preemptable spin locks for $m = 8$, $U = 0.3n$, 8 resources, $rsf = 0.25$, $N^{max} = 1$, and medium critical sections. The schedulability of the considered preemptable lock types in this configuration is shown in Fig. 1075.

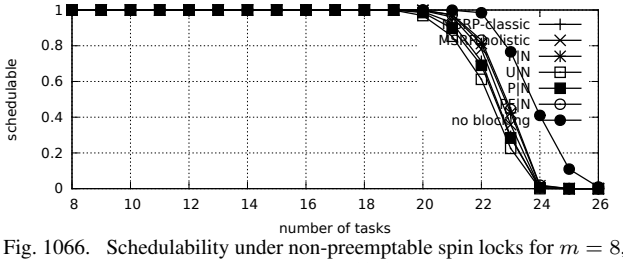

Fig. 1066. Schedulability under non-preemptable spin locks for $m = 8$, $U = 0.3n$, 8 resources, $rsf = 0.25$, $N^{max} = 2$, and medium critical sections. The schedulability of the considered preemptable lock types in this configuration is shown in Fig. 1076.

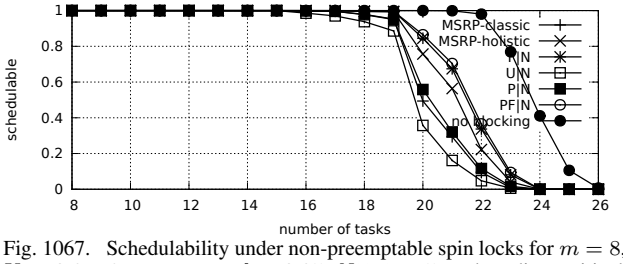

Fig. 1067. Schedulability under non-preemptable spin locks for $m = 8$, $U = 0.3n$, 8 resources, $rsf = 0.25$, $N^{max} = 5$, and medium critical sections. The schedulability of the considered preemptable lock types in this configuration is shown in Fig. 1077.

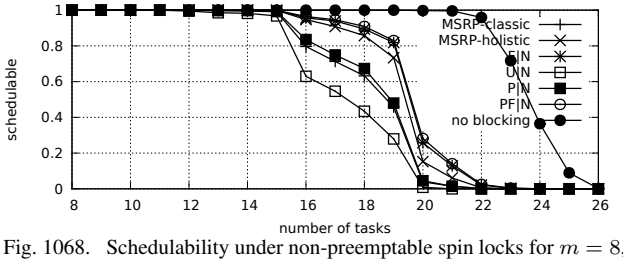

Fig. 1068. Schedulability under non-preemptable spin locks for $m = 8$, $U = 0.3n$, 8 resources, $rsf = 0.25$, $N^{max} = 10$, and medium critical sections. The schedulability of the considered preemptable lock types in this configuration is shown in Fig. 1078.

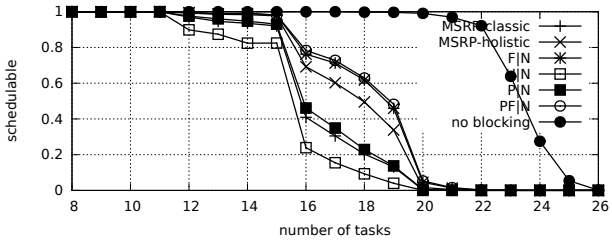

Fig. 1069. Schedulability under non-preemptable spin locks for $m = 8$, $U = 0.3n$, 8 resources, $rsf = 0.25$, $N^{max} = 15$, and medium critical sections. The schedulability of the considered preemptable lock types in this configuration is shown in Fig. 1079.

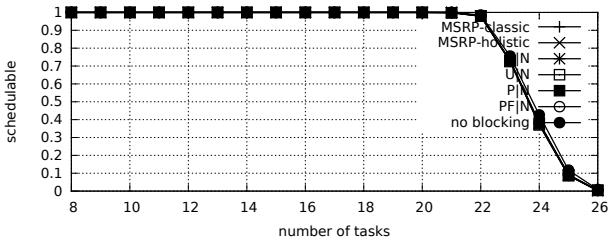

Fig. 1070. Schedulability under non-preemptable spin locks for $m = 8$, $U = 0.3n$, 8 resources, $rsf = 0.25$, $N^{max} = 1$, and short critical sections. The schedulability of the considered preemptable lock types in this configuration is shown in Fig. 1080.

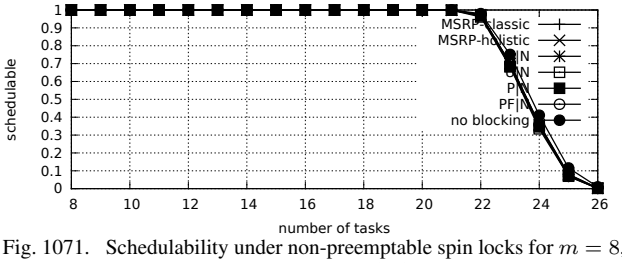

Fig. 1071. Schedulability under non-preemptable spin locks for $m = 8$, $U = 0.3n$, 8 resources, $rsf = 0.25$, $N^{max} = 2$, and short critical sections. The schedulability of the considered preemptable lock types in this configuration is shown in Fig. 1081.

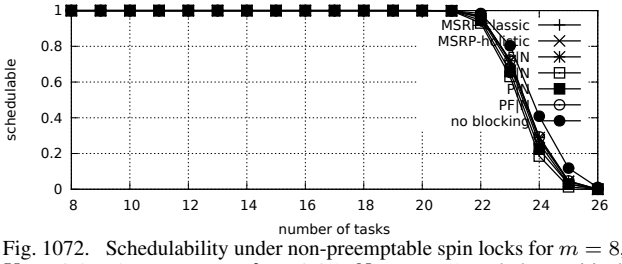

Fig. 1072. Schedulability under non-preemptable spin locks for $m = 8$, $U = 0.3n$, 8 resources, $rsf = 0.25$, $N^{max} = 5$, and short critical sections. The schedulability of the considered preemptable lock types in this configuration is shown in Fig. 1082.

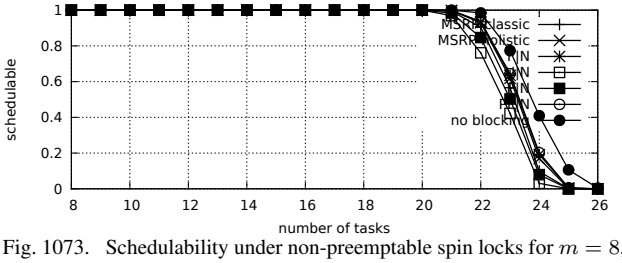

Fig. 1073. Schedulability under non-preemptable spin locks for $m = 8$, $U = 0.3n$, 8 resources, $rsf = 0.25$, $N^{max} = 10$, and short critical sections. The schedulability of the considered preemptable lock types in this configuration is shown in Fig. 1083.

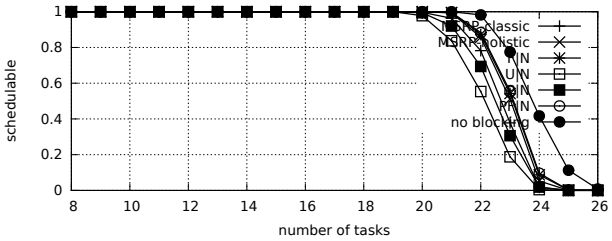

Fig. 1074. Schedulability under non-preemptable spin locks for $m = 8$, $U = 0.3n$, 8 resources, $rsf = 0.25$, $N^{max} = 15$, and short critical sections. The schedulability of the considered preemptable lock types in this configuration is shown in Fig. 1084.

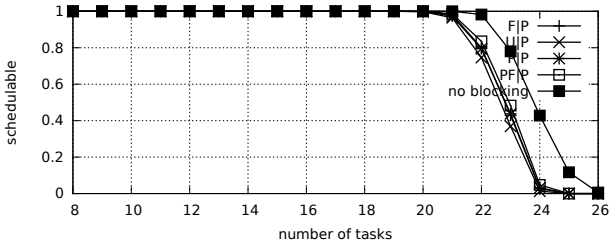

Fig. 1075. Schedulability under preemptable spin locks for $m = 8$, $U = 0.3n$, 8 resources, $rsf = 0.25$, $N^{max} = 1$, and medium critical sections. The schedulability of the considered non-preemptable lock types in this configuration is shown in Fig. 1065.

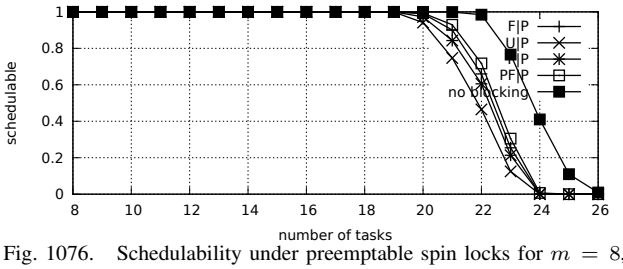

Fig. 1076. Schedulability under preemptable spin locks for $m = 8$, $U = 0.3n$, 8 resources, $rsf = 0.25$, $N^{max} = 2$, and medium critical sections. The schedulability of the considered non-preemptable lock types in this configuration is shown in Fig. 1066.

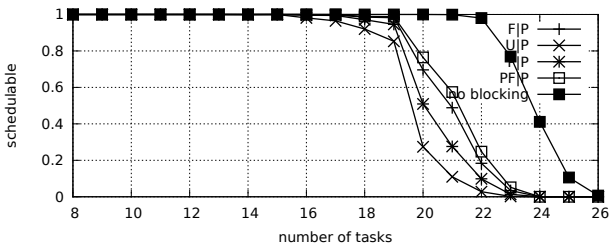

Fig. 1077. Schedulability under preemptable spin locks for $m = 8$, $U = 0.3n$, 8 resources, $rsf = 0.25$, $N^{max} = 5$, and medium critical sections. The schedulability of the considered non-preemptable lock types in this configuration is shown in Fig. 1067.

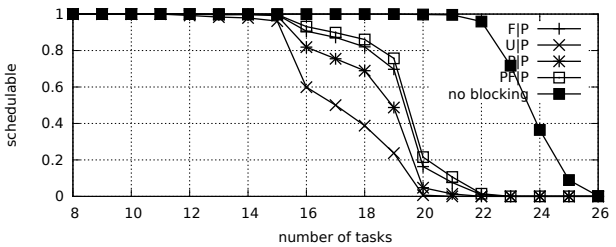

Fig. 1078. Schedulability under preemptable spin locks for $m = 8$, $U = 0.3n$, 8 resources, $rsf = 0.25$, $N^{max} = 10$, and medium critical sections. The schedulability of the considered non-preemptable lock types in this configuration is shown in Fig. 1068.

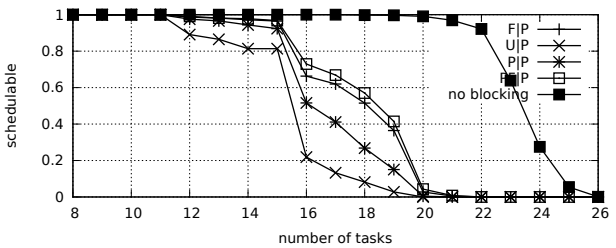

Fig. 1079. Schedulability under preemptable spin locks for $m = 8$, $U = 0.3n$, 8 resources, $rsf = 0.25$, $N^{max} = 15$, and medium critical sections. The schedulability of the considered non-preemptable lock types in this configuration is shown in Fig. 1069.

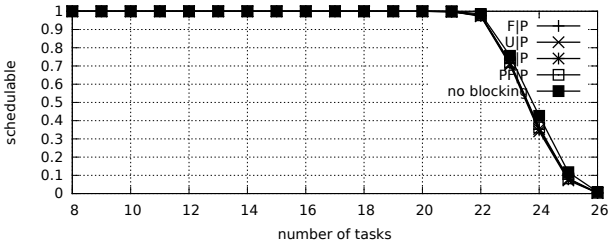

Fig. 1080. Schedulability under preemptable spin locks for $m = 8$, $U = 0.3n$, 8 resources, $rsf = 0.25$, $N^{max} = 1$, and short critical sections. The schedulability of the considered non-preemptable lock types in this configuration is shown in Fig. 1070.

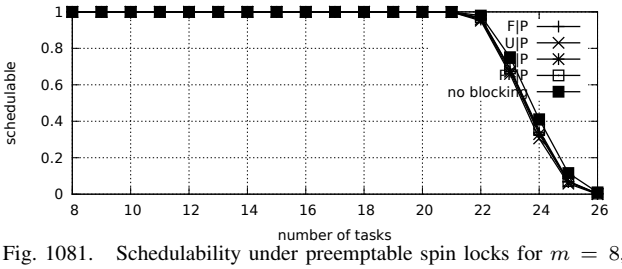

Fig. 1081. Schedulability under preemptable spin locks for $m = 8$, $U = 0.3n$, 8 resources, $rsf = 0.25$, $N^{max} = 2$, and short critical sections. The schedulability of the considered non-preemptable lock types in this configuration is shown in Fig. 1071.

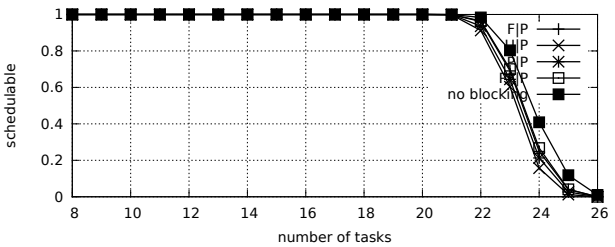

Fig. 1082. Schedulability under preemptable spin locks for $m = 8$, $U = 0.3n$, 8 resources, $rsf = 0.25$, $N^{max} = 5$, and short critical sections. The schedulability of the considered non-preemptable lock types in this configuration is shown in Fig. 1072.

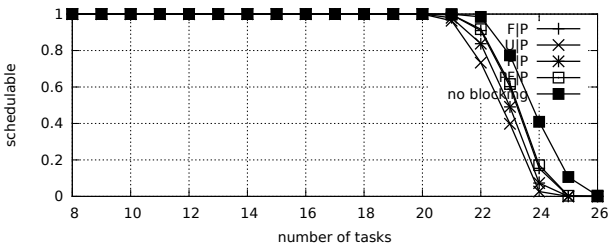

Fig. 1083. Schedulability under preemptable spin locks for $m = 8$, $U = 0.3n$, 8 resources, $rsf = 0.25$, $N^{max} = 10$, and short critical sections. The schedulability of the considered non-preemptable lock types in this configuration is shown in Fig. 1073.

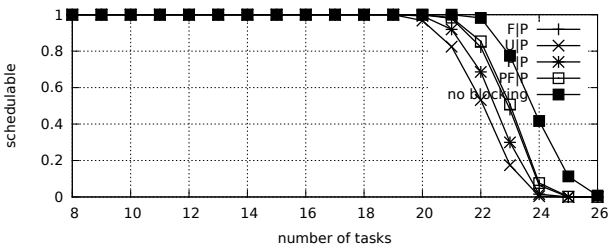

Fig. 1084. Schedulability under preemptable spin locks for $m = 8$, $U = 0.3n$, 8 resources, $rsf = 0.25$, $N^{max} = 15$, and short critical sections. The schedulability of the considered non-preemptable lock types in this configuration is shown in Fig. 1074.

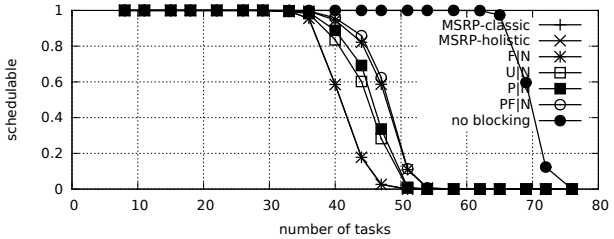

Fig. 1085. Schedulability under non-preemptable spin locks for $m = 8$, $U = 0.1n$, 8 resources, $rsf = 0.4$, $N^{max} = 1$, and medium critical sections. The schedulability of the considered preemptable lock types in this configuration is shown in Fig. 1095.

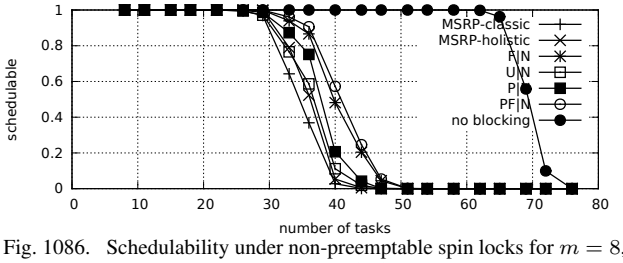

Fig. 1086. Schedulability under non-preemptable spin locks for $m = 8$, $U = 0.1n$, 8 resources, $rsf = 0.4$, $N^{max} = 2$, and medium critical sections. The schedulability of the considered preemptable lock types in this configuration is shown in Fig. 1096.

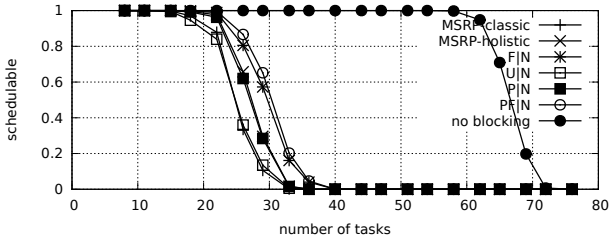

Fig. 1087. Schedulability under non-preemptable spin locks for $m = 8$, $U = 0.1n$, 8 resources, $rsf = 0.4$, $N^{max} = 5$, and medium critical sections. The schedulability of the considered preemptable lock types in this configuration is shown in Fig. 1097.

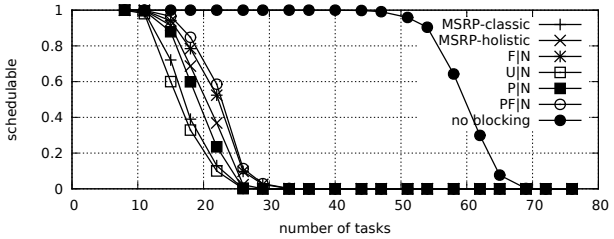

Fig. 1088. Schedulability under non-preemptable spin locks for $m = 8$, $U = 0.1n$, 8 resources, $rsf = 0.4$, $N^{max} = 10$, and medium critical sections. The schedulability of the considered preemptable lock types in this configuration is shown in Fig. 1098.

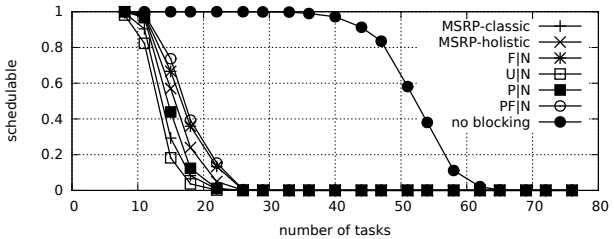

Fig. 1089. Schedulability under non-preemptable spin locks for $m = 8$, $U = 0.1n$, 8 resources, $rsf = 0.4$, $N^{max} = 15$, and medium critical sections. The schedulability of the considered preemptable lock types in this configuration is shown in Fig. 1099.

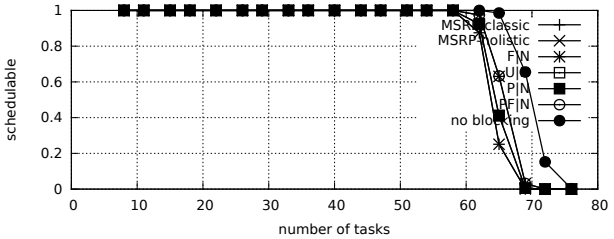

Fig. 1090. Schedulability under non-preemptable spin locks for $m = 8$, $U = 0.1n$, 8 resources, $rsf = 0.4$, $N^{max} = 1$, and short critical sections. The schedulability of the considered preemptable lock types in this configuration is shown in Fig. 1100.

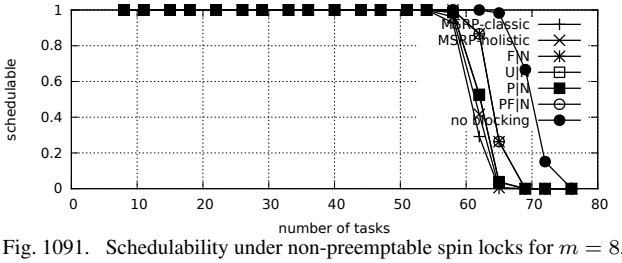

Fig. 1091. Schedulability under non-preemptable spin locks for $m = 8$, $U = 0.1n$, 8 resources, $rsf = 0.4$, $N^{max} = 2$, and short critical sections. The schedulability of the considered preemptable lock types in this configuration is shown in Fig. 1101.

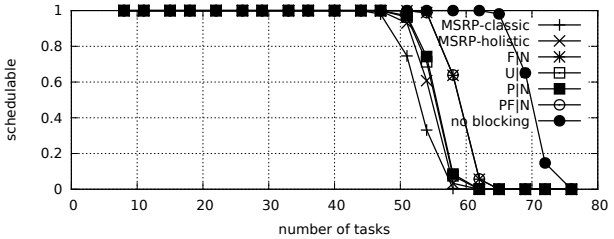

Fig. 1092. Schedulability under non-preemptable spin locks for $m = 8$, $U = 0.1n$, 8 resources, $rsf = 0.4$, $N^{max} = 5$, and short critical sections. The schedulability of the considered preemptable lock types in this configuration is shown in Fig. 1102.

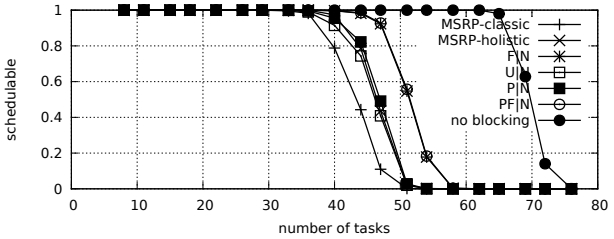

Fig. 1093. Schedulability under non-preemptable spin locks for $m = 8$, $U = 0.1n$, 8 resources, $rsf = 0.4$, $N^{max} = 10$, and short critical sections. The schedulability of the considered preemptable lock types in this configuration is shown in Fig. 1103.

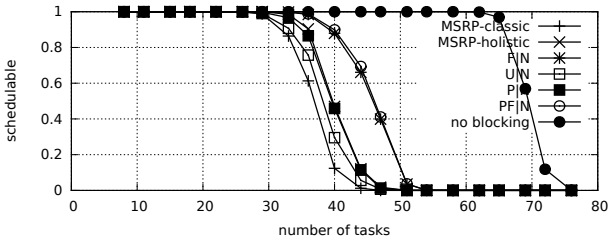

Fig. 1094. Schedulability under non-preemptable spin locks for $m = 8$, $U = 0.1n$, 8 resources, $rsf = 0.4$, $N^{max} = 15$, and short critical sections. The schedulability of the considered preemptable lock types in this configuration is shown in Fig. 1104.

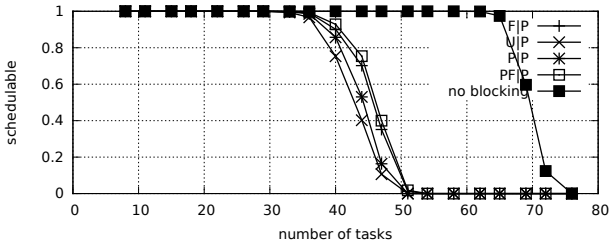

Fig. 1095. Schedulability under preemptable spin locks for $m = 8$, $U = 0.1n$, 8 resources, $rsf = 0.4$, $N^{max} = 1$, and medium critical sections. The schedulability of the considered non-preemptable lock types in this configuration is shown in Fig. 1085.

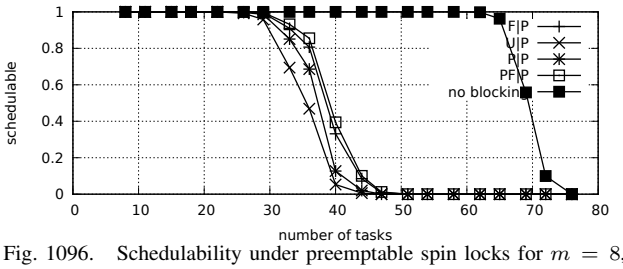

Fig. 1096. Schedulability under preemptable spin locks for $m = 8$, $U = 0.1n$, 8 resources, $rsf = 0.4$, $N^{max} = 2$, and medium critical sections. The schedulability of the considered non-preemptable lock types in this configuration is shown in Fig. 1086.

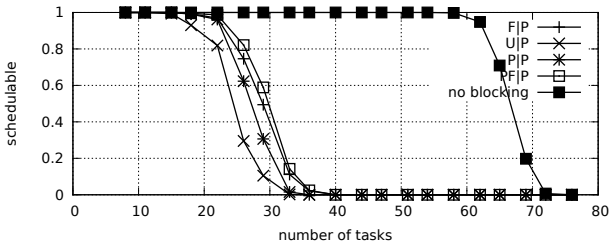

Fig. 1097. Schedulability under preemptable spin locks for $m = 8$, $U = 0.1n$, 8 resources, $rsf = 0.4$, $N^{max} = 5$, and medium critical sections. The schedulability of the considered non-preemptable lock types in this configuration is shown in Fig. 1087.

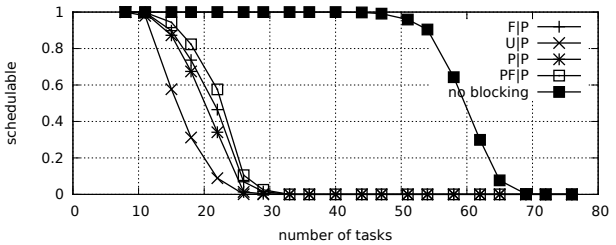

Fig. 1098. Schedulability under preemptable spin locks for $m = 8$, $U = 0.1n$, 8 resources, $rsf = 0.4$, $N^{max} = 10$, and medium critical sections. The schedulability of the considered non-preemptable lock types in this configuration is shown in Fig. 1088.

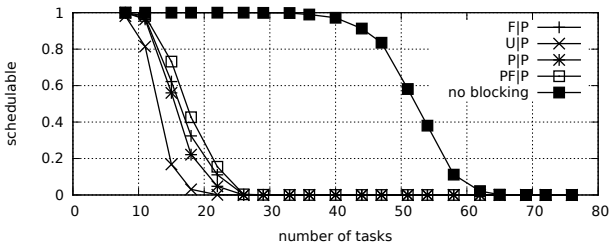

Fig. 1099. Schedulability under preemptable spin locks for $m = 8$, $U = 0.1n$, 8 resources, $rsf = 0.4$, $N^{max} = 15$, and medium critical sections. The schedulability of the considered non-preemptable lock types in this configuration is shown in Fig. 1089.

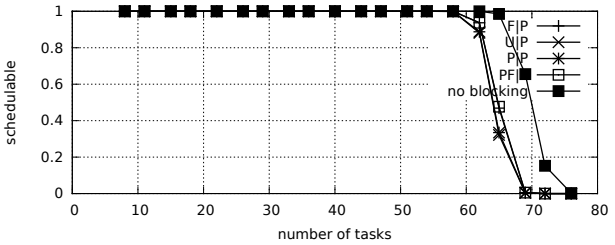

Fig. 1100. Schedulability under preemptable spin locks for $m = 8$, $U = 0.1n$, 8 resources, $rsf = 0.4$, $N^{max} = 1$, and short critical sections. The schedulability of the considered non-preemptable lock types in this configuration is shown in Fig. 1090.

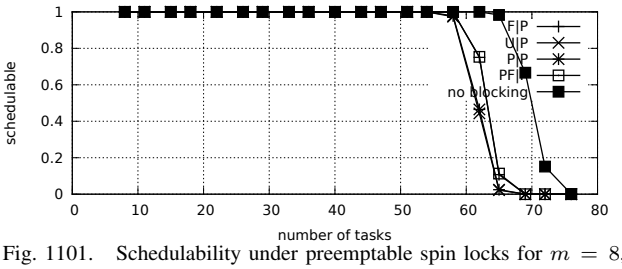

Fig. 1101. Schedulability under preemptable spin locks for $m = 8$, $U = 0.1n$, 8 resources, $rsf = 0.4$, $N^{max} = 2$, and short critical sections. The schedulability of the considered non-preemptable lock types in this configuration is shown in Fig. 1091.

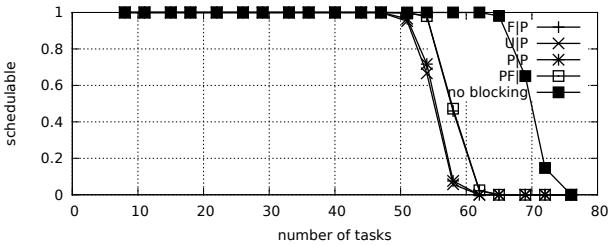

Fig. 1102. Schedulability under preemptable spin locks for $m = 8$, $U = 0.1n$, 8 resources, $rsf = 0.4$, $N^{max} = 5$, and short critical sections. The schedulability of the considered non-preemptable lock types in this configuration is shown in Fig. 1092.

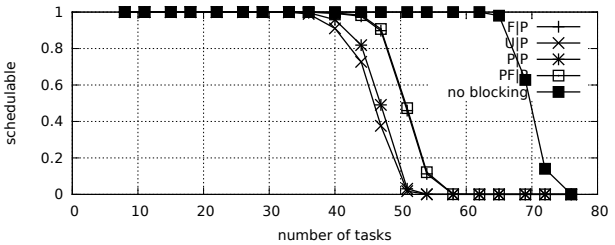

Fig. 1103. Schedulability under preemptable spin locks for $m = 8$, $U = 0.1n$, 8 resources, $rsf = 0.4$, $N^{max} = 10$, and short critical sections. The schedulability of the considered non-preemptable lock types in this configuration is shown in Fig. 1093.

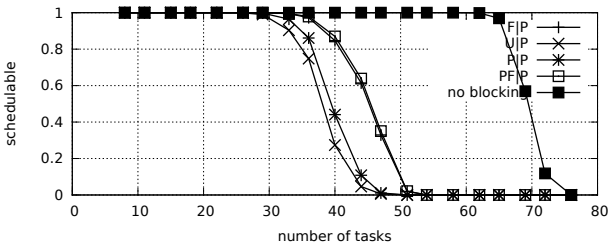

Fig. 1104. Schedulability under preemptable spin locks for $m = 8$, $U = 0.1n$, 8 resources, $rsf = 0.4$, $N^{max} = 15$, and short critical sections. The schedulability of the considered non-preemptable lock types in this configuration is shown in Fig. 1094.

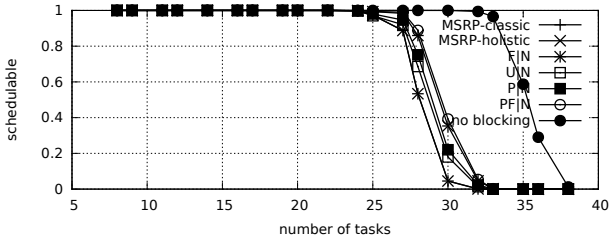

Fig. 1105. Schedulability under non-preemptable spin locks for $m = 8$, $U = 0.2n$, 8 resources, $rsf = 0.4$, $N^{max} = 1$, and medium critical sections. The schedulability of the considered preemptable lock types in this configuration is shown in Fig. 1115.

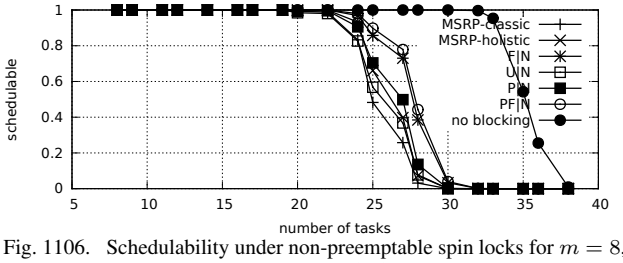

Fig. 1106. Schedulability under non-preemptable spin locks for $m = 8$, $U = 0.2n$, 8 resources, $rsf = 0.4$, $N^{max} = 2$, and medium critical sections. The schedulability of the considered preemptable lock types in this configuration is shown in Fig. 1116.

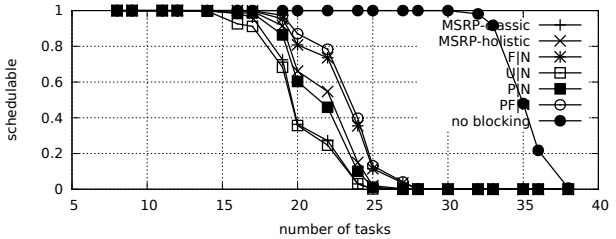

Fig. 1107. Schedulability under non-preemptable spin locks for $m = 8$, $U = 0.2n$, 8 resources, $rsf = 0.4$, $N^{max} = 5$, and medium critical sections. The schedulability of the considered preemptable lock types in this configuration is shown in Fig. 1117.

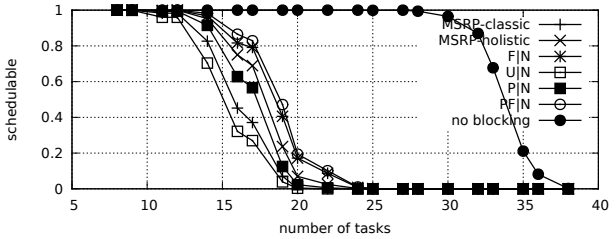

Fig. 1108. Schedulability under non-preemptable spin locks for $m = 8$, $U = 0.2n$, 8 resources, $rsf = 0.4$, $N^{max} = 10$, and medium critical sections. The schedulability of the considered preemptable lock types in this configuration is shown in Fig. 1118.

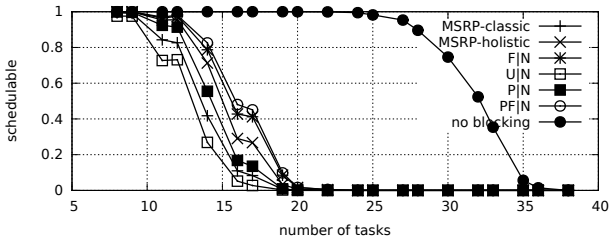

Fig. 1109. Schedulability under non-preemptable spin locks for $m = 8$, $U = 0.2n$, 8 resources, $rsf = 0.4$, $N^{max} = 15$, and medium critical sections. The schedulability of the considered preemptable lock types in this configuration is shown in Fig. 1119.

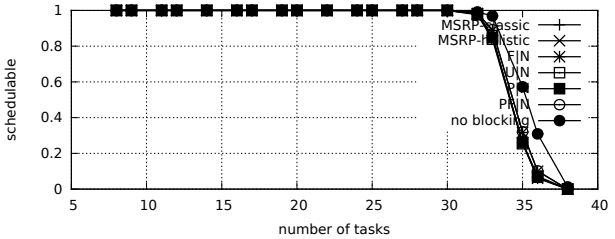

Fig. 1110. Schedulability under non-preemptable spin locks for $m = 8$, $U = 0.2n$, 8 resources, $rsf = 0.4$, $N^{max} = 1$, and short critical sections. The schedulability of the considered preemptable lock types in this configuration is shown in Fig. 1120.

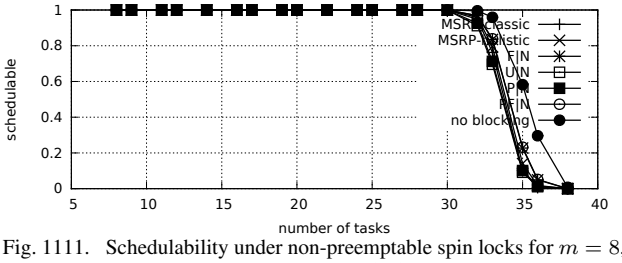

Fig. 1111. Schedulability under non-preemptable spin locks for $m = 8$, $U = 0.2n$, 8 resources, $rsf = 0.4$, $N^{max} = 2$, and short critical sections. The schedulability of the considered preemptable lock types in this configuration is shown in Fig. 1121.

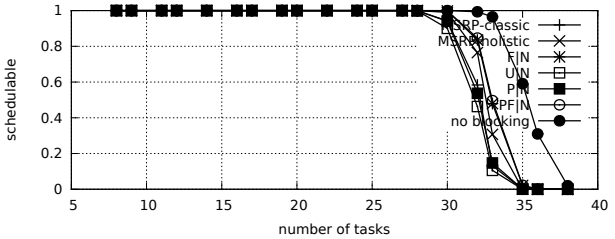

Fig. 1112. Schedulability under non-preemptable spin locks for $m = 8$, $U = 0.2n$, 8 resources, $rsf = 0.4$, $N^{max} = 5$, and short critical sections. The schedulability of the considered preemptable lock types in this configuration is shown in Fig. 1122.

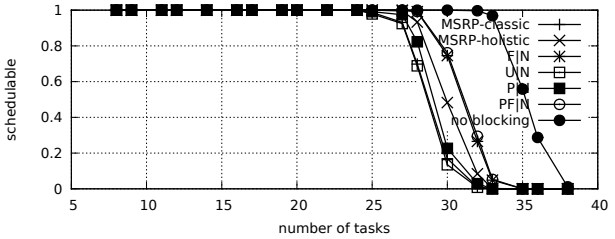

Fig. 1113. Schedulability under non-preemptable spin locks for $m = 8$, $U = 0.2n$, 8 resources, $rsf = 0.4$, $N^{max} = 10$, and short critical sections. The schedulability of the considered preemptable lock types in this configuration is shown in Fig. 1123.

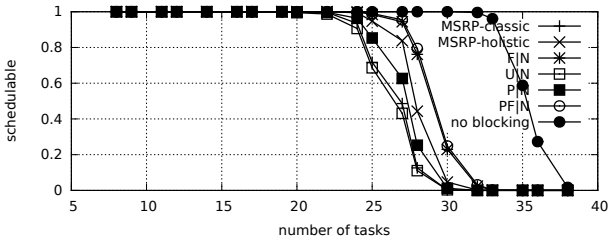

Fig. 1114. Schedulability under non-preemptable spin locks for $m = 8$, $U = 0.2n$, 8 resources, $rsf = 0.4$, $N^{max} = 15$, and short critical sections. The schedulability of the considered preemptable lock types in this configuration is shown in Fig. 1124.

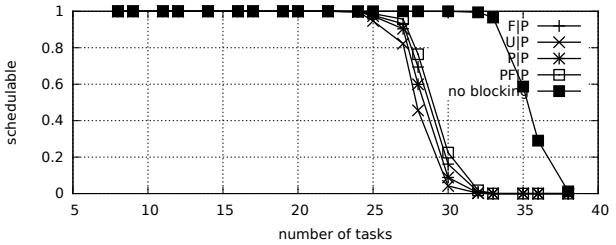

Fig. 1115. Schedulability under preemptable spin locks for $m = 8$, $U = 0.2n$, 8 resources, $rsf = 0.4$, $N^{max} = 1$, and medium critical sections. The schedulability of the considered non-preemptable lock types in this configuration is shown in Fig. 1105.

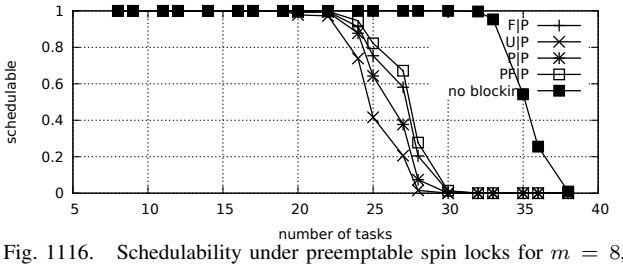

Fig. 1116. Schedulability under preemptable spin locks for $m = 8$, $U = 0.2n$, 8 resources, $rsf = 0.4$, $N^{max} = 2$, and medium critical sections. The schedulability of the considered non-preemptable lock types in this configuration is shown in Fig. 1106.

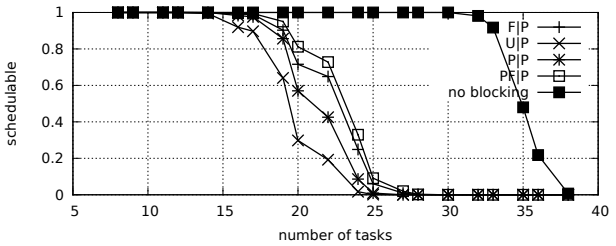

Fig. 1117. Schedulability under preemptable spin locks for $m = 8$, $U = 0.2n$, 8 resources, $rsf = 0.4$, $N^{max} = 5$, and medium critical sections. The schedulability of the considered non-preemptable lock types in this configuration is shown in Fig. 1107.

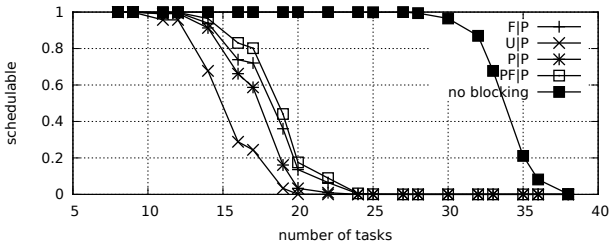

Fig. 1118. Schedulability under preemptable spin locks for $m = 8$, $U = 0.2n$, 8 resources, $rsf = 0.4$, $N^{max} = 10$, and medium critical sections. The schedulability of the considered non-preemptable lock types in this configuration is shown in Fig. 1108.

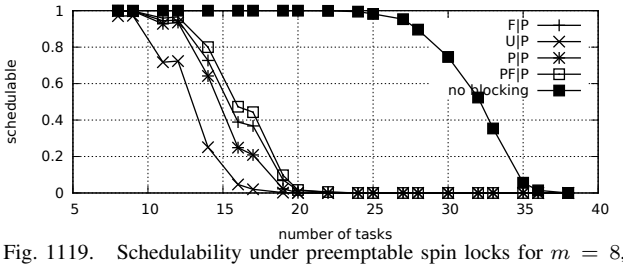

Fig. 1119. Schedulability under preemptable spin locks for $m = 8$, $U = 0.2n$, 8 resources, $rsf = 0.4$, $N^{max} = 15$, and medium critical sections. The schedulability of the considered non-preemptable lock types in this configuration is shown in Fig. 1109.

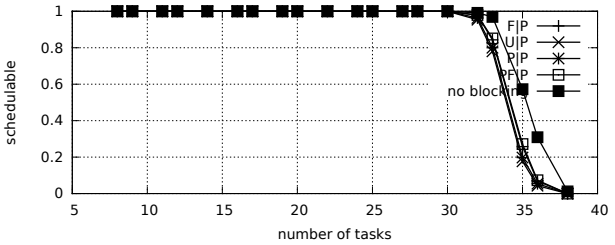

Fig. 1120. Schedulability under preemptable spin locks for $m = 8$, $U = 0.2n$, 8 resources, $rsf = 0.4$, $N^{max} = 1$, and short critical sections. The schedulability of the considered non-preemptable lock types in this configuration is shown in Fig. 1110.

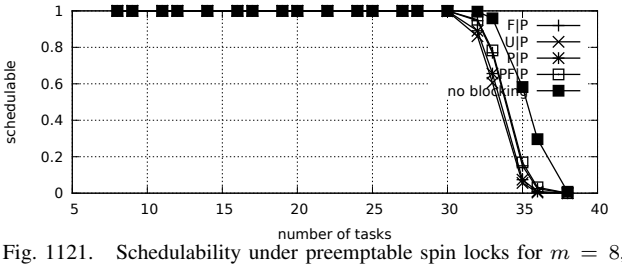

Fig. 1121. Schedulability under preemptable spin locks for $m = 8$, $U = 0.2n$, 8 resources, $rsf = 0.4$, $N^{max} = 2$, and short critical sections. The schedulability of the considered non-preemptable lock types in this configuration is shown in Fig. 1111.

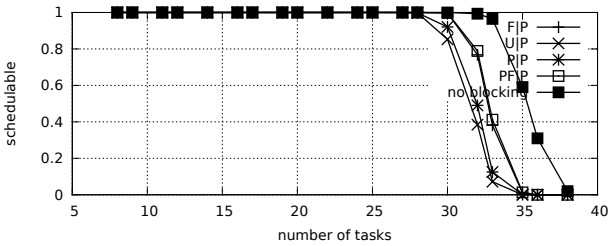

Fig. 1122. Schedulability under preemptable spin locks for $m = 8$, $U = 0.2n$, 8 resources, $rsf = 0.4$, $N^{max} = 5$, and short critical sections. The schedulability of the considered non-preemptable lock types in this configuration is shown in Fig. 1112.

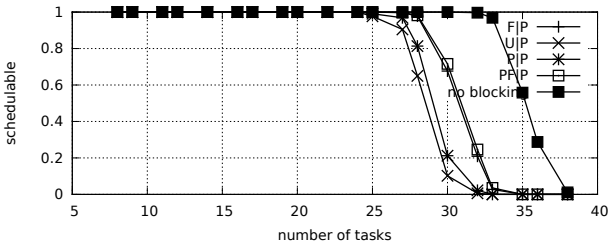

Fig. 1123. Schedulability under preemptable spin locks for $m = 8$, $U = 0.2n$, 8 resources, $rsf = 0.4$, $N^{max} = 10$, and short critical sections. The schedulability of the considered non-preemptable lock types in this configuration is shown in Fig. 1113.

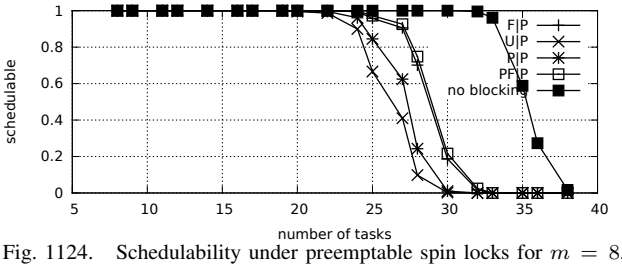

Fig. 1124. Schedulability under preemptable spin locks for $m = 8$, $U = 0.2n$, 8 resources, $rsf = 0.4$, $N^{max} = 15$, and short critical sections. The schedulability of the considered non-preemptable lock types in this configuration is shown in Fig. 1114.

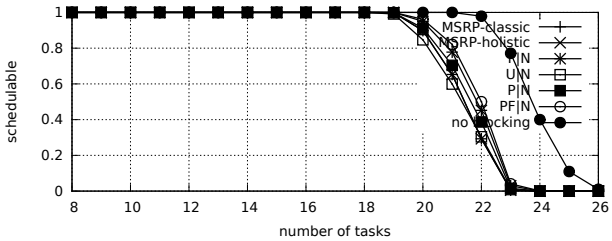

Fig. 1125. Schedulability under non-preemptable spin locks for $m = 8$, $U = 0.3n$, 8 resources, $rsf = 0.4$, $N^{max} = 1$, and medium critical sections. The schedulability of the considered preemptable lock types in this configuration is shown in Fig. 1135.

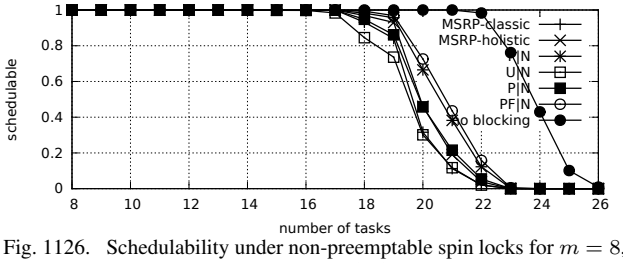

Fig. 1126. Schedulability under non-preemptable spin locks for $m = 8$, $U = 0.3n$, 8 resources, $rsf = 0.4$, $N^{max} = 2$, and medium critical sections. The schedulability of the considered preemptable lock types in this configuration is shown in Fig. 1136.

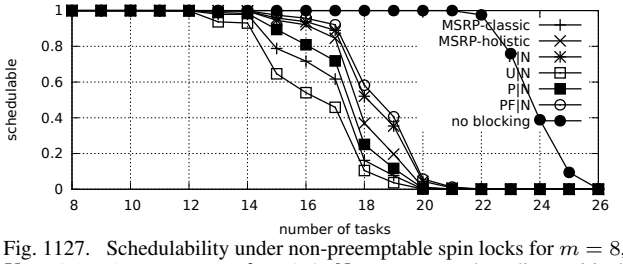

Fig. 1127. Schedulability under non-preemptable spin locks for $m = 8$, $U = 0.3n$, 8 resources, $rsf = 0.4$, $N^{max} = 5$, and medium critical sections. The schedulability of the considered preemptable lock types in this configuration is shown in Fig. 1137.

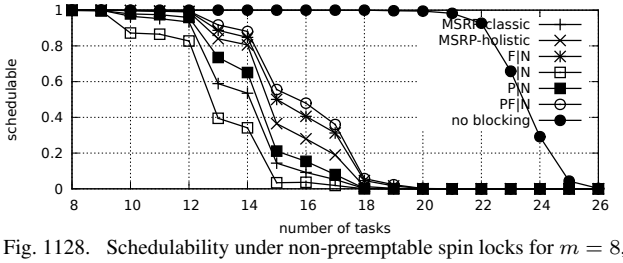

Fig. 1128. Schedulability under non-preemptable spin locks for $m = 8$, $U = 0.3n$, 8 resources, $rsf = 0.4$, $N^{max} = 10$, and medium critical sections. The schedulability of the considered preemptable lock types in this configuration is shown in Fig. 1138.

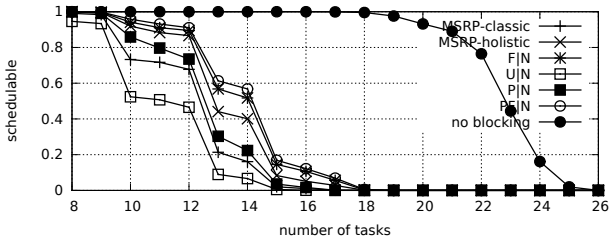

Fig. 1129. Schedulability under non-preemptable spin locks for $m = 8$, $U = 0.3n$, 8 resources, $rsf = 0.4$, $N^{max} = 15$, and medium critical sections. The schedulability of the considered preemptable lock types in this configuration is shown in Fig. 1139.

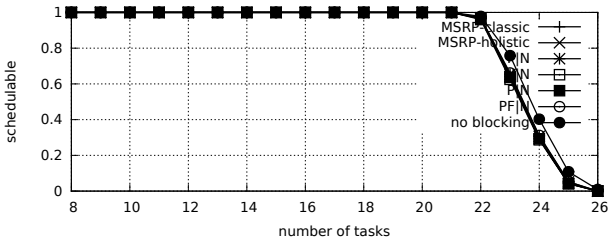

Fig. 1130. Schedulability under non-preemptable spin locks for $m = 8$, $U = 0.3n$, 8 resources, $rsf = 0.4$, $N^{max} = 1$, and short critical sections. The schedulability of the considered preemptable lock types in this configuration is shown in Fig. 1140.

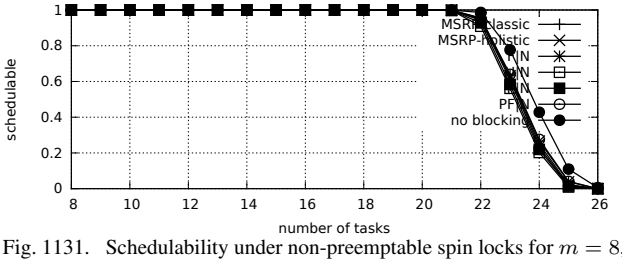

Fig. 1131. Schedulability under non-preemptable spin locks for $m = 8$, $U = 0.3n$, 8 resources, $rsf = 0.4$, $N^{max} = 2$, and short critical sections. The schedulability of the considered preemptable lock types in this configuration is shown in Fig. 1141.

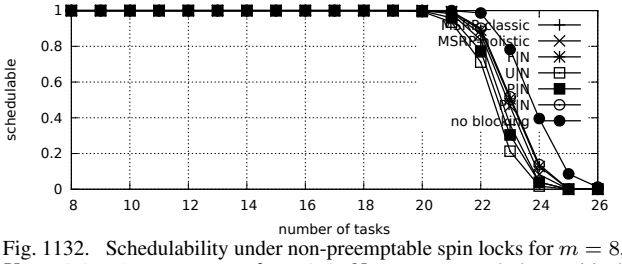

Fig. 1132. Schedulability under non-preemptable spin locks for $m = 8$, $U = 0.3n$, 8 resources, $rsf = 0.4$, $N^{max} = 5$, and short critical sections. The schedulability of the considered preemptable lock types in this configuration is shown in Fig. 1142.

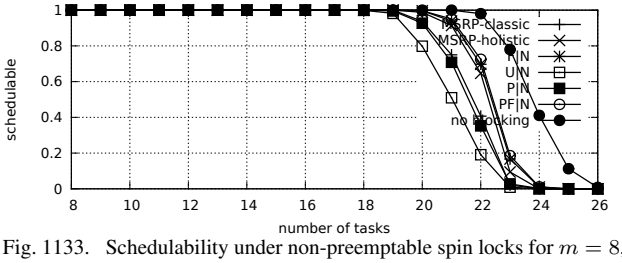

Fig. 1133. Schedulability under non-preemptable spin locks for $m = 8$, $U = 0.3n$, 8 resources, $rsf = 0.4$, $N^{max} = 10$, and short critical sections. The schedulability of the considered preemptable lock types in this configuration is shown in Fig. 1143.

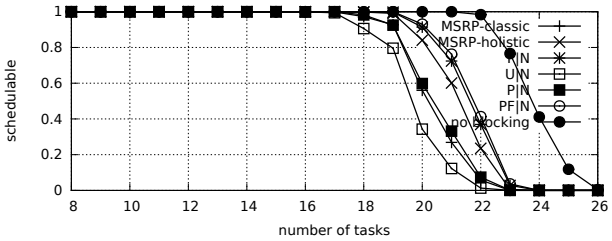

Fig. 1134. Schedulability under non-preemptable spin locks for $m = 8$, $U = 0.3n$, 8 resources, $rsf = 0.4$, $N^{max} = 15$, and short critical sections. The schedulability of the considered preemptable lock types in this configuration is shown in Fig. 1144.

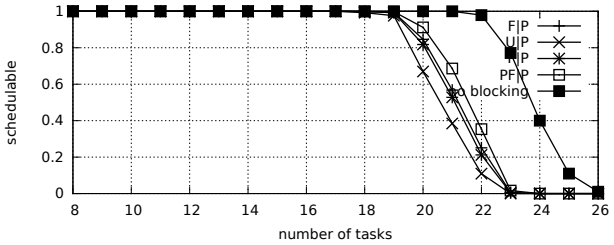

Fig. 1135. Schedulability under preemptable spin locks for $m = 8$, $U = 0.3n$, 8 resources, $rsf = 0.4$, $N^{max} = 1$, and medium critical sections. The schedulability of the considered non-preemptable lock types in this configuration is shown in Fig. 1125.

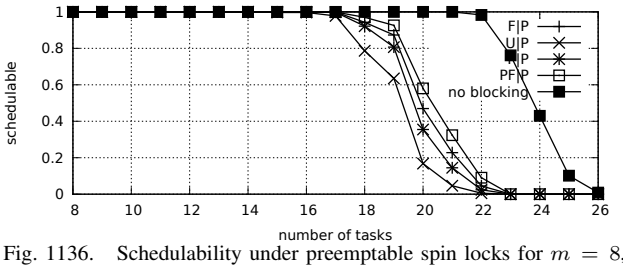

Fig. 1136. Schedulability under preemptable spin locks for $m = 8$, $U = 0.3n$, 8 resources, $rsf = 0.4$, $N^{max} = 2$, and medium critical sections. The schedulability of the considered non-preemptable lock types in this configuration is shown in Fig. 1126.

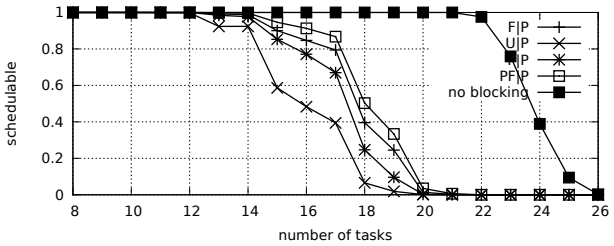

Fig. 1137. Schedulability under preemptable spin locks for $m = 8$, $U = 0.3n$, 8 resources, $rsf = 0.4$, $N^{max} = 5$, and medium critical sections. The schedulability of the considered non-preemptable lock types in this configuration is shown in Fig. 1127.

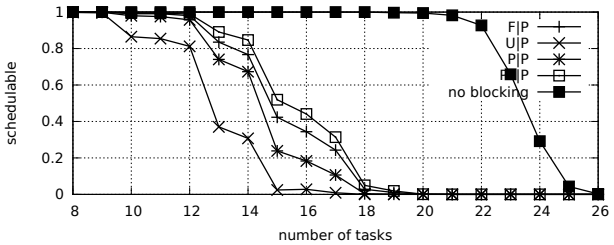

Fig. 1138. Schedulability under preemptable spin locks for $m = 8$, $U = 0.3n$, 8 resources, $rsf = 0.4$, $N^{max} = 10$, and medium critical sections. The schedulability of the considered non-preemptable lock types in this configuration is shown in Fig. 1128.

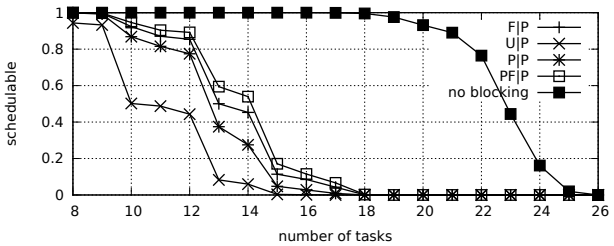

Fig. 1139. Schedulability under preemptable spin locks for $m = 8$, $U = 0.3n$, 8 resources, $rsf = 0.4$, $N^{max} = 15$, and medium critical sections. The schedulability of the considered non-preemptable lock types in this configuration is shown in Fig. 1129.

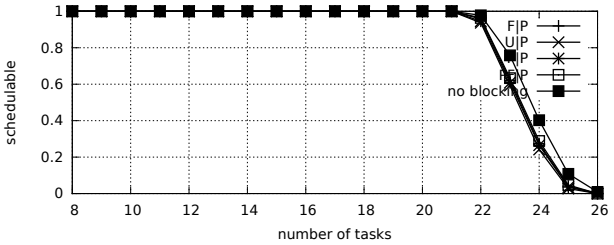

Fig. 1140. Schedulability under preemptable spin locks for $m = 8$, $U = 0.3n$, 8 resources, $rsf = 0.4$, $N^{max} = 1$, and short critical sections. The schedulability of the considered non-preemptable lock types in this configuration is shown in Fig. 1130.

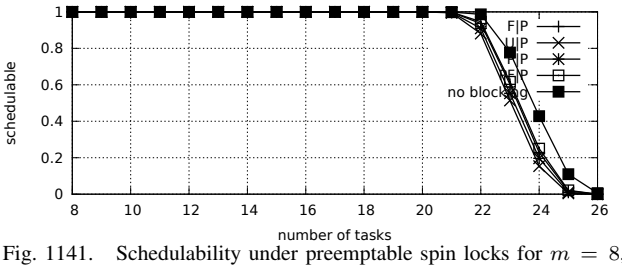

Fig. 1141. Schedulability under preemptable spin locks for $m = 8$, $U = 0.3n$, 8 resources, $rsf = 0.4$, $N^{max} = 2$, and short critical sections. The schedulability of the considered non-preemptable lock types in this configuration is shown in Fig. 1131.

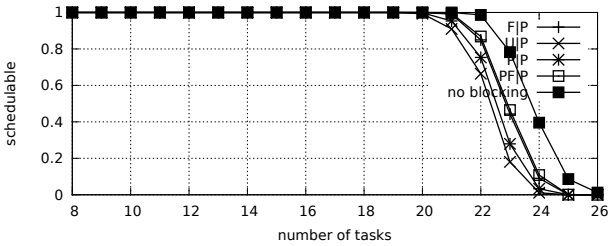

Fig. 1142. Schedulability under preemptable spin locks for $m = 8$, $U = 0.3n$, 8 resources, $rsf = 0.4$, $N^{max} = 5$, and short critical sections. The schedulability of the considered non-preemptable lock types in this configuration is shown in Fig. 1132.

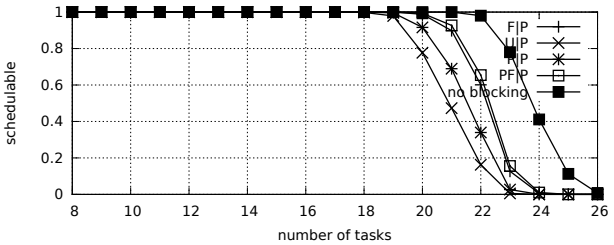

Fig. 1143. Schedulability under preemptable spin locks for $m = 8$, $U = 0.3n$, 8 resources, $rsf = 0.4$, $N^{max} = 10$, and short critical sections. The schedulability of the considered non-preemptable lock types in this configuration is shown in Fig. 1133.

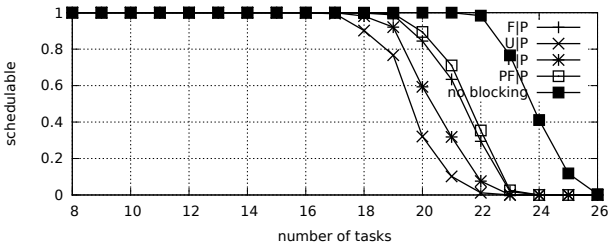

Fig. 1144. Schedulability under preemptable spin locks for $m = 8$, $U = 0.3n$, 8 resources, $rsf = 0.4$, $N^{max} = 15$, and short critical sections. The schedulability of the considered non-preemptable lock types in this configuration is shown in Fig. 1134.

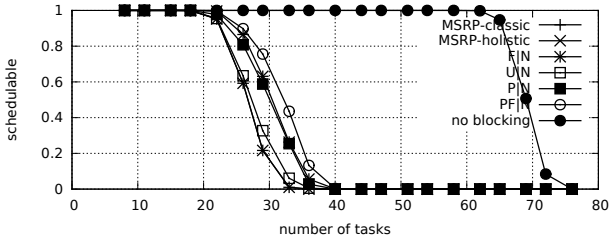

Fig. 1145. Schedulability under non-preemptable spin locks for $m = 8$, $U = 0.1n$, 8 resources, $rsf = 0.75$, $N^{max} = 1$, and medium critical sections. The schedulability of the considered preemptable lock types in this configuration is shown in Fig. 1155.

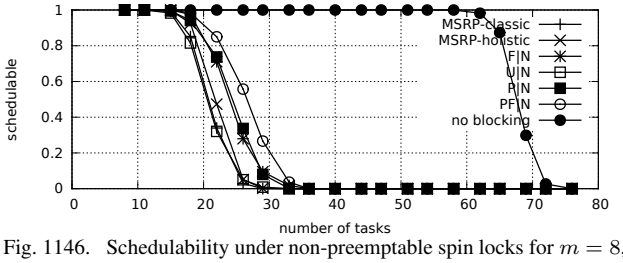

Fig. 1146. Schedulability under non-preemptable spin locks for $m = 8$, $U = 0.1n$, 8 resources, $rsf = 0.75$, $N^{max} = 2$, and medium critical sections. The schedulability of the considered preemptable lock types in this configuration is shown in Fig. 1156.

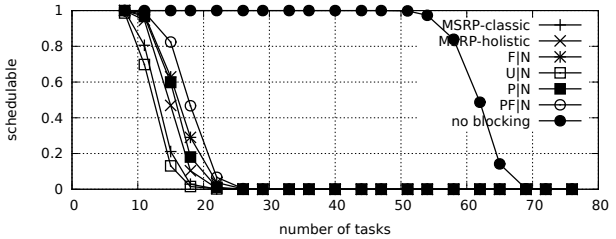

Fig. 1147. Schedulability under non-preemptable spin locks for $m = 8$, $U = 0.1n$, 8 resources, $rsf = 0.75$, $N^{max} = 5$, and medium critical sections. The schedulability of the considered preemptable lock types in this configuration is shown in Fig. 1157.

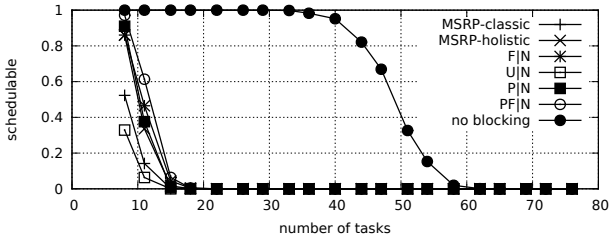

Fig. 1148. Schedulability under non-preemptable spin locks for $m = 8$, $U = 0.1n$, 8 resources, $rsf = 0.75$, $N^{max} = 10$, and medium critical sections. The schedulability of the considered preemptable lock types in this configuration is shown in Fig. 1158.

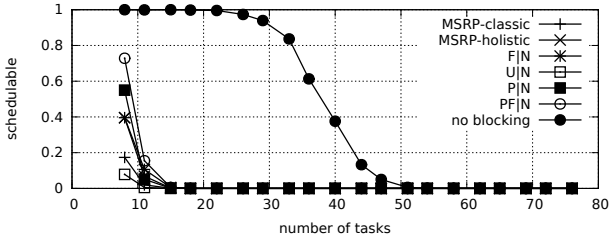

Fig. 1149. Schedulability under non-preemptable spin locks for $m = 8$, $U = 0.1n$, 8 resources, $rsf = 0.75$, $N^{max} = 15$, and medium critical sections. The schedulability of the considered preemptable lock types in this configuration is shown in Fig. 1159.

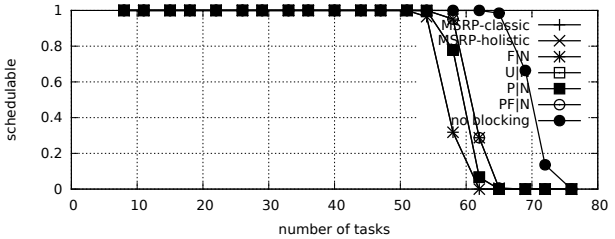

Fig. 1150. Schedulability under non-preemptable spin locks for $m = 8$, $U = 0.1n$, 8 resources, $rsf = 0.75$, $N^{max} = 1$, and short critical sections. The schedulability of the considered preemptable lock types in this configuration is shown in Fig. 1160.

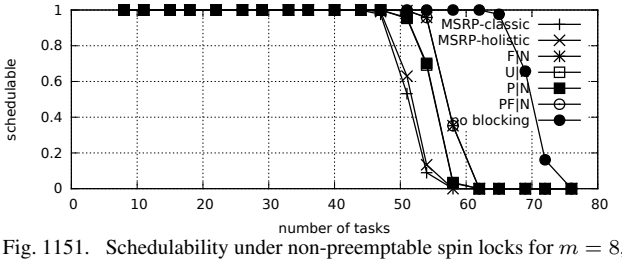

Fig. 1151. Schedulability under non-preemptable spin locks for $m = 8$, $U = 0.1n$, 8 resources, $rsf = 0.75$, $N^{max} = 2$, and short critical sections. The schedulability of the considered preemptable lock types in this configuration is shown in Fig. 1161.

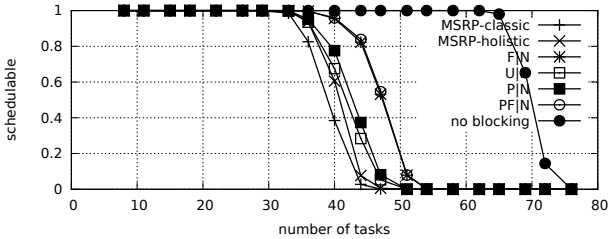

Fig. 1152. Schedulability under non-preemptable spin locks for $m = 8$, $U = 0.1n$, 8 resources, $rsf = 0.75$, $N^{max} = 5$, and short critical sections. The schedulability of the considered preemptable lock types in this configuration is shown in Fig. 1162.

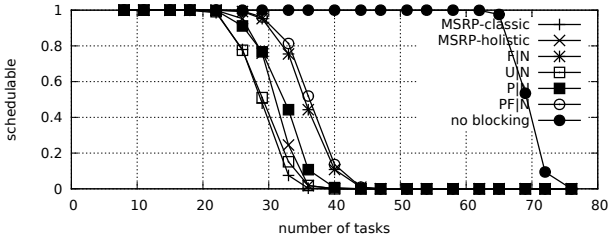

Fig. 1153. Schedulability under non-preemptable spin locks for $m = 8$, $U = 0.1n$, 8 resources, $rsf = 0.75$, $N^{max} = 10$, and short critical sections. The schedulability of the considered preemptable lock types in this configuration is shown in Fig. 1163.

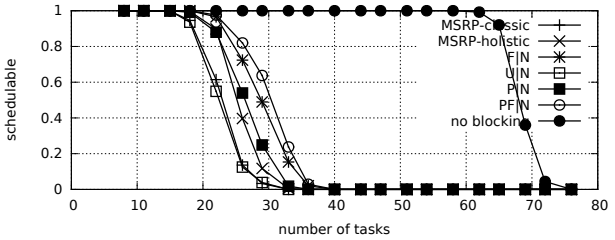

Fig. 1154. Schedulability under non-preemptable spin locks for $m = 8$, $U = 0.1n$, 8 resources, $rsf = 0.75$, $N^{max} = 15$, and short critical sections. The schedulability of the considered preemptable lock types in this configuration is shown in Fig. 1164.

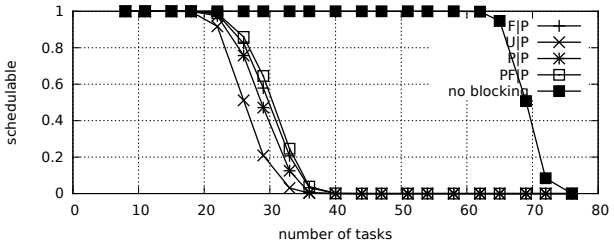

Fig. 1155. Schedulability under preemptable spin locks for $m = 8$, $U = 0.1n$, 8 resources, $rsf = 0.75$, $N^{max} = 1$, and medium critical sections. The schedulability of the considered non-preemptable lock types in this configuration is shown in Fig. 1145.

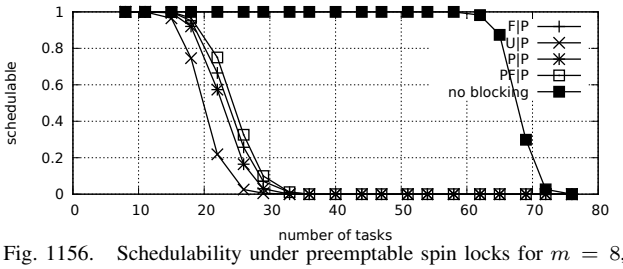

Fig. 1156. Schedulability under preemptable spin locks for $m = 8$, $U = 0.1n$, 8 resources, $rsf = 0.75$, $N^{max} = 2$, and medium critical sections. The schedulability of the considered non-preemptable lock types in this configuration is shown in Fig. 1146.

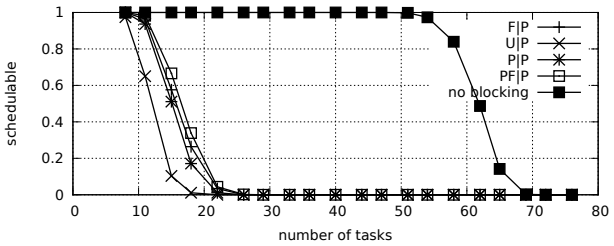

Fig. 1157. Schedulability under preemptable spin locks for $m = 8$, $U = 0.1n$, 8 resources, $rsf = 0.75$, $N^{max} = 5$, and medium critical sections. The schedulability of the considered non-preemptable lock types in this configuration is shown in Fig. 1147.

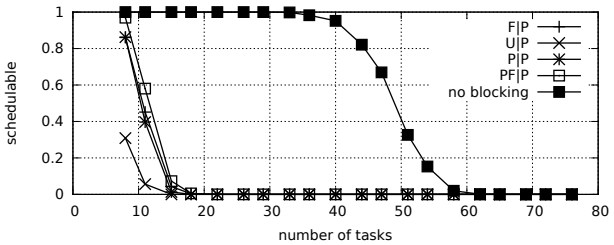

Fig. 1158. Schedulability under preemptable spin locks for $m = 8$, $U = 0.1n$, 8 resources, $rsf = 0.75$, $N^{max} = 10$, and medium critical sections. The schedulability of the considered non-preemptable lock types in this configuration is shown in Fig. 1148.

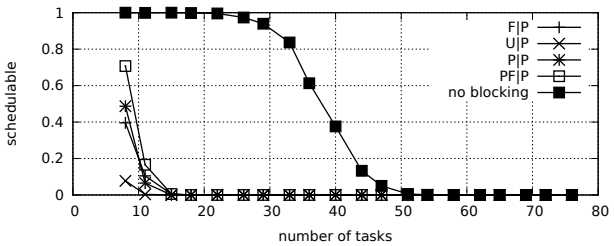

Fig. 1159. Schedulability under preemptable spin locks for $m = 8$, $U = 0.1n$, 8 resources, $rsf = 0.75$, $N^{max} = 15$, and medium critical sections. The schedulability of the considered non-preemptable lock types in this configuration is shown in Fig. 1149.

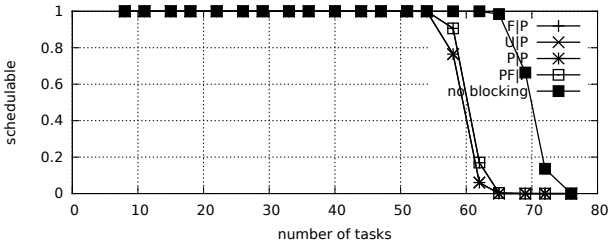

Fig. 1160. Schedulability under preemptable spin locks for $m = 8$, $U = 0.1n$, 8 resources, $rsf = 0.75$, $N^{max} = 1$, and short critical sections. The schedulability of the considered non-preemptable lock types in this configuration is shown in Fig. 1150.

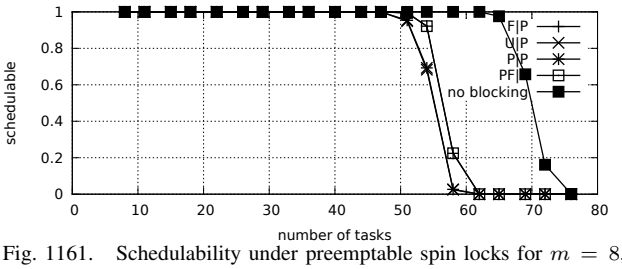

Fig. 1161. Schedulability under preemptable spin locks for $m = 8$, $U = 0.1n$, 8 resources, $rsf = 0.75$, $N^{max} = 2$, and short critical sections. The schedulability of the considered non-preemptable lock types in this configuration is shown in Fig. 1151.

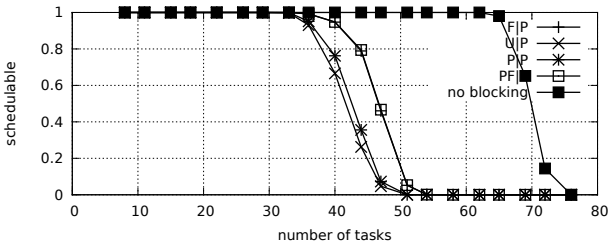

Fig. 1162. Schedulability under preemptable spin locks for $m = 8$, $U = 0.1n$, 8 resources, $rsf = 0.75$, $N^{max} = 5$, and short critical sections. The schedulability of the considered non-preemptable lock types in this configuration is shown in Fig. 1152.

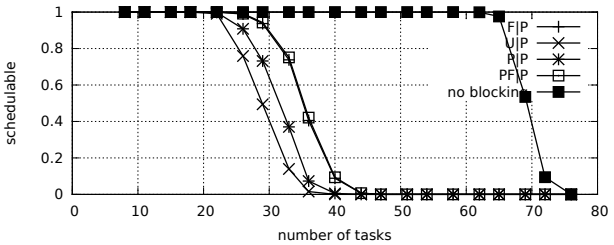

Fig. 1163. Schedulability under preemptable spin locks for $m = 8$, $U = 0.1n$, 8 resources, $rsf = 0.75$, $N^{max} = 10$, and short critical sections. The schedulability of the considered non-preemptable lock types in this configuration is shown in Fig. 1153.

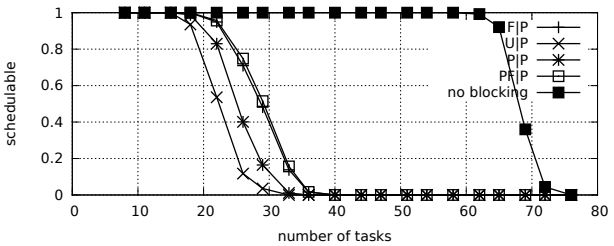

Fig. 1164. Schedulability under preemptable spin locks for $m = 8$, $U = 0.1n$, 8 resources, $rsf = 0.75$, $N^{max} = 15$, and short critical sections. The schedulability of the considered non-preemptable lock types in this configuration is shown in Fig. 1154.

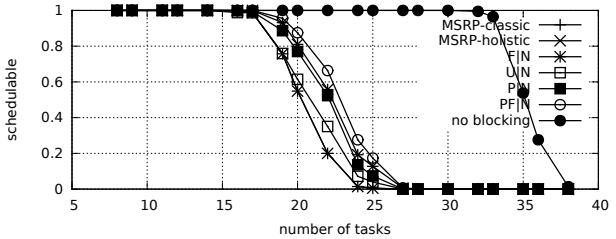

Fig. 1165. Schedulability under non-preemptable spin locks for $m = 8$, $U = 0.2n$, 8 resources, $rsf = 0.75$, $N^{max} = 1$, and medium critical sections. The schedulability of the considered preemptable lock types in this configuration is shown in Fig. 1175.

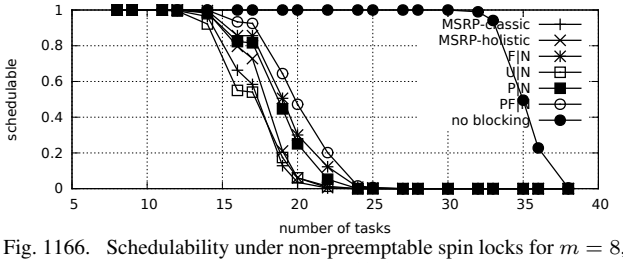

Fig. 1166. Schedulability under non-preemptable spin locks for $m = 8$, $U = 0.2n$, 8 resources, $rsf = 0.75$, $N^{max} = 2$, and medium critical sections. The schedulability of the considered preemptable lock types in this configuration is shown in Fig. 1176.

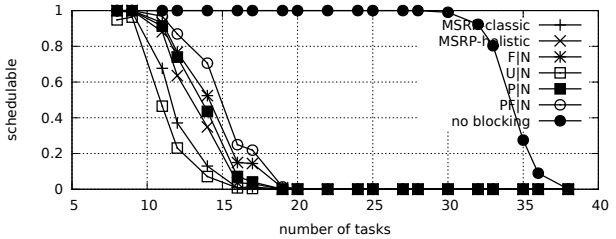

Fig. 1167. Schedulability under non-preemptable spin locks for $m = 8$, $U = 0.2n$, 8 resources, $rsf = 0.75$, $N^{max} = 5$, and medium critical sections. The schedulability of the considered preemptable lock types in this configuration is shown in Fig. 1177.

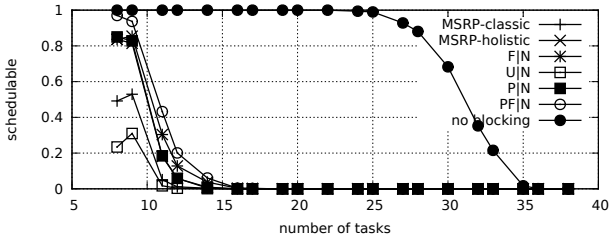

Fig. 1168. Schedulability under non-preemptable spin locks for $m = 8$, $U = 0.2n$, 8 resources, $rsf = 0.75$, $N^{max} = 10$, and medium critical sections. The schedulability of the considered preemptable lock types in this configuration is shown in Fig. 1178.

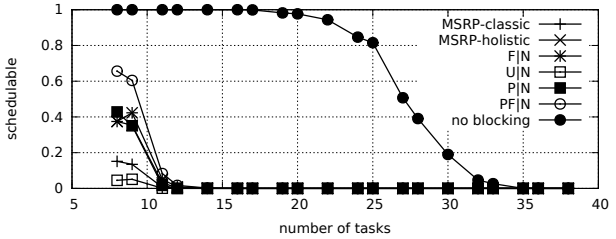

Fig. 1169. Schedulability under non-preemptable spin locks for $m = 8$, $U = 0.2n$, 8 resources, $rsf = 0.75$, $N^{max} = 15$, and medium critical sections. The schedulability of the considered preemptable lock types in this configuration is shown in Fig. 1179.

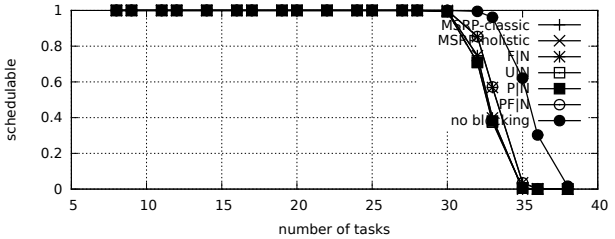

Fig. 1170. Schedulability under non-preemptable spin locks for $m = 8$, $U = 0.2n$, 8 resources, $rsf = 0.75$, $N^{max} = 1$, and short critical sections. The schedulability of the considered preemptable lock types in this configuration is shown in Fig. 1180.

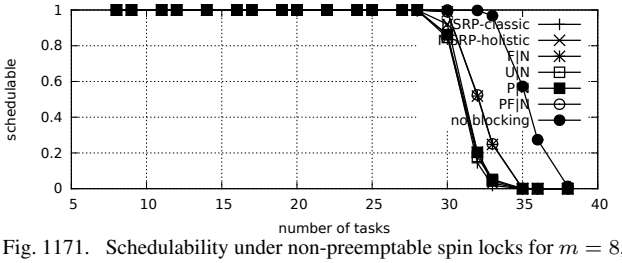

Fig. 1171. Schedulability under non-preemptable spin locks for $m = 8$, $U = 0.2n$, 8 resources, $rsf = 0.75$, $N^{max} = 2$, and short critical sections. The schedulability of the considered preemptable lock types in this configuration is shown in Fig. 1181.

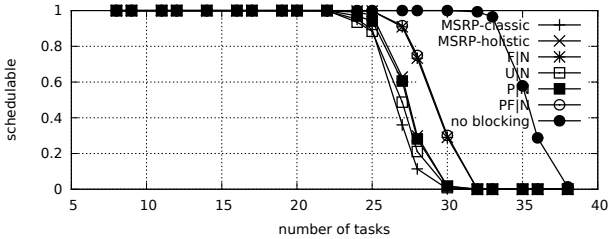

Fig. 1172. Schedulability under non-preemptable spin locks for $m = 8$, $U = 0.2n$, 8 resources, $rsf = 0.75$, $N^{max} = 5$, and short critical sections. The schedulability of the considered preemptable lock types in this configuration is shown in Fig. 1182.

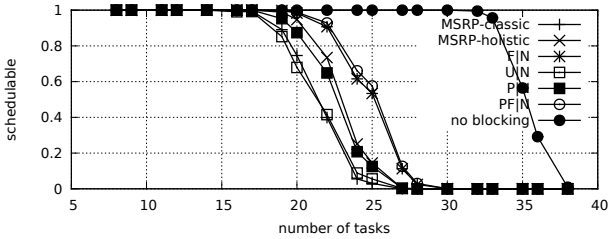

Fig. 1173. Schedulability under non-preemptable spin locks for $m = 8$, $U = 0.2n$, 8 resources, $rsf = 0.75$, $N^{max} = 10$, and short critical sections. The schedulability of the considered preemptable lock types in this configuration is shown in Fig. 1183.

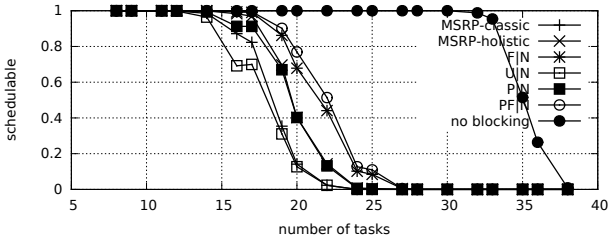

Fig. 1174. Schedulability under non-preemptable spin locks for $m = 8$, $U = 0.2n$, 8 resources, $rsf = 0.75$, $N^{max} = 15$, and short critical sections. The schedulability of the considered preemptable lock types in this configuration is shown in Fig. 1184.

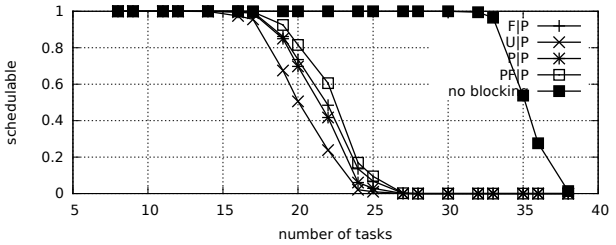

Fig. 1175. Schedulability under preemptable spin locks for $m = 8$, $U = 0.2n$, 8 resources, $rsf = 0.75$, $N^{max} = 1$, and medium critical sections. The schedulability of the considered non-preemptable lock types in this configuration is shown in Fig. 1165.

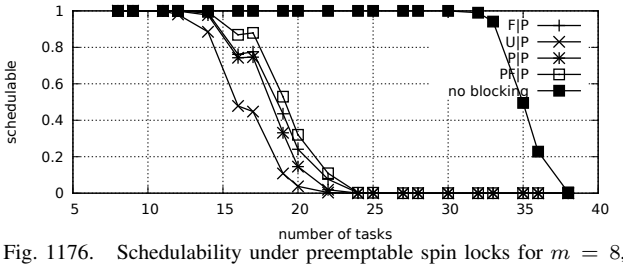

Fig. 1176. Schedulability under preemptable spin locks for $m = 8$, $U = 0.2n$, 8 resources, $rsf = 0.75$, $N^{max} = 2$, and medium critical sections. The schedulability of the considered non-preemptable lock types in this configuration is shown in Fig. 1166.

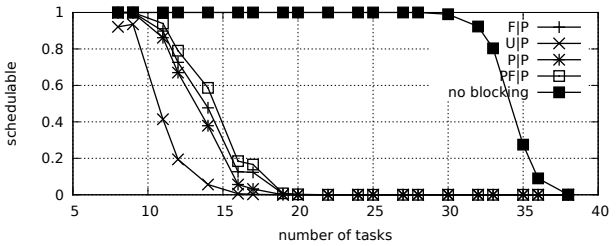

Fig. 1177. Schedulability under preemptable spin locks for $m = 8$, $U = 0.2n$, 8 resources, $rsf = 0.75$, $N^{max} = 5$, and medium critical sections. The schedulability of the considered non-preemptable lock types in this configuration is shown in Fig. 1167.

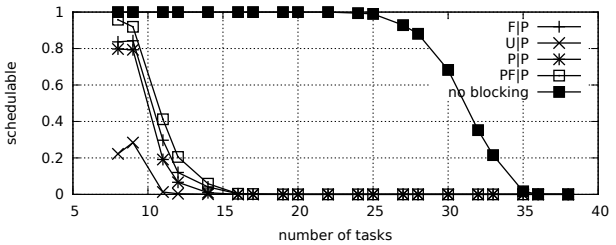

Fig. 1178. Schedulability under preemptable spin locks for $m = 8$, $U = 0.2n$, 8 resources, $rsf = 0.75$, $N^{max} = 10$, and medium critical sections. The schedulability of the considered non-preemptable lock types in this configuration is shown in Fig. 1168.

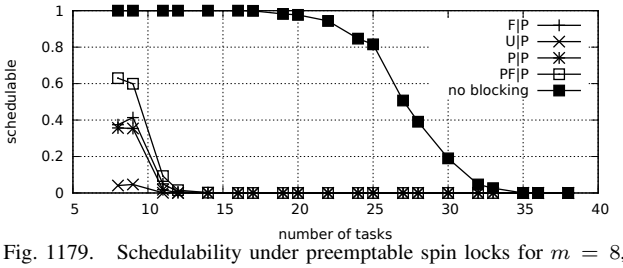

Fig. 1179. Schedulability under preemptable spin locks for $m = 8$, $U = 0.2n$, 8 resources, $rsf = 0.75$, $N^{max} = 15$, and medium critical sections. The schedulability of the considered non-preemptable lock types in this configuration is shown in Fig. 1169.

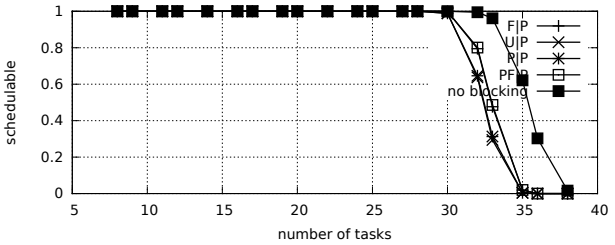

Fig. 1180. Schedulability under preemptable spin locks for $m = 8$, $U = 0.2n$, 8 resources, $rsf = 0.75$, $N^{max} = 1$, and short critical sections. The schedulability of the considered non-preemptable lock types in this configuration is shown in Fig. 1170.

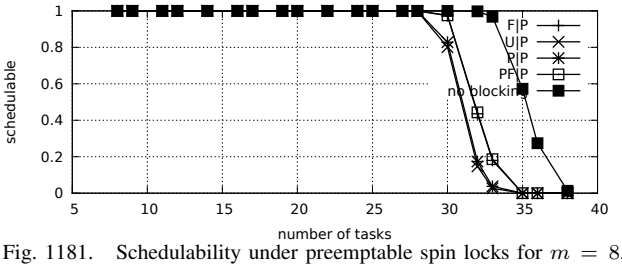

Fig. 1181. Schedulability under preemptable spin locks for $m = 8$, $U = 0.2n$, 8 resources, $rsf = 0.75$, $N^{max} = 2$, and short critical sections. The schedulability of the considered non-preemptable lock types in this configuration is shown in Fig. 1171.

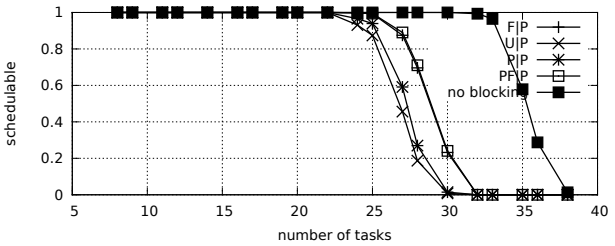

Fig. 1182. Schedulability under preemptable spin locks for $m = 8$, $U = 0.2n$, 8 resources, $rsf = 0.75$, $N^{max} = 5$, and short critical sections. The schedulability of the considered non-preemptable lock types in this configuration is shown in Fig. 1172.

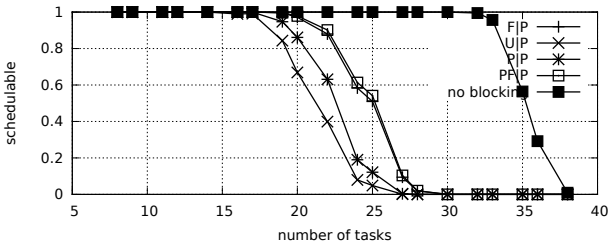

Fig. 1183. Schedulability under preemptable spin locks for $m = 8$, $U = 0.2n$, 8 resources, $rsf = 0.75$, $N^{max} = 10$, and short critical sections. The schedulability of the considered non-preemptable lock types in this configuration is shown in Fig. 1173.

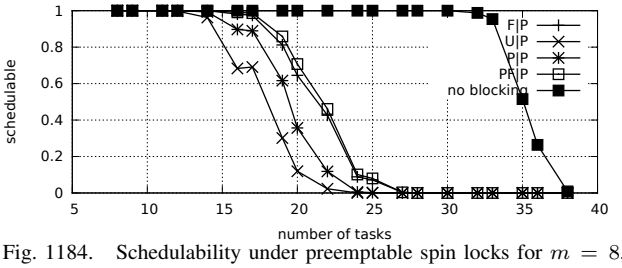

Fig. 1184. Schedulability under preemptable spin locks for $m = 8$, $U = 0.2n$, 8 resources, $rsf = 0.75$, $N^{max} = 15$, and short critical sections. The schedulability of the considered non-preemptable lock types in this configuration is shown in Fig. 1174.

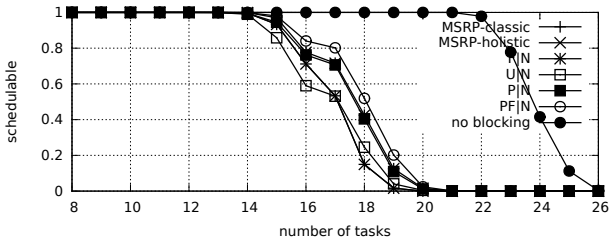

Fig. 1185. Schedulability under non-preemptable spin locks for $m = 8$, $U = 0.3n$, 8 resources, $rsf = 0.75$, $N^{max} = 1$, and medium critical sections. The schedulability of the considered preemptable lock types in this configuration is shown in Fig. 1195.

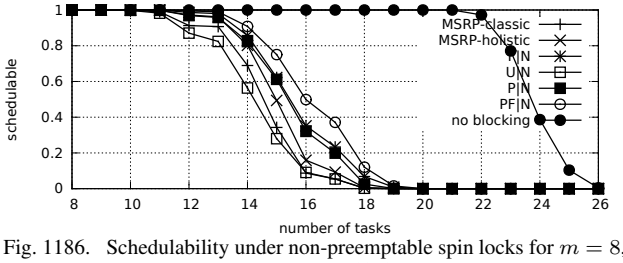

Fig. 1186. Schedulability under non-preemptable spin locks for $m = 8$, $U = 0.3n$, 8 resources, $rsf = 0.75$, $N^{max} = 2$, and medium critical sections. The schedulability of the considered preemptable lock types in this configuration is shown in Fig. 1196.

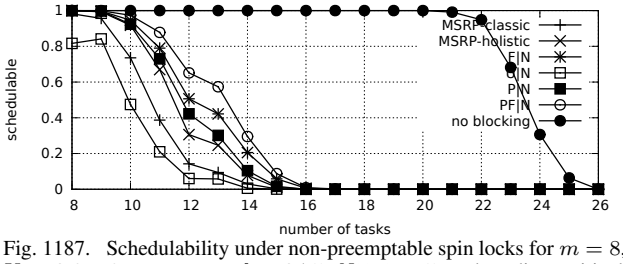

Fig. 1187. Schedulability under non-preemptable spin locks for $m = 8$, $U = 0.3n$, 8 resources, $rsf = 0.75$, $N^{max} = 5$, and medium critical sections. The schedulability of the considered preemptable lock types in this configuration is shown in Fig. 1197.

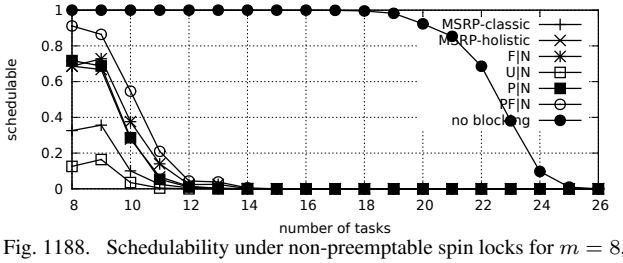

Fig. 1188. Schedulability under non-preemptable spin locks for $m = 8$, $U = 0.3n$, 8 resources, $rsf = 0.75$, $N^{max} = 10$, and medium critical sections. The schedulability of the considered preemptable lock types in this configuration is shown in Fig. 1198.

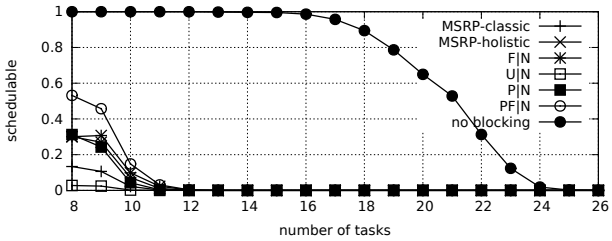

Fig. 1189. Schedulability under non-preemptable spin locks for $m = 8$, $U = 0.3n$, 8 resources, $rsf = 0.75$, $N^{max} = 15$, and medium critical sections. The schedulability of the considered preemptable lock types in this configuration is shown in Fig. 1199.

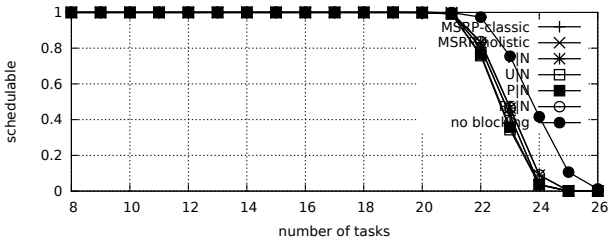

Fig. 1190. Schedulability under non-preemptable spin locks for $m = 8$, $U = 0.3n$, 8 resources, $rsf = 0.75$, $N^{max} = 1$, and short critical sections. The schedulability of the considered preemptable lock types in this configuration is shown in Fig. 1200.

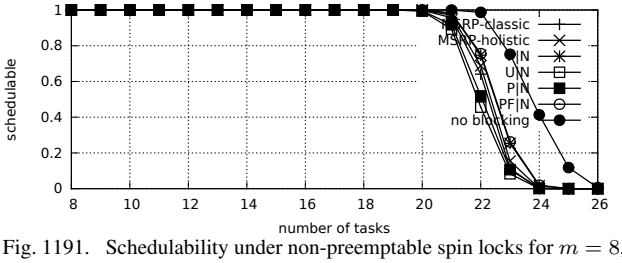

Fig. 1191. Schedulability under non-preemptable spin locks for $m = 8$, $U = 0.3n$, 8 resources, $rsf = 0.75$, $N^{max} = 2$, and short critical sections. The schedulability of the considered preemptable lock types in this configuration is shown in Fig. 1201.

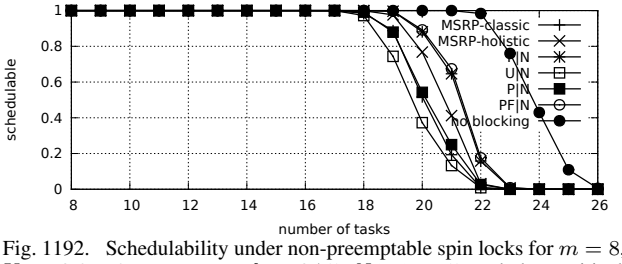

Fig. 1192. Schedulability under non-preemptable spin locks for $m = 8$, $U = 0.3n$, 8 resources, $rsf = 0.75$, $N^{max} = 5$, and short critical sections. The schedulability of the considered preemptable lock types in this configuration is shown in Fig. 1202.

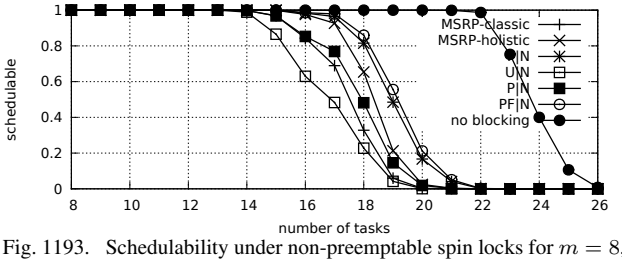

Fig. 1193. Schedulability under non-preemptable spin locks for $m = 8$, $U = 0.3n$, 8 resources, $rsf = 0.75$, $N^{max} = 10$, and short critical sections. The schedulability of the considered preemptable lock types in this configuration is shown in Fig. 1203.

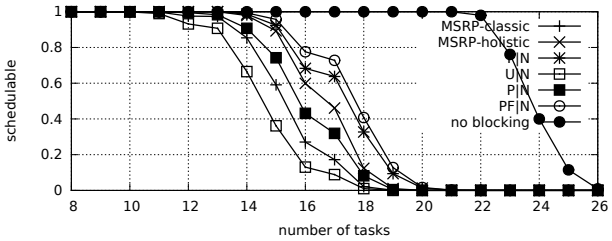

Fig. 1194. Schedulability under non-preemptable spin locks for $m = 8$, $U = 0.3n$, 8 resources, $rsf = 0.75$, $N^{max} = 15$, and short critical sections. The schedulability of the considered preemptable lock types in this configuration is shown in Fig. 1204.

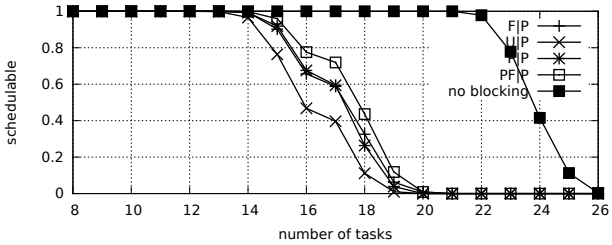

Fig. 1195. Schedulability under preemptable spin locks for $m = 8$, $U = 0.3n$, 8 resources, $rsf = 0.75$, $N^{max} = 1$, and medium critical sections. The schedulability of the considered non-preemptable lock types in this configuration is shown in Fig. 1185.

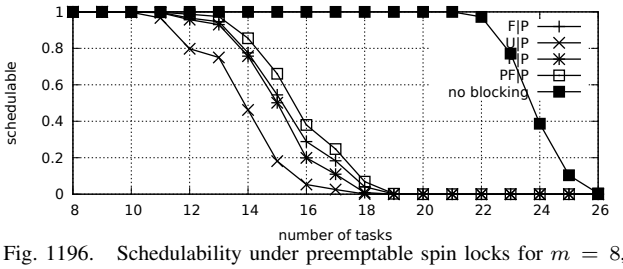

Fig. 1196. Schedulability under preemptable spin locks for $m = 8$, $U = 0.3n$, 8 resources, $rsf = 0.75$, $N^{max} = 2$, and medium critical sections. The schedulability of the considered non-preemptable lock types in this configuration is shown in Fig. 1186.

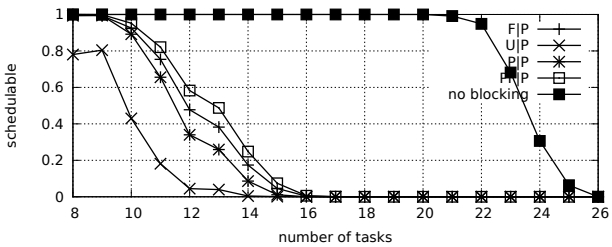

Fig. 1197. Schedulability under preemptable spin locks for $m = 8$, $U = 0.3n$, 8 resources, $rsf = 0.75$, $N^{max} = 5$, and medium critical sections. The schedulability of the considered non-preemptable lock types in this configuration is shown in Fig. 1187.

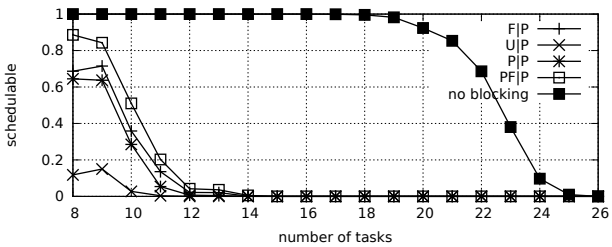

Fig. 1198. Schedulability under preemptable spin locks for $m = 8$, $U = 0.3n$, 8 resources, $rsf = 0.75$, $N^{max} = 10$, and medium critical sections. The schedulability of the considered non-preemptable lock types in this configuration is shown in Fig. 1188.

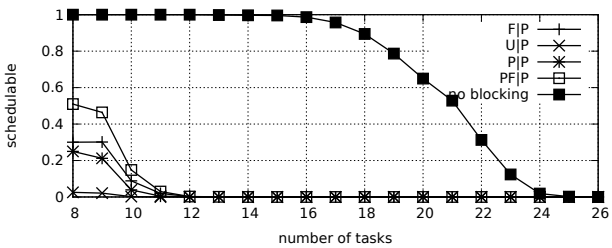

Fig. 1199. Schedulability under preemptable spin locks for $m = 8$, $U = 0.3n$, 8 resources, $rsf = 0.75$, $N^{max} = 15$, and medium critical sections. The schedulability of the considered non-preemptable lock types in this configuration is shown in Fig. 1189.

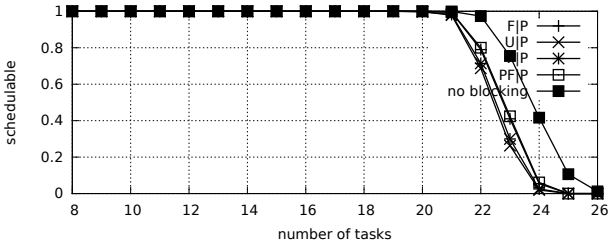

Fig. 1200. Schedulability under preemptable spin locks for $m = 8$, $U = 0.3n$, 8 resources, $rsf = 0.75$, $N^{max} = 1$, and short critical sections. The schedulability of the considered non-preemptable lock types in this configuration is shown in Fig. 1190.

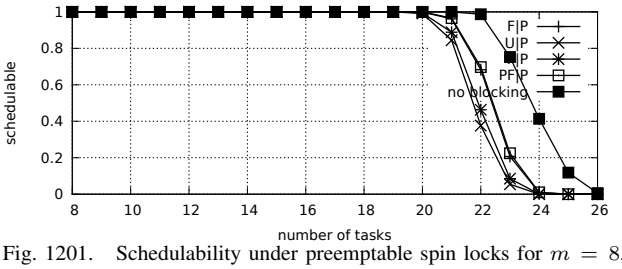

Fig. 1201. Schedulability under preemptable spin locks for $m = 8$, $U = 0.3n$, 8 resources, $rsf = 0.75$, $N^{max} = 2$, and short critical sections. The schedulability of the considered non-preemptable lock types in this configuration is shown in Fig. 1191.

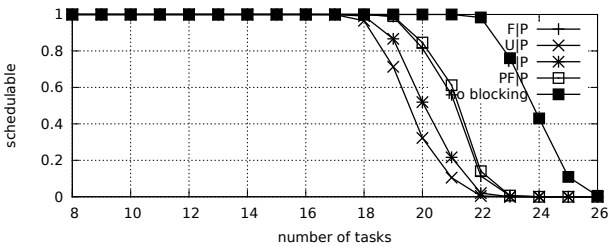

Fig. 1202. Schedulability under preemptable spin locks for $m = 8$, $U = 0.3n$, 8 resources, $rsf = 0.75$, $N^{max} = 5$, and short critical sections. The schedulability of the considered non-preemptable lock types in this configuration is shown in Fig. 1192.

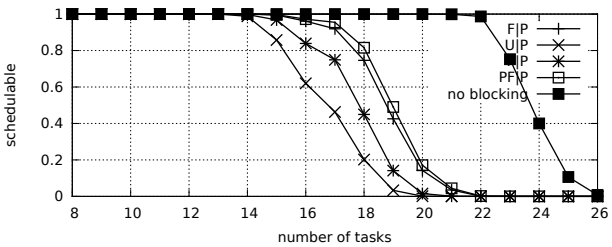

Fig. 1203. Schedulability under preemptable spin locks for $m = 8$, $U = 0.3n$, 8 resources, $rsf = 0.75$, $N^{max} = 10$, and short critical sections. The schedulability of the considered non-preemptable lock types in this configuration is shown in Fig. 1193.

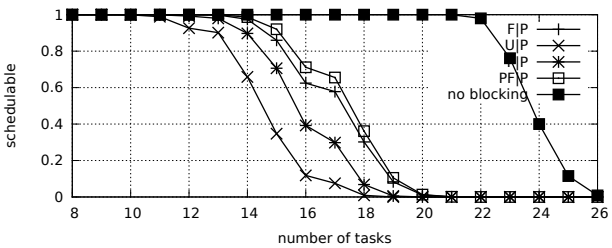

Fig. 1204. Schedulability under preemptable spin locks for $m = 8$, $U = 0.3n$, 8 resources, $rsf = 0.75$, $N^{max} = 15$, and short critical sections. The schedulability of the considered non-preemptable lock types in this configuration is shown in Fig. 1194.

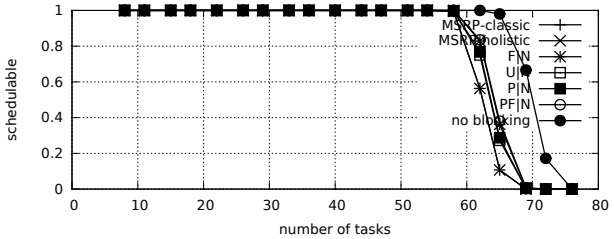

Fig. 1205. Schedulability under non-preemptable spin locks for $m = 8$, $U = 0.1n$, 16 resources, $rsf = 0.1$, $N^{max} = 1$, and medium critical sections. The schedulability of the considered preemptable lock types in this configuration is shown in Fig. 1215.

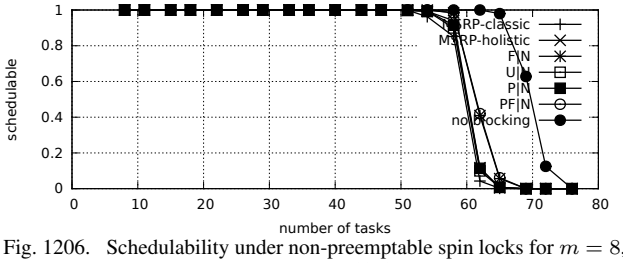

Fig. 1206. Schedulability under non-preemptable spin locks for $m = 8$, $U = 0.1n$, 16 resources, $rsf = 0.1$, $N^{max} = 2$, and medium critical sections. The schedulability of the considered preemptable lock types in this configuration is shown in Fig. 1216.

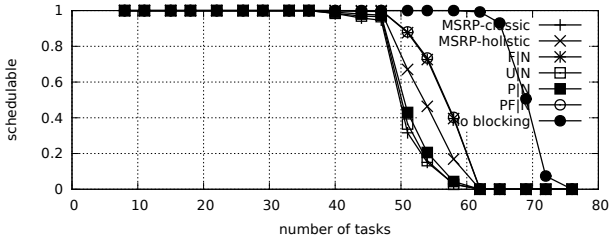

Fig. 1207. Schedulability under non-preemptable spin locks for $m = 8$, $U = 0.1n$, 16 resources, $rsf = 0.1$, $N^{max} = 5$, and medium critical sections. The schedulability of the considered preemptable lock types in this configuration is shown in Fig. 1217.

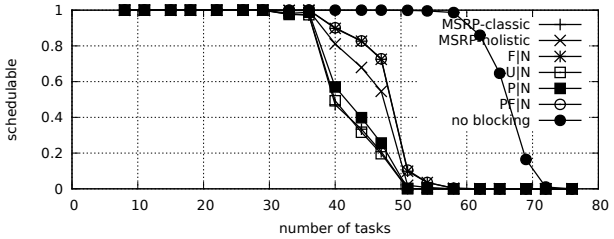

Fig. 1208. Schedulability under non-preemptable spin locks for $m = 8$, $U = 0.1n$, 16 resources, $rsf = 0.1$, $N^{max} = 10$, and medium critical sections. The schedulability of the considered preemptable lock types in this configuration is shown in Fig. 1218.

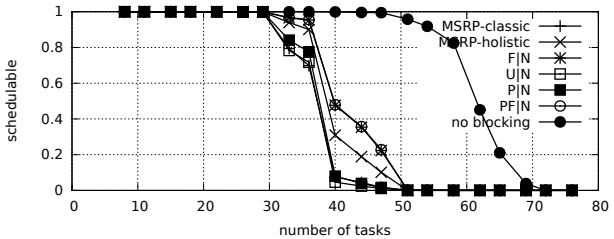

Fig. 1209. Schedulability under non-preemptable spin locks for $m = 8$, $U = 0.1n$, 16 resources, $rsf = 0.1$, $N^{max} = 15$, and medium critical sections. The schedulability of the considered preemptable lock types in this configuration is shown in Fig. 1219.

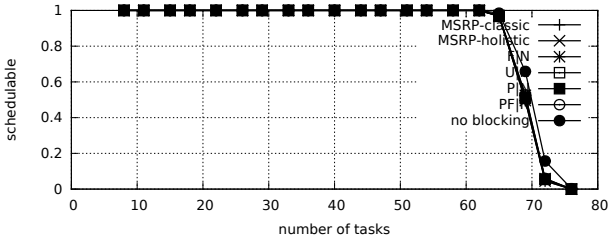

Fig. 1210. Schedulability under non-preemptable spin locks for $m = 8$, $U = 0.1n$, 16 resources, $rsf = 0.1$, $N^{max} = 1$, and short critical sections. The schedulability of the considered preemptable lock types in this configuration is shown in Fig. 1220.

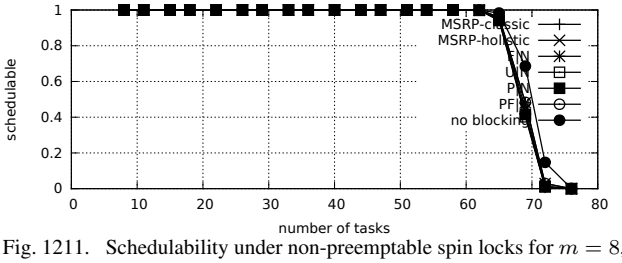

Fig. 1211. Schedulability under non-preemptable spin locks for $m = 8$, $U = 0.1n$, 16 resources, $rsf = 0.1$, $N^{max} = 2$, and short critical sections. The schedulability of the considered preemptable lock types in this configuration is shown in Fig. 1221.

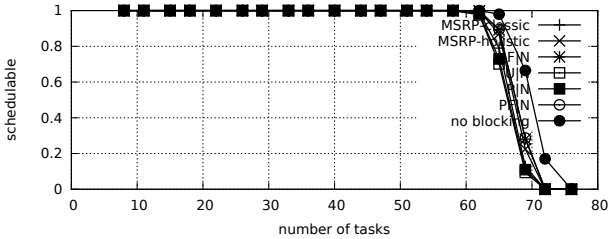

Fig. 1212. Schedulability under non-preemptable spin locks for $m = 8$, $U = 0.1n$, 16 resources, $rsf = 0.1$, $N^{max} = 5$, and short critical sections. The schedulability of the considered preemptable lock types in this configuration is shown in Fig. 1222.

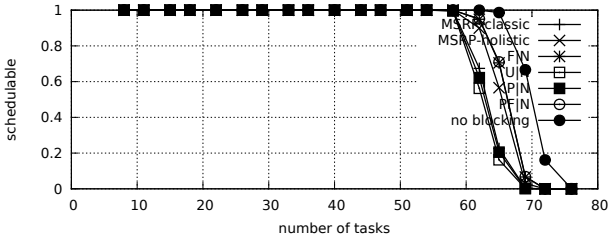

Fig. 1213. Schedulability under non-preemptable spin locks for $m = 8$, $U = 0.1n$, 16 resources, $rsf = 0.1$, $N^{max} = 10$, and short critical sections. The schedulability of the considered preemptable lock types in this configuration is shown in Fig. 1223.

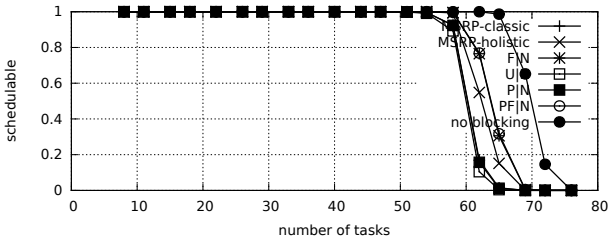

Fig. 1214. Schedulability under non-preemptable spin locks for $m = 8$, $U = 0.1n$, 16 resources, $rsf = 0.1$, $N^{max} = 15$, and short critical sections. The schedulability of the considered preemptable lock types in this configuration is shown in Fig. 1224.

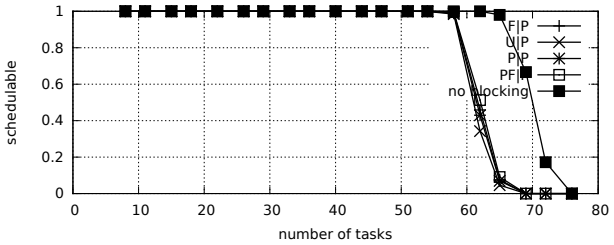

Fig. 1215. Schedulability under preemptable spin locks for $m = 8$, $U = 0.1n$, 16 resources, $rsf = 0.1$, $N^{max} = 1$, and medium critical sections. The schedulability of the considered non-preemptable lock types in this configuration is shown in Fig. 1205.

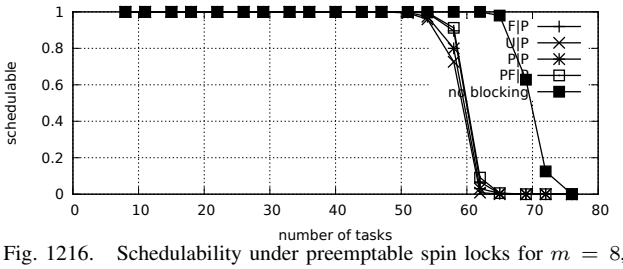

Fig. 1216. Schedulability under preemptable spin locks for $m = 8$, $U = 0.1n$, 16 resources, $rsf = 0.1$, $N^{max} = 2$, and medium critical sections. The schedulability of the considered non-preemptable lock types in this configuration is shown in Fig. 1206.

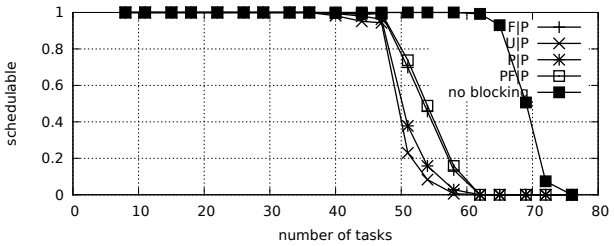

Fig. 1217. Schedulability under preemptable spin locks for $m = 8$, $U = 0.1n$, 16 resources, $rsf = 0.1$, $N^{max} = 5$, and medium critical sections. The schedulability of the considered non-preemptable lock types in this configuration is shown in Fig. 1207.

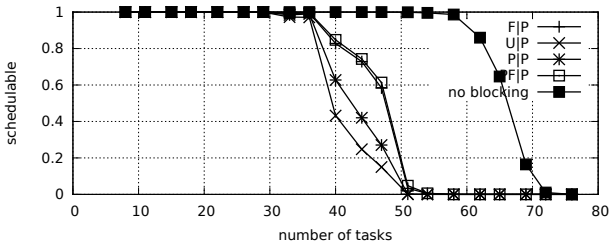

Fig. 1218. Schedulability under preemptable spin locks for $m = 8$, $U = 0.1n$, 16 resources, $rsf = 0.1$, $N^{max} = 10$, and medium critical sections. The schedulability of the considered non-preemptable lock types in this configuration is shown in Fig. 1208.

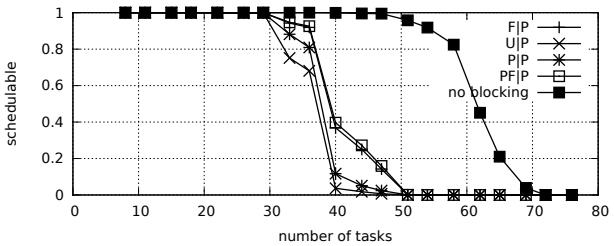

Fig. 1219. Schedulability under preemptable spin locks for $m = 8$, $U = 0.1n$, 16 resources, $rsf = 0.1$, $N^{max} = 15$, and medium critical sections. The schedulability of the considered non-preemptable lock types in this configuration is shown in Fig. 1209.

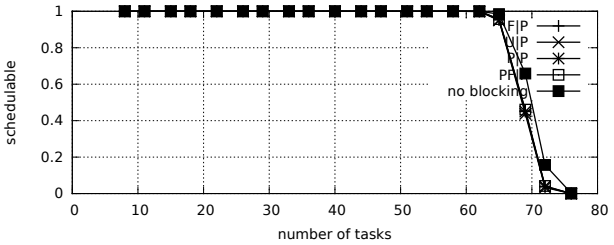

Fig. 1220. Schedulability under preemptable spin locks for $m = 8$, $U = 0.1n$, 16 resources, $rsf = 0.1$, $N^{max} = 1$, and short critical sections. The schedulability of the considered non-preemptable lock types in this configuration is shown in Fig. 1210.

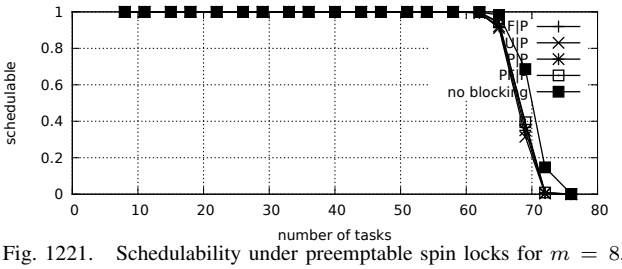

Fig. 1221. Schedulability under preemptable spin locks for $m = 8$, $U = 0.1n$, 16 resources, $rsf = 0.1$, $N^{max} = 2$, and short critical sections. The schedulability of the considered non-preemptable lock types in this configuration is shown in Fig. 1211.

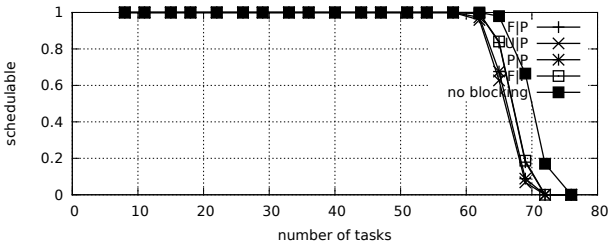

Fig. 1222. Schedulability under preemptable spin locks for $m = 8$, $U = 0.1n$, 16 resources, $rsf = 0.1$, $N^{max} = 5$, and short critical sections. The schedulability of the considered non-preemptable lock types in this configuration is shown in Fig. 1212.

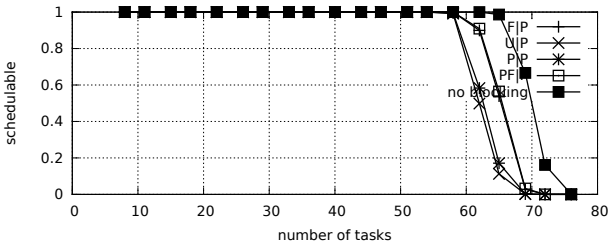

Fig. 1223. Schedulability under preemptable spin locks for $m = 8$, $U = 0.1n$, 16 resources, $rsf = 0.1$, $N^{max} = 10$, and short critical sections. The schedulability of the considered non-preemptable lock types in this configuration is shown in Fig. 1213.

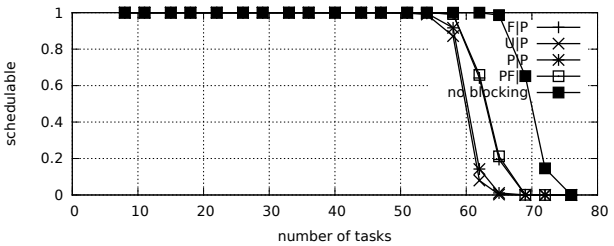

Fig. 1224. Schedulability under preemptable spin locks for $m = 8$, $U = 0.1n$, 16 resources, $rsf = 0.1$, $N^{max} = 15$, and short critical sections. The schedulability of the considered non-preemptable lock types in this configuration is shown in Fig. 1214.

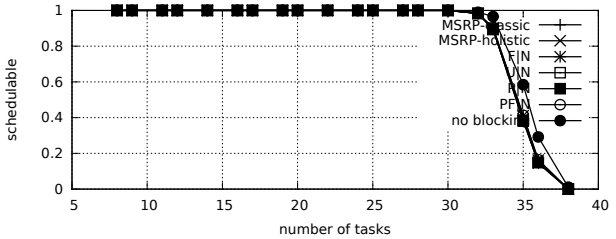

Fig. 1225. Schedulability under non-preemptable spin locks for $m = 8$, $U = 0.2n$, 16 resources, $rsf = 0.1$, $N^{max} = 1$, and medium critical sections. The schedulability of the considered preemptable lock types in this configuration is shown in Fig. 1235.

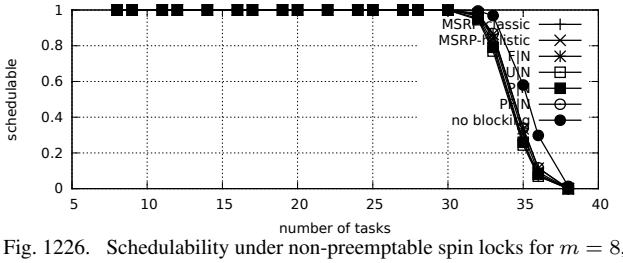

Fig. 1226. Schedulability under non-preemptable spin locks for $m = 8$, $U = 0.2n$, 16 resources, $rsf = 0.1$, $N^{max} = 2$, and medium critical sections. The schedulability of the considered preemptable lock types in this configuration is shown in Fig. 1236.

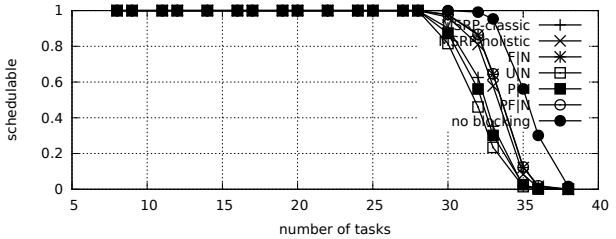

Fig. 1227. Schedulability under non-preemptable spin locks for $m = 8$, $U = 0.2n$, 16 resources, $rsf = 0.1$, $N^{max} = 5$, and medium critical sections. The schedulability of the considered preemptable lock types in this configuration is shown in Fig. 1237.

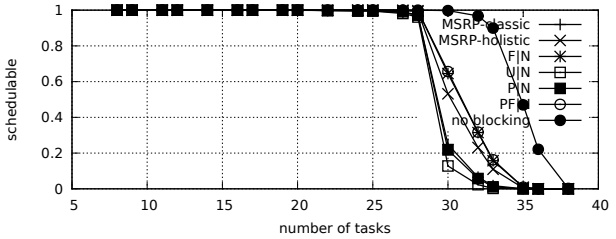

Fig. 1228. Schedulability under non-preemptable spin locks for $m = 8$, $U = 0.2n$, 16 resources, $rsf = 0.1$, $N^{max} = 10$, and medium critical sections. The schedulability of the considered preemptable lock types in this configuration is shown in Fig. 1238.

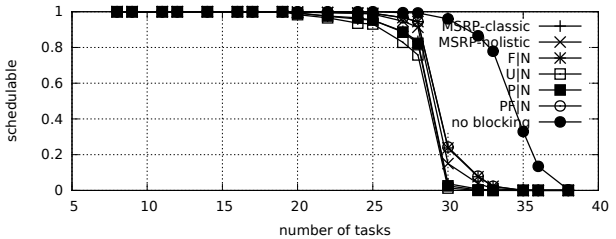

Fig. 1229. Schedulability under non-preemptable spin locks for $m = 8$, $U = 0.2n$, 16 resources, $rsf = 0.1$, $N^{max} = 15$, and medium critical sections. The schedulability of the considered preemptable lock types in this configuration is shown in Fig. 1239.

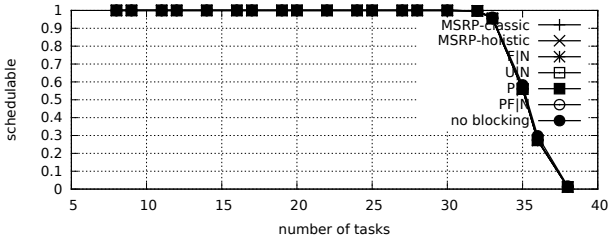

Fig. 1230. Schedulability under non-preemptable spin locks for $m = 8$, $U = 0.2n$, 16 resources, $rsf = 0.1$, $N^{max} = 1$, and short critical sections. The schedulability of the considered preemptable lock types in this configuration is shown in Fig. 1240.

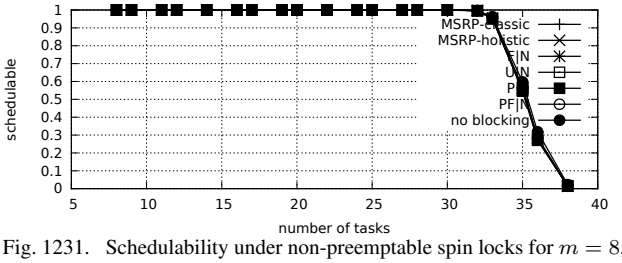

Fig. 1231. Schedulability under non-preemptable spin locks for $m = 8$, $U = 0.2n$, 16 resources, $rsf = 0.1$, $N^{max} = 2$, and short critical sections. The schedulability of the considered preemptable lock types in this configuration is shown in Fig. 1241.

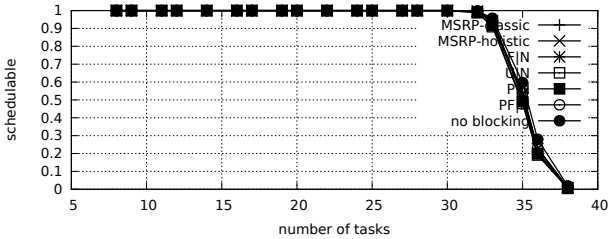

Fig. 1232. Schedulability under non-preemptable spin locks for $m = 8$, $U = 0.2n$, 16 resources, $rsf = 0.1$, $N^{max} = 5$, and short critical sections. The schedulability of the considered preemptable lock types in this configuration is shown in Fig. 1242.

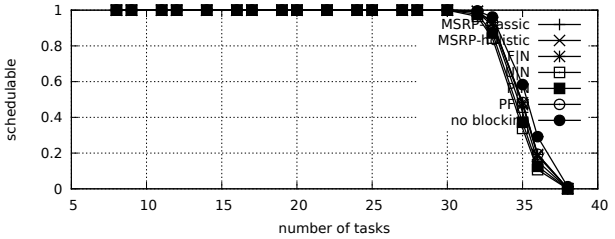

Fig. 1233. Schedulability under non-preemptable spin locks for $m = 8$, $U = 0.2n$, 16 resources, $rsf = 0.1$, $N^{max} = 10$, and short critical sections. The schedulability of the considered preemptable lock types in this configuration is shown in Fig. 1243.

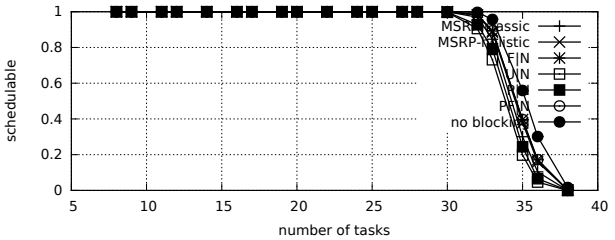

Fig. 1234. Schedulability under non-preemptable spin locks for $m = 8$, $U = 0.2n$, 16 resources, $rsf = 0.1$, $N^{max} = 15$, and short critical sections. The schedulability of the considered preemptable lock types in this configuration is shown in Fig. 1244.

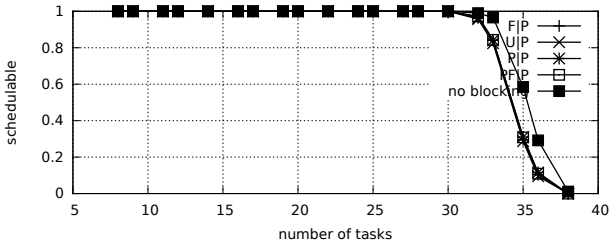

Fig. 1235. Schedulability under preemptable spin locks for $m = 8$, $U = 0.2n$, 16 resources, $rsf = 0.1$, $N^{max} = 1$, and medium critical sections. The schedulability of the considered non-preemptable lock types in this configuration is shown in Fig. 1225.

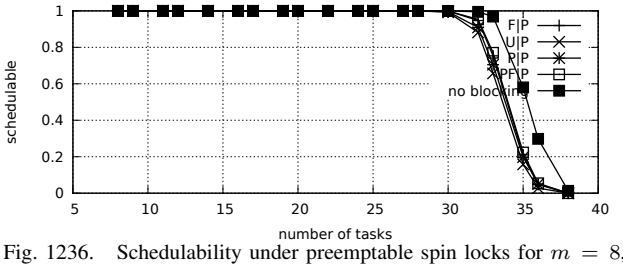

Fig. 1236. Schedulability under preemptable spin locks for $m = 8$, $U = 0.2n$, 16 resources, $rsf = 0.1$, $N^{max} = 2$, and medium critical sections. The schedulability of the considered non-preemptable lock types in this configuration is shown in Fig. 1226.

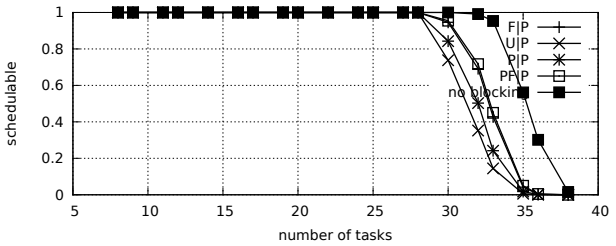

Fig. 1237. Schedulability under preemptable spin locks for $m = 8$, $U = 0.2n$, 16 resources, $rsf = 0.1$, $N^{max} = 5$, and medium critical sections. The schedulability of the considered non-preemptable lock types in this configuration is shown in Fig. 1227.

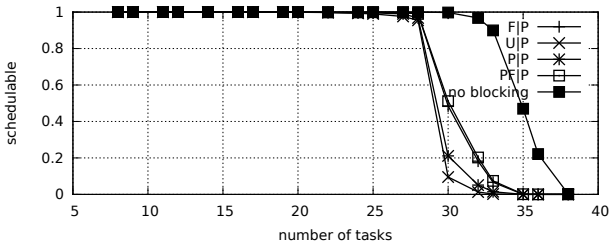

Fig. 1238. Schedulability under preemptable spin locks for $m = 8$, $U = 0.2n$, 16 resources, $rsf = 0.1$, $N^{max} = 10$, and medium critical sections. The schedulability of the considered non-preemptable lock types in this configuration is shown in Fig. 1228.

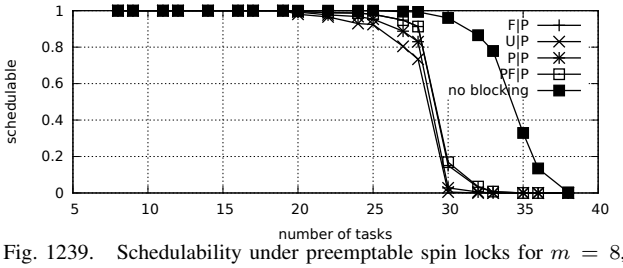

Fig. 1239. Schedulability under preemptable spin locks for $m = 8$, $U = 0.2n$, 16 resources, $rsf = 0.1$, $N^{max} = 15$, and medium critical sections. The schedulability of the considered non-preemptable lock types in this configuration is shown in Fig. 1229.

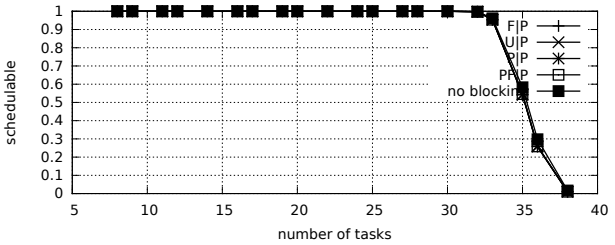

Fig. 1240. Schedulability under preemptable spin locks for $m = 8$, $U = 0.2n$, 16 resources, $rsf = 0.1$, $N^{max} = 1$, and short critical sections. The schedulability of the considered non-preemptable lock types in this configuration is shown in Fig. 1230.

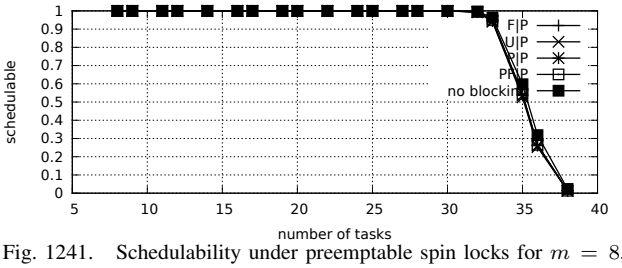

Fig. 1241. Schedulability under preemptable spin locks for $m = 8$, $U = 0.2n$, 16 resources, $rsf = 0.1$, $N^{max} = 2$, and short critical sections. The schedulability of the considered non-preemptable lock types in this configuration is shown in Fig. 1231.

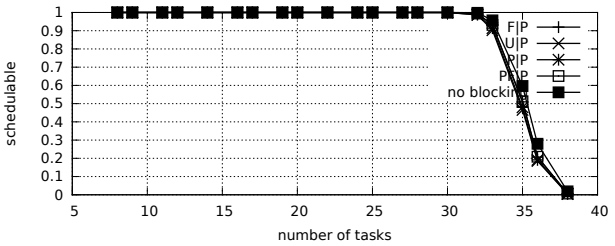

Fig. 1242. Schedulability under preemptable spin locks for $m = 8$, $U = 0.2n$, 16 resources, $rsf = 0.1$, $N^{max} = 5$, and short critical sections. The schedulability of the considered non-preemptable lock types in this configuration is shown in Fig. 1232.

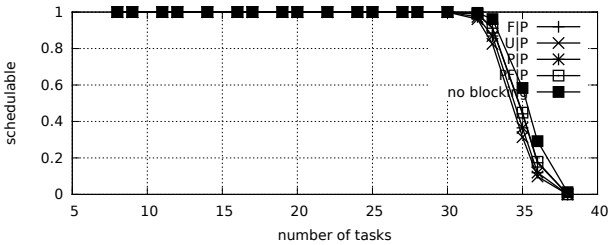

Fig. 1243. Schedulability under preemptable spin locks for $m = 8$, $U = 0.2n$, 16 resources, $rsf = 0.1$, $N^{max} = 10$, and short critical sections. The schedulability of the considered non-preemptable lock types in this configuration is shown in Fig. 1233.

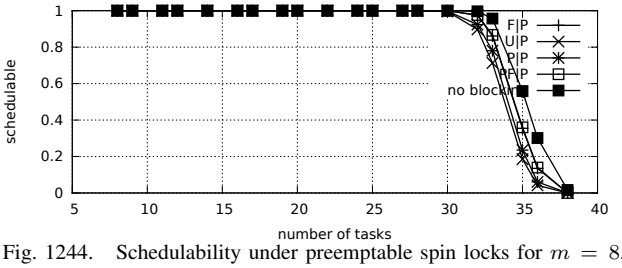

Fig. 1244. Schedulability under preemptable spin locks for $m = 8$, $U = 0.2n$, 16 resources, $rsf = 0.1$, $N^{max} = 15$, and short critical sections. The schedulability of the considered non-preemptable lock types in this configuration is shown in Fig. 1234.

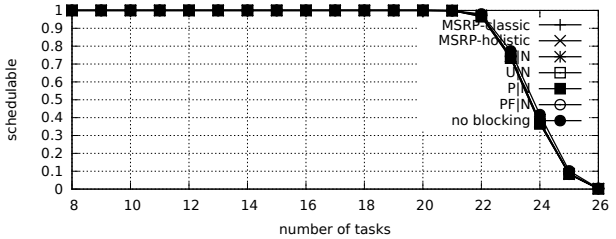

Fig. 1245. Schedulability under non-preemptable spin locks for $m = 8$, $U = 0.3n$, 16 resources, $rsf = 0.1$, $N^{max} = 1$, and medium critical sections. The schedulability of the considered preemptable lock types in this configuration is shown in Fig. 1255.

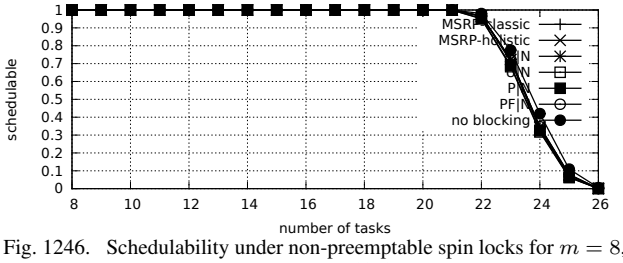

Fig. 1246. Schedulability under non-preemptable spin locks for $m = 8$, $U = 0.3n$, 16 resources, $rsf = 0.1$, $N^{max} = 2$, and medium critical sections. The schedulability of the considered preemptable lock types in this configuration is shown in Fig. 1256.

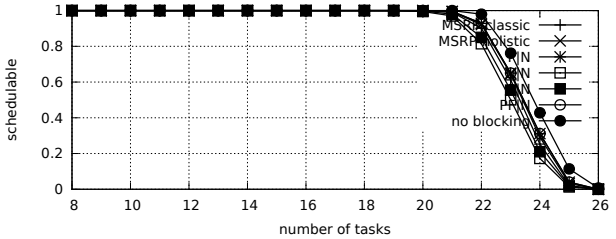

Fig. 1247. Schedulability under non-preemptable spin locks for $m = 8$, $U = 0.3n$, 16 resources, $rsf = 0.1$, $N^{max} = 5$, and medium critical sections. The schedulability of the considered preemptable lock types in this configuration is shown in Fig. 1257.

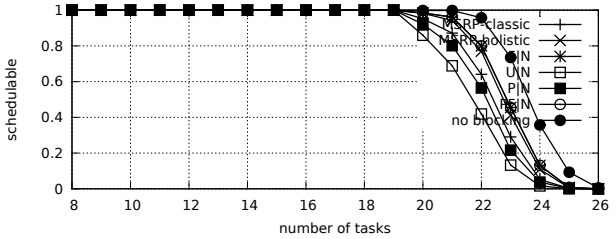

Fig. 1248. Schedulability under non-preemptable spin locks for $m = 8$, $U = 0.3n$, 16 resources, $rsf = 0.1$, $N^{max} = 10$, and medium critical sections. The schedulability of the considered preemptable lock types in this configuration is shown in Fig. 1258.

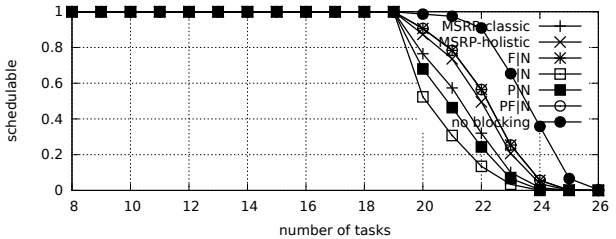

Fig. 1249. Schedulability under non-preemptable spin locks for $m = 8$, $U = 0.3n$, 16 resources, $rsf = 0.1$, $N^{max} = 15$, and medium critical sections. The schedulability of the considered preemptable lock types in this configuration is shown in Fig. 1259.

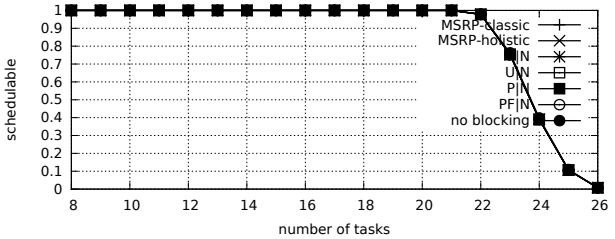

Fig. 1250. Schedulability under non-preemptable spin locks for $m = 8$, $U = 0.3n$, 16 resources, $rsf = 0.1$, $N^{max} = 1$, and short critical sections. The schedulability of the considered preemptable lock types in this configuration is shown in Fig. 1260.

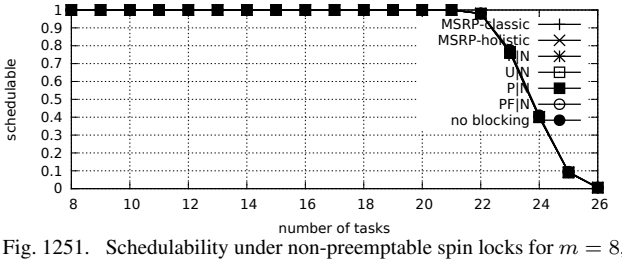

Fig. 1251. Schedulability under non-preemptable spin locks for $m = 8$, $U = 0.3n$, 16 resources, $rsf = 0.1$, $N^{max} = 2$, and short critical sections. The schedulability of the considered preemptable lock types in this configuration is shown in Fig. 1261.

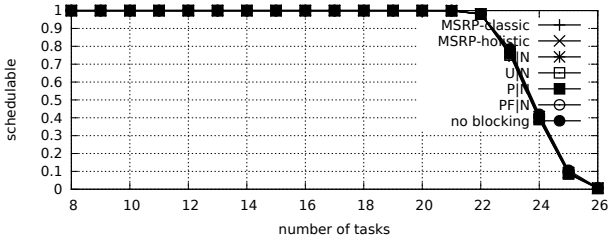

Fig. 1252. Schedulability under non-preemptable spin locks for $m = 8$, $U = 0.3n$, 16 resources, $rsf = 0.1$, $N^{max} = 5$, and short critical sections. The schedulability of the considered preemptable lock types in this configuration is shown in Fig. 1262.

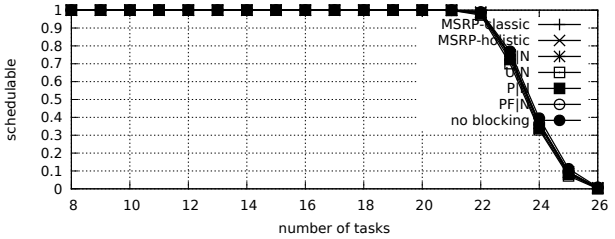

Fig. 1253. Schedulability under non-preemptable spin locks for $m = 8$, $U = 0.3n$, 16 resources, $rsf = 0.1$, $N^{max} = 10$, and short critical sections. The schedulability of the considered preemptable lock types in this configuration is shown in Fig. 1263.

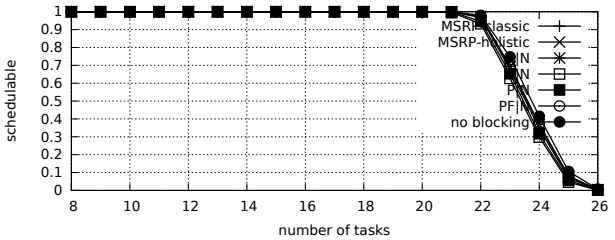

Fig. 1254. Schedulability under non-preemptable spin locks for $m = 8$, $U = 0.3n$, 16 resources, $rsf = 0.1$, $N^{max} = 15$, and short critical sections. The schedulability of the considered preemptable lock types in this configuration is shown in Fig. 1264.

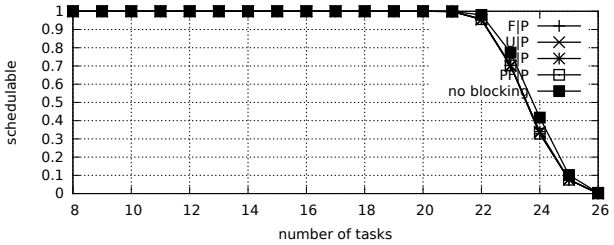

Fig. 1255. Schedulability under preemptable spin locks for $m = 8$, $U = 0.3n$, 16 resources, $rsf = 0.1$, $N^{max} = 1$, and medium critical sections. The schedulability of the considered non-preemptable lock types in this configuration is shown in Fig. 1245.

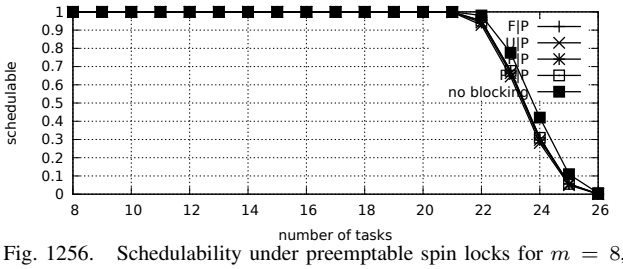

Fig. 1256. Schedulability under preemptable spin locks for $m = 8$, $U = 0.3n$, 16 resources, $rsf = 0.1$, $N^{max} = 2$, and medium critical sections. The schedulability of the considered non-preemptable lock types in this configuration is shown in Fig. 1246.

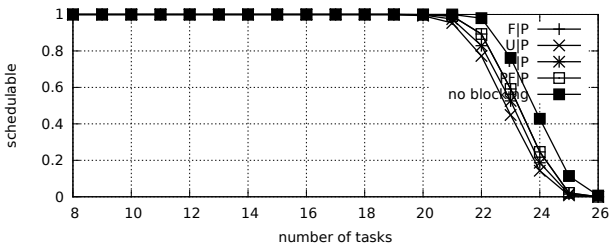

Fig. 1257. Schedulability under preemptable spin locks for $m = 8$, $U = 0.3n$, 16 resources, $rsf = 0.1$, $N^{max} = 5$, and medium critical sections. The schedulability of the considered non-preemptable lock types in this configuration is shown in Fig. 1247.

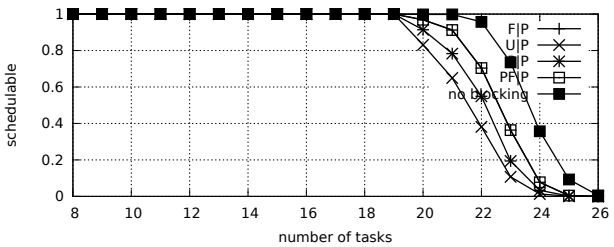

Fig. 1258. Schedulability under preemptable spin locks for $m = 8$, $U = 0.3n$, 16 resources, $rsf = 0.1$, $N^{max} = 10$, and medium critical sections. The schedulability of the considered non-preemptable lock types in this configuration is shown in Fig. 1248.

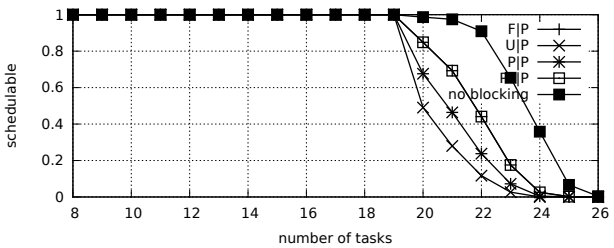

Fig. 1259. Schedulability under preemptable spin locks for $m = 8$, $U = 0.3n$, 16 resources, $rsf = 0.1$, $N^{max} = 15$, and medium critical sections. The schedulability of the considered non-preemptable lock types in this configuration is shown in Fig. 1249.

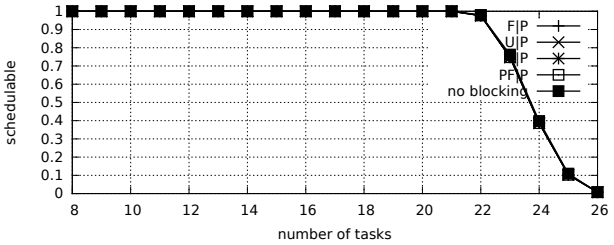

Fig. 1260. Schedulability under preemptable spin locks for $m = 8$, $U = 0.3n$, 16 resources, $rsf = 0.1$, $N^{max} = 1$, and short critical sections. The schedulability of the considered non-preemptable lock types in this configuration is shown in Fig. 1250.

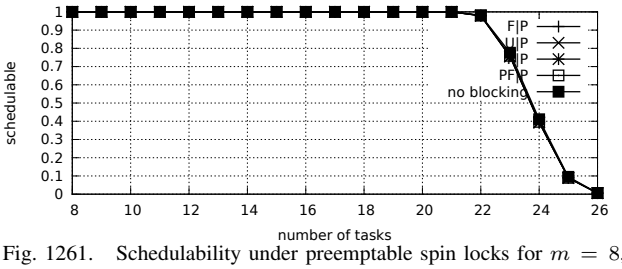

Fig. 1261. Schedulability under preemptable spin locks for $m = 8$, $U = 0.3n$, 16 resources, $rsf = 0.1$, $N^{max} = 2$, and short critical sections. The schedulability of the considered non-preemptable lock types in this configuration is shown in Fig. 1251.

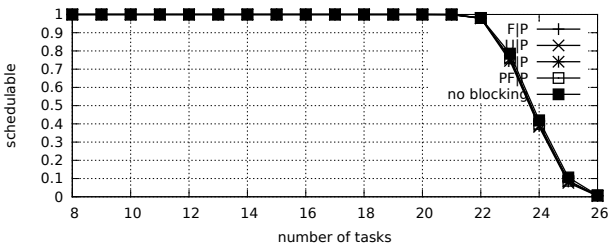

Fig. 1262. Schedulability under preemptable spin locks for $m = 8$, $U = 0.3n$, 16 resources, $rsf = 0.1$, $N^{max} = 5$, and short critical sections. The schedulability of the considered non-preemptable lock types in this configuration is shown in Fig. 1252.

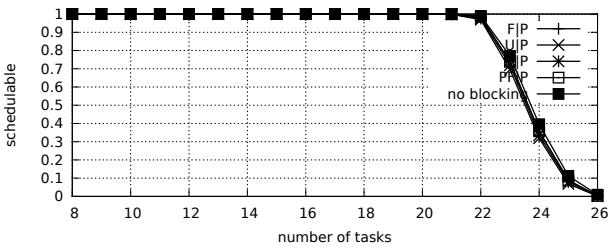

Fig. 1263. Schedulability under preemptable spin locks for $m = 8$, $U = 0.3n$, 16 resources, $rsf = 0.1$, $N^{max} = 10$, and short critical sections. The schedulability of the considered non-preemptable lock types in this configuration is shown in Fig. 1253.

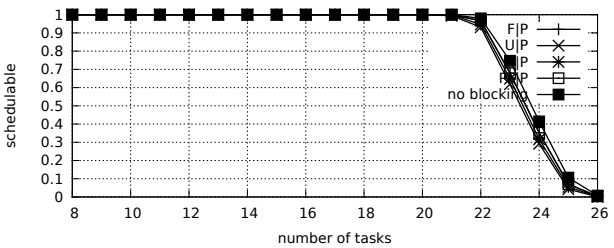

Fig. 1264. Schedulability under preemptable spin locks for $m = 8$, $U = 0.3n$, 16 resources, $rsf = 0.1$, $N^{max} = 15$, and short critical sections. The schedulability of the considered non-preemptable lock types in this configuration is shown in Fig. 1254.

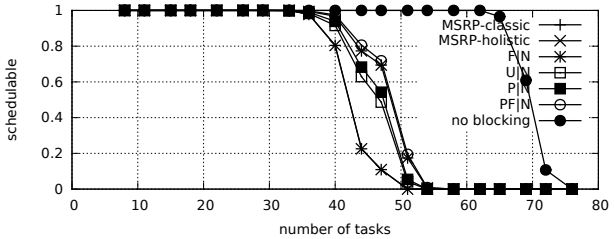

Fig. 1265. Schedulability under non-preemptable spin locks for $m = 8$, $U = 0.1n$, 16 resources, $rsf = 0.25$, $N^{max} = 1$, and medium critical sections. The schedulability of the considered preemptable lock types in this configuration is shown in Fig. 1275.

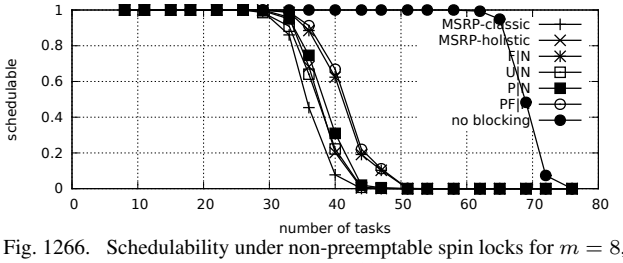

Fig. 1266. Schedulability under non-preemptable spin locks for $m = 8$, $U = 0.1n$, 16 resources, $rsf = 0.25$, $N^{max} = 2$, and medium critical sections. The schedulability of the considered preemptable lock types in this configuration is shown in Fig. 1276.

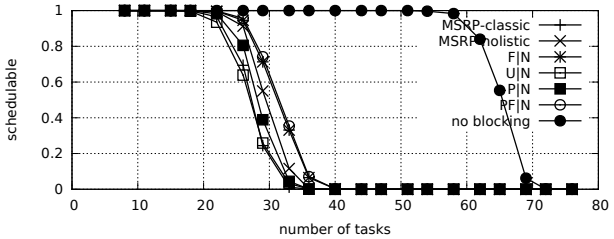

Fig. 1267. Schedulability under non-preemptable spin locks for $m = 8$, $U = 0.1n$, 16 resources, $rsf = 0.25$, $N^{max} = 5$, and medium critical sections. The schedulability of the considered preemptable lock types in this configuration is shown in Fig. 1277.

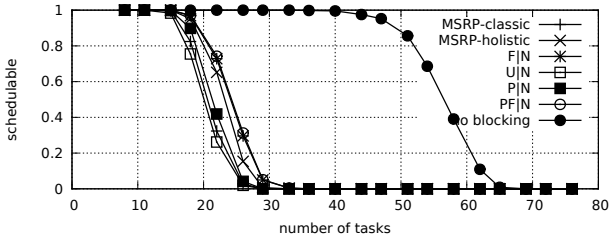

Fig. 1268. Schedulability under non-preemptable spin locks for $m = 8$, $U = 0.1n$, 16 resources, $rsf = 0.25$, $N^{max} = 10$, and medium critical sections. The schedulability of the considered preemptable lock types in this configuration is shown in Fig. 1278.

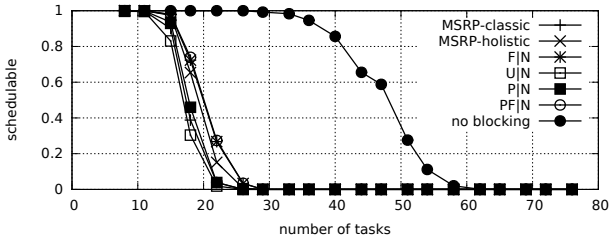

Fig. 1269. Schedulability under non-preemptable spin locks for $m = 8$, $U = 0.1n$, 16 resources, $rsf = 0.25$, $N^{max} = 15$, and medium critical sections. The schedulability of the considered preemptable lock types in this configuration is shown in Fig. 1279.

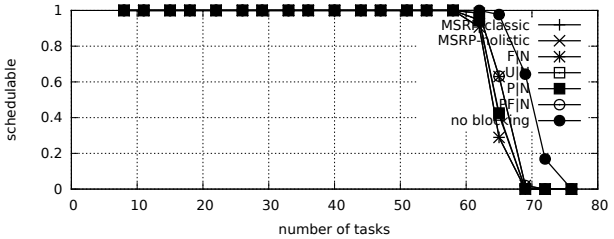

Fig. 1270. Schedulability under non-preemptable spin locks for $m = 8$, $U = 0.1n$, 16 resources, $rsf = 0.25$, $N^{max} = 1$, and short critical sections. The schedulability of the considered preemptable lock types in this configuration is shown in Fig. 1280.

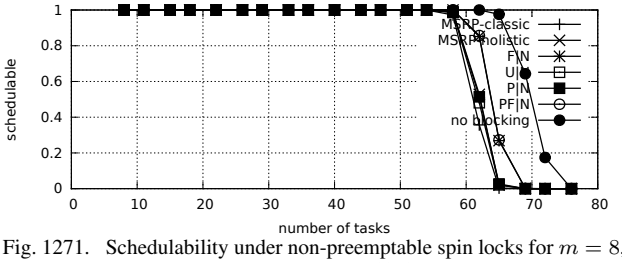

Fig. 1271. Schedulability under non-preemptable spin locks for $m = 8$, $U = 0.1n$, 16 resources, $rsf = 0.25$, $N^{max} = 2$, and short critical sections. The schedulability of the considered preemptable lock types in this configuration is shown in Fig. 1281.

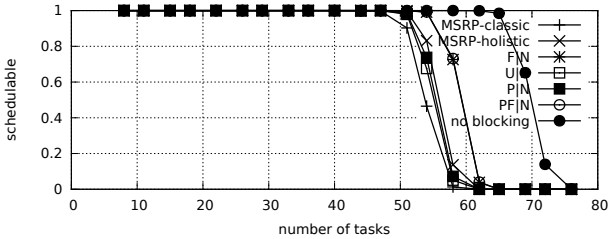

Fig. 1272. Schedulability under non-preemptable spin locks for $m = 8$, $U = 0.1n$, 16 resources, $rsf = 0.25$, $N^{max} = 5$, and short critical sections. The schedulability of the considered preemptable lock types in this configuration is shown in Fig. 1282.

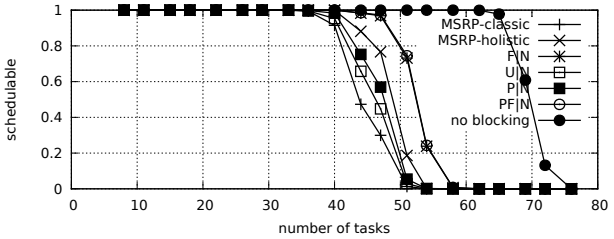

Fig. 1273. Schedulability under non-preemptable spin locks for $m = 8$, $U = 0.1n$, 16 resources, $rsf = 0.25$, $N^{max} = 10$, and short critical sections. The schedulability of the considered preemptable lock types in this configuration is shown in Fig. 1283.

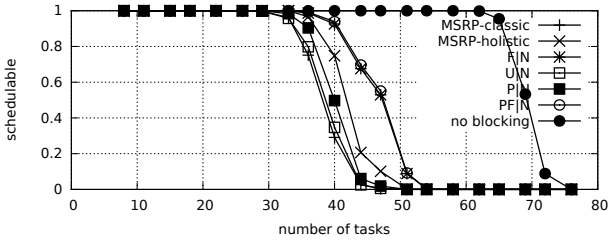

Fig. 1274. Schedulability under non-preemptable spin locks for $m = 8$, $U = 0.1n$, 16 resources, $rsf = 0.25$, $N^{max} = 15$, and short critical sections. The schedulability of the considered preemptable lock types in this configuration is shown in Fig. 1284.

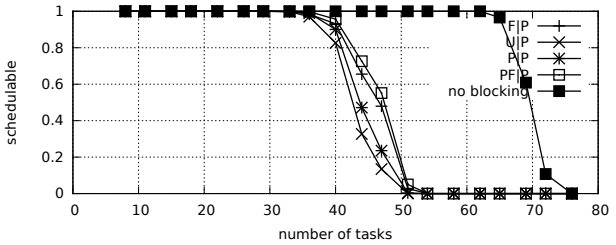

Fig. 1275. Schedulability under preemptable spin locks for $m = 8$, $U = 0.1n$, 16 resources, $rsf = 0.25$, $N^{max} = 1$, and medium critical sections. The schedulability of the considered non-preemptable lock types in this configuration is shown in Fig. 1265.

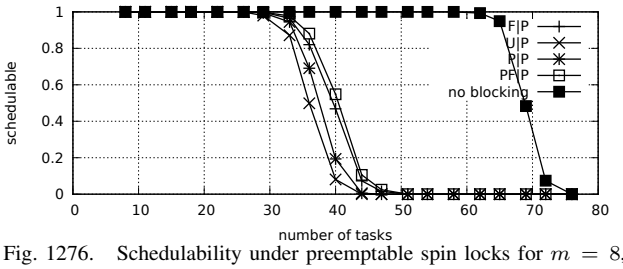

Fig. 1276. Schedulability under preemptable spin locks for $m = 8$, $U = 0.1n$, 16 resources, $rsf = 0.25$, $N^{max} = 2$, and medium critical sections. The schedulability of the considered non-preemptable lock types in this configuration is shown in Fig. 1266.

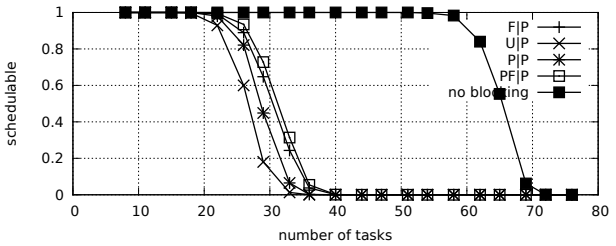

Fig. 1277. Schedulability under preemptable spin locks for $m = 8$, $U = 0.1n$, 16 resources, $rsf = 0.25$, $N^{max} = 5$, and medium critical sections. The schedulability of the considered non-preemptable lock types in this configuration is shown in Fig. 1267.

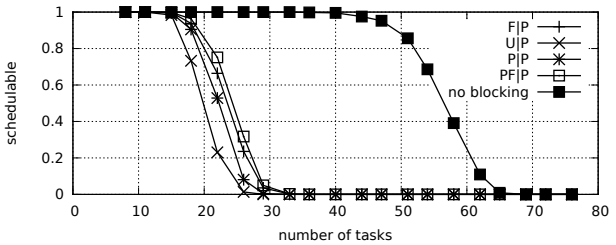

Fig. 1278. Schedulability under preemptable spin locks for $m = 8$, $U = 0.1n$, 16 resources, $rsf = 0.25$, $N^{max} = 10$, and medium critical sections. The schedulability of the considered non-preemptable lock types in this configuration is shown in Fig. 1268.

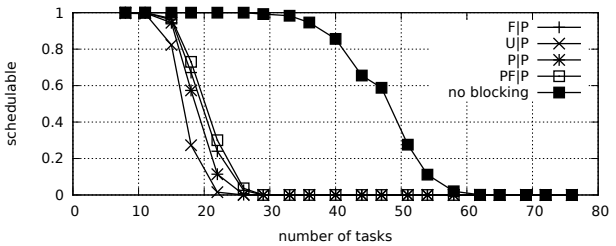

Fig. 1279. Schedulability under preemptable spin locks for $m = 8$, $U = 0.1n$, 16 resources, $rsf = 0.25$, $N^{max} = 15$, and medium critical sections. The schedulability of the considered non-preemptable lock types in this configuration is shown in Fig. 1269.

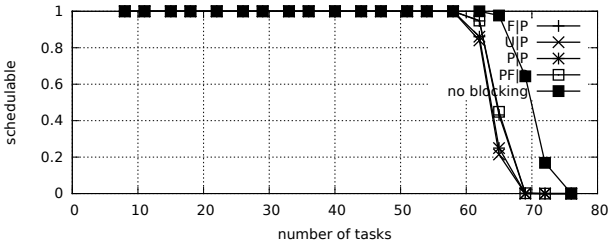

Fig. 1280. Schedulability under preemptable spin locks for $m = 8$, $U = 0.1n$, 16 resources, $rsf = 0.25$, $N^{max} = 1$, and short critical sections. The schedulability of the considered non-preemptable lock types in this configuration is shown in Fig. 1270.

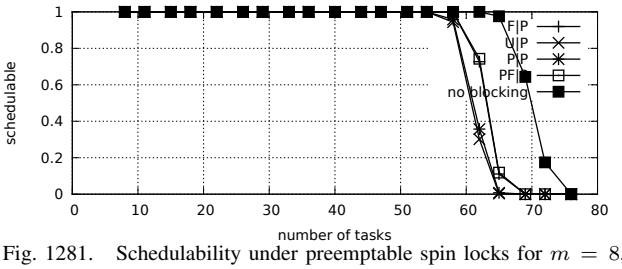

Fig. 1281. Schedulability under preemptable spin locks for $m = 8$, $U = 0.1n$, 16 resources, $rsf = 0.25$, $N^{max} = 2$, and short critical sections. The schedulability of the considered non-preemptable lock types in this configuration is shown in Fig. 1271.

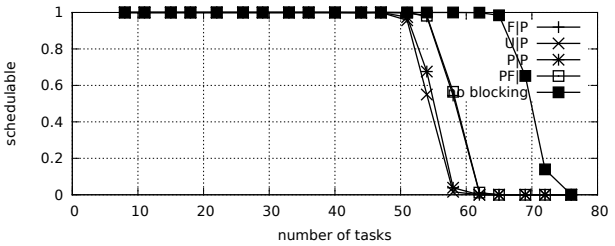

Fig. 1282. Schedulability under preemptable spin locks for $m = 8$, $U = 0.1n$, 16 resources, $rsf = 0.25$, $N^{max} = 5$, and short critical sections. The schedulability of the considered non-preemptable lock types in this configuration is shown in Fig. 1272.

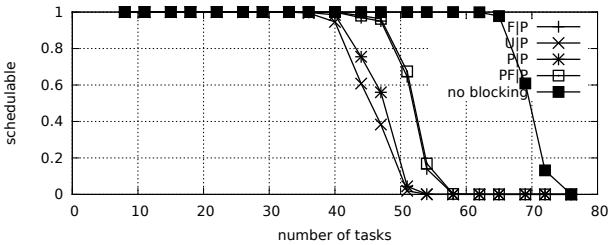

Fig. 1283. Schedulability under preemptable spin locks for $m = 8$, $U = 0.1n$, 16 resources, $rsf = 0.25$, $N^{max} = 10$, and short critical sections. The schedulability of the considered non-preemptable lock types in this configuration is shown in Fig. 1273.

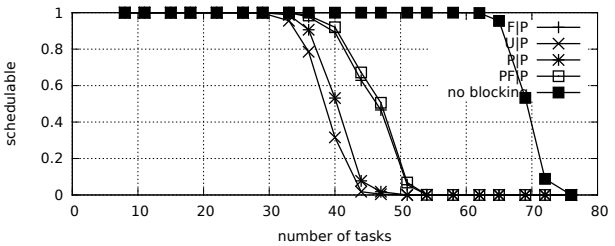

Fig. 1284. Schedulability under preemptable spin locks for $m = 8$, $U = 0.1n$, 16 resources, $rsf = 0.25$, $N^{max} = 15$, and short critical sections. The schedulability of the considered non-preemptable lock types in this configuration is shown in Fig. 1274.

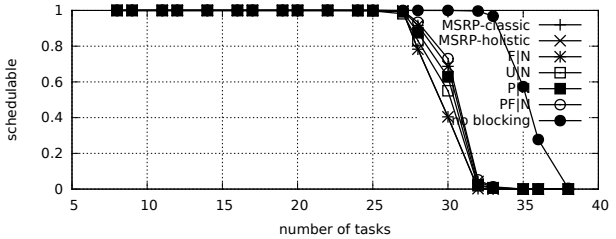

Fig. 1285. Schedulability under non-preemptable spin locks for $m = 8$, $U = 0.2n$, 16 resources, $rsf = 0.25$, $N^{max} = 1$, and medium critical sections. The schedulability of the considered preemptable lock types in this configuration is shown in Fig. 1295.

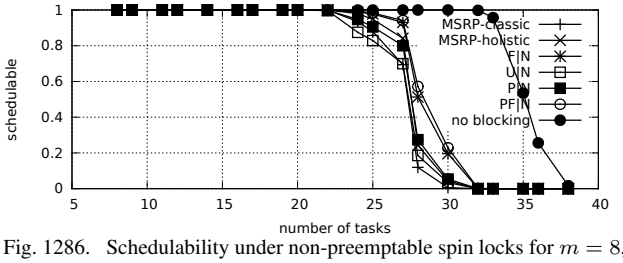

Fig. 1286. Schedulability under non-preemptable spin locks for $m = 8$, $U = 0.2n$, 16 resources, $rsf = 0.25$, $N^{max} = 2$, and medium critical sections. The schedulability of the considered preemptable lock types in this configuration is shown in Fig. 1296.

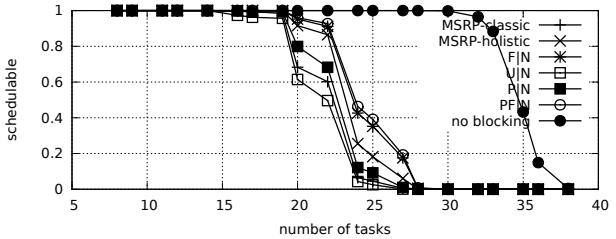

Fig. 1287. Schedulability under non-preemptable spin locks for $m = 8$, $U = 0.2n$, 16 resources, $rsf = 0.25$, $N^{max} = 5$, and medium critical sections. The schedulability of the considered preemptable lock types in this configuration is shown in Fig. 1297.

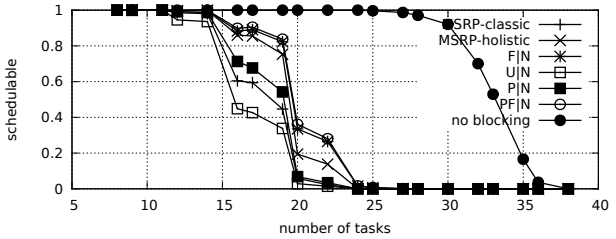

Fig. 1288. Schedulability under non-preemptable spin locks for $m = 8$, $U = 0.2n$, 16 resources, $rsf = 0.25$, $N^{max} = 10$, and medium critical sections. The schedulability of the considered preemptable lock types in this configuration is shown in Fig. 1298.

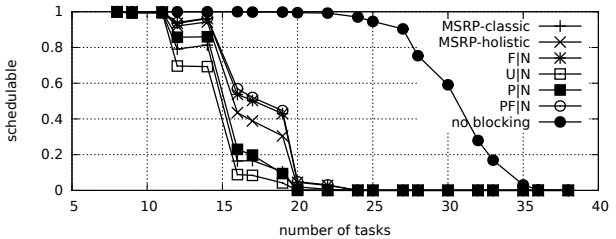

Fig. 1289. Schedulability under non-preemptable spin locks for $m = 8$, $U = 0.2n$, 16 resources, $rsf = 0.25$, $N^{max} = 15$, and medium critical sections. The schedulability of the considered preemptable lock types in this configuration is shown in Fig. 1299.

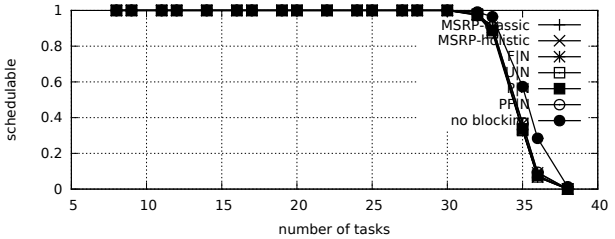

Fig. 1290. Schedulability under non-preemptable spin locks for $m = 8$, $U = 0.2n$, 16 resources, $rsf = 0.25$, $N^{max} = 1$, and short critical sections. The schedulability of the considered preemptable lock types in this configuration is shown in Fig. 1300.

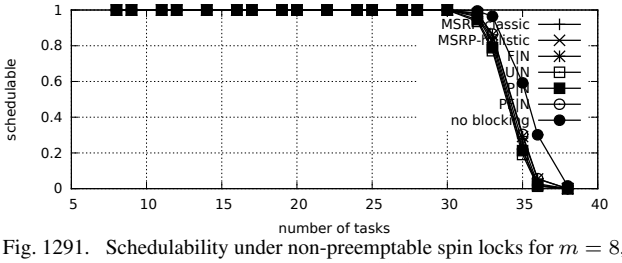

Fig. 1291. Schedulability under non-preemptable spin locks for $m = 8$, $U = 0.2n$, 16 resources, $rsf = 0.25$, $N^{max} = 2$, and short critical sections. The schedulability of the considered preemptable lock types in this configuration is shown in Fig. 1301.

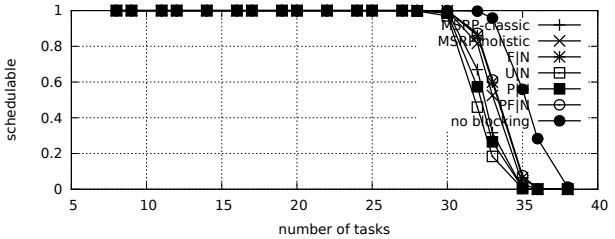

Fig. 1292. Schedulability under non-preemptable spin locks for $m = 8$, $U = 0.2n$, 16 resources, $rsf = 0.25$, $N^{max} = 5$, and short critical sections. The schedulability of the considered preemptable lock types in this configuration is shown in Fig. 1302.

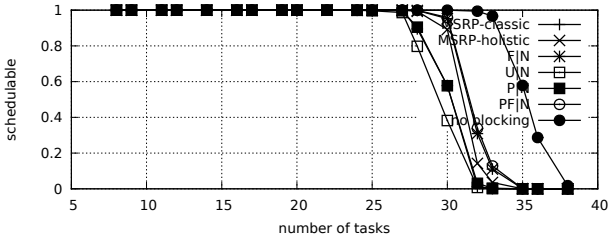

Fig. 1293. Schedulability under non-preemptable spin locks for $m = 8$, $U = 0.2n$, 16 resources, $rsf = 0.25$, $N^{max} = 10$, and short critical sections. The schedulability of the considered preemptable lock types in this configuration is shown in Fig. 1303.

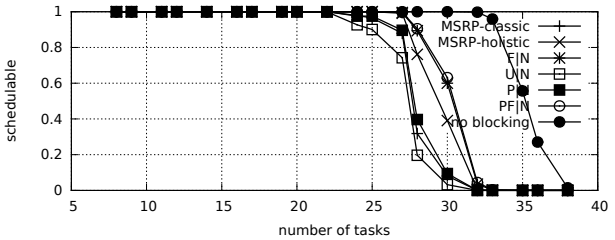

Fig. 1294. Schedulability under non-preemptable spin locks for $m = 8$, $U = 0.2n$, 16 resources, $rsf = 0.25$, $N^{max} = 15$, and short critical sections. The schedulability of the considered preemptable lock types in this configuration is shown in Fig. 1304.

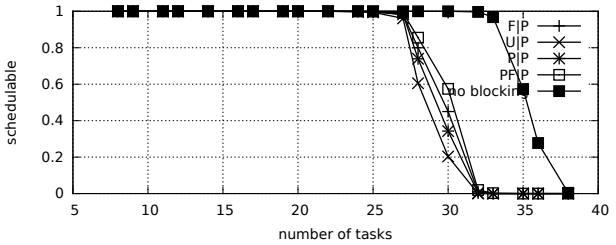

Fig. 1295. Schedulability under preemptable spin locks for $m = 8$, $U = 0.2n$, 16 resources, $rsf = 0.25$, $N^{max} = 1$, and medium critical sections. The schedulability of the considered non-preemptable lock types in this configuration is shown in Fig. 1285.

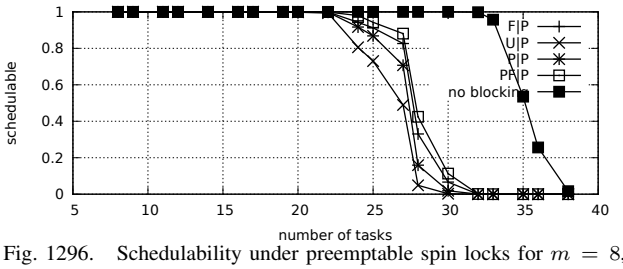

Fig. 1296. Schedulability under preemptable spin locks for $m = 8$, $U = 0.2n$, 16 resources, $rsf = 0.25$, $N^{max} = 2$, and medium critical sections. The schedulability of the considered non-preemptable lock types in this configuration is shown in Fig. 1286.

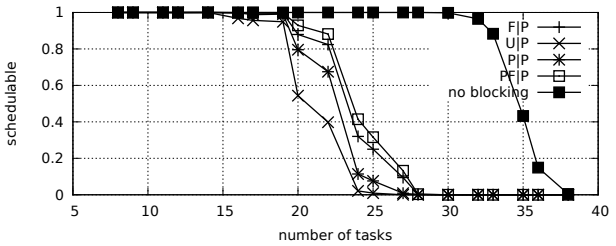

Fig. 1297. Schedulability under preemptable spin locks for $m = 8$, $U = 0.2n$, 16 resources, $rsf = 0.25$, $N^{max} = 5$, and medium critical sections. The schedulability of the considered non-preemptable lock types in this configuration is shown in Fig. 1287.

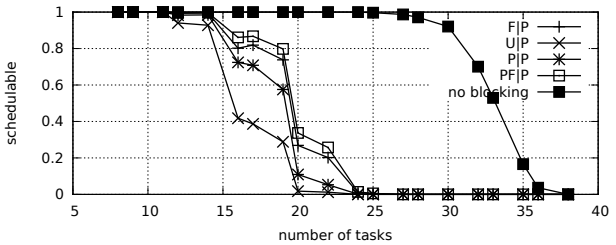

Fig. 1298. Schedulability under preemptable spin locks for $m = 8$, $U = 0.2n$, 16 resources, $rsf = 0.25$, $N^{max} = 10$, and medium critical sections. The schedulability of the considered non-preemptable lock types in this configuration is shown in Fig. 1288.

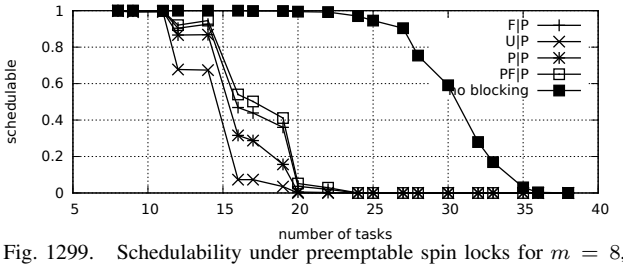

Fig. 1299. Schedulability under preemptable spin locks for $m = 8$, $U = 0.2n$, 16 resources, $rsf = 0.25$, $N^{max} = 15$, and medium critical sections. The schedulability of the considered non-preemptable lock types in this configuration is shown in Fig. 1289.

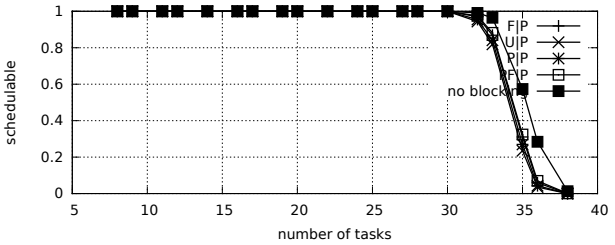

Fig. 1300. Schedulability under preemptable spin locks for $m = 8$, $U = 0.2n$, 16 resources, $rsf = 0.25$, $N^{max} = 1$, and short critical sections. The schedulability of the considered non-preemptable lock types in this configuration is shown in Fig. 1290.

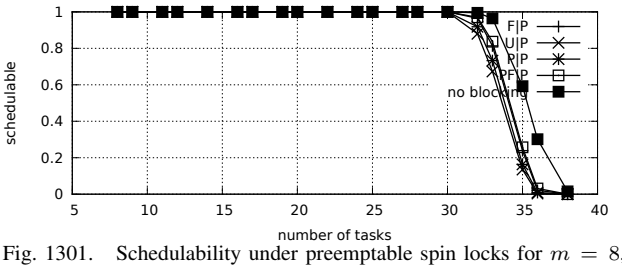

Fig. 1301. Schedulability under preemptable spin locks for $m = 8$, $U = 0.2n$, 16 resources, $rsf = 0.25$, $N^{max} = 2$, and short critical sections. The schedulability of the considered non-preemptable lock types in this configuration is shown in Fig. 1291.

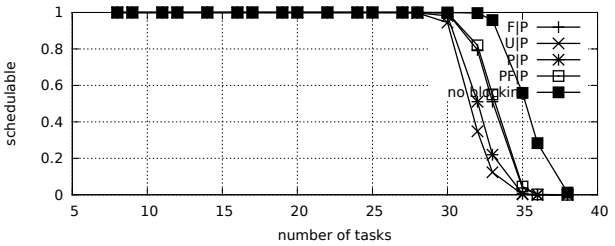

Fig. 1302. Schedulability under preemptable spin locks for $m = 8$, $U = 0.2n$, 16 resources, $rsf = 0.25$, $N^{max} = 5$, and short critical sections. The schedulability of the considered non-preemptable lock types in this configuration is shown in Fig. 1292.

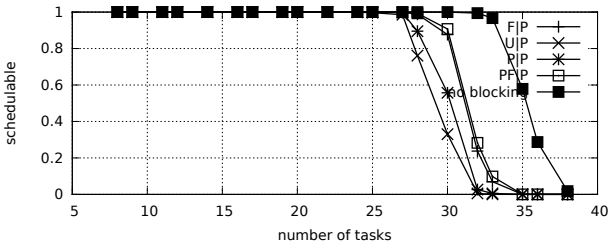

Fig. 1303. Schedulability under preemptable spin locks for $m = 8$, $U = 0.2n$, 16 resources, $rsf = 0.25$, $N^{max} = 10$, and short critical sections. The schedulability of the considered non-preemptable lock types in this configuration is shown in Fig. 1293.

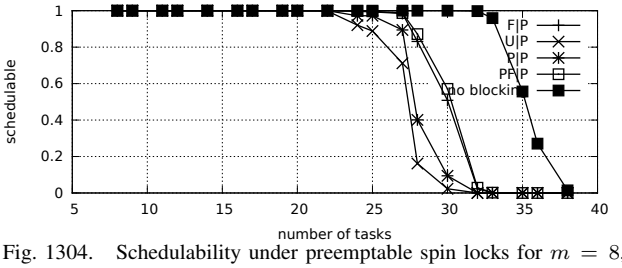

Fig. 1304. Schedulability under preemptable spin locks for $m = 8$, $U = 0.2n$, 16 resources, $rsf = 0.25$, $N^{max} = 15$, and short critical sections. The schedulability of the considered non-preemptable lock types in this configuration is shown in Fig. 1294.

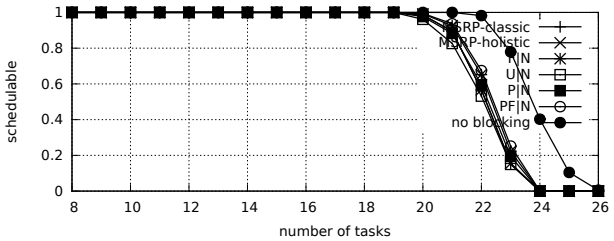

Fig. 1305. Schedulability under non-preemptable spin locks for $m = 8$, $U = 0.3n$, 16 resources, $rsf = 0.25$, $N^{max} = 1$, and medium critical sections. The schedulability of the considered preemptable lock types in this configuration is shown in Fig. 1315.

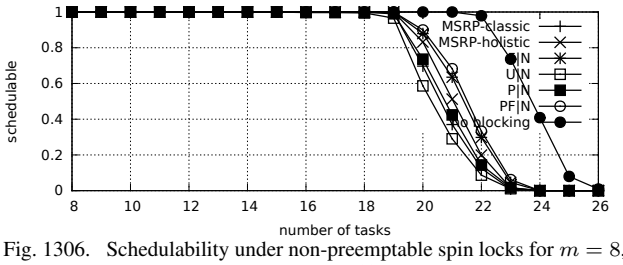

Fig. 1306. Schedulability under non-preemptable spin locks for $m = 8$, $U = 0.3n$, 16 resources, $rsf = 0.25$, $N^{max} = 2$, and medium critical sections. The schedulability of the considered preemptable lock types in this configuration is shown in Fig. 1316.

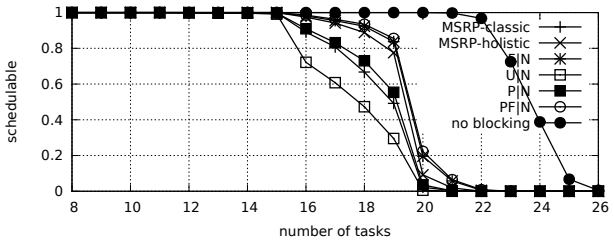

Fig. 1307. Schedulability under non-preemptable spin locks for $m = 8$, $U = 0.3n$, 16 resources, $rsf = 0.25$, $N^{max} = 5$, and medium critical sections. The schedulability of the considered preemptable lock types in this configuration is shown in Fig. 1317.

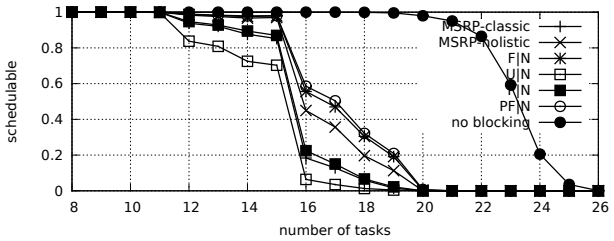

Fig. 1308. Schedulability under non-preemptable spin locks for $m = 8$, $U = 0.3n$, 16 resources, $rsf = 0.25$, $N^{max} = 10$, and medium critical sections. The schedulability of the considered preemptable lock types in this configuration is shown in Fig. 1318.

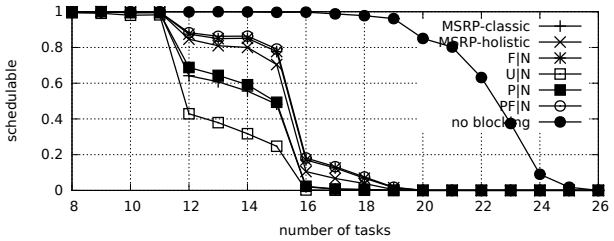

Fig. 1309. Schedulability under non-preemptable spin locks for $m = 8$, $U = 0.3n$, 16 resources, $rsf = 0.25$, $N^{max} = 15$, and medium critical sections. The schedulability of the considered preemptable lock types in this configuration is shown in Fig. 1319.

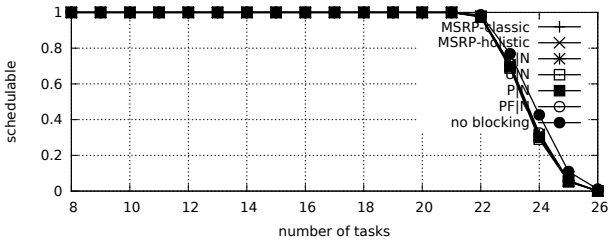

Fig. 1310. Schedulability under non-preemptable spin locks for $m = 8$, $U = 0.3n$, 16 resources, $rsf = 0.25$, $N^{max} = 1$, and short critical sections. The schedulability of the considered preemptable lock types in this configuration is shown in Fig. 1320.

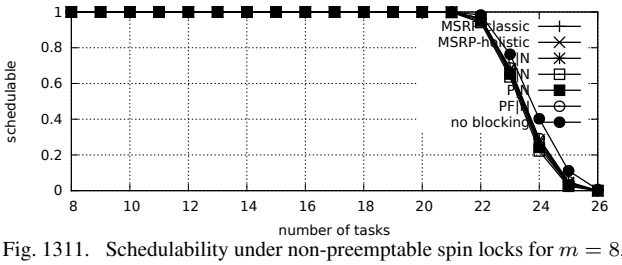

Fig. 1311. Schedulability under non-preemptable spin locks for $m = 8$, $U = 0.3n$, 16 resources, $rsf = 0.25$, $N^{max} = 2$, and short critical sections. The schedulability of the considered preemptable lock types in this configuration is shown in Fig. 1321.

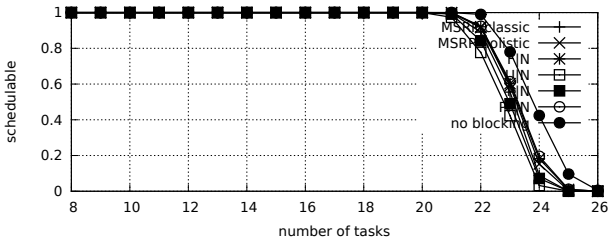

Fig. 1312. Schedulability under non-preemptable spin locks for $m = 8$, $U = 0.3n$, 16 resources, $rsf = 0.25$, $N^{max} = 5$, and short critical sections. The schedulability of the considered preemptable lock types in this configuration is shown in Fig. 1322.

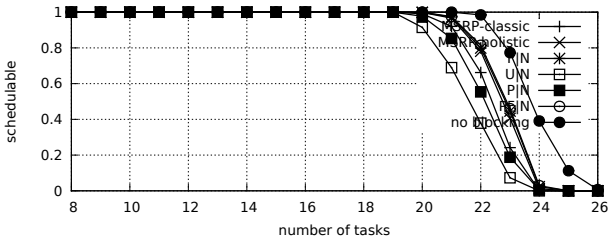

Fig. 1313. Schedulability under non-preemptable spin locks for $m = 8$, $U = 0.3n$, 16 resources, $rsf = 0.25$, $N^{max} = 10$, and short critical sections. The schedulability of the considered preemptable lock types in this configuration is shown in Fig. 1323.

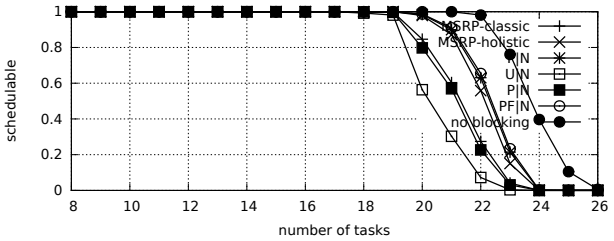

Fig. 1314. Schedulability under non-preemptable spin locks for $m = 8$, $U = 0.3n$, 16 resources, $rsf = 0.25$, $N^{max} = 15$, and short critical sections. The schedulability of the considered preemptable lock types in this configuration is shown in Fig. 1324.

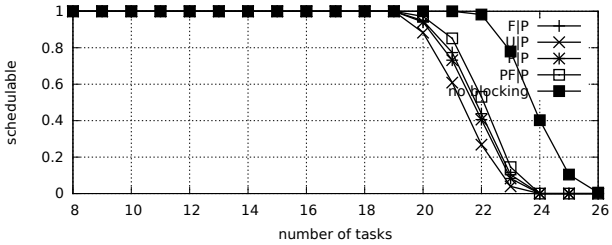

Fig. 1315. Schedulability under preemptable spin locks for $m = 8$, $U = 0.3n$, 16 resources, $rsf = 0.25$, $N^{max} = 1$, and medium critical sections. The schedulability of the considered non-preemptable lock types in this configuration is shown in Fig. 1305.

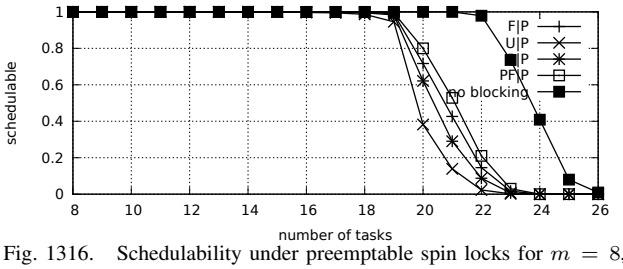

Fig. 1316. Schedulability under preemptable spin locks for $m = 8$, $U = 0.3n$, 16 resources, $rsf = 0.25$, $N^{max} = 2$, and medium critical sections. The schedulability of the considered non-preemptable lock types in this configuration is shown in Fig. 1306.

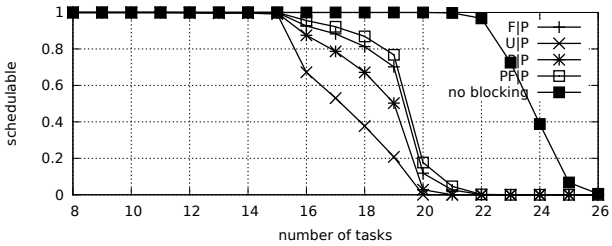

Fig. 1317. Schedulability under preemptable spin locks for $m = 8$, $U = 0.3n$, 16 resources, $rsf = 0.25$, $N^{max} = 5$, and medium critical sections. The schedulability of the considered non-preemptable lock types in this configuration is shown in Fig. 1307.

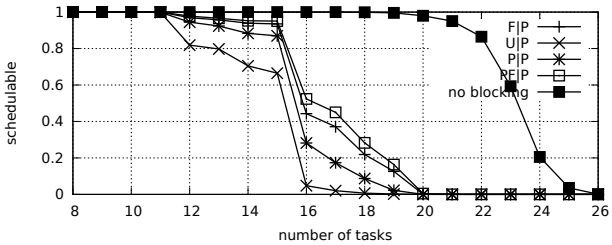

Fig. 1318. Schedulability under preemptable spin locks for $m = 8$, $U = 0.3n$, 16 resources, $rsf = 0.25$, $N^{max} = 10$, and medium critical sections. The schedulability of the considered non-preemptable lock types in this configuration is shown in Fig. 1308.

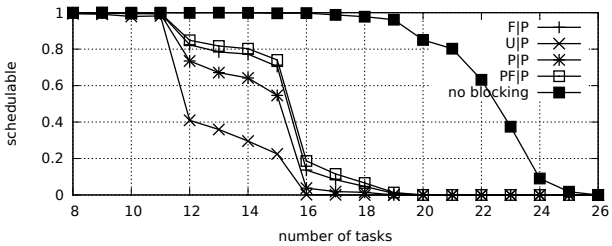

Fig. 1319. Schedulability under preemptable spin locks for $m = 8$, $U = 0.3n$, 16 resources, $rsf = 0.25$, $N^{max} = 15$, and medium critical sections. The schedulability of the considered non-preemptable lock types in this configuration is shown in Fig. 1309.

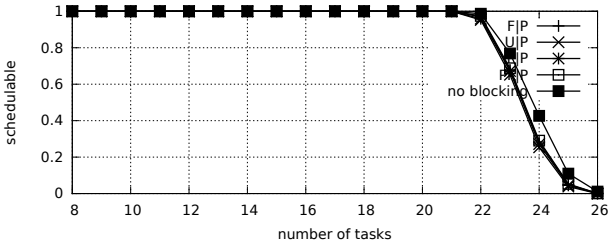

Fig. 1320. Schedulability under preemptable spin locks for $m = 8$, $U = 0.3n$, 16 resources, $rsf = 0.25$, $N^{max} = 1$, and short critical sections. The schedulability of the considered non-preemptable lock types in this configuration is shown in Fig. 1310.

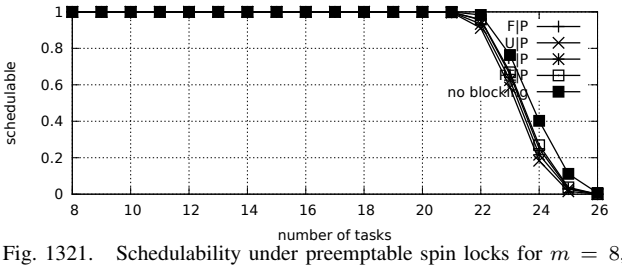

Fig. 1321. Schedulability under preemptable spin locks for $m = 8$, $U = 0.3n$, 16 resources, $rsf = 0.25$, $N^{max} = 2$, and short critical sections. The schedulability of the considered non-preemptable lock types in this configuration is shown in Fig. 1311.

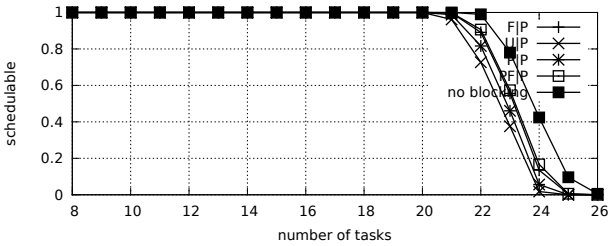

Fig. 1322. Schedulability under preemptable spin locks for $m = 8$, $U = 0.3n$, 16 resources, $rsf = 0.25$, $N^{max} = 5$, and short critical sections. The schedulability of the considered non-preemptable lock types in this configuration is shown in Fig. 1312.

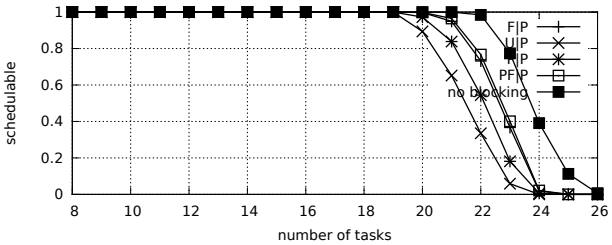

Fig. 1323. Schedulability under preemptable spin locks for $m = 8$, $U = 0.3n$, 16 resources, $rsf = 0.25$, $N^{max} = 10$, and short critical sections. The schedulability of the considered non-preemptable lock types in this configuration is shown in Fig. 1313.

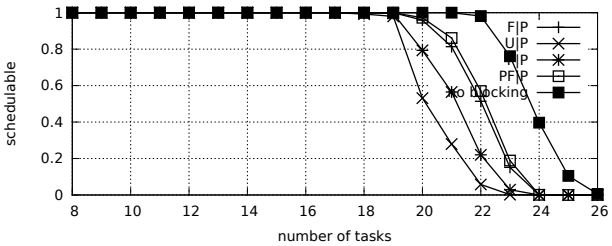

Fig. 1324. Schedulability under preemptable spin locks for $m = 8$, $U = 0.3n$, 16 resources, $rsf = 0.25$, $N^{max} = 15$, and short critical sections. The schedulability of the considered non-preemptable lock types in this configuration is shown in Fig. 1314.

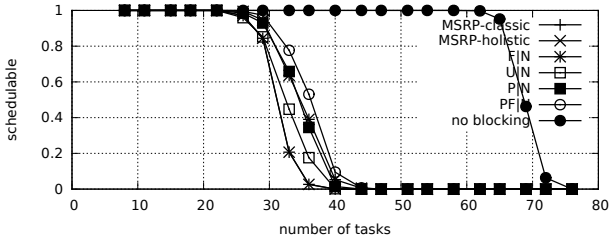

Fig. 1325. Schedulability under non-preemptable spin locks for $m = 8$, $U = 0.1n$, 16 resources, $rsf = 0.4$, $N^{max} = 1$, and medium critical sections. The schedulability of the considered preemptable lock types in this configuration is shown in Fig. 1335.

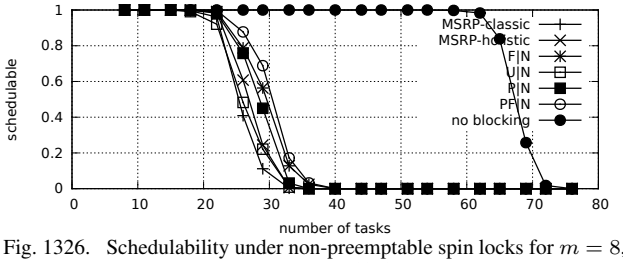

Fig. 1326. Schedulability under non-preemptable spin locks for $m = 8$, $U = 0.1n$, 16 resources, $rsf = 0.4$, $N^{max} = 2$, and medium critical sections. The schedulability of the considered preemptable lock types in this configuration is shown in Fig. 1336.

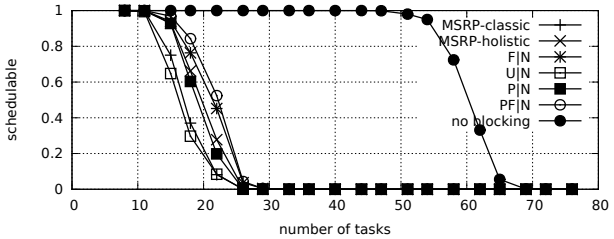

Fig. 1327. Schedulability under non-preemptable spin locks for $m = 8$, $U = 0.1n$, 16 resources, $rsf = 0.4$, $N^{max} = 5$, and medium critical sections. The schedulability of the considered preemptable lock types in this configuration is shown in Fig. 1337.

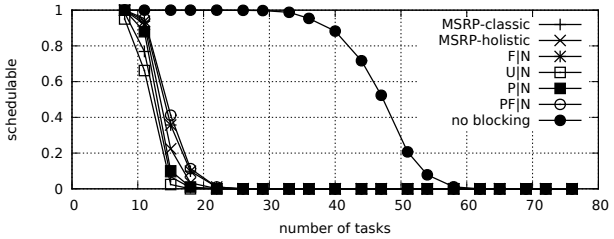

Fig. 1328. Schedulability under non-preemptable spin locks for $m = 8$, $U = 0.1n$, 16 resources, $rsf = 0.4$, $N^{max} = 10$, and medium critical sections. The schedulability of the considered preemptable lock types in this configuration is shown in Fig. 1338.

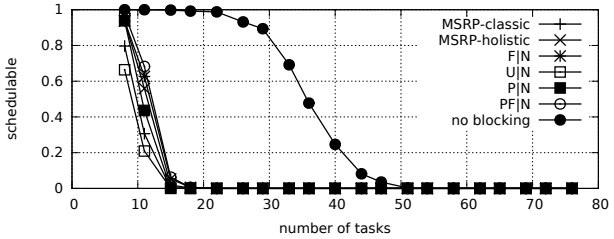

Fig. 1329. Schedulability under non-preemptable spin locks for $m = 8$, $U = 0.1n$, 16 resources, $rsf = 0.4$, $N^{max} = 15$, and medium critical sections. The schedulability of the considered preemptable lock types in this configuration is shown in Fig. 1339.

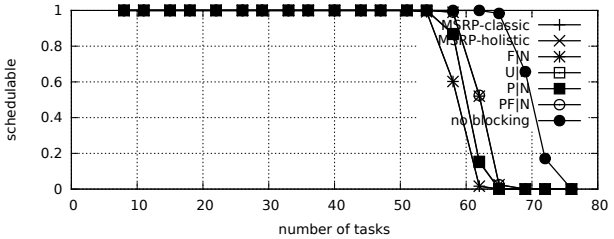

Fig. 1330. Schedulability under non-preemptable spin locks for $m = 8$, $U = 0.1n$, 16 resources, $rsf = 0.4$, $N^{max} = 1$, and short critical sections. The schedulability of the considered preemptable lock types in this configuration is shown in Fig. 1340.

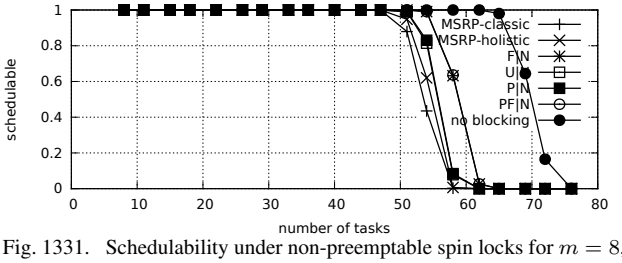

Fig. 1331. Schedulability under non-preemptable spin locks for $m = 8$, $U = 0.1n$, 16 resources, $rsf = 0.4$, $N^{max} = 2$, and short critical sections. The schedulability of the considered preemptable lock types in this configuration is shown in Fig. 1341.

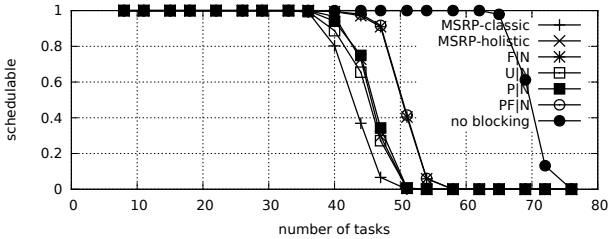

Fig. 1332. Schedulability under non-preemptable spin locks for $m = 8$, $U = 0.1n$, 16 resources, $rsf = 0.4$, $N^{max} = 5$, and short critical sections. The schedulability of the considered preemptable lock types in this configuration is shown in Fig. 1342.

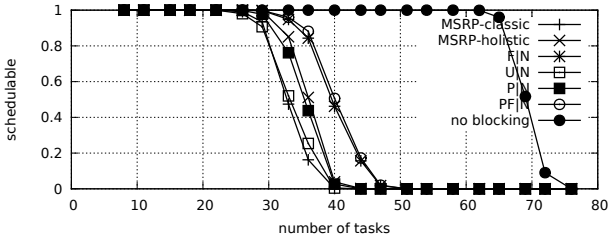

Fig. 1333. Schedulability under non-preemptable spin locks for $m = 8$, $U = 0.1n$, 16 resources, $rsf = 0.4$, $N^{max} = 10$, and short critical sections. The schedulability of the considered preemptable lock types in this configuration is shown in Fig. 1343.

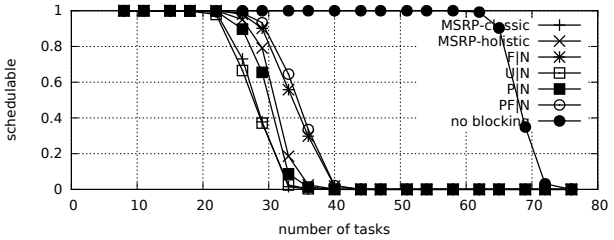

Fig. 1334. Schedulability under non-preemptable spin locks for $m = 8$, $U = 0.1n$, 16 resources, $rsf = 0.4$, $N^{max} = 15$, and short critical sections. The schedulability of the considered preemptable lock types in this configuration is shown in Fig. 1344.

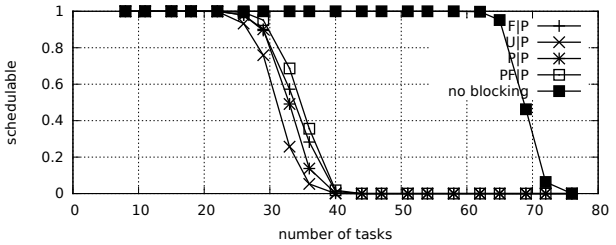

Fig. 1335. Schedulability under preemptable spin locks for $m = 8$, $U = 0.1n$, 16 resources, $rsf = 0.4$, $N^{max} = 1$, and medium critical sections. The schedulability of the considered non-preemptable lock types in this configuration is shown in Fig. 1325.

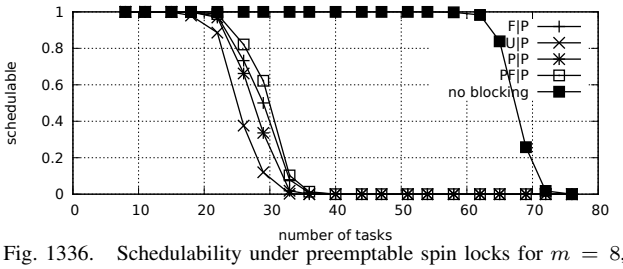

Fig. 1336. Schedulability under preemptable spin locks for $m = 8$, $U = 0.1n$, 16 resources, $rsf = 0.4$, $N^{max} = 2$, and medium critical sections. The schedulability of the considered non-preemptable lock types in this configuration is shown in Fig. 1326.

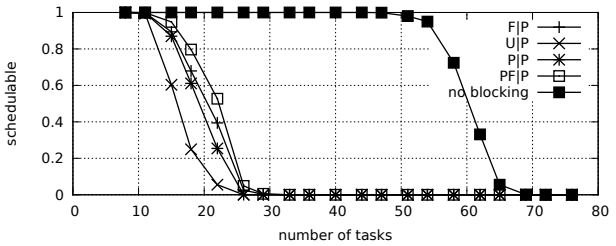

Fig. 1337. Schedulability under preemptable spin locks for $m = 8$, $U = 0.1n$, 16 resources, $rsf = 0.4$, $N^{max} = 5$, and medium critical sections. The schedulability of the considered non-preemptable lock types in this configuration is shown in Fig. 1327.

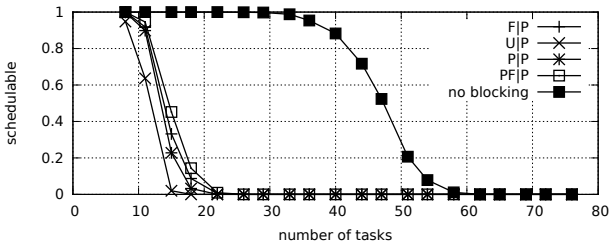

Fig. 1338. Schedulability under preemptable spin locks for $m = 8$, $U = 0.1n$, 16 resources, $rsf = 0.4$, $N^{max} = 10$, and medium critical sections. The schedulability of the considered non-preemptable lock types in this configuration is shown in Fig. 1328.

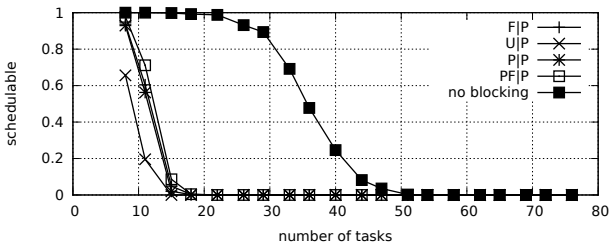

Fig. 1339. Schedulability under preemptable spin locks for $m = 8$, $U = 0.1n$, 16 resources, $rsf = 0.4$, $N^{max} = 15$, and medium critical sections. The schedulability of the considered non-preemptable lock types in this configuration is shown in Fig. 1329.

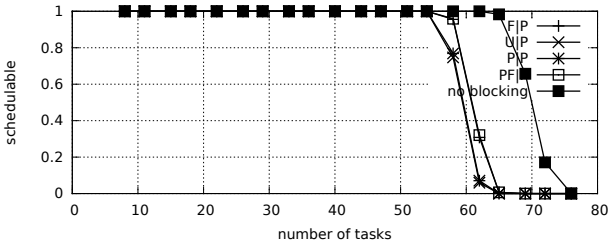

Fig. 1340. Schedulability under preemptable spin locks for $m = 8$, $U = 0.1n$, 16 resources, $rsf = 0.4$, $N^{max} = 1$, and short critical sections. The schedulability of the considered non-preemptable lock types in this configuration is shown in Fig. 1330.

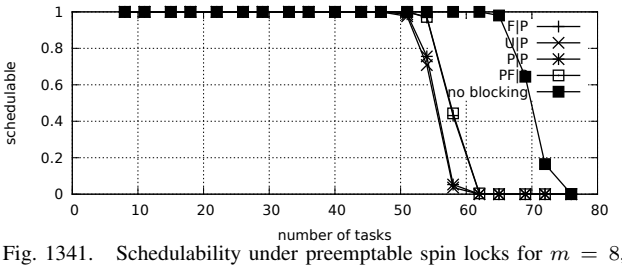

Fig. 1341. Schedulability under preemptable spin locks for $m = 8$, $U = 0.1n$, 16 resources, $rsf = 0.4$, $N^{max} = 2$, and short critical sections. The schedulability of the considered non-preemptable lock types in this configuration is shown in Fig. 1331.

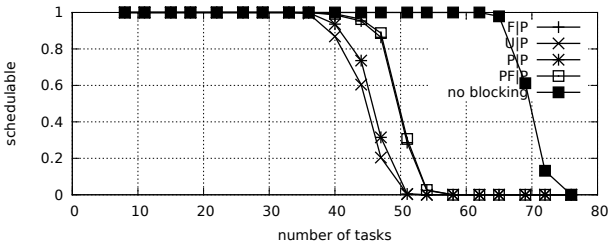

Fig. 1342. Schedulability under preemptable spin locks for $m = 8$, $U = 0.1n$, 16 resources, $rsf = 0.4$, $N^{max} = 5$, and short critical sections. The schedulability of the considered non-preemptable lock types in this configuration is shown in Fig. 1332.

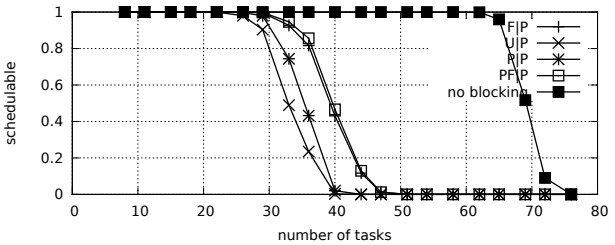

Fig. 1343. Schedulability under preemptable spin locks for $m = 8$, $U = 0.1n$, 16 resources, $rsf = 0.4$, $N^{max} = 10$, and short critical sections. The schedulability of the considered non-preemptable lock types in this configuration is shown in Fig. 1333.

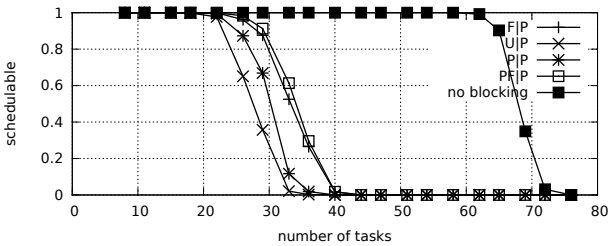

Fig. 1344. Schedulability under preemptable spin locks for $m = 8$, $U = 0.1n$, 16 resources, $rsf = 0.4$, $N^{max} = 15$, and short critical sections. The schedulability of the considered non-preemptable lock types in this configuration is shown in Fig. 1334.

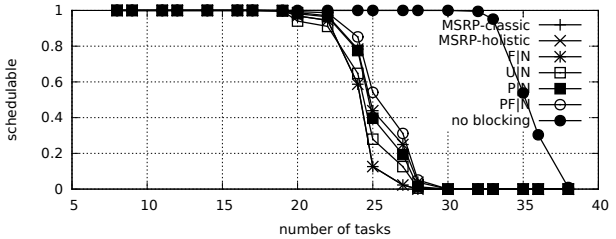

Fig. 1345. Schedulability under non-preemptable spin locks for $m = 8$, $U = 0.2n$, 16 resources, $rsf = 0.4$, $N^{max} = 1$, and medium critical sections. The schedulability of the considered preemptable lock types in this configuration is shown in Fig. 1355.

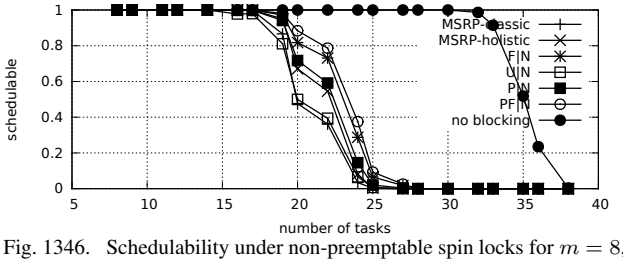

Fig. 1346. Schedulability under non-preemptable spin locks for $m = 8$, $U = 0.2n$, 16 resources, $rsf = 0.4$, $N^{max} = 2$, and medium critical sections. The schedulability of the considered preemptable lock types in this configuration is shown in Fig. 1356.

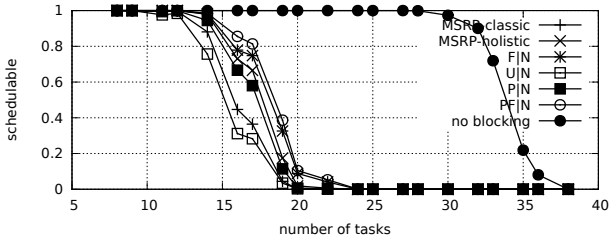

Fig. 1347. Schedulability under non-preemptable spin locks for $m = 8$, $U = 0.2n$, 16 resources, $rsf = 0.4$, $N^{max} = 5$, and medium critical sections. The schedulability of the considered preemptable lock types in this configuration is shown in Fig. 1357.

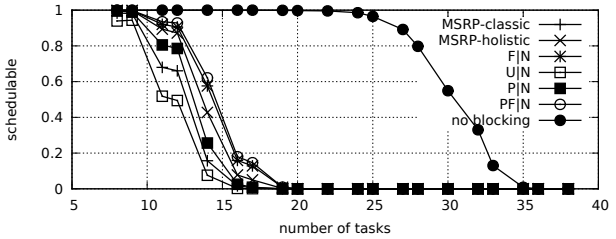

Fig. 1348. Schedulability under non-preemptable spin locks for $m = 8$, $U = 0.2n$, 16 resources, $rsf = 0.4$, $N^{max} = 10$, and medium critical sections. The schedulability of the considered preemptable lock types in this configuration is shown in Fig. 1358.

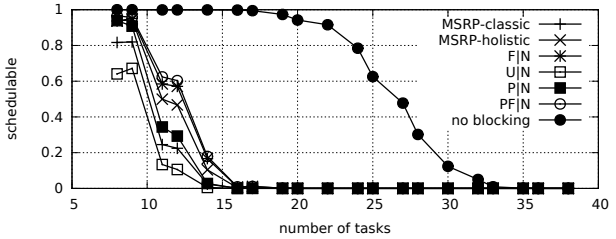

Fig. 1349. Schedulability under non-preemptable spin locks for $m = 8$, $U = 0.2n$, 16 resources, $rsf = 0.4$, $N^{max} = 15$, and medium critical sections. The schedulability of the considered preemptable lock types in this configuration is shown in Fig. 1359.

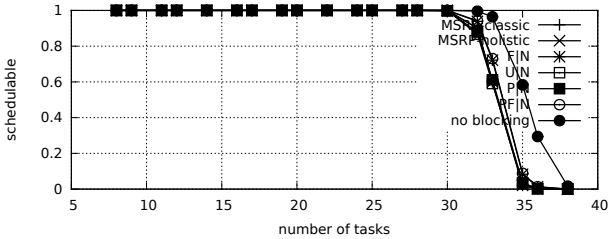

Fig. 1350. Schedulability under non-preemptable spin locks for $m = 8$, $U = 0.2n$, 16 resources, $rsf = 0.4$, $N^{max} = 1$, and short critical sections. The schedulability of the considered preemptable lock types in this configuration is shown in Fig. 1360.

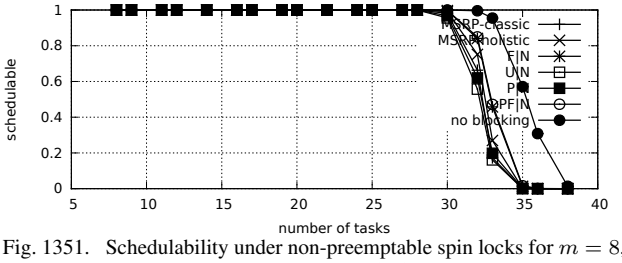

Fig. 1351. Schedulability under non-preemptable spin locks for $m = 8$, $U = 0.2n$, 16 resources, $rsf = 0.4$, $N^{max} = 2$, and short critical sections. The schedulability of the considered preemptable lock types in this configuration is shown in Fig. 1361.

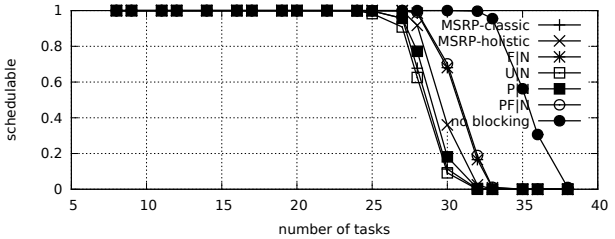

Fig. 1352. Schedulability under non-preemptable spin locks for $m = 8$, $U = 0.2n$, 16 resources, $rsf = 0.4$, $N^{max} = 5$, and short critical sections. The schedulability of the considered preemptable lock types in this configuration is shown in Fig. 1362.

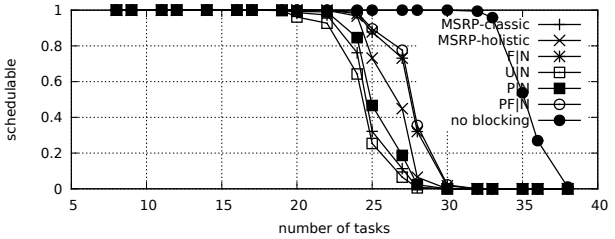

Fig. 1353. Schedulability under non-preemptable spin locks for $m = 8$, $U = 0.2n$, 16 resources, $rsf = 0.4$, $N^{max} = 10$, and short critical sections. The schedulability of the considered preemptable lock types in this configuration is shown in Fig. 1363.

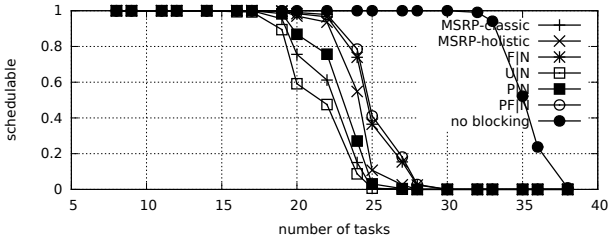

Fig. 1354. Schedulability under non-preemptable spin locks for $m = 8$, $U = 0.2n$, 16 resources, $rsf = 0.4$, $N^{max} = 15$, and short critical sections. The schedulability of the considered preemptable lock types in this configuration is shown in Fig. 1364.

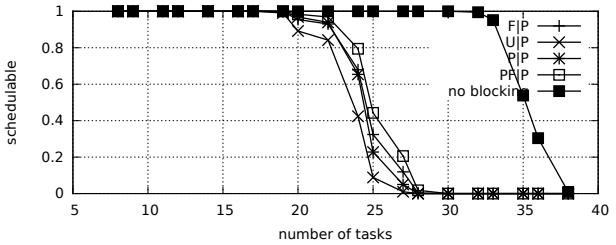

Fig. 1355. Schedulability under preemptable spin locks for $m = 8$, $U = 0.2n$, 16 resources, $rsf = 0.4$, $N^{max} = 1$, and medium critical sections. The schedulability of the considered non-preemptable lock types in this configuration is shown in Fig. 1345.

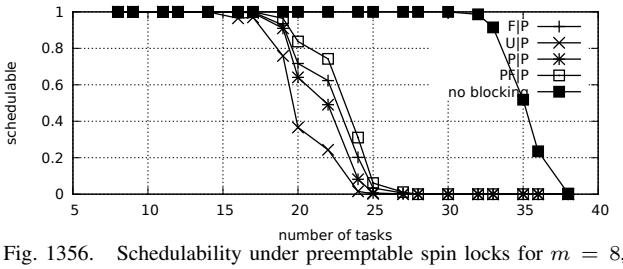

Fig. 1356. Schedulability under preemptable spin locks for $m = 8$, $U = 0.2n$, 16 resources, $rsf = 0.4$, $N^{max} = 2$, and medium critical sections. The schedulability of the considered non-preemptable lock types in this configuration is shown in Fig. 1346.

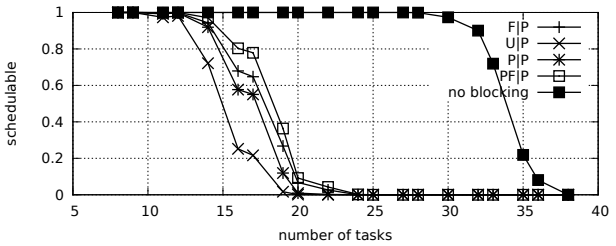

Fig. 1357. Schedulability under preemptable spin locks for $m = 8$, $U = 0.2n$, 16 resources, $rsf = 0.4$, $N^{max} = 5$, and medium critical sections. The schedulability of the considered non-preemptable lock types in this configuration is shown in Fig. 1347.

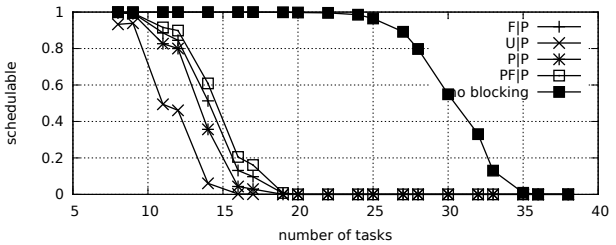

Fig. 1358. Schedulability under preemptable spin locks for $m = 8$, $U = 0.2n$, 16 resources, $rsf = 0.4$, $N^{max} = 10$, and medium critical sections. The schedulability of the considered non-preemptable lock types in this configuration is shown in Fig. 1348.

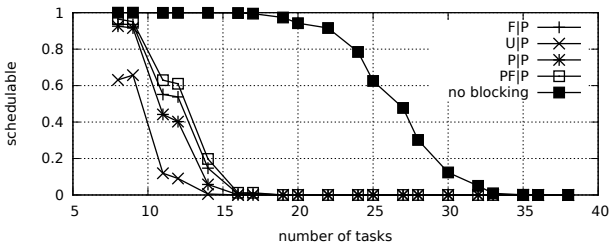

Fig. 1359. Schedulability under preemptable spin locks for $m = 8$, $U = 0.2n$, 16 resources, $rsf = 0.4$, $N^{max} = 15$, and medium critical sections. The schedulability of the considered non-preemptable lock types in this configuration is shown in Fig. 1349.

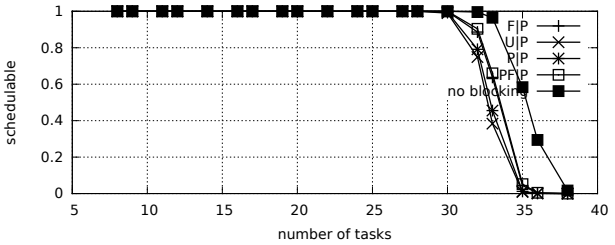

Fig. 1360. Schedulability under preemptable spin locks for $m = 8$, $U = 0.2n$, 16 resources, $rsf = 0.4$, $N^{max} = 1$, and short critical sections. The schedulability of the considered non-preemptable lock types in this configuration is shown in Fig. 1350.

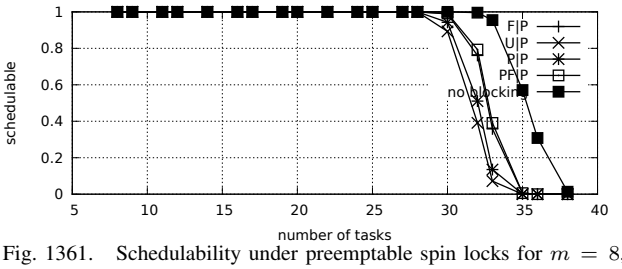

Fig. 1361. Schedulability under preemptable spin locks for $m = 8$, $U = 0.2n$, 16 resources, $rsf = 0.4$, $N^{max} = 2$, and short critical sections. The schedulability of the considered non-preemptable lock types in this configuration is shown in Fig. 1351.

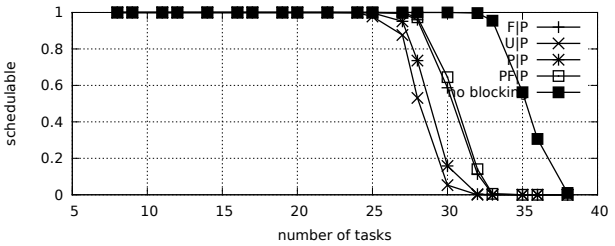

Fig. 1362. Schedulability under preemptable spin locks for $m = 8$, $U = 0.2n$, 16 resources, $rsf = 0.4$, $N^{max} = 5$, and short critical sections. The schedulability of the considered non-preemptable lock types in this configuration is shown in Fig. 1352.

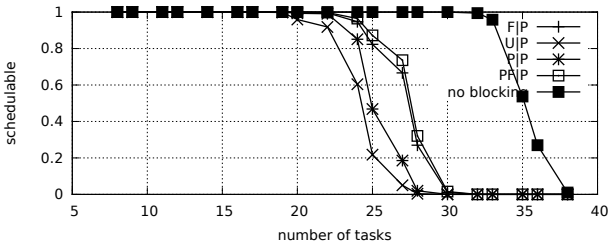

Fig. 1363. Schedulability under preemptable spin locks for $m = 8$, $U = 0.2n$, 16 resources, $rsf = 0.4$, $N^{max} = 10$, and short critical sections. The schedulability of the considered non-preemptable lock types in this configuration is shown in Fig. 1353.

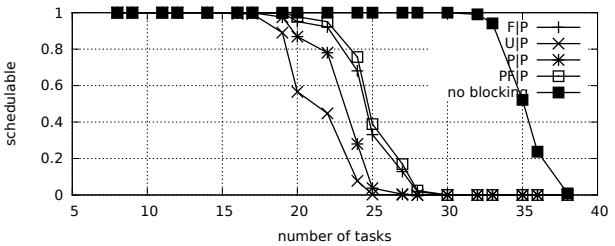

Fig. 1364. Schedulability under preemptable spin locks for $m = 8$, $U = 0.2n$, 16 resources, $rsf = 0.4$, $N^{max} = 15$, and short critical sections. The schedulability of the considered non-preemptable lock types in this configuration is shown in Fig. 1354.

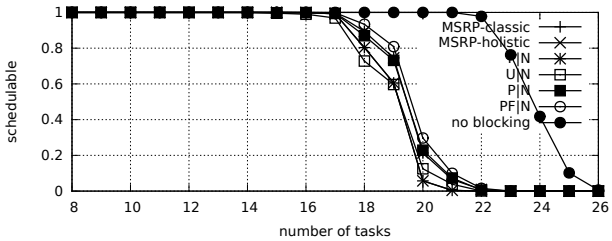

Fig. 1365. Schedulability under non-preemptable spin locks for $m = 8$, $U = 0.3n$, 16 resources, $rsf = 0.4$, $N^{max} = 1$, and medium critical sections. The schedulability of the considered preemptable lock types in this configuration is shown in Fig. 1375.

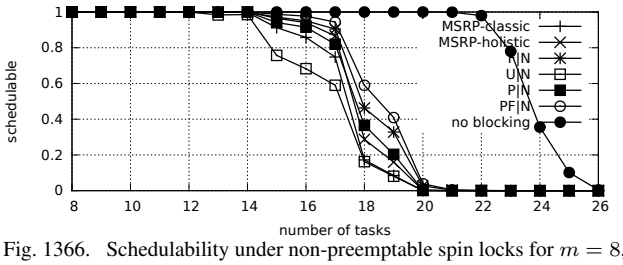

Fig. 1366. Schedulability under non-preemptable spin locks for $m = 8$, $U = 0.3n$, 16 resources, $rsf = 0.4$, $N^{max} = 2$, and medium critical sections. The schedulability of the considered preemptable lock types in this configuration is shown in Fig. 1376.

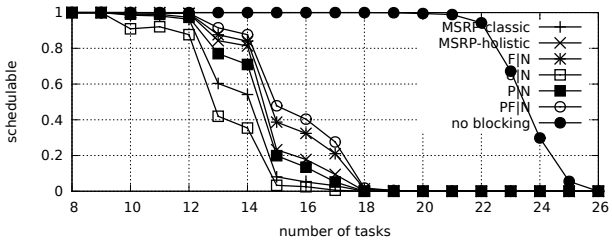

Fig. 1367. Schedulability under non-preemptable spin locks for $m = 8$, $U = 0.3n$, 16 resources, $rsf = 0.4$, $N^{max} = 5$, and medium critical sections. The schedulability of the considered preemptable lock types in this configuration is shown in Fig. 1377.

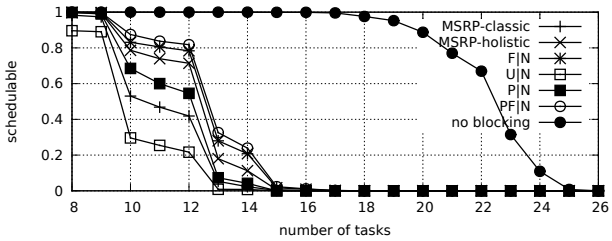

Fig. 1368. Schedulability under non-preemptable spin locks for $m = 8$, $U = 0.3n$, 16 resources, $rsf = 0.4$, $N^{max} = 10$, and medium critical sections. The schedulability of the considered preemptable lock types in this configuration is shown in Fig. 1378.

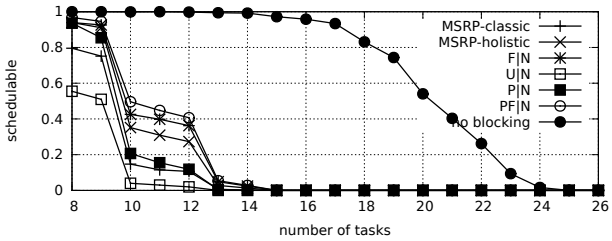

Fig. 1369. Schedulability under non-preemptable spin locks for $m = 8$, $U = 0.3n$, 16 resources, $rsf = 0.4$, $N^{max} = 15$, and medium critical sections. The schedulability of the considered preemptable lock types in this configuration is shown in Fig. 1379.

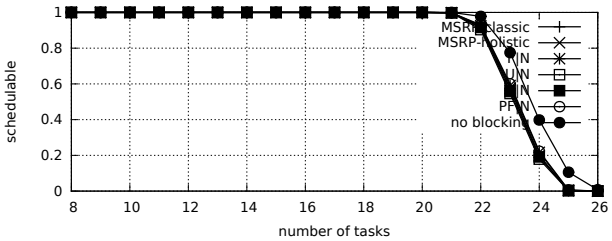

Fig. 1370. Schedulability under non-preemptable spin locks for $m = 8$, $U = 0.3n$, 16 resources, $rsf = 0.4$, $N^{max} = 1$, and short critical sections. The schedulability of the considered preemptable lock types in this configuration is shown in Fig. 1380.

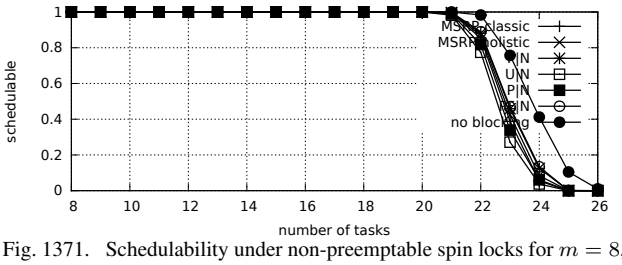

Fig. 1371. Schedulability under non-preemptable spin locks for $m = 8$, $U = 0.3n$, 16 resources, $rsf = 0.4$, $N^{max} = 2$, and short critical sections. The schedulability of the considered preemptable lock types in this configuration is shown in Fig. 1381.

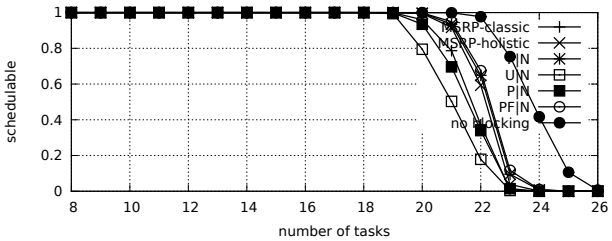

Fig. 1372. Schedulability under non-preemptable spin locks for $m = 8$, $U = 0.3n$, 16 resources, $rsf = 0.4$, $N^{max} = 5$, and short critical sections. The schedulability of the considered preemptable lock types in this configuration is shown in Fig. 1382.

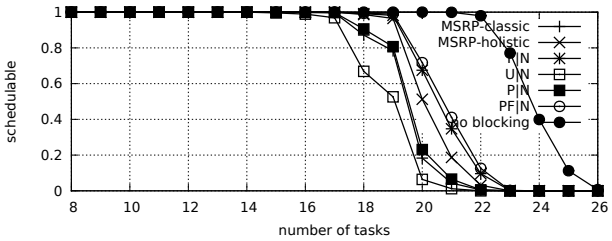

Fig. 1373. Schedulability under non-preemptable spin locks for $m = 8$, $U = 0.3n$, 16 resources, $rsf = 0.4$, $N^{max} = 10$, and short critical sections. The schedulability of the considered preemptable lock types in this configuration is shown in Fig. 1383.

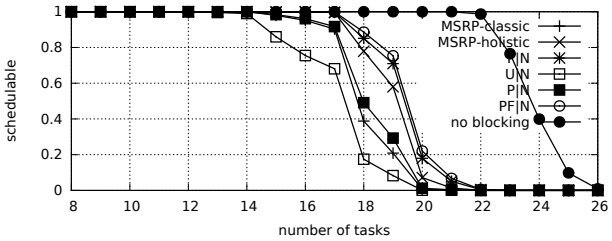

Fig. 1374. Schedulability under non-preemptable spin locks for $m = 8$, $U = 0.3n$, 16 resources, $rsf = 0.4$, $N^{max} = 15$, and short critical sections. The schedulability of the considered preemptable lock types in this configuration is shown in Fig. 1384.

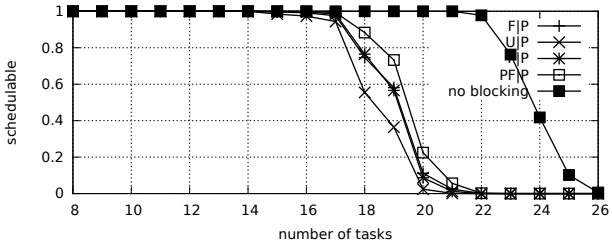

Fig. 1375. Schedulability under preemptable spin locks for $m = 8$, $U = 0.3n$, 16 resources, $rsf = 0.4$, $N^{max} = 1$, and medium critical sections. The schedulability of the considered non-preemptable lock types in this configuration is shown in Fig. 1365.

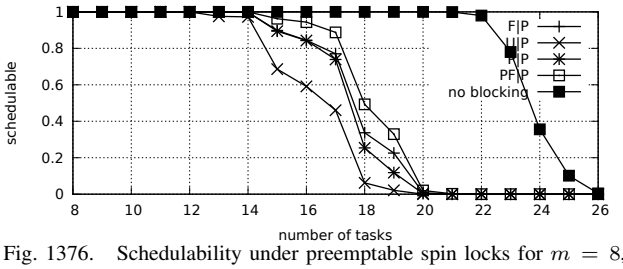

Fig. 1376. Schedulability under preemptable spin locks for $m = 8$, $U = 0.3n$, 16 resources, $rsf = 0.4$, $N^{max} = 2$, and medium critical sections. The schedulability of the considered non-preemptable lock types in this configuration is shown in Fig. 1366.

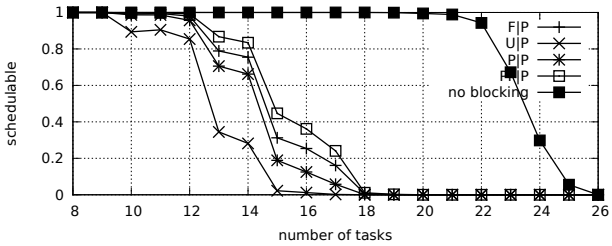

Fig. 1377. Schedulability under preemptable spin locks for $m = 8$, $U = 0.3n$, 16 resources, $rsf = 0.4$, $N^{max} = 5$, and medium critical sections. The schedulability of the considered non-preemptable lock types in this configuration is shown in Fig. 1367.

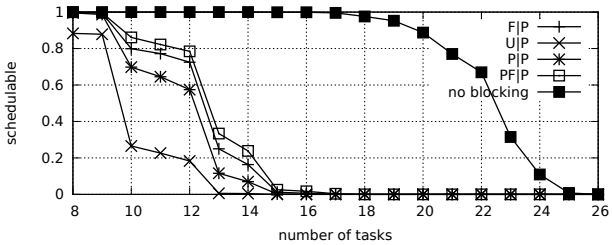

Fig. 1378. Schedulability under preemptable spin locks for $m = 8$, $U = 0.3n$, 16 resources, $rsf = 0.4$, $N^{max} = 10$, and medium critical sections. The schedulability of the considered non-preemptable lock types in this configuration is shown in Fig. 1368.

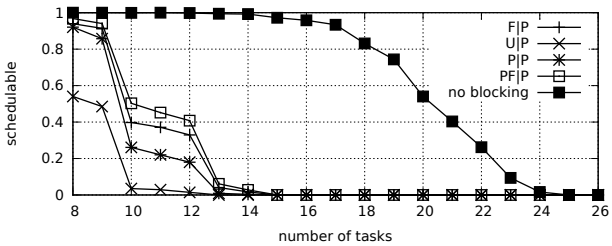

Fig. 1379. Schedulability under preemptable spin locks for $m = 8$, $U = 0.3n$, 16 resources, $rsf = 0.4$, $N^{max} = 15$, and medium critical sections. The schedulability of the considered non-preemptable lock types in this configuration is shown in Fig. 1369.

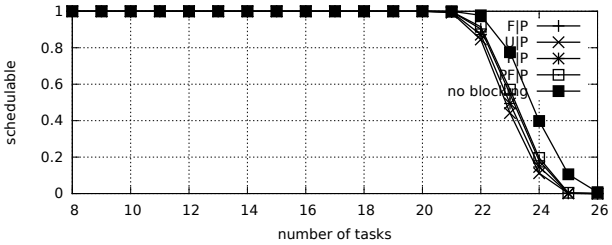

Fig. 1380. Schedulability under preemptable spin locks for $m = 8$, $U = 0.3n$, 16 resources, $rsf = 0.4$, $N^{max} = 1$, and short critical sections. The schedulability of the considered non-preemptable lock types in this configuration is shown in Fig. 1370.

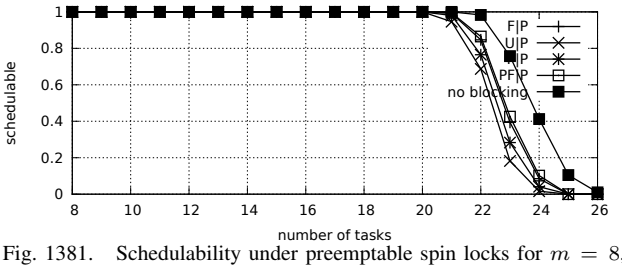

Fig. 1381. Schedulability under preemptable spin locks for $m = 8$, $U = 0.3n$, 16 resources, $rsf = 0.4$, $N^{max} = 2$, and short critical sections. The schedulability of the considered non-preemptable lock types in this configuration is shown in Fig. 1371.

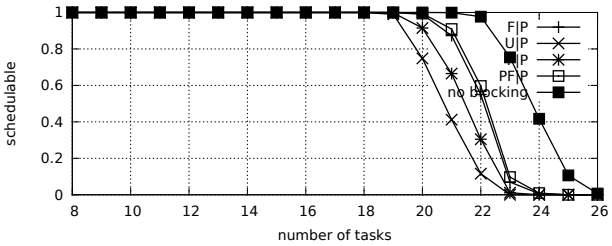

Fig. 1382. Schedulability under preemptable spin locks for $m = 8$, $U = 0.3n$, 16 resources, $rsf = 0.4$, $N^{max} = 5$, and short critical sections. The schedulability of the considered non-preemptable lock types in this configuration is shown in Fig. 1372.

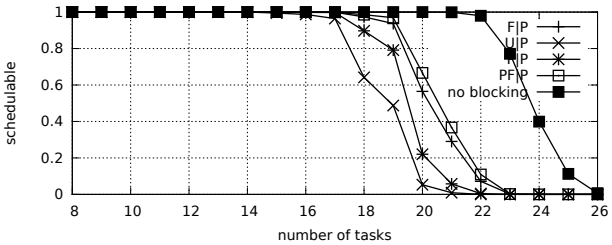

Fig. 1383. Schedulability under preemptable spin locks for $m = 8$, $U = 0.3n$, 16 resources, $rsf = 0.4$, $N^{max} = 10$, and short critical sections. The schedulability of the considered non-preemptable lock types in this configuration is shown in Fig. 1373.

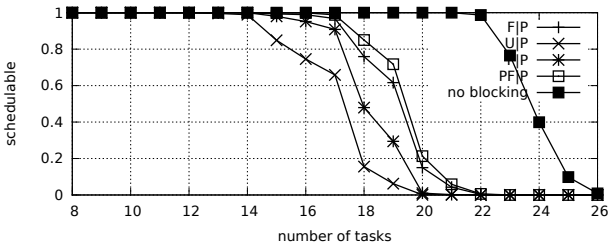

Fig. 1384. Schedulability under preemptable spin locks for $m = 8$, $U = 0.3n$, 16 resources, $rsf = 0.4$, $N^{max} = 15$, and short critical sections. The schedulability of the considered non-preemptable lock types in this configuration is shown in Fig. 1374.

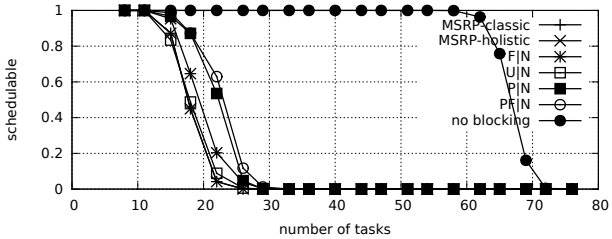

Fig. 1385. Schedulability under non-preemptable spin locks for $m = 8$, $U = 0.1n$, 16 resources, $rsf = 0.75$, $N^{max} = 1$, and medium critical sections. The schedulability of the considered preemptable lock types in this configuration is shown in Fig. 1395.

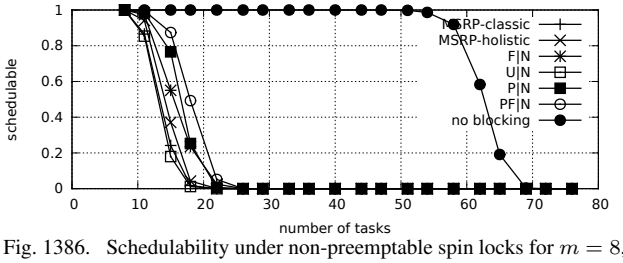

Fig. 1386. Schedulability under non-preemptable spin locks for $m = 8$, $U = 0.1n$, 16 resources, $rsf = 0.75$, $N^{max} = 2$, and medium critical sections. The schedulability of the considered preemptable lock types in this configuration is shown in Fig. 1396.

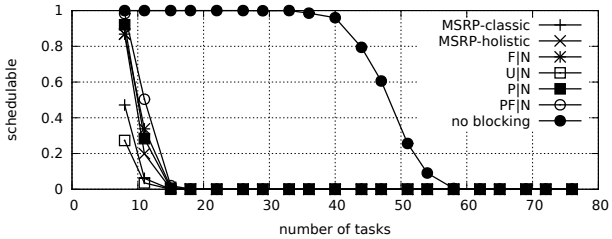

Fig. 1387. Schedulability under non-preemptable spin locks for $m = 8$, $U = 0.1n$, 16 resources, $rsf = 0.75$, $N^{max} = 5$, and medium critical sections. The schedulability of the considered preemptable lock types in this configuration is shown in Fig. 1397.

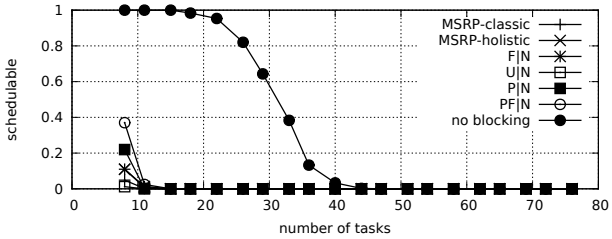

Fig. 1388. Schedulability under non-preemptable spin locks for $m = 8$, $U = 0.1n$, 16 resources, $rsf = 0.75$, $N^{max} = 10$, and medium critical sections. The schedulability of the considered preemptable lock types in this configuration is shown in Fig. 1398.

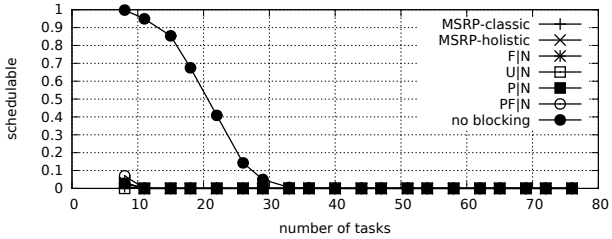

Fig. 1389. Schedulability under non-preemptable spin locks for $m = 8$, $U = 0.1n$, 16 resources, $rsf = 0.75$, $N^{max} = 15$, and medium critical sections. The schedulability of the considered preemptable lock types in this configuration is shown in Fig. 1399.

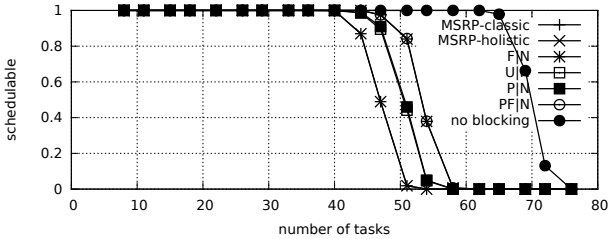

Fig. 1390. Schedulability under non-preemptable spin locks for $m = 8$, $U = 0.1n$, 16 resources, $rsf = 0.75$, $N^{max} = 1$, and short critical sections. The schedulability of the considered preemptable lock types in this configuration is shown in Fig. 1400.

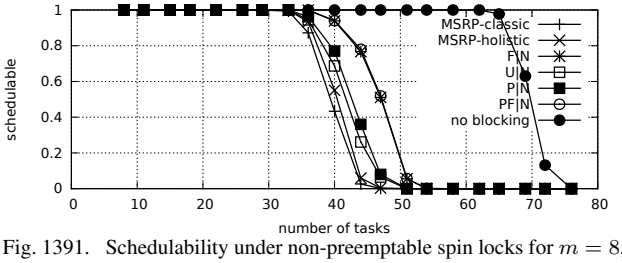

Fig. 1391. Schedulability under non-preemptable spin locks for $m = 8$, $U = 0.1n$, 16 resources, $rsf = 0.75$, $N^{max} = 2$, and short critical sections. The schedulability of the considered preemptable lock types in this configuration is shown in Fig. 1401.

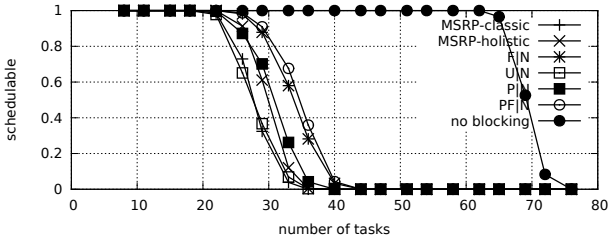

Fig. 1392. Schedulability under non-preemptable spin locks for $m = 8$, $U = 0.1n$, 16 resources, $rsf = 0.75$, $N^{max} = 5$, and short critical sections. The schedulability of the considered preemptable lock types in this configuration is shown in Fig. 1402.

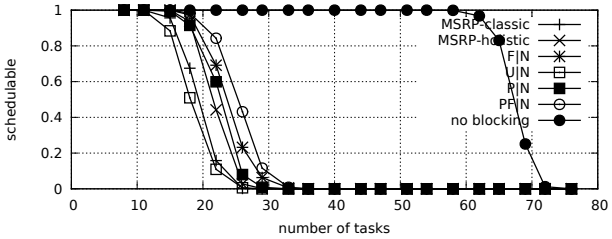

Fig. 1393. Schedulability under non-preemptable spin locks for $m = 8$, $U = 0.1n$, 16 resources, $rsf = 0.75$, $N^{max} = 10$, and short critical sections. The schedulability of the considered preemptable lock types in this configuration is shown in Fig. 1403.

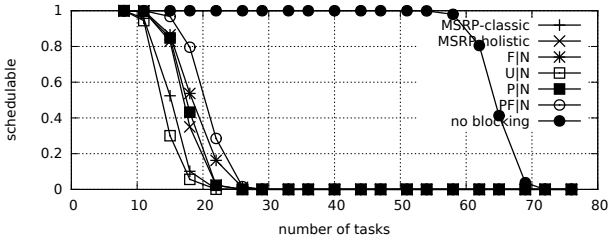

Fig. 1394. Schedulability under non-preemptable spin locks for $m = 8$, $U = 0.1n$, 16 resources, $rsf = 0.75$, $N^{max} = 15$, and short critical sections. The schedulability of the considered preemptable lock types in this configuration is shown in Fig. 1404.

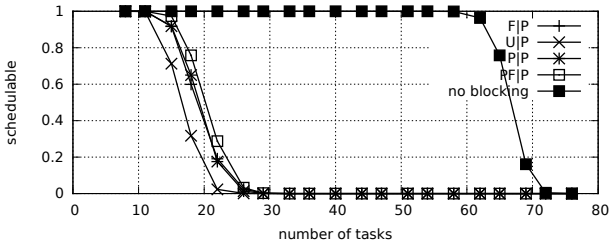

Fig. 1395. Schedulability under preemptable spin locks for $m = 8$, $U = 0.1n$, 16 resources, $rsf = 0.75$, $N^{max} = 1$, and medium critical sections. The schedulability of the considered non-preemptable lock types in this configuration is shown in Fig. 1385.

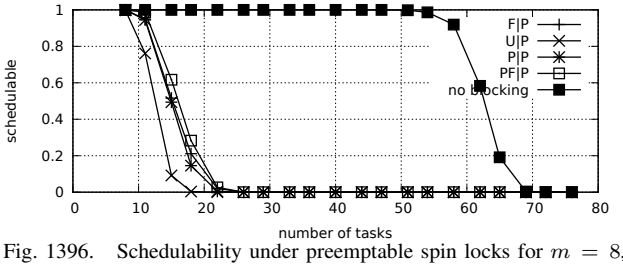

Fig. 1396. Schedulability under preemptable spin locks for $m = 8$, $U = 0.1n$, 16 resources, $rsf = 0.75$, $N^{max} = 2$, and medium critical sections. The schedulability of the considered non-preemptable lock types in this configuration is shown in Fig. 1386.

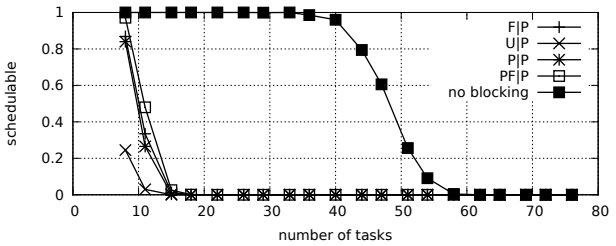

Fig. 1397. Schedulability under preemptable spin locks for $m = 8$, $U = 0.1n$, 16 resources, $rsf = 0.75$, $N^{max} = 5$, and medium critical sections. The schedulability of the considered non-preemptable lock types in this configuration is shown in Fig. 1387.

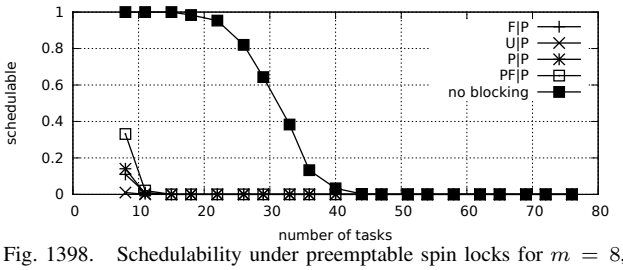

Fig. 1398. Schedulability under preemptable spin locks for $m = 8$, $U = 0.1n$, 16 resources, $rsf = 0.75$, $N^{max} = 10$, and medium critical sections. The schedulability of the considered non-preemptable lock types in this configuration is shown in Fig. 1388.

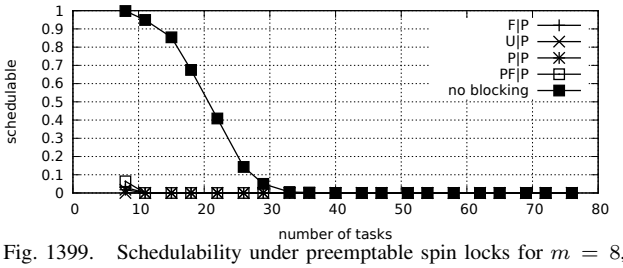

Fig. 1399. Schedulability under preemptable spin locks for $m = 8$, $U = 0.1n$, 16 resources, $rsf = 0.75$, $N^{max} = 15$, and medium critical sections. The schedulability of the considered non-preemptable lock types in this configuration is shown in Fig. 1389.

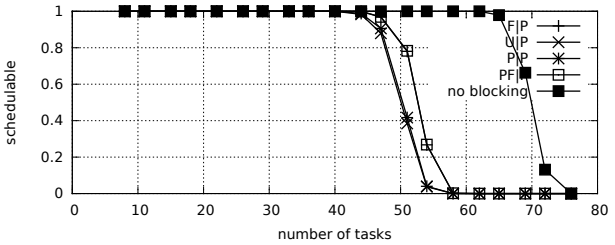

Fig. 1400. Schedulability under preemptable spin locks for $m = 8$, $U = 0.1n$, 16 resources, $rsf = 0.75$, $N^{max} = 1$, and short critical sections. The schedulability of the considered non-preemptable lock types in this configuration is shown in Fig. 1390.

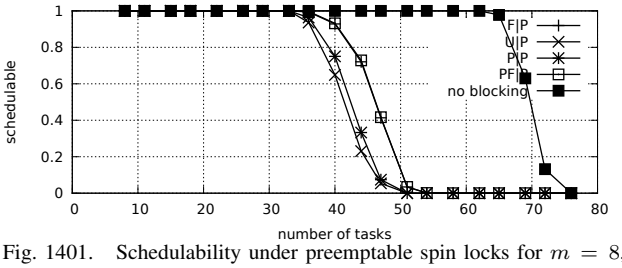

Fig. 1401. Schedulability under preemptable spin locks for $m = 8$, $U = 0.1n$, 16 resources, $rsf = 0.75$, $N^{max} = 2$, and short critical sections. The schedulability of the considered non-preemptable lock types in this configuration is shown in Fig. 1391.

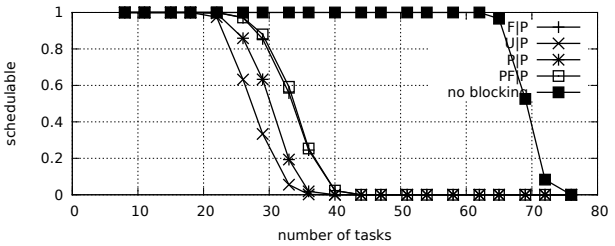

Fig. 1402. Schedulability under preemptable spin locks for $m = 8$, $U = 0.1n$, 16 resources, $rsf = 0.75$, $N^{max} = 5$, and short critical sections. The schedulability of the considered non-preemptable lock types in this configuration is shown in Fig. 1392.

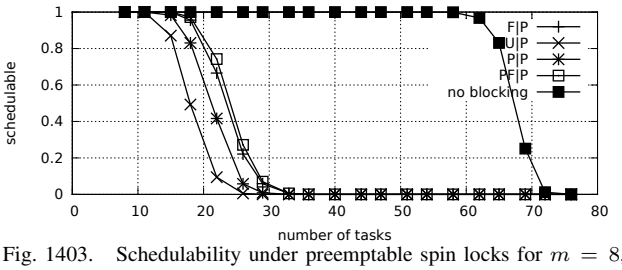

Fig. 1403. Schedulability under preemptable spin locks for $m = 8$, $U = 0.1n$, 16 resources, $rsf = 0.75$, $N^{max} = 10$, and short critical sections. The schedulability of the considered non-preemptable lock types in this configuration is shown in Fig. 1393.

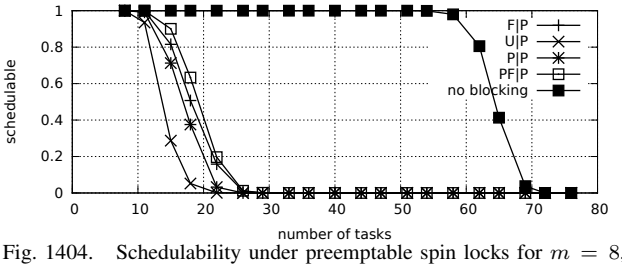

Fig. 1404. Schedulability under preemptable spin locks for $m = 8$, $U = 0.1n$, 16 resources, $rsf = 0.75$, $N^{max} = 15$, and short critical sections. The schedulability of the considered non-preemptable lock types in this configuration is shown in Fig. 1394.

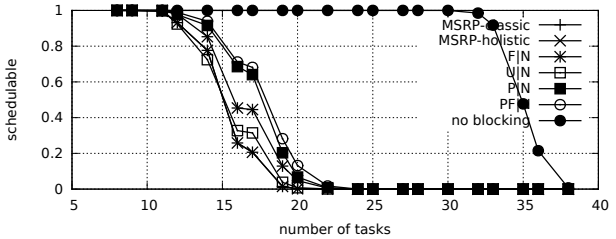

Fig. 1405. Schedulability under non-preemptable spin locks for $m = 8$, $U = 0.2n$, 16 resources, $rsf = 0.75$, $N^{max} = 1$, and medium critical sections. The schedulability of the considered preemptable lock types in this configuration is shown in Fig. 1415.

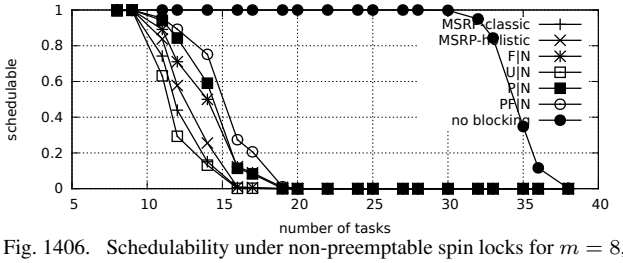

Fig. 1406. Schedulability under non-preemptable spin locks for $m = 8$, $U = 0.2n$, 16 resources, $rsf = 0.75$, $N^{max} = 2$, and medium critical sections. The schedulability of the considered preemptable lock types in this configuration is shown in Fig. 1416.

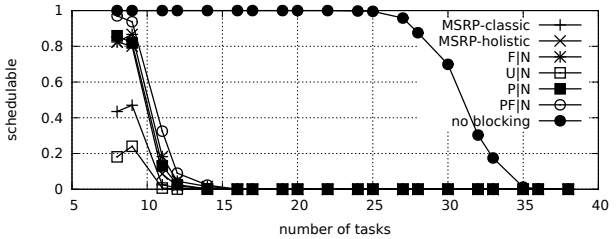

Fig. 1407. Schedulability under non-preemptable spin locks for $m = 8$, $U = 0.2n$, 16 resources, $rsf = 0.75$, $N^{max} = 5$, and medium critical sections. The schedulability of the considered preemptable lock types in this configuration is shown in Fig. 1417.

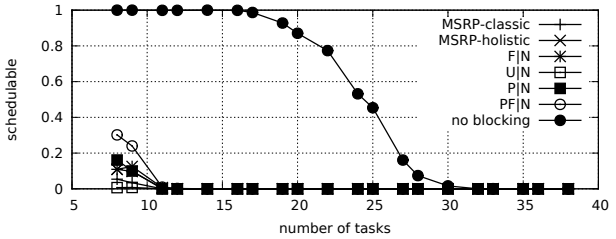

Fig. 1408. Schedulability under non-preemptable spin locks for $m = 8$, $U = 0.2n$, 16 resources, $rsf = 0.75$, $N^{max} = 10$, and medium critical sections. The schedulability of the considered preemptable lock types in this configuration is shown in Fig. 1418.

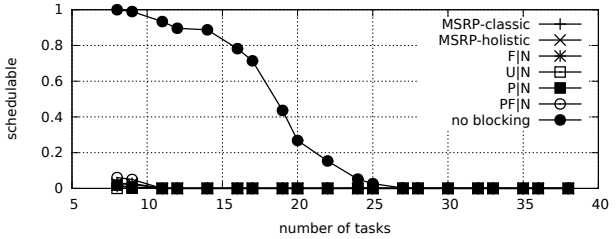

Fig. 1409. Schedulability under non-preemptable spin locks for $m = 8$, $U = 0.2n$, 16 resources, $rsf = 0.75$, $N^{max} = 15$, and medium critical sections. The schedulability of the considered preemptable lock types in this configuration is shown in Fig. 1419.

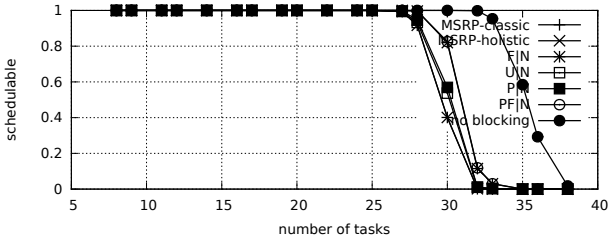

Fig. 1410. Schedulability under non-preemptable spin locks for $m = 8$, $U = 0.2n$, 16 resources, $rsf = 0.75$, $N^{max} = 1$, and short critical sections. The schedulability of the considered preemptable lock types in this configuration is shown in Fig. 1420.

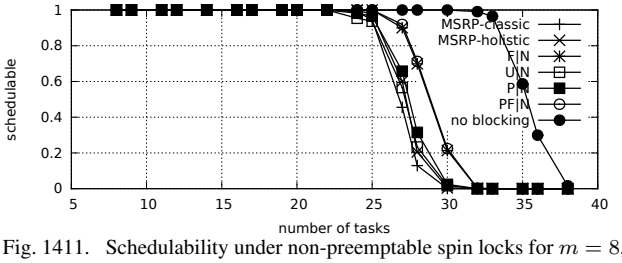

Fig. 1411. Schedulability under non-preemptable spin locks for $m = 8$, $U = 0.2n$, 16 resources, $rsf = 0.75$, $N^{max} = 2$, and short critical sections. The schedulability of the considered preemptable lock types in this configuration is shown in Fig. 1421.

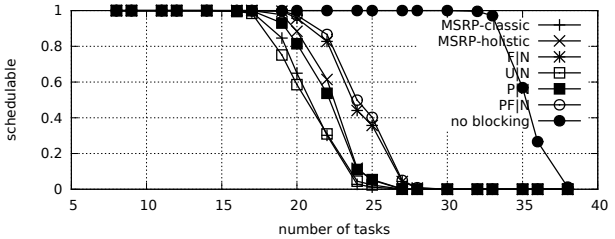

Fig. 1412. Schedulability under non-preemptable spin locks for $m = 8$, $U = 0.2n$, 16 resources, $rsf = 0.75$, $N^{max} = 5$, and short critical sections. The schedulability of the considered preemptable lock types in this configuration is shown in Fig. 1422.

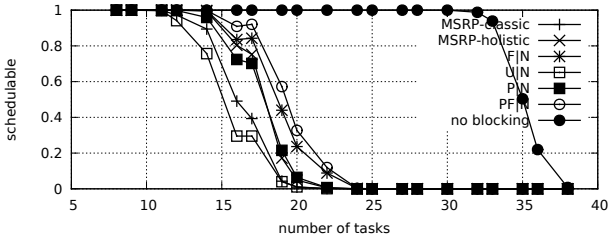

Fig. 1413. Schedulability under non-preemptable spin locks for $m = 8$, $U = 0.2n$, 16 resources, $rsf = 0.75$, $N^{max} = 10$, and short critical sections. The schedulability of the considered preemptable lock types in this configuration is shown in Fig. 1423.

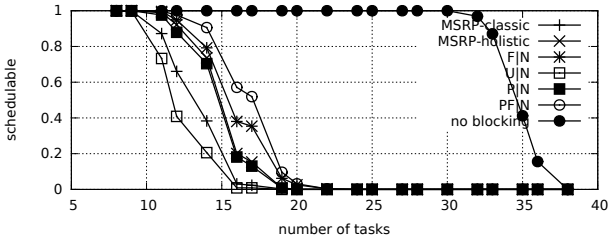

Fig. 1414. Schedulability under non-preemptable spin locks for $m = 8$, $U = 0.2n$, 16 resources, $rsf = 0.75$, $N^{max} = 15$, and short critical sections. The schedulability of the considered preemptable lock types in this configuration is shown in Fig. 1424.

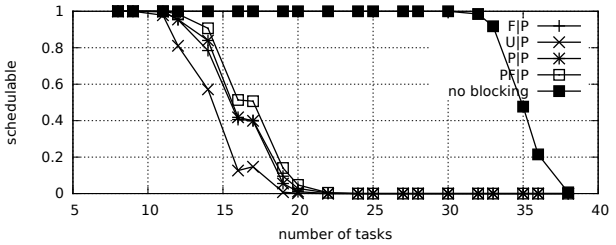

Fig. 1415. Schedulability under preemptable spin locks for $m = 8$, $U = 0.2n$, 16 resources, $rsf = 0.75$, $N^{max} = 1$, and medium critical sections. The schedulability of the considered non-preemptable lock types in this configuration is shown in Fig. 1405.

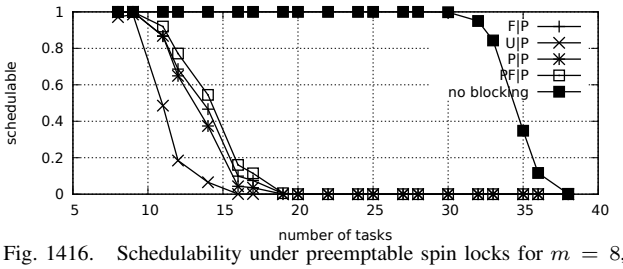

Fig. 1416. Schedulability under preemptable spin locks for $m = 8$, $U = 0.2n$, 16 resources, $rsf = 0.75$, $N^{max} = 2$, and medium critical sections. The schedulability of the considered non-preemptable lock types in this configuration is shown in Fig. 1406.

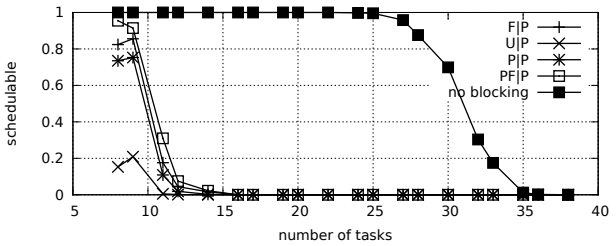

Fig. 1417. Schedulability under preemptable spin locks for $m = 8$, $U = 0.2n$, 16 resources, $rsf = 0.75$, $N^{max} = 5$, and medium critical sections. The schedulability of the considered non-preemptable lock types in this configuration is shown in Fig. 1407.

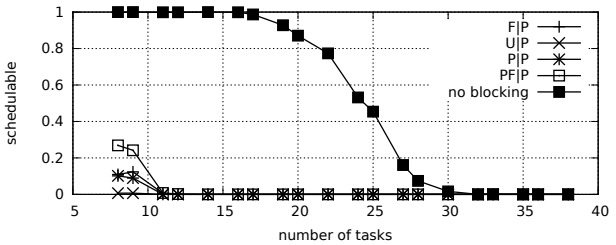

Fig. 1418. Schedulability under preemptable spin locks for $m = 8$, $U = 0.2n$, 16 resources, $rsf = 0.75$, $N^{max} = 10$, and medium critical sections. The schedulability of the considered non-preemptable lock types in this configuration is shown in Fig. 1408.

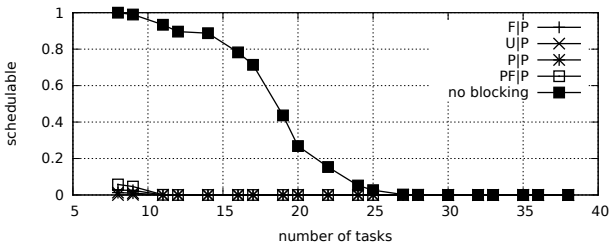

Fig. 1419. Schedulability under preemptable spin locks for $m = 8$, $U = 0.2n$, 16 resources, $rsf = 0.75$, $N^{max} = 15$, and medium critical sections. The schedulability of the considered non-preemptable lock types in this configuration is shown in Fig. 1409.

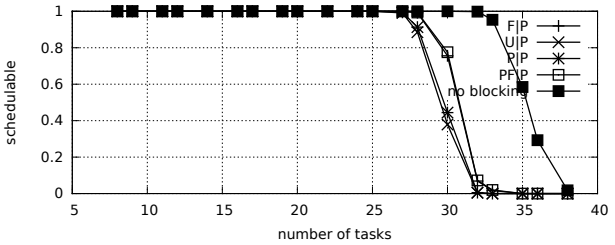

Fig. 1420. Schedulability under preemptable spin locks for $m = 8$, $U = 0.2n$, 16 resources, $rsf = 0.75$, $N^{max} = 1$, and short critical sections. The schedulability of the considered non-preemptable lock types in this configuration is shown in Fig. 1410.

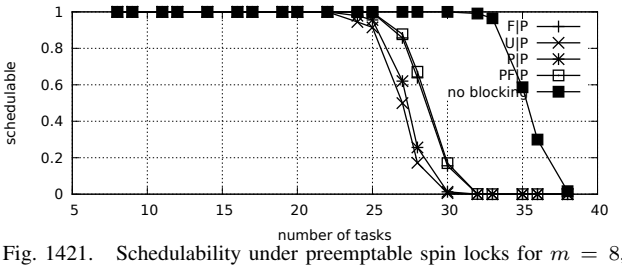

Fig. 1421. Schedulability under preemptable spin locks for $m = 8$, $U = 0.2n$, 16 resources, $rsf = 0.75$, $N^{max} = 2$, and short critical sections. The schedulability of the considered non-preemptable lock types in this configuration is shown in Fig. 1411.

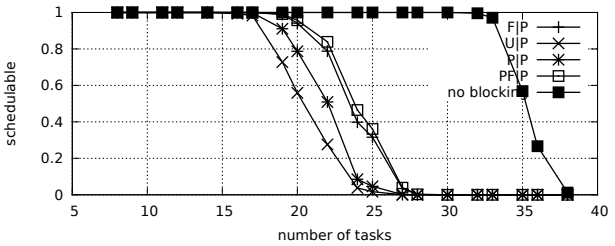

Fig. 1422. Schedulability under preemptable spin locks for $m = 8$, $U = 0.2n$, 16 resources, $rsf = 0.75$, $N^{max} = 5$, and short critical sections. The schedulability of the considered non-preemptable lock types in this configuration is shown in Fig. 1412.

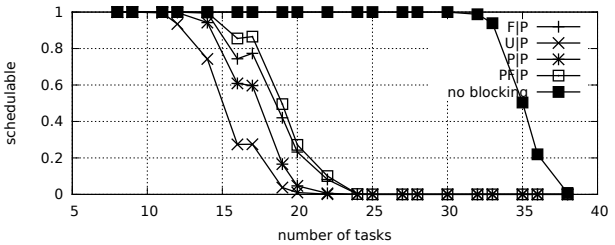

Fig. 1423. Schedulability under preemptable spin locks for $m = 8$, $U = 0.2n$, 16 resources, $rsf = 0.75$, $N^{max} = 10$, and short critical sections. The schedulability of the considered non-preemptable lock types in this configuration is shown in Fig. 1413.

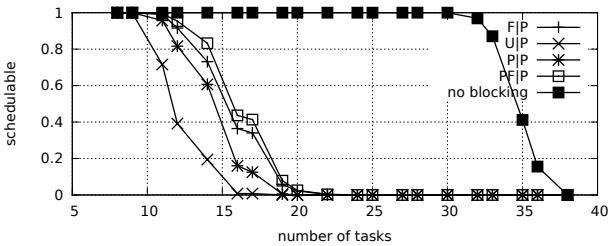

Fig. 1424. Schedulability under preemptable spin locks for $m = 8$, $U = 0.2n$, 16 resources, $rsf = 0.75$, $N^{max} = 15$, and short critical sections. The schedulability of the considered non-preemptable lock types in this configuration is shown in Fig. 1414.

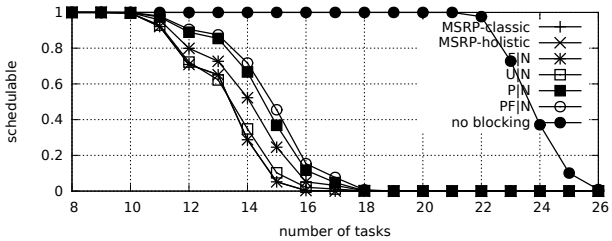

Fig. 1425. Schedulability under non-preemptable spin locks for $m = 8$, $U = 0.3n$, 16 resources, $rsf = 0.75$, $N^{max} = 1$, and medium critical sections. The schedulability of the considered preemptable lock types in this configuration is shown in Fig. 1435.

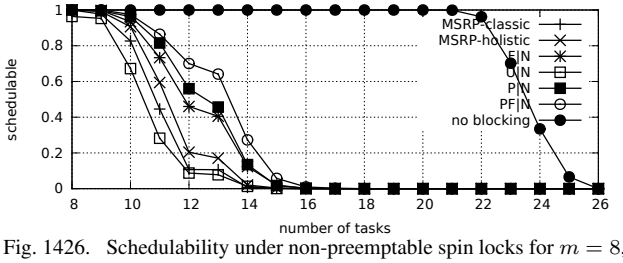

Fig. 1426. Schedulability under non-preemptable spin locks for $m = 8$, $U = 0.3n$, 16 resources, $rsf = 0.75$, $N^{max} = 2$, and medium critical sections. The schedulability of the considered preemptable lock types in this configuration is shown in Fig. 1436.

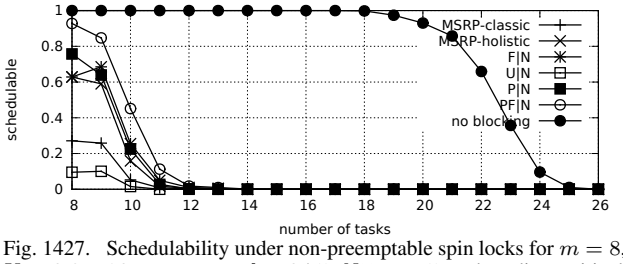

Fig. 1427. Schedulability under non-preemptable spin locks for $m = 8$, $U = 0.3n$, 16 resources, $rsf = 0.75$, $N^{max} = 5$, and medium critical sections. The schedulability of the considered preemptable lock types in this configuration is shown in Fig. 1437.

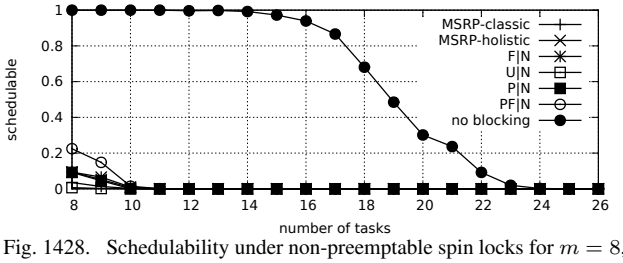

Fig. 1428. Schedulability under non-preemptable spin locks for $m = 8$, $U = 0.3n$, 16 resources, $rsf = 0.75$, $N^{max} = 10$, and medium critical sections. The schedulability of the considered preemptable lock types in this configuration is shown in Fig. 1438.

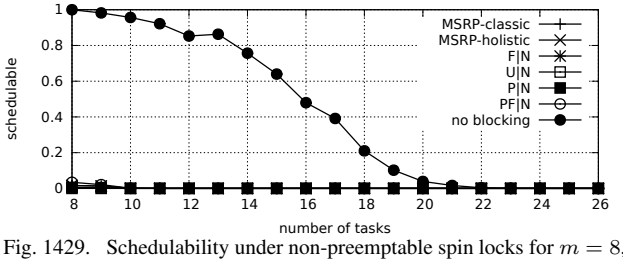

Fig. 1429. Schedulability under non-preemptable spin locks for $m = 8$, $U = 0.3n$, 16 resources, $rsf = 0.75$, $N^{max} = 15$, and medium critical sections. The schedulability of the considered preemptable lock types in this configuration is shown in Fig. 1439.

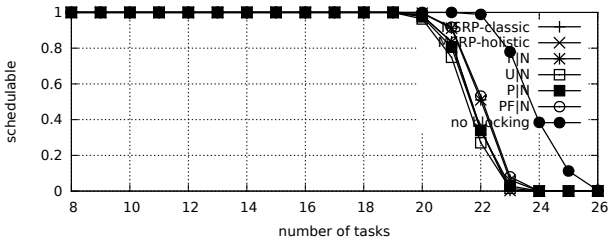

Fig. 1430. Schedulability under non-preemptable spin locks for $m = 8$, $U = 0.3n$, 16 resources, $rsf = 0.75$, $N^{max} = 1$, and short critical sections. The schedulability of the considered preemptable lock types in this configuration is shown in Fig. 1440.

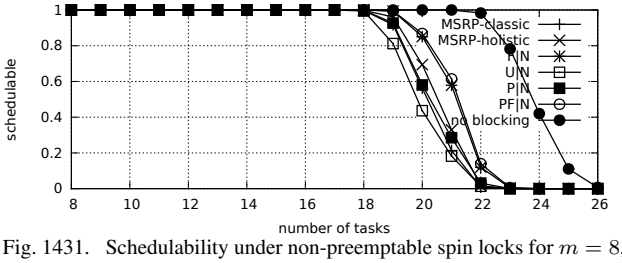

Fig. 1431. Schedulability under non-preemptable spin locks for $m = 8$, $U = 0.3n$, 16 resources, $rsf = 0.75$, $N^{max} = 2$, and short critical sections. The schedulability of the considered preemptable lock types in this configuration is shown in Fig. 1441.

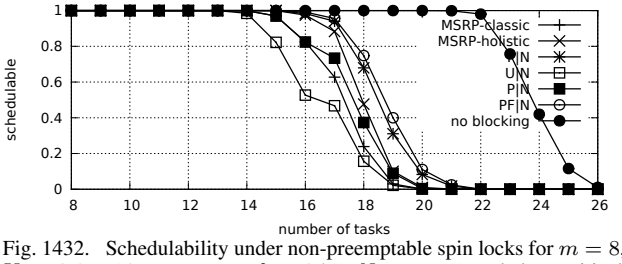

Fig. 1432. Schedulability under non-preemptable spin locks for $m = 8$, $U = 0.3n$, 16 resources, $rsf = 0.75$, $N^{max} = 5$, and short critical sections. The schedulability of the considered preemptable lock types in this configuration is shown in Fig. 1442.

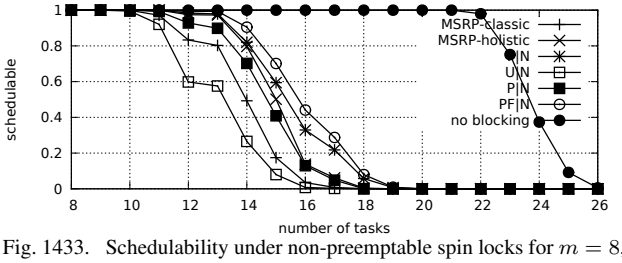

Fig. 1433. Schedulability under non-preemptable spin locks for $m = 8$, $U = 0.3n$, 16 resources, $rsf = 0.75$, $N^{max} = 10$, and short critical sections. The schedulability of the considered preemptable lock types in this configuration is shown in Fig. 1443.

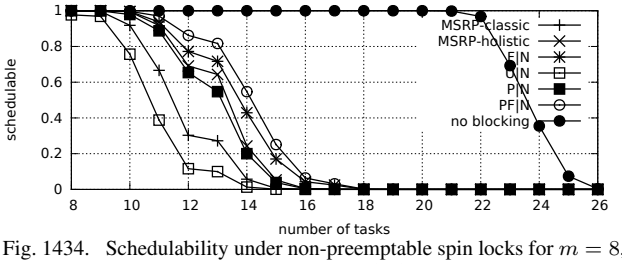

Fig. 1434. Schedulability under non-preemptable spin locks for $m = 8$, $U = 0.3n$, 16 resources, $rsf = 0.75$, $N^{max} = 15$, and short critical sections. The schedulability of the considered preemptable lock types in this configuration is shown in Fig. 1444.

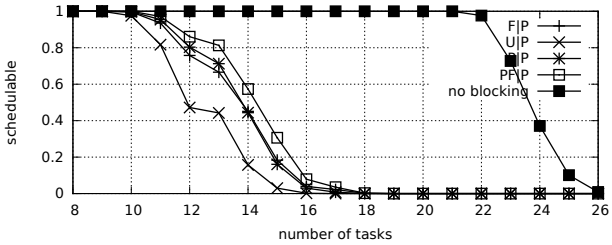

Fig. 1435. Schedulability under preemptable spin locks for $m = 8$, $U = 0.3n$, 16 resources, $rsf = 0.75$, $N^{max} = 1$, and medium critical sections. The schedulability of the considered non-preemptable lock types in this configuration is shown in Fig. 1425.

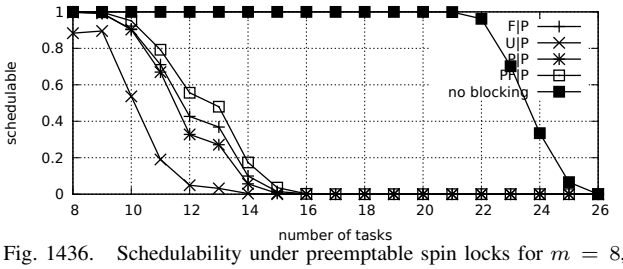

Fig. 1436. Schedulability under preemptable spin locks for $m = 8$, $U = 0.3n$, 16 resources, $rsf = 0.75$, $N^{max} = 2$, and medium critical sections. The schedulability of the considered non-preemptable lock types in this configuration is shown in Fig. 1426.

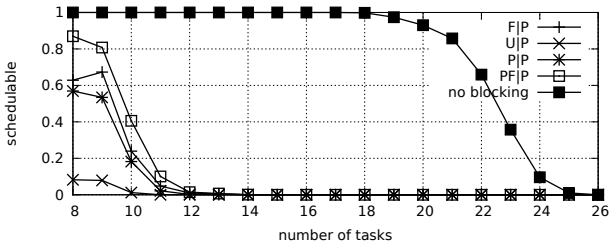

Fig. 1437. Schedulability under preemptable spin locks for $m = 8$, $U = 0.3n$, 16 resources, $rsf = 0.75$, $N^{max} = 5$, and medium critical sections. The schedulability of the considered non-preemptable lock types in this configuration is shown in Fig. 1427.

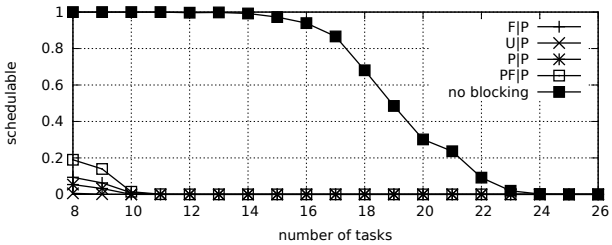

Fig. 1438. Schedulability under preemptable spin locks for $m = 8$, $U = 0.3n$, 16 resources, $rsf = 0.75$, $N^{max} = 10$, and medium critical sections. The schedulability of the considered non-preemptable lock types in this configuration is shown in Fig. 1428.

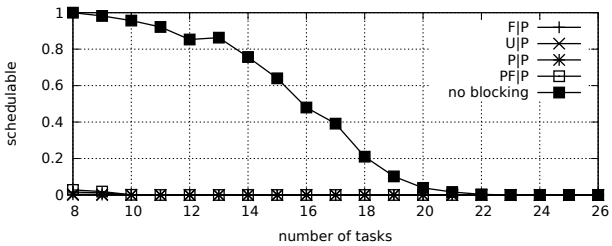

Fig. 1439. Schedulability under preemptable spin locks for $m = 8$, $U = 0.3n$, 16 resources, $rsf = 0.75$, $N^{max} = 15$, and medium critical sections. The schedulability of the considered non-preemptable lock types in this configuration is shown in Fig. 1429.

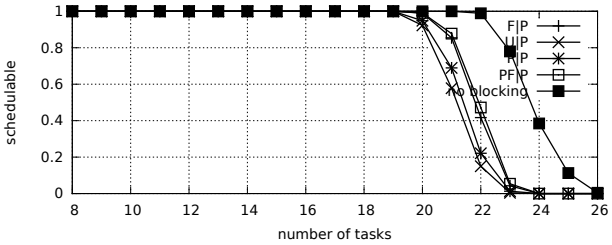

Fig. 1440. Schedulability under preemptable spin locks for $m = 8$, $U = 0.3n$, 16 resources, $rsf = 0.75$, $N^{max} = 1$, and short critical sections. The schedulability of the considered non-preemptable lock types in this configuration is shown in Fig. 1430.

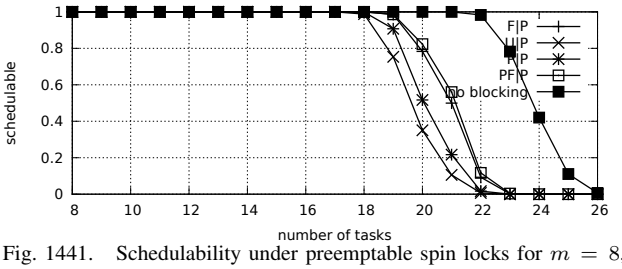

Fig. 1441. Schedulability under preemptable spin locks for $m = 8$, $U = 0.3n$, 16 resources, $rsf = 0.75$, $N^{max} = 2$, and short critical sections. The schedulability of the considered non-preemptable lock types in this configuration is shown in Fig. 1431.

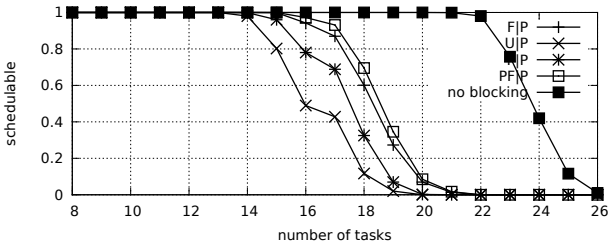

Fig. 1442. Schedulability under preemptable spin locks for $m = 8$, $U = 0.3n$, 16 resources, $rsf = 0.75$, $N^{max} = 5$, and short critical sections. The schedulability of the considered non-preemptable lock types in this configuration is shown in Fig. 1432.

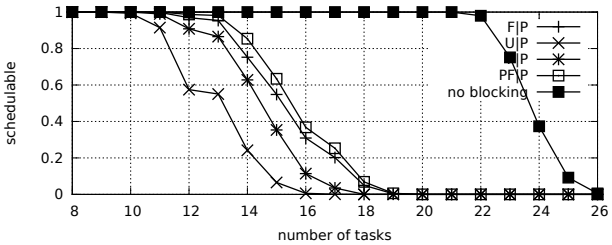

Fig. 1443. Schedulability under preemptable spin locks for $m = 8$, $U = 0.3n$, 16 resources, $rsf = 0.75$, $N^{max} = 10$, and short critical sections. The schedulability of the considered non-preemptable lock types in this configuration is shown in Fig. 1433.

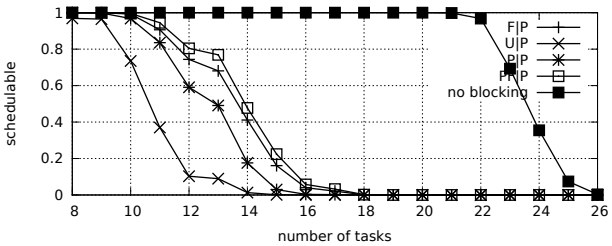

Fig. 1444. Schedulability under preemptable spin locks for $m = 8$, $U = 0.3n$, 16 resources, $rsf = 0.75$, $N^{max} = 15$, and short critical sections. The schedulability of the considered non-preemptable lock types in this configuration is shown in Fig. 1434.

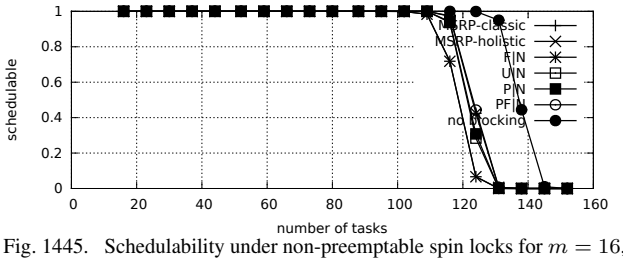

Fig. 1445. Schedulability under non-preemptable spin locks for $m = 16$, $U = 0.1n$, 8 resources, $rsf = 0.1$, $N^{max} = 1$, and medium critical sections. The schedulability of the considered preemptable lock types in this configuration is shown in Fig. 1455.

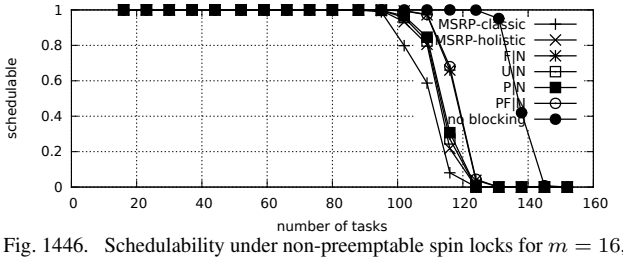

Fig. 1446. Schedulability under non-preemptable spin locks for $m = 16$, $U = 0.1n$, 8 resources, $rsf = 0.1$, $N^{max} = 2$, and medium critical sections. The schedulability of the considered preemptable lock types in this configuration is shown in Fig. 1456.

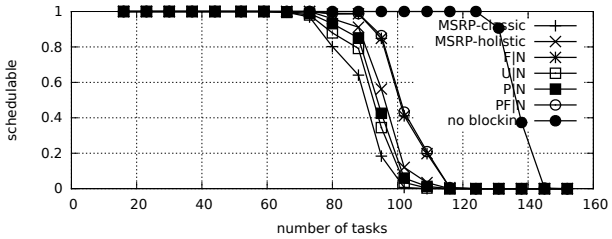

Fig. 1447. Schedulability under non-preemptable spin locks for $m = 16$, $U = 0.1n$, 8 resources, $rsf = 0.1$, $N^{max} = 5$, and medium critical sections. The schedulability of the considered preemptable lock types in this configuration is shown in Fig. 1457.

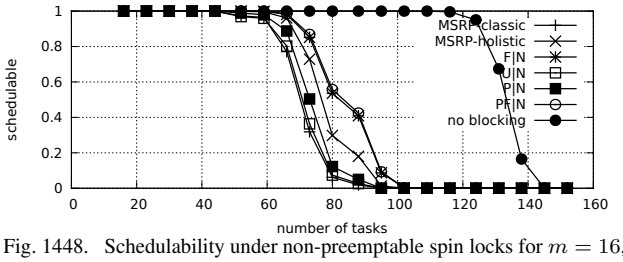

Fig. 1448. Schedulability under non-preemptable spin locks for $m = 16$, $U = 0.1n$, 8 resources, $rsf = 0.1$, $N^{max} = 10$, and medium critical sections. The schedulability of the considered preemptable lock types in this configuration is shown in Fig. 1458.

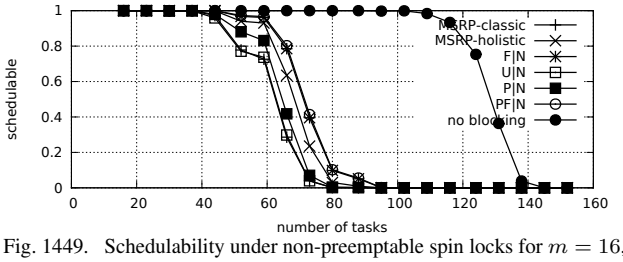

Fig. 1449. Schedulability under non-preemptable spin locks for $m = 16$, $U = 0.1n$, 8 resources, $rsf = 0.1$, $N^{max} = 15$, and medium critical sections. The schedulability of the considered preemptable lock types in this configuration is shown in Fig. 1459.

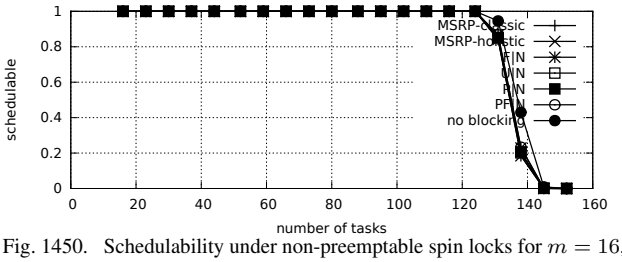

Fig. 1450. Schedulability under non-preemptable spin locks for $m = 16$, $U = 0.1n$, 8 resources, $rsf = 0.1$, $N^{max} = 1$, and short critical sections. The schedulability of the considered preemptable lock types in this configuration is shown in Fig. 1460.

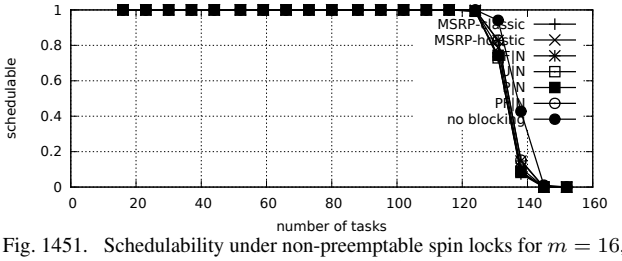

Fig. 1451. Schedulability under non-preemptable spin locks for $m = 16$, $U = 0.1n$, 8 resources, $rsf = 0.1$, $N^{max} = 2$, and short critical sections. The schedulability of the considered preemptable lock types in this configuration is shown in Fig. 1461.

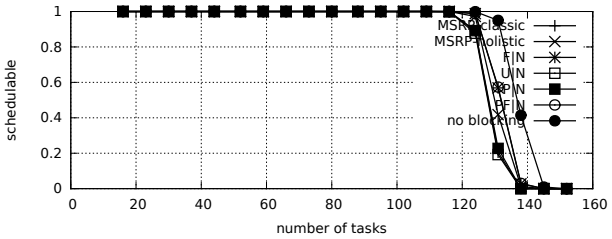

Fig. 1452. Schedulability under non-preemptable spin locks for $m = 16$, $U = 0.1n$, 8 resources, $rsf = 0.1$, $N^{max} = 5$, and short critical sections. The schedulability of the considered preemptable lock types in this configuration is shown in Fig. 1462.

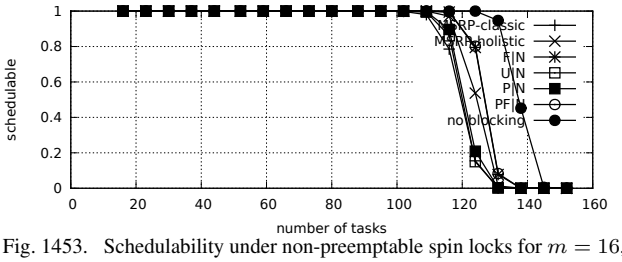

Fig. 1453. Schedulability under non-preemptable spin locks for $m = 16$, $U = 0.1n$, 8 resources, $rsf = 0.1$, $N^{max} = 10$, and short critical sections. The schedulability of the considered preemptable lock types in this configuration is shown in Fig. 1463.

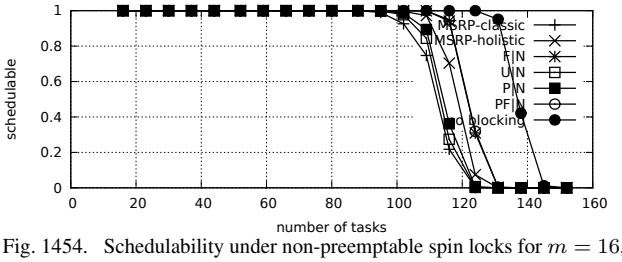

Fig. 1454. Schedulability under non-preemptable spin locks for $m = 16$, $U = 0.1n$, 8 resources, $rsf = 0.1$, $N^{max} = 15$, and short critical sections. The schedulability of the considered preemptable lock types in this configuration is shown in Fig. 1464.

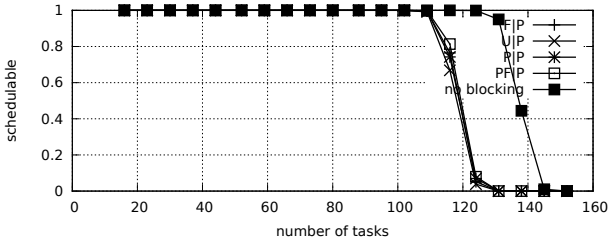

Fig. 1455. Schedulability under preemptable spin locks for $m = 16$, $U = 0.1n$, 8 resources, $rsf = 0.1$, $N^{max} = 1$, and medium critical sections. The schedulability of the considered non-preemptable lock types in this configuration is shown in Fig. 1445.

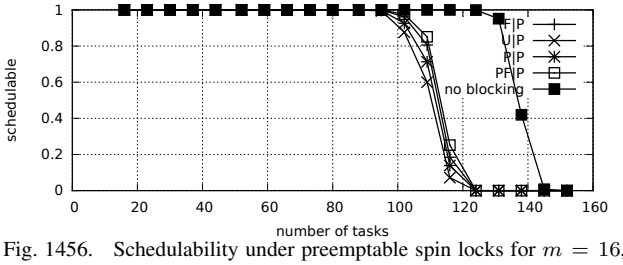

Fig. 1456. Schedulability under preemptable spin locks for $m = 16$, $U = 0.1n$, 8 resources, $rsf = 0.1$, $N^{max} = 2$, and medium critical sections. The schedulability of the considered non-preemptable lock types in this configuration is shown in Fig. 1446.

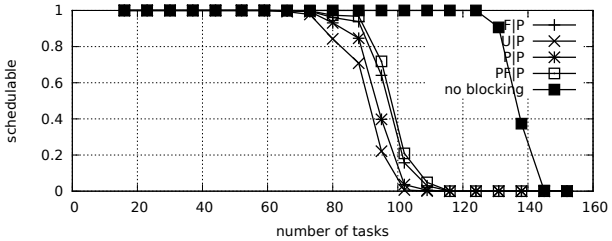

Fig. 1457. Schedulability under preemptable spin locks for $m = 16$, $U = 0.1n$, 8 resources, $rsf = 0.1$, $N^{max} = 5$, and medium critical sections. The schedulability of the considered non-preemptable lock types in this configuration is shown in Fig. 1447.

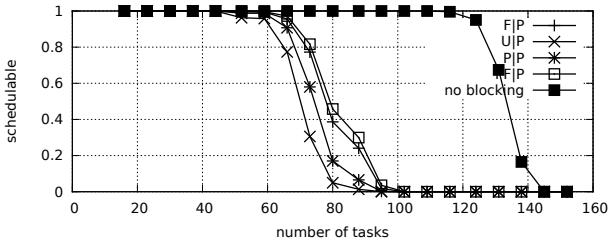

Fig. 1458. Schedulability under preemptable spin locks for $m = 16$, $U = 0.1n$, 8 resources, $rsf = 0.1$, $N^{max} = 10$, and medium critical sections. The schedulability of the considered non-preemptable lock types in this configuration is shown in Fig. 1448.

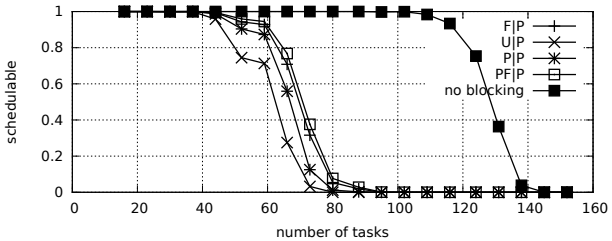

Fig. 1459. Schedulability under preemptable spin locks for $m = 16$, $U = 0.1n$, 8 resources, $rsf = 0.1$, $N^{max} = 15$, and medium critical sections. The schedulability of the considered non-preemptable lock types in this configuration is shown in Fig. 1449.

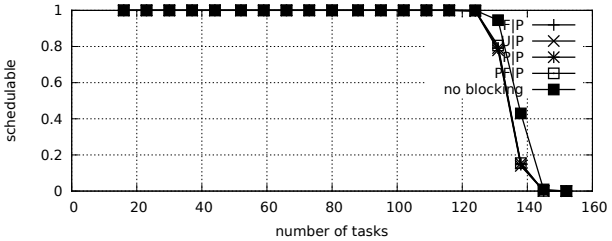

Fig. 1460. Schedulability under preemptable spin locks for $m = 16$, $U = 0.1n$, 8 resources, $rsf = 0.1$, $N^{max} = 1$, and short critical sections. The schedulability of the considered non-preemptable lock types in this configuration is shown in Fig. 1450.

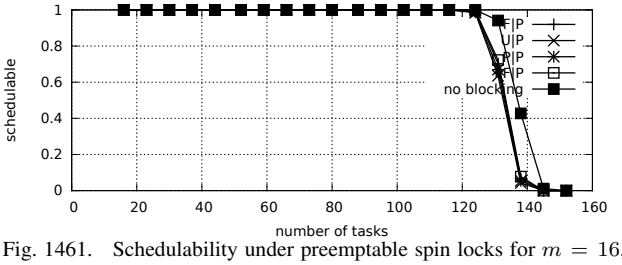

Fig. 1461. Schedulability under preemptable spin locks for $m = 16$, $U = 0.1n$, 8 resources, $rsf = 0.1$, $N^{max} = 2$, and short critical sections. The schedulability of the considered non-preemptable lock types in this configuration is shown in Fig. 1451.

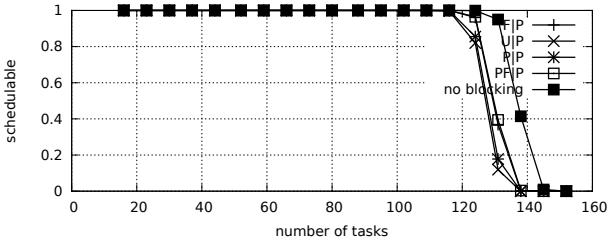

Fig. 1462. Schedulability under preemptable spin locks for $m = 16$, $U = 0.1n$, 8 resources, $rsf = 0.1$, $N^{max} = 5$, and short critical sections. The schedulability of the considered non-preemptable lock types in this configuration is shown in Fig. 1452.

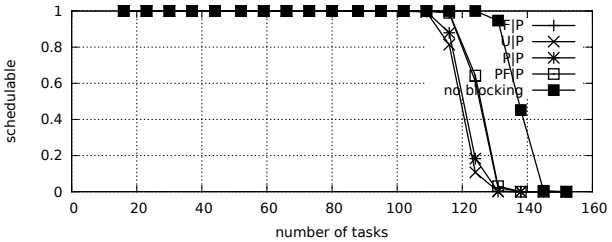

Fig. 1463. Schedulability under preemptable spin locks for $m = 16$, $U = 0.1n$, 8 resources, $rsf = 0.1$, $N^{max} = 10$, and short critical sections. The schedulability of the considered non-preemptable lock types in this configuration is shown in Fig. 1453.

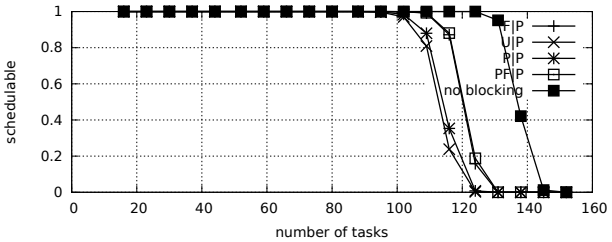

Fig. 1464. Schedulability under preemptable spin locks for $m = 16$, $U = 0.1n$, 8 resources, $rsf = 0.1$, $N^{max} = 15$, and short critical sections. The schedulability of the considered non-preemptable lock types in this configuration is shown in Fig. 1454.

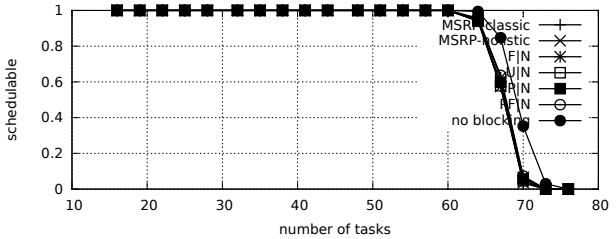

Fig. 1465. Schedulability under non-preemptable spin locks for $m = 16$, $U = 0.2n$, 8 resources, $rsf = 0.1$, $N^{max} = 1$, and medium critical sections. The schedulability of the considered preemptable lock types in this configuration is shown in Fig. 1475.

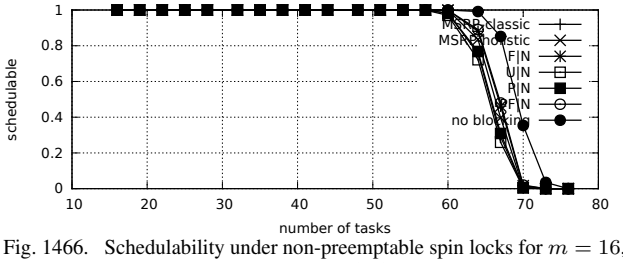

Fig. 1466. Schedulability under non-preemptable spin locks for $m = 16$, $U = 0.2n$, 8 resources, $rsf = 0.1$, $N^{max} = 2$, and medium critical sections. The schedulability of the considered preemptable lock types in this configuration is shown in Fig. 1476.

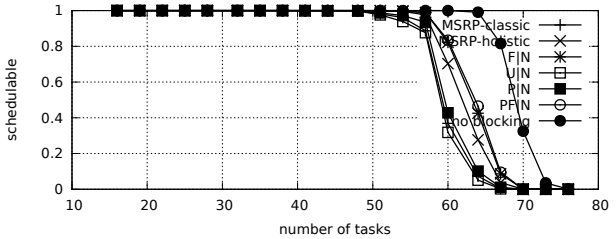

Fig. 1467. Schedulability under non-preemptable spin locks for $m = 16$, $U = 0.2n$, 8 resources, $rsf = 0.1$, $N^{max} = 5$, and medium critical sections. The schedulability of the considered preemptable lock types in this configuration is shown in Fig. 1477.

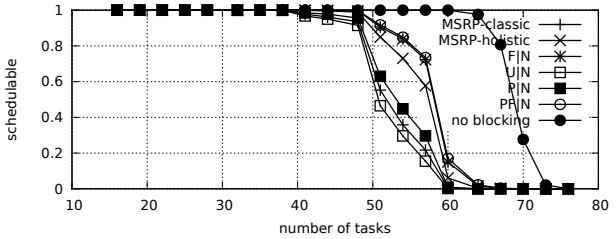

Fig. 1468. Schedulability under non-preemptable spin locks for $m = 16$, $U = 0.2n$, 8 resources, $rsf = 0.1$, $N^{max} = 10$, and medium critical sections. The schedulability of the considered preemptable lock types in this configuration is shown in Fig. 1478.

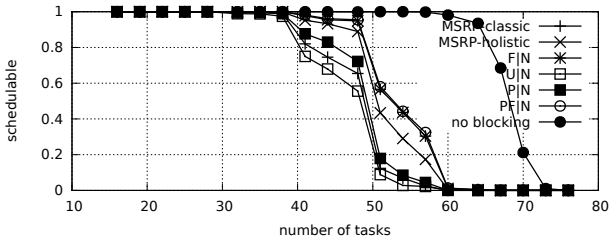

Fig. 1469. Schedulability under non-preemptable spin locks for $m = 16$, $U = 0.2n$, 8 resources, $rsf = 0.1$, $N^{max} = 15$, and medium critical sections. The schedulability of the considered preemptable lock types in this configuration is shown in Fig. 1479.

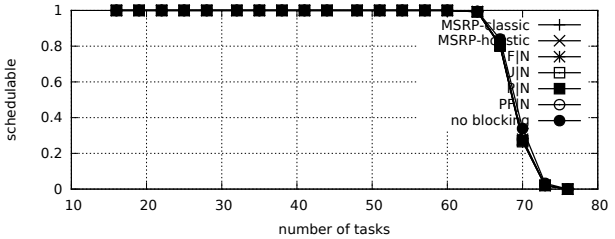

Fig. 1470. Schedulability under non-preemptable spin locks for $m = 16$, $U = 0.2n$, 8 resources, $rsf = 0.1$, $N^{max} = 1$, and short critical sections. The schedulability of the considered preemptable lock types in this configuration is shown in Fig. 1480.

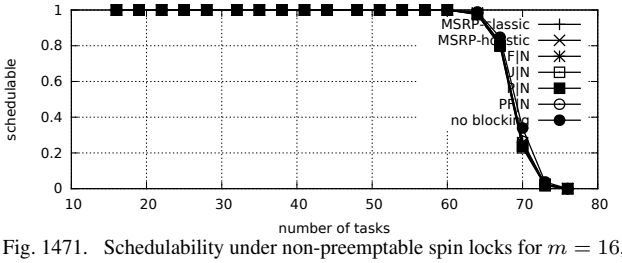

Fig. 1471. Schedulability under non-preemptable spin locks for $m = 16$, $U = 0.2n$, 8 resources, $rsf = 0.1$, $N^{max} = 2$, and short critical sections. The schedulability of the considered preemptable lock types in this configuration is shown in Fig. 1481.

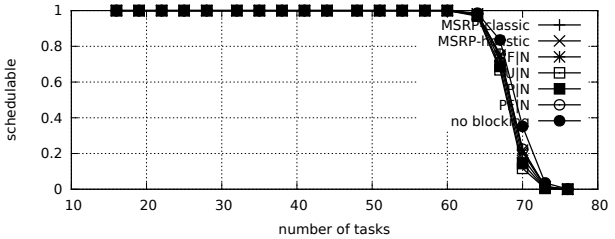

Fig. 1472. Schedulability under non-preemptable spin locks for $m = 16$, $U = 0.2n$, 8 resources, $rsf = 0.1$, $N^{max} = 5$, and short critical sections. The schedulability of the considered preemptable lock types in this configuration is shown in Fig. 1482.

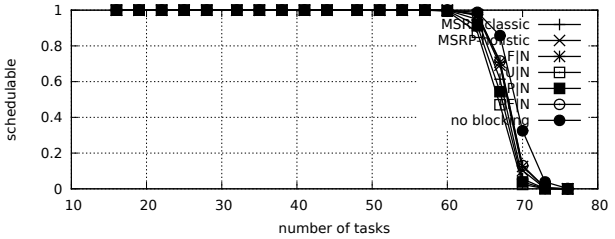

Fig. 1473. Schedulability under non-preemptable spin locks for $m = 16$, $U = 0.2n$, 8 resources, $rsf = 0.1$, $N^{max} = 10$, and short critical sections. The schedulability of the considered preemptable lock types in this configuration is shown in Fig. 1483.

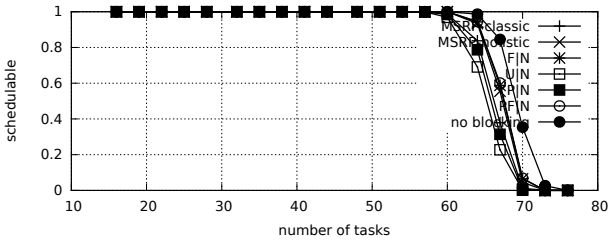

Fig. 1474. Schedulability under non-preemptable spin locks for $m = 16$, $U = 0.2n$, 8 resources, $rsf = 0.1$, $N^{max} = 15$, and short critical sections. The schedulability of the considered preemptable lock types in this configuration is shown in Fig. 1484.

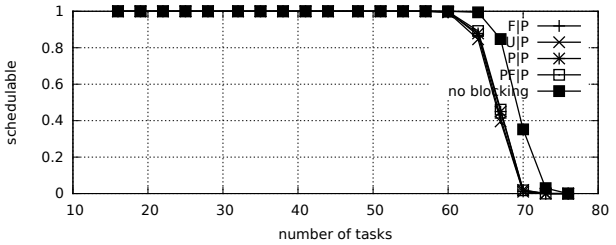

Fig. 1475. Schedulability under preemptable spin locks for $m = 16$, $U = 0.2n$, 8 resources, $rsf = 0.1$, $N^{max} = 1$, and medium critical sections. The schedulability of the considered non-preemptable lock types in this configuration is shown in Fig. 1465.

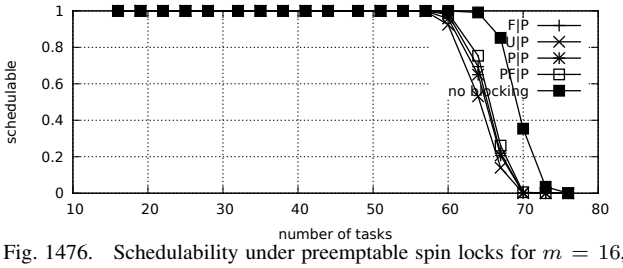

Fig. 1476. Schedulability under preemptable spin locks for $m = 16$, $U = 0.2n$, 8 resources, $rsf = 0.1$, $N^{max} = 2$, and medium critical sections. The schedulability of the considered non-preemptable lock types in this configuration is shown in Fig. 1466.

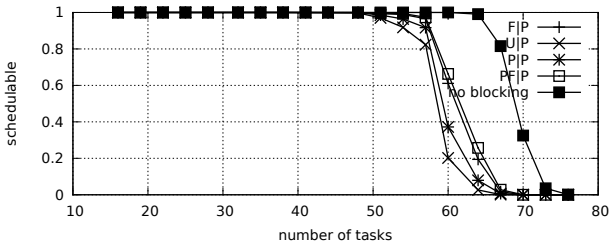

Fig. 1477. Schedulability under preemptable spin locks for $m = 16$, $U = 0.2n$, 8 resources, $rsf = 0.1$, $N^{max} = 5$, and medium critical sections. The schedulability of the considered non-preemptable lock types in this configuration is shown in Fig. 1467.

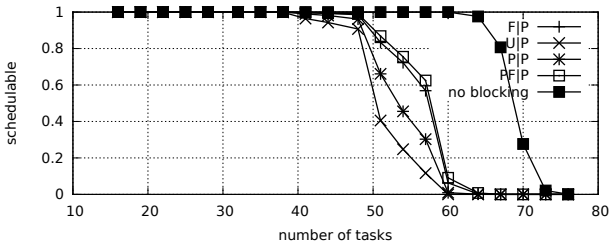

Fig. 1478. Schedulability under preemptable spin locks for $m = 16$, $U = 0.2n$, 8 resources, $rsf = 0.1$, $N^{max} = 10$, and medium critical sections. The schedulability of the considered non-preemptable lock types in this configuration is shown in Fig. 1468.

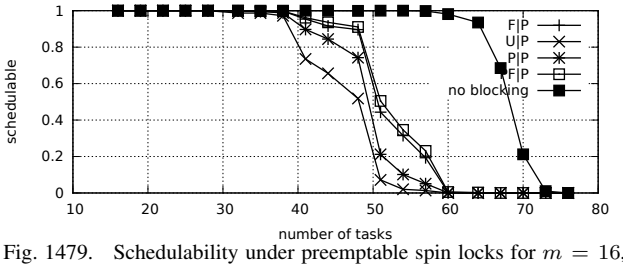

Fig. 1479. Schedulability under preemptable spin locks for $m = 16$, $U = 0.2n$, 8 resources, $rsf = 0.1$, $N^{max} = 15$, and medium critical sections. The schedulability of the considered non-preemptable lock types in this configuration is shown in Fig. 1469.

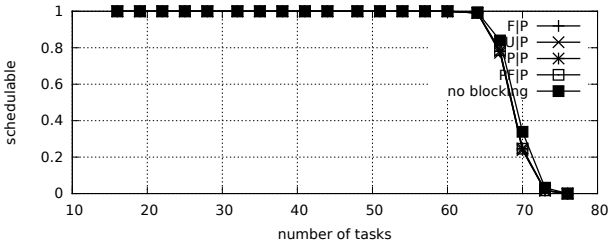

Fig. 1480. Schedulability under preemptable spin locks for $m = 16$, $U = 0.2n$, 8 resources, $rsf = 0.1$, $N^{max} = 1$, and short critical sections. The schedulability of the considered non-preemptable lock types in this configuration is shown in Fig. 1470.

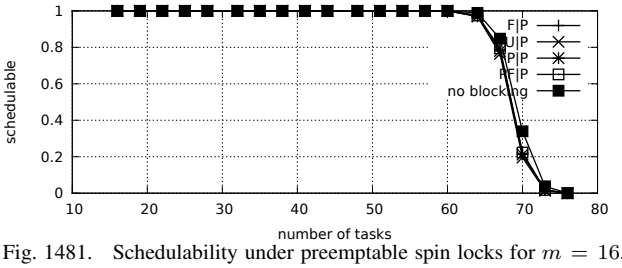

Fig. 1481. Schedulability under preemptable spin locks for $m = 16$, $U = 0.2n$, 8 resources, $rsf = 0.1$, $N^{max} = 2$, and short critical sections. The schedulability of the considered non-preemptable lock types in this configuration is shown in Fig. 1471.

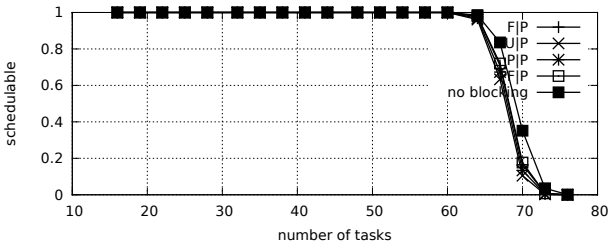

Fig. 1482. Schedulability under preemptable spin locks for $m = 16$, $U = 0.2n$, 8 resources, $rsf = 0.1$, $N^{max} = 5$, and short critical sections. The schedulability of the considered non-preemptable lock types in this configuration is shown in Fig. 1472.

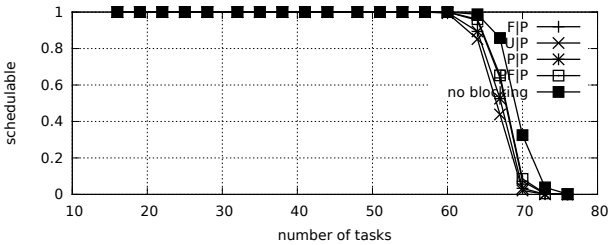

Fig. 1483. Schedulability under preemptable spin locks for $m = 16$, $U = 0.2n$, 8 resources, $rsf = 0.1$, $N^{max} = 10$, and short critical sections. The schedulability of the considered non-preemptable lock types in this configuration is shown in Fig. 1473.

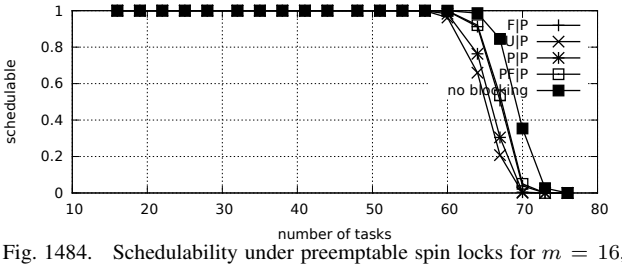

Fig. 1484. Schedulability under preemptable spin locks for $m = 16$, $U = 0.2n$, 8 resources, $rsf = 0.1$, $N^{max} = 15$, and short critical sections. The schedulability of the considered non-preemptable lock types in this configuration is shown in Fig. 1474.

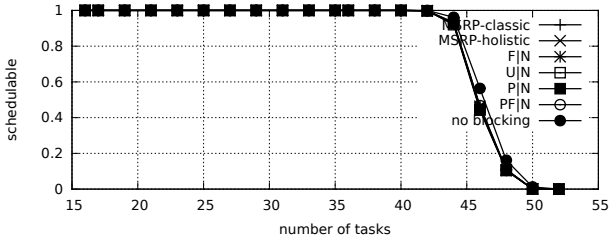

Fig. 1485. Schedulability under non-preemptable spin locks for $m = 16$, $U = 0.3n$, 8 resources, $rsf = 0.1$, $N^{max} = 1$, and medium critical sections. The schedulability of the considered preemptable lock types in this configuration is shown in Fig. 1495.

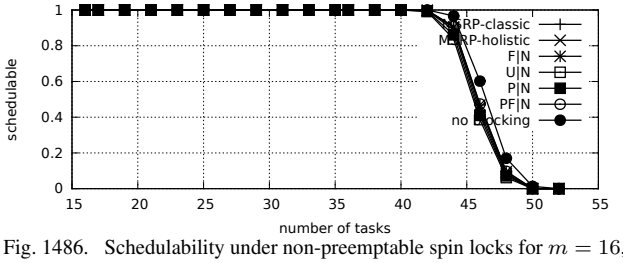

Fig. 1486. Schedulability under non-preemptable spin locks for $m = 16$, $U = 0.3n$, 8 resources, $rsf = 0.1$, $N^{max} = 2$, and medium critical sections. The schedulability of the considered preemptable lock types in this configuration is shown in Fig. 1496.

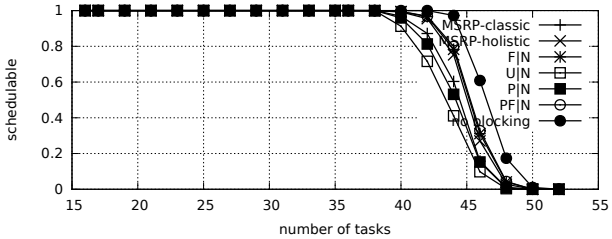

Fig. 1487. Schedulability under non-preemptable spin locks for $m = 16$, $U = 0.3n$, 8 resources, $rsf = 0.1$, $N^{max} = 5$, and medium critical sections. The schedulability of the considered preemptable lock types in this configuration is shown in Fig. 1497.

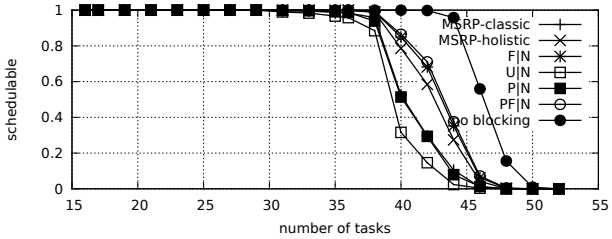

Fig. 1488. Schedulability under non-preemptable spin locks for $m = 16$, $U = 0.3n$, 8 resources, $rsf = 0.1$, $N^{max} = 10$, and medium critical sections. The schedulability of the considered preemptable lock types in this configuration is shown in Fig. 1498.

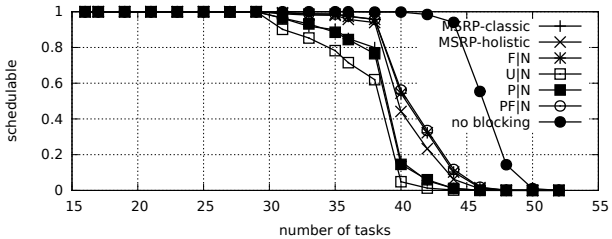

Fig. 1489. Schedulability under non-preemptable spin locks for $m = 16$, $U = 0.3n$, 8 resources, $rsf = 0.1$, $N^{max} = 15$, and medium critical sections. The schedulability of the considered preemptable lock types in this configuration is shown in Fig. 1499.

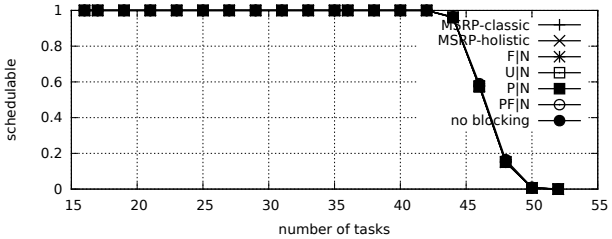

Fig. 1490. Schedulability under non-preemptable spin locks for $m = 16$, $U = 0.3n$, 8 resources, $rsf = 0.1$, $N^{max} = 1$, and short critical sections. The schedulability of the considered preemptable lock types in this configuration is shown in Fig. 1500.

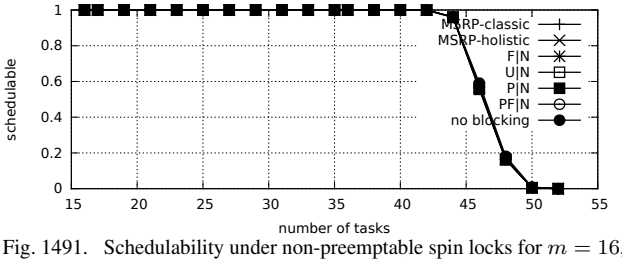

Fig. 1491. Schedulability under non-preemptable spin locks for $m = 16$, $U = 0.3n$, 8 resources, $rsf = 0.1$, $N^{max} = 2$, and short critical sections. The schedulability of the considered preemptable lock types in this configuration is shown in Fig. 1501.

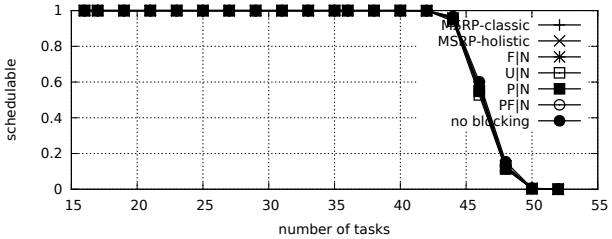

Fig. 1492. Schedulability under non-preemptable spin locks for $m = 16$, $U = 0.3n$, 8 resources, $rsf = 0.1$, $N^{max} = 5$, and short critical sections. The schedulability of the considered preemptable lock types in this configuration is shown in Fig. 1502.

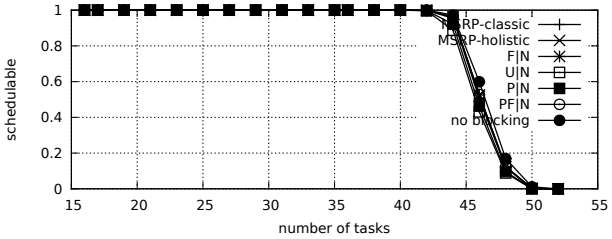

Fig. 1493. Schedulability under non-preemptable spin locks for $m = 16$, $U = 0.3n$, 8 resources, $rsf = 0.1$, $N^{max} = 10$, and short critical sections. The schedulability of the considered preemptable lock types in this configuration is shown in Fig. 1503.

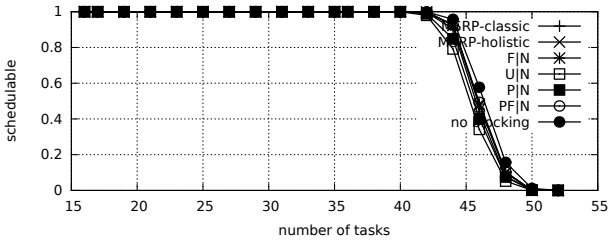

Fig. 1494. Schedulability under non-preemptable spin locks for $m = 16$, $U = 0.3n$, 8 resources, $rsf = 0.1$, $N^{max} = 15$, and short critical sections. The schedulability of the considered preemptable lock types in this configuration is shown in Fig. 1504.

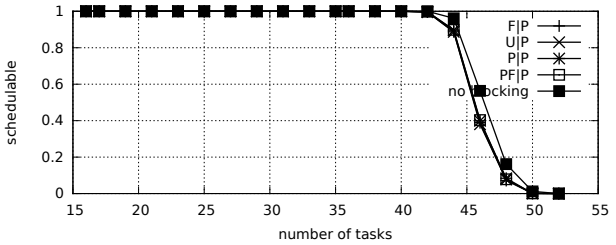

Fig. 1495. Schedulability under preemptable spin locks for $m = 16$, $U = 0.3n$, 8 resources, $rsf = 0.1$, $N^{max} = 1$, and medium critical sections. The schedulability of the considered non-preemptable lock types in this configuration is shown in Fig. 1485.

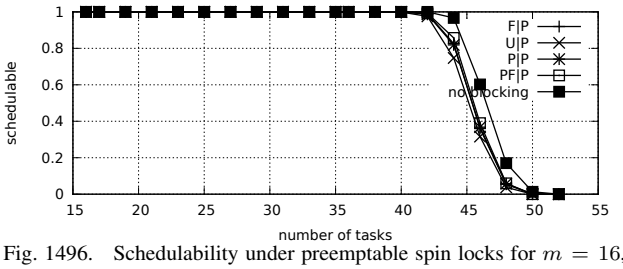

Fig. 1496. Schedulability under preemptable spin locks for $m = 16$, $U = 0.3n$, 8 resources, $rsf = 0.1$, $N^{max} = 2$, and medium critical sections. The schedulability of the considered non-preemptable lock types in this configuration is shown in Fig. 1486.

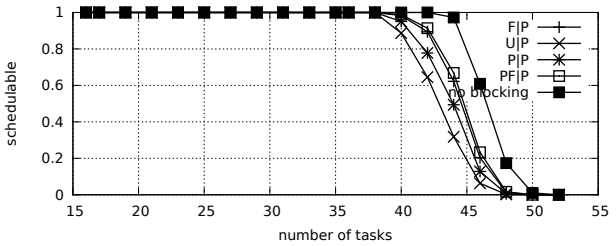

Fig. 1497. Schedulability under preemptable spin locks for $m = 16$, $U = 0.3n$, 8 resources, $rsf = 0.1$, $N^{max} = 5$, and medium critical sections. The schedulability of the considered non-preemptable lock types in this configuration is shown in Fig. 1487.

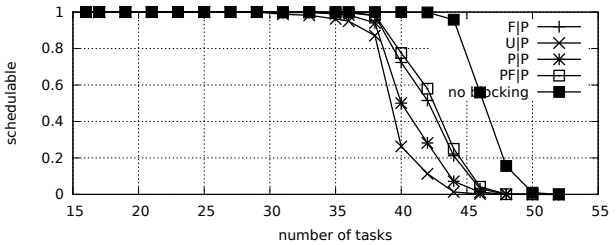

Fig. 1498. Schedulability under preemptable spin locks for $m = 16$, $U = 0.3n$, 8 resources, $rsf = 0.1$, $N^{max} = 10$, and medium critical sections. The schedulability of the considered non-preemptable lock types in this configuration is shown in Fig. 1488.

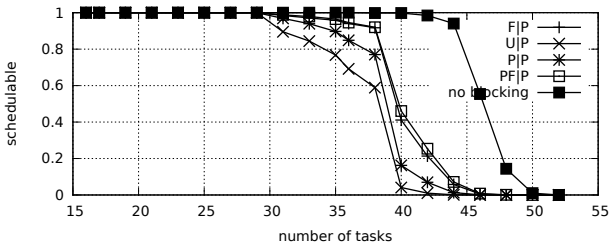

Fig. 1499. Schedulability under preemptable spin locks for $m = 16$, $U = 0.3n$, 8 resources, $rsf = 0.1$, $N^{max} = 15$, and medium critical sections. The schedulability of the considered non-preemptable lock types in this configuration is shown in Fig. 1489.

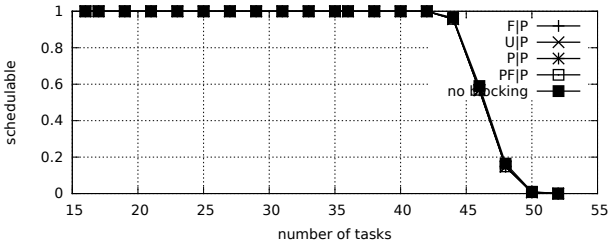

Fig. 1500. Schedulability under preemptable spin locks for $m = 16$, $U = 0.3n$, 8 resources, $rsf = 0.1$, $N^{max} = 1$, and short critical sections. The schedulability of the considered non-preemptable lock types in this configuration is shown in Fig. 1490.

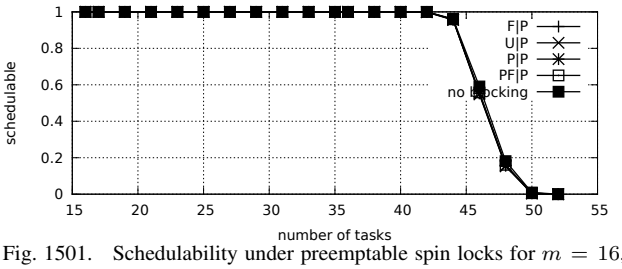

Fig. 1501. Schedulability under preemptable spin locks for $m = 16$, $U = 0.3n$, 8 resources, $rsf = 0.1$, $N^{max} = 2$, and short critical sections. The schedulability of the considered non-preemptable lock types in this configuration is shown in Fig. 1491.

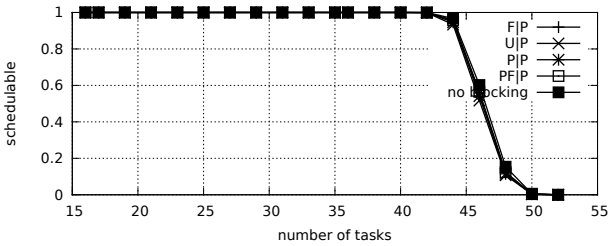

Fig. 1502. Schedulability under preemptable spin locks for $m = 16$, $U = 0.3n$, 8 resources, $rsf = 0.1$, $N^{max} = 5$, and short critical sections. The schedulability of the considered non-preemptable lock types in this configuration is shown in Fig. 1492.

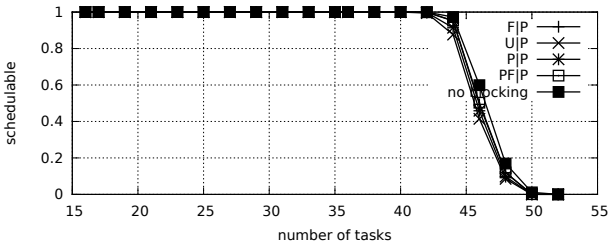

Fig. 1503. Schedulability under preemptable spin locks for $m = 16$, $U = 0.3n$, 8 resources, $rsf = 0.1$, $N^{max} = 10$, and short critical sections. The schedulability of the considered non-preemptable lock types in this configuration is shown in Fig. 1493.

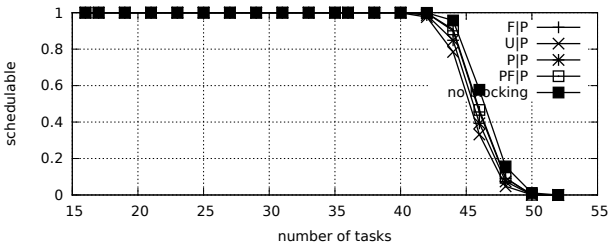

Fig. 1504. Schedulability under preemptable spin locks for $m = 16$, $U = 0.3n$, 8 resources, $rsf = 0.1$, $N^{max} = 15$, and short critical sections. The schedulability of the considered non-preemptable lock types in this configuration is shown in Fig. 1494.

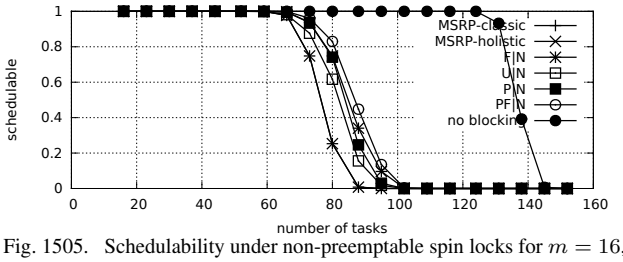

Fig. 1505. Schedulability under non-preemptable spin locks for $m = 16$, $U = 0.1n$, 8 resources, $rsf = 0.25$, $N^{max} = 1$, and medium critical sections. The schedulability of the considered preemptable lock types in this configuration is shown in Fig. 1515.

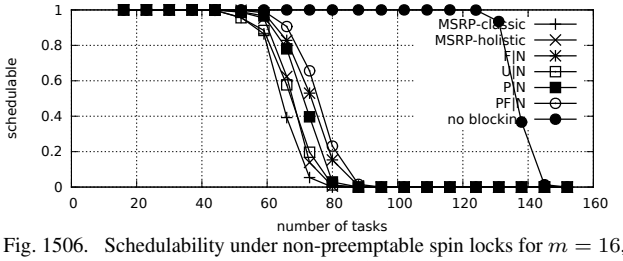

Fig. 1506. Schedulability under non-preemptable spin locks for $m = 16$, $U = 0.1n$, 8 resources, $rsf = 0.25$, $N^{max} = 2$, and medium critical sections. The schedulability of the considered preemptable lock types in this configuration is shown in Fig. 1516.

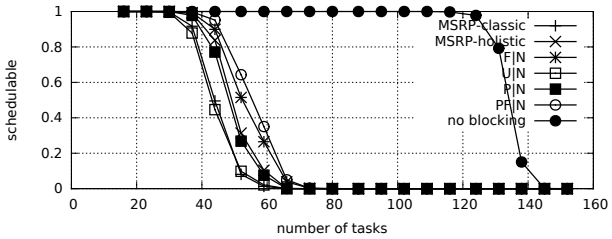

Fig. 1507. Schedulability under non-preemptable spin locks for $m = 16$, $U = 0.1n$, 8 resources, $rsf = 0.25$, $N^{max} = 5$, and medium critical sections. The schedulability of the considered preemptable lock types in this configuration is shown in Fig. 1517.

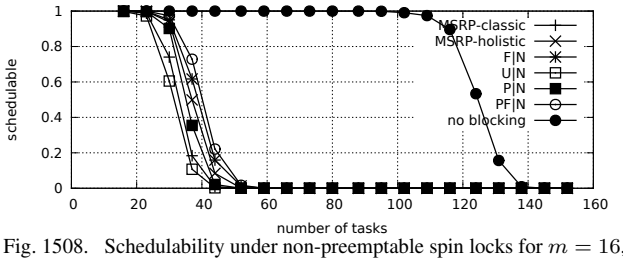

Fig. 1508. Schedulability under non-preemptable spin locks for $m = 16$, $U = 0.1n$, 8 resources, $rsf = 0.25$, $N^{max} = 10$, and medium critical sections. The schedulability of the considered preemptable lock types in this configuration is shown in Fig. 1518.

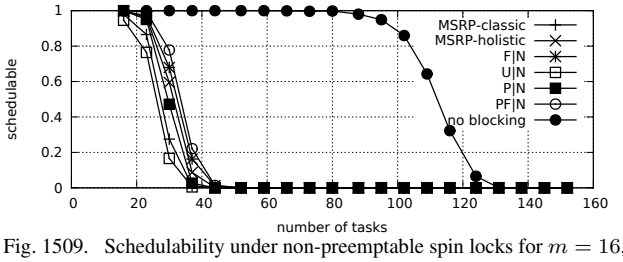

Fig. 1509. Schedulability under non-preemptable spin locks for $m = 16$, $U = 0.1n$, 8 resources, $rsf = 0.25$, $N^{max} = 15$, and medium critical sections. The schedulability of the considered preemptable lock types in this configuration is shown in Fig. 1519.

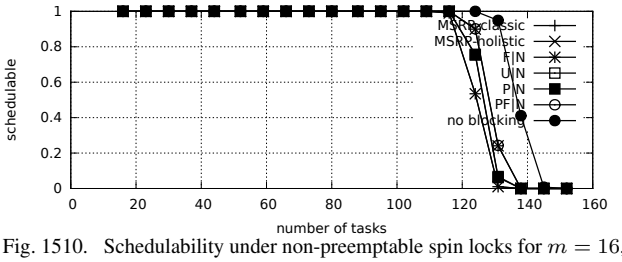

Fig. 1510. Schedulability under non-preemptable spin locks for $m = 16$, $U = 0.1n$, 8 resources, $rsf = 0.25$, $N^{max} = 1$, and short critical sections. The schedulability of the considered preemptable lock types in this configuration is shown in Fig. 1520.

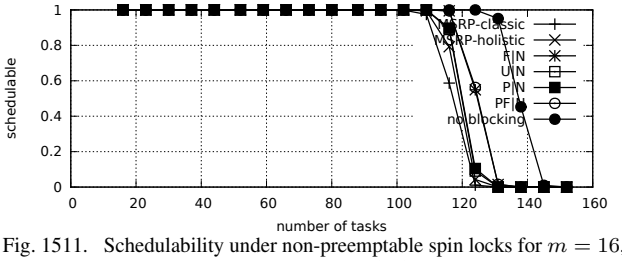

Fig. 1511. Schedulability under non-preemptable spin locks for $m = 16$, $U = 0.1n$, 8 resources, $rsf = 0.25$, $N^{max} = 2$, and short critical sections. The schedulability of the considered preemptable lock types in this configuration is shown in Fig. 1521.

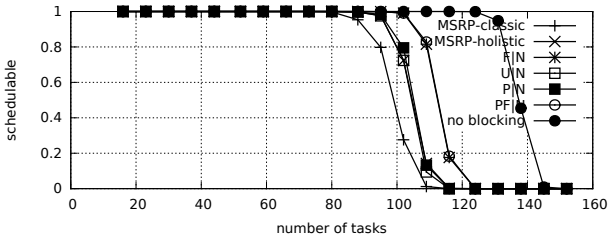

Fig. 1512. Schedulability under non-preemptable spin locks for $m = 16$, $U = 0.1n$, 8 resources, $rsf = 0.25$, $N^{max} = 5$, and short critical sections. The schedulability of the considered preemptable lock types in this configuration is shown in Fig. 1522.

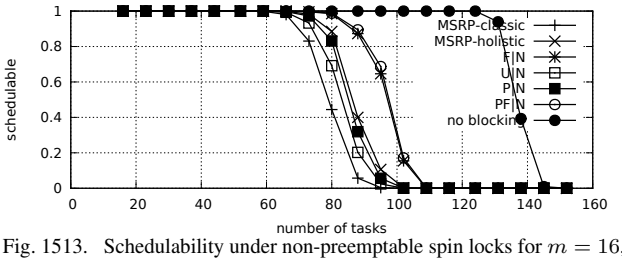

Fig. 1513. Schedulability under non-preemptable spin locks for $m = 16$, $U = 0.1n$, 8 resources, $rsf = 0.25$, $N^{max} = 10$, and short critical sections. The schedulability of the considered preemptable lock types in this configuration is shown in Fig. 1523.

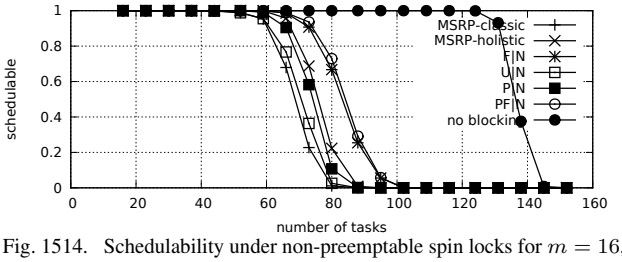

Fig. 1514. Schedulability under non-preemptable spin locks for $m = 16$, $U = 0.1n$, 8 resources, $rsf = 0.25$, $N^{max} = 15$, and short critical sections. The schedulability of the considered preemptable lock types in this configuration is shown in Fig. 1524.

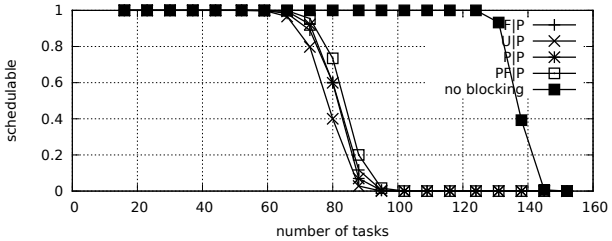

Fig. 1515. Schedulability under preemptable spin locks for $m = 16$, $U = 0.1n$, 8 resources, $rsf = 0.25$, $N^{max} = 1$, and medium critical sections. The schedulability of the considered non-preemptable lock types in this configuration is shown in Fig. 1505.

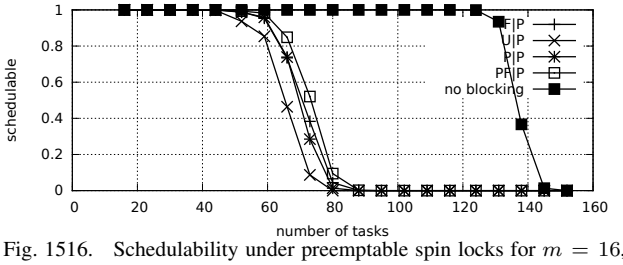

Fig. 1516. Schedulability under preemptable spin locks for $m = 16$, $U = 0.1n$, 8 resources, $rsf = 0.25$, $N^{max} = 2$, and medium critical sections. The schedulability of the considered non-preemptable lock types in this configuration is shown in Fig. 1506.

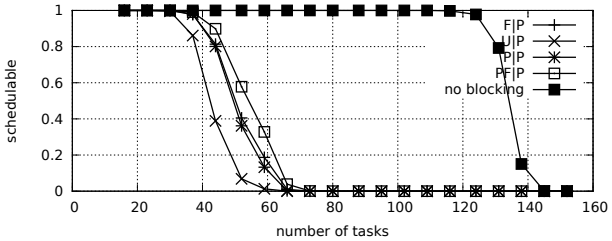

Fig. 1517. Schedulability under preemptable spin locks for $m = 16$, $U = 0.1n$, 8 resources, $rsf = 0.25$, $N^{max} = 5$, and medium critical sections. The schedulability of the considered non-preemptable lock types in this configuration is shown in Fig. 1507.

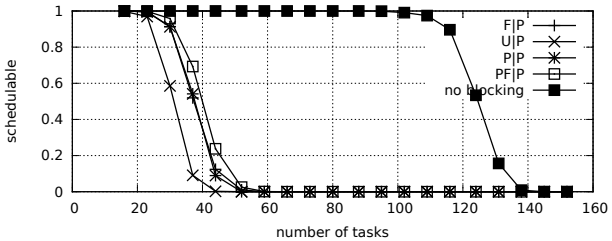

Fig. 1518. Schedulability under preemptable spin locks for $m = 16$, $U = 0.1n$, 8 resources, $rsf = 0.25$, $N^{max} = 10$, and medium critical sections. The schedulability of the considered non-preemptable lock types in this configuration is shown in Fig. 1508.

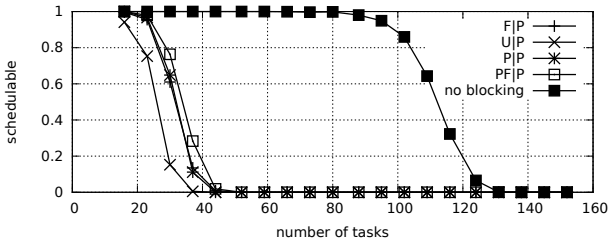

Fig. 1519. Schedulability under preemptable spin locks for $m = 16$, $U = 0.1n$, 8 resources, $rsf = 0.25$, $N^{max} = 15$, and medium critical sections. The schedulability of the considered non-preemptable lock types in this configuration is shown in Fig. 1509.

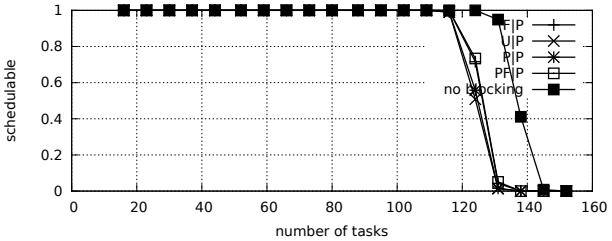

Fig. 1520. Schedulability under preemptable spin locks for $m = 16$, $U = 0.1n$, 8 resources, $rsf = 0.25$, $N^{max} = 1$, and short critical sections. The schedulability of the considered non-preemptable lock types in this configuration is shown in Fig. 1510.

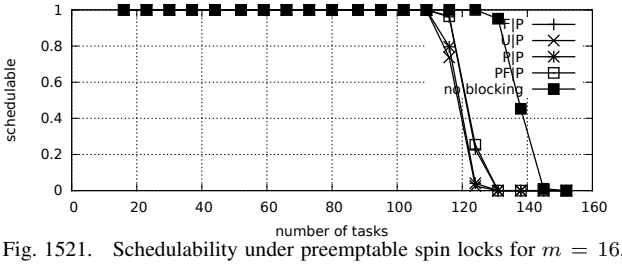

Fig. 1521. Schedulability under preemptable spin locks for $m = 16$, $U = 0.1n$, 8 resources, $rsf = 0.25$, $N^{max} = 2$, and short critical sections. The schedulability of the considered non-preemptable lock types in this configuration is shown in Fig. 1511.

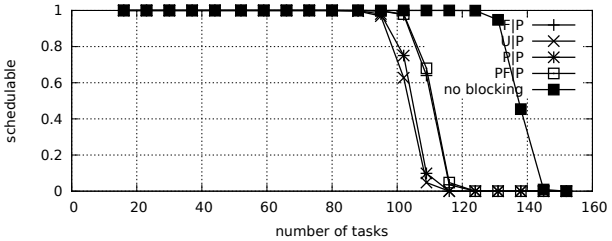

Fig. 1522. Schedulability under preemptable spin locks for $m = 16$, $U = 0.1n$, 8 resources, $rsf = 0.25$, $N^{max} = 5$, and short critical sections. The schedulability of the considered non-preemptable lock types in this configuration is shown in Fig. 1512.

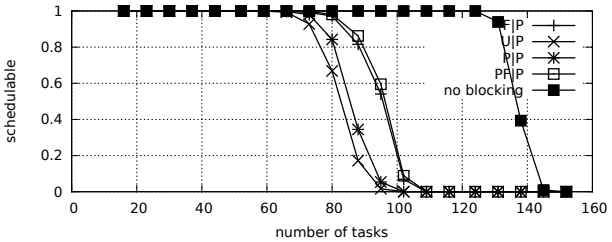

Fig. 1523. Schedulability under preemptable spin locks for $m = 16$, $U = 0.1n$, 8 resources, $rsf = 0.25$, $N^{max} = 10$, and short critical sections. The schedulability of the considered non-preemptable lock types in this configuration is shown in Fig. 1513.

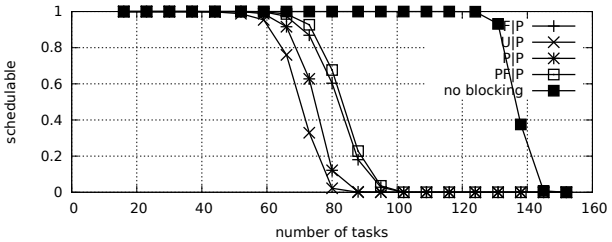

Fig. 1524. Schedulability under preemptable spin locks for $m = 16$, $U = 0.1n$, 8 resources, $rsf = 0.25$, $N^{max} = 15$, and short critical sections. The schedulability of the considered non-preemptable lock types in this configuration is shown in Fig. 1514.

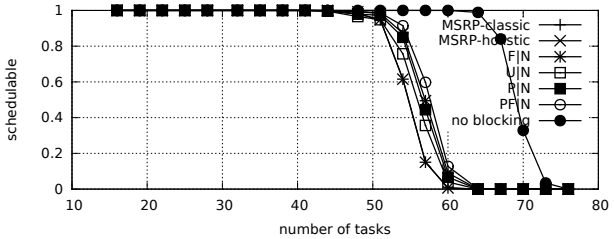

Fig. 1525. Schedulability under non-preemptable spin locks for $m = 16$, $U = 0.2n$, 8 resources, $rsf = 0.25$, $N^{max} = 1$, and medium critical sections. The schedulability of the considered preemptable lock types in this configuration is shown in Fig. 1535.

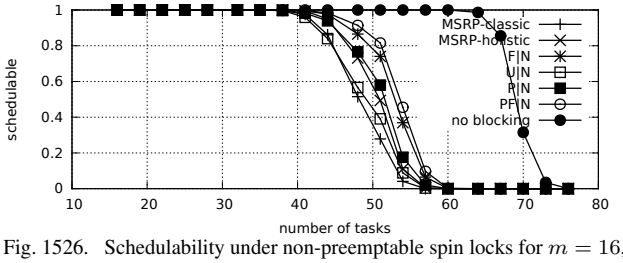

Fig. 1526. Schedulability under non-preemptable spin locks for $m = 16$, $U = 0.2n$, 8 resources, $rsf = 0.25$, $N^{max} = 2$, and medium critical sections. The schedulability of the considered preemptable lock types in this configuration is shown in Fig. 1536.

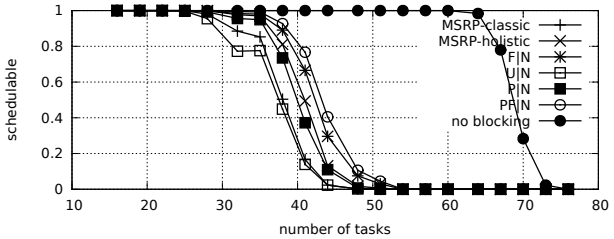

Fig. 1527. Schedulability under non-preemptable spin locks for $m = 16$, $U = 0.2n$, 8 resources, $rsf = 0.25$, $N^{max} = 5$, and medium critical sections. The schedulability of the considered preemptable lock types in this configuration is shown in Fig. 1537.

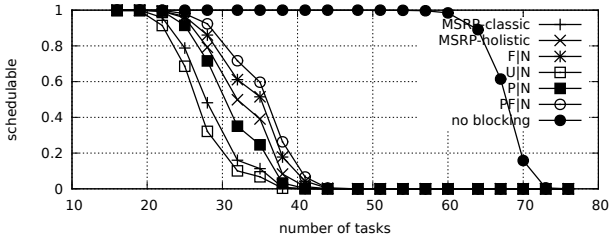

Fig. 1528. Schedulability under non-preemptable spin locks for $m = 16$, $U = 0.2n$, 8 resources, $rsf = 0.25$, $N^{max} = 10$, and medium critical sections. The schedulability of the considered preemptable lock types in this configuration is shown in Fig. 1538.

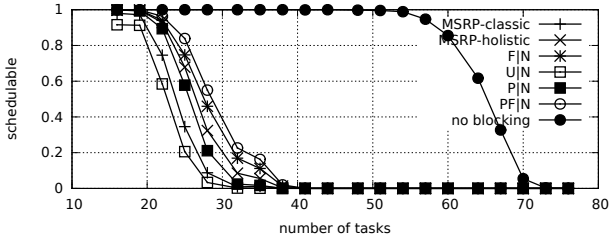

Fig. 1529. Schedulability under non-preemptable spin locks for $m = 16$, $U = 0.2n$, 8 resources, $rsf = 0.25$, $N^{max} = 15$, and medium critical sections. The schedulability of the considered preemptable lock types in this configuration is shown in Fig. 1539.

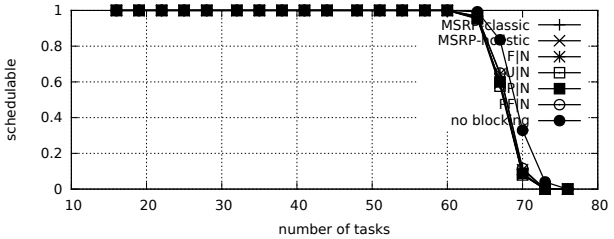

Fig. 1530. Schedulability under non-preemptable spin locks for $m = 16$, $U = 0.2n$, 8 resources, $rsf = 0.25$, $N^{max} = 1$, and short critical sections. The schedulability of the considered preemptable lock types in this configuration is shown in Fig. 1540.

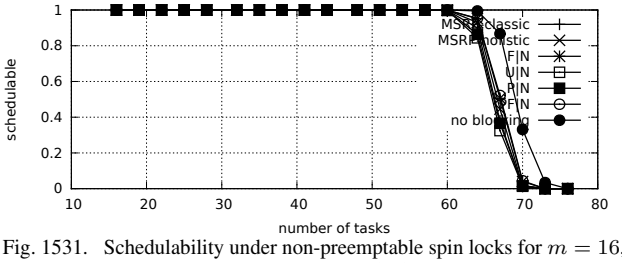

Fig. 1531. Schedulability under non-preemptable spin locks for $m = 16$, $U = 0.2n$, 8 resources, $rsf = 0.25$, $N^{max} = 2$, and short critical sections. The schedulability of the considered preemptable lock types in this configuration is shown in Fig. 1541.

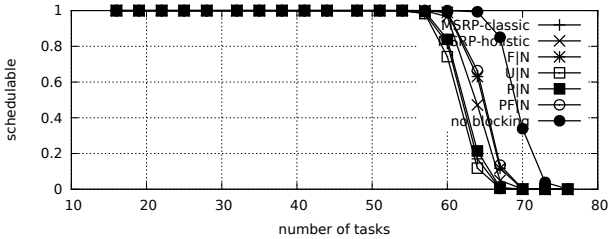

Fig. 1532. Schedulability under non-preemptable spin locks for $m = 16$, $U = 0.2n$, 8 resources, $rsf = 0.25$, $N^{max} = 5$, and short critical sections. The schedulability of the considered preemptable lock types in this configuration is shown in Fig. 1542.

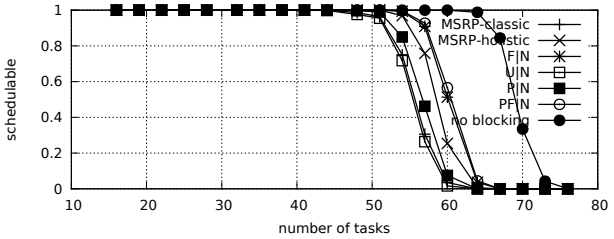

Fig. 1533. Schedulability under non-preemptable spin locks for $m = 16$, $U = 0.2n$, 8 resources, $rsf = 0.25$, $N^{max} = 10$, and short critical sections. The schedulability of the considered preemptable lock types in this configuration is shown in Fig. 1543.

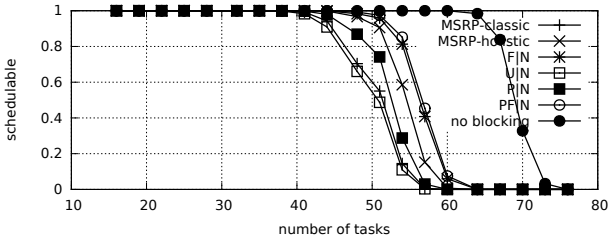

Fig. 1534. Schedulability under non-preemptable spin locks for $m = 16$, $U = 0.2n$, 8 resources, $rsf = 0.25$, $N^{max} = 15$, and short critical sections. The schedulability of the considered preemptable lock types in this configuration is shown in Fig. 1544.

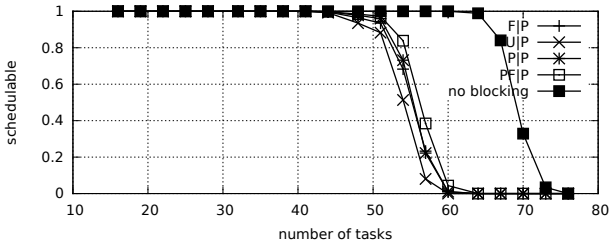

Fig. 1535. Schedulability under preemptable spin locks for $m = 16$, $U = 0.2n$, 8 resources, $rsf = 0.25$, $N^{max} = 1$, and medium critical sections. The schedulability of the considered non-preemptable lock types in this configuration is shown in Fig. 1525.

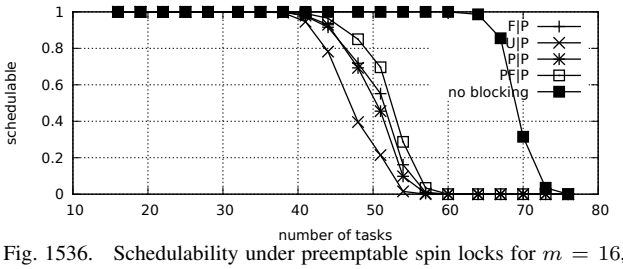

Fig. 1536. Schedulability under preemptable spin locks for $m = 16$, $U = 0.2n$, 8 resources, $rsf = 0.25$, $N^{max} = 2$, and medium critical sections. The schedulability of the considered non-preemptable lock types in this configuration is shown in Fig. 1526.

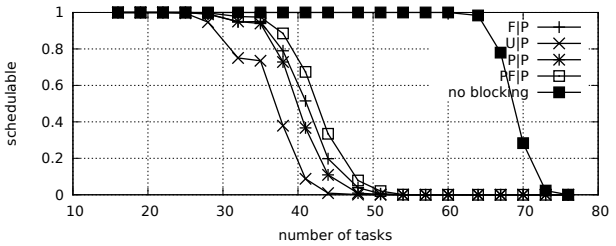

Fig. 1537. Schedulability under preemptable spin locks for $m = 16$, $U = 0.2n$, 8 resources, $rsf = 0.25$, $N^{max} = 5$, and medium critical sections. The schedulability of the considered non-preemptable lock types in this configuration is shown in Fig. 1527.

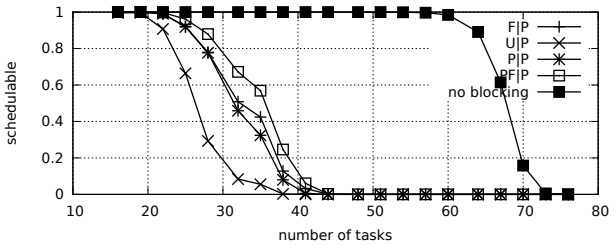

Fig. 1538. Schedulability under preemptable spin locks for $m = 16$, $U = 0.2n$, 8 resources, $rsf = 0.25$, $N^{max} = 10$, and medium critical sections. The schedulability of the considered non-preemptable lock types in this configuration is shown in Fig. 1528.

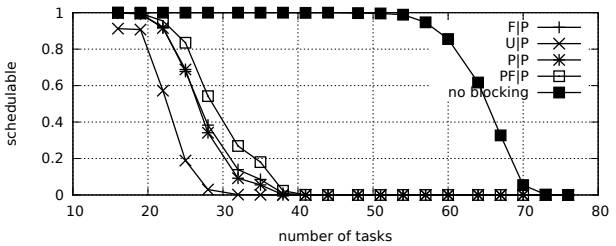

Fig. 1539. Schedulability under preemptable spin locks for $m = 16$, $U = 0.2n$, 8 resources, $rsf = 0.25$, $N^{max} = 15$, and medium critical sections. The schedulability of the considered non-preemptable lock types in this configuration is shown in Fig. 1529.

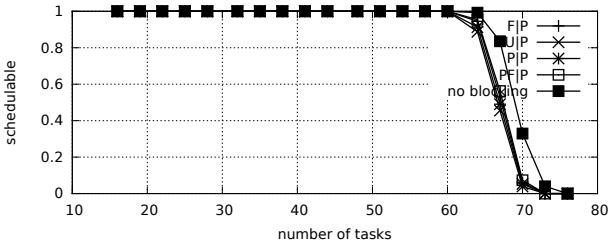

Fig. 1540. Schedulability under preemptable spin locks for $m = 16$, $U = 0.2n$, 8 resources, $rsf = 0.25$, $N^{max} = 1$, and short critical sections. The schedulability of the considered non-preemptable lock types in this configuration is shown in Fig. 1530.

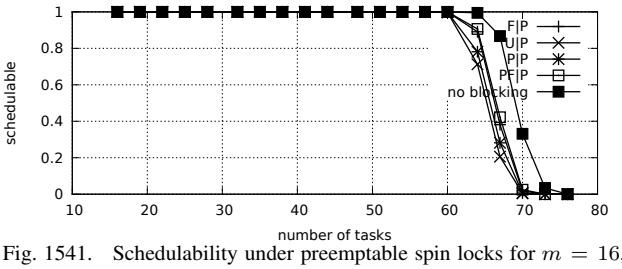

Fig. 1541. Schedulability under preemptable spin locks for $m = 16$, $U = 0.2n$, 8 resources, $rsf = 0.25$, $N^{max} = 2$, and short critical sections. The schedulability of the considered non-preemptable lock types in this configuration is shown in Fig. 1531.

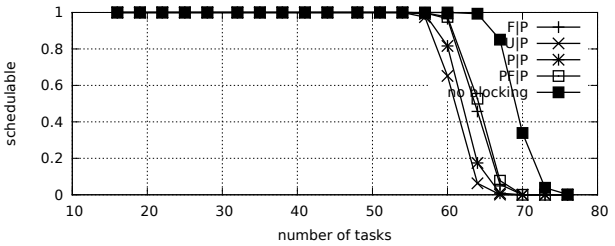

Fig. 1542. Schedulability under preemptable spin locks for $m = 16$, $U = 0.2n$, 8 resources, $rsf = 0.25$, $N^{max} = 5$, and short critical sections. The schedulability of the considered non-preemptable lock types in this configuration is shown in Fig. 1532.

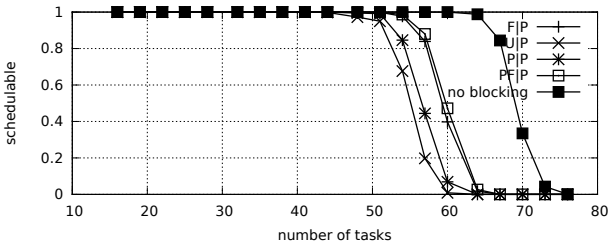

Fig. 1543. Schedulability under preemptable spin locks for $m = 16$, $U = 0.2n$, 8 resources, $rsf = 0.25$, $N^{max} = 10$, and short critical sections. The schedulability of the considered non-preemptable lock types in this configuration is shown in Fig. 1533.

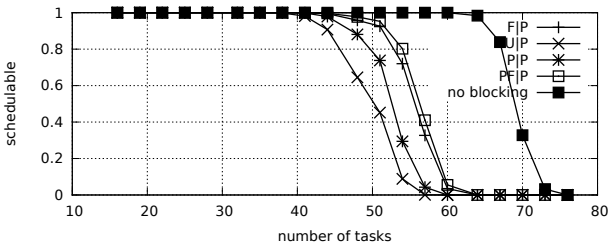

Fig. 1544. Schedulability under preemptable spin locks for $m = 16$, $U = 0.2n$, 8 resources, $rsf = 0.25$, $N^{max} = 15$, and short critical sections. The schedulability of the considered non-preemptable lock types in this configuration is shown in Fig. 1534.

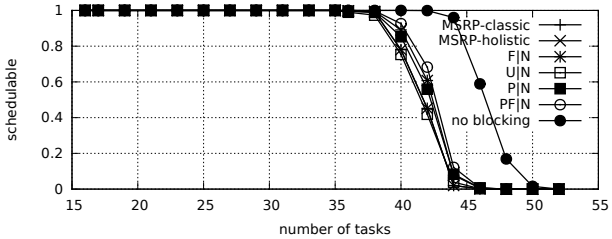

Fig. 1545. Schedulability under non-preemptable spin locks for $m = 16$, $U = 0.3n$, 8 resources, $rsf = 0.25$, $N^{max} = 1$, and medium critical sections. The schedulability of the considered preemptable lock types in this configuration is shown in Fig. 1555.

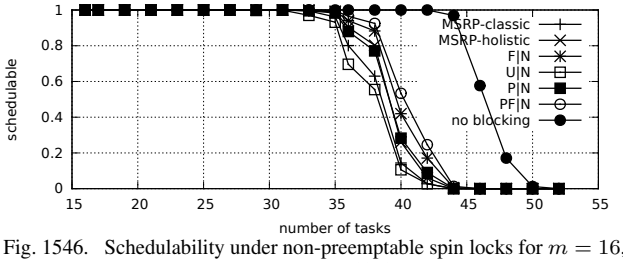

Fig. 1546. Schedulability under non-preemptable spin locks for $m = 16$, $U = 0.3n$, 8 resources, $rsf = 0.25$, $N^{max} = 2$, and medium critical sections. The schedulability of the considered preemptable lock types in this configuration is shown in Fig. 1556.

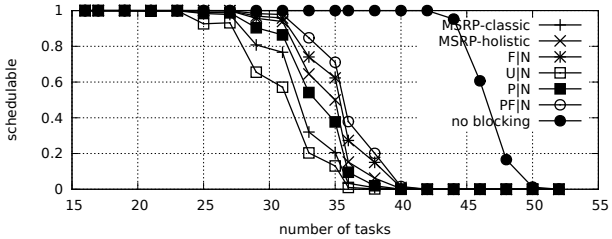

Fig. 1547. Schedulability under non-preemptable spin locks for $m = 16$, $U = 0.3n$, 8 resources, $rsf = 0.25$, $N^{max} = 5$, and medium critical sections. The schedulability of the considered preemptable lock types in this configuration is shown in Fig. 1557.

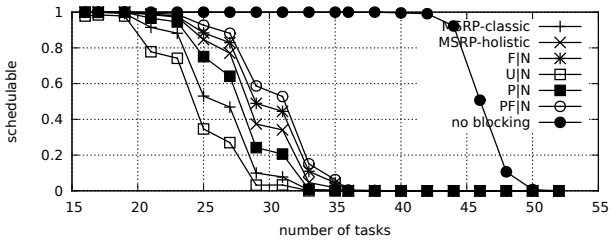

Fig. 1548. Schedulability under non-preemptable spin locks for $m = 16$, $U = 0.3n$, 8 resources, $rsf = 0.25$, $N^{max} = 10$, and medium critical sections. The schedulability of the considered preemptable lock types in this configuration is shown in Fig. 1558.

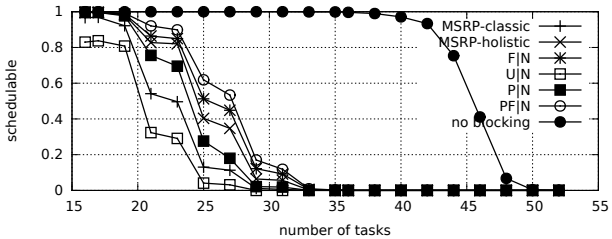

Fig. 1549. Schedulability under non-preemptable spin locks for $m = 16$, $U = 0.3n$, 8 resources, $rsf = 0.25$, $N^{max} = 15$, and medium critical sections. The schedulability of the considered preemptable lock types in this configuration is shown in Fig. 1559.

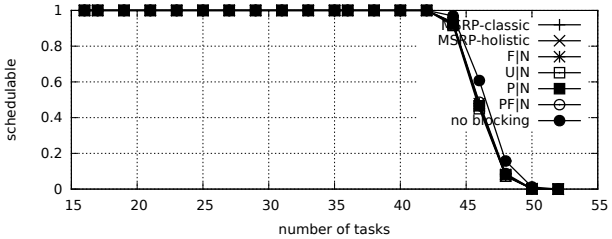

Fig. 1550. Schedulability under non-preemptable spin locks for $m = 16$, $U = 0.3n$, 8 resources, $rsf = 0.25$, $N^{max} = 1$, and short critical sections. The schedulability of the considered preemptable lock types in this configuration is shown in Fig. 1560.

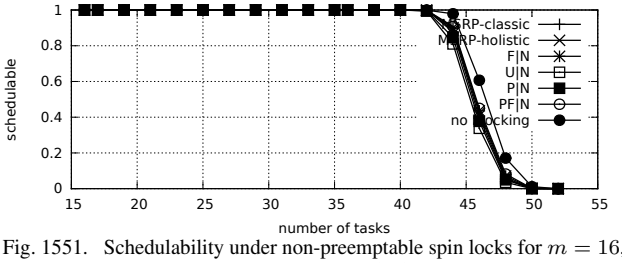

Fig. 1551. Schedulability under non-preemptable spin locks for $m = 16$, $U = 0.3n$, 8 resources, $rsf = 0.25$, $N^{max} = 2$, and short critical sections. The schedulability of the considered preemptable lock types in this configuration is shown in Fig. 1561.

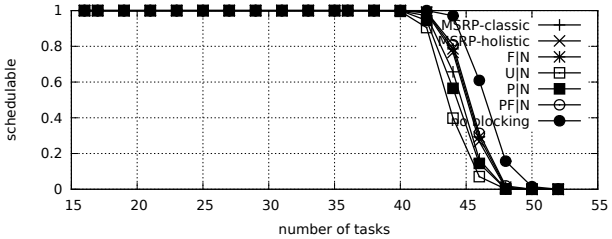

Fig. 1552. Schedulability under non-preemptable spin locks for $m = 16$, $U = 0.3n$, 8 resources, $rsf = 0.25$, $N^{max} = 5$, and short critical sections. The schedulability of the considered preemptable lock types in this configuration is shown in Fig. 1562.

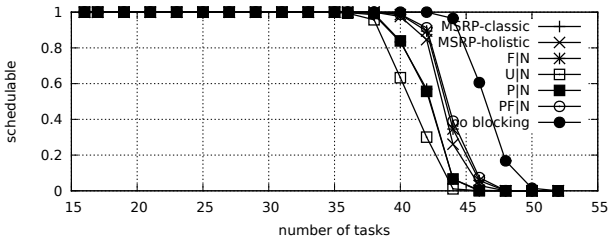

Fig. 1553. Schedulability under non-preemptable spin locks for $m = 16$, $U = 0.3n$, 8 resources, $rsf = 0.25$, $N^{max} = 10$, and short critical sections. The schedulability of the considered preemptable lock types in this configuration is shown in Fig. 1563.

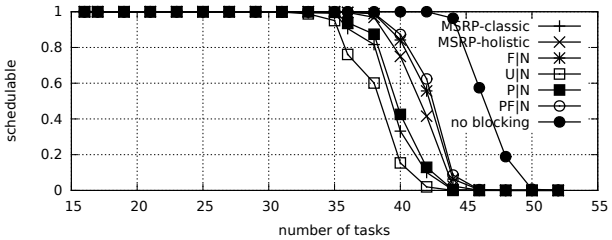

Fig. 1554. Schedulability under non-preemptable spin locks for $m = 16$, $U = 0.3n$, 8 resources, $rsf = 0.25$, $N^{max} = 15$, and short critical sections. The schedulability of the considered preemptable lock types in this configuration is shown in Fig. 1564.

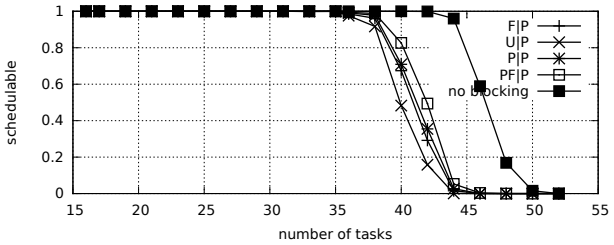

Fig. 1555. Schedulability under preemptable spin locks for $m = 16$, $U = 0.3n$, 8 resources, $rsf = 0.25$, $N^{max} = 1$, and medium critical sections. The schedulability of the considered non-preemptable lock types in this configuration is shown in Fig. 1545.

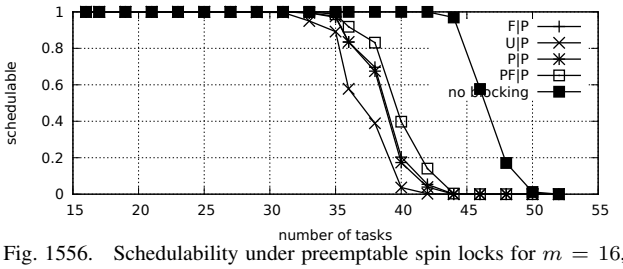

Fig. 1556. Schedulability under preemptable spin locks for $m = 16$, $U = 0.3n$, 8 resources, $rsf = 0.25$, $N^{max} = 2$, and medium critical sections. The schedulability of the considered non-preemptable lock types in this configuration is shown in Fig. 1546.

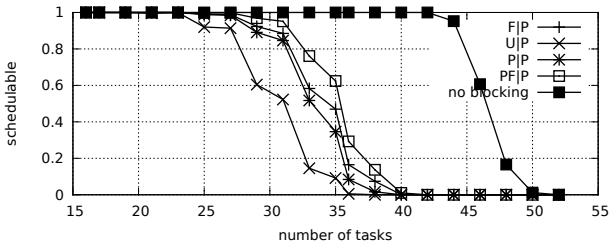

Fig. 1557. Schedulability under preemptable spin locks for $m = 16$, $U = 0.3n$, 8 resources, $rsf = 0.25$, $N^{max} = 5$, and medium critical sections. The schedulability of the considered non-preemptable lock types in this configuration is shown in Fig. 1547.

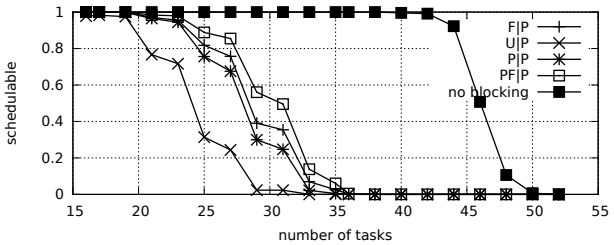

Fig. 1558. Schedulability under preemptable spin locks for $m = 16$, $U = 0.3n$, 8 resources, $rsf = 0.25$, $N^{max} = 10$, and medium critical sections. The schedulability of the considered non-preemptable lock types in this configuration is shown in Fig. 1548.

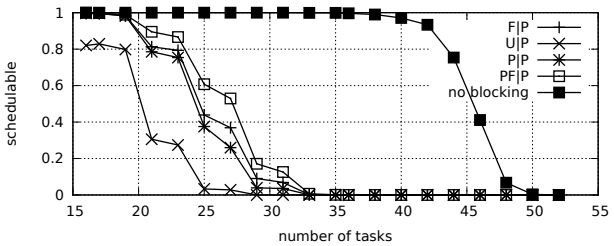

Fig. 1559. Schedulability under preemptable spin locks for $m = 16$, $U = 0.3n$, 8 resources, $rsf = 0.25$, $N^{max} = 15$, and medium critical sections. The schedulability of the considered non-preemptable lock types in this configuration is shown in Fig. 1549.

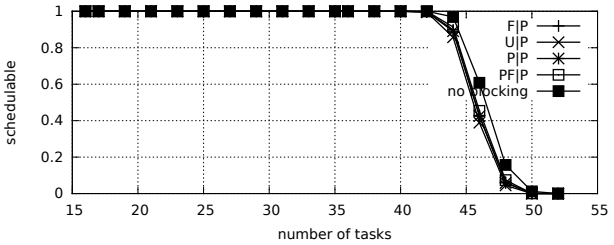

Fig. 1560. Schedulability under preemptable spin locks for $m = 16$, $U = 0.3n$, 8 resources, $rsf = 0.25$, $N^{max} = 1$, and short critical sections. The schedulability of the considered non-preemptable lock types in this configuration is shown in Fig. 1550.

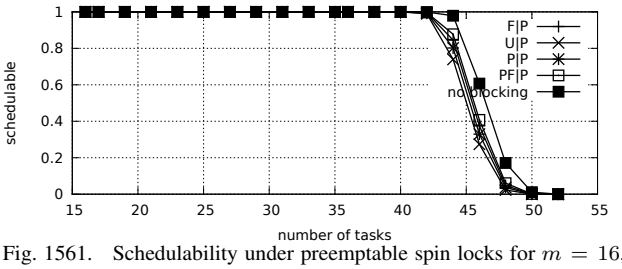

Fig. 1561. Schedulability under preemptable spin locks for $m = 16$, $U = 0.3n$, 8 resources, $rsf = 0.25$, $N^{max} = 2$, and short critical sections. The schedulability of the considered non-preemptable lock types in this configuration is shown in Fig. 1551.

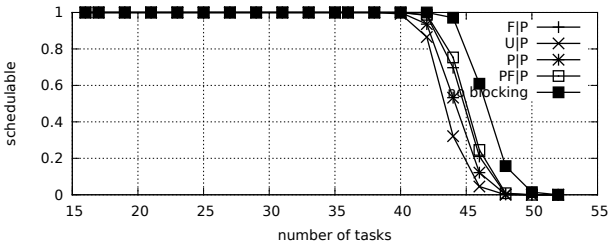

Fig. 1562. Schedulability under preemptable spin locks for $m = 16$, $U = 0.3n$, 8 resources, $rsf = 0.25$, $N^{max} = 5$, and short critical sections. The schedulability of the considered non-preemptable lock types in this configuration is shown in Fig. 1552.

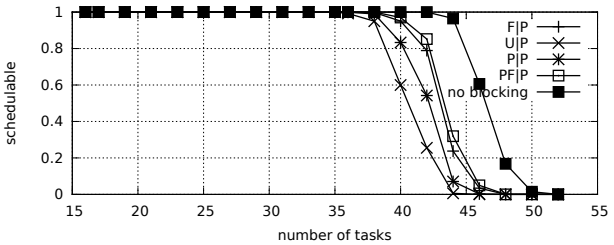

Fig. 1563. Schedulability under preemptable spin locks for $m = 16$, $U = 0.3n$, 8 resources, $rsf = 0.25$, $N^{max} = 10$, and short critical sections. The schedulability of the considered non-preemptable lock types in this configuration is shown in Fig. 1553.

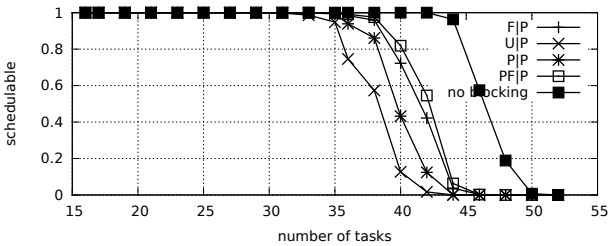

Fig. 1564. Schedulability under preemptable spin locks for $m = 16$, $U = 0.3n$, 8 resources, $rsf = 0.25$, $N^{max} = 15$, and short critical sections. The schedulability of the considered non-preemptable lock types in this configuration is shown in Fig. 1554.

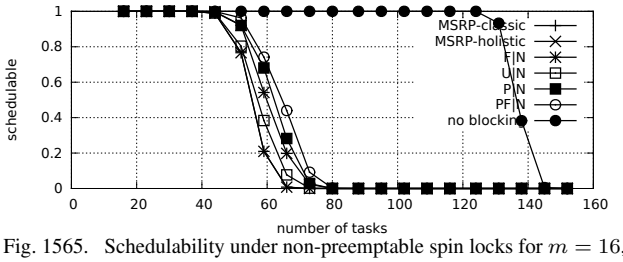

Fig. 1565. Schedulability under non-preemptable spin locks for $m = 16$, $U = 0.1n$, 8 resources, $rsf = 0.4$, $N^{max} = 1$, and medium critical sections. The schedulability of the considered preemptable lock types in this configuration is shown in Fig. 1575.

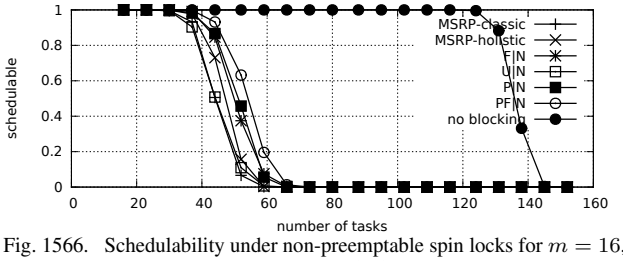

Fig. 1566. Schedulability under non-preemptable spin locks for $m = 16$, $U = 0.1n$, 8 resources, $rsf = 0.4$, $N^{max} = 2$, and medium critical sections. The schedulability of the considered preemptable lock types in this configuration is shown in Fig. 1576.

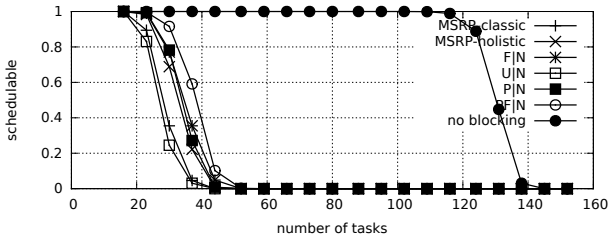

Fig. 1567. Schedulability under non-preemptable spin locks for $m = 16$, $U = 0.1n$, 8 resources, $rsf = 0.4$, $N^{max} = 5$, and medium critical sections. The schedulability of the considered preemptable lock types in this configuration is shown in Fig. 1577.

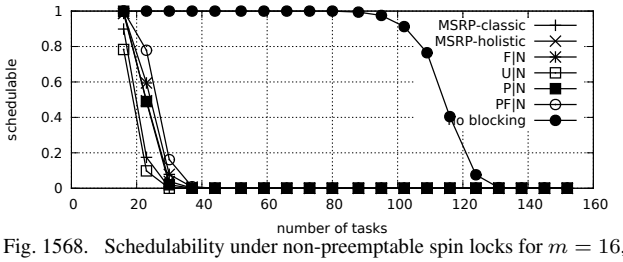

Fig. 1568. Schedulability under non-preemptable spin locks for $m = 16$, $U = 0.1n$, 8 resources, $rsf = 0.4$, $N^{max} = 10$, and medium critical sections. The schedulability of the considered preemptable lock types in this configuration is shown in Fig. 1578.

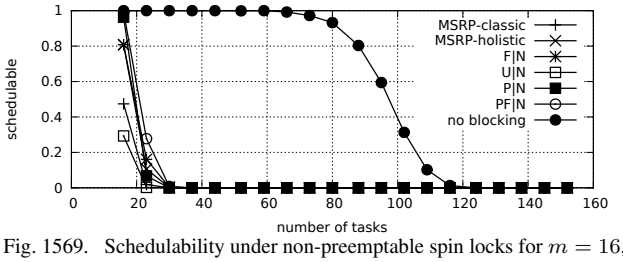

Fig. 1569. Schedulability under non-preemptable spin locks for $m = 16$, $U = 0.1n$, 8 resources, $rsf = 0.4$, $N^{max} = 15$, and medium critical sections. The schedulability of the considered preemptable lock types in this configuration is shown in Fig. 1579.

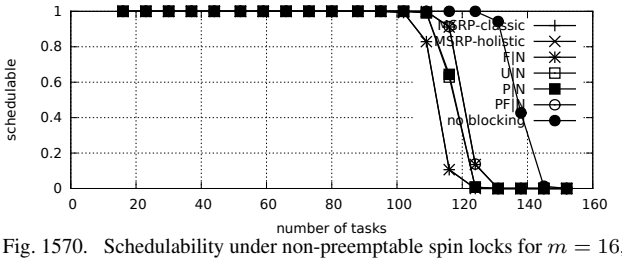

Fig. 1570. Schedulability under non-preemptable spin locks for $m = 16$, $U = 0.1n$, 8 resources, $rsf = 0.4$, $N^{max} = 1$, and short critical sections. The schedulability of the considered preemptable lock types in this configuration is shown in Fig. 1580.

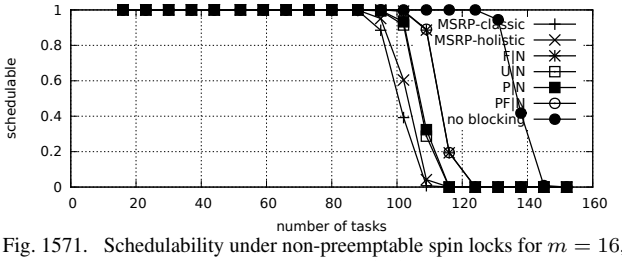

Fig. 1571. Schedulability under non-preemptable spin locks for $m = 16$, $U = 0.1n$, 8 resources, $rsf = 0.4$, $N^{max} = 2$, and short critical sections. The schedulability of the considered preemptable lock types in this configuration is shown in Fig. 1581.

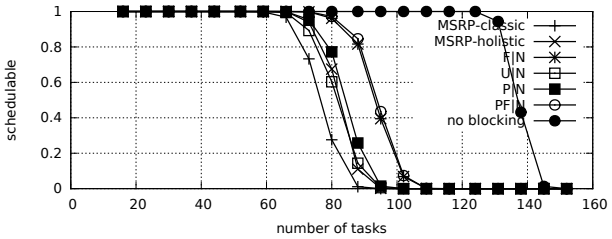

Fig. 1572. Schedulability under non-preemptable spin locks for $m = 16$, $U = 0.1n$, 8 resources, $rsf = 0.4$, $N^{max} = 5$, and short critical sections. The schedulability of the considered preemptable lock types in this configuration is shown in Fig. 1582.

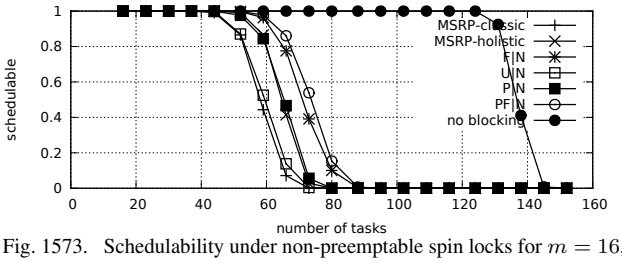

Fig. 1573. Schedulability under non-preemptable spin locks for $m = 16$, $U = 0.1n$, 8 resources, $rsf = 0.4$, $N^{max} = 10$, and short critical sections. The schedulability of the considered preemptable lock types in this configuration is shown in Fig. 1583.

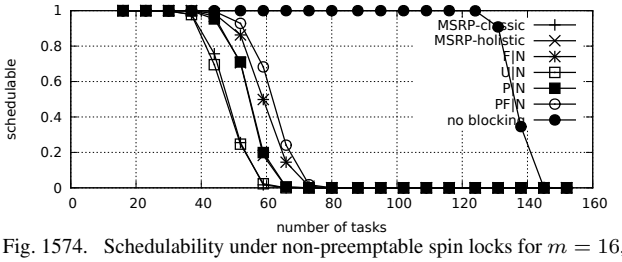

Fig. 1574. Schedulability under non-preemptable spin locks for $m = 16$, $U = 0.1n$, 8 resources, $rsf = 0.4$, $N^{max} = 15$, and short critical sections. The schedulability of the considered preemptable lock types in this configuration is shown in Fig. 1584.

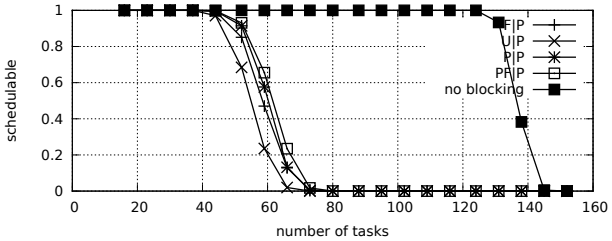

Fig. 1575. Schedulability under preemptable spin locks for $m = 16$, $U = 0.1n$, 8 resources, $rsf = 0.4$, $N^{max} = 1$, and medium critical sections. The schedulability of the considered non-preemptable lock types in this configuration is shown in Fig. 1565.

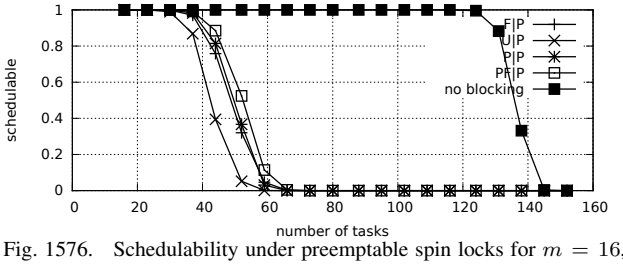

Fig. 1576. Schedulability under preemptable spin locks for $m = 16$, $U = 0.1n$, 8 resources, $rsf = 0.4$, $N^{max} = 2$, and medium critical sections. The schedulability of the considered non-preemptable lock types in this configuration is shown in Fig. 1566.

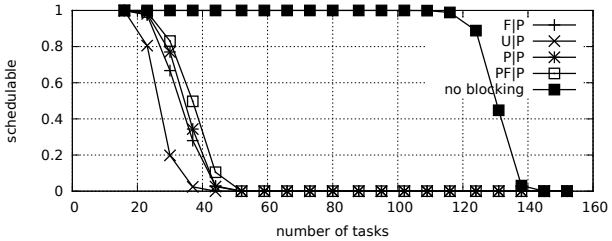

Fig. 1577. Schedulability under preemptable spin locks for $m = 16$, $U = 0.1n$, 8 resources, $rsf = 0.4$, $N^{max} = 5$, and medium critical sections. The schedulability of the considered non-preemptable lock types in this configuration is shown in Fig. 1567.

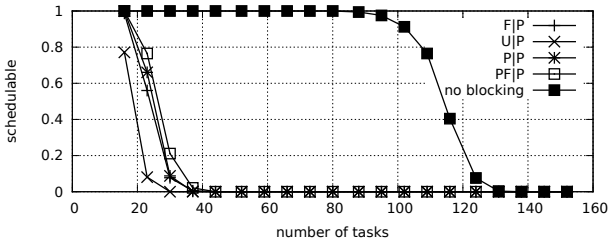

Fig. 1578. Schedulability under preemptable spin locks for $m = 16$, $U = 0.1n$, 8 resources, $rsf = 0.4$, $N^{max} = 10$, and medium critical sections. The schedulability of the considered non-preemptable lock types in this configuration is shown in Fig. 1568.

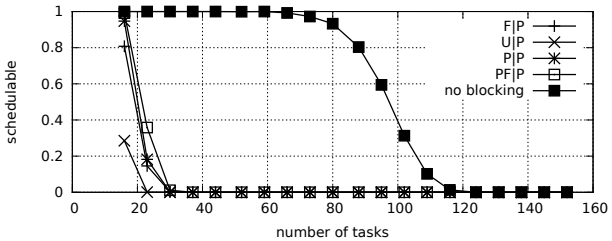

Fig. 1579. Schedulability under preemptable spin locks for $m = 16$, $U = 0.1n$, 8 resources, $rsf = 0.4$, $N^{max} = 15$, and medium critical sections. The schedulability of the considered non-preemptable lock types in this configuration is shown in Fig. 1569.

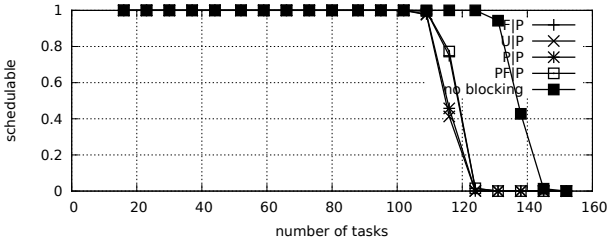

Fig. 1580. Schedulability under preemptable spin locks for $m = 16$, $U = 0.1n$, 8 resources, $rsf = 0.4$, $N^{max} = 1$, and short critical sections. The schedulability of the considered non-preemptable lock types in this configuration is shown in Fig. 1570.

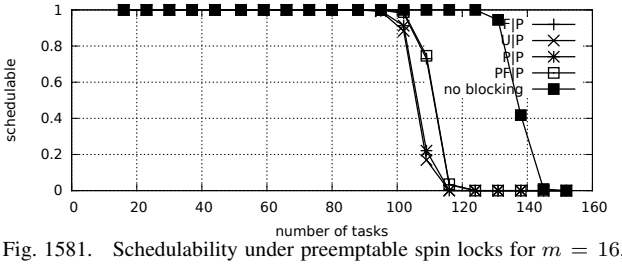

Fig. 1581. Schedulability under preemptable spin locks for $m = 16$, $U = 0.1n$, 8 resources, $rsf = 0.4$, $N^{max} = 2$, and short critical sections. The schedulability of the considered non-preemptable lock types in this configuration is shown in Fig. 1571.

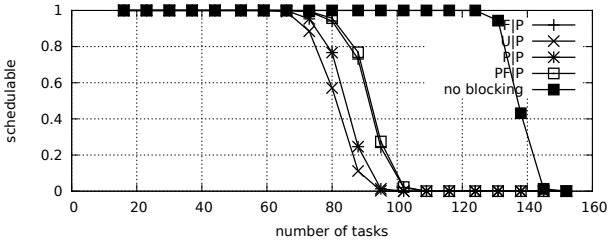

Fig. 1582. Schedulability under preemptable spin locks for $m = 16$, $U = 0.1n$, 8 resources, $rsf = 0.4$, $N^{max} = 5$, and short critical sections. The schedulability of the considered non-preemptable lock types in this configuration is shown in Fig. 1572.

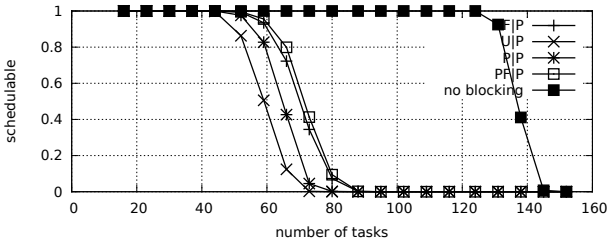

Fig. 1583. Schedulability under preemptable spin locks for $m = 16$, $U = 0.1n$, 8 resources, $rsf = 0.4$, $N^{max} = 10$, and short critical sections. The schedulability of the considered non-preemptable lock types in this configuration is shown in Fig. 1573.

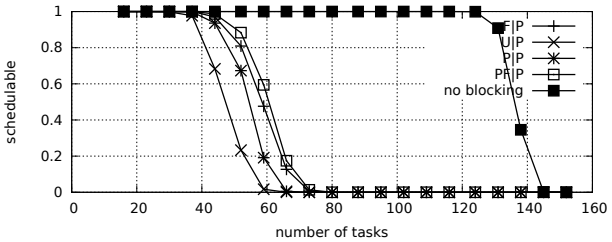

Fig. 1584. Schedulability under preemptable spin locks for $m = 16$, $U = 0.1n$, 8 resources, $rsf = 0.4$, $N^{max} = 15$, and short critical sections. The schedulability of the considered non-preemptable lock types in this configuration is shown in Fig. 1574.

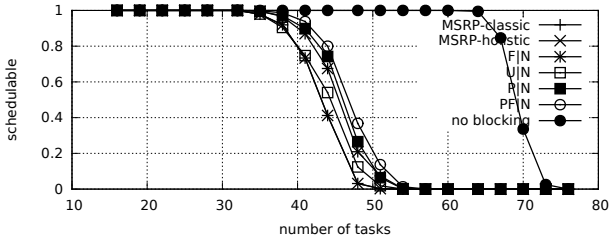

Fig. 1585. Schedulability under non-preemptable spin locks for $m = 16$, $U = 0.2n$, 8 resources, $rsf = 0.4$, $N^{max} = 1$, and medium critical sections. The schedulability of the considered preemptable lock types in this configuration is shown in Fig. 1595.

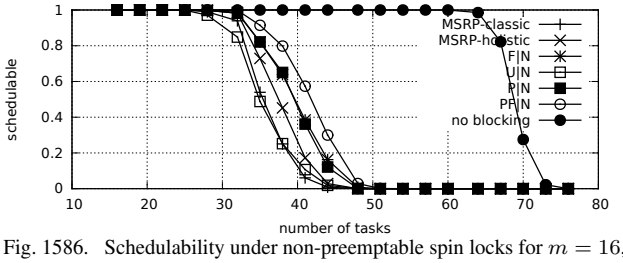

Fig. 1586. Schedulability under non-preemptable spin locks for $m = 16$, $U = 0.2n$, 8 resources, $rsf = 0.4$, $N^{max} = 2$, and medium critical sections. The schedulability of the considered preemptable lock types in this configuration is shown in Fig. 1596.

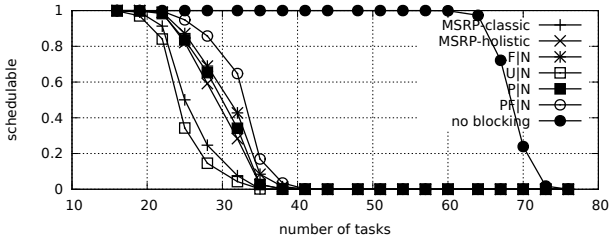

Fig. 1587. Schedulability under non-preemptable spin locks for $m = 16$, $U = 0.2n$, 8 resources, $rsf = 0.4$, $N^{max} = 5$, and medium critical sections. The schedulability of the considered preemptable lock types in this configuration is shown in Fig. 1597.

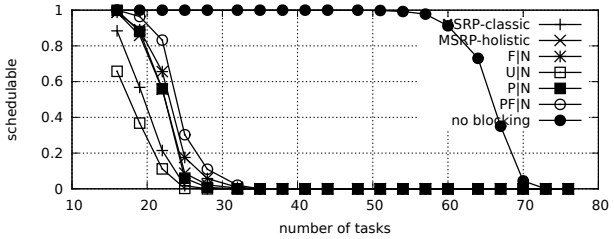

Fig. 1588. Schedulability under non-preemptable spin locks for $m = 16$, $U = 0.2n$, 8 resources, $rsf = 0.4$, $N^{max} = 10$, and medium critical sections. The schedulability of the considered preemptable lock types in this configuration is shown in Fig. 1598.

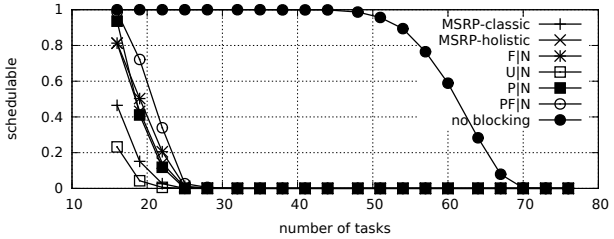

Fig. 1589. Schedulability under non-preemptable spin locks for $m = 16$, $U = 0.2n$, 8 resources, $rsf = 0.4$, $N^{max} = 15$, and medium critical sections. The schedulability of the considered preemptable lock types in this configuration is shown in Fig. 1599.

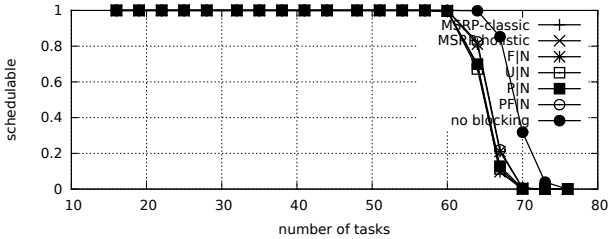

Fig. 1590. Schedulability under non-preemptable spin locks for $m = 16$, $U = 0.2n$, 8 resources, $rsf = 0.4$, $N^{max} = 1$, and short critical sections. The schedulability of the considered preemptable lock types in this configuration is shown in Fig. 1600.

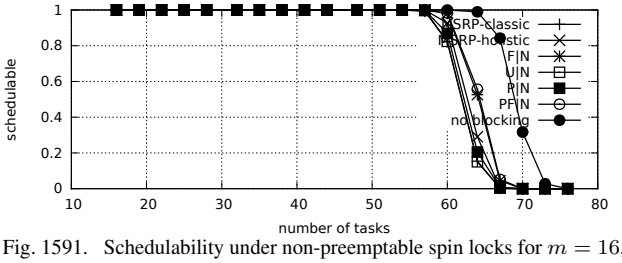

Fig. 1591. Schedulability under non-preemptable spin locks for $m = 16$, $U = 0.2n$, 8 resources, $rsf = 0.4$, $N^{max} = 2$, and short critical sections. The schedulability of the considered preemptable lock types in this configuration is shown in Fig. 1601.

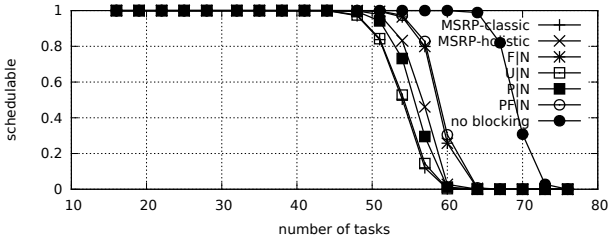

Fig. 1592. Schedulability under non-preemptable spin locks for $m = 16$, $U = 0.2n$, 8 resources, $rsf = 0.4$, $N^{max} = 5$, and short critical sections. The schedulability of the considered preemptable lock types in this configuration is shown in Fig. 1602.

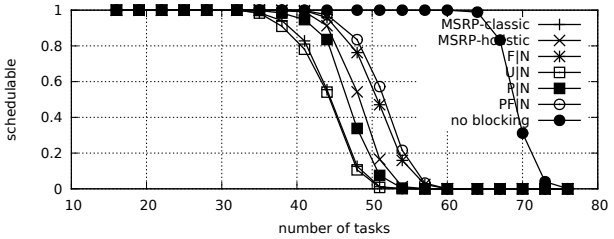

Fig. 1593. Schedulability under non-preemptable spin locks for $m = 16$, $U = 0.2n$, 8 resources, $rsf = 0.4$, $N^{max} = 10$, and short critical sections. The schedulability of the considered preemptable lock types in this configuration is shown in Fig. 1603.

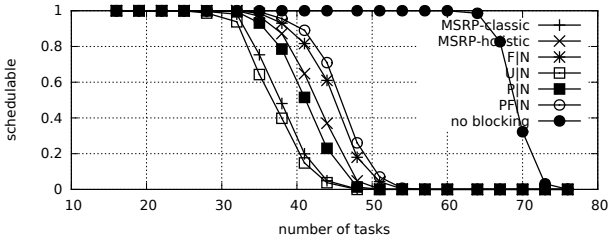

Fig. 1594. Schedulability under non-preemptable spin locks for $m = 16$, $U = 0.2n$, 8 resources, $rsf = 0.4$, $N^{max} = 15$, and short critical sections. The schedulability of the considered preemptable lock types in this configuration is shown in Fig. 1604.

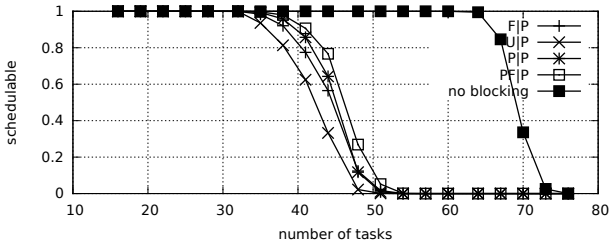

Fig. 1595. Schedulability under preemptable spin locks for $m = 16$, $U = 0.2n$, 8 resources, $rsf = 0.4$, $N^{max} = 1$, and medium critical sections. The schedulability of the considered non-preemptable lock types in this configuration is shown in Fig. 1585.

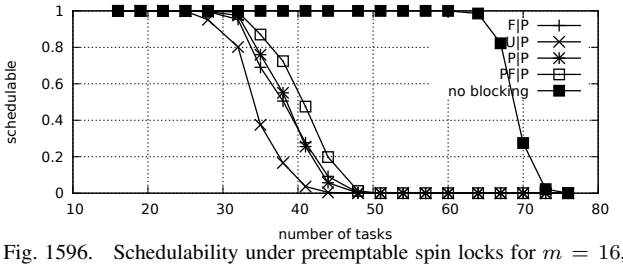

Fig. 1596. Schedulability under preemptable spin locks for $m = 16$, $U = 0.2n$, 8 resources, $rsf = 0.4$, $N^{max} = 2$, and medium critical sections. The schedulability of the considered non-preemptable lock types in this configuration is shown in Fig. 1586.

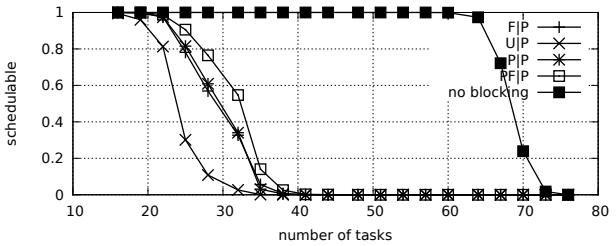

Fig. 1597. Schedulability under preemptable spin locks for $m = 16$, $U = 0.2n$, 8 resources, $rsf = 0.4$, $N^{max} = 5$, and medium critical sections. The schedulability of the considered non-preemptable lock types in this configuration is shown in Fig. 1587.

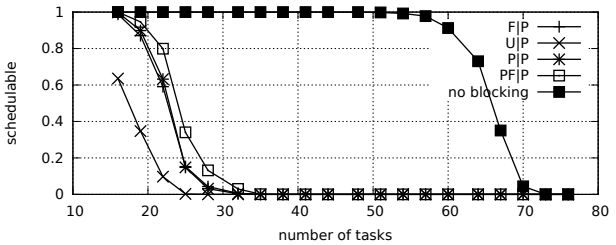

Fig. 1598. Schedulability under preemptable spin locks for $m = 16$, $U = 0.2n$, 8 resources, $rsf = 0.4$, $N^{max} = 10$, and medium critical sections. The schedulability of the considered non-preemptable lock types in this configuration is shown in Fig. 1588.

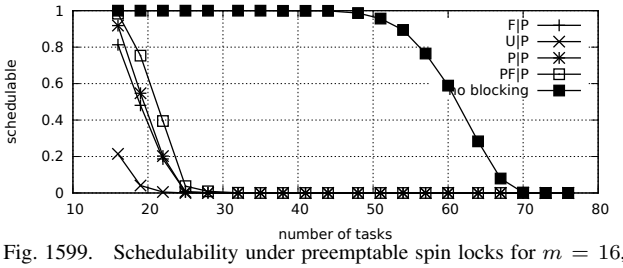

Fig. 1599. Schedulability under preemptable spin locks for $m = 16$, $U = 0.2n$, 8 resources, $rsf = 0.4$, $N^{max} = 15$, and medium critical sections. The schedulability of the considered non-preemptable lock types in this configuration is shown in Fig. 1589.

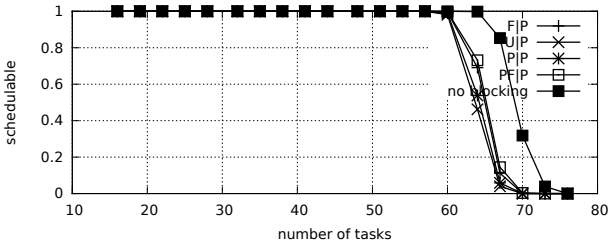

Fig. 1600. Schedulability under preemptable spin locks for $m = 16$, $U = 0.2n$, 8 resources, $rsf = 0.4$, $N^{max} = 1$, and short critical sections. The schedulability of the considered non-preemptable lock types in this configuration is shown in Fig. 1590.

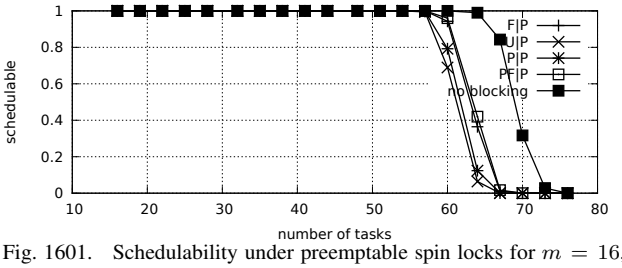

Fig. 1601. Schedulability under preemptable spin locks for $m = 16$, $U = 0.2n$, 8 resources, $rsf = 0.4$, $N^{max} = 2$, and short critical sections. The schedulability of the considered non-preemptable lock types in this configuration is shown in Fig. 1591.

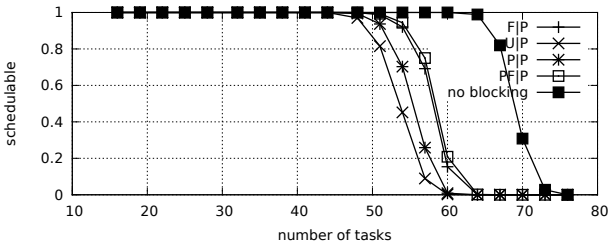

Fig. 1602. Schedulability under preemptable spin locks for $m = 16$, $U = 0.2n$, 8 resources, $rsf = 0.4$, $N^{max} = 5$, and short critical sections. The schedulability of the considered non-preemptable lock types in this configuration is shown in Fig. 1592.

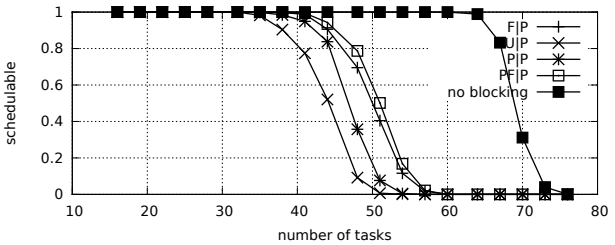

Fig. 1603. Schedulability under preemptable spin locks for $m = 16$, $U = 0.2n$, 8 resources, $rsf = 0.4$, $N^{max} = 10$, and short critical sections. The schedulability of the considered non-preemptable lock types in this configuration is shown in Fig. 1593.

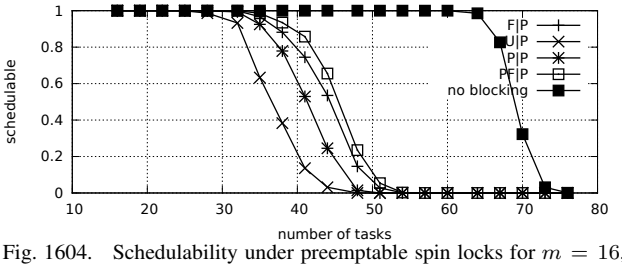

Fig. 1604. Schedulability under preemptable spin locks for $m = 16$, $U = 0.2n$, 8 resources, $rsf = 0.4$, $N^{max} = 15$, and short critical sections. The schedulability of the considered non-preemptable lock types in this configuration is shown in Fig. 1594.

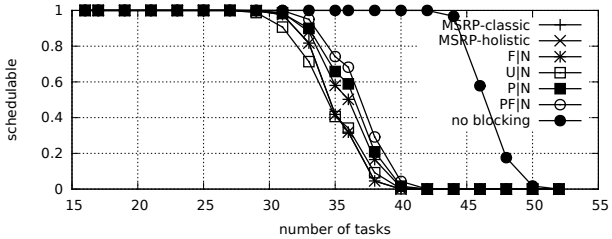

Fig. 1605. Schedulability under non-preemptable spin locks for $m = 16$, $U = 0.3n$, 8 resources, $rsf = 0.4$, $N^{max} = 1$, and medium critical sections. The schedulability of the considered preemptable lock types in this configuration is shown in Fig. 1615.

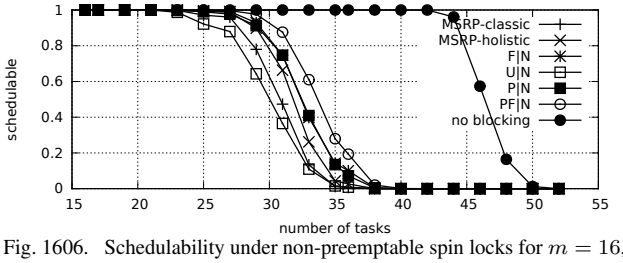

Fig. 1606. Schedulability under non-preemptable spin locks for $m = 16$, $U = 0.3n$, 8 resources, $rsf = 0.4$, $N^{max} = 2$, and medium critical sections. The schedulability of the considered preemptable lock types in this configuration is shown in Fig. 1616.

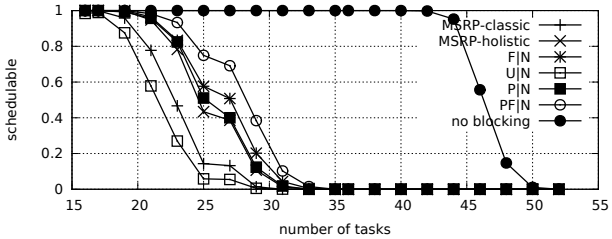

Fig. 1607. Schedulability under non-preemptable spin locks for $m = 16$, $U = 0.3n$, 8 resources, $rsf = 0.4$, $N^{max} = 5$, and medium critical sections. The schedulability of the considered preemptable lock types in this configuration is shown in Fig. 1617.

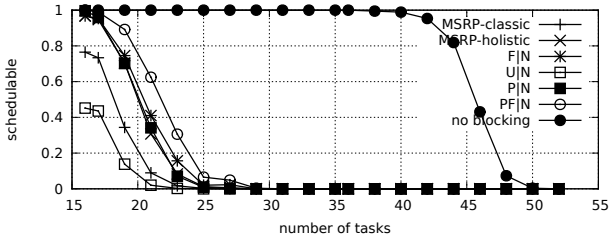

Fig. 1608. Schedulability under non-preemptable spin locks for $m = 16$, $U = 0.3n$, 8 resources, $rsf = 0.4$, $N^{max} = 10$, and medium critical sections. The schedulability of the considered preemptable lock types in this configuration is shown in Fig. 1618.

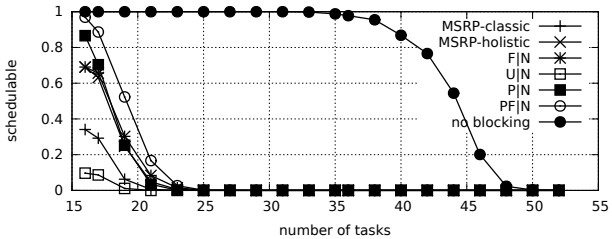

Fig. 1609. Schedulability under non-preemptable spin locks for $m = 16$, $U = 0.3n$, 8 resources, $rsf = 0.4$, $N^{max} = 15$, and medium critical sections. The schedulability of the considered preemptable lock types in this configuration is shown in Fig. 1619.

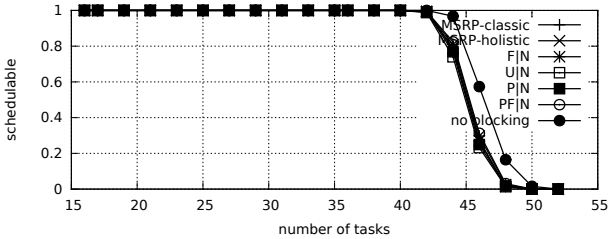

Fig. 1610. Schedulability under non-preemptable spin locks for $m = 16$, $U = 0.3n$, 8 resources, $rsf = 0.4$, $N^{max} = 1$, and short critical sections. The schedulability of the considered preemptable lock types in this configuration is shown in Fig. 1620.

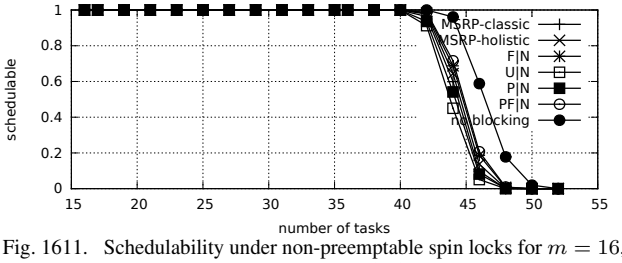

Fig. 1611. Schedulability under non-preemptable spin locks for $m = 16$, $U = 0.3n$, 8 resources, $rsf = 0.4$, $N^{max} = 2$, and short critical sections. The schedulability of the considered preemptable lock types in this configuration is shown in Fig. 1621.

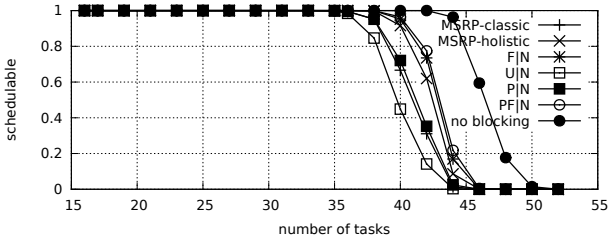

Fig. 1612. Schedulability under non-preemptable spin locks for $m = 16$, $U = 0.3n$, 8 resources, $rsf = 0.4$, $N^{max} = 5$, and short critical sections. The schedulability of the considered preemptable lock types in this configuration is shown in Fig. 1622.

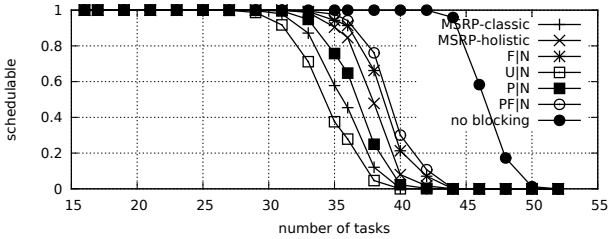

Fig. 1613. Schedulability under non-preemptable spin locks for $m = 16$, $U = 0.3n$, 8 resources, $rsf = 0.4$, $N^{max} = 10$, and short critical sections. The schedulability of the considered preemptable lock types in this configuration is shown in Fig. 1623.

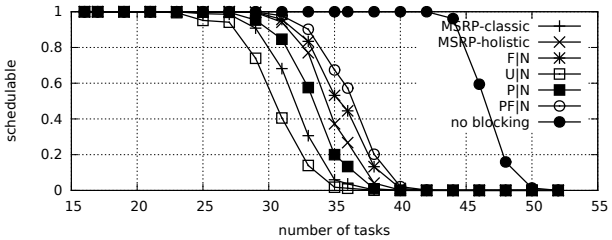

Fig. 1614. Schedulability under non-preemptable spin locks for $m = 16$, $U = 0.3n$, 8 resources, $rsf = 0.4$, $N^{max} = 15$, and short critical sections. The schedulability of the considered preemptable lock types in this configuration is shown in Fig. 1624.

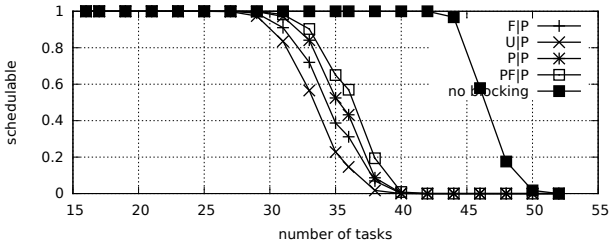

Fig. 1615. Schedulability under preemptable spin locks for $m = 16$, $U = 0.3n$, 8 resources, $rsf = 0.4$, $N^{max} = 1$, and medium critical sections. The schedulability of the considered non-preemptable lock types in this configuration is shown in Fig. 1605.

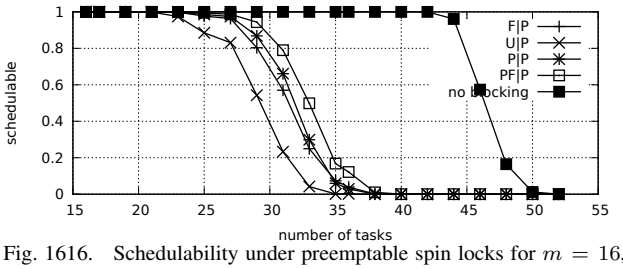

Fig. 1616. Schedulability under preemptable spin locks for $m = 16$, $U = 0.3n$, 8 resources, $rsf = 0.4$, $N^{max} = 2$, and medium critical sections. The schedulability of the considered non-preemptable lock types in this configuration is shown in Fig. 1606.

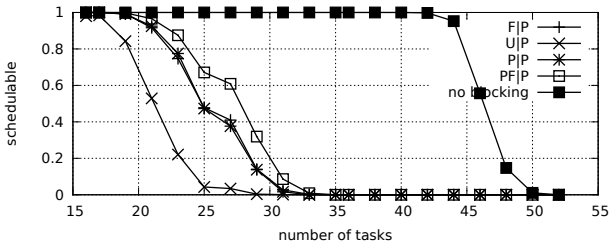

Fig. 1617. Schedulability under preemptable spin locks for $m = 16$, $U = 0.3n$, 8 resources, $rsf = 0.4$, $N^{max} = 5$, and medium critical sections. The schedulability of the considered non-preemptable lock types in this configuration is shown in Fig. 1607.

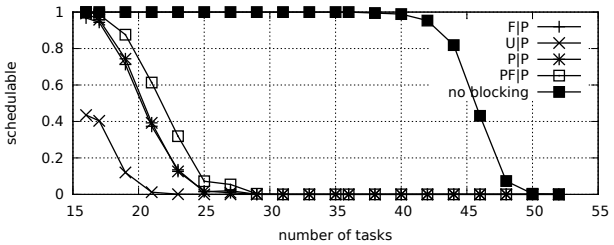

Fig. 1618. Schedulability under preemptable spin locks for $m = 16$, $U = 0.3n$, 8 resources, $rsf = 0.4$, $N^{max} = 10$, and medium critical sections. The schedulability of the considered non-preemptable lock types in this configuration is shown in Fig. 1608.

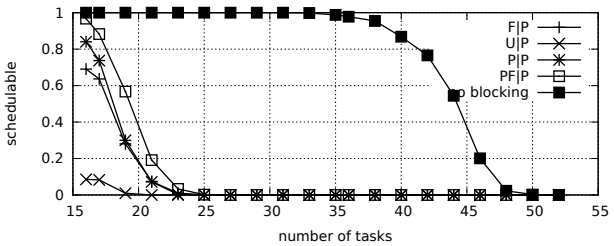

Fig. 1619. Schedulability under preemptable spin locks for $m = 16$, $U = 0.3n$, 8 resources, $rsf = 0.4$, $N^{max} = 15$, and medium critical sections. The schedulability of the considered non-preemptable lock types in this configuration is shown in Fig. 1609.

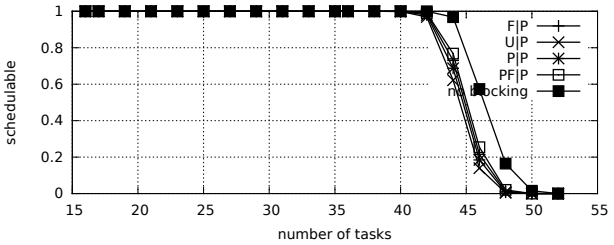

Fig. 1620. Schedulability under preemptable spin locks for $m = 16$, $U = 0.3n$, 8 resources, $rsf = 0.4$, $N^{max} = 1$, and short critical sections. The schedulability of the considered non-preemptable lock types in this configuration is shown in Fig. 1610.

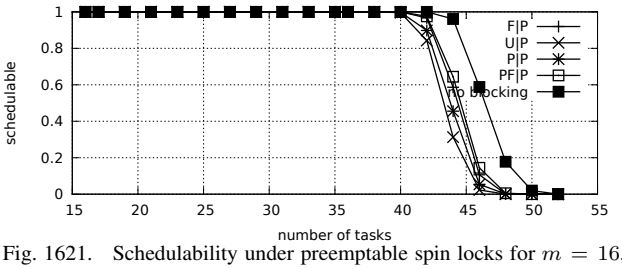

Fig. 1621. Schedulability under preemptable spin locks for $m = 16$, $U = 0.3n$, 8 resources, $rsf = 0.4$, $N^{max} = 2$, and short critical sections. The schedulability of the considered non-preemptable lock types in this configuration is shown in Fig. 1611.

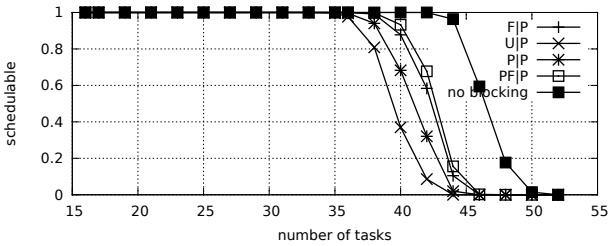

Fig. 1622. Schedulability under preemptable spin locks for $m = 16$, $U = 0.3n$, 8 resources, $rsf = 0.4$, $N^{max} = 5$, and short critical sections. The schedulability of the considered non-preemptable lock types in this configuration is shown in Fig. 1612.

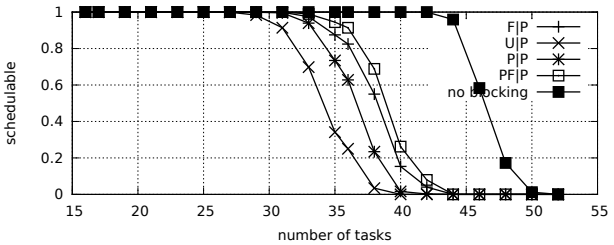

Fig. 1623. Schedulability under preemptable spin locks for $m = 16$, $U = 0.3n$, 8 resources, $rsf = 0.4$, $N^{max} = 10$, and short critical sections. The schedulability of the considered non-preemptable lock types in this configuration is shown in Fig. 1613.

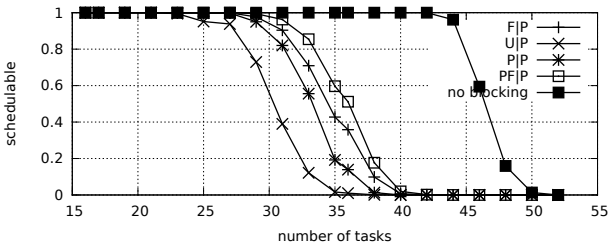

Fig. 1624. Schedulability under preemptable spin locks for $m = 16$, $U = 0.3n$, 8 resources, $rsf = 0.4$, $N^{max} = 15$, and short critical sections. The schedulability of the considered non-preemptable lock types in this configuration is shown in Fig. 1614.

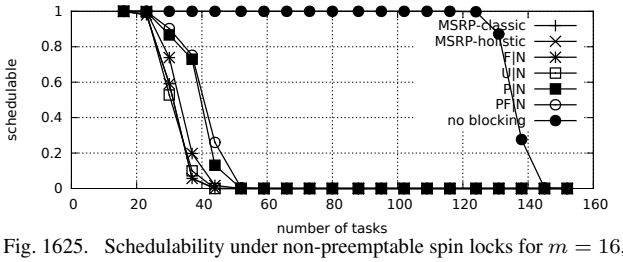

Fig. 1625. Schedulability under non-preemptable spin locks for $m = 16$, $U = 0.1n$, 8 resources, $rsf = 0.75$, $N^{max} = 1$, and medium critical sections. The schedulability of the considered preemptable lock types in this configuration is shown in Fig. 1635.

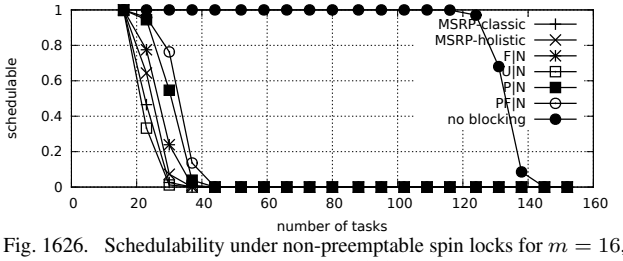

Fig. 1626. Schedulability under non-preemptable spin locks for $m = 16$, $U = 0.1n$, 8 resources, $rsf = 0.75$, $N^{max} = 2$, and medium critical sections. The schedulability of the considered preemptable lock types in this configuration is shown in Fig. 1636.

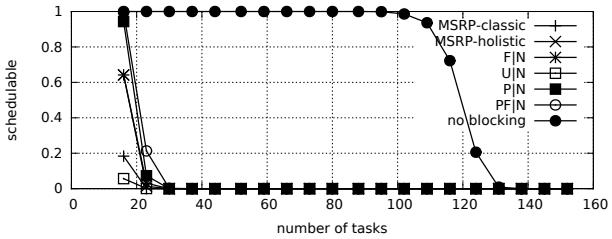

Fig. 1627. Schedulability under non-preemptable spin locks for $m = 16$, $U = 0.1n$, 8 resources, $rsf = 0.75$, $N^{max} = 5$, and medium critical sections. The schedulability of the considered preemptable lock types in this configuration is shown in Fig. 1637.

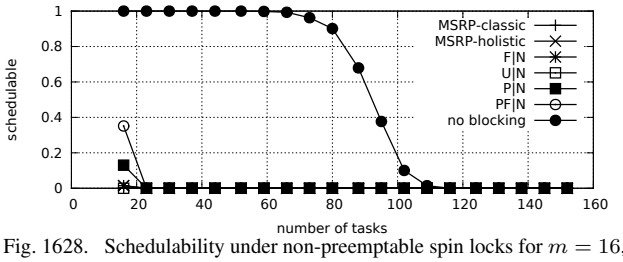

Fig. 1628. Schedulability under non-preemptable spin locks for $m = 16$, $U = 0.1n$, 8 resources, $rsf = 0.75$, $N^{max} = 10$, and medium critical sections. The schedulability of the considered preemptable lock types in this configuration is shown in Fig. 1638.

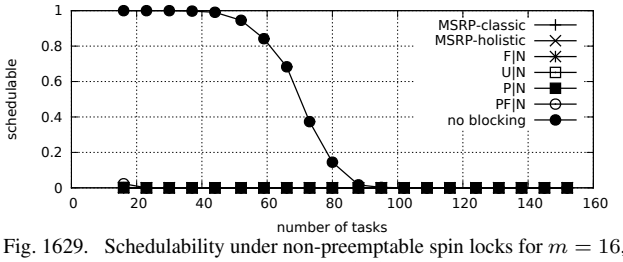

Fig. 1629. Schedulability under non-preemptable spin locks for $m = 16$, $U = 0.1n$, 8 resources, $rsf = 0.75$, $N^{max} = 15$, and medium critical sections. The schedulability of the considered preemptable lock types in this configuration is shown in Fig. 1639.

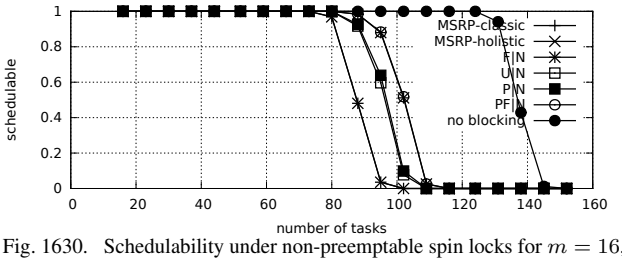

Fig. 1630. Schedulability under non-preemptable spin locks for $m = 16$, $U = 0.1n$, 8 resources, $rsf = 0.75$, $N^{max} = 1$, and short critical sections. The schedulability of the considered preemptable lock types in this configuration is shown in Fig. 1640.

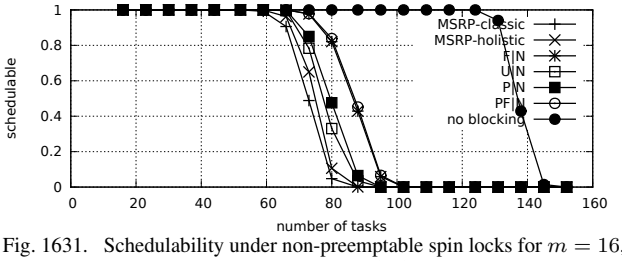

Fig. 1631. Schedulability under non-preemptable spin locks for $m = 16$, $U = 0.1n$, 8 resources, $rsf = 0.75$, $N^{max} = 2$, and short critical sections. The schedulability of the considered preemptable lock types in this configuration is shown in Fig. 1641.

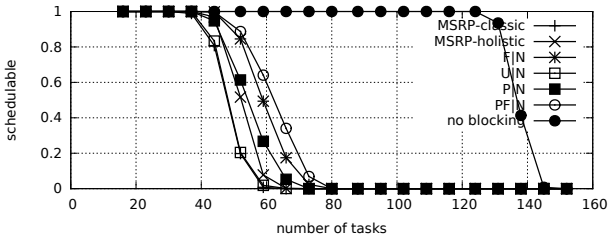

Fig. 1632. Schedulability under non-preemptable spin locks for $m = 16$, $U = 0.1n$, 8 resources, $rsf = 0.75$, $N^{max} = 5$, and short critical sections. The schedulability of the considered preemptable lock types in this configuration is shown in Fig. 1642.

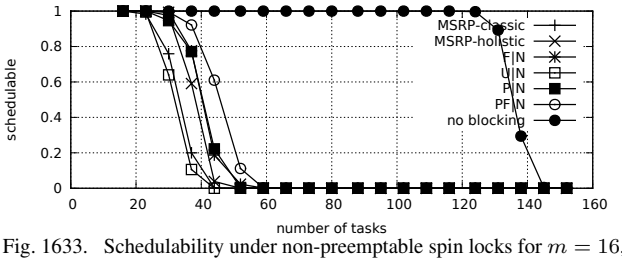

Fig. 1633. Schedulability under non-preemptable spin locks for $m = 16$, $U = 0.1n$, 8 resources, $rsf = 0.75$, $N^{max} = 10$, and short critical sections. The schedulability of the considered preemptable lock types in this configuration is shown in Fig. 1643.

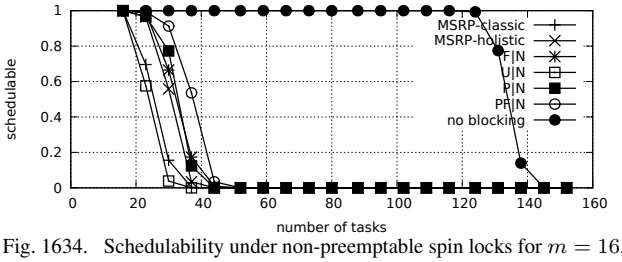

Fig. 1634. Schedulability under non-preemptable spin locks for $m = 16$, $U = 0.1n$, 8 resources, $rsf = 0.75$, $N^{max} = 15$, and short critical sections. The schedulability of the considered preemptable lock types in this configuration is shown in Fig. 1644.

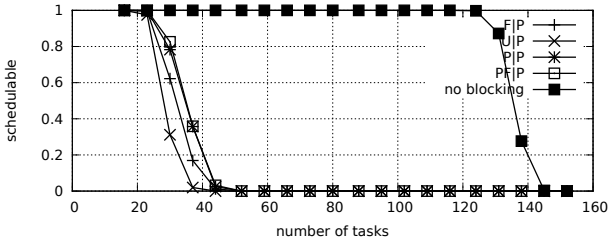

Fig. 1635. Schedulability under preemptable spin locks for $m = 16$, $U = 0.1n$, 8 resources, $rsf = 0.75$, $N^{max} = 1$, and medium critical sections. The schedulability of the considered non-preemptable lock types in this configuration is shown in Fig. 1625.

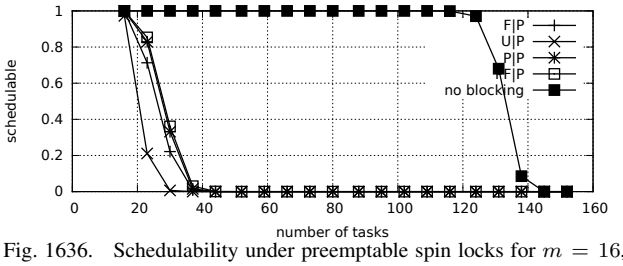

Fig. 1636. Schedulability under preemptable spin locks for $m = 16$, $U = 0.1n$, 8 resources, $rsf = 0.75$, $N^{max} = 2$, and medium critical sections. The schedulability of the considered non-preemptable lock types in this configuration is shown in Fig. 1626.

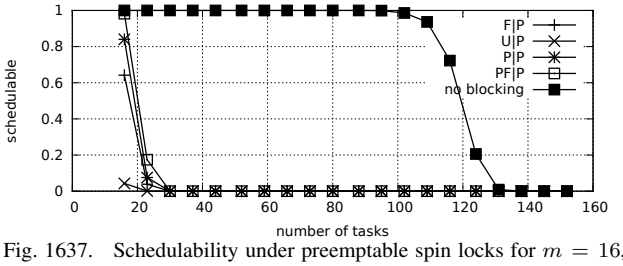

Fig. 1637. Schedulability under preemptable spin locks for $m = 16$, $U = 0.1n$, 8 resources, $rsf = 0.75$, $N^{max} = 5$, and medium critical sections. The schedulability of the considered non-preemptable lock types in this configuration is shown in Fig. 1627.

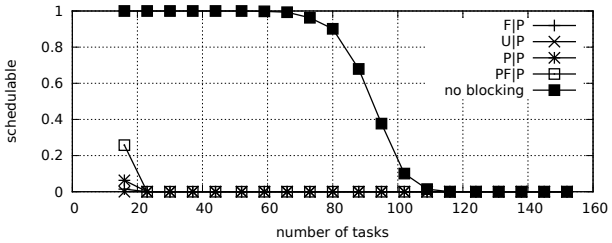

Fig. 1638. Schedulability under preemptable spin locks for $m = 16$, $U = 0.1n$, 8 resources, $rsf = 0.75$, $N^{max} = 10$, and medium critical sections. The schedulability of the considered non-preemptable lock types in this configuration is shown in Fig. 1628.

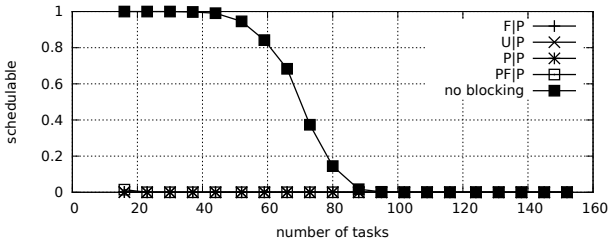

Fig. 1639. Schedulability under preemptable spin locks for $m = 16$, $U = 0.1n$, 8 resources, $rsf = 0.75$, $N^{max} = 15$, and medium critical sections. The schedulability of the considered non-preemptable lock types in this configuration is shown in Fig. 1629.

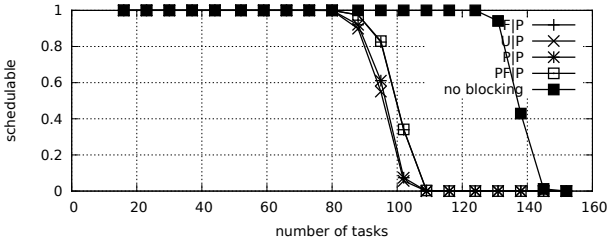

Fig. 1640. Schedulability under preemptable spin locks for $m = 16$, $U = 0.1n$, 8 resources, $rsf = 0.75$, $N^{max} = 1$, and short critical sections. The schedulability of the considered non-preemptable lock types in this configuration is shown in Fig. 1630.

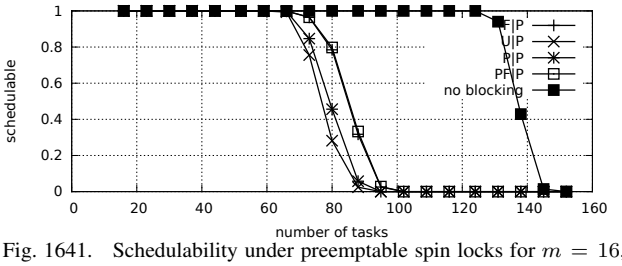

Fig. 1641. Schedulability under preemptable spin locks for $m = 16$, $U = 0.1n$, 8 resources, $rsf = 0.75$, $N^{max} = 2$, and short critical sections. The schedulability of the considered non-preemptable lock types in this configuration is shown in Fig. 1631.

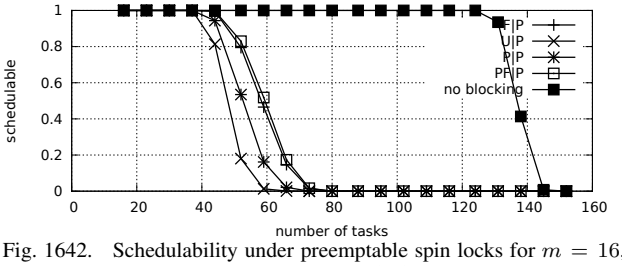

Fig. 1642. Schedulability under preemptable spin locks for $m = 16$, $U = 0.1n$, 8 resources, $rsf = 0.75$, $N^{max} = 5$, and short critical sections. The schedulability of the considered non-preemptable lock types in this configuration is shown in Fig. 1632.

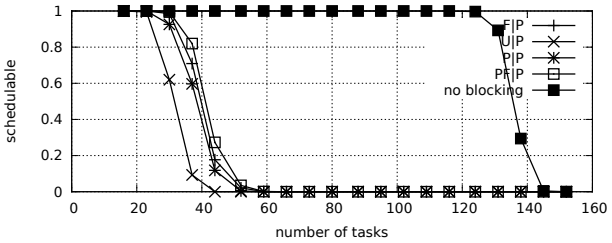

Fig. 1643. Schedulability under preemptable spin locks for $m = 16$, $U = 0.1n$, 8 resources, $rsf = 0.75$, $N^{max} = 10$, and short critical sections. The schedulability of the considered non-preemptable lock types in this configuration is shown in Fig. 1633.

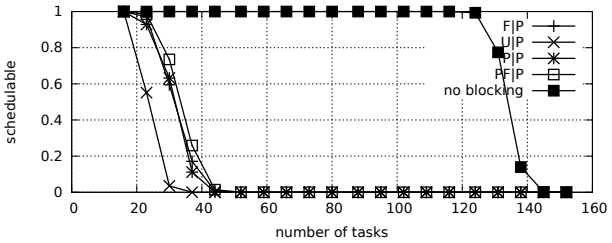

Fig. 1644. Schedulability under preemptable spin locks for $m = 16$, $U = 0.1n$, 8 resources, $rsf = 0.75$, $N^{max} = 15$, and short critical sections. The schedulability of the considered non-preemptable lock types in this configuration is shown in Fig. 1634.

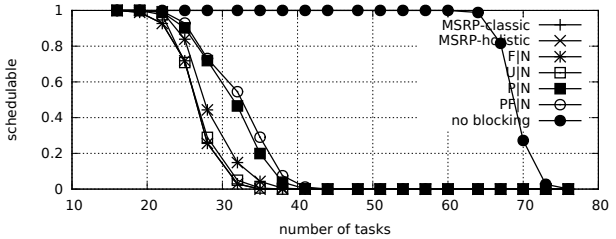

Fig. 1645. Schedulability under non-preemptable spin locks for $m = 16$, $U = 0.2n$, 8 resources, $rsf = 0.75$, $N^{max} = 1$, and medium critical sections. The schedulability of the considered preemptable lock types in this configuration is shown in Fig. 1655.

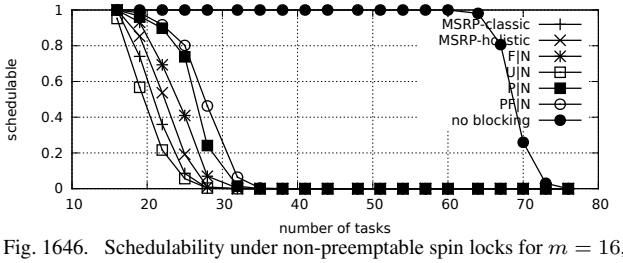

Fig. 1646. Schedulability under non-preemptable spin locks for $m = 16$, $U = 0.2n$, 8 resources, $rsf = 0.75$, $N^{max} = 2$, and medium critical sections. The schedulability of the considered preemptable lock types in this configuration is shown in Fig. 1656.

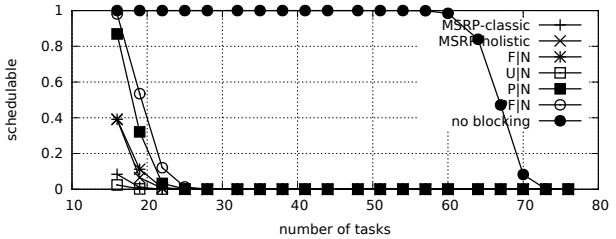

Fig. 1647. Schedulability under non-preemptable spin locks for $m = 16$, $U = 0.2n$, 8 resources, $rsf = 0.75$, $N^{max} = 5$, and medium critical sections. The schedulability of the considered preemptable lock types in this configuration is shown in Fig. 1657.

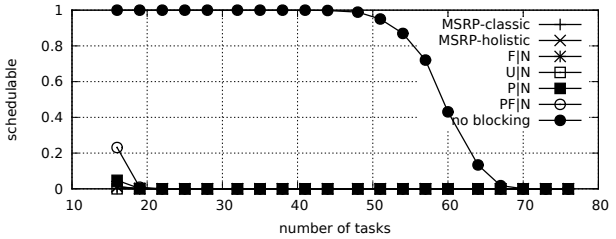

Fig. 1648. Schedulability under non-preemptable spin locks for $m = 16$, $U = 0.2n$, 8 resources, $rsf = 0.75$, $N^{max} = 10$, and medium critical sections. The schedulability of the considered preemptable lock types in this configuration is shown in Fig. 1658.

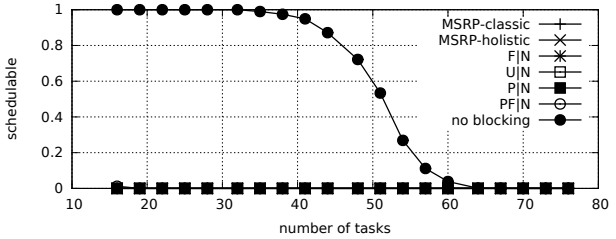

Fig. 1649. Schedulability under non-preemptable spin locks for $m = 16$, $U = 0.2n$, 8 resources, $rsf = 0.75$, $N^{max} = 15$, and medium critical sections. The schedulability of the considered preemptable lock types in this configuration is shown in Fig. 1659.

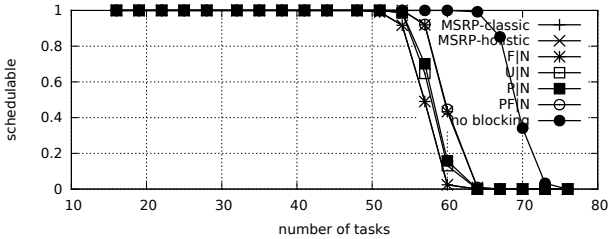

Fig. 1650. Schedulability under non-preemptable spin locks for $m = 16$, $U = 0.2n$, 8 resources, $rsf = 0.75$, $N^{max} = 1$, and short critical sections. The schedulability of the considered preemptable lock types in this configuration is shown in Fig. 1660.

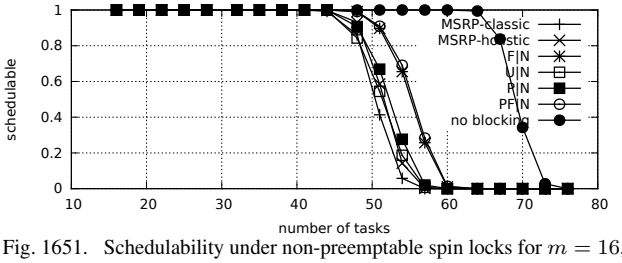

Fig. 1651. Schedulability under non-preemptable spin locks for $m = 16$, $U = 0.2n$, 8 resources, $rsf = 0.75$, $N^{max} = 2$, and short critical sections. The schedulability of the considered preemptable lock types in this configuration is shown in Fig. 1661.

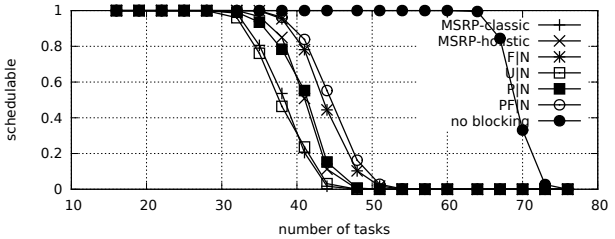

Fig. 1652. Schedulability under non-preemptable spin locks for $m = 16$, $U = 0.2n$, 8 resources, $rsf = 0.75$, $N^{max} = 5$, and short critical sections. The schedulability of the considered preemptable lock types in this configuration is shown in Fig. 1662.

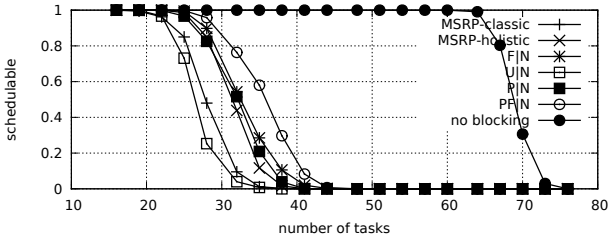

Fig. 1653. Schedulability under non-preemptable spin locks for $m = 16$, $U = 0.2n$, 8 resources, $rsf = 0.75$, $N^{max} = 10$, and short critical sections. The schedulability of the considered preemptable lock types in this configuration is shown in Fig. 1663.

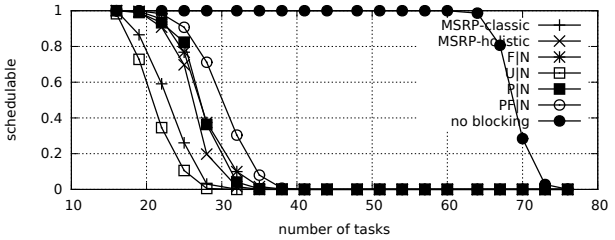

Fig. 1654. Schedulability under non-preemptable spin locks for $m = 16$, $U = 0.2n$, 8 resources, $rsf = 0.75$, $N^{max} = 15$, and short critical sections. The schedulability of the considered preemptable lock types in this configuration is shown in Fig. 1664.

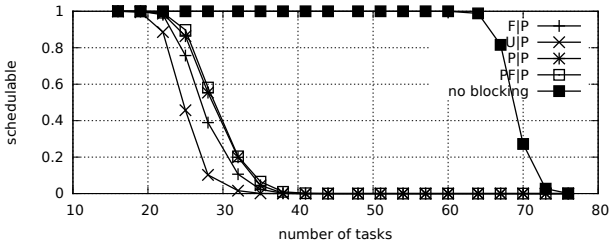

Fig. 1655. Schedulability under preemptable spin locks for $m = 16$, $U = 0.2n$, 8 resources, $rsf = 0.75$, $N^{max} = 1$, and medium critical sections. The schedulability of the considered non-preemptable lock types in this configuration is shown in Fig. 1645.

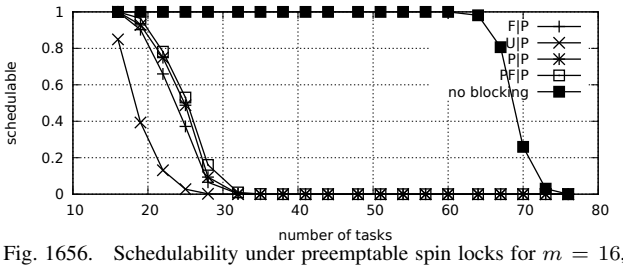

Fig. 1656. Schedulability under preemptable spin locks for $m = 16$, $U = 0.2n$, 8 resources, $rsf = 0.75$, $N^{max} = 2$, and medium critical sections. The schedulability of the considered non-preemptable lock types in this configuration is shown in Fig. 1646.

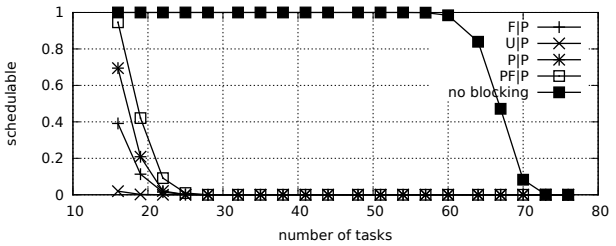

Fig. 1657. Schedulability under preemptable spin locks for $m = 16$, $U = 0.2n$, 8 resources, $rsf = 0.75$, $N^{max} = 5$, and medium critical sections. The schedulability of the considered non-preemptable lock types in this configuration is shown in Fig. 1647.

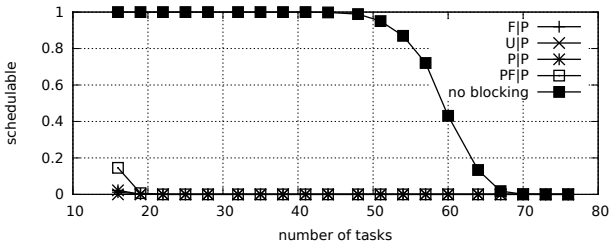

Fig. 1658. Schedulability under preemptable spin locks for $m = 16$, $U = 0.2n$, 8 resources, $rsf = 0.75$, $N^{max} = 10$, and medium critical sections. The schedulability of the considered non-preemptable lock types in this configuration is shown in Fig. 1648.

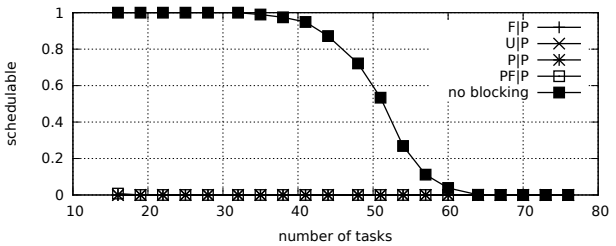

Fig. 1659. Schedulability under preemptable spin locks for $m = 16$, $U = 0.2n$, 8 resources, $rsf = 0.75$, $N^{max} = 15$, and medium critical sections. The schedulability of the considered non-preemptable lock types in this configuration is shown in Fig. 1649.

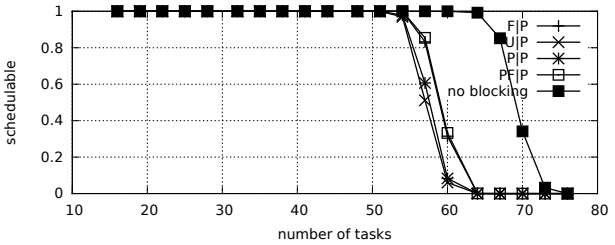

Fig. 1660. Schedulability under preemptable spin locks for $m = 16$, $U = 0.2n$, 8 resources, $rsf = 0.75$, $N^{max} = 1$, and short critical sections. The schedulability of the considered non-preemptable lock types in this configuration is shown in Fig. 1650.

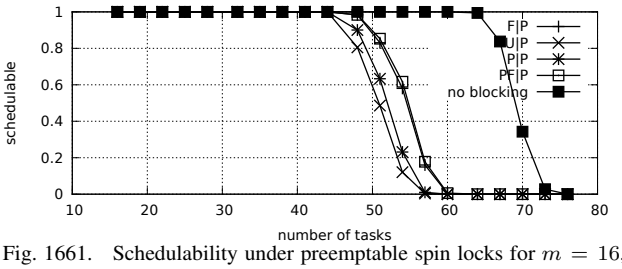

Fig. 1661. Schedulability under preemptable spin locks for $m = 16$, $U = 0.2n$, 8 resources, $rsf = 0.75$, $N^{max} = 2$, and short critical sections. The schedulability of the considered non-preemptable lock types in this configuration is shown in Fig. 1651.

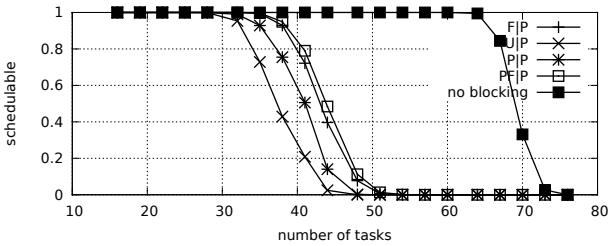

Fig. 1662. Schedulability under preemptable spin locks for $m = 16$, $U = 0.2n$, 8 resources, $rsf = 0.75$, $N^{max} = 5$, and short critical sections. The schedulability of the considered non-preemptable lock types in this configuration is shown in Fig. 1652.

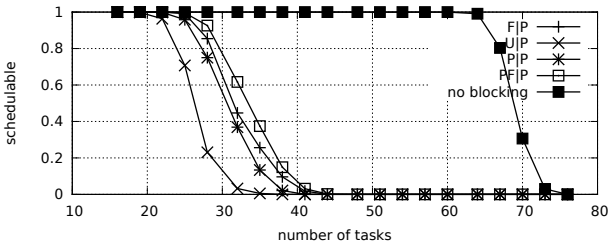

Fig. 1663. Schedulability under preemptable spin locks for $m = 16$, $U = 0.2n$, 8 resources, $rsf = 0.75$, $N^{max} = 10$, and short critical sections. The schedulability of the considered non-preemptable lock types in this configuration is shown in Fig. 1653.

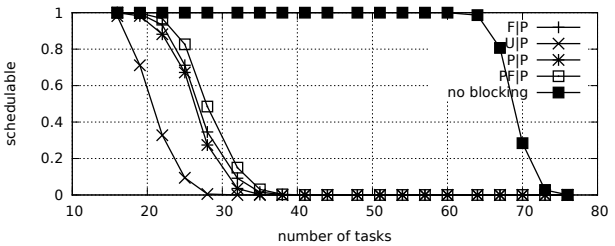

Fig. 1664. Schedulability under preemptable spin locks for $m = 16$, $U = 0.2n$, 8 resources, $rsf = 0.75$, $N^{max} = 15$, and short critical sections. The schedulability of the considered non-preemptable lock types in this configuration is shown in Fig. 1654.

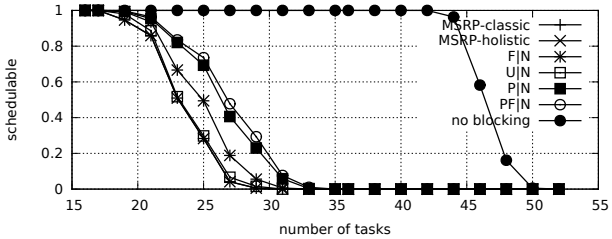

Fig. 1665. Schedulability under non-preemptable spin locks for $m = 16$, $U = 0.3n$, 8 resources, $rsf = 0.75$, $N^{max} = 1$, and medium critical sections. The schedulability of the considered preemptable lock types in this configuration is shown in Fig. 1675.

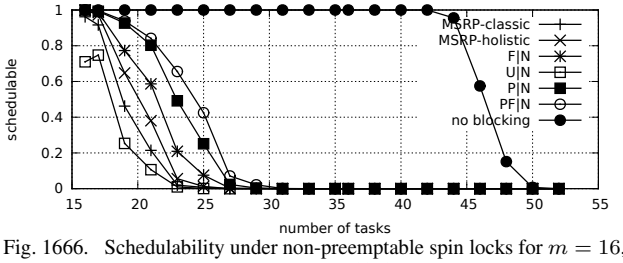

Fig. 1666. Schedulability under non-preemptable spin locks for $m = 16$, $U = 0.3n$, 8 resources, $rsf = 0.75$, $N^{max} = 2$, and medium critical sections. The schedulability of the considered preemptable lock types in this configuration is shown in Fig. 1676.

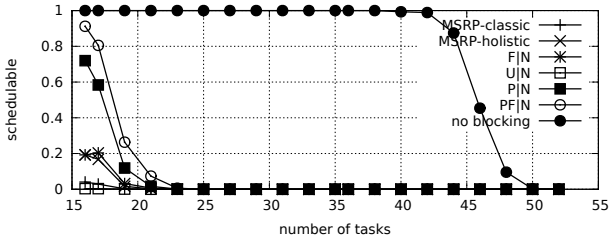

Fig. 1667. Schedulability under non-preemptable spin locks for $m = 16$, $U = 0.3n$, 8 resources, $rsf = 0.75$, $N^{max} = 5$, and medium critical sections. The schedulability of the considered preemptable lock types in this configuration is shown in Fig. 1677.

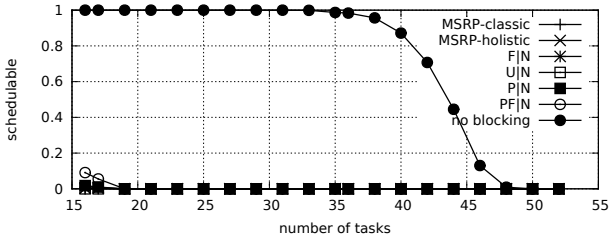

Fig. 1668. Schedulability under non-preemptable spin locks for $m = 16$, $U = 0.3n$, 8 resources, $rsf = 0.75$, $N^{max} = 10$, and medium critical sections. The schedulability of the considered preemptable lock types in this configuration is shown in Fig. 1678.

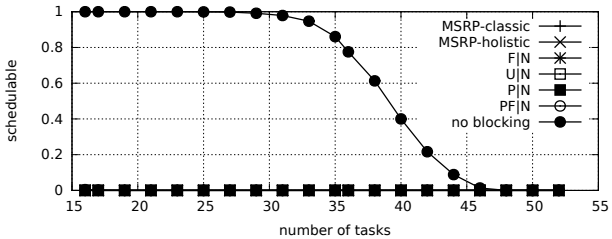

Fig. 1669. Schedulability under non-preemptable spin locks for $m = 16$, $U = 0.3n$, 8 resources, $rsf = 0.75$, $N^{max} = 15$, and medium critical sections. The schedulability of the considered preemptable lock types in this configuration is shown in Fig. 1679.

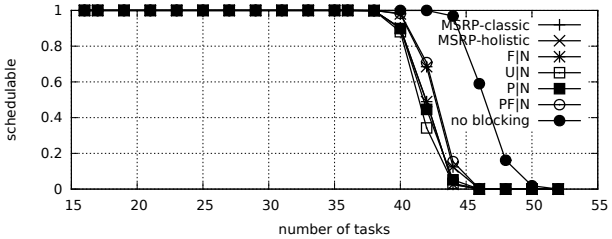

Fig. 1670. Schedulability under non-preemptable spin locks for $m = 16$, $U = 0.3n$, 8 resources, $rsf = 0.75$, $N^{max} = 1$, and short critical sections. The schedulability of the considered preemptable lock types in this configuration is shown in Fig. 1680.

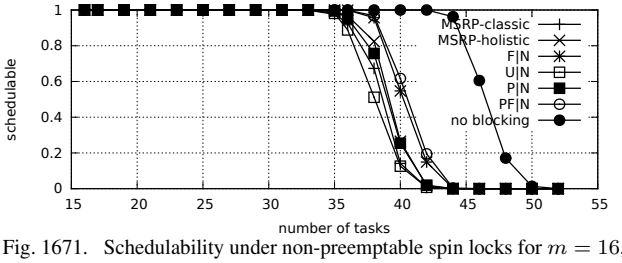

Fig. 1671. Schedulability under non-preemptable spin locks for $m = 16$, $U = 0.3n$, 8 resources, $rsf = 0.75$, $N^{max} = 2$, and short critical sections. The schedulability of the considered preemptable lock types in this configuration is shown in Fig. 1681.

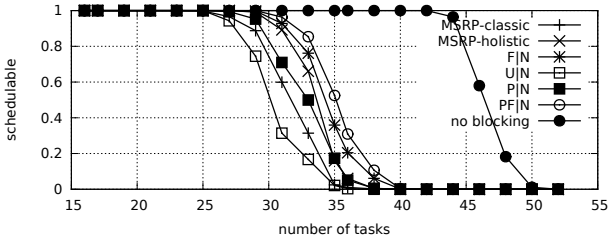

Fig. 1672. Schedulability under non-preemptable spin locks for $m = 16$, $U = 0.3n$, 8 resources, $rsf = 0.75$, $N^{max} = 5$, and short critical sections. The schedulability of the considered preemptable lock types in this configuration is shown in Fig. 1682.

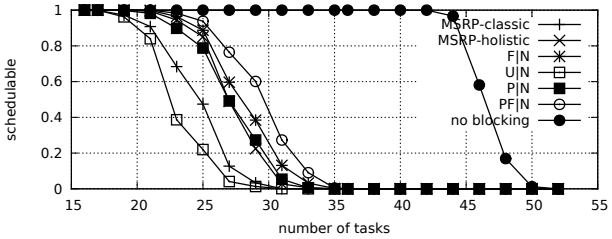

Fig. 1673. Schedulability under non-preemptable spin locks for $m = 16$, $U = 0.3n$, 8 resources, $rsf = 0.75$, $N^{max} = 10$, and short critical sections. The schedulability of the considered preemptable lock types in this configuration is shown in Fig. 1683.

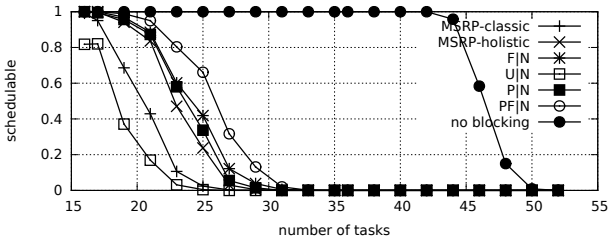

Fig. 1674. Schedulability under non-preemptable spin locks for $m = 16$, $U = 0.3n$, 8 resources, $rsf = 0.75$, $N^{max} = 15$, and short critical sections. The schedulability of the considered preemptable lock types in this configuration is shown in Fig. 1684.

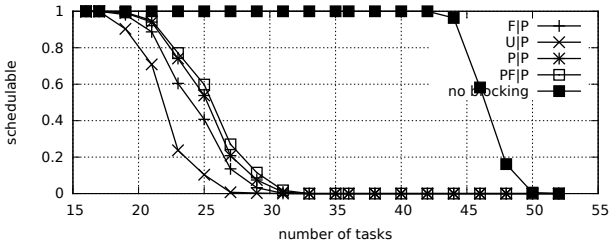

Fig. 1675. Schedulability under preemptable spin locks for $m = 16$, $U = 0.3n$, 8 resources, $rsf = 0.75$, $N^{max} = 1$, and medium critical sections. The schedulability of the considered non-preemptable lock types in this configuration is shown in Fig. 1665.

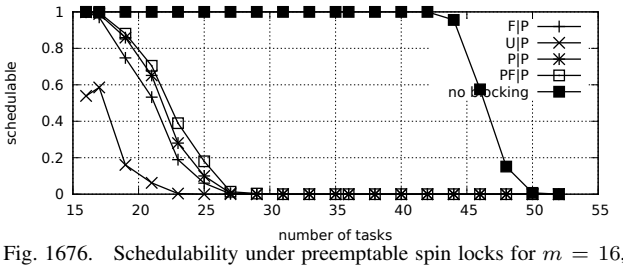

Fig. 1676. Schedulability under preemptable spin locks for $m = 16$, $U = 0.3n$, 8 resources, $rsf = 0.75$, $N^{max} = 2$, and medium critical sections. The schedulability of the considered non-preemptable lock types in this configuration is shown in Fig. 1666.

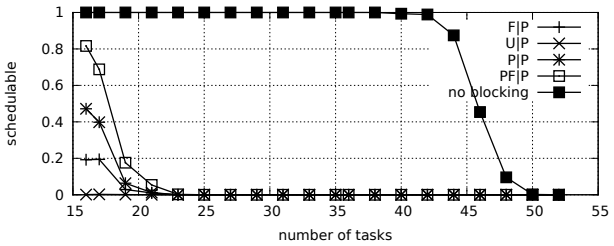

Fig. 1677. Schedulability under preemptable spin locks for $m = 16$, $U = 0.3n$, 8 resources, $rsf = 0.75$, $N^{max} = 5$, and medium critical sections. The schedulability of the considered non-preemptable lock types in this configuration is shown in Fig. 1667.

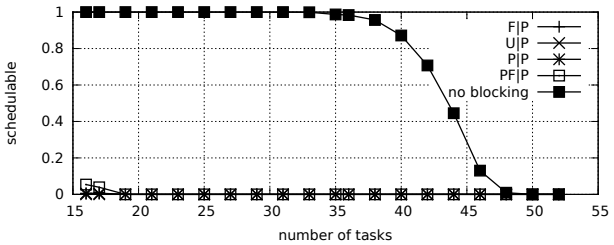

Fig. 1678. Schedulability under preemptable spin locks for $m = 16$, $U = 0.3n$, 8 resources, $rsf = 0.75$, $N^{max} = 10$, and medium critical sections. The schedulability of the considered non-preemptable lock types in this configuration is shown in Fig. 1668.

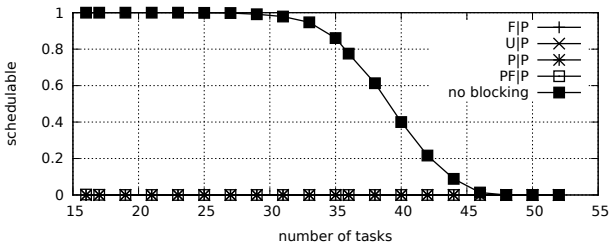

Fig. 1679. Schedulability under preemptable spin locks for $m = 16$, $U = 0.3n$, 8 resources, $rsf = 0.75$, $N^{max} = 15$, and medium critical sections. The schedulability of the considered non-preemptable lock types in this configuration is shown in Fig. 1669.

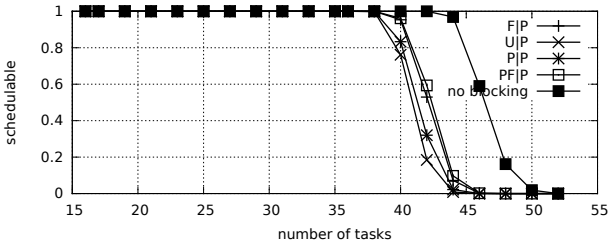

Fig. 1680. Schedulability under preemptable spin locks for $m = 16$, $U = 0.3n$, 8 resources, $rsf = 0.75$, $N^{max} = 1$, and short critical sections. The schedulability of the considered non-preemptable lock types in this configuration is shown in Fig. 1670.

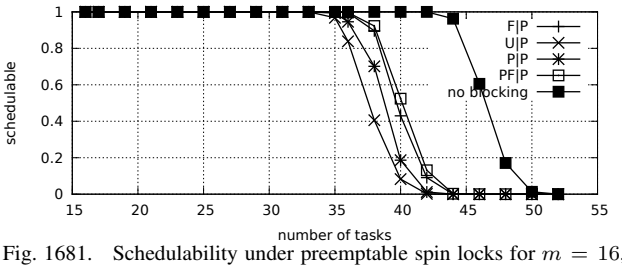

Fig. 1681. Schedulability under preemptable spin locks for $m = 16$, $U = 0.3n$, 8 resources, $rsf = 0.75$, $N^{max} = 2$, and short critical sections. The schedulability of the considered non-preemptable lock types in this configuration is shown in Fig. 1671.

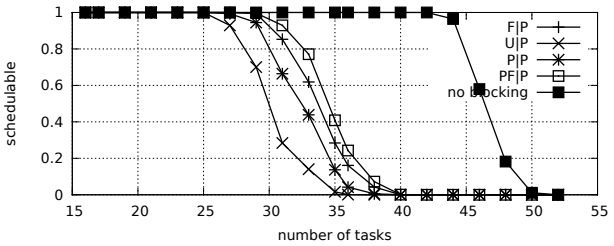

Fig. 1682. Schedulability under preemptable spin locks for $m = 16$, $U = 0.3n$, 8 resources, $rsf = 0.75$, $N^{max} = 5$, and short critical sections. The schedulability of the considered non-preemptable lock types in this configuration is shown in Fig. 1672.

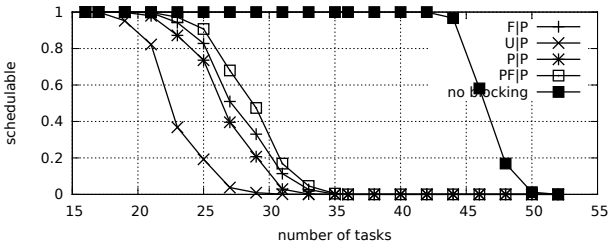

Fig. 1683. Schedulability under preemptable spin locks for $m = 16$, $U = 0.3n$, 8 resources, $rsf = 0.75$, $N^{max} = 10$, and short critical sections. The schedulability of the considered non-preemptable lock types in this configuration is shown in Fig. 1673.

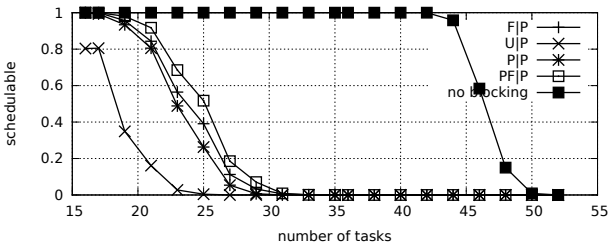

Fig. 1684. Schedulability under preemptable spin locks for $m = 16$, $U = 0.3n$, 8 resources, $rsf = 0.75$, $N^{max} = 15$, and short critical sections. The schedulability of the considered non-preemptable lock types in this configuration is shown in Fig. 1674.

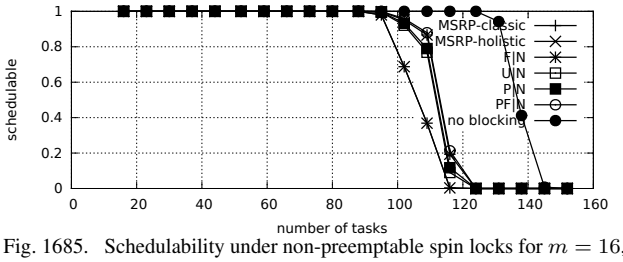

Fig. 1685. Schedulability under non-preemptable spin locks for $m = 16$, $U = 0.1n$, 16 resources, $rsf = 0.1$, $N^{max} = 1$, and medium critical sections. The schedulability of the considered preemptable lock types in this configuration is shown in Fig. 1695.

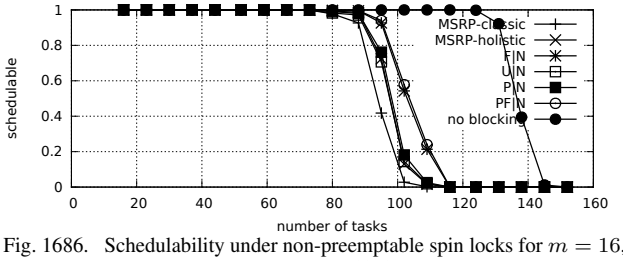

Fig. 1686. Schedulability under non-preemptable spin locks for $m = 16$, $U = 0.1n$, 16 resources, $rsf = 0.1$, $N^{max} = 2$, and medium critical sections. The schedulability of the considered preemptable lock types in this configuration is shown in Fig. 1696.

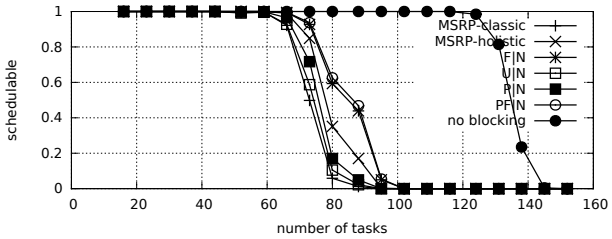

Fig. 1687. Schedulability under non-preemptable spin locks for $m = 16$, $U = 0.1n$, 16 resources, $rsf = 0.1$, $N^{max} = 5$, and medium critical sections. The schedulability of the considered preemptable lock types in this configuration is shown in Fig. 1697.

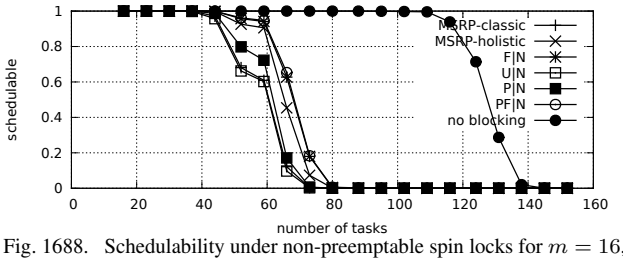

Fig. 1688. Schedulability under non-preemptable spin locks for $m = 16$, $U = 0.1n$, 16 resources, $rsf = 0.1$, $N^{max} = 10$, and medium critical sections. The schedulability of the considered preemptable lock types in this configuration is shown in Fig. 1698.

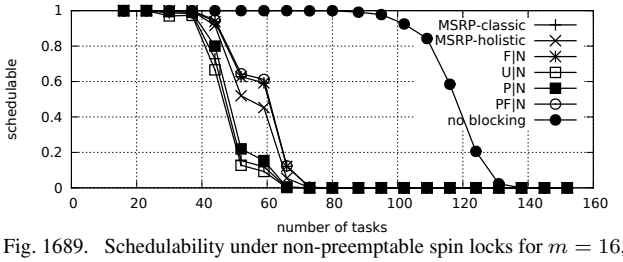

Fig. 1689. Schedulability under non-preemptable spin locks for $m = 16$, $U = 0.1n$, 16 resources, $rsf = 0.1$, $N^{max} = 15$, and medium critical sections. The schedulability of the considered preemptable lock types in this configuration is shown in Fig. 1699.

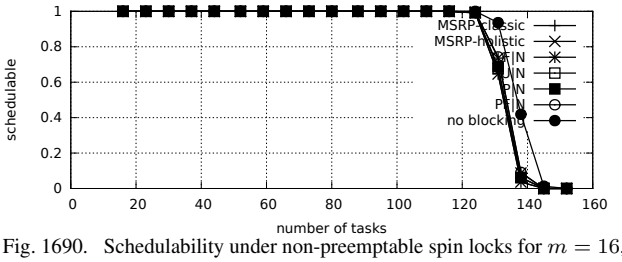

Fig. 1690. Schedulability under non-preemptable spin locks for $m = 16$, $U = 0.1n$, 16 resources, $rsf = 0.1$, $N^{max} = 1$, and short critical sections. The schedulability of the considered preemptable lock types in this configuration is shown in Fig. 1700.

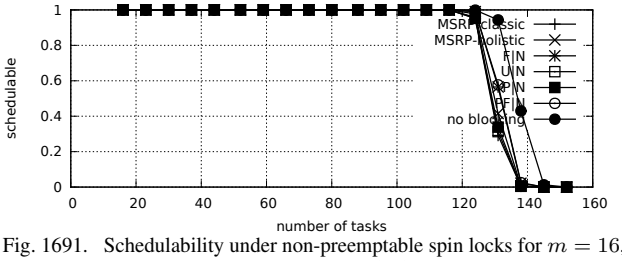

Fig. 1691. Schedulability under non-preemptable spin locks for $m = 16$, $U = 0.1n$, 16 resources, $rsf = 0.1$, $N^{max} = 2$, and short critical sections. The schedulability of the considered preemptable lock types in this configuration is shown in Fig. 1701.

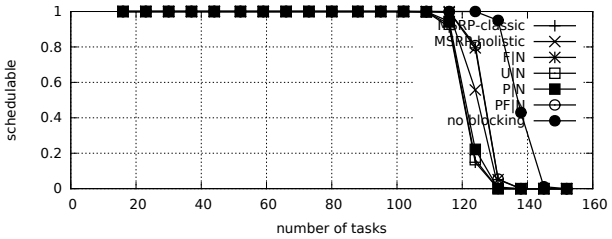

Fig. 1692. Schedulability under non-preemptable spin locks for $m = 16$, $U = 0.1n$, 16 resources, $rsf = 0.1$, $N^{max} = 5$, and short critical sections. The schedulability of the considered preemptable lock types in this configuration is shown in Fig. 1702.

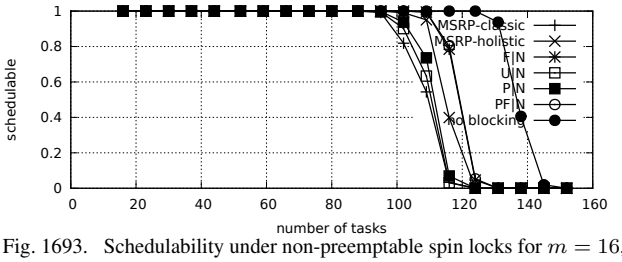

Fig. 1693. Schedulability under non-preemptable spin locks for $m = 16$, $U = 0.1n$, 16 resources, $rsf = 0.1$, $N^{max} = 10$, and short critical sections. The schedulability of the considered preemptable lock types in this configuration is shown in Fig. 1703.

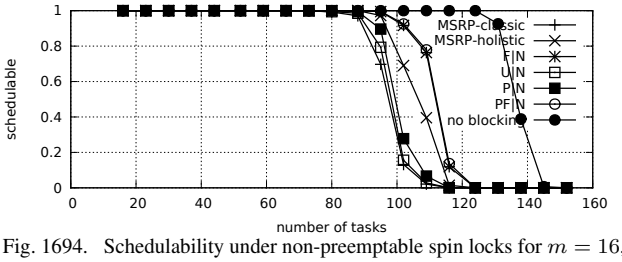

Fig. 1694. Schedulability under non-preemptable spin locks for $m = 16$, $U = 0.1n$, 16 resources, $rsf = 0.1$, $N^{max} = 15$, and short critical sections. The schedulability of the considered preemptable lock types in this configuration is shown in Fig. 1704.

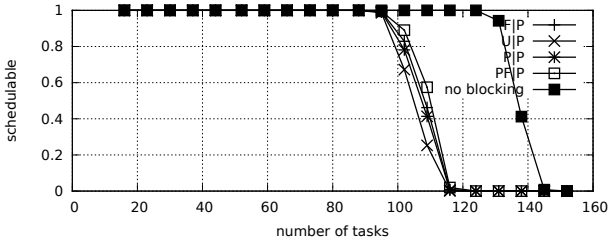

Fig. 1695. Schedulability under preemptable spin locks for $m = 16$, $U = 0.1n$, 16 resources, $rsf = 0.1$, $N^{max} = 1$, and medium critical sections. The schedulability of the considered non-preemptable lock types in this configuration is shown in Fig. 1685.

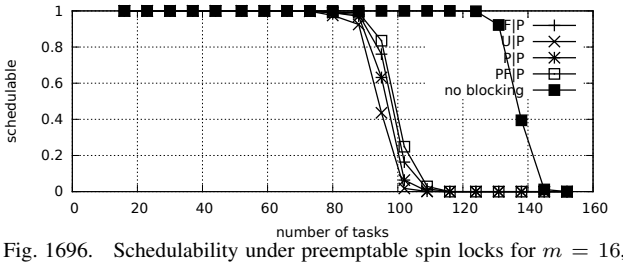

Fig. 1696. Schedulability under preemptable spin locks for $m = 16$, $U = 0.1n$, 16 resources, $rsf = 0.1$, $N^{max} = 2$, and medium critical sections. The schedulability of the considered non-preemptable lock types in this configuration is shown in Fig. 1686.

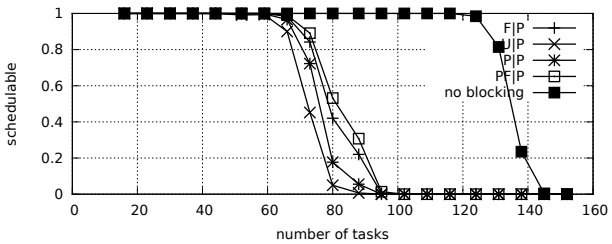

Fig. 1697. Schedulability under preemptable spin locks for $m = 16$, $U = 0.1n$, 16 resources, $rsf = 0.1$, $N^{max} = 5$, and medium critical sections. The schedulability of the considered non-preemptable lock types in this configuration is shown in Fig. 1687.

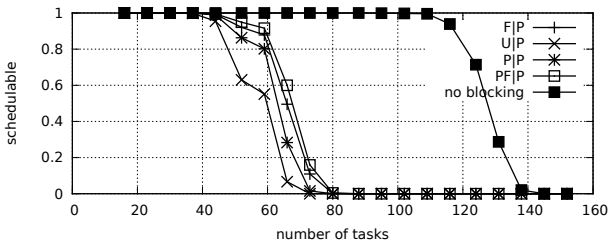

Fig. 1698. Schedulability under preemptable spin locks for $m = 16$, $U = 0.1n$, 16 resources, $rsf = 0.1$, $N^{max} = 10$, and medium critical sections. The schedulability of the considered non-preemptable lock types in this configuration is shown in Fig. 1688.

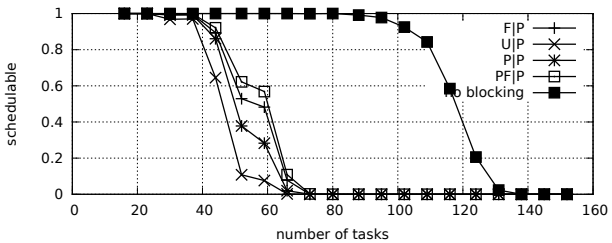

Fig. 1699. Schedulability under preemptable spin locks for $m = 16$, $U = 0.1n$, 16 resources, $rsf = 0.1$, $N^{max} = 15$, and medium critical sections. The schedulability of the considered non-preemptable lock types in this configuration is shown in Fig. 1689.

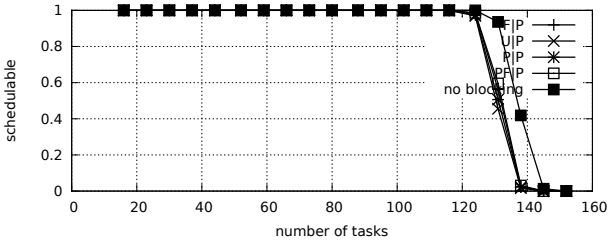

Fig. 1700. Schedulability under preemptable spin locks for $m = 16$, $U = 0.1n$, 16 resources, $rsf = 0.1$, $N^{max} = 1$, and short critical sections. The schedulability of the considered non-preemptable lock types in this configuration is shown in Fig. 1690.

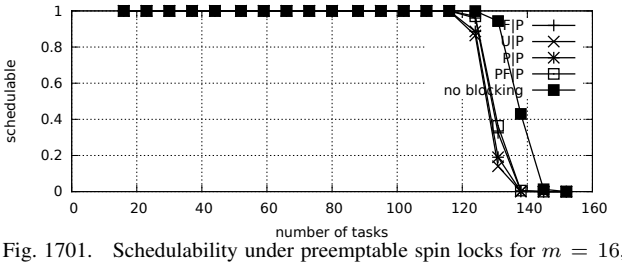

Fig. 1701. Schedulability under preemptable spin locks for $m = 16$, $U = 0.1n$, 16 resources, $rsf = 0.1$, $N^{max} = 2$, and short critical sections. The schedulability of the considered non-preemptable lock types in this configuration is shown in Fig. 1691.

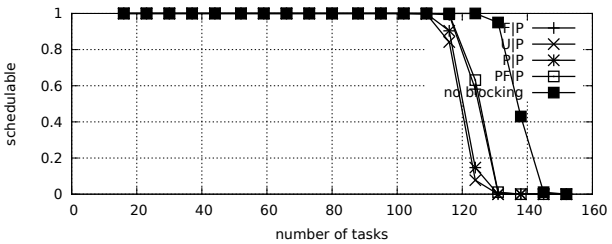

Fig. 1702. Schedulability under preemptable spin locks for $m = 16$, $U = 0.1n$, 16 resources, $rsf = 0.1$, $N^{max} = 5$, and short critical sections. The schedulability of the considered non-preemptable lock types in this configuration is shown in Fig. 1692.

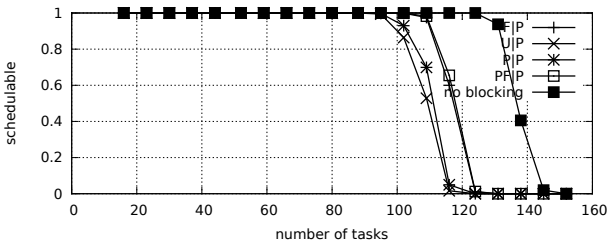

Fig. 1703. Schedulability under preemptable spin locks for $m = 16$, $U = 0.1n$, 16 resources, $rsf = 0.1$, $N^{max} = 10$, and short critical sections. The schedulability of the considered non-preemptable lock types in this configuration is shown in Fig. 1693.

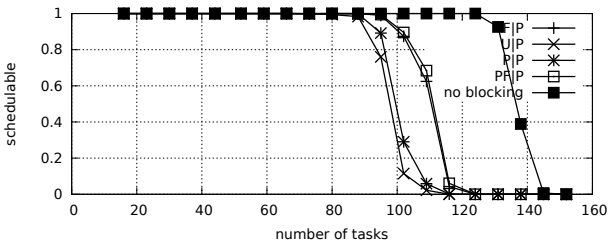

Fig. 1704. Schedulability under preemptable spin locks for $m = 16$, $U = 0.1n$, 16 resources, $rsf = 0.1$, $N^{max} = 15$, and short critical sections. The schedulability of the considered non-preemptable lock types in this configuration is shown in Fig. 1694.

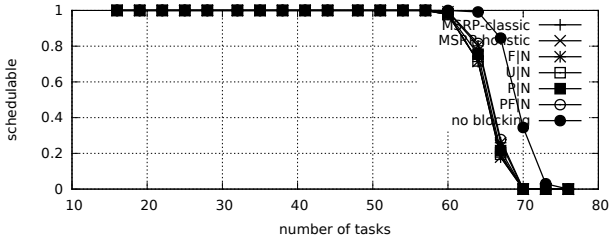

Fig. 1705. Schedulability under non-preemptable spin locks for $m = 16$, $U = 0.2n$, 16 resources, $rsf = 0.1$, $N^{max} = 1$, and medium critical sections. The schedulability of the considered preemptable lock types in this configuration is shown in Fig. 1715.

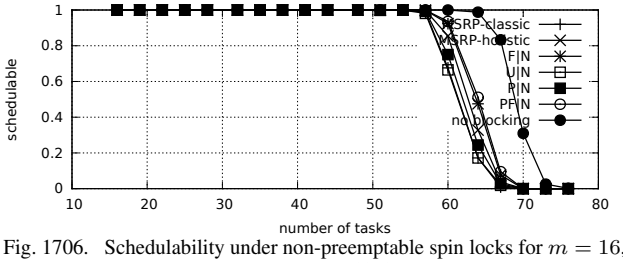

Fig. 1706. Schedulability under non-preemptable spin locks for $m = 16$, $U = 0.2n$, 16 resources, $rsf = 0.1$, $N^{max} = 2$, and medium critical sections. The schedulability of the considered preemptable lock types in this configuration is shown in Fig. 1716.

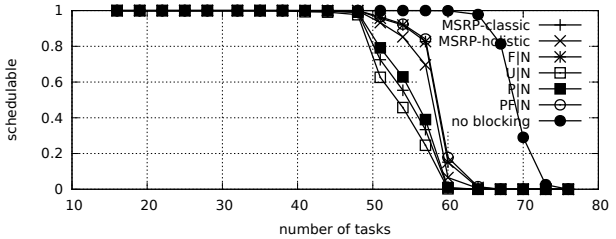

Fig. 1707. Schedulability under non-preemptable spin locks for $m = 16$, $U = 0.2n$, 16 resources, $rsf = 0.1$, $N^{max} = 5$, and medium critical sections. The schedulability of the considered preemptable lock types in this configuration is shown in Fig. 1717.

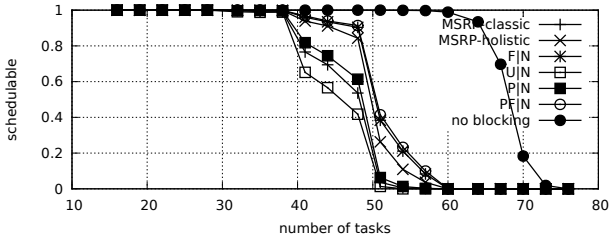

Fig. 1708. Schedulability under non-preemptable spin locks for $m = 16$, $U = 0.2n$, 16 resources, $rsf = 0.1$, $N^{max} = 10$, and medium critical sections. The schedulability of the considered preemptable lock types in this configuration is shown in Fig. 1718.

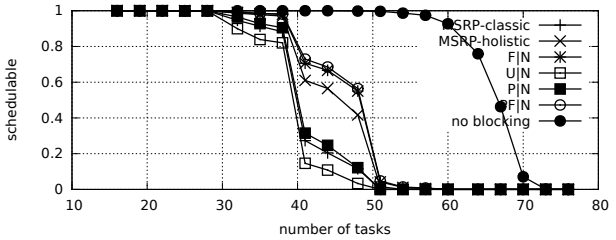

Fig. 1709. Schedulability under non-preemptable spin locks for $m = 16$, $U = 0.2n$, 16 resources, $rsf = 0.1$, $N^{max} = 15$, and medium critical sections. The schedulability of the considered preemptable lock types in this configuration is shown in Fig. 1719.

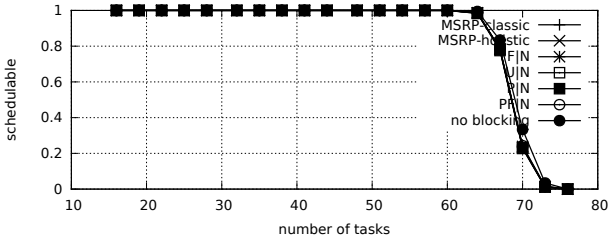

Fig. 1710. Schedulability under non-preemptable spin locks for $m = 16$, $U = 0.2n$, 16 resources, $rsf = 0.1$, $N^{max} = 1$, and short critical sections. The schedulability of the considered preemptable lock types in this configuration is shown in Fig. 1720.

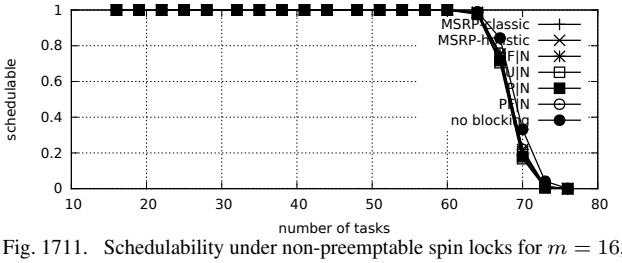

Fig. 1711. Schedulability under non-preemptable spin locks for $m = 16$, $U = 0.2n$, 16 resources, $rsf = 0.1$, $N^{max} = 2$, and short critical sections. The schedulability of the considered preemptable lock types in this configuration is shown in Fig. 1721.

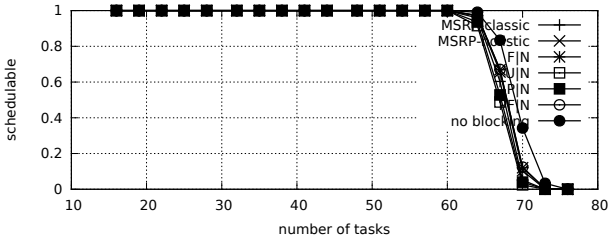

Fig. 1712. Schedulability under non-preemptable spin locks for $m = 16$, $U = 0.2n$, 16 resources, $rsf = 0.1$, $N^{max} = 5$, and short critical sections. The schedulability of the considered preemptable lock types in this configuration is shown in Fig. 1722.

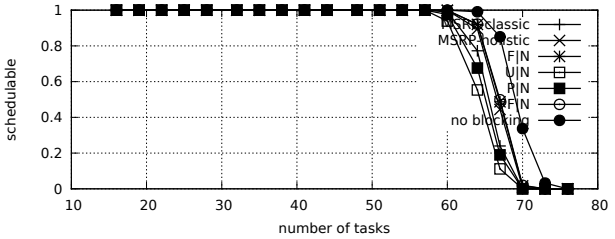

Fig. 1713. Schedulability under non-preemptable spin locks for $m = 16$, $U = 0.2n$, 16 resources, $rsf = 0.1$, $N^{max} = 10$, and short critical sections. The schedulability of the considered preemptable lock types in this configuration is shown in Fig. 1723.

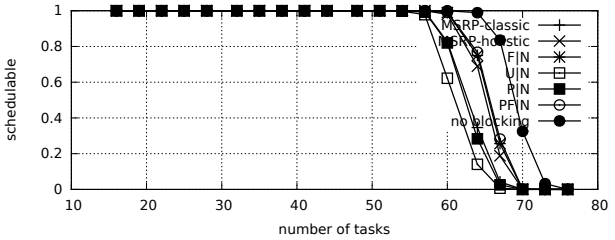

Fig. 1714. Schedulability under non-preemptable spin locks for $m = 16$, $U = 0.2n$, 16 resources, $rsf = 0.1$, $N^{max} = 15$, and short critical sections. The schedulability of the considered preemptable lock types in this configuration is shown in Fig. 1724.

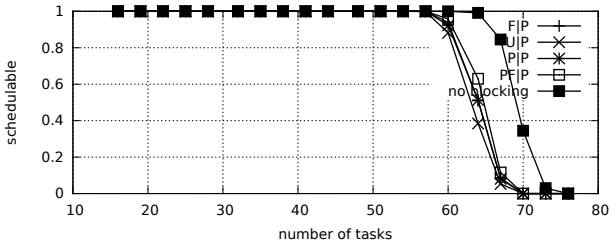

Fig. 1715. Schedulability under preemptable spin locks for $m = 16$, $U = 0.2n$, 16 resources, $rsf = 0.1$, $N^{max} = 1$, and medium critical sections. The schedulability of the considered non-preemptable lock types in this configuration is shown in Fig. 1705.

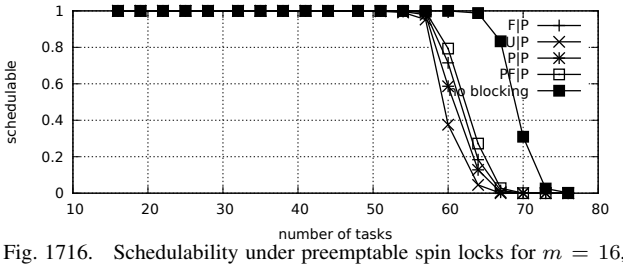

Fig. 1716. Schedulability under preemptable spin locks for $m = 16$, $U = 0.2n$, 16 resources, $rsf = 0.1$, $N^{max} = 2$, and medium critical sections. The schedulability of the considered non-preemptable lock types in this configuration is shown in Fig. 1706.

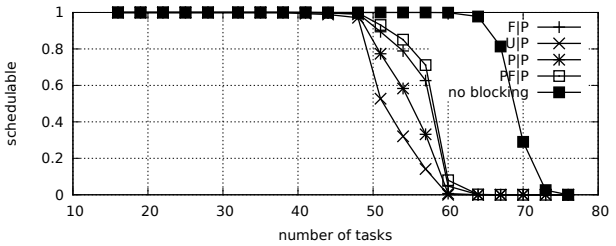

Fig. 1717. Schedulability under preemptable spin locks for $m = 16$, $U = 0.2n$, 16 resources, $rsf = 0.1$, $N^{max} = 5$, and medium critical sections. The schedulability of the considered non-preemptable lock types in this configuration is shown in Fig. 1707.

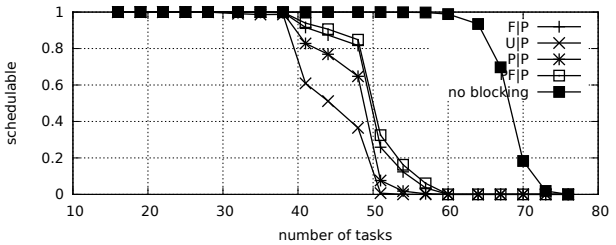

Fig. 1718. Schedulability under preemptable spin locks for $m = 16$, $U = 0.2n$, 16 resources, $rsf = 0.1$, $N^{max} = 10$, and medium critical sections. The schedulability of the considered non-preemptable lock types in this configuration is shown in Fig. 1708.

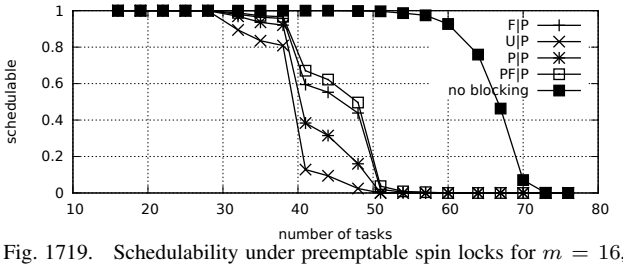

Fig. 1719. Schedulability under preemptable spin locks for $m = 16$, $U = 0.2n$, 16 resources, $rsf = 0.1$, $N^{max} = 15$, and medium critical sections. The schedulability of the considered non-preemptable lock types in this configuration is shown in Fig. 1709.

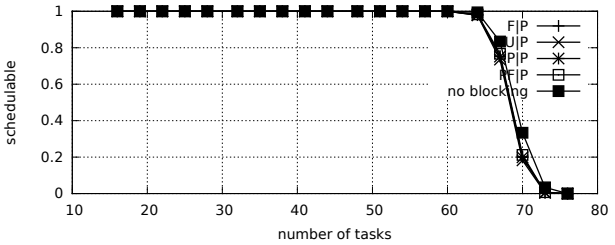

Fig. 1720. Schedulability under preemptable spin locks for $m = 16$, $U = 0.2n$, 16 resources, $rsf = 0.1$, $N^{max} = 1$, and short critical sections. The schedulability of the considered non-preemptable lock types in this configuration is shown in Fig. 1710.

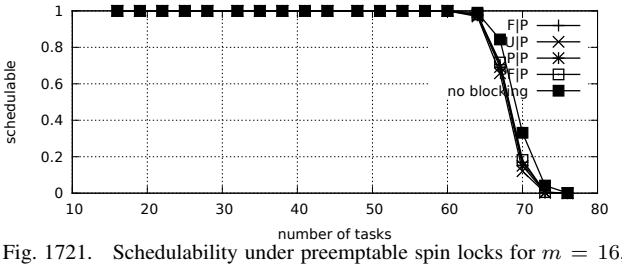

Fig. 1721. Schedulability under preemptable spin locks for $m = 16$, $U = 0.2n$, 16 resources, $rsf = 0.1$, $N^{max} = 2$, and short critical sections. The schedulability of the considered non-preemptable lock types in this configuration is shown in Fig. 1711.

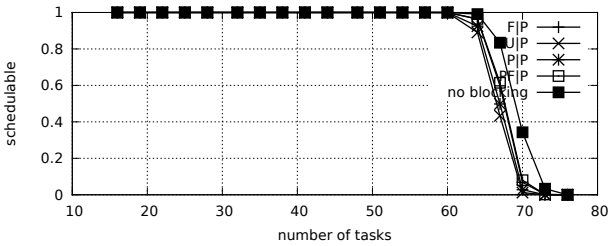

Fig. 1722. Schedulability under preemptable spin locks for $m = 16$, $U = 0.2n$, 16 resources, $rsf = 0.1$, $N^{max} = 5$, and short critical sections. The schedulability of the considered non-preemptable lock types in this configuration is shown in Fig. 1712.

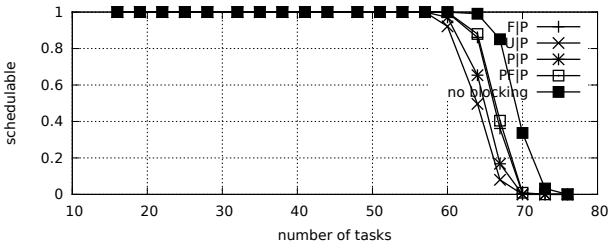

Fig. 1723. Schedulability under preemptable spin locks for $m = 16$, $U = 0.2n$, 16 resources, $rsf = 0.1$, $N^{max} = 10$, and short critical sections. The schedulability of the considered non-preemptable lock types in this configuration is shown in Fig. 1713.

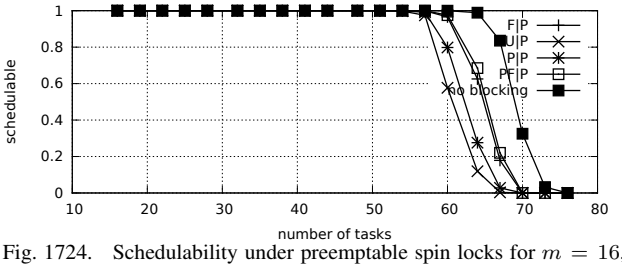

Fig. 1724. Schedulability under preemptable spin locks for $m = 16$, $U = 0.2n$, 16 resources, $rsf = 0.1$, $N^{max} = 15$, and short critical sections. The schedulability of the considered non-preemptable lock types in this configuration is shown in Fig. 1714.

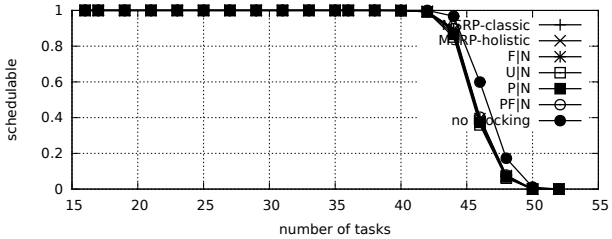

Fig. 1725. Schedulability under non-preemptable spin locks for $m = 16$, $U = 0.3n$, 16 resources, $rsf = 0.1$, $N^{max} = 1$, and medium critical sections. The schedulability of the considered preemptable lock types in this configuration is shown in Fig. 1735.

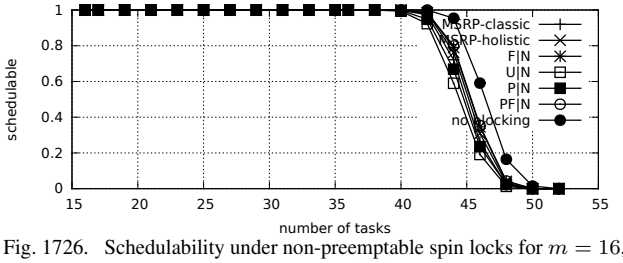

Fig. 1726. Schedulability under non-preemptable spin locks for $m = 16$, $U = 0.3n$, 16 resources, $rsf = 0.1$, $N^{max} = 2$, and medium critical sections. The schedulability of the considered preemptable lock types in this configuration is shown in Fig. 1736.

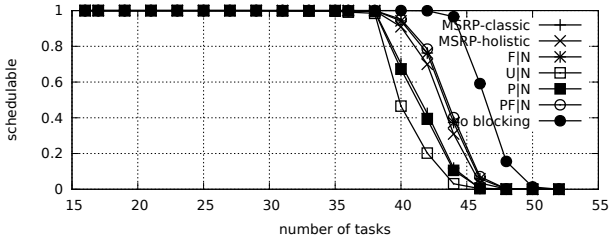

Fig. 1727. Schedulability under non-preemptable spin locks for $m = 16$, $U = 0.3n$, 16 resources, $rsf = 0.1$, $N^{max} = 5$, and medium critical sections. The schedulability of the considered preemptable lock types in this configuration is shown in Fig. 1737.

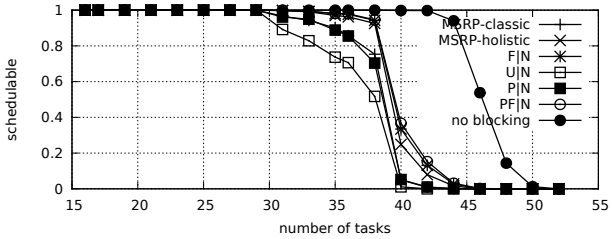

Fig. 1728. Schedulability under non-preemptable spin locks for $m = 16$, $U = 0.3n$, 16 resources, $rsf = 0.1$, $N^{max} = 10$, and medium critical sections. The schedulability of the considered preemptable lock types in this configuration is shown in Fig. 1738.

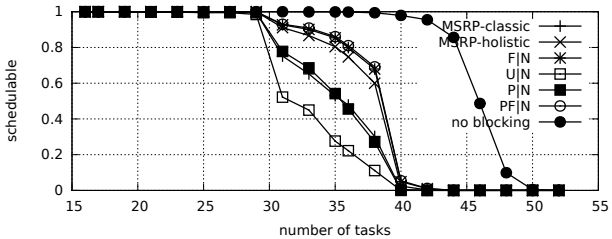

Fig. 1729. Schedulability under non-preemptable spin locks for $m = 16$, $U = 0.3n$, 16 resources, $rsf = 0.1$, $N^{max} = 15$, and medium critical sections. The schedulability of the considered preemptable lock types in this configuration is shown in Fig. 1739.

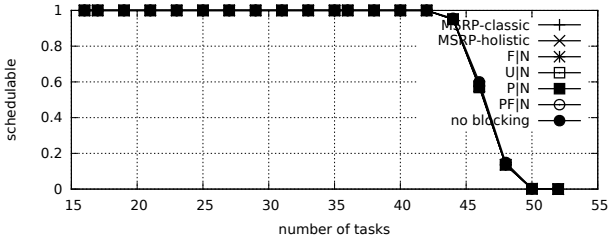

Fig. 1730. Schedulability under non-preemptable spin locks for $m = 16$, $U = 0.3n$, 16 resources, $rsf = 0.1$, $N^{max} = 1$, and short critical sections. The schedulability of the considered preemptable lock types in this configuration is shown in Fig. 1740.

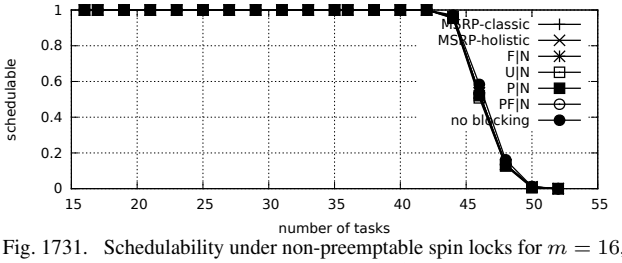

Fig. 1731. Schedulability under non-preemptable spin locks for $m = 16$, $U = 0.3n$, 16 resources, $rsf = 0.1$, $N^{max} = 2$, and short critical sections. The schedulability of the considered preemptable lock types in this configuration is shown in Fig. 1741.

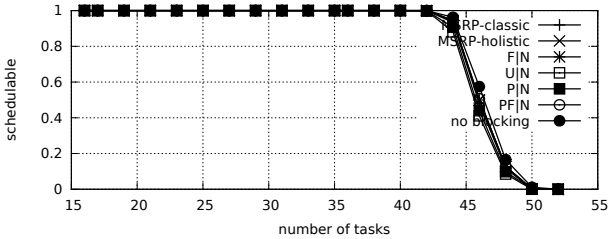

Fig. 1732. Schedulability under non-preemptable spin locks for $m = 16$, $U = 0.3n$, 16 resources, $rsf = 0.1$, $N^{max} = 5$, and short critical sections. The schedulability of the considered preemptable lock types in this configuration is shown in Fig. 1742.

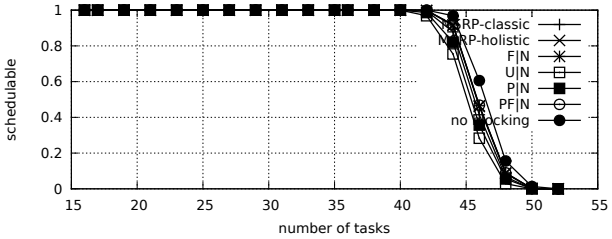

Fig. 1733. Schedulability under non-preemptable spin locks for $m = 16$, $U = 0.3n$, 16 resources, $rsf = 0.1$, $N^{max} = 10$, and short critical sections. The schedulability of the considered preemptable lock types in this configuration is shown in Fig. 1743.

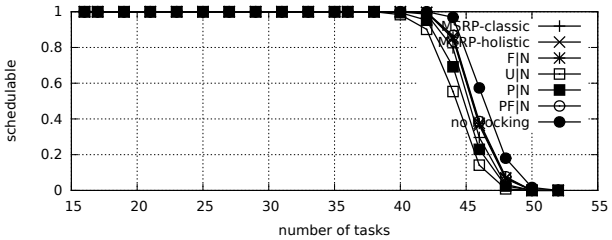

Fig. 1734. Schedulability under non-preemptable spin locks for $m = 16$, $U = 0.3n$, 16 resources, $rsf = 0.1$, $N^{max} = 15$, and short critical sections. The schedulability of the considered preemptable lock types in this configuration is shown in Fig. 1744.

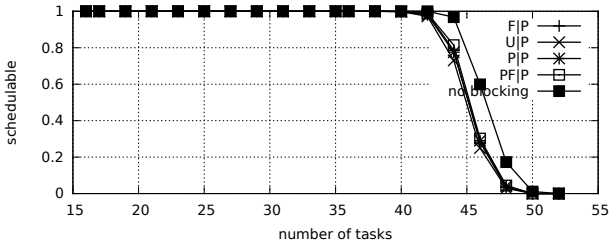

Fig. 1735. Schedulability under preemptable spin locks for $m = 16$, $U = 0.3n$, 16 resources, $rsf = 0.1$, $N^{max} = 1$, and medium critical sections. The schedulability of the considered non-preemptable lock types in this configuration is shown in Fig. 1725.

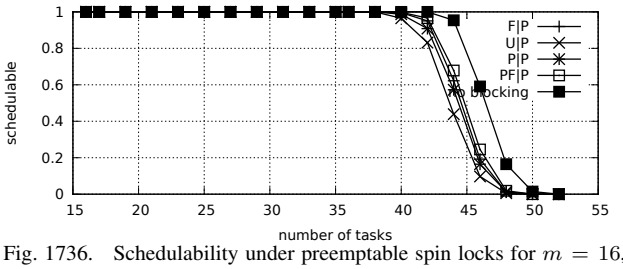

Fig. 1736. Schedulability under preemptable spin locks for $m = 16$, $U = 0.3n$, 16 resources, $rsf = 0.1$, $N^{max} = 2$, and medium critical sections. The schedulability of the considered non-preemptable lock types in this configuration is shown in Fig. 1726.

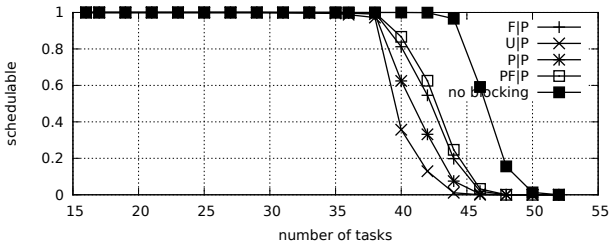

Fig. 1737. Schedulability under preemptable spin locks for $m = 16$, $U = 0.3n$, 16 resources, $rsf = 0.1$, $N^{max} = 5$, and medium critical sections. The schedulability of the considered non-preemptable lock types in this configuration is shown in Fig. 1727.

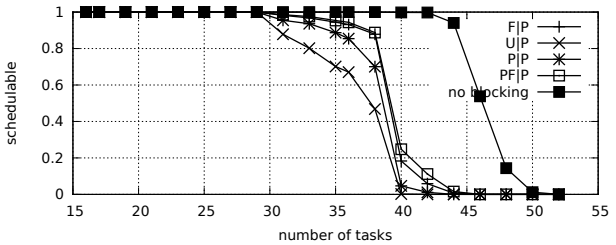

Fig. 1738. Schedulability under preemptable spin locks for $m = 16$, $U = 0.3n$, 16 resources, $rsf = 0.1$, $N^{max} = 10$, and medium critical sections. The schedulability of the considered non-preemptable lock types in this configuration is shown in Fig. 1728.

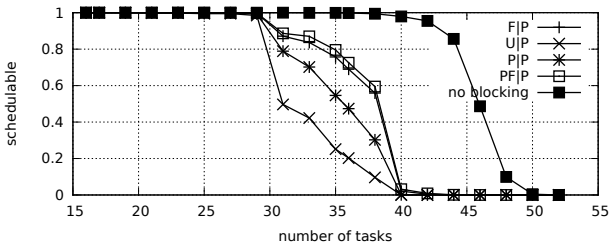

Fig. 1739. Schedulability under preemptable spin locks for $m = 16$, $U = 0.3n$, 16 resources, $rsf = 0.1$, $N^{max} = 15$, and medium critical sections. The schedulability of the considered non-preemptable lock types in this configuration is shown in Fig. 1729.

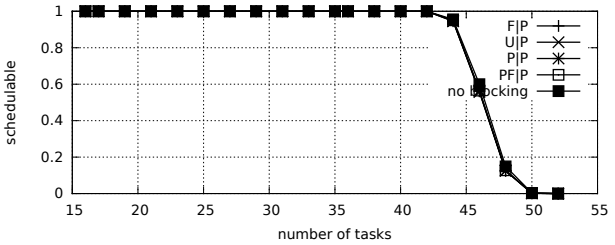

Fig. 1740. Schedulability under preemptable spin locks for $m = 16$, $U = 0.3n$, 16 resources, $rsf = 0.1$, $N^{max} = 1$, and short critical sections. The schedulability of the considered non-preemptable lock types in this configuration is shown in Fig. 1730.

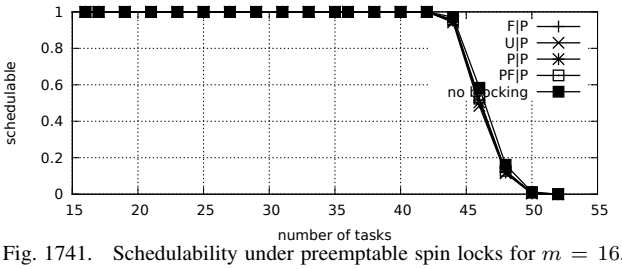

Fig. 1741. Schedulability under preemptable spin locks for $m = 16$, $U = 0.3n$, 16 resources, $rsf = 0.1$, $N^{max} = 2$, and short critical sections. The schedulability of the considered non-preemptable lock types in this configuration is shown in Fig. 1731.

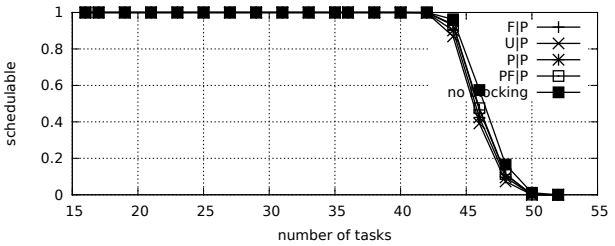

Fig. 1742. Schedulability under preemptable spin locks for $m = 16$, $U = 0.3n$, 16 resources, $rsf = 0.1$, $N^{max} = 5$, and short critical sections. The schedulability of the considered non-preemptable lock types in this configuration is shown in Fig. 1732.

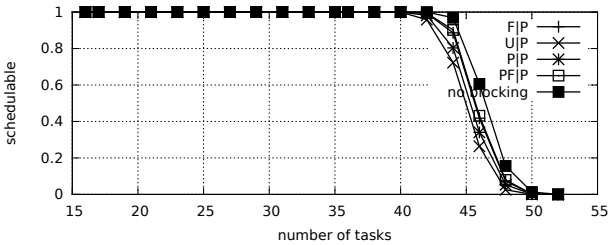

Fig. 1743. Schedulability under preemptable spin locks for $m = 16$, $U = 0.3n$, 16 resources, $rsf = 0.1$, $N^{max} = 10$, and short critical sections. The schedulability of the considered non-preemptable lock types in this configuration is shown in Fig. 1733.

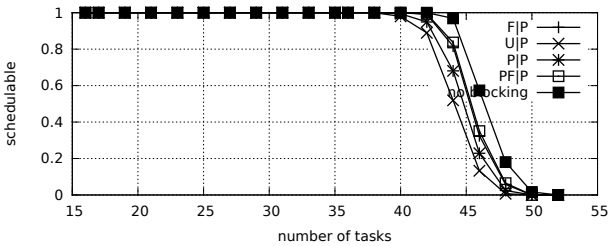

Fig. 1744. Schedulability under preemptable spin locks for $m = 16$, $U = 0.3n$, 16 resources, $rsf = 0.1$, $N^{max} = 15$, and short critical sections. The schedulability of the considered non-preemptable lock types in this configuration is shown in Fig. 1734.

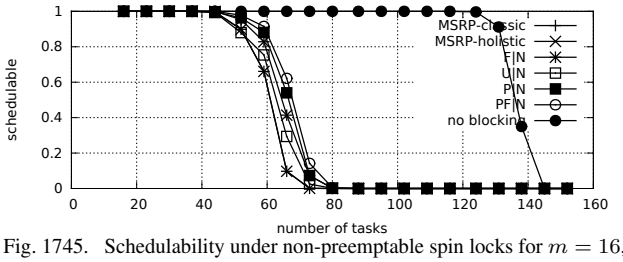

Fig. 1745. Schedulability under non-preemptable spin locks for $m = 16$, $U = 0.1n$, 16 resources, $rsf = 0.25$, $N^{max} = 1$, and medium critical sections. The schedulability of the considered preemptable lock types in this configuration is shown in Fig. 1755.

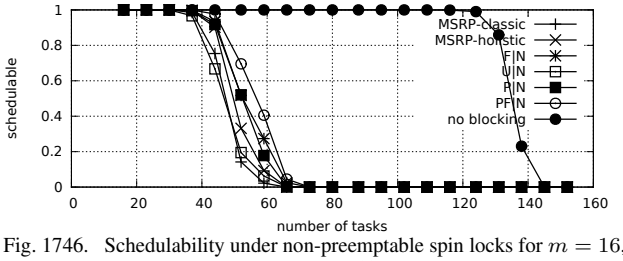

Fig. 1746. Schedulability under non-preemptable spin locks for $m = 16$, $U = 0.1n$, 16 resources, $rsf = 0.25$, $N^{max} = 2$, and medium critical sections. The schedulability of the considered preemptable lock types in this configuration is shown in Fig. 1756.

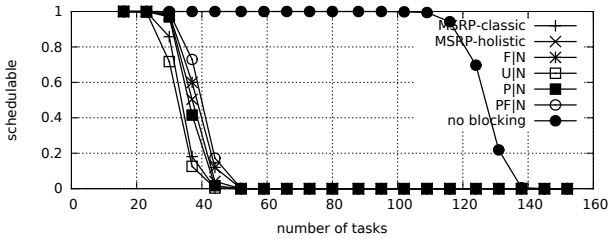

Fig. 1747. Schedulability under non-preemptable spin locks for $m = 16$, $U = 0.1n$, 16 resources, $rsf = 0.25$, $N^{max} = 5$, and medium critical sections. The schedulability of the considered preemptable lock types in this configuration is shown in Fig. 1757.

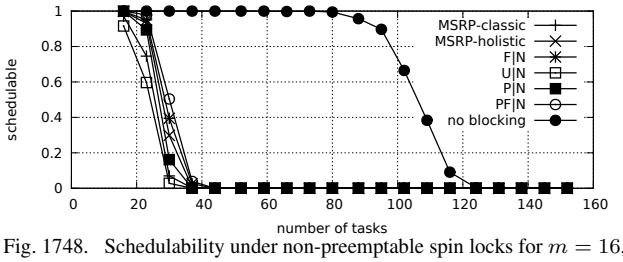

Fig. 1748. Schedulability under non-preemptable spin locks for $m = 16$, $U = 0.1n$, 16 resources, $rsf = 0.25$, $N^{max} = 10$, and medium critical sections. The schedulability of the considered preemptable lock types in this configuration is shown in Fig. 1758.

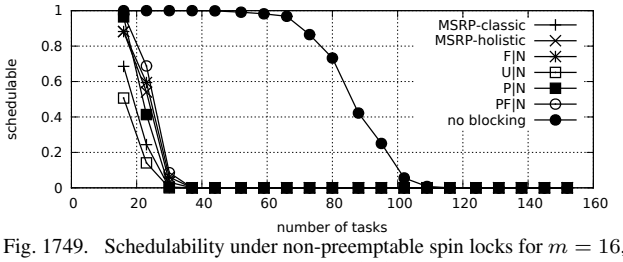

Fig. 1749. Schedulability under non-preemptable spin locks for $m = 16$, $U = 0.1n$, 16 resources, $rsf = 0.25$, $N^{max} = 15$, and medium critical sections. The schedulability of the considered preemptable lock types in this configuration is shown in Fig. 1759.

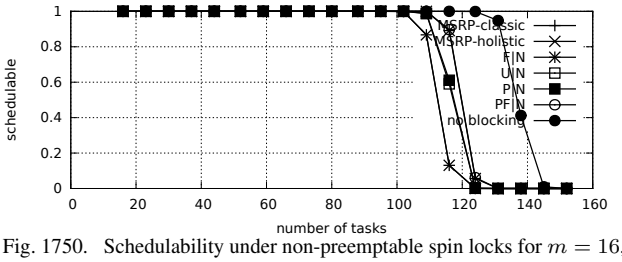

Fig. 1750. Schedulability under non-preemptable spin locks for $m = 16$, $U = 0.1n$, 16 resources, $rsf = 0.25$, $N^{max} = 1$, and short critical sections. The schedulability of the considered preemptable lock types in this configuration is shown in Fig. 1760.

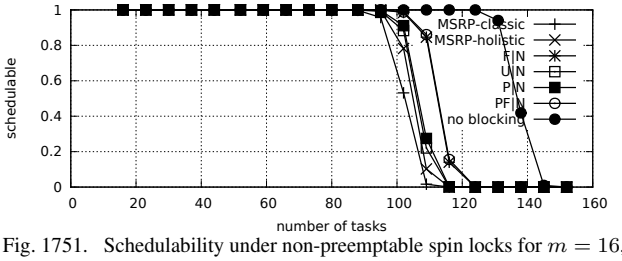

Fig. 1751. Schedulability under non-preemptable spin locks for $m = 16$, $U = 0.1n$, 16 resources, $rsf = 0.25$, $N^{max} = 2$, and short critical sections. The schedulability of the considered preemptable lock types in this configuration is shown in Fig. 1761.

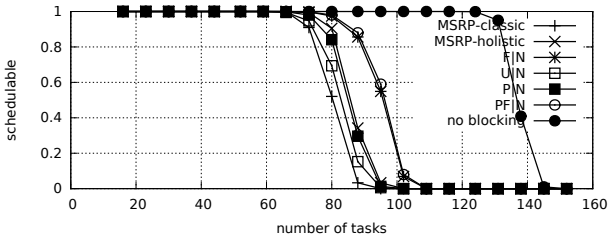

Fig. 1752. Schedulability under non-preemptable spin locks for $m = 16$, $U = 0.1n$, 16 resources, $rsf = 0.25$, $N^{max} = 5$, and short critical sections. The schedulability of the considered preemptable lock types in this configuration is shown in Fig. 1762.

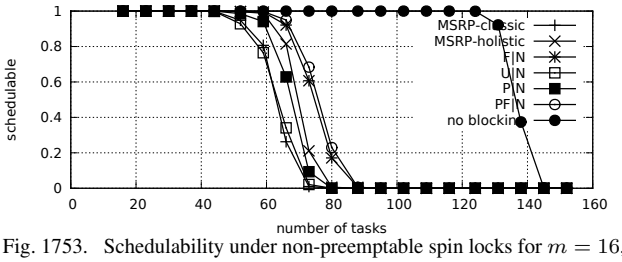

Fig. 1753. Schedulability under non-preemptable spin locks for $m = 16$, $U = 0.1n$, 16 resources, $rsf = 0.25$, $N^{max} = 10$, and short critical sections. The schedulability of the considered preemptable lock types in this configuration is shown in Fig. 1763.

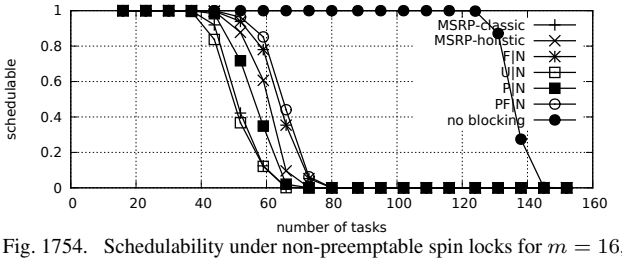

Fig. 1754. Schedulability under non-preemptable spin locks for $m = 16$, $U = 0.1n$, 16 resources, $rsf = 0.25$, $N^{max} = 15$, and short critical sections. The schedulability of the considered preemptable lock types in this configuration is shown in Fig. 1764.

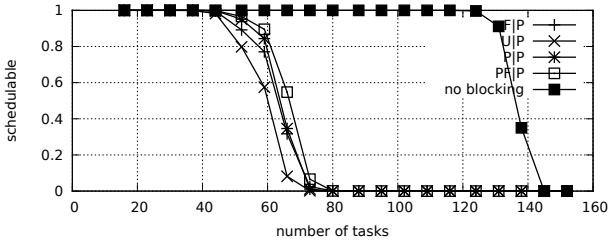

Fig. 1755. Schedulability under preemptable spin locks for $m = 16$, $U = 0.1n$, 16 resources, $rsf = 0.25$, $N^{max} = 1$, and medium critical sections. The schedulability of the considered non-preemptable lock types in this configuration is shown in Fig. 1745.

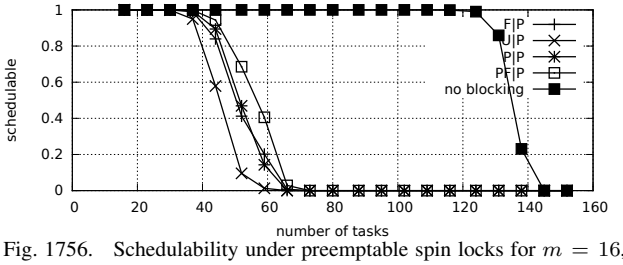

Fig. 1756. Schedulability under preemptable spin locks for $m = 16$, $U = 0.1n$, 16 resources, $rsf = 0.25$, $N^{max} = 2$, and medium critical sections. The schedulability of the considered non-preemptable lock types in this configuration is shown in Fig. 1746.

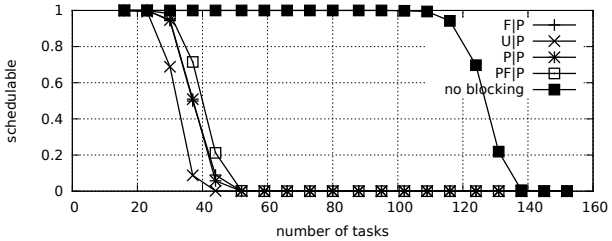

Fig. 1757. Schedulability under preemptable spin locks for $m = 16$, $U = 0.1n$, 16 resources, $rsf = 0.25$, $N^{max} = 5$, and medium critical sections. The schedulability of the considered non-preemptable lock types in this configuration is shown in Fig. 1747.

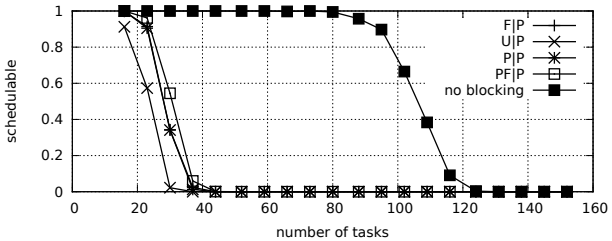

Fig. 1758. Schedulability under preemptable spin locks for $m = 16$, $U = 0.1n$, 16 resources, $rsf = 0.25$, $N^{max} = 10$, and medium critical sections. The schedulability of the considered non-preemptable lock types in this configuration is shown in Fig. 1748.

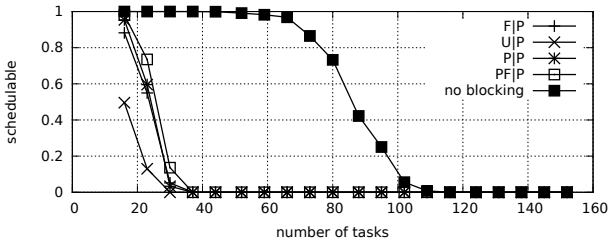

Fig. 1759. Schedulability under preemptable spin locks for $m = 16$, $U = 0.1n$, 16 resources, $rsf = 0.25$, $N^{max} = 15$, and medium critical sections. The schedulability of the considered non-preemptable lock types in this configuration is shown in Fig. 1749.

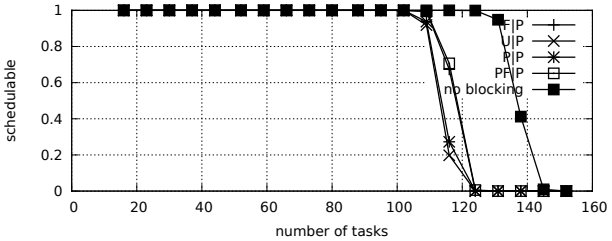

Fig. 1760. Schedulability under preemptable spin locks for $m = 16$, $U = 0.1n$, 16 resources, $rsf = 0.25$, $N^{max} = 1$, and short critical sections. The schedulability of the considered non-preemptable lock types in this configuration is shown in Fig. 1750.

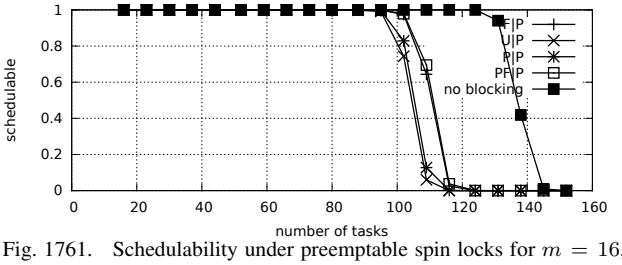

Fig. 1761. Schedulability under preemptable spin locks for $m = 16$, $U = 0.1n$, 16 resources, $rsf = 0.25$, $N^{max} = 2$, and short critical sections. The schedulability of the considered non-preemptable lock types in this configuration is shown in Fig. 1751.

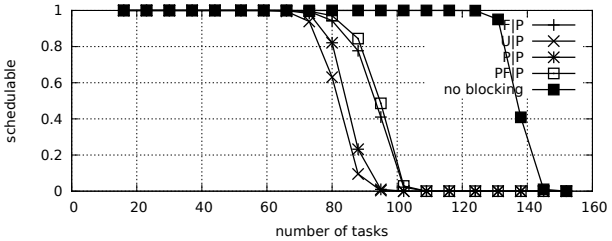

Fig. 1762. Schedulability under preemptable spin locks for $m = 16$, $U = 0.1n$, 16 resources, $rsf = 0.25$, $N^{max} = 5$, and short critical sections. The schedulability of the considered non-preemptable lock types in this configuration is shown in Fig. 1752.

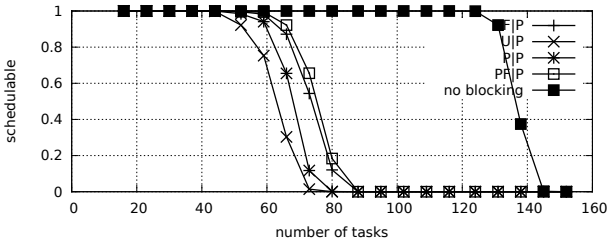

Fig. 1763. Schedulability under preemptable spin locks for $m = 16$, $U = 0.1n$, 16 resources, $rsf = 0.25$, $N^{max} = 10$, and short critical sections. The schedulability of the considered non-preemptable lock types in this configuration is shown in Fig. 1753.

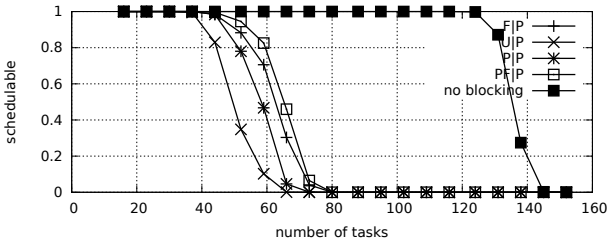

Fig. 1764. Schedulability under preemptable spin locks for $m = 16$, $U = 0.1n$, 16 resources, $rsf = 0.25$, $N^{max} = 15$, and short critical sections. The schedulability of the considered non-preemptable lock types in this configuration is shown in Fig. 1754.

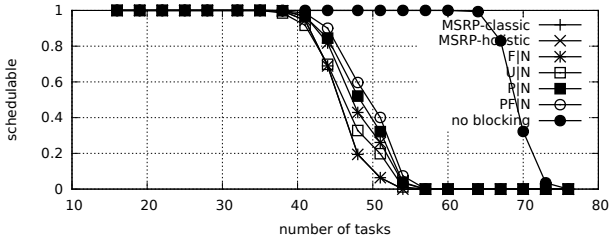

Fig. 1765. Schedulability under non-preemptable spin locks for $m = 16$, $U = 0.2n$, 16 resources, $rsf = 0.25$, $N^{max} = 1$, and medium critical sections. The schedulability of the considered preemptable lock types in this configuration is shown in Fig. 1775.

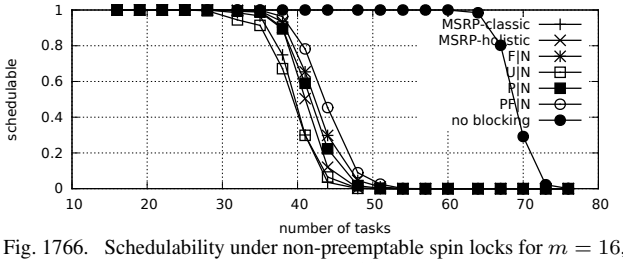

Fig. 1766. Schedulability under non-preemptable spin locks for $m = 16$, $U = 0.2n$, 16 resources, $rsf = 0.25$, $N^{max} = 2$, and medium critical sections. The schedulability of the considered preemptable lock types in this configuration is shown in Fig. 1776.

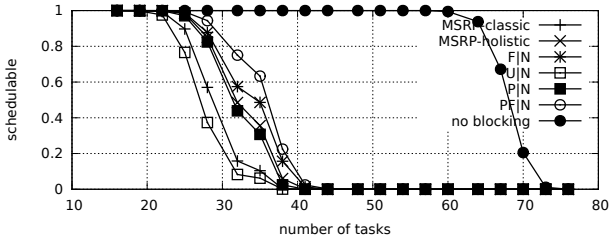

Fig. 1767. Schedulability under non-preemptable spin locks for $m = 16$, $U = 0.2n$, 16 resources, $rsf = 0.25$, $N^{max} = 5$, and medium critical sections. The schedulability of the considered preemptable lock types in this configuration is shown in Fig. 1777.

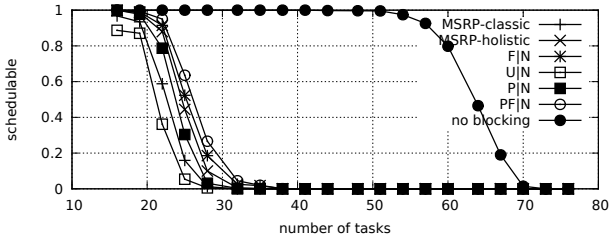

Fig. 1768. Schedulability under non-preemptable spin locks for $m = 16$, $U = 0.2n$, 16 resources, $rsf = 0.25$, $N^{max} = 10$, and medium critical sections. The schedulability of the considered preemptable lock types in this configuration is shown in Fig. 1778.

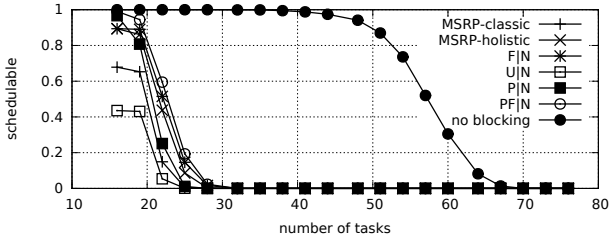

Fig. 1769. Schedulability under non-preemptable spin locks for $m = 16$, $U = 0.2n$, 16 resources, $rsf = 0.25$, $N^{max} = 15$, and medium critical sections. The schedulability of the considered preemptable lock types in this configuration is shown in Fig. 1779.

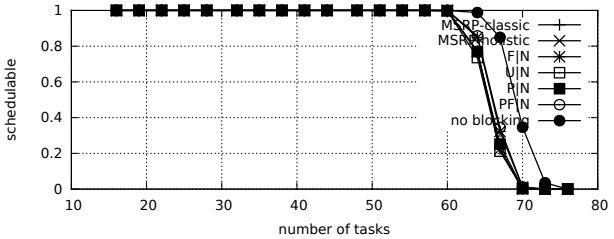

Fig. 1770. Schedulability under non-preemptable spin locks for $m = 16$, $U = 0.2n$, 16 resources, $rsf = 0.25$, $N^{max} = 1$, and short critical sections. The schedulability of the considered preemptable lock types in this configuration is shown in Fig. 1780.

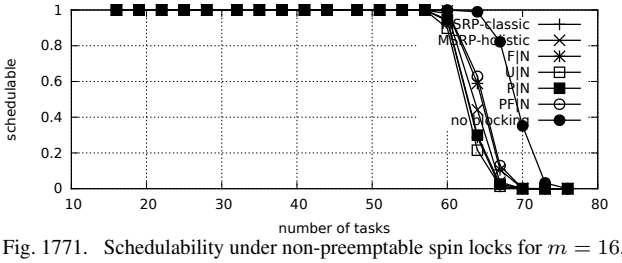

Fig. 1771. Schedulability under non-preemptable spin locks for $m = 16$, $U = 0.2n$, 16 resources, $rsf = 0.25$, $N^{max} = 2$, and short critical sections. The schedulability of the considered preemptable lock types in this configuration is shown in Fig. 1781.

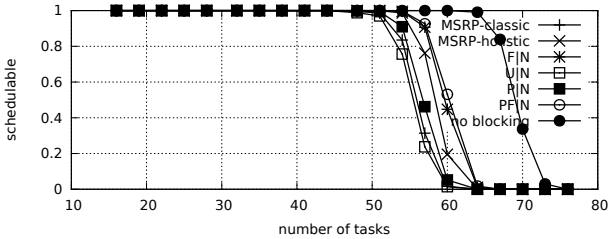

Fig. 1772. Schedulability under non-preemptable spin locks for $m = 16$, $U = 0.2n$, 16 resources, $rsf = 0.25$, $N^{max} = 5$, and short critical sections. The schedulability of the considered preemptable lock types in this configuration is shown in Fig. 1782.

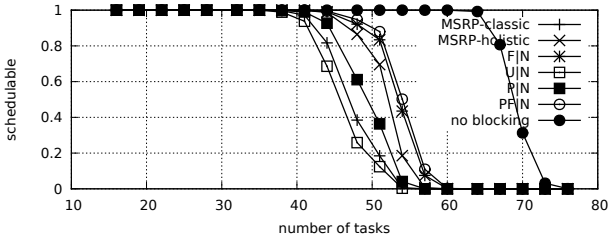

Fig. 1773. Schedulability under non-preemptable spin locks for $m = 16$, $U = 0.2n$, 16 resources, $rsf = 0.25$, $N^{max} = 10$, and short critical sections. The schedulability of the considered preemptable lock types in this configuration is shown in Fig. 1783.

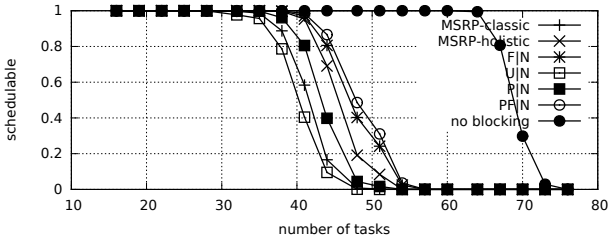

Fig. 1774. Schedulability under non-preemptable spin locks for $m = 16$, $U = 0.2n$, 16 resources, $rsf = 0.25$, $N^{max} = 15$, and short critical sections. The schedulability of the considered preemptable lock types in this configuration is shown in Fig. 1784.

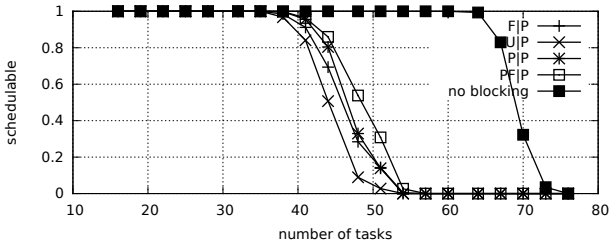

Fig. 1775. Schedulability under preemptable spin locks for $m = 16$, $U = 0.2n$, 16 resources, $rsf = 0.25$, $N^{max} = 1$, and medium critical sections. The schedulability of the considered non-preemptable lock types in this configuration is shown in Fig. 1765.

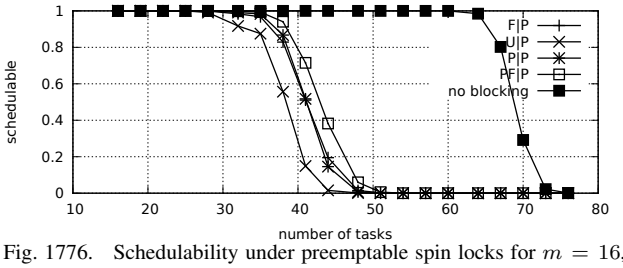

Fig. 1776. Schedulability under preemptable spin locks for $m = 16$, $U = 0.2n$, 16 resources, $rsf = 0.25$, $N^{max} = 2$, and medium critical sections. The schedulability of the considered non-preemptable lock types in this configuration is shown in Fig. 1766.

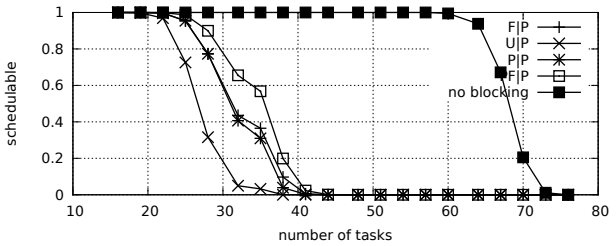

Fig. 1777. Schedulability under preemptable spin locks for $m = 16$, $U = 0.2n$, 16 resources, $rsf = 0.25$, $N^{max} = 5$, and medium critical sections. The schedulability of the considered non-preemptable lock types in this configuration is shown in Fig. 1767.

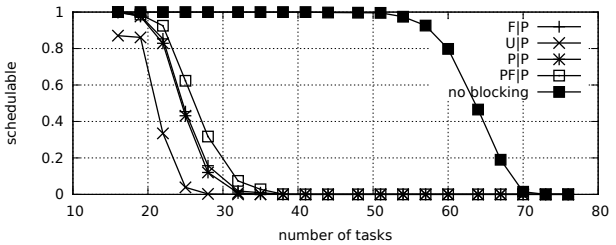

Fig. 1778. Schedulability under preemptable spin locks for $m = 16$, $U = 0.2n$, 16 resources, $rsf = 0.25$, $N^{max} = 10$, and medium critical sections. The schedulability of the considered non-preemptable lock types in this configuration is shown in Fig. 1768.

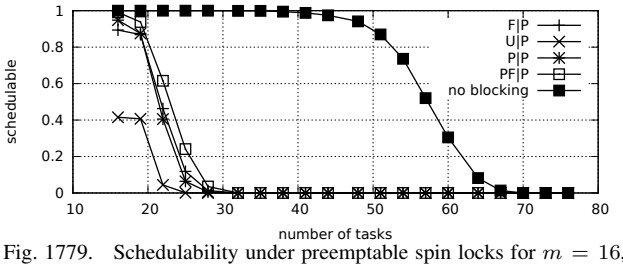

Fig. 1779. Schedulability under preemptable spin locks for $m = 16$, $U = 0.2n$, 16 resources, $rsf = 0.25$, $N^{max} = 15$, and medium critical sections. The schedulability of the considered non-preemptable lock types in this configuration is shown in Fig. 1769.

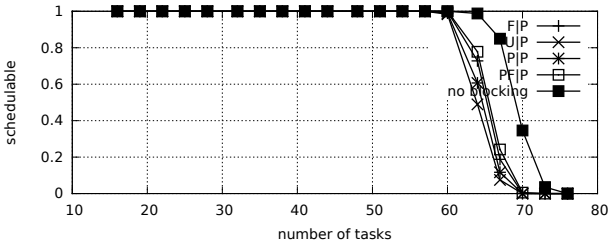

Fig. 1780. Schedulability under preemptable spin locks for $m = 16$, $U = 0.2n$, 16 resources, $rsf = 0.25$, $N^{max} = 1$, and short critical sections. The schedulability of the considered non-preemptable lock types in this configuration is shown in Fig. 1770.

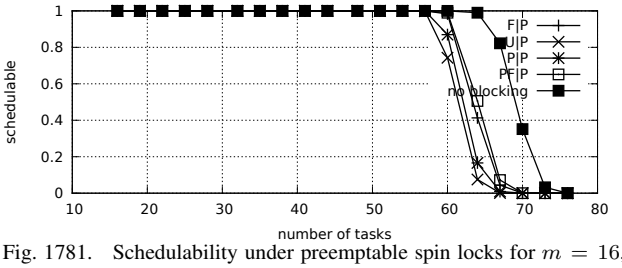

Fig. 1781. Schedulability under preemptable spin locks for $m = 16$, $U = 0.2n$, 16 resources, $rsf = 0.25$, $N^{max} = 2$, and short critical sections. The schedulability of the considered non-preemptable lock types in this configuration is shown in Fig. 1771.

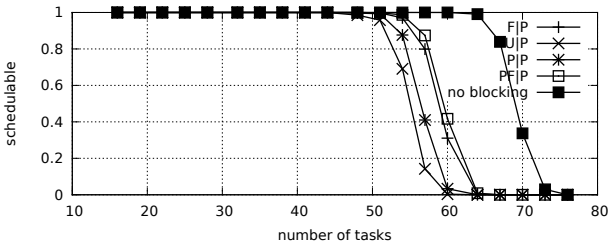

Fig. 1782. Schedulability under preemptable spin locks for $m = 16$, $U = 0.2n$, 16 resources, $rsf = 0.25$, $N^{max} = 5$, and short critical sections. The schedulability of the considered non-preemptable lock types in this configuration is shown in Fig. 1772.

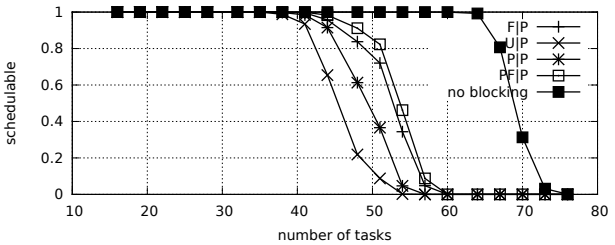

Fig. 1783. Schedulability under preemptable spin locks for $m = 16$, $U = 0.2n$, 16 resources, $rsf = 0.25$, $N^{max} = 10$, and short critical sections. The schedulability of the considered non-preemptable lock types in this configuration is shown in Fig. 1773.

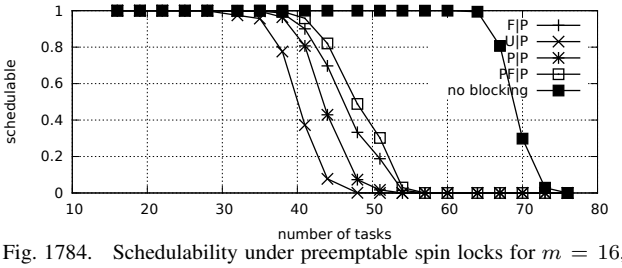

Fig. 1784. Schedulability under preemptable spin locks for $m = 16$, $U = 0.2n$, 16 resources, $rsf = 0.25$, $N^{max} = 15$, and short critical sections. The schedulability of the considered non-preemptable lock types in this configuration is shown in Fig. 1774.

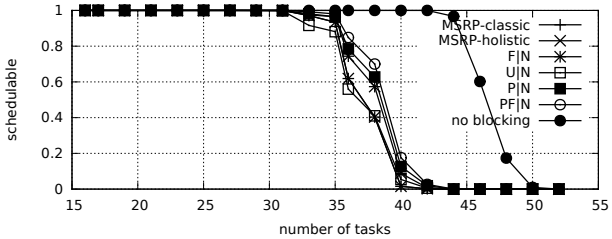

Fig. 1785. Schedulability under non-preemptable spin locks for $m = 16$, $U = 0.3n$, 16 resources, $rsf = 0.25$, $N^{max} = 1$, and medium critical sections. The schedulability of the considered preemptable lock types in this configuration is shown in Fig. 1795.

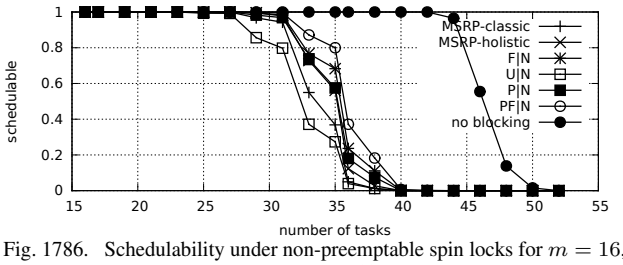

Fig. 1786. Schedulability under non-preemptable spin locks for $m = 16$, $U = 0.3n$, 16 resources, $rsf = 0.25$, $N^{max} = 2$, and medium critical sections. The schedulability of the considered preemptable lock types in this configuration is shown in Fig. 1796.

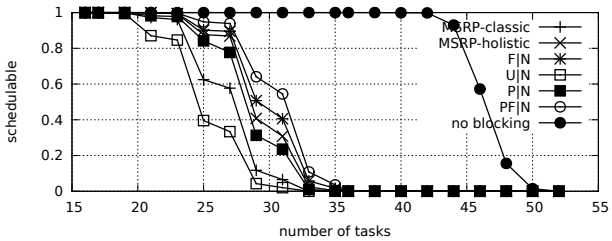

Fig. 1787. Schedulability under non-preemptable spin locks for $m = 16$, $U = 0.3n$, 16 resources, $rsf = 0.25$, $N^{max} = 5$, and medium critical sections. The schedulability of the considered preemptable lock types in this configuration is shown in Fig. 1797.

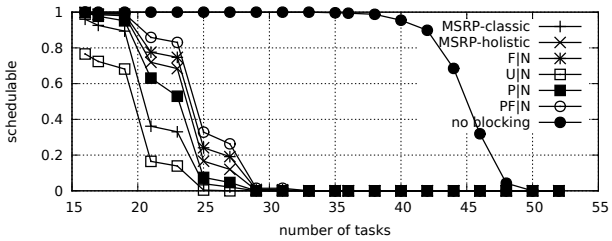

Fig. 1788. Schedulability under non-preemptable spin locks for $m = 16$, $U = 0.3n$, 16 resources, $rsf = 0.25$, $N^{max} = 10$, and medium critical sections. The schedulability of the considered preemptable lock types in this configuration is shown in Fig. 1798.

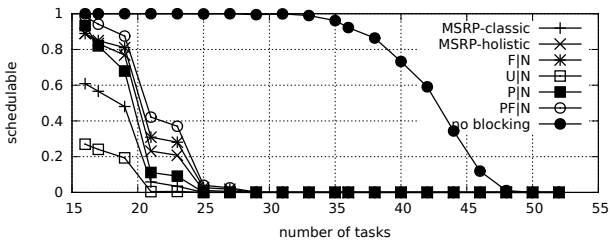

Fig. 1789. Schedulability under non-preemptable spin locks for $m = 16$, $U = 0.3n$, 16 resources, $rsf = 0.25$, $N^{max} = 15$, and medium critical sections. The schedulability of the considered preemptable lock types in this configuration is shown in Fig. 1799.

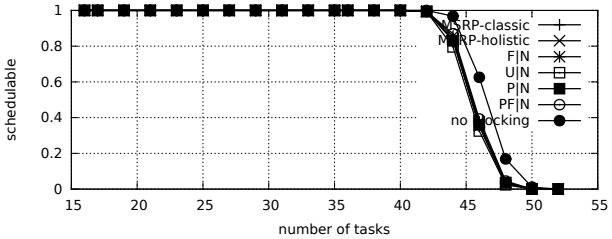

Fig. 1790. Schedulability under non-preemptable spin locks for $m = 16$, $U = 0.3n$, 16 resources, $rsf = 0.25$, $N^{max} = 1$, and short critical sections. The schedulability of the considered preemptable lock types in this configuration is shown in Fig. 1800.

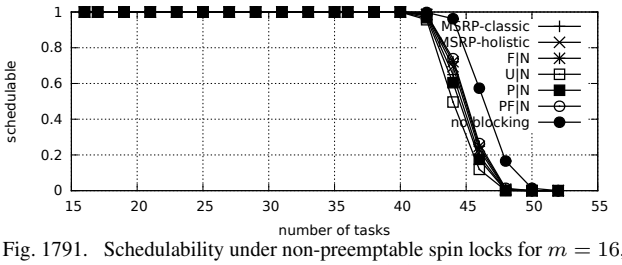

Fig. 1791. Schedulability under non-preemptable spin locks for $m = 16$, $U = 0.3n$, 16 resources, $rsf = 0.25$, $N^{max} = 2$, and short critical sections. The schedulability of the considered preemptable lock types in this configuration is shown in Fig. 1801.

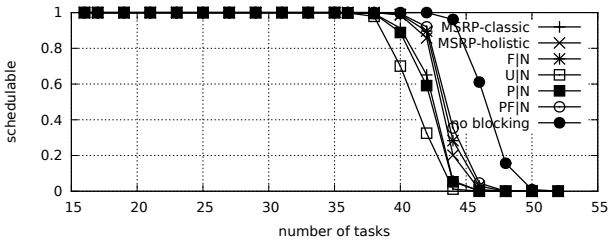

Fig. 1792. Schedulability under non-preemptable spin locks for $m = 16$, $U = 0.3n$, 16 resources, $rsf = 0.25$, $N^{max} = 5$, and short critical sections. The schedulability of the considered preemptable lock types in this configuration is shown in Fig. 1802.

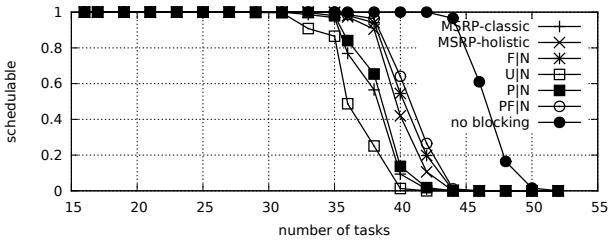

Fig. 1793. Schedulability under non-preemptable spin locks for $m = 16$, $U = 0.3n$, 16 resources, $rsf = 0.25$, $N^{max} = 10$, and short critical sections. The schedulability of the considered preemptable lock types in this configuration is shown in Fig. 1803.

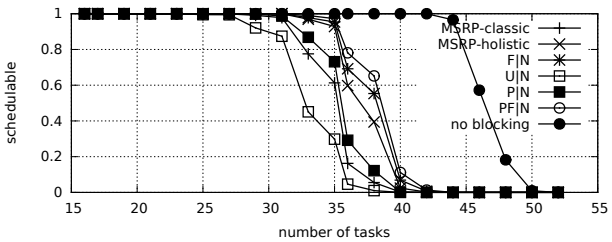

Fig. 1794. Schedulability under non-preemptable spin locks for $m = 16$, $U = 0.3n$, 16 resources, $rsf = 0.25$, $N^{max} = 15$, and short critical sections. The schedulability of the considered preemptable lock types in this configuration is shown in Fig. 1804.

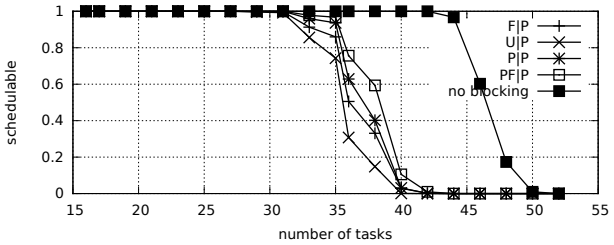

Fig. 1795. Schedulability under preemptable spin locks for $m = 16$, $U = 0.3n$, 16 resources, $rsf = 0.25$, $N^{max} = 1$, and medium critical sections. The schedulability of the considered non-preemptable lock types in this configuration is shown in Fig. 1785.

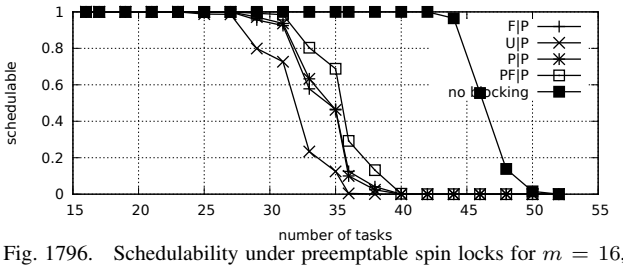

Fig. 1796. Schedulability under preemptable spin locks for $m = 16$, $U = 0.3n$, 16 resources, $rsf = 0.25$, $N^{max} = 2$, and medium critical sections. The schedulability of the considered non-preemptable lock types in this configuration is shown in Fig. 1786.

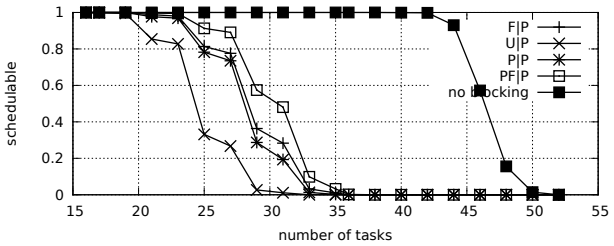

Fig. 1797. Schedulability under preemptable spin locks for $m = 16$, $U = 0.3n$, 16 resources, $rsf = 0.25$, $N^{max} = 5$, and medium critical sections. The schedulability of the considered non-preemptable lock types in this configuration is shown in Fig. 1787.

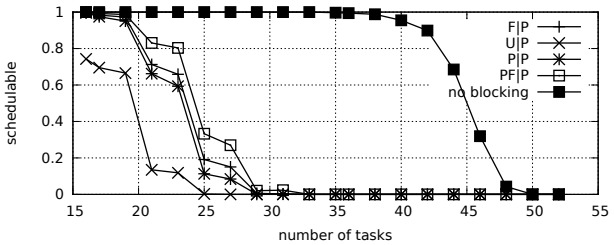

Fig. 1798. Schedulability under preemptable spin locks for $m = 16$, $U = 0.3n$, 16 resources, $rsf = 0.25$, $N^{max} = 10$, and medium critical sections. The schedulability of the considered non-preemptable lock types in this configuration is shown in Fig. 1788.

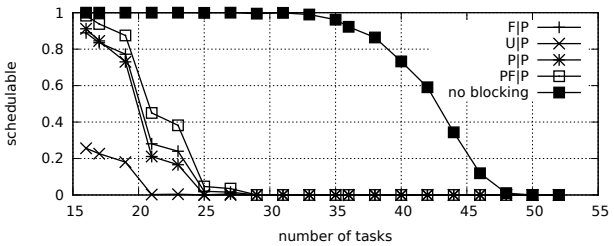

Fig. 1799. Schedulability under preemptable spin locks for $m = 16$, $U = 0.3n$, 16 resources, $rsf = 0.25$, $N^{max} = 15$, and medium critical sections. The schedulability of the considered non-preemptable lock types in this configuration is shown in Fig. 1789.

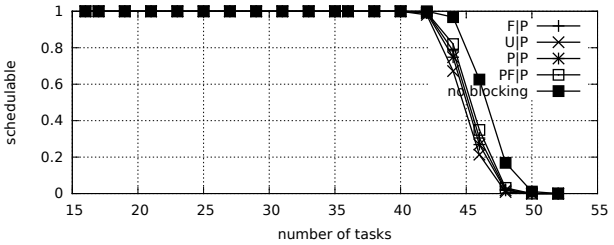

Fig. 1800. Schedulability under preemptable spin locks for $m = 16$, $U = 0.3n$, 16 resources, $rsf = 0.25$, $N^{max} = 1$, and short critical sections. The schedulability of the considered non-preemptable lock types in this configuration is shown in Fig. 1790.

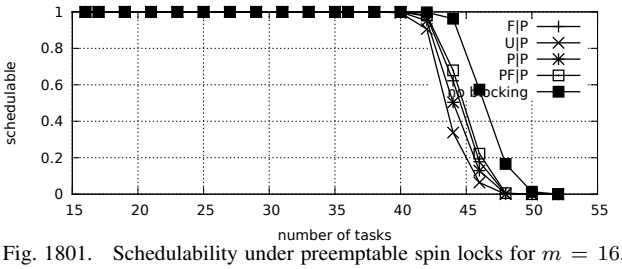

Fig. 1801. Schedulability under preemptable spin locks for $m = 16$, $U = 0.3n$, 16 resources, $rsf = 0.25$, $N^{max} = 2$, and short critical sections. The schedulability of the considered non-preemptable lock types in this configuration is shown in Fig. 1791.

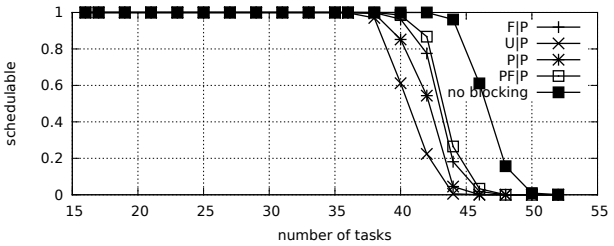

Fig. 1802. Schedulability under preemptable spin locks for $m = 16$, $U = 0.3n$, 16 resources, $rsf = 0.25$, $N^{max} = 5$, and short critical sections. The schedulability of the considered non-preemptable lock types in this configuration is shown in Fig. 1792.

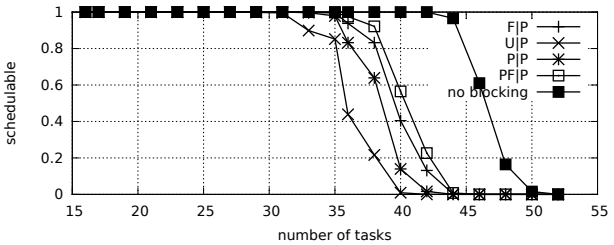

Fig. 1803. Schedulability under preemptable spin locks for $m = 16$, $U = 0.3n$, 16 resources, $rsf = 0.25$, $N^{max} = 10$, and short critical sections. The schedulability of the considered non-preemptable lock types in this configuration is shown in Fig. 1793.

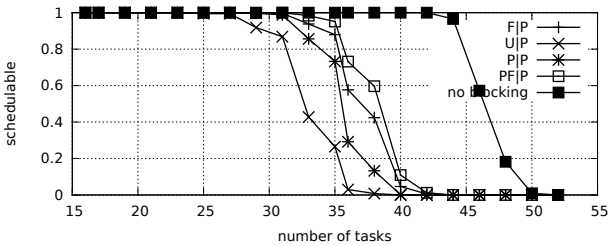

Fig. 1804. Schedulability under preemptable spin locks for $m = 16$, $U = 0.3n$, 16 resources, $rsf = 0.25$, $N^{max} = 15$, and short critical sections. The schedulability of the considered non-preemptable lock types in this configuration is shown in Fig. 1794.

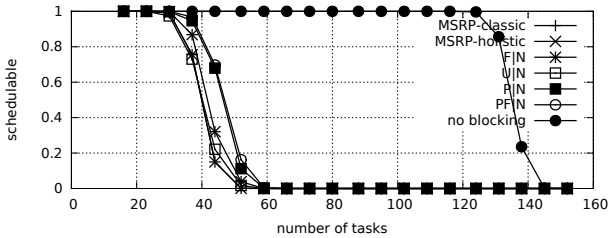

Fig. 1805. Schedulability under non-preemptable spin locks for $m = 16$, $U = 0.1n$, 16 resources, $rsf = 0.4$, $N^{max} = 1$, and medium critical sections. The schedulability of the considered preemptable lock types in this configuration is shown in Fig. 1815.

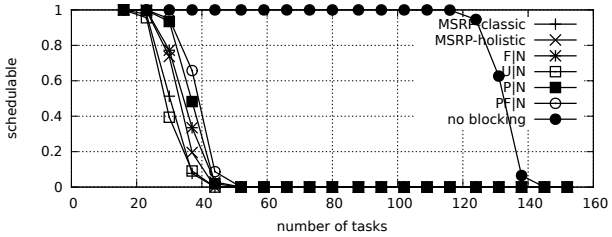

Fig. 1806. Schedulability under non-preemptable spin locks for $m = 16$, $U = 0.1n$, 16 resources, $rsf = 0.4$, $N^{max} = 2$, and medium critical sections. The schedulability of the considered preemptable lock types in this configuration is shown in Fig. 1816.

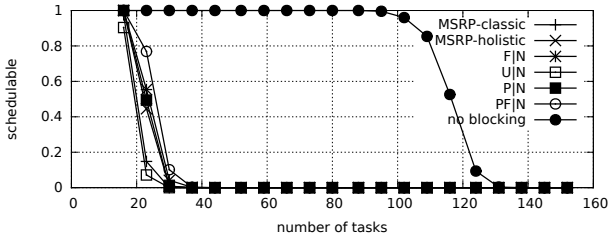

Fig. 1807. Schedulability under non-preemptable spin locks for $m = 16$, $U = 0.1n$, 16 resources, $rsf = 0.4$, $N^{max} = 5$, and medium critical sections. The schedulability of the considered preemptable lock types in this configuration is shown in Fig. 1817.

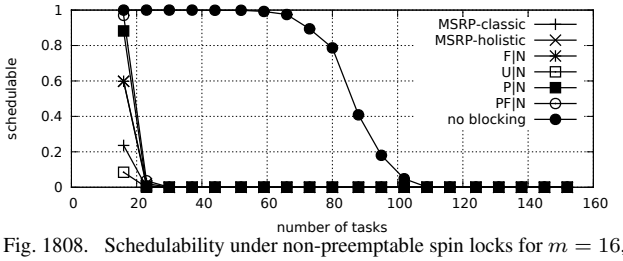

Fig. 1808. Schedulability under non-preemptable spin locks for $m = 16$, $U = 0.1n$, 16 resources, $rsf = 0.4$, $N^{max} = 10$, and medium critical sections. The schedulability of the considered preemptable lock types in this configuration is shown in Fig. 1818.

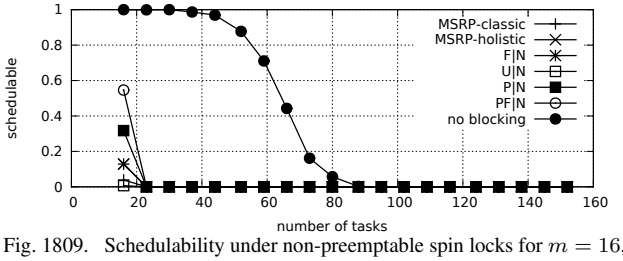

Fig. 1809. Schedulability under non-preemptable spin locks for $m = 16$, $U = 0.1n$, 16 resources, $rsf = 0.4$, $N^{max} = 15$, and medium critical sections. The schedulability of the considered preemptable lock types in this configuration is shown in Fig. 1819.

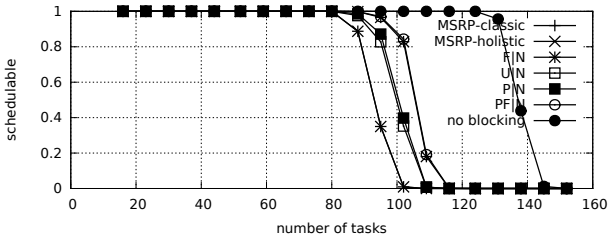

Fig. 1810. Schedulability under non-preemptable spin locks for $m = 16$, $U = 0.1n$, 16 resources, $rsf = 0.4$, $N^{max} = 1$, and short critical sections. The schedulability of the considered preemptable lock types in this configuration is shown in Fig. 1820.

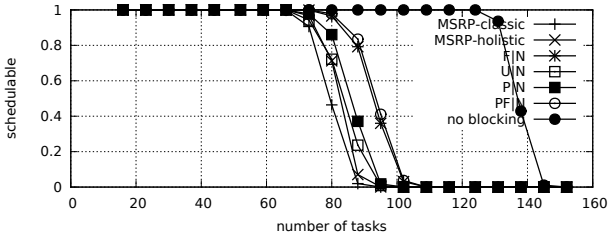

Fig. 1811. Schedulability under non-preemptable spin locks for $m = 16$, $U = 0.1n$, 16 resources, $rsf = 0.4$, $N^{max} = 2$, and short critical sections. The schedulability of the considered preemptable lock types in this configuration is shown in Fig. 1821.

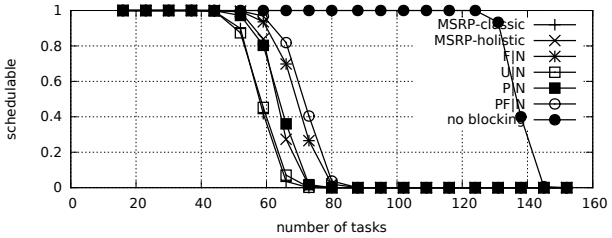

Fig. 1812. Schedulability under non-preemptable spin locks for $m = 16$, $U = 0.1n$, 16 resources, $rsf = 0.4$, $N^{max} = 5$, and short critical sections. The schedulability of the considered preemptable lock types in this configuration is shown in Fig. 1822.

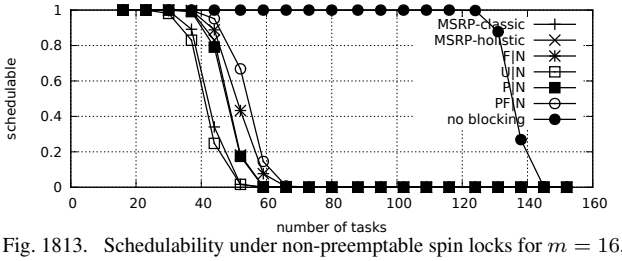

Fig. 1813. Schedulability under non-preemptable spin locks for $m = 16$, $U = 0.1n$, 16 resources, $rsf = 0.4$, $N^{max} = 10$, and short critical sections. The schedulability of the considered preemptable lock types in this configuration is shown in Fig. 1823.

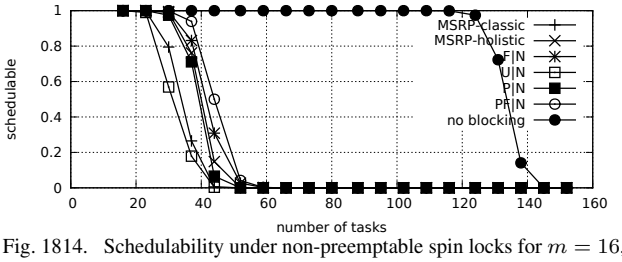

Fig. 1814. Schedulability under non-preemptable spin locks for $m = 16$, $U = 0.1n$, 16 resources, $rsf = 0.4$, $N^{max} = 15$, and short critical sections. The schedulability of the considered preemptable lock types in this configuration is shown in Fig. 1824.

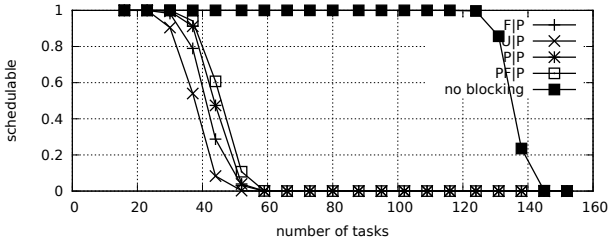

Fig. 1815. Schedulability under preemptable spin locks for $m = 16$, $U = 0.1n$, 16 resources, $rsf = 0.4$, $N^{max} = 1$, and medium critical sections. The schedulability of the considered non-preemptable lock types in this configuration is shown in Fig. 1805.

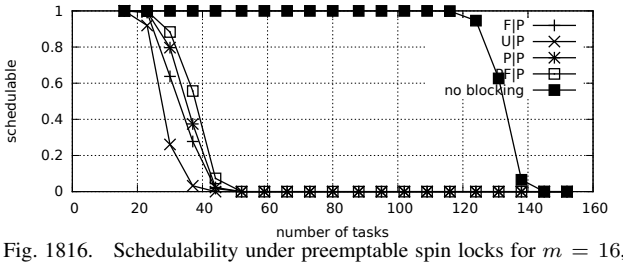

Fig. 1816. Schedulability under preemptable spin locks for $m = 16$, $U = 0.1n$, 16 resources, $rsf = 0.4$, $N^{max} = 2$, and medium critical sections. The schedulability of the considered non-preemptable lock types in this configuration is shown in Fig. 1806.

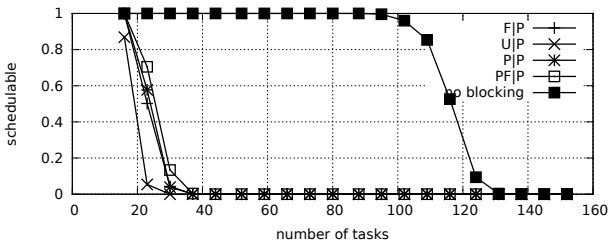

Fig. 1817. Schedulability under preemptable spin locks for $m = 16$, $U = 0.1n$, 16 resources, $rsf = 0.4$, $N^{max} = 5$, and medium critical sections. The schedulability of the considered non-preemptable lock types in this configuration is shown in Fig. 1807.

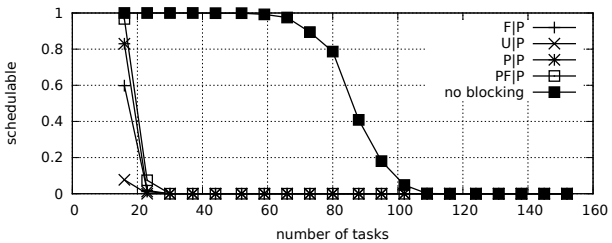

Fig. 1818. Schedulability under preemptable spin locks for $m = 16$, $U = 0.1n$, 16 resources, $rsf = 0.4$, $N^{max} = 10$, and medium critical sections. The schedulability of the considered non-preemptable lock types in this configuration is shown in Fig. 1808.

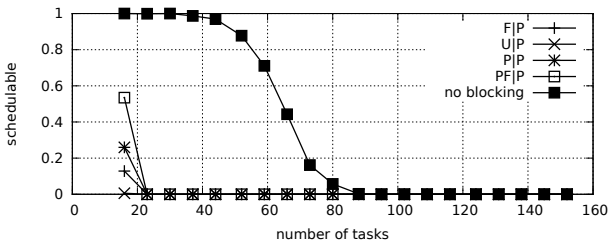

Fig. 1819. Schedulability under preemptable spin locks for $m = 16$, $U = 0.1n$, 16 resources, $rsf = 0.4$, $N^{max} = 15$, and medium critical sections. The schedulability of the considered non-preemptable lock types in this configuration is shown in Fig. 1809.

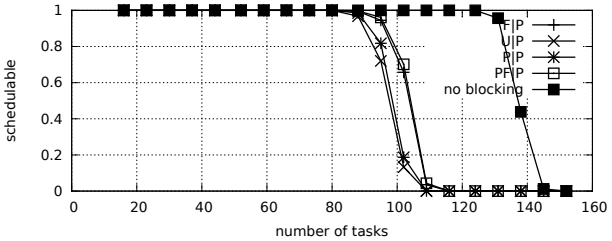

Fig. 1820. Schedulability under preemptable spin locks for $m = 16$, $U = 0.1n$, 16 resources, $rsf = 0.4$, $N^{max} = 1$, and short critical sections. The schedulability of the considered non-preemptable lock types in this configuration is shown in Fig. 1810.

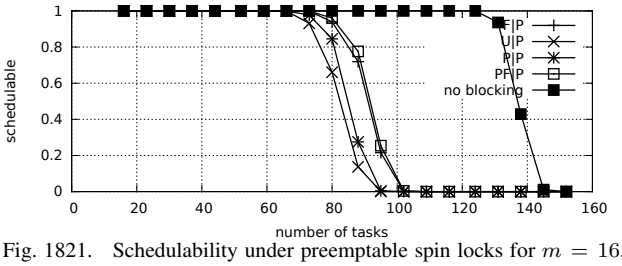

Fig. 1821. Schedulability under preemptable spin locks for $m = 16$, $U = 0.1n$, 16 resources, $rsf = 0.4$, $N^{max} = 2$, and short critical sections. The schedulability of the considered non-preemptable lock types in this configuration is shown in Fig. 1811.

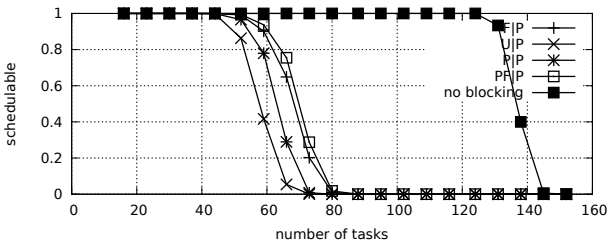

Fig. 1822. Schedulability under preemptable spin locks for $m = 16$, $U = 0.1n$, 16 resources, $rsf = 0.4$, $N^{max} = 5$, and short critical sections. The schedulability of the considered non-preemptable lock types in this configuration is shown in Fig. 1812.

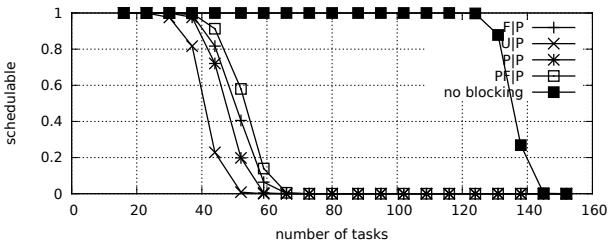

Fig. 1823. Schedulability under preemptable spin locks for $m = 16$, $U = 0.1n$, 16 resources, $rsf = 0.4$, $N^{max} = 10$, and short critical sections. The schedulability of the considered non-preemptable lock types in this configuration is shown in Fig. 1813.

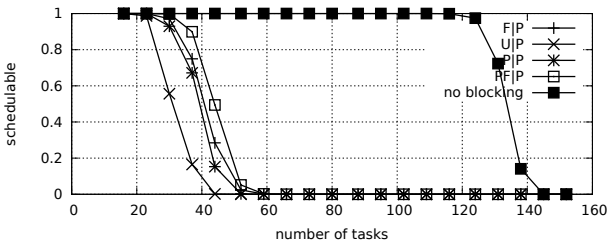

Fig. 1824. Schedulability under preemptable spin locks for $m = 16$, $U = 0.1n$, 16 resources, $rsf = 0.4$, $N^{max} = 15$, and short critical sections. The schedulability of the considered non-preemptable lock types in this configuration is shown in Fig. 1814.

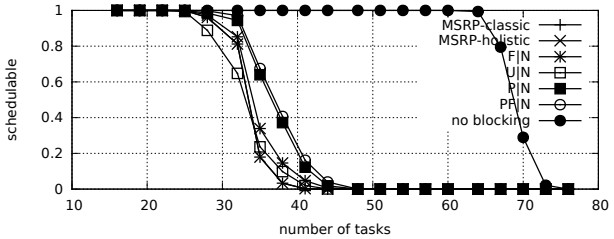

Fig. 1825. Schedulability under non-preemptable spin locks for $m = 16$, $U = 0.2n$, 16 resources, $rsf = 0.4$, $N^{max} = 1$, and medium critical sections. The schedulability of the considered preemptable lock types in this configuration is shown in Fig. 1835.

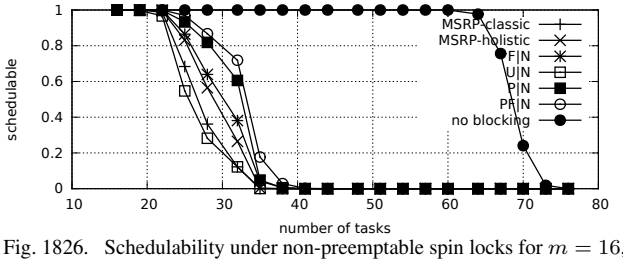

Fig. 1826. Schedulability under non-preemptable spin locks for $m = 16$, $U = 0.2n$, 16 resources, $rsf = 0.4$, $N^{max} = 2$, and medium critical sections. The schedulability of the considered preemptable lock types in this configuration is shown in Fig. 1836.

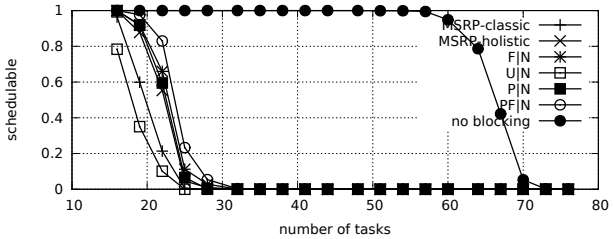

Fig. 1827. Schedulability under non-preemptable spin locks for $m = 16$, $U = 0.2n$, 16 resources, $rsf = 0.4$, $N^{max} = 5$, and medium critical sections. The schedulability of the considered preemptable lock types in this configuration is shown in Fig. 1837.

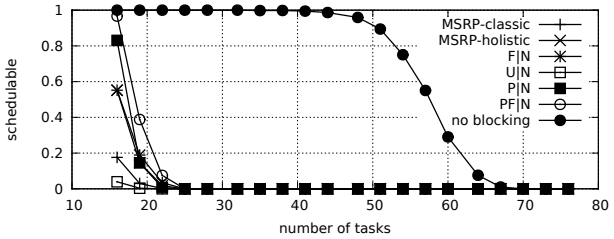

Fig. 1828. Schedulability under non-preemptable spin locks for $m = 16$, $U = 0.2n$, 16 resources, $rsf = 0.4$, $N^{max} = 10$, and medium critical sections. The schedulability of the considered preemptable lock types in this configuration is shown in Fig. 1838.

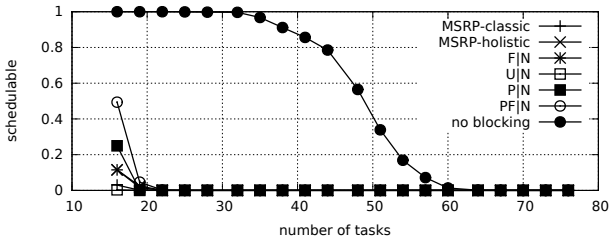

Fig. 1829. Schedulability under non-preemptable spin locks for $m = 16$, $U = 0.2n$, 16 resources, $rsf = 0.4$, $N^{max} = 15$, and medium critical sections. The schedulability of the considered preemptable lock types in this configuration is shown in Fig. 1839.

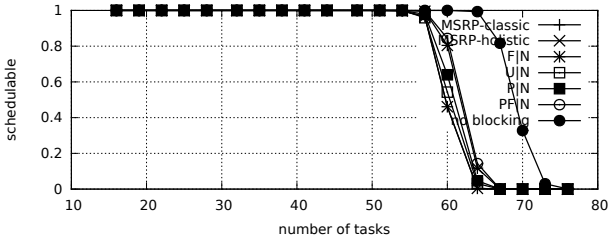

Fig. 1830. Schedulability under non-preemptable spin locks for $m = 16$, $U = 0.2n$, 16 resources, $rsf = 0.4$, $N^{max} = 1$, and short critical sections. The schedulability of the considered preemptable lock types in this configuration is shown in Fig. 1840.

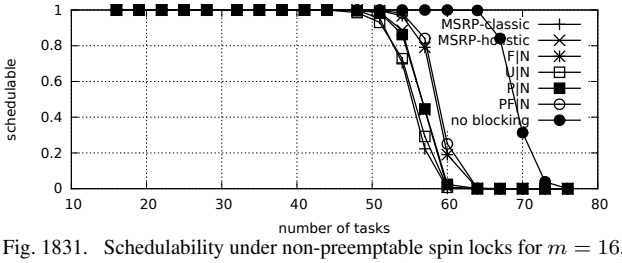

Fig. 1831. Schedulability under non-preemptable spin locks for $m = 16$, $U = 0.2n$, 16 resources, $rsf = 0.4$, $N^{max} = 2$, and short critical sections. The schedulability of the considered preemptable lock types in this configuration is shown in Fig. 1841.

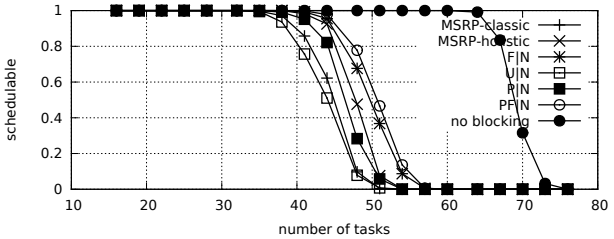

Fig. 1832. Schedulability under non-preemptable spin locks for $m = 16$, $U = 0.2n$, 16 resources, $rsf = 0.4$, $N^{max} = 5$, and short critical sections. The schedulability of the considered preemptable lock types in this configuration is shown in Fig. 1842.

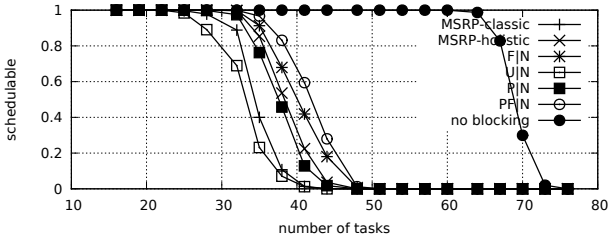

Fig. 1833. Schedulability under non-preemptable spin locks for $m = 16$, $U = 0.2n$, 16 resources, $rsf = 0.4$, $N^{max} = 10$, and short critical sections. The schedulability of the considered preemptable lock types in this configuration is shown in Fig. 1843.

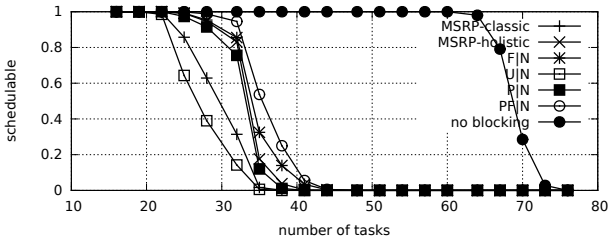

Fig. 1834. Schedulability under non-preemptable spin locks for $m = 16$, $U = 0.2n$, 16 resources, $rsf = 0.4$, $N^{max} = 15$, and short critical sections. The schedulability of the considered preemptable lock types in this configuration is shown in Fig. 1844.

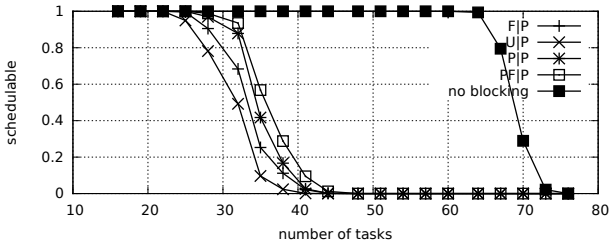

Fig. 1835. Schedulability under preemptable spin locks for $m = 16$, $U = 0.2n$, 16 resources, $rsf = 0.4$, $N^{max} = 1$, and medium critical sections. The schedulability of the considered non-preemptable lock types in this configuration is shown in Fig. 1825.

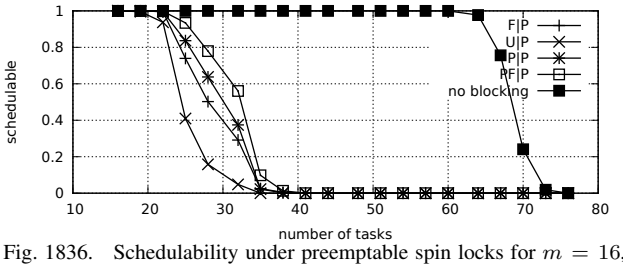

Fig. 1836. Schedulability under preemptable spin locks for $m = 16$, $U = 0.2n$, 16 resources, $rsf = 0.4$, $N^{max} = 2$, and medium critical sections. The schedulability of the considered non-preemptable lock types in this configuration is shown in Fig. 1826.

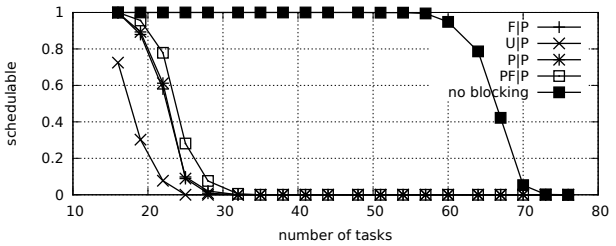

Fig. 1837. Schedulability under preemptable spin locks for $m = 16$, $U = 0.2n$, 16 resources, $rsf = 0.4$, $N^{max} = 5$, and medium critical sections. The schedulability of the considered non-preemptable lock types in this configuration is shown in Fig. 1827.

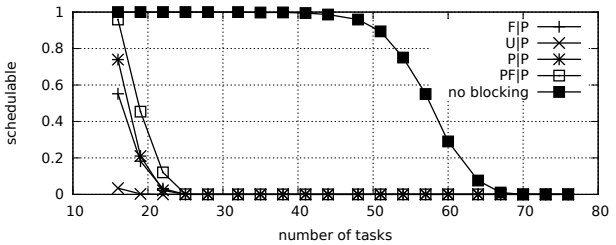

Fig. 1838. Schedulability under preemptable spin locks for $m = 16$, $U = 0.2n$, 16 resources, $rsf = 0.4$, $N^{max} = 10$, and medium critical sections. The schedulability of the considered non-preemptable lock types in this configuration is shown in Fig. 1828.

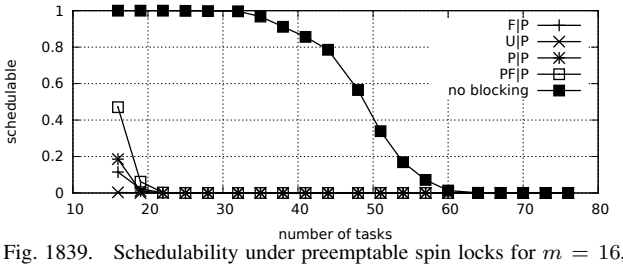

Fig. 1839. Schedulability under preemptable spin locks for $m = 16$, $U = 0.2n$, 16 resources, $rsf = 0.4$, $N^{max} = 15$, and medium critical sections. The schedulability of the considered non-preemptable lock types in this configuration is shown in Fig. 1829.

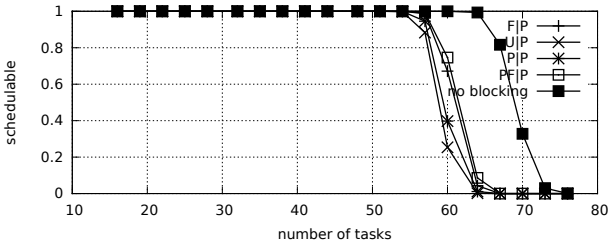

Fig. 1840. Schedulability under preemptable spin locks for $m = 16$, $U = 0.2n$, 16 resources, $rsf = 0.4$, $N^{max} = 1$, and short critical sections. The schedulability of the considered non-preemptable lock types in this configuration is shown in Fig. 1830.

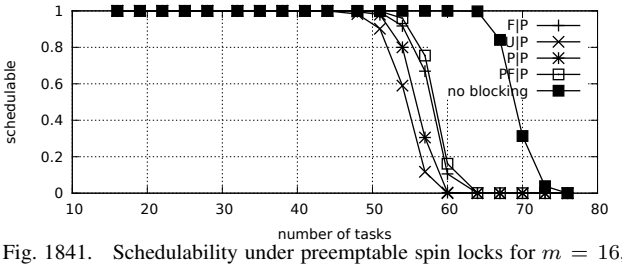

Fig. 1841. Schedulability under preemptable spin locks for $m = 16$, $U = 0.2n$, 16 resources, $rsf = 0.4$, $N^{max} = 2$, and short critical sections. The schedulability of the considered non-preemptable lock types in this configuration is shown in Fig. 1831.

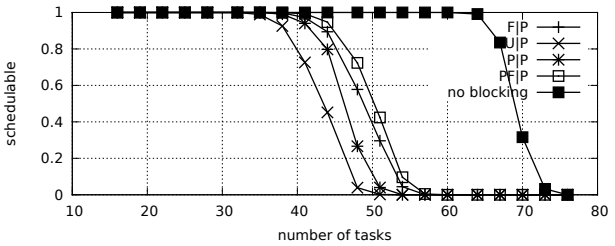

Fig. 1842. Schedulability under preemptable spin locks for $m = 16$, $U = 0.2n$, 16 resources, $rsf = 0.4$, $N^{max} = 5$, and short critical sections. The schedulability of the considered non-preemptable lock types in this configuration is shown in Fig. 1832.

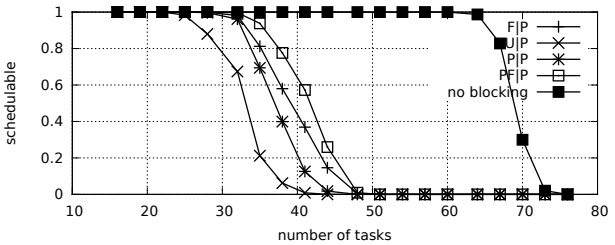

Fig. 1843. Schedulability under preemptable spin locks for $m = 16$, $U = 0.2n$, 16 resources, $rsf = 0.4$, $N^{max} = 10$, and short critical sections. The schedulability of the considered non-preemptable lock types in this configuration is shown in Fig. 1833.

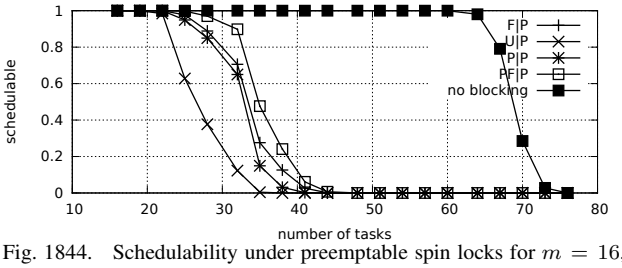

Fig. 1844. Schedulability under preemptable spin locks for $m = 16$, $U = 0.2n$, 16 resources, $rsf = 0.4$, $N^{max} = 15$, and short critical sections. The schedulability of the considered non-preemptable lock types in this configuration is shown in Fig. 1834.

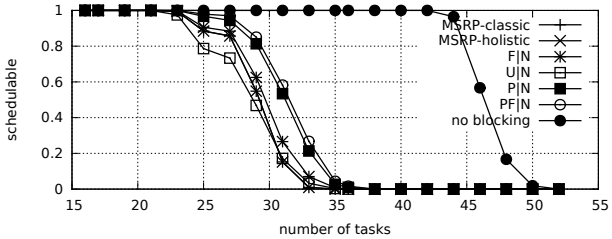

Fig. 1845. Schedulability under non-preemptable spin locks for $m = 16$, $U = 0.3n$, 16 resources, $rsf = 0.4$, $N^{max} = 1$, and medium critical sections. The schedulability of the considered preemptable lock types in this configuration is shown in Fig. 1855.

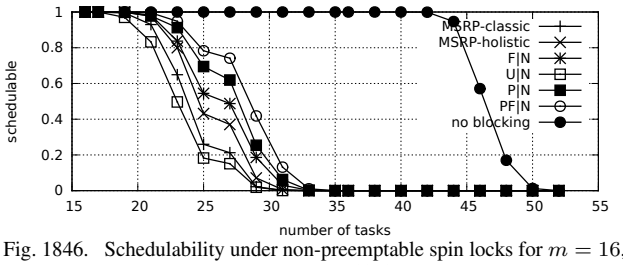

Fig. 1846. Schedulability under non-preemptable spin locks for $m = 16$, $U = 0.3n$, 16 resources, $rsf = 0.4$, $N^{max} = 2$, and medium critical sections. The schedulability of the considered preemptable lock types in this configuration is shown in Fig. 1856.

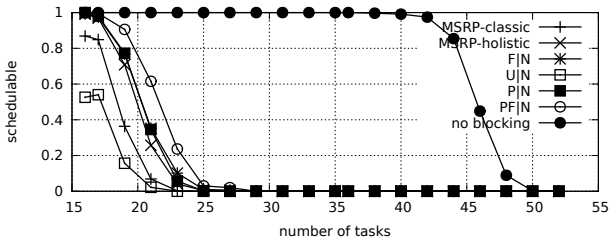

Fig. 1847. Schedulability under non-preemptable spin locks for $m = 16$, $U = 0.3n$, 16 resources, $rsf = 0.4$, $N^{max} = 5$, and medium critical sections. The schedulability of the considered preemptable lock types in this configuration is shown in Fig. 1857.

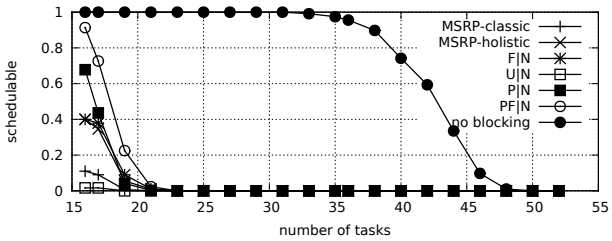

Fig. 1848. Schedulability under non-preemptable spin locks for $m = 16$, $U = 0.3n$, 16 resources, $rsf = 0.4$, $N^{max} = 10$, and medium critical sections. The schedulability of the considered preemptable lock types in this configuration is shown in Fig. 1858.

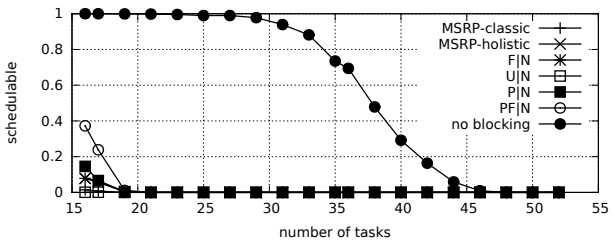

Fig. 1849. Schedulability under non-preemptable spin locks for $m = 16$, $U = 0.3n$, 16 resources, $rsf = 0.4$, $N^{max} = 15$, and medium critical sections. The schedulability of the considered preemptable lock types in this configuration is shown in Fig. 1859.

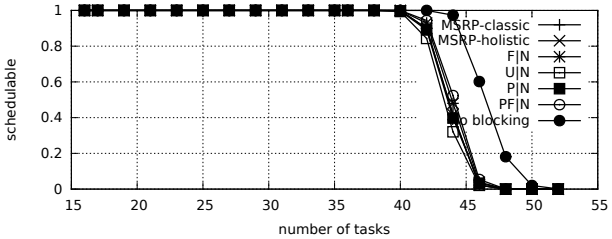

Fig. 1850. Schedulability under non-preemptable spin locks for $m = 16$, $U = 0.3n$, 16 resources, $rsf = 0.4$, $N^{max} = 1$, and short critical sections. The schedulability of the considered preemptable lock types in this configuration is shown in Fig. 1860.

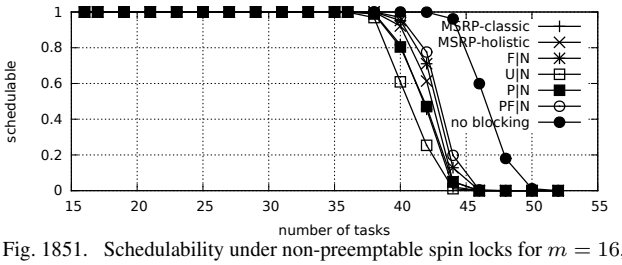

Fig. 1851. Schedulability under non-preemptable spin locks for $m = 16$, $U = 0.3n$, 16 resources, $rsf = 0.4$, $N^{max} = 2$, and short critical sections. The schedulability of the considered preemptable lock types in this configuration is shown in Fig. 1861.

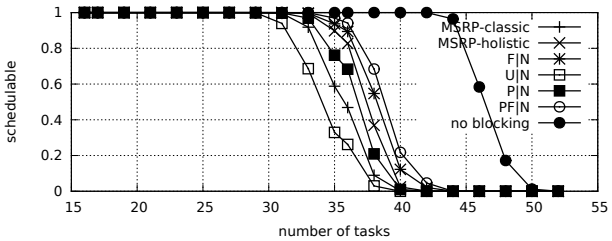

Fig. 1852. Schedulability under non-preemptable spin locks for $m = 16$, $U = 0.3n$, 16 resources, $rsf = 0.4$, $N^{max} = 5$, and short critical sections. The schedulability of the considered preemptable lock types in this configuration is shown in Fig. 1862.

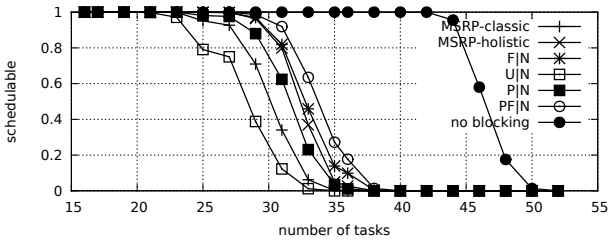

Fig. 1853. Schedulability under non-preemptable spin locks for $m = 16$, $U = 0.3n$, 16 resources, $rsf = 0.4$, $N^{max} = 10$, and short critical sections. The schedulability of the considered preemptable lock types in this configuration is shown in Fig. 1863.

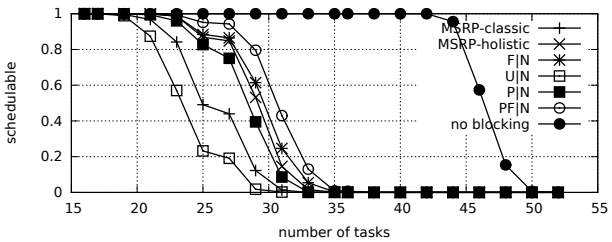

Fig. 1854. Schedulability under non-preemptable spin locks for $m = 16$, $U = 0.3n$, 16 resources, $rsf = 0.4$, $N^{max} = 15$, and short critical sections. The schedulability of the considered preemptable lock types in this configuration is shown in Fig. 1864.

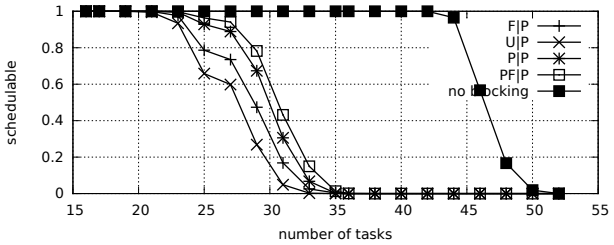

Fig. 1855. Schedulability under preemptable spin locks for $m = 16$, $U = 0.3n$, 16 resources, $rsf = 0.4$, $N^{max} = 1$, and medium critical sections. The schedulability of the considered non-preemptable lock types in this configuration is shown in Fig. 1845.

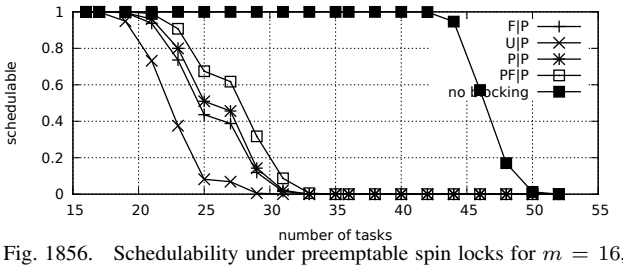

Fig. 1856. Schedulability under preemptable spin locks for $m = 16$, $U = 0.3n$, 16 resources, $rsf = 0.4$, $N^{max} = 2$, and medium critical sections. The schedulability of the considered non-preemptable lock types in this configuration is shown in Fig. 1846.

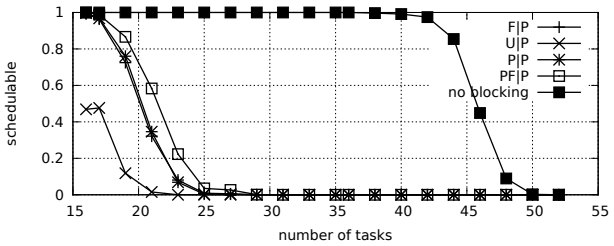

Fig. 1857. Schedulability under preemptable spin locks for $m = 16$, $U = 0.3n$, 16 resources, $rsf = 0.4$, $N^{max} = 5$, and medium critical sections. The schedulability of the considered non-preemptable lock types in this configuration is shown in Fig. 1847.

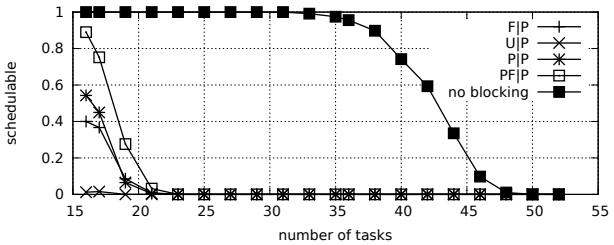

Fig. 1858. Schedulability under preemptable spin locks for $m = 16$, $U = 0.3n$, 16 resources, $rsf = 0.4$, $N^{max} = 10$, and medium critical sections. The schedulability of the considered non-preemptable lock types in this configuration is shown in Fig. 1848.

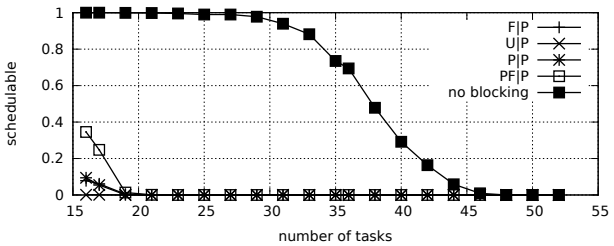

Fig. 1859. Schedulability under preemptable spin locks for $m = 16$, $U = 0.3n$, 16 resources, $rsf = 0.4$, $N^{max} = 15$, and medium critical sections. The schedulability of the considered non-preemptable lock types in this configuration is shown in Fig. 1849.

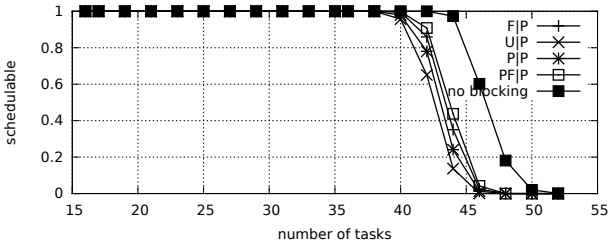

Fig. 1860. Schedulability under preemptable spin locks for $m = 16$, $U = 0.3n$, 16 resources, $rsf = 0.4$, $N^{max} = 1$, and short critical sections. The schedulability of the considered non-preemptable lock types in this configuration is shown in Fig. 1850.

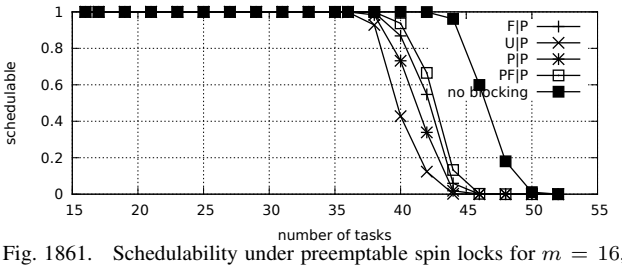

Fig. 1861. Schedulability under preemptable spin locks for $m = 16$, $U = 0.3n$, 16 resources, $rsf = 0.4$, $N^{max} = 2$, and short critical sections. The schedulability of the considered non-preemptable lock types in this configuration is shown in Fig. 1851.

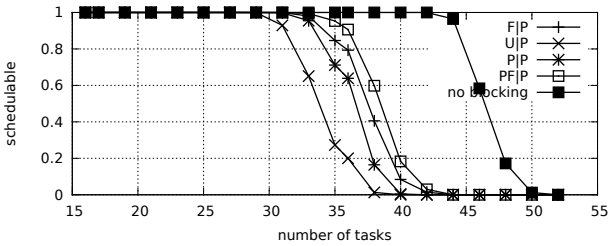

Fig. 1862. Schedulability under preemptable spin locks for $m = 16$, $U = 0.3n$, 16 resources, $rsf = 0.4$, $N^{max} = 5$, and short critical sections. The schedulability of the considered non-preemptable lock types in this configuration is shown in Fig. 1852.

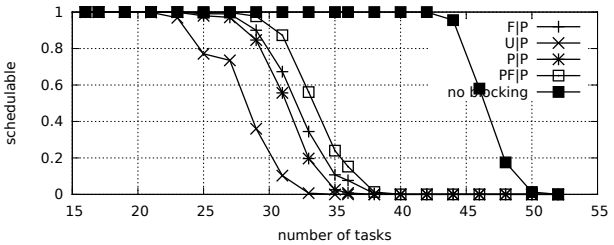

Fig. 1863. Schedulability under preemptable spin locks for $m = 16$, $U = 0.3n$, 16 resources, $rsf = 0.4$, $N^{max} = 10$, and short critical sections. The schedulability of the considered non-preemptable lock types in this configuration is shown in Fig. 1853.

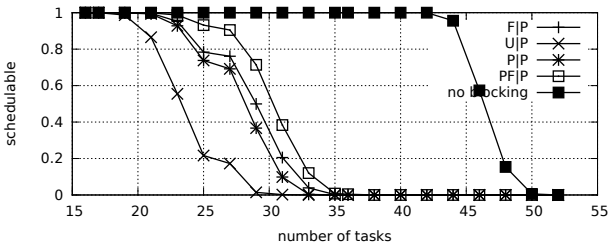

Fig. 1864. Schedulability under preemptable spin locks for $m = 16$, $U = 0.3n$, 16 resources, $rsf = 0.4$, $N^{max} = 15$, and short critical sections. The schedulability of the considered non-preemptable lock types in this configuration is shown in Fig. 1854.

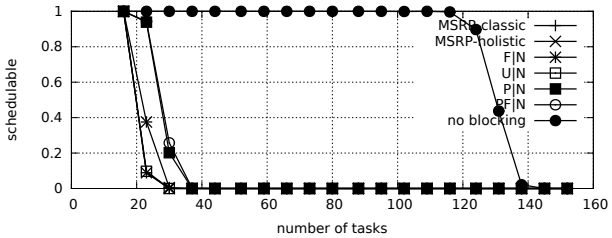

Fig. 1865. Schedulability under non-preemptable spin locks for $m = 16$, $U = 0.1n$, 16 resources, $rsf = 0.75$, $N^{max} = 1$, and medium critical sections. The schedulability of the considered preemptable lock types in this configuration is shown in Fig. 1875.

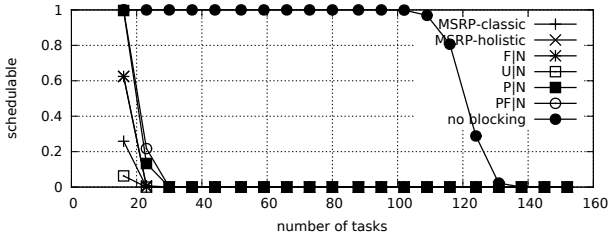

Fig. 1866. Schedulability under non-preemptable spin locks for $m = 16$, $U = 0.1n$, 16 resources, $rsf = 0.75$, $N^{max} = 2$, and medium critical sections. The schedulability of the considered preemptable lock types in this configuration is shown in Fig. 1876.

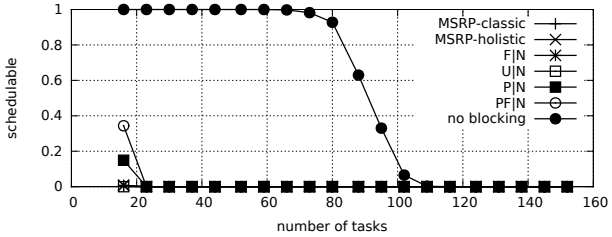

Fig. 1867. Schedulability under non-preemptable spin locks for $m = 16$, $U = 0.1n$, 16 resources, $rsf = 0.75$, $N^{max} = 5$, and medium critical sections. The schedulability of the considered preemptable lock types in this configuration is shown in Fig. 1877.

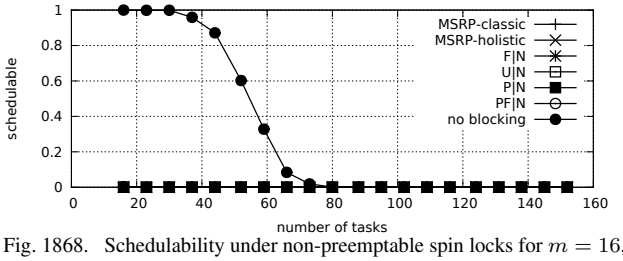

Fig. 1868. Schedulability under non-preemptable spin locks for $m = 16$, $U = 0.1n$, 16 resources, $rsf = 0.75$, $N^{max} = 10$, and medium critical sections. The schedulability of the considered preemptable lock types in this configuration is shown in Fig. 1878.

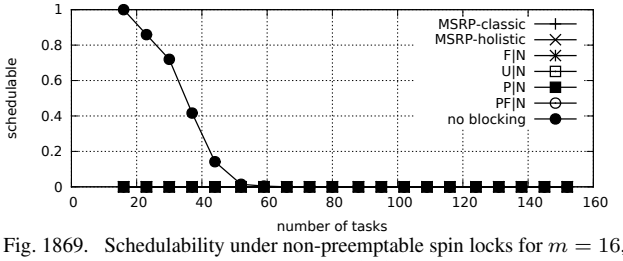

Fig. 1869. Schedulability under non-preemptable spin locks for $m = 16$, $U = 0.1n$, 16 resources, $rsf = 0.75$, $N^{max} = 15$, and medium critical sections. The schedulability of the considered preemptable lock types in this configuration is shown in Fig. 1879.

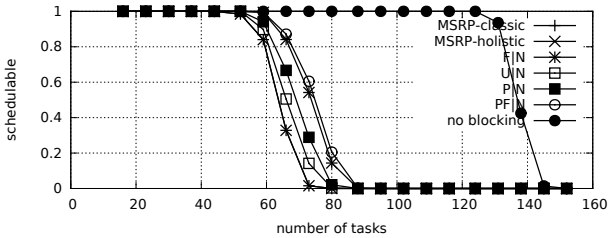

Fig. 1870. Schedulability under non-preemptable spin locks for $m = 16$, $U = 0.1n$, 16 resources, $rsf = 0.75$, $N^{max} = 1$, and short critical sections. The schedulability of the considered preemptable lock types in this configuration is shown in Fig. 1880.

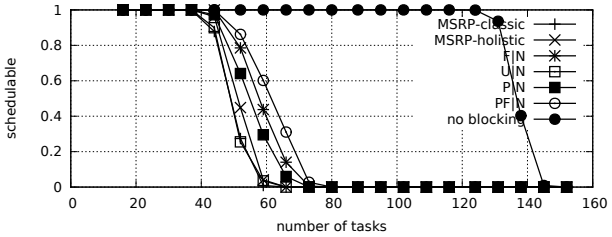

Fig. 1871. Schedulability under non-preemptable spin locks for $m = 16$, $U = 0.1n$, 16 resources, $rsf = 0.75$, $N^{max} = 2$, and short critical sections. The schedulability of the considered preemptable lock types in this configuration is shown in Fig. 1881.

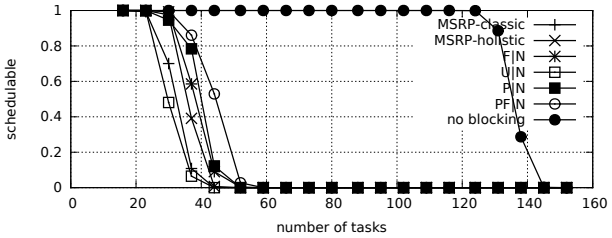

Fig. 1872. Schedulability under non-preemptable spin locks for $m = 16$, $U = 0.1n$, 16 resources, $rsf = 0.75$, $N^{max} = 5$, and short critical sections. The schedulability of the considered preemptable lock types in this configuration is shown in Fig. 1882.

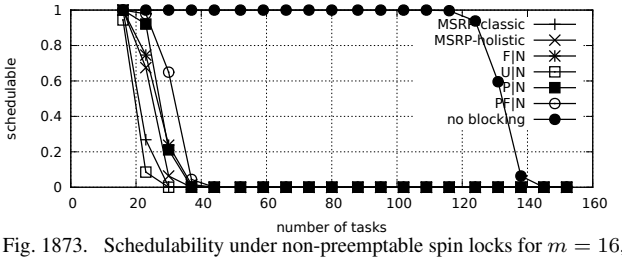

Fig. 1873. Schedulability under non-preemptable spin locks for $m = 16$, $U = 0.1n$, 16 resources, $rsf = 0.75$, $N^{max} = 10$, and short critical sections. The schedulability of the considered preemptable lock types in this configuration is shown in Fig. 1883.

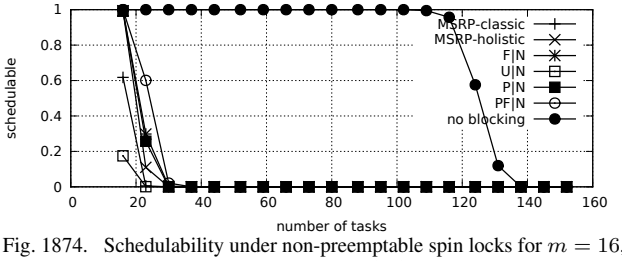

Fig. 1874. Schedulability under non-preemptable spin locks for $m = 16$, $U = 0.1n$, 16 resources, $rsf = 0.75$, $N^{max} = 15$, and short critical sections. The schedulability of the considered preemptable lock types in this configuration is shown in Fig. 1884.

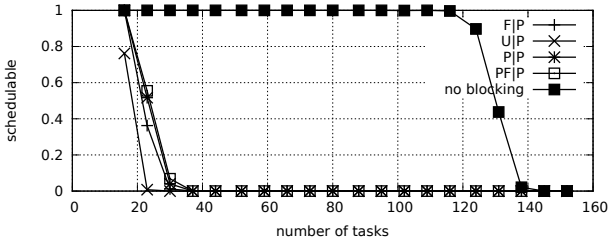

Fig. 1875. Schedulability under preemptable spin locks for $m = 16$, $U = 0.1n$, 16 resources, $rsf = 0.75$, $N^{max} = 1$, and medium critical sections. The schedulability of the considered non-preemptable lock types in this configuration is shown in Fig. 1865.

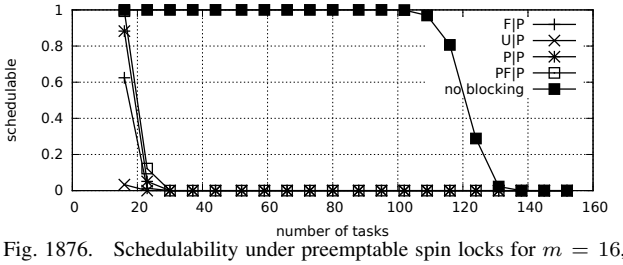

Fig. 1876. Schedulability under preemptable spin locks for $m = 16$, $U = 0.1n$, 16 resources, $rsf = 0.75$, $N^{max} = 2$, and medium critical sections. The schedulability of the considered non-preemptable lock types in this configuration is shown in Fig. 1866.

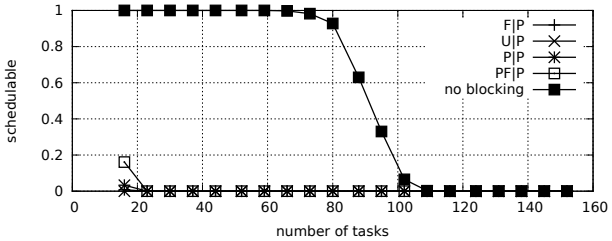

Fig. 1877. Schedulability under preemptable spin locks for $m = 16$, $U = 0.1n$, 16 resources, $rsf = 0.75$, $N^{max} = 5$, and medium critical sections. The schedulability of the considered non-preemptable lock types in this configuration is shown in Fig. 1867.

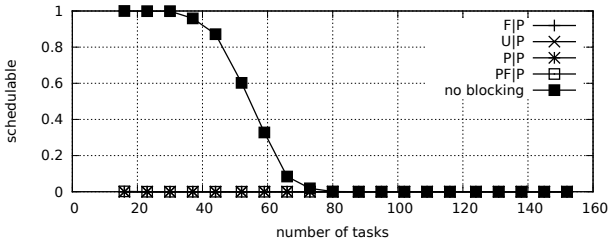

Fig. 1878. Schedulability under preemptable spin locks for $m = 16$, $U = 0.1n$, 16 resources, $rsf = 0.75$, $N^{max} = 10$, and medium critical sections. The schedulability of the considered non-preemptable lock types in this configuration is shown in Fig. 1868.

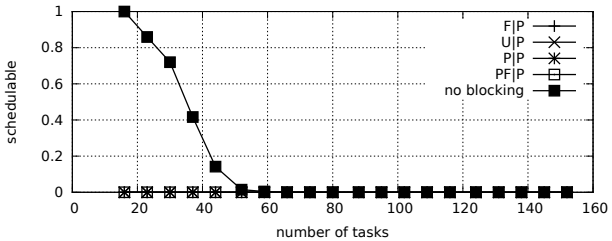

Fig. 1879. Schedulability under preemptable spin locks for $m = 16$, $U = 0.1n$, 16 resources, $rsf = 0.75$, $N^{max} = 15$, and medium critical sections. The schedulability of the considered non-preemptable lock types in this configuration is shown in Fig. 1869.

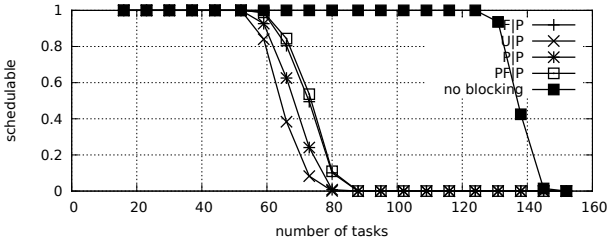

Fig. 1880. Schedulability under preemptable spin locks for $m = 16$, $U = 0.1n$, 16 resources, $rsf = 0.75$, $N^{max} = 1$, and short critical sections. The schedulability of the considered non-preemptable lock types in this configuration is shown in Fig. 1870.

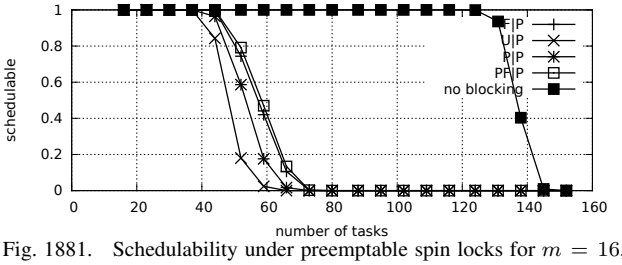

Fig. 1881. Schedulability under preemptable spin locks for $m = 16$, $U = 0.1n$, 16 resources, $rsf = 0.75$, $N^{max} = 2$, and short critical sections. The schedulability of the considered non-preemptable lock types in this configuration is shown in Fig. 1871.

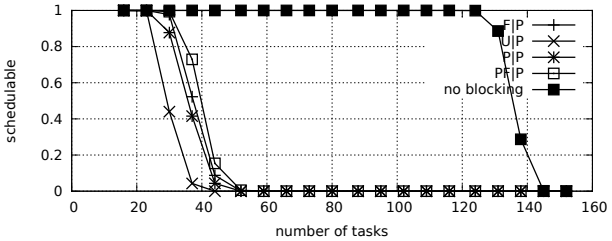

Fig. 1882. Schedulability under preemptable spin locks for $m = 16$, $U = 0.1n$, 16 resources, $rsf = 0.75$, $N^{max} = 5$, and short critical sections. The schedulability of the considered non-preemptable lock types in this configuration is shown in Fig. 1872.

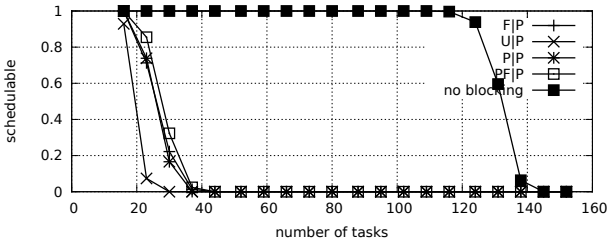

Fig. 1883. Schedulability under preemptable spin locks for $m = 16$, $U = 0.1n$, 16 resources, $rsf = 0.75$, $N^{max} = 10$, and short critical sections. The schedulability of the considered non-preemptable lock types in this configuration is shown in Fig. 1873.

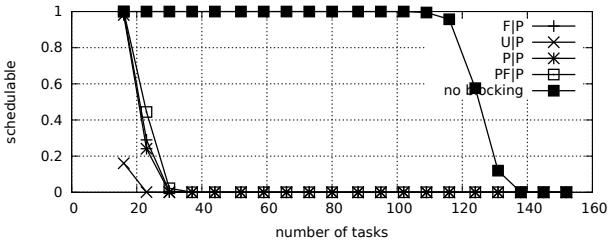

Fig. 1884. Schedulability under preemptable spin locks for $m = 16$, $U = 0.1n$, 16 resources, $rsf = 0.75$, $N^{max} = 15$, and short critical sections. The schedulability of the considered non-preemptable lock types in this configuration is shown in Fig. 1874.

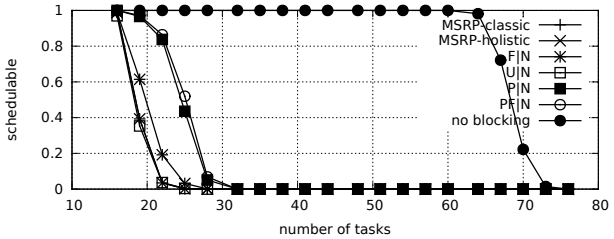

Fig. 1885. Schedulability under non-preemptable spin locks for $m = 16$, $U = 0.2n$, 16 resources, $rsf = 0.75$, $N^{max} = 1$, and medium critical sections. The schedulability of the considered preemptable lock types in this configuration is shown in Fig. 1895.

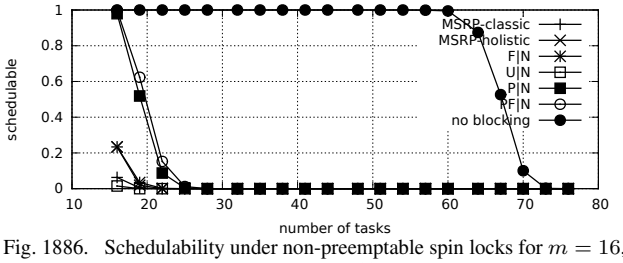

Fig. 1886. Schedulability under non-preemptable spin locks for $m = 16$, $U = 0.2n$, 16 resources, $rsf = 0.75$, $N^{max} = 2$, and medium critical sections. The schedulability of the considered preemptable lock types in this configuration is shown in Fig. 1896.

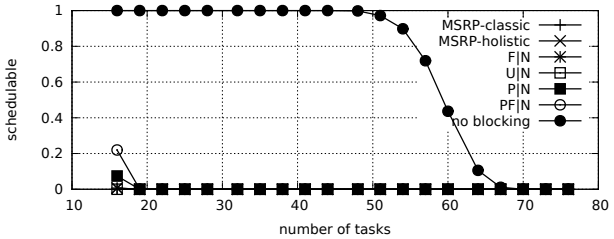

Fig. 1887. Schedulability under non-preemptable spin locks for $m = 16$, $U = 0.2n$, 16 resources, $rsf = 0.75$, $N^{max} = 5$, and medium critical sections. The schedulability of the considered preemptable lock types in this configuration is shown in Fig. 1897.

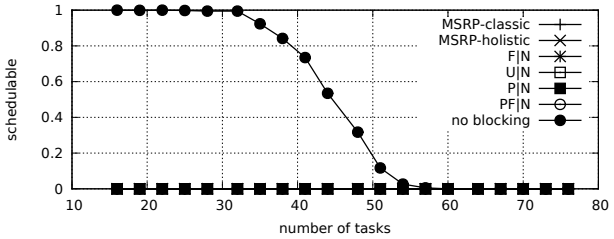

Fig. 1888. Schedulability under non-preemptable spin locks for $m = 16$, $U = 0.2n$, 16 resources, $rsf = 0.75$, $N^{max} = 10$, and medium critical sections. The schedulability of the considered preemptable lock types in this configuration is shown in Fig. 1898.

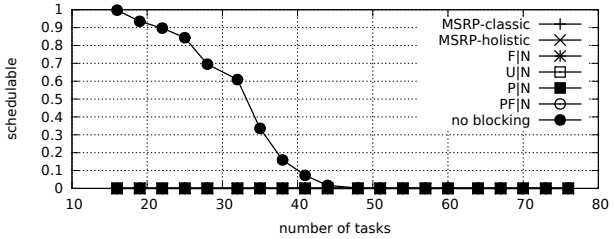

Fig. 1889. Schedulability under non-preemptable spin locks for $m = 16$, $U = 0.2n$, 16 resources, $rsf = 0.75$, $N^{max} = 15$, and medium critical sections. The schedulability of the considered preemptable lock types in this configuration is shown in Fig. 1899.

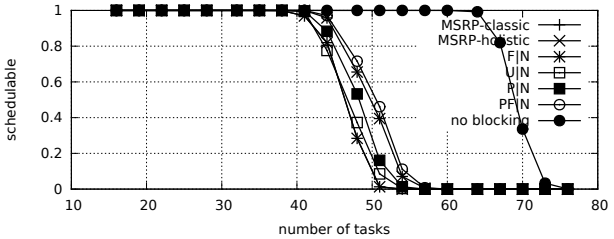

Fig. 1890. Schedulability under non-preemptable spin locks for $m = 16$, $U = 0.2n$, 16 resources, $rsf = 0.75$, $N^{max} = 1$, and short critical sections. The schedulability of the considered preemptable lock types in this configuration is shown in Fig. 1900.

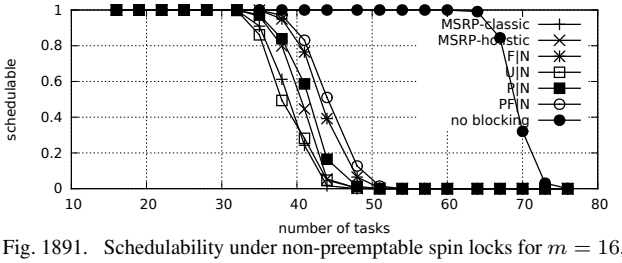

Fig. 1891. Schedulability under non-preemptable spin locks for $m = 16$, $U = 0.2n$, 16 resources, $rsf = 0.75$, $N^{max} = 2$, and short critical sections. The schedulability of the considered preemptable lock types in this configuration is shown in Fig. 1901.

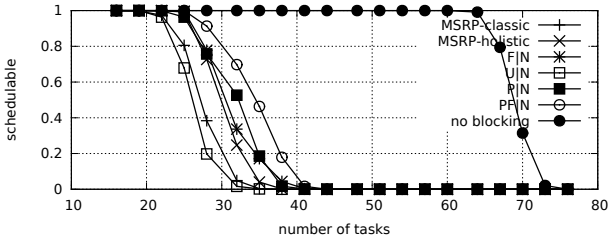

Fig. 1892. Schedulability under non-preemptable spin locks for $m = 16$, $U = 0.2n$, 16 resources, $rsf = 0.75$, $N^{max} = 5$, and short critical sections. The schedulability of the considered preemptable lock types in this configuration is shown in Fig. 1902.

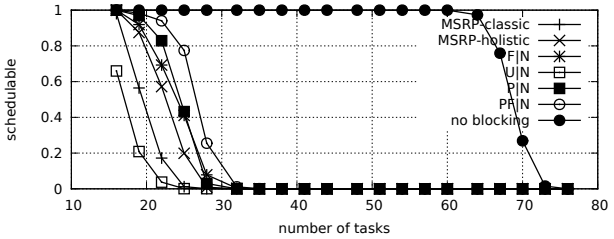

Fig. 1893. Schedulability under non-preemptable spin locks for $m = 16$, $U = 0.2n$, 16 resources, $rsf = 0.75$, $N^{max} = 10$, and short critical sections. The schedulability of the considered preemptable lock types in this configuration is shown in Fig. 1903.

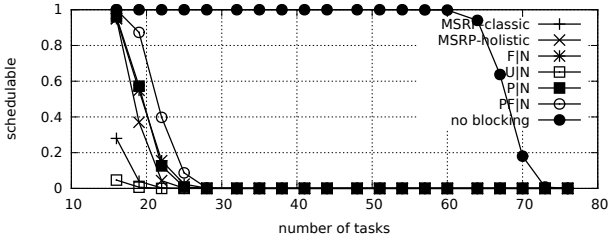

Fig. 1894. Schedulability under non-preemptable spin locks for $m = 16$, $U = 0.2n$, 16 resources, $rsf = 0.75$, $N^{max} = 15$, and short critical sections. The schedulability of the considered preemptable lock types in this configuration is shown in Fig. 1904.

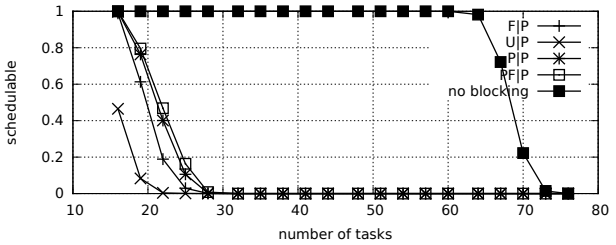

Fig. 1895. Schedulability under preemptable spin locks for $m = 16$, $U = 0.2n$, 16 resources, $rsf = 0.75$, $N^{max} = 1$, and medium critical sections. The schedulability of the considered non-preemptable lock types in this configuration is shown in Fig. 1885.

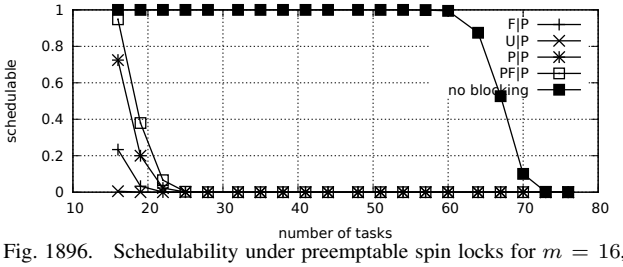

Fig. 1896. Schedulability under preemptable spin locks for $m = 16$, $U = 0.2n$, 16 resources, $rsf = 0.75$, $N^{max} = 2$, and medium critical sections. The schedulability of the considered non-preemptable lock types in this configuration is shown in Fig. 1886.

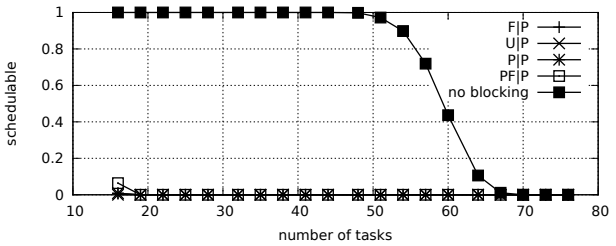

Fig. 1897. Schedulability under preemptable spin locks for $m = 16$, $U = 0.2n$, 16 resources, $rsf = 0.75$, $N^{max} = 5$, and medium critical sections. The schedulability of the considered non-preemptable lock types in this configuration is shown in Fig. 1887.

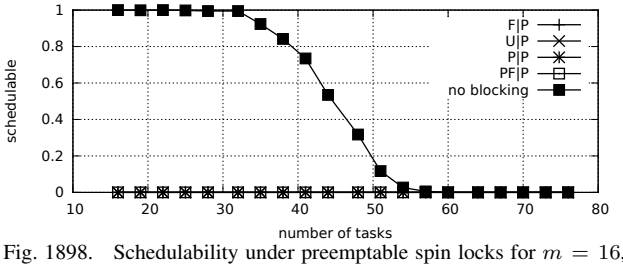

Fig. 1898. Schedulability under preemptable spin locks for $m = 16$, $U = 0.2n$, 16 resources, $rsf = 0.75$, $N^{max} = 10$, and medium critical sections. The schedulability of the considered non-preemptable lock types in this configuration is shown in Fig. 1888.

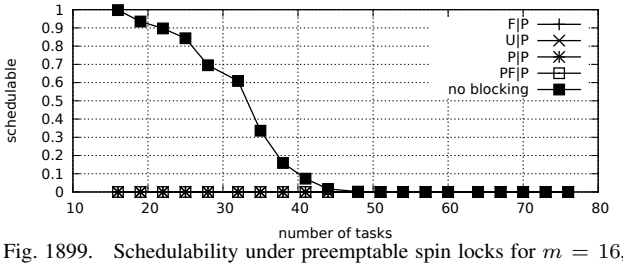

Fig. 1899. Schedulability under preemptable spin locks for $m = 16$, $U = 0.2n$, 16 resources, $rsf = 0.75$, $N^{max} = 15$, and medium critical sections. The schedulability of the considered non-preemptable lock types in this configuration is shown in Fig. 1889.

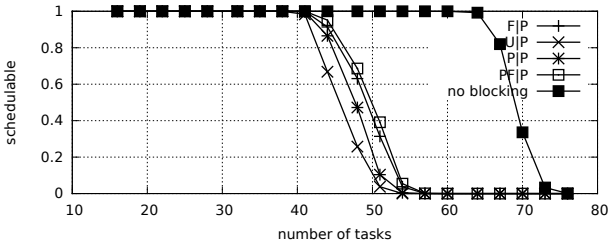

Fig. 1900. Schedulability under preemptable spin locks for $m = 16$, $U = 0.2n$, 16 resources, $rsf = 0.75$, $N^{max} = 1$, and short critical sections. The schedulability of the considered non-preemptable lock types in this configuration is shown in Fig. 1890.

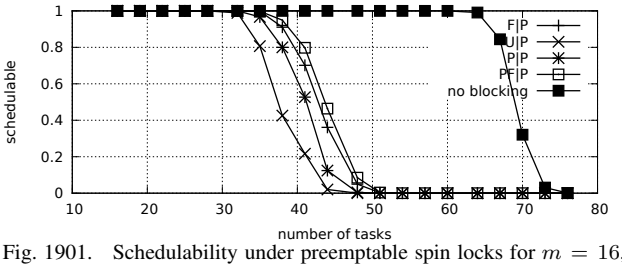

Fig. 1901. Schedulability under preemptable spin locks for $m = 16$, $U = 0.2n$, 16 resources, $rsf = 0.75$, $N^{max} = 2$, and short critical sections. The schedulability of the considered non-preemptable lock types in this configuration is shown in Fig. 1891.

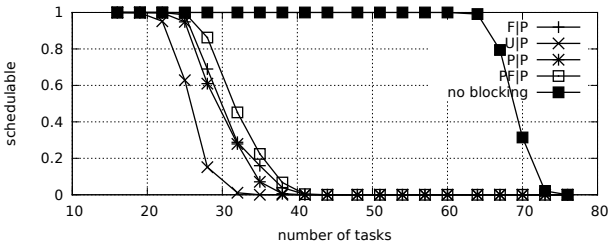

Fig. 1902. Schedulability under preemptable spin locks for $m = 16$, $U = 0.2n$, 16 resources, $rsf = 0.75$, $N^{max} = 5$, and short critical sections. The schedulability of the considered non-preemptable lock types in this configuration is shown in Fig. 1892.

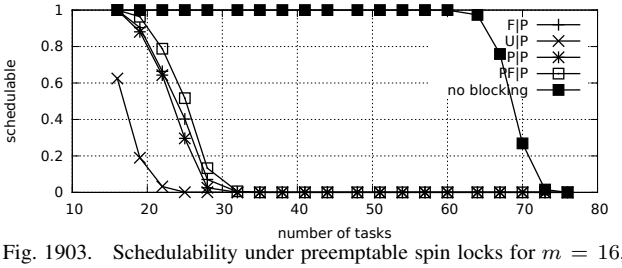

Fig. 1903. Schedulability under preemptable spin locks for $m = 16$, $U = 0.2n$, 16 resources, $rsf = 0.75$, $N^{max} = 10$, and short critical sections. The schedulability of the considered non-preemptable lock types in this configuration is shown in Fig. 1893.

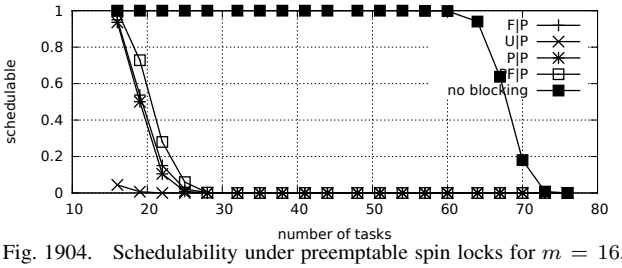

Fig. 1904. Schedulability under preemptable spin locks for $m = 16$, $U = 0.2n$, 16 resources, $rsf = 0.75$, $N^{max} = 15$, and short critical sections. The schedulability of the considered non-preemptable lock types in this configuration is shown in Fig. 1894.

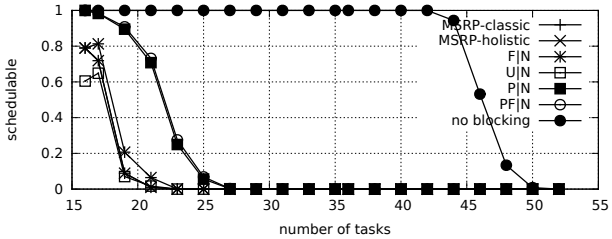

Fig. 1905. Schedulability under non-preemptable spin locks for $m = 16$, $U = 0.3n$, 16 resources, $rsf = 0.75$, $N^{max} = 1$, and medium critical sections. The schedulability of the considered preemptable lock types in this configuration is shown in Fig. 1915.

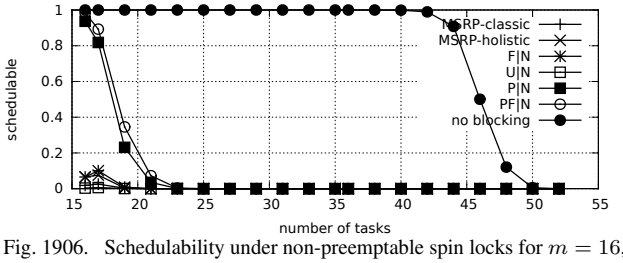

Fig. 1906. Schedulability under non-preemptable spin locks for $m = 16$, $U = 0.3n$, 16 resources, $rsf = 0.75$, $N^{max} = 2$, and medium critical sections. The schedulability of the considered preemptable lock types in this configuration is shown in Fig. 1916.

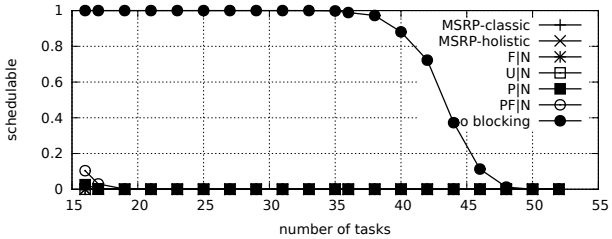

Fig. 1907. Schedulability under non-preemptable spin locks for $m = 16$, $U = 0.3n$, 16 resources, $rsf = 0.75$, $N^{max} = 5$, and medium critical sections. The schedulability of the considered preemptable lock types in this configuration is shown in Fig. 1917.

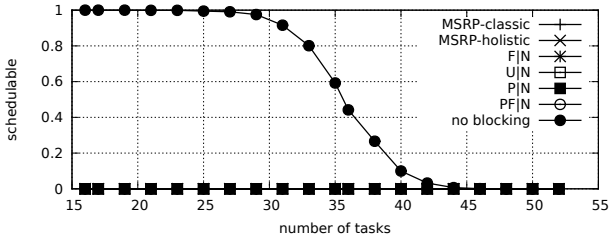

Fig. 1908. Schedulability under non-preemptable spin locks for $m = 16$, $U = 0.3n$, 16 resources, $rsf = 0.75$, $N^{max} = 10$, and medium critical sections. The schedulability of the considered preemptable lock types in this configuration is shown in Fig. 1918.

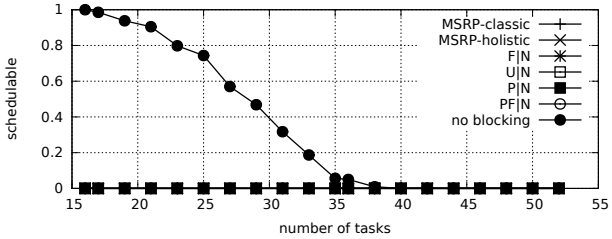

Fig. 1909. Schedulability under non-preemptable spin locks for $m = 16$, $U = 0.3n$, 16 resources, $rsf = 0.75$, $N^{max} = 15$, and medium critical sections. The schedulability of the considered preemptable lock types in this configuration is shown in Fig. 1919.

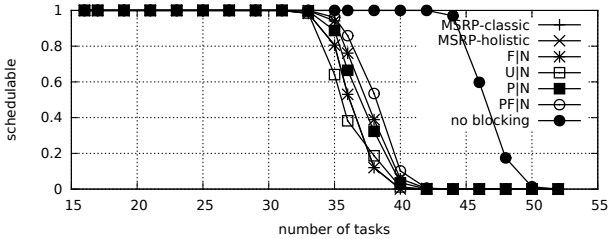

Fig. 1910. Schedulability under non-preemptable spin locks for $m = 16$, $U = 0.3n$, 16 resources, $rsf = 0.75$, $N^{max} = 1$, and short critical sections. The schedulability of the considered preemptable lock types in this configuration is shown in Fig. 1920.

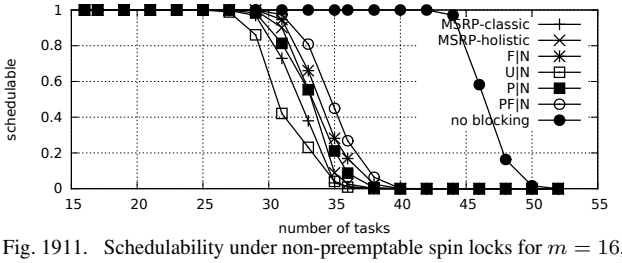

Fig. 1911. Schedulability under non-preemptable spin locks for $m = 16$, $U = 0.3n$, 16 resources, $rsf = 0.75$, $N^{max} = 2$, and short critical sections. The schedulability of the considered preemptable lock types in this configuration is shown in Fig. 1921.

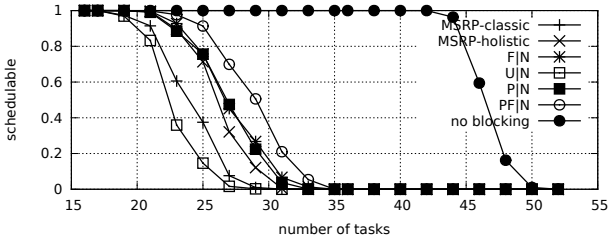

Fig. 1912. Schedulability under non-preemptable spin locks for $m = 16$, $U = 0.3n$, 16 resources, $rsf = 0.75$, $N^{max} = 5$, and short critical sections. The schedulability of the considered preemptable lock types in this configuration is shown in Fig. 1922.

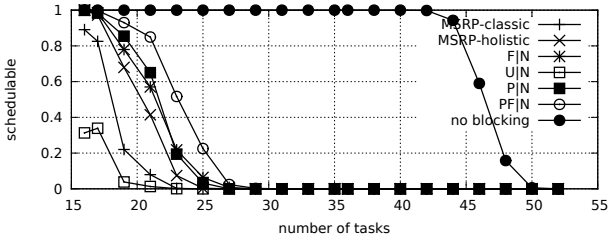

Fig. 1913. Schedulability under non-preemptable spin locks for $m = 16$, $U = 0.3n$, 16 resources, $rsf = 0.75$, $N^{max} = 10$, and short critical sections. The schedulability of the considered preemptable lock types in this configuration is shown in Fig. 1923.

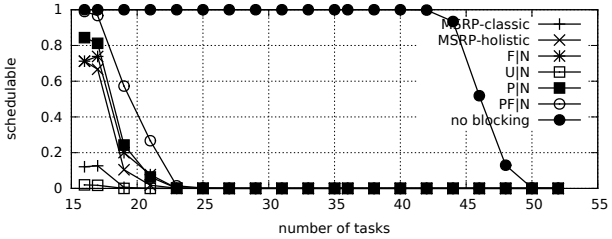

Fig. 1914. Schedulability under non-preemptable spin locks for $m = 16$, $U = 0.3n$, 16 resources, $rsf = 0.75$, $N^{max} = 15$, and short critical sections. The schedulability of the considered preemptable lock types in this configuration is shown in Fig. 1924.

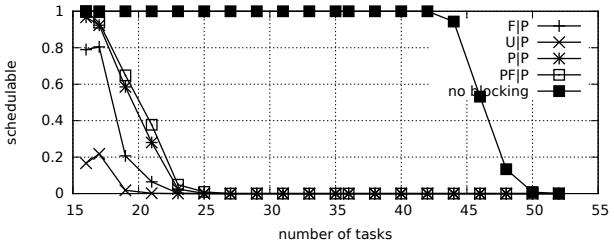

Fig. 1915. Schedulability under preemptable spin locks for $m = 16$, $U = 0.3n$, 16 resources, $rsf = 0.75$, $N^{max} = 1$, and medium critical sections. The schedulability of the considered non-preemptable lock types in this configuration is shown in Fig. 1905.

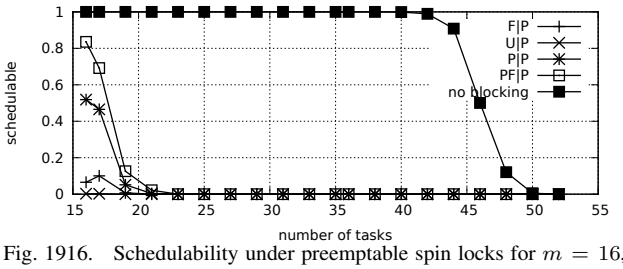

Fig. 1916. Schedulability under preemptable spin locks for $m = 16$, $U = 0.3n$, 16 resources, $rsf = 0.75$, $N^{max} = 2$, and medium critical sections. The schedulability of the considered non-preemptable lock types in this configuration is shown in Fig. 1906.

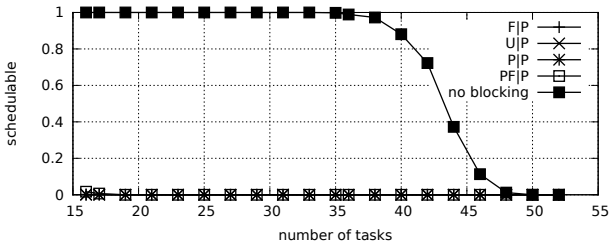

Fig. 1917. Schedulability under preemptable spin locks for $m = 16$, $U = 0.3n$, 16 resources, $rsf = 0.75$, $N^{max} = 5$, and medium critical sections. The schedulability of the considered non-preemptable lock types in this configuration is shown in Fig. 1907.

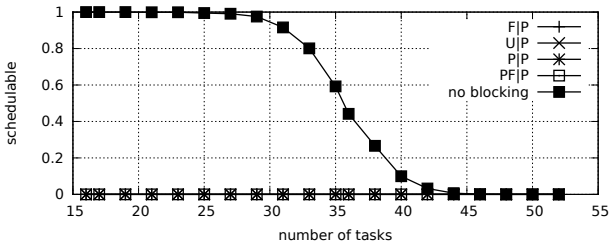

Fig. 1918. Schedulability under preemptable spin locks for $m = 16$, $U = 0.3n$, 16 resources, $rsf = 0.75$, $N^{max} = 10$, and medium critical sections. The schedulability of the considered non-preemptable lock types in this configuration is shown in Fig. 1908.

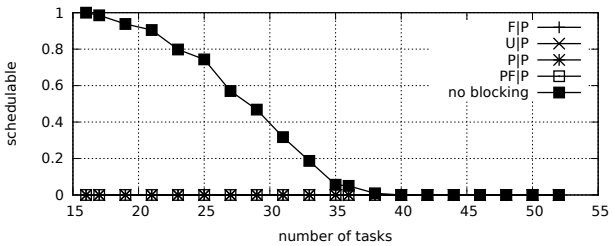

Fig. 1919. Schedulability under preemptable spin locks for $m = 16$, $U = 0.3n$, 16 resources, $rsf = 0.75$, $N^{max} = 15$, and medium critical sections. The schedulability of the considered non-preemptable lock types in this configuration is shown in Fig. 1909.

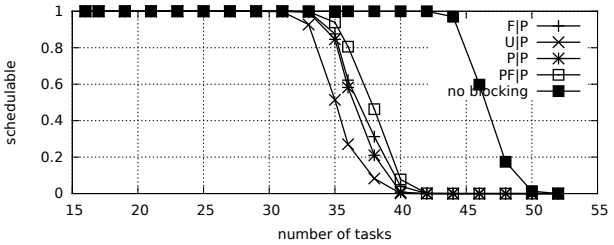

Fig. 1920. Schedulability under preemptable spin locks for $m = 16$, $U = 0.3n$, 16 resources, $rsf = 0.75$, $N^{max} = 1$, and short critical sections. The schedulability of the considered non-preemptable lock types in this configuration is shown in Fig. 1910.

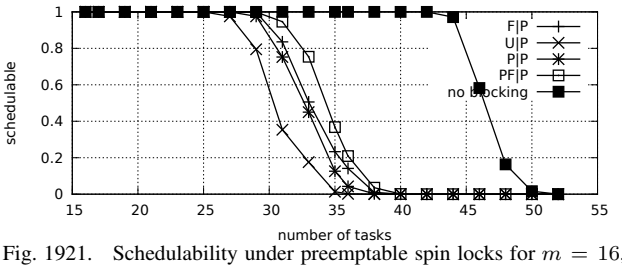

Fig. 1921. Schedulability under preemptable spin locks for $m = 16$, $U = 0.3n$, 16 resources, $rsf = 0.75$, $N^{max} = 2$, and short critical sections. The schedulability of the considered non-preemptable lock types in this configuration is shown in Fig. 1911.

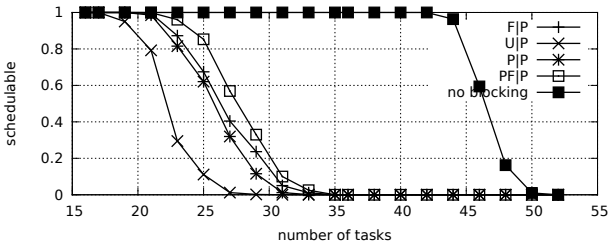

Fig. 1922. Schedulability under preemptable spin locks for $m = 16$, $U = 0.3n$, 16 resources, $rsf = 0.75$, $N^{max} = 5$, and short critical sections. The schedulability of the considered non-preemptable lock types in this configuration is shown in Fig. 1912.

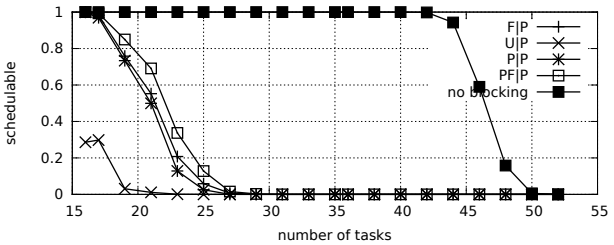

Fig. 1923. Schedulability under preemptable spin locks for $m = 16$, $U = 0.3n$, 16 resources, $rsf = 0.75$, $N^{max} = 10$, and short critical sections. The schedulability of the considered non-preemptable lock types in this configuration is shown in Fig. 1913.

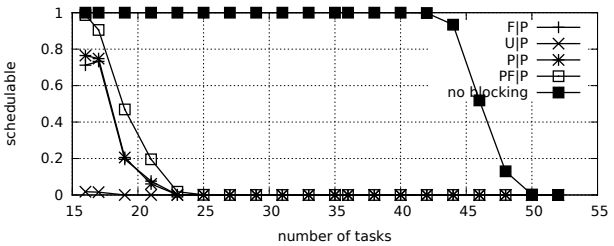

Fig. 1924. Schedulability under preemptable spin locks for $m = 16$, $U = 0.3n$, 16 resources, $rsf = 0.75$, $N^{max} = 15$, and short critical sections. The schedulability of the considered non-preemptable lock types in this configuration is shown in Fig. 1914.

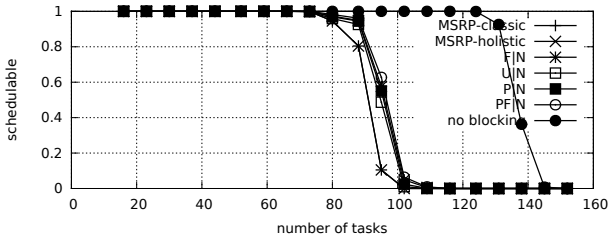

Fig. 1925. Schedulability under non-preemptable spin locks for $m = 16$, $U = 0.1n$, 32 resources, $rsf = 0.1$, $N^{max} = 1$, and medium critical sections. The schedulability of the considered preemptable lock types in this configuration is shown in Fig. 1935.

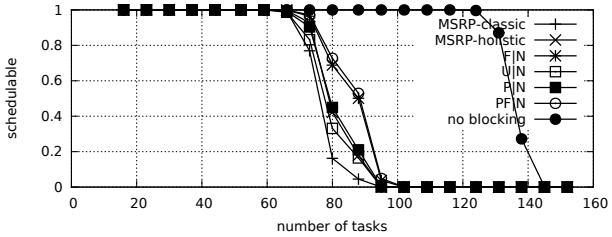

Fig. 1926. Schedulability under non-preemptable spin locks for $m = 16$, $U = 0.1n$, 32 resources, $rsf = 0.1$, $N^{max} = 2$, and medium critical sections. The schedulability of the considered preemptable lock types in this configuration is shown in Fig. 1936.

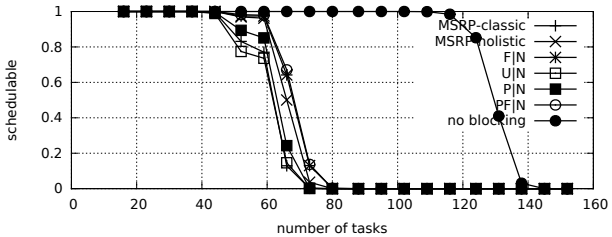

Fig. 1927. Schedulability under non-preemptable spin locks for $m = 16$, $U = 0.1n$, 32 resources, $rsf = 0.1$, $N^{max} = 5$, and medium critical sections. The schedulability of the considered preemptable lock types in this configuration is shown in Fig. 1937.

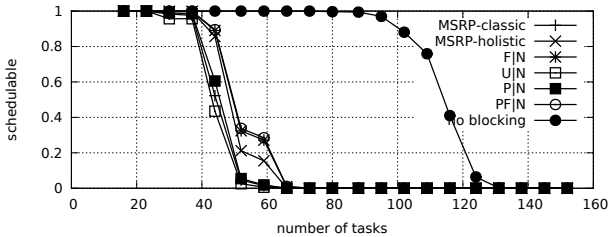

Fig. 1928. Schedulability under non-preemptable spin locks for $m = 16$, $U = 0.1n$, 32 resources, $rsf = 0.1$, $N^{max} = 10$, and medium critical sections. The schedulability of the considered preemptable lock types in this configuration is shown in Fig. 1938.

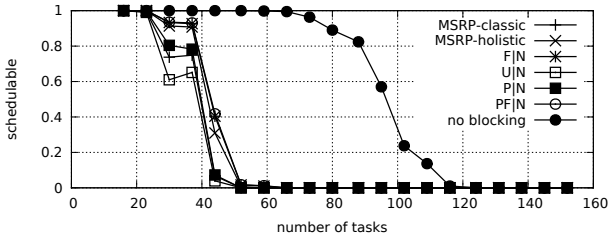

Fig. 1929. Schedulability under non-preemptable spin locks for $m = 16$, $U = 0.1n$, 32 resources, $rsf = 0.1$, $N^{max} = 15$, and medium critical sections. The schedulability of the considered preemptable lock types in this configuration is shown in Fig. 1939.

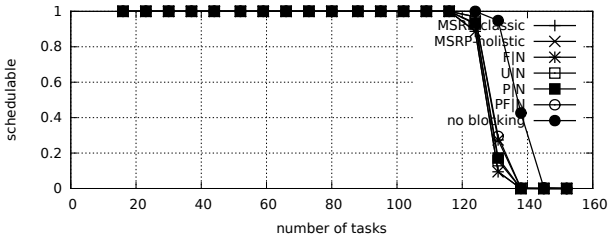

Fig. 1930. Schedulability under non-preemptable spin locks for $m = 16$, $U = 0.1n$, 32 resources, $rsf = 0.1$, $N^{max} = 1$, and short critical sections. The schedulability of the considered preemptable lock types in this configuration is shown in Fig. 1940.

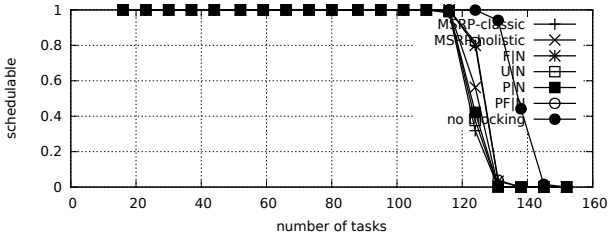

Fig. 1931. Schedulability under non-preemptable spin locks for $m = 16$, $U = 0.1n$, 32 resources, $rsf = 0.1$, $N^{max} = 2$, and short critical sections. The schedulability of the considered preemptable lock types in this configuration is shown in Fig. 1941.

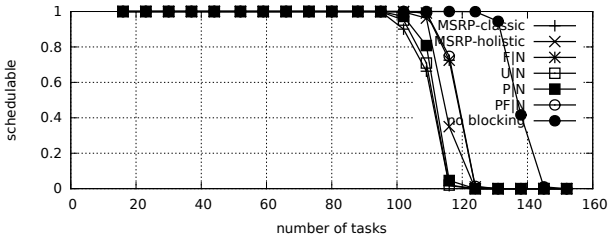

Fig. 1932. Schedulability under non-preemptable spin locks for $m = 16$, $U = 0.1n$, 32 resources, $rsf = 0.1$, $N^{max} = 5$, and short critical sections. The schedulability of the considered preemptable lock types in this configuration is shown in Fig. 1942.

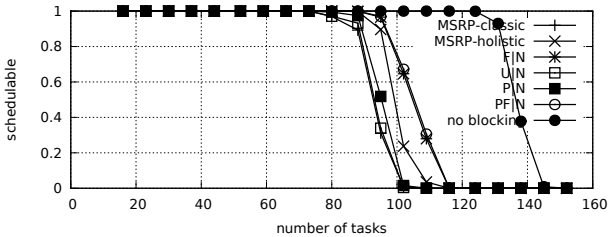

Fig. 1933. Schedulability under non-preemptable spin locks for $m = 16$, $U = 0.1n$, 32 resources, $rsf = 0.1$, $N^{max} = 10$, and short critical sections. The schedulability of the considered preemptable lock types in this configuration is shown in Fig. 1943.

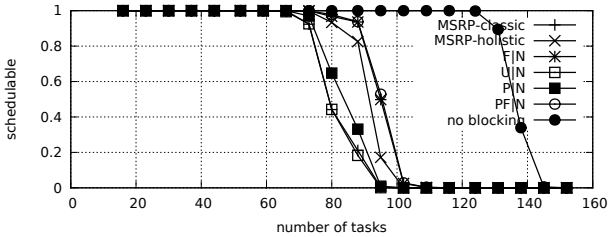

Fig. 1934. Schedulability under non-preemptable spin locks for $m = 16$, $U = 0.1n$, 32 resources, $rsf = 0.1$, $N^{max} = 15$, and short critical sections. The schedulability of the considered preemptable lock types in this configuration is shown in Fig. 1944.

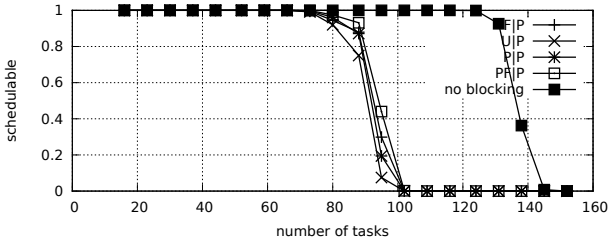

Fig. 1935. Schedulability under preemptable spin locks for $m = 16$, $U = 0.1n$, 32 resources, $rsf = 0.1$, $N^{max} = 1$, and medium critical sections. The schedulability of the considered non-preemptable lock types in this configuration is shown in Fig. 1925.

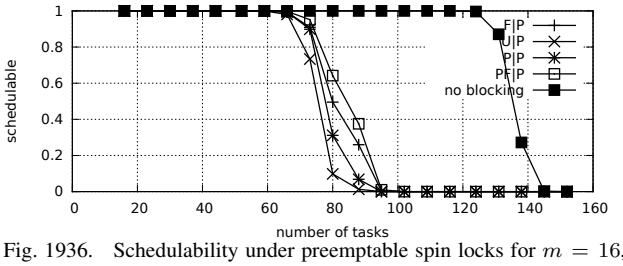

Fig. 1936. Schedulability under preemptable spin locks for $m = 16$, $U = 0.1n$, 32 resources, $rsf = 0.1$, $N^{max} = 2$, and medium critical sections. The schedulability of the considered non-preemptable lock types in this configuration is shown in Fig. 1926.

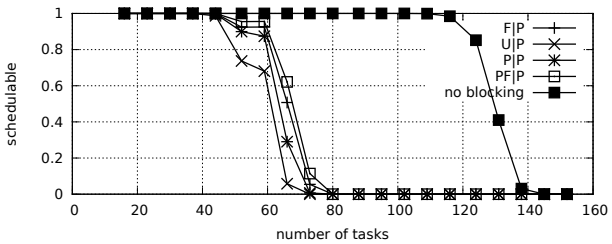

Fig. 1937. Schedulability under preemptable spin locks for $m = 16$, $U = 0.1n$, 32 resources, $rsf = 0.1$, $N^{max} = 5$, and medium critical sections. The schedulability of the considered non-preemptable lock types in this configuration is shown in Fig. 1927.

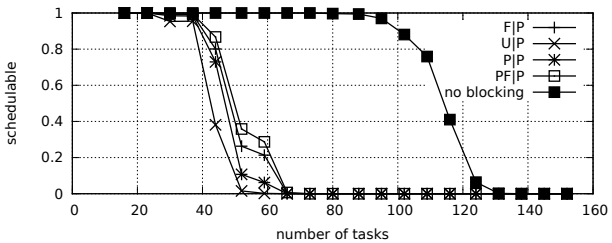

Fig. 1938. Schedulability under preemptable spin locks for $m = 16$, $U = 0.1n$, 32 resources, $rsf = 0.1$, $N^{max} = 10$, and medium critical sections. The schedulability of the considered non-preemptable lock types in this configuration is shown in Fig. 1928.

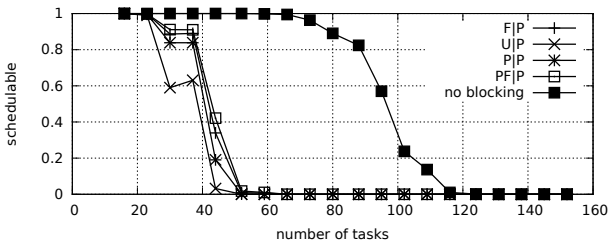

Fig. 1939. Schedulability under preemptable spin locks for $m = 16$, $U = 0.1n$, 32 resources, $rsf = 0.1$, $N^{max} = 15$, and medium critical sections. The schedulability of the considered non-preemptable lock types in this configuration is shown in Fig. 1929.

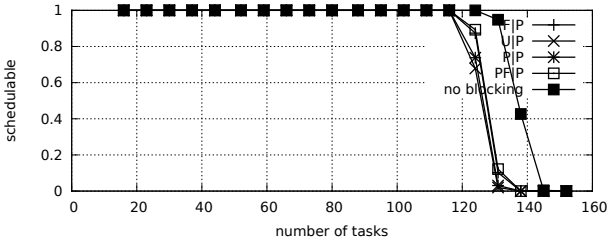

Fig. 1940. Schedulability under preemptable spin locks for $m = 16$, $U = 0.1n$, 32 resources, $rsf = 0.1$, $N^{max} = 1$, and short critical sections. The schedulability of the considered non-preemptable lock types in this configuration is shown in Fig. 1930.

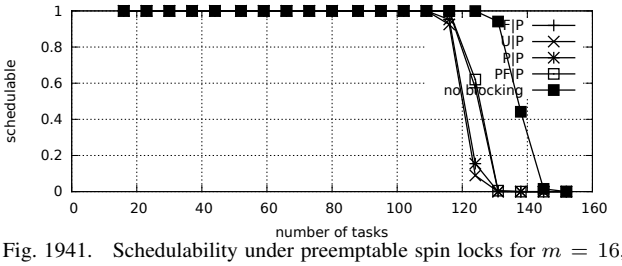

Fig. 1941. Schedulability under preemptable spin locks for $m = 16$, $U = 0.1n$, 32 resources, $rsf = 0.1$, $N^{max} = 2$, and short critical sections. The schedulability of the considered non-preemptable lock types in this configuration is shown in Fig. 1931.

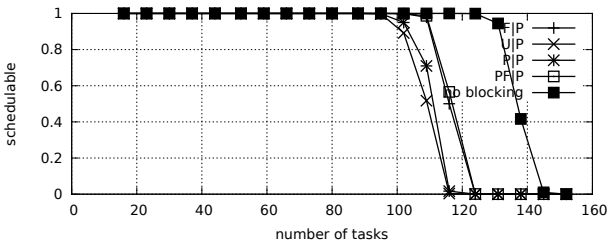

Fig. 1942. Schedulability under preemptable spin locks for $m = 16$, $U = 0.1n$, 32 resources, $rsf = 0.1$, $N^{max} = 5$, and short critical sections. The schedulability of the considered non-preemptable lock types in this configuration is shown in Fig. 1932.

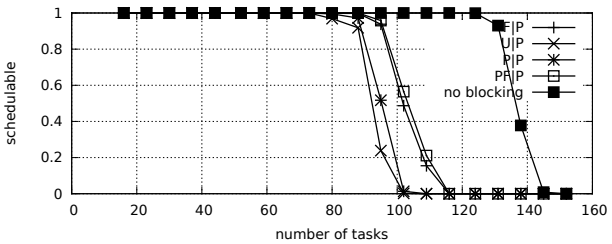

Fig. 1943. Schedulability under preemptable spin locks for $m = 16$, $U = 0.1n$, 32 resources, $rsf = 0.1$, $N^{max} = 10$, and short critical sections. The schedulability of the considered non-preemptable lock types in this configuration is shown in Fig. 1933.

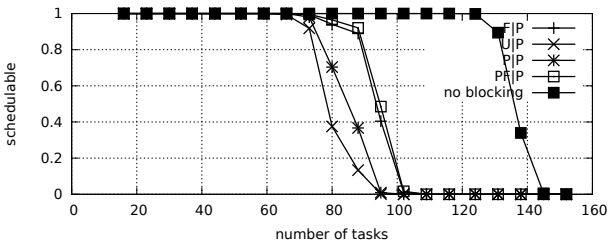

Fig. 1944. Schedulability under preemptable spin locks for $m = 16$, $U = 0.1n$, 32 resources, $rsf = 0.1$, $N^{max} = 15$, and short critical sections. The schedulability of the considered non-preemptable lock types in this configuration is shown in Fig. 1934.

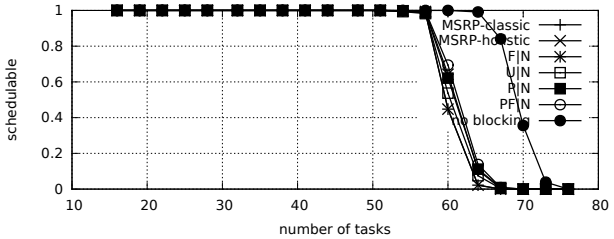

Fig. 1945. Schedulability under non-preemptable spin locks for $m = 16$, $U = 0.2n$, 32 resources, $rsf = 0.1$, $N^{max} = 1$, and medium critical sections. The schedulability of the considered preemptable lock types in this configuration is shown in Fig. 1955.

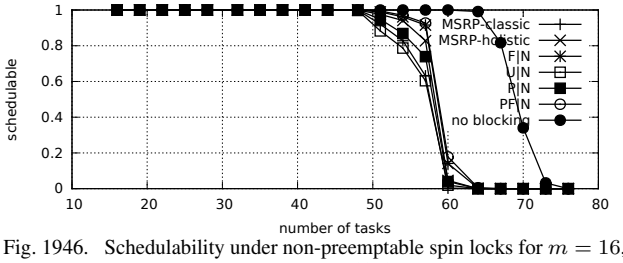

Fig. 1946. Schedulability under non-preemptable spin locks for $m = 16$, $U = 0.2n$, 32 resources, $rsf = 0.1$, $N^{max} = 2$, and medium critical sections. The schedulability of the considered preemptable lock types in this configuration is shown in Fig. 1956.

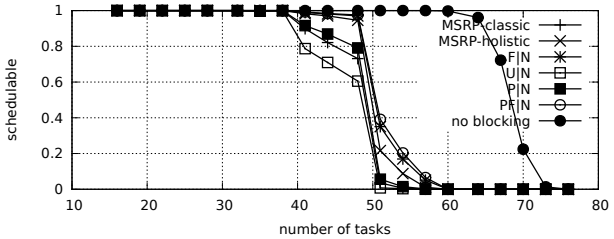

Fig. 1947. Schedulability under non-preemptable spin locks for $m = 16$, $U = 0.2n$, 32 resources, $rsf = 0.1$, $N^{max} = 5$, and medium critical sections. The schedulability of the considered preemptable lock types in this configuration is shown in Fig. 1957.

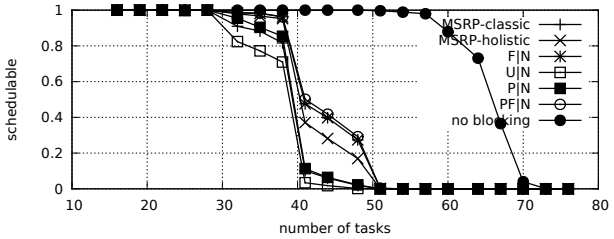

Fig. 1948. Schedulability under non-preemptable spin locks for $m = 16$, $U = 0.2n$, 32 resources, $rsf = 0.1$, $N^{max} = 10$, and medium critical sections. The schedulability of the considered preemptable lock types in this configuration is shown in Fig. 1958.

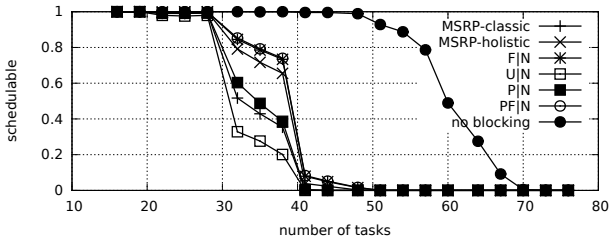

Fig. 1949. Schedulability under non-preemptable spin locks for $m = 16$, $U = 0.2n$, 32 resources, $rsf = 0.1$, $N^{max} = 15$, and medium critical sections. The schedulability of the considered preemptable lock types in this configuration is shown in Fig. 1959.

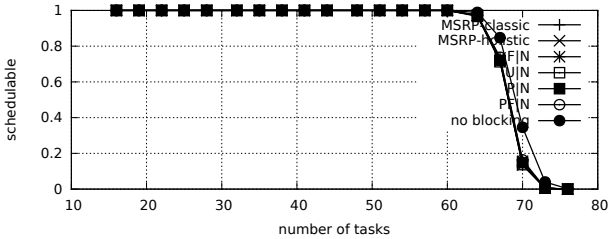

Fig. 1950. Schedulability under non-preemptable spin locks for $m = 16$, $U = 0.2n$, 32 resources, $rsf = 0.1$, $N^{max} = 1$, and short critical sections. The schedulability of the considered preemptable lock types in this configuration is shown in Fig. 1960.

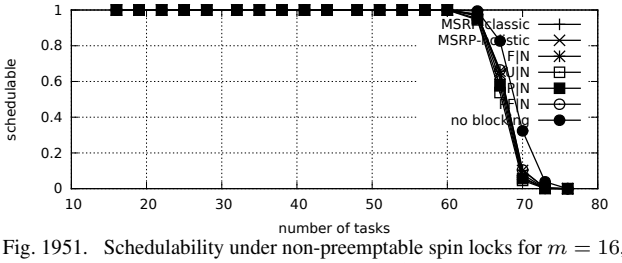

Fig. 1951. Schedulability under non-preemptable spin locks for $m = 16$, $U = 0.2n$, 32 resources, $rsf = 0.1$, $N^{max} = 2$, and short critical sections. The schedulability of the considered preemptable lock types in this configuration is shown in Fig. 1961.

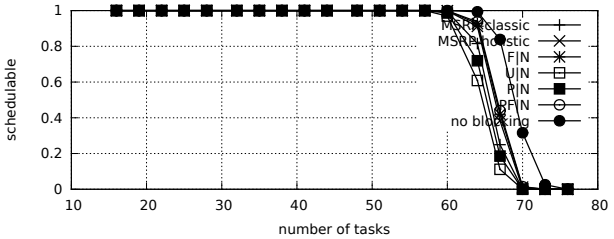

Fig. 1952. Schedulability under non-preemptable spin locks for $m = 16$, $U = 0.2n$, 32 resources, $rsf = 0.1$, $N^{max} = 5$, and short critical sections. The schedulability of the considered preemptable lock types in this configuration is shown in Fig. 1962.

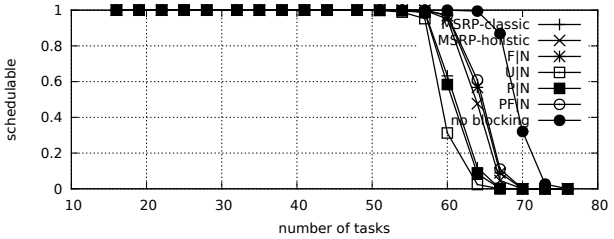

Fig. 1953. Schedulability under non-preemptable spin locks for $m = 16$, $U = 0.2n$, 32 resources, $rsf = 0.1$, $N^{max} = 10$, and short critical sections. The schedulability of the considered preemptable lock types in this configuration is shown in Fig. 1963.

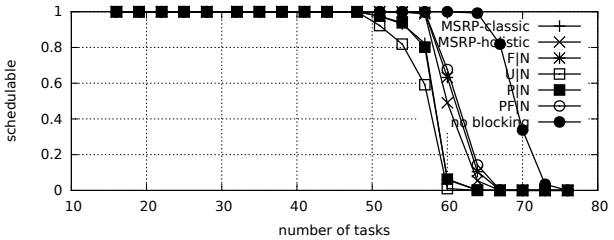

Fig. 1954. Schedulability under non-preemptable spin locks for $m = 16$, $U = 0.2n$, 32 resources, $rsf = 0.1$, $N^{max} = 15$, and short critical sections. The schedulability of the considered preemptable lock types in this configuration is shown in Fig. 1964.

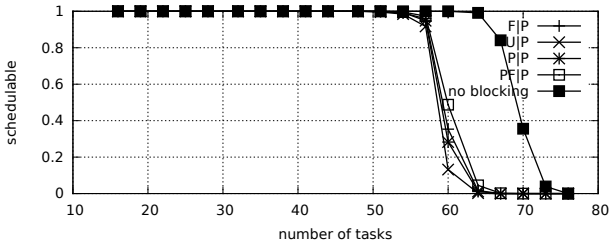

Fig. 1955. Schedulability under preemptable spin locks for $m = 16$, $U = 0.2n$, 32 resources, $rsf = 0.1$, $N^{max} = 1$, and medium critical sections. The schedulability of the considered non-preemptable lock types in this configuration is shown in Fig. 1945.

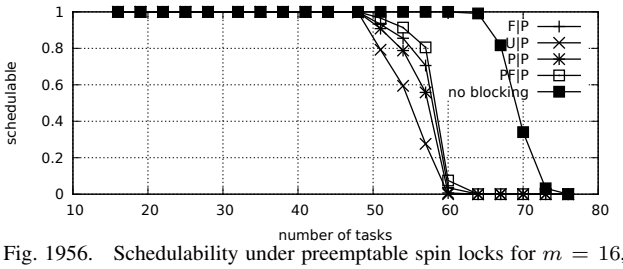

Fig. 1956. Schedulability under preemptable spin locks for $m = 16$, $U = 0.2n$, 32 resources, $rsf = 0.1$, $N^{max} = 2$, and medium critical sections. The schedulability of the considered non-preemptable lock types in this configuration is shown in Fig. 1946.

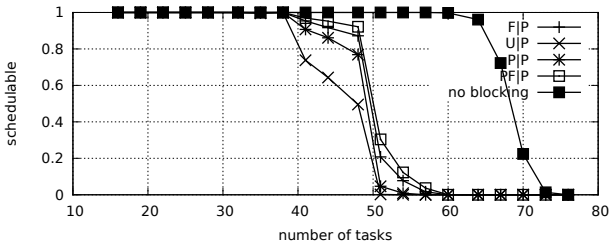

Fig. 1957. Schedulability under preemptable spin locks for $m = 16$, $U = 0.2n$, 32 resources, $rsf = 0.1$, $N^{max} = 5$, and medium critical sections. The schedulability of the considered non-preemptable lock types in this configuration is shown in Fig. 1947.

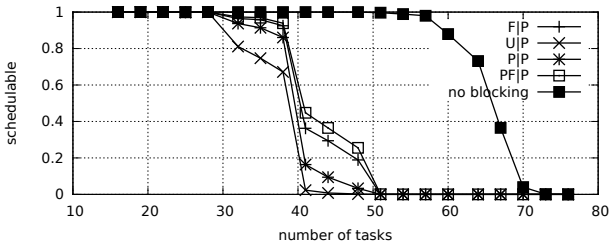

Fig. 1958. Schedulability under preemptable spin locks for $m = 16$, $U = 0.2n$, 32 resources, $rsf = 0.1$, $N^{max} = 10$, and medium critical sections. The schedulability of the considered non-preemptable lock types in this configuration is shown in Fig. 1948.

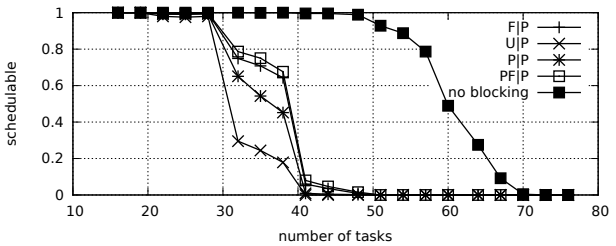

Fig. 1959. Schedulability under preemptable spin locks for $m = 16$, $U = 0.2n$, 32 resources, $rsf = 0.1$, $N^{max} = 15$, and medium critical sections. The schedulability of the considered non-preemptable lock types in this configuration is shown in Fig. 1949.

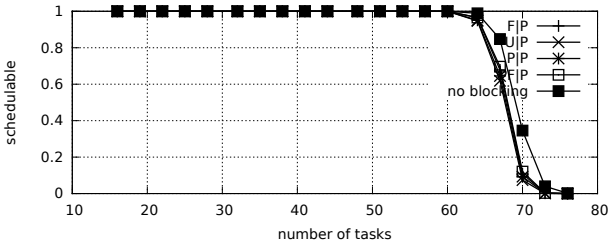

Fig. 1960. Schedulability under preemptable spin locks for $m = 16$, $U = 0.2n$, 32 resources, $rsf = 0.1$, $N^{max} = 1$, and short critical sections. The schedulability of the considered non-preemptable lock types in this configuration is shown in Fig. 1950.

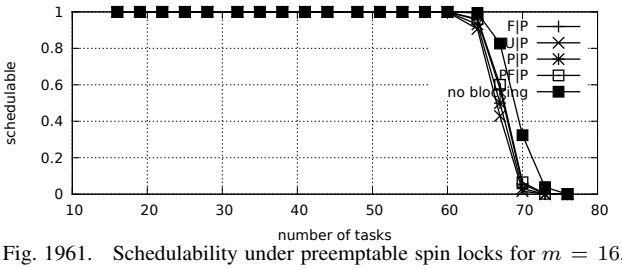

Fig. 1961. Schedulability under preemptable spin locks for $m = 16$, $U = 0.2n$, 32 resources, $rsf = 0.1$, $N^{max} = 2$, and short critical sections. The schedulability of the considered non-preemptable lock types in this configuration is shown in Fig. 1951.

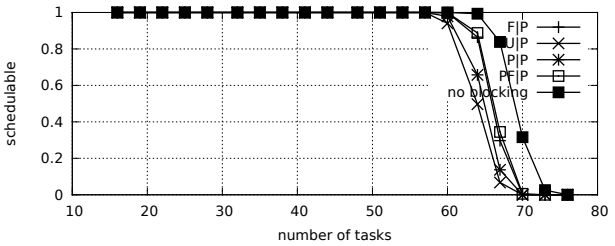

Fig. 1962. Schedulability under preemptable spin locks for $m = 16$, $U = 0.2n$, 32 resources, $rsf = 0.1$, $N^{max} = 5$, and short critical sections. The schedulability of the considered non-preemptable lock types in this configuration is shown in Fig. 1952.

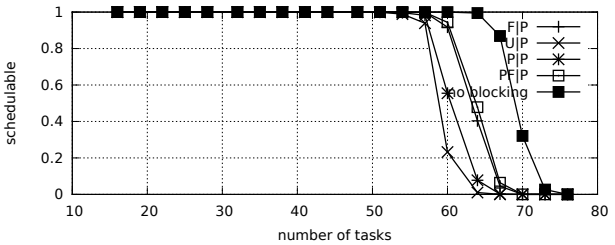

Fig. 1963. Schedulability under preemptable spin locks for $m = 16$, $U = 0.2n$, 32 resources, $rsf = 0.1$, $N^{max} = 10$, and short critical sections. The schedulability of the considered non-preemptable lock types in this configuration is shown in Fig. 1953.

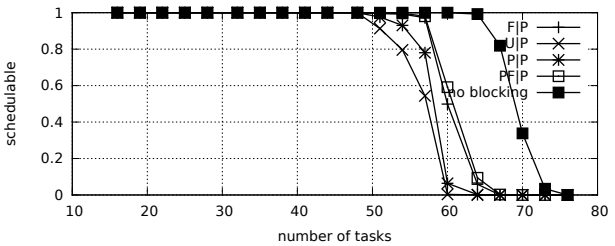

Fig. 1964. Schedulability under preemptable spin locks for $m = 16$, $U = 0.2n$, 32 resources, $rsf = 0.1$, $N^{max} = 15$, and short critical sections. The schedulability of the considered non-preemptable lock types in this configuration is shown in Fig. 1954.

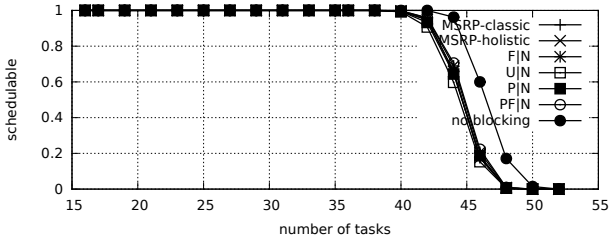

Fig. 1965. Schedulability under non-preemptable spin locks for $m = 16$, $U = 0.3n$, 32 resources, $rsf = 0.1$, $N^{max} = 1$, and medium critical sections. The schedulability of the considered preemptable lock types in this configuration is shown in Fig. 1975.

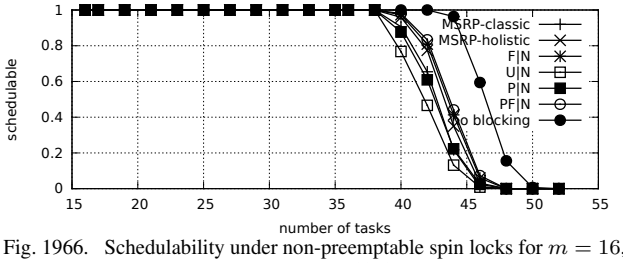

Fig. 1966. Schedulability under non-preemptable spin locks for $m = 16$, $U = 0.3n$, 32 resources, $rsf = 0.1$, $N^{max} = 2$, and medium critical sections. The schedulability of the considered preemptable lock types in this configuration is shown in Fig. 1976.

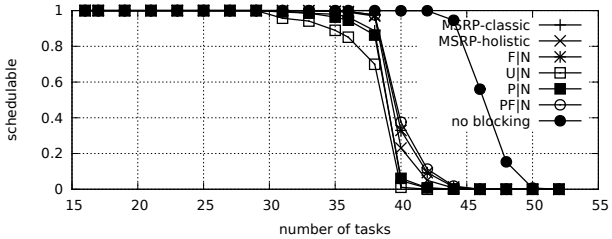

Fig. 1967. Schedulability under non-preemptable spin locks for $m = 16$, $U = 0.3n$, 32 resources, $rsf = 0.1$, $N^{max} = 5$, and medium critical sections. The schedulability of the considered preemptable lock types in this configuration is shown in Fig. 1977.

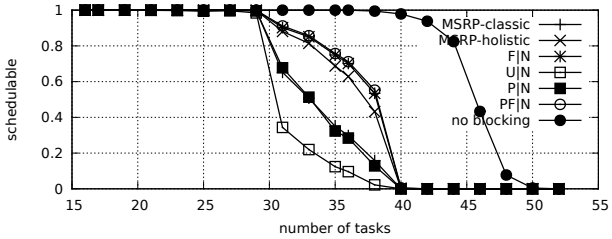

Fig. 1968. Schedulability under non-preemptable spin locks for $m = 16$, $U = 0.3n$, 32 resources, $rsf = 0.1$, $N^{max} = 10$, and medium critical sections. The schedulability of the considered preemptable lock types in this configuration is shown in Fig. 1978.

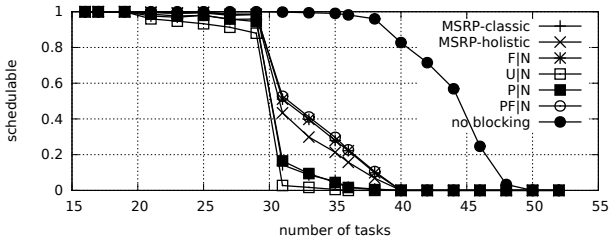

Fig. 1969. Schedulability under non-preemptable spin locks for $m = 16$, $U = 0.3n$, 32 resources, $rsf = 0.1$, $N^{max} = 15$, and medium critical sections. The schedulability of the considered preemptable lock types in this configuration is shown in Fig. 1979.

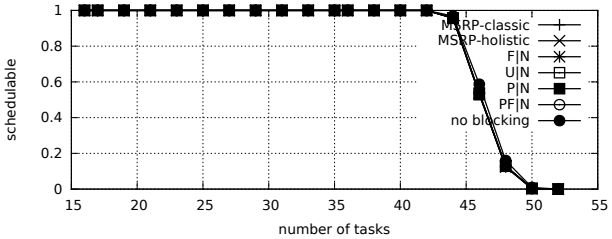

Fig. 1970. Schedulability under non-preemptable spin locks for $m = 16$, $U = 0.3n$, 32 resources, $rsf = 0.1$, $N^{max} = 1$, and short critical sections. The schedulability of the considered preemptable lock types in this configuration is shown in Fig. 1980.

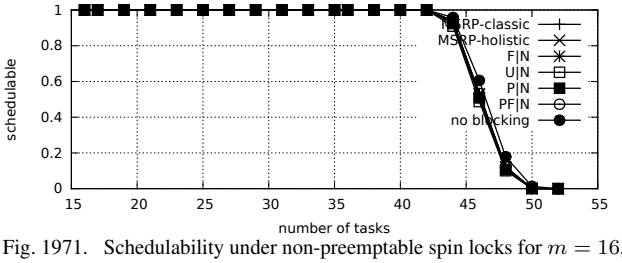

Fig. 1971. Schedulability under non-preemptable spin locks for $m = 16$, $U = 0.3n$, 32 resources, $rsf = 0.1$, $N^{max} = 2$, and short critical sections. The schedulability of the considered preemptable lock types in this configuration is shown in Fig. 1981.

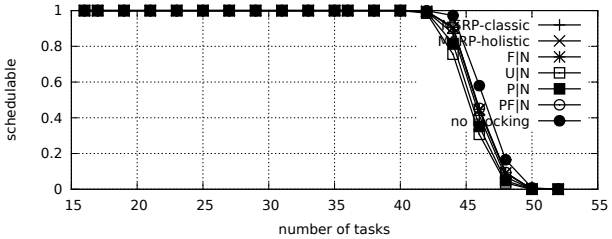

Fig. 1972. Schedulability under non-preemptable spin locks for $m = 16$, $U = 0.3n$, 32 resources, $rsf = 0.1$, $N^{max} = 5$, and short critical sections. The schedulability of the considered preemptable lock types in this configuration is shown in Fig. 1982.

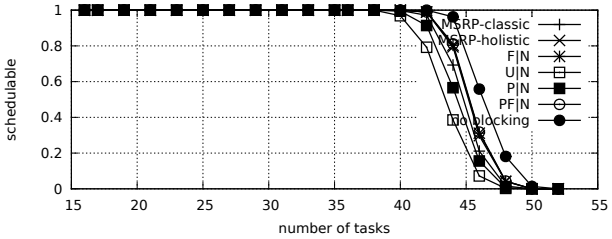

Fig. 1973. Schedulability under non-preemptable spin locks for $m = 16$, $U = 0.3n$, 32 resources, $rsf = 0.1$, $N^{max} = 10$, and short critical sections. The schedulability of the considered preemptable lock types in this configuration is shown in Fig. 1983.

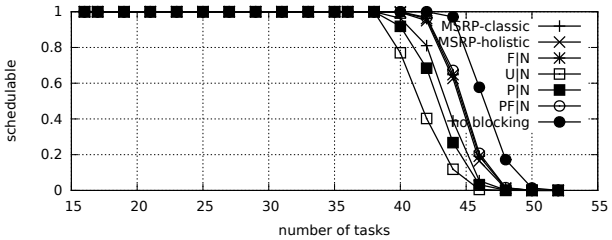

Fig. 1974. Schedulability under non-preemptable spin locks for $m = 16$, $U = 0.3n$, 32 resources, $rsf = 0.1$, $N^{max} = 15$, and short critical sections. The schedulability of the considered preemptable lock types in this configuration is shown in Fig. 1984.

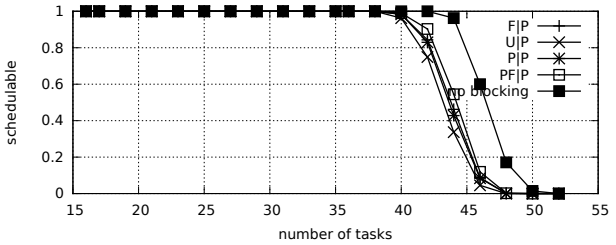

Fig. 1975. Schedulability under preemptable spin locks for $m = 16$, $U = 0.3n$, 32 resources, $rsf = 0.1$, $N^{max} = 1$, and medium critical sections. The schedulability of the considered non-preemptable lock types in this configuration is shown in Fig. 1965.

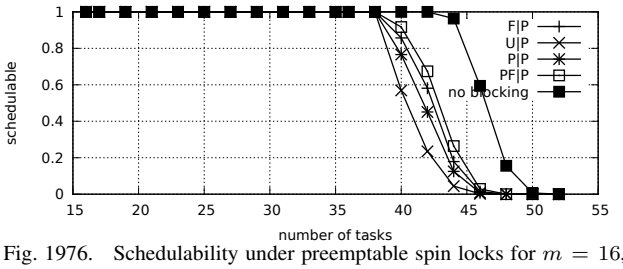

Fig. 1976. Schedulability under preemptable spin locks for $m = 16$, $U = 0.3n$, 32 resources, $rsf = 0.1$, $N^{max} = 2$, and medium critical sections. The schedulability of the considered non-preemptable lock types in this configuration is shown in Fig. 1966.

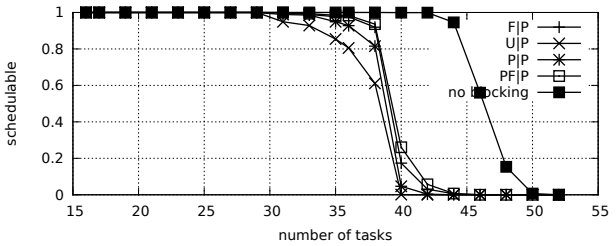

Fig. 1977. Schedulability under preemptable spin locks for $m = 16$, $U = 0.3n$, 32 resources, $rsf = 0.1$, $N^{max} = 5$, and medium critical sections. The schedulability of the considered non-preemptable lock types in this configuration is shown in Fig. 1967.

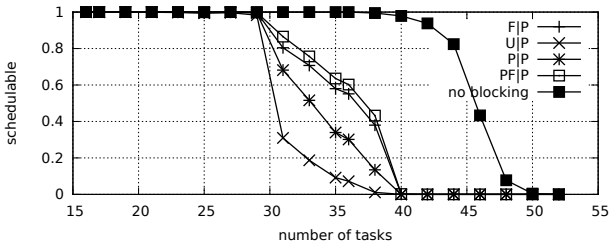

Fig. 1978. Schedulability under preemptable spin locks for $m = 16$, $U = 0.3n$, 32 resources, $rsf = 0.1$, $N^{max} = 10$, and medium critical sections. The schedulability of the considered non-preemptable lock types in this configuration is shown in Fig. 1968.

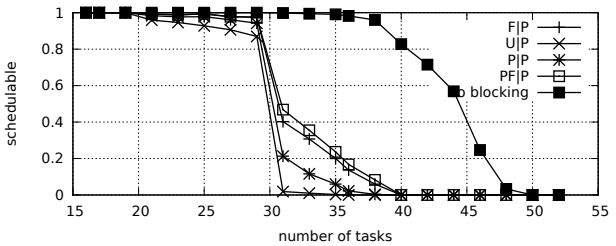

Fig. 1979. Schedulability under preemptable spin locks for $m = 16$, $U = 0.3n$, 32 resources, $rsf = 0.1$, $N^{max} = 15$, and medium critical sections. The schedulability of the considered non-preemptable lock types in this configuration is shown in Fig. 1969.

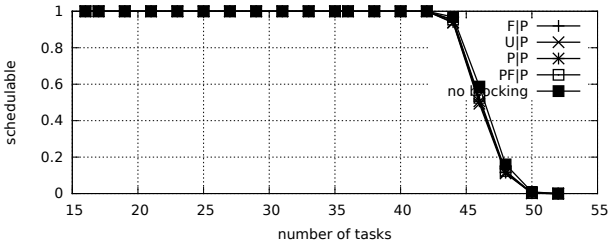

Fig. 1980. Schedulability under preemptable spin locks for $m = 16$, $U = 0.3n$, 32 resources, $rsf = 0.1$, $N^{max} = 1$, and short critical sections. The schedulability of the considered non-preemptable lock types in this configuration is shown in Fig. 1970.

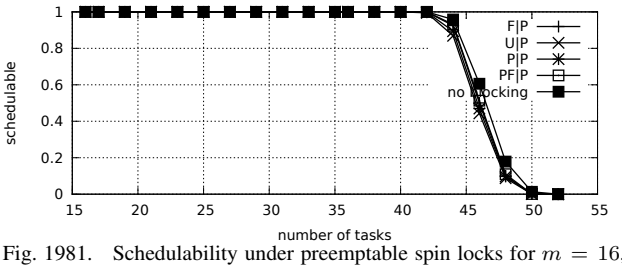

Fig. 1981. Schedulability under preemptable spin locks for $m = 16$, $U = 0.3n$, 32 resources, $rsf = 0.1$, $N^{max} = 2$, and short critical sections. The schedulability of the considered non-preemptable lock types in this configuration is shown in Fig. 1971.

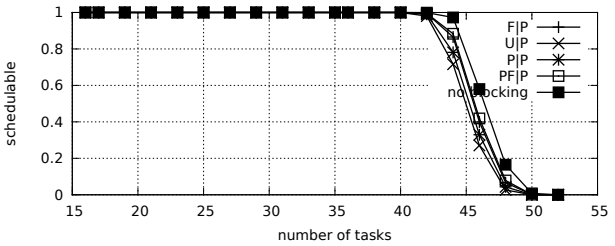

Fig. 1982. Schedulability under preemptable spin locks for $m = 16$, $U = 0.3n$, 32 resources, $rsf = 0.1$, $N^{max} = 5$, and short critical sections. The schedulability of the considered non-preemptable lock types in this configuration is shown in Fig. 1972.

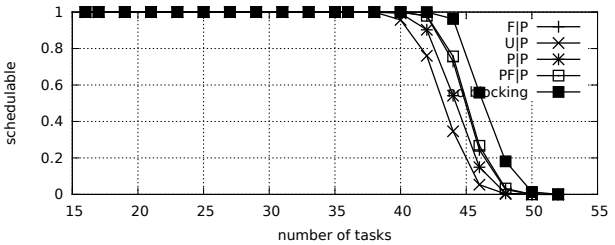

Fig. 1983. Schedulability under preemptable spin locks for $m = 16$, $U = 0.3n$, 32 resources, $rsf = 0.1$, $N^{max} = 10$, and short critical sections. The schedulability of the considered non-preemptable lock types in this configuration is shown in Fig. 1973.

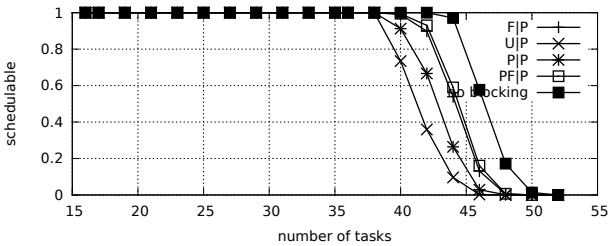

Fig. 1984. Schedulability under preemptable spin locks for $m = 16$, $U = 0.3n$, 32 resources, $rsf = 0.1$, $N^{max} = 15$, and short critical sections. The schedulability of the considered non-preemptable lock types in this configuration is shown in Fig. 1974.

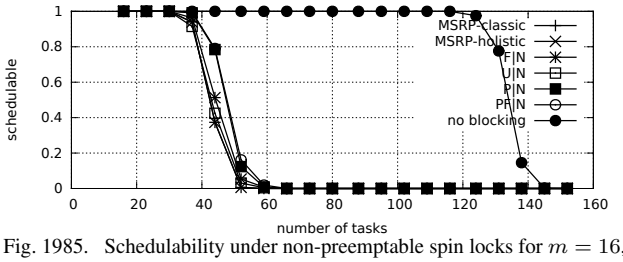

Fig. 1985. Schedulability under non-preemptable spin locks for $m = 16$, $U = 0.1n$, 32 resources, $rsf = 0.25$, $N^{max} = 1$, and medium critical sections. The schedulability of the considered preemptable lock types in this configuration is shown in Fig. 1995.

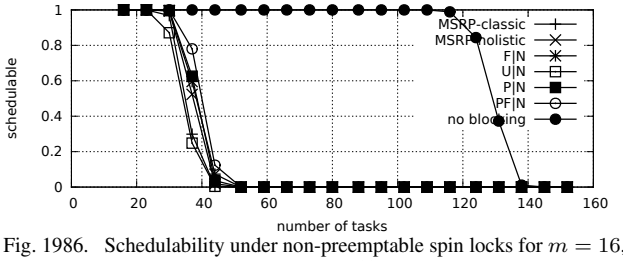

Fig. 1986. Schedulability under non-preemptable spin locks for $m = 16$, $U = 0.1n$, 32 resources, $rsf = 0.25$, $N^{max} = 2$, and medium critical sections. The schedulability of the considered preemptable lock types in this configuration is shown in Fig. 1996.

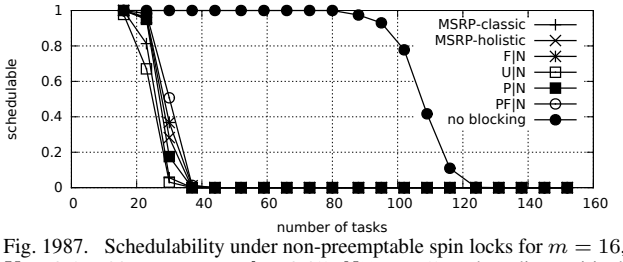

Fig. 1987. Schedulability under non-preemptable spin locks for $m = 16$, $U = 0.1n$, 32 resources, $rsf = 0.25$, $N^{max} = 5$, and medium critical sections. The schedulability of the considered preemptable lock types in this configuration is shown in Fig. 1997.

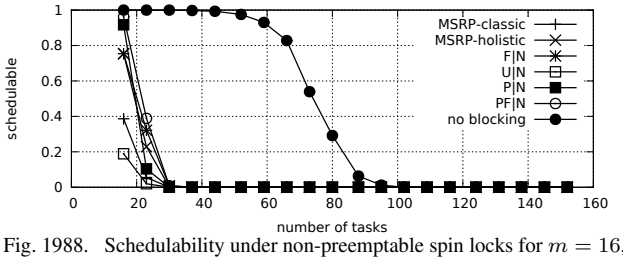

Fig. 1988. Schedulability under non-preemptable spin locks for $m = 16$, $U = 0.1n$, 32 resources, $rsf = 0.25$, $N^{max} = 10$, and medium critical sections. The schedulability of the considered preemptable lock types in this configuration is shown in Fig. 1998.

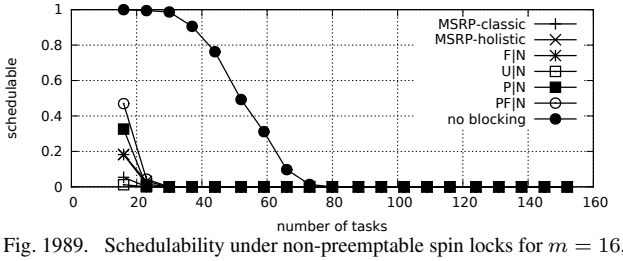

Fig. 1989. Schedulability under non-preemptable spin locks for $m = 16$, $U = 0.1n$, 32 resources, $rsf = 0.25$, $N^{max} = 15$, and medium critical sections. The schedulability of the considered preemptable lock types in this configuration is shown in Fig. 1999.

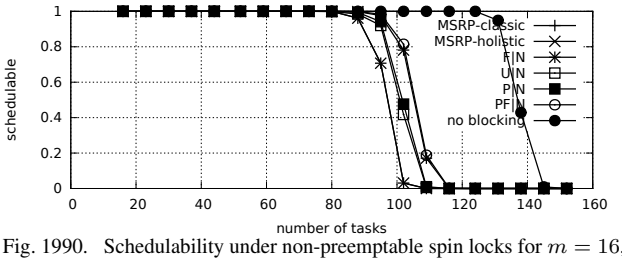

Fig. 1990. Schedulability under non-preemptable spin locks for $m = 16$, $U = 0.1n$, 32 resources, $rsf = 0.25$, $N^{max} = 1$, and short critical sections. The schedulability of the considered preemptable lock types in this configuration is shown in Fig. 2000.

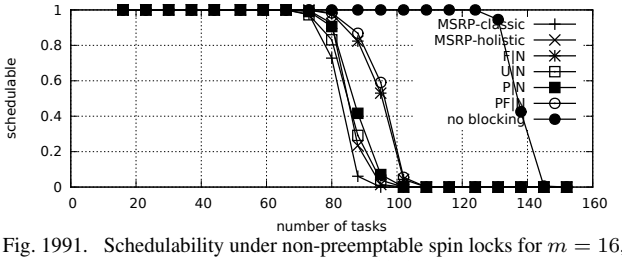

Fig. 1991. Schedulability under non-preemptable spin locks for $m = 16$, $U = 0.1n$, 32 resources, $rsf = 0.25$, $N^{max} = 2$, and short critical sections. The schedulability of the considered preemptable lock types in this configuration is shown in Fig. 2001.

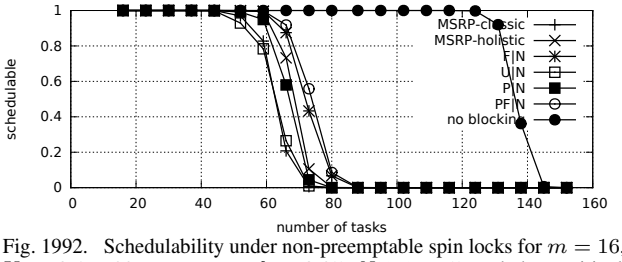

Fig. 1992. Schedulability under non-preemptable spin locks for $m = 16$, $U = 0.1n$, 32 resources, $rsf = 0.25$, $N^{max} = 5$, and short critical sections. The schedulability of the considered preemptable lock types in this configuration is shown in Fig. 2002.

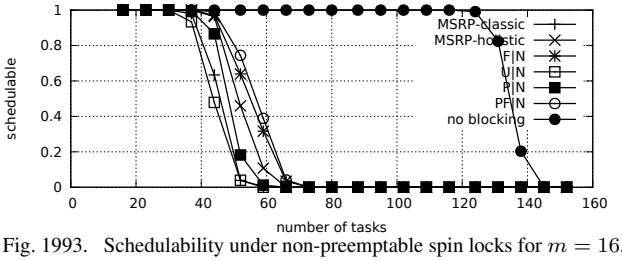

Fig. 1993. Schedulability under non-preemptable spin locks for $m = 16$, $U = 0.1n$, 32 resources, $rsf = 0.25$, $N^{max} = 10$, and short critical sections. The schedulability of the considered preemptable lock types in this configuration is shown in Fig. 2003.

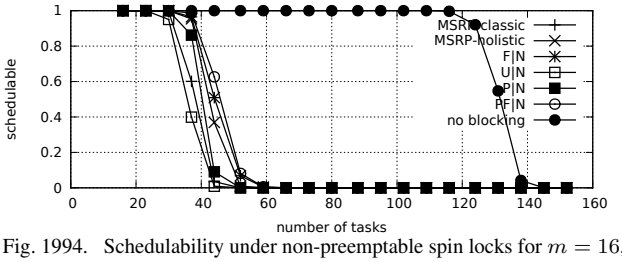

Fig. 1994. Schedulability under non-preemptable spin locks for $m = 16$, $U = 0.1n$, 32 resources, $rsf = 0.25$, $N^{max} = 15$, and short critical sections. The schedulability of the considered preemptable lock types in this configuration is shown in Fig. 2004.

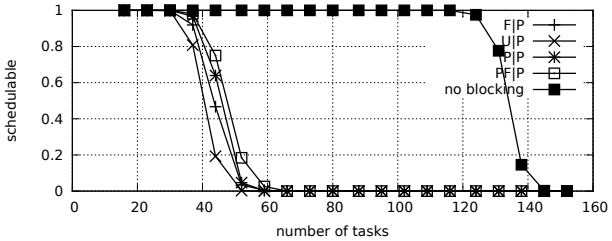

Fig. 1995. Schedulability under preemptable spin locks for $m = 16$, $U = 0.1n$, 32 resources, $rsf = 0.25$, $N^{max} = 1$, and medium critical sections. The schedulability of the considered non-preemptable lock types in this configuration is shown in Fig. 1985.

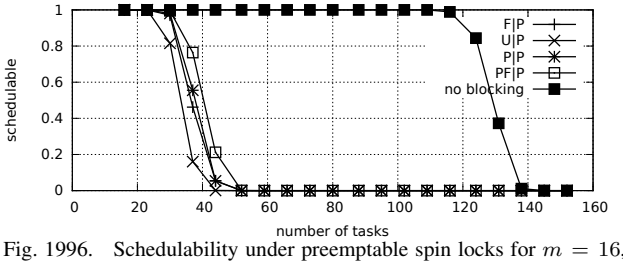

Fig. 1996. Schedulability under preemptable spin locks for $m = 16$, $U = 0.1n$, 32 resources, $rsf = 0.25$, $N^{max} = 2$, and medium critical sections. The schedulability of the considered non-preemptable lock types in this configuration is shown in Fig. 1986.

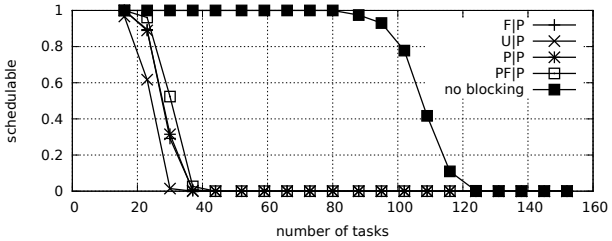

Fig. 1997. Schedulability under preemptable spin locks for $m = 16$, $U = 0.1n$, 32 resources, $rsf = 0.25$, $N^{max} = 5$, and medium critical sections. The schedulability of the considered non-preemptable lock types in this configuration is shown in Fig. 1987.

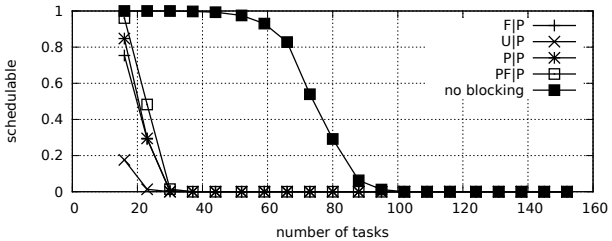

Fig. 1998. Schedulability under preemptable spin locks for $m = 16$, $U = 0.1n$, 32 resources, $rsf = 0.25$, $N^{max} = 10$, and medium critical sections. The schedulability of the considered non-preemptable lock types in this configuration is shown in Fig. 1988.

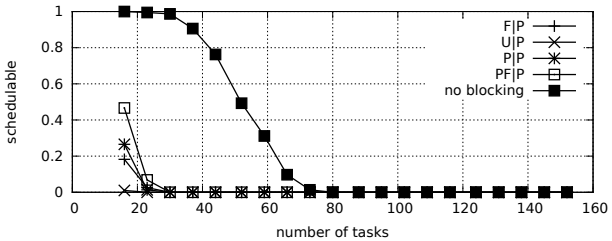

Fig. 1999. Schedulability under preemptable spin locks for $m = 16$, $U = 0.1n$, 32 resources, $rsf = 0.25$, $N^{max} = 15$, and medium critical sections. The schedulability of the considered non-preemptable lock types in this configuration is shown in Fig. 1989.

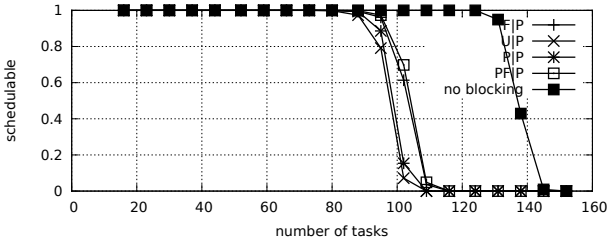

Fig. 2000. Schedulability under preemptable spin locks for $m = 16$, $U = 0.1n$, 32 resources, $rsf = 0.25$, $N^{max} = 1$, and short critical sections. The schedulability of the considered non-preemptable lock types in this configuration is shown in Fig. 1990.

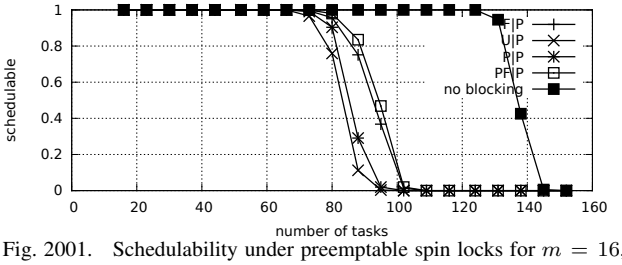

Fig. 2001. Schedulability under preemptable spin locks for $m = 16$, $U = 0.1n$, 32 resources, $rsf = 0.25$, $N^{max} = 2$, and short critical sections. The schedulability of the considered non-preemptable lock types in this configuration is shown in Fig. 1991.

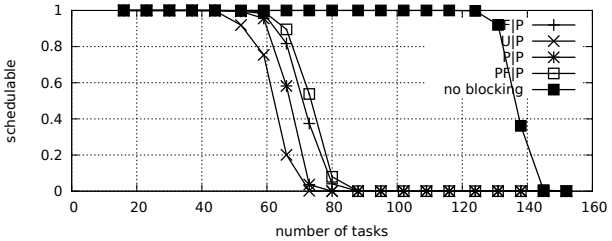

Fig. 2002. Schedulability under preemptable spin locks for $m = 16$, $U = 0.1n$, 32 resources, $rsf = 0.25$, $N^{max} = 5$, and short critical sections. The schedulability of the considered non-preemptable lock types in this configuration is shown in Fig. 1992.

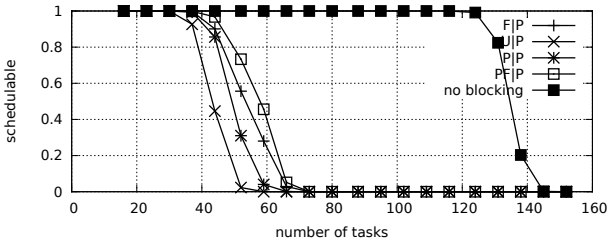

Fig. 2003. Schedulability under preemptable spin locks for $m = 16$, $U = 0.1n$, 32 resources, $rsf = 0.25$, $N^{max} = 10$, and short critical sections. The schedulability of the considered non-preemptable lock types in this configuration is shown in Fig. 1993.

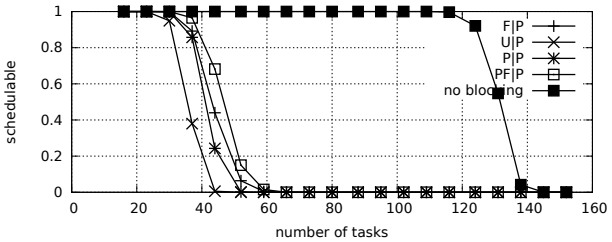

Fig. 2004. Schedulability under preemptable spin locks for $m = 16$, $U = 0.1n$, 32 resources, $rsf = 0.25$, $N^{max} = 15$, and short critical sections. The schedulability of the considered non-preemptable lock types in this configuration is shown in Fig. 1994.

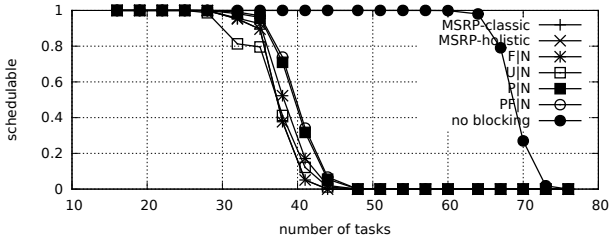

Fig. 2005. Schedulability under non-preemptable spin locks for $m = 16$, $U = 0.2n$, 32 resources, $rsf = 0.25$, $N^{max} = 1$, and medium critical sections. The schedulability of the considered preemptable lock types in this configuration is shown in Fig. 2015.

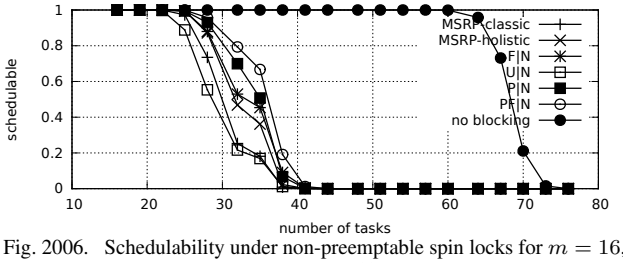

Fig. 2006. Schedulability under non-preemptable spin locks for $m = 16$, $U = 0.2n$, 32 resources, $rsf = 0.25$, $N^{max} = 2$, and medium critical sections. The schedulability of the considered preemptable lock types in this configuration is shown in Fig. 2016.

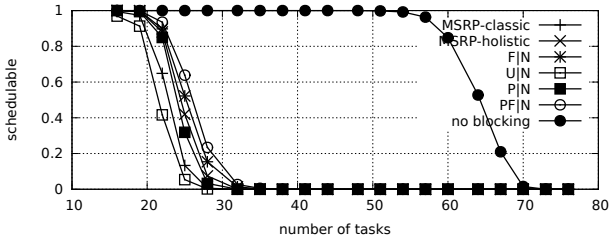

Fig. 2007. Schedulability under non-preemptable spin locks for $m = 16$, $U = 0.2n$, 32 resources, $rsf = 0.25$, $N^{max} = 5$, and medium critical sections. The schedulability of the considered preemptable lock types in this configuration is shown in Fig. 2017.

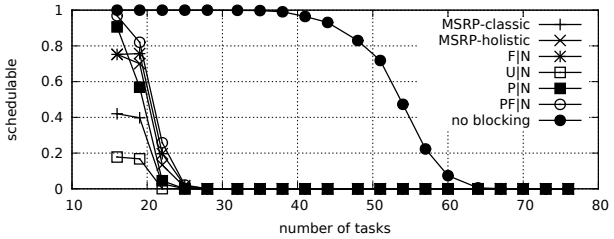

Fig. 2008. Schedulability under non-preemptable spin locks for $m = 16$, $U = 0.2n$, 32 resources, $rsf = 0.25$, $N^{max} = 10$, and medium critical sections. The schedulability of the considered preemptable lock types in this configuration is shown in Fig. 2018.

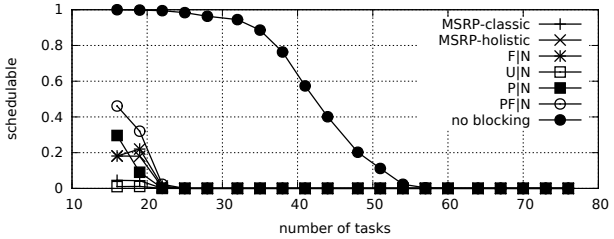

Fig. 2009. Schedulability under non-preemptable spin locks for $m = 16$, $U = 0.2n$, 32 resources, $rsf = 0.25$, $N^{max} = 15$, and medium critical sections. The schedulability of the considered preemptable lock types in this configuration is shown in Fig. 2019.

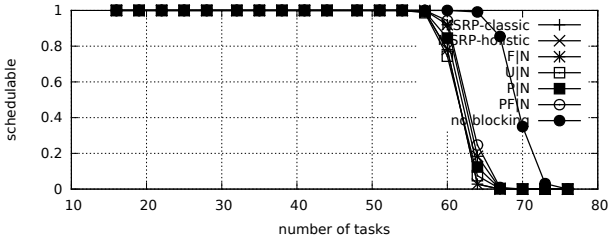

Fig. 2010. Schedulability under non-preemptable spin locks for $m = 16$, $U = 0.2n$, 32 resources, $rsf = 0.25$, $N^{max} = 1$, and short critical sections. The schedulability of the considered preemptable lock types in this configuration is shown in Fig. 2020.

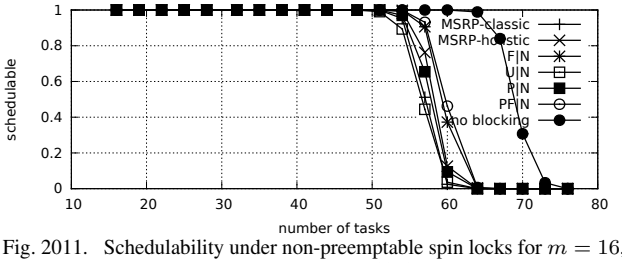

Fig. 2011. Schedulability under non-preemptable spin locks for $m = 16$, $U = 0.2n$, 32 resources, $rsf = 0.25$, $N^{max} = 2$, and short critical sections. The schedulability of the considered preemptable lock types in this configuration is shown in Fig. 2021.

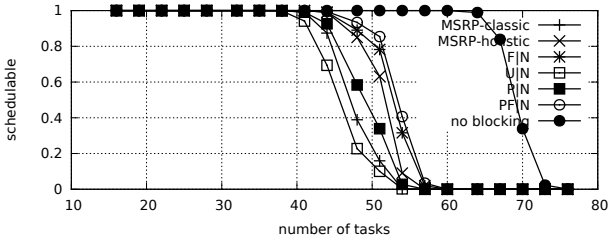

Fig. 2012. Schedulability under non-preemptable spin locks for $m = 16$, $U = 0.2n$, 32 resources, $rsf = 0.25$, $N^{max} = 5$, and short critical sections. The schedulability of the considered preemptable lock types in this configuration is shown in Fig. 2022.

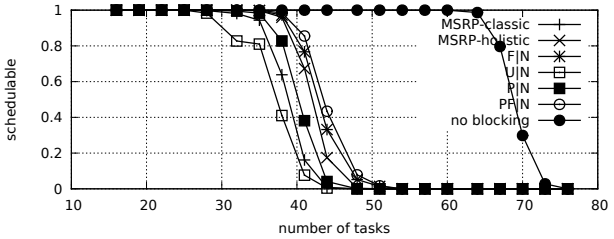

Fig. 2013. Schedulability under non-preemptable spin locks for $m = 16$, $U = 0.2n$, 32 resources, $rsf = 0.25$, $N^{max} = 10$, and short critical sections. The schedulability of the considered preemptable lock types in this configuration is shown in Fig. 2023.

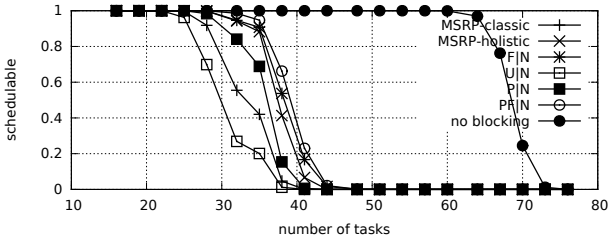

Fig. 2014. Schedulability under non-preemptable spin locks for $m = 16$, $U = 0.2n$, 32 resources, $rsf = 0.25$, $N^{max} = 15$, and short critical sections. The schedulability of the considered preemptable lock types in this configuration is shown in Fig. 2024.

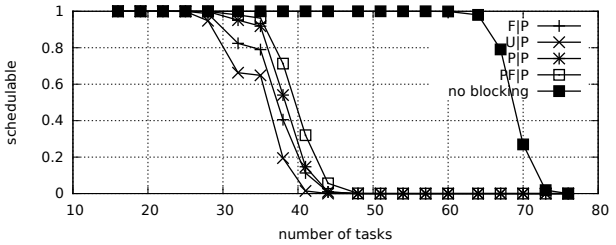

Fig. 2015. Schedulability under preemptable spin locks for $m = 16$, $U = 0.2n$, 32 resources, $rsf = 0.25$, $N^{max} = 1$, and medium critical sections. The schedulability of the considered non-preemptable lock types in this configuration is shown in Fig. 2005.

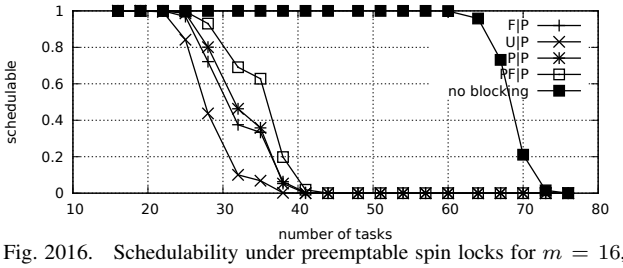

Fig. 2016. Schedulability under preemptable spin locks for $m = 16$, $U = 0.2n$, 32 resources, $rsf = 0.25$, $N^{max} = 2$, and medium critical sections. The schedulability of the considered non-preemptable lock types in this configuration is shown in Fig. 2006.

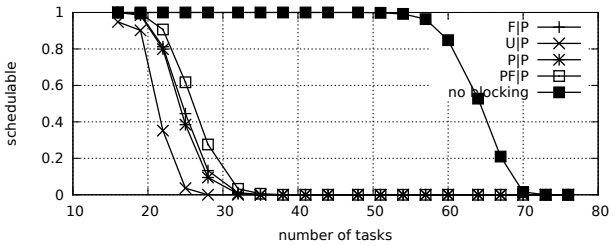

Fig. 2017. Schedulability under preemptable spin locks for $m = 16$, $U = 0.2n$, 32 resources, $rsf = 0.25$, $N^{max} = 5$, and medium critical sections. The schedulability of the considered non-preemptable lock types in this configuration is shown in Fig. 2007.

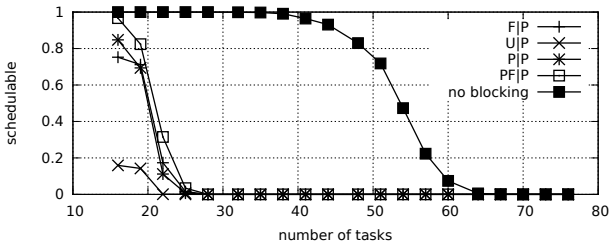

Fig. 2018. Schedulability under preemptable spin locks for $m = 16$, $U = 0.2n$, 32 resources, $rsf = 0.25$, $N^{max} = 10$, and medium critical sections. The schedulability of the considered non-preemptable lock types in this configuration is shown in Fig. 2008.

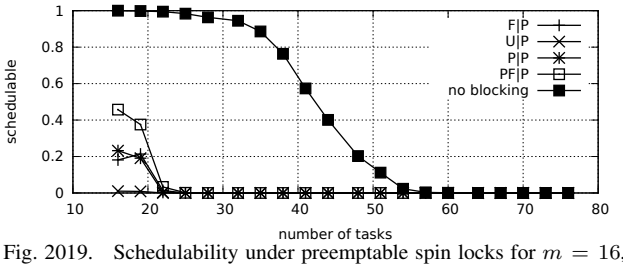

Fig. 2019. Schedulability under preemptable spin locks for $m = 16$, $U = 0.2n$, 32 resources, $rsf = 0.25$, $N^{max} = 15$, and medium critical sections. The schedulability of the considered non-preemptable lock types in this configuration is shown in Fig. 2009.

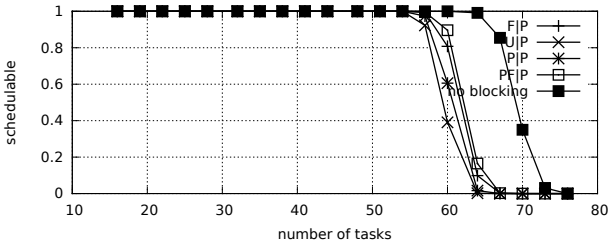

Fig. 2020. Schedulability under preemptable spin locks for $m = 16$, $U = 0.2n$, 32 resources, $rsf = 0.25$, $N^{max} = 1$, and short critical sections. The schedulability of the considered non-preemptable lock types in this configuration is shown in Fig. 2010.

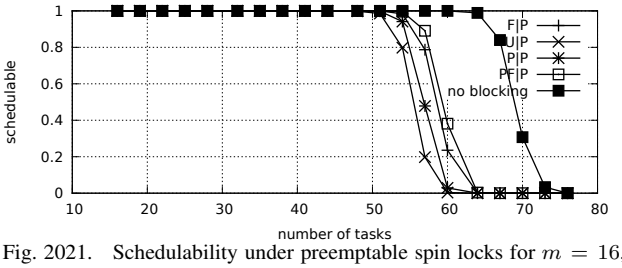

Fig. 2021. Schedulability under preemptable spin locks for $m = 16$, $U = 0.2n$, 32 resources, $rsf = 0.25$, $N^{max} = 2$, and short critical sections. The schedulability of the considered non-preemptable lock types in this configuration is shown in Fig. 2011.

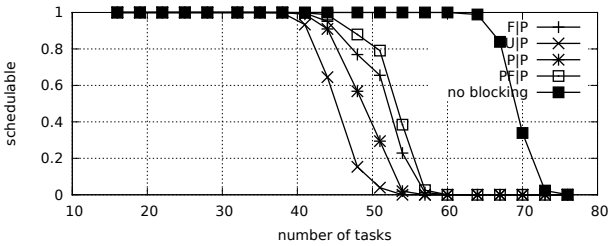

Fig. 2022. Schedulability under preemptable spin locks for $m = 16$, $U = 0.2n$, 32 resources, $rsf = 0.25$, $N^{max} = 5$, and short critical sections. The schedulability of the considered non-preemptable lock types in this configuration is shown in Fig. 2012.

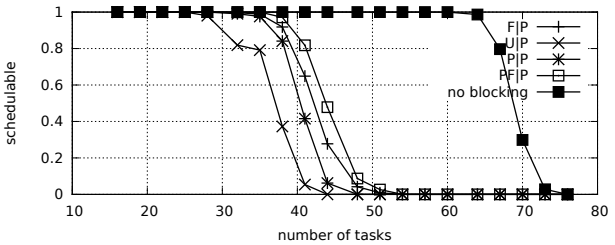

Fig. 2023. Schedulability under preemptable spin locks for $m = 16$, $U = 0.2n$, 32 resources, $rsf = 0.25$, $N^{max} = 10$, and short critical sections. The schedulability of the considered non-preemptable lock types in this configuration is shown in Fig. 2013.

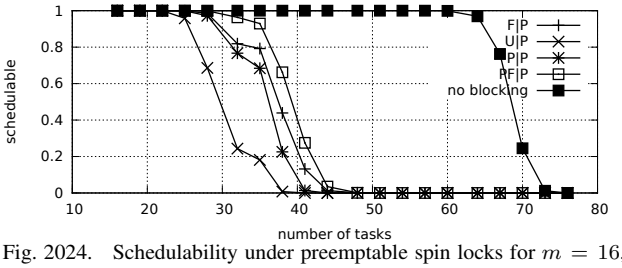

Fig. 2024. Schedulability under preemptable spin locks for $m = 16$, $U = 0.2n$, 32 resources, $rsf = 0.25$, $N^{max} = 15$, and short critical sections. The schedulability of the considered non-preemptable lock types in this configuration is shown in Fig. 2014.

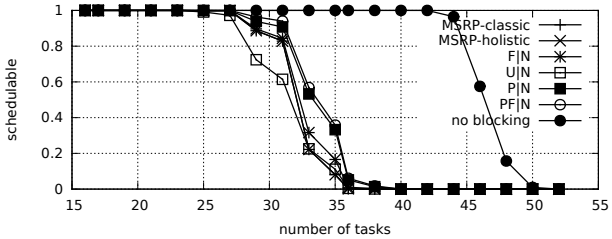

Fig. 2025. Schedulability under non-preemptable spin locks for $m = 16$, $U = 0.3n$, 32 resources, $rsf = 0.25$, $N^{max} = 1$, and medium critical sections. The schedulability of the considered preemptable lock types in this configuration is shown in Fig. 2035.

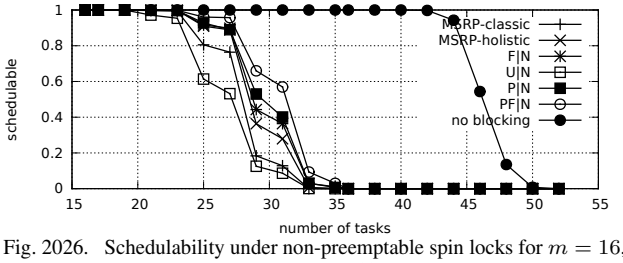

Fig. 2026. Schedulability under non-preemptable spin locks for $m = 16$, $U = 0.3n$, 32 resources, $rsf = 0.25$, $N^{max} = 2$, and medium critical sections. The schedulability of the considered preemptable lock types in this configuration is shown in Fig. 2036.

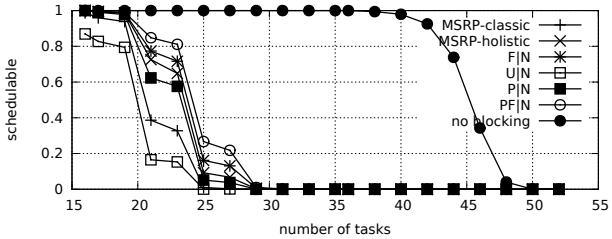

Fig. 2027. Schedulability under non-preemptable spin locks for $m = 16$, $U = 0.3n$, 32 resources, $rsf = 0.25$, $N^{max} = 5$, and medium critical sections. The schedulability of the considered preemptable lock types in this configuration is shown in Fig. 2037.

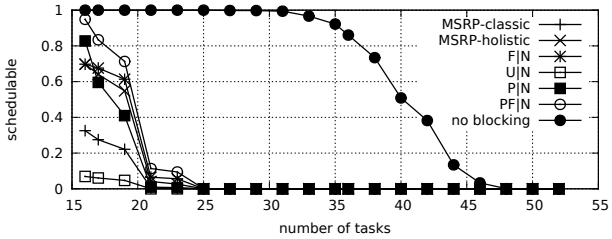

Fig. 2028. Schedulability under non-preemptable spin locks for $m = 16$, $U = 0.3n$, 32 resources, $rsf = 0.25$, $N^{max} = 10$, and medium critical sections. The schedulability of the considered preemptable lock types in this configuration is shown in Fig. 2038.

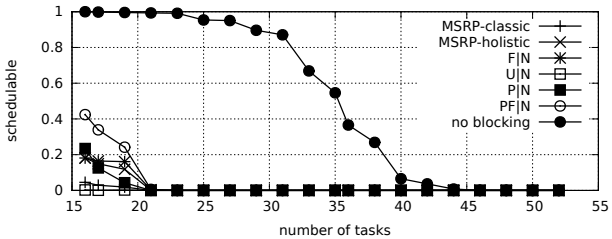

Fig. 2029. Schedulability under non-preemptable spin locks for $m = 16$, $U = 0.3n$, 32 resources, $rsf = 0.25$, $N^{max} = 15$, and medium critical sections. The schedulability of the considered preemptable lock types in this configuration is shown in Fig. 2039.

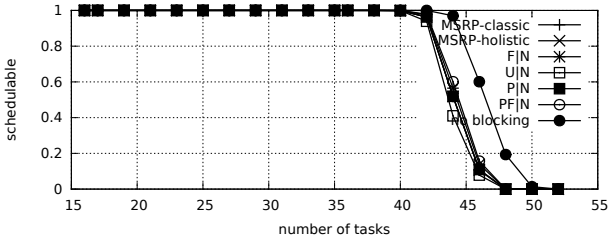

Fig. 2030. Schedulability under non-preemptable spin locks for $m = 16$, $U = 0.3n$, 32 resources, $rsf = 0.25$, $N^{max} = 1$, and short critical sections. The schedulability of the considered preemptable lock types in this configuration is shown in Fig. 2040.

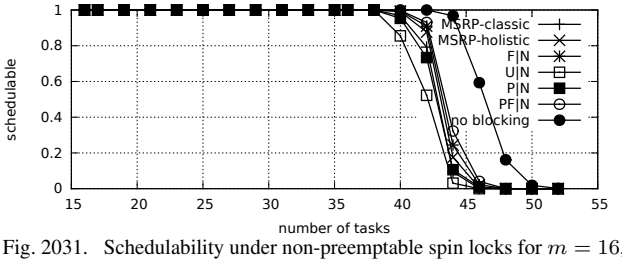

Fig. 2031. Schedulability under non-preemptable spin locks for $m = 16$, $U = 0.3n$, 32 resources, $rsf = 0.25$, $N^{max} = 2$, and short critical sections. The schedulability of the considered preemptable lock types in this configuration is shown in Fig. 2041.

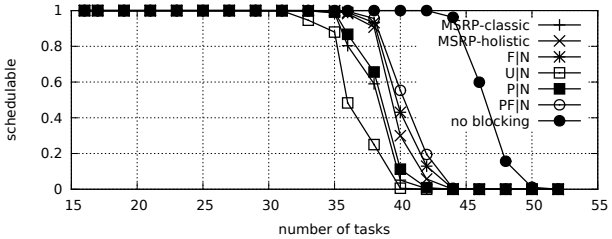

Fig. 2032. Schedulability under non-preemptable spin locks for $m = 16$, $U = 0.3n$, 32 resources, $rsf = 0.25$, $N^{max} = 5$, and short critical sections. The schedulability of the considered preemptable lock types in this configuration is shown in Fig. 2042.

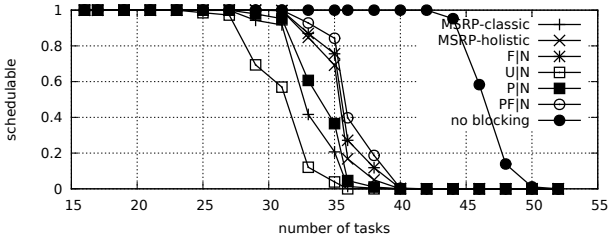

Fig. 2033. Schedulability under non-preemptable spin locks for $m = 16$, $U = 0.3n$, 32 resources, $rsf = 0.25$, $N^{max} = 10$, and short critical sections. The schedulability of the considered preemptable lock types in this configuration is shown in Fig. 2043.

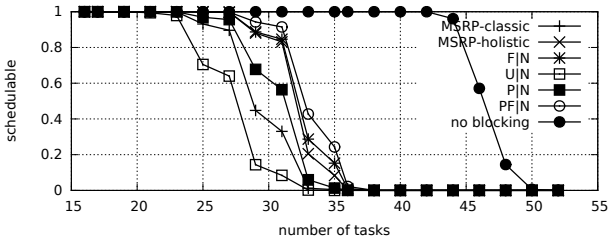

Fig. 2034. Schedulability under non-preemptable spin locks for $m = 16$, $U = 0.3n$, 32 resources, $rsf = 0.25$, $N^{max} = 15$, and short critical sections. The schedulability of the considered preemptable lock types in this configuration is shown in Fig. 2044.

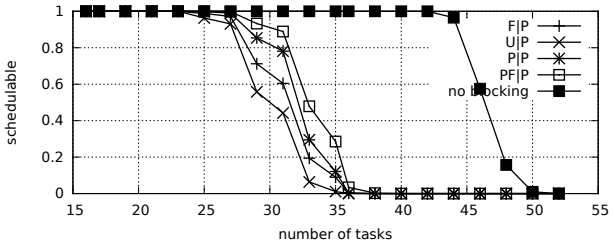

Fig. 2035. Schedulability under preemptable spin locks for $m = 16$, $U = 0.3n$, 32 resources, $rsf = 0.25$, $N^{max} = 1$, and medium critical sections. The schedulability of the considered non-preemptable lock types in this configuration is shown in Fig. 2025.

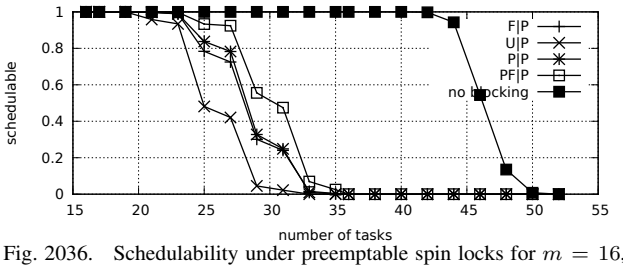

Fig. 2036. Schedulability under preemptable spin locks for $m = 16$, $U = 0.3n$, 32 resources, $rsf = 0.25$, $N^{max} = 2$, and medium critical sections. The schedulability of the considered non-preemptable lock types in this configuration is shown in Fig. 2026.

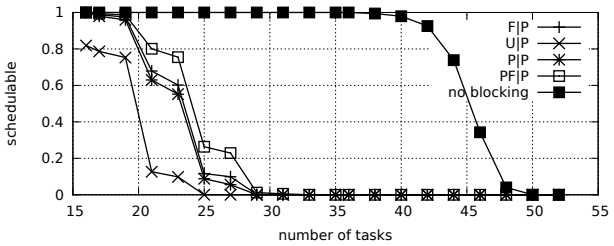

Fig. 2037. Schedulability under preemptable spin locks for $m = 16$, $U = 0.3n$, 32 resources, $rsf = 0.25$, $N^{max} = 5$, and medium critical sections. The schedulability of the considered non-preemptable lock types in this configuration is shown in Fig. 2027.

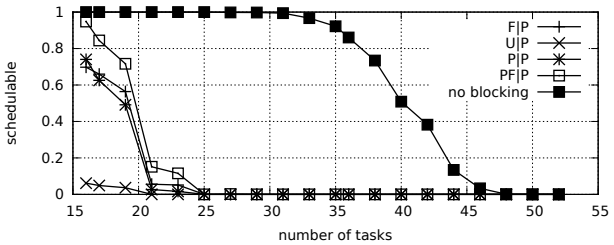

Fig. 2038. Schedulability under preemptable spin locks for $m = 16$, $U = 0.3n$, 32 resources, $rsf = 0.25$, $N^{max} = 10$, and medium critical sections. The schedulability of the considered non-preemptable lock types in this configuration is shown in Fig. 2028.

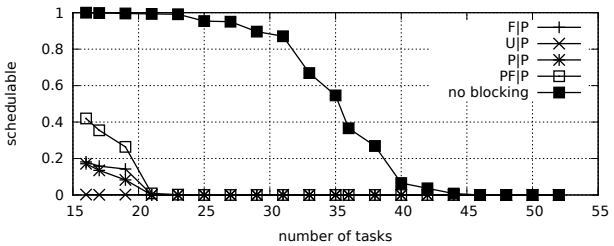

Fig. 2039. Schedulability under preemptable spin locks for $m = 16$, $U = 0.3n$, 32 resources, $rsf = 0.25$, $N^{max} = 15$, and medium critical sections. The schedulability of the considered non-preemptable lock types in this configuration is shown in Fig. 2029.

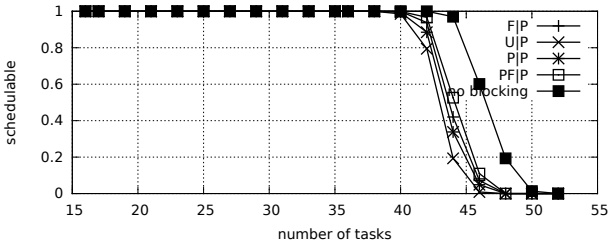

Fig. 2040. Schedulability under preemptable spin locks for $m = 16$, $U = 0.3n$, 32 resources, $rsf = 0.25$, $N^{max} = 1$, and short critical sections. The schedulability of the considered non-preemptable lock types in this configuration is shown in Fig. 2030.

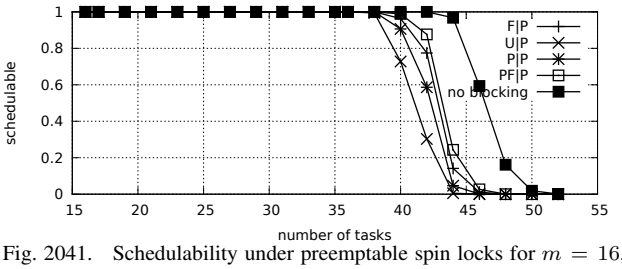

Fig. 2041. Schedulability under preemptable spin locks for $m = 16$, $U = 0.3n$, 32 resources, $rsf = 0.25$, $N^{max} = 2$, and short critical sections. The schedulability of the considered non-preemptable lock types in this configuration is shown in Fig. 2031.

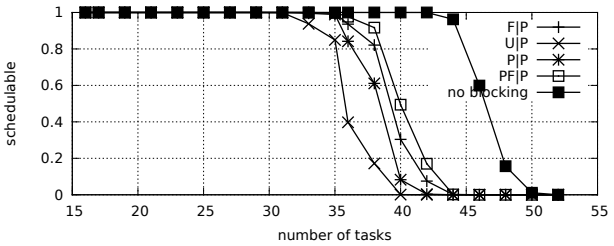

Fig. 2042. Schedulability under preemptable spin locks for $m = 16$, $U = 0.3n$, 32 resources, $rsf = 0.25$, $N^{max} = 5$, and short critical sections. The schedulability of the considered non-preemptable lock types in this configuration is shown in Fig. 2032.

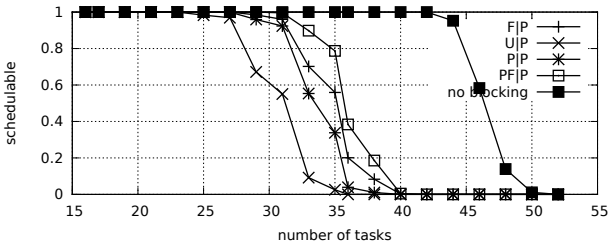

Fig. 2043. Schedulability under preemptable spin locks for $m = 16$, $U = 0.3n$, 32 resources, $rsf = 0.25$, $N^{max} = 10$, and short critical sections. The schedulability of the considered non-preemptable lock types in this configuration is shown in Fig. 2033.

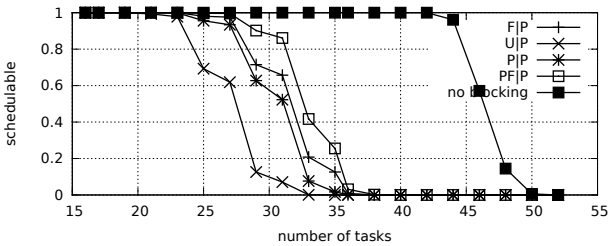

Fig. 2044. Schedulability under preemptable spin locks for $m = 16$, $U = 0.3n$, 32 resources, $rsf = 0.25$, $N^{max} = 15$, and short critical sections. The schedulability of the considered non-preemptable lock types in this configuration is shown in Fig. 2034.

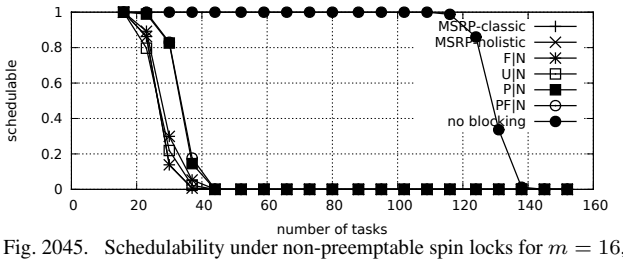

Fig. 2045. Schedulability under non-preemptable spin locks for $m = 16$, $U = 0.1n$, 32 resources, $rsf = 0.4$, $N^{max} = 1$, and medium critical sections. The schedulability of the considered preemptable lock types in this configuration is shown in Fig. 2055.

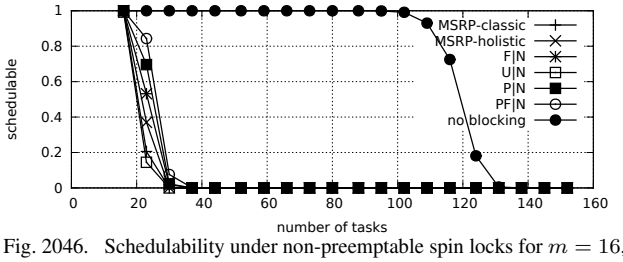

Fig. 2046. Schedulability under non-preemptable spin locks for $m = 16$, $U = 0.1n$, 32 resources, $rsf = 0.4$, $N^{max} = 2$, and medium critical sections. The schedulability of the considered preemptable lock types in this configuration is shown in Fig. 2056.

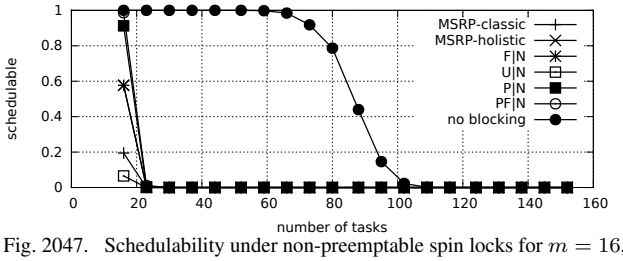

Fig. 2047. Schedulability under non-preemptable spin locks for $m = 16$, $U = 0.1n$, 32 resources, $rsf = 0.4$, $N^{max} = 5$, and medium critical sections. The schedulability of the considered preemptable lock types in this configuration is shown in Fig. 2057.

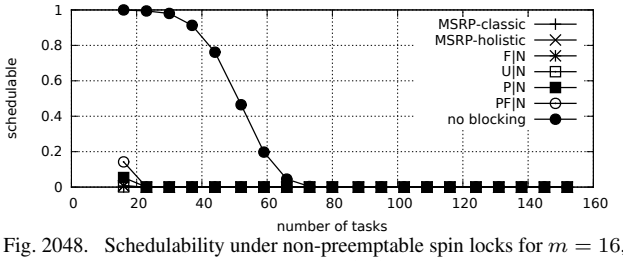

Fig. 2048. Schedulability under non-preemptable spin locks for $m = 16$, $U = 0.1n$, 32 resources, $rsf = 0.4$, $N^{max} = 10$, and medium critical sections. The schedulability of the considered preemptable lock types in this configuration is shown in Fig. 2058.

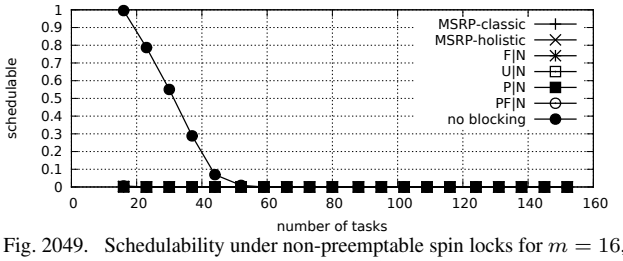

Fig. 2049. Schedulability under non-preemptable spin locks for $m = 16$, $U = 0.1n$, 32 resources, $rsf = 0.4$, $N^{max} = 15$, and medium critical sections. The schedulability of the considered preemptable lock types in this configuration is shown in Fig. 2059.

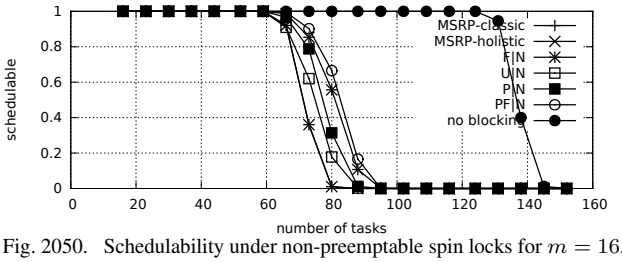

Fig. 2050. Schedulability under non-preemptable spin locks for $m = 16$, $U = 0.1n$, 32 resources, $rsf = 0.4$, $N^{max} = 1$, and short critical sections. The schedulability of the considered preemptable lock types in this configuration is shown in Fig. 2060.

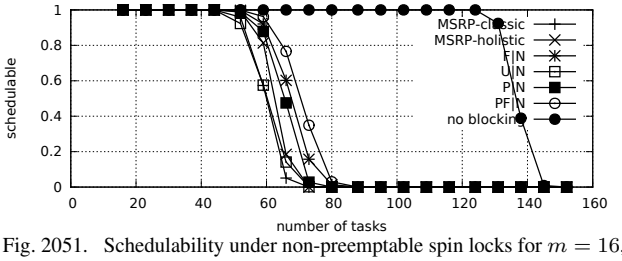

Fig. 2051. Schedulability under non-preemptable spin locks for $m = 16$, $U = 0.1n$, 32 resources, $rsf = 0.4$, $N^{max} = 2$, and short critical sections. The schedulability of the considered preemptable lock types in this configuration is shown in Fig. 2061.

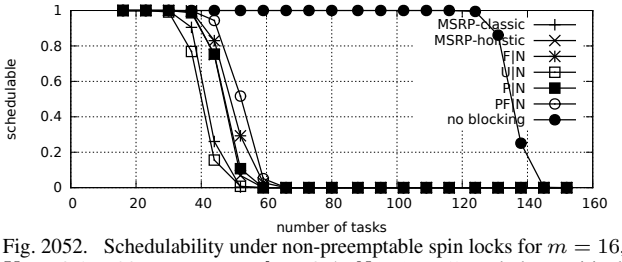

Fig. 2052. Schedulability under non-preemptable spin locks for $m = 16$, $U = 0.1n$, 32 resources, $rsf = 0.4$, $N^{max} = 5$, and short critical sections. The schedulability of the considered preemptable lock types in this configuration is shown in Fig. 2062.

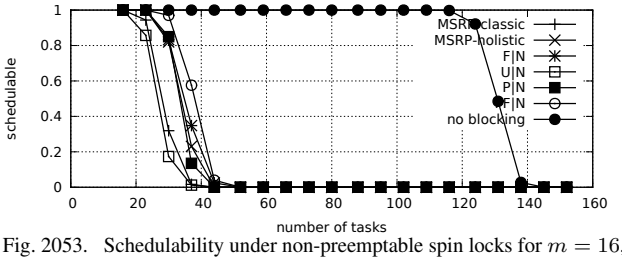

Fig. 2053. Schedulability under non-preemptable spin locks for $m = 16$, $U = 0.1n$, 32 resources, $rsf = 0.4$, $N^{max} = 10$, and short critical sections. The schedulability of the considered preemptable lock types in this configuration is shown in Fig. 2063.

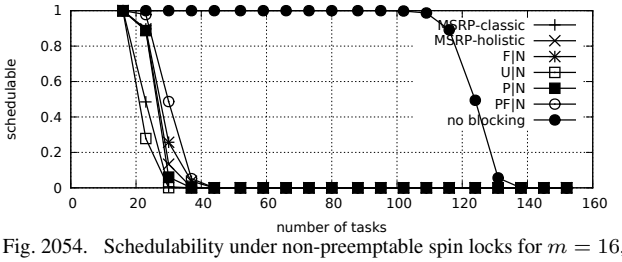

Fig. 2054. Schedulability under non-preemptable spin locks for $m = 16$, $U = 0.1n$, 32 resources, $rsf = 0.4$, $N^{max} = 15$, and short critical sections. The schedulability of the considered preemptable lock types in this configuration is shown in Fig. 2064.

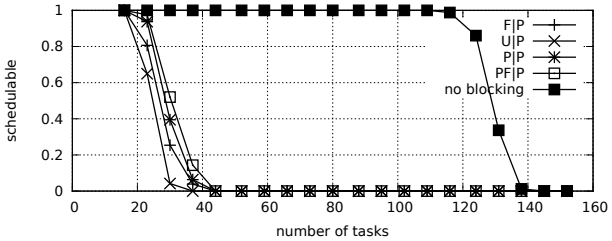

Fig. 2055. Schedulability under preemptable spin locks for $m = 16$, $U = 0.1n$, 32 resources, $rsf = 0.4$, $N^{max} = 1$, and medium critical sections. The schedulability of the considered non-preemptable lock types in this configuration is shown in Fig. 2045.

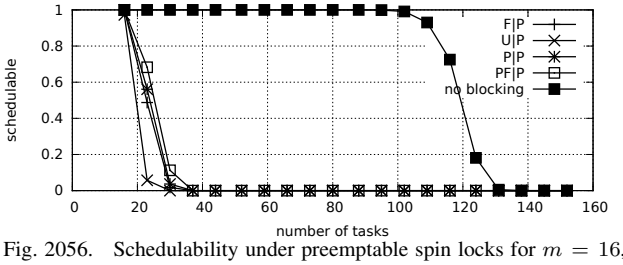

Fig. 2056. Schedulability under preemptable spin locks for $m = 16$, $U = 0.1n$, 32 resources, $rsf = 0.4$, $N^{max} = 2$, and medium critical sections. The schedulability of the considered non-preemptable lock types in this configuration is shown in Fig. 2046.

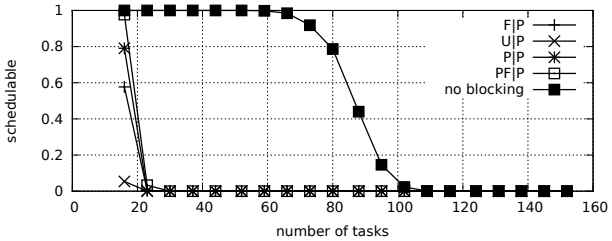

Fig. 2057. Schedulability under preemptable spin locks for $m = 16$, $U = 0.1n$, 32 resources, $rsf = 0.4$, $N^{max} = 5$, and medium critical sections. The schedulability of the considered non-preemptable lock types in this configuration is shown in Fig. 2047.

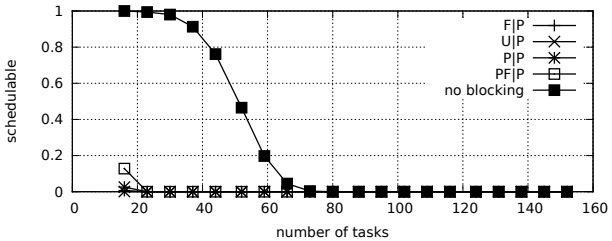

Fig. 2058. Schedulability under preemptable spin locks for $m = 16$, $U = 0.1n$, 32 resources, $rsf = 0.4$, $N^{max} = 10$, and medium critical sections. The schedulability of the considered non-preemptable lock types in this configuration is shown in Fig. 2048.

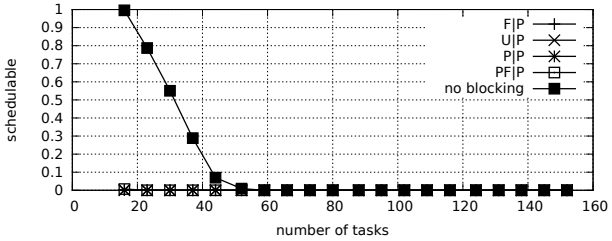

Fig. 2059. Schedulability under preemptable spin locks for $m = 16$, $U = 0.1n$, 32 resources, $rsf = 0.4$, $N^{max} = 15$, and medium critical sections. The schedulability of the considered non-preemptable lock types in this configuration is shown in Fig. 2049.

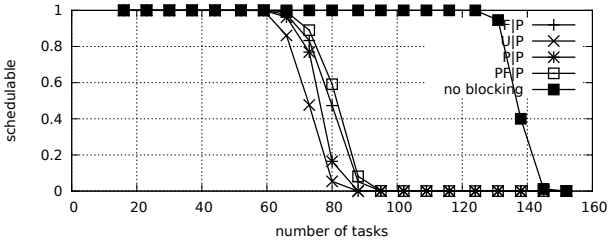

Fig. 2060. Schedulability under preemptable spin locks for $m = 16$, $U = 0.1n$, 32 resources, $rsf = 0.4$, $N^{max} = 1$, and short critical sections. The schedulability of the considered non-preemptable lock types in this configuration is shown in Fig. 2050.

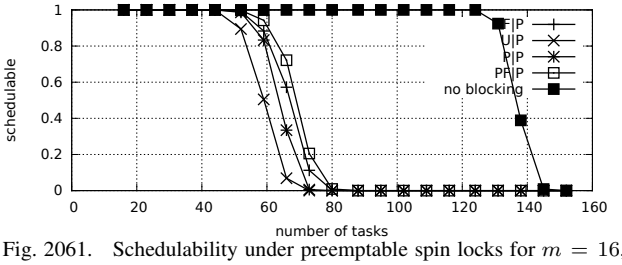

Fig. 2061. Schedulability under preemptable spin locks for $m = 16$, $U = 0.1n$, 32 resources, $rsf = 0.4$, $N^{max} = 2$, and short critical sections. The schedulability of the considered non-preemptable lock types in this configuration is shown in Fig. 2051.

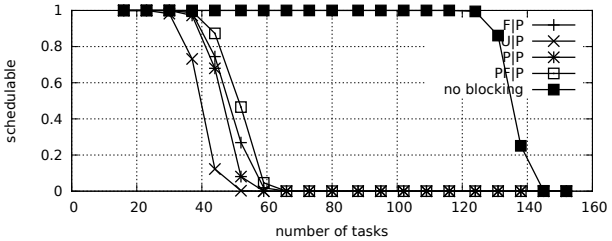

Fig. 2062. Schedulability under preemptable spin locks for $m = 16$, $U = 0.1n$, 32 resources, $rsf = 0.4$, $N^{max} = 5$, and short critical sections. The schedulability of the considered non-preemptable lock types in this configuration is shown in Fig. 2052.

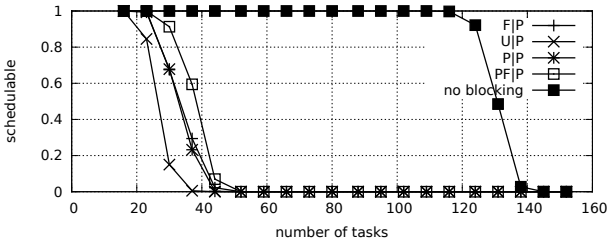

Fig. 2063. Schedulability under preemptable spin locks for $m = 16$, $U = 0.1n$, 32 resources, $rsf = 0.4$, $N^{max} = 10$, and short critical sections. The schedulability of the considered non-preemptable lock types in this configuration is shown in Fig. 2053.

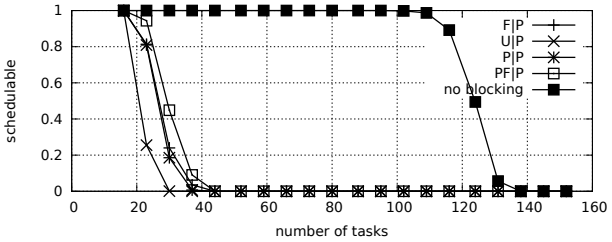

Fig. 2064. Schedulability under preemptable spin locks for $m = 16$, $U = 0.1n$, 32 resources, $rsf = 0.4$, $N^{max} = 15$, and short critical sections. The schedulability of the considered non-preemptable lock types in this configuration is shown in Fig. 2054.

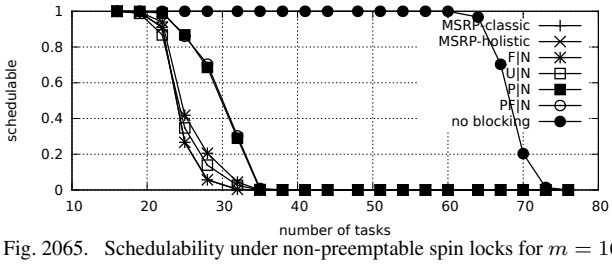

Fig. 2065. Schedulability under non-preemptable spin locks for $m = 16$, $U = 0.2n$, 32 resources, $rsf = 0.4$, $N^{max} = 1$, and medium critical sections. The schedulability of the considered preemptable lock types in this configuration is shown in Fig. 2075.

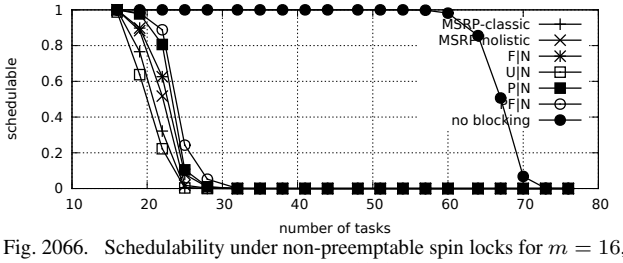

Fig. 2066. Schedulability under non-preemptable spin locks for $m = 16$, $U = 0.2n$, 32 resources, $rsf = 0.4$, $N^{max} = 2$, and medium critical sections. The schedulability of the considered preemptable lock types in this configuration is shown in Fig. 2076.

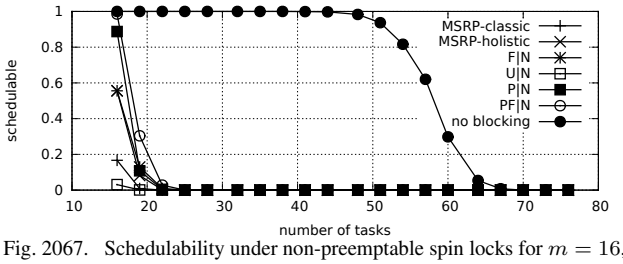

Fig. 2067. Schedulability under non-preemptable spin locks for $m = 16$, $U = 0.2n$, 32 resources, $rsf = 0.4$, $N^{max} = 5$, and medium critical sections. The schedulability of the considered preemptable lock types in this configuration is shown in Fig. 2077.

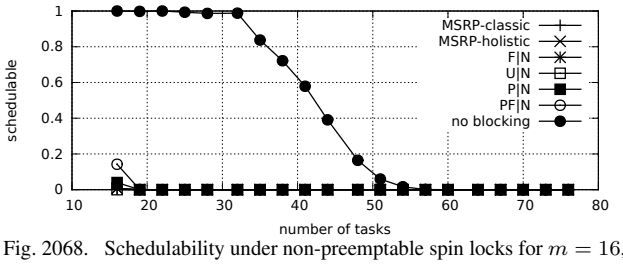

Fig. 2068. Schedulability under non-preemptable spin locks for $m = 16$, $U = 0.2n$, 32 resources, $rsf = 0.4$, $N^{max} = 10$, and medium critical sections. The schedulability of the considered preemptable lock types in this configuration is shown in Fig. 2078.

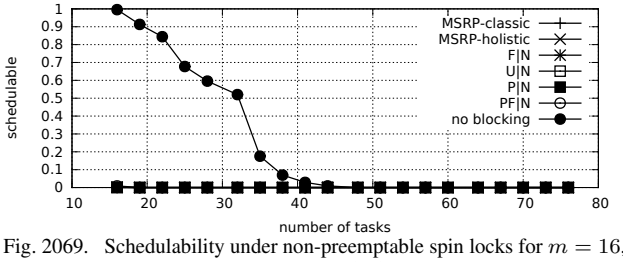

Fig. 2069. Schedulability under non-preemptable spin locks for $m = 16$, $U = 0.2n$, 32 resources, $rsf = 0.4$, $N^{max} = 15$, and medium critical sections. The schedulability of the considered preemptable lock types in this configuration is shown in Fig. 2079.

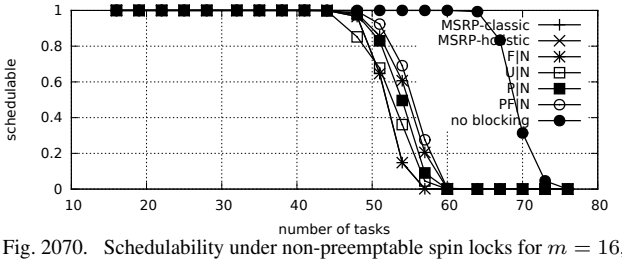

Fig. 2070. Schedulability under non-preemptable spin locks for $m = 16$, $U = 0.2n$, 32 resources, $rsf = 0.4$, $N^{max} = 1$, and short critical sections. The schedulability of the considered preemptable lock types in this configuration is shown in Fig. 2080.

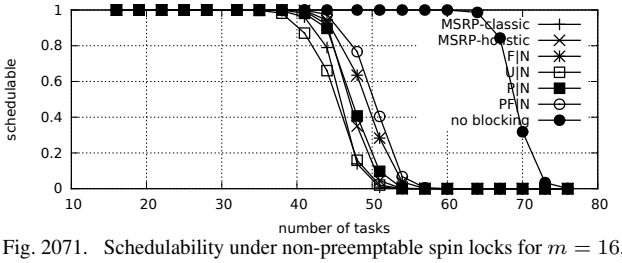

Fig. 2071. Schedulability under non-preemptable spin locks for $m = 16$, $U = 0.2n$, 32 resources, $rsf = 0.4$, $N^{max} = 2$, and short critical sections. The schedulability of the considered preemptable lock types in this configuration is shown in Fig. 2081.

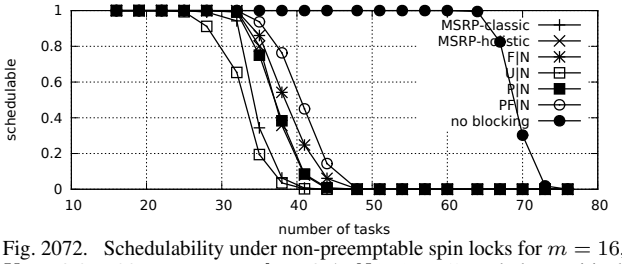

Fig. 2072. Schedulability under non-preemptable spin locks for $m = 16$, $U = 0.2n$, 32 resources, $rsf = 0.4$, $N^{max} = 5$, and short critical sections. The schedulability of the considered preemptable lock types in this configuration is shown in Fig. 2082.

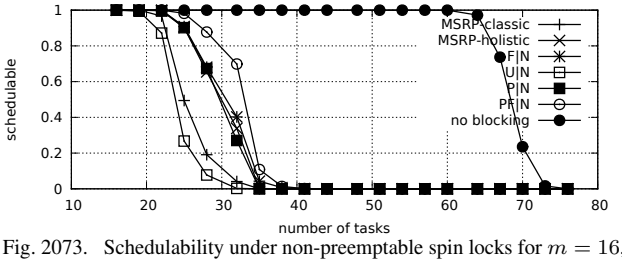

Fig. 2073. Schedulability under non-preemptable spin locks for $m = 16$, $U = 0.2n$, 32 resources, $rsf = 0.4$, $N^{max} = 10$, and short critical sections. The schedulability of the considered preemptable lock types in this configuration is shown in Fig. 2083.

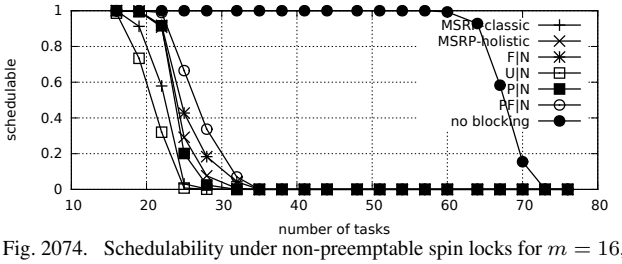

Fig. 2074. Schedulability under non-preemptable spin locks for $m = 16$, $U = 0.2n$, 32 resources, $rsf = 0.4$, $N^{max} = 15$, and short critical sections. The schedulability of the considered preemptable lock types in this configuration is shown in Fig. 2084.

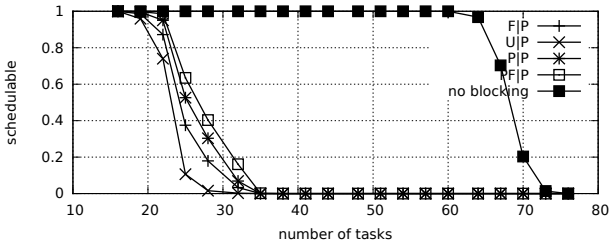

Fig. 2075. Schedulability under preemptable spin locks for $m = 16$, $U = 0.2n$, 32 resources, $rsf = 0.4$, $N^{max} = 1$, and medium critical sections. The schedulability of the considered non-preemptable lock types in this configuration is shown in Fig. 2065.

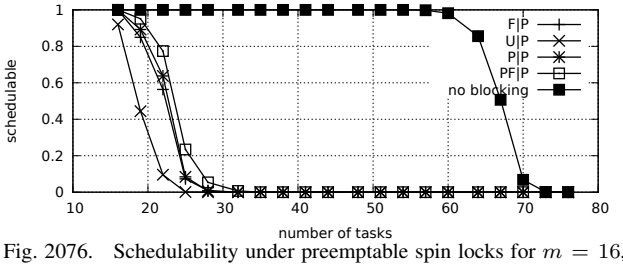

Fig. 2076. Schedulability under preemptable spin locks for $m = 16$, $U = 0.2n$, 32 resources, $rsf = 0.4$, $N^{max} = 2$, and medium critical sections. The schedulability of the considered non-preemptable lock types in this configuration is shown in Fig. 2066.

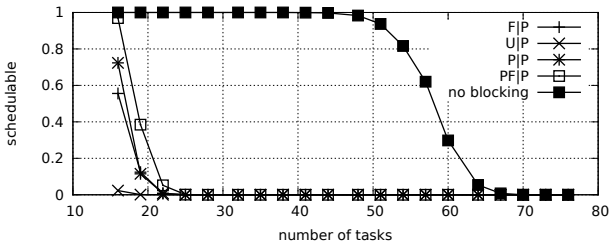

Fig. 2077. Schedulability under preemptable spin locks for $m = 16$, $U = 0.2n$, 32 resources, $rsf = 0.4$, $N^{max} = 5$, and medium critical sections. The schedulability of the considered non-preemptable lock types in this configuration is shown in Fig. 2067.

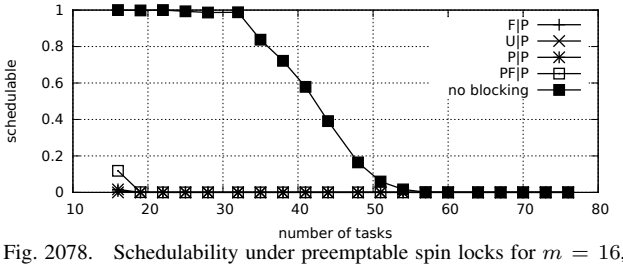

Fig. 2078. Schedulability under preemptable spin locks for $m = 16$, $U = 0.2n$, 32 resources, $rsf = 0.4$, $N^{max} = 10$, and medium critical sections. The schedulability of the considered non-preemptable lock types in this configuration is shown in Fig. 2068.

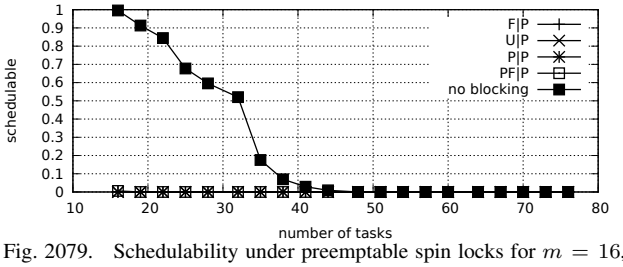

Fig. 2079. Schedulability under preemptable spin locks for $m = 16$, $U = 0.2n$, 32 resources, $rsf = 0.4$, $N^{max} = 15$, and medium critical sections. The schedulability of the considered non-preemptable lock types in this configuration is shown in Fig. 2069.

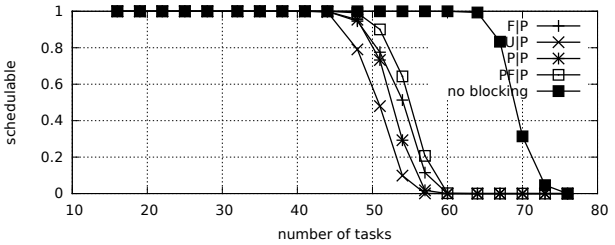

Fig. 2080. Schedulability under preemptable spin locks for $m = 16$, $U = 0.2n$, 32 resources, $rsf = 0.4$, $N^{max} = 1$, and short critical sections. The schedulability of the considered non-preemptable lock types in this configuration is shown in Fig. 2070.

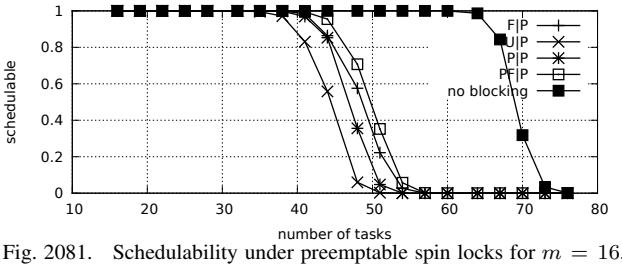

Fig. 2081. Schedulability under preemptable spin locks for $m = 16$, $U = 0.2n$, 32 resources, $rsf = 0.4$, $N^{max} = 2$, and short critical sections. The schedulability of the considered non-preemptable lock types in this configuration is shown in Fig. 2071.

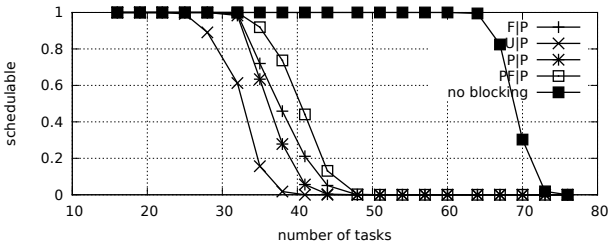

Fig. 2082. Schedulability under preemptable spin locks for $m = 16$, $U = 0.2n$, 32 resources, $rsf = 0.4$, $N^{max} = 5$, and short critical sections. The schedulability of the considered non-preemptable lock types in this configuration is shown in Fig. 2072.

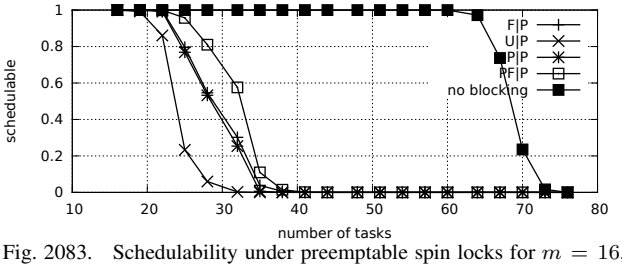

Fig. 2083. Schedulability under preemptable spin locks for $m = 16$, $U = 0.2n$, 32 resources, $rsf = 0.4$, $N^{max} = 10$, and short critical sections. The schedulability of the considered non-preemptable lock types in this configuration is shown in Fig. 2073.

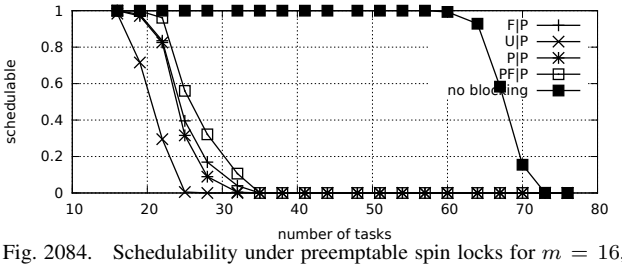

Fig. 2084. Schedulability under preemptable spin locks for $m = 16$, $U = 0.2n$, 32 resources, $rsf = 0.4$, $N^{max} = 15$, and short critical sections. The schedulability of the considered non-preemptable lock types in this configuration is shown in Fig. 2074.

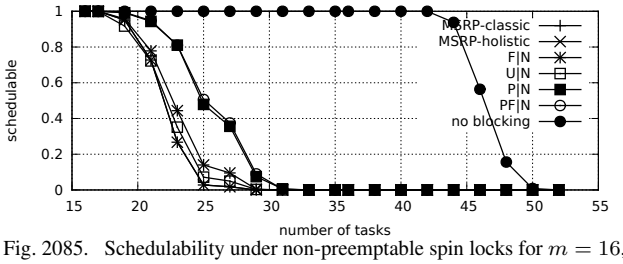

Fig. 2085. Schedulability under non-preemptable spin locks for $m = 16$, $U = 0.3n$, 32 resources, $rsf = 0.4$, $N^{max} = 1$, and medium critical sections. The schedulability of the considered preemptable lock types in this configuration is shown in Fig. 2095.

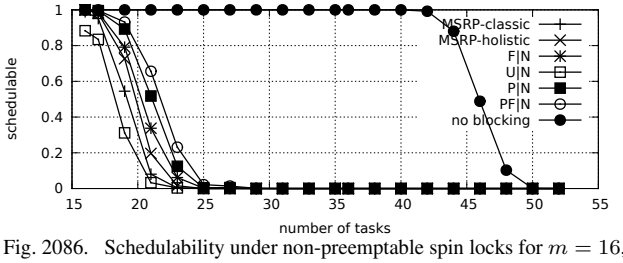

Fig. 2086. Schedulability under non-preemptable spin locks for $m = 16$, $U = 0.3n$, 32 resources, $rsf = 0.4$, $N^{max} = 2$, and medium critical sections. The schedulability of the considered preemptable lock types in this configuration is shown in Fig. 2096.

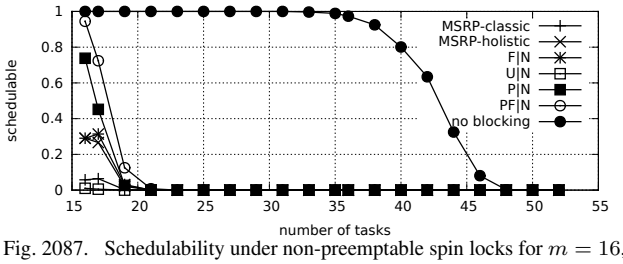

Fig. 2087. Schedulability under non-preemptable spin locks for $m = 16$, $U = 0.3n$, 32 resources, $rsf = 0.4$, $N^{max} = 5$, and medium critical sections. The schedulability of the considered preemptable lock types in this configuration is shown in Fig. 2097.

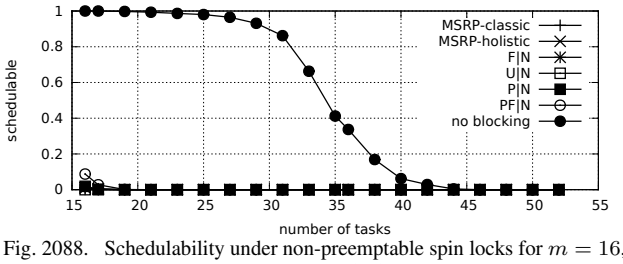

Fig. 2088. Schedulability under non-preemptable spin locks for $m = 16$, $U = 0.3n$, 32 resources, $rsf = 0.4$, $N^{max} = 10$, and medium critical sections. The schedulability of the considered preemptable lock types in this configuration is shown in Fig. 2098.

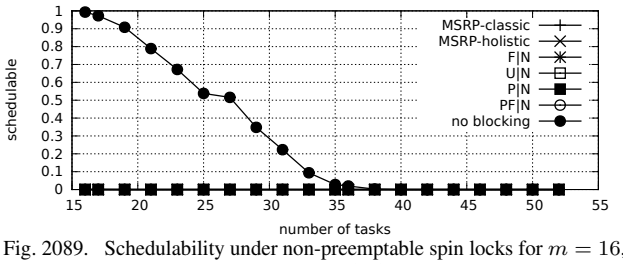

Fig. 2089. Schedulability under non-preemptable spin locks for $m = 16$, $U = 0.3n$, 32 resources, $rsf = 0.4$, $N^{max} = 15$, and medium critical sections. The schedulability of the considered preemptable lock types in this configuration is shown in Fig. 2099.

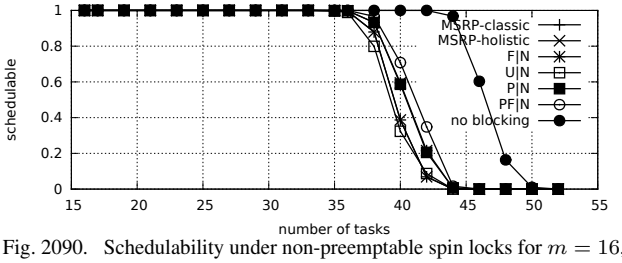

Fig. 2090. Schedulability under non-preemptable spin locks for $m = 16$, $U = 0.3n$, 32 resources, $rsf = 0.4$, $N^{max} = 1$, and short critical sections. The schedulability of the considered preemptable lock types in this configuration is shown in Fig. 2100.

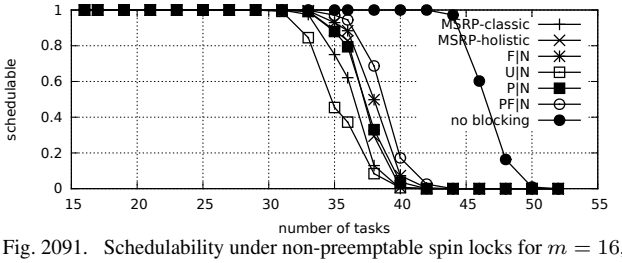

Fig. 2091. Schedulability under non-preemptable spin locks for $m = 16$, $U = 0.3n$, 32 resources, $rsf = 0.4$, $N^{max} = 2$, and short critical sections. The schedulability of the considered preemptable lock types in this configuration is shown in Fig. 2101.

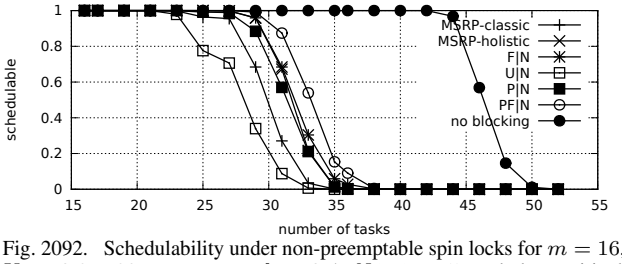

Fig. 2092. Schedulability under non-preemptable spin locks for $m = 16$, $U = 0.3n$, 32 resources, $rsf = 0.4$, $N^{max} = 5$, and short critical sections. The schedulability of the considered preemptable lock types in this configuration is shown in Fig. 2102.

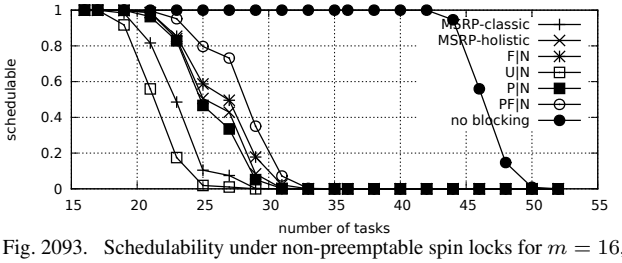

Fig. 2093. Schedulability under non-preemptable spin locks for $m = 16$, $U = 0.3n$, 32 resources, $rsf = 0.4$, $N^{max} = 10$, and short critical sections. The schedulability of the considered preemptable lock types in this configuration is shown in Fig. 2103.

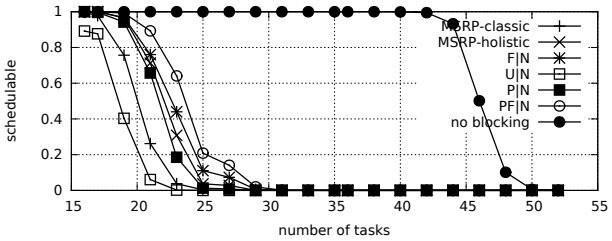

Fig. 2094. Schedulability under non-preemptable spin locks for $m = 16$, $U = 0.3n$, 32 resources, $rsf = 0.4$, $N^{max} = 15$, and short critical sections. The schedulability of the considered preemptable lock types in this configuration is shown in Fig. 2104.

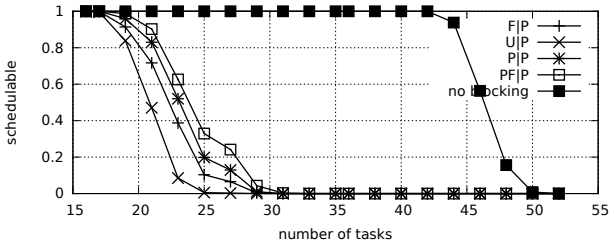

Fig. 2095. Schedulability under preemptable spin locks for $m = 16$, $U = 0.3n$, 32 resources, $rsf = 0.4$, $N^{max} = 1$, and medium critical sections. The schedulability of the considered non-preemptable lock types in this configuration is shown in Fig. 2085.

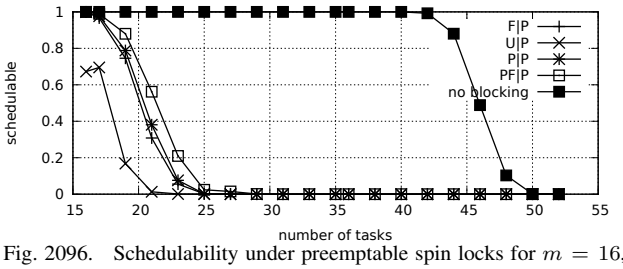

Fig. 2096. Schedulability under preemptable spin locks for $m = 16$, $U = 0.3n$, 32 resources, $rsf = 0.4$, $N^{max} = 2$, and medium critical sections. The schedulability of the considered non-preemptable lock types in this configuration is shown in Fig. 2086.

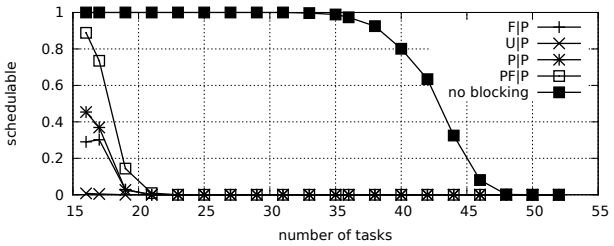

Fig. 2097. Schedulability under preemptable spin locks for $m = 16$, $U = 0.3n$, 32 resources, $rsf = 0.4$, $N^{max} = 5$, and medium critical sections. The schedulability of the considered non-preemptable lock types in this configuration is shown in Fig. 2087.

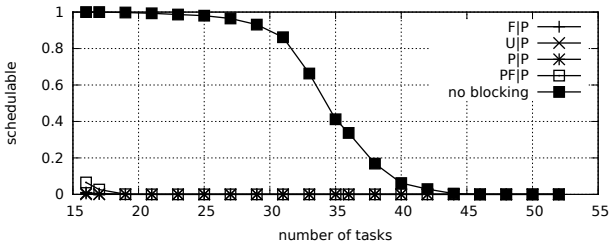

Fig. 2098. Schedulability under preemptable spin locks for $m = 16$, $U = 0.3n$, 32 resources, $rsf = 0.4$, $N^{max} = 10$, and medium critical sections. The schedulability of the considered non-preemptable lock types in this configuration is shown in Fig. 2088.

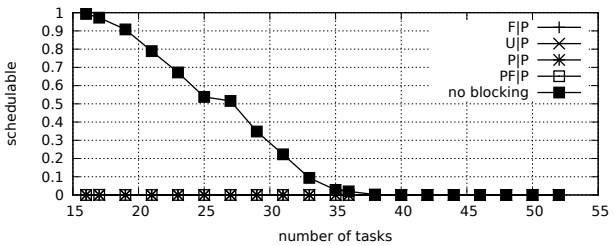

Fig. 2099. Schedulability under preemptable spin locks for $m = 16$, $U = 0.3n$, 32 resources, $rsf = 0.4$, $N^{max} = 15$, and medium critical sections. The schedulability of the considered non-preemptable lock types in this configuration is shown in Fig. 2089.

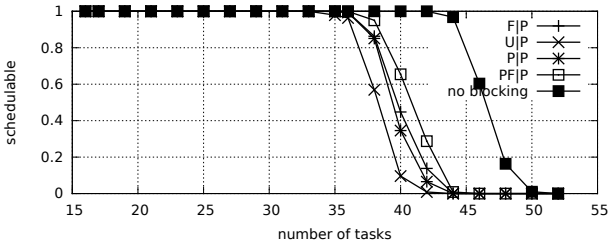

Fig. 2100. Schedulability under preemptable spin locks for $m = 16$, $U = 0.3n$, 32 resources, $rsf = 0.4$, $N^{max} = 1$, and short critical sections. The schedulability of the considered non-preemptable lock types in this configuration is shown in Fig. 2090.

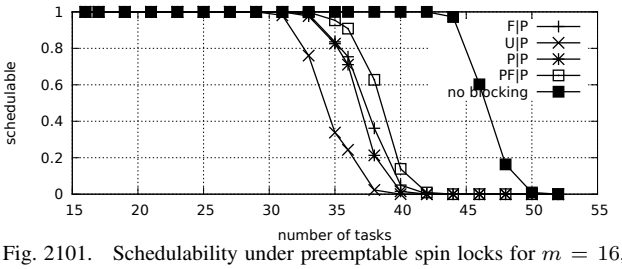

Fig. 2101. Schedulability under preemptable spin locks for $m = 16$, $U = 0.3n$, 32 resources, $rsf = 0.4$, $N^{max} = 2$, and short critical sections. The schedulability of the considered non-preemptable lock types in this configuration is shown in Fig. 2091.

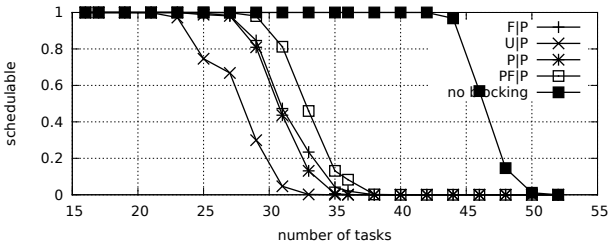

Fig. 2102. Schedulability under preemptable spin locks for $m = 16$, $U = 0.3n$, 32 resources, $rsf = 0.4$, $N^{max} = 5$, and short critical sections. The schedulability of the considered non-preemptable lock types in this configuration is shown in Fig. 2092.

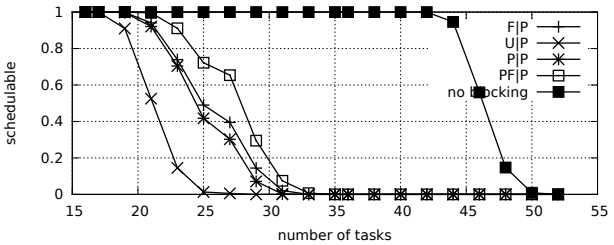

Fig. 2103. Schedulability under preemptable spin locks for $m = 16$, $U = 0.3n$, 32 resources, $rsf = 0.4$, $N^{max} = 10$, and short critical sections. The schedulability of the considered non-preemptable lock types in this configuration is shown in Fig. 2093.

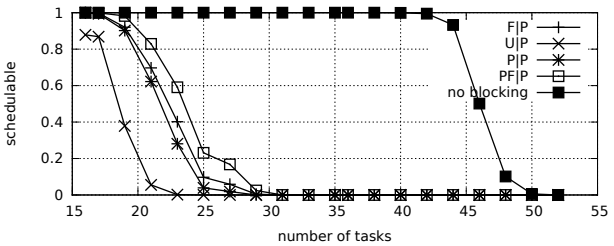

Fig. 2104. Schedulability under preemptable spin locks for $m = 16$, $U = 0.3n$, 32 resources, $rsf = 0.4$, $N^{max} = 15$, and short critical sections. The schedulability of the considered non-preemptable lock types in this configuration is shown in Fig. 2094.

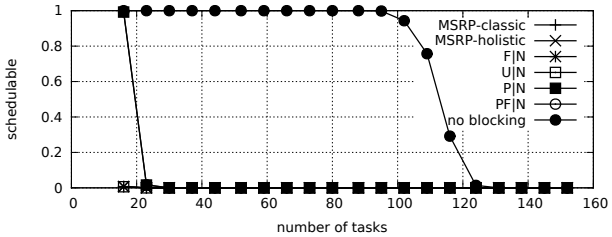

Fig. 2105. Schedulability under non-preemptable spin locks for $m = 16$, $U = 0.1n$, 32 resources, $rsf = 0.75$, $N^{max} = 1$, and medium critical sections. The schedulability of the considered preemptable lock types in this configuration is shown in Fig. 2115.

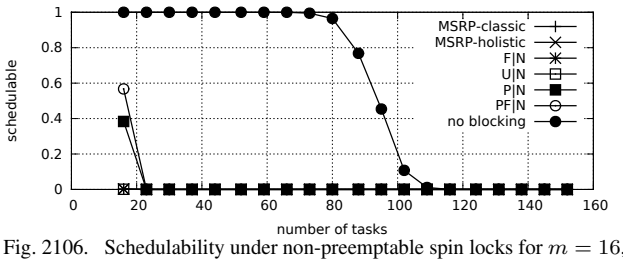

Fig. 2106. Schedulability under non-preemptable spin locks for $m = 16$, $U = 0.1n$, 32 resources, $rsf = 0.75$, $N^{max} = 2$, and medium critical sections. The schedulability of the considered preemptable lock types in this configuration is shown in Fig. 2116.

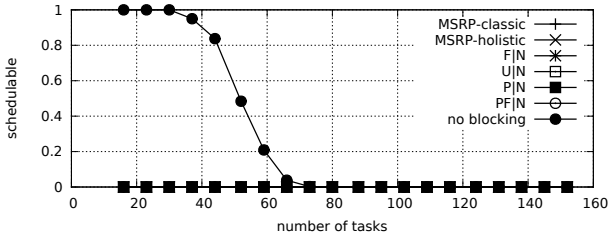

Fig. 2107. Schedulability under non-preemptable spin locks for $m = 16$, $U = 0.1n$, 32 resources, $rsf = 0.75$, $N^{max} = 5$, and medium critical sections. The schedulability of the considered preemptable lock types in this configuration is shown in Fig. 2117.

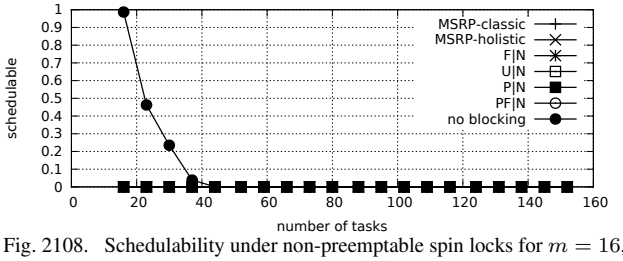

Fig. 2108. Schedulability under non-preemptable spin locks for $m = 16$, $U = 0.1n$, 32 resources, $rsf = 0.75$, $N^{max} = 10$, and medium critical sections. The schedulability of the considered preemptable lock types in this configuration is shown in Fig. 2118.

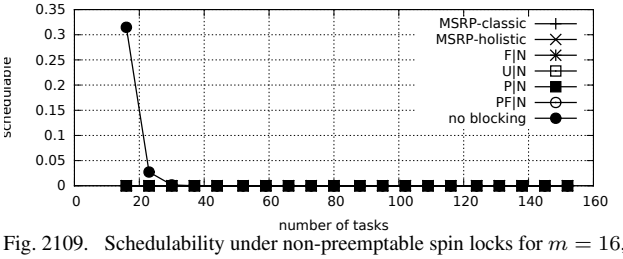

Fig. 2109. Schedulability under non-preemptable spin locks for $m = 16$, $U = 0.1n$, 32 resources, $rsf = 0.75$, $N^{max} = 15$, and medium critical sections. The schedulability of the considered preemptable lock types in this configuration is shown in Fig. 2119.

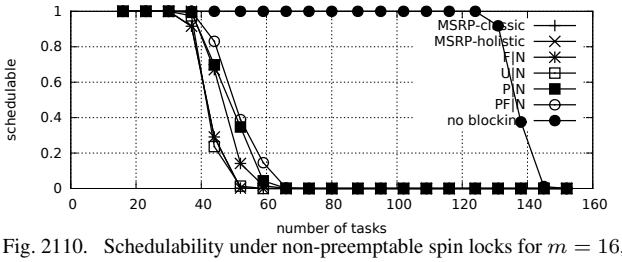

Fig. 2110. Schedulability under non-preemptable spin locks for $m = 16$, $U = 0.1n$, 32 resources, $rsf = 0.75$, $N^{max} = 1$, and short critical sections. The schedulability of the considered preemptable lock types in this configuration is shown in Fig. 2120.

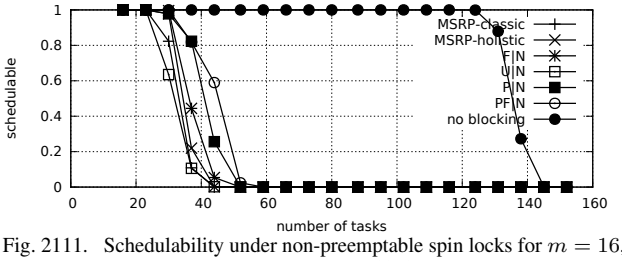

Fig. 2111. Schedulability under non-preemptable spin locks for $m = 16$, $U = 0.1n$, 32 resources, $rsf = 0.75$, $N^{max} = 2$, and short critical sections. The schedulability of the considered preemptable lock types in this configuration is shown in Fig. 2121.

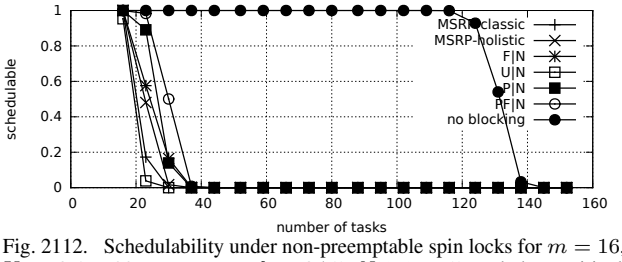

Fig. 2112. Schedulability under non-preemptable spin locks for $m = 16$, $U = 0.1n$, 32 resources, $rsf = 0.75$, $N^{max} = 5$, and short critical sections. The schedulability of the considered preemptable lock types in this configuration is shown in Fig. 2122.

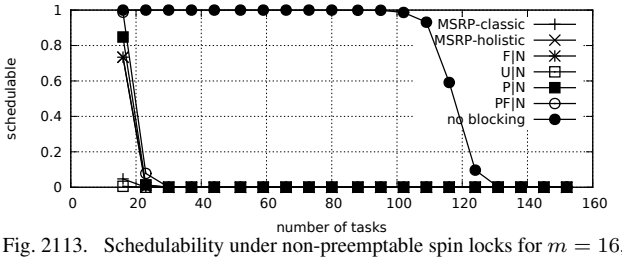

Fig. 2113. Schedulability under non-preemptable spin locks for $m = 16$, $U = 0.1n$, 32 resources, $rsf = 0.75$, $N^{max} = 10$, and short critical sections. The schedulability of the considered preemptable lock types in this configuration is shown in Fig. 2123.

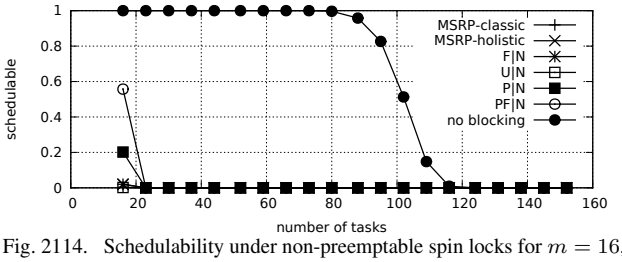

Fig. 2114. Schedulability under non-preemptable spin locks for $m = 16$, $U = 0.1n$, 32 resources, $rsf = 0.75$, $N^{max} = 15$, and short critical sections. The schedulability of the considered preemptable lock types in this configuration is shown in Fig. 2124.

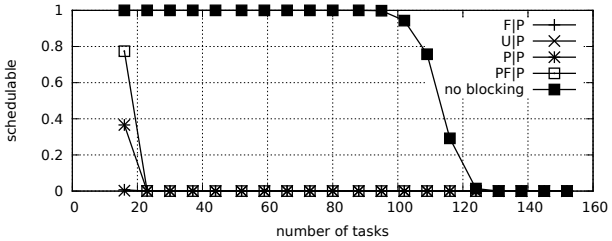

Fig. 2115. Schedulability under preemptable spin locks for $m = 16$, $U = 0.1n$, 32 resources, $rsf = 0.75$, $N^{max} = 1$, and medium critical sections. The schedulability of the considered non-preemptable lock types in this configuration is shown in Fig. 2105.

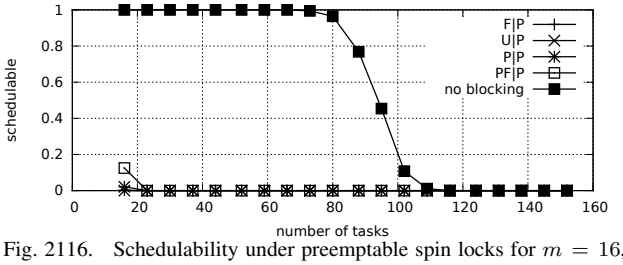

Fig. 2116. Schedulability under preemptable spin locks for $m = 16$, $U = 0.1n$, 32 resources, $rsf = 0.75$, $N^{max} = 2$, and medium critical sections. The schedulability of the considered non-preemptable lock types in this configuration is shown in Fig. 2106.

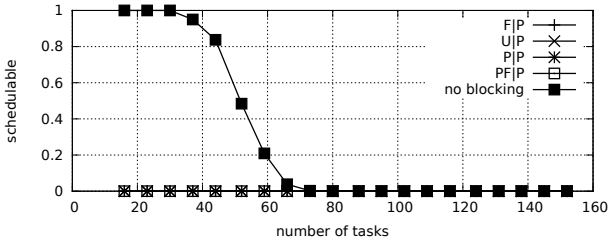

Fig. 2117. Schedulability under preemptable spin locks for $m = 16$, $U = 0.1n$, 32 resources, $rsf = 0.75$, $N^{max} = 5$, and medium critical sections. The schedulability of the considered non-preemptable lock types in this configuration is shown in Fig. 2107.

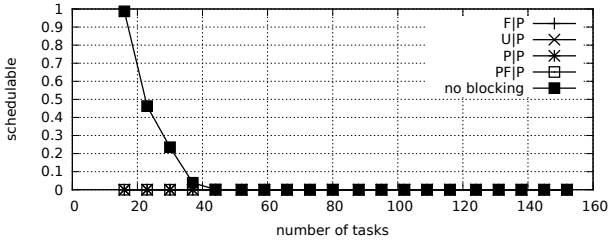

Fig. 2118. Schedulability under preemptable spin locks for $m = 16$, $U = 0.1n$, 32 resources, $rsf = 0.75$, $N^{max} = 10$, and medium critical sections. The schedulability of the considered non-preemptable lock types in this configuration is shown in Fig. 2108.

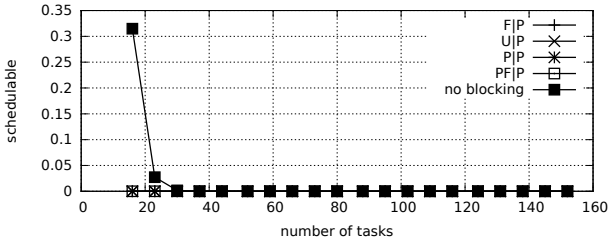

Fig. 2119. Schedulability under preemptable spin locks for $m = 16$, $U = 0.1n$, 32 resources, $rsf = 0.75$, $N^{max} = 15$, and medium critical sections. The schedulability of the considered non-preemptable lock types in this configuration is shown in Fig. 2109.

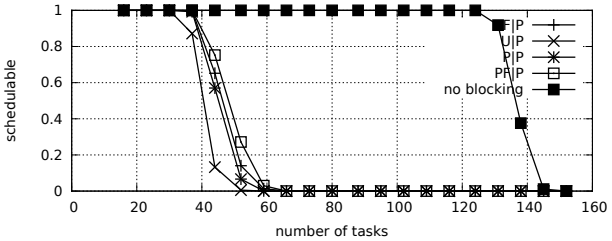

Fig. 2120. Schedulability under preemptable spin locks for $m = 16$, $U = 0.1n$, 32 resources, $rsf = 0.75$, $N^{max} = 1$, and short critical sections. The schedulability of the considered non-preemptable lock types in this configuration is shown in Fig. 2110.

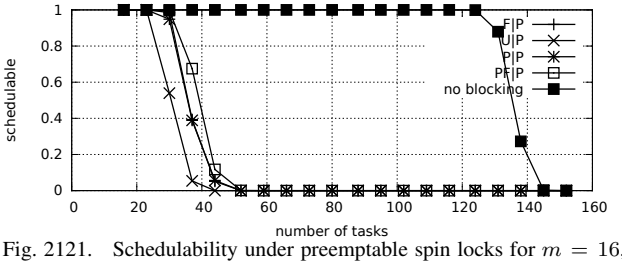

Fig. 2121. Schedulability under preemptable spin locks for $m = 16$, $U = 0.1n$, 32 resources, $rsf = 0.75$, $N^{max} = 2$, and short critical sections. The schedulability of the considered non-preemptable lock types in this configuration is shown in Fig. 2111.

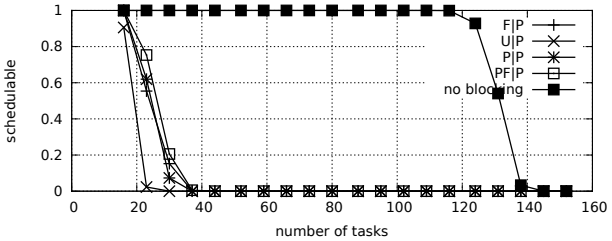

Fig. 2122. Schedulability under preemptable spin locks for $m = 16$, $U = 0.1n$, 32 resources, $rsf = 0.75$, $N^{max} = 5$, and short critical sections. The schedulability of the considered non-preemptable lock types in this configuration is shown in Fig. 2112.

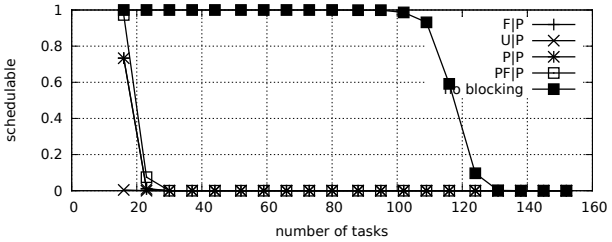

Fig. 2123. Schedulability under preemptable spin locks for $m = 16$, $U = 0.1n$, 32 resources, $rsf = 0.75$, $N^{max} = 10$, and short critical sections. The schedulability of the considered non-preemptable lock types in this configuration is shown in Fig. 2113.

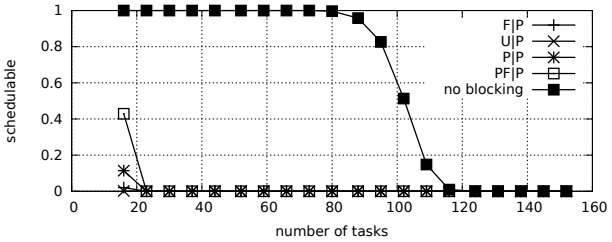

Fig. 2124. Schedulability under preemptable spin locks for $m = 16$, $U = 0.1n$, 32 resources, $rsf = 0.75$, $N^{max} = 15$, and short critical sections. The schedulability of the considered non-preemptable lock types in this configuration is shown in Fig. 2114.

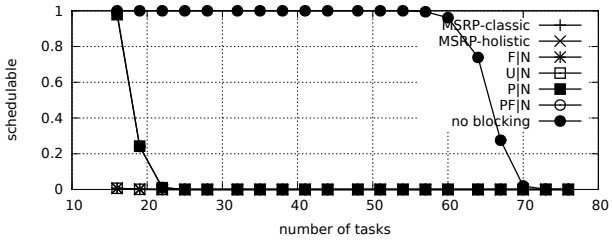

Fig. 2125. Schedulability under non-preemptable spin locks for $m = 16$, $U = 0.2n$, 32 resources, $rsf = 0.75$, $N^{max} = 1$, and medium critical sections. The schedulability of the considered preemptable lock types in this configuration is shown in Fig. 2135.

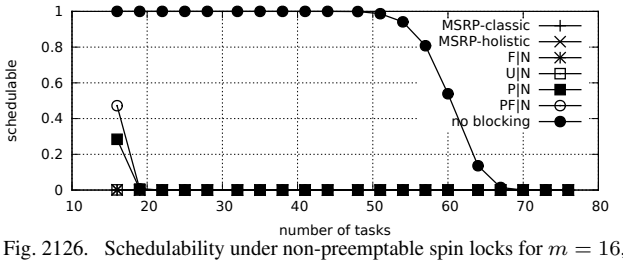

Fig. 2126. Schedulability under non-preemptable spin locks for $m = 16$, $U = 0.2n$, 32 resources, $rsf = 0.75$, $N^{max} = 2$, and medium critical sections. The schedulability of the considered preemptable lock types in this configuration is shown in Fig. 2136.

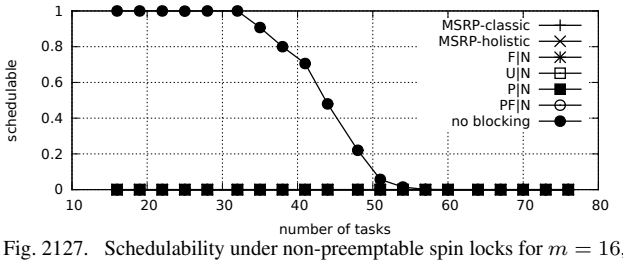

Fig. 2127. Schedulability under non-preemptable spin locks for $m = 16$, $U = 0.2n$, 32 resources, $rsf = 0.75$, $N^{max} = 5$, and medium critical sections. The schedulability of the considered preemptable lock types in this configuration is shown in Fig. 2137.

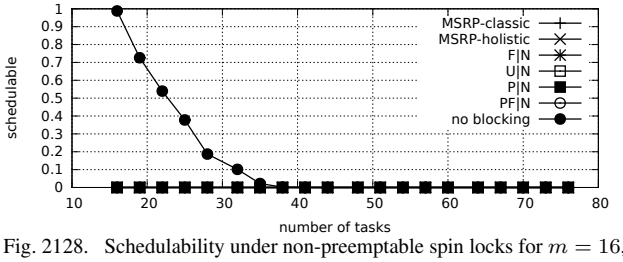

Fig. 2128. Schedulability under non-preemptable spin locks for $m = 16$, $U = 0.2n$, 32 resources, $rsf = 0.75$, $N^{max} = 10$, and medium critical sections. The schedulability of the considered preemptable lock types in this configuration is shown in Fig. 2138.

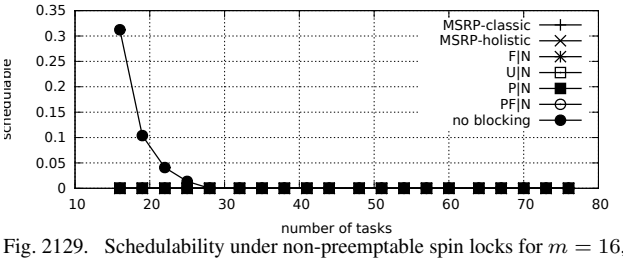

Fig. 2129. Schedulability under non-preemptable spin locks for $m = 16$, $U = 0.2n$, 32 resources, $rsf = 0.75$, $N^{max} = 15$, and medium critical sections. The schedulability of the considered preemptable lock types in this configuration is shown in Fig. 2139.

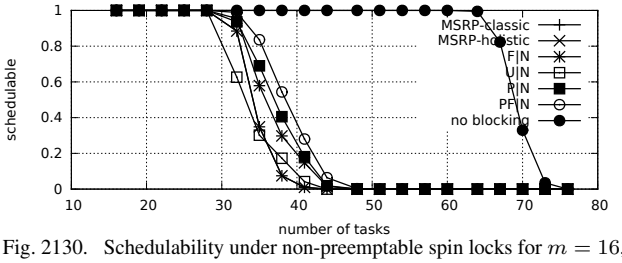

Fig. 2130. Schedulability under non-preemptable spin locks for $m = 16$, $U = 0.2n$, 32 resources, $rsf = 0.75$, $N^{max} = 1$, and short critical sections. The schedulability of the considered preemptable lock types in this configuration is shown in Fig. 2140.

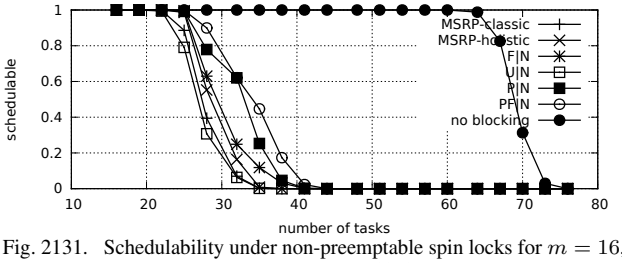

Fig. 2131. Schedulability under non-preemptable spin locks for $m = 16$, $U = 0.2n$, 32 resources, $rsf = 0.75$, $N^{max} = 2$, and short critical sections. The schedulability of the considered preemptable lock types in this configuration is shown in Fig. 2141.

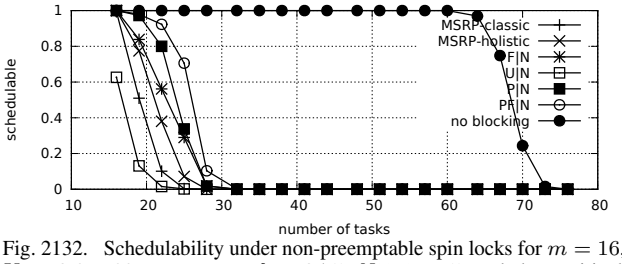

Fig. 2132. Schedulability under non-preemptable spin locks for $m = 16$, $U = 0.2n$, 32 resources, $rsf = 0.75$, $N^{max} = 5$, and short critical sections. The schedulability of the considered preemptable lock types in this configuration is shown in Fig. 2142.

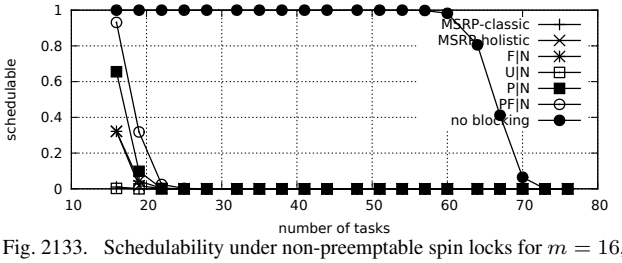

Fig. 2133. Schedulability under non-preemptable spin locks for $m = 16$, $U = 0.2n$, 32 resources, $rsf = 0.75$, $N^{max} = 10$, and short critical sections. The schedulability of the considered preemptable lock types in this configuration is shown in Fig. 2143.

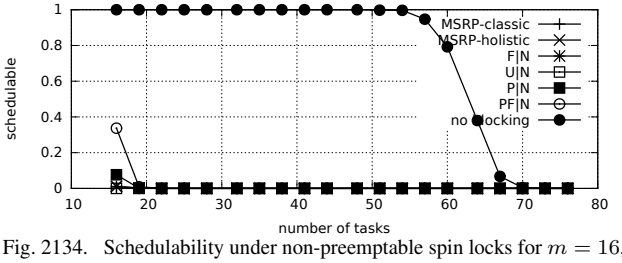

Fig. 2134. Schedulability under non-preemptable spin locks for $m = 16$, $U = 0.2n$, 32 resources, $rsf = 0.75$, $N^{max} = 15$, and short critical sections. The schedulability of the considered preemptable lock types in this configuration is shown in Fig. 2144.

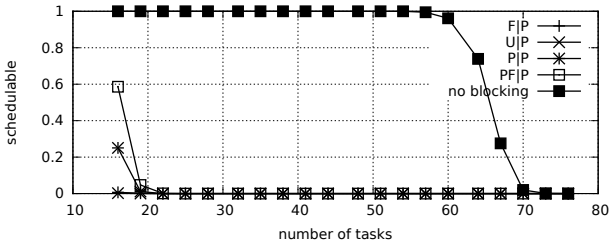

Fig. 2135. Schedulability under preemptable spin locks for $m = 16$, $U = 0.2n$, 32 resources, $rsf = 0.75$, $N^{max} = 1$, and medium critical sections. The schedulability of the considered non-preemptable lock types in this configuration is shown in Fig. 2125.

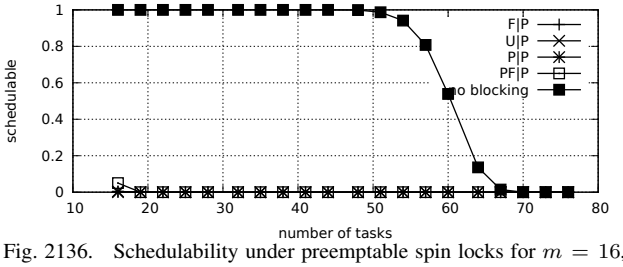

Fig. 2136. Schedulability under preemptable spin locks for $m = 16$, $U = 0.2n$, 32 resources, $rsf = 0.75$, $N^{max} = 2$, and medium critical sections. The schedulability of the considered non-preemptable lock types in this configuration is shown in Fig. 2126.

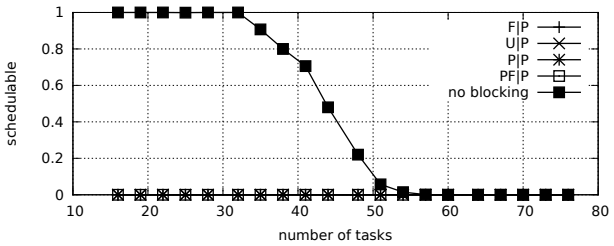

Fig. 2137. Schedulability under preemptable spin locks for $m = 16$, $U = 0.2n$, 32 resources, $rsf = 0.75$, $N^{max} = 5$, and medium critical sections. The schedulability of the considered non-preemptable lock types in this configuration is shown in Fig. 2127.

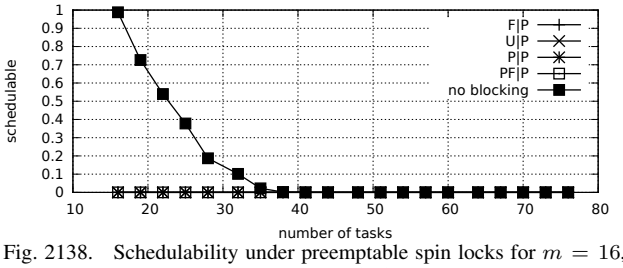

Fig. 2138. Schedulability under preemptable spin locks for $m = 16$, $U = 0.2n$, 32 resources, $rsf = 0.75$, $N^{max} = 10$, and medium critical sections. The schedulability of the considered non-preemptable lock types in this configuration is shown in Fig. 2128.

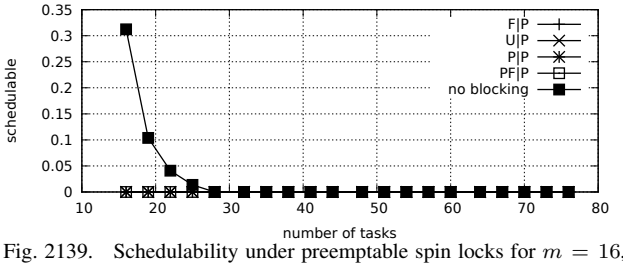

Fig. 2139. Schedulability under preemptable spin locks for $m = 16$, $U = 0.2n$, 32 resources, $rsf = 0.75$, $N^{max} = 15$, and medium critical sections. The schedulability of the considered non-preemptable lock types in this configuration is shown in Fig. 2129.

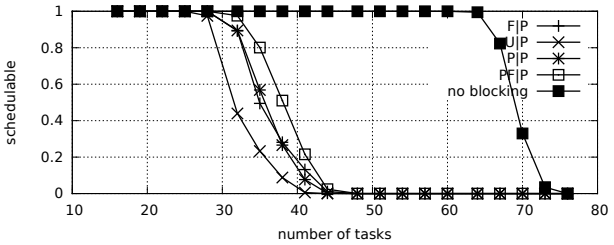

Fig. 2140. Schedulability under preemptable spin locks for $m = 16$, $U = 0.2n$, 32 resources, $rsf = 0.75$, $N^{max} = 1$, and short critical sections. The schedulability of the considered non-preemptable lock types in this configuration is shown in Fig. 2130.

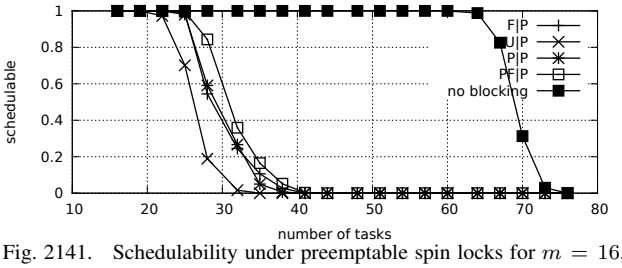

Fig. 2141. Schedulability under preemptable spin locks for $m = 16$, $U = 0.2n$, 32 resources, $rsf = 0.75$, $N^{max} = 2$, and short critical sections. The schedulability of the considered non-preemptable lock types in this configuration is shown in Fig. 2131.

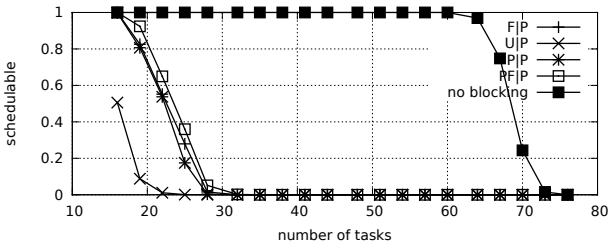

Fig. 2142. Schedulability under preemptable spin locks for $m = 16$, $U = 0.2n$, 32 resources, $rsf = 0.75$, $N^{max} = 5$, and short critical sections. The schedulability of the considered non-preemptable lock types in this configuration is shown in Fig. 2132.

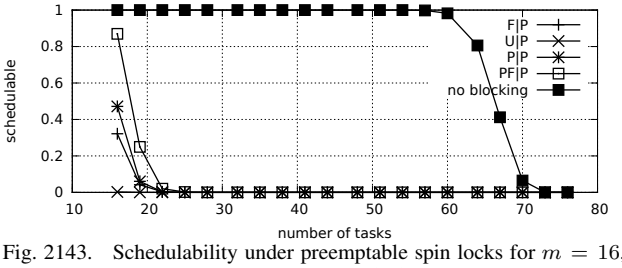

Fig. 2143. Schedulability under preemptable spin locks for $m = 16$, $U = 0.2n$, 32 resources, $rsf = 0.75$, $N^{max} = 10$, and short critical sections. The schedulability of the considered non-preemptable lock types in this configuration is shown in Fig. 2133.

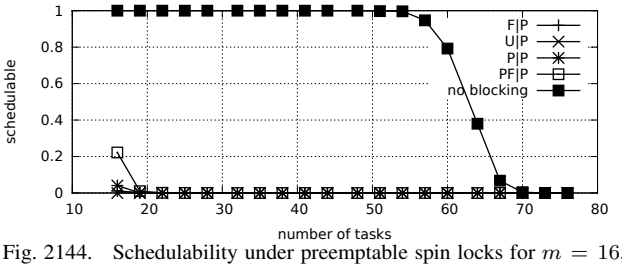

Fig. 2144. Schedulability under preemptable spin locks for $m = 16$, $U = 0.2n$, 32 resources, $rsf = 0.75$, $N^{max} = 15$, and short critical sections. The schedulability of the considered non-preemptable lock types in this configuration is shown in Fig. 2134.

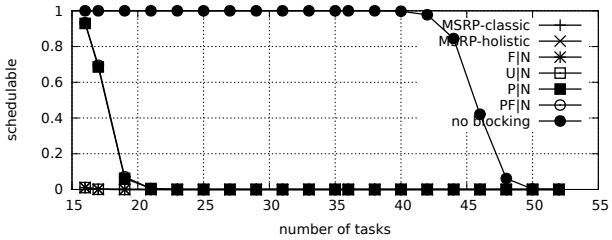

Fig. 2145. Schedulability under non-preemptable spin locks for $m = 16$, $U = 0.3n$, 32 resources, $rsf = 0.75$, $N^{max} = 1$, and medium critical sections. The schedulability of the considered preemptable lock types in this configuration is shown in Fig. 2155.

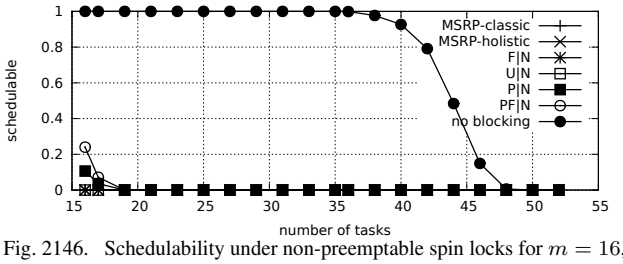

Fig. 2146. Schedulability under non-preemptable spin locks for $m = 16$, $U = 0.3n$, 32 resources, $rsf = 0.75$, $N^{max} = 2$, and medium critical sections. The schedulability of the considered preemptable lock types in this configuration is shown in Fig. 2156.

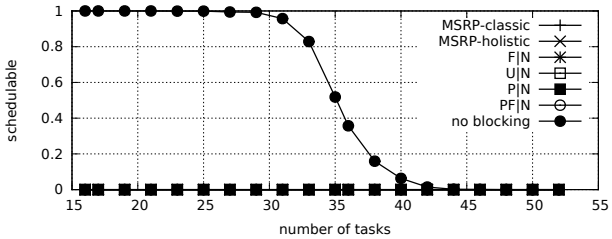

Fig. 2147. Schedulability under non-preemptable spin locks for $m = 16$, $U = 0.3n$, 32 resources, $rsf = 0.75$, $N^{max} = 5$, and medium critical sections. The schedulability of the considered preemptable lock types in this configuration is shown in Fig. 2157.

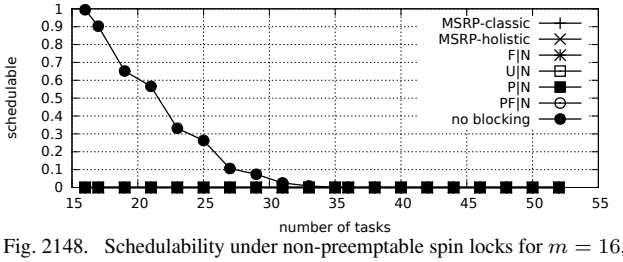

Fig. 2148. Schedulability under non-preemptable spin locks for $m = 16$, $U = 0.3n$, 32 resources, $rsf = 0.75$, $N^{max} = 10$, and medium critical sections. The schedulability of the considered preemptable lock types in this configuration is shown in Fig. 2158.

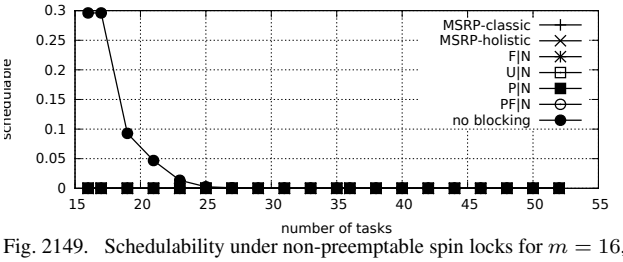

Fig. 2149. Schedulability under non-preemptable spin locks for $m = 16$, $U = 0.3n$, 32 resources, $rsf = 0.75$, $N^{max} = 15$, and medium critical sections. The schedulability of the considered preemptable lock types in this configuration is shown in Fig. 2159.

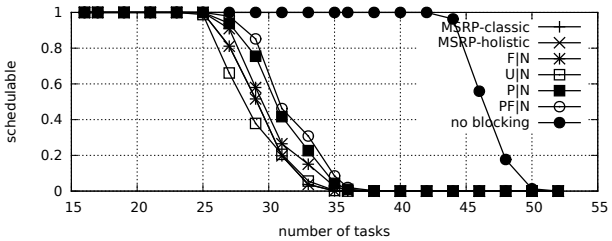

Fig. 2150. Schedulability under non-preemptable spin locks for $m = 16$, $U = 0.3n$, 32 resources, $rsf = 0.75$, $N^{max} = 1$, and short critical sections. The schedulability of the considered preemptable lock types in this configuration is shown in Fig. 2160.

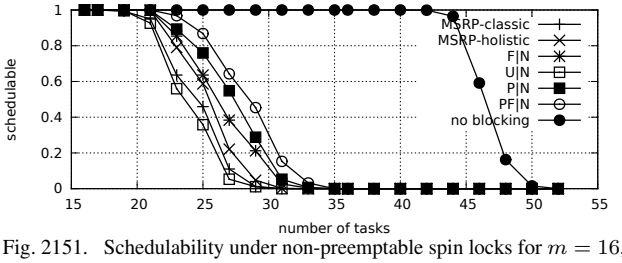

Fig. 2151. Schedulability under non-preemptable spin locks for $m = 16$, $U = 0.3n$, 32 resources, $rsf = 0.75$, $N^{max} = 2$, and short critical sections. The schedulability of the considered preemptable lock types in this configuration is shown in Fig. 2161.

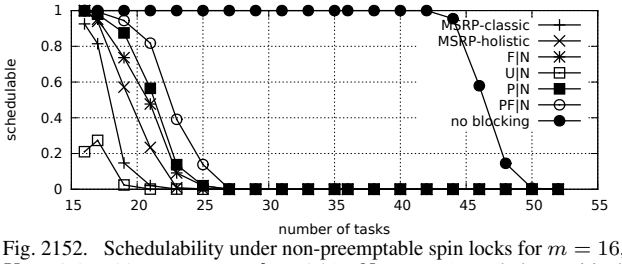

Fig. 2152. Schedulability under non-preemptable spin locks for $m = 16$, $U = 0.3n$, 32 resources, $rsf = 0.75$, $N^{max} = 5$, and short critical sections. The schedulability of the considered preemptable lock types in this configuration is shown in Fig. 2162.

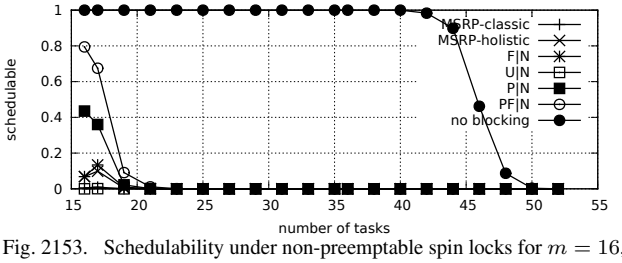

Fig. 2153. Schedulability under non-preemptable spin locks for $m = 16$, $U = 0.3n$, 32 resources, $rsf = 0.75$, $N^{max} = 10$, and short critical sections. The schedulability of the considered preemptable lock types in this configuration is shown in Fig. 2163.

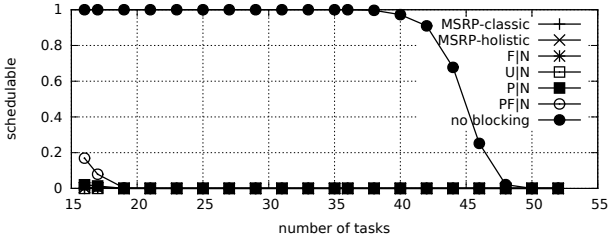

Fig. 2154. Schedulability under non-preemptable spin locks for $m = 16$, $U = 0.3n$, 32 resources, $rsf = 0.75$, $N^{max} = 15$, and short critical sections. The schedulability of the considered preemptable lock types in this configuration is shown in Fig. 2164.

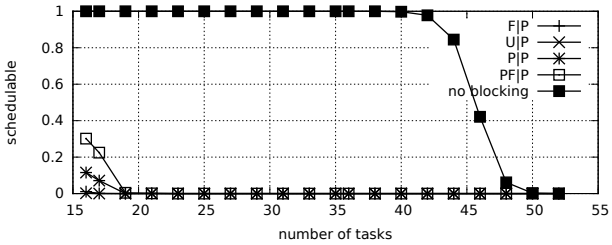

Fig. 2155. Schedulability under preemptable spin locks for $m = 16$, $U = 0.3n$, 32 resources, $rsf = 0.75$, $N^{max} = 1$, and medium critical sections. The schedulability of the considered non-preemptable lock types in this configuration is shown in Fig. 2145.

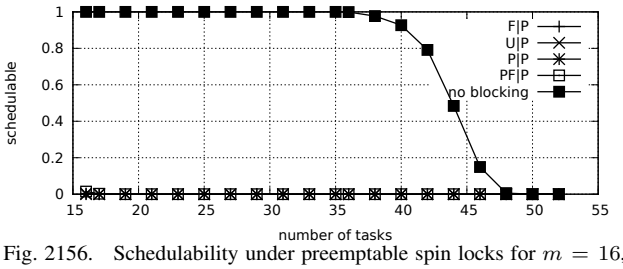

Fig. 2156. Schedulability under preemptable spin locks for $m = 16$, $U = 0.3n$, 32 resources, $rsf = 0.75$, $N^{max} = 2$, and medium critical sections. The schedulability of the considered non-preemptable lock types in this configuration is shown in Fig. 2146.

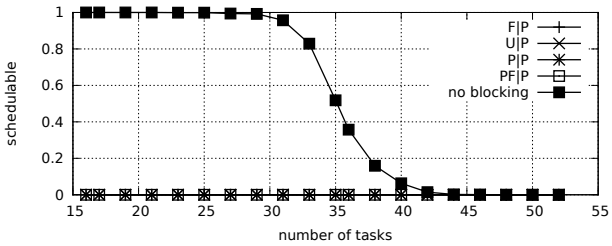

Fig. 2157. Schedulability under preemptable spin locks for $m = 16$, $U = 0.3n$, 32 resources, $rsf = 0.75$, $N^{max} = 5$, and medium critical sections. The schedulability of the considered non-preemptable lock types in this configuration is shown in Fig. 2147.

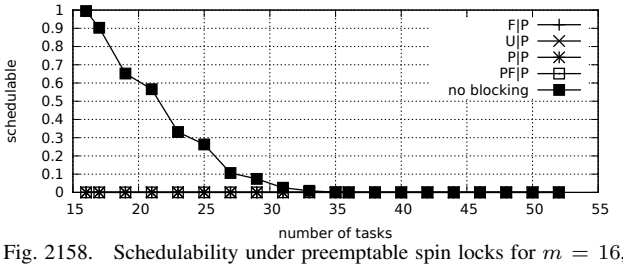

Fig. 2158. Schedulability under preemptable spin locks for $m = 16$, $U = 0.3n$, 32 resources, $rsf = 0.75$, $N^{max} = 10$, and medium critical sections. The schedulability of the considered non-preemptable lock types in this configuration is shown in Fig. 2148.

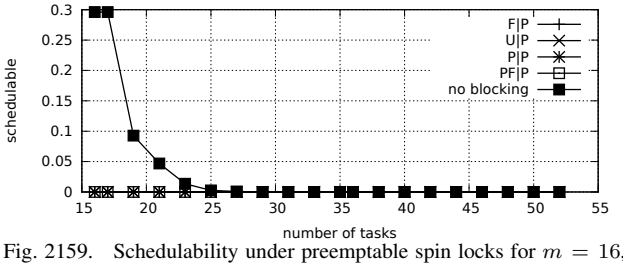

Fig. 2159. Schedulability under preemptable spin locks for $m = 16$, $U = 0.3n$, 32 resources, $rsf = 0.75$, $N^{max} = 15$, and medium critical sections. The schedulability of the considered non-preemptable lock types in this configuration is shown in Fig. 2149.

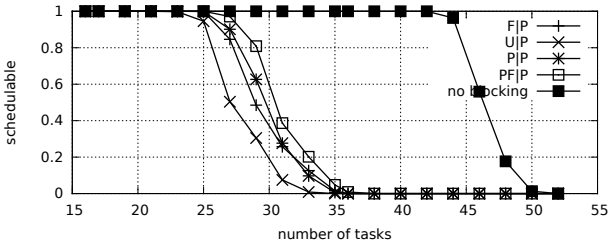

Fig. 2160. Schedulability under preemptable spin locks for $m = 16$, $U = 0.3n$, 32 resources, $rsf = 0.75$, $N^{max} = 1$, and short critical sections. The schedulability of the considered non-preemptable lock types in this configuration is shown in Fig. 2150.

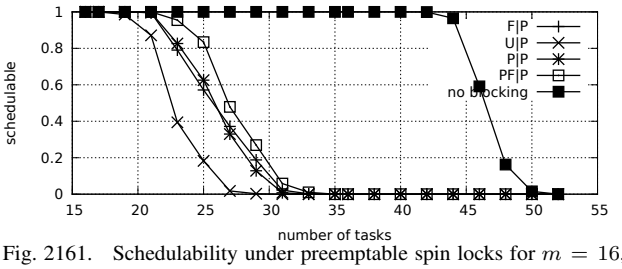

Fig. 2161. Schedulability under preemptable spin locks for $m = 16$, $U = 0.3n$, 32 resources, $rsf = 0.75$, $N^{max} = 2$, and short critical sections. The schedulability of the considered non-preemptable lock types in this configuration is shown in Fig. 2151.

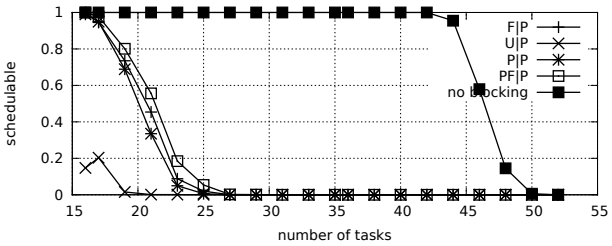

Fig. 2162. Schedulability under preemptable spin locks for $m = 16$, $U = 0.3n$, 32 resources, $rsf = 0.75$, $N^{max} = 5$, and short critical sections. The schedulability of the considered non-preemptable lock types in this configuration is shown in Fig. 2152.

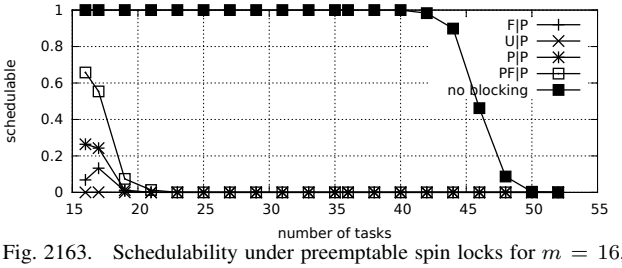

Fig. 2163. Schedulability under preemptable spin locks for $m = 16$, $U = 0.3n$, 32 resources, $rsf = 0.75$, $N^{max} = 10$, and short critical sections. The schedulability of the considered non-preemptable lock types in this configuration is shown in Fig. 2153.

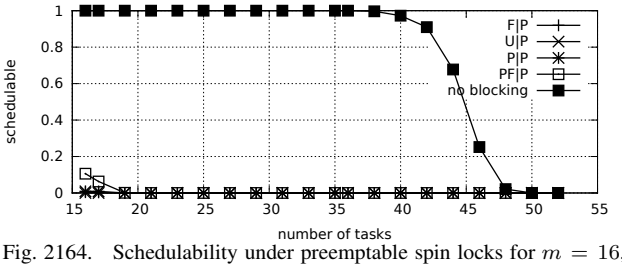

Fig. 2164. Schedulability under preemptable spin locks for $m = 16$, $U = 0.3n$, 32 resources, $rsf = 0.75$, $N^{max} = 15$, and short critical sections. The schedulability of the considered non-preemptable lock types in this configuration is shown in Fig. 2154.

Configurations with $U = 0.1n$

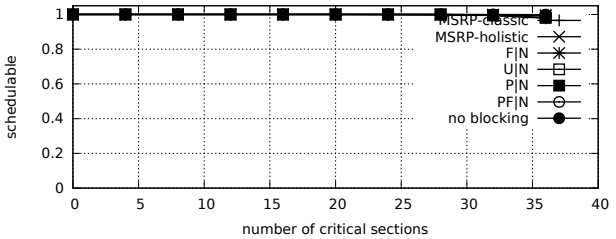

Fig. 2165. Schedulability under non-preemptable spin locks for $m = 4$, $U = 0.1n$, 2 resources, $rsf = 0.1$, and medium critical sections. The schedulability of the considered preemptable lock types in this configuration is shown in Fig. 2167.

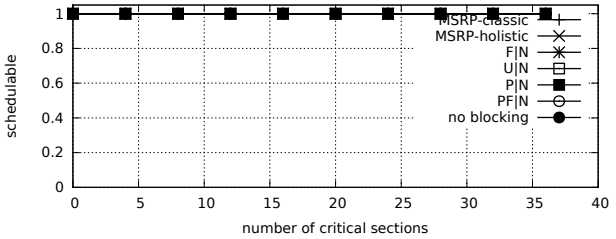

Fig. 2166. Schedulability under non-preemptable spin locks for $m = 4$, $U = 0.1n$, 2 resources, $rsf = 0.1$, and short critical sections. The schedulability of the considered preemptable lock types in this configuration is shown in Fig. 2168.

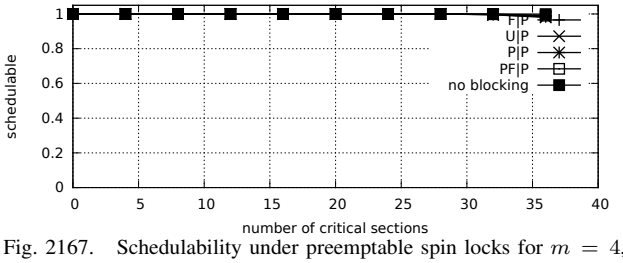

Fig. 2167. Schedulability under preemptable spin locks for $m = 4$, $U = 0.1n$, 2 resources, $rsf = 0.1$, and medium critical sections. The schedulability of the considered non-preemptable lock types in this configuration is shown in Fig. 2165.

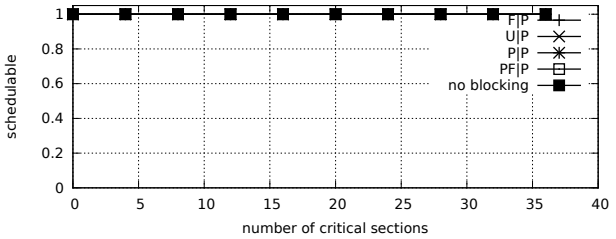

Fig. 2168. Schedulability under preemptable spin locks for $m = 4$, $U = 0.1n$, 2 resources, $rsf = 0.1$, and short critical sections. The schedulability of the considered non-preemptable lock types in this configuration is shown in Fig. 2166.

Configurations with $U = 0.2n$

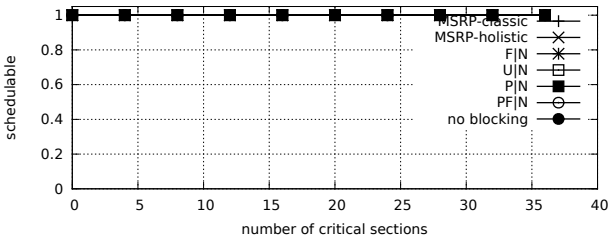

Fig. 2169. Schedulability under non-preemptable spin locks for $m = 4$, $U = 0.2n$, 2 resources, $rsf = 0.1$, and medium critical sections. The schedulability of the considered preemptable lock types in this configuration is shown in Fig. 2171.

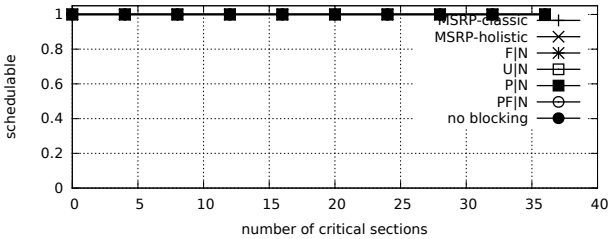

Fig. 2170. Schedulability under non-preemptable spin locks for $m = 4$, $U = 0.2n$, 2 resources, $rsf = 0.1$, and short critical sections. The schedulability of the considered preemptable lock types in this configuration is shown in Fig. 2172.

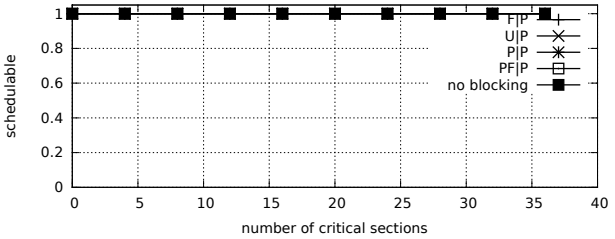

Fig. 2171. Schedulability under preemptable spin locks for $m = 4$, $U = 0.2n$, 2 resources, $rsf = 0.1$, and medium critical sections. The schedulability of the considered non-preemptable lock types in this configuration is shown in Fig. 2169.

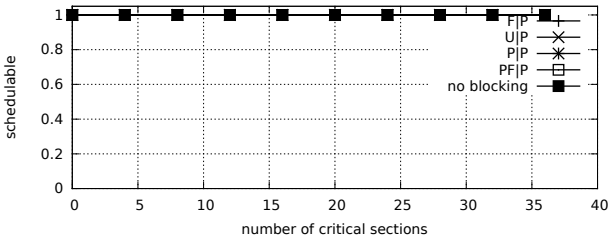

Fig. 2172. Schedulability under preemptable spin locks for $m = 4$, $U = 0.2n$, 2 resources, $rsf = 0.1$, and short critical sections. The schedulability of the considered non-preemptable lock types in this configuration is shown in Fig. 2170.

Configurations with $U = 0.3n$

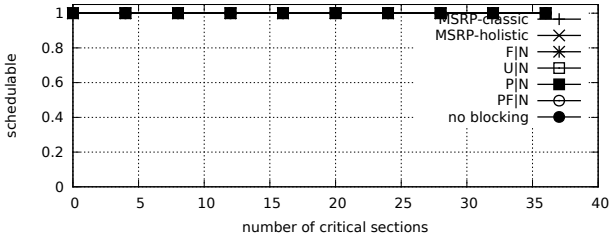

Fig. 2173. Schedulability under non-preemptable spin locks for $m = 4$, $U = 0.3n$, 2 resources, $rsf = 0.1$, and medium critical sections. The schedulability of the considered preemptable lock types in this configuration is shown in Fig. 2175.

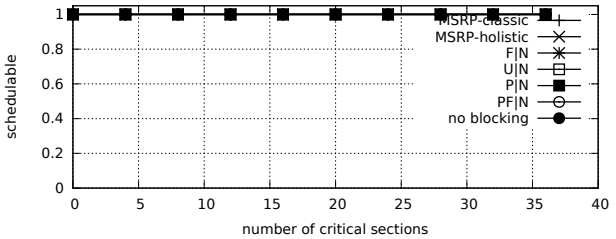

Fig. 2174. Schedulability under non-preemptable spin locks for $m = 4$, $U = 0.3n$, 2 resources, $rsf = 0.1$, and short critical sections. The schedulability of the considered preemptable lock types in this configuration is shown in Fig. 2176.

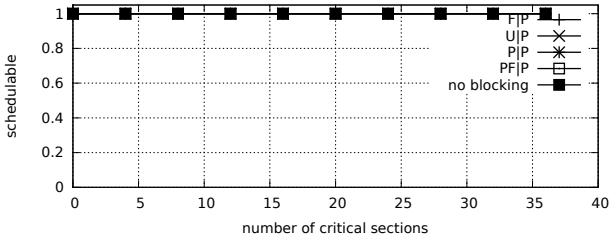

Fig. 2175. Schedulability under preemptable spin locks for $m = 4$, $U = 0.3n$, 2 resources, $rsf = 0.1$, and medium critical sections. The schedulability of the considered non-preemptable lock types in this configuration is shown in Fig. 2173.

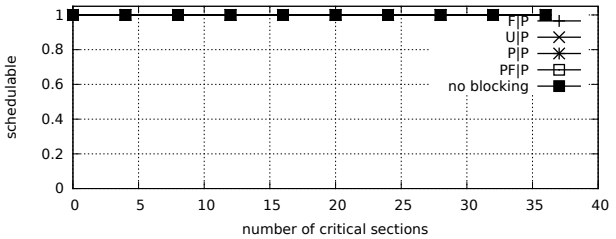

Fig. 2176. Schedulability under preemptable spin locks for $m = 4$, $U = 0.3n$, 2 resources, $rsf = 0.1$, and short critical sections. The schedulability of the considered non-preemptable lock types in this configuration is shown in Fig. 2174.

Configurations with $U = 0.1n$

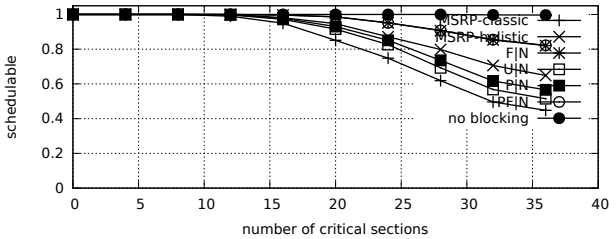

Fig. 2177. Schedulability under non-preemptable spin locks for $m = 4$, $U = 0.1n$, 2 resources, $rsf = 0.25$, and medium critical sections. The schedulability of the considered preemptable lock types in this configuration is shown in Fig. 2179.

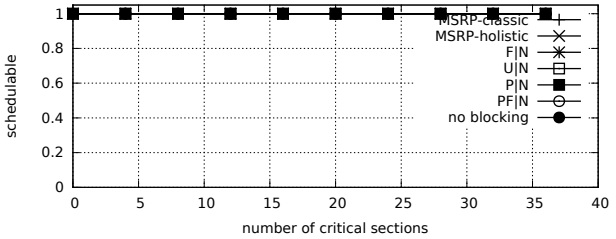

Fig. 2178. Schedulability under non-preemptable spin locks for $m = 4$, $U = 0.1n$, 2 resources, $rsf = 0.25$, and short critical sections. The schedulability of the considered preemptable lock types in this configuration is shown in Fig. 2180.

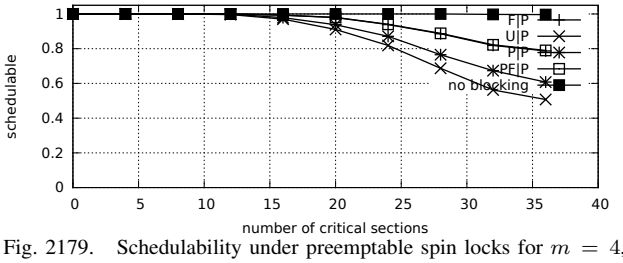

Fig. 2179. Schedulability under preemptable spin locks for $m = 4$, $U = 0.1n$, 2 resources, $rsf = 0.25$, and medium critical sections. The schedulability of the considered non-preemptable lock types in this configuration is shown in Fig. 2177.

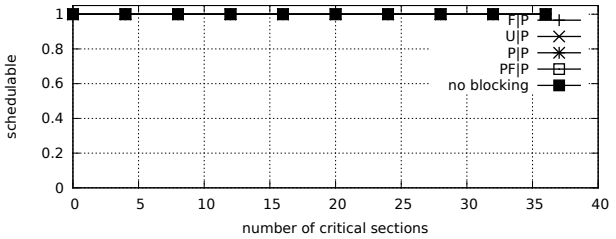

Fig. 2180. Schedulability under preemptable spin locks for $m = 4$, $U = 0.1n$, 2 resources, $rsf = 0.25$, and short critical sections. The schedulability of the considered non-preemptable lock types in this configuration is shown in Fig. 2178.

Configurations with $U = 0.2n$

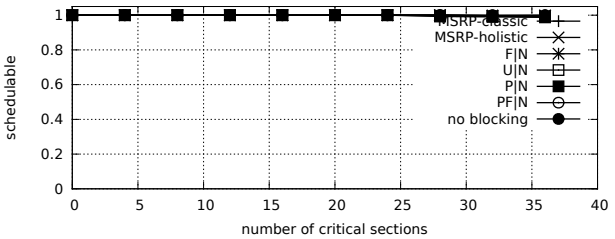

Fig. 2181. Schedulability under non-preemptable spin locks for $m = 4$, $U = 0.2n$, 2 resources, $rsf = 0.25$, and medium critical sections. The schedulability of the considered preemptable lock types in this configuration is shown in Fig. 2183.

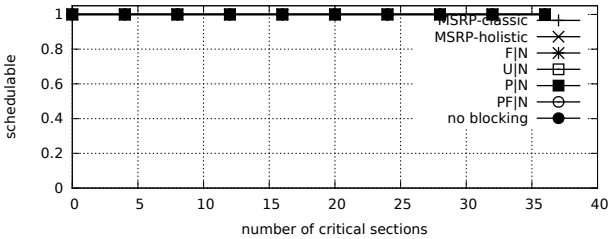

Fig. 2182. Schedulability under non-preemptable spin locks for $m = 4$, $U = 0.2n$, 2 resources, $rsf = 0.25$, and short critical sections. The schedulability of the considered preemptable lock types in this configuration is shown in Fig. 2184.

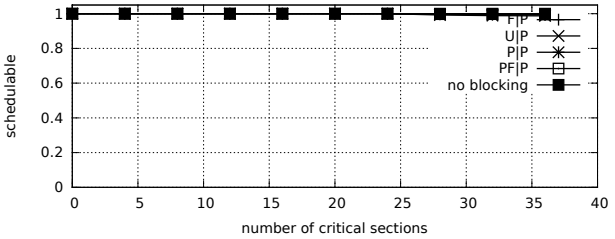

Fig. 2183. Schedulability under preemptable spin locks for $m = 4$, $U = 0.2n$, 2 resources, $rsf = 0.25$, and medium critical sections. The schedulability of the considered non-preemptable lock types in this configuration is shown in Fig. 2181.

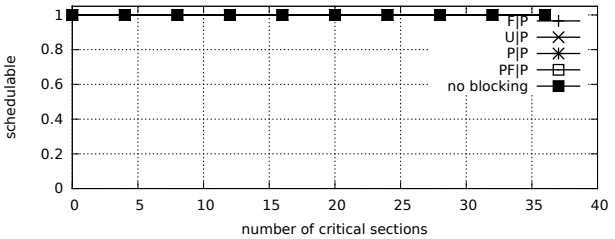

Fig. 2184. Schedulability under preemptable spin locks for $m = 4$, $U = 0.2n$, 2 resources, $rsf = 0.25$, and short critical sections. The schedulability of the considered non-preemptable lock types in this configuration is shown in Fig. 2182.

Configurations with $U = 0.3n$

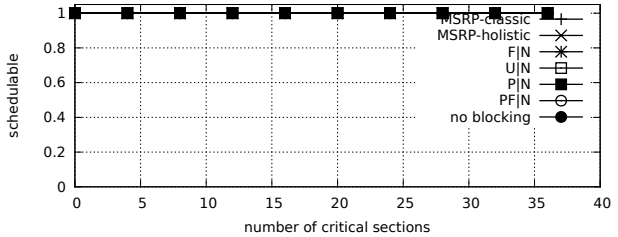

Fig. 2185. Schedulability under non-preemptable spin locks for $m = 4$, $U = 0.3n$, 2 resources, $rsf = 0.25$, and medium critical sections. The schedulability of the considered preemptable lock types in this configuration is shown in Fig. 2187.

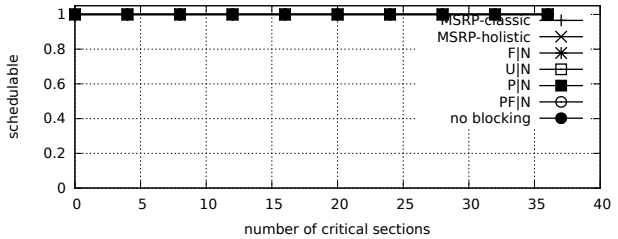

Fig. 2186. Schedulability under non-preemptable spin locks for $m = 4$, $U = 0.3n$, 2 resources, $rsf = 0.25$, and short critical sections. The schedulability of the considered preemptable lock types in this configuration is shown in Fig. 2188.

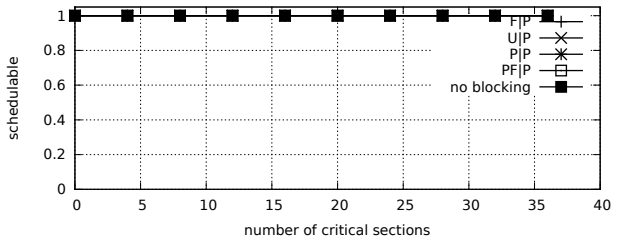

Fig. 2187. Schedulability under preemptable spin locks for $m = 4$, $U = 0.3n$, 2 resources, $rsf = 0.25$, and medium critical sections. The schedulability of the considered non-preemptable lock types in this configuration is shown in Fig. 2185.

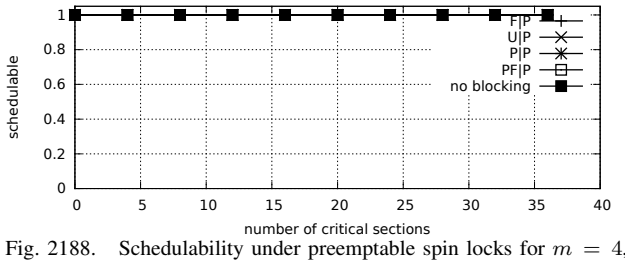

Fig. 2188. Schedulability under preemptable spin locks for $m = 4$, $U = 0.3n$, 2 resources, $rsf = 0.25$, and short critical sections. The schedulability of the considered non-preemptable lock types in this configuration is shown in Fig. 2186.

Configurations with $U = 0.1n$

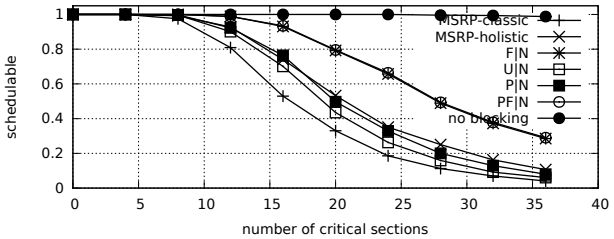

Fig. 2189. Schedulability under non-preemptable spin locks for $m = 4$, $U = 0.1n$, 2 resources, $rsf = 0.4$, and medium critical sections. The schedulability of the considered preemptable lock types in this configuration is shown in Fig. 2191.

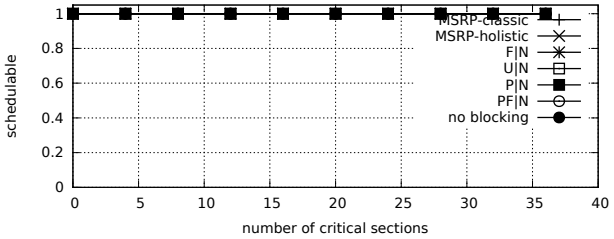

Fig. 2190. Schedulability under non-preemptable spin locks for $m = 4$, $U = 0.1n$, 2 resources, $rsf = 0.4$, and short critical sections. The schedulability of the considered preemptable lock types in this configuration is shown in Fig. 2192.

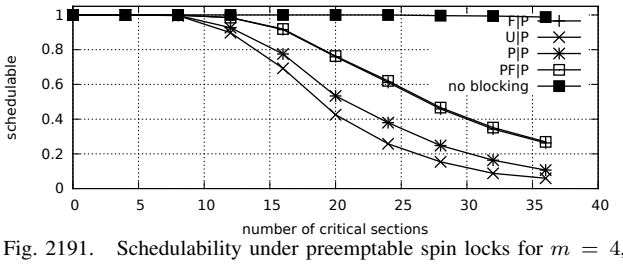

Fig. 2191. Schedulability under preemptable spin locks for $m = 4$, $U = 0.1n$, 2 resources, $rsf = 0.4$, and medium critical sections. The schedulability of the considered non-preemptable lock types in this configuration is shown in Fig. 2189.

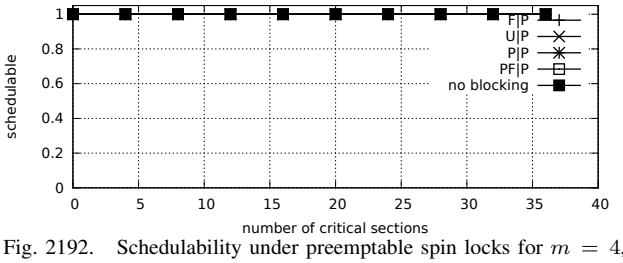

Fig. 2192. Schedulability under preemptable spin locks for $m = 4$, $U = 0.1n$, 2 resources, $rsf = 0.4$, and short critical sections. The schedulability of the considered non-preemptable lock types in this configuration is shown in Fig. 2190.

Configurations with $U = 0.2n$

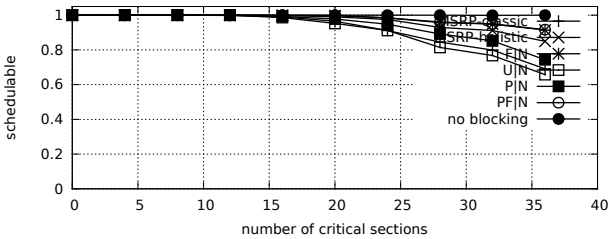

Fig. 2193. Schedulability under non-preemptable spin locks for $m = 4$, $U = 0.2n$, 2 resources, $rsf = 0.4$, and medium critical sections. The schedulability of the considered preemptable lock types in this configuration is shown in Fig. 2195.

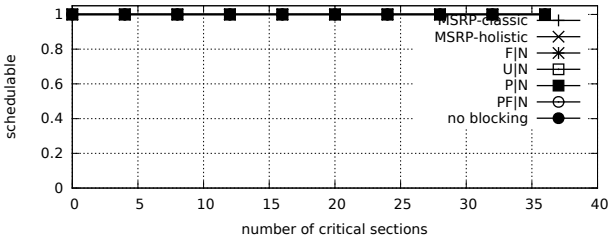

Fig. 2194. Schedulability under non-preemptable spin locks for $m = 4$, $U = 0.2n$, 2 resources, $rsf = 0.4$, and short critical sections. The schedulability of the considered preemptable lock types in this configuration is shown in Fig. 2196.

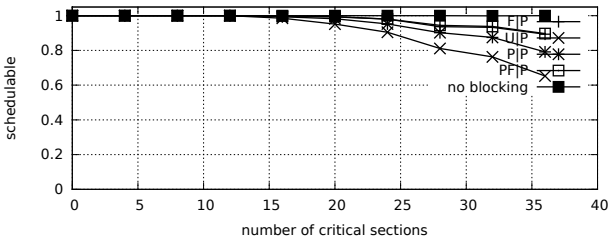

Fig. 2195. Schedulability under preemptable spin locks for $m = 4$, $U = 0.2n$, 2 resources, $rsf = 0.4$, and medium critical sections. The schedulability of the considered non-preemptable lock types in this configuration is shown in Fig. 2193.

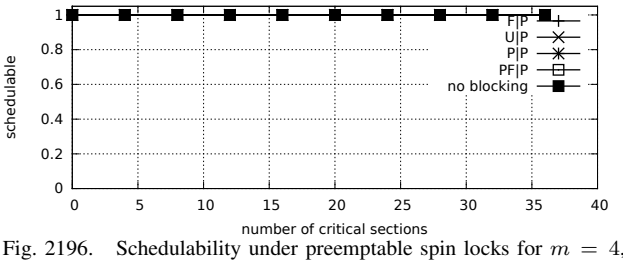

Fig. 2196. Schedulability under preemptable spin locks for $m = 4$, $U = 0.2n$, 2 resources, $rsf = 0.4$, and short critical sections. The schedulability of the considered non-preemptable lock types in this configuration is shown in Fig. 2194.

Configurations with $U = 0.3n$

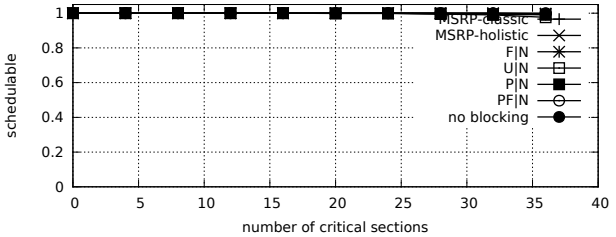

Fig. 2197. Schedulability under non-preemptable spin locks for $m = 4$, $U = 0.3n$, 2 resources, $rsf = 0.4$, and medium critical sections. The schedulability of the considered preemptable lock types in this configuration is shown in Fig. 2199.

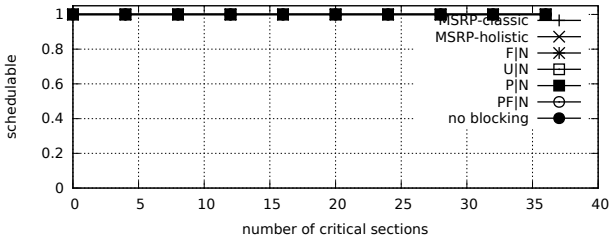

Fig. 2198. Schedulability under non-preemptable spin locks for $m = 4$, $U = 0.3n$, 2 resources, $rsf = 0.4$, and short critical sections. The schedulability of the considered preemptable lock types in this configuration is shown in Fig. 2200.

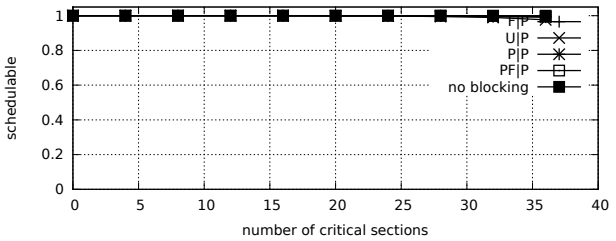

Fig. 2199. Schedulability under preemptable spin locks for $m = 4$, $U = 0.3n$, 2 resources, $rsf = 0.4$, and medium critical sections. The schedulability of the considered non-preemptable lock types in this configuration is shown in Fig. 2197.

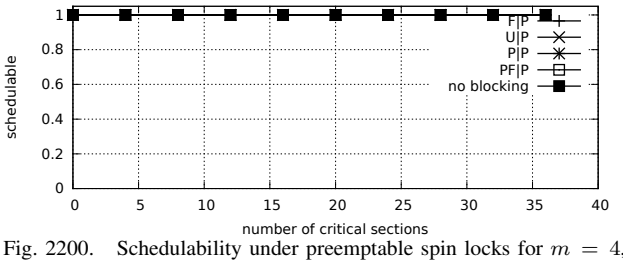

Fig. 2200. Schedulability under preemptable spin locks for $m = 4$, $U = 0.3n$, 2 resources, $rsf = 0.4$, and short critical sections. The schedulability of the considered non-preemptable lock types in this configuration is shown in Fig. 2198.

Configurations with $U = 0.1n$

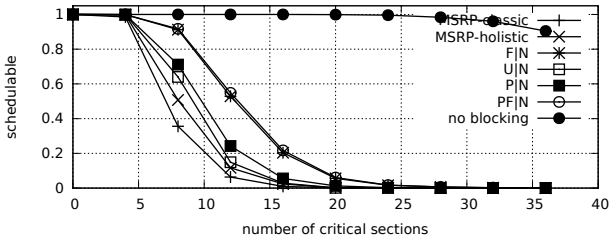

Fig. 2201. Schedulability under non-preemptable spin locks for $m = 4$, $U = 0.1n$, 2 resources, $rsf = 0.75$, and medium critical sections. The schedulability of the considered preemptable lock types in this configuration is shown in Fig. 2203.

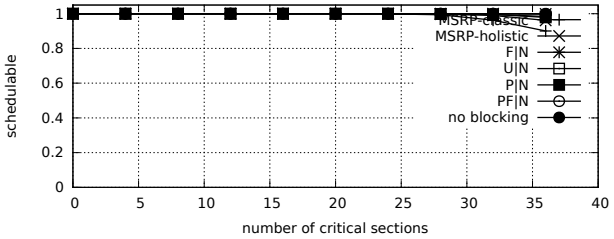

Fig. 2202. Schedulability under non-preemptable spin locks for $m = 4$, $U = 0.1n$, 2 resources, $rsf = 0.75$, and short critical sections. The schedulability of the considered preemptable lock types in this configuration is shown in Fig. 2204.

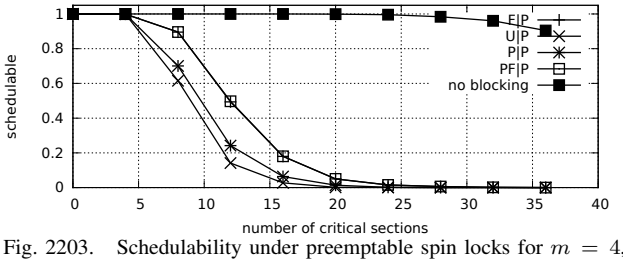

Fig. 2203. Schedulability under preemptable spin locks for $m = 4$, $U = 0.1n$, 2 resources, $rsf = 0.75$, and medium critical sections. The schedulability of the considered non-preemptable lock types in this configuration is shown in Fig. 2201.

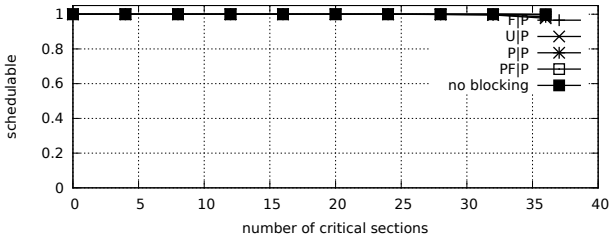

Fig. 2204. Schedulability under preemptable spin locks for $m = 4$, $U = 0.1n$, 2 resources, $rsf = 0.75$, and short critical sections. The schedulability of the considered non-preemptable lock types in this configuration is shown in Fig. 2202.

Configurations with $U = 0.2n$

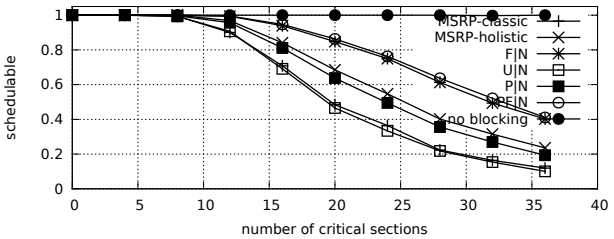

Fig. 2205. Schedulability under non-preemptable spin locks for $m = 4$, $U = 0.2n$, 2 resources, $rsf = 0.75$, and medium critical sections. The schedulability of the considered preemptable lock types in this configuration is shown in Fig. 2207.

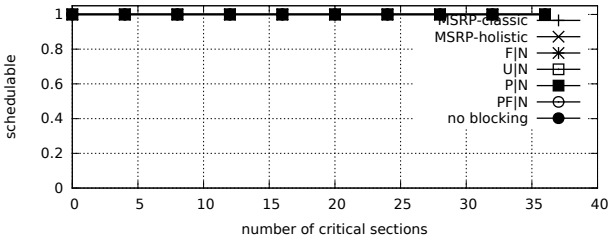

Fig. 2206. Schedulability under non-preemptable spin locks for $m = 4$, $U = 0.2n$, 2 resources, $rsf = 0.75$, and short critical sections. The schedulability of the considered preemptable lock types in this configuration is shown in Fig. 2208.

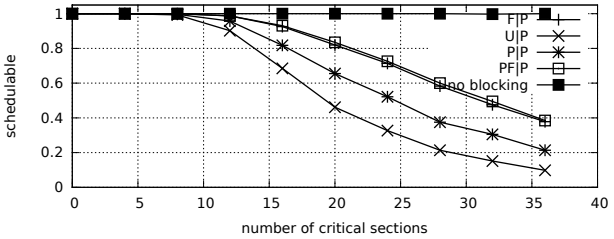

Fig. 2207. Schedulability under preemptable spin locks for $m = 4$, $U = 0.2n$, 2 resources, $rsf = 0.75$, and medium critical sections. The schedulability of the considered non-preemptable lock types in this configuration is shown in Fig. 2205.

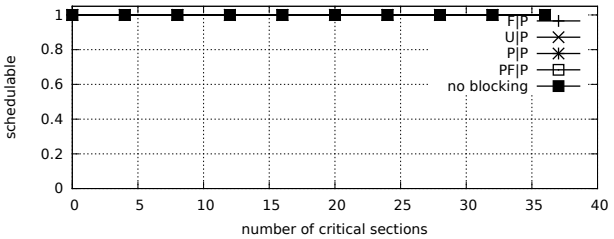

Fig. 2208. Schedulability under preemptable spin locks for $m = 4$, $U = 0.2n$, 2 resources, $rsf = 0.75$, and short critical sections. The schedulability of the considered non-preemptable lock types in this configuration is shown in Fig. 2206.

Configurations with $U = 0.3n$

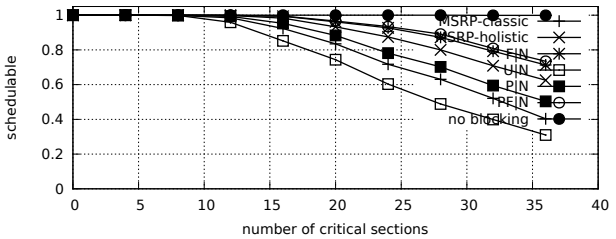

Fig. 2209. Schedulability under non-preemptable spin locks for $m = 4$, $U = 0.3n$, 2 resources, $rsf = 0.75$, and medium critical sections. The schedulability of the considered preemptable lock types in this configuration is shown in Fig. 2211.

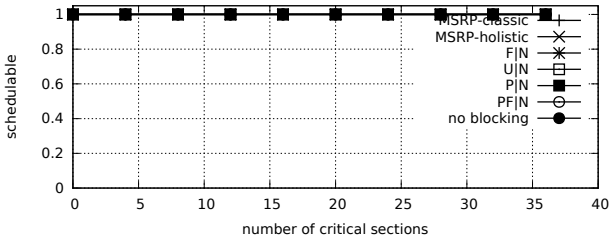

Fig. 2210. Schedulability under non-preemptable spin locks for $m = 4$, $U = 0.3n$, 2 resources, $rsf = 0.75$, and short critical sections. The schedulability of the considered preemptable lock types in this configuration is shown in Fig. 2212.

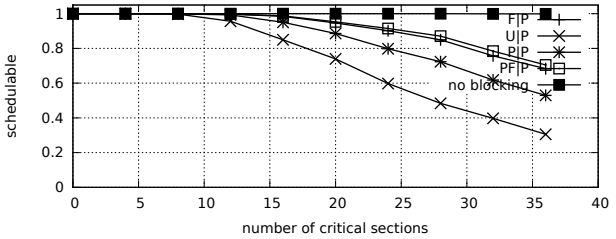

Fig. 2211. Schedulability under preemptable spin locks for $m = 4$, $U = 0.3n$, 2 resources, $rsf = 0.75$, and medium critical sections. The schedulability of the considered non-preemptable lock types in this configuration is shown in Fig. 2209.

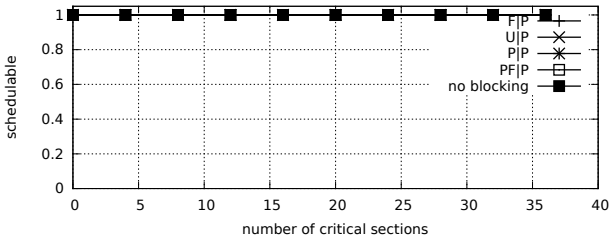

Fig. 2212. Schedulability under preemptable spin locks for $m = 4$, $U = 0.3n$, 2 resources, $rsf = 0.75$, and short critical sections. The schedulability of the considered non-preemptable lock types in this configuration is shown in Fig. 2210.

Configurations with $U = 0.1n$

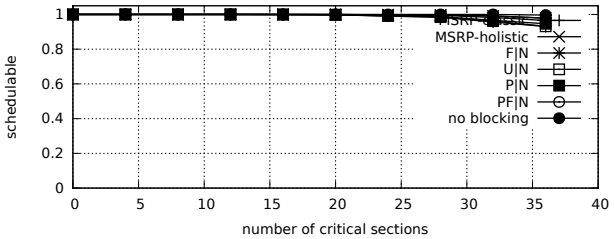

Fig. 2213. Schedulability under non-preemptable spin locks for $m = 4$, $U = 0.1n$, 4 resources, $rsf = 0.1$, and medium critical sections. The schedulability of the considered preemptable lock types in this configuration is shown in Fig. 2215.

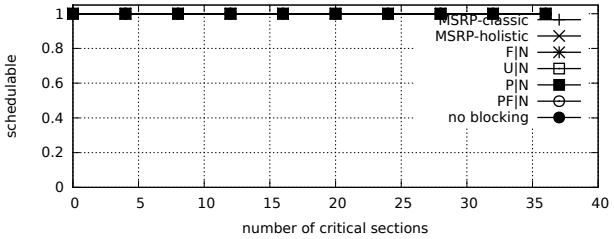

Fig. 2214. Schedulability under non-preemptable spin locks for $m = 4$, $U = 0.1n$, 4 resources, $rsf = 0.1$, and short critical sections. The schedulability of the considered preemptable lock types in this configuration is shown in Fig. 2216.

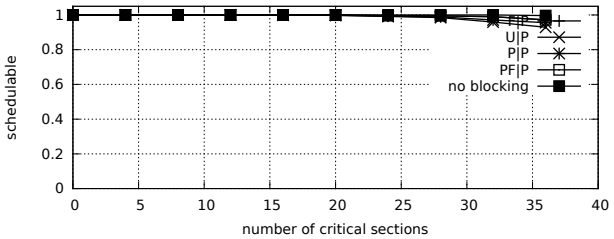

Fig. 2215. Schedulability under preemptable spin locks for $m = 4$, $U = 0.1n$, 4 resources, $rsf = 0.1$, and medium critical sections. The schedulability of the considered non-preemptable lock types in this configuration is shown in Fig. 2213.

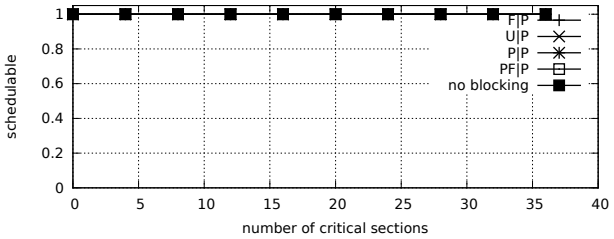

Fig. 2216. Schedulability under preemptable spin locks for $m = 4$, $U = 0.1n$, 4 resources, $rsf = 0.1$, and short critical sections. The schedulability of the considered non-preemptable lock types in this configuration is shown in Fig. 2214.

Configurations with $U = 0.2n$

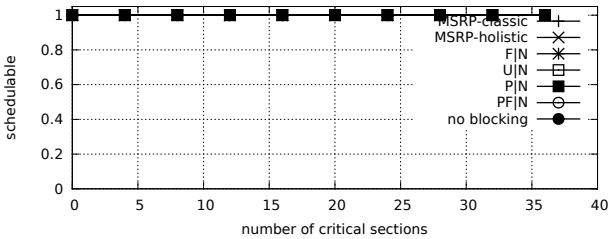

Fig. 2217. Schedulability under non-preemptable spin locks for $m = 4$, $U = 0.2n$, 4 resources, $rsf = 0.1$, and medium critical sections. The schedulability of the considered preemptable lock types in this configuration is shown in Fig. 2219.

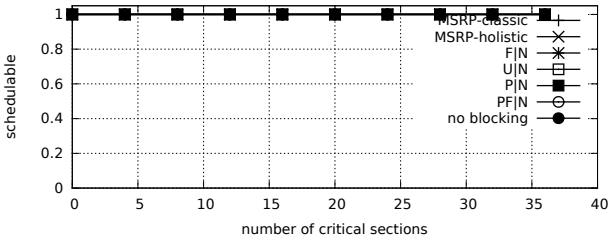

Fig. 2218. Schedulability under non-preemptable spin locks for $m = 4$, $U = 0.2n$, 4 resources, $rsf = 0.1$, and short critical sections. The schedulability of the considered preemptable lock types in this configuration is shown in Fig. 2220.

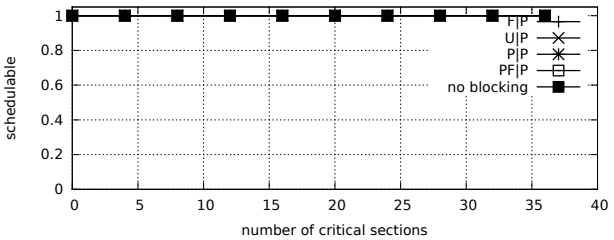

Fig. 2219. Schedulability under preemptable spin locks for $m = 4$, $U = 0.2n$, 4 resources, $rsf = 0.1$, and medium critical sections. The schedulability of the considered non-preemptable lock types in this configuration is shown in Fig. 2217.

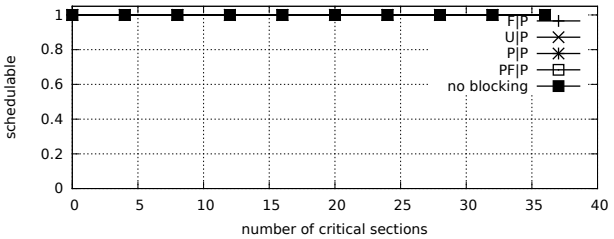

Fig. 2220. Schedulability under preemptable spin locks for $m = 4$, $U = 0.2n$, 4 resources, $rsf = 0.1$, and short critical sections. The schedulability of the considered non-preemptable lock types in this configuration is shown in Fig. 2218.

Configurations with $U = 0.3n$

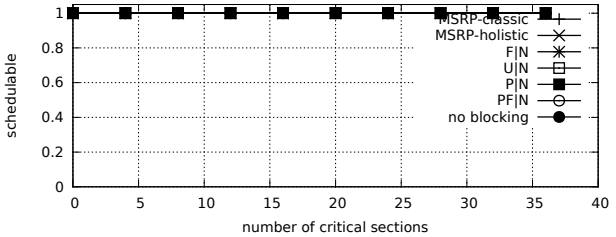

Fig. 2221. Schedulability under non-preemptable spin locks for $m = 4$, $U = 0.3n$, 4 resources, $rsf = 0.1$, and medium critical sections. The schedulability of the considered preemptable lock types in this configuration is shown in Fig. 2223.

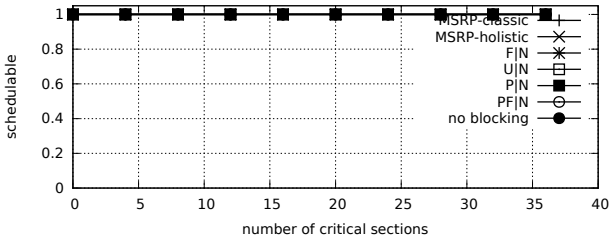

Fig. 2222. Schedulability under non-preemptable spin locks for $m = 4$, $U = 0.3n$, 4 resources, $rsf = 0.1$, and short critical sections. The schedulability of the considered preemptable lock types in this configuration is shown in Fig. 2224.

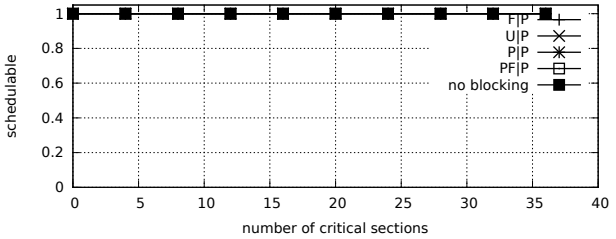

Fig. 2223. Schedulability under preemptable spin locks for $m = 4$, $U = 0.3n$, 4 resources, $rsf = 0.1$, and medium critical sections. The schedulability of the considered non-preemptable lock types in this configuration is shown in Fig. 2221.

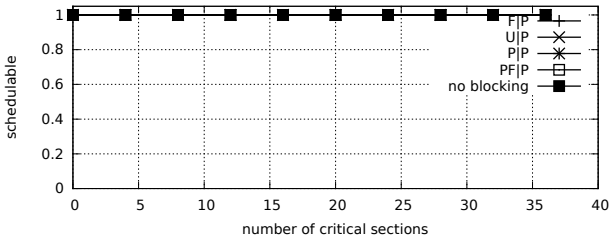

Fig. 2224. Schedulability under preemptable spin locks for $m = 4$, $U = 0.3n$, 4 resources, $rsf = 0.1$, and short critical sections. The schedulability of the considered non-preemptable lock types in this configuration is shown in Fig. 2222.

Configurations with $U = 0.1n$

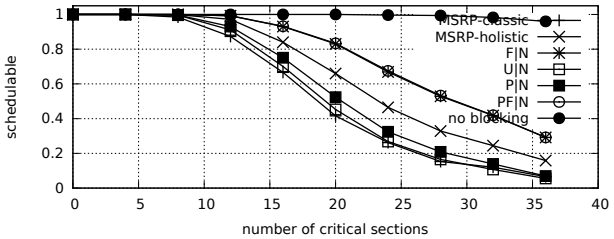

Fig. 2225. Schedulability under non-preemptable spin locks for $m = 4$, $U = 0.1n$, 4 resources, $rsf = 0.25$, and medium critical sections. The schedulability of the considered preemptable lock types in this configuration is shown in Fig. 2227.

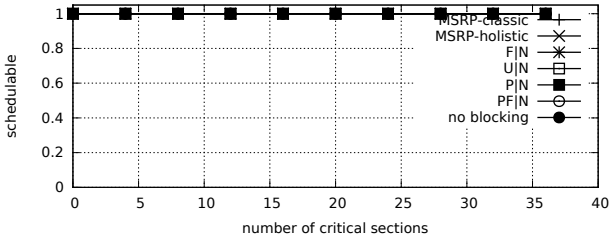

Fig. 2226. Schedulability under non-preemptable spin locks for $m = 4$, $U = 0.1n$, 4 resources, $rsf = 0.25$, and short critical sections. The schedulability of the considered preemptable lock types in this configuration is shown in Fig. 2228.

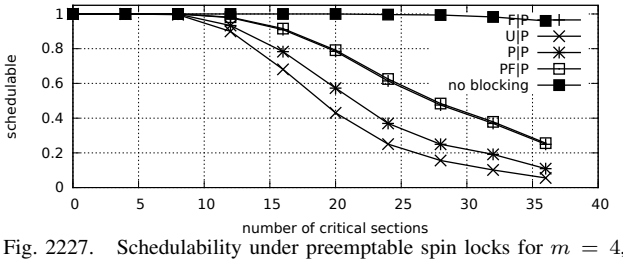

Fig. 2227. Schedulability under preemptable spin locks for $m = 4$, $U = 0.1n$, 4 resources, $rsf = 0.25$, and medium critical sections. The schedulability of the considered non-preemptable lock types in this configuration is shown in Fig. 2225.

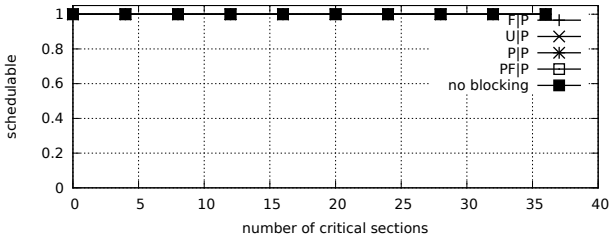

Fig. 2228. Schedulability under preemptable spin locks for $m = 4$, $U = 0.1n$, 4 resources, $rsf = 0.25$, and short critical sections. The schedulability of the considered non-preemptable lock types in this configuration is shown in Fig. 2226.

Configurations with $U = 0.2n$

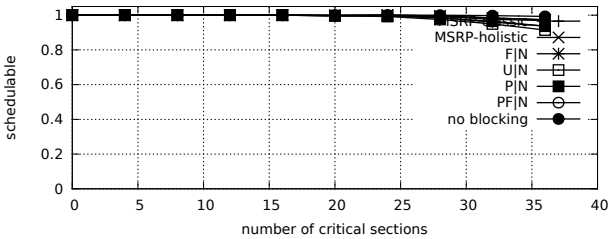

Fig. 2229. Schedulability under non-preemptable spin locks for $m = 4$, $U = 0.2n$, 4 resources, $rsf = 0.25$, and medium critical sections. The schedulability of the considered preemptable lock types in this configuration is shown in Fig. 2231.

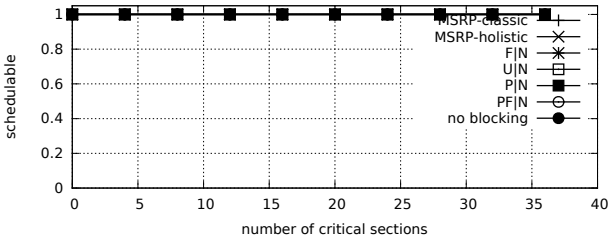

Fig. 2230. Schedulability under non-preemptable spin locks for $m = 4$, $U = 0.2n$, 4 resources, $rsf = 0.25$, and short critical sections. The schedulability of the considered preemptable lock types in this configuration is shown in Fig. 2232.

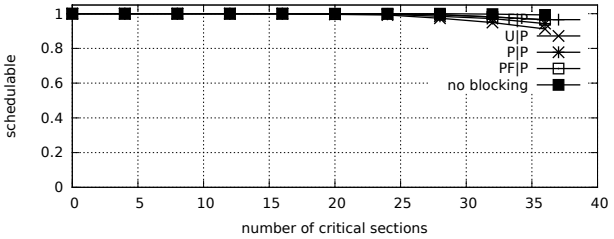

Fig. 2231. Schedulability under preemptable spin locks for $m = 4$, $U = 0.2n$, 4 resources, $rsf = 0.25$, and medium critical sections. The schedulability of the considered non-preemptable lock types in this configuration is shown in Fig. 2229.

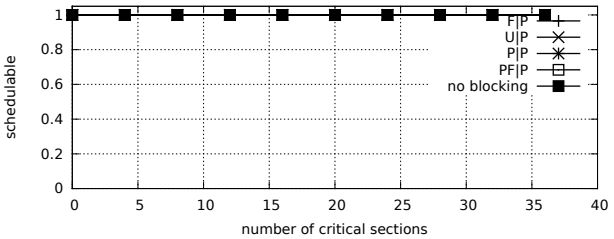

Fig. 2232. Schedulability under preemptable spin locks for $m = 4$, $U = 0.2n$, 4 resources, $rsf = 0.25$, and short critical sections. The schedulability of the considered non-preemptable lock types in this configuration is shown in Fig. 2230.

Configurations with $U = 0.3n$

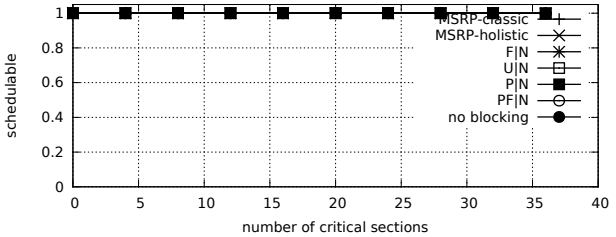

Fig. 2233. Schedulability under non-preemptable spin locks for $m = 4$, $U = 0.3n$, 4 resources, $rsf = 0.25$, and medium critical sections. The schedulability of the considered preemptable lock types in this configuration is shown in Fig. 2235.

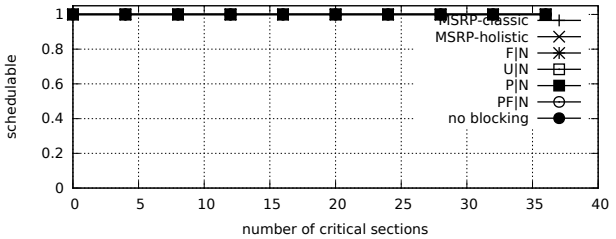

Fig. 2234. Schedulability under non-preemptable spin locks for $m = 4$, $U = 0.3n$, 4 resources, $rsf = 0.25$, and short critical sections. The schedulability of the considered preemptable lock types in this configuration is shown in Fig. 2236.

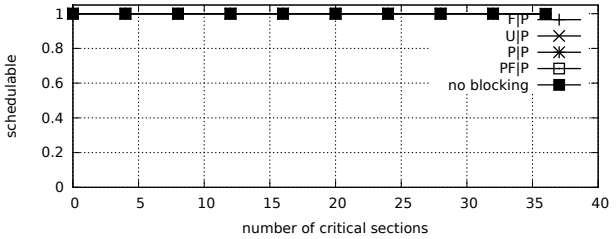

Fig. 2235. Schedulability under preemptable spin locks for $m = 4$, $U = 0.3n$, 4 resources, $rsf = 0.25$, and medium critical sections. The schedulability of the considered non-preemptable lock types in this configuration is shown in Fig. 2233.

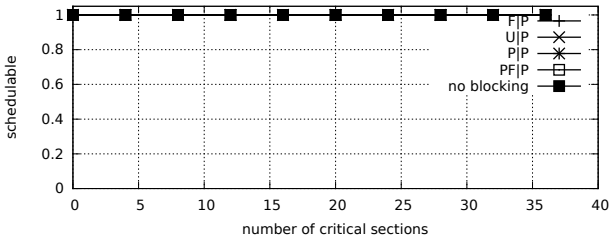

Fig. 2236. Schedulability under preemptable spin locks for $m = 4$, $U = 0.3n$, 4 resources, $rsf = 0.25$, and short critical sections. The schedulability of the considered non-preemptable lock types in this configuration is shown in Fig. 2234.

Configurations with $U = 0.1n$

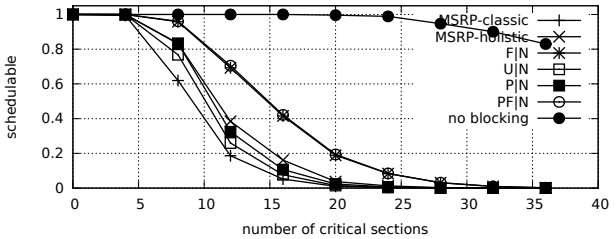

Fig. 2237. Schedulability under non-preemptable spin locks for $m = 4$, $U = 0.1n$, 4 resources, $rsf = 0.4$, and medium critical sections. The schedulability of the considered preemptable lock types in this configuration is shown in Fig. 2239.

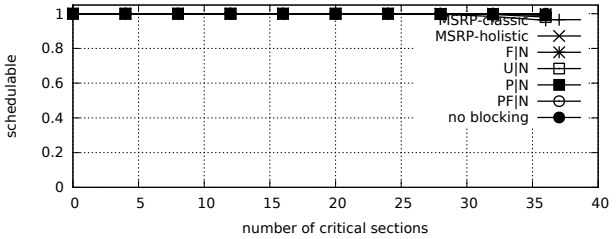

Fig. 2238. Schedulability under non-preemptable spin locks for $m = 4$, $U = 0.1n$, 4 resources, $rsf = 0.4$, and short critical sections. The schedulability of the considered preemptable lock types in this configuration is shown in Fig. 2240.

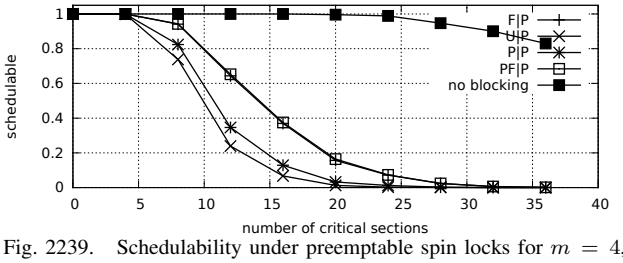

Fig. 2239. Schedulability under preemptable spin locks for $m = 4$, $U = 0.1n$, 4 resources, $rsf = 0.4$, and medium critical sections. The schedulability of the considered non-preemptable lock types in this configuration is shown in Fig. 2237.

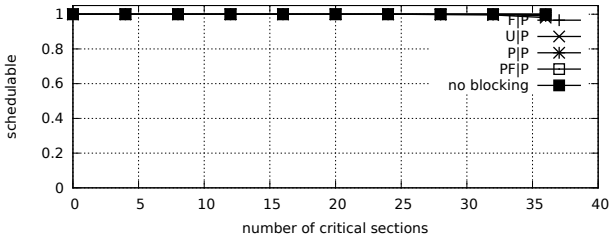

Fig. 2240. Schedulability under preemptable spin locks for $m = 4$, $U = 0.1n$, 4 resources, $rsf = 0.4$, and short critical sections. The schedulability of the considered non-preemptable lock types in this configuration is shown in Fig. 2238.

Configurations with $U = 0.2n$

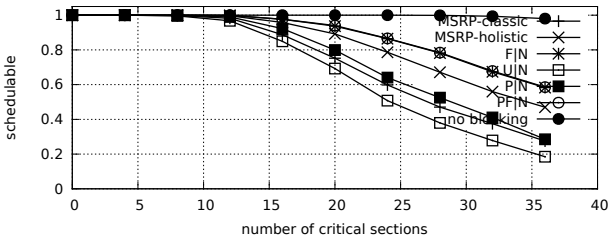

Fig. 2241. Schedulability under non-preemptable spin locks for $m = 4$, $U = 0.2n$, 4 resources, $rsf = 0.4$, and medium critical sections. The schedulability of the considered preemptable lock types in this configuration is shown in Fig. 2243.

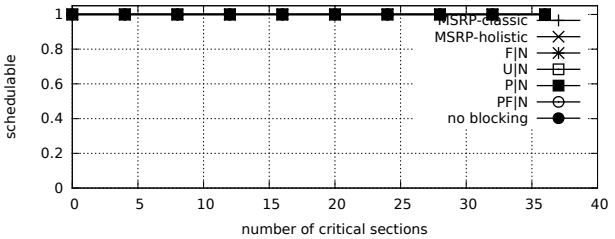

Fig. 2242. Schedulability under non-preemptable spin locks for $m = 4$, $U = 0.2n$, 4 resources, $rsf = 0.4$, and short critical sections. The schedulability of the considered preemptable lock types in this configuration is shown in Fig. 2244.

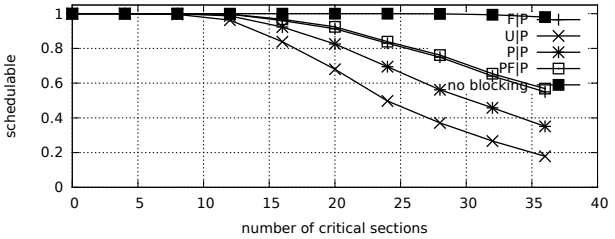

Fig. 2243. Schedulability under preemptable spin locks for $m = 4$, $U = 0.2n$, 4 resources, $rsf = 0.4$, and medium critical sections. The schedulability of the considered non-preemptable lock types in this configuration is shown in Fig. 2241.

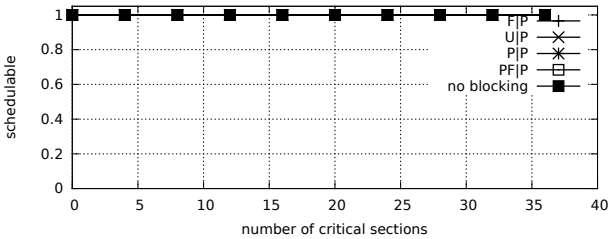

Fig. 2244. Schedulability under preemptable spin locks for $m = 4$, $U = 0.2n$, 4 resources, $rsf = 0.4$, and short critical sections. The schedulability of the considered non-preemptable lock types in this configuration is shown in Fig. 2242.

Configurations with $U = 0.3n$

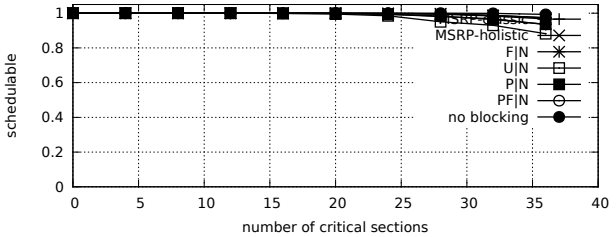

Fig. 2245. Schedulability under non-preemptable spin locks for $m = 4$, $U = 0.3n$, 4 resources, $rsf = 0.4$, and medium critical sections. The schedulability of the considered preemptable lock types in this configuration is shown in Fig. 2247.

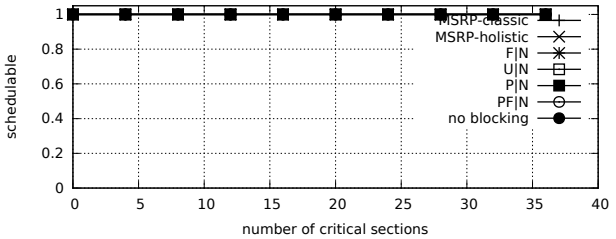

Fig. 2246. Schedulability under non-preemptable spin locks for $m = 4$, $U = 0.3n$, 4 resources, $rsf = 0.4$, and short critical sections. The schedulability of the considered preemptable lock types in this configuration is shown in Fig. 2248.

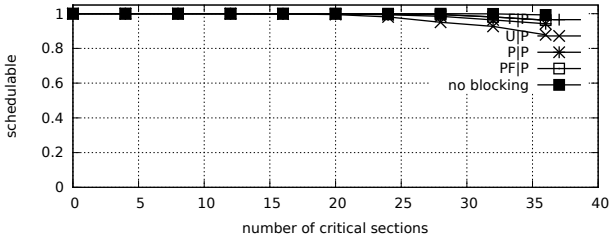

Fig. 2247. Schedulability under preemptable spin locks for $m = 4$, $U = 0.3n$, 4 resources, $rsf = 0.4$, and medium critical sections. The schedulability of the considered non-preemptable lock types in this configuration is shown in Fig. 2245.

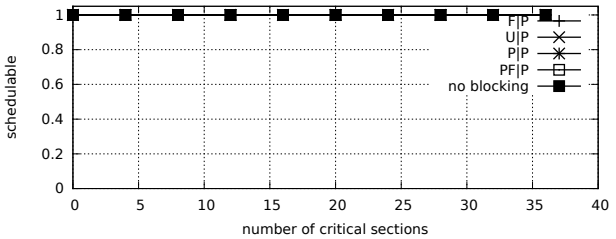

Fig. 2248. Schedulability under preemptable spin locks for $m = 4$, $U = 0.3n$, 4 resources, $rsf = 0.4$, and short critical sections. The schedulability of the considered non-preemptable lock types in this configuration is shown in Fig. 2246.

Configurations with $U = 0.1n$

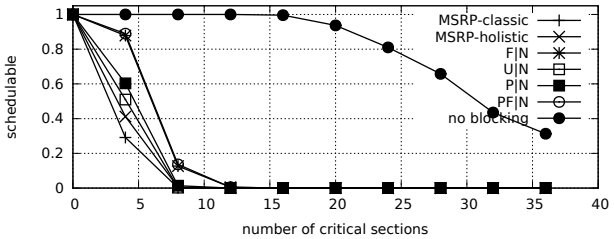

Fig. 2249. Schedulability under non-preemptable spin locks for $m = 4$, $U = 0.1n$, 4 resources, $rsf = 0.75$, and medium critical sections. The schedulability of the considered preemptable lock types in this configuration is shown in Fig. 2251.

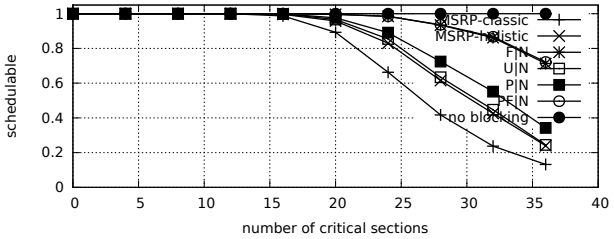

Fig. 2250. Schedulability under non-preemptable spin locks for $m = 4$, $U = 0.1n$, 4 resources, $rsf = 0.75$, and short critical sections. The schedulability of the considered preemptable lock types in this configuration is shown in Fig. 2252.

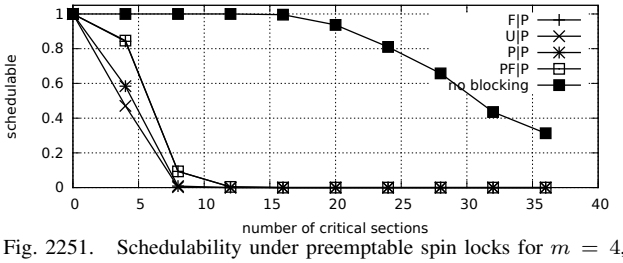

Fig. 2251. Schedulability under preemptable spin locks for $m = 4$, $U = 0.1n$, 4 resources, $rsf = 0.75$, and medium critical sections. The schedulability of the considered non-preemptable lock types in this configuration is shown in Fig. 2249.

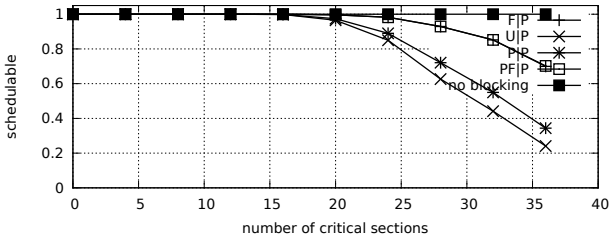

Fig. 2252. Schedulability under preemptable spin locks for $m = 4$, $U = 0.1n$, 4 resources, $rsf = 0.75$, and short critical sections. The schedulability of the considered non-preemptable lock types in this configuration is shown in Fig. 2250.

Configurations with $U = 0.2n$

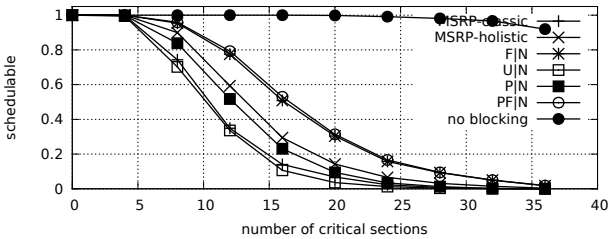

Fig. 2253. Schedulability under non-preemptable spin locks for $m = 4$, $U = 0.2n$, 4 resources, $rsf = 0.75$, and medium critical sections. The schedulability of the considered preemptable lock types in this configuration is shown in Fig. 2255.

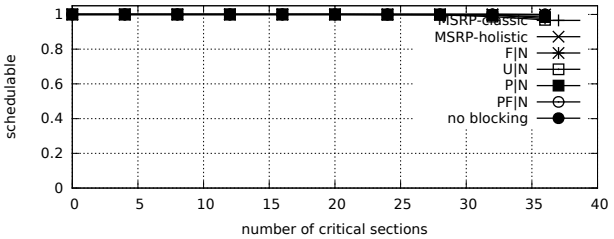

Fig. 2254. Schedulability under non-preemptable spin locks for $m = 4$, $U = 0.2n$, 4 resources, $rsf = 0.75$, and short critical sections. The schedulability of the considered preemptable lock types in this configuration is shown in Fig. 2256.

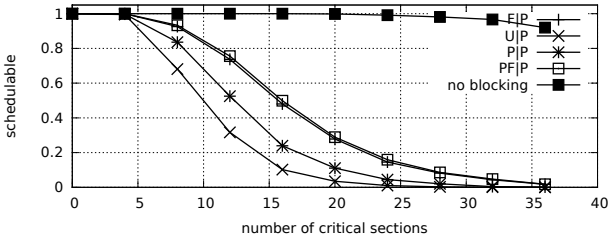

Fig. 2255. Schedulability under preemptable spin locks for $m = 4$, $U = 0.2n$, 4 resources, $rsf = 0.75$, and medium critical sections. The schedulability of the considered non-preemptable lock types in this configuration is shown in Fig. 2253.

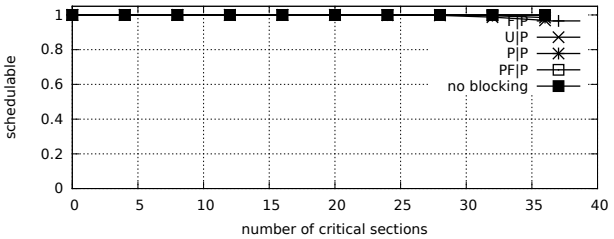

Fig. 2256. Schedulability under preemptable spin locks for $m = 4$, $U = 0.2n$, 4 resources, $rsf = 0.75$, and short critical sections. The schedulability of the considered non-preemptable lock types in this configuration is shown in Fig. 2254.

Configurations with $U = 0.3n$

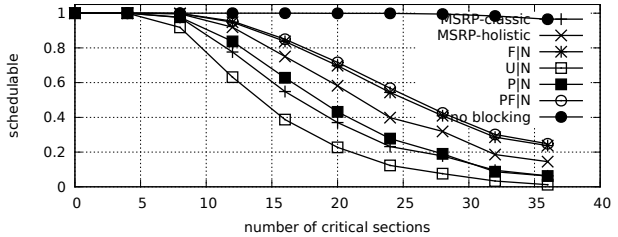

Fig. 2257. Schedulability under non-preemptable spin locks for $m = 4$, $U = 0.3n$, 4 resources, $rsf = 0.75$, and medium critical sections. The schedulability of the considered preemptable lock types in this configuration is shown in Fig. 2259.

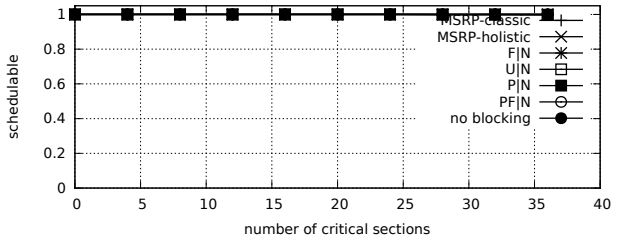

Fig. 2258. Schedulability under non-preemptable spin locks for $m = 4$, $U = 0.3n$, 4 resources, $rsf = 0.75$, and short critical sections. The schedulability of the considered preemptable lock types in this configuration is shown in Fig. 2260.

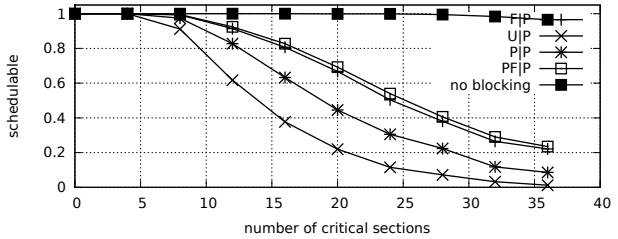

Fig. 2259. Schedulability under preemptable spin locks for $m = 4$, $U = 0.3n$, 4 resources, $rsf = 0.75$, and medium critical sections. The schedulability of the considered non-preemptable lock types in this configuration is shown in Fig. 2257.

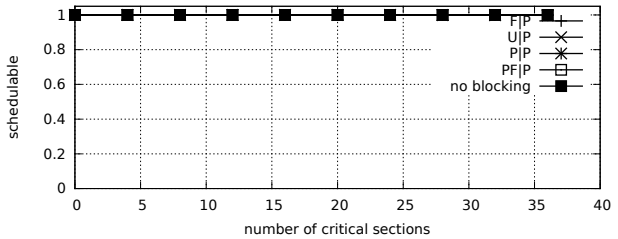

Fig. 2260. Schedulability under preemptable spin locks for $m = 4$, $U = 0.3n$, 4 resources, $rsf = 0.75$, and short critical sections. The schedulability of the considered non-preemptable lock types in this configuration is shown in Fig. 2258.

Configurations with $U = 0.1n$

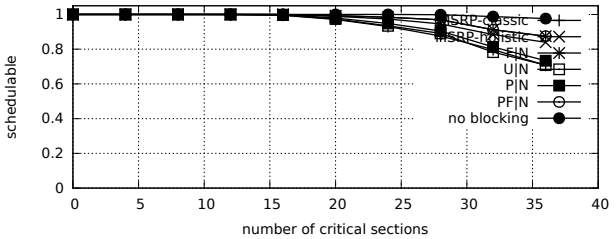

Fig. 2261. Schedulability under non-preemptable spin locks for $m = 4$, $U = 0.1n$, 8 resources, $rsf = 0.1$, and medium critical sections. The schedulability of the considered preemptable lock types in this configuration is shown in Fig. 2263.

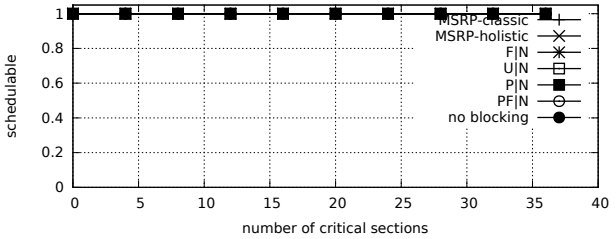

Fig. 2262. Schedulability under non-preemptable spin locks for $m = 4$, $U = 0.1n$, 8 resources, $rsf = 0.1$, and short critical sections. The schedulability of the considered preemptable lock types in this configuration is shown in Fig. 2264.

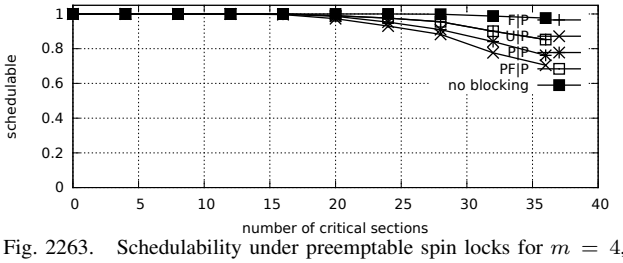

Fig. 2263. Schedulability under preemptable spin locks for $m = 4$, $U = 0.1n$, 8 resources, $rsf = 0.1$, and medium critical sections. The schedulability of the considered non-preemptable lock types in this configuration is shown in Fig. 2261.

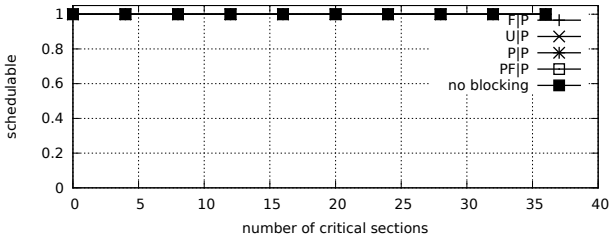

Fig. 2264. Schedulability under preemptable spin locks for $m = 4$, $U = 0.1n$, 8 resources, $rsf = 0.1$, and short critical sections. The schedulability of the considered non-preemptable lock types in this configuration is shown in Fig. 2262.

Configurations with $U = 0.2n$

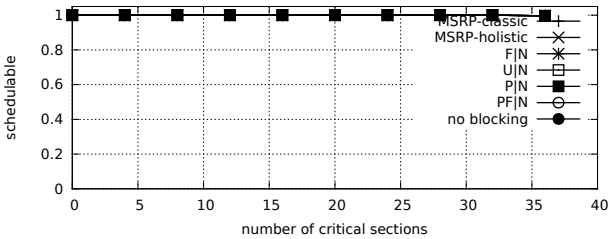

Fig. 2265. Schedulability under non-preemptable spin locks for $m = 4$, $U = 0.2n$, 8 resources, $rsf = 0.1$, and medium critical sections. The schedulability of the considered preemptable lock types in this configuration is shown in Fig. 2267.

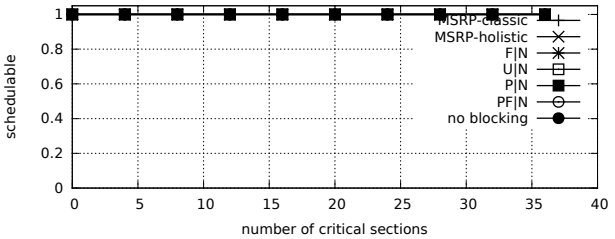

Fig. 2266. Schedulability under non-preemptable spin locks for $m = 4$, $U = 0.2n$, 8 resources, $rsf = 0.1$, and short critical sections. The schedulability of the considered preemptable lock types in this configuration is shown in Fig. 2268.

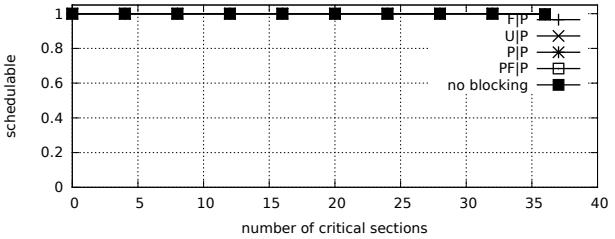

Fig. 2267. Schedulability under preemptable spin locks for $m = 4$, $U = 0.2n$, 8 resources, $rsf = 0.1$, and medium critical sections. The schedulability of the considered non-preemptable lock types in this configuration is shown in Fig. 2265.

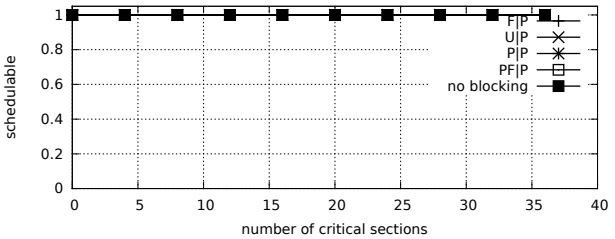

Fig. 2268. Schedulability under preemptable spin locks for $m = 4$, $U = 0.2n$, 8 resources, $rsf = 0.1$, and short critical sections. The schedulability of the considered non-preemptable lock types in this configuration is shown in Fig. 2266.

Configurations with $U = 0.3n$

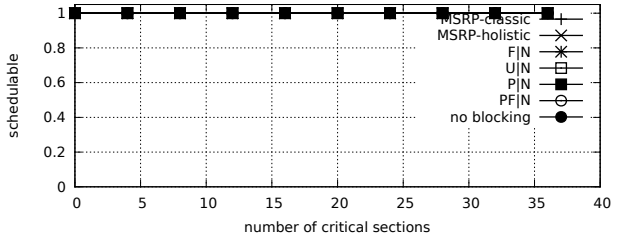

Fig. 2269. Schedulability under non-preemptable spin locks for $m = 4$, $U = 0.3n$, 8 resources, $rsf = 0.1$, and medium critical sections. The schedulability of the considered preemptable lock types in this configuration is shown in Fig. 2271.

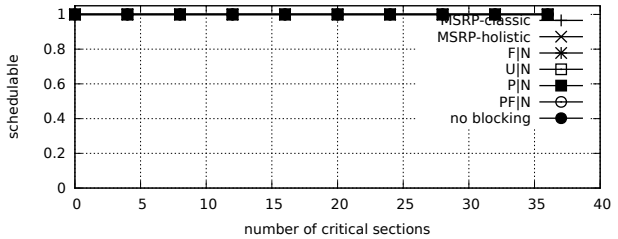

Fig. 2270. Schedulability under non-preemptable spin locks for $m = 4$, $U = 0.3n$, 8 resources, $rsf = 0.1$, and short critical sections. The schedulability of the considered preemptable lock types in this configuration is shown in Fig. 2272.

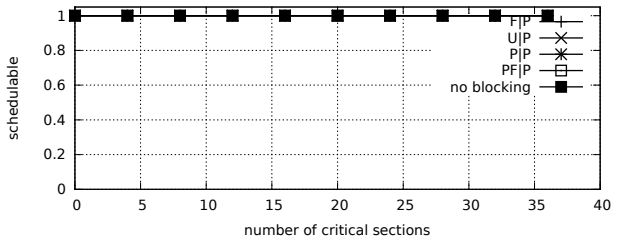

Fig. 2271. Schedulability under preemptable spin locks for $m = 4$, $U = 0.3n$, 8 resources, $rsf = 0.1$, and medium critical sections. The schedulability of the considered non-preemptable lock types in this configuration is shown in Fig. 2269.

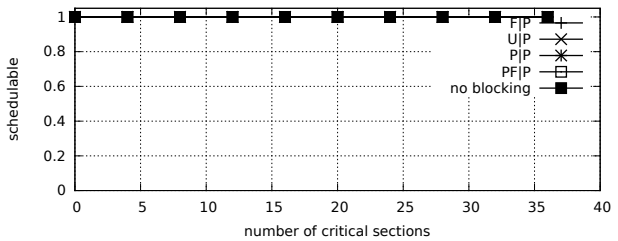

Fig. 2272. Schedulability under preemptable spin locks for $m = 4$, $U = 0.3n$, 8 resources, $rsf = 0.1$, and short critical sections. The schedulability of the considered non-preemptable lock types in this configuration is shown in Fig. 2270.

Configurations with $U = 0.1n$

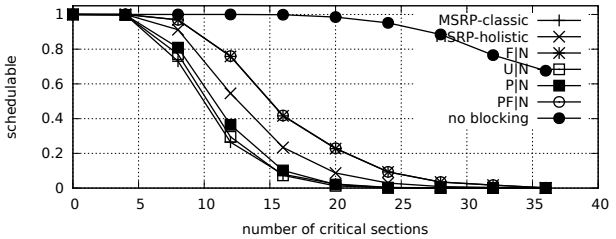

Fig. 2273. Schedulability under non-preemptable spin locks for $m = 4$, $U = 0.1n$, 8 resources, $rsf = 0.25$, and medium critical sections. The schedulability of the considered preemptable lock types in this configuration is shown in Fig. 2275.

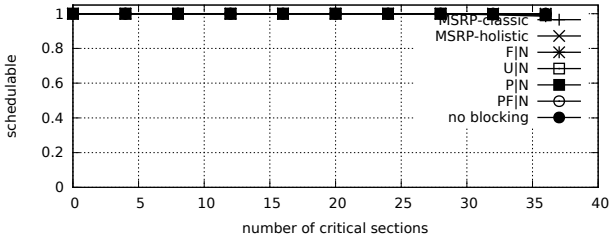

Fig. 2274. Schedulability under non-preemptable spin locks for $m = 4$, $U = 0.1n$, 8 resources, $rsf = 0.25$, and short critical sections. The schedulability of the considered preemptable lock types in this configuration is shown in Fig. 2276.

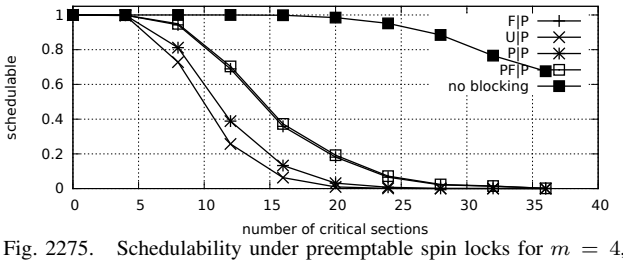

Fig. 2275. Schedulability under preemptable spin locks for $m = 4$, $U = 0.1n$, 8 resources, $rsf = 0.25$, and medium critical sections. The schedulability of the considered non-preemptable lock types in this configuration is shown in Fig. 2273.

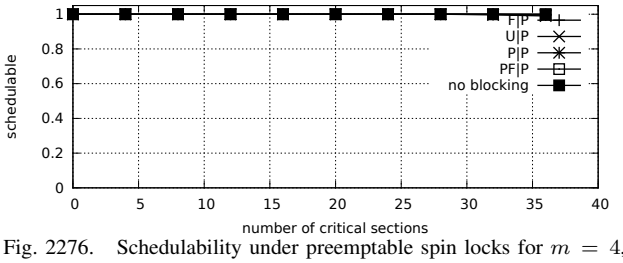

Fig. 2276. Schedulability under preemptable spin locks for $m = 4$, $U = 0.1n$, 8 resources, $rsf = 0.25$, and short critical sections. The schedulability of the considered non-preemptable lock types in this configuration is shown in Fig. 2274.

Configurations with $U = 0.2n$

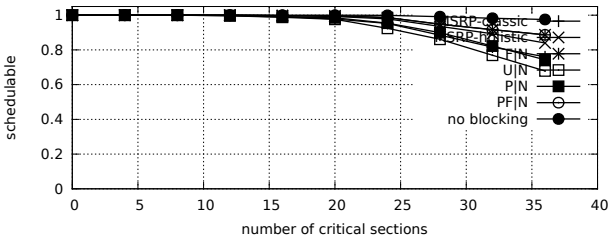

Fig. 2277. Schedulability under non-preemptable spin locks for $m = 4$, $U = 0.2n$, 8 resources, $rsf = 0.25$, and medium critical sections. The schedulability of the considered preemptable lock types in this configuration is shown in Fig. 2279.

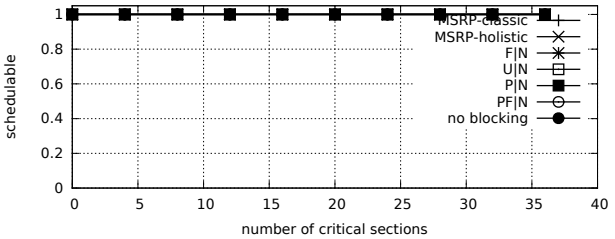

Fig. 2278. Schedulability under non-preemptable spin locks for $m = 4$, $U = 0.2n$, 8 resources, $rsf = 0.25$, and short critical sections. The schedulability of the considered preemptable lock types in this configuration is shown in Fig. 2280.

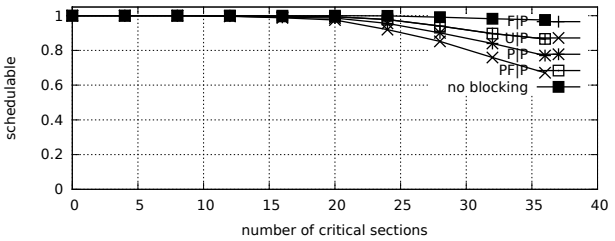

Fig. 2279. Schedulability under preemptable spin locks for $m = 4$, $U = 0.2n$, 8 resources, $rsf = 0.25$, and medium critical sections. The schedulability of the considered non-preemptable lock types in this configuration is shown in Fig. 2277.

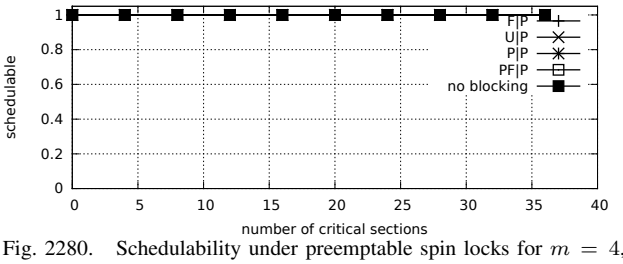

Fig. 2280. Schedulability under preemptable spin locks for $m = 4$, $U = 0.2n$, 8 resources, $rsf = 0.25$, and short critical sections. The schedulability of the considered non-preemptable lock types in this configuration is shown in Fig. 2278.

Configurations with $U = 0.3n$

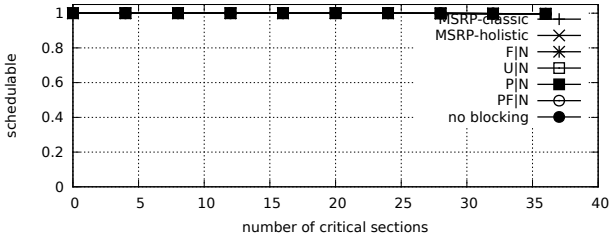

Fig. 2281. Schedulability under non-preemptable spin locks for $m = 4$, $U = 0.3n$, 8 resources, $rsf = 0.25$, and medium critical sections. The schedulability of the considered preemptable lock types in this configuration is shown in Fig. 2283.

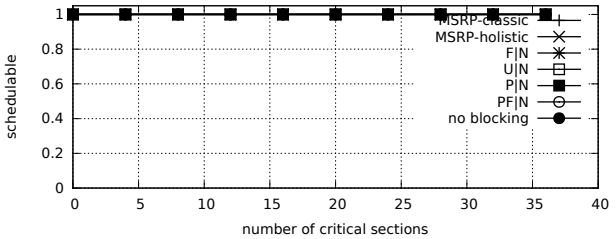

Fig. 2282. Schedulability under non-preemptable spin locks for $m = 4$, $U = 0.3n$, 8 resources, $rsf = 0.25$, and short critical sections. The schedulability of the considered preemptable lock types in this configuration is shown in Fig. 2284.

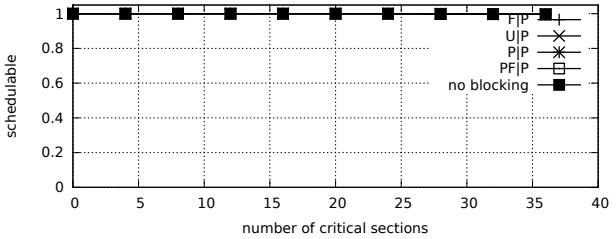

Fig. 2283. Schedulability under preemptable spin locks for $m = 4$, $U = 0.3n$, 8 resources, $rsf = 0.25$, and medium critical sections. The schedulability of the considered non-preemptable lock types in this configuration is shown in Fig. 2281.

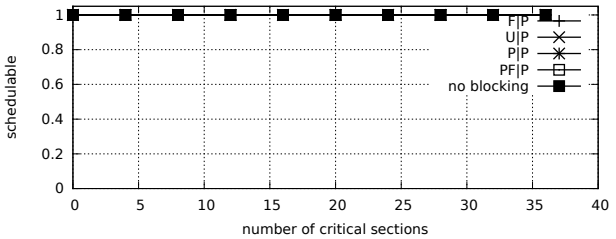

Fig. 2284. Schedulability under preemptable spin locks for $m = 4$, $U = 0.3n$, 8 resources, $rsf = 0.25$, and short critical sections. The schedulability of the considered non-preemptable lock types in this configuration is shown in Fig. 2282.

Configurations with $U = 0.1n$

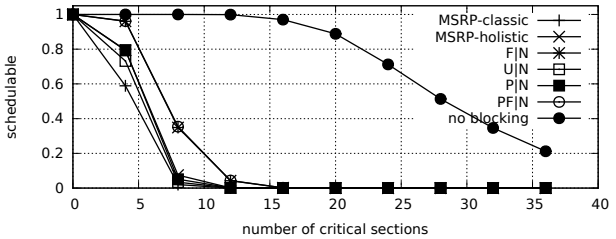

Fig. 2285. Schedulability under non-preemptable spin locks for $m = 4$, $U = 0.1n$, 8 resources, $rsf = 0.4$, and medium critical sections. The schedulability of the considered preemptable lock types in this configuration is shown in Fig. 2287.

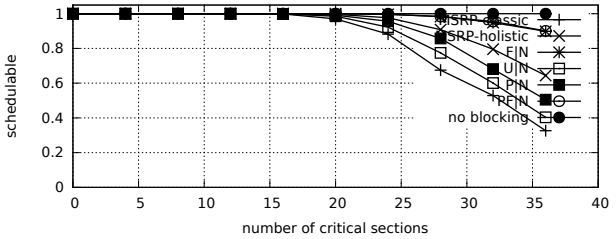

Fig. 2286. Schedulability under non-preemptable spin locks for $m = 4$, $U = 0.1n$, 8 resources, $rsf = 0.4$, and short critical sections. The schedulability of the considered preemptable lock types in this configuration is shown in Fig. 2288.

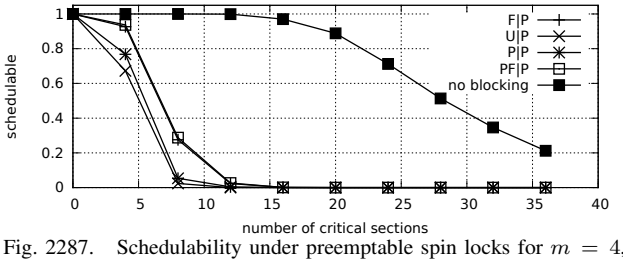

Fig. 2287. Schedulability under preemptable spin locks for $m = 4$, $U = 0.1n$, 8 resources, $rsf = 0.4$, and medium critical sections. The schedulability of the considered non-preemptable lock types in this configuration is shown in Fig. 2285.

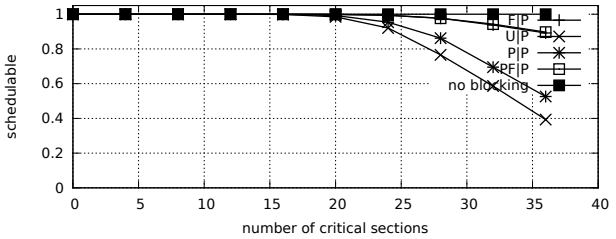

Fig. 2288. Schedulability under preemptable spin locks for $m = 4$, $U = 0.1n$, 8 resources, $rsf = 0.4$, and short critical sections. The schedulability of the considered non-preemptable lock types in this configuration is shown in Fig. 2286.

Configurations with $U = 0.2n$

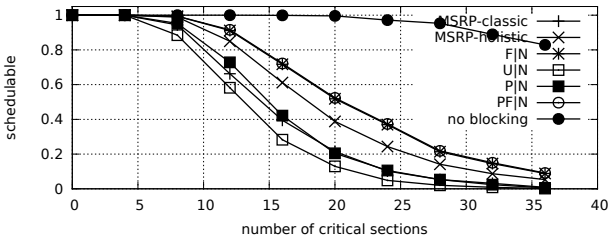

Fig. 2289. Schedulability under non-preemptable spin locks for $m = 4$, $U = 0.2n$, 8 resources, $rsf = 0.4$, and medium critical sections. The schedulability of the considered preemptable lock types in this configuration is shown in Fig. 2291.

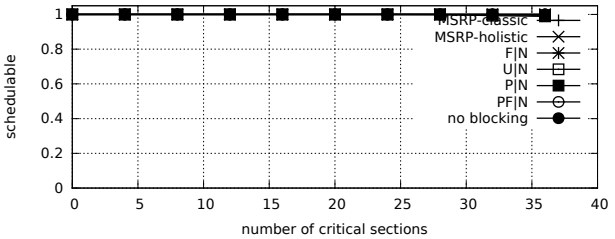

Fig. 2290. Schedulability under non-preemptable spin locks for $m = 4$, $U = 0.2n$, 8 resources, $rsf = 0.4$, and short critical sections. The schedulability of the considered preemptable lock types in this configuration is shown in Fig. 2292.

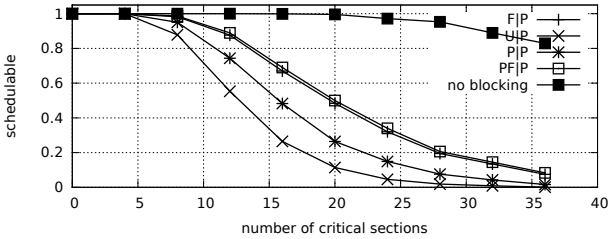

Fig. 2291. Schedulability under preemptable spin locks for $m = 4$, $U = 0.2n$, 8 resources, $rsf = 0.4$, and medium critical sections. The schedulability of the considered non-preemptable lock types in this configuration is shown in Fig. 2289.

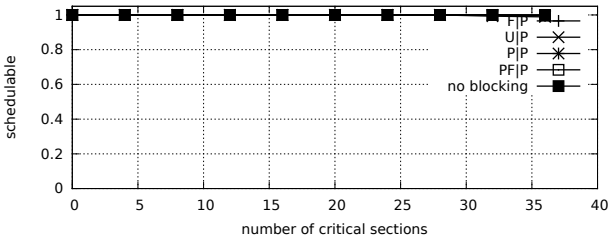

Fig. 2292. Schedulability under preemptable spin locks for $m = 4$, $U = 0.2n$, 8 resources, $rsf = 0.4$, and short critical sections. The schedulability of the considered non-preemptable lock types in this configuration is shown in Fig. 2290.

Configurations with $U = 0.3n$

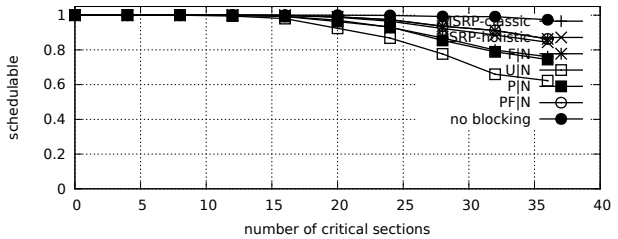

Fig. 2293. Schedulability under non-preemptable spin locks for $m = 4$, $U = 0.3n$, 8 resources, $rsf = 0.4$, and medium critical sections. The schedulability of the considered preemptable lock types in this configuration is shown in Fig. 2295.

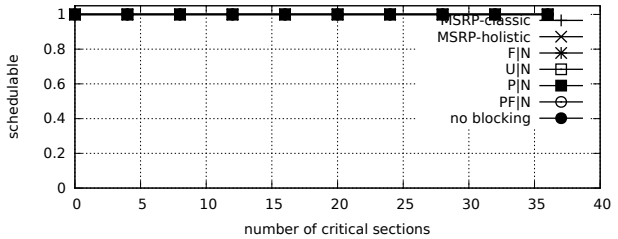

Fig. 2294. Schedulability under non-preemptable spin locks for $m = 4$, $U = 0.3n$, 8 resources, $rsf = 0.4$, and short critical sections. The schedulability of the considered preemptable lock types in this configuration is shown in Fig. 2296.

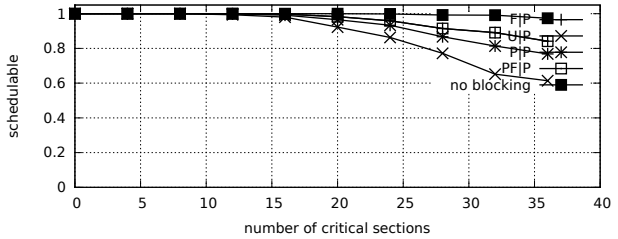

Fig. 2295. Schedulability under preemptable spin locks for $m = 4$, $U = 0.3n$, 8 resources, $rsf = 0.4$, and medium critical sections. The schedulability of the considered non-preemptable lock types in this configuration is shown in Fig. 2293.

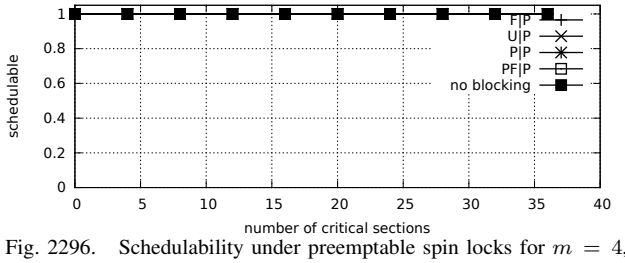

Fig. 2296. Schedulability under preemptable spin locks for $m = 4$, $U = 0.3n$, 8 resources, $rsf = 0.4$, and short critical sections. The schedulability of the considered non-preemptable lock types in this configuration is shown in Fig. 2294.

Configurations with $U = 0.1n$

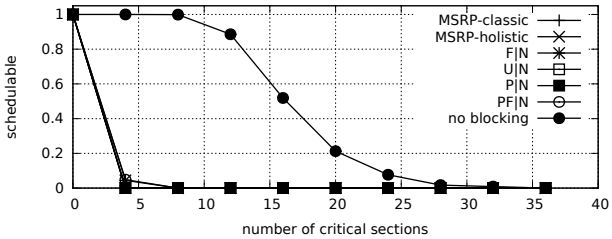

Fig. 2297. Schedulability under non-preemptable spin locks for $m = 4$, $U = 0.1n$, 8 resources, $rsf = 0.75$, and medium critical sections. The schedulability of the considered preemptable lock types in this configuration is shown in Fig. 2299.

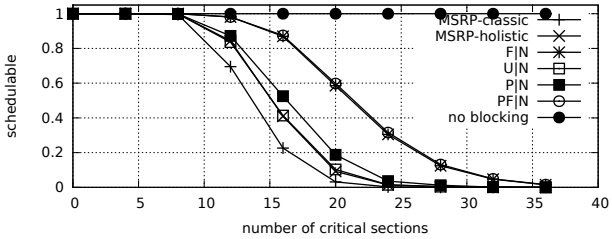

Fig. 2298. Schedulability under non-preemptable spin locks for $m = 4$, $U = 0.1n$, 8 resources, $rsf = 0.75$, and short critical sections. The schedulability of the considered preemptable lock types in this configuration is shown in Fig. 2300.

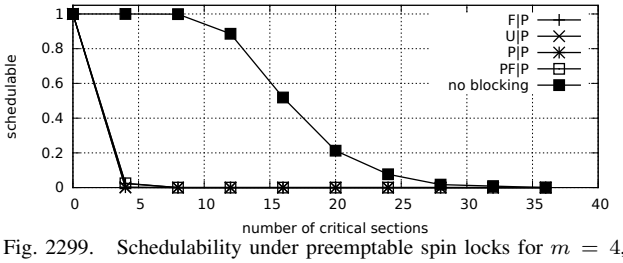

Fig. 2299. Schedulability under preemptable spin locks for $m = 4$, $U = 0.1n$, 8 resources, $rsf = 0.75$, and medium critical sections. The schedulability of the considered non-preemptable lock types in this configuration is shown in Fig. 2297.

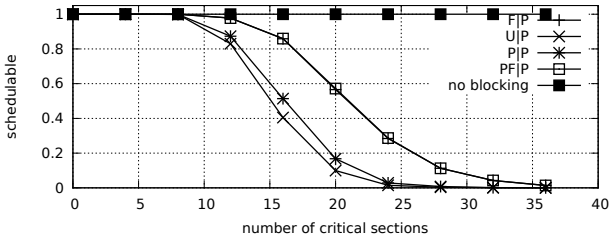

Fig. 2300. Schedulability under preemptable spin locks for $m = 4$, $U = 0.1n$, 8 resources, $rsf = 0.75$, and short critical sections. The schedulability of the considered non-preemptable lock types in this configuration is shown in Fig. 2298.

Configurations with $U = 0.2n$

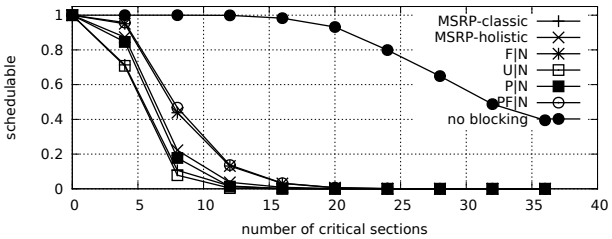

Fig. 2301. Schedulability under non-preemptable spin locks for $m = 4$, $U = 0.2n$, 8 resources, $rsf = 0.75$, and medium critical sections. The schedulability of the considered preemptable lock types in this configuration is shown in Fig. 2303.

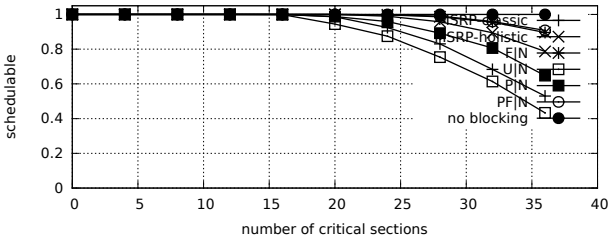

Fig. 2302. Schedulability under non-preemptable spin locks for $m = 4$, $U = 0.2n$, 8 resources, $rsf = 0.75$, and short critical sections. The schedulability of the considered preemptable lock types in this configuration is shown in Fig. 2304.

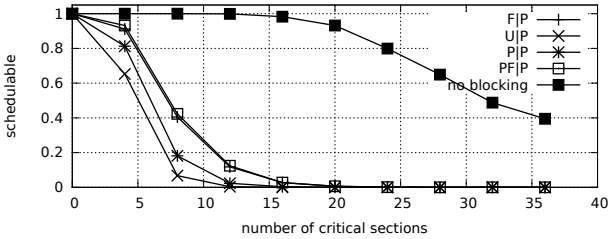

Fig. 2303. Schedulability under preemptable spin locks for $m = 4$, $U = 0.2n$, 8 resources, $rsf = 0.75$, and medium critical sections. The schedulability of the considered non-preemptable lock types in this configuration is shown in Fig. 2301.

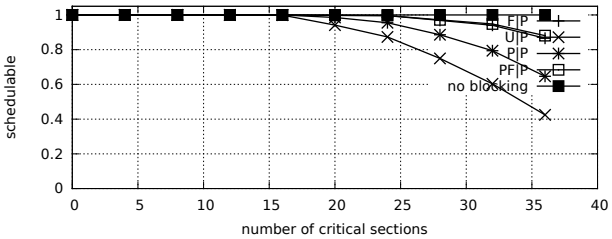

Fig. 2304. Schedulability under preemptable spin locks for $m = 4$, $U = 0.2n$, 8 resources, $rsf = 0.75$, and short critical sections. The schedulability of the considered non-preemptable lock types in this configuration is shown in Fig. 2302.

Configurations with $U = 0.3n$

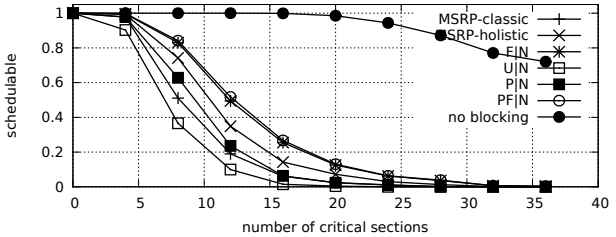

Fig. 2305. Schedulability under non-preemptable spin locks for $m = 4$, $U = 0.3n$, 8 resources, $rsf = 0.75$, and medium critical sections. The schedulability of the considered preemptable lock types in this configuration is shown in Fig. 2307.

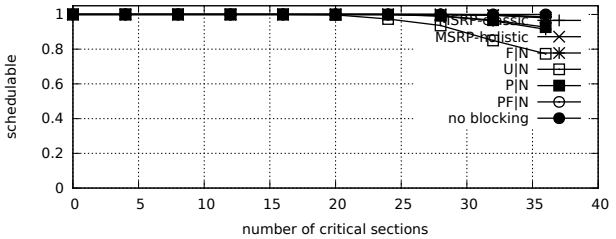

Fig. 2306. Schedulability under non-preemptable spin locks for $m = 4$, $U = 0.3n$, 8 resources, $rsf = 0.75$, and short critical sections. The schedulability of the considered preemptable lock types in this configuration is shown in Fig. 2308.

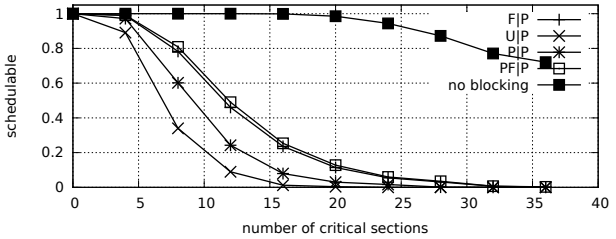

Fig. 2307. Schedulability under preemptable spin locks for $m = 4$, $U = 0.3n$, 8 resources, $rsf = 0.75$, and medium critical sections. The schedulability of the considered non-preemptable lock types in this configuration is shown in Fig. 2305.

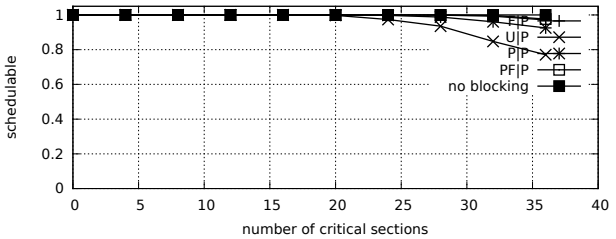

Fig. 2308. Schedulability under preemptable spin locks for $m = 4$, $U = 0.3n$, 8 resources, $rsf = 0.75$, and short critical sections. The schedulability of the considered non-preemptable lock types in this configuration is shown in Fig. 2306.

Configurations with $U = 0.1n$

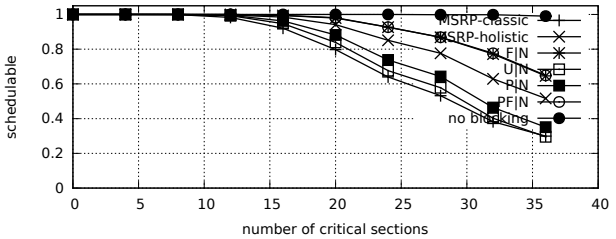

Fig. 2309. Schedulability under non-preemptable spin locks for $m = 8$, $U = 0.1n$, 4 resources, $rsf = 0.1$, and medium critical sections. The schedulability of the considered preemptable lock types in this configuration is shown in Fig. 2311.

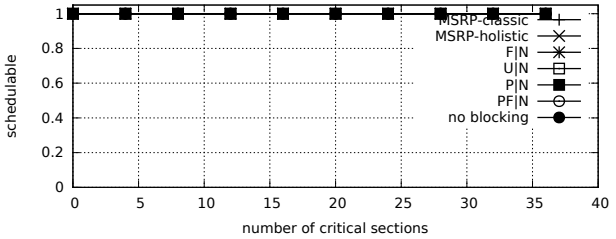

Fig. 2310. Schedulability under non-preemptable spin locks for $m = 8$, $U = 0.1n$, 4 resources, $rsf = 0.1$, and short critical sections. The schedulability of the considered preemptable lock types in this configuration is shown in Fig. 2312.

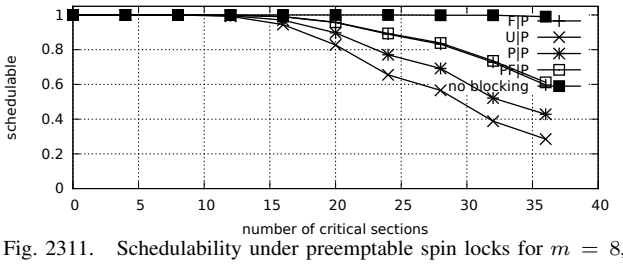

Fig. 2311. Schedulability under preemptable spin locks for $m = 8$, $U = 0.1n$, 4 resources, $rsf = 0.1$, and medium critical sections. The schedulability of the considered non-preemptable lock types in this configuration is shown in Fig. 2309.

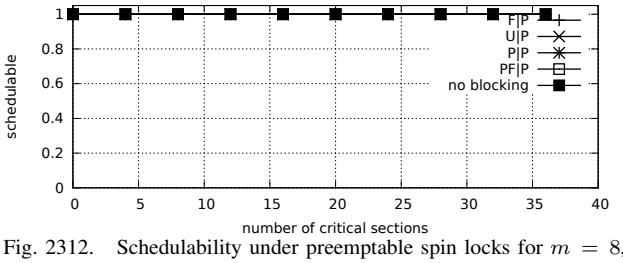

Fig. 2312. Schedulability under preemptable spin locks for $m = 8$, $U = 0.1n$, 4 resources, $rsf = 0.1$, and short critical sections. The schedulability of the considered non-preemptable lock types in this configuration is shown in Fig. 2310.

Configurations with $U = 0.2n$

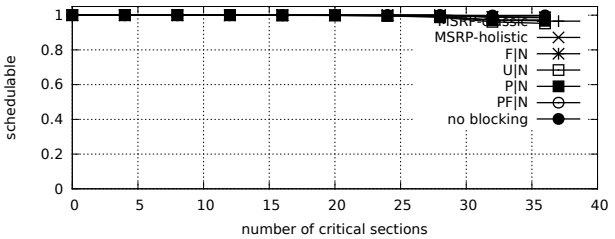

Fig. 2313. Schedulability under non-preemptable spin locks for $m = 8$, $U = 0.2n$, 4 resources, $rsf = 0.1$, and medium critical sections. The schedulability of the considered preemptable lock types in this configuration is shown in Fig. 2315.

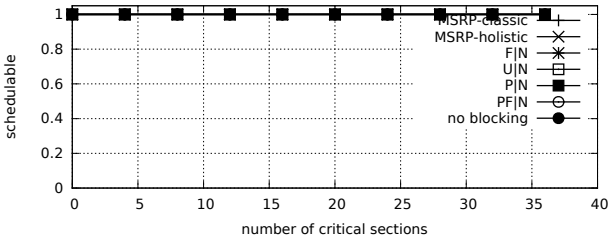

Fig. 2314. Schedulability under non-preemptable spin locks for $m = 8$, $U = 0.2n$, 4 resources, $rsf = 0.1$, and short critical sections. The schedulability of the considered preemptable lock types in this configuration is shown in Fig. 2316.

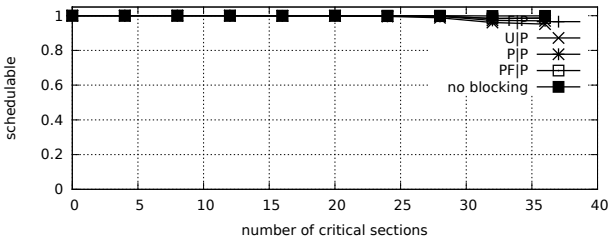

Fig. 2315. Schedulability under preemptable spin locks for $m = 8$, $U = 0.2n$, 4 resources, $rsf = 0.1$, and medium critical sections. The schedulability of the considered non-preemptable lock types in this configuration is shown in Fig. 2313.

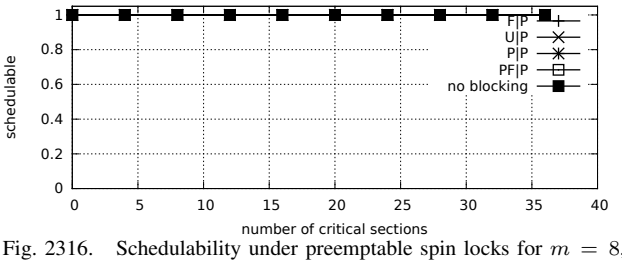

Fig. 2316. Schedulability under preemptable spin locks for $m = 8$, $U = 0.2n$, 4 resources, $rsf = 0.1$, and short critical sections. The schedulability of the considered non-preemptable lock types in this configuration is shown in Fig. 2314.

Configurations with $U = 0.3n$

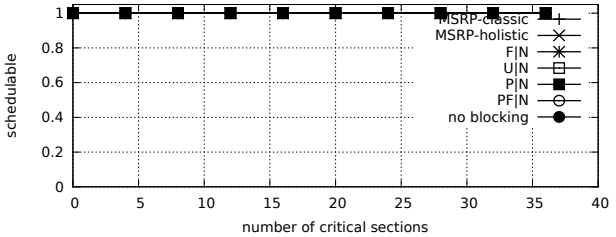

Fig. 2317. Schedulability under non-preemptable spin locks for $m = 8$, $U = 0.3n$, 4 resources, $rsf = 0.1$, and medium critical sections. The schedulability of the considered preemptable lock types in this configuration is shown in Fig. 2319.

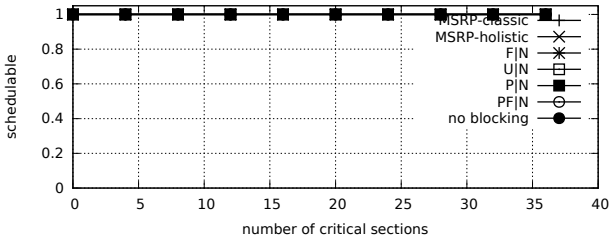

Fig. 2318. Schedulability under non-preemptable spin locks for $m = 8$, $U = 0.3n$, 4 resources, $rsf = 0.1$, and short critical sections. The schedulability of the considered preemptable lock types in this configuration is shown in Fig. 2320.

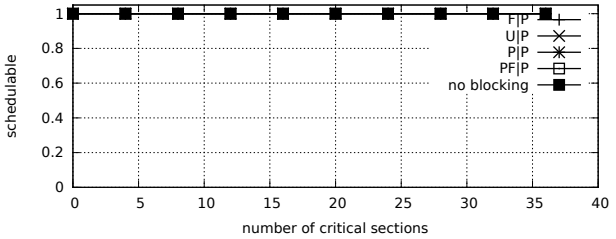

Fig. 2319. Schedulability under preemptable spin locks for $m = 8$, $U = 0.3n$, 4 resources, $rsf = 0.1$, and medium critical sections. The schedulability of the considered non-preemptable lock types in this configuration is shown in Fig. 2317.

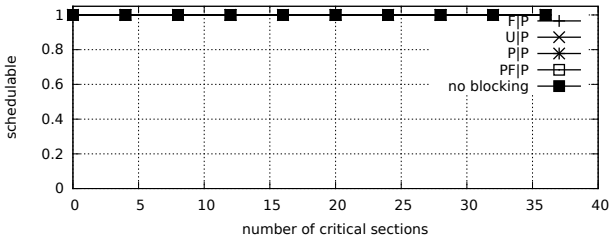

Fig. 2320. Schedulability under preemptable spin locks for $m = 8$, $U = 0.3n$, 4 resources, $rsf = 0.1$, and short critical sections. The schedulability of the considered non-preemptable lock types in this configuration is shown in Fig. 2318.

Configurations with $U = 0.1n$

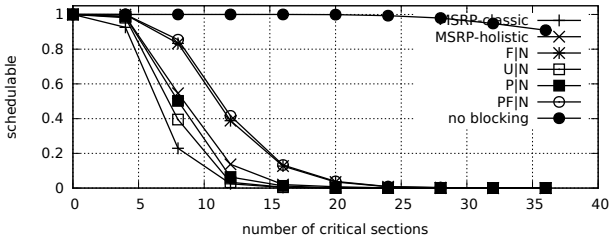

Fig. 2321. Schedulability under non-preemptable spin locks for $m = 8$, $U = 0.1n$, 4 resources, $rsf = 0.25$, and medium critical sections. The schedulability of the considered preemptable lock types in this configuration is shown in Fig. 2323.

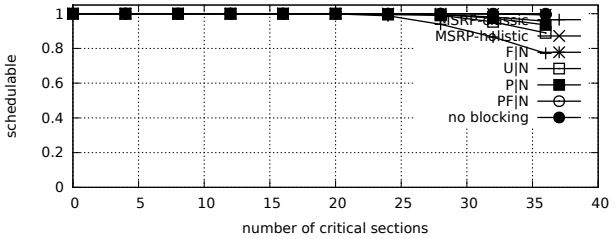

Fig. 2322. Schedulability under non-preemptable spin locks for $m = 8$, $U = 0.1n$, 4 resources, $rsf = 0.25$, and short critical sections. The schedulability of the considered preemptable lock types in this configuration is shown in Fig. 2324.

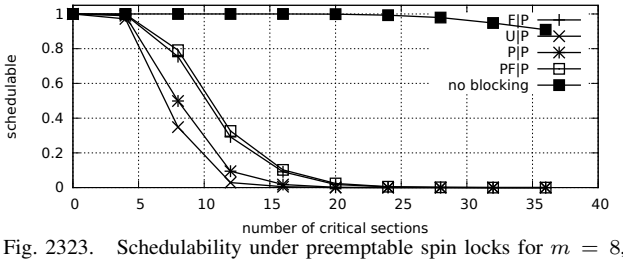

Fig. 2323. Schedulability under preemptable spin locks for $m = 8$, $U = 0.1n$, 4 resources, $rsf = 0.25$, and medium critical sections. The schedulability of the considered non-preemptable lock types in this configuration is shown in Fig. 2321.

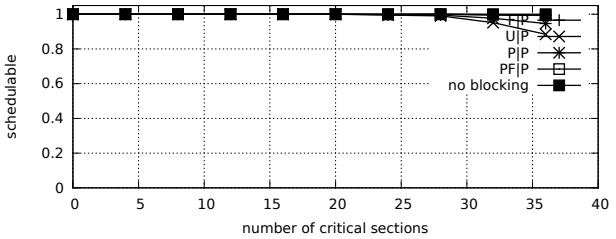

Fig. 2324. Schedulability under preemptable spin locks for $m = 8$, $U = 0.1n$, 4 resources, $rsf = 0.25$, and short critical sections. The schedulability of the considered non-preemptable lock types in this configuration is shown in Fig. 2322.

Configurations with $U = 0.2n$

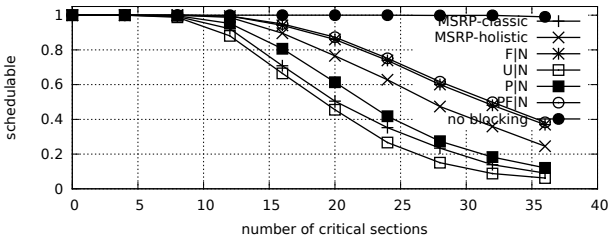

Fig. 2325. Schedulability under non-preemptable spin locks for $m = 8$, $U = 0.2n$, 4 resources, $rsf = 0.25$, and medium critical sections. The schedulability of the considered preemptable lock types in this configuration is shown in Fig. 2327.

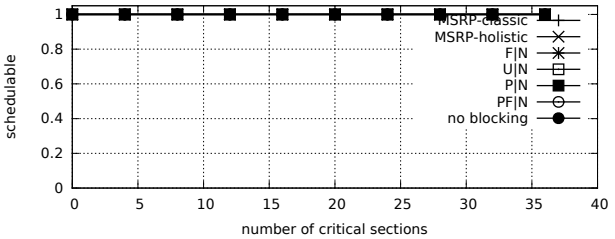

Fig. 2326. Schedulability under non-preemptable spin locks for $m = 8$, $U = 0.2n$, 4 resources, $rsf = 0.25$, and short critical sections. The schedulability of the considered preemptable lock types in this configuration is shown in Fig. 2328.

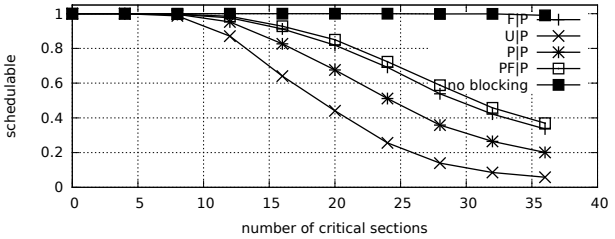

Fig. 2327. Schedulability under preemptable spin locks for $m = 8$, $U = 0.2n$, 4 resources, $rsf = 0.25$, and medium critical sections. The schedulability of the considered non-preemptable lock types in this configuration is shown in Fig. 2325.

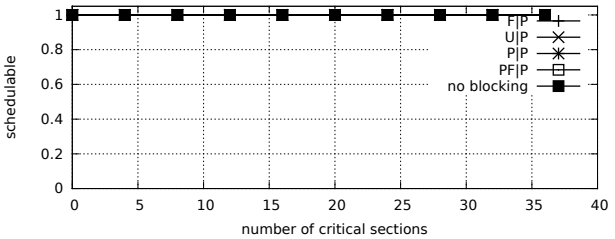

Fig. 2328. Schedulability under preemptable spin locks for $m = 8$, $U = 0.2n$, 4 resources, $rsf = 0.25$, and short critical sections. The schedulability of the considered non-preemptable lock types in this configuration is shown in Fig. 2326.

Configurations with $U = 0.3n$

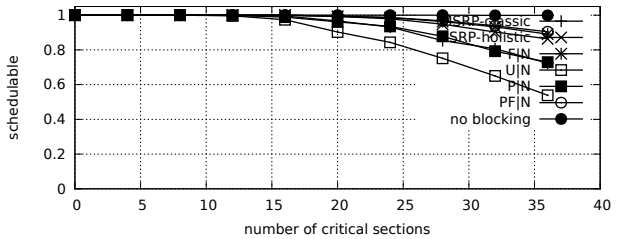

Fig. 2329. Schedulability under non-preemptable spin locks for $m = 8$, $U = 0.3n$, 4 resources, $rsf = 0.25$, and medium critical sections. The schedulability of the considered preemptable lock types in this configuration is shown in Fig. 2331.

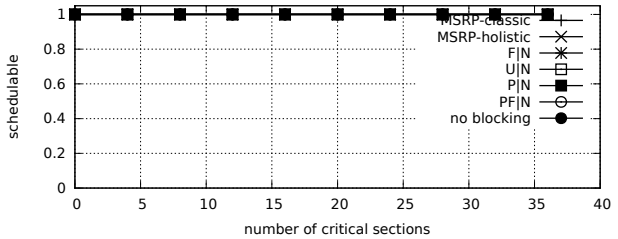

Fig. 2330. Schedulability under non-preemptable spin locks for $m = 8$, $U = 0.3n$, 4 resources, $rsf = 0.25$, and short critical sections. The schedulability of the considered preemptable lock types in this configuration is shown in Fig. 2332.

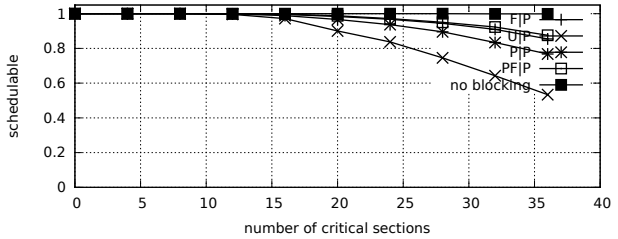

Fig. 2331. Schedulability under preemptable spin locks for $m = 8$, $U = 0.3n$, 4 resources, $rsf = 0.25$, and medium critical sections. The schedulability of the considered non-preemptable lock types in this configuration is shown in Fig. 2329.

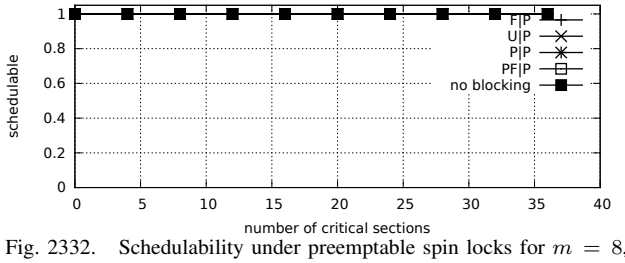

Fig. 2332. Schedulability under preemptable spin locks for $m = 8$, $U = 0.3n$, 4 resources, $rsf = 0.25$, and short critical sections. The schedulability of the considered non-preemptable lock types in this configuration is shown in Fig. 2330.

Configurations with $U = 0.1n$

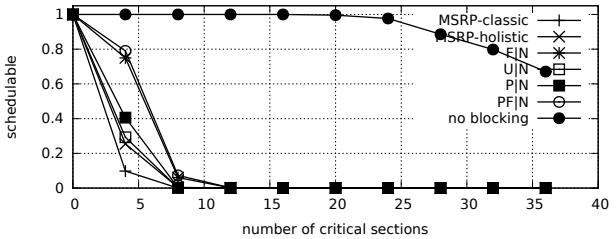

Fig. 2333. Schedulability under non-preemptable spin locks for $m = 8$, $U = 0.1n$, 4 resources, $rsf = 0.4$, and medium critical sections. The schedulability of the considered preemptable lock types in this configuration is shown in Fig. 2335.

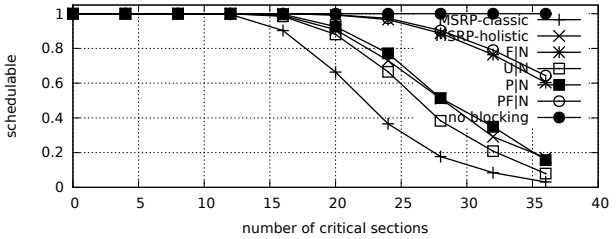

Fig. 2334. Schedulability under non-preemptable spin locks for $m = 8$, $U = 0.1n$, 4 resources, $rsf = 0.4$, and short critical sections. The schedulability of the considered preemptable lock types in this configuration is shown in Fig. 2336.

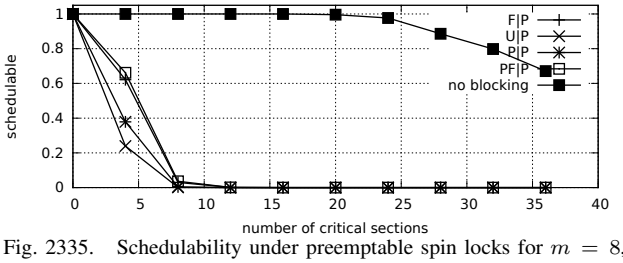

Fig. 2335. Schedulability under preemptable spin locks for $m = 8$, $U = 0.1n$, 4 resources, $rsf = 0.4$, and medium critical sections. The schedulability of the considered non-preemptable lock types in this configuration is shown in Fig. 2333.

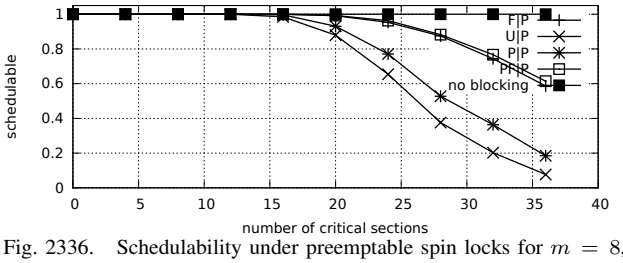

Fig. 2336. Schedulability under preemptable spin locks for $m = 8$, $U = 0.1n$, 4 resources, $rsf = 0.4$, and short critical sections. The schedulability of the considered non-preemptable lock types in this configuration is shown in Fig. 2334.

Configurations with $U = 0.2n$

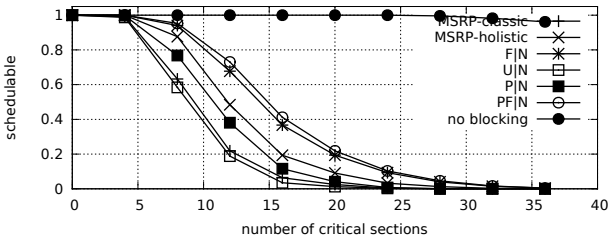

Fig. 2337. Schedulability under non-preemptable spin locks for $m = 8$, $U = 0.2n$, 4 resources, $rsf = 0.4$, and medium critical sections. The schedulability of the considered preemptable lock types in this configuration is shown in Fig. 2339.

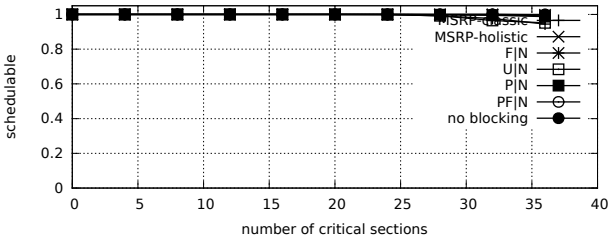

Fig. 2338. Schedulability under non-preemptable spin locks for $m = 8$, $U = 0.2n$, 4 resources, $rsf = 0.4$, and short critical sections. The schedulability of the considered preemptable lock types in this configuration is shown in Fig. 2340.

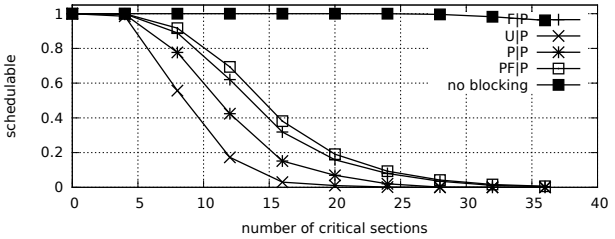

Fig. 2339. Schedulability under preemptable spin locks for $m = 8$, $U = 0.2n$, 4 resources, $rsf = 0.4$, and medium critical sections. The schedulability of the considered non-preemptable lock types in this configuration is shown in Fig. 2337.

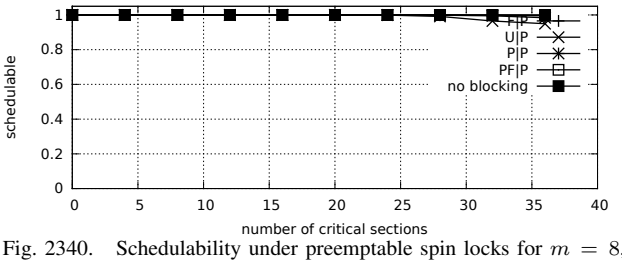

Fig. 2340. Schedulability under preemptable spin locks for $m = 8$, $U = 0.2n$, 4 resources, $rsf = 0.4$, and short critical sections. The schedulability of the considered non-preemptable lock types in this configuration is shown in Fig. 2338.

Configurations with $U = 0.3n$

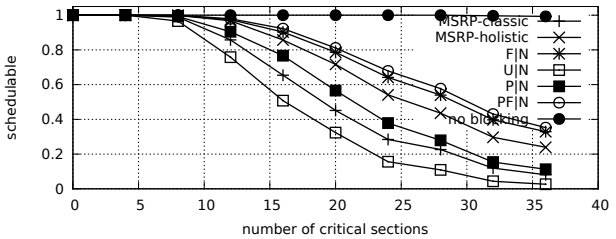

Fig. 2341. Schedulability under non-preemptable spin locks for $m = 8$, $U = 0.3n$, 4 resources, $rsf = 0.4$, and medium critical sections. The schedulability of the considered preemptable lock types in this configuration is shown in Fig. 2343.

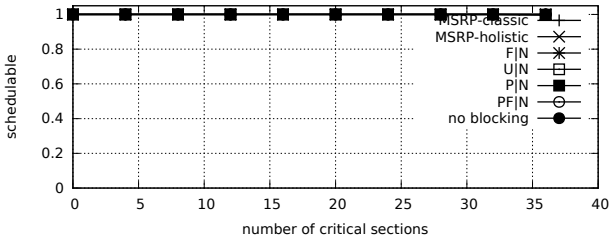

Fig. 2342. Schedulability under non-preemptable spin locks for $m = 8$, $U = 0.3n$, 4 resources, $rsf = 0.4$, and short critical sections. The schedulability of the considered preemptable lock types in this configuration is shown in Fig. 2344.

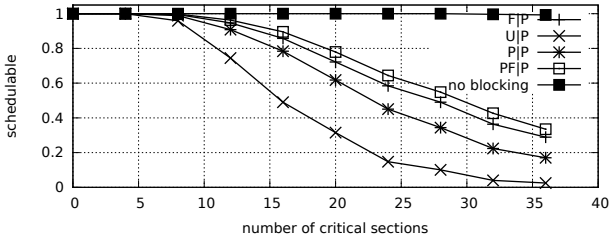

Fig. 2343. Schedulability under preemptable spin locks for $m = 8$, $U = 0.3n$, 4 resources, $rsf = 0.4$, and medium critical sections. The schedulability of the considered non-preemptable lock types in this configuration is shown in Fig. 2341.

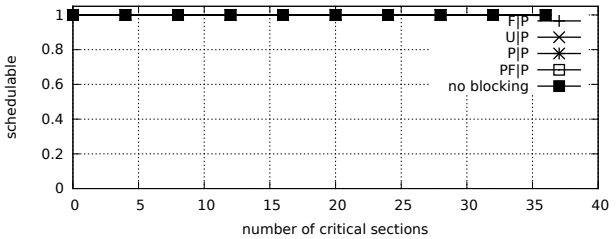

Fig. 2344. Schedulability under preemptable spin locks for $m = 8$, $U = 0.3n$, 4 resources, $rsf = 0.4$, and short critical sections. The schedulability of the considered non-preemptable lock types in this configuration is shown in Fig. 2342.

Configurations with $U = 0.1n$

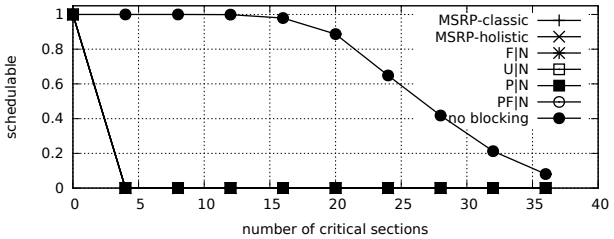

Fig. 2345. Schedulability under non-preemptable spin locks for $m = 8$, $U = 0.1n$, 4 resources, $rsf = 0.75$, and medium critical sections. The schedulability of the considered preemptable lock types in this configuration is shown in Fig. 2347.

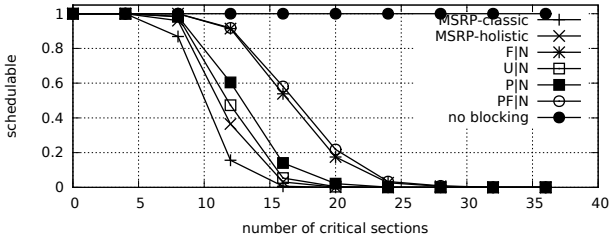

Fig. 2346. Schedulability under non-preemptable spin locks for $m = 8$, $U = 0.1n$, 4 resources, $rsf = 0.75$, and short critical sections. The schedulability of the considered preemptable lock types in this configuration is shown in Fig. 2348.

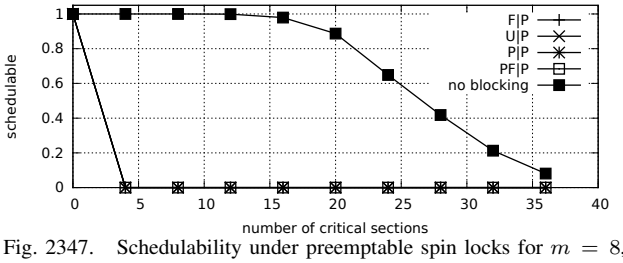

Fig. 2347. Schedulability under preemptable spin locks for $m = 8$, $U = 0.1n$, 4 resources, $rsf = 0.75$, and medium critical sections. The schedulability of the considered non-preemptable lock types in this configuration is shown in Fig. 2345.

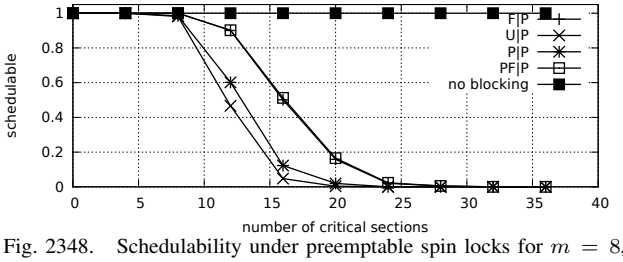

Fig. 2348. Schedulability under preemptable spin locks for $m = 8$, $U = 0.1n$, 4 resources, $rsf = 0.75$, and short critical sections. The schedulability of the considered non-preemptable lock types in this configuration is shown in Fig. 2346.

Configurations with $U = 0.2n$

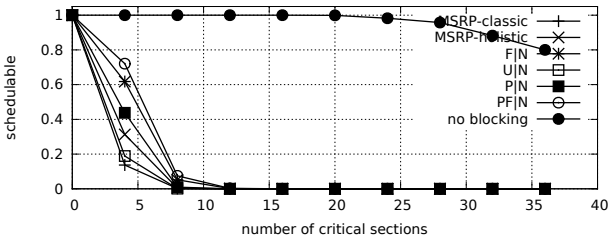

Fig. 2349. Schedulability under non-preemptable spin locks for $m = 8$, $U = 0.2n$, 4 resources, $rsf = 0.75$, and medium critical sections. The schedulability of the considered preemptable lock types in this configuration is shown in Fig. 2351.

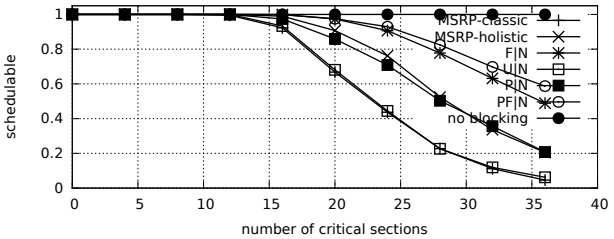

Fig. 2350. Schedulability under non-preemptable spin locks for $m = 8$, $U = 0.2n$, 4 resources, $rsf = 0.75$, and short critical sections. The schedulability of the considered preemptable lock types in this configuration is shown in Fig. 2352.

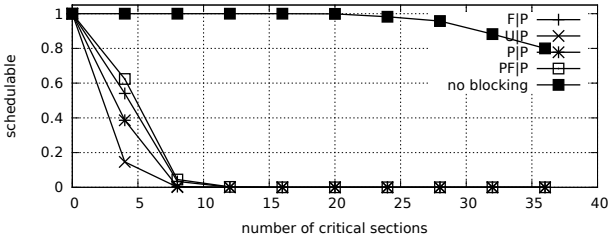

Fig. 2351. Schedulability under preemptable spin locks for $m = 8$, $U = 0.2n$, 4 resources, $rsf = 0.75$, and medium critical sections. The schedulability of the considered non-preemptable lock types in this configuration is shown in Fig. 2349.

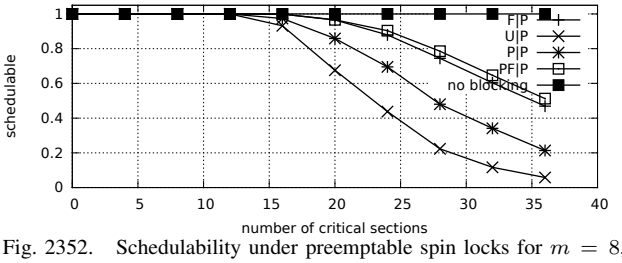

Fig. 2352. Schedulability under preemptable spin locks for $m = 8$, $U = 0.2n$, 4 resources, $rsf = 0.75$, and short critical sections. The schedulability of the considered non-preemptable lock types in this configuration is shown in Fig. 2350.

Configurations with $U = 0.3n$

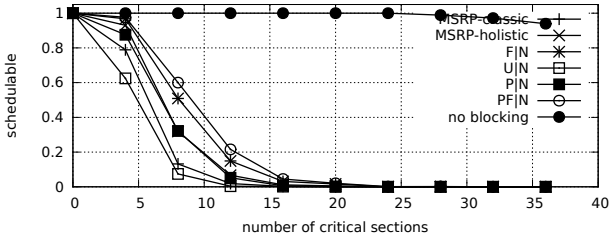

Fig. 2353. Schedulability under non-preemptable spin locks for $m = 8$, $U = 0.3n$, 4 resources, $rsf = 0.75$, and medium critical sections. The schedulability of the considered preemptable lock types in this configuration is shown in Fig. 2355.

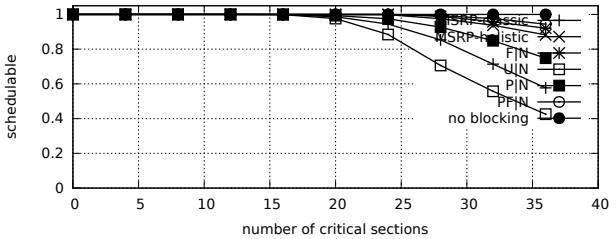

Fig. 2354. Schedulability under non-preemptable spin locks for $m = 8$, $U = 0.3n$, 4 resources, $rsf = 0.75$, and short critical sections. The schedulability of the considered preemptable lock types in this configuration is shown in Fig. 2356.

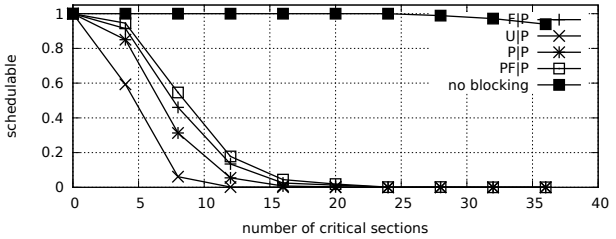

Fig. 2355. Schedulability under preemptable spin locks for $m = 8$, $U = 0.3n$, 4 resources, $rsf = 0.75$, and medium critical sections. The schedulability of the considered non-preemptable lock types in this configuration is shown in Fig. 2353.

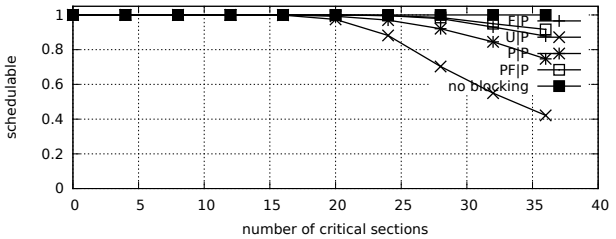

Fig. 2356. Schedulability under preemptable spin locks for $m = 8$, $U = 0.3n$, 4 resources, $rsf = 0.75$, and short critical sections. The schedulability of the considered non-preemptable lock types in this configuration is shown in Fig. 2354.

Configurations with $U = 0.1n$

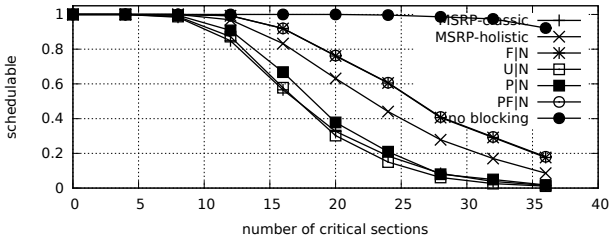

Fig. 2357. Schedulability under non-preemptable spin locks for $m = 8$, $U = 0.1n$, 8 resources, $rsf = 0.1$, and medium critical sections. The schedulability of the considered preemptable lock types in this configuration is shown in Fig. 2359.

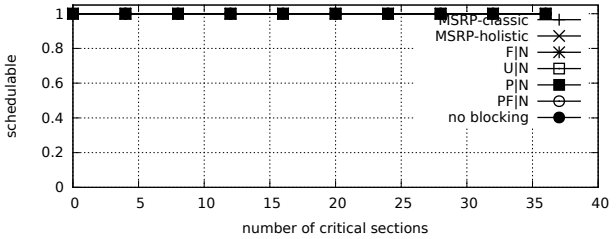

Fig. 2358. Schedulability under non-preemptable spin locks for $m = 8$, $U = 0.1n$, 8 resources, $rsf = 0.1$, and short critical sections. The schedulability of the considered preemptable lock types in this configuration is shown in Fig. 2360.

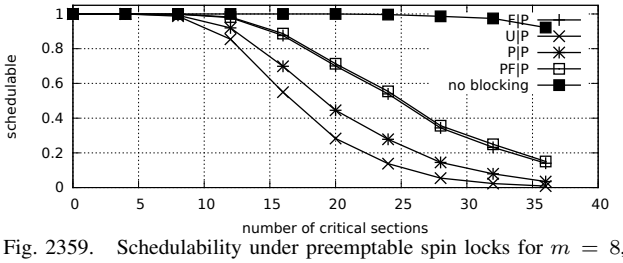

Fig. 2359. Schedulability under preemptable spin locks for $m = 8$, $U = 0.1n$, 8 resources, $rsf = 0.1$, and medium critical sections. The schedulability of the considered non-preemptable lock types in this configuration is shown in Fig. 2357.

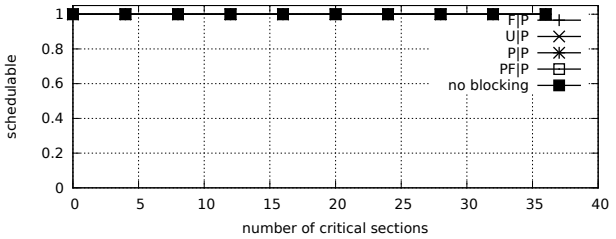

Fig. 2360. Schedulability under preemptable spin locks for $m = 8$, $U = 0.1n$, 8 resources, $rsf = 0.1$, and short critical sections. The schedulability of the considered non-preemptable lock types in this configuration is shown in Fig. 2358.

Configurations with $U = 0.2n$

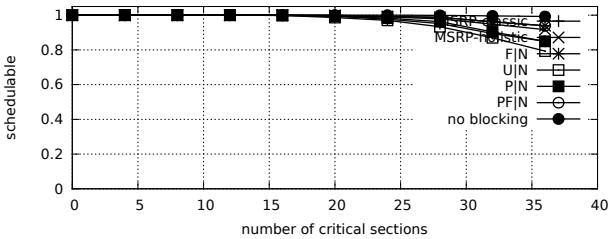

Fig. 2361. Schedulability under non-preemptable spin locks for $m = 8$, $U = 0.2n$, 8 resources, $rsf = 0.1$, and medium critical sections. The schedulability of the considered preemptable lock types in this configuration is shown in Fig. 2363.

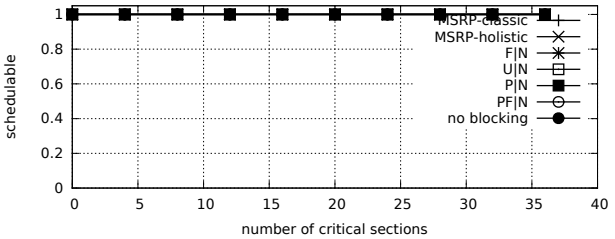

Fig. 2362. Schedulability under non-preemptable spin locks for $m = 8$, $U = 0.2n$, 8 resources, $rsf = 0.1$, and short critical sections. The schedulability of the considered preemptable lock types in this configuration is shown in Fig. 2364.

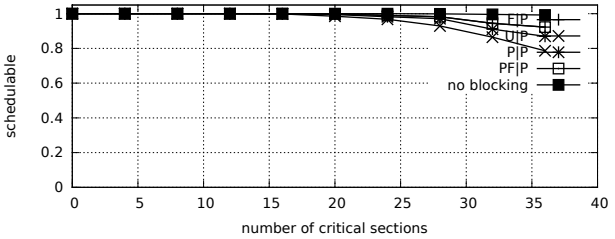

Fig. 2363. Schedulability under preemptable spin locks for $m = 8$, $U = 0.2n$, 8 resources, $rsf = 0.1$, and medium critical sections. The schedulability of the considered non-preemptable lock types in this configuration is shown in Fig. 2361.

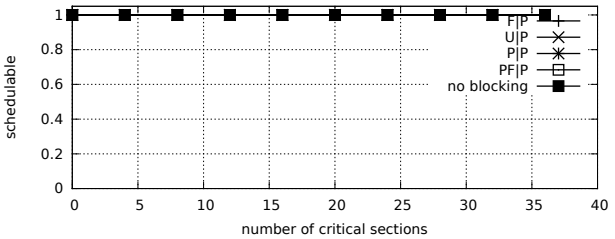

Fig. 2364. Schedulability under preemptable spin locks for $m = 8$, $U = 0.2n$, 8 resources, $rsf = 0.1$, and short critical sections. The schedulability of the considered non-preemptable lock types in this configuration is shown in Fig. 2362.

Configurations with $U = 0.3n$

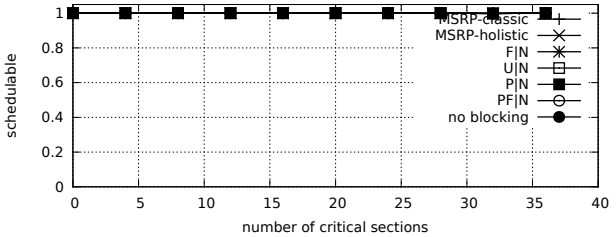

Fig. 2365. Schedulability under non-preemptable spin locks for $m = 8$, $U = 0.3n$, 8 resources, $rsf = 0.1$, and medium critical sections. The schedulability of the considered preemptable lock types in this configuration is shown in Fig. 2367.

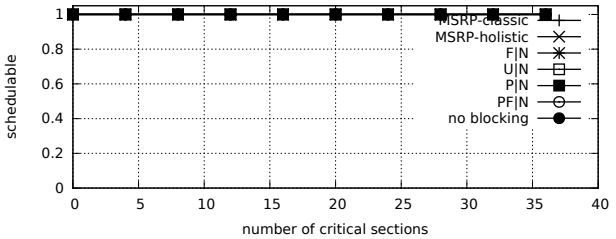

Fig. 2366. Schedulability under non-preemptable spin locks for $m = 8$, $U = 0.3n$, 8 resources, $rsf = 0.1$, and short critical sections. The schedulability of the considered preemptable lock types in this configuration is shown in Fig. 2368.

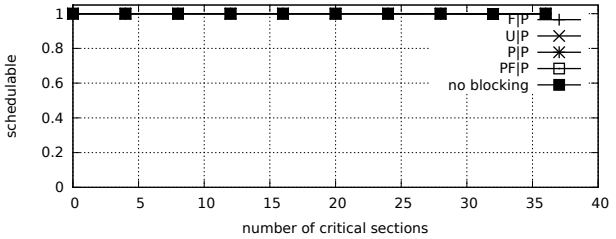

Fig. 2367. Schedulability under preemptable spin locks for $m = 8$, $U = 0.3n$, 8 resources, $rsf = 0.1$, and medium critical sections. The schedulability of the considered non-preemptable lock types in this configuration is shown in Fig. 2365.

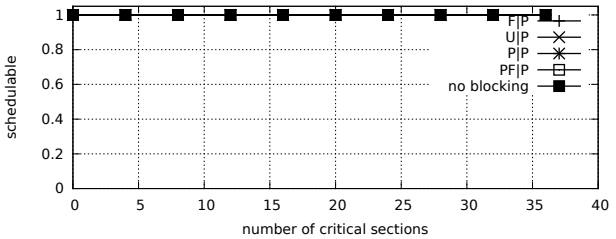

Fig. 2368. Schedulability under preemptable spin locks for $m = 8$, $U = 0.3n$, 8 resources, $rsf = 0.1$, and short critical sections. The schedulability of the considered non-preemptable lock types in this configuration is shown in Fig. 2366.

Configurations with $U = 0.1n$

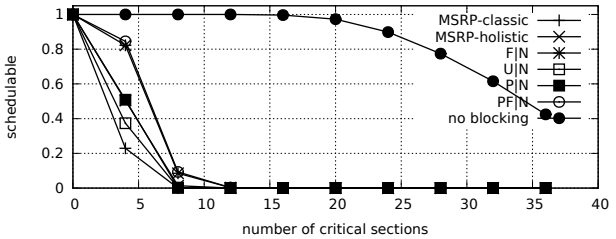

Fig. 2369. Schedulability under non-preemptable spin locks for $m = 8$, $U = 0.1n$, 8 resources, $rsf = 0.25$, and medium critical sections. The schedulability of the considered preemptable lock types in this configuration is shown in Fig. 2371.

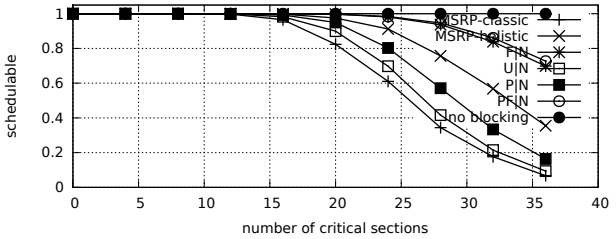

Fig. 2370. Schedulability under non-preemptable spin locks for $m = 8$, $U = 0.1n$, 8 resources, $rsf = 0.25$, and short critical sections. The schedulability of the considered preemptable lock types in this configuration is shown in Fig. 2372.

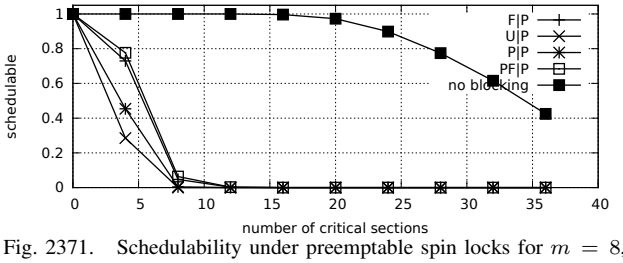

Fig. 2371. Schedulability under preemptable spin locks for $m = 8$, $U = 0.1n$, 8 resources, $rsf = 0.25$, and medium critical sections. The schedulability of the considered non-preemptable lock types in this configuration is shown in Fig. 2369.

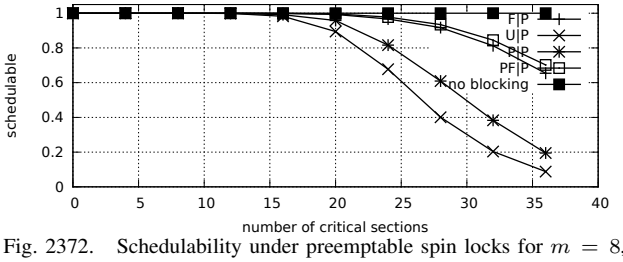

Fig. 2372. Schedulability under preemptable spin locks for $m = 8$, $U = 0.1n$, 8 resources, $rsf = 0.25$, and short critical sections. The schedulability of the considered non-preemptable lock types in this configuration is shown in Fig. 2370.

Configurations with $U = 0.2n$

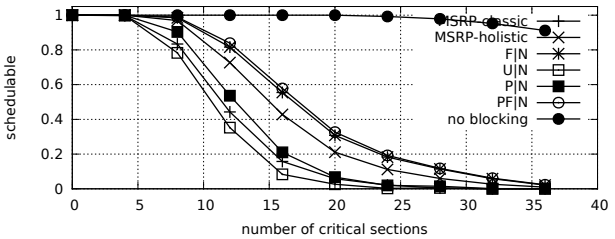

Fig. 2373. Schedulability under non-preemptable spin locks for $m = 8$, $U = 0.2n$, 8 resources, $rsf = 0.25$, and medium critical sections. The schedulability of the considered preemptable lock types in this configuration is shown in Fig. 2375.

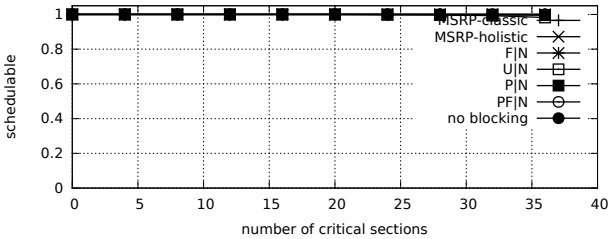

Fig. 2374. Schedulability under non-preemptable spin locks for $m = 8$, $U = 0.2n$, 8 resources, $rsf = 0.25$, and short critical sections. The schedulability of the considered preemptable lock types in this configuration is shown in Fig. 2376.

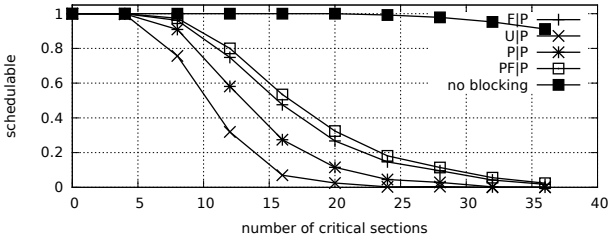

Fig. 2375. Schedulability under preemptable spin locks for $m = 8$, $U = 0.2n$, 8 resources, $rsf = 0.25$, and medium critical sections. The schedulability of the considered non-preemptable lock types in this configuration is shown in Fig. 2373.

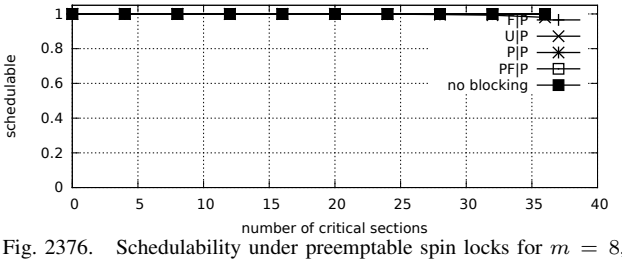

Fig. 2376. Schedulability under preemptable spin locks for $m = 8$, $U = 0.2n$, 8 resources, $rsf = 0.25$, and short critical sections. The schedulability of the considered non-preemptable lock types in this configuration is shown in Fig. 2374.

Configurations with $U = 0.3n$

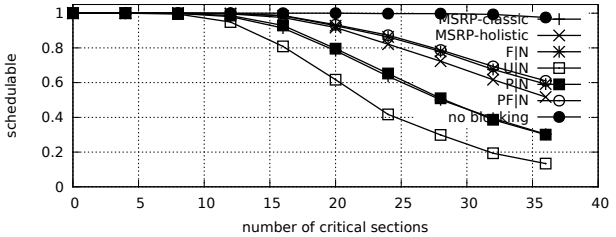

Fig. 2377. Schedulability under non-preemptable spin locks for $m = 8$, $U = 0.3n$, 8 resources, $rsf = 0.25$, and medium critical sections. The schedulability of the considered preemptable lock types in this configuration is shown in Fig. 2379.

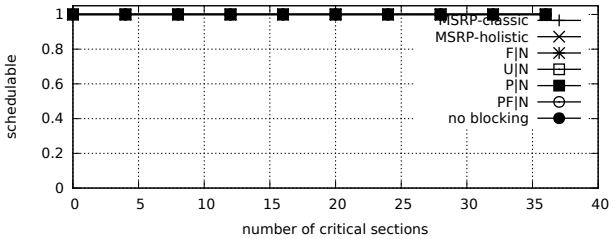

Fig. 2378. Schedulability under non-preemptable spin locks for $m = 8$, $U = 0.3n$, 8 resources, $rsf = 0.25$, and short critical sections. The schedulability of the considered preemptable lock types in this configuration is shown in Fig. 2380.

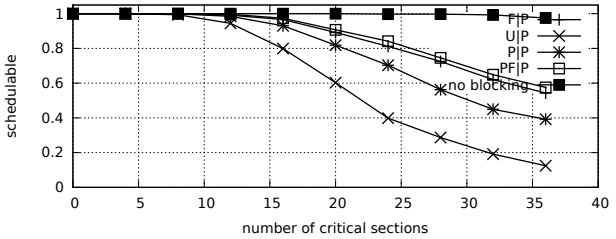

Fig. 2379. Schedulability under preemptable spin locks for $m = 8$, $U = 0.3n$, 8 resources, $rsf = 0.25$, and medium critical sections. The schedulability of the considered non-preemptable lock types in this configuration is shown in Fig. 2377.

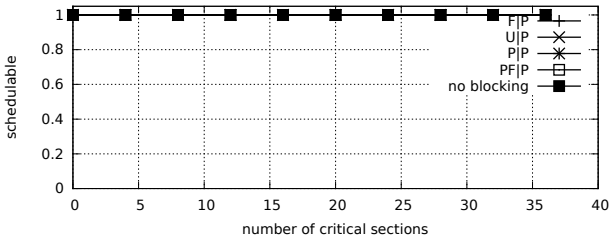

Fig. 2380. Schedulability under preemptable spin locks for $m = 8$, $U = 0.3n$, 8 resources, $rsf = 0.25$, and short critical sections. The schedulability of the considered non-preemptable lock types in this configuration is shown in Fig. 2378.

Configurations with $U = 0.1n$

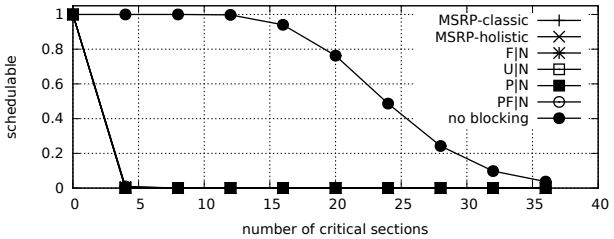

Fig. 2381. Schedulability under non-preemptable spin locks for $m = 8$, $U = 0.1n$, 8 resources, $rsf = 0.4$, and medium critical sections. The schedulability of the considered preemptable lock types in this configuration is shown in Fig. 2383.

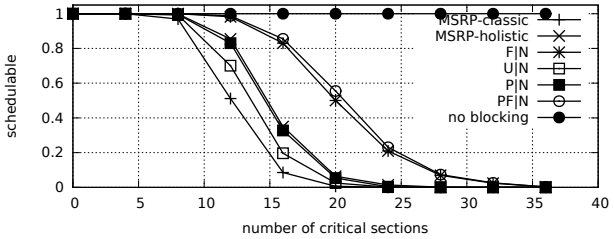

Fig. 2382. Schedulability under non-preemptable spin locks for $m = 8$, $U = 0.1n$, 8 resources, $rsf = 0.4$, and short critical sections. The schedulability of the considered preemptable lock types in this configuration is shown in Fig. 2384.

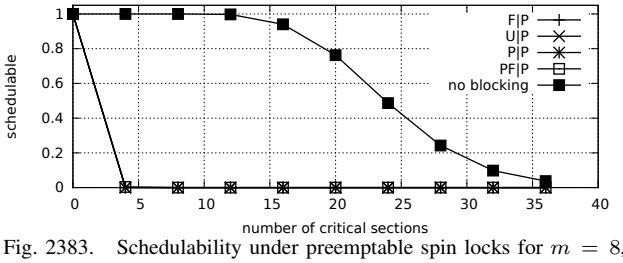

Fig. 2383. Schedulability under preemptable spin locks for $m = 8$, $U = 0.1n$, 8 resources, $rsf = 0.4$, and medium critical sections. The schedulability of the considered non-preemptable lock types in this configuration is shown in Fig. 2381.

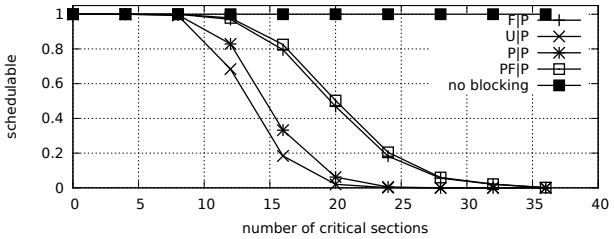

Fig. 2384. Schedulability under preemptable spin locks for $m = 8$, $U = 0.1n$, 8 resources, $rsf = 0.4$, and short critical sections. The schedulability of the considered non-preemptable lock types in this configuration is shown in Fig. 2382.

Configurations with $U = 0.2n$

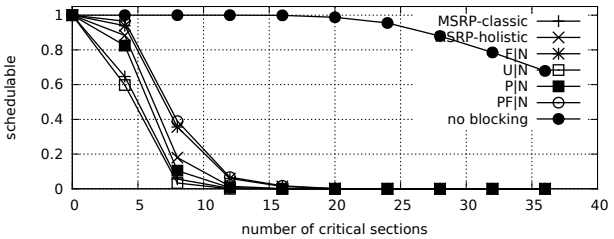

Fig. 2385. Schedulability under non-preemptable spin locks for $m = 8$, $U = 0.2n$, 8 resources, $rsf = 0.4$, and medium critical sections. The schedulability of the considered preemptable lock types in this configuration is shown in Fig. 2387.

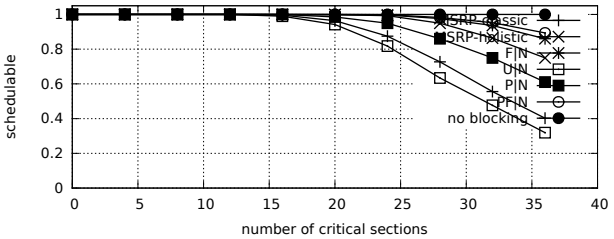

Fig. 2386. Schedulability under non-preemptable spin locks for $m = 8$, $U = 0.2n$, 8 resources, $rsf = 0.4$, and short critical sections. The schedulability of the considered preemptable lock types in this configuration is shown in Fig. 2388.

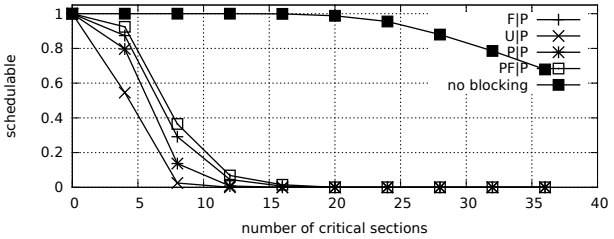

Fig. 2387. Schedulability under preemptable spin locks for $m = 8$, $U = 0.2n$, 8 resources, $rsf = 0.4$, and medium critical sections. The schedulability of the considered non-preemptable lock types in this configuration is shown in Fig. 2385.

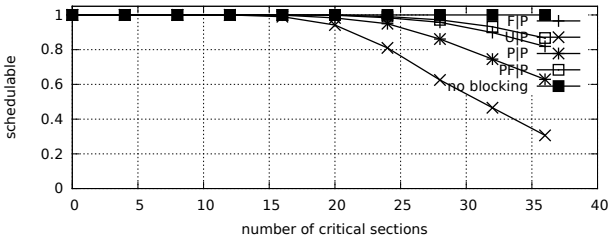

Fig. 2388. Schedulability under preemptable spin locks for $m = 8$, $U = 0.2n$, 8 resources, $rsf = 0.4$, and short critical sections. The schedulability of the considered non-preemptable lock types in this configuration is shown in Fig. 2386.

Configurations with $U = 0.3n$

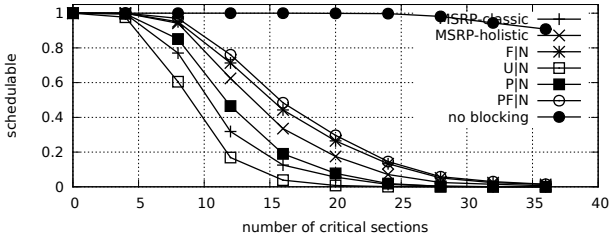

Fig. 2389. Schedulability under non-preemptable spin locks for $m = 8$, $U = 0.3n$, 8 resources, $rsf = 0.4$, and medium critical sections. The schedulability of the considered preemptable lock types in this configuration is shown in Fig. 2391.

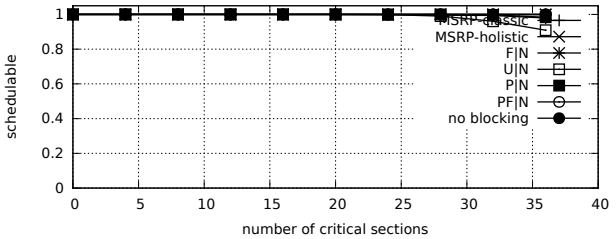

Fig. 2390. Schedulability under non-preemptable spin locks for $m = 8$, $U = 0.3n$, 8 resources, $rsf = 0.4$, and short critical sections. The schedulability of the considered preemptable lock types in this configuration is shown in Fig. 2392.

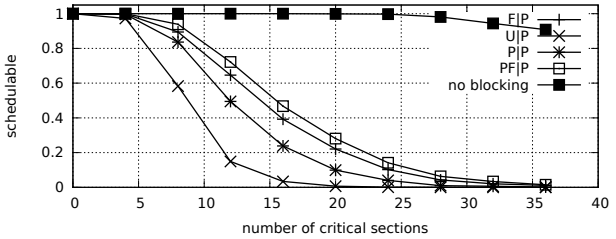

Fig. 2391. Schedulability under preemptable spin locks for $m = 8$, $U = 0.3n$, 8 resources, $rsf = 0.4$, and medium critical sections. The schedulability of the considered non-preemptable lock types in this configuration is shown in Fig. 2389.

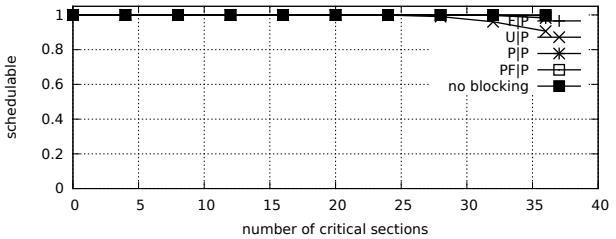

Fig. 2392. Schedulability under preemptable spin locks for $m = 8$, $U = 0.3n$, 8 resources, $rsf = 0.4$, and short critical sections. The schedulability of the considered non-preemptable lock types in this configuration is shown in Fig. 2390.

Configurations with $U = 0.1n$

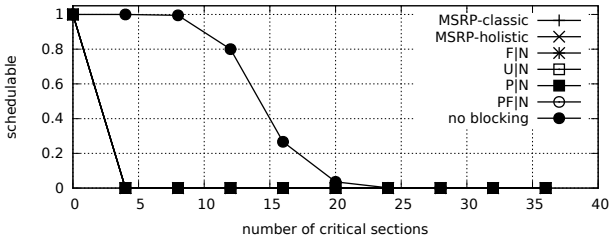

Fig. 2393. Schedulability under non-preemptable spin locks for $m = 8$, $U = 0.1n$, 8 resources, $rsf = 0.75$, and medium critical sections. The schedulability of the considered preemptable lock types in this configuration is shown in Fig. 2395.

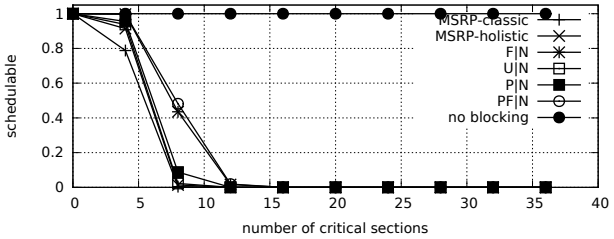

Fig. 2394. Schedulability under non-preemptable spin locks for $m = 8$, $U = 0.1n$, 8 resources, $rsf = 0.75$, and short critical sections. The schedulability of the considered preemptable lock types in this configuration is shown in Fig. 2396.

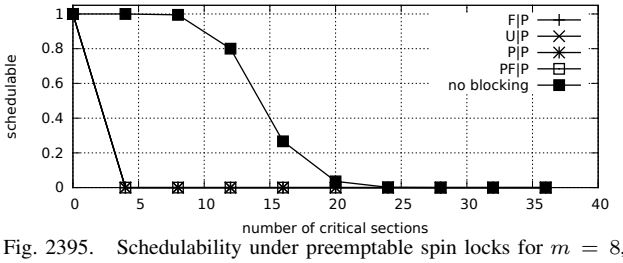

Fig. 2395. Schedulability under preemptable spin locks for $m = 8$, $U = 0.1n$, 8 resources, $rsf = 0.75$, and medium critical sections. The schedulability of the considered non-preemptable lock types in this configuration is shown in Fig. 2393.

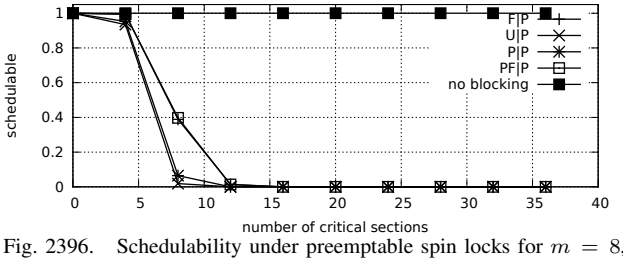

Fig. 2396. Schedulability under preemptable spin locks for $m = 8$, $U = 0.1n$, 8 resources, $rsf = 0.75$, and short critical sections. The schedulability of the considered non-preemptable lock types in this configuration is shown in Fig. 2394.

Configurations with $U = 0.2n$

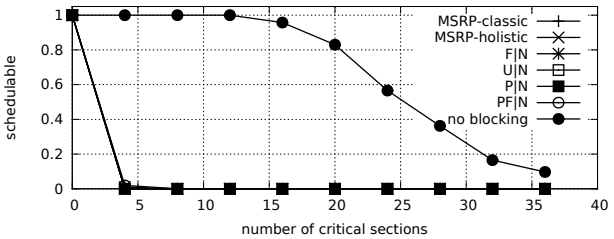

Fig. 2397. Schedulability under non-preemptable spin locks for $m = 8$, $U = 0.2n$, 8 resources, $rsf = 0.75$, and medium critical sections. The schedulability of the considered preemptable lock types in this configuration is shown in Fig. 2399.

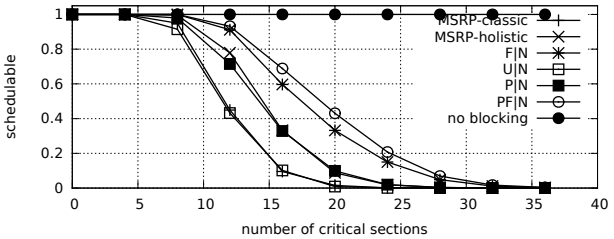

Fig. 2398. Schedulability under non-preemptable spin locks for $m = 8$, $U = 0.2n$, 8 resources, $rsf = 0.75$, and short critical sections. The schedulability of the considered preemptable lock types in this configuration is shown in Fig. 2400.

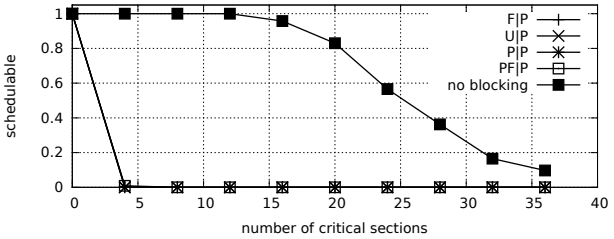

Fig. 2399. Schedulability under preemptable spin locks for $m = 8$, $U = 0.2n$, 8 resources, $rsf = 0.75$, and medium critical sections. The schedulability of the considered non-preemptable lock types in this configuration is shown in Fig. 2397.

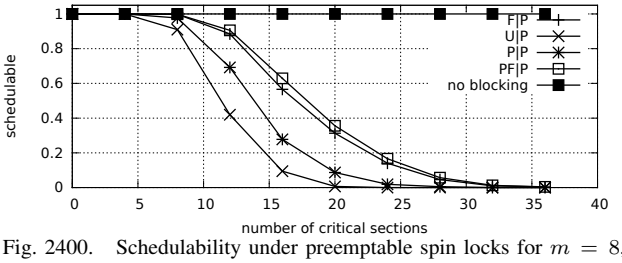

Fig. 2400. Schedulability under preemptable spin locks for $m = 8$, $U = 0.2n$, 8 resources, $rsf = 0.75$, and short critical sections. The schedulability of the considered non-preemptable lock types in this configuration is shown in Fig. 2398.

Configurations with $U = 0.3n$

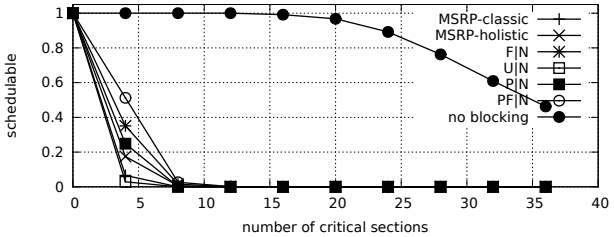

Fig. 2401. Schedulability under non-preemptable spin locks for $m = 8$, $U = 0.3n$, 8 resources, $rsf = 0.75$, and medium critical sections. The schedulability of the considered preemptable lock types in this configuration is shown in Fig. 2403.

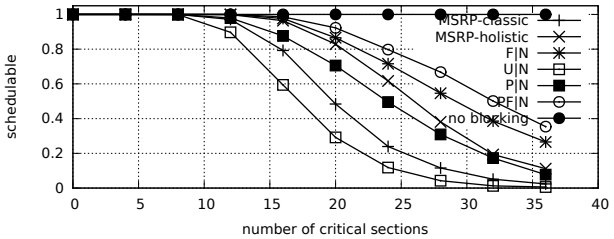

Fig. 2402. Schedulability under non-preemptable spin locks for $m = 8$, $U = 0.3n$, 8 resources, $rsf = 0.75$, and short critical sections. The schedulability of the considered preemptable lock types in this configuration is shown in Fig. 2404.

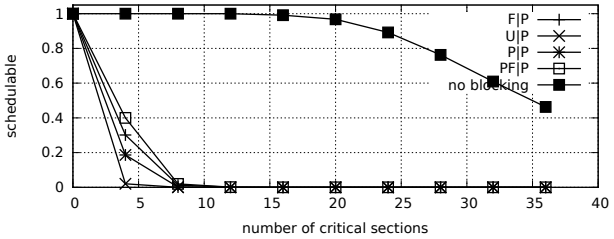

Fig. 2403. Schedulability under preemptable spin locks for $m = 8$, $U = 0.3n$, 8 resources, $rsf = 0.75$, and medium critical sections. The schedulability of the considered non-preemptable lock types in this configuration is shown in Fig. 2401.

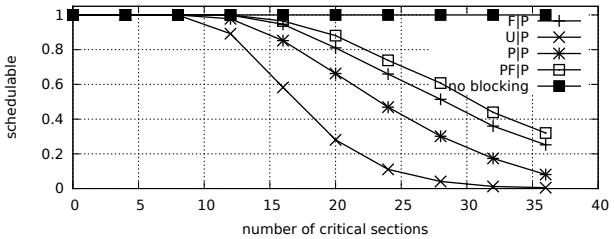

Fig. 2404. Schedulability under preemptable spin locks for $m = 8$, $U = 0.3n$, 8 resources, $rsf = 0.75$, and short critical sections. The schedulability of the considered non-preemptable lock types in this configuration is shown in Fig. 2402.

Configurations with $U = 0.1n$

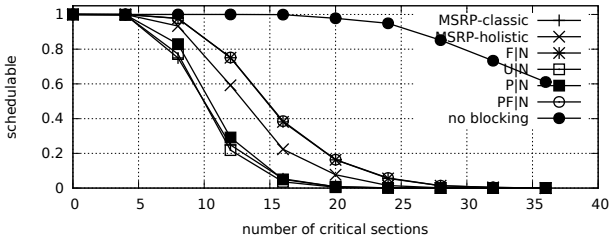

Fig. 2405. Schedulability under non-preemptable spin locks for $m = 8$, $U = 0.1n$, 16 resources, $rsf = 0.1$, and medium critical sections. The schedulability of the considered preemptable lock types in this configuration is shown in Fig. 2407.

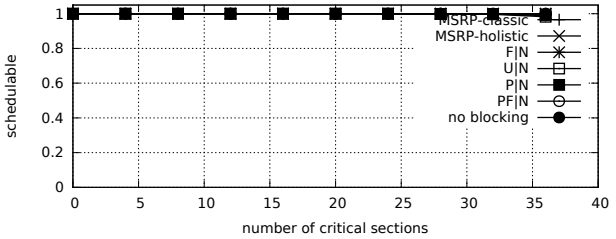

Fig. 2406. Schedulability under non-preemptable spin locks for $m = 8$, $U = 0.1n$, 16 resources, $rsf = 0.1$, and short critical sections. The schedulability of the considered preemptable lock types in this configuration is shown in Fig. 2408.

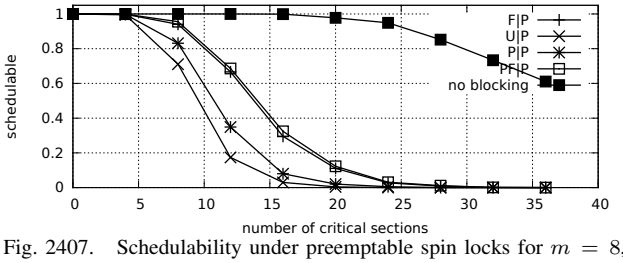

Fig. 2407. Schedulability under preemptable spin locks for $m = 8$, $U = 0.1n$, 16 resources, $rsf = 0.1$, and medium critical sections. The schedulability of the considered non-preemptable lock types in this configuration is shown in Fig. 2405.

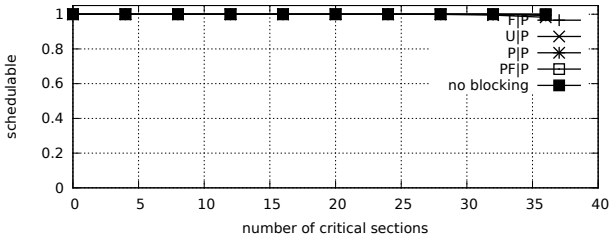

Fig. 2408. Schedulability under preemptable spin locks for $m = 8$, $U = 0.1n$, 16 resources, $rsf = 0.1$, and short critical sections. The schedulability of the considered non-preemptable lock types in this configuration is shown in Fig. 2406.

Configurations with $U = 0.2n$

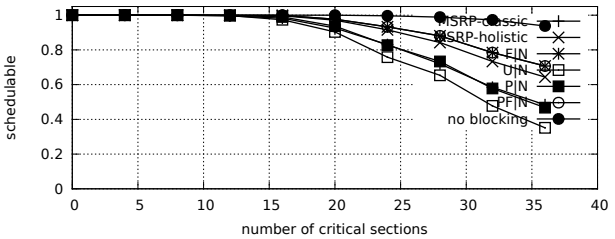

Fig. 2409. Schedulability under non-preemptable spin locks for $m = 8$, $U = 0.2n$, 16 resources, $rsf = 0.1$, and medium critical sections. The schedulability of the considered preemptable lock types in this configuration is shown in Fig. 2411.

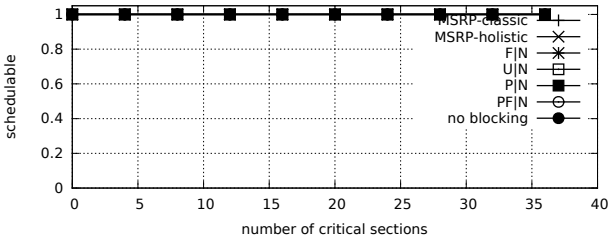

Fig. 2410. Schedulability under non-preemptable spin locks for $m = 8$, $U = 0.2n$, 16 resources, $rsf = 0.1$, and short critical sections. The schedulability of the considered preemptable lock types in this configuration is shown in Fig. 2412.

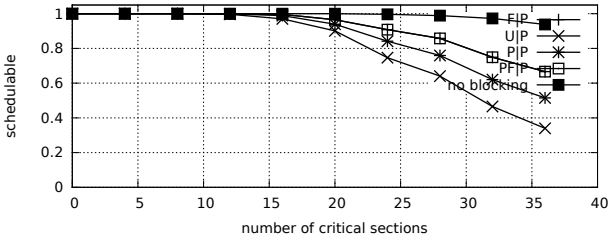

Fig. 2411. Schedulability under preemptable spin locks for $m = 8$, $U = 0.2n$, 16 resources, $rsf = 0.1$, and medium critical sections. The schedulability of the considered non-preemptable lock types in this configuration is shown in Fig. 2409.

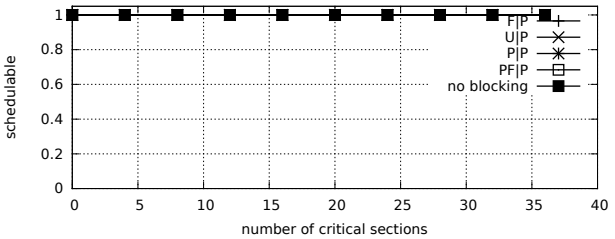

Fig. 2412. Schedulability under preemptable spin locks for $m = 8$, $U = 0.2n$, 16 resources, $rsf = 0.1$, and short critical sections. The schedulability of the considered non-preemptable lock types in this configuration is shown in Fig. 2410.

Configurations with $U = 0.3n$

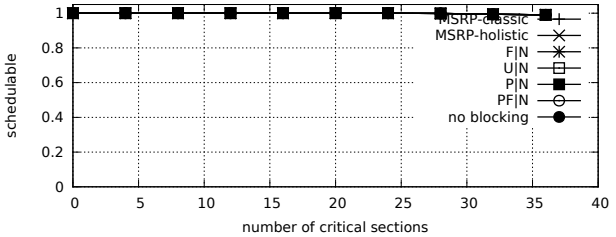

Fig. 2413. Schedulability under non-preemptable spin locks for $m = 8$, $U = 0.3n$, 16 resources, $rsf = 0.1$, and medium critical sections. The schedulability of the considered preemptable lock types in this configuration is shown in Fig. 2415.

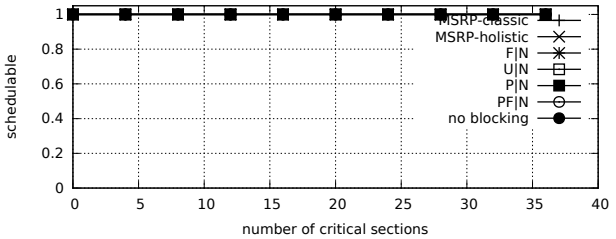

Fig. 2414. Schedulability under non-preemptable spin locks for $m = 8$, $U = 0.3n$, 16 resources, $rsf = 0.1$, and short critical sections. The schedulability of the considered preemptable lock types in this configuration is shown in Fig. 2416.

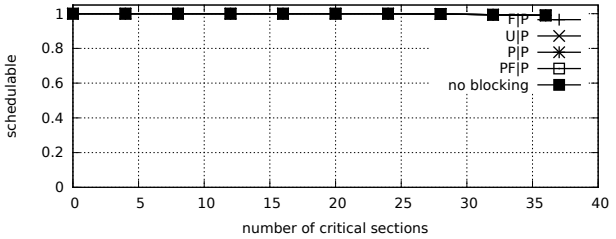

Fig. 2415. Schedulability under preemptable spin locks for $m = 8$, $U = 0.3n$, 16 resources, $rsf = 0.1$, and medium critical sections. The schedulability of the considered non-preemptable lock types in this configuration is shown in Fig. 2413.

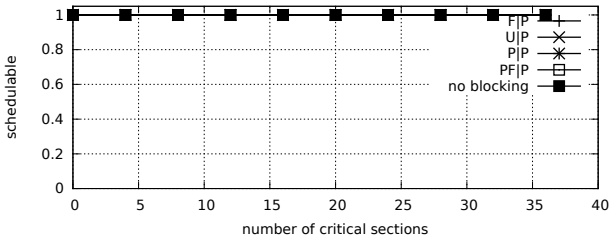

Fig. 2416. Schedulability under preemptable spin locks for $m = 8$, $U = 0.3n$, 16 resources, $rsf = 0.1$, and short critical sections. The schedulability of the considered non-preemptable lock types in this configuration is shown in Fig. 2414.

Configurations with $U = 0.1n$

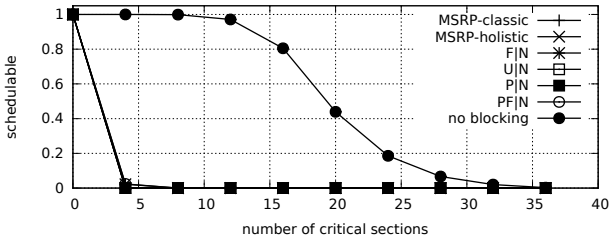

Fig. 2417. Schedulability under non-preemptable spin locks for $m = 8$, $U = 0.1n$, 16 resources, $rsf = 0.25$, and medium critical sections. The schedulability of the considered preemptable lock types in this configuration is shown in Fig. 2419.

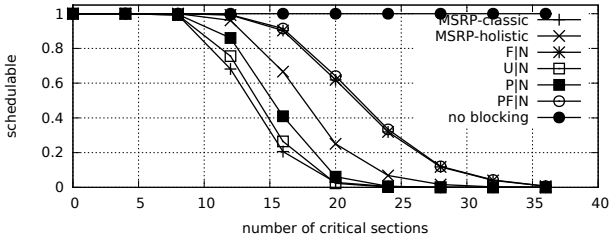

Fig. 2418. Schedulability under non-preemptable spin locks for $m = 8$, $U = 0.1n$, 16 resources, $rsf = 0.25$, and short critical sections. The schedulability of the considered preemptable lock types in this configuration is shown in Fig. 2420.

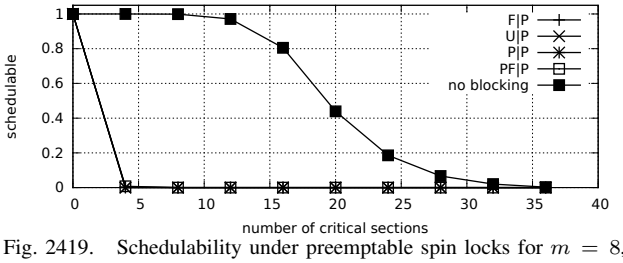

Fig. 2419. Schedulability under preemptable spin locks for $m = 8$, $U = 0.1n$, 16 resources, $rsf = 0.25$, and medium critical sections. The schedulability of the considered non-preemptable lock types in this configuration is shown in Fig. 2417.

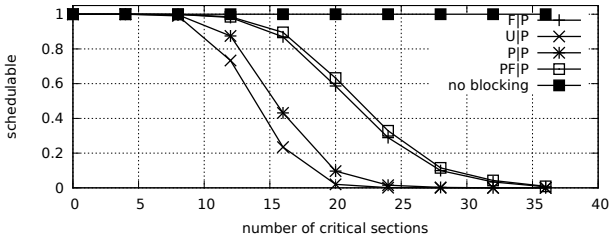

Fig. 2420. Schedulability under preemptable spin locks for $m = 8$, $U = 0.1n$, 16 resources, $rsf = 0.25$, and short critical sections. The schedulability of the considered non-preemptable lock types in this configuration is shown in Fig. 2418.

Configurations with $U = 0.2n$

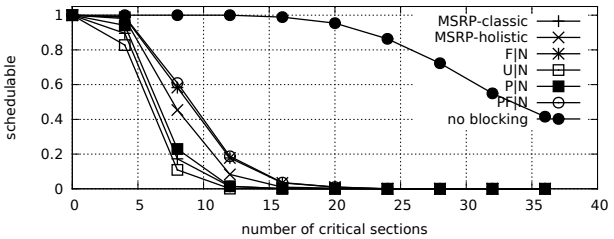

Fig. 2421. Schedulability under non-preemptable spin locks for $m = 8$, $U = 0.2n$, 16 resources, $rsf = 0.25$, and medium critical sections. The schedulability of the considered preemptable lock types in this configuration is shown in Fig. 2423.

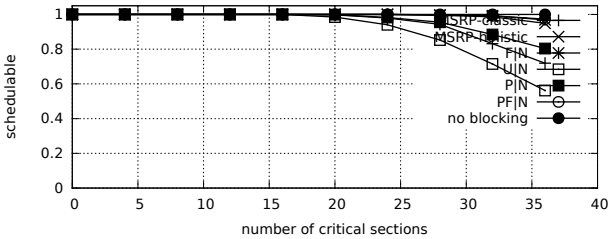

Fig. 2422. Schedulability under non-preemptable spin locks for $m = 8$, $U = 0.2n$, 16 resources, $rsf = 0.25$, and short critical sections. The schedulability of the considered preemptable lock types in this configuration is shown in Fig. 2424.

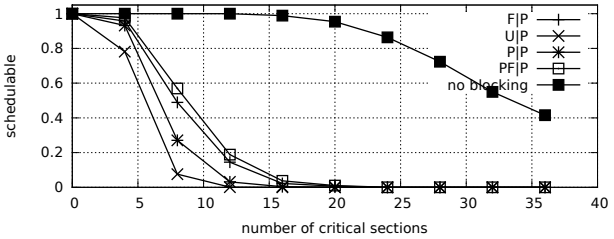

Fig. 2423. Schedulability under preemptable spin locks for $m = 8$, $U = 0.2n$, 16 resources, $rsf = 0.25$, and medium critical sections. The schedulability of the considered non-preemptable lock types in this configuration is shown in Fig. 2421.

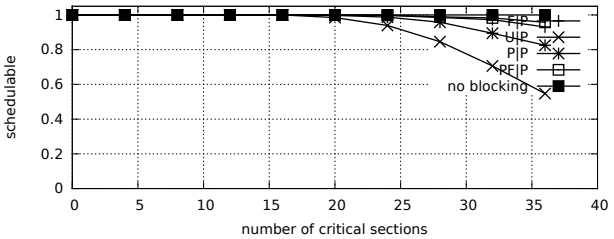

Fig. 2424. Schedulability under preemptable spin locks for $m = 8$, $U = 0.2n$, 16 resources, $rsf = 0.25$, and short critical sections. The schedulability of the considered non-preemptable lock types in this configuration is shown in Fig. 2422.

Configurations with $U = 0.3n$

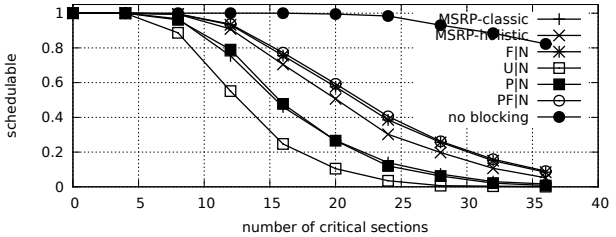

Fig. 2425. Schedulability under non-preemptable spin locks for $m = 8$, $U = 0.3n$, 16 resources, $rsf = 0.25$, and medium critical sections. The schedulability of the considered preemptable lock types in this configuration is shown in Fig. 2427.

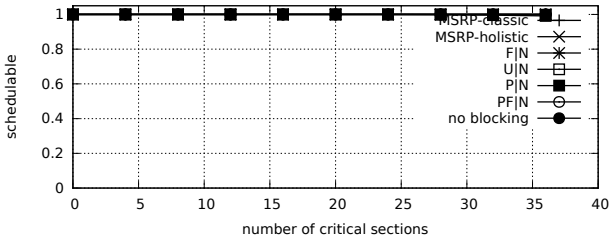

Fig. 2426. Schedulability under non-preemptable spin locks for $m = 8$, $U = 0.3n$, 16 resources, $rsf = 0.25$, and short critical sections. The schedulability of the considered preemptable lock types in this configuration is shown in Fig. 2428.

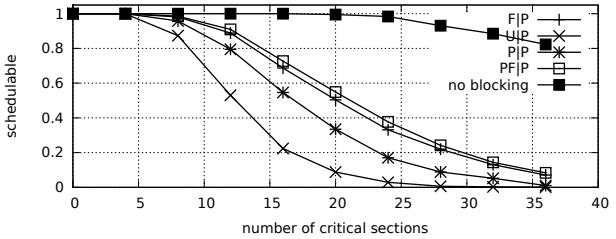

Fig. 2427. Schedulability under preemptable spin locks for $m = 8$, $U = 0.3n$, 16 resources, $rsf = 0.25$, and medium critical sections. The schedulability of the considered non-preemptable lock types in this configuration is shown in Fig. 2425.

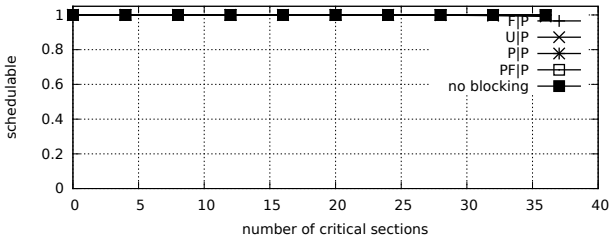

Fig. 2428. Schedulability under preemptable spin locks for $m = 8$, $U = 0.3n$, 16 resources, $rsf = 0.25$, and short critical sections. The schedulability of the considered non-preemptable lock types in this configuration is shown in Fig. 2426.

Configurations with $U = 0.1n$

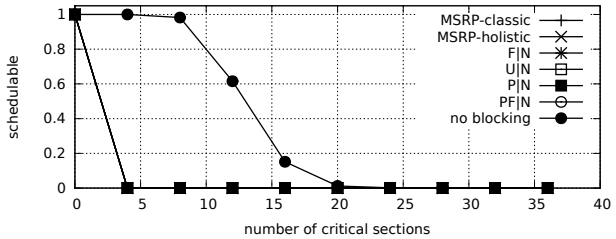

Fig. 2429. Schedulability under non-preemptable spin locks for $m = 8$, $U = 0.1n$, 16 resources, $rsf = 0.4$, and medium critical sections. The schedulability of the considered preemptable lock types in this configuration is shown in Fig. 2431.

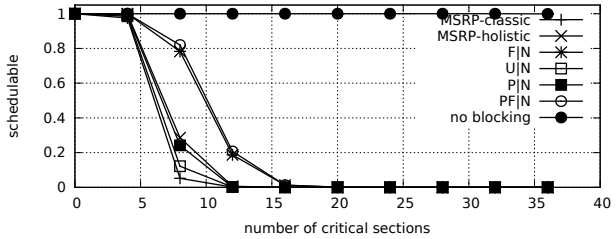

Fig. 2430. Schedulability under non-preemptable spin locks for $m = 8$, $U = 0.1n$, 16 resources, $rsf = 0.4$, and short critical sections. The schedulability of the considered preemptable lock types in this configuration is shown in Fig. 2432.

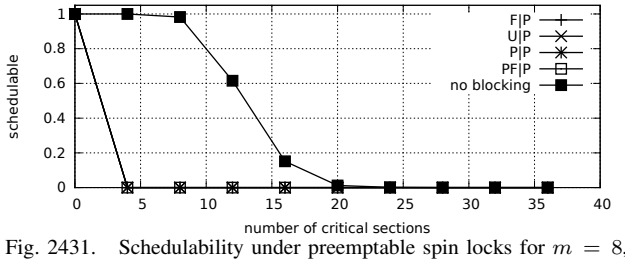

Fig. 2431. Schedulability under preemptable spin locks for $m = 8$, $U = 0.1n$, 16 resources, $rsf = 0.4$, and medium critical sections. The schedulability of the considered non-preemptable lock types in this configuration is shown in Fig. 2429.

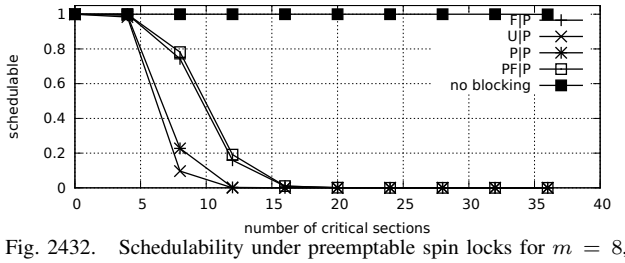

Fig. 2432. Schedulability under preemptable spin locks for $m = 8$, $U = 0.1n$, 16 resources, $rsf = 0.4$, and short critical sections. The schedulability of the considered non-preemptable lock types in this configuration is shown in Fig. 2430.

Configurations with $U = 0.2n$

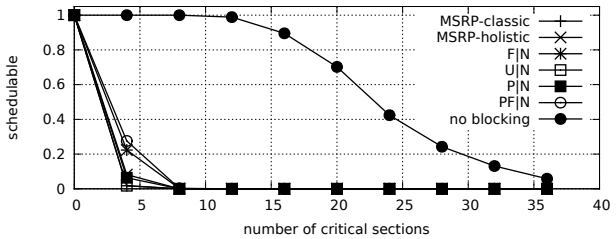

Fig. 2433. Schedulability under non-preemptable spin locks for $m = 8$, $U = 0.2n$, 16 resources, $rsf = 0.4$, and medium critical sections. The schedulability of the considered preemptable lock types in this configuration is shown in Fig. 2435.

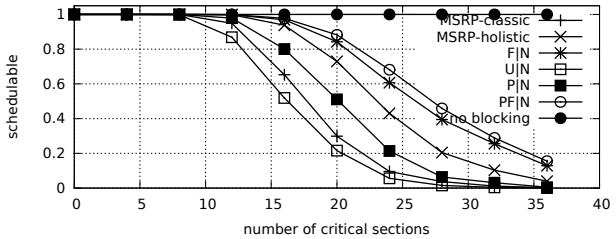

Fig. 2434. Schedulability under non-preemptable spin locks for $m = 8$, $U = 0.2n$, 16 resources, $rsf = 0.4$, and short critical sections. The schedulability of the considered preemptable lock types in this configuration is shown in Fig. 2436.

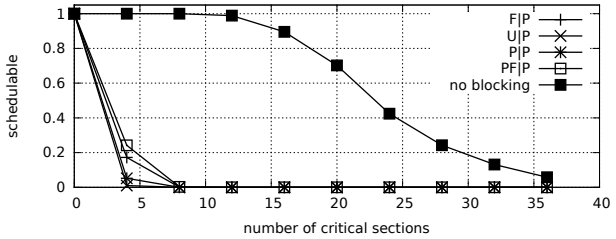

Fig. 2435. Schedulability under preemptable spin locks for $m = 8$, $U = 0.2n$, 16 resources, $rsf = 0.4$, and medium critical sections. The schedulability of the considered non-preemptable lock types in this configuration is shown in Fig. 2433.

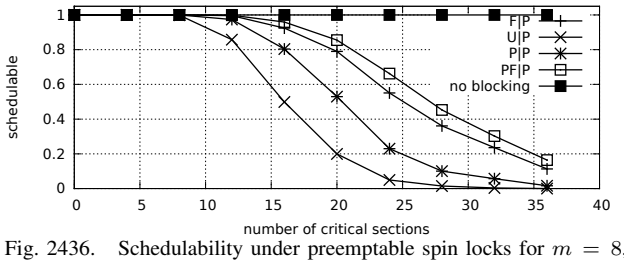

Fig. 2436. Schedulability under preemptable spin locks for $m = 8$, $U = 0.2n$, 16 resources, $rsf = 0.4$, and short critical sections. The schedulability of the considered non-preemptable lock types in this configuration is shown in Fig. 2434.

Configurations with $U = 0.3n$

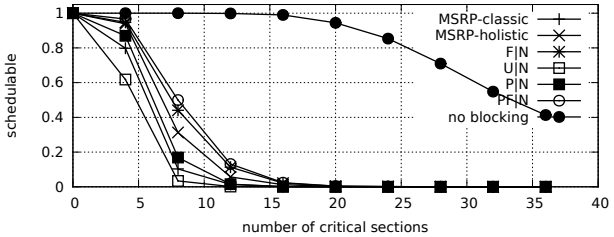

Fig. 2437. Schedulability under non-preemptable spin locks for $m = 8$, $U = 0.3n$, 16 resources, $rsf = 0.4$, and medium critical sections. The schedulability of the considered preemptable lock types in this configuration is shown in Fig. 2439.

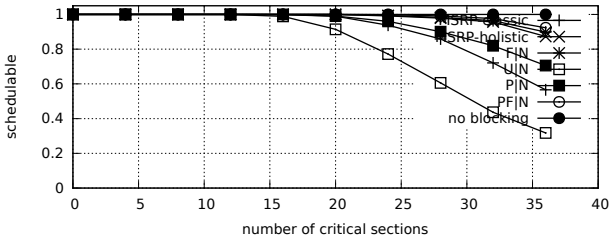

Fig. 2438. Schedulability under non-preemptable spin locks for $m = 8$, $U = 0.3n$, 16 resources, $rsf = 0.4$, and short critical sections. The schedulability of the considered preemptable lock types in this configuration is shown in Fig. 2440.

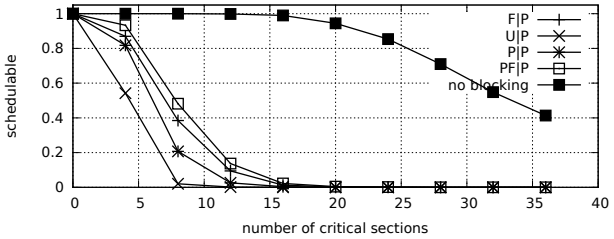

Fig. 2439. Schedulability under preemptable spin locks for $m = 8$, $U = 0.3n$, 16 resources, $rsf = 0.4$, and medium critical sections. The schedulability of the considered non-preemptable lock types in this configuration is shown in Fig. 2437.

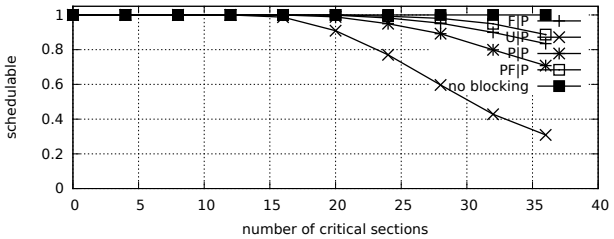

Fig. 2440. Schedulability under preemptable spin locks for $m = 8$, $U = 0.3n$, 16 resources, $rsf = 0.4$, and short critical sections. The schedulability of the considered non-preemptable lock types in this configuration is shown in Fig. 2438.

Configurations with $U = 0.1n$

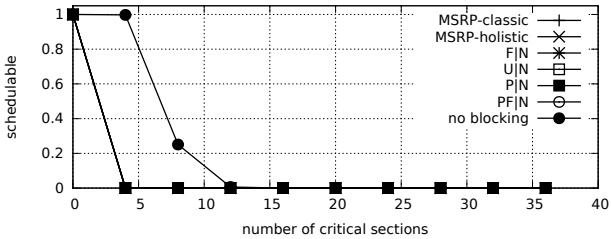

Fig. 2441. Schedulability under non-preemptable spin locks for $m = 8$, $U = 0.1n$, 16 resources, $rsf = 0.75$, and medium critical sections. The schedulability of the considered preemptable lock types in this configuration is shown in Fig. 2443.

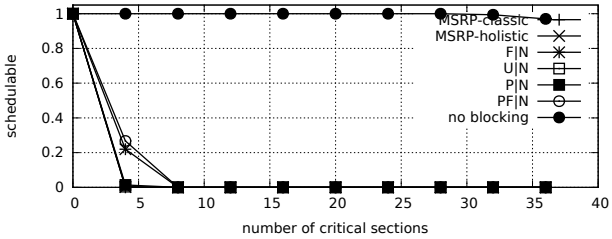

Fig. 2442. Schedulability under non-preemptable spin locks for $m = 8$, $U = 0.1n$, 16 resources, $rsf = 0.75$, and short critical sections. The schedulability of the considered preemptable lock types in this configuration is shown in Fig. 2444.

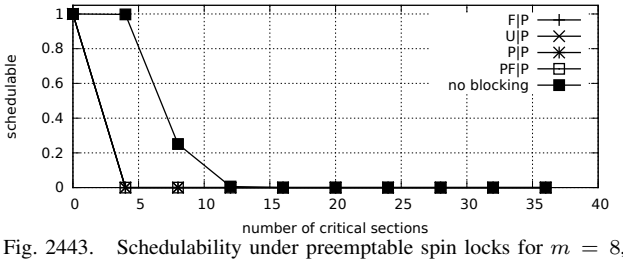

Fig. 2443. Schedulability under preemptable spin locks for $m = 8$, $U = 0.1n$, 16 resources, $rsf = 0.75$, and medium critical sections. The schedulability of the considered non-preemptable lock types in this configuration is shown in Fig. 2441.

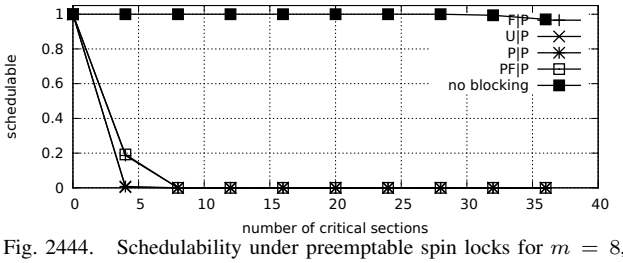

Fig. 2444. Schedulability under preemptable spin locks for $m = 8$, $U = 0.1n$, 16 resources, $rsf = 0.75$, and short critical sections. The schedulability of the considered non-preemptable lock types in this configuration is shown in Fig. 2442.

Configurations with $U = 0.2n$

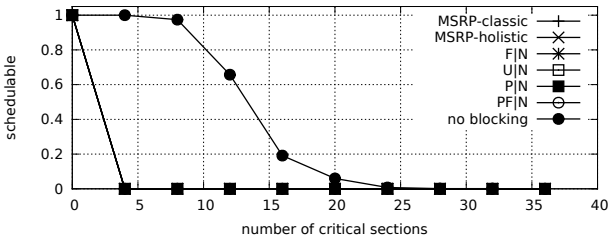

Fig. 2445. Schedulability under non-preemptable spin locks for $m = 8$, $U = 0.2n$, 16 resources, $rsf = 0.75$, and medium critical sections. The schedulability of the considered preemptable lock types in this configuration is shown in Fig. 2447.

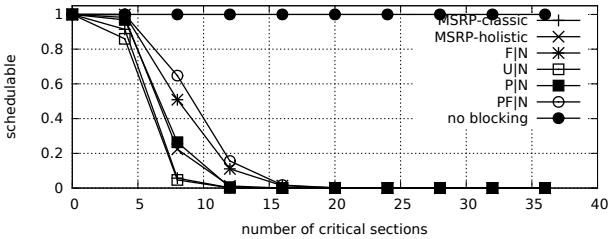

Fig. 2446. Schedulability under non-preemptable spin locks for $m = 8$, $U = 0.2n$, 16 resources, $rsf = 0.75$, and short critical sections. The schedulability of the considered preemptable lock types in this configuration is shown in Fig. 2448.

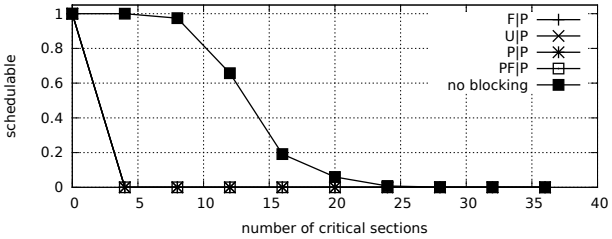

Fig. 2447. Schedulability under preemptable spin locks for $m = 8$, $U = 0.2n$, 16 resources, $rsf = 0.75$, and medium critical sections. The schedulability of the considered non-preemptable lock types in this configuration is shown in Fig. 2445.

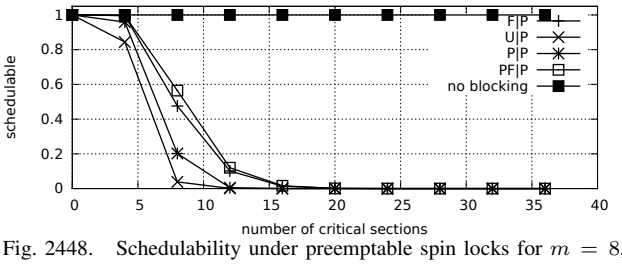

Fig. 2448. Schedulability under preemptable spin locks for $m = 8$, $U = 0.2n$, 16 resources, $rsf = 0.75$, and short critical sections. The schedulability of the considered non-preemptable lock types in this configuration is shown in Fig. 2446.

Configurations with $U = 0.3n$

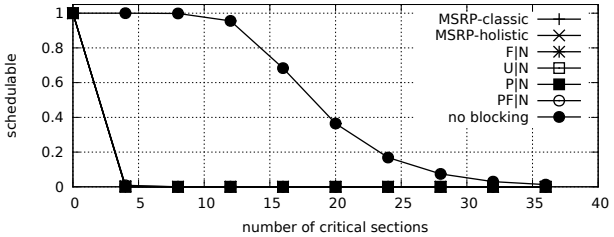

Fig. 2449. Schedulability under non-preemptable spin locks for $m = 8$, $U = 0.3n$, 16 resources, $rsf = 0.75$, and medium critical sections. The schedulability of the considered preemptable lock types in this configuration is shown in Fig. 2451.

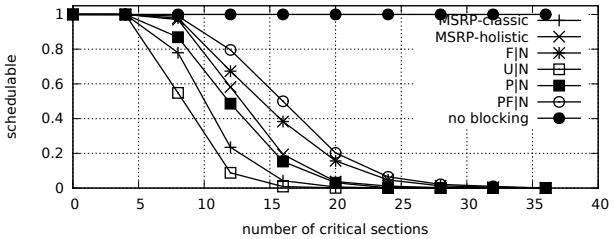

Fig. 2450. Schedulability under non-preemptable spin locks for $m = 8$, $U = 0.3n$, 16 resources, $rsf = 0.75$, and short critical sections. The schedulability of the considered preemptable lock types in this configuration is shown in Fig. 2452.

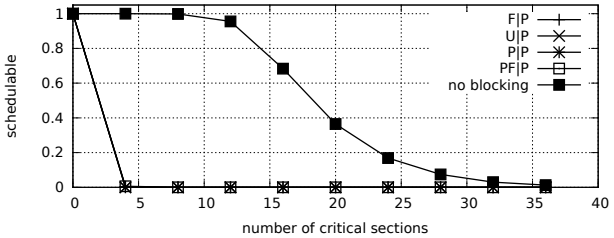

Fig. 2451. Schedulability under preemptable spin locks for $m = 8$, $U = 0.3n$, 16 resources, $rsf = 0.75$, and medium critical sections. The schedulability of the considered non-preemptable lock types in this configuration is shown in Fig. 2449.

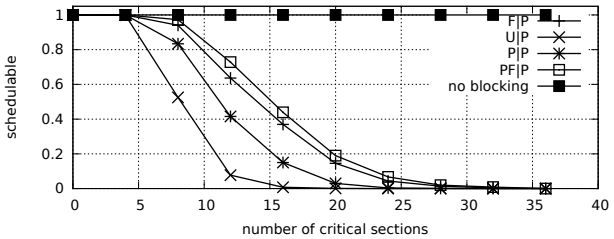

Fig. 2452. Schedulability under preemptable spin locks for $m = 8$, $U = 0.3n$, 16 resources, $rsf = 0.75$, and short critical sections. The schedulability of the considered non-preemptable lock types in this configuration is shown in Fig. 2450.

Configurations with $U = 0.1n$

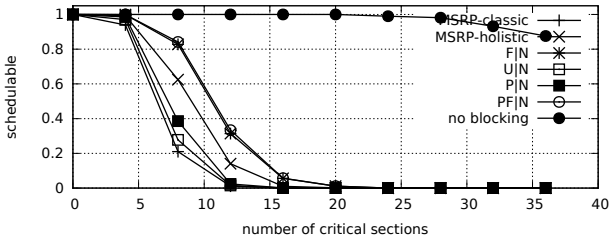

Fig. 2453. Schedulability under non-preemptable spin locks for $m = 16$, $U = 0.1n$, 8 resources, $rsf = 0.1$, and medium critical sections. The schedulability of the considered preemptable lock types in this configuration is shown in Fig. 2455.

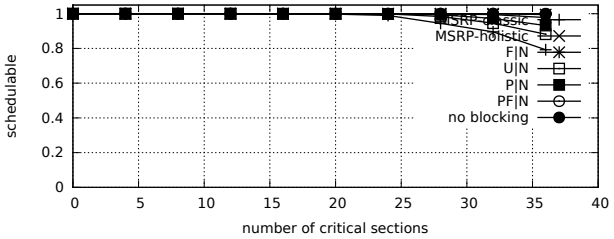

Fig. 2454. Schedulability under non-preemptable spin locks for $m = 16$, $U = 0.1n$, 8 resources, $rsf = 0.1$, and short critical sections. The schedulability of the considered preemptable lock types in this configuration is shown in Fig. 2456.

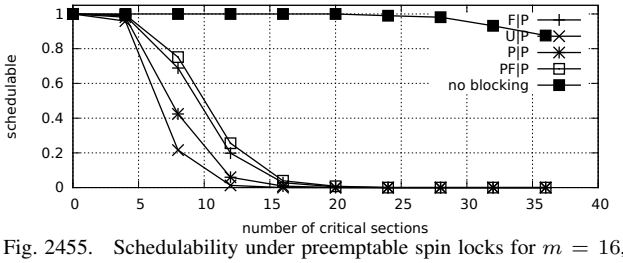

Fig. 2455. Schedulability under preemptable spin locks for $m = 16$, $U = 0.1n$, 8 resources, $rsf = 0.1$, and medium critical sections. The schedulability of the considered non-preemptable lock types in this configuration is shown in Fig. 2453.

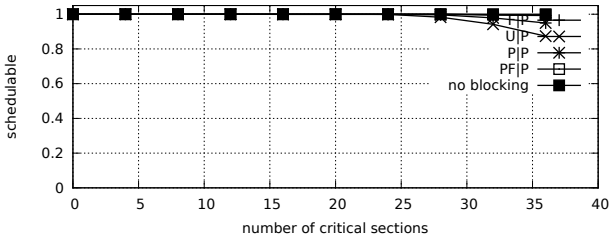

Fig. 2456. Schedulability under preemptable spin locks for $m = 16$, $U = 0.1n$, 8 resources, $rsf = 0.1$, and short critical sections. The schedulability of the considered non-preemptable lock types in this configuration is shown in Fig. 2454.

Configurations with $U = 0.2n$

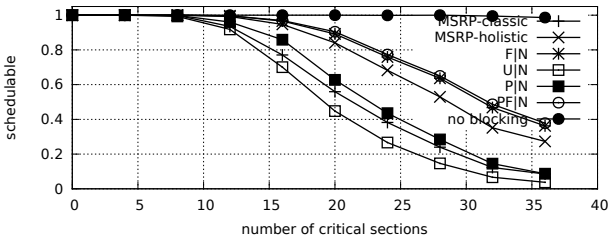

Fig. 2457. Schedulability under non-preemptable spin locks for $m = 16$, $U = 0.2n$, 8 resources, $rsf = 0.1$, and medium critical sections. The schedulability of the considered preemptable lock types in this configuration is shown in Fig. 2459.

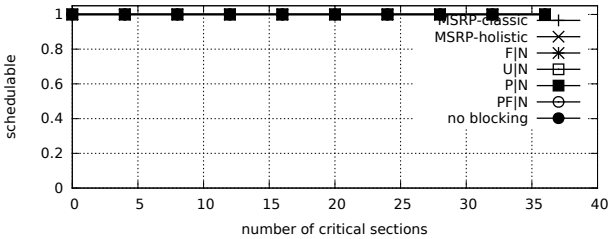

Fig. 2458. Schedulability under non-preemptable spin locks for $m = 16$, $U = 0.2n$, 8 resources, $rsf = 0.1$, and short critical sections. The schedulability of the considered preemptable lock types in this configuration is shown in Fig. 2460.

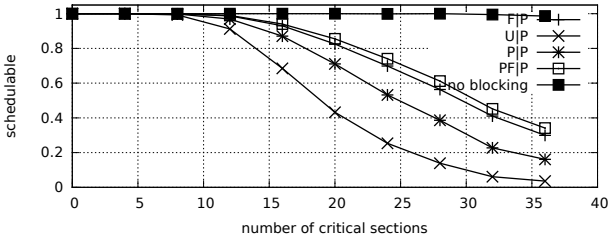

Fig. 2459. Schedulability under preemptable spin locks for $m = 16$, $U = 0.2n$, 8 resources, $rsf = 0.1$, and medium critical sections. The schedulability of the considered non-preemptable lock types in this configuration is shown in Fig. 2457.

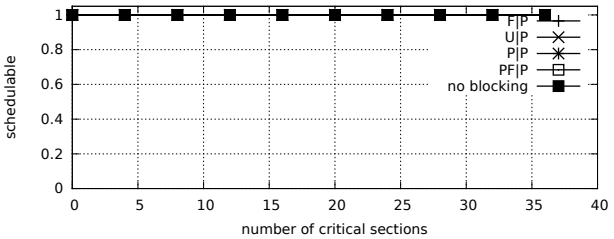

Fig. 2460. Schedulability under preemptable spin locks for $m = 16$, $U = 0.2n$, 8 resources, $rsf = 0.1$, and short critical sections. The schedulability of the considered non-preemptable lock types in this configuration is shown in Fig. 2458.

Configurations with $U = 0.3n$

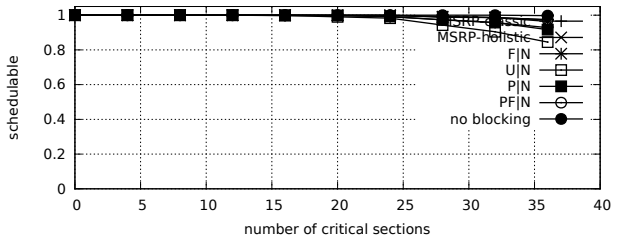

Fig. 2461. Schedulability under non-preemptable spin locks for $m = 16$, $U = 0.3n$, 8 resources, $rsf = 0.1$, and medium critical sections. The schedulability of the considered preemptable lock types in this configuration is shown in Fig. 2463.

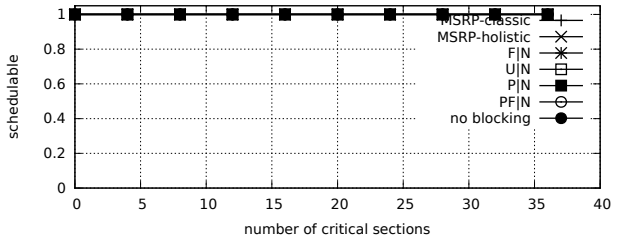

Fig. 2462. Schedulability under non-preemptable spin locks for $m = 16$, $U = 0.3n$, 8 resources, $rsf = 0.1$, and short critical sections. The schedulability of the considered preemptable lock types in this configuration is shown in Fig. 2464.

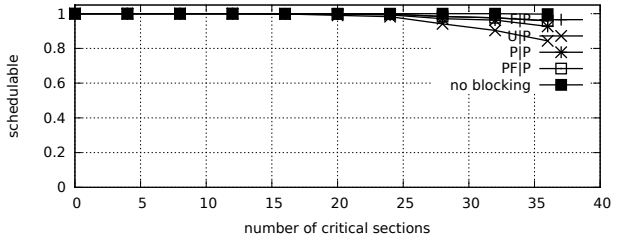

Fig. 2463. Schedulability under preemptable spin locks for $m = 16$, $U = 0.3n$, 8 resources, $rsf = 0.1$, and medium critical sections. The schedulability of the considered non-preemptable lock types in this configuration is shown in Fig. 2461.

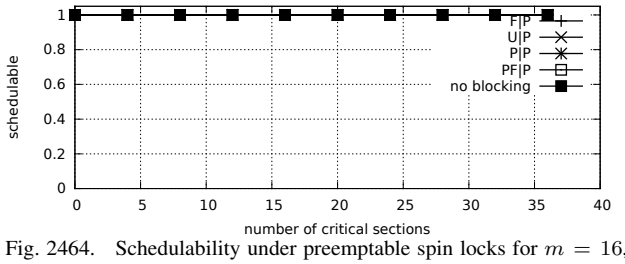

Fig. 2464. Schedulability under preemptable spin locks for $m = 16$, $U = 0.3n$, 8 resources, $rsf = 0.1$, and short critical sections. The schedulability of the considered non-preemptable lock types in this configuration is shown in Fig. 2462.

Configurations with $U = 0.1n$

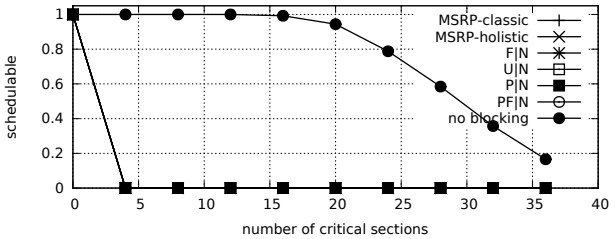

Fig. 2465. Schedulability under non-preemptable spin locks for $m = 16$, $U = 0.1n$, 8 resources, $rsf = 0.25$, and medium critical sections. The schedulability of the considered preemptable lock types in this configuration is shown in Fig. 2467.

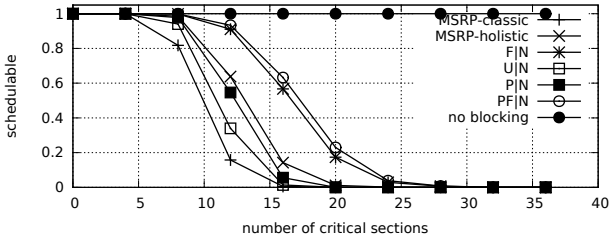

Fig. 2466. Schedulability under non-preemptable spin locks for $m = 16$, $U = 0.1n$, 8 resources, $rsf = 0.25$, and short critical sections. The schedulability of the considered preemptable lock types in this configuration is shown in Fig. 2468.

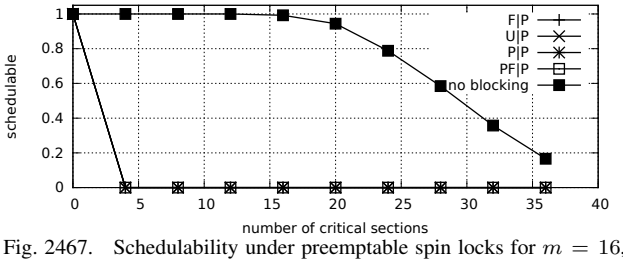

Fig. 2467. Schedulability under preemptable spin locks for $m = 16$, $U = 0.1n$, 8 resources, $rsf = 0.25$, and medium critical sections. The schedulability of the considered non-preemptable lock types in this configuration is shown in Fig. 2465.

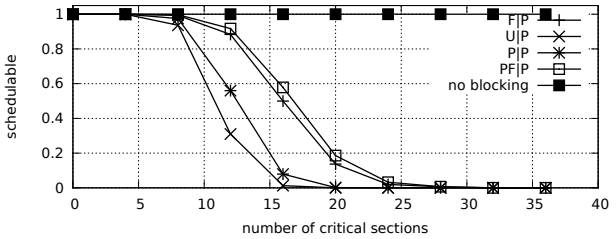

Fig. 2468. Schedulability under preemptable spin locks for $m = 16$, $U = 0.1n$, 8 resources, $rsf = 0.25$, and short critical sections. The schedulability of the considered non-preemptable lock types in this configuration is shown in Fig. 2466.

Configurations with $U = 0.2n$

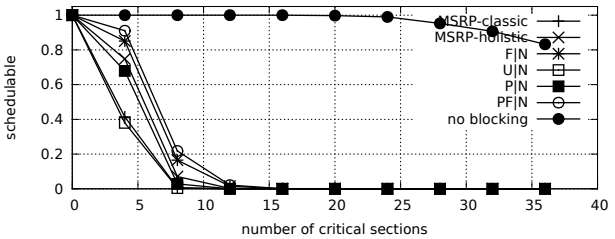

Fig. 2469. Schedulability under non-preemptable spin locks for $m = 16$, $U = 0.2n$, 8 resources, $rsf = 0.25$, and medium critical sections. The schedulability of the considered preemptable lock types in this configuration is shown in Fig. 2471.

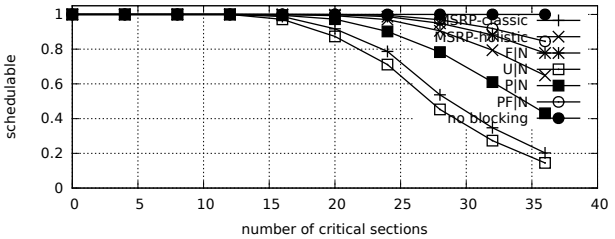

Fig. 2470. Schedulability under non-preemptable spin locks for $m = 16$, $U = 0.2n$, 8 resources, $rsf = 0.25$, and short critical sections. The schedulability of the considered preemptable lock types in this configuration is shown in Fig. 2472.

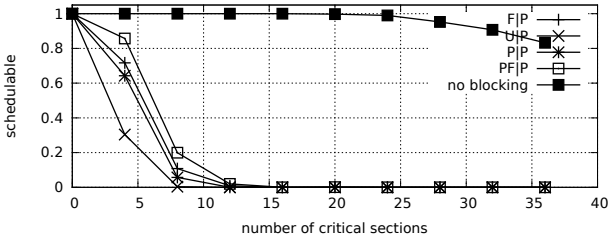

Fig. 2471. Schedulability under preemptable spin locks for $m = 16$, $U = 0.2n$, 8 resources, $rsf = 0.25$, and medium critical sections. The schedulability of the considered non-preemptable lock types in this configuration is shown in Fig. 2469.

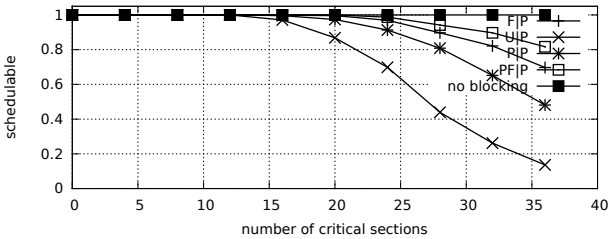

Fig. 2472. Schedulability under preemptable spin locks for $m = 16$, $U = 0.2n$, 8 resources, $rsf = 0.25$, and short critical sections. The schedulability of the considered non-preemptable lock types in this configuration is shown in Fig. 2470.

Configurations with $U = 0.3n$

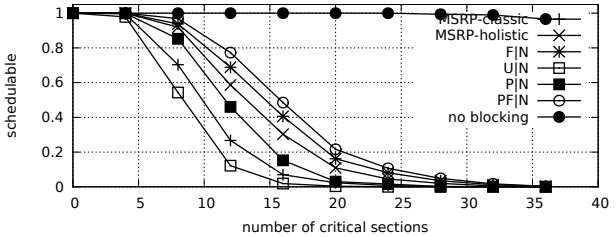

Fig. 2473. Schedulability under non-preemptable spin locks for $m = 16$, $U = 0.3n$, 8 resources, $rsf = 0.25$, and medium critical sections. The schedulability of the considered preemptable lock types in this configuration is shown in Fig. 2475.

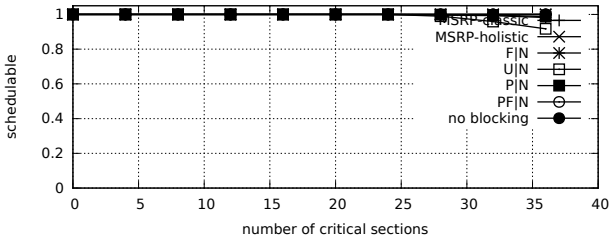

Fig. 2474. Schedulability under non-preemptable spin locks for $m = 16$, $U = 0.3n$, 8 resources, $rsf = 0.25$, and short critical sections. The schedulability of the considered preemptable lock types in this configuration is shown in Fig. 2476.

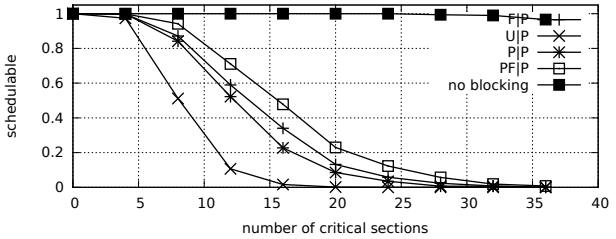

Fig. 2475. Schedulability under preemptable spin locks for $m = 16$, $U = 0.3n$, 8 resources, $rsf = 0.25$, and medium critical sections. The schedulability of the considered non-preemptable lock types in this configuration is shown in Fig. 2473.

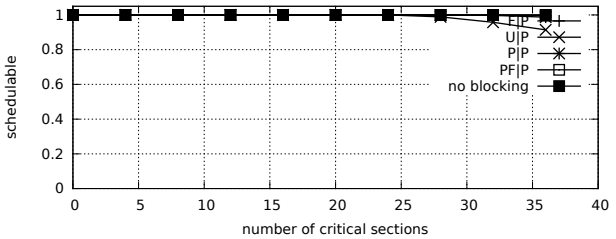

Fig. 2476. Schedulability under preemptable spin locks for $m = 16$, $U = 0.3n$, 8 resources, $rsf = 0.25$, and short critical sections. The schedulability of the considered non-preemptable lock types in this configuration is shown in Fig. 2474.

Configurations with $U = 0.1n$

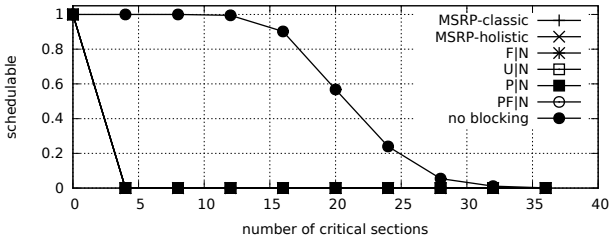

Fig. 2477. Schedulability under non-preemptable spin locks for $m = 16$, $U = 0.1n$, 8 resources, $rsf = 0.4$, and medium critical sections. The schedulability of the considered preemptable lock types in this configuration is shown in Fig. 2479.

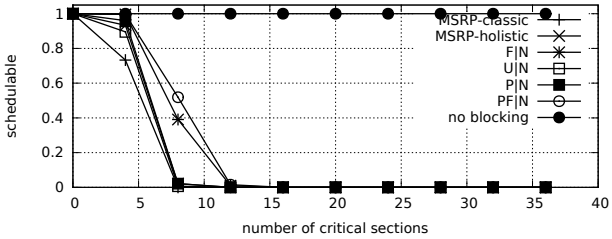

Fig. 2478. Schedulability under non-preemptable spin locks for $m = 16$, $U = 0.1n$, 8 resources, $rsf = 0.4$, and short critical sections. The schedulability of the considered preemptable lock types in this configuration is shown in Fig. 2480.

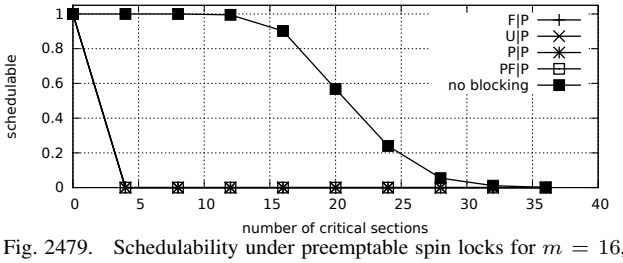

Fig. 2479. Schedulability under preemptable spin locks for $m = 16$, $U = 0.1n$, 8 resources, $rsf = 0.4$, and medium critical sections. The schedulability of the considered non-preemptable lock types in this configuration is shown in Fig. 2477.

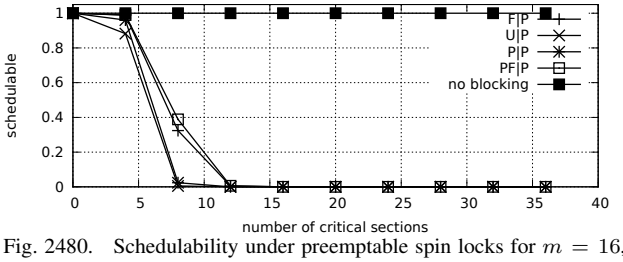

Fig. 2480. Schedulability under preemptable spin locks for $m = 16$, $U = 0.1n$, 8 resources, $rsf = 0.4$, and short critical sections. The schedulability of the considered non-preemptable lock types in this configuration is shown in Fig. 2478.

Configurations with $U = 0.2n$

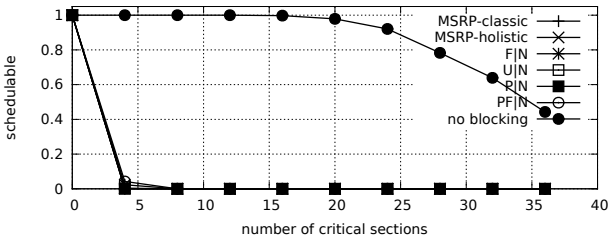

Fig. 2481. Schedulability under non-preemptable spin locks for $m = 16$, $U = 0.2n$, 8 resources, $rsf = 0.4$, and medium critical sections. The schedulability of the considered preemptable lock types in this configuration is shown in Fig. 2483.

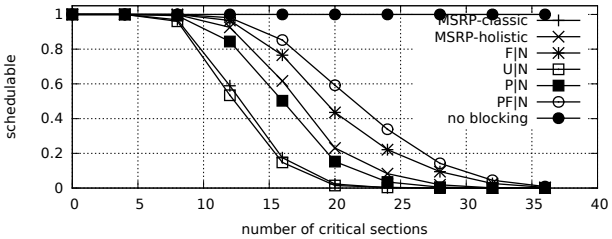

Fig. 2482. Schedulability under non-preemptable spin locks for $m = 16$, $U = 0.2n$, 8 resources, $rsf = 0.4$, and short critical sections. The schedulability of the considered preemptable lock types in this configuration is shown in Fig. 2484.

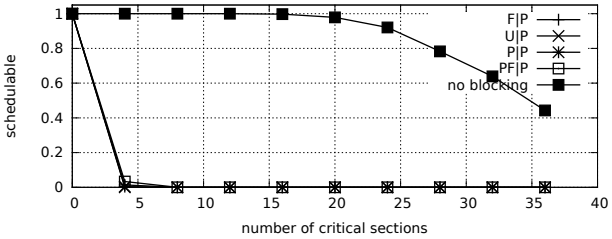

Fig. 2483. Schedulability under preemptable spin locks for $m = 16$, $U = 0.2n$, 8 resources, $rsf = 0.4$, and medium critical sections. The schedulability of the considered non-preemptable lock types in this configuration is shown in Fig. 2481.

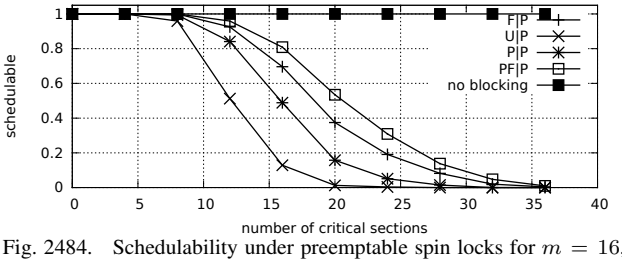

Fig. 2484. Schedulability under preemptable spin locks for $m = 16$, $U = 0.2n$, 8 resources, $rsf = 0.4$, and short critical sections. The schedulability of the considered non-preemptable lock types in this configuration is shown in Fig. 2482.

Configurations with $U = 0.3n$

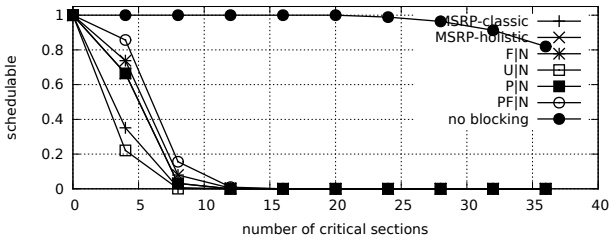

Fig. 2485. Schedulability under non-preemptable spin locks for $m = 16$, $U = 0.3n$, 8 resources, $rsf = 0.4$, and medium critical sections. The schedulability of the considered preemptable lock types in this configuration is shown in Fig. 2487.

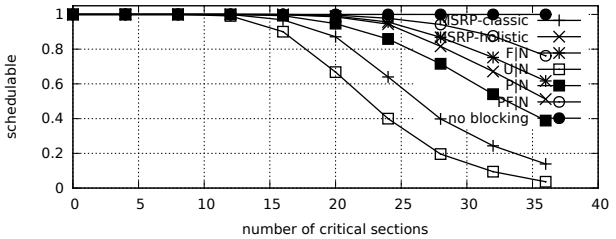

Fig. 2486. Schedulability under non-preemptable spin locks for $m = 16$, $U = 0.3n$, 8 resources, $rsf = 0.4$, and short critical sections. The schedulability of the considered preemptable lock types in this configuration is shown in Fig. 2488.

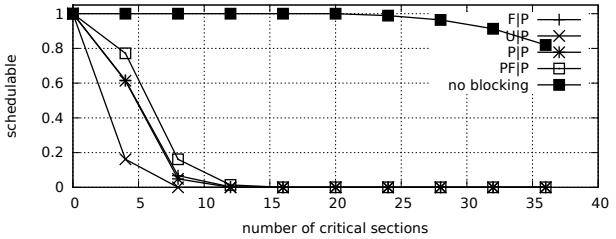

Fig. 2487. Schedulability under preemptable spin locks for $m = 16$, $U = 0.3n$, 8 resources, $rsf = 0.4$, and medium critical sections. The schedulability of the considered non-preemptable lock types in this configuration is shown in Fig. 2485.

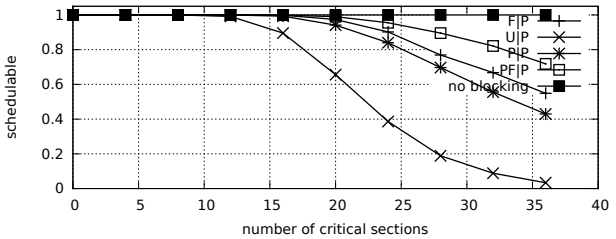

Fig. 2488. Schedulability under preemptable spin locks for $m = 16$, $U = 0.3n$, 8 resources, $rsf = 0.4$, and short critical sections. The schedulability of the considered non-preemptable lock types in this configuration is shown in Fig. 2486.

Configurations with $U = 0.1n$

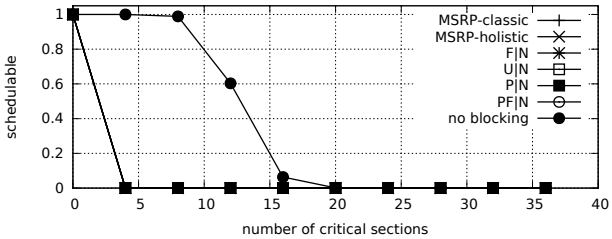

Fig. 2489. Schedulability under non-preemptable spin locks for $m = 16$, $U = 0.1n$, 8 resources, $rsf = 0.75$, and medium critical sections. The schedulability of the considered preemptable lock types in this configuration is shown in Fig. 2491.

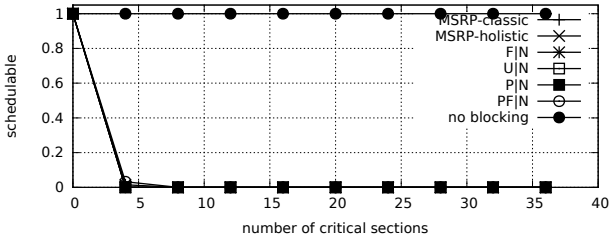

Fig. 2490. Schedulability under non-preemptable spin locks for $m = 16$, $U = 0.1n$, 8 resources, $rsf = 0.75$, and short critical sections. The schedulability of the considered preemptable lock types in this configuration is shown in Fig. 2492.

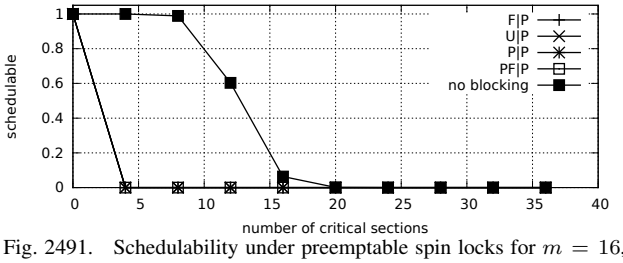

Fig. 2491. Schedulability under preemptable spin locks for $m = 16$, $U = 0.1n$, 8 resources, $rsf = 0.75$, and medium critical sections. The schedulability of the considered non-preemptable lock types in this configuration is shown in Fig. 2489.

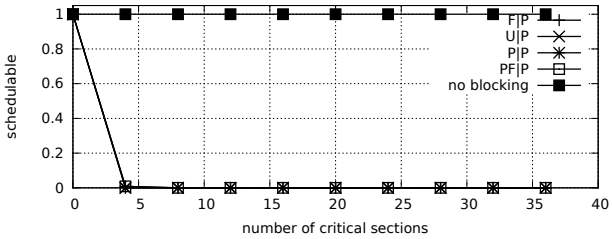

Fig. 2492. Schedulability under preemptable spin locks for $m = 16$, $U = 0.1n$, 8 resources, $rsf = 0.75$, and short critical sections. The schedulability of the considered non-preemptable lock types in this configuration is shown in Fig. 2490.

Configurations with $U = 0.2n$

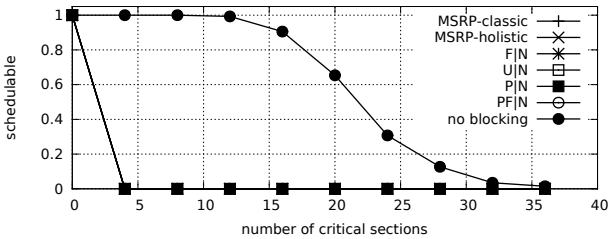

Fig. 2493. Schedulability under non-preemptable spin locks for $m = 16$, $U = 0.2n$, 8 resources, $rsf = 0.75$, and medium critical sections. The schedulability of the considered preemptable lock types in this configuration is shown in Fig. 2495.

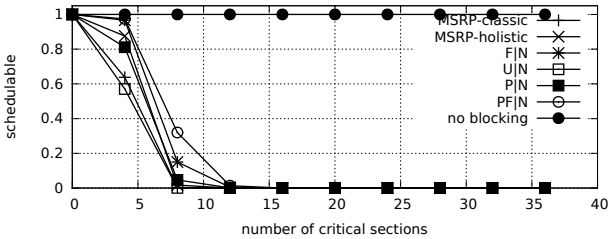

Fig. 2494. Schedulability under non-preemptable spin locks for $m = 16$, $U = 0.2n$, 8 resources, $rsf = 0.75$, and short critical sections. The schedulability of the considered preemptable lock types in this configuration is shown in Fig. 2496.

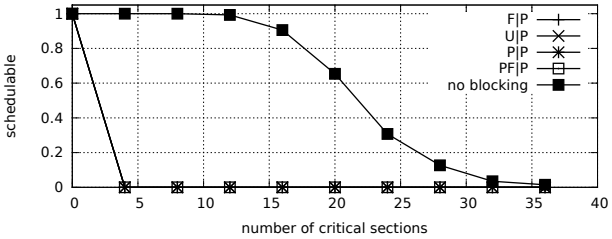

Fig. 2495. Schedulability under preemptable spin locks for $m = 16$, $U = 0.2n$, 8 resources, $rsf = 0.75$, and medium critical sections. The schedulability of the considered non-preemptable lock types in this configuration is shown in Fig. 2493.

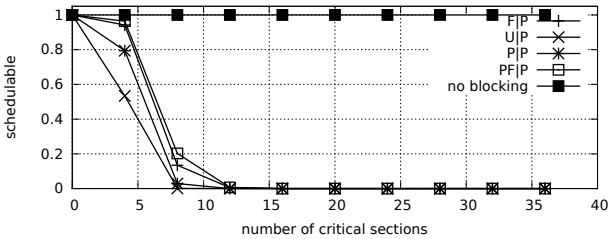

Fig. 2496. Schedulability under preemptable spin locks for $m = 16$, $U = 0.2n$, 8 resources, $rsf = 0.75$, and short critical sections. The schedulability of the considered non-preemptable lock types in this configuration is shown in Fig. 2494.

Configurations with $U = 0.3n$

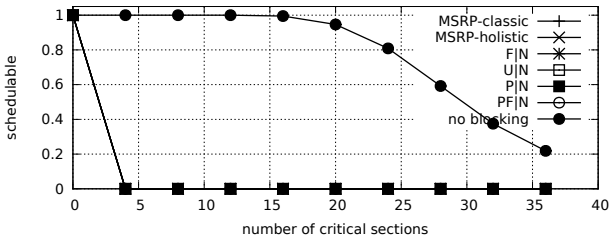

Fig. 2497. Schedulability under non-preemptable spin locks for $m = 16$, $U = 0.3n$, 8 resources, $rsf = 0.75$, and medium critical sections. The schedulability of the considered preemptable lock types in this configuration is shown in Fig. 2499.

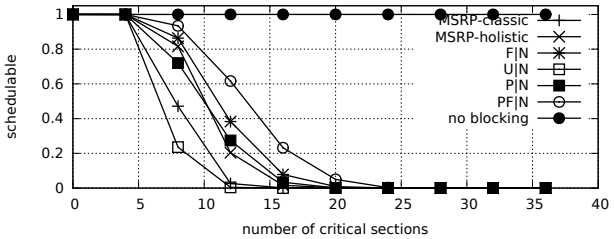

Fig. 2498. Schedulability under non-preemptable spin locks for $m = 16$, $U = 0.3n$, 8 resources, $rsf = 0.75$, and short critical sections. The schedulability of the considered preemptable lock types in this configuration is shown in Fig. 2500.

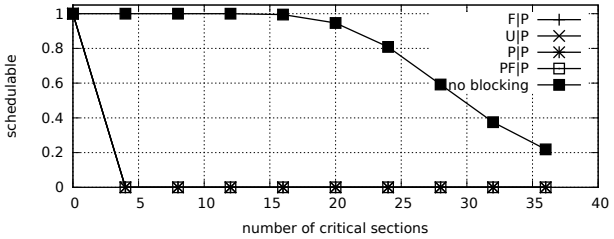

Fig. 2499. Schedulability under preemptable spin locks for $m = 16$, $U = 0.3n$, 8 resources, $rsf = 0.75$, and medium critical sections. The schedulability of the considered non-preemptable lock types in this configuration is shown in Fig. 2497.

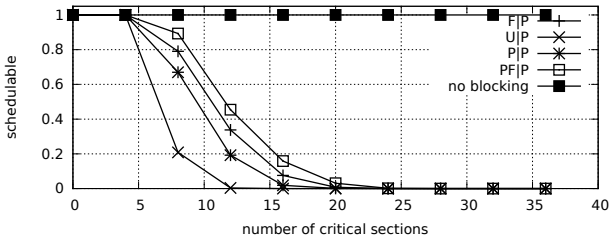

Fig. 2500. Schedulability under preemptable spin locks for $m = 16$, $U = 0.3n$, 8 resources, $rsf = 0.75$, and short critical sections. The schedulability of the considered non-preemptable lock types in this configuration is shown in Fig. 2498.

Configurations with $U = 0.1n$

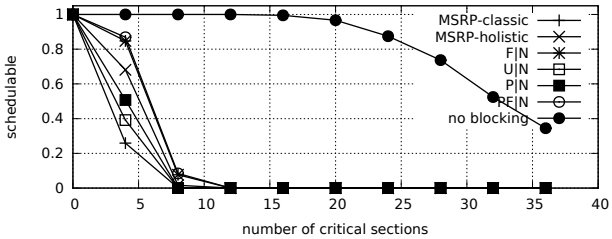

Fig. 2501. Schedulability under non-preemptable spin locks for $m = 16$, $U = 0.1n$, 16 resources, $rsf = 0.1$, and medium critical sections. The schedulability of the considered preemptable lock types in this configuration is shown in Fig. 2503.

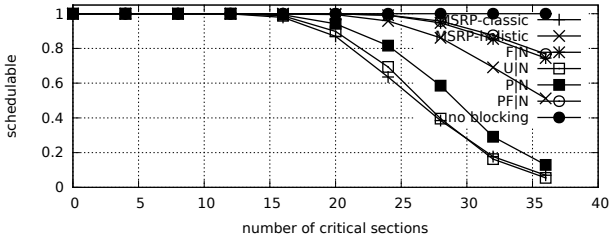

Fig. 2502. Schedulability under non-preemptable spin locks for $m = 16$, $U = 0.1n$, 16 resources, $rsf = 0.1$, and short critical sections. The schedulability of the considered preemptable lock types in this configuration is shown in Fig. 2504.

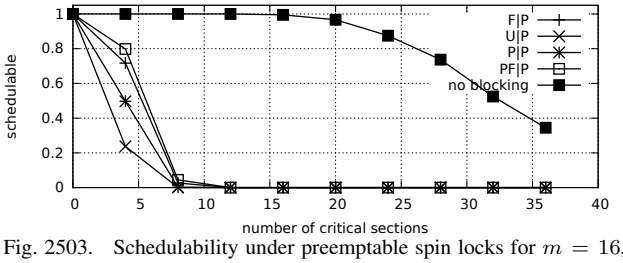

Fig. 2503. Schedulability under preemptable spin locks for $m = 16$, $U = 0.1n$, 16 resources, $rsf = 0.1$, and medium critical sections. The schedulability of the considered non-preemptable lock types in this configuration is shown in Fig. 2501.

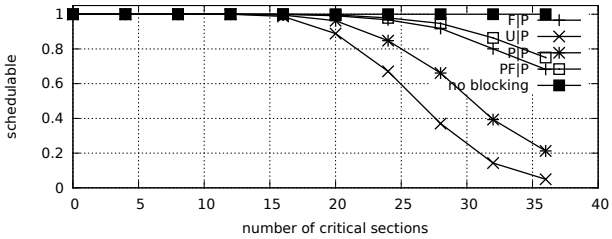

Fig. 2504. Schedulability under preemptable spin locks for $m = 16$, $U = 0.1n$, 16 resources, $rsf = 0.1$, and short critical sections. The schedulability of the considered non-preemptable lock types in this configuration is shown in Fig. 2502.

Configurations with $U = 0.2n$

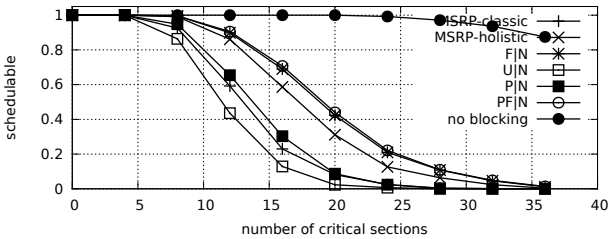

Fig. 2505. Schedulability under non-preemptable spin locks for $m = 16$, $U = 0.2n$, 16 resources, $rsf = 0.1$, and medium critical sections. The schedulability of the considered preemptable lock types in this configuration is shown in Fig. 2507.

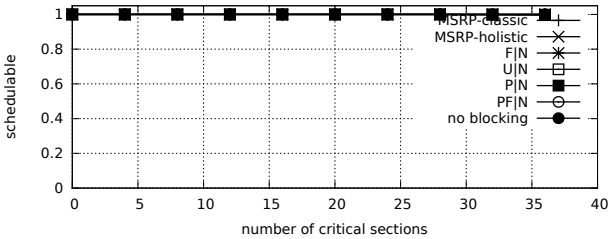

Fig. 2506. Schedulability under non-preemptable spin locks for $m = 16$, $U = 0.2n$, 16 resources, $rsf = 0.1$, and short critical sections. The schedulability of the considered preemptable lock types in this configuration is shown in Fig. 2508.

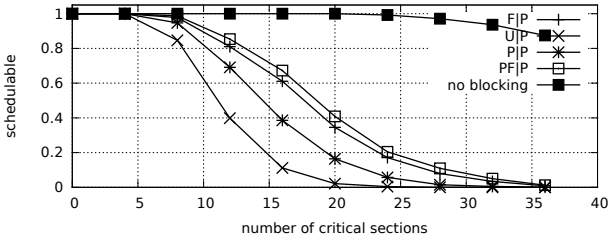

Fig. 2507. Schedulability under preemptable spin locks for $m = 16$, $U = 0.2n$, 16 resources, $rsf = 0.1$, and medium critical sections. The schedulability of the considered non-preemptable lock types in this configuration is shown in Fig. 2505.

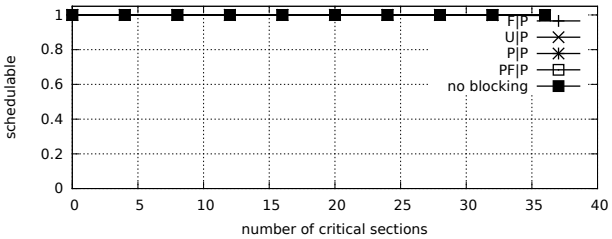

Fig. 2508. Schedulability under preemptable spin locks for $m = 16$, $U = 0.2n$, 16 resources, $rsf = 0.1$, and short critical sections. The schedulability of the considered non-preemptable lock types in this configuration is shown in Fig. 2506.

Configurations with $U = 0.3n$

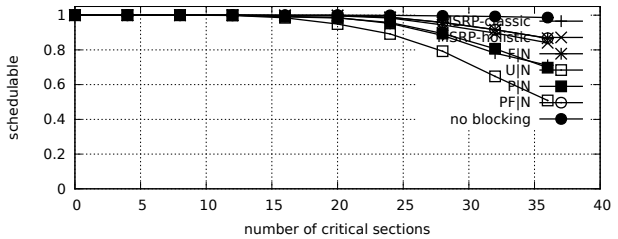

Fig. 2509. Schedulability under non-preemptable spin locks for $m = 16$, $U = 0.3n$, 16 resources, $rsf = 0.1$, and medium critical sections. The schedulability of the considered preemptable lock types in this configuration is shown in Fig. 2511.

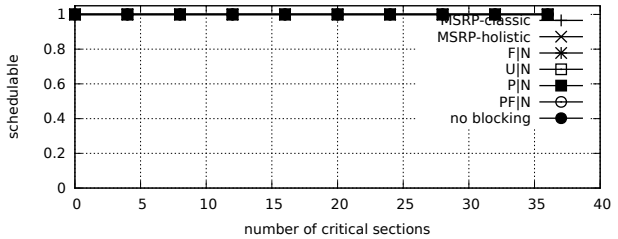

Fig. 2510. Schedulability under non-preemptable spin locks for $m = 16$, $U = 0.3n$, 16 resources, $rsf = 0.1$, and short critical sections. The schedulability of the considered preemptable lock types in this configuration is shown in Fig. 2512.

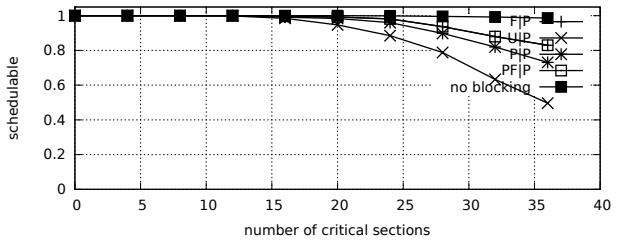

Fig. 2511. Schedulability under preemptable spin locks for $m = 16$, $U = 0.3n$, 16 resources, $rsf = 0.1$, and medium critical sections. The schedulability of the considered non-preemptable lock types in this configuration is shown in Fig. 2509.

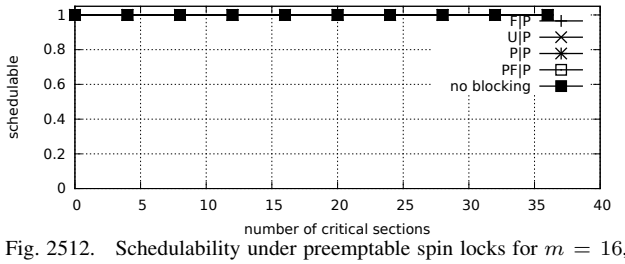

Fig. 2512. Schedulability under preemptable spin locks for $m = 16$, $U = 0.3n$, 16 resources, $rsf = 0.1$, and short critical sections. The schedulability of the considered non-preemptable lock types in this configuration is shown in Fig. 2510.

Configurations with $U = 0.1n$

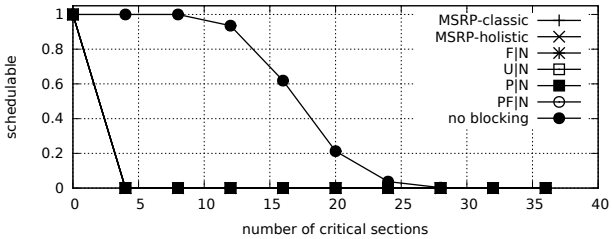

Fig. 2513. Schedulability under non-preemptable spin locks for $m = 16$, $U = 0.1n$, 16 resources, $rsf = 0.25$, and medium critical sections. The schedulability of the considered preemptable lock types in this configuration is shown in Fig. 2515.

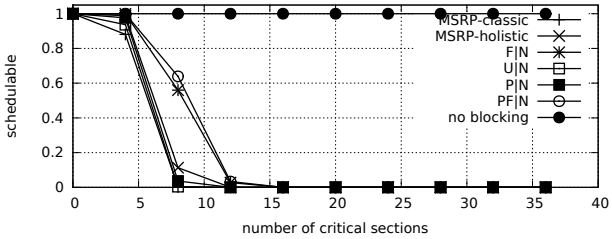

Fig. 2514. Schedulability under non-preemptable spin locks for $m = 16$, $U = 0.1n$, 16 resources, $rsf = 0.25$, and short critical sections. The schedulability of the considered preemptable lock types in this configuration is shown in Fig. 2516.

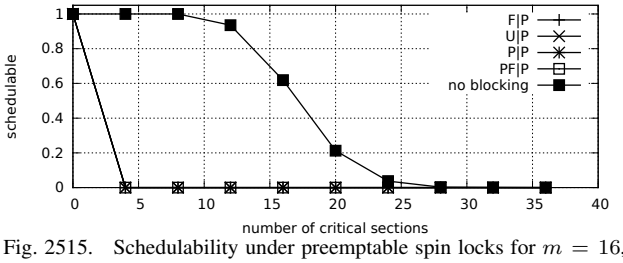

Fig. 2515. Schedulability under preemptable spin locks for $m = 16$, $U = 0.1n$, 16 resources, $rsf = 0.25$, and medium critical sections. The schedulability of the considered non-preemptable lock types in this configuration is shown in Fig. 2513.

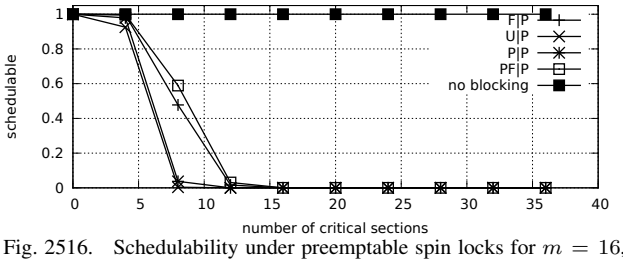

Fig. 2516. Schedulability under preemptable spin locks for $m = 16$, $U = 0.1n$, 16 resources, $rsf = 0.25$, and short critical sections. The schedulability of the considered non-preemptable lock types in this configuration is shown in Fig. 2514.

Configurations with $U = 0.2n$

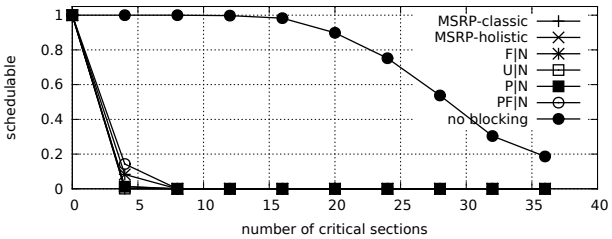

Fig. 2517. Schedulability under non-preemptable spin locks for $m = 16$, $U = 0.2n$, 16 resources, $rsf = 0.25$, and medium critical sections. The schedulability of the considered preemptable lock types in this configuration is shown in Fig. 2519.

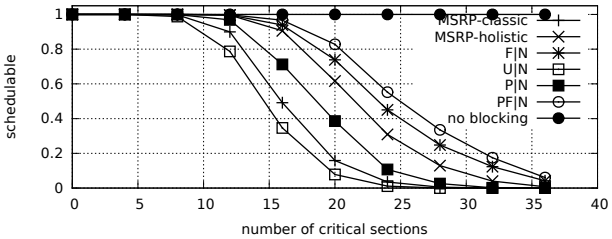

Fig. 2518. Schedulability under non-preemptable spin locks for $m = 16$, $U = 0.2n$, 16 resources, $rsf = 0.25$, and short critical sections. The schedulability of the considered preemptable lock types in this configuration is shown in Fig. 2520.

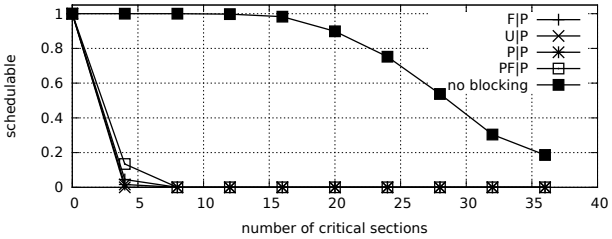

Fig. 2519. Schedulability under preemptable spin locks for $m = 16$, $U = 0.2n$, 16 resources, $rsf = 0.25$, and medium critical sections. The schedulability of the considered non-preemptable lock types in this configuration is shown in Fig. 2517.

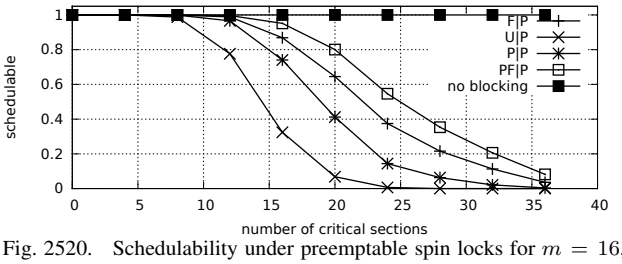

Fig. 2520. Schedulability under preemptable spin locks for $m = 16$, $U = 0.2n$, 16 resources, $rsf = 0.25$, and short critical sections. The schedulability of the considered non-preemptable lock types in this configuration is shown in Fig. 2518.

Configurations with $U = 0.3n$

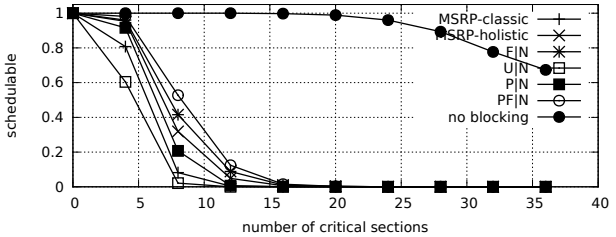

Fig. 2521. Schedulability under non-preemptable spin locks for $m = 16$, $U = 0.3n$, 16 resources, $rsf = 0.25$, and medium critical sections. The schedulability of the considered preemptable lock types in this configuration is shown in Fig. 2523.

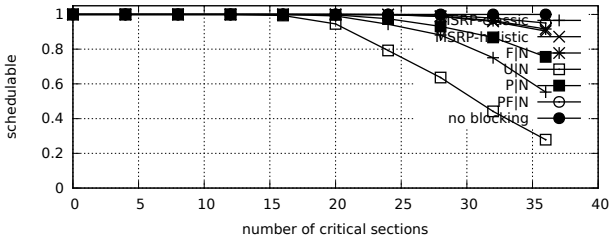

Fig. 2522. Schedulability under non-preemptable spin locks for $m = 16$, $U = 0.3n$, 16 resources, $rsf = 0.25$, and short critical sections. The schedulability of the considered preemptable lock types in this configuration is shown in Fig. 2524.

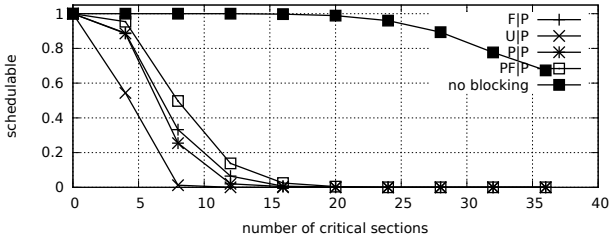

Fig. 2523. Schedulability under preemptable spin locks for $m = 16$, $U = 0.3n$, 16 resources, $rsf = 0.25$, and medium critical sections. The schedulability of the considered non-preemptable lock types in this configuration is shown in Fig. 2521.

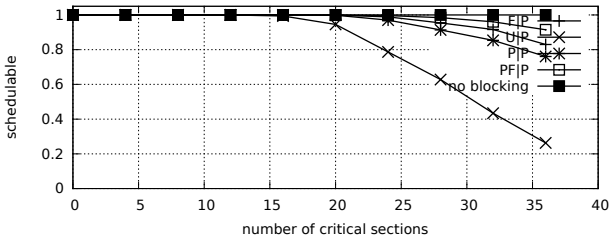

Fig. 2524. Schedulability under preemptable spin locks for $m = 16$, $U = 0.3n$, 16 resources, $rsf = 0.25$, and short critical sections. The schedulability of the considered non-preemptable lock types in this configuration is shown in Fig. 2522.

Configurations with $U = 0.1n$

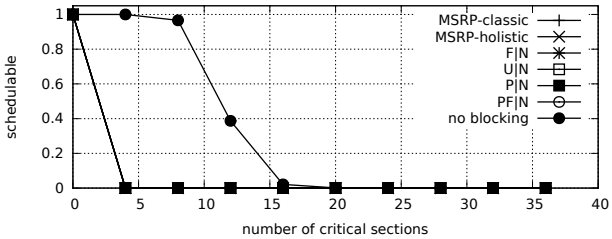

Fig. 2525. Schedulability under non-preemptable spin locks for $m = 16$, $U = 0.1n$, 16 resources, $rsf = 0.4$, and medium critical sections. The schedulability of the considered preemptable lock types in this configuration is shown in Fig. 2527.

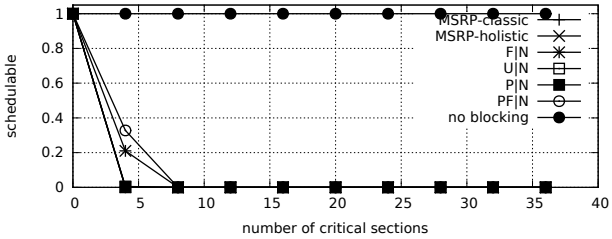

Fig. 2526. Schedulability under non-preemptable spin locks for $m = 16$, $U = 0.1n$, 16 resources, $rsf = 0.4$, and short critical sections. The schedulability of the considered preemptable lock types in this configuration is shown in Fig. 2528.

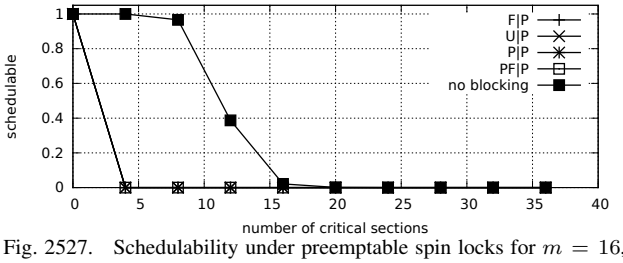

Fig. 2527. Schedulability under preemptable spin locks for $m = 16$, $U = 0.1n$, 16 resources, $rsf = 0.4$, and medium critical sections. The schedulability of the considered non-preemptable lock types in this configuration is shown in Fig. 2525.

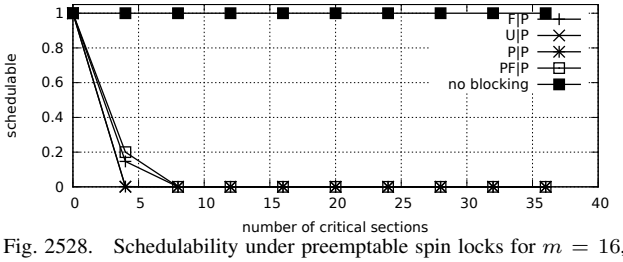

Fig. 2528. Schedulability under preemptable spin locks for $m = 16$, $U = 0.1n$, 16 resources, $rsf = 0.4$, and short critical sections. The schedulability of the considered non-preemptable lock types in this configuration is shown in Fig. 2526.

Configurations with $U = 0.2n$

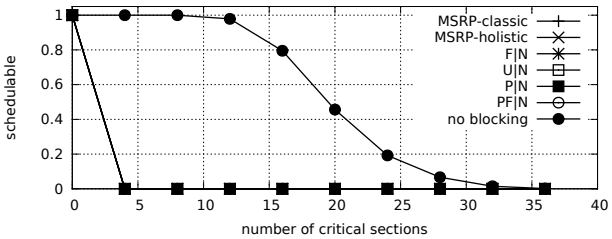

Fig. 2529. Schedulability under non-preemptable spin locks for $m = 16$, $U = 0.2n$, 16 resources, $rsf = 0.4$, and medium critical sections. The schedulability of the considered preemptable lock types in this configuration is shown in Fig. 2531.

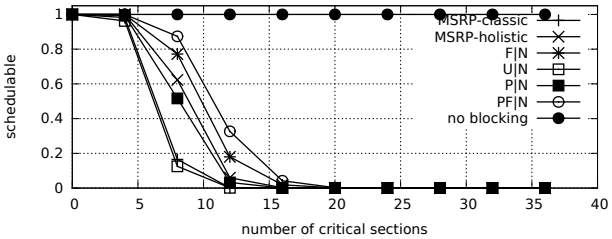

Fig. 2530. Schedulability under non-preemptable spin locks for $m = 16$, $U = 0.2n$, 16 resources, $rsf = 0.4$, and short critical sections. The schedulability of the considered preemptable lock types in this configuration is shown in Fig. 2532.

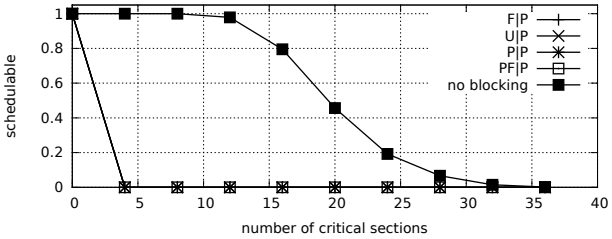

Fig. 2531. Schedulability under preemptable spin locks for $m = 16$, $U = 0.2n$, 16 resources, $rsf = 0.4$, and medium critical sections. The schedulability of the considered non-preemptable lock types in this configuration is shown in Fig. 2529.

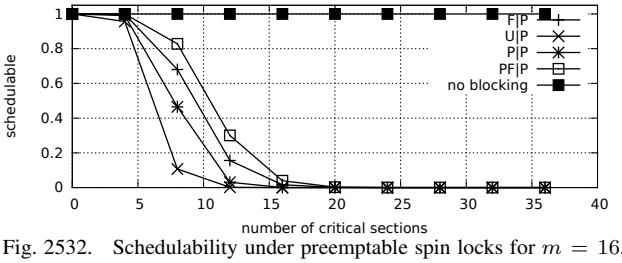

Fig. 2532. Schedulability under preemptable spin locks for $m = 16$, $U = 0.2n$, 16 resources, $rsf = 0.4$, and short critical sections. The schedulability of the considered non-preemptable lock types in this configuration is shown in Fig. 2530.

Configurations with $U = 0.3n$

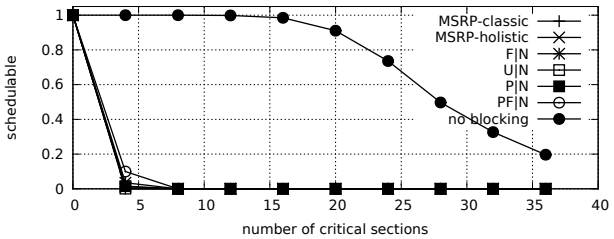

Fig. 2533. Schedulability under non-preemptable spin locks for $m = 16$, $U = 0.3n$, 16 resources, $rsf = 0.4$, and medium critical sections. The schedulability of the considered preemptable lock types in this configuration is shown in Fig. 2535.

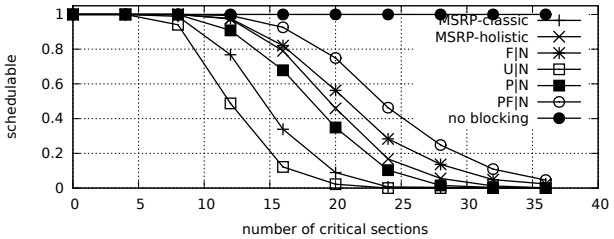

Fig. 2534. Schedulability under non-preemptable spin locks for $m = 16$, $U = 0.3n$, 16 resources, $rsf = 0.4$, and short critical sections. The schedulability of the considered preemptable lock types in this configuration is shown in Fig. 2536.

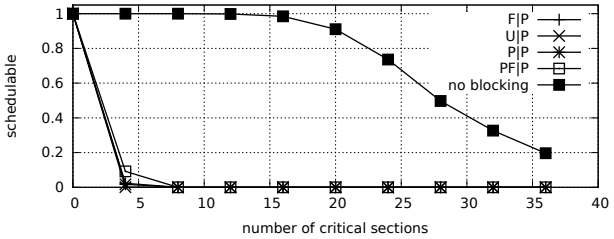

Fig. 2535. Schedulability under preemptable spin locks for $m = 16$, $U = 0.3n$, 16 resources, $rsf = 0.4$, and medium critical sections. The schedulability of the considered non-preemptable lock types in this configuration is shown in Fig. 2533.

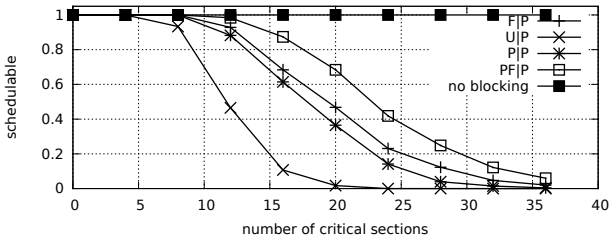

Fig. 2536. Schedulability under preemptable spin locks for $m = 16$, $U = 0.3n$, 16 resources, $rsf = 0.4$, and short critical sections. The schedulability of the considered non-preemptable lock types in this configuration is shown in Fig. 2534.

Configurations with $U = 0.1n$

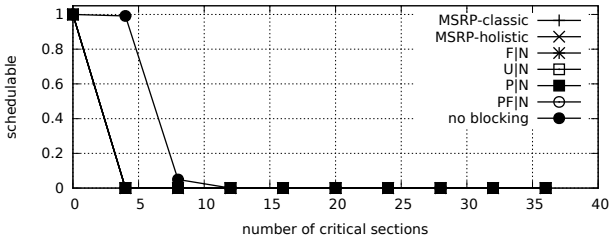

Fig. 2537. Schedulability under non-preemptable spin locks for $m = 16$, $U = 0.1n$, 16 resources, $rsf = 0.75$, and medium critical sections. The schedulability of the considered preemptable lock types in this configuration is shown in Fig. 2539.

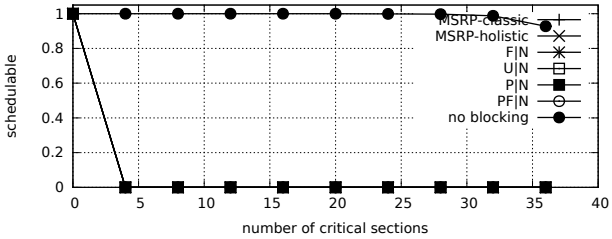

Fig. 2538. Schedulability under non-preemptable spin locks for $m = 16$, $U = 0.1n$, 16 resources, $rsf = 0.75$, and short critical sections. The schedulability of the considered preemptable lock types in this configuration is shown in Fig. 2540.

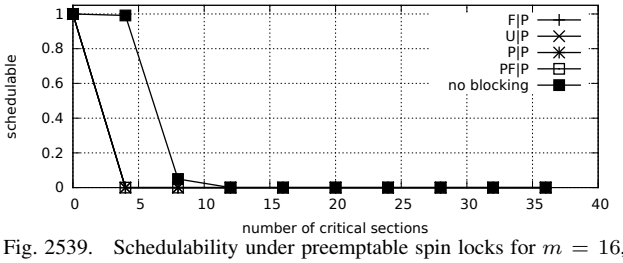

Fig. 2539. Schedulability under preemptable spin locks for $m = 16$, $U = 0.1n$, 16 resources, $rsf = 0.75$, and medium critical sections. The schedulability of the considered non-preemptable lock types in this configuration is shown in Fig. 2537.

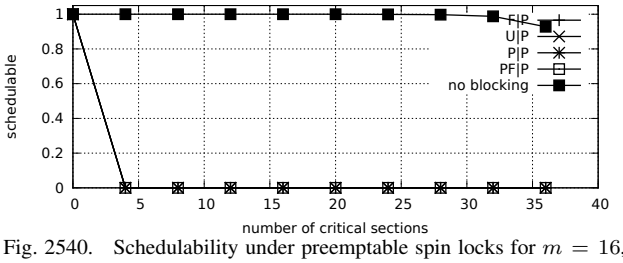

Fig. 2540. Schedulability under preemptable spin locks for $m = 16$, $U = 0.1n$, 16 resources, $rsf = 0.75$, and short critical sections. The schedulability of the considered non-preemptable lock types in this configuration is shown in Fig. 2538.

Configurations with $U = 0.2n$

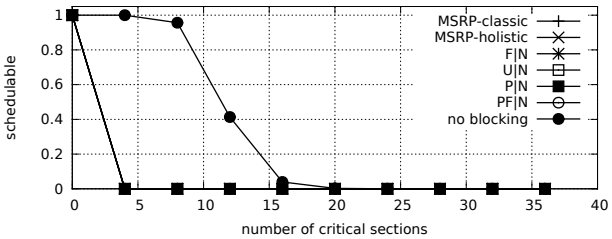

Fig. 2541. Schedulability under non-preemptable spin locks for $m = 16$, $U = 0.2n$, 16 resources, $rsf = 0.75$, and medium critical sections. The schedulability of the considered preemptable lock types in this configuration is shown in Fig. 2543.

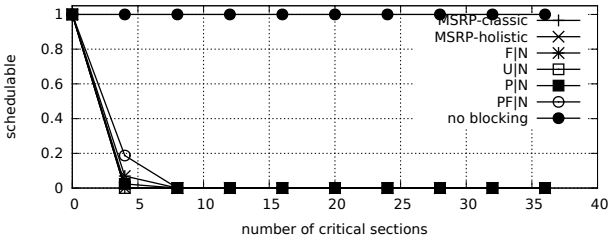

Fig. 2542. Schedulability under non-preemptable spin locks for $m = 16$, $U = 0.2n$, 16 resources, $rsf = 0.75$, and short critical sections. The schedulability of the considered preemptable lock types in this configuration is shown in Fig. 2544.

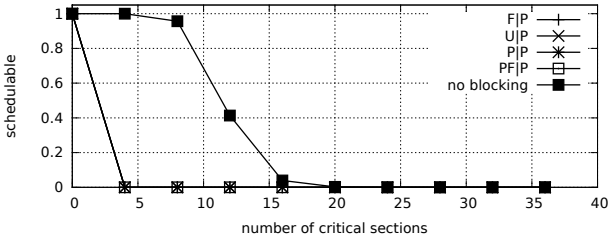

Fig. 2543. Schedulability under preemptable spin locks for $m = 16$, $U = 0.2n$, 16 resources, $rsf = 0.75$, and medium critical sections. The schedulability of the considered non-preemptable lock types in this configuration is shown in Fig. 2541.

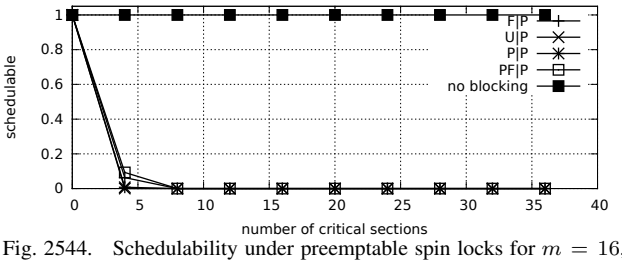

Fig. 2544. Schedulability under preemptable spin locks for $m = 16$, $U = 0.2n$, 16 resources, $rsf = 0.75$, and short critical sections. The schedulability of the considered non-preemptable lock types in this configuration is shown in Fig. 2542.

Configurations with $U = 0.3n$

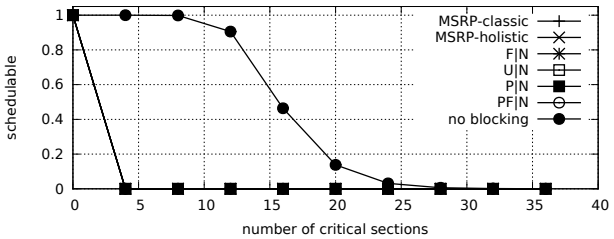

Fig. 2545. Schedulability under non-preemptable spin locks for $m = 16$, $U = 0.3n$, 16 resources, $rsf = 0.75$, and medium critical sections. The schedulability of the considered preemptable lock types in this configuration is shown in Fig. 2547.

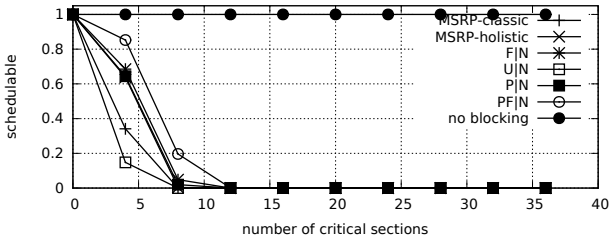

Fig. 2546. Schedulability under non-preemptable spin locks for $m = 16$, $U = 0.3n$, 16 resources, $rsf = 0.75$, and short critical sections. The schedulability of the considered preemptable lock types in this configuration is shown in Fig. 2548.

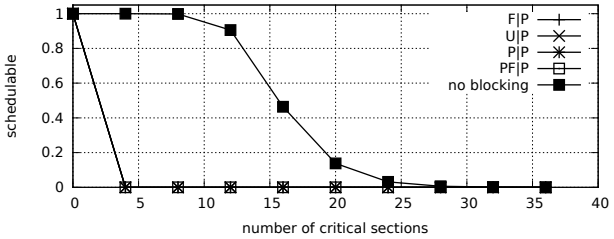

Fig. 2547. Schedulability under preemptable spin locks for $m = 16$, $U = 0.3n$, 16 resources, $rsf = 0.75$, and medium critical sections. The schedulability of the considered non-preemptable lock types in this configuration is shown in Fig. 2545.

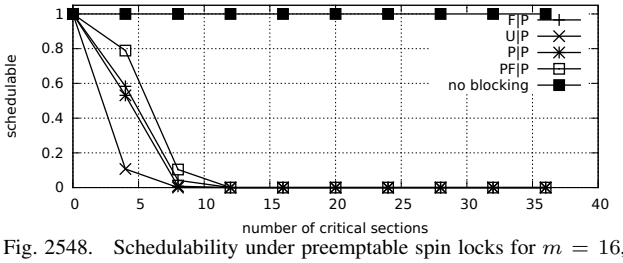

Fig. 2548. Schedulability under preemptable spin locks for $m = 16$, $U = 0.3n$, 16 resources, $rsf = 0.75$, and short critical sections. The schedulability of the considered non-preemptable lock types in this configuration is shown in Fig. 2546.

Configurations with $U = 0.1n$

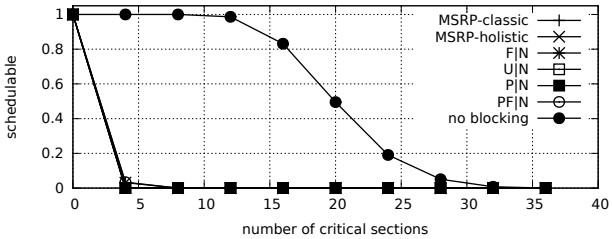

Fig. 2549. Schedulability under non-preemptable spin locks for $m = 16$, $U = 0.1n$, 32 resources, $rsf = 0.1$, and medium critical sections. The schedulability of the considered preemptable lock types in this configuration is shown in Fig. 2551.

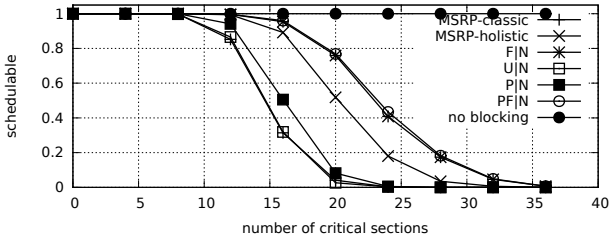

Fig. 2550. Schedulability under non-preemptable spin locks for $m = 16$, $U = 0.1n$, 32 resources, $rsf = 0.1$, and short critical sections. The schedulability of the considered preemptable lock types in this configuration is shown in Fig. 2552.

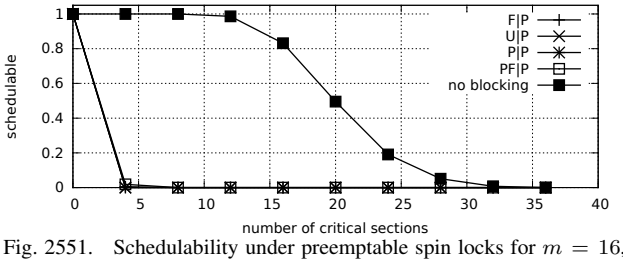

Fig. 2551. Schedulability under preemptable spin locks for $m = 16$, $U = 0.1n$, 32 resources, $rsf = 0.1$, and medium critical sections. The schedulability of the considered non-preemptable lock types in this configuration is shown in Fig. 2549.

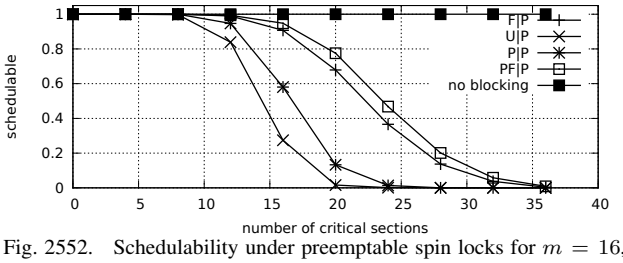

Fig. 2552. Schedulability under preemptable spin locks for $m = 16$, $U = 0.1n$, 32 resources, $rsf = 0.1$, and short critical sections. The schedulability of the considered non-preemptable lock types in this configuration is shown in Fig. 2550.

Configurations with $U = 0.2n$

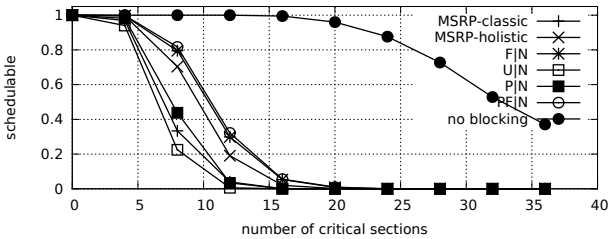

Fig. 2553. Schedulability under non-preemptable spin locks for $m = 16$, $U = 0.2n$, 32 resources, $rsf = 0.1$, and medium critical sections. The schedulability of the considered preemptable lock types in this configuration is shown in Fig. 2555.

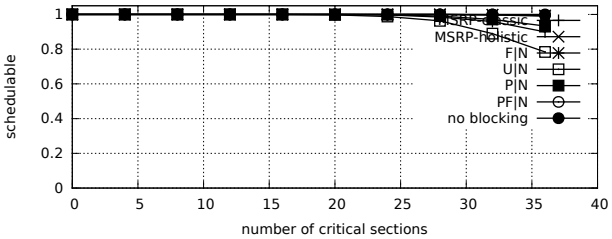

Fig. 2554. Schedulability under non-preemptable spin locks for $m = 16$, $U = 0.2n$, 32 resources, $rsf = 0.1$, and short critical sections. The schedulability of the considered preemptable lock types in this configuration is shown in Fig. 2556.

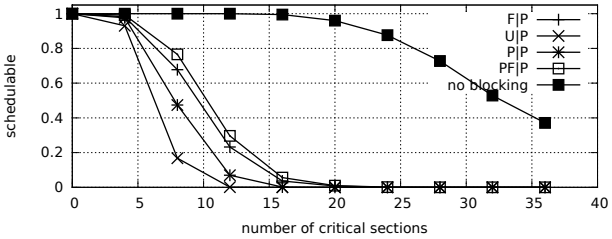

Fig. 2555. Schedulability under preemptable spin locks for $m = 16$, $U = 0.2n$, 32 resources, $rsf = 0.1$, and medium critical sections. The schedulability of the considered non-preemptable lock types in this configuration is shown in Fig. 2553.

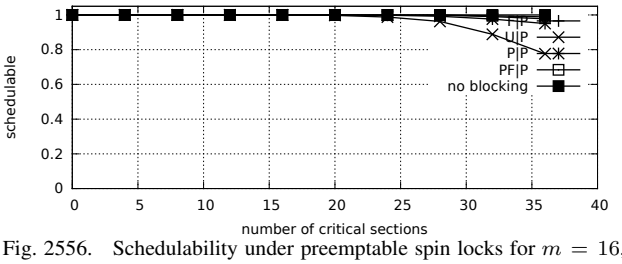

Fig. 2556. Schedulability under preemptable spin locks for $m = 16$, $U = 0.2n$, 32 resources, $rsf = 0.1$, and short critical sections. The schedulability of the considered non-preemptable lock types in this configuration is shown in Fig. 2554.

Configurations with $U = 0.3n$

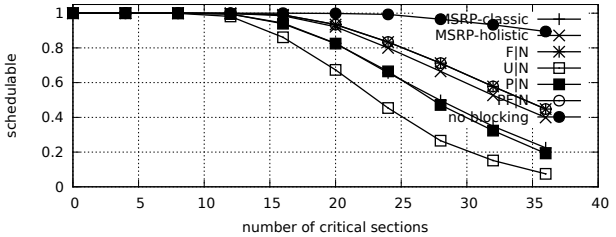

Fig. 2557. Schedulability under non-preemptable spin locks for $m = 16$, $U = 0.3n$, 32 resources, $rsf = 0.1$, and medium critical sections. The schedulability of the considered preemptable lock types in this configuration is shown in Fig. 2559.

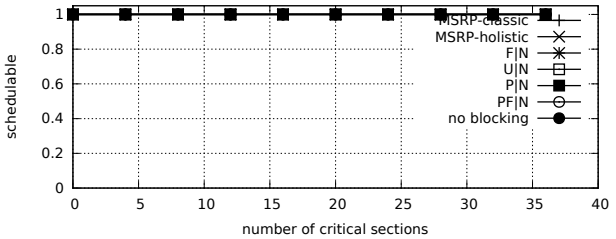

Fig. 2558. Schedulability under non-preemptable spin locks for $m = 16$, $U = 0.3n$, 32 resources, $rsf = 0.1$, and short critical sections. The schedulability of the considered preemptable lock types in this configuration is shown in Fig. 2560.

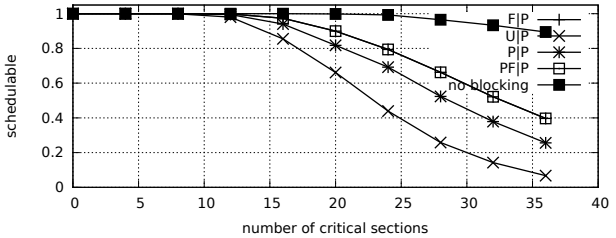

Fig. 2559. Schedulability under preemptable spin locks for $m = 16$, $U = 0.3n$, 32 resources, $rsf = 0.1$, and medium critical sections. The schedulability of the considered non-preemptable lock types in this configuration is shown in Fig. 2557.

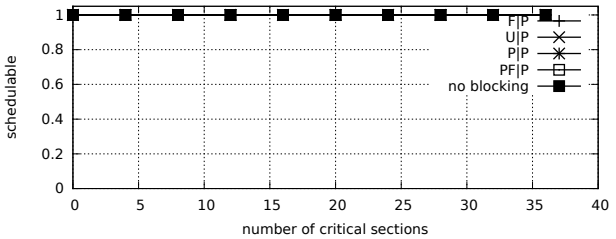

Fig. 2560. Schedulability under preemptable spin locks for $m = 16$, $U = 0.3n$, 32 resources, $rsf = 0.1$, and short critical sections. The schedulability of the considered non-preemptable lock types in this configuration is shown in Fig. 2558.

Configurations with $U = 0.1n$

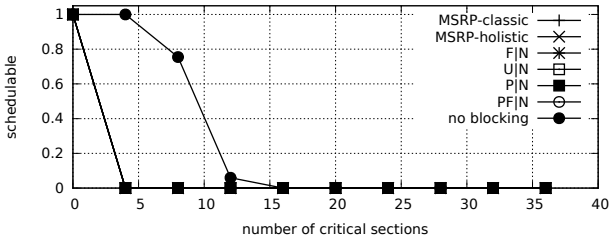

Fig. 2561. Schedulability under non-preemptable spin locks for $m = 16$, $U = 0.1n$, 32 resources, $rsf = 0.25$, and medium critical sections. The schedulability of the considered preemptable lock types in this configuration is shown in Fig. 2563.

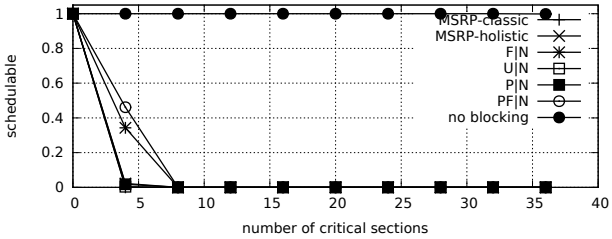

Fig. 2562. Schedulability under non-preemptable spin locks for $m = 16$, $U = 0.1n$, 32 resources, $rsf = 0.25$, and short critical sections. The schedulability of the considered preemptable lock types in this configuration is shown in Fig. 2564.

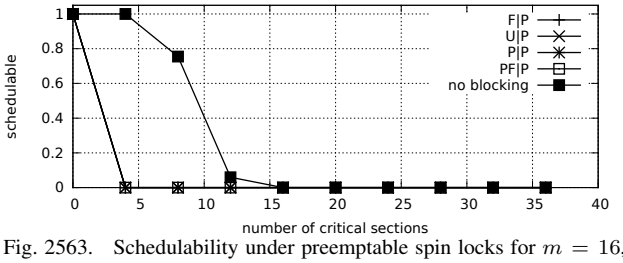

Fig. 2563. Schedulability under preemptable spin locks for $m = 16$, $U = 0.1n$, 32 resources, $rsf = 0.25$, and medium critical sections. The schedulability of the considered non-preemptable lock types in this configuration is shown in Fig. 2561.

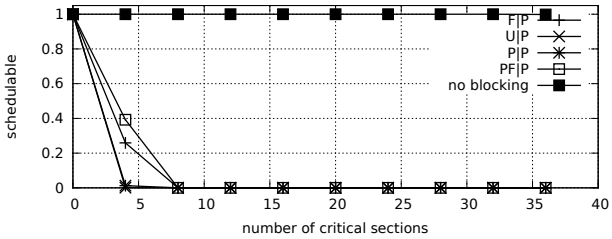

Fig. 2564. Schedulability under preemptable spin locks for $m = 16$, $U = 0.1n$, 32 resources, $rsf = 0.25$, and short critical sections. The schedulability of the considered non-preemptable lock types in this configuration is shown in Fig. 2562.

Configurations with $U = 0.2n$

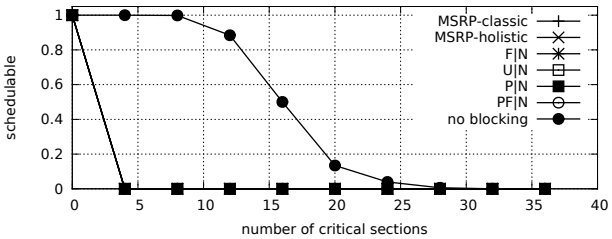

Fig. 2565. Schedulability under non-preemptable spin locks for $m = 16$, $U = 0.2n$, 32 resources, $rsf = 0.25$, and medium critical sections. The schedulability of the considered preemptable lock types in this configuration is shown in Fig. 2567.

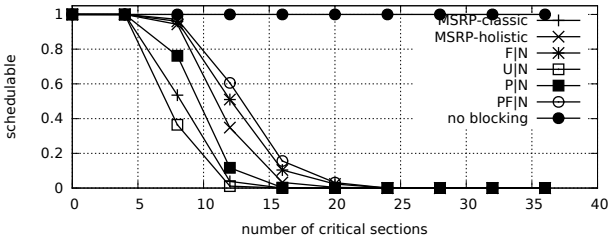

Fig. 2566. Schedulability under non-preemptable spin locks for $m = 16$, $U = 0.2n$, 32 resources, $rsf = 0.25$, and short critical sections. The schedulability of the considered preemptable lock types in this configuration is shown in Fig. 2568.

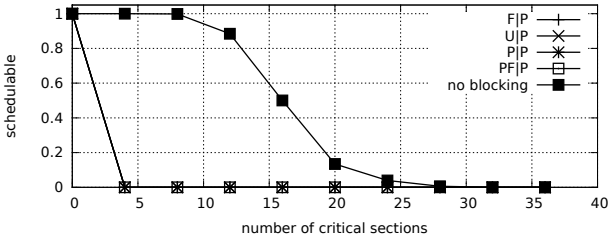

Fig. 2567. Schedulability under preemptable spin locks for $m = 16$, $U = 0.2n$, 32 resources, $rsf = 0.25$, and medium critical sections. The schedulability of the considered non-preemptable lock types in this configuration is shown in Fig. 2565.

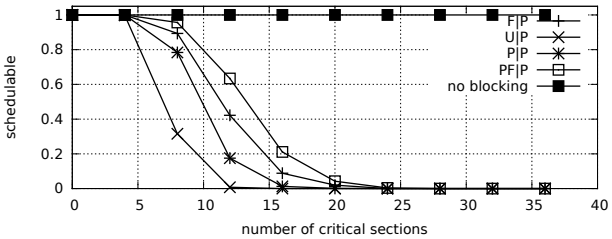

Fig. 2568. Schedulability under preemptable spin locks for $m = 16$, $U = 0.2n$, 32 resources, $rsf = 0.25$, and short critical sections. The schedulability of the considered non-preemptable lock types in this configuration is shown in Fig. 2566.

Configurations with $U = 0.3n$

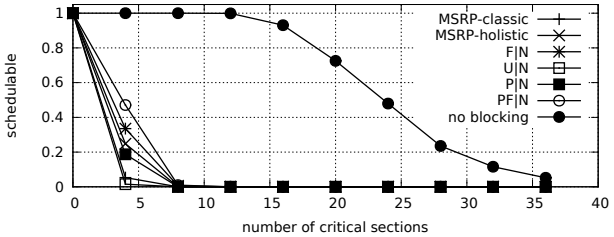

Fig. 2569. Schedulability under non-preemptable spin locks for $m = 16$, $U = 0.3n$, 32 resources, $rsf = 0.25$, and medium critical sections. The schedulability of the considered preemptable lock types in this configuration is shown in Fig. 2571.

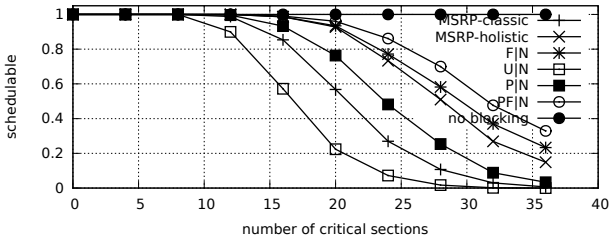

Fig. 2570. Schedulability under non-preemptable spin locks for $m = 16$, $U = 0.3n$, 32 resources, $rsf = 0.25$, and short critical sections. The schedulability of the considered preemptable lock types in this configuration is shown in Fig. 2572.

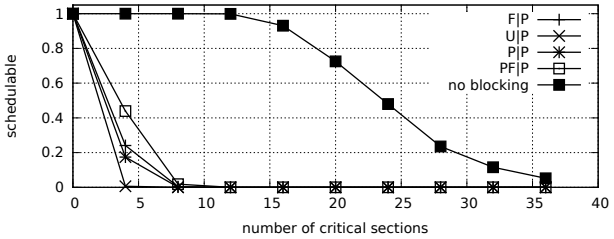

Fig. 2571. Schedulability under preemptable spin locks for $m = 16$, $U = 0.3n$, 32 resources, $rsf = 0.25$, and medium critical sections. The schedulability of the considered non-preemptable lock types in this configuration is shown in Fig. 2569.

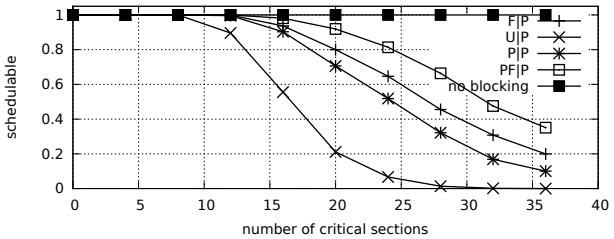

Fig. 2572. Schedulability under preemptable spin locks for $m = 16$, $U = 0.3n$, 32 resources, $rsf = 0.25$, and short critical sections. The schedulability of the considered non-preemptable lock types in this configuration is shown in Fig. 2570.

Configurations with $U = 0.1n$

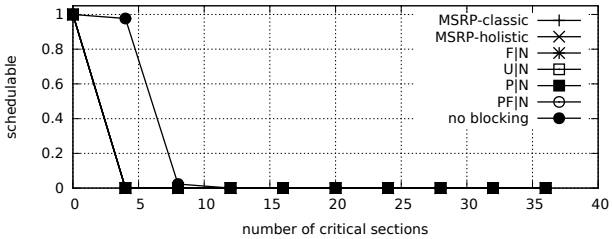

Fig. 2573. Schedulability under non-preemptable spin locks for $m = 16$, $U = 0.1n$, 32 resources, $rsf = 0.4$, and medium critical sections. The schedulability of the considered preemptable lock types in this configuration is shown in Fig. 2575.

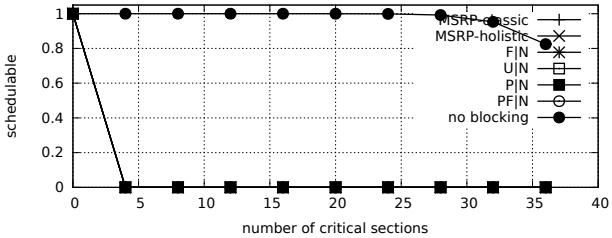

Fig. 2574. Schedulability under non-preemptable spin locks for $m = 16$, $U = 0.1n$, 32 resources, $rsf = 0.4$, and short critical sections. The schedulability of the considered preemptable lock types in this configuration is shown in Fig. 2576.

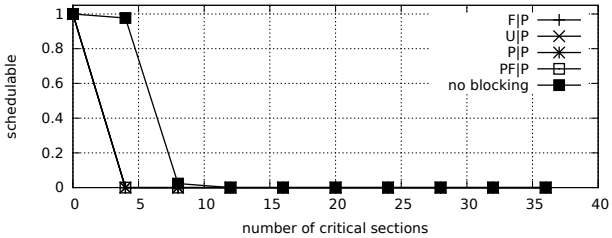

Fig. 2575. Schedulability under preemptable spin locks for $m = 16$, $U = 0.1n$, 32 resources, $rsf = 0.4$, and medium critical sections. The schedulability of the considered non-preemptable lock types in this configuration is shown in Fig. 2573.

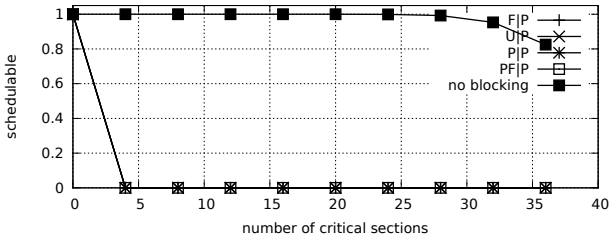

Fig. 2576. Schedulability under preemptable spin locks for $m = 16$, $U = 0.1n$, 32 resources, $rsf = 0.4$, and short critical sections. The schedulability of the considered non-preemptable lock types in this configuration is shown in Fig. 2574.

Configurations with $U = 0.2n$

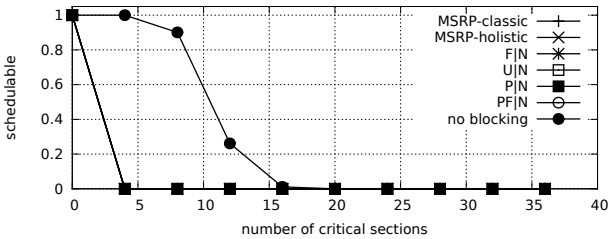

Fig. 2577. Schedulability under non-preemptable spin locks for $m = 16$, $U = 0.2n$, 32 resources, $rsf = 0.4$, and medium critical sections. The schedulability of the considered preemptable lock types in this configuration is shown in Fig. 2579.

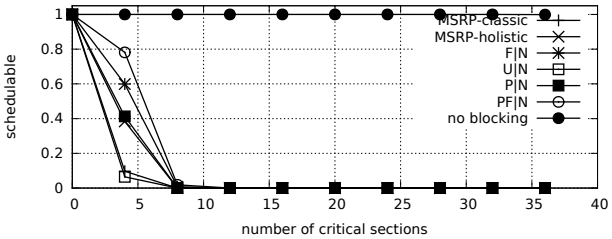

Fig. 2578. Schedulability under non-preemptable spin locks for $m = 16$, $U = 0.2n$, 32 resources, $rsf = 0.4$, and short critical sections. The schedulability of the considered preemptable lock types in this configuration is shown in Fig. 2580.

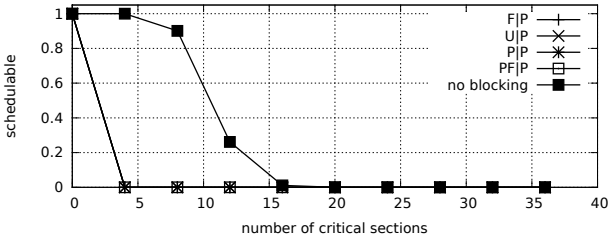

Fig. 2579. Schedulability under preemptable spin locks for $m = 16$, $U = 0.2n$, 32 resources, $rsf = 0.4$, and medium critical sections. The schedulability of the considered non-preemptable lock types in this configuration is shown in Fig. 2577.

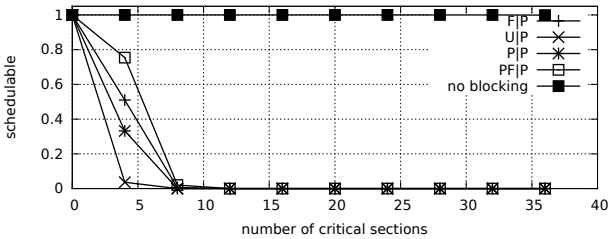

Fig. 2580. Schedulability under preemptable spin locks for $m = 16$, $U = 0.2n$, 32 resources, $rsf = 0.4$, and short critical sections. The schedulability of the considered non-preemptable lock types in this configuration is shown in Fig. 2578.

Configurations with $U = 0.3n$

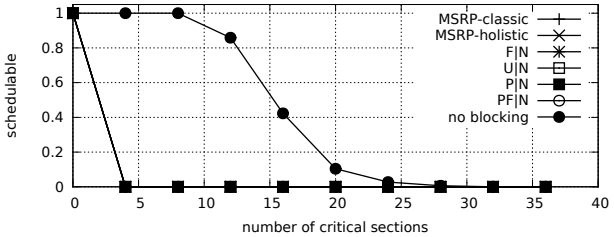

Fig. 2581. Schedulability under non-preemptable spin locks for $m = 16$, $U = 0.3n$, 32 resources, $rsf = 0.4$, and medium critical sections. The schedulability of the considered preemptable lock types in this configuration is shown in Fig. 2583.

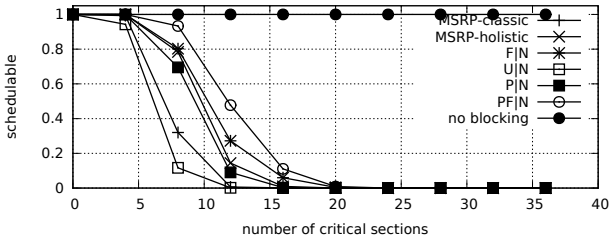

Fig. 2582. Schedulability under non-preemptable spin locks for $m = 16$, $U = 0.3n$, 32 resources, $rsf = 0.4$, and short critical sections. The schedulability of the considered preemptable lock types in this configuration is shown in Fig. 2584.

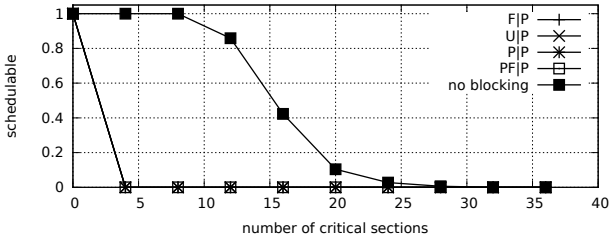

Fig. 2583. Schedulability under preemptable spin locks for $m = 16$, $U = 0.3n$, 32 resources, $rsf = 0.4$, and medium critical sections. The schedulability of the considered non-preemptable lock types in this configuration is shown in Fig. 2581.

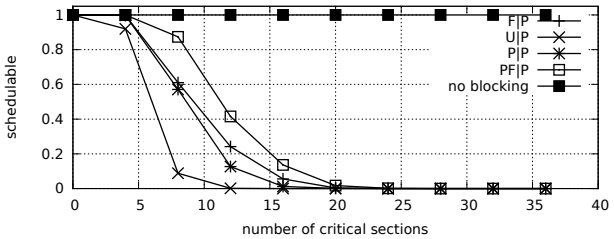

Fig. 2584. Schedulability under preemptable spin locks for $m = 16$, $U = 0.3n$, 32 resources, $rsf = 0.4$, and short critical sections. The schedulability of the considered non-preemptable lock types in this configuration is shown in Fig. 2582.

Configurations with $U = 0.1n$

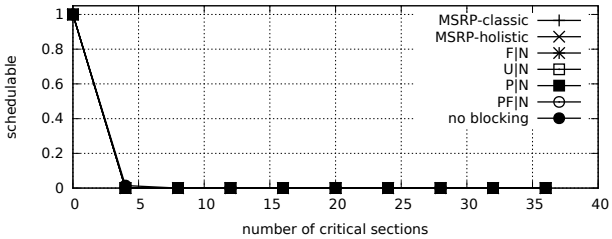

Fig. 2585. Schedulability under non-preemptable spin locks for $m = 16$, $U = 0.1n$, 32 resources, $rsf = 0.75$, and medium critical sections. The schedulability of the considered preemptable lock types in this configuration is shown in Fig. 2587.

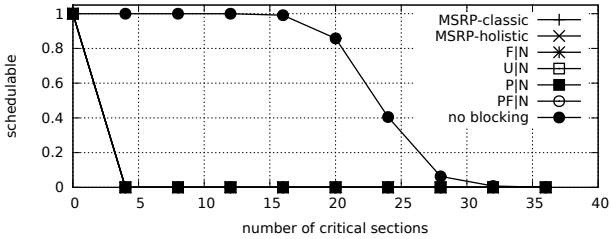

Fig. 2586. Schedulability under non-preemptable spin locks for $m = 16$, $U = 0.1n$, 32 resources, $rsf = 0.75$, and short critical sections. The schedulability of the considered preemptable lock types in this configuration is shown in Fig. 2588.

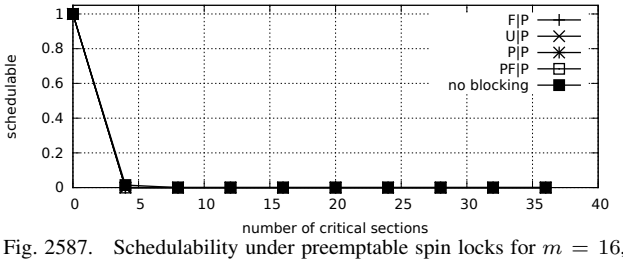

Fig. 2587. Schedulability under preemptable spin locks for $m = 16$, $U = 0.1n$, 32 resources, $rsf = 0.75$, and medium critical sections. The schedulability of the considered non-preemptable lock types in this configuration is shown in Fig. 2585.

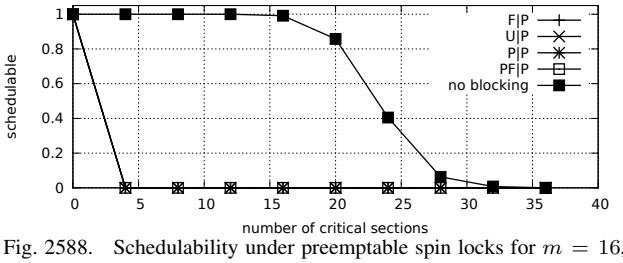

Fig. 2588. Schedulability under preemptable spin locks for $m = 16$, $U = 0.1n$, 32 resources, $rsf = 0.75$, and short critical sections. The schedulability of the considered non-preemptable lock types in this configuration is shown in Fig. 2586.

Configurations with $U = 0.2n$

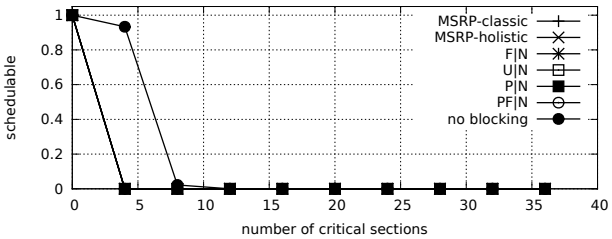

Fig. 2589. Schedulability under non-preemptable spin locks for $m = 16$, $U = 0.2n$, 32 resources, $rsf = 0.75$, and medium critical sections. The schedulability of the considered preemptable lock types in this configuration is shown in Fig. 2591.

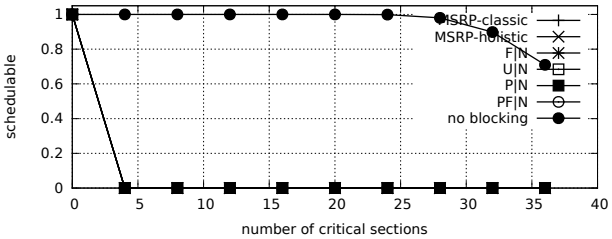

Fig. 2590. Schedulability under non-preemptable spin locks for $m = 16$, $U = 0.2n$, 32 resources, $rsf = 0.75$, and short critical sections. The schedulability of the considered preemptable lock types in this configuration is shown in Fig. 2592.

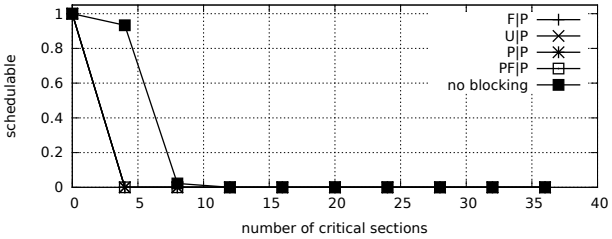

Fig. 2591. Schedulability under preemptable spin locks for $m = 16$, $U = 0.2n$, 32 resources, $rsf = 0.75$, and medium critical sections. The schedulability of the considered non-preemptable lock types in this configuration is shown in Fig. 2589.

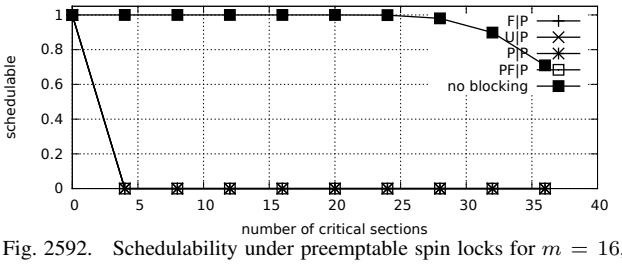

Fig. 2592. Schedulability under preemptable spin locks for $m = 16$, $U = 0.2n$, 32 resources, $rsf = 0.75$, and short critical sections. The schedulability of the considered non-preemptable lock types in this configuration is shown in Fig. 2590.

Configurations with $U = 0.3n$

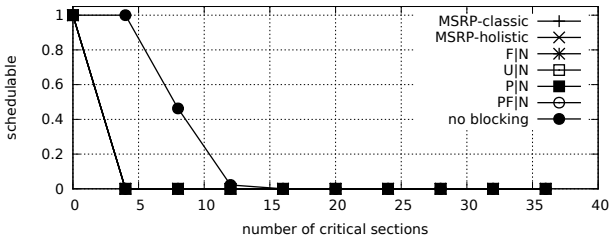

Fig. 2593. Schedulability under non-preemptable spin locks for $m = 16$, $U = 0.3n$, 32 resources, $rsf = 0.75$, and medium critical sections. The schedulability of the considered preemptable lock types in this configuration is shown in Fig. 2595.

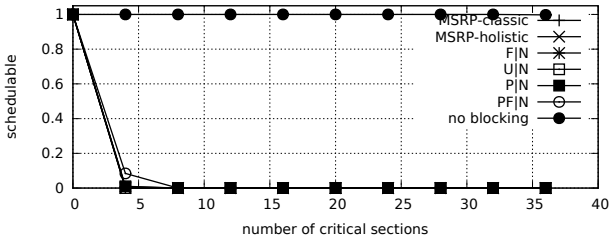

Fig. 2594. Schedulability under non-preemptable spin locks for $m = 16$, $U = 0.3n$, 32 resources, $rsf = 0.75$, and short critical sections. The schedulability of the considered preemptable lock types in this configuration is shown in Fig. 2596.

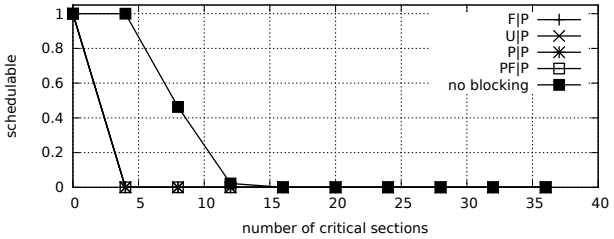

Fig. 2595. Schedulability under preemptable spin locks for $m = 16$, $U = 0.3n$, 32 resources, $rsf = 0.75$, and medium critical sections. The schedulability of the considered non-preemptable lock types in this configuration is shown in Fig. 2593.

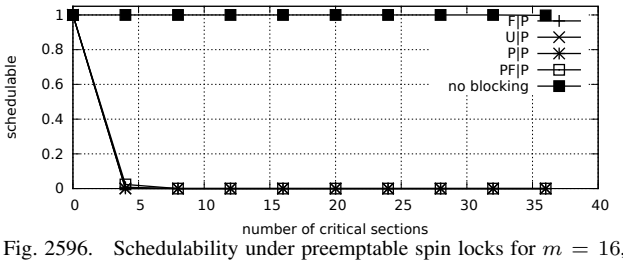

Fig. 2596. Schedulability under preemptable spin locks for $m = 16$, $U = 0.3n$, 32 resources, $rsf = 0.75$, and short critical sections. The schedulability of the considered non-preemptable lock types in this configuration is shown in Fig. 2594.